AD-763 699

# DEFENSE NUCLEAR AGENCY REACTION RATE HANDBOOK, SECOND EDITION

GENERAL ELECTRIC Co.

PREPARED FOR
DEFENSE NUCLEAR AGENCY

MARCH 1972

Distributed By:

NTIS
National Technical Information Service
U. S. DEPARTMENT OF COMMERCE

AD 763699

DNA 1948H
(Formerly DASA 1948)

# DEFENSE NUCLEAR AGENCY
# REACTION RATE HANDBOOK

## SECOND EDITION

MARCH 1972

APPROVED FOR PUBLIC RELEASE; DISTRIBUTION UNLIMITED

Unclassified
Security Classification

**DOCUMENT CONTROL DATA - R & D**

*(Security classification of title, body of abstract and indexing annotation must be entered when the overall report is classified)*

| | |
|---|---|
| 1. ORIGINATING ACTIVITY (Corporate author)<br>General Electric Co.<br>Space Sciences Laboratory<br>P.O. Box 8555, Philadelphia, Pa. 19101 | 2a. REPORT SECURITY CLASSIFICATION<br>Unclassified<br>2b. GROUP |

3. REPORT TITLE

DNA Reaction Rate Handbook

4. DESCRIPTIVE NOTES (Type of report and inclusive dates)
Final Report

5. AUTHOR(S) (First name, middle initial, last name)

Editors-in-Chief: Dr. M.H. Bortner, Dr. Theo. Baurer; Project Officer: Dr. C.A. Blank; and various authors contributing chapters on their specialties.

| | | |
|---|---|---|
| 6. REPORT DATE<br>March 1972 | 7a. TOTAL NO. OF PAGES<br~~980~~ 1033 | 7b. NO. OF REFS |
| 8a. CONTRACT OR GRANT NO.<br>DASA-01-70-C-0082, DASA-01-71-C-0145<br>b. PROJECT NO.<br>NWED Subtask Code HD028,<br>c. Work Unit 11<br>d. | 9a. ORIGINATOR'S REPORT NUMBER(S)<br>DNA 1948H<br>9b. OTHER REPORT NO(S) (Any other numbers that may be assigned this report)<br>None | |

10. DISTRIBUTION STATEMENT

Approved for Public Release; Distribution Unlimited

| | |
|---|---|
| 11. SUPPLEMENTARY NOTES<br>Published by DASIAC<br>DoD Nuclear Information & Analysis Center | 12. SPONSORING MILITARY ACTIVITY<br>Defense Nuclear Agency<br>Washington, D.C. 20305 |

13. ABSTRACT

This DNA-sponsored handbook contains the latest and most accurate information on upper atmospheric chemical and physical processes. Such information is required for the solution of various problems involving military radar and communication blackout. Periodic additions to, and revisions of, this handbook are planned to accommodate new information, revise data, etc. The twenty-four chapters are divided into four major groups: Group A—Chapters on Atmospheric Background; Group B—Methods of Gathering Data; Group C—Chapters on Pertinent Rate Data; Group D—Chapters on Data Application. Appropriate appendices are included.

DD FORM 1 NOV 65 1473 REPLACES DD FORM 1473, 1 JAN 64, WHICH IS OBSOLETE FOR ARMY USE.

Unclassified
Security Classification

| 14. KEY WORDS | LINK A | | LINK B | | LINK C | |
|---|---|---|---|---|---|---|
| | ROLE | WT | ROLE | WT | ROLE | WT |
| Reaction rate<br>Upper atmospheric physical and chemical processes<br>Electromagnetic blackaut | | | | | | |

AD763699

MEMORANDUM

To: All Authorized Recipients of the DNA Reaction Rate Handbook (DNA 1948H)

From: The Editors

Enclosed herewith you will find a copy of Revision Number 1 to the Handbook. It comprises:

1. Revised interim version of Chapter 2.
2. Revised pages applicable to Appendices A, F, and G.

You should immediately substitute the enclosed items into your copy of the Handbook, discarding the corresponding pages which they replace.

You should also enter on page iii in front of your Handbook the following information: Revision No. 1; Date of Issue- November 1972; Date of Receipt-whatever day you receive this; and sign your name in the last column.

Revision Number 2 is expected to be issued during the late spring or early summer of 1973. Thank you for your patience and cooperation.

DNA 1948H
(Farmerly DASA 1948)
Revisian No.1

DEFENSE NUCLEAR AGENCY

# REACTION RATE HANDBOOK

SECOND EDITION
REVISION NUMBER 1

Editars-in-Chief:
Dr. M.H. Bartner
Dr. T. Baurer

NOVEMBER 1972

Project Officer: Dr. C.A. Blank

APPROVED FOR PUBLIC RELEASE; DISTRIBUTION UNLIMITED

Organized by General Electric Space Sciences Laboratary
For The Defense Nuclear Agency Under Cantracts
DASA 01-70-C-0052 and DASA 01-71-C-0145

This effort supported by Defense Nuclear Agency
NWED Subtask Cade HD028, Work Unit 11

Published by DASIAC
DaD Nucleor Infarmation and Analysis Center
Generol Electric, TEMPO
Santa Borbora, California 93102

# 2. THE NATURAL ATMOSPHERE: ATMOSPHERIC STRUCTURE

K.S.W. Champion, Air Force Cambridge Research Laboratories
(Latest Revision 16 March 1972)

N. B.: This chapter is not ready for publication, as of the latest revision date, cited above. However, the author has supplied selected reference data for the use of other authors elsewhere in the Handbook, and those authors therefore are enabled to cite Chapter 2 as the source of the information thus utilized. Chapter 2 will be prepared and distributed to authorized recipients of the Handbook at an early date. In the meantime, readers are encouraged to refer to the predecessor chapter by the same author in the First Edition of the Handbook, to other chapters in this Edition (numbers 4, 5, 13) in which data supplied by Dr. Champion are used as noted above, and to two papers* presented by Dr. Champion and his co-workers at the Fourteenth COSPAR Meeting, Seattle, Washington, June 1971. One of the two preprints referenced below is included herewith, in expanded form, as an interim version of Chapter 2.

---

*Champion, K. S. W., "The Properties of the Neutral Atmosphere", Paper R. 5; Champion, K. S. W., and R. A. Schweinfurth, "The Mean COSPAR International Reference Atmosphere", Paper F. 2, Fourteenth COSPAR Meeting, Seattle, Washington, June, 1971.

# THE MEAN COSPAR INTERNATIONAL REFERENCE ATMOSPHERE

K. S. W. Champion and R. A. Schweinfurth
Air Force Cambridge Research Laboratories
Bedford, Massachusetts, U. S. A.

This contributed paper has been prepared for presentation at the Fourteenth COSPAR Meeting, June 1971 in Seattle. Paper F.2.

# THE MEAN COSPAR INTERNATIONAL REFERENCE ATMOSPHERE

K. S. W. Champion and R. A. Schweinfurth
Air Force Cambridge Research Laboratories
Bedford, Massachusetts, U. S. A.

## 1. INTRODUCTION

The new mean atmosphere has been developed for the altitude range 25 to 500 km. The basis of the reference atmosphere is as follows:

Between 25 and 75 km the model represents annual mean conditions for latitudes near 30°.

Between 120 and 500 km the model corresponds to diurnal, seasonal, and semiannual variation average conditions for a latitude near 30° and a solar flux $\overline{F}$ of $145 \times 10^{-22}$ W/m$^2$/Hz.

Between 75 and 120 km a model has been developed which provides a smooth connection between the lower and upper sections of the mean atmosphere.

In addition, a basis is suggested for extending the model from 25 km to ground-level.

It should be noted that throughout the Mean Reference Atmosphere the same formula (appropriate to a latitude of 30°) has been used for the acceleration due to gravity.

This atmosphere contains temperature, density, pressure, density and pressure scale heights, mean molecular weight, densities of major constituents, and total number densities.

The reasons for providing a Mean Reference Atmosphere are twofold:

(1) For many computations it is unnecessary to include a variety of atmospheric conditions and it is sufficient and economical to use a single typical model of the atmosphere.

(2) The respective low and high altitude models of the Reference Atmospheres are functions of different parameters and do not match at 110 km. Thus, if computations are to span this altitude it will, in general, be most satisfactory to use the mean model.

## 2. MODEL BETWEEN 25 AND 75 km

The data used to develop this model were the annual mean pressure value at 25 km at 30° latitude and the annual mean temperature values at 30° latitude at 5 km intervals starting at 25 km derived from Groves [1]. The actual values are as follows:

Pressure at 25 km: $2.483 \times 10^3$ newtons/$m^2$

| Altitude (km) | 25 | 30 | 35 | 40 | 45 | 50 |
|---|---|---|---|---|---|---|
| Temperature (K) | 221.7 | 230.7 | 241.5 | 255.3 | 267.7 | 271.6 |
| Altitude (km) | 55 | 60 | 65 | 70 | 75 | |
| Temperature (K) | 263.9 | 249.3 | 232.7 | 216.2 | 205.0 | |

Starting at 25 km the atmospheric properties were computed using the following equations. Simpson's Rule was used to integrate numerically the pressure equation:

$$p = p_1 \exp\left[-\frac{M_o}{R}\int_{z_1}^{z} g\,dz/T_M\right] \qquad (1)$$

where: $p_1$ = pressure at reference altitude $z_1$

$p$ = pressure at altitude $z$

$M_o$ = sea level value of mean molecular weight = 28.96

$R$ = universal gas constant = $8.31432 \times 10^7$ ergs $K^{-1}$ $gmole^{-1}$

$g$ = acceleration due to gravity

$T_M$ = molecular-scale temperature

$$T_M = \frac{M_o}{M} T \ , \qquad (2)$$

where M = mean molecular weight

T = kinetic temperature.

The total density was calculated from the relation:

$$\rho = \frac{pM}{RT} = \frac{pM_o}{RT_M} \quad . \tag{3}$$

The pressure scale height was calculated from:

$$Hp = \frac{RT}{Mg} = \frac{RT_M}{M_o g} \quad . \tag{4}$$

As the aim of the computations was to derive a model for the altitude region 25 to 500 km using a single expression for the acceleration due to gravity the expressions used respectively for the low and high altitude models were investigated. Unfortunately, neither formula was adequate. The formula used by Groves was the same as in CIRA 1965 and was sufficient in all respects except that its accuracy at high altitudes was not acceptable. The error was 1 in $10^4$ at 200 km, 4 in $10^4$ at 300 km, and increased rapidly with altitude. On the other hand, the expression used by Jacchia [2] is valid only for a latitude near 45° (45°32'33"). The problem was solved by adding another term to the expression used in CIRA 1965. The basic expression due to Lambert [3] includes dependence on latitude $\phi$:

$$\begin{aligned} g = g\phi &- (3.085462 \times 10^{-6} + 2.27 \times 10^{-9} \cos 2\phi)z \\ &+ (7.254 \times 10^{-13} + 1.0 \times 10^{-15} \cos 2\phi)z^2 \\ &- (1.517 \times 10^{-19} + 6 \times 10^{-22} \cos 2\phi)z^3 \ \text{m/sec}^2 \end{aligned} \tag{5}$$

where z is in meters.

The form applicable to 30° latitude is

$$\begin{aligned} g = 9.79324 &- 3.086597 \times 10^{-6}\, z + 7.259 \times 10^{-13}\, z^2 \\ &- 1.520 \times 10^{-19}\, z^3 \ \text{m/sec}^2 \quad . \end{aligned} \tag{6}$$

## 3. MODEL BETWEEN 75 AND 120 km

The model in this region has to provide a transition between the low altitude model based on Groves' data [1] and Jacchia's high altitude models [2]. Jacchia's models start at 90 km and Groves' models extend to 110 km and they are not only different but they are functions of different parameters. Obviously a compromise must be devised.

As a starting point a temperature profile had to be chosen. As inputs for this it is interesting to compare the values from several models given below:

| Altitude (km) | Temperature ($T_M$, K) | | | |
|---|---|---|---|---|
| | US Std Atm 1962 | CIRA 1965 | Groves* | Jacchia+ |
| 80 | 180.65 | 186.0 | 197.3 | - |
| 90 | 180.65 | 186.0 | 189.0 | 183.8 |
| 100 | 210.65 | 213.0 | 215.1 | 203.5 |
| 110 | 260.65 | 263.0 | 284.0 | 265.5 |
| 120 | 360.65 | 380.7 | - | 380.6 |

*Average annual values for 30° latitude converted from kinetic temperatures using the values of M in reference [1].

+Average values for 45° latitude from model with 1000 K exospheric temperature using the values of M in reference [2] to convert the kinctic temperatures.

Two points should be noted. One is that Groves' temperature at 80 km is substantially higher than that in other models. The second is the differences between the temperatures of the Groves and Jacchia models. A further constraint on the temperature profile used in this altitude region is that it must yield a specified density value at 120 km. The values determined for the molecular-scale temperature ($T_M$) are:

| Altitude (km) | 80 | 90 | 100 | 110 | 120 |
|---|---|---|---|---|---|
| Temperature ($T_M$, K) | 195.0 | 183.8 | 203.5 | 265.5 | 380.6 |

The adjustments in the temperature profile were made between 75 and 90 km.

Composition was calculated for this region by J. D. George using the techniques of George, Zimmerman, and Keneshea [4], which include the effects of chemistry and atmospheric dynamics.

The equations used are a system of mass and momentum conservation equations given below for the i'th species:

$$\frac{\partial n_i}{\partial t} = F_i - n_i R_i - \frac{\partial (n_i u_i)}{\partial z} - \frac{\partial \varphi_i}{\partial z} \tag{7}$$

$$\frac{\partial u_i}{\partial t} = \frac{-kT}{m_1}\left(\frac{1}{n_i}\frac{\partial n_i}{\partial z} + \frac{1}{T}\frac{\partial T}{\partial z} + \frac{1}{H_i}\right) - [N_2]C_i u_i \tag{8}$$

where:

$n_i$ = the concentration of the i'th species

$u_i$ = the mean velocity of the i'th species

$= V_i + \bar{u}$

$V_i$ = the diffusion velocity of the i'th species

$\bar{u}$ = the mean mass velocity

$t$ = time

$z$ = altitude

$F_i$ = chemical formation rate of the i'th species

$n_i R_i$ = chemical removal rate of the i'th species

$k$ = Boltzmann constant

$m_i$ = mass of the i'th species

$H_i$ = scale height of the i'th species

$n_i[N_2]C_i$ is proportional to the frequency of collisions between $N_2$ and the i'th species.

$\varphi_i$ is the turbulent mixing flux for the i'th species given by:

$$\varphi_i = -K_t\left[\frac{\partial n_i}{\partial z} + n_i\left(\frac{1}{T}\frac{\partial T}{\partial z} + \frac{1}{H_m}\right)\right] , \tag{9}$$

where $K_t$ is the turbulent diffusion coefficient and $H_m$ is the scale height of a species with the mean mass.

At the lower boundary at 75 km $N_2$, $O_2$, Ar, and He were assumed to have the same mixing ratio as at ground level taken from the U. S. Standard Atmosphere, 1962. At this boundary the species O and $O_3$ were chemically determined by:

$$\frac{\partial n_i}{\partial t} = F_i - n_i R_i \quad . \tag{10}$$

Although not printed in the tables the following species were included in the computations and their densities determined: $H_2O$ (ground level mixing ratio at 75 km), OH, H, $H_2$, $HO_2$, and $H_2O_2$ (chemically determined at 75 km).

The mean velocity ($u_i$) was assumed to be zero for all species at the upper boundary at 120 km. The turbulent flux for all species is also zero at that altitude since the assumed turbulent diffusion coefficient $K_t$ is zero above the turbopause at 100 km. The concentrations of $N_2$, $O_2$, O, Ar, and He were fixed at the upper boundary at the values for the high altitude portion of the model. The remaining species were assumed to be in diffusive equilibrium.

Since a diurnally varying solar flux was used with equations (7), (8), and (9) periodic solutions are obtained. The solution was continued for 32 problem days for a latitude of 30°N using a fixed declination angle (0° or equinox) resulting in a periodically varying zenith angle. The choice of 32 days was arbitrary but did result in adequate accuracy. The variation in the densities of all species was less than one part per thousand from noon of day 31 to noon of day 32. The mean profiles presented here were obtained by averaging over the final 24 hours at 15-minute intervals. One of the constraints of the solution was to maintain a fixed molecular scale temperature profile. The kinetic temperature profile was derived using the solution mean molecular weight. The kinetic temperatures were used to compute the $N_2$ concentrations in the diffusive equilibrium region from 101 to 120 km. A transition from diffusive equilibrium at 101 km to mixing at 99 km was made using a cubic to represent $\log_{10}[N_2]$. Below 99 km, the mixing region for $N_2$, the initial $N_2$ profile was not changed.

In performing the computations the variation with temperature of the reaction rate constants $R_i$ was included, as well as the effects of absorption by the $O_2$ and $O_3$ column densities on the dissociation rates by solar ultraviolet radiation. The finite difference analogues used are essentially those given by Shimazaki [5] with modifications as cited by George, Zimmerman, and Keneshea [4]. However, the technique used is modified in that the equations are treated as fully implicit throughout the solution. This approach should preserve the conservation of atoms within the solution altitude region (75 to 120 km) with the exception of the loss of atoms through the lower boundary.

## 4. MODEL ABOVE 120 km

The exospheric temperature was calculated to correspond to average diurnal, seasonal, semi-annual, and geomagnetic conditions for 30° latitude and a solar flux of $145 \times 10^{-22}$ W/m$^2$/Hz. The resultant exospheric temperature is 1000 K.

Jacchia's models were recomputed from 90 km upwards using the expression for g given in equation (6). This results in a change in the total density and number densities of the constituents at higher altitudes. The densities were then changed (at all altitudes) so that at 120 km they matched the density computed for the intermediate altitude model. These densities are very close to those of the 1000 K Jacchia model at 120 km as shown immediately below, but are slightly different at other altitudes.

| Altitude (km) | Temp (K) | Log [$N_2$]($m^{-3}$) | Log [$O_2$]($m^{-3}$) |
|---|---|---|---|
| 120 | 334.5 | 17.5789 | 16.7338 |

| Log [O]($m^{-3}$) | Log [Ar]($m^{-3}$) | Log [He]($m^{-3}$) | M |
|---|---|---|---|
| 17.1532 | 15.1732 | 13.5376 | 25.45 |

| Density ($kgm^{-3}$) |
|---|
| $2.438 \times 10^{-8}$ |

Above the turbopause (assumed to be at 100 km) the number densities of each individual species $n_i$ were computed by integrating the equation for diffusive equilibrium:

$$\frac{dn_i}{n_i} = -\frac{M_i g}{RT}\,dz - (1 + \alpha_i)\frac{dT}{T} \quad , \tag{11}$$

where $\alpha_i$ is the thermal diffusion coefficient taken to be -0.33 for helium and zero for other constituents.

## 5. MEAN REFERENCE ATMOSPHERE

The properties of the Mean Reference Atmosphere are presented in Tables 1-4. Table 1 contains values of molecular scale temperature, density, log density, pressure, log pressure, number density, pressure scale height, and acceleration due to gravity over the altitude range 25 to 120 km.* Table 2 contains values of kinetic temperature, mean molecular weight, and log number densities of $N_2$, $O_2$, O, Ar. He, and $O_3$ over the altitude range 75 to 120 km. Densities of O and $O_3$ are not presented below 80 km because at these altitudes their diurnal variation is so large that average values would have little significance. The $O_3$ densities presented are for noon. In Table 3 are given molecular scale temperature, density, log density, pressure, log pressure, pressure scale height, and acceleration due to gravity for the altitude range 120 to 500 km. Table 4 contains the corresponding values of kinetic temperature, mean molecular weight, number density, and log number densities of $N_2$, $O_2$, O, Ar, and He for the altitudes 120 to 500 km.

The properties of the Mean Reference Atmosphere are illustrated in Figures 1-7. Figure 1 shows the pressure scale height as a function of altitude. Figure 2 shows the kinetic temperature (T) and the molecular-scale temperature ($T_M$). Figure 3 contains the kinetic

*The Mean CIRA has been developed for the altitude range 25 to 500 km. At 25 km the Mean CIRA values are almost identical with those of the US Standard Atmosphere Supplements, 1966 midlatitude spring/fall model. Thus the values in Table 1 can be extended to ground level by using the numbers in Table 5.1, page 119 of the Supplements. If an exact match is required for a given parameter, e.g., temperature, density, or pressure, then the Mean CIRA 25-km value can be matched to the Supplement value slightly above 25 km (25.15 km for temperature) and then the Supplement altitude values scaled accordingly. Physically this can be justified because different g values were used in developing the two models (45° N and 30° N values for the Supplement and the Mean CIRA, respectively).

temperature of the mean atmosphere plus curves indicating low extreme and high extreme temperatures whose frequency of occurrence is one per cent or less. The extreme curves attain exospheric temperatures of 550 and 1900 K, respectively. The pressure curve for the Mean Atmosphere is shown in Figure 4. Low extreme, high extreme and mean density values are plotted in Figure 5. Above 180 km these curves correspond to the temperature profiles in Figure 3. The mean molecular weights for the mean atmosphere are plotted in Figure 6. The corresponding number densities of $N_2$, $O_2$, O, $O_3$, Ar, He, and H are shown in Figure 7.

To illustrate very large seasonal variations, Figure 8 contains the mean June-July temperature profile for 80° N and Figure 9 the mean December-January temperature profile for the same location. These profiles are based primarily on data from Heiss Island and are from Reference [6]. At 50 km the temperatures range from 279 K in summer to 247 K in winter, compared with the mean reference value of 271.6 K. At 80 km they range from 177 K in summer to 218 K in winter, compared with the reference value of 195 K.

Figure 10 contains the mean CIRA temperatures, median warm temperatures and those exceeded 10% and 1% of the time and, similarly, median cold temperatures and those above which 90% and 99%, respectively, of the temperatures lie. The extreme temperature profiles are a revised version of those in Reference [7]. The corresponding density curves are shown in Figure 11. In general, the mean atmosphere values are in excellent agreement with the other curves.

## 6. REFERENCES

[1] G. V. Groves, Seasonal and latitudinal models of atmospheric temperature, pressure and density, 25 to 100 km, AFCRL-70-0261 (1970).

[2] L. G. Jacchia, Revised static models of the thermosphere and exosphere with empirical temperature profiles, Smithson. Astrophys. Obs. Spec. Report 332 (1971).

[3] W. D. Lambert, Acceleration of gravity in the free air, in Smithsonian Meteorological Tables, sixth edition, Washington (1951) p. 490.

[4] J. D. George, S. P. Zimmerman and T. J. Keneshea, The latitudinal variation of major and minor neutral species in the upper atmosphere, to be published in Space Research XII, Berlin (1972).

[5] T. S. Shimazaki, J. Atmos. Terr. Phys. 29, 723 (1967).

[6] Supplements to the Project of the International Standard Atmosphere Model, ISO/TC-20/SC-6 (Secretariat-30) (1970).

[7] A. E. Cole, in: Space Research XI, Akademie-Verlag, Berlin (1971) p. 813.

## Table 1. Mean Reference Atmosphere structure parameters, 25 to 120 km.

| HEIGHT KM | MOLEC TEMP K | DENSITY KG/M3 | LOG DEN (KG/M3) | PRESSURE NT/M2 | LOG PRESSURE (NT/M2) | NUMBER DENSITY /M3 | PRESSURE SCALE HT KM | G M/SEC2 |
|---|---|---|---|---|---|---|---|---|
| 25 | 221.7 | 3.899E-02 | -1.409 | 2.483E+03 | 3.395 | 8.111E+23 | 6.55 | 9.716 |
| 26 | 223.4 | 3.327E-02 | -1.478 | 2.133E+03 | 3.329 | 6.916E+23 | 6.60 | 9.714 |
| 27 | 225.1 | 2.838E-02 | -1.547 | 1.832E+03 | 3.263 | 5.902E+23 | 6.65 | 9.710 |
| 28 | 226.9 | 2.427E-02 | -1.615 | 1.578E+03 | 3.198 | 5.042E+23 | 6.71 | 9.707 |
| 29 | 228.7 | 2.075E-02 | -1.683 | 1.361E+03 | 3.134 | 4.311E+23 | 6.77 | 9.704 |
| 30 | 230.7 | 1.774E-02 | -1.751 | 1.175E+03 | 3.070 | 3.690E+23 | 6.83 | 9.701 |
| 31 | 232.6 | 1.521E-02 | -1.818 | 1.016E+03 | 3.007 | 3.162E+23 | 6.89 | 9.698 |
| 32 | 234.6 | 1.306E-02 | -1.884 | 8.790E+02 | 2.944 | 2.713E+23 | 6.95 | 9.695 |
| 33 | 236.8 | 1.119E-02 | -1.951 | 7.621E+02 | 2.882 | 2.329E+23 | 7.01 | 9.692 |
| 34 | 239.1 | 9.638E-03 | -2.016 | 6.607E+02 | 2.820 | 2.002E+23 | 7.08 | 9.689 |
| 35 | 241.5 | 8.279E-03 | -2.082 | 5.741E+02 | 2.759 | 1.722E+23 | 7.16 | 9.686 |
| 36 | 244.4 | 7.129E-03 | -2.147 | 5.000E+02 | 2.699 | 1.481E+23 | 7.25 | 9.683 |
| 37 | 247.2 | 6.138E-03 | -2.212 | 4.355E+02 | 2.639 | 1.277E+23 | 7.33 | 9.680 |
| 38 | 250.0 | 5.297E-03 | -2.276 | 3.802E+02 | 2.580 | 1.102E+23 | 7.42 | 9.677 |
| 39 | 252.7 | 4.581E-03 | -2.339 | 3.327E+02 | 2.522 | 9.536E+22 | 7.50 | 9.674 |
| 40 | 255.3 | 3.972E-03 | -2.401 | 2.911E+02 | 2.464 | 8.265E+22 | 7.58 | 9.671 |
| 41 | 258.5 | 3.443E-03 | -2.463 | 2.553E+02 | 2.407 | 7.160E+22 | 7.68 | 9.668 |
| 42 | 261.3 | 2.992E-03 | -2.524 | 2.244E+02 | 2.351 | 6.222E+22 | 7.76 | 9.665 |
| 43 | 263.8 | 2.606E-03 | -2.584 | 1.972E+02 | 2.295 | 5.422E+22 | 7.84 | 9.662 |
| 44 | 266.0 | 2.280E-03 | -2.642 | 1.738E+02 | 2.240 | 4.737E+22 | 7.90 | 9.659 |
| 45 | 267.7 | 1.995E-03 | -2.700 | 1.535E+02 | 2.186 | 4.148E+22 | 7.96 | 9.656 |
| 46 | 269.4 | 1.750E-03 | -2.757 | 1.352E+02 | 2.131 | 3.637E+22 | 8.01 | 9.653 |
| 47 | 270.7 | 1.538E-03 | -2.813 | 1.194E+02 | 2.077 | 3.197E+22 | 8.05 | 9.650 |
| 48 | 271.4 | 1.355E-03 | -2.868 | 1.054E+02 | 2.023 | 2.816E+22 | 8.08 | 9.647 |
| 49 | 271.7 | 1.194E-03 | -2.923 | 9.333E+01 | 1.970 | 2.485E+22 | 8.09 | 9.644 |
| 50 | 271.6 | 1.057E-03 | -2.976 | 8.241E+01 | 1.916 | 2.198E+22 | 8.09 | 9.641 |
| 51 | 270.6 | 9.376E-04 | -3.028 | 7.276E+01 | 1.862 | 1.949E+22 | 8.06 | 9.638 |
| 52 | 269.4 | 8.318E-04 | -3.080 | 6.427E+01 | 1.808 | 1.729E+22 | 8.03 | 9.635 |
| 53 | 267.8 | 7.379E-04 | -3.132 | 5.675E+01 | 1.754 | 1.534E+22 | 7.98 | 9.632 |
| 54 | 266.0 | 6.546E-04 | -3.184 | 5.000E+01 | 1.699 | 1.362E+22 | 7.93 | 9.629 |
| 55 | 263.9 | 5.821E-04 | -3.235 | 4.406E+01 | 1.644 | 1.210E+22 | 7.87 | 9.626 |
| 56 | 261.2 | 5.176E-04 | -3.286 | 3.882E+01 | 1.589 | 1.076E+22 | 7.79 | 9.623 |
| 57 | 258.3 | 4.603E-04 | -3.337 | 3.412E+01 | 1.533 | 9.563E+21 | 7.71 | 9.620 |
| 58 | 255.4 | 4.083E-04 | -3.389 | 2.992E+01 | 1.476 | 8.489E+21 | 7.62 | 9.617 |
| 59 | 252.4 | 3.622E-04 | -3.441 | 2.624E+01 | 1.419 | 7.528E+21 | 7.54 | 9.614 |
| 60 | 249.3 | 3.206E-04 | -3.494 | 2.296E+01 | 1.361 | 6.669E+21 | 7.45 | 9.611 |
| 61 | 246.0 | 2.838E-04 | -3.547 | 2.004E+01 | 1.302 | 5.904E+21 | 7.35 | 9.608 |
| 62 | 242.7 | 2.512E-04 | -3.600 | 1.750E+01 | 1.243 | 5.219E+21 | 7.25 | 9.605 |
| 63 | 239.4 | 2.213E-04 | -3.655 | 1.521E+01 | 1.182 | 4.606E+21 | 7.16 | 9.602 |
| 64 | 236.1 | 1.950E-04 | -3.710 | 1.321E+01 | 1.121 | 4.057E+21 | 7.06 | 9.599 |
| 65 | 232.7 | 1.718E-04 | -3.765 | 1.146E+01 | 1.059 | 3.568E+21 | 6.96 | 9.596 |
| 66 | 229.0 | 1.510E-04 | -3.821 | 9.908E+00 | .996 | 3.137E+21 | 6.85 | 9.593 |
| 67 | 225.5 | 1.321E-04 | -3.879 | 8.570E+00 | .933 | 2.751E+21 | 6.75 | 9.590 |
| 68 | 222.2 | 1.156E-04 | -3.937 | 7.379E+00 | .868 | 2.404E+21 | 6.65 | 9.587 |
| 69 | 219.1 | 1.007E-04 | -3.997 | 6.339E+00 | .802 | 2.096E+21 | 6.56 | 9.584 |
| 70 | 216.2 | 8.770E-05 | -4.057 | 5.445E+00 | .736 | 1.822E+21 | 6.48 | 9.581 |
| 71 | 213.7 | 7.586E-05 | -4.120 | 4.656E+00 | .668 | 1.578E+21 | 6.41 | 9.578 |
| 72 | 211.3 | 6.561E-05 | -4.183 | 3.981E+00 | .600 | 1.364E+21 | 6.34 | 9.575 |

Table 1. (Cont'd.)

| HEIGHT KM | MOLEC TEMP K | DENSITY KG/M3 | LOG DEN (KG/M3) | PRESSURE NT/M2 | LOG PRESSURE (NT/M2) | NUMBER DENSITY /M3 | PRESSURE SCALE HT KM | G M/SEC2 |
|---|---|---|---|---|---|---|---|---|
| 73 | 209.1 | 5.662E-05 | -4.247 | 3.396E+00 | .531 | 1.177E+21 | 6.27 | 9.572 |
| 74 | 207.0 | 4.875E-05 | -4.312 | 2.891E+00 | .461 | 1.013E+21 | 6.21 | 9.569 |
| 75 | 205.0 | 4.178E-05 | -4.379 | 2.460E+00 | .391 | 8.696E+20 | 6.15 | 9.566 |
| 76 | 203.0 | 3.581E-05 | -4.446 | 2.089E+00 | .320 | 7.455E+20 | 6.09 | 9.563 |
| 77 | 201.0 | 3.069E-05 | -4.513 | 1.770E+00 | .248 | 6.381E+20 | 6.04 | 9.560 |
| 78 | 199.0 | 2.624E-05 | -4.581 | 1.496E+00 | .175 | 5.453E+20 | 5.98 | 9.557 |
| 79 | 197.0 | 2.239E-05 | -4.650 | 1.265E+00 | .102 | 4.653E+20 | 5.92 | 9.554 |
| 80 | 195.0 | 1.905E-05 | -4.720 | 1.067E+00 | .028 | 3.964E+20 | 5.86 | 9.551 |
| 81 | 193.0 | 1.622E-05 | -4.790 | 8.974E-01 | -.047 | 3.371E+20 | 5.80 | 9.548 |
| 82 | 191.0 | 1.377E-05 | -4.861 | 7.551E-01 | -.122 | 2.864E+20 | 5.75 | 9.545 |
| 83 | 189.0 | 1.167E-05 | -4.933 | 6.324E-01 | -.199 | 2.428E+20 | 5.69 | 9.542 |
| 84 | 187.1 | 9.863E-06 | -5.006 | 5.297E-01 | -.276 | 2.055E+20 | 5.63 | 9.539 |
| 85 | 185.1 | 8.337E-06 | -5.079 | 4.426E-01 | -.354 | 1.736E+20 | 5.57 | 9.536 |
| 86 | 184.8 | 6.982E-06 | -5.156 | 3.698E-01 | -.432 | 1.453E+20 | 5.57 | 9.533 |
| 87 | 184.5 | 5.834E-06 | -5.234 | 3.090E-01 | -.510 | 1.215E+20 | 5.56 | 9.530 |
| 88 | 184.2 | 4.875E-06 | -5.312 | 2.576E-01 | -.589 | 1.015E+20 | 5.55 | 9.527 |
| 89 | 184.0 | 4.074E-06 | -5.390 | 2.148E-01 | -.668 | 8.482E+19 | 5.55 | 9.524 |
| 90 | 183.8 | 3.396E-06 | -5.469 | 1.795E-01 | -.746 | 7.087E+19 | 5.54 | 9.521 |
| 91 | 184.6 | 2.825E-06 | -5.549 | 1.496E-01 | -.825 | 5.890E+19 | 5.57 | 9.518 |
| 92 | 185.4 | 2.350E-06 | -5.629 | 1.250E-01 | -.903 | 4.901E+19 | 5.59 | 9.515 |
| 93 | 186.7 | 1.950E-06 | -5.710 | 1.045E-01 | -.981 | 4.072E+19 | 5.64 | 9.512 |
| 94 | 188.0 | 1.622E-06 | -5.790 | 8.750E-02 | -1.058 | 3.386E+19 | 5.68 | 9.509 |
| 95 | 190.3 | 1.343E-06 | -5.872 | 7.345E-02 | -1.134 | 2.808E+19 | 5.75 | 9.506 |
| 96 | 192.0 | 1.119E-06 | -5.951 | 6.166E-02 | -1.210 | 2.344E+19 | 5.80 | 9.503 |
| 97 | 194.5 | 9.311E-07 | -6.031 | 5.200E-02 | -1.284 | 1.952E+19 | 5.88 | 9.500 |
| 98 | 197.1 | 7.745E-07 | -6.111 | 4.385E-02 | -1.358 | 1.630E+19 | 5.96 | 9.498 |
| 99 | 200.3 | 6.442E-07 | -6.191 | 3.707E-02 | -1.431 | 1.362E+19 | 6.06 | 9.495 |
| 100 | 203.5 | 5.297E-07 | -6.276 | 3.090E-02 | -1.510 | 1.125E+19 | 6.16 | 9.492 |
| 101 | 207.3 | 4.355E-07 | -6.361 | 2.588E-02 | -1.587 | 9.305E+18 | 6.27 | 9.489 |
| 102 | 211.6 | 3.648E-07 | -6.438 | 2.218E-02 | -1.654 | 7.856E+18 | 6.40 | 9.486 |
| 103 | 216.7 | 3.062E-07 | -6.514 | 1.905E-02 | -1.720 | 6.634E+18 | 6.56 | 9.483 |
| 104 | 221.7 | 2.582E-07 | -6.588 | 1.644E-02 | -1.784 | 5.628E+18 | 6.71 | 9.480 |
| 105 | 228.0 | 2.173E-07 | -6.663 | 1.422E-02 | -1.847 | 4.768E+18 | 6.91 | 9.477 |
| 106 | 234.2 | 1.841E-07 | -6.735 | 1.236E-02 | -1.908 | 4.060E+18 | 7.10 | 9.474 |
| 107 | 241.1 | 1.560E-07 | -6.807 | 1.079E-02 | -1.967 | 3.463E+18 | 7.31 | 9.471 |
| 108 | 248.6 | 1.327E-07 | -6.877 | 9.462E-03 | -2.024 | 2.961E+18 | 7.54 | 9.468 |
| 109 | 256.8 | 1.130E-07 | -6.947 | 8.337E-03 | -2.079 | 2.538E+18 | 7.79 | 9.465 |
| 110 | 265.5 | 9.661E-08 | -7.015 | 7.362E-03 | -2.133 | 2.182E+18 | 8.06 | 9.462 |
| 111 | 274.9 | 8.279E-08 | -7.082 | 6.546E-03 | -2.184 | 1.881E+18 | 8.34 | 9.459 |
| 112 | 284.8 | 7.129E-08 | -7.147 | 5.834E-03 | -2.234 | 1.627E+18 | 8.65 | 9.456 |
| 113 | 295.1 | 6.166E-08 | -7.210 | 5.224E-03 | -2.282 | 1.413E+18 | 8.96 | 9.454 |
| 114 | 305.9 | 5.346E-08 | -7.272 | 4.688E-03 | -2.329 | 1.231E+18 | 9.29 | 9.451 |
| 115 | 317.1 | 4.645E-08 | -7.333 | 4.236E-03 | -2.373 | 1.076E+18 | 9.64 | 9.448 |
| 116 | 329.2 | 4.055E-08 | -7.392 | 3.837E-03 | -2.416 | 9.433E+17 | 10.01 | 9.445 |
| 117 | 341.6 | 3.548E-08 | -7.450 | 3.483E-03 | -2.458 | 8.298E+17 | 10.39 | 9.442 |
| 118 | 354.3 | 3.126E-08 | -7.505 | 3.177E-03 | -2.498 | 7.327E+17 | 10.78 | 9.439 |
| 119 | 366.9 | 2.761E-08 | -7.559 | 2.904E-03 | -2.537 | 6.499E+17 | 11.16 | 9.436 |
| 120 | 380.6 | 2.438E-08 | -7.613 | 2.667E-03 | -2.574 | 5.772E+17 | 11.58 | 9.433 |

Table 2. Kinetic temperature and composition of the Mean Reference Atmosphere, 75 to 120 km.

| HEIGHT KM | TEMP K | MEAN MOL WT | LOG N(N2) (/M3) | LOG N(O2) (/M3) | LOG N(O) (/M3) | LOG N(AR) (/M3) | LOG N(HE) (/M3) | LOG N(O3) (/M3) |
|---|---|---|---|---|---|---|---|---|
| 75 | 205.0 | 28.96 | 20.832 | 20.261 | | 18.910 | 15.659 | |
| 76 | 203.0 | 28.96 | 20.765 | 20.193 | | 18.842 | 15.591 | |
| 77 | 201.0 | 28.96 | 20.698 | 20.124 | | 18.773 | 15.523 | |
| 78 | 198.9 | 28.95 | 20.630 | 20.055 | | 18.704 | 15.454 | |
| 79 | 196.9 | 28.95 | 20.562 | 19.985 | | 18.634 | 15.385 | |
| 80 | 194.9 | 28.95 | 20.492 | 19.914 | 16.794 | 18.563 | 15.315 | 14.495 |
| 81 | 192.9 | 28.94 | 20.422 | 19.843 | 16.896 | 18.492 | 15.244 | 14.434 |
| 82 | 190.9 | 28.94 | 20.352 | 19.771 | 16.981 | 18.420 | 15.172 | 14.364 |
| 83 | 188.8 | 28.94 | 20.280 | 19.698 | 17.049 | 18.347 | 15.100 | 14.284 |
| 84 | 186.9 | 28.93 | 20.208 | 19.624 | 17.102 | 18.273 | 15.027 | 14.195 |
| 85 | 184.9 | 28.93 | 20.135 | 19.550 | 17.144 | 18.199 | 14.954 | 14.098 |
| 86 | 184.6 | 28.92 | 20.058 | 19.471 | 17.173 | 18.120 | 14.876 | 13.975 |
| 87 | 184.2 | 28.91 | 19.980 | 19.392 | 17.194 | 18.041 | 14.798 | 13.845 |
| 88 | 183.9 | 28.91 | 19.903 | 19.312 | 17.208 | 17.962 | 14.721 | 13.710 |
| 89 | 183.6 | 28.90 | 19.825 | 19.232 | 17.216 | 17.882 | 14.643 | 13.570 |
| 90 | 183.4 | 28.89 | 19.747 | 19.153 | 17.220 | 17.802 | 14.565 | 13.425 |
| 91 | 184.1 | 28.88 | 19.667 | 19.070 | 17.222 | 17.720 | 14.486 | 13.269 |
| 92 | 184.8 | 28.87 | 19.587 | 18.988 | 17.227 | 17.638 | 14.407 | 13.115 |
| 93 | 186.0 | 28.86 | 19.507 | 18.904 | 17.235 | 17.556 | 14.329 | 12.959 |
| 94 | 187.2 | 28.84 | 19.427 | 18.823 | 17.251 | 17.473 | 14.252 | 12.810 |
| 95 | 189.3 | 28.81 | 19.346 | 18.739 | 17.280 | 17.389 | 14.178 | 12.665 |
| 96 | 190.8 | 28.77 | 19.267 | 18.656 | 17.334 | 17.306 | 14.110 | 12.549 |
| 97 | 192.9 | 28.72 | 19.187 | 18.570 | 17.407 | 17.221 | 14.050 | 12.445 |
| 98 | 194.9 | 28.63 | 19.107 | 18.483 | 17.489 | 17.133 | 14.000 | 12.348 |
| 99 | 197.2 | 28.51 | 19.028 | 18.392 | 17.562 | 17.041 | 13.960 | 12.236 |
| 100 | 199.4 | 28.37 | 18.940 | 18.299 | 17.618 | 16.945 | 13.928 | 12.099 |
| 101 | 201.9 | 28.20 | 18.853 | 18.201 | 17.654 | 16.842 | 13.902 | 11.938 |
| 102 | 204.8 | 28.03 | 18.778 | 18.105 | 17.670 | 16.739 | 13.879 | 11.766 |
| 103 | 208.4 | 27.85 | 18.703 | 18.009 | 17.672 | 16.636 | 13.855 | 11.577 |
| 104 | 211.9 | 27.68 | 18.630 | 17.916 | 17.664 | 16.536 | 13.833 | 11.385 |
| 105 | 216.6 | 27.51 | 18.556 | 17.823 | 17.647 | 16.435 | 13.811 | 11.178 |
| 106 | 221.2 | 27.35 | 18.483 | 17.734 | 17.627 | 16.337 | 13.791 | 10.974 |
| 107 | 226.4 | 27.19 | 18.411 | 17.647 | 17.602 | 16.241 | 13.770 | 10.766 |
| 108 | 232.1 | 27.03 | 18.340 | 17.561 | 17.573 | 16.146 | 13.750 | 10.555 |
| 109 | 238.4 | 26.88 | 18.270 | 17.479 | 17.542 | 16.053 | 13.730 | 10.343 |
| 110 | 245.1 | 26.73 | 18.200 | 17.398 | 17.509 | 15.961 | 13.711 | 10.132 |
| 111 | 252.4 | 26.59 | 18.132 | 17.320 | 17.475 | 15.872 | 13.692 | 9.920 |
| 112 | 260.1 | 26.45 | 18.065 | 17.245 | 17.440 | 15.785 | 13.673 | 9.710 |
| 113 | 268.1 | 26.31 | 17.999 | 17.173 | 17.404 | 15.701 | 13.655 | 9.503 |
| 114 | 276.5 | 26.18 | 17.935 | 17.103 | 17.368 | 15.619 | 13.637 | 9.299 |
| 115 | 285.2 | 26.05 | 17.872 | 17.036 | 17.332 | 15.539 | 13.620 | 9.098 |
| 116 | 294.7 | 25.92 | 17.811 | 16.971 | 17.295 | 15.461 | 13.603 | 8.899 |
| 117 | 304.3 | 25.80 | 17.750 | 16.908 | 17.259 | 15.385 | 13.586 | 8.703 |
| 118 | 314.2 | 25.68 | 17.692 | 16.847 | 17.223 | 15.312 | 13.569 | 8.514 |
| 119 | 323.9 | 25.57 | 17.635 | 16.790 | 17.188 | 15.242 | 13.553 | 8.332 |
| 120 | 334.5 | 25.45 | 17.579 | 16.734 | 17.153 | 15.173 | 13.538 | 8.167 |

Table 3. Mean Reference Atmosphere structure parameters, 120 to 500 km.

| HEIGHT KM | MOLEC TEMP K | DENSITY KG/M3 | LOG DEN (KG/M3) | DENSITY SCALE HT KM | PRESSURE NT/M2 | LOG PRESSURE (NT/M2) | PRESSURE SCALE HT KM | G M/SEC2 |
|---|---|---|---|---|---|---|---|---|
| 120 | 380.6 | 2.440E-08 | -7.613 | 8.17 | 2.666E-03 | -2.574 | 11.58 | 9.433 |
| 121 | 394.5 | 2.162E-08 | -7.665 | 8.42 | 2.449E-03 | -2.611 | 12.01 | 9.430 |
| 122 | 408.6 | 1.924E-08 | -7.716 | 8.67 | 2.257E-03 | -2.647 | 12.44 | 9.427 |
| 123 | 423.0 | 1.717E-08 | -7.765 | 8.94 | 2.085E-03 | -2.681 | 12.89 | 9.424 |
| 124 | 437.6 | 1.538E-08 | -7.813 | 9.21 | 1.932E-03 | -2.714 | 13.33 | 9.421 |
| 125 | 452.3 | 1.382E-08 | -7.859 | 9.51 | 1.795E-03 | -2.746 | 13.79 | 9.418 |
| 126 | 467.1 | 1.246E-08 | -7.904 | 9.80 | 1.671E-03 | -2.777 | 14.24 | 9.416 |
| 127 | 482.0 | 1.127E-08 | -7.948 | 10.10 | 1.560E-03 | -2.807 | 14.70 | 9.413 |
| 128 | 497.0 | 1.022E-08 | -7.990 | 10.41 | 1.459E-03 | -2.836 | 15.16 | 9.410 |
| 129 | 511.9 | 9.300E-09 | -8.032 | 10.73 | 1.367E-03 | -2.864 | 15.62 | 9.407 |
| 130 | 526.9 | 8.484E-09 | -8.071 | 11.05 | 1.283E-03 | -2.892 | 16.08 | 9.404 |
| 131 | 541.8 | 7.759E-09 | -8.110 | 11.37 | 1.207E-03 | -2.918 | 16.55 | 9.401 |
| 132 | 556.7 | 7.115E-09 | -8.148 | 11.70 | 1.137E-03 | -2.944 | 17.01 | 9.398 |
| 133 | 571.5 | 6.546E-09 | -8.184 | 12.03 | 1.073E-03 | -2.969 | 17.46 | 9.395 |
| 134 | 586.3 | 6.025E-09 | -8.220 | 12.36 | 1.014E-03 | -2.994 | 17.92 | 9.392 |
| 135 | 600.9 | 5.563E-09 | -8.255 | 12.70 | 9.597E-04 | -3.018 | 18.37 | 9.389 |
| 136 | 615.5 | 5.147E-09 | -8.288 | 13.04 | 9.094E-04 | -3.041 | 18.83 | 9.387 |
| 137 | 629.9 | 4.772E-09 | -8.321 | 13.39 | 8.629E-04 | -3.064 | 19.27 | 9.384 |
| 138 | 644.2 | 4.432E-09 | -8.353 | 13.73 | 8.198E-04 | -3.086 | 19.72 | 9.381 |
| 139 | 658.4 | 4.125E-09 | -8.385 | 14.08 | 7.797E-04 | -3.108 | 20.16 | 9.378 |
| 140 | 672.4 | 3.845E-09 | -8.415 | 14.44 | 7.423E-04 | -3.129 | 20.59 | 9.375 |
| 141 | 686.2 | 3.591E-09 | -8.445 | 14.79 | 7.075E-04 | -3.150 | 21.02 | 9.372 |
| 142 | 699.9 | 3.359E-09 | -8.474 | 15.14 | 6.749E-04 | -3.171 | 21.45 | 9.369 |
| 143 | 713.4 | 3.147E-09 | -8.502 | 15.50 | 6.443E-04 | -3.191 | 21.87 | 9.366 |
| 144 | 726.7 | 2.952E-09 | -8.530 | 15.85 | 6.159E-04 | -3.210 | 22.28 | 9.363 |
| 145 | 739.8 | 2.774E-09 | -8.557 | 16.21 | 5.891E-04 | -3.230 | 22.69 | 9.360 |
| 146 | 752.8 | 2.609E-09 | -8.583 | 16.56 | 5.640E-04 | -3.249 | 23.10 | 9.358 |
| 147 | 765.6 | 2.458E-09 | -8.609 | 16.92 | 5.403E-04 | -3.267 | 23.50 | 9.355 |
| 148 | 778.1 | 2.318E-09 | -8.635 | 17.27 | 5.179E-04 | -3.286 | 23.89 | 9.352 |
| 149 | 790.5 | 2.189E-09 | -8.660 | 17.63 | 4.969E-04 | -3.304 | 24.28 | 9.349 |
| 150 | 802.7 | 2.070E-09 | -8.684 | 17.98 | 4.770E-04 | -3.321 | 24.66 | 9.346 |
| 151 | 814.7 | 1.959E-09 | -8.708 | 18.32 | 4.582E-04 | -3.339 | 25.04 | 9.343 |
| 152 | 826.6 | 1.856E-09 | -8.731 | 18.67 | 4.404E-04 | -3.356 | 25.41 | 9.340 |
| 153 | 838.2 | 1.760E-09 | -8.755 | 19.02 | 4.235E-04 | -3.373 | 25.77 | 9.337 |
| 154 | 849.7 | 1.670E-09 | -8.777 | 19.36 | 4.075E-04 | -3.390 | 26.13 | 9.335 |
| 155 | 861.0 | 1.587E-09 | -8.799 | 19.70 | 3.923E-04 | -3.406 | 26.49 | 9.332 |
| 156 | 872.1 | 1.509E-09 | -8.821 | 20.04 | 3.778E-04 | -3.423 | 26.84 | 9.329 |
| 157 | 883.0 | 1.436E-09 | -8.843 | 20.37 | 3.641E-04 | -3.439 | 27.18 | 9.326 |
| 158 | 893.8 | 1.368E-09 | -8.864 | 20.71 | 3.510E-04 | -3.455 | 27.52 | 9.323 |
| 159 | 904.4 | 1.304E-09 | -8.885 | 21.04 | 3.386E-04 | -3.470 | 27.86 | 9.320 |
| 160 | 914.8 | 1.244E-09 | -8.905 | 21.37 | 3.267E-04 | -3.486 | 28.19 | 9.317 |

## Table 3. (Cont'd.)

| HEIGHT KM | MOLEC TEMP K | DENSITY KG/M3 | LOG DEN (KG/M3) | DENSITY SCALE HT KM | PRESSURE NT/M2 | LOG PRESSURE (NT/M2) | PRESSURE SCALE HT KM | G M/SEC2 |
|---|---|---|---|---|---|---|---|---|
| 161 | 925.1 | 1.188E-09 | -8.925 | 21.69 | 3.154E-04 | -3.501 | 28.51 | 9.314 |
| 162 | 935.2 | 1.134E-09 | -8.945 | 22.01 | 3.046E-04 | -3.516 | 28.83 | 9.312 |
| 163 | 945.2 | 1.084E-09 | -8.965 | 22.33 | 2.943E-04 | -3.531 | 29.15 | 9.309 |
| 164 | 955.0 | 1.037E-09 | -8.984 | 22.65 | 2.844E-04 | -3.546 | 29.46 | 9.306 |
| 165 | 964.7 | 9.927E-10 | -9.003 | 22.96 | 2.749E-04 | -3.561 | 29.77 | 9.303 |
| 166 | 974.2 | 9.507E-10 | -9.022 | 23.28 | 2.659E-04 | -3.575 | 30.07 | 9.300 |
| 167 | 983.6 | 9.110E-10 | -9.040 | 23.58 | 2.573E-04 | -3.590 | 30.37 | 9.297 |
| 168 | 992.9 | 8.734E-10 | -9.059 | 23.88 | 2.490E-04 | -3.604 | 30.67 | 9.294 |
| 169 | 1002.1 | 8.378E-10 | -9.077 | 24.17 | 2.410E-04 | -3.618 | 30.96 | 9.292 |
| 170 | 1011.1 | 8.040E-10 | -9.095 | 24.48 | 2.334E-04 | -3.632 | 31.25 | 9.289 |
| 171 | 1020.0 | 7.720E-10 | -9.112 | 24.78 | 2.261E-04 | -3.646 | 31.53 | 9.286 |
| 172 | 1028.7 | 7.417E-10 | -9.130 | 25.06 | 2.191E-04 | -3.659 | 31.82 | 9.283 |
| 173 | 1037.4 | 7.128E-10 | -9.147 | 25.35 | 2.123E-04 | -3.673 | 32.09 | 9.280 |
| 174 | 1045.9 | 6.854E-10 | -9.164 | 25.64 | 2.058E-04 | -3.687 | 32.37 | 9.277 |
| 175 | 1054.4 | 6.593E-10 | -9.181 | 25.92 | 1.996E-04 | -3.700 | 32.64 | 9.274 |
| 176 | 1062.7 | 6.345E-10 | -9.198 | 26.20 | 1.936E-04 | -3.713 | 32.91 | 9.272 |
| 177 | 1070.9 | 6.109E-10 | -9.214 | 26.47 | 1.878E-04 | -3.726 | 33.17 | 9.269 |
| 178 | 1079.0 | 5.883E-10 | -9.230 | 26.75 | 1.823E-04 | -3.739 | 33.43 | 9.266 |
| 179 | 1087.1 | 5.669E-10 | -9.247 | 27.02 | 1.769E-04 | -3.752 | 33.69 | 9.263 |
| 180 | 1095.0 | 5.464E-10 | -9.263 | 27.29 | 1.718E-04 | -3.765 | 33.95 | 9.260 |
| 181 | 1102.8 | 5.268E-10 | -9.278 | 27.56 | 1.668E-04 | -3.778 | 34.20 | 9.257 |
| 182 | 1110.5 | 5.081E-10 | -9.294 | 27.82 | 1.620E-04 | -3.790 | 34.45 | 9.255 |
| 183 | 1118.2 | 4.903E-10 | -9.310 | 28.08 | 1.574E-04 | -3.803 | 34.70 | 9.252 |
| 184 | 1125.7 | 4.732E-10 | -9.325 | 28.34 | 1.529E-04 | -3.816 | 34.94 | 9.249 |
| 185 | 1133.2 | 4.568E-10 | -9.340 | 28.60 | 1.486E-04 | -3.828 | 35.19 | 9.246 |
| 186 | 1140.6 | 4.412E-10 | -9.355 | 28.86 | 1.445E-04 | -3.840 | 35.43 | 9.243 |
| 187 | 1147.9 | 4.262E-10 | -9.370 | 29.11 | 1.405E-04 | -3.852 | 35.66 | 9.240 |
| 188 | 1155.1 | 4.119E-10 | -9.385 | 29.35 | 1.366E-04 | -3.865 | 35.90 | 9.238 |
| 189 | 1162.2 | 3.982E-10 | -9.400 | 29.60 | 1.329E-04 | -3.877 | 36.13 | 9.235 |
| 190 | 1169.3 | 3.850E-10 | -9.415 | 29.85 | 1.292E-04 | -3.889 | 36.36 | 9.232 |
| 191 | 1176.2 | 3.724E-10 | -9.429 | 30.09 | 1.257E-04 | -3.901 | 36.59 | 9.229 |
| 192 | 1183.1 | 3.602E-10 | -9.443 | 30.34 | 1.224E-04 | -3.912 | 36.82 | 9.226 |
| 193 | 1190.0 | 3.486E-10 | -9.458 | 30.58 | 1.191E-04 | -3.924 | 37.04 | 9.223 |
| 194 | 1196.7 | 3.374E-10 | -9.472 | 30.82 | 1.159E-04 | -3.936 | 37.26 | 9.221 |
| 195 | 1203.4 | 3.267E-10 | -9.486 | 31.05 | 1.129E-04 | -3.947 | 37.48 | 9.218 |
| 196 | 1210.0 | 3.164E-10 | -9.500 | 31.28 | 1.099E-04 | -3.959 | 37.70 | 9.215 |
| 197 | 1216.6 | 3.065E-10 | -9.514 | 31.51 | 1.070E-04 | -3.970 | 37.91 | 9.212 |
| 198 | 1223.1 | 2.969E-10 | -9.527 | 31.74 | 1.043E-04 | -3.982 | 38.12 | 9.209 |
| 199 | 1229.5 | 2.878E-10 | -9.541 | 31.98 | 1.016E-04 | -3.993 | 38.34 | 9.207 |
| 200 | 1235.8 | 2.789E-10 | -9.555 | 32.21 | 9.896E-05 | -4.005 | 38.55 | 9.204 |

## Table 3. (Cont'd.)

| HEIGHT KM | MOLEC TEMP K | DENSITY KG/M3 | LOG DEN (KG/M3) | DENSITY SCALE HT KM | PRESSURE NT/M2 | LOG PRESSURE (NT/M2) | PRESSURE SCALE HT KM | G M/SEC2 |
|---|---|---|---|---|---|---|---|---|
| 202 | 1248.3 | 2.622E-10 | -9.581 | 32.66 | 9.399E-05 | -4.027 | 38.96 | 9.198 |
| 204 | 1260.6 | 2.468E-10 | -9.608 | 33.10 | 8.931E-05 | -4.049 | 39.37 | 9.192 |
| 206 | 1272.6 | 2.324E-10 | -9.634 | 33.54 | 8.491E-05 | -4.071 | 39.77 | 9.187 |
| 208 | 1284.4 | 2.190E-10 | -9.660 | 33.97 | 8.076E-05 | -4.093 | 40.16 | 9.181 |
| 210 | 1295.9 | 2.066E-10 | -9.685 | 34.40 | 7.686E-05 | -4.114 | 40.55 | 9.176 |
| 212 | 1307.2 | 1.950E-10 | -9.710 | 34.82 | 7.317E-05 | -4.136 | 40.93 | 9.170 |
| 214 | 1318.3 | 1.842E-10 | -9.735 | 35.24 | 6.970E-05 | -4.157 | 41.30 | 9.164 |
| 216 | 1329.2 | 1.741E-10 | -9.759 | 35.65 | 6.642E-05 | -4.178 | 41.66 | 9.159 |
| 218 | 1339.9 | 1.646E-10 | -9.784 | 36.06 | 6.332E-05 | -4.198 | 42.03 | 9.153 |
| 220 | 1350.3 | 1.558E-10 | -9.808 | 36.45 | 6.039E-05 | -4.219 | 42.38 | 9.148 |
| 222 | 1360.6 | 1.475E-10 | -9.831 | 36.85 | 5.762E-05 | -4.239 | 42.73 | 9.142 |
| 224 | 1370.6 | 1.398E-10 | -9.855 | 37.24 | 5.499E-05 | -4.260 | 43.07 | 9.137 |
| 226 | 1380.5 | 1.325E-10 | -9.878 | 37.63 | 5.251E-05 | -4.280 | 43.41 | 9.131 |
| 228 | 1390.2 | 1.257E-10 | -9.901 | 38.01 | 5.015E-05 | -4.300 | 43.74 | 9.125 |
| 230 | 1399.6 | 1.192E-10 | -9.924 | 38.39 | 4.792E-05 | -4.320 | 44.06 | 9.120 |
| 232 | 1408.9 | 1.132E-10 | -9.946 | 38.77 | 4.580E-05 | -4.339 | 44.38 | 9.114 |
| 234 | 1418.1 | 1.076E-10 | -9.968 | 39.13 | 4.379E-05 | -4.359 | 44.70 | 9.109 |
| 236 | 1427.0 | 1.022E-10 | -9.990 | 39.49 | 4.188E-05 | -4.378 | 45.00 | 9.103 |
| 238 | 1435.8 | 9.720E-11 | -10.012 | 39.85 | 4.006E-05 | -4.397 | 45.31 | 9.098 |
| 240 | 1444.4 | 9.246E-11 | -10.034 | 40.21 | 3.834E-05 | -4.416 | 45.61 | 9.092 |
| 242 | 1452.8 | 8.799E-11 | -10.056 | 40.56 | 3.670E-05 | -4.435 | 45.90 | 9.087 |
| 244 | 1461.0 | 8.378E-11 | -10.077 | 40.91 | 3.514E-05 | -4.454 | 46.19 | 9.081 |
| 246 | 1469.1 | 7.979E-11 | -10.098 | 41.25 | 3.366E-05 | -4.473 | 46.47 | 9.076 |
| 248 | 1477.1 | 7.603E-11 | -10.119 | 41.59 | 3.224E-05 | -4.492 | 46.75 | 9.070 |
| 250 | 1484.9 | 7.248E-11 | -10.140 | 41.92 | 3.090E-05 | -4.510 | 47.03 | 9.065 |
| 252 | 1492.5 | 6.911E-11 | -10.160 | 42.25 | 2.961E-05 | -4.529 | 47.30 | 9.059 |
| 254 | 1499.9 | 6.593E-11 | -10.181 | 42.58 | 2.839E-05 | -4.547 | 47.56 | 9.054 |
| 256 | 1507.3 | 6.292E-11 | -10.201 | 42.90 | 2.723E-05 | -4.565 | 47.83 | 9.048 |
| 258 | 1514.4 | 6.006E-11 | -10.221 | 43.21 | 2.611E-05 | -4.583 | 48.08 | 9.043 |
| 260 | 1521.5 | 5.735E-11 | -10.241 | 43.52 | 2.505E-05 | -4.601 | 48.33 | 9.037 |
| 262 | 1528.4 | 5.478E-11 | -10.261 | 43.83 | 2.404E-05 | -4.619 | 48.58 | 9.032 |
| 264 | 1535.1 | 5.235E-11 | -10.281 | 44.13 | 2.307E-05 | -4.637 | 48.83 | 9.026 |
| 266 | 1541.7 | 5.004E-11 | -10.301 | 44.44 | 2.215E-05 | -4.655 | 49.07 | 9.021 |
| 268 | 1548.2 | 4.784E-11 | -10.320 | 44.74 | 2.127E-05 | -4.672 | 49.30 | 9.015 |
| 270 | 1554.6 | 4.576E-11 | -10.340 | 45.03 | 2.042E-05 | -4.690 | 49.54 | 9.010 |
| 272 | 1560.8 | 4.378E-11 | -10.359 | 45.32 | 1.962E-05 | -4.707 | 49.76 | 9.004 |
| 274 | 1566.9 | 4.189E-11 | -10.378 | 45.60 | 1.885E-05 | -4.725 | 49.99 | 8.999 |
| 276 | 1572.9 | 4.010E-11 | -10.397 | 45.88 | 1.811E-05 | -4.742 | 50.21 | 8.993 |
| 278 | 1578.7 | 3.839E-11 | -10.416 | 46.16 | 1.740E-05 | -4.759 | 50.43 | 8.988 |
| 280 | 1584.5 | 3.677E-11 | -10.434 | 46.43 | 1.673E-05 | -4.777 | 50.64 | 8.983 |
| 282 | 1590.1 | 3.522E-11 | -10.453 | 46.70 | 1.608E-05 | -4.794 | 50.85 | 8.977 |
| 284 | 1595.6 | 3.375E-11 | -10.472 | 46.96 | 1.546E-05 | -4.811 | 51.06 | 8.972 |
| 286 | 1601.0 | 3.235E-11 | -10.490 | 47.22 | 1.487E-05 | -4.828 | 51.26 | 8.966 |
| 288 | 1606.3 | 3.101E-11 | -10.508 | 47.48 | 1.430E-05 | -4.845 | 51.46 | 8.961 |
| 290 | 1611.5 | 2.974E-11 | -10.527 | 47.73 | 1.376E-05 | -4.861 | 51.66 | 8.955 |
| 292 | 1616.6 | 2.852E-11 | -10.545 | 47.98 | 1.324E-05 | -4.878 | 51.86 | 8.950 |
| 294 | 1621.6 | 2.736E-11 | -10.563 | 48.23 | 1.274E-05 | -4.895 | 52.05 | 8.945 |
| 296 | 1626.5 | 2.625E-11 | -10.581 | 48.47 | 1.226E-05 | -4.912 | 52.24 | 8.939 |
| 298 | 1631.2 | 2.519E-11 | -10.599 | 48.71 | 1.180E-05 | -4.928 | 52.42 | 8.934 |
| 300 | 1636.0 | 2.418E-11 | -10.617 | 48.95 | 1.136E-05 | -4.945 | 52.60 | 8.928 |

## Table 3. (Cont'd.)

| HEIGHT KM | MOLEC TEMP K | DENSITY KG/M3 | LOG DEN (KG/M3) | DENSITY SCALE HT KM | PRESSURE NT/M2 | LOG PRESSURE (N/M2) | PRESSURE SCALE HT KM | G M/SEC2 |
|---|---|---|---|---|---|---|---|---|
| 302 | 1640.6 | 2.321E-11 | -10.634 | 49.19 | 1.093E-05 | -4.961 | 52.78 | 8.923 |
| 304 | 1645.1 | 2.229E-11 | -10.652 | 49.42 | 1.053E-05 | -4.978 | 52.96 | 8.918 |
| 306 | 1649.5 | 2.141E-11 | -10.669 | 49.64 | 1.014E-05 | -4.994 | 53.14 | 8.912 |
| 308 | 1653.8 | 2.056E-11 | -10.687 | 49.86 | 9.764E-06 | -5.010 | 53.31 | 8.907 |
| 310 | 1658.1 | 1.976E-11 | -10.704 | 50.07 | 9.405E-06 | -5.027 | 53.48 | 8.902 |
| 312 | 1662.3 | 1.899E-11 | -10.722 | 50.28 | 9.061E-06 | -5.043 | 53.64 | 8.896 |
| 314 | 1666.4 | 1.825E-11 | -10.739 | 50.50 | 8.730E-06 | -5.059 | 53.81 | 8.891 |
| 316 | 1670.4 | 1.754E-11 | -10.756 | 50.70 | 8.412E-06 | -5.075 | 53.97 | 8.886 |
| 318 | 1674.3 | 1.686E-11 | -10.773 | 50.91 | 8.106E-06 | -5.091 | 54.13 | 8.880 |
| 320 | 1678.2 | 1.621E-11 | -10.790 | 51.12 | 7.812E-06 | -5.107 | 54.29 | 8.875 |
| 322 | 1682.0 | 1.559E-11 | -10.807 | 51.32 | 7.530E-06 | -5.123 | 54.44 | 8.870 |
| 324 | 1685.7 | 1.500E-11 | -10.824 | 51.51 | 7.259E-06 | -5.139 | 54.60 | 8.864 |
| 326 | 1689.4 | 1.443E-11 | -10.841 | 51.71 | 6.998E-06 | -5.155 | 54.75 | 8.859 |
| 328 | 1693.0 | 1.388E-11 | -10.858 | 51.90 | 6.747E-06 | -5.171 | 54.90 | 8.854 |
| 330 | 1696.5 | 1.336E-11 | -10.874 | 52.09 | 6.507E-06 | -5.187 | 55.05 | 8.848 |
| 332 | 1700.0 | 1.286E-11 | -10.891 | 52.28 | 6.275E-06 | -5.202 | 55.19 | 8.843 |
| 334 | 1703.4 | 1.237E-11 | -10.907 | 52.46 | 6.052E-06 | -5.218 | 55.34 | 8.838 |
| 336 | 1706.8 | 1.191E-11 | -10.924 | 52.64 | 5.837E-06 | -5.234 | 55.48 | 8.832 |
| 338 | 1710.1 | 1.147E-11 | -10.940 | 52.81 | 5.631E-06 | -5.249 | 55.62 | 8.827 |
| 340 | 1713.4 | 1.104E-11 | -10.957 | 52.98 | 5.432E-06 | -5.265 | 55.76 | 8.822 |
| 342 | 1716.6 | 1.063E-11 | -10.973 | 53.16 | 5.241E-06 | -5.281 | 55.90 | 8.816 |
| 344 | 1719.7 | 1.024E-11 | -10.990 | 53.32 | 5.057E-06 | -5.296 | 56.03 | 8.811 |
| 346 | 1722.8 | 9.866E-12 | -11.006 | 53.49 | 4.880E-06 | -5.312 | 56.17 | 8.806 |
| 348 | 1725.8 | 9.505E-12 | -11.022 | 53.65 | 4.709E-06 | -5.327 | 56.30 | 8.801 |
| 350 | 1728.8 | 9.158E-12 | -11.038 | 53.81 | 4.545E-06 | -5.342 | 56.43 | 8.795 |
| 352 | 1731.8 | 8.824E-12 | -11.054 | 53.97 | 4.387E-06 | -5.358 | 56.56 | 8.790 |
| 354 | 1734.7 | 8.503E-12 | -11.070 | 54.13 | 4.235E-06 | -5.373 | 56.69 | 8.785 |
| 356 | 1737.6 | 8.195E-12 | -11.086 | 54.29 | 4.088E-06 | -5.388 | 56.82 | 8.780 |
| 358 | 1740.4 | 7.899E-12 | -11.102 | 54.44 | 3.947E-06 | -5.404 | 56.95 | 8.774 |
| 360 | 1743.2 | 7.615E-12 | -11.118 | 54.59 | 3.811E-06 | -5.419 | 57.07 | 8.769 |
| 362 | 1746.0 | 7.341E-12 | -11.134 | 54.74 | 3.680E-06 | -5.434 | 57.20 | 8.764 |
| 364 | 1748.7 | 7.078E-12 | -11.150 | 54.89 | 3.554E-06 | -5.449 | 57.32 | 8.759 |
| 366 | 1751.4 | 6.825E-12 | -11.166 | 55.03 | 3.432E-06 | -5.464 | 57.44 | 8.753 |
| 368 | 1754.1 | 6.582E-12 | -11.182 | 55.17 | 3.315E-06 | -5.480 | 57.57 | 8.748 |
| 370 | 1756.7 | 6.348E-12 | -11.197 | 55.31 | 3.202E-06 | -5.495 | 57.69 | 8.743 |
| 372 | 1759.3 | 6.123E-12 | -11.213 | 55.45 | 3.093E-06 | -5.510 | 57.81 | 8.738 |
| 374 | 1761.9 | 5.906E-12 | -11.229 | 55.59 | 2.988E-06 | -5.525 | 57.93 | 8.732 |
| 376 | 1764.5 | 5.698E-12 | -11.244 | 55.72 | 2.886E-06 | -5.540 | 58.05 | 8.727 |
| 378 | 1767.0 | 5.497E-12 | -11.260 | 55.85 | 2.789E-06 | -5.555 | 58.16 | 8.722 |
| 380 | 1769.5 | 5.304E-12 | -11.275 | 55.98 | 2.694E-06 | -5.570 | 58.28 | 8.717 |
| 382 | 1772.0 | 5.118E-12 | -11.291 | 56.11 | 2.604E-06 | -5.584 | 58.40 | 8.712 |
| 384 | 1774.5 | 4.939E-12 | -11.306 | 56.24 | 2.516E-06 | -5.599 | 58.51 | 8.706 |
| 386 | 1776.9 | 4.767E-12 | -11.322 | 56.35 | 2.432E-06 | -5.614 | 58.63 | 8.701 |
| 388 | 1779.4 | 4.600E-12 | -11.337 | 56.48 | 2.350E-06 | -5.629 | 58.74 | 8.696 |
| 390 | 1781.8 | 4.441E-12 | -11.353 | 56.60 | 2.272E-06 | -5.644 | 58.86 | 8.691 |
| 392 | 1784.2 | 4.287E-12 | -11.368 | 56.72 | 2.196E-06 | -5.658 | 58.97 | 8.686 |
| 394 | 1786.6 | 4.138E-12 | -11.383 | 56.84 | 2.123E-06 | -5.673 | 59.09 | 8.681 |
| 396 | 1788.9 | 3.995E-12 | -11.398 | 56.96 | 2.052E-06 | -5.688 | 59.20 | 8.675 |
| 398 | 1791.3 | 3.858E-12 | -11.414 | 57.09 | 1.984E-06 | -5.702 | 59.32 | 8.670 |
| 400 | 1793.7 | 3.725E-12 | -11.429 | 57.20 | 1.918E-06 | -5.717 | 59.43 | 8.665 |

Table 3. (Cont'd.)

| HEIGHT KM | MOLEC TEMP K | DENSITY KG/M3 | LOG DEN (KG/M3) | DENSITY SCALE HT KM | PRESSURE NT/M2 | LOG PRESSURE (NT/M2) | PRESSURE SCALE HT KM | G M/SEC2 |
|---|---|---|---|---|---|---|---|---|
| 402 | 1796.0 | 3.597E-12 | -11.444 | 57.32 | 1.855E-06 | -5.732 | 59.54 | 8.660 |
| 404 | 1796.4 | 3.474E-12 | -11.459 | 57.43 | 1.794E-06 | -5.746 | 59.66 | 8.655 |
| 406 | 1800.7 | 3.355E-12 | -11.474 | 57.54 | 1.735E-06 | -5.761 | 59.77 | 8.650 |
| 408 | 1803.1 | 3.241E-12 | -11.489 | 57.65 | 1.677E-06 | -5.775 | 59.88 | 8.644 |
| 410 | 1805.4 | 3.130E-12 | -11.504 | 57.75 | 1.622E-06 | -5.790 | 60.00 | 8.639 |
| 412 | 1807.8 | 3.024E-12 | -11.519 | 57.86 | 1.569E-06 | -5.804 | 60.11 | 8.634 |
| 414 | 1810.1 | 2.921E-12 | -11.534 | 57.97 | 1.518E-06 | -5.819 | 60.22 | 8.629 |
| 416 | 1812.5 | 2.822E-12 | -11.549 | 58.07 | 1.468E-06 | -5.833 | 60.34 | 8.624 |
| 418 | 1814.8 | 2.727E-12 | -11.564 | 58.18 | 1.421E-06 | -5.848 | 60.45 | 8.619 |
| 420 | 1817.2 | 2.635E-12 | -11.579 | 58.28 | 1.374E-06 | -5.862 | 60.57 | 8.614 |
| 422 | 1819.5 | 2.546E-12 | -11.594 | 58.38 | 1.330E-06 | -5.876 | 60.68 | 8.609 |
| 424 | 1821.9 | 2.460E-12 | -11.609 | 58.49 | 1.287E-06 | -5.890 | 60.80 | 8.603 |
| 426 | 1824.3 | 2.377E-12 | -11.624 | 58.59 | 1.245E-06 | -5.905 | 60.91 | 8.598 |
| 428 | 1826.7 | 2.298E-12 | -11.639 | 58.69 | 1.205E-06 | -5.919 | 61.03 | 8.593 |
| 430 | 1829.1 | 2.221E-12 | -11.653 | 58.79 | 1.166E-06 | -5.933 | 61.14 | 8.588 |
| 432 | 1831.5 | 2.147E-12 | -11.668 | 58.89 | 1.129E-06 | -5.947 | 61.26 | 8.583 |
| 434 | 1833.9 | 2.075E-12 | -11.683 | 58.98 | 1.092E-06 | -5.962 | 61.38 | 8.578 |
| 436 | 1836.3 | 2.006E-12 | -11.698 | 59.08 | 1.057E-06 | -5.976 | 61.50 | 8.573 |
| 438 | 1838.8 | 1.939E-12 | -11.712 | 59.17 | 1.024E-06 | -5.990 | 61.62 | 8.568 |
| 440 | 1841.3 | 1.875E-12 | -11.727 | 59.26 | 9.910E-07 | -6.004 | 61.74 | 8.563 |
| 442 | 1843.8 | 1.813E-12 | -11.742 | 59.36 | 9.595E-07 | -6.018 | 61.86 | 8.558 |
| 444 | 1846.3 | 1.753E-12 | -11.756 | 59.45 | 9.290E-07 | -6.032 | 61.98 | 8.553 |
| 446 | 1848.8 | 1.695E-12 | -11.771 | 59.54 | 8.995E-07 | -6.046 | 62.10 | 8.548 |
| 448 | 1851.4 | 1.639E-12 | -11.786 | 59.64 | 8.710E-07 | -6.060 | 62.22 | 8.542 |
| 450 | 1854.0 | 1.585E-12 | -11.800 | 59.73 | 8.435E-07 | -6.074 | 62.35 | 8.537 |
| 452 | 1856.6 | 1.533E-12 | -11.815 | 59.82 | 8.169E-07 | -6.088 | 62.47 | 8.532 |
| 454 | 1859.3 | 1.482E-12 | -11.829 | 59.91 | 7.912E-07 | -6.102 | 62.60 | 8.527 |
| 456 | 1861.9 | 1.434E-12 | -11.844 | 60.00 | 7.663E-07 | -6.116 | 62.72 | 8.522 |
| 458 | 1864.6 | 1.387E-12 | -11.858 | 60.09 | 7.423E-07 | -6.129 | 62.85 | 8.517 |
| 460 | 1867.4 | 1.341E-12 | -11.872 | 60.18 | 7.191E-07 | -6.143 | 62.98 | 8.512 |
| 462 | 1870.2 | 1.297E-12 | -11.887 | 60.27 | 6.966E-07 | -6.157 | 63.11 | 8.507 |
| 464 | 1873.0 | 1.255E-12 | -11.901 | 60.36 | 6.749E-07 | -6.171 | 63.25 | 8.502 |
| 466 | 1875.8 | 1.214E-12 | -11.916 | 60.45 | 6.539E-07 | -6.184 | 63.38 | 8.497 |
| 468 | 1878.7 | 1.175E-12 | -11.930 | 60.54 | 6.337E-07 | -6.198 | 63.51 | 8.492 |
| 470 | 1881.6 | 1.137E-12 | -11.944 | 60.63 | 6.140E-07 | -6.212 | 63.65 | 8.487 |
| 472 | 1884.6 | 1.100E-12 | -11.959 | 60.72 | 5.950E-07 | -6.225 | 63.79 | 8.482 |
| 474 | 1887.6 | 1.064E-12 | -11.973 | 60.81 | 5.767E-07 | -6.239 | 63.93 | 8.477 |
| 476 | 1890.7 | 1.030E-12 | -11.987 | 60.90 | 5.590E-07 | -6.253 | 64.07 | 8.472 |
| 478 | 1893.8 | 9.965E-13 | -12.002 | 60.98 | 5.418E-07 | -6.266 | 64.21 | 8.467 |
| 480 | 1895.9 | 9.644E-13 | -12.016 | 61.08 | 5.252E-07 | -6.280 | 64.36 | 8.462 |
| 482 | 1900.1 | 9.333E-13 | -12.030 | 61.16 | 5.092E-07 | -6.293 | 64.50 | 8.457 |
| 484 | 1903.4 | 9.033E-13 | -12.044 | 61.25 | 4.936E-07 | -6.307 | 64.65 | 8.452 |
| 486 | 1906.7 | 8.743E-13 | -12.058 | 61.34 | 4.786E-07 | -6.320 | 64.80 | 8.447 |
| 488 | 1910.0 | 8.463E-13 | -12.072 | 61.43 | 4.641E-07 | -6.333 | 64.96 | 8.442 |
| 490 | 1913.4 | 8.192E-13 | -12.087 | 61.52 | 4.500E-07 | -6.347 | 65.11 | 8.437 |
| 492 | 1916.9 | 7.930E-13 | -12.101 | 61.60 | 4.364E-07 | -6.360 | 65.27 | 8.432 |
| 494 | 1920.5 | 7.677E-13 | -12.115 | 61.69 | 4.232E-07 | -6.373 | 65.43 | 8.427 |
| 496 | 1924.0 | 7.432E-13 | -12.129 | 61.78 | 4.106E-07 | -6.387 | 65.59 | 8.422 |
| 498 | 1927.7 | 7.196E-13 | -12.143 | 61.87 | 3.982E-07 | -6.400 | 65.75 | 8.417 |
| 500 | 1931.4 | 6.967E-13 | -12.157 | 61.95 | 3.863E-07 | -6.413 | 65.91 | 8.412 |

Table 4. Kinetic temperature and composition of the Mean Reference Atmosphere, 120 to 500 km.

| HEIGHT KM | TEMP K | MEAN MOL WT | NUMBER DENSITY /M3 | LOG N(N2) (/M3) | LOG N(O2) (/M3) | LOG N(O) (/M3) | LOG N(AR) (/M3) | LOG N(HE) (/M3) |
|---|---|---|---|---|---|---|---|---|
| 120 | 334.5 | 25.45 | 5.772E+17 | 17.579 | 16.734 | 17.153 | 15.173 | 13.538 |
| 121 | 345.3 | 25.35 | 5.137E+17 | 17.524 | 16.674 | 17.116 | 15.102 | 13.523 |
| 122 | 356.2 | 25.25 | 4.589E+17 | 17.472 | 16.615 | 17.080 | 15.032 | 13.509 |
| 123 | 367.3 | 25.15 | 4.112E+17 | 17.420 | 16.558 | 17.045 | 14.964 | 13.496 |
| 124 | 378.5 | 25.05 | 3.698E+17 | 17.370 | 16.503 | 17.011 | 14.898 | 13.482 |
| 125 | 389.7 | 24.95 | 3.336E+17 | 17.322 | 16.449 | 16.978 | 14.835 | 13.469 |
| 126 | 400.9 | 24.85 | 3.019E+17 | 17.274 | 16.397 | 16.946 | 14.773 | 13.457 |
| 127 | 412.1 | 24.76 | 2.741E+17 | 17.229 | 16.347 | 16.914 | 14.712 | 13.444 |
| 128 | 423.3 | 24.66 | 2.496E+17 | 17.184 | 16.297 | 16.884 | 14.654 | 13.432 |
| 129 | 434.4 | 24.57 | 2.279E+17 | 17.141 | 16.249 | 16.854 | 14.597 | 13.421 |
| 130 | 445.4 | 24.48 | 2.087E+17 | 17.098 | 16.203 | 16.826 | 14.541 | 13.410 |
| 131 | 456.4 | 24.39 | 1.916E+17 | 17.057 | 16.157 | 16.798 | 14.487 | 13.399 |
| 132 | 467.2 | 24.31 | 1.763E+17 | 17.017 | 16.113 | 16.770 | 14.434 | 13.388 |
| 133 | 478.0 | 24.22 | 1.626E+17 | 16.978 | 16.070 | 16.747 | 14.383 | 13.378 |
| 134 | 488.6 | 24.13 | 1.503E+17 | 16.940 | 16.028 | 16.718 | 14.333 | 13.368 |
| 135 | 499.0 | 24.05 | 1.393E+17 | 16.903 | 15.987 | 16.69_ | 14.284 | 13.358 |
| 136 | 509.4 | 23.97 | 1.293E+17 | 16.867 | 15.947 | 16.668 | 14.236 | 13.349 |
| 137 | 519.6 | 23.89 | 1.203E+17 | 16.832 | 15.908 | 16.645 | 14.190 | 13.340 |
| 138 | 529.6 | 23.81 | 1.121E+17 | 16.798 | 15.870 | 16.621 | 14.144 | 13.331 |
| 139 | 539.4 | 23.73 | 1.047E+17 | 16.764 | 15.832 | 16.599 | 14.099 | 13.322 |
| 140 | 549.0 | 23.65 | 9.793E+16 | 16.731 | 15.796 | 16.577 | 14.056 | 13.314 |
| 141 | 558.5 | 23.57 | 9.176E+16 | 16.699 | 15.760 | 16.555 | 14.013 | 13.306 |
| 142 | 567.8 | 23.49 | 8.610E+16 | 16.667 | 15.725 | 16.534 | 13.971 | 13.298 |
| 143 | 576.9 | 23.42 | 8.092E+16 | 16.636 | 15.691 | 16.513 | 13.930 | 13.290 |
| 144 | 585.8 | 23.35 | 7.616E+16 | 16.606 | 15.657 | 16.493 | 13.890 | 13.282 |
| 145 | 594.5 | 23.27 | 7.178E+16 | 16.577 | 15.624 | 16.474 | 13.850 | 13.275 |
| 146 | 603.0 | 23.20 | 6.774E+16 | 16.548 | 15.592 | 16.454 | 13.811 | 13.268 |
| 147 | 611.4 | 23.13 | 6.401E+16 | 16.519 | 15.560 | 16.436 | 13.773 | 13.261 |
| 148 | 619.5 | 23.06 | 6.056E+16 | 16.491 | 15.529 | 16.417 | 13.736 | 13.254 |
| 149 | 627.4 | 22.99 | 5.736E+16 | 16.464 | 15.499 | 16.399 | 13.699 | 13.248 |
| 150 | 635.2 | 22.92 | 5.439E+16 | 16.437 | 15.469 | 16.381 | 13.663 | 13.241 |
| 151 | 642.8 | 22.85 | 5.163E+16 | 16.410 | 15.439 | 16.364 | 13.627 | 13.235 |
| 152 | 650.2 | 22.78 | 4.906E+16 | 16.384 | 15.410 | 16.347 | 13.592 | 13.229 |
| 153 | 657.4 | 22.71 | 4.666E+16 | 16.358 | 15.381 | 16.330 | 13.557 | 13.223 |
| 154 | 664.4 | 22.65 | 4.442E+16 | 16.333 | 15.353 | 16.314 | 13.523 | 13.217 |
| 155 | 671.3 | 22.58 | 4.233E+16 | 16.308 | 15.325 | 16.298 | 13.490 | 13.212 |
| 156 | 678.0 | 22.51 | 4.037E+16 | 16.283 | 15.298 | 16.282 | 13.457 | 13.206 |
| 157 | 684.5 | 22.45 | 3.853E+16 | 16.259 | 15.271 | 16.266 | 13.424 | 13.201 |
| 158 | 690.9 | 22.39 | 3.681E+16 | 16.235 | 15.244 | 16.251 | 13.392 | 13.195 |
| 159 | 697.1 | 22.32 | 3.518E+16 | 16.212 | 15.218 | 16.236 | 13.360 | 13.190 |
| 160 | 703.1 | 22.26 | 3.366E+16 | 16.189 | 15.192 | 16.221 | 13.328 | 13.185 |

## Table 4. (Conr'd.)

| HEIGHT KM | TEMP K | MEAN MOL WT | NUMBER DENSITY /M3 | LOG N(N2) (/M3) | LOG N(O2) (/M3) | LOG N(O) (/M3) | LOG N(AR) (/M3) | LOG N(HE) (/M3) |
|---|---|---|---|---|---|---|---|---|
| 161 | 709.0 | 22.20 | 3.222E+16 | 16.166 | 15.166 | 16.206 | 13.297 | 13.180 |
| 162 | 714.8 | 22.13 | 3.087E+16 | 16.143 | 15.141 | 16.192 | 13.266 | 13.175 |
| 163 | 720.4 | 22.07 | 2.959E+16 | 16.121 | 15.115 | 16.177 | 13.236 | 13.170 |
| 164 | 725.9 | 22.01 | 2.838E+16 | 16.099 | 15.091 | 16.163 | 13.205 | 13.166 |
| 165 | 731.3 | 21.95 | 2.723E+16 | 16.077 | 15.066 | 16.150 | 13.176 | 13.161 |
| 166 | 736.5 | 21.89 | 2.615E+16 | 16.055 | 15.042 | 16.136 | 13.146 | 13.156 |
| 167 | 741.6 | 21.83 | 2.513E+16 | 16.034 | 15.018 | 16.122 | 13.117 | 13.152 |
| 168 | 746.6 | 21.78 | 2.416E+16 | 16.012 | 14.994 | 16.109 | 13.088 | 13.147 |
| 169 | 751.5 | 21.72 | 2.323E+16 | 15.991 | 14.970 | 16.096 | 13.059 | 13.143 |
| 170 | 756.2 | 21.66 | 2.236E+16 | 15.971 | 14.947 | 16.082 | 13.031 | 13.139 |
| 171 | 760.8 | 21.60 | 2.152E+16 | 15.950 | 14.924 | 16.070 | 13.003 | 13.135 |
| 172 | 765.4 | 21.55 | 2.073E+16 | 15.930 | 14.901 | 16.057 | 12.975 | 13.130 |
| 173 | 769.8 | 21.49 | 1.998E+16 | 15.909 | 14.878 | 16.045 | 12.947 | 13.126 |
| 174 | 774.1 | 21.43 | 1.926E+16 | 15.889 | 14.85 | 16.032 | 12.919 | 13.122 |
| 175 | 778.4 | 21.38 | 1.857E+16 | 15.870 | 14.83 | 16.020 | 12.892 | 13.118 |
| 176 | 782.5 | 21.32 | 1.792E+16 | 15.850 | 14.811 | 16.007 | 12.865 | 13.114 |
| 177 | 786.5 | 21.27 | 1.730E+16 | 15.830 | 14.789 | 15.995 | 12.838 | 13.111 |
| 178 | 790.5 | 21.22 | 1.670E+16 | 15.811 | 14.768 | 15.983 | 12.811 | 13.107 |
| 179 | 794.4 | 21.16 | 1.613E+16 | 15.792 | 14.746 | 15.971 | 12.785 | 13.103 |
| 180 | 798.1 | 21.11 | 1.559E+16 | 15.773 | 14.724 | 15.960 | 12.758 | 13.099 |
| 181 | 801.8 | 21.06 | 1.507E+16 | 15.754 | 14.703 | 15.948 | 12.732 | 13.096 |
| 182 | 805.5 | 21.00 | 1.457E+16 | 15.735 | 14.682 | 15.936 | 12.706 | 13.092 |
| 183 | 809.0 | 20.95 | 1.409E+16 | 15.716 | 14.661 | 15.925 | 12.680 | 13.088 |
| 184 | 812.5 | 20.90 | 1.363E+16 | 15.698 | 14.640 | 15.914 | 12.655 | 13.085 |
| 185 | 815.9 | 20.85 | 1.319E+16 | 15.679 | 14.619 | 15.902 | 12.629 | 13.081 |
| 186 | 819.2 | 20.80 | 1.277E+16 | 15.661 | 14.598 | 15.891 | 12.604 | 13.078 |
| 187 | 822.5 | 20.75 | 1.237E+16 | 15.643 | 14.576 | 15.880 | 12.579 | 13.075 |
| 188 | 825.7 | 20.70 | 1.198E+16 | 15.625 | 14.557 | 15.869 | 12.554 | 13.071 |
| 189 | 828.8 | 20.65 | 1.161E+16 | 15.607 | 14.537 | 15.858 | 12.529 | 13.068 |
| 190 | 831.9 | 20.60 | 1.125E+16 | 15.589 | 14.517 | 15.847 | 12.504 | 13.064 |
| 191 | 834.9 | 20.55 | 1.091E+16 | 15.571 | 14.497 | 15.836 | 12.479 | 13.061 |
| 192 | 837.8 | 20.51 | 1.058E+16 | 15.553 | 14.477 | 15.825 | 12.455 | 13.058 |
| 193 | 840.7 | 20.46 | 1.026E+16 | 15.536 | 14.457 | 15.815 | 12.430 | 13.055 |
| 194 | 843.5 | 20.41 | 9.956E+15 | 15.518 | 14.437 | 15.804 | 12.406 | 13.052 |
| 195 | 846.3 | 20.37 | 9.661E+15 | 15.501 | 14.418 | 15.794 | 12.382 | 13.048 |
| 196 | 849.0 | 20.32 | 9.378E+15 | 15.484 | 14.398 | 15.783 | 12.358 | 13.045 |
| 197 | 851.7 | 20.27 | 9.104E+15 | 15.466 | 14.379 | 15.773 | 12.334 | 13.042 |
| 198 | 854.3 | 20.23 | 8.841E+15 | 15.449 | 14.359 | 15.762 | 12.310 | 13.039 |
| 199 | 856.8 | 20.18 | 8.587E+15 | 15.432 | 14.340 | 15.752 | 12.286 | 13.036 |
| 200 | 859.3 | 20.14 | 8.342E+15 | 15.415 | 14.321 | 15.742 | 12.262 | 13.033 |

Table 4. (Cont'd.)

| HEIGHT KM | TEMP K | MEAN MOL WT | NUMBER DENSITY /M3 | LOG N(N2) (/M3) | LOG N(O2) (/M3) | LOG N(O) (/M3) | LOG N(AR) (/M3) | LOG N(HE) (/M3) |
|---|---|---|---|---|---|---|---|---|
| 202 | 864.2 | 20.05 | 7.878E+15 | 15.382 | 14.283 | 15.721 | 12.215 | 13.027 |
| 204 | 868.9 | 19.96 | 7.445E+15 | 15.348 | 14.245 | 15.701 | 12.169 | 13.021 |
| 206 | 873.4 | 19.88 | 7.041E+15 | 15.315 | 14.207 | 15.682 | 12.122 | 13.015 |
| 208 | 877.8 | 19.79 | 6.665E+15 | 15.282 | 14.170 | 15.662 | 12.077 | 13.010 |
| 210 | 882.0 | 19.71 | 6.312E+15 | 15.250 | 14.133 | 15.642 | 12.031 | 13.004 |
| 212 | 886.0 | 19.63 | 5.982E+15 | 15.217 | 14.096 | 15.623 | 11.986 | 12.998 |
| 214 | 889.9 | 19.55 | 5.673E+15 | 15.185 | 14.060 | 15.604 | 11.941 | 12.993 |
| 216 | 893.7 | 19.47 | 5.384E+15 | 15.153 | 14.024 | 15.585 | 11.896 | 12.987 |
| 218 | 897.3 | 19.39 | 5.112E+15 | 15.122 | 13.988 | 15.566 | 11.852 | 12.982 |
| 220 | 900.7 | 19.32 | 4.856E+15 | 15.090 | 13.952 | 15.547 | 11.807 | 12.977 |
| 222 | 904.1 | 19.24 | 4.616E+15 | 15.059 | 13.917 | 15.529 | 11.763 | 12.971 |
| 224 | 907.3 | 19.17 | 4.390E+15 | 15.028 | 13.881 | 15.510 | 11.720 | 12.966 |
| 226 | 910.5 | 19.10 | 4.177E+15 | 14.997 | 13.846 | 15.492 | 11.676 | 12.961 |
| 228 | 913.5 | 19.03 | 3.977E+15 | 14.966 | 13.811 | 15.474 | 11.633 | 12.956 |
| 230 | 916.4 | 18.96 | 3.788E+15 | 14.936 | 13.777 | 15.456 | 11.590 | 12.951 |
| 232 | 919.2 | 18.89 | 3.609E+15 | 14.905 | 13.742 | 15.438 | 11.547 | 12.946 |
| 234 | 921.8 | 18.83 | 3.441E+15 | 14.875 | 13.708 | 15.420 | 11.505 | 12.941 |
| 236 | 924.4 | 18.76 | 3.281E+15 | 14.845 | 13.674 | 15.402 | 11.462 | 12.936 |
| 238 | 927.0 | 18.70 | 3.131E+15 | 14.815 | 13.640 | 15.385 | 11.420 | 12.931 |
| 240 | 929.4 | 18.63 | 2.988E+15 | 14.785 | 13.606 | 15.367 | 11.378 | 12.927 |
| 242 | 931.7 | 18.57 | 2.853E+15 | 14.755 | 13.572 | 15.350 | 11.336 | 12.922 |
| 244 | 933.9 | 18.51 | 2.725E+15 | 14.726 | 13.538 | 15.333 | 11.295 | 12.917 |
| 246 | 936.1 | 18.45 | 2.604E+15 | 14.696 | 13.505 | 15.315 | 11.253 | 12.913 |
| 248 | 938.2 | 18.39 | 2.489E+15 | 14.667 | 13.472 | 15.298 | 11.212 | 12.908 |
| 250 | 940.2 | 18.34 | 2.380E+15 | 14.638 | 13.438 | 15.281 | 11.171 | 12.903 |
| 252 | 942.2 | 18.28 | 2.277E+15 | 14.609 | 13.405 | 15.264 | 11.129 | 12.899 |
| 254 | 944.0 | 18.23 | 2.178E+15 | 14.580 | 13.372 | 15.247 | 11.089 | 12.894 |
| 256 | 945.8 | 18.17 | 2.085E+15 | 14.551 | 13.339 | 15.230 | 11.048 | 12.890 |
| 258 | 947.6 | 18.12 | 1.996E+15 | 14.522 | 13.307 | 15.214 | 11.007 | 12.885 |
| 260 | 949.3 | 18.07 | 1.912E+15 | 14.494 | 13.274 | 15.197 | 10.967 | 12.881 |
| 262 | 950.9 | 18.02 | 1.831E+15 | 14.465 | 13.242 | 15.180 | 10.926 | 12.876 |
| 264 | 952.4 | 17.97 | 1.755E+15 | 14.437 | 13.209 | 15.164 | 10.886 | 12.872 |
| 266 | 953.9 | 17.92 | 1.682E+15 | 14.408 | 13.177 | 15.147 | 10.846 | 12.867 |
| 268 | 955.4 | 17.87 | 1.612E+15 | 14.380 | 13.145 | 15.131 | 10.805 | 12.863 |
| 270 | 956.8 | 17.82 | 1.546E+15 | 14.352 | 13.112 | 15.114 | 10.766 | 12.859 |
| 272 | 958.2 | 17.78 | 1.483E+15 | 14.324 | 13.080 | 15.098 | 10.726 | 12.854 |
| 274 | 959.5 | 17.73 | 1.423E+15 | 14.295 | 13.048 | 15.082 | 10.686 | 12.850 |
| 276 | 960.7 | 17.69 | 1.365E+15 | 14.267 | 13.016 | 15.065 | 10.646 | 12.846 |
| 278 | 961.9 | 17.65 | 1.310E+15 | 14.240 | 12.985 | 15.049 | 10.607 | 12.842 |
| 280 | 963.1 | 17.60 | 1.258E+15 | 14.212 | 12.953 | 15.033 | 10.567 | 12.837 |
| 282 | 964.2 | 17.56 | 1.208E+15 | 14.184 | 12.921 | 15.017 | 10.528 | 12.833 |
| 284 | 965.3 | 17.52 | 1.160E+15 | 14.156 | 12.890 | 15.001 | 10.488 | 12.829 |
| 286 | 966.4 | 17.48 | 1.114E+15 | 14.129 | 12.858 | 14.985 | 10.449 | 12.825 |
| 288 | 967.4 | 17.44 | 1.071E+15 | 14.101 | 12.827 | 14.969 | 10.410 | 12.821 |
| 290 | 968.4 | 17.40 | 1.029E+15 | 14.073 | 12.795 | 14.953 | 10.371 | 12.816 |
| 292 | 969.3 | 17.36 | 9.891E+14 | 14.046 | 12.764 | 14.937 | 10.332 | 12.812 |
| 294 | 970.2 | 17.33 | 9.508E+14 | 14.019 | 12.733 | 14.921 | 10.293 | 12.808 |
| 296 | 971.1 | 17.29 | 9.142E+14 | 13.991 | 12.702 | 14.906 | 10.254 | 12.804 |
| 298 | 972.0 | 17.26 | 8.792E+14 | 13.964 | 12.670 | 14.890 | 10.215 | 12.800 |
| 300 | 972.8 | 17.22 | 8.456E+14 | 13.937 | 12.639 | 14.874 | 10.177 | 12.796 |

## Table 4. (Cont'd.)

| HEIGHT KM | TEMP K | MEAN MOL WT | NUMBER DENSITY /M3 | LOG N(N2) (/M3) | LOG N(O2) (/M3) | LOG N(O) (/M3) | LOG N(AR) (/M3) | LOG N(HE) (/M3) |
|---|---|---|---|---|---|---|---|---|
| 302 | 973.6 | 17.19 | 8.134E+14 | 13.909 | 12.608 | 14.859 | 10.138 | 12.792 |
| 304 | 974.4 | 17.15 | 7.826E+14 | 13.882 | 12.577 | 14.843 | 10.100 | 12.788 |
| 306 | 975.1 | 17.12 | 7.531E+14 | 13.855 | 12.546 | 14.827 | 10.061 | 12.784 |
| 308 | 975.8 | 17.09 | 7.248E+14 | 13.828 | 12.516 | 14.812 | 10.023 | 12.780 |
| 310 | 976.5 | 17.06 | 6.977E+14 | 13.801 | 12.485 | 14.796 | 9.984 | 12.776 |
| 312 | 977.2 | 17.02 | 6.716E+14 | 13.774 | 12.454 | 14.781 | 9.946 | 12.772 |
| 314 | 977.8 | 16.99 | 6.467E+14 | 13.747 | 12.423 | 14.765 | 9.908 | 12.768 |
| 316 | 978.5 | 16.96 | 6.227E+14 | 13.720 | 12.393 | 14.750 | 9.870 | 12.764 |
| 318 | 979.1 | 16.93 | 5.997E+14 | 13.694 | 12.362 | 14.734 | 9.831 | 12.760 |
| 320 | 979.7 | 16.91 | 5.776E+14 | 13.667 | 12.332 | 14.719 | 9.793 | 12.756 |
| 322 | 980.2 | 16.88 | 5.565E+14 | 13.640 | 12.301 | 14.703 | 9.755 | 12.752 |
| 324 | 980.8 | 16.85 | 5.361E+14 | 13.613 | 12.271 | 14.688 | 9.717 | 12.748 |
| 326 | 981.3 | 16.82 | 5.166E+14 | 13.587 | 12.240 | 14.673 | 9.679 | 12.744 |
| 328 | 981.8 | 16.79 | 4.978E+14 | 13.560 | 12.210 | 14.657 | 9.641 | 12.740 |
| 330 | 982.3 | 16.77 | 4.798E+14 | 13.533 | 12.179 | 14.642 | 9.604 | 12.736 |
| 332 | 982.8 | 16.74 | 4.625E+14 | 13.507 | 12.149 | 14.627 | 9.566 | 12.732 |
| 334 | 983.3 | 16.72 | 4.458E+14 | 13.480 | 12.119 | 14.612 | 9.528 | 12.729 |
| 336 | 983.7 | 16.69 | 4.298E+14 | 13.454 | 12.089 | 14.596 | 9.490 | 12.725 |
| 338 | 984.1 | 16.67 | 4.144E+14 | 13.427 | 12.058 | 14.581 | 9.453 | 12.721 |
| 340 | 984.6 | 16.64 | 3.997E+14 | 13.401 | 12.028 | 14.566 | 9.415 | 12.717 |
| 342 | 985.0 | 16.62 | 3.854E+14 | 13.375 | 11.998 | 14.551 | 9.378 | 12.713 |
| 344 | 985.4 | 16.59 | 3.718E+14 | 13.348 | 11.968 | 14.536 | 9.340 | 12.709 |
| 346 | 985.7 | 16.57 | 3.586E+14 | 13.322 | 11.938 | 14.521 | 9.303 | 12.705 |
| 348 | 986.1 | 16.55 | 3.459E+14 | 13.296 | 11.908 | 14.506 | 9.265 | 12.702 |
| 350 | 986.5 | 16.52 | 3.338E+14 | 13.269 | 11.878 | 14.490 | 9.228 | 12.698 |
| 352 | 986.8 | 16.50 | 3.220E+14 | 13.243 | 11.848 | 14.475 | 9.190 | 12.694 |
| 354 | 987.2 | 16.48 | 3.108E+14 | 13.217 | 11.818 | 14.460 | 9.153 | 12.690 |
| 356 | 987.5 | 16.46 | 2.999E+14 | 13.191 | 11.788 | 14.445 | 9.116 | 12.686 |
| 358 | 987.8 | 16.44 | 2.894E+14 | 13.165 | 11.758 | 14.430 | 9.079 | 12.683 |
| 360 | 988.1 | 16.42 | 2.794E+14 | 13.139 | 11.729 | 14.415 | 9.041 | 12.679 |
| 362 | 988.4 | 16.39 | 2.697E+14 | 13.112 | 11.699 | 14.400 | 9.004 | 12.675 |
| 364 | 988.7 | 16.37 | 2.604E+14 | 13.086 | 11.669 | 14.386 | 8.967 | 12.671 |
| 366 | 989.0 | 16.35 | 2.514E+14 | 13.060 | 11.639 | 14.371 | 8.930 | 12.667 |
| 368 | 989.2 | 16.33 | 2.427E+14 | 13.034 | 11.610 | 14.356 | 8.893 | 12.664 |
| 370 | 989.5 | 16.31 | 2.344E+14 | 13.008 | 11.580 | 14.341 | 8.856 | 12.660 |
| 372 | 989.8 | 16.29 | 2.263E+14 | 12.982 | 11.550 | 14.326 | 8.819 | 12.656 |
| 374 | 990.0 | 16.27 | 2.186E+14 | 12.956 | 11.521 | 14.311 | 8.782 | 12.652 |
| 376 | 990.2 | 16.25 | 2.111E+14 | 12.931 | 11.491 | 14.296 | 8.745 | 12.649 |
| 378 | 990.5 | 16.23 | 2.039E+14 | 12.905 | 11.462 | 14.281 | 8.708 | 12.645 |
| 380 | 990.7 | 16.21 | 1.970E+14 | 12.879 | 11.432 | 14.267 | 8.672 | 12.641 |
| 382 | 990.9 | 16.19 | 1.903E+14 | 12.853 | 11.403 | 14.252 | 8.635 | 12.637 |
| 384 | 991.1 | 16.18 | 1.839E+14 | 12.827 | 11.373 | 14.237 | 8.598 | 12.634 |
| 386 | 991.3 | 16.16 | 1.777E+14 | 12.801 | 11.344 | 14.222 | 8.561 | 12.630 |
| 388 | 991.5 | 16.14 | 1.717E+14 | 12.776 | 11.314 | 14.208 | 8.525 | 12.626 |
| 390 | 991.7 | 16.12 | 1.659E+14 | 12.750 | 11.285 | 14.193 | 8.488 | 12.622 |
| 392 | 991.9 | 16.10 | 1.603E+14 | 12.724 | 11.255 | 14.178 | 8.451 | 12.619 |
| 394 | 992.1 | 16.08 | 1.550E+14 | 12.698 | 11.226 | 14.163 | 8.415 | 12.615 |
| 396 | 992.3 | 16.06 | 1.498E+14 | 12.673 | 11.197 | 14.149 | 8.378 | 12.611 |
| 398 | 992.5 | 16.04 | 1.448E+14 | 12.647 | 11.168 | 14.134 | 8.342 | 12.608 |
| 400 | 992.6 | 16.03 | 1.400E+14 | 12.621 | 11.138 | 14.119 | 8.305 | 12.604 |

## Table 4. (Cont'd.)

| HEIGHT KM | TEMP K | MEAN MOL WT | NUMBER DENSITY /M3 | LOG N(N2) (/M3) | LOG N(O2) (/M3) | LOG N(O) (/M3) | LOG N(AR) (/M3) | LOG N(HE) (/M3) |
|---|---|---|---|---|---|---|---|---|
| 402 | 992.8 | 16.01 | 1.353E+14 | 12.596 | 11.109 | 14.105 | 8.269 | 12.600 |
| 404 | 993.0 | 15.99 | 1.308E+14 | 12.570 | 11.060 | 14.090 | 8.242 | 12.596 |
| 406 | 993.1 | 15.97 | 1.265E+14 | 12.545 | 11.051 | 14.075 | 8.196 | 12.593 |
| 408 | 993.3 | 15.95 | 1.223E+14 | 12.519 | 11.021 | 14.061 | 8.159 | 12.589 |
| 410 | 993.4 | 15.93 | 1.183E+14 | 12.494 | 10.992 | 14.046 | 8.123 | 12.585 |
| 412 | 993.5 | 15.92 | 1.144E+14 | 12.468 | 10.963 | 14.032 | 8.087 | 12.582 |
| 414 | 993.7 | 15.90 | 1.107E+14 | 12.443 | 10.934 | 14.017 | 8.050 | 12.578 |
| 416 | 993.8 | 15.88 | 1.070E+14 | 12.417 | 10.905 | 14.002 | 8.014 | 12.574 |
| 418 | 994.0 | 15.86 | 1.035E+14 | 12.392 | 10.876 | 13.988 | 7.978 | 12.571 |
| 420 | 994.1 | 15.84 | 1.001E+14 | 12.366 | 10.847 | 13.973 | 7.941 | 12.567 |
| 422 | 994.2 | 15.82 | 9.689E+13 | 12.341 | 10.818 | 13.959 | 7.905 | 12.563 |
| 424 | 994.3 | 15.81 | 9.374E+13 | 12.316 | 10.789 | 13.944 | 7.869 | 12.560 |
| 426 | 994.5 | 15.79 | 9.070E+13 | 12.290 | 10.760 | 13.930 | 7.833 | 12.556 |
| 428 | 994.6 | 15.77 | 8.776E+13 | 12.265 | 10.731 | 13.915 | 7.797 | 12.553 |
| 430 | 994.7 | 15.75 | 8.493E+13 | 12.239 | 10.702 | 13.901 | 7.761 | 12.549 |
| 432 | 994.8 | 15.73 | 8.219E+13 | 12.214 | 10.673 | 13.886 | 7.725 | 12.545 |
| 434 | 994.9 | 15.71 | 7.954E+13 | 12.189 | 10.644 | 13.872 | 7.689 | 12.542 |
| 436 | 995.0 | 15.69 | 7.699E+13 | 12.164 | 10.615 | 13.857 | 7.653 | 12.538 |
| 438 | 995.1 | 15.67 | 7.452E+13 | 12.138 | 10.587 | 13.843 | 7.617 | 12.534 |
| 440 | 995.2 | 15.65 | 7.213E+13 | 12.113 | 10.558 | 13.829 | 7.581 | 12.531 |
| 442 | 995.3 | 15.63 | 6.983E+13 | 12.088 | 10.529 | 13.814 | 7.545 | 12.527 |
| 444 | 995.4 | 15.61 | 6.760E+13 | 12.063 | 10.500 | 13.800 | 7.509 | 12.523 |
| 446 | 995.5 | 15.59 | 6.545E+13 | 12.038 | 10.471 | 13.785 | 7.473 | 12.520 |
| 448 | 995.6 | 15.57 | 6.337E+13 | 12.012 | 10.443 | 13.771 | 7.437 | 12.516 |
| 450 | 995.7 | 15.55 | 6.136E+13 | 11.987 | 10.414 | 13.757 | 7.401 | 12.513 |
| 452 | 995.8 | 15.53 | 5.942E+13 | 11.962 | 10.385 | 13.742 | 7.365 | 12.509 |
| 454 | 995.8 | 15.51 | 5.755E+13 | 11.937 | 10.357 | 13.728 | 7.330 | 12.505 |
| 456 | 995.9 | 15.49 | 5.574E+13 | 11.912 | 10.328 | 13.713 | 7.294 | 12.502 |
| 458 | 996.0 | 15.47 | 5.399E+13 | 11.887 | 10.299 | 13.699 | 7.258 | 12.498 |
| 460 | 996.1 | 15.45 | 5.229E+13 | 11.862 | 10.271 | 13.685 | 7.222 | 12.495 |
| 462 | 996.2 | 15.43 | 5.066E+13 | 11.837 | 10.242 | 13.670 | 7.187 | 12.491 |
| 464 | 996.2 | 15.40 | 4.907E+13 | 11.812 | 10.214 | 13.656 | 7.151 | 12.487 |
| 466 | 996.3 | 15.38 | 4.754E+13 | 11.787 | 10.185 | 13.642 | 7.115 | 12.484 |
| 468 | 996.4 | 15.36 | 4.607E+13 | 11.762 | 10.157 | 13.628 | 7.080 | 12.480 |
| 470 | 996.4 | 15.34 | 4.464E+13 | 11.737 | 10.128 | 13.613 | 7.044 | 12.477 |
| 472 | 996.5 | 15.31 | 4.325E+13 | 11.712 | 10.100 | 13.599 | 7.009 | 12.473 |
| 474 | 996.6 | 15.29 | 4.192E+13 | 11.687 | 10.071 | 13.585 | 6.973 | 12.470 |
| 476 | 996.6 | 15.27 | 4.063E+13 | 11.662 | 10.043 | 13.571 | 6.938 | 12.466 |
| 478 | 996.7 | 15.24 | 3.938E+13 | 11.637 | 10.014 | 13.556 | 6.902 | 12.462 |
| 480 | 996.8 | 15.22 | 3.817E+13 | 11.612 | 9.986 | 13.542 | 6.867 | 12.459 |
| 482 | 996.8 | 15.19 | 3.700E+13 | 11.587 | 9.957 | 13.528 | 6.831 | 12.455 |
| 484 | 996.9 | 15.17 | 3.587E+13 | 11.563 | 9.929 | 13.514 | 6.796 | 12.452 |
| 486 | 996.9 | 15.14 | 3.478E+13 | 11.538 | 9.901 | 13.500 | 6.760 | 12.448 |
| 488 | 997.0 | 15.12 | 3.372E+13 | 11.513 | 9.872 | 13.485 | 6.725 | 12.445 |
| 490 | 997.0 | 15.09 | 3.269E+13 | 11.488 | 9.844 | 13.471 | 6.690 | 12.441 |
| 492 | 997.1 | 15.06 | 3.171E+13 | 11.463 | 9.816 | 13.457 | 6.654 | 12.437 |
| 494 | 997.1 | 15.04 | 3.075E+13 | 11.439 | 9.787 | 13.443 | 6.619 | 12.434 |
| 496 | 997.2 | 15.01 | 2.982E+13 | 11.414 | 9.759 | 13.429 | 6.584 | 12.430 |
| 498 | 997.2 | 14.98 | 2.893E+13 | 11.389 | 9.731 | 13.415 | 6.548 | 12.427 |
| 500 | 997.3 | 14.95 | 2.806E+13 | 11.364 | 9.703 | 13.400 | 6.513 | 12.423 |

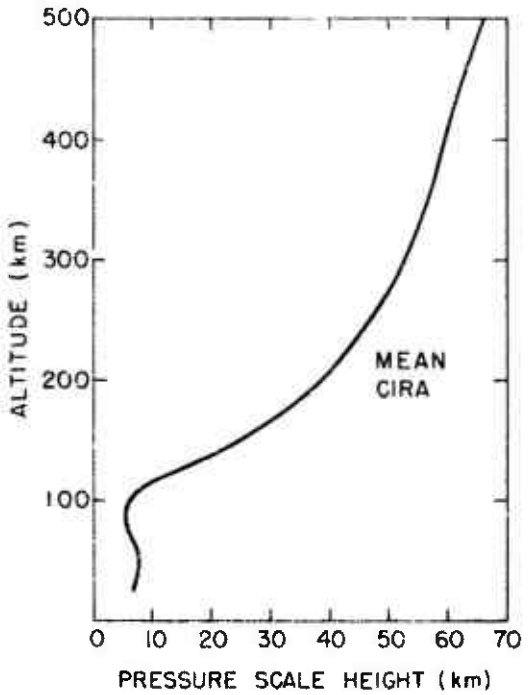


Figure 1. Pressure scale heights of the mean CIRA atmosphere.

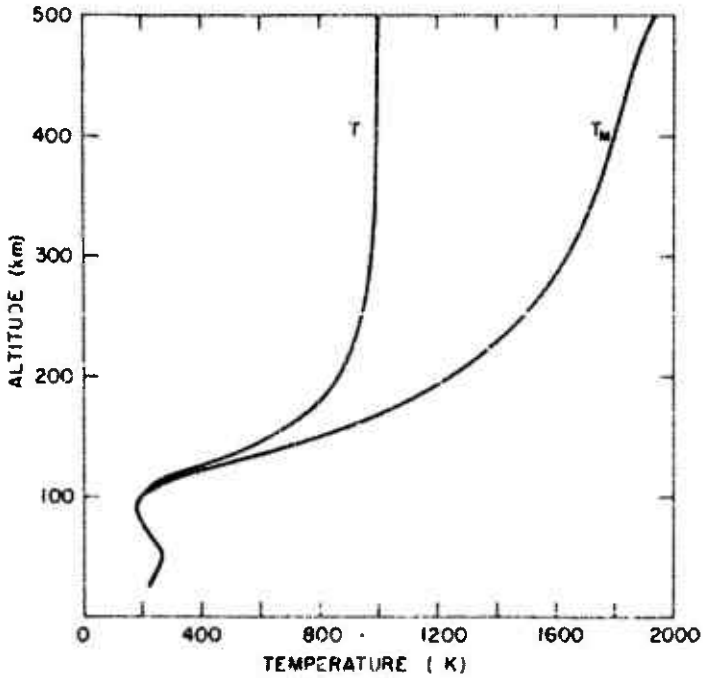


Figure 2. Kinetic temperatures (T) and molecular-scale temperatures ($T_M$) of the mean atmosphere.

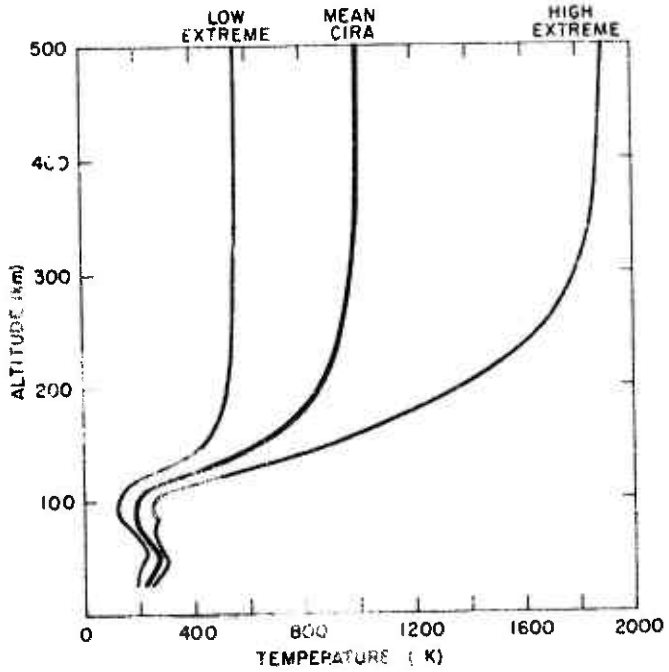


Figure 3. Mean CIRA temperatures and low extreme and high extreme temperatures.

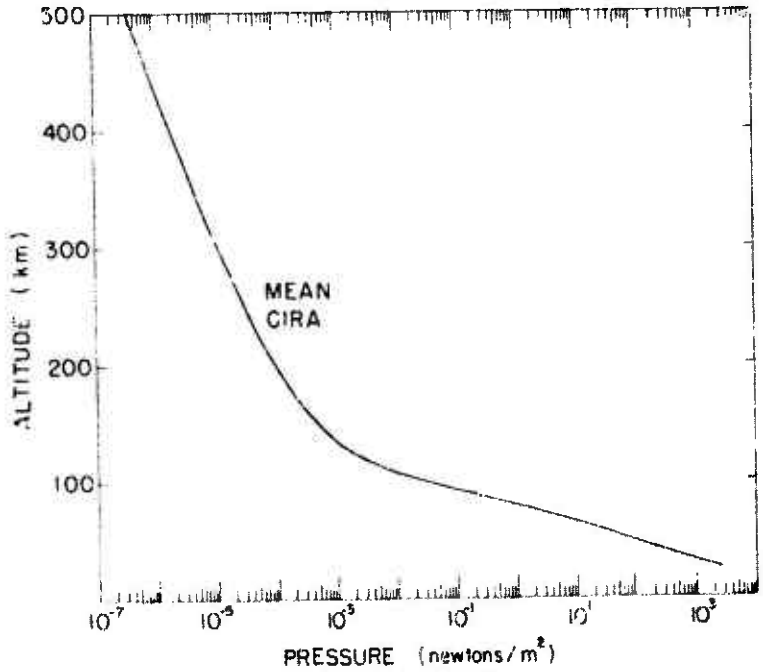


Figure 4. Pressure curve of the mean atmosphere, from 25 to 500 km.

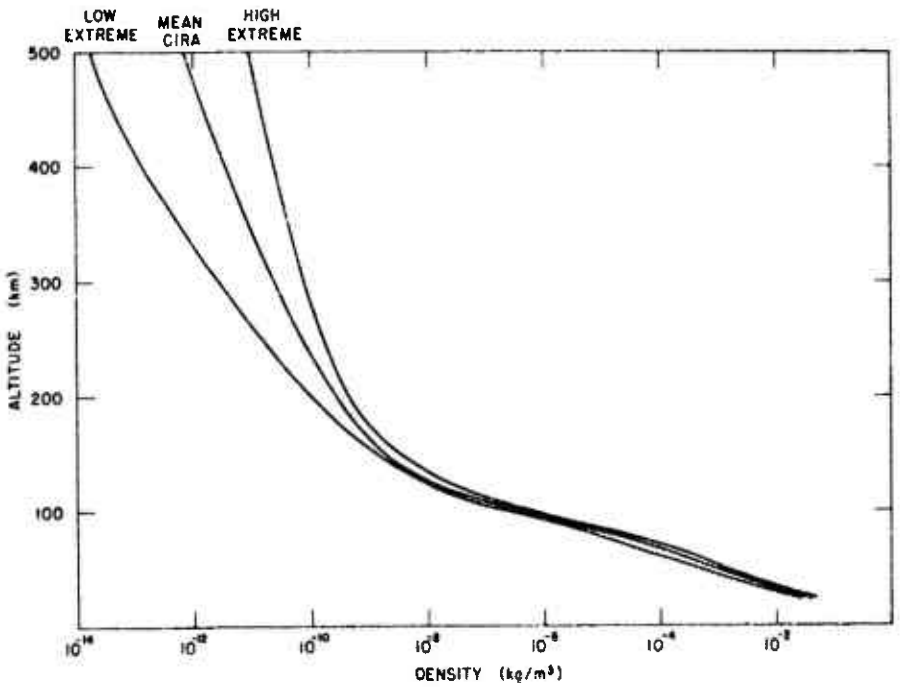


Figure 5. Mean CIRA densities and curves of extreme densities.

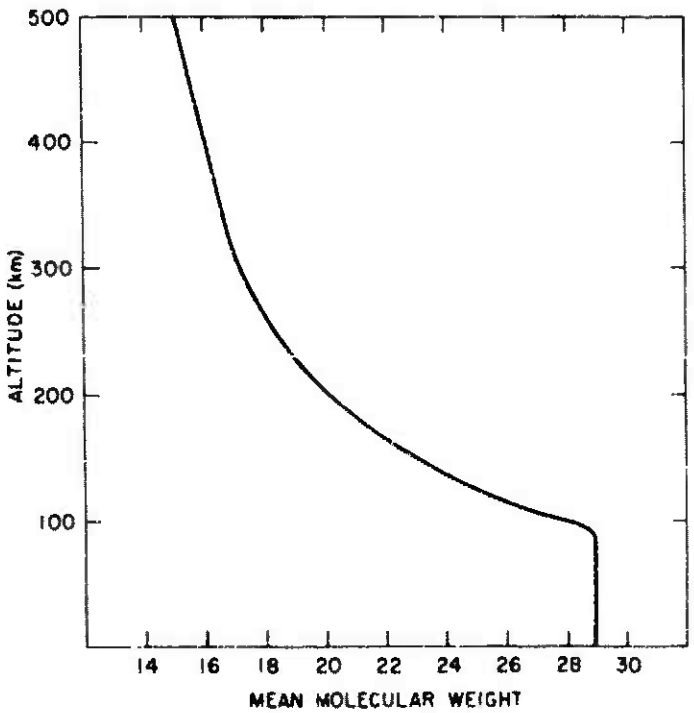


Figure 6. Mean molecular weights of Mean CIRA atmosphere.

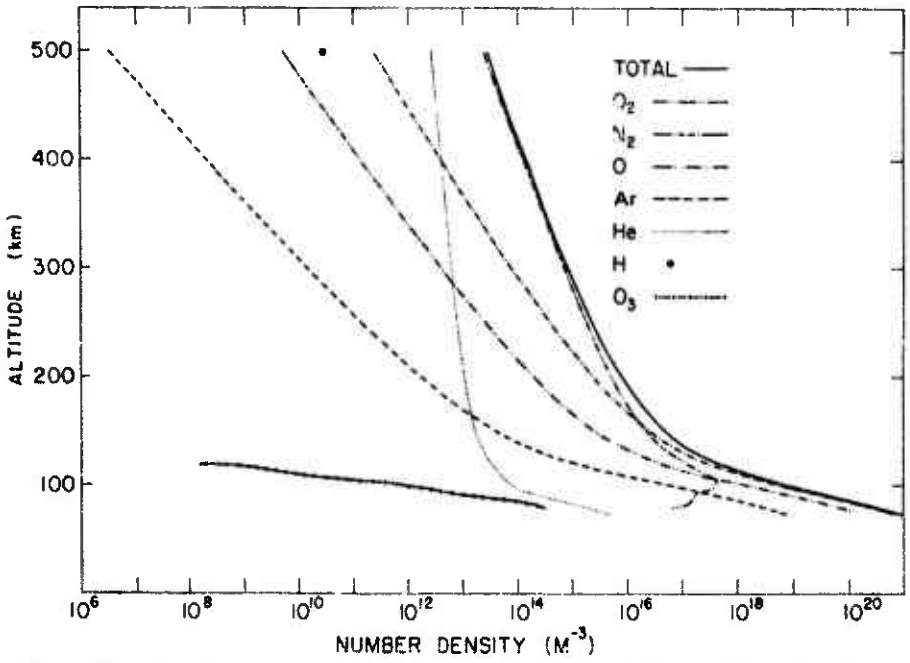


Figure 7. Total number densities and densities of $N_2$, $O_2$, O, $O_3$, Ar, He, and H.

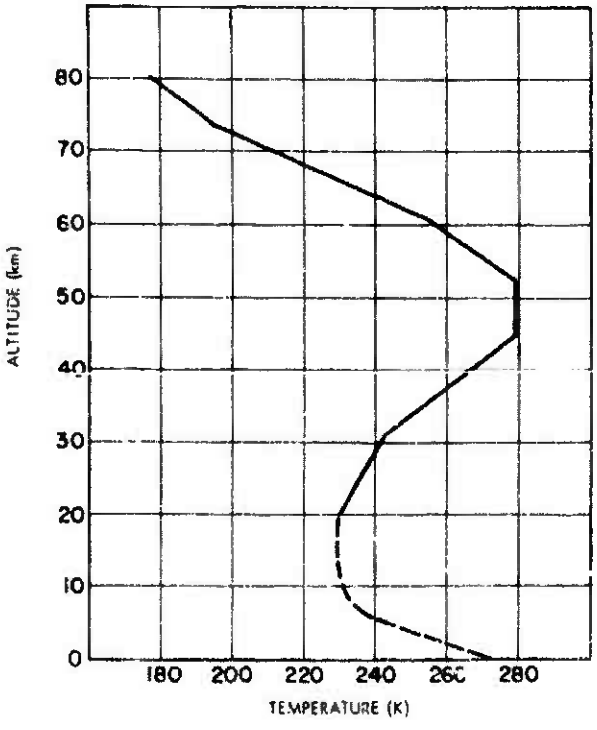


Figure 8. Mean June-July temperature profile for 80°N.

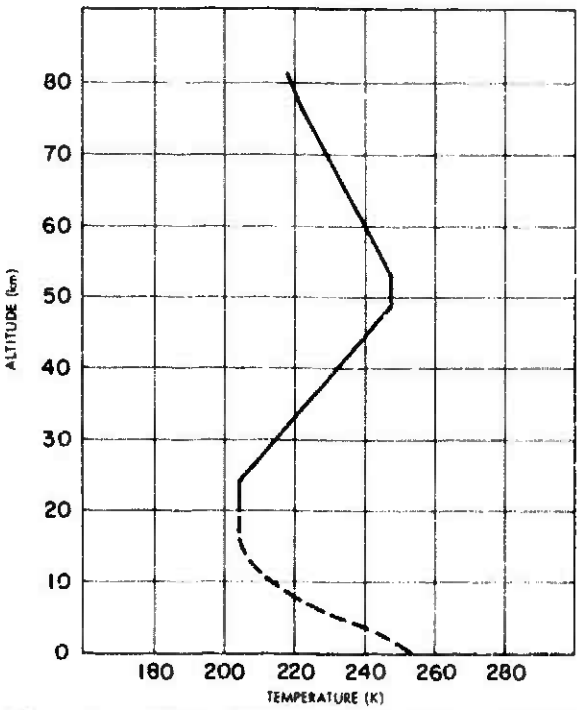


Figure 9. Mean December-January temperature profile for 80° N.

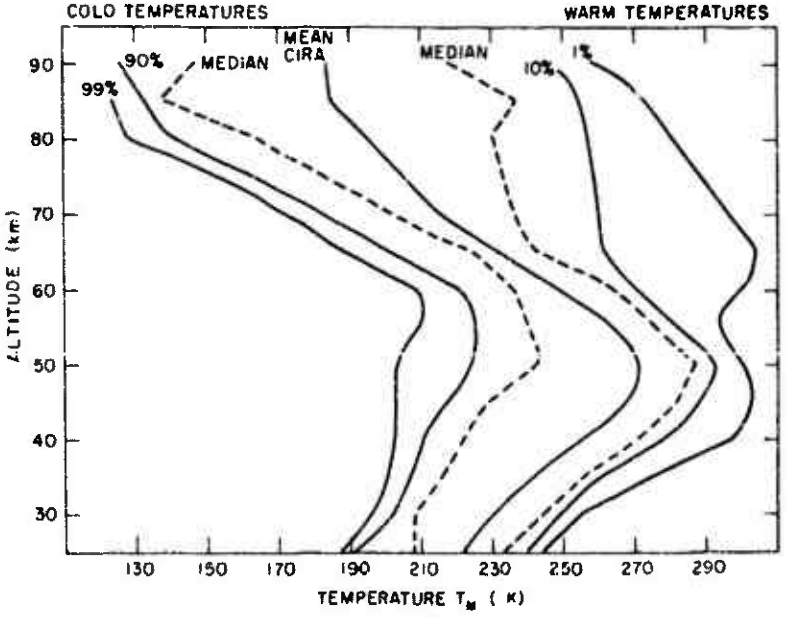


Figure 10. Mean CIRA temperatures, temperatures which are exceeded 50, 10, and 1% of the time during warmest months and temperatures exceeded 50, 90, and 99% of the time during coldest months at latitudes between 0° and 80° N.

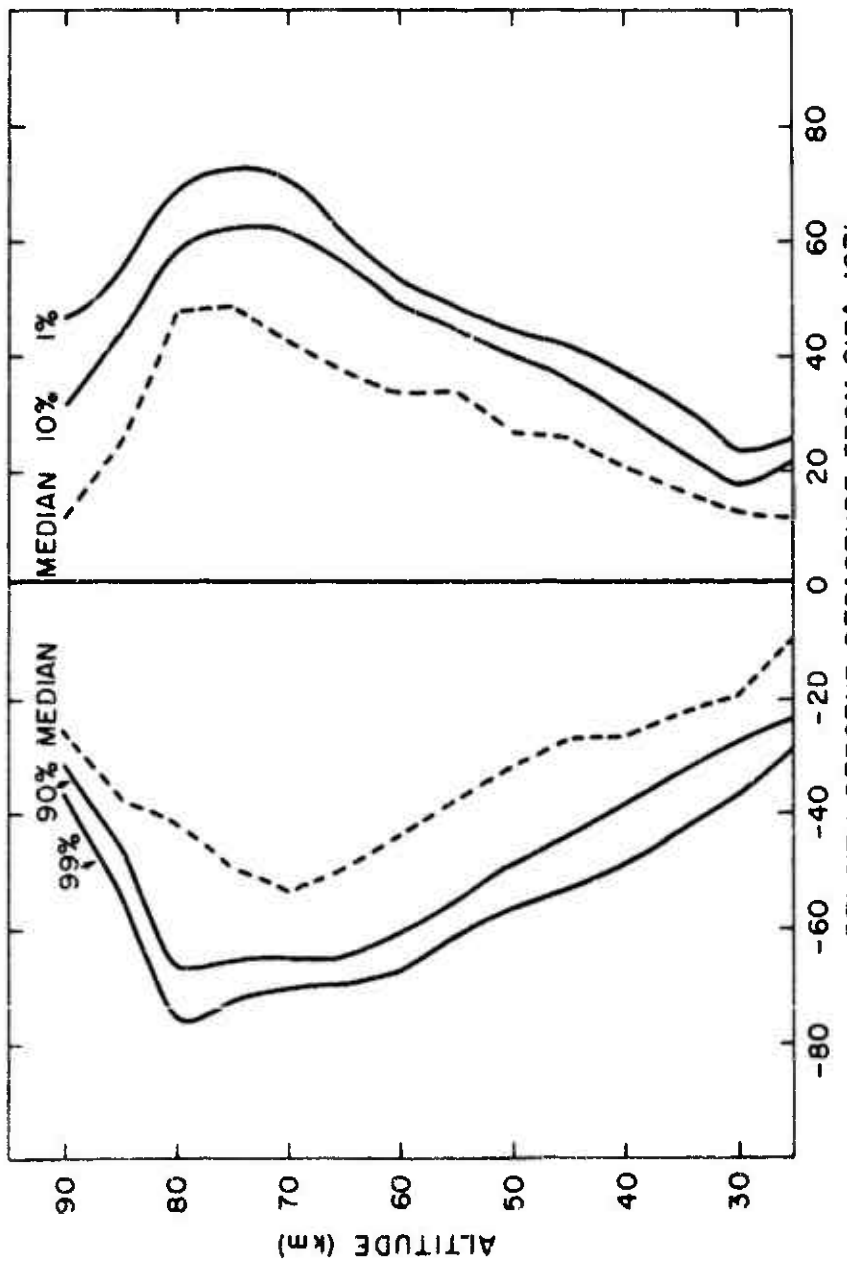


Figure 11. Densities relative to mean CIRA exceeded 50, 10, and 1% of the time during months with highest densities and densities exceeded 50, 90, and 99% of the time during months with lowest densities at latitudes between 0° and 80°N.

B (cont'd) Designation in Figure 16-2, for work of Bardsley, Reference 16-28 (16).

Power of the pre-exponential thermal dependence, a characteristic term of the rate-constant function (19).

Magnetic field strength (21).

Indexing use: target species (15).

BH Designation for Birge-Hopfield system (9).

$B_o$ Comparison real function plotted in Figure 21-2, from Reference 21-2, assuming $j = 0$ and $\nu(\epsilon) = \nu_o$ (21).

B&T Designation in Figure 20-6, for work of Bauer and Tsang, Reference 20-143 (20).

$B_2$ Real function plotted in Figure 21-2, from Equation 21-5 (21).

b Power of the pre-exponential thermal dependence, a characteristic term of the rate-constant function (6, 16, 19, 24).

Parameter defined in Equation 15-10 (15).

Impact parameter (15).

Indexing uses: bound state of species (8).
trajectory point (15).
impact parameter (15).
colliding species in the Firsov model (15).
magnetic field (21).

$b_j$ Interaction or capture radius (15).

$|b_j|^2$ Capture probability (15).

buoy Indexing use only; buoyancy subrange (3).

$b_1$ Cut-off radius (15).

C Designation for unspecified chemical species (6, 19, 20).

Linear slope in a Boltzmann system (6).

Designation in Table 9-5, for chemical association process (9).

C (cont'd) Designation in Table 15-2, for fast-particle detection (15).

Constant ≅ 3.49 in the Thomas theory (15).

Least-squares fit constant (16).

$C_i$ Collision proportionality constant for species "i" (2).

$\mathfrak{C}_p(X)$ Integral function of X used in Equation 21-5 and explained and tabulated in Reference 21-28 (21).

c Speed of sound (3).

Speed of light (4, 7, 11).

Activation temperature of chemical reaction, a characteristic term of the rate-constant function (6, 19, 24).

Indexing uses: chemical change (3).
chemical energy (3).
cyclotron (7).
cone (7).
collisional (20).

$\bar{c}$ Mean thermal speed (3).

$\bar{c}_j$ Mean thermal speed of species "j" (3).

$c_o$ Speed of sound in unperturbed medium (3).

col Indexing use only; column (11).

crit Indexing use only; critical value (3).

$c_v$ Specific heat at constant volume per unit mass (3).

$c(\rho)$ $= \left| b_j(+\infty) \right|^2$ (15).

D Effective diffusion coefficient (3).

Dissociation energy (4).

Distance from nuclear burst measured along surface of earth (5).

Designation for unspecified chemical species (6).

Designation in Table 15-2, for slow-particle detection (15).

Least-squares fit constant (16).

$E_{XA}$ Activation energy for collisional excitation (X→A) reaction (20).

$E_1$ $\equiv MR^2(E_i/13.6)^2$, in the method of Fleischmann, Dehmel, and Lee (15).

Kinetic energy of incident ion before collision (15).

$E_2$ Kinetic energy of incident ion after collision (15).

e Ionic or electronic charge (7, 11, 15, 21).

Designation in Table 9-5, for photoelectron process (9).

Indexing uses: energy equation (3).
electron (4, 5, 7, 8, 11, 16, 20, 21, 22, 24).
electronic transition (11).
bound electron (15).
electron acting as third body (16).

eddy Indexing use only; eddy (3).

eff Indexing use only; effective (9, 15).

ex Indexing use only; excitation (4, 11).

F Solar flux at 10.7-cm wavelength (5).

Designation in Table 9-5, for fluorescence process (9).

Free energy (10).

Fraction of optically active molecules under irradiation, which are radiatively excited per second (11).

Designation on Page 18A-8, of work of Ferguson, from Reference 18A-9 (18A).

Designation on Page 18A-9, of work of Felsenfeld et al, from Reference 18A-40 (18A).

$\bar{F}$ Mean solar flux (2).

$\underset{\sim}{F}$ Total external force per unit mass (3).

$\underset{\sim}{F}'$ Miscellaneous external forces acting on atmosphere (3).

$\underset{\sim}{F}_a$ External force per unit mass on species "a" (3).

$F_i$ Chemical formation rate of species "i" (2).

$F(k)$ Turbulent power spectrum, in wavenumber space (3).

$F(k)_{Kolm}$ F(k) in the inertial subrange, according to Kolmogoroff's Law (3).

$f$ Oscillator strength or "f-number" of transition (11).

Range of reciprocal electron densities over which a linear variation with time is obtained, to within one percent (16).

Indexing uses: fluorescence (11).
final (11).

$f_o$ Resonant frequency (7).

$f_v$ Fraction of collisions having relative velocities between v and v+dv (6).

$f(X)$ Fractional atmospheric concentration of species "X" (4).

$f(\epsilon)$ Electron energy distribution function (21).

$G$ Fractional energy loss per collision (21).

$G(\ell, t)$ Probability for separation distance "$\ell$" between two particles (3).

GS Designation in Figure 16-2, of work of Gunton and Shaw, from Reference 16-7 (16).

$g$ Gravitational acceleration (2, 4).

Production rate factor (9).

Statistical weight (11).

Indexing use: gas-kinetic (21).

$\underset{\sim}{g}$ Gravitational force per unit mass (3).

gas Indexing use only; gas-kinetic (16).

$g_{io.}$ Statistical weight of ionic ground state (11).

$g_{n\ell}$ Statistical weight of a recombining level "$n\ell$" (11).

$g_n(\nu)$ Statistical weight of a recombining level in a hydrogenic species (11).

g(X) Electronic statistical weight of species "X" (4).

g(y) Firsov model parameter $\equiv \left[ y^{0.1} - 1 \right]$ (15).

H Atmospheric scale height (3).

Magnetic field (7).

Scale height of atomic oxygen (9).

Enthalpy (10, 17, 19).

Total Hamiltonian (15).

Designation in Figure 16-1, of work of Hagen, from Reference 16-22 (16).

Designation on Page 18A-9, of work of Howard et al, from Reference 18A-12 (18A).

Scale height (20).

Indexing use: hydrogen atom (15).

Ha Designation in Figure 16-1, of work of Hackam, from Reference 16-19 (16).

HCE Designation for Handbook Committee Estimate (24).

$H_i$ Scale height of species "i" (2).

$H_m$ Scale height of species having mean mass (2).

$H_p$ Pressure scale height (2).

H(X) Scale height of species "X" (4).

h Planck constant (3, 4, 6, 7, 11, 17, 19, 20, 24).

Altitude (4, 5).

Indexing use: altitude (4).

$\hbar$ Modified Planck constant, $h/2\pi$ (11, 15).

$h_{ii} \equiv (\phi_i, V_b \phi_i)$

$h_{ij} \equiv (\phi_i, V_a \phi_j)$ (15).

$h_{ji} \equiv (\phi_j, V_b\phi_i)$
$h_{ji} \equiv (\phi_j, V_a\phi_j)$ } (15).

$\bar{h}_j^{-1}$ A measure of chemical effect in turbulence, from Equation 3-67a (3).

$h_o$ Turbopause altitude (4).

Indexing use: turbopause altitude (4).

horiz Indexing use only; horizontal (3).

$h_q$ Quenching height (9).

I Ionization potential (4, 15).

Photon flux after transmission (7).

Intensity of indicated radiation (9).

Geomagnetic dip angle (9).

Designation in Table 9-5, of ionic reaction process (9).

$I_{col}$ Line-of-sight column emission rate = line integral of $I_{vol}$ (11).

ICR Designation for Ion Cyclotron Resonance (7).

IGY Designation for International Geophysical Year (9).

$I_H$ Ionization potential (13.6 eV) of ground-state hydrogen atom (15).

Im Designation for imaginary portion of function (21).

$\mathrm{Im}\Delta K_i$ Imaginary portion of $\Delta K_i$, in the low-frequency limit (21).

$I_o$ Photon flux before transmission (7).

$I_o(\lambda)$ Incident light intensity (12).

IP Ionization potential (18A).

IR Infrared.

| | |
|---|---|
| $K_t$ | Turbulent diffusion coefficient (2). |
| $K'$ | Collisional rate (11). |
| $K'_{01}$ | Collisional excitation rate (11). |
| $K'_{10}$ | Collisional deexcitation rate (11). |
| **K** | Thermal conductivity coefficient (3). |
| $\mathbf{K}_i$ | Degree of ionization of plasma (3). |
| k | Wavenumber (3). |
| | Boltzmann constant (2, 4, 11, 20, 21). |
| | Rate constant or rate-constant function, of chemical reaction, in the forward direction as written (6, 11, 18A, 19, 20, 24). |
| | Total absorption coefficient (7). |
| | Rate coefficient of ion-molecule reaction (8). |
| | Total three-body recombination rate coefficient (16). |
| | Indexing use: kinetic (4). |
| $\underset{\sim}{k}$ | Wavenumber vector (3). |
| $k_g$ | Upper limit of wavenumber for buoyancy subrange (3). |
| $k_i$ | Photoionization coefficient (7). |
| | Rate constant for inelastic scattering from species "i" (20). |
| $k^i_{3n}$ | Rate coefficient for Thomson recombination, three-body neutral-molecule-stabilized, positive-ion negative ion recombination (16). |
| kin | Indexing use only; kinetic (11). |
| $k_j(z)$ | First-order rate constant for photoionization of species "j", at altitude "z" (13). |
| $k_M$ | Rate constant for quenching reaction where "M" is the quenchant (20). |
| kn | Reactive collision frequency (20). |

$k(NO^+)$ Rate coefficient for $NO^+$ production (13).

$k_o$ $= 2\pi/L_o$ (3).

$k_r$ Rate constant for reverse reaction (18A).

$k_T$ Rate constant for a system having Maxwellian distribution (6, 14).

Absorption coefficient (12).

$k(v)$ Rate constant for formation of vibrationally excited species in level "v" (11).

$k_x$, $k_y$, $k_z$ Wavenumber directional components (3).

$k_\nu$ $= 2\pi/L_\nu = (\epsilon_\nu/\nu^3)^{1/4}$ (3).

$k_{10}$ Rate constant for deactivation of first vibrational level (20).

$k_{3e}$ Three-body recombination rate coefficient with electron as third body (16).

$k_{3n}$ Three-body recombination rate coefficient with neutral species as third body (16).

$k_{3r}$ Three-body recombination rate coefficient (16).

$k_{300}$ Rate constant at 300 K (24).

$k'$ Rate constant or rate-constant function of chemical reaction, in the reverse direction as written (6).

$k$ Boltzmann constant (3, 6).

L Designation for Lyman radiation (5).

Optical pathlength (13).

LBH Designation for Lyman-Birge-Hopfield system (9).

$L_{ij}(\epsilon)$ Inelastic cross-section for low-energy electron in gas (21).

$L_j$ Rate of process "j" leading to electron loss (16).

$L_j^{-1}$ A measure of the effect of wind shear in turbulence, in Equation 3-67b (3).

$L_j(\epsilon)$ Energy loss function for the jth vibrational level (21).

$L_o$ Length scale of large (turbulent) disturbances (3).

LT Designation in Figure 16-2, of work of Lin and Teare, from Reference 16-27 (16).

LTE Designation for Local Thermodynamic Equilibrium (4, 11).

Ly Designation for Lyman radiation (12).

$L(\epsilon)$ Energy loss function (21).

$L_\nu$ Length scale of the smallest of eddies (3).

$L_{2r}$ Rate of electron loss via two-body electron-ion recombination (16).

$L_{3r}$ Rate of electron loss via three-body electron-ion recombination (16).

$\ell$ Distance (3).

Charged rearrangement rate constant for negative ions (9).

Light path (12).

$\ell_m$ Gas-kinetic mean free path (3).

M Mean molecular weight (2).

Gram molecular weight (3).

Reduced molecular weight (6).

Designation for third body or collisional partner (6, 16, 17, 18A, 19, 20, 24).

Reduced mass of ion-molecule reaction pair (8).

M (cont'd) Projectile mass, in the method of Fleischmann, Dehmel, and Lee (15).

Designation for unspecified chemical species (17, 18A, 20).

Number of density of collision partner (20).

Mass number (21).

Indexing use: molecular-scale (2).

MB Designation in Figures 16-1 and 16-3, of work of Mehr and Biondi, from Reference 16-21 (16).

Me Designation for unspecified metallic species (11).

$M_i$ Molecular weight of species "i" (2).

Mass number for an ionic species (21).

Reduced mass of ion + neutral pair (21).

$M_o$ Sea-level mean atmospheric molecular weight = 28.96 (2).

M(X) Mass of species "X" (4).

m Mean mass of an "air molecule" (3).

Unspecified function of altitude, time of day, and sunspot cycle (5).

Ionic mass (7, 15).

Concentration of attaching neutral species (9).

Mass of electron (21).

Indexing uses: mean-mass (2).
equation of motion (3).
combining proportions (6).
molecular (9).
momentum-transfer (11, 21).
number of electrons stripped (15).

$m_a$ Molecular mass of species "a" (3).

$m_{av}$ Mass of average "air molecule" (3).

max Indexing use only; maximum (11).

| | |
|---|---|
| $m_e$ | Mass of electron (4, 11). |
| | Mass of bound electron on target atom (15). |
| $m_i$ | Mass of species "i" (2). |
| $m_j$ | Molecular mass of species "j" (3). |
| mn | Indexing use only; mutual neutralization (16). |
| mol | Indexing use only; molecular (3). |
| $m_l$ | Mass of incident ion (15). |
| N | Designation for north latitude (2). |
| | Number of observations (3). |
| | Brunt-Väisälä frequency (3). |
| | Electron concentration (9). |
| | Number of collisions per second per molecule at altitude (11). |
| | Total number of optically active molecules under irradiation (11). |
| | Designation for unspecified chemical species (16). |
| | Molecular density (21). |
| | Indexing use: neutral product (12). |
| $N_{col}$ | Column density of molecules under radiative excitation (11). |
| NED | Designation for No Experimental Data (24). |
| $N_{ex}$ | Total number of optically active molecules under irradiation which become excited (11). |
| $N_i$ | Positive-ion density (21). |
| $[N_j]$ | Concentration of species "j" (13). |
| $N^+$ | Positive-ion concentration (9). |
| $N_a^+$ | Density of atomic ions (9). |
| $N_{mi}^+$ | Density of molecular ions (9). |

$N^-$ Negative-ion concentration (9).

$n$ Species concentration (3).

Gas density (7).

Concentration of detaching neutral species (9).

Level of hydrogenic species into which recombination is taking place (11).

Density of absorbing gas (12).

= -b for certain recombination reactions (19).

Electron density (21).

Indexing uses: combining proportions (5, 6, 16, 17, 21, 24).
level of hydrogenic species (11).
final charge on initially neutral target species (15).
neutral species acting as third body (16).
electron noise (21).

$n_B$ Number density of target species (15).

$n_e$ Electron density (4, 5, 7, 8, 11, 16, 22).

$\langle n_e(t) \rangle$ Space-averaged electron density at time "t" (16).

$\langle n_e(0) \rangle$ Space-averaged electron density at zero time (16).

$n_e(\infty)$ Stationary electron density long after ionizing source is turned on (16).

$n_{eff}$ Number of electrons effectively available for ionization in the outer shell of projectile species, in the method of Fleischmann, Dehmel, and Lee (15).

$n_i$ Number density of species "i" (2, 20).

Ion density (11).

$n_i R_i$ Chemical removal rate of species "i" (2).

$n_j$ Number density of species "j" (3).

$n_j'$ Fluctuation of $n_j$ (3).

$\bar{n}_j$ Mean value of $n_j$ (3).

$n\ell$ A particular level into which radiative recombination is taking place (11).

Indexing use: level into which radiative recombination is taking place (11).

$n_{N_2}$ $N_2$ species density (24).

$n_o$ Loschmidt number (7, 12).

$n_s$ Density of stabilizing agent (16).

$n_{tot}$ Total species density (4).

n(X) Species density of "X" (4).

$n_1$ Vertical distribution of atomic-oxygen concentration (3).

$n_2$ Vertical distribution of molecular-oxygen concentration (3).

$n_+$ Positive-ion density (16).

$n_-$ Negative-ion density (16).

o Indexing uses: sea-level (2).
unperturbed-medium (3).
reference (3).
turbopause (4).
pre-magnetic storm (5).
pre-transmission (7).
resonant (7).
Loschmidt (7, 12).
standard-state (10).
band-origin (11).
atomic species (11).
incidence (12).
impact, in the Firsov model (15).
Bohr (15, 21).
collision-free (20).
free-space (21).
energy-independent (21).
pre-integration (21).

P — Designation on Page 18A-9, of work of Puckett and Teague, from Reference 18A-41 (18A).

P(b, u) — Probability for charge transfer on collision at impact parameter "b" and relative velocity "u" (15).

PCA — Designation for Polar Cap Absorption (5, 9).

$P_i$ — Rate of process "i" leading to electron production (16).

p — Pressure at altitude (2).

Pressure or partial pressure (3, 8, 10, 20, 21).

Indexing uses: pressure (2).
combining proportions (6).
projectile species (15).
plasma (21).
half-integer spacing (21).

p' — Pressure for small perturbation or fluctuation (3).

$\bar{p}$ — Mean pressure (3).

$p_a$ — Partial pressure for species "a" (3).

$p_{N_2}$ — Pressure of $N_2$ (20).

$p_o$ — Pressure for unperturbed background (3).

pop — Indexing use only; population (4).

$p_i$ — Pressure at reference altitude (2).

Q — Diffusional rate (3).

Characteristic Q-number of a resonant cavity (7).

Partition function (11).

Cross-section (15).

Capture cross-section (15).

Source term (21).

Indexing use: quenching (11).

$Q_a$ Net rate of radiative heat absorption by species "a" (3).

$Q_c$ Net rate of chemical energy evolution per unit mass (3).

$Q_m(\epsilon)$ Source term for electron momentum-transfer collisions (21).

$Q_n$ Specific slow-ion production cross-section (15).

$Q_R$ Net rate of radiant energy absorption per unit mass (3).

$Q_{rot}(X)$ Rotational partition function for a rigid rotator (4).

$Q_v$ Vibrational partition function (11).

$Q_{vib}(X)$ Vibrational partition function for a harmonic oscillator (4).

$Q(X)$ Partition function of (molecular)species "X" (4).

$Q_{ii}^{0n}$ Ionization cross-section (ambiguous term) where i = j (15).

$Q_{ij}^{0n}$ Cross-section for collisional charge exchange in heavy-particle collisions, where i = n+ j (15).

$Q_{10}^{01}$ Cross-section for collisional charge exchange where i = 1 (15).

$Q_+$ Total slow positive-charge production cross-section (15).

$Q_-$ Electron production cross-section (15).

$q$ Ion-pair production rate due to beta-particle ionization of air (5).

Electron production rate (9).

Bremsstrahlung radiation (11).

Electron source function (22).

Indexing use: quenching (9).

$\underset{\sim}{q}$ Total heat flux vector (3).

$\underset{\sim}{q}_a$ Heat flux carried by species "a" (3).

$q_o$ $\equiv \sum_j \sigma_{0j} \approx \sigma_{01}$ at low energies (15).

$q_{v'v''}$ Franck-Condon factor for electronic transition involving $v=v'$ in excited state and $v=v''$ in ground state (11).

R Gas constant (2, 3, 19).

Designation in Table 9-5, for resonance scattering process (9).

Interaction distance, in the method of Fleischmann, Dehmel, and Lee (15).

Internuclear separation (15).

Indexing uses: radiant energy (3).
chemical destruction (11).

Re Reynolds number (3).

Designation for real portion of function (21).

$Re\Delta K_i$ Real portion of $\Delta K_i$, in the low-frequency limit (21).

Ri Richardson number (3).

$R_i$ Chemical removal rate constant of species "i" (2).

$R_o$ Impact parameter, in the Firsov model (15).

Ryd Indexing use only; Rydberg (11).

$R_{\lambda\mu}$ Irradiance incident on volume element (11).

$R_{\lambda\mu e}$ Solar irradiance upon the atmosphere at center wavelength $\lambda_e$ of electronic transition (11).

r Radius of interaction (15).

Indexing uses: radiative recombination (8, 9).
recombination (16).
reference (16, 19).
reverse (18A).

$\underset{\sim}{r}$ Position vector measured from earth center (3).

Electron position vector, with respect to trajectory midpoint (15).

Indexing use: trajectory midpoint electron position vector (15).

| | |
|---|---|
| TID | Designation for Traveling Ionospheric Disturbance (3). |
| $T_{ion}$ | Ion-kinetic temperature (17). |
| $T_j$ | Effective temperature of species "j" (3). |
| $T_j'$ | Fluctuation of $T_j$ (3). |
| $\overline{T}_j$ | Mean value of $T_j$ (3). |
| $T_k$ | Kinetic temperature (4). |
| $T_{kin}$ | Kinetic temperature (11). |
| $T_M$ | Molecular-scale temperature (2). |
| TM | Indexing use only; normalization, in the method of Fleischmann, Dehmel, and Lee (15). |
| $T_n$ | Electron noise "temperature" (21). |
| TOF | Designation for Time-of-Flight (7). |
| $T_{pop}$ | Population temperature (4). |
| $T_r$ | Reference temperature (16, 19). |
| $T_{ref}$ | Reference temperature (24). |
| $T_{rot}$ | Rotational temperature (11). |
| $T_{tr}$ | Translational temperature (20). |
| $T_v$ | Vibrational temperature (4, 20, 24). |
| $T_{vib}$ | Vibrational temperature (11, 18A). |
| T-V | Designation for translational-vibrational energy transfer (11). |
| $T_+$ | Positive-ion temperature (16). |

$t$ Time (2, 3, 5, 11, 15, 16, 19, 20, 21).

Indexing uses: turbulent (2).
threshold (6).
target species (15).

th Indexing use only; thermal (3).

$t_o$ Initial time of integration (21).

tot Indexing use only; total (4).

tr Indexing use only; translational (20).

$U_e$ Potential energy of bound electron (15).

UHF Designation for Ultra High Frequency (7).

UV Designation for Ultraviolet.

$u$ Speed (3).

$\equiv 2.855\ \theta/\lambda$ (11).

Relative velocity (15).

Radial component of relative velocity on collision, in the Firsov model (15).

Indexing uses: relative velocity (15).
energy exchange (21).

$\bar{u}$ Mean mass velocity (2).

$\underset{\sim}{u}$ Velocity vector (3).

$\underset{\sim}{u}'$ Velocity vector for small perturbation or fluctuation (3).

$\underset{\sim}{\bar{u}}$ Mean velocity vector (3).

$\underset{\sim}{u}_a$ Velocity vector for species "a" (3).

$u_c$ Arhitrary reference velocity (3).

$u_i$ Mean velocity of species "i" (2).

Directional components of velocity (3).

$\bar{u}_i$ Mean directional components of velocity (3).

$u_o$ Ionizational impact velocity, in the Firsov model (15).

uv Designation for ultraviolet.

$u_1$ Vertical component of diffusion velocity of atomic oxygen (3).

$u_2$ Vertical component of diffusion velocity of molecular oxygen (3).

V Volume (10).

$V_a(r_a)$ Potential centered on trajectory point (15).

$V_b(r_b)$ Potential centered on trajectory point (15).

$V_i$ Diffusion velocity of species "i" (2).

VT Designation for vibrational-translational energy transfer (20).

V-T Designation for vibrational-translational energy transfer (11).

VV Designation for vibrational-vibrational energy transfer (20, 24).

V-V Designation for vibrational-vibrational energy transfer (11).

v Initial velocity (3).

Relative collisional velocity (6).

Vibrational level or quantum number (9, 11, 16, 20, 24).

Velocity (15, 21).

Indexing uses: constant volume (3).
vibrational (4, 11, 20, 24).

$\underset{\sim}{v}$ Velocity vector (15).

$\vec{v}$ Velocity vector (15).

v' Vibrational level in excited electronic state (11).

Vibrational level in unspecified electronic state (20).

| | |
|---|---|
| $v'v''$ | Indexing use only; electronic transition involving two states for which $v = v'$ and $v = v''$, respectively (11). |
| $v''$ | Vibrational level in ground electronic state (11). |
| | Vibrational level in unspecified electronic state (20). |
| $\bar{v}'$ | Mean number of vibrational quanta excited in ground electronic state through fluorescence (11). |
| $v_e$ | Velocity of bound electron on target atom (15). |
| $v'_e$ | Parameter defined in Equation 15-11 (15). |
| vib | Indexing use only; vibrational (4, 11, 18A). |
| $v_{max}$ | Maximum vibrational level (11). |
| vol | Indexing use only; volume (11). |
| $v_1$ | Velocity of incident ion (15). |
| $v'_j$ | Parameter defined in Equation 15-11 (15). |
| W | Designation for west (3). |
| | Designation for unspecified chemical species (6, 10). |
| WB | Designation in Figure 16-2, for work of Weller and Biondi, from Reference 16-24 (16). |
| W-K | Designation for Watson-Koontz system (9). |
| w | Electron drift velocity (21). |
| X | Designation for unspecified chemical species (6, 9, 10, 11, 14, 16, 17, 24). |
| | Indexing uses: chemical species (4, 8, 14).<br>functional (21). |
| [X] | Concentration of species "x" (11). |
| X' | Indexing use only; chemical species for product atom which may be in a bound excited state (8). |

$\sigma_0$ Absorption cross-section for $O_2$ at zero atmosphere pressure, by extrapolation (Herzberg continuum) (12).

$\sigma_{01}$ $\approx \sum_j \sigma_{0j}$ at low energies (15).

$\sigma_{0j}$ Electron stripping cross-section from neutrals (15).

$\sigma_1$ Absorption cross-section for $O_2$ at one atmosphere pressure (Herzberg continuum) (12).

$\sigma_{1m}$ Cross-section for stripping "m" electrons in $N^+$ up $\cdots$ $N_2$ impact (15).

$\sigma_{10}$ $\sigma_{10}^{01}$ in the low-energy limit (15).

$\tau$ Time for onset of turbulent dispersion (3).

Recovery time (9).

Relaxation time, or the e-folding time of $\epsilon$ (20).

$\tau_c$ Effective lifetime for collisional deexcitation (20).

$\tau_j(\Delta\lambda)$ Optical depth in wavelength range "$\Delta\lambda$" for species "j" (13).

$\tau_o$ Collision-free radiative lifetime of excited species (20).

$\tau(\Delta\lambda)$ Optical depth in wavelength range "$\Delta\lambda$" (13).

$\Phi$ Rayleigh dissipation function (3).

$\Phi_z(\Delta\lambda)$ Local photon flux in the wavelength range "$\Delta\lambda$" at altitude "z" (13).

$\Phi_\infty(\Delta\lambda)$ Photon flux in the wavelength range "$\Delta\lambda$" at the top of the atmosphere (13).

$\omega_i$ Turbulent mixing flux for species "i" (2).

$\phi$ Latitude (2, 3).

$\phi_i(\underset{\sim}{r}_a)$ Bound-state wavefunction for the charge state "i" at a trajectory point (15).

$\phi_i(\underset{\sim}{r}_a, \underset{\sim}{r})$ Wavefunction defined in Equation 15-18 (15).

$\phi_j(\underset{\sim}{r}_b)$ Bound-state wavefunction for the charge state "j" at a trajectory point (15).

$\phi_j(\underset{\sim}{r}_b, \underset{\sim}{r})$ Wavefunction defined in Equation 15-19 (15).

$\psi$ Total wavefunction (15).

$\Omega$ $\equiv \omega$ or $\omega \pm \omega_{be}$ or $\omega \pm \omega_{bi}$ (21).

$\underset{\sim}{\Omega}$ Angular velocity of earth's rotation (3).

$\omega$ Frequency (3).

Frequency of alternating electric field (7).

Angular frequency of applied electric field (21).

$\omega_a$ $\equiv c_o/2H$ (3).

$\omega_{be}$ Cyclotron frequency for electrons in a magnetic field (21).

$\omega_{bi}$ Cyclotron frequency for ions in a magnetic field (21).

$\omega_c$ Angular or cyclotron frequency of orbital motion (7).

$\omega_e$ Vibrational constant (4, 11).

$\omega_e x_e$ First anharmonic correction term (11).

$\omega_{pe}$ Plasma resonance frequency for electrons (21).

$\omega_s$ Wind shear (3).

Numbers used as indices:

0 Reference condition (3).

Temperature of 0 K (10, 19).

Zero atmosphere pressure (12).

Initial charge on neutral target species (15).

Zero time (16).

Functional (21).

| | |
|---|---|
| 01 | Excitation (11). |
| 1 | Reference condition (2). |
| | Atomic oxygen (3). |
| | Molecular (3). |
| | Vibrational level (10). |
| | One atmosphere pressure (12). |
| | Incident particles before collision (15). |
| | Cut-off (15). |
| | Stripping, in collision of $N^+$ on $N_2$ (15). |
| 10 | Deexcitation (11). |
| | Deactivation of first vibrational level (20). |
| 2 | Molecular oxygen (3). |
| | Turbulent (3). |
| | Vibrational level (10). |
| | Incident particles after collision (15). |
| | Number of electrons stripped, in collision of $N^+$ on $N_2$ (15). |
| | Two-body process (16). |
| | Functional (21). |
| 3 | Vibrational level (10). |
| | Number of electrons stripped, in collision of $N^+$ on $N_2$ (15). |
| | Three-body process (16). |
| 4 | Number of electrons stripped, in collision of $N^+$ on $N_2$ (15). |
| 300 | Temperature of 300 K (24). |

$\infty$ Top of atmosphere (13).

End of trajectory (15).

Designation of long time after ionizing source is turned on (16).

Miscellaneous symbols used as indices (where "X" is taken as an anonymous symbol modified by each index):

$X'$ Fluctuation or perturbation (3).

Miscellaneous (3).

Reverse (6).

Bound excited state (8).

Collisional (11).

Excited electronic state (11).

Ionization (13).

Secondary of a type (14).

Upper electronic state (14).

For special parameter (15).

Unspecified electronic state (20).

$X''$ Ground electronic state (11).

Lower electronic state (14).

Unspecified electronic state (20).

$\underset{\sim}{X}$ Vector (3, 15).

$\underset{\approx}{X}$ Tensor (3).

$\vec{X}$ Vector (15, 16).

$\overline{X}$ Mean (2, 3, 11, 21).

$\langle X \rangle$ Space-averaged (16, 21).

$\{X\}$ Variation (3, 16).

# APPENDIX F
# SPECIES INDEX

N. B. : The entries are listed by chapter and page. For instance, the designation 5-7, 8 indicates the presence of information on pages 7 and 8 of Chapter 5, and 5-(6-9) designates information on pages 6 through 9 of Chapter 5. In a few cases, a species is treated continuously throughout an entire chapter; when this occurs, the chapter number is given. Where information is contained in a figure or table, the figure number or table number is given separately from the chapter and page numbers, which are used only for textual reference. Certain tables are subdivided, e.g., 16-1 into 16-1.1, 16-1.2, etc., and 24-1 into Roman Numeral categories. These subdivisions are included in the designations, where applicable, for greater clarity. Entries are listed alphabetically by standard chemical symbol, with the added features that the invented symbol "Me" is used to indicate metallic species generally, and that "air", "air ions", "electron", and "teflon" are entered as words, in their proper alphabetical order. Electronically excited states are listed either as specific state designations (in alphabetical and numerical order) where these are known, or by the use of the asterisk (*) to indicate electronic excitation generally. Vibrationally excited states are designated by the double-dagger (‡). Unless otherwise noted, all species listed are gas-phase species. A few solids and liquids are included, and are appropriately designated as such, viz., by the respective standard indicators (s) and (ℓ).

Ag Figure 15-2.

$Ag^+$ Page 15-36.

| | |
|---|---|
| Air | Pages 3-5, 33; 5-18; 7-27, 29; 17-7; 21-4, 5, (7-9), (16-18), 25.<br>Tables 11-2; 16-1.2; 21-2, 4; 24-1 (VI).<br>Figures 7-8; 9-2, 3; 21-3, 5. |
| Air Ions | Pages 16-21, 23.<br>Tables 16-1.1; 24-1 (VI). |
| Al | Pages 5-13; 7-20; 15-1, 21, 29.<br>Figures 5-10; 15-1, 5. |
| $Al^+$ | Pages 15-6, 15, 31, 35, 39, 44, 45, 47; 16-18; 20-18.<br>Table 16-1.1.<br>Figure 15-4. |
| $Al(CH_3)_3$ | Page 5-19. |
| AlO | Pages 11-23, 25.<br>Table 11-1. |
| $AlO^*$ | Page 11-25. |
| Ar | Pages 2-(9-12); 4-1; 10-2; 11-27; 15-21, 25, 34, 36, 37, 43; 16-14, 16, 17, 24; 17-3; 18A-9; 19-8, 9, 12; 21-5, 24.<br>Tables 2-2, 4; 10-1, 10; 15-1; 18A-5; 20-2, 6, 8; 24-1 (XXVI).<br>Figures 2-7; 4-1; 10-10; 14-10; 15-1, 2, 5. |
| $Ar^*$ | Table 10-10. |
| $Ar^+$ | Pages 15-31, 43; 16-18.<br>Tables 10-1, 11; 16-1.1. |
| $Ar^{+*}$ | Table 10-11. |
| $Ar^{++}$ | Page 15-43.<br>Table 10-1. |
| $Ar^{3+}$ | Page 15-43. |
| $Ar^{4+}$ | Page 15-43. |
| $Ar^{5+}$ | Page 15-43. |

| | |
|---|---|
| $Cs^+$ | Pages 15-37, 41.<br>Table 20-10. |
| $D^-$ | Pages 16-22, 23.<br>Table 16-I.2. |
| $D_2$ | Page 16-24. |
| Electron | Chapters 17; 21.<br>Pages 4-6, 13; 5-(5-8), 19; 6-2, 3, (7-12), 14; 7-2, 4, 8, 11, 20, 23, 25, 27, 29; 8-(1-7), 10, 11; 9-1, 4, 6, (8-16), 30; 11-(25-33); 12-1, 5; 13-1; 15-1, (5-7), 20, 25, (29-47); 16-(1-21); 20-3, 5, 7, 8, 10, 11, (13-17); 22-2.<br>Tables 6-1; 8-(1-3); 9-1, 4; 12-1; 16-1.1; 18A-4; 20-7, 9, 10; 24-1 (I, II, III, IV, VII, VIII, IX, X, XI, XII, XXX).<br>Figures 4-3; 5-9; 7-6, 7; 9-1; 14-17; 16-(1-4); 20-(3-5), (7-9). |
| F | Page 17-18.<br>Table 17-7.<br>Figures 15-1, 2. |
| $F^+$ | Page 16-18.<br>Table 16-1.1. |
| Fe | Pages 11-20; 15-1, 21, 30; 20-7.<br>Table 18A-7.<br>Figures 15-1, 5. |
| $Fe^+$ | Pages 15-6, 15, 32, 35, 40, 44, 46, 47; 20-18.<br>Tables 18A-3, 5, 7; 24-1 (XIV).<br>Figures 15-3; 20-1. |
| FeO | Page 11-20.<br>Table 11-1. |
| $FeO^+$ | Tables 18A-3; 24-1 (XIV). |
| $FeO_2^+$ | Table 18A-5. |

| | |
|---|---|
| H | Pages 2-9, 12; 6-8; 7-7; 8-(6-8); 10-4; 11-15, 17; 15-1, 18, 19; 19-3, 12; 20-16.<br>Tables 6-1; 8-2; 9-1, 5, 6; 10-1, 2; 12-2; 18A-(1-4), 7; 19-1; 20-10; 24-1 (I, IV, XIII, XIV, XV, XXIV, XXV, XXVII).<br>Figures 2-7; 10-1, 10; 14-1, 3, 4, 17; 15-1, 2. |
| $H^*$ | Tables 10-2; 20-10.<br>Figure 10-1. |
| $H(3\,^2P)$ | Tables 9-5; 20-10. |
| $H(^2S)$ | Table 20-10. |
| $H^+$ | Pages 6-8; 7-17; 8-1, 8; 9-6, 8; 10-3; 16-18, 20, 22, 23.<br>Tables 8-1; 9-1; 10-1; 16-1.1, 1.2; 18A-1, 3, 7; 20-10; 24-1 (I, XIII).<br>Figures 14-3, 4, 64, 89; 16-4. |
| $H^-$ | Pages 7-17; 8-6, 7; 10-3; 16-22, 23; 17-2, 8.<br>Tables 10-1; 16-1.2; 17-3; 18A-2; 24-1 (XV).<br>Figures 10-9; 14-1, 16. |
| $HCO^+$ | See $CHO^+$ |
| $HNO_2$ | Page 18A-9.<br>Tables 18A-3, 4; 24-1 (XIV). |
| $HNO_3$ | Page 11-13.<br>Table 11-1. |
| $HO_2$ | Pages 2-9; 11-16; 19-12; 20-16.<br>Tables 11-1; 19-1; 24-1 (XII, XXIV, XXV, XXVII). |
| $HO_2^-$ | Page 17-2. |
| HS | Table 18A-2. |
| $HS^-$ | Table 18A-2. |

$H_2$ Pages 2-9; 10-2; 11-31, 33; 16-17, 18, 24; 17-4; 19-4, 12; 20-16.
Tables 9-5; 10-1, 19; 17-4; 18A-3; 20-10; 24-I (XII, XIV, XXV, XXVII).
Figures 10-8; 14-(12-20); I5-1, 2.

$H_2^{\ddagger}$ Table 20-10.

$H_2^+$ Page 16-18.
Tables 10-1, 19; 16-1.2.
Figures 14-13, 64, 89.

$H_2^{+\ddagger}$ Page 16-I8.

$H_2^-$ Page 17-9.

$H_2NO_2^+$ See $NO^+(H_2O)$.

$H_2NO_3^-$ See $NO_2^-(H_2O)$.

$H_2NO_4^-$ See $NO_3^-(H_2O)$.

$H_2O$ Pages 2-9; 4-15; 6-8; 9-11; 11-1, 11; 12-6, 29; 17-3, 4, 8, 12; 18A-2, 3, (8-10); 19-12; 20-15, 16; 21-5, 6, 8, 16, 18, 27, 28.
Tables 6-I; 10-1, 20; 11-1, 2; 12-2; 17-(3-5), 7; 18A-1. (3-7); 20-5, 6, 8, 10; 21-1, 2; 24-1 (IV, IX, XII, XIII, XIV, XVI, XVIII, XIX, XXI, XXIV, XXV, XXVII, XXX, XXXIII).
Figures 4-2, 8; 11-1; 12-17; 14-(62-65); 20-6; 21-1, 3, 5.

$H_2O^{\ddagger}$ Page 4-15.
Tables 10-20; 20-5; 24-1 (XXXIII).

$H_2O^+$ Tables 10-1, 20; 18A-1, 3, 7; 24-1 (XIII, XIV).
Figure 14-63.

$H_2O^{+\ddagger}$ Table 10-20.

$H_2O^-$ Page 17-9.

$H_2O_2$ Page 2-9.
Table 24-1 (XXIV, XXVII).

$H_2O_2^-$ See $O^-(H_2O)$.

$H_2O_3^+$ See $O_2^+(H_2O)$.

$H_2O_3^-$ See $O_2^-(H_2O)$.

$H_2O_4^-$ See $O_3^-(H_2O)$.

$H_2SO_4(\ell)$ Page 19-4.

$H_3O$ Table 18A-7.

$H_3O^+$ Pages 9-11; 16-17; 18A-8; 21-20.
Tables 16-1.1; 18A-3, 5, 7; 21-4; 24-1 (IV, XIV, XVIII, XIX).

$H_3O^+(H_2O)$ Pages 18A-8; 21-25.
Tables 16-1.1; 18A-3, 5; 21-4; 24-1 (IV, XIV, XVIII, XIX).

$H_3O^+(H_2O)_2$ Pages 16-17; 18A-9.
Tables 16-1.1; 18A-3, 5; 24-1 (IV, XIV, XVIII, XIX).

$H_3O^+(H_2O)_3$ Tables 16-1.1; 18A-5; 24-1 (IV, XVIII, XIX).

$H_3O^+(H_2O)_4$ Tables 16-1.1; 18A-5; 24-1 (IV, XVIII, XIX).

$H_3O^+(H_2O)_5$ Page 16-17.
Tables 16-1.1; 24-1 (IV).

$H_3O^+(H_2O)_n$ Pages 9-11; 16-17; 18A-8; 21-20.
Tables 16-1.1; 24-1 (IV, XVIII, XIX).

$H_3O^+(OH)$ Page 18A-8.
Tables 18A-3; 24-1 (IV, XIV, XIX).

$H_3O_2^-$ See $OH^-(H_2O)$.

$H_3PO_4(\ell)$ Page 19-4.

$H_4NO_3^+$ See $NO^+(H_2O)_2$.

$H_4O_2^+$ See $H_3O^+(OH)$.

| | |
|---|---|
| $H_4O_4^-$ | See $O_2^-(H_2O)_2$. |
| $H_5O_2^+$ | See $H_3O^+(H_2O)$. |
| $H_6NO_4^+$ | See $NO^+(H_2O)_3$. |
| $H_6O_5^-$ | See $O_2^-(H_2O)_3$. |
| $H_7O_3^+$ | See $H_3O^+(H_2O)_2$. |
| $H_8O_6^-$ | See $O_2^-(H_2O)_4$. |
| $H_9O_4^+$ | See $H_3O^+(H_2O)_3$. |
| $H_{10}O_7^-$ | See $O_2^-(H_2O)_5$. |
| $H_{11}O_5^+$ | See $H_3O^+(H_2O)_4$. |
| $H_{13}O_6^+$ | See $H_3O^+(H_2O)_5$. |
| $H_{2n}NO_{n+3}^-$ | See $NO_3^-(H_2O)_n$. |
| $H_{2n}O_{n+2}^-$ | See $O_2^-(H_2O)_n$. |
| $H_{2n+3}O_{n+1}^+$ | See $H_3O^+(H_2O)_n$. |
| He | Pages 2-(9-12); 4-1; 7-4, 10, 23; 8-4; 11-33; 15-1; 16-12, 14, 15, 17, 20, 21, 24; 18A-4, 7, 9; 19-12; 20-15; 21-17.<br>Tables 2-2, 4; 8-2; 9-1, 3, 5; 12-2; 16-1.1, 1.2; 18A-1, 5, 6; 20-8, 10; 21-3; 24-1 (XVIII, XXI).<br>Figures 2-7; 4-1; 7-3, 6; 15-1, 2; 21-4. |
| $He^*$ | Table 20-10. |
| $He(^3P)$ | Table 9-5. |
| $He(2\,^1S)$ | Table 20-10. |
| $He(^3S)$ | Tables 9-5; 20-10. |
| $He^+$ | Pages 8-3; 15-45, 46; 16-18, 20, 22, 23; 18A-3, 4.<br>Tables 9-1, 3, 5; 16-1.1; 18A-1; 20-10. |

| | |
|---|---|
| $He_2^+$ | Page 16-20.<br>Tables 16-1.1; 18A-1. |
| Hg | Page 20-7. |
| I | Pages 15-21; 19-3.<br>Table 18A-2.<br>Figures 15-5, 7. |
| $I^+$ | Pages 15-37, 41.<br>Table 15-1. |
| $I^-$ | Page 16-21.<br>Tables 16-1.2; 18A-2. |
| $I_2$ | Page 16-21. |
| $I_2^+$ | Page 16-21.<br>Table 16-1.2. |
| K | Pages 15-21, 29.<br>Table 8-2.<br>Figures 15-2, 5, 8. |
| $K^*$ | Table 9-5. |
| $K^+$ | Pages 15-32, 35, 40; 16-18.<br>Tables 15-1; 16-1.1; 18A-3, 5. |
| $K^+(CO_2)$ | Table 18A-5. |
| $KO^+$ | Table 18A-3. |
| Kr | Pages 15-30; 16-24.<br>Table 20-8.<br>Figures 15-1, 2. |
| $Kr^+$ | Pages 15-32, 36, 40. |
| Li | Page 15-1.<br>Table 8-2.<br>Figures 15-1, 2. |
| $Li^*$ | Table 9-5. |

$N_2$

Pages 2-(9-12); 4-1, 8, 13; 6-8, 14, 15; 8-11, 12; 9-4, 12, 13, 31; 10-2, 4; 11-13, 14, 18, 27, 32; 12-6, 16, 17, 30; 13-(1-4); 14-1; 15-1, 21, 22, 25, (34-38); 16-8, 10, 22, 24; 17-3, 5, 8; 18A-(3-5), 7, 9; 19-4, (7-10), (12-14); 20-(3-10), 13, (15-17); 21-4, 5, 8, 15, 20, 25, 26, 28, 31; 22-1.

Tables 2-2, 4; 9-2, 3, 6, 7; 10-1, 13; 11-2; 12-(2-4), 6a, 6b; 13-1, 2, 4, 6; 14-(1-3); 15-1; 16-1.2; 17-(4-6); 18A-1, (3-7); 19-1; 20-1, 2, (4-6), (8-10); 21-(1-4); 24-1 (I, II, IV, IX, X, XII, XIII, XIV, XVI, XVIII, XXI, XXIII, XXIV, XXV, XXVI, XXVII, XXVIII, XXX, XXXII, XXXIII).

Figures 2-7; 4-1, 4, 8; 10-5, 8, 11; 12-7; 14-(29-41); 15-1, 2, (6-9); 20-1, 3, 4, 6; 21-1, 3, 4.

$N_2^{\ddagger}$

Pages 4-13; 5-17; 6-7; 11-14, 34; 19-7, 14; 20-(3-6); 21-4; 22-1.

Tables 9-6; 20-2, 3, 10; 24-1 (XXVII, XXXII, XXXIII).

Figures 10-5; 20-1, 3, 4.

$N_2^{*}$

Pages 20-3, (6-8).

Tables 10-13; 20-1, 10.

Figures 10-5; 20-1.

$N_2(a\,^1\Pi_g)$

Tables 9-5, 6; 10-13; 20-1, 10.

Figure 10-5.

$N_2(a\,^1\Pi_g)^{\ddagger}$

Table 20-10.

$N_2(a'\,^1\Sigma_u^-)$

Tables 10-13; 20-1.

Figure 10-5.

$N_2(A\,^3\Sigma_u^+)$

Pages 6-15; 20-3, (6-8).

Tables 9-6, 7; 10-13; 20-1, 4, 10; 24-1 (XXVIII, XXX).

Figures 10-5; 20-1.

$N_2(A\,^3\Sigma_u^+)^{\ddagger}$

Pages 20-3, 7.

Figure 20-1.

$N_2(b'\,^1\Sigma_u^+)$

Figure 10-5.

$N_2(B\ ^3\Pi_g)$ Pages 6-15; 20-6, 7.
Tables 9-5, 6; 10-13; 20-1, 10; 24-1 (XXV).
Figures 10-5; 20-1.

$N_2(B\ ^3\Pi_g)^{\ddagger}$ Figure 20-1.

$N_2(B'\ ^3\Sigma_u^-)$ Page 20-7.
Tables 9-5; 10-13; 20-1.
Figure 10-5.

$N_2(C\ ^3\Pi_u)$ Pages 20-6, 7.
Tables 9-5, 6; 20-10.
Figure 10-5.

$N_2(C\ ^3\Pi_u)^{\ddagger}$ Table 20-10.

$N_2(C'\ ^3\Pi_u)$ Figure 10-5.

$N_2(D\ ^3\Sigma_u^+)$ Page 20-7.

$N_2(E\ ^3\Sigma_g^+)$ Page 20-7.
Figure 10-5.

$N_2(h\ ^1\Sigma_u^+)$ Tables 9-6; 12-6a.

$N_2(w\ ^1\Delta_u)$ Tables 10-13; 20-1.
Figure 10-5.

$N_2(W\ ^3\Delta_u)$ Page 20-7.
Tables 10-13; 20-1.

$N_2(^1\Pi_u)$ Tables 12-6a, 6b.

$N_2(^5\Pi_u)$ Figure 10-5.

$N_2^+$ Pages 6-15; 8-12; 9-4, 11, 21, 31; 13-1, 3, 4; 14-1; 15-5, 43; 16-7, 8, 10, 18, 22; 18A-(4-7); 20-(6-10), 15, 17; 21-20.
Tables 9-2, 3, 6; 10-1, 14; 13-3, 5, 7; 14-1, 2; 16-1.1, 1.2; 18A-1, 3, 5, 7; 20-1, 9, 10; 21-4; 24-1 (I, II, IV, V, XIII, XIV, XVII, XXX).
Figures 10-5; 12-7; 14-(30-37), 90; 16-1; 20-2.

| | |
|---|---|
| $N_3^+$ | Pages 16-7, 8, 10; 20-9.<br>Tables I8A-3; 21-4; 24-1 (IV, XIV, XVIII). |
| $N_4^+$ | Pages I6-7, 10, 16; I8A-7.<br>Tables I6-1.1; 18A-1, 3, 5; 21-4; 24-1 (IV, XIV, XVIII).<br>Figure 16-1. |
| Na | Pages 5-19; 18A-3, 6; 20-7.<br>Tables 8-2; 9-6; 18A-I, 3, 7; 20-10; 24-I (XIII, XIV).<br>Figures I5-2; 20-I. |
| $Na^*$ | Tables 9-5; 20-I, I0. |
| $Na^+$ | Pages 16-18, 23; I8A-6; 20-18.<br>Tables 16-I.1; 18A-I, 3, 5, 7; 24-1 (XIII).<br>Figure 20-1. |
| $Na^+(CO_2)$ | Table I8A-5. |
| $Na^+(CO_2)_2$ | Table I8A-5. |
| $NaO^+$ | Tables I8A-3; 24-1 (XIV). |
| Ne | Pages 15-25, 43, 44; 16-8, I0, 11, 14, 16, 24.<br>Tables 8-2; 15-I.<br>Figures I5-1, 2. |
| $Ne^*$ | Page 16-8. |
| $Ne^+$ | Pages 15-34, 39, 43; 16-18.<br>Table 16-1.1. |
| $Ne^{++}$ | Page 15-43. |
| $Ne^{3+}$ | Page 15-43. |
| $Ne^{4+}$ | Page 15-43. |
| $Ne^{5+}$ | Page 15-43. |
| $Ne_2^+$ | Page 16-16. |

| | |
|---|---|
| O | Pages 2-(9-12); 3-33, 34; 4-13, 15; 5-18; 6-2, 8, 12, 14, 15; 7-7; 8-7, 8, 10, 11; 9-12, 13, 15, 30, 31; 10-4; 11-13, (16-20), 31, 32; 12-6, (8-23), 30; 13-1, 3, 4; 15-1, 6, 15, 25, (29-33); 16-10, 11, 16; 17-2, 6, 9, 12, 14; 18A-5, 6, 8; 19-(2-14); 20-3, 6, 7, (10-12), (14-18); 21-6, 16, 20, 25, 29.<br>Tables 2-2, 4; 6-1; 8-2; 9-(2-6); 10-1, 8; 12-(1-5), 7a, 7b, 8a, 8b; 13-1, 2, 4, 6; 15-2; 17-(1-4), 6, 7; 18A-(1-4), 6, 7; 19-1; 20-1, 2, (4-7), 9, 10; 21-(1-4); 24-1 (I, II, IV, V, VII, VIII, IX, X, XI, XII, XIII, XIV, XV, XVI, XVIII, XXIII, XXIV, XXV, XXVI, XXVII, XXVIII, XXX, XXXII).<br>Figures 2-7; 4-1, 7; 10-3, 6, 7, 10; 12-(8-10); 14-2, (7-9); 15-(1-4); 20-1, 4, 6, 9; 21-1, 4. |
| $O^*$ | Pages 12-(17-23).<br>Tables 10-8; 12-5; 20-1, 7, 10.<br>Figures 10-3; 12-8, 9; 20-1, 9. |
| $O(^1D)$ | Pages 4-13; 5-17, 18; 6-15; 8-10; 12-9, 21, 27, 28; 16-16; 19-14; 20-3, 4, 12, (14-16); 22-1.<br>Tables 9-(5-7); 12-3, 5, 7a, 7b; 20-1, 7, 8, 10; 24-1 (IV, XXIV, XXVII, XXVIII, XXX).<br>Figures 4-2, 4, 5; 10-6, 7, 10; 20-1, 9. |
| $O(4\,^3P)$ | Table 9-5. |
| $O(^5P)$ | Table 9-6. |
| $O(^1S)$ | Pages 5-18; 8-10; 9-31; 12-21; 16-16; 19-14; 20-4, 14, 15.<br>Tables 9-(5-7); 12-7a, 7b; 20-1, 7, 10; 24-1 (IV, XXV, XXVIII, XXX).<br>Figures 10-6, 7; 12-10; 20-1, 9. |
| $O(^3S)$ | Tables 9-5, 6; 20-1. |
| $O(^5S)$ | Tables 9-5, 6; 20-1.<br>Figure 20-1. |
| $O^+$ | Pages 4-6; 6-7, 14, 15; 8-2, 8; 9-(11-13), 15; 10-4; 12-14, 21; 13-3, 4; 15-31, 34, 39, (43-45), 47; 16-18, 22, 23; 18A-5; 20-5, 11, (15-17). |

$O^+$ (Cont'd.) Tables 9-2, 3, 5, 6; 10-1, 9; I2-I, 7b, 8a, 8b; 13-3, 5, ', 16-I.I, I.2; 18A-1, 3, 5, 7; 20-1, 3; 21-4; 24-I (I, II, V, XIII, XIV, XVIII, XXVIII, XXX).

Figures 4-3, 4; 10-4, 6, 7; 12-8, I0, I1; 14-8, 64, 73, 74; 20-2, 4.

$O^{+*}$ Pages 12-20, 21; 20-(I5-I7).
Tables 10-9; 20-1.
Figures I0-4; I2-(8-II); 20-2.

$O^+(^2D)$ Pages 6-15; I2-20; 20-8, (16-18).
Tables 9-3, 6; 12-8a, 8b; 20-I, 9, I0; 24-I (II, XIII, XXVIII, XXX).
Figures 10-7; 12-8, 9, 11; I4-73; 20-2.

$O^+(^2P)$ Pages 12-21; 20-I6, 17.
Tables 9-6; 12-8a, 8b; 20-1; 24-1 (II, XXVIII).
Figures 12-(9-11).

$O^+(^4P)$ Figure I4-74.

$O^{++}$ Page I5-43.
Tables 10-1; 12-I.

$O^{3+}$ Page 15-43.

$O^-$ Pages 5-7; 6-12, 14; 8-7; 9-I5, 30; I0-3; I1-25; 16-22, 23; 17-2, 4, 5, 8, 9, 12, I3; I8A-3; 20-II, 13.
Tables I0-1, 7; 16-I.2; I7-(1-4). 6, 7; 18A-2, 4, 6; 20-I0; 24-1 (V, VII, VIII, IX, X, XI, XII, XV, XVI, XX, XXI).
Figures 10-6, 7, 9; 14-2.

$O^{-*}$ Table I0-7.

$O^-(CO_2)$ See $CO_3^-$.

$O^-(H_2O)$ Tables 18A-6; 24-1 (XXI).

OCS Page 19-6.

| | |
|---|---|
| OH | Pages 2-9; 7-7; 11-1, 16, 17; 17-2; 18A-8; 19-3, 12; 20-16; 21-6.<br>Tables 6-1; 10-1, 19; 11-1; 17-(1-3); 18A-(1-3); 19-1; 20-10; 24-1 (VII, VIII, XIII, XIV, XV, XIX) XXIV, XXV, XXVII).<br>Figure 4-6. |
| $OH^{\ddagger}$ | Pages 11-(15-17).<br>Tables 9-5; 20-10. |
| $OH^{*}$ | Page 12-29.<br>Tables 10-19; 20-10. |
| $OH^{+}$ | Tables 10-I, 19; 18A-1, 3; 24-1 (XIII, XIV).<br>Figure 14-64. |
| $OH^{+*}$ | Table 10-19. |
| $OH^{-}$ | Page 17-2.<br>Tables 10-1, 19; 17-1, 2, 7; 18A-2, 4; 24-1 (VII, VIII, XII, XV). |
| $OH^{-}(H_2O)$ | Table 17-7. |
| $OONO^{-}$<br>(Cf. $NO_3^{-}$) | Page 18A-7.<br>Tables 18A-4; 24-1 (XVI). |
| $O_2$ | Pages 2-(9-12); 3-33, 38; 4-1, 6, 8, 10, 15; 5-19; 6-2, 8, 12, 14, 15; 8-11; 9-12, 15, 30; 10-2, 4; 11-(13-20), 27, 32, 33; 12-(6-16), 20, 27, 28, 30; 13-1, 3, 4; 15-1, 21, 34, 36, (39-43), 46, 47; 16-14, 15, 17, 22, 23; 17-2, 4, (6-8), 12, 14, 17; 18A-(5-9); 19-(4-6), (8-14); 20-6, (9-18); 21-4, 5, 8, 16, 20, 25, 27, 28.<br>Tables 2-2, 4; 9-2, 4, 6, 7; 10-1, 17; 11-2; 12-(1-4), 7a, 7b; 13-1, 2, 4, 6; 15-1; 16-1.2; 17-(1-7); 18A-(1-7); 19-1; 20-1, 2, (4-6), (8-10); 21-(1-4); 24-1 (I, II, IV, VII, VIII, IX, X, XI, XII, XIII, XIV, XV, XVI, XVIII, XIX, XX, XXI, XXII, XXIII, XXIV, XXV, XXVI, XXVII, XXVIII, XXIX, XXX, XXXII, XXXIII).<br>Figures 2-7; 3-7; 4-1, 4, (6-8); 10-7, 8, 11; 11-(8-10); 12-(1-6); 14-(45-61); 15-1, 2, (6-8); 20-1, 4 (6-o); 21-1, 3, 4. |

$O_2^+(H_2O)$ Page 18A-8.
Tables 18A-3, 5; 24-1 (IV, XIV, XVIII).

$O_2^+(N_2)$ Tables 18A-3, 5; 24-1 (XIV, XVIII).

$O_2^+(N_2O)$ Table 18A-5.

$O_2^+(O_2)$ See $O_4^+$.

$O_2^{++}$ Table 10-1.

$O_2^-$ Pages 5-7; 6-12; 9-30; 16-22; 17-2, 4, (7-9), (12-14); 18A-3, 7; 20-13.
Tables 9-4; 10-1, 19; 12-1; 16-1.2; 17-1, 2, (4-7); 18A-2, 4, 6; 20-10; 21-4; 24-1 (V, VII, VIII, IX, X, XI, XII, XV, XVI, XXI, XXII).
Figures 10-7, 9.

$O_2^-(CO_2)$ See $CO_4^-$.

$O_2^-(H_2O)$ Pages 17-2, 9, 17.
Tables 17-7; 18A-4, 6; 24-1 (XVI, XXI).

$O_2^-(H_2O)_2$ Tables 17-7; 18A-6; 24-1 (XXI).

$O_2^-(H_2O)_3$ Table 17-7.

$O_2^-(H_2C)_4$ Table 17-7.

$O_2^-(H_2O)_5$ Table 17-7.

$O_2^-(H_2O)_n$ Page 17-16.

$O_2^-(N_2)$ Tables 18A-6; 24-1 (XXI).

$O_2^-(O_2)$ See $O_4^-$.

$O_3$ Pages 2-9-12); 4-15; 5-18; 6-2, 12; 9-30; 11-1, 11, 15, 17, 19; 12-6, 24, 27; 17-2, 4, 9, 12; 18A-6, 8; 19-2, (4-8), 14; 20-12, 13; 21-17.
Tables 2-2; 10-1, 20; 11-1; 12-2; 17-(1-4), 7; 18A-(2-4); 19-1; 20-6, 10; 21-2; 24-1 (VII, VIII, XI, XII, XIV, XV, XVI, XXIV, XXV, XXVI, XXVII, XXX).
Figures 2-7; 4-2, 7, 8; 11-1, 2; 12-14, 15; 21-3.

| | |
|---|---|
| $O_3^{\ddagger}$ | Page 11-19.<br>Table 10-20. |
| $O_3^{+}$ | Page 16-14.<br>Tables 10-1, 20; 24-1 (XVIII). |
| $O_3^{+\ddagger}$ | Table 10-20. |
| $O_3^{-}$ | Pages 17-2, 9, 12.<br>Tables 10-1, 20; 17-1, 2, 4, 7; 18A-2, 4, 6; 21-4; 24-1 (VII, VIII, XII, XV, XVI, XX, XXI). |
| $O_3^{-\ddagger}$ | Table 10-20. |
| $O_3^{-}(H_2O)$ | Tables 18A-6; 24-1 (XXI). |
| $O_4^{*}$ | Page 20-13. |
| $O_4^{+}$ | Pages 16-14, 16; 18A-(6-8).<br>Tables 16-1.1; 18A-3, 5; 21-4; 24-1 (IV, XIV, XVIII, XIX). |
| $O_4^{-}$ | Pages 17-9, 14, 17; 18A-7.<br>Tables 17-7; 18A-4, 6; 21-4; 24-1 (XVI, XXI, XXII). |
| $P^{+}$ | Page 16-18.<br>Table 16-1.1. |
| $PH_2^{-}$ | Page 7-9. |
| Pt | Page 7-22. |
| $Rb^{+}$ | Page 15-36. |
| $S^{+}$ | Page 16-18.<br>Table 16-1.1. |
| $SF_5^{-}$ | Page 17-18.<br>Table 17-7. |
| $SF_6$ | Pages 17-17, 18.<br>Table 17-7. |

Aubrey, B. B.: 21-7

Awajobi, O. A.: 9-34

Axworthy, A. E., Jr.: 19-4

Bachynski, M. P.: 21-10

Badger, R. M.: 20-32

Bahr, J. L.: 12-88

Baiamonte, V.: 6-17

Bailey, A. D.: 9-19, 27; 17-10; 20-203; 21-61

Bailey, D. K.: 9-22

Bailey, T. L.: 17-25

Bailey, V. A.: 21-16

Bair, E.: 6-17

Baisley, V. C.: 12-72

Baker, A. D.: 7-78

Baker, C.: 7-78

Baker, D. M.: 3-33; 20-166

Baker, K.: 20-166

Baldeschwieler, J. D.: 7-22

Baldwin, R. R.: 19-33

Bamford, C. H.: 11-18 (Ed.)

Banks, P.: 21-70

Bardsley, J. N.: 8-15, 21, 61, 64; 11-66; 16-28; 17-39, 60

Barrow, R. F.: 10-32

Barth, C. A.: 9-74, 92; 19-35; 20-69

Basco, N.: 20-217

Bates, D. R.: 4-4 (Ed.); 7-9 (Ed.), 57 (Ed.), 89 (Ed.); 8-1, 4, 6, 7, 8, 9, 10, 12, 14, 16, 17, 25, 26, 30; 9-25; 11-68, 69; 15-2 (Ed.), 4, 19, 20 (Ed.), 32; 16-42 (Ed.), 43; 17-21; 20-4, 43, 76, 235

Bauer, E.: 3 (Author) -2, 44; 4 (Author) -14, 15; 20-6, 7, 55, 56, 80, 143, 222, 232

Baulch, D. L.: 15-54; 24-16, 35, 32

Baum, C. E.: 21-58

Baurer, T.: 1 (Author); 6 (Author); 19-37; 23 (Author); 24 (Author)

Bayes, K.: 20-155

Beaty, E. C.: 10-36; 17-5, 44, 45; 21-41; 24-3

Beauchamp, J. L.: 7-20, 21; 21-74

Becker, R. A.: 7-70; 12-42

Bederson, B.: 7-2 (Ed.), 58 (Ed.); 21-7

Bekefi, G.: 21-45

Bell, G.: 15-13

Belles, F. E.: 20-236

Belon, A. E.: 9-11

Belrose, J. S.: 5-14; 9-95; 21-29

Belyaev, V. A.: 7-61

Benesch, W.: 10-52; 20-19

Bennett, R. A.: 17-40, 62

Bennett, W. R.: 20-46 (Ed.)

Benson, S. W.: 19-4

Berkowitz, J.: 7-85; 17-58

Berlande, J.: 16-47

Berning, W. W.: 9-53

Bernstein, R.: 20-220

Berry, R. E.: 16-40

Berry, R. S.: 7-64; 8-75; 10-14, 43; 16-62

Bethe, H. A.: 11-44

Bethke, G. W.: 12-15

Beyer, R. A.: 18-65, 66

Beynon, W. J. G.: 9-58 (Ed.), 62 (Ed.)

Copy No. _____

DNA 1948H
(Formerly DASA 1948)

DEFENSE NUCLEAR AGENCY

# REACTION RATE HANDBOOK
## SECOND EDITION

Editors-in-Chief:
Dr. M.H. Bartner
Dr. T. Bourer

MARCH 1972

Project Officer: Dr. C.A. Blank

*APPROVED FOR PUBLIC RELEASE; DISTRIBUTION UNLIMITED*

Organized by General Electric Space Sciences Laboratory
for Defense Nuclear Agency Under Contracts
DASA 01-70-C-0082 and DASA 01-71-C-0145

This effort supported by Defense Nuclear Agency
NWED Subtask Code HD028, Work Unit 11

Published by DASIAC
DoD Nuclear Information and Analysis Center
General Electric, TEMPO
Santa Barbara, California

DDC
RECEIVED
JUL 27 1973
B

RECORD OF REVISIONS

| Revision No. | Date of Issue | Date of Receipt | Entered By |
|---|---|---|---|
| | | | |



Preceding page blank

# FOREWORD
# TO THE SECOND EDITION

The original DASA Reaction Rate Handbook was prepared as an aid to those associated in various ways with the DASA (now DNA) Reaction Rate Program, including those who direct and coordinate the program, those who provide the basic data, and those who use these data to calculate the phenomenological effects of perturbing influences in the atmosphere, and to predict therefrom the resultant variations in atmospheric chemistry and electromagnetic transmission. At the time of its original publication, a need was foreseen for periodic updating of the Handbook contents, in order to permit such calculations to be carried out with accuracy and precision commensurate with the most advanced information available. In the recent past, the quality and quantity of candidate revisions and additions to the Handbook have reached the level where it is now obvious that the needs of the interested scientific communities would be best served by the publication of a Second Edition of the Handbook incorporating many new areas of coverage not previously included.

Hence, the present publication represents a major revision of what is now the DNA Reaction Rate Handbook. Data obtained since the dissemination and an earlier updating of the First Edition are included, both replacing and adding to the original contents. Much of the information newly incorporated into many of the older chapters has been suggested for inclusion by data users interested in enhancing, thereby, the ultilitarian value of the Handbook. In addition, an attempt has been made to render the overall coverage more complete than it had been previously, by including several new chapters encompassing subject matter which, while closely related to the more traditional material, had been omitted in the First Edition. As before, further revisions may be anticipated from time to time, and suggestions for improvements will continue to be welcomed by the DNA project officer, Dr. C. A. Blank.



Preceding page blank

# FOREWORD
# TO THE FIRST EDITION

Several years ago the Defense Atomic Support Agency initiated a concerted effort to explore the effects upon the upper atmosphere arising from high-altitude nuclear detonations. As a result of this endeavor, it was ascertained that rather profound effects upon atmospheric physical and chemical processes can occur, leading to extensive degradation of the performance of military radar and communication systems. (This situation is discussed in detail in Chapter 10 of the unclassified publication, The Effects of Nuclear Weapons, S. Glasstone, ed., U. S. Government Printing Office, 1962.) In seeking to obtain a more complete and thorough understanding of the fundamental scientific nature and problems of the upper atmosphere which underlie such military problem areas, a comprehensive reaction rate program comprising theoretical, laboratory and field measurement studies was undertaken in 1961. One of the long-range objectives established early in this program was the future publication of a DASA-sponsored handbook containing certain useful, accurate, and reliable information on upper atmospheric chemical and physical processes. Such information is required for the solution of various problems involving military radar and communication blackout. The publication of this first edition of such a handbook thus represents fulfillment of that goal. Periodic additions to, and revisions of this handbook are planned to accommodate new information, revision of older data, corrections, etc. Suggestions for improving the nature and utility of this document are most welcome and should be directed to the indicated DASA Project Officer.



Preceding page blank

# ACKNOWLEDGMENTS

In an undertaking of the magnitude of this one, that is, the preparation and publication of a Revised Edition of the DNA Reaction Rate Handbook, where virtually the entire DNA-oriented scientific community has become involved at one level or another, it is a virtual impossibility to acknowledge each and every individual contribution. Therefore, the lists of those to whom appreciation is explicitly expressed, below, are necessarily limited to those whose efforts have seemed most noteworthy. This in no way detracts from the value of those lesser contributions which cannot be recorded here.

In order to give the maximum amount of credit in the minimum amount of space, each name is listed only once (alphabetically according to institutional affiliation), and is followed by a group of code letters and numbers designating the qualitative and quantitative aspects of the person's efforts in behalf of the Handbook. Thus the code letter "A" followed by one or more numbers indicates authorship or co-authorship of the chapters so numbered. The letter "C" denotes consultative or other contributory aid to the authors of the chapters designated. The letter "R" means that a person acted as a reviewer of the indicated chapters. The letter "E" followed by numbers 1 and/or 2 in parentheses shows that a person served on the first and/or second of two sessions of the Handbook Editorial Advisory Committee, held in Washington, D. C. during the spring of 1971. The letters "S" and "P", respectively, designate those who have been instrumental in providing support for the Handbook project, and the person under whose direction the actual publication has been carried out.

As suggested above, this listing still omits from mention the virtual army of typists, copyists, conveyors of casual suggestions, photographers, artists, "personal communicators" appropriately referenced elsewhere, librarians, and probably several other cate-



Preceding page blank

gories of helpers, without whose combined output the majority of those listed below might never have got their own efforts off the ground.

Air Force Cambridge Research Laboratories, Hanscom Field, Bedford, Massachusetts:

K. S. W. Champion: A-2; C-5, 13; R-8, 9; E (1, 2).

F. P. DelGreco: A-11; E (2).

J. D. George: A-13.

R. E. Good: R-3.

R. E. Huffman: A-12, 13; C-5; R-7; E (2).

T. J Keneshea: A-13.

J. P. Kennealy: A-11.

R. S. Narcisi: C-5.

R. O'Neil: C-4.

J. F. Paulson: A-7; R-24; E (2).

R. A. Schweinfurth: A-2.

S. P. Zimmerman: R-3.

Air Force Weapons Laboratory, Kirtland Air Force Base, New Mexico:

G. H. Canavan: C-22.

J. S. Greene, Jr.: A-15; E (2).

S. D. Rockwood: A-22; E (2).

W. A. Whitaker: C-15, 22.

Ballistic Research Laboratories, Aberdeen Proving Ground, Maryland:

F. W. Niles: A-22, C-10; R-16, 17, 18A, 19, 24; E (1, 2).

Bishop College, Dallas, Texas:

B. Gottlieb: C-4.

College of the City of New York, New York, New York:

C. M. Tchen: A-3.

Defense Nuclear Agency, Washington, District of Columbia:

W. W. Berning: S.

C. A. Blank: A-1, 23; R-24; E (1, 2); S.

J. D. Brown: S.

H. C. Fitz, Jr.: S.

G. R. Und-hill: S.

Dewey Electronics Corporation, New York, New York:

M. N. Hirsh: C-7.

GCA Corporation, Bedford, Massachusetts:

A. Dalgarno: A-8; C-15.

H. Miranda: C-8.

G. Victor: C-8; E (2).

General Electric Company, Space Sciences Laboratory, King of Prussia, Pennsylvania:

T. Baurer: A-1, 6, 23, 24; C-11, 15; E (1, 2).

M. H. Bortner: A-1, 4, 6, 23, 24; R-2, 3, 14; E (1, 2).

I. M. Pikus: A-15.

General Electric Company, TEMPO, Santa Barbara, California:

A. A. Feryok: E (2); P.

W. S. Knapp: A-5, 22; E (2).

Gulf Energy and Environmental Systems Company, San Diego, California:

J. K. Layton: A-7.

J. W. McGowan (formerly): A-20

R. H. Neynaber: A-7.

B. R. Turner (formerly): C-7.

D. A. Vroom: A-7.

Institute for Defense Analyses, Arlington, Virginia:

E. Bauer: A-3, 4; E (2).

P. A. Selwyn: A-3.

Joint Institute for Laboratory Astrophysics, University of Colorado, Boulder, Colorado:

G. E. Chamberlain: A-14.

L. J. Kieffer: A-14.

A. V. Phelps: A-17, 21; R-24.

Lockheed Palo Alto Research Laboratories, Palo Alto, California:

J. E. Evans: A-9.

R. C. Gunton: A-9.

E. G. Joki: A-9.

R. D. Sears: R-3, 6, 11, 15, 21, 23; E (1, 2).

Mission Research Corporation, Santa Barbara, California:

D. H. Archer: A-5.

P. G. Fischer: R-15.

D. Sappenfield: C-15.

M. Scheibe: E (1).

D. H. Sowle: R-15.

National Aeronautics and Space Administration, Ames Research Center, Moffett Naval Air Station, California:

I. G. Poppoff: A-9.

R. C. Whitten: A-9.

National Bureau of Standards, Gaithersburg, Maryland:

J. W. Cooper: C-11.

National Oceanic and Atmospheric Administration, Boulder, Colorado:

E. E. Ferguson: A-18A; R-7, 24; E (2).

G. C. Reid: C-23.

Naval Research Laboratories, Washington, District of Columbia:

A. W. Ali: A-15; R-6, 13, 20; E (1, 2).

C. Y. Johnson: C-2.

R & D Associates, Santa Monica, California:

F. R. Gilmore: A-1, 10, 20; C-8, 11; R-3, 4, 6, 11, 23; E (1, 2).

Science Applications, Inc., La Jolla, California:

D. A. Hamlin: C-15; R-15.

Southwest Center for Advanced Studies, Dallas, Texas:

F. S. Johnson: C-4.

Stanford Research Institute, Menlo Park, California:

J. R. Peterson: C-16.

University of Michigan, Ann Arbor, Michigan:

S. R. Drayson: C-4.

University of Pittsburgh, Pittsburgh, Pennsylvania:

M. A. Biondi: A-16; R-8, 24; E (1).

W. L. Fite: A-15; C-14, 18A; R-14; E (1, 2).

F. Kaufman: A-19; R-24.

Wayne State University, Detroit, Michigan:

R. H. Kummler: A-4, 20, 24; R-2, 3, 9, 11, 13, 21; E (1, 2).

# TABLE OF CONTENTS


RECORD OF REVISIONS iii

FOREWORD TO THE SECOND EDITION v

FOREWORD TO THE FIRST EDITION vii

ACKNOWLEDGMENTS ix

LIST OF ILLUSTRATIONS xxiii

LIST OF TABLES xxxi

1. INTRODUCTION 1-1

1.1. The Purpose and Scope of the Handbook 1-1

1.2. Contents of the Handbook 1-2

1.3. Environmental Definitions Relevant to Nuclear-Disturbed Atmospheres 1-3

1.4. Simulation Problems 1-5

GROUP A—CHAPTERS ON ATMOSPHERIC BACKGROUND

2. THE NATURAL ATMOSPHERE: ATMOSPHERIC STRUCTURE 2-1

3. THE NATURAL ATMOSPHERE: FLUID MECHANICS AND AERONOMY 3-1

3.1. Introduction 3-1

3.2. Equations of Fluid Mechanical Motions of the Atmosphere 3-2

3.3. The Dominant Fluid Motions in the Atmosphere 3-7

3.4. Wave Motions in the Atmosphere 3-12

3.5. Atmospheric Turbulence 3-21

3.6. Effect of Turbulence on Chemistry in the Upper Atmosphere 3-31

3.7. Conclusions 3-38




Preceding page blank

References 3-40

Supplementary Bibliography 3-44

4. THE NATURAL ATMOSPHERE: ENERGY BALANCE IN THE UPPER ATMOSPHERE 4-1

4.1. Intraductian 4-1

4.2. Cancentratians and Population Temperatures 4-1

4.3. Energy Partitian 4-8

4.4. Energy Transfer and Energy Balance 4-10

4.5. The Vibrational Population 4-10

References 4-15

5. THE DISTURBED ATMOSPHERE 5-1

5.1. The Naturally Disturbed Atmasphere 5-1

5.2. The Nuclear-Perturbed Atmasphere 5-8

5.3. Excited Species 5-18

5.4. Chemical Releases 5-19

References 5-20

6. THE CHEMICAL KINETICS OF THE DISTURBED ATMOSPHERE 6-1

6.1. Intraductian 6-1

6.2. Reactian Mechanisms 6-1

6.3. Temperature Dependence 6-3

6.4. Ian Recombination Pracesses 6-7

6.5. Other Kinetic Cansideratians; the Rale af Metastable States 6-12

6.6. Data Gathering, Interpretatian, and Use 6-16

References 6-19

GROUP B—CHAPTERS ON METHODS OF GATHERING DATA

7. DATA-GATHERING METHODS BASED ON LABORATORY EXPERIMENTATION 7-1

7.1. Introduction 7-1

7.2. Afterglow Studies 7-2

7.3. Mass-Spectrometer Ion-Source Measurements 7-7
7.4. Ion Cyclotron Resonance 7-8
7.5. Drift-Tube Measurements 7-9
7.6. Beam Techniques 7-11
7.7. Photon Measurements 7-19
7.8. Studies of Irradiated Air 7-27
References 7-29
8. DATA-GATHERING METHODS BASED ON THEORETICAL ANALYSIS 8-1
8.1. Introduction 8-1
8.2. Electron-Ion Recombination Processes 8-1
8.3. Removal of Negative Ions 8-6
8.4. Charge Transfer 8-7
8.5. Ion-Molecule Reactions 8-9
8.6. Quenching Collisions 8-9
8.7. Vibrational Deactivation 8-10
8.8. Electron Impact 8-10
8.9. Vibrational Excitation 8-11
8.10. Photoionization 8-11
References 8-12
9. DATA-GATHERING METHODS BASED ON ATMOSPHERIC MEASUREMENTS 9-1
9.1. Introduction 9-1
9.2. Types of Atmospheric Measurements 9-2
9.3. Determinations of Effective Recombination Coefficients in the D, E, and F Regions 9-8
9.4. Measurements and Results for Other Parameters 9-15
References 9-32

GROUP C—CHAPTERS ON PERTINENT RATE DATA

10. BASIC ENERGY-LEVEL AND EQUILIBRIUM DATA 10-1
10.1. Introduction 10-1
10.2. Reaction Energies 10-1
10.3. Energy Levels and Potential Curves 10-3
10.4. Equilibrium Constants 10-5
References 10-6
11. THE KINETICS OF ATMOSPHERIC RADIATIVE PROCESSES IN THE INFRARED 11-1
11.1. Introduction 11-1
11.2. Collisional Excitation Processes 11-10
11.3. Radiative Excitation 11-20
11.4. Radiative Processes in Low-Density Plasmas 11-25
11.5. Conclusions 11-34
Appendix I: Band Shapes and Band Widths 11-35
Appendix II: Resonance Fluorescence Excitation Relationships 11-40
References 11-41
12. PHOTOCHEMICAL PROCESSES: CROSS-SECTION DATA 12-1
12.1. Introduction 12-1
12.2. Types of Absorption Processes 12-2
12.3. Photon Cross-Section Data 12-6
12.4. Photon Cross-Sections for Ultraviolet Deposition Codes 12-29
References 12-41
13. PHOTOCHEMICAL PROCESSES: SOLAR PHOTOIONIZATION RATE CONSTANTS AND ULTRAVIOLET INTENSITIES 13-1
13.1. First-Order Rate Constants 13-1
13.2. Solar Ultraviolet Intensities 13-4
References 13-6

14. KINETICS OF LOW-ENERGY ELECTRON COLLISION PROCESSES 14-1
14.1. Introduction 14-1
14.2. Figure Labels 14-2
14.3. Data Sources 14-5
14.4. Bibliography 14-5
14.5. Preparation of Figures 14-6
References 14-6
Bibliography 14-54
15. KINETICS OF HIGH-ENERGY HEAVY-PARTICLE COLLISIONAL PROCESSES 15-1
15.1. Introduction 15-1
15.2. Cross-Section Definitions 15-2
15.3. Experimental Methods 15-4
15.4. Theoretical Methods 15-5
15.5. Sample Experimental Data 15-25
References 15-48
16. CHARGED-PARTICLE RECOMBINATION PROCESSES 16-1
16.1. Introduction 16-1
16.2. Methods of Measurement and Analysis 16-2
16.3. Results 16-6
16.4. Summary 16-25
References 16-30
17. ELECTRON ATTACHMENT AND DETACHMENT PROCESSES 17-1
17.1. Introduction 17-1
17.2. Types of Attachment-Detachment Processes 17-1
17.3. Stability of Negative Ions 17-9
17.4. Ionospheric Significance 17-12
References 17-13

18. ION-NEUTRAL REACTIONS

A. THERMAL PROCESSES 18A-1

18A.1. Introduction 18A-1

18A.2. Techniques 18A-2

18A.3. Examples of Important Ionospheric Reactions 18A-4

18A.4. Summary of Reaction Rate Constants 18A-10

References 18A-29

B. NON-THERMAL PROCESSES 18B-1

19. NEUTRAL REACTIONS 19-1

19.1. Introduction 19-1

19.2. Experimental Methods 19-2

19.3. Detailed Discussion of Some Important Reactions 19-4

19.4. Brief Discussion of Other Reactions 19-10

19.5. Conclusions 19-14

References 19-19

20. EXCITATION AND DEEXCITATION PROCESSES 20-1

20.1. General Considerations 20-1

20.2. Lifetimes of, and Energy Stored in, Excited States 20-2

20.3. The Excitation and Deexcitation of Specific States 20-2

20.4. Reaction Rates for Reactions Involving Excited Species 20-18

References 20-51

21. ELECTRON COLLISION FREQUENCIES AND RADIO FREQUENCY ABSORPTION 21-1

21.1. Introduction 21-1

21.2. Electron Collision Frequencies 21-1

21.3. Radio-Frequency Transmission Coefficients 21-7

21.4. Weakly Ionized, Dry Air 21-8

21.5. Electron Energy Relaxation 21-10

21.6. Application of Electron Energy Loss Data 21-18

21.7. Radio-Frequency Transmission Coefficients for Ions 21-20
21.8. Summary 21-26
References 21-26

GROUP D—CHAPTERS ON DATA APPLICATION

22. DEIONIZATION SOLUTIONS 22-1
22.1. Introduction 22-1
22.2. Multi-Species Codes 22-1
22.3. Codes for Systems 22-2
23. PROBLEM AREAS IN ATMOSPHERIC DEIONIZATION 23-1
24. SUMMARY OF SUGGESTED RATE CONSTANTS 24-1
24.1. Introduction 24-1
24.2. Presentation of Reactions and Rate Data 24-1
References 24-47

APPENDICES

APPENDIX A SYMBOLS A-1
APPENDIX B CONSTANTS B-1
APPENDIX C CONVERSION FACTORS C-1
APPENDIX D GLOSSARY D-1
APPENDIX E SUBJECT INDEX E-1
APPENDIX F SPECIES INDEX F-1
APPENDIX G AUTHOR INDEX G-1
APPENDIX H GENERAL REFERENCES H-1

# LIST OF ILLUSTRATIONS


| FIGURE NO. | TITLE | PAGE |
|---|---|---|
| 3-1 | Latitudinal cross-section of mean zonal winds. | 3-10 |
| 3-2a | Horizontal wind components in a vertical plane normal to the line of sight, on one representative occasion. | 3-11 |
| 3-2b | Vertical wind sheors based on sodium cloud data from Wallops Island. | 3-11 |
| 3-3 | Wind speed spectra at sea level. | 3-19 |
| 3-4 | General character of the turbulent power spectrum F(k). | 3-24 |
| 3-5 | Effective atmospheric diffusion coefficient D as a function of altitude. | 3-30 |
| 3-6 | Change of horizontal diffusion coefficient with time. | 3-32 |
| 3-7 | Distribution of molecular oxygen. | 3-35 |
| 4-1 | Fractional concentrations of the major neutral species in the atmosphere. | 4-2 |
| 4-2 | Fractional concentrations of the minor neutral species in the atmosphere. | 4-3 |
| 4-3 | Fractional concentrations of the ionic species in the daytime atmosphere. | 4-4 |
| 4-4 | Population temperatures of atmospheric species. | 4-7 |
| 4-5 | Distribution of energy among different degrees of freedom. | 4-9 |
| 4-6 | Schematic heat budget constituents between 80 and 105 km. | 4-11 |
| 4-7 | Altitude dependence of energy absorption and emission. | 4-12 |
| 4-8 | Summary of vibrational temperatures in the normal atmosphere, compared to dissociation and kinetic temperatures. | 4-14 |




Preceding page blank

| | | |
|---|---|---|
| 5-1 | Normolized density as o function of altitude for selected days prior to, during, ond following the magnetic storm of 13 November 1960. | 5-2 |
| 5-2 | Temperoture increose for oltitudes obove about 300 km for selected days prior to, during, and following the magnetic storm of 13 November 1960. | 5-3 |
| 5-3 | A comparison of the average height dependence of $T_e$ and $T_i$ on (a) the magnetically quiet ond disturbed days in September, and (b) the magnetically quiet and disturbed nights. | 5-4 |
| 5-4 | Daytime D-region ionization rates. | 5-6 |
| 5-5 | Electron density profiles for the D-region of the ionosphere. | 5-7 |
| 5-6 | Idealized typical $n_e$-h profiles showing negotive and positive variations of the peak electron density. | 5-9 |
| 5-7 | Examples of fireboll temperatures for three detanation regions. | 5-10 |
| 5-8 | Examples of fireboll density for three detonation regions. | 5-12 |
| 5-9 | Examples of fireball electron density for three detonotion regions. | 5-14 |
| 5-10 | Ionization due to o medium-yield weapon (with 600 lb Al) detonated at 40 km. | 5-14 |
| 5-11 | Ion-pair density due to prompt radiation from a 1-MT burst detonated at 120 km, t = 0. | 5-15 |
| 5-12 | Ion-pair production rates from beta and gamma rodiation beneoth a 1-MT fission debris regior | 5-16 |
| 5-13 | Electron density profiles corresponding to the ion-pair productian rates shown in Figure 5-12. | 5-17 |
| 7-1 | Simplified diogram of microwave afterglow moss-spectrometer apparotus used by Mehr and Biondi in ion-electron recombination studies. | 7-3 |
| 7-2 | Schematic diogram of stationary afterglow apparatus used by Lineberger and Puckett. | 7-5 |
| 7-3 | Simplified schematic diagram of the flowing-afterglow opparotus of Ferguson, Fehsenfeld, and Schmeltekopf. | 7-6 |

| | | |
|---|---|---|
| 7-4 | Schematic diagram of part of the double mass-spectrometer system of Giese and Maier. | 7-14 |
| 7-5 | Schematic diagram of the apparatus used by Stebbings, Turner, and Rutherford. | 7-15 |
| 7-6 | System for photoionization and for collection and retarding-potentiol analysis of photoelectrons, used by Frost, McDowell, and Vroom. | 7-24 |
| 7-7 | Block diagram of photodetochment apparatus of Smith and Branscomb. | 7-26 |
| 7-8 | Schematic of the apparatus used by Hirsh et al for studies of irrodiated gases. | 7-28 |
| 9-1 | Schematic diagram of coordinated experiment. | 9-7 |
| 9-2 | Effective recombination rate coefficients measured in the upper atmosphere. | 9-14 |
| 9-3 | Collision frequency measurements. | 9-20 |
| 10-1 | Partial Grotrian diagram of hydrogen atom. | 10-42 |
| 10-2 | Partial Grotrian diagram of atomic nitrogen. | 10-43 |
| 10-3 | Partial Grotrian diagram of atomic oxygen. | 10-44 |
| 10-4 | Partial Grotrian diagram of $O^+$. | 10-45 |
| 10-5 | Potential-energy curves for $N_2^-$ (unstable), $N_2$, and $N_2^+$. | 10-46 |
| 10-6 | Potential-energy curves for $NO^-$, NO, and $NO^+$. | 10-47 |
| 10-7 | Potential-energy curves for $O_2^-$, $O_2$, and $O_2^+$. | 10-48 |
| 10-8 | Equilibrium constants for dissociation. | 10-49 |
| 10-9 | Equilibrium constants for ionization (detochment) of negative ions. | 10-49 |
| 10-10 | Equilibrium constants for ianization of atoms. | 10-50 |
| 10-11 | Equilibrium constants far ionization of diatomic molecules. | 10-50 |
| 11-1 | Spectrum of the airglow between 4 and 8 μm. | 11-2 |
| 11-2 | Atmospheric emission spectrum between 8 and 16 μm (altitude ≈ 12 km). | 11-3 |

| | | |
|---|---|---|
| 11-3 | Infrared spectrum of a high-altitude nuclear detonation in the 1.5-3 μm region. | 11-4 |
| 11-4 | Infrared spectrum of a high-altitude nuclear detonation in the 3-6 μm region. | 11-5 |
| 11-5 | Earthshine in the 1000-1450 $cm^{-1}$ region. | 11-21 |
| 11-6 | Earthshine in the 400-1000 $cm^{-1}$ region. | 11-21 |
| 11-7 | Irradionce at the top of the atmosphere, for quiet sun and two blackbody sources. | 11-22 |
| 11-8 | Calculated emissivities of oxygen plasma at 500 K. | 11-29 |
| 11-9 | Calculated emissivities of oxygen plasma at 2000 K. | 11-30 |
| 11-10 | Calculated emissivities of oxygen plasma at 6000 K. | 11-30 |
| 11-11 | CO spectral band shapes in the 4.30-5.30 μm range (vibrational temperature = 300 K; rotational temperature = 300 K). | 11-36 |
| 11-12 | CO spectral band shapes in the 4.30-5.30 μm range (vibrational temperature = 1000 K; rotational temperature = 1000 K). | 11-37 |
| 11-13 | CO spectral band shapes in the 4.30-5.30 μm range (vibrational temperature = 5000 K; rotational temperature = 300 K). | 11-38 |
| 11-14 | CO spectral band shapes in the 4.30-5.30 μm range (vibrational temperature = 5000 K; rotational temperature = 5000 K). | 11-39 |
| 12-1 | Oxygen absorption cross-sections in the Herzberg continuum. | 12-8 |
| 12-2 | Oxygen absorption cross-sections, Schumann-Runge bands (1,0 to 6,0). | 12-9 |
| 12-3 | Oxygen absorption cross-sections, Schumann-Runge bands (4,0 to 16,0). | 12-10 |
| 12-4 | Oxygen absorption cross-sections in the Schumann-Runge continuum. | 12-10 |
| 12-5 | Oxygen partial cross-sections for molecular ions. | 12-15 |
| 12-6 | Oxygen partial cross-sections for molecular ions. | 12-15 |
| 12-7 | Nitrogen partial cross-sections for molecular ions. | 12-17 |

| | | |
|---|---|---|
| 12-8 | Atomic oxygen cross-sections: Ionization threshold ($^4S$) to $^2D$ limit. | 12-18 |
| 12-9 | Atomic oxygen cross-sections: $^2D$ threshold to $^2P$ limit. | 12-19 |
| 12-10 | Atomic oxygen cross-sections. $^2P$ threshold to shorter wavelengths. | 12-20 |
| 12-11 | Atomic oxygen photoionization cross-sections for specific initial and final states. | 12-23 |
| 12-12 | Atomic nitrogen photoionization cross-sections for specific initial and final states. | 12-25 |
| 12-13 | Nitric oxide cross-sections. | 12-26 |
| 12-14 | Ozone cross-sections. Wavelength 3000-3600 A. | 12-26 |
| 12-15 | Ozone cross-sections. Wavelength 2000-3000 A. | 12-27 |
| 12-16 | Carbon dioxide cross-sections. | 12-28 |
| 12-17 | Water vapor cross-sections. | 12-29 |
| 13-1 | Solar flux incident on upper atmosphere. | 13-5 |
| | Figures 14-1 through 14-90 are untitled. (See pages 14-7 through 14-53.) | |
| 15-1 | Result of published data scaled according to Equation (15-13) to give a normalized universal curve. | 15-11 |
| 15-2 | Experimental data scaled according to Equation (15-13) and compared with the statistical theory of Firsov. | 15-12 |
| 15-3 | Electron capture and loss cross-sections of $Fe^+$ on O. | 15-16 |
| 15-4 | Electron capture and loss cross-sections of $Al^+$ on O. | 15-17 |
| 15-5 | Stripping cross-sections for various projectile atoms on argon. | 15-21 |
| 15-6 | Stripping cross-sections for uranium on nitrogen and oxygen. | 15-22 |
| 15-7 | Stripping cross-sections as indicated. | 15-23 |
| 15-8 | Stripping cross-sections for potassium atoms on nitrogen and on oxygen. | 15-24 |
| 15-9 | Comparison of the combined Russek-Firsov models for $N^+$ on $N_2$. | 15-26 |

A group of 71 unnumbered figures are found on pages 15-29 through 15-47.


| | | |
|---|---|---|
| 16-1 | Two-body electron-ion recombination coefficients, $\alpha(N_2^+)$ and $\alpha(N_4^+)$. | 16-9 |
| 16-2 | Two-body electron-ion recombination coefficient $\alpha(NO^+)$ as a function of temperature. | 16-13 |
| 16-3 | Two-body electron-ion recombination coefficient $\alpha(O_2^+)$ as a function of temperature. | 16-15 |
| 16-4 | Effective two-body recombination coefficient for collisional-radiative recombination of electrons and $H^+$ ions as a function of electron density, over a range of electron temperatures. | 16-19 |
| 20-1 | Energy levels of pertinent atoms, molecules, and metallic ions. | 20-42 |
| 20-2 | Energy levels of pertinent ions above those of corresponding ground-state neutral species. | 20-43 |
| 20-3 | Nitrogen vibrational excitation rate constants as a function of the electron kinetic temperature for 300 K $N_2$ kinetic temperature. | 20-44 |
| 20-4 | Loss frequencies for $N_2$ vibration as a function of altitude. | 20-45 |
| 20-5 | Excitation of atomic nitrogen by electron impact. | 20-46 |
| 20-6 | Deactivation of $O_2^{\ddagger}$ (v = 1). | 20-47 |
| 20-7 | The rate coefficient for $O_2$ vibrational excitation by electron impact. | 20-48 |
| 20-8 | Cross-section for electron-impact excitation of $O_2$. | 20-49 |
| 20-9 | Electron-impact excitation of atomic oxygen. | 20-50 |
| 21-1 | Electron collision frequencies in various atmospheric gases. | 21-2 |
| 21-2 | Real and imaginary parts of normalized conductivity showing effect of energy-dependent collision frequency. | 21-9 |
| 21-3 | Electron energy exchange frequencies for various atmospheric gases. | 21-12 |

| | | |
|---|---|---|
| 21-4 | Electron cooling rates in atmospheric gases. | 21-13 |
| 21-5 | Relaxation of characteristic energy and momentum-transfer collision frequency for dry air at 230 K and relaxation of characteristic energy in moist air (1.5 percent $H_2O$) at 300 K. | 21-19 |

# LIST OF TABLES


| TABLE NO. | TITLE | PAGE |
|---|---|---|
| 3-1 | Evidence for the occurrence of gravity waves ond tides in the atmosphere. | 3-17 |
| 3-2 | Possible mechanisms for the generation of grovity waves in the otmosphere. | 3-18 |
| 3-3 | Possible mechanisms for the dissipotion of otmospheric gravity woves. | 3-19 |
| 6-1 | Types of reoction. | 6-4 |
| 8-1 | Coefficient of rodiative recombination of $H^+$ and e. | 8-2 |
| 8-2 | Coefficient of radiative recombination of $X^+$ and e ot 250 K. | 8-2 |
| 8-3 | Coefficient of collisional radiative recombination. | 8-4 |
| 9-1 | Types of atmospheric measurements. | 9-3 |
| 9-2 | Ion-neutral reaction rate coefficients derived from analysis of ion composition meosurements. | 9-17 |
| 9-3 | Ion-neutral reaction rote coefficients—single rate measurements. | 9-18 |
| 9-4 | Rote coefficients for ion-ion, neutral-neutral, and attachment. | 9-19 |
| 9-5 | Known oirglow emissions for the eorth. | 9-22 |
| 9-6 | Fluorescence efficiencies meosured in auroras. | 9-24 |
| 9-7 | Quenching rate coefficients of important otmospheric species. | 9-29 |
| 10-1 | Molecular weights and energies of formation, dissociation, and ionization for selected atoms and molecules. | 10-11 |




Preceding page blank

| | | |
|---|---|---|
| 10-2 | Energy levels and equilibrium fractional electronic populations of H . | 10-18 |
| 10-3 | Energy levels and equilibrium fractional electronic populations of C . | 10-19 |
| 10-4 | Energy levels and equilibrium fractional electronic populations of $C^+$ . | 10-21 |
| 10-5 | Energy levels and equilibrium fractional electronic populations of N . | 10-23 |
| 10-6 | Energy levels and equilibrium fractional electronic populations of $N^+$ . | 10-24 |
| 10-7 | Energy levels and equilibrium fractional electronic populations of $O^-$ . | 10-26 |
| 10-8 | Energy levels and equilibrium fractional electronic populations of O . | 10-27 |
| 10-9 | Energy levels and equilibrium fractional electronic populations of $O^+$ . | 10-29 |
| 10-10 | Energy levels and equilibrium fractional electronic populations of Ar . | 10-30 |
| 10-11 | Energy levels and equilibrium fractional electronic populations of $Ar^+$ . | 10-31 |
| 10-12 | Energy levels and equilibrium fractional electronic populations of CO . | 10-33 |
| 10-13 | Energy levels and equilibrium fractional electronic populations of $N_2$ . | 10-34 |
| 10-14 | Energy levels and equilibrium fractional electronic populations of $N_2^+$ . | 10-35 |
| 10-15 | Energy levels and equilibrium fractional electronic populations of NO . | 10-36 |
| 10-16 | Energy levels and equilibrium fractional electronic populations of $NO^+$ . | 10-37 |
| 10-17 | Energy levels and equilibrium fractional electronic populations of $O_2$ . | 10-38 |
| 10-18 | Energy levels and equilibrium fractional electronic populations of $O_2^+$ . | 10-39 |

| | | |
|---|---|---|
| 10-19 | Lower electronic and vibrational energy levels of selected diatomic molecules. | 10-40 |
| 10-20 | Vibrotional spacing of triotomic molecules. | 10-41 |
| 11-1 | Data on infrared bands of atmospheric interest. | 11-6 |
| 11-2 | Collisional excitation parameters. | 11-12 |
| 12-1 | Photon absorption processes. | 12-3 |
| 12-2 | First ionization thresholds. | 12-4 |
| 12-3 | Absorption and ionization cross-sections of $O_2$, $N_2$, and O at solar lines. | 12-11 |
| 12-4 | Absorption cross-sections at wavelengths less than 304 A. | 12-14 |
| 12-5 | Atomic oxygen lines which may absorb solar lines. | 12-22 |
| 12-6a | Molecular nitrogen, $N_2$: photon cross-sections for very strong emission lines. | 12-31 |
| 12-6b | Molecular nitrogen, $N_2$: photon cross-sections for strong emission lines. | 12-32 |
| 12-7a | Molecular oxygen, $O_2$: photon cross-sections for very strong emission lines. | 12-34 |
| 12-7b | Molecular oxygen, $O_2$: photon cross-sections for strong emission lines. | 12-35 |
| 12-8a | Atomic oxygen O, and atomic nitrogen, N: photon cross-sections for very strong emission lines. | 12-36 |
| 12-8b | Atomic oxygen, O, and atomic nitrogen, N: photon cross-sections for strong emission lines. | 12-37 |
| 12-9a | Nitric oxide, NO: photon cross-sections for very strong emission lines. | 12-39 |
| 12-9b | Nitric oxide, NO: photon cross-sections for strong emission lines. | 12-40 |
| 13-1 | | 13-7 |
| 13-2 | (No titles included.) | 13-9 |
| 13-3 | | 13-10 |
| 13-4 | | 13-11 |

| | | |
|---|---|---|
| 13-5 | | 13-12 |
| 13-6 | (No titles included.) | 13-13 |
| 13-7 | | 13-14 |
| 14-1 | Effective line excitation cross-sections of the Meinel bands of $N_2^+$. | 14-23 |
| 14-2 | Effective line excitation cross-sections of the 1st negative bands of $N_2^+$. | 14-26 |
| 14-3 | Effective dissociative ionization cross-sections of $N_2$. | 14-28 |
| 15-1 | Comparison of classical theoretical predictions with experimental data for ion-atom charge transfer. | 15-8 |
| 15-2 | Summary of experimental techniques and detection methods used by various authors. | 15-27 |
| 15-3 | Symbols for measured cross-section values. | 15-28 |
| 16-1 | Recombination coefficient tabulation. | 16-26 |
| 17-1 | Radiative attachment. | 17-3 |
| 17-2 | Photodetachment. | 17-3 |
| 17-3 | Dissociative attachment. | 17-5 |
| 17-4 | Associative detachment. | 17-5 |
| 17-5 | Three-body attachment. | 17-7 |
| 17-6 | Collisional detachment. | 17-8 |
| 17-7 | Stability of negative ions of possible ionospheric interest. | 17-10 |
| 18A-1 | Positive-ion charge-transfer. | 18A-11 |
| 18A-2 | Negative-ion charge-transfer. | 18A-15 |
| 18A-3 | Positive-ion atom-interchange. | 18A-16 |
| 18A-4 | Negative-ion atom-interchange. | 18A-19 |
| 18A-5 | Three-body positive-ion reactions. | 18A-22 |
| 18A-6 | Three-body negative-ion reactions. | 18A-25 |
| 18A-7 | Charge transfer to neutral metals. | 18A-27 |
| 19-1 | Neutral reaction rate constants. | 19-16 |

| | | |
|---|---|---|
| 20-1 | Radiative lifetimes and transitions for principal atmospheric species. | 20-20 |
| 20-2 | Energy transfer from $N_2^{\ddagger}$. | 20-26 |
| 20-3 | Rate constonts for the reaction $N_2^{\ddagger} + O^+ \rightarrow NO^+ + N$ for a ronge of vibrational and tronslatian temperatures. | 20-27 |
| 20-4 | Quenching data for $N_2(A\,^3\Sigma_u^+)$. | 20-28 |
| 20-5 | Deactivation of $O_2^{\ddagger}$ (v = 1). | 20-29 |
| 20-6 | Quenching data for $O_2(^1\Delta_g)$. | 20-30 |
| 20-7 | Dissociative recombination of $O_2^+$ with electrans. | 20-30 |
| 20-8 | Quenching of $O(^1D)$ by various gases, relative to molecular nitrogen. | 20-31 |
| 20-9 | Calculated reactian coefficients. | 20-31 |
| 20-10 | Excitatian and deexcitation rate coefficients or cross-sections. | 20-32 |
| 21-1 | Electron collisian frequencies per molecule. | 21-3 |
| 21-2 | Electron energy exchange frequencies in atmospheric gases. | 21-14 |
| 21-3 | Electron cooling rate coefficient. | 21-15 |
| 21-4 | Mobilities of ians in atmospheric gases. | 21-21 |
| 24-1 | Reoctions and suggested rate constants. | 24-4 |

# 1. INTRODUCTION

C.A. Blank, Defense Nuclear Agency
F.R. Gilmore, R&D Associates
T. Baurer, General Electric Company
M.H. Bortner, General Electric Company
(Latest Revision 26 August 1971)

## 1.1 THE PURPOSE AND SCOPE OF THE HANDBOOK

The recovery of the atmosphere, following its disturbance by any of several natural or manmade events of the magnitude of a solar-flare impingement or a nuclear burst, may be characterized in terms of certain extremely important chemical and physical processes. Such events tend to introduce electromagnetic radiation, high temperatures, matter including atomic and subatomic particles, shock waves, and other phenomena related to these, in broadly varying ranges of energy and intensity, and all capable of producing remarkable changes in the atmospheric structure and chemical composition in very short time periods. Typically, the electron density and ionization levels thus generated may be many orders of magnitude higher than those of the normal, quiescent atmosphere. Since the propagation of directed electromagnetic radiation (e.g., transmitted radar, radio, and optical signals) is related to the intensity of these levels, and since the perturbation of the affected atmospheric region may last for minutes or hours and spread over hundreds of square miles in area, serious problems may ensue in relation to operational military systems designed to survive and to function during or subsequent to such disturbances.

It is the purpose of this Handbook to provide the best available detailed information concerning both chemical and physical mechanisms of the sort indicated above, and the roles which these processes play in atmospheric ionization and deionization. The processes by which increased ionization levels are produced, for example, in the event of a nuclear detonation, have been described in general elsewhere in the open literature. The high electron density levels created thereby may be diminished, as free electrons are

removed, by a variety of mechanisms which are termed collectively "atmospheric deionization". The chemical kinetics of such induced "atmospheric deionization" is highly complex, and in its present state of knowledge it involves many areas of uncertainty. Nevertheless, it is possible to carry out reasonable and useful theoretical calculations involving the rate chemistry of highly ionized air produced in the above manner. Based on these considerations, this Handbook presents what are believed to be the best available chemical kinetic data relevant to this problem area, as well as related information required for the associated calculations. The material thus presented can also serve as a guide to experimenters engaged in the acquisition of additional data of the same type. Although a considerable portion of the contents of this Handbook has been obtained directly from DNA-sponsored programs, much has been acquired or gleaned from the results of other efforts described in many other scientific and technical source-works.

## 1.2 CONTENTS OF THE HANDBOOK

For organizational purposes this Handbook is divided into four major groups, each comprising several chapters of related content. The first of these, Group A (Chapters 2 through 6), deals with general background material. Conditions of temperature, density, and chemical composition which are usually needed to determine the importance of specific processes or to assess particular instances of highly ionized atmospheres, are presented in Chapter 2 for the normal, and in Chapter 5 for the disturbed atmosphere. The effects of fluid mechanics upon the phenomenology of atmospheric chemistry are discussed in Chapter 3, and the partition of energy among the various modes available in the atmosphere in Chapter 4. The most important general types of rate processes which need to be considered are described in some detail in Chapter 6.

In Group B (Chapters 7 through 9), various aspects of the different methods employed to obtain data pertaining to the important chemical processes are examined. These chapters cover, respectively; experimental techniques, theoretical methods, and the extraction of useful data from direct atmospheric measurements.

The nature and scope of the data revealed through such investigations, and the state of our knowledge concerning several classes of reactions, are reviewed and evaluated in Group C (Chapters 10 through 21). Fundamental thermodynamic data, e.g., energy levels

and populations of states, as well as energies and equilibrium constants of reactions, are provided in Chapter 10, while Chapter 11 explores in depth the chemical kinetics controlling atmospheric radiative processes. Specific coverage of the remaining chapters in this group is as follows: experimental photochemical cross-section data, atmospheric fluxes and calculated photochemical rates, low-energy electron-collisional processes, the kinetics of high-energy heavy-particle collisions related to the nuclear-burst problem, recombination processes, electron attachment-detachment, ion-neutral reactions, neutral reactions, excitation-deexcitation processes, and electron collision frequencies (and radio-frequency absorption) in air.

The final Group D (Chapters 22 through 24) concerns the utilization, status, uncertainties, and problems associated with the determination of reaction rates. Thus these three chapters cover, respectively: the utilization of lumped-parameter systems as compared with detailed kinetic systems, outstanding problems involving atmospheric chemical processes, and a detailed summary of rate constants recommended for use in atmospheric deionization calculations Since many such calculations are performed using special computer codes, the availability of the recommended or standard rate constants listed in Chapter 24 is important, particularly for the sake of comparative studies or calculations.

## 1.3 ENVIRONMENTAL DEFINITIONS RELEVANT TO NUCLEAR-DISTURBED ATMOSPHERES

In the immediate aftermath of atmospheric perturbations induced by nuclear detonations several arbitrary environmental regions become of particular concern from the standpoint of chemical rate processes. These may be designated as: (a) the fireball proper; (b) the fireball halo; and (c) the cool but disturbed region beyond. In general, the phenomenology of the latter region was stressed in the information presented in the First Edition of this Handbook, and continues to figure prominently in this Second Edition. However, the processes occurring in the inner two regions are beginning to receive increased attention, a fact which is certainly reflected in the substance of the Handbook as here published, and which will undoubtedly continue to be made manifest in all future revisions thereof. In the paragraphs following, working definitions are provided, within the combined contexts of their interest for and relevance to

chemical kinetics, for each of the three regions cited above.

The fireball proper is the locale of high-temperature and high-energy processes, many of which lie beyond the regime of conventional chemistry and fall within the realm of plasma physics, especially at very early times after a nuclear detonation. The very early fireball contains within it a core of debris matter generated in the burst. With the passage of time, the very high energy of the fireball is dissipated, through expansion into, and interaction with, its surroundings. Reaction-rate information pertaining to this region is to be found in Chapter 15 of the Handbook.

The fireball halo may be characterized by the prevalence of very warm temperatures due both to radiation and to shock-front passage. Elevated translational, rotational, vibrational, and electronic temperatures are created, which vary in space and time, and which maintain an overall state of nonequilibrium at high altitudes. Endothermic reactions can also occur, in addition to high-energy radiation-induced processes. Cooling of this region to ambient temperatures occurs during a time period on the order of minutes. At lower altitudes, the actual volume thus affected is diminished in size. Therefore, the nature and scope of the chemical phenomenology would appear generally to assume greater significance at higher than at lower altitudes. However, the applicability of such a generalization to particular circumstances will vary with the individual case, and with the system performance under consideration.

In the outermost, or cool disturbed region, high electron densities are created by the radiation emitted by the nuclear burst, but the temperature does not rise significantly. The chemical processes are mainly exothermic and, in general, tend to reduce the electron density. Since this is a very large region, it has been traditionally the subject of greatest interest, especially to those concerned with electromagnetic or optical systems which must survive and continue to operate effectively within the field of disturbance.

The characteristics of these spatial regions obviously will vary with the size, nature, and other parameters associated with the nuclear detonation. Consequently, the effects created may be grouped arbitrarily into several altitude regimes (cf. Chapter 2) and time frames, depending upon the situation under consideration. The continuously changing nature of the post-nuclear-burst environment, overlaid upon a simultaneously varying "normal" atmosphere, makes

it even more difficult to perform pertinent phenomenological and simulation studies in any given context. In other words, without a prior detailed knowledge of the "normally" varying atmospheric constituents, processes, and behavior, the integrated effects of a nuclear burst superimposed upon the effects of such natural atmospheric disturbances as solar eclipses, auroras, and polar-cap absorption events (cf. Chapter 9) make it very difficult to achieve the degree of comprehension which is desired in all studies which involve perturbations of the real atmosphere. Indeed, the use of the suggested terminology of "n-dimensional chemistry" may be an appropriate descriptive phrase to employ in attempting to describe the processes encountered under such circumstances.

## 1.4 SIMULATION PROBLEMS

Atmospheric modeling studies are most often based upon the analysis of direct measurements of the neutral, ionic, and electronic composition, and radiative fluxes characteristic of the ionosphere under normal conditions, as well as during such natural geophysical disturbances as were mentioned above, and during those nuclear tests performed prior to the moratorium on atmospheric detonations. In the usual alternative, laboratory experiments are performed in which two well-defined ionospheric constituents are allowed to interact as an isolated phenomenon, with the rate of the ensuing reaction measured as a function of the various parameters at the experimenter's disposal. Such laboratory experiments provide data for incorporation into modeling studies of all degrees of complexity.

Each method of gathering data has its advantages and its constraints. In the direct atmospheric measurements approach, the temperature, pressure, and other pertinent physical and chemical parameters cannot be controlled to the extent required for reliable extrapolations to more extreme conditions. Often it is impractical even to measure all these variables with an accuracy as sufficient as is desired. Nevertheless, atmospheric measurements do offer a rather direct, and at times, singular approach to the analysis of phenomena which must be understood, for given practical applications, under the conditions prevailing in the ionosphere. In the laboratory, on the other hand, nearly complete control of the pressure, temperature, and chemical composition of the experimental environment can be achieved, so that a given isolated reaction often may be investigated with adequate confidence and intimacy. However, some reactions important in the upper atmosphere are not measurable at

the higher pressures usually used in laboratory investigations, simply because they are dominated by or subject to the response of other reactions. At lower working pressures in the laboratory, useful measurements are often prevented by recombination and quenching at the container walls, as well as extremely low signal-to-noise response levels. Moreover, the number of individual reactions of possible importance in the upper atmosphere may be quite substantial both in number and effect, especially since each significant excited state must be treated as a separate reactive species.

To circumvent this difficulty and provide an artificial environment which combines the convenience and controls characteristic of the laboratory with the relevance of direct atmospheric observation, the so-called "lumped-parameter" experiment concept—essentially experimentation with irradiated air—has been devised and implemented. Ideally, this technique utilizes an apparatus into which one introduces air-like gaseous mixtures and subjects them to the combined influences which are characteristic of a given geophysical environment. If it is certain that the procedure employed has not altered the processes resulting therefrom in a manner such as to invalidate the attempted duplication of a given ionospheric situation, then the values of appropriate variables of particular interest, e.g., the complex conductivity of the resulting gaseous mixture, can be measured by pertinent techniques. Thus in principle the "real world" is introduced into the equipment, and data are acquired which characterize selected environments and situations closely enough to be considered a valid "simulation".

In reality of course, all laboratory experiment differs from the ionosphere, in at least three important particulars. Even the so-called "lumped-parameter" approach is vulnerable in these respects. First, the container walls tend to modify processes under investigation, by removing electrons, ions, and other species through surface recombination, and by deexcitation of otherwise long-lived states through collision phenomena. Second, the laboratory experiment is never completely free of system-contributed impurities which either do not exist in, or differ from, those found in the ionosphere, but which may actively influence the course of the laboratory phenomenology. Finally, inasmuch as the actual atmospheric composition is not known with sufficient accuracy for most situations of interest, and unstable species are difficult to produce and control in the laboratory, the effects of minor constituents cannot usually be duplicated with any reasonable degree of satisfaction. As a result,

a large part of the effort involved in conducting such laboratory experiments must be concerned with the determination of those factors which tend to exert some extraneous influence upon the behavior of the "simulated" atmosphere. This requires in turn the interpretation of the observed gross behavior in terms of the elementary microscopic processes which govern the variation of ionization levels in the medium under study. Although somewhat out of keeping with "lumped-parameter" philosophy, the need for such interpretive effort is quite obviously unavoidable in the context of any realistic experiment. Nevertheless, "lumped-parameter" experiments may offer a unique and valuable contribution, provided they are conducted with a full realization of their shortcomings and constraints, and are interpreted in such a manner as to provide fresh insights into the complexities of the atmospheric processes under investigation.

It may be concluded from this discussion that since the true "simulation" of atmospheric systems to the degree required for the empirical evaluation of burst effects is not possible at present, reliance must continue to be placed largely on the direct investigation of specific individual processes found by experience and analysis to be relevant and important. Computational procedures which utilize all the appropriate data in an effort to determine overall system effects may then be employed in a selective, utilitarian manner, to enhance further the existing state of knowledge, and to guide future explorations into those areas of endeavor which offer the optimum chance for successful advancement in one of the most difficult and complex areas of investigation concerned with our environment.

## GROUP A

## CHAPTERS ON ATMOSPHERIC BACKGROUND

CHAPTER 2 The Natural Atmosphere: Atmospheric Structure

CHAPTER 3 The Natural Atmosphere: Fluid Mechanics and Aeronomy

CHAPTER 4 The Naturel Atmosphere: Energy Balance in the Upper Atmosphere

CHAPTER 5 The Disturbed Atmosphere

CHAPTER 6 The Chemical Kinetics of the Disturbed Atmosphere

# 2. THE NATURAL ATMOSPHERE: ATMOSPHERIC STRUCTURE

K.S.W. Champion, Air Force Cambridge Research Laboratories
(Latest Revision 29 September 1971)

N. B.: This chapter was not ready for publication in time to be distributed with the rest of the Handbook. Much work involving the reduction and interpretation of recently acquired data remained to be done, and could not be completed on schedule. However, it has been possible for the author to supply selected reference data for the use of other authors elsewhere in the Handbook, and for those other authors therefore to cite Chapter 2 as the source of the information thus utilized. Chapter 2 will be prepared and distributed to authorized recipients of the Handbook at an early date. In the meantime, readers are encouraged to refer to the predecessor chapter by the same author in the First Edition of the Handbook, to other chapters in this Edition (numbers 4, 5, 13) in which data supplied by Dr. Champion are used as noted above, and to two papers* presented by Dr. Champion and his co-workers at the Fourteenth COSPAR Meeting, Seattle, Washington, June 1971. One of the two preprints referenced below is included herewith as a tentative version of Chapter 2.

---

*Champion, K. S. W., "The Properties of the Neutral Atmosphere", Paper R. 5; Champion, K. S. W., and R. A. Schweinfurth, "The Mean COSPAR International Reference Atmosphere", Paper F. 2, Fourteenth COSPAR Meeting, Seattle, Washington, June, 1971.

# THE MEAN COSPAR INTERNATIONAL REFERENCE ATMOSPHERE

K. S. W. Champion and R. A. Schweinfurth
Air Force Cambridge Research Laboratories
Bedford, Massachusetts, U. S. A.

This contributed paper has been prepared for presentation at the Fourteenth COSPAR Meeting, June 1971 in Seattle. Paper f. 2.

# THE MEAN COSPAR INTERNATIONAL REFERENCE ATMOSPHERE

K. S. W. Champion and R. A. Schweinfurth
Air Force Cambridge Research Laboratories
Bedford, Massachusetts, U. S. A.

## ABSTRACT

The new mean atmosphere has been developed for the altitude range 25 to 500 km. The basis of the reference atmosphere is as follows:

Between 25 and 75 km the model represents annual mean conditions for latitudes near $30^{\circ}$.

Between 120 and 500 km the model corresponds to diurnal, seasonal and semiannual variation average conditions for a latitude near $30^{\circ}$ and a solar flux $\overline{F}$ of $145 \times 10^{-22}$ $W/m^2/Hz$.

Between 75 and 120 km a model has been developed which provides a smooth connection between the lower and upper sections of the mean atmosphere.

Note that throughout the Mean Reference Atmosphere the same formula (appropriate to a latitude of $30^{\circ}$) has been used for the acceleration due to gravity.

## 1. INTRODUCTION

The new COSPAR International Reference Atmospheres will contain:

(1) Seasonal and latitudinal models of density, temperature, pressure and winds between 25 and 110 km.

(2) Models from 110 to 2500 km for various solar fluxes and times of day. These models contain density, temperature, mean molecular weight and major constituents.

(3) A Mean Reference Atmosphere for the altitude range 25 to 500 km. This atmosphere contains density, temperature, pressure, mean molecular weight and major constituents.

The reasons for providing a Mean Reference Atmosphere are twofold:

(1) For many computations it is unnecessary to include a variety of atmospheric conditions and it is sufficient and economical to use a single typical model of the atmosphere.

(2) The respective low and high altitude models described above are functions of different parameters and do not match at 110 km. Thus, if computations are to span this altitude it will, in general, be most satisfactory to use the mean model.

The specifications for the new Mean Reference Atmosphere are given in the abstract.

## 2. MODEL BETWEEN 25 AND 75 KM

The data used to develop this model were the annual mean pressure value at 25 km at $30^{\circ}$ latitude and the annual mean temperature values at $30^{\circ}$ latitude at 5 km intervals

starting at 25 km derived from Groves [17]. The actual values are:

Pressure at 25 km $2.483 \times 10^3$ newtons/$m^2$

| Altitude (km) | 25 | 30 | 35 | 40 | 45 | 50 |
|---|---|---|---|---|---|---|
| Temperature ($^oK$) | 221.8 | 230.7 | 241.5 | 255.3 | 267.8 | 271.6 |
| | 55 | 60 | 65 | 70 | 75 | |
| | 263.9 | 249.3 | 232.8 | 216.3 | 205.0 | |

Starting at 25 km the atmospheric properties were computed using the following equations. Simpson's Rule was used to integrate numerically the pressure equation

$$p = p_1 \exp \left[ - \frac{M_o}{R} \int_{z_1}^{z} g dz / T_M \right] \qquad (1)$$

where: $p_1$ = pressure at reference altitude $z_1$

$p$ = pressure at altitude $z$

$M_o$ = sea level value of mean molecular weight = 28.96

$R$ = universal gas constant = $8.31432 \times 10^7$ ergs $K^{-1}$ $gmole^{-1}$

$g$ = acceleration due to gravity

$T_M$ = molecular-scale temperature

$$T_M = \frac{M_o}{M} T \qquad (2)$$

where $M$ = mean molecular weight

$T$ = kinetic temperature.

The total density was calculated from the relation

$$\rho = \frac{pM}{RT} = \frac{pM_o}{RT_M} \qquad (3)$$

The pressure scale height was calculated from

$$H = \frac{RT}{Mg} = \frac{RT_M}{M_o g} \qquad (4)$$

As the aim of the computations was to derive a model for the altitude region 25 to 500 km using a single expression for the acceleration due to gravity the expressions used respectively for the low and high altitude models were investigated. Unfortunately, neither formula was adequate. The formula used by Groves was the same as in CIRA 1965 and was sufficient in all respects except that its accuracy at high altitudes was not acceptable. The error was 1 in $10^4$ at 200 km, 4 in $10^4$ at 300 km and rapidly increased with altitude. On the other hand, the expression used by Jacchia [2] is valid only for a latitude near $45^\circ$ ($45^\circ$ 32' 33"). The problem was solved by adding another term to the expression used in CIRA 1965. The basic expression due to Lambert [3] includes dependence on latitude $\phi$

$$g = g\phi - (3.085462 \times 10^{-6} + 2.27 \times 10^{-9} \cos 2\phi)Z + (7.254 \times 10^{-13} + 1.0 \times 10^{-15} \cos 2\phi)Z^2 - (1.517 \times 10^{-19} + 6 \times 10^{-22} \cos 2\phi)Z^3 \text{ m/sec}^2 \quad (5)$$

where Z is in meters.

The form applicable to $30^\circ$ latitude is

$$g = 9.79324 - 3.086597 \times 10^{-6} Z - 7.259 \times 10^{-13} Z^2 - 1.520 \times 10^{-19} Z^3 \text{ m/sec}^2 \quad (6)$$

## 3. MODEL BETWEEN 75 AND 120 KM

The model in this region has to provide a transition between the low altitude model based on Groves' data [1] and Jacchia's high altitude models [2]. Jacchia's models start at 90 km and Groves' models extend to 110 km and they are not only different but they are functions of different parameters. Obviously a compromise must be devised.

As a starting point a temperature profile had to be chosen. As inputs for this it is interesting to compare the values from several models given in Table 1.

TABLE 1

| Altitude | Temperature ($T_M$) | | | |
|---|---|---|---|---|
| | USSA 1962 | CIRA 1965 | Groves* | Jacchia+ |
| 80 km | 130.65 K | 186.0 K | 197.3 K | - - - |
| 90 | 180.65 | 186.0 | 189.0 | 183.8 K |
| 100 | 210.65 | 213.0 | 215.1 | 203.5 |
| 110 | 260.65 | 263.0 | 284.0 | 265.5 |
| 120 | 360.65 | 380.7 | - - - | 380.6 |

*Average annual values for 30° latitude converted from kinetic temperatures using the values of M in reference [1].

+Average values for 45° latitude from model with 1000°K exospheric temperature using the values of M in reference [2] to convert the kinetic temperatures.

Two points should be noted. One is that Groves temperature at 80 km is substantially higher than that in other models. The second is the differences between the temperatures of the Groves and Jacchia models. A further constraint on the temperature profile used in this altitude region is that it must yield a specified density value at 120 km. The values determined for the molecular-scale temperature ($T_M$) are:

| Altitude (km) | 80 | 90 | 100 | 110 | 120 |
|---|---|---|---|---|---|
| Temperature ($T_M$, K) | 195.0 | 183.8 | 203.5 | 265.5 | 380.6 |

The adjustments in the temperature profile were made between 75 and 90 km.

Composition is to be calculated for this region using the techniques of Keneshea, Zimmerman and George [4], which include the effects of chemistry and atmospheric dynamics.

## 4. MODEL ABOVE 120 KM

The exospheric temperature was calculated to correspond to average diurnal, seasonal, semi-annual and geomagnetic conditions for $30^{\circ}$ latitude and a solar flux of $145 \times 10^{-22}$ $W/m^2/Hz$. The resultant exospheric temperature is $1000^{\circ}K$.

Jacchia's models were recomputed from 90 km upwards using the expression for g given in equation (6). This results in a change in the total density and number densities of the constituents at higher altitudes. The densities were then changed (at all altitudes) so that at 120 km they matched the density computed for the intermediate altitude model. These densities are very close to those of the $1000^{\circ}K$ Jacchia model at 120 km (see Table 2), but are slightly different at other altitudes.

TABLE 2

| Altitude | Temp | Log $N_2$ ($m^{-3}$) | Log $O_2$($m^{-3}$) | Log O($m^{-3}$) |
|---|---|---|---|---|
| 120 km | 334.5K | 17.5789 | 16.7338 | 17.1532 |

| Log A($m^{-3}$) | Log He ($m^{-3}$) | M | Density ($kgm^{-3}$) |
|---|---|---|---|
| 15.1732 | 13.5376 | 25.45 | 2.440 -8 |

Above the turbopause (assumed to be at 100 km) the number densities of each individual species $n_i$ were computed by integrating the equation for diffusive equilibrium

$$\frac{dn_i}{n_i} = - \frac{M_i g}{RT} dz - (1 + \alpha_i) \frac{dT}{T} \qquad (7)$$

where $\alpha_i$ is the thermal diffusion coefficient taken to be -0.38 for helium and zero for other constituents.

## 5. MEAN REFERENCE ATMOSPHERE

The properties of the Mean Reference Atmosphere are shown in figs. 1-7. Fig. 1 shows the pressure scale height as a function of altitude. Fig. 2 shows the kinetic temperature (T) and the molecular-scale temperature ($T_M$). Fig. 3 contains the kinetic temperature of the mean atmosphere plus curves indicating low extreme and high extreme temperatures. The latter attain exospheric temperatures of 500° and 1900°K, respectively. The pressure curve for the Mean Atmosphere is shown in fig. 4. Low extreme, high extreme and mean density values are plotted in fig. 5. These curves correspond to the temperature profiles in fig. 3. The mean molecular weights for the mean atmosphere are plotted in fig. 6. The corresponding number densities of $N_2$, $O_2$, O, A, He and H are shown in fig. 7.

To illustrate extreme conditions fig. 8 contains the mean June-July temperature profile for 80°N and fig. 9 the mean December-January temperature profile for the same location. These profiles are based primarily on data from Heiss Island and are from reference [57]. At 50 km the temperatures range from 279°K in summer to 247°K in winter, compared with the mean reference value of 271.6°K. At 80 km they range from 177°K in summer to 218°K in winter, compared with the reference value of 195°K.

Fig. 10 contains the mean CIRA temperatures, median warm temperatures and those exceeded 10% and 1% of the time and, similarly, median cold temperatures and

those above which 90% and 99%, respectively, of the temperatures lie. The extreme temperature profiles are a revised version of those in reference [6]. The corresponding density curves are shown in fig. 11. In general, the mean atmosphere values are in excellent agreement with the other curves. However, in fig. 10 the low median temperature crosses the mean profile near 65 km. The median values should be looked at again in this region. In fig. 11 the high median touches the mean at 90 km. Again the extremes are symmetrical with regard to the mean and the median value should be investigated.

REFERENCES

[1] G. V. Groves. Seasonal and latitudinal models of atmospheric temperature, pressure and density, 25 to 100 km, AFCRL-70-0261 (1970).

[2] L. G. Jacchia, Revised static models of the thermosphere and exosphere with empirical temperature profiles, Smithson. Astrophys. Obs., Spec. Report 332 (1971).

[3] W. D. Lambert, Acceleration of gravity in the free air, in: Smithsonian Meteorological Tables, sixth edition, Washington (1951) p. 490.

[4] T. J. Keneshea, S. P. Zimmerman and J. D. George, The latitudinal variation of major and minor neutral species in the upper atmosphere, to be presented at COSPAR, Seattle (1971).

[5] Supplements to the Project of the International Standard Atmosphere Model, ISO/TC-20/SC-6 (Secretariat-30) (1970).

[6] A. E. Cole, Extreme variations in temperature and density between 30 and 90 km, presented at COSPAR, Leningrad (1970).

LIST OF ILLUSTRATIONS

Fig. 1 Pressure scale heights of the mean CIRA atmosphere.

Fig. 2 Kinetic temperatures (T) and molecular-scale temperatures ($T_M$) of the mean atmosphere.

Fig. 3 Mean CIRA temperatures and low extreme and high extreme temperatures.

Fig. 4 Pressure curve of the mean atmosphere, from 25 to 500 km.

Fig. 5 Mean CIRA densities and curves of extreme densities.

Fig. 6 Mean molecular weights of Mean CIRA atmosphere.

Fig. 7 number densities and densities of $N_2$, $O_2$, O, He and H.

Fig. 8 Mean June-July temperature profile for 80°N.

Fig. 9 Mean December-January temperature profile for 80°N.

Fig. 10 Mean CIRA temperatures, temperatures which are exceeded 50, 10 and 1% of the time during warmest months and temperatures exceeded 50, 90 and 99% of the time during the coldest months at latitudes between 0° and 75°N.

Fig. 11 Densities relative to mean CIRA exceeded 50, 10 and 1% of the time during months with highest densities and densities exceeded 50, 90 and 99% of the time during months with lowest densities at latitudes between 0° and 75°N.

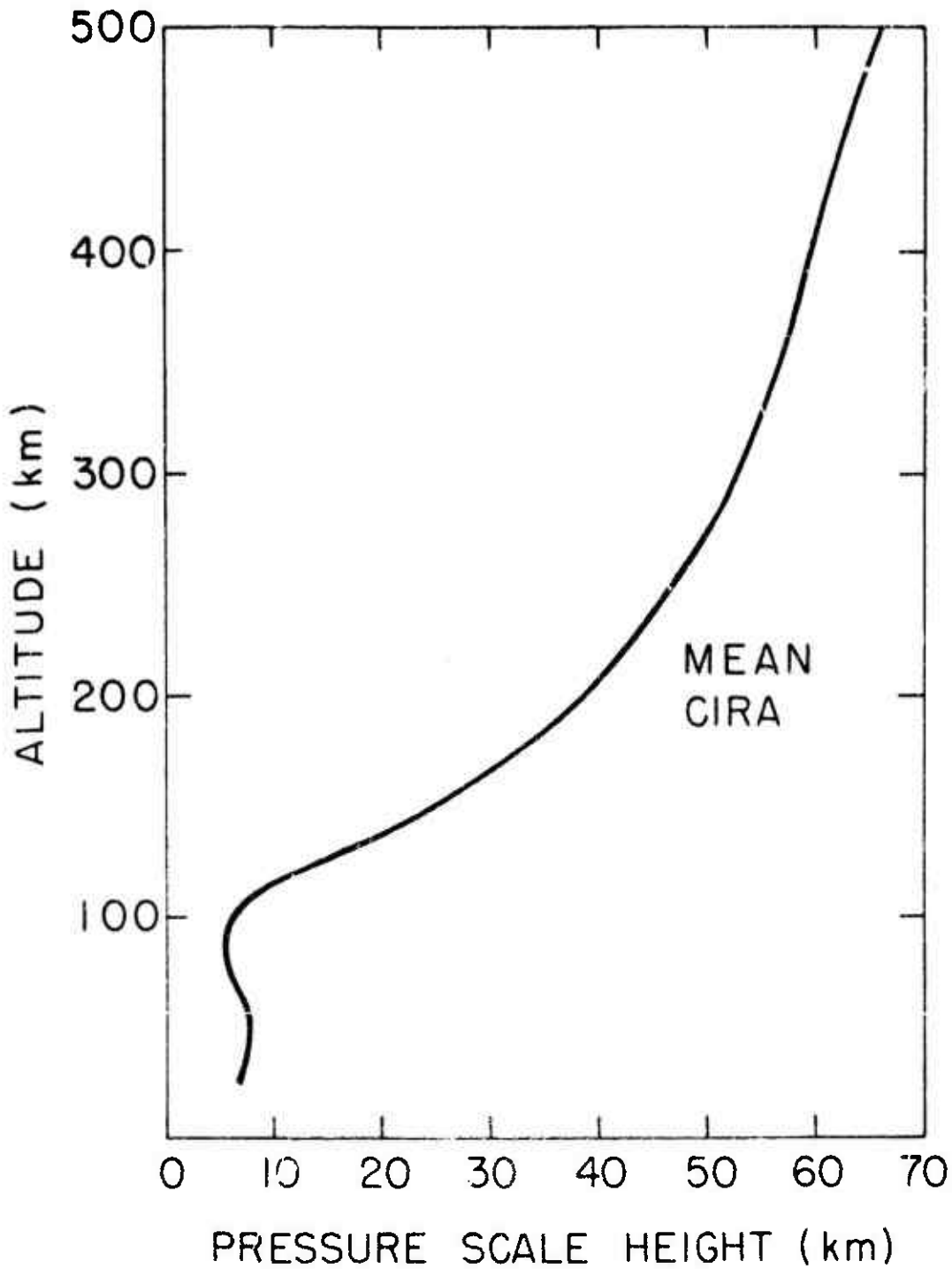
500
400
300
200
100
ALTITUDE (km)
MEAN
CIRA
0
10
20
30
40
50
60
70
PRESSURE SCALE HEIGHT (km)

FIGURE 1

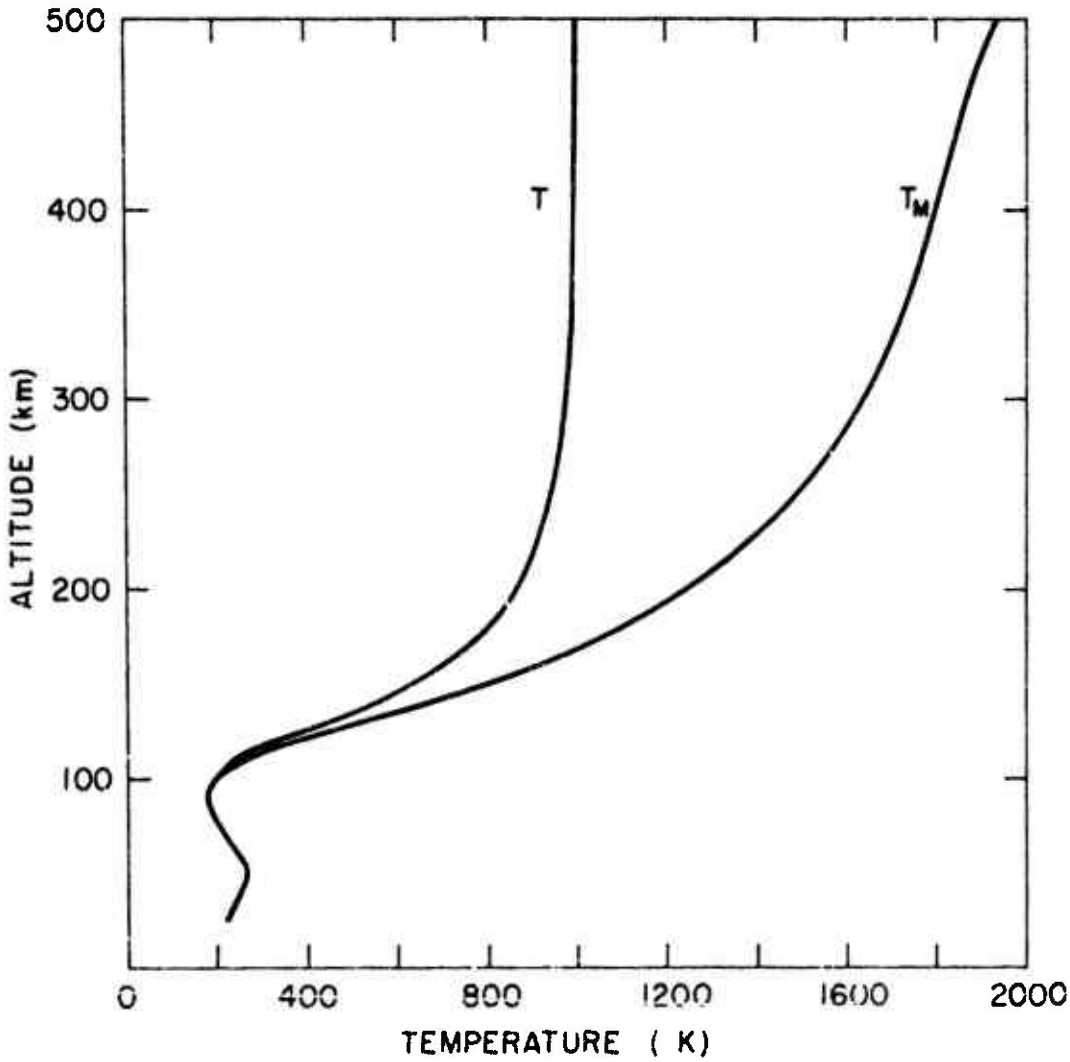
500
400
300
200
100
ALTITUDE (km)
T
$T_M$
0
400
800
1200
1600
2000
TEMPERATURE ( K)

FIGURE 2

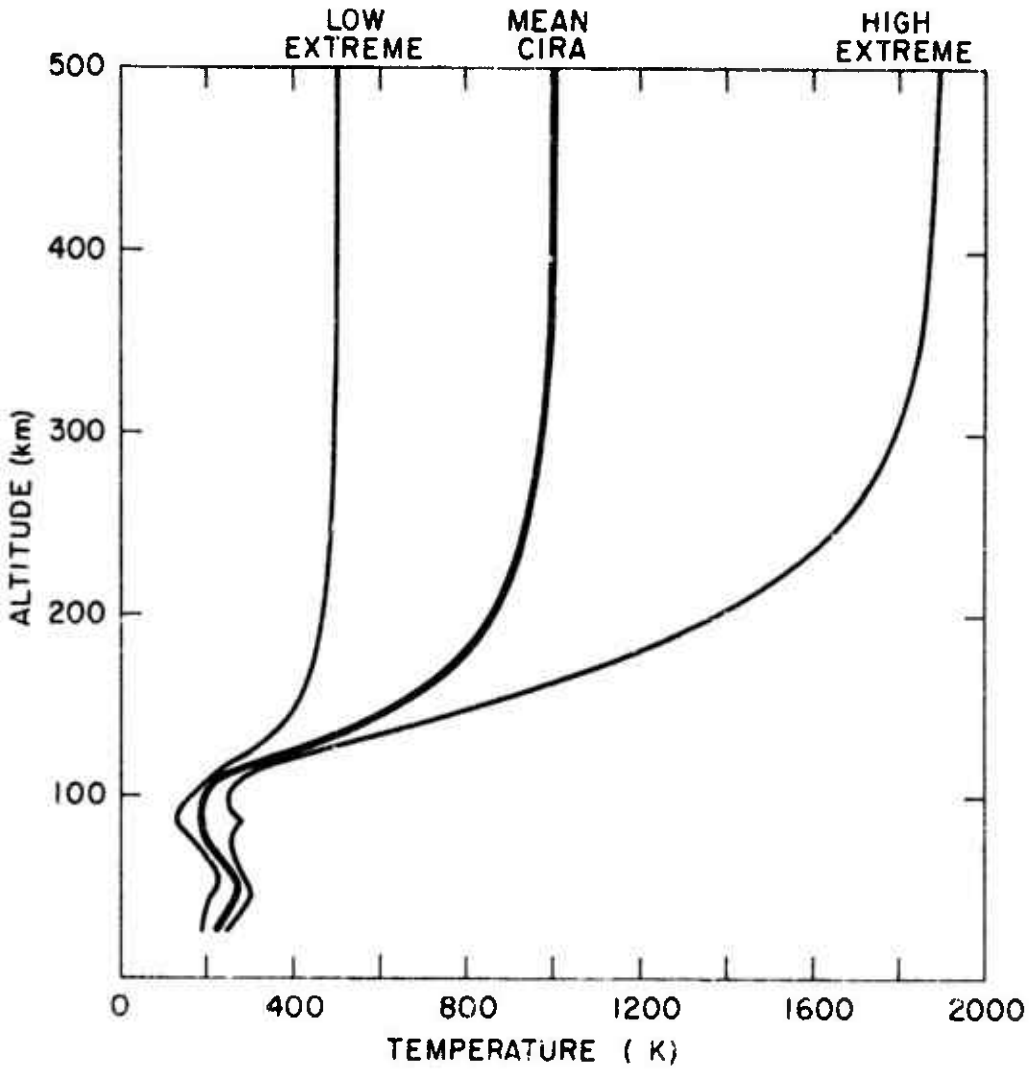
LOW
EXTREME
MEAN
CIRA
HIGH
EXTREME
500
400
300
200
100
ALTITUDE (km)
0
400
800
1200
1600
2000
TEMPERATURE ( K)

FIGURE 3

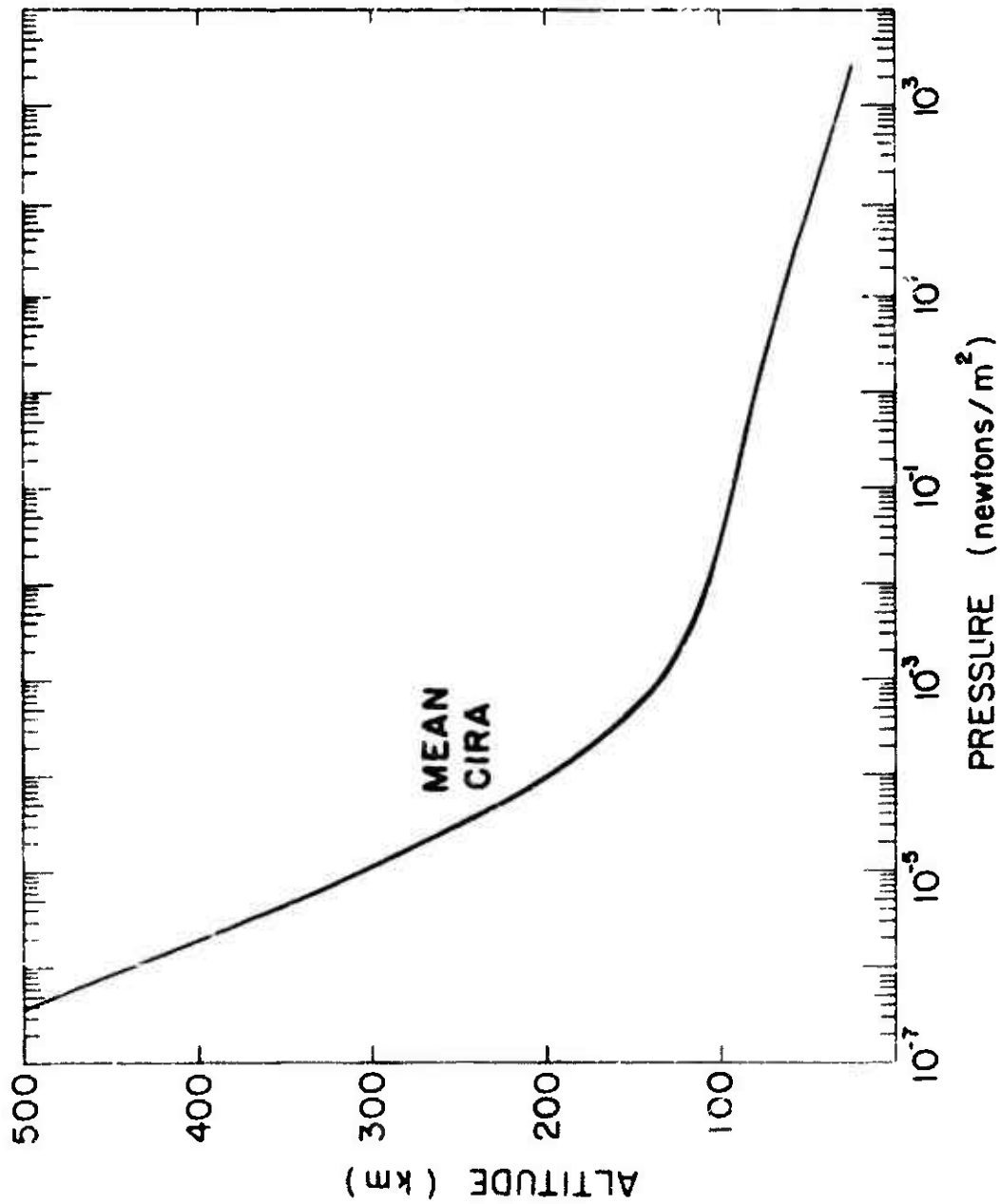
ALTITUDE (km)
500
400
300
200
100
MEAN
CIRA
$10^{-7}$
$10^{-5}$
$10^{-3}$
$10^{-1}$
$10^{1}$
$10^{3}$
PRESSURE (newtons/$m^2$)

FIGURE 4

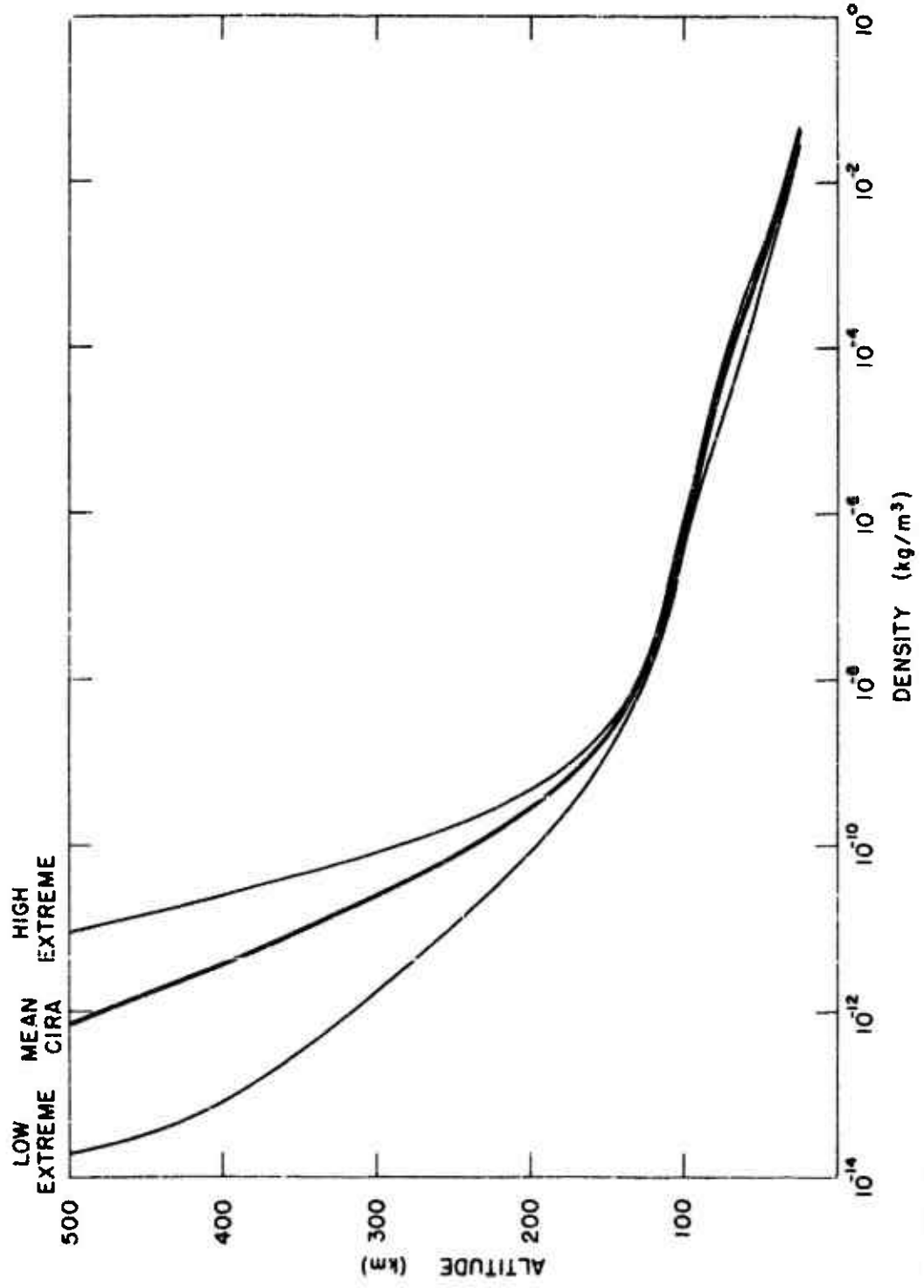
HIGH EXTREME
MEAN CIRA
LOW EXTREME
500
400
300
200
100
ALTITUDE (km)
$10^{0}$
$10^{-2}$
$10^{-4}$
$10^{-6}$
$10^{-8}$
$10^{-10}$
$10^{-12}$
$10^{-14}$
DENSITY (kg/m$^3$)

FIGURE 5

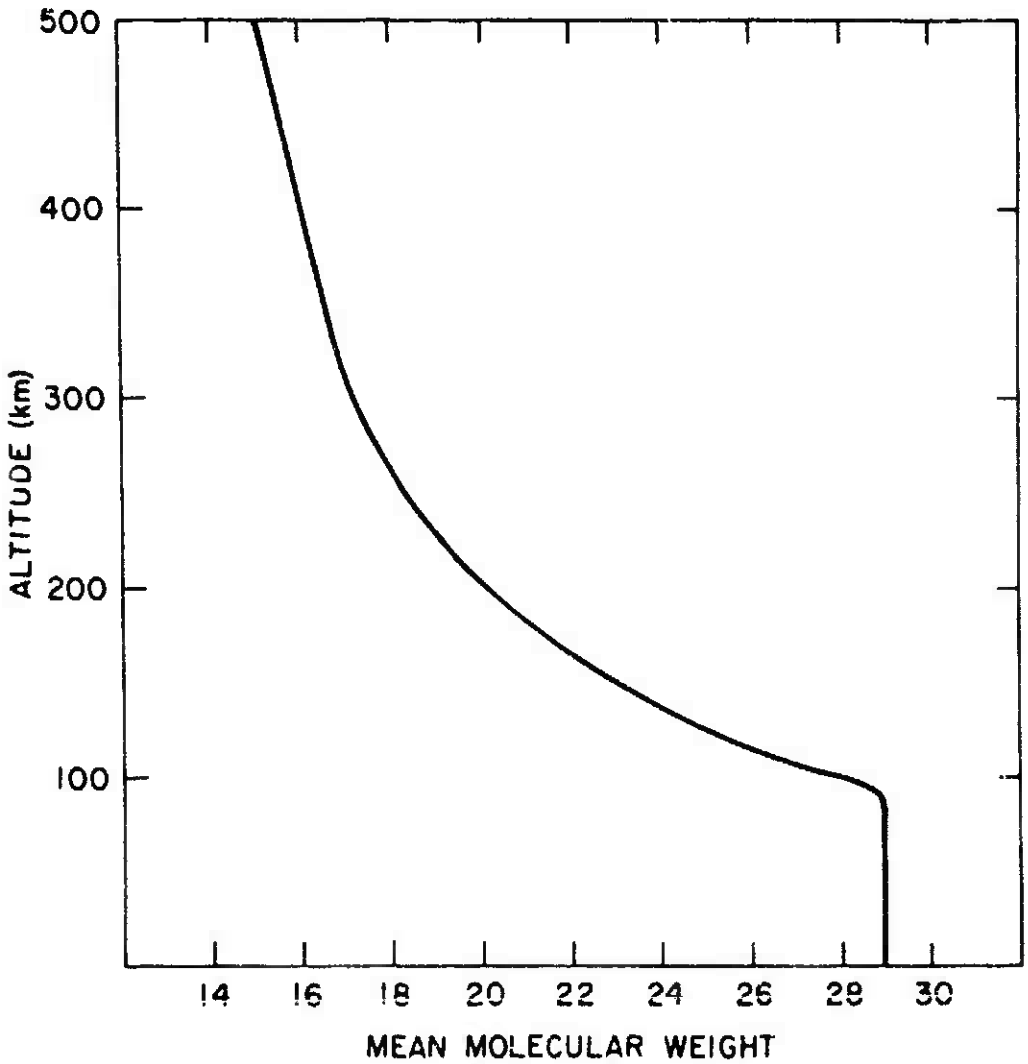
500
400
300
200
100
ALTITUDE (km)
14
16
18
20
22
24
26
28
30
MEAN MOLECULAR WEIGHT

FIGURE 6

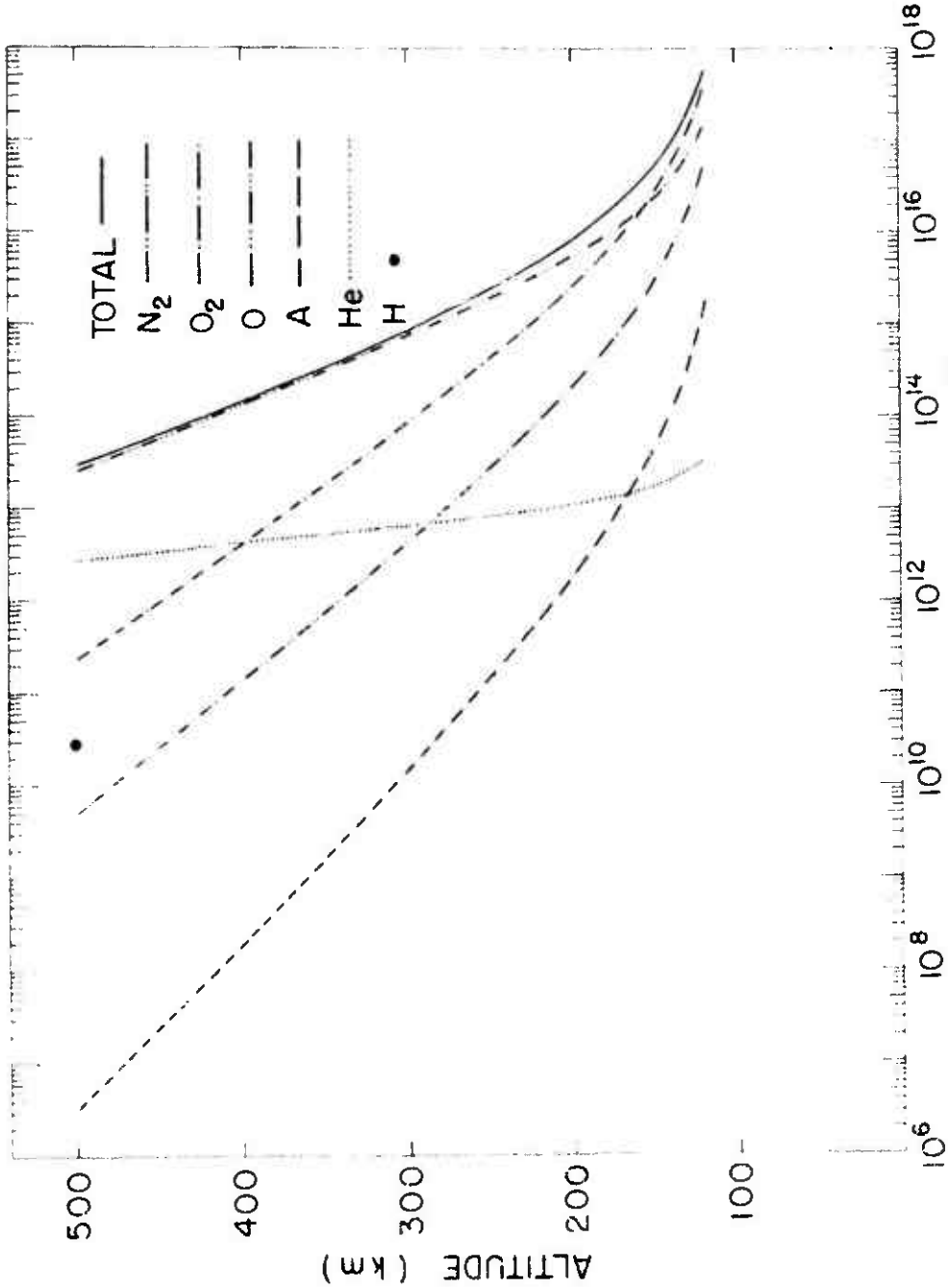
TOTAL
$N_2$
$O_2$
O
A
He
H
ALTITUDE (km)
500
400
300
200
100
NUMBER DENSITY ($M^{-3}$)
$10^{6}$
$10^{8}$
$10^{10}$
$10^{12}$
$10^{14}$
$10^{16}$
$10^{18}$

FIGURE 7

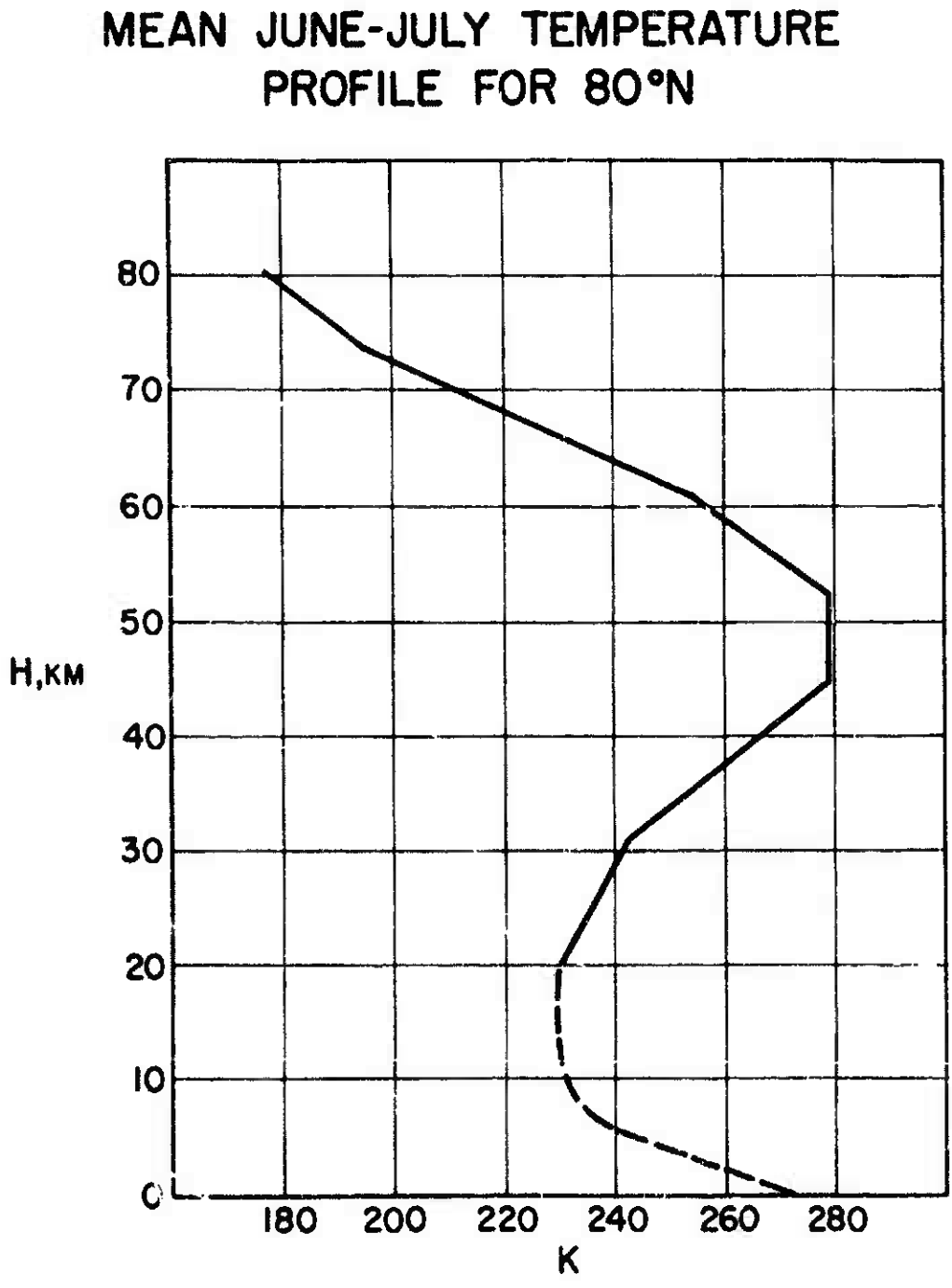
MEAN JUNE-JULY TEMPERATURE
PROFILE FOR 80°N
H,KM
80
70
60
50
40
30
20
10
0
180
200
220
240
260
280
K

FIGURE 8

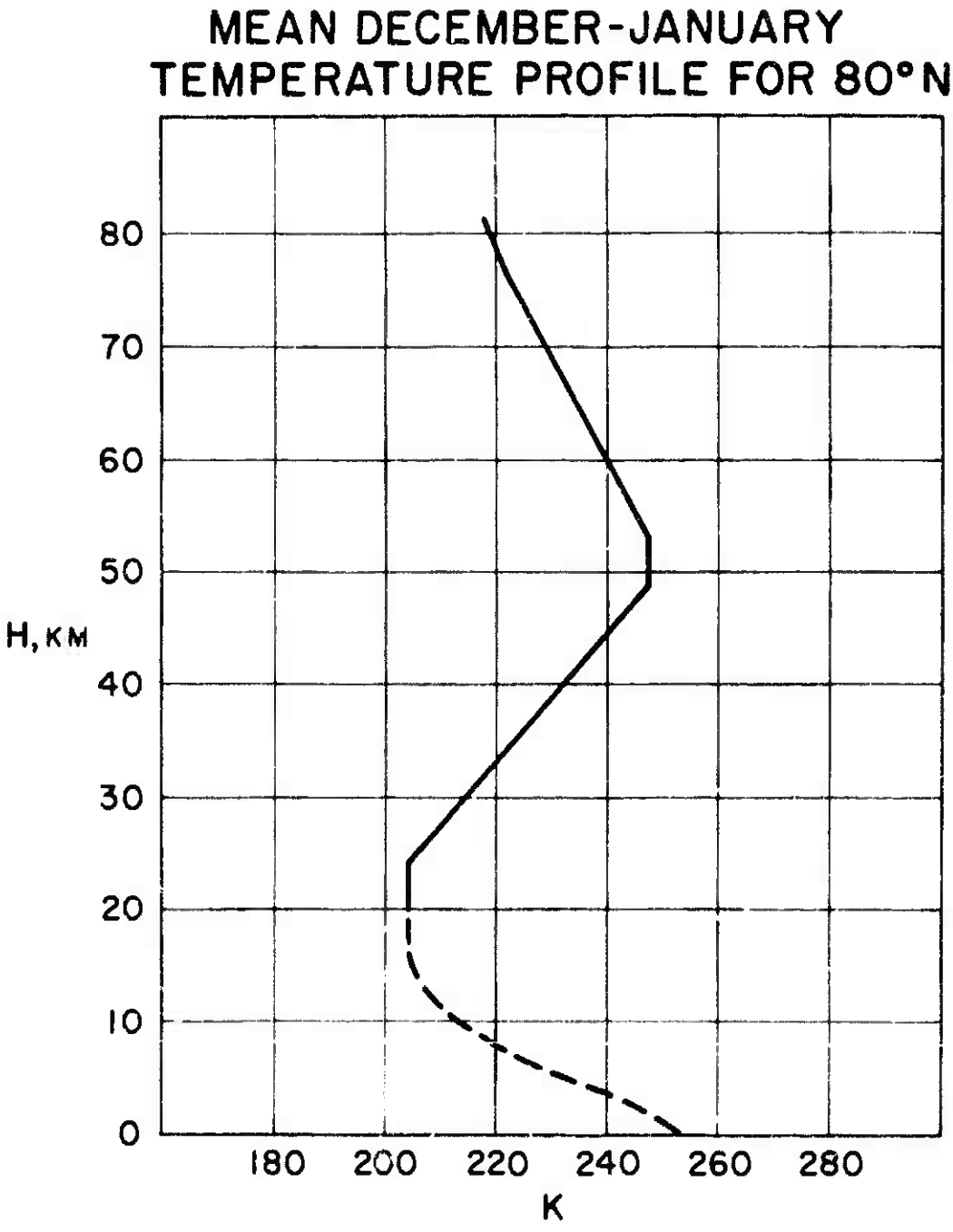
MEAN DECEMBER-JANUARY
TEMPERATURE PROFILE FOR 80°N
H, KM
80
70
60
50
40
30
20
10
0
180
200
220
240
260
280
K

FIGURE 9

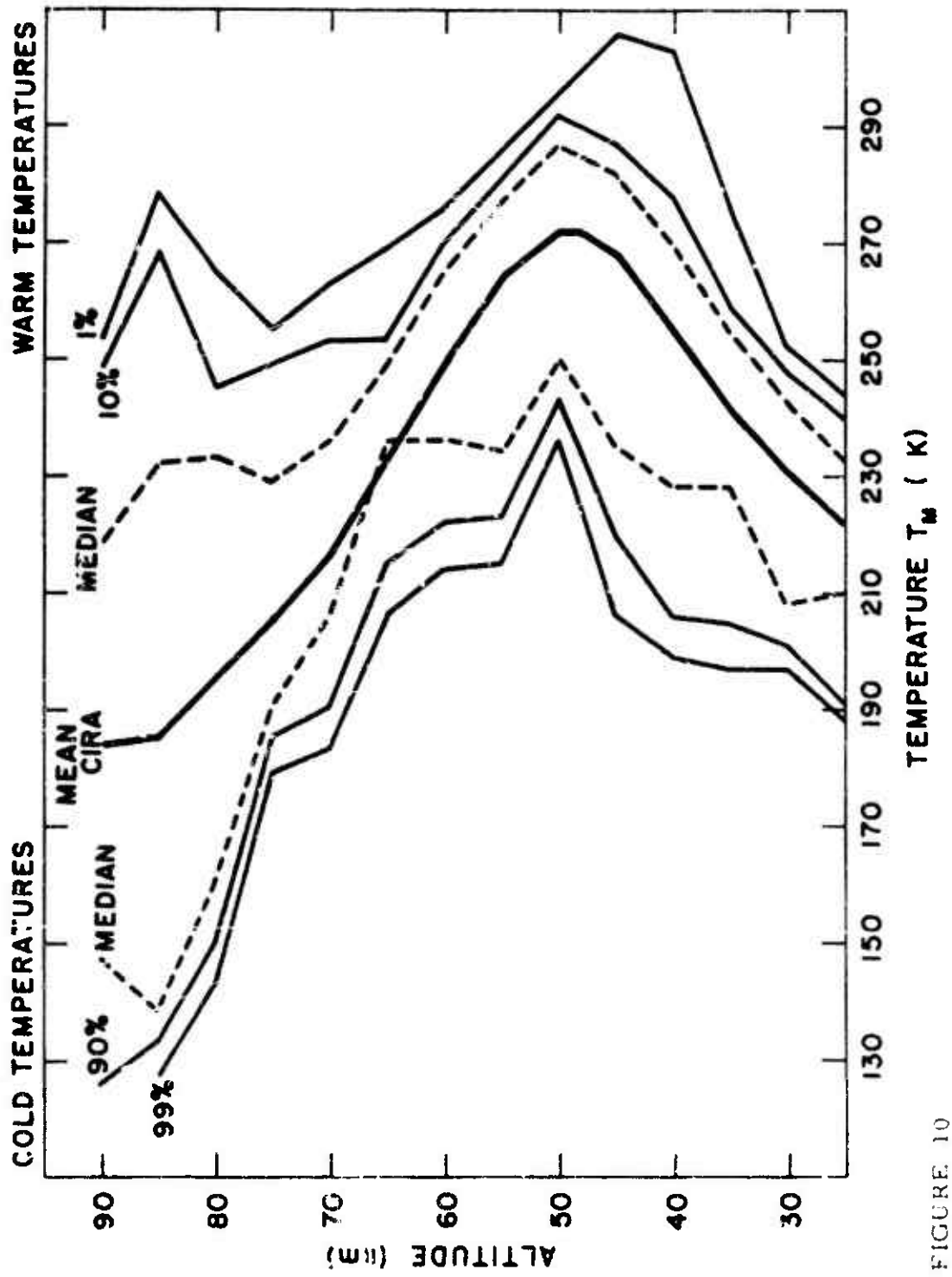
WARM TEMPERATURES
COLD TEMPERATURES
1%
10%
MEDIAN
MEAN CIRA
MEDIAN
90%
99%
ALTITUDE (km)
TEMPERATURE $T_M$ ( K)
90
80
70
60
50
40
30
130
150
170
190
210
230
250
270
290

FIGURE 10

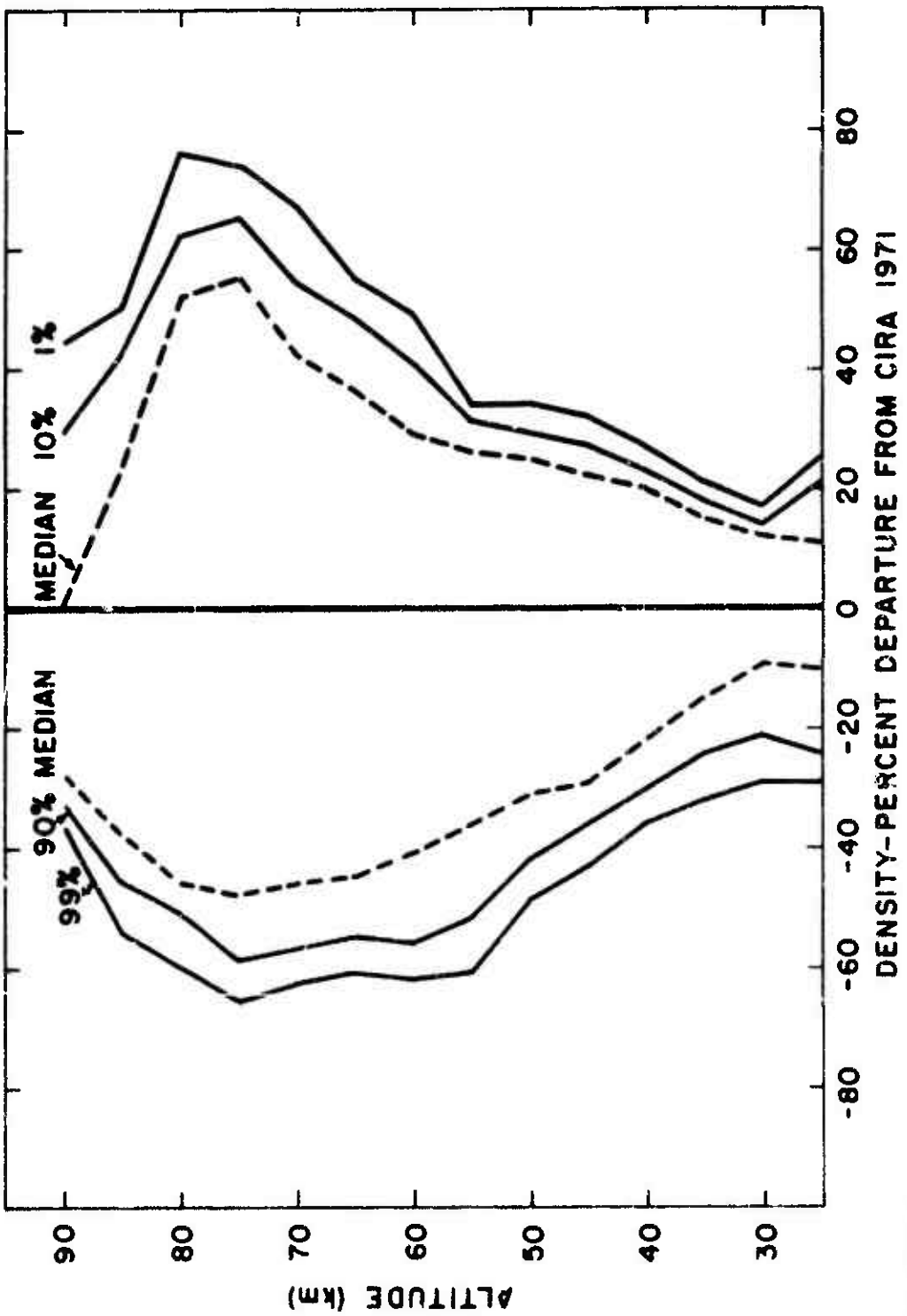
MEDIAN
10%
1%
90% MEDIAN
99%
80
60
40
20
0
-20
-40
-60
-80
DENSITY-PERCENT DEPARTURE FROM CIRA 1971
90
80
70
60
50
40
30
ALTITUDE (km)

FIGURE 11

# 3. THE NATURAL ATMOSPHERE: FLUID MECHANICS AND AERONOMY*

E. Bauer and P.A. Selwyn
Institute for Defense Anolyses
C.M. Tchen
City College of New York
(Lotest Revision 24 September 1971)

## 3.1 INTRODUCTION

The earth's upper atmosphere is sometimes treated as a quiescent and static medium in which radiative absorption and emission processes and the related chemical reactions of aeronomic interest take place. However, local heating and cooling arising from the absorption of solar ultraviolet radiation and of infrared "earthshine" and from infrared emission from atmospheric gases cause pressure gradients which give rise to atmospheric motions. These motions are complex; they include (on a steadily decreasing time scale) dominant motions or mean winds, atmospheric tides, acoustic-gravity waves, and ultimately, turbulence. The effects of all these different fluid motions and of their interactions on the aeronomic photochemistry have not been completely analyzed.

The scope of the present chapter is limited by the neglect of plasma phenomena to altitudes below about 180-250 km. Because of the long range of Coulomb interactions, plasma effects on fluid motions become significant for rather small degrees of ionization $K_i$. Thus Delcroix (Reference 3-1) characterizes a strongly ionized plasma as one for which $K_i > 10^{-4}$, which corresponds to an altitude $h > 220$ km; if one chose $K_i > 10^{-5}$, this would give $h > 180$ km. For altitudes below about 180 km the overall fluid motions are not significantly affected by plasma effects; above 220 km this is no longer true.

Anotner limit is set by the assumption of continuum fluid mechanics, as characterized by the Navier-Stokes equations and corresponding dissipation terms. This assumption also tends to fail at high altitudes or low densities where the flow tends to be free-

*This work was performed under Contract DAHC-15-67-C-0011, ARPA Assignment 5.

molecular rather than continuum in character. However, these effects do not extend to as low an altitude as do the plasma effects.

An extensive supplementary bibliography at the end of this chapter provides sources of further information. A somewhat more detailed discussion of this subject is given by Bauer, Selwyn, and Tchen (Reference 3-2). For a current survey of fluid mechanical energy sources and sinks in the upper atmosphere, see Moe (Reference 3-3).

## 3.2 EQUATIONS OF FLUID MECHANICAL MOTIONS OF THE ATMOSPHERE

### 3.2.1 Introduction

The dynamical equations of fluid motions in a form applicable to the earth's atmosphere are the equations of continuity (conservation of mass), motion (conservation of momentum), energy transport (conservation of energy), and state. Thus there are one vector and three scalar equations for one vector variable $\underset{\sim}{u}$ (velocity) and three scalar variables p (pressure), $\rho$ (mass density), and T (temperature).

Collisional interactions are described below in terms of the transport coefficients for viscosity, diffusion, and heat conduction; the mechanisms for chemical interactions are also presented in macroscopic form. (For more details, see Hirschfelder, Curtiss, and Bird (Reference 3-4), especially Chapter 11, and Burgers (Reference 3-5).)

### 3.2.2 Equations for the Individual Constituents

The equation of continuity for a species a , having mass density $\rho_a$ and a bulk or number-averaged velocity $\underset{\sim}{u}_a$ , is:

$$(\partial/\partial t)\,\rho_a + \nabla \cdot (\rho_a \underset{\sim}{u}_a) = S_{c;a} \quad , \tag{3-1}$$

where $S_{c;a}$ denotes the rate of production or loss of species a owing to chemical reactions with other species.

The equation of motion for species a is:

$$\rho_a(D_a/Dt)\underset{\sim}{u}_a - \nabla p_a + \nabla \cdot \underset{\approx}{\pi}_a = \rho_a \underset{\sim}{F}_a + \underset{\sim}{S}_{m;a} , \qquad (3\text{-}2)$$

where:

$$(D_a/Dt) \equiv (\partial/\partial t) + \underset{\sim}{u}_a \cdot \nabla . \qquad (3\text{-}3)$$

In addition:

$p_a$ = partial pressure of species a ;

$\underset{\approx}{\pi}_a$ = viscous stress tensor of species a ; (When the usual constitutive relations are employed, as in Reference 3-4, Equation (11.2-13), the expression for $\underset{\approx}{\pi}_a$ contains a proportionality constant equal to the viscosity coefficient $\mu_a$ .)

$\underset{\sim}{F}_a$ = external force per unit mass on species a ;

$\underset{\sim}{S}_{m;a}$ = effect of collisions, including the effect of chemical reactions, on the equation of motion. (The chemical terms included here depend on the angular distribution of reactants and products in a reactive collision, but are generally negligible compared to the effect of non-reactive collisions.)

To the same order of collisional interactions, the equation of energy transport for species a is:

$$\rho_a(D_a/Dt)E_a + p_a(\nabla \cdot \underset{\sim}{u}_a) + (\underset{\approx}{\pi}_a \cdot \nabla) \cdot \underset{\sim}{u}_a + \nabla \cdot \underset{\sim}{q}_a = S_{e;a} + Q_a , \qquad (3\text{-}4)$$

where

$E_a$ = internal energy of species a per unit mass;

$\underset{\sim}{q}_a$ = heat flux carried by species a ;

$S_{e;a}$ = effect of collisions and reactions on the energy equation;

$Q_a$ = net rate of radiative heat absorption by species a .

Finally, the appropriate approximation for the equation of state is the perfect gas law:

$$p_a = \rho_a \mathfrak{k} T / m_a \ , \tag{3-5}$$

where

$T$ = temperature;

$m_a$ = mass of a molecule of species a ;

$\mathfrak{k}$ = Boltzmann constant.

(If the gas constant R is used, it should be noted that there is a chance of confusion between the universal gas constant $R = 8.31 \times 10^7$ erg/K-mole and the gas constant per gram = R/M, where M is the gram molecular weight of the gas. The symbol R is occasionally used for both of these quantities.)

Details of the chemical terms $S_{c;a}$ , $\underset{\sim}{S}_{m;a}$ , $S_{e;a}$ may be found in Reference 3-5.

### 3.2.3 Equations for the Medium as a Whole

Summation of equations (3-1), (3-2), (3-4), and (3-5) for all the interacting species a leads to some significant simplifications. For example, in the equation of continuity,

$$\sum_a S_{c;a} = 0 \ , \tag{3-6}$$

because no net matter is created or destroyed. Thus the overall equation of continuity becomes:

$$(\partial/\partial t)\rho + \nabla \cdot (\rho \underset{\sim}{u}) = 0 \ , \tag{3-7}$$

where $\underset{\sim}{u} = (1/\rho) \sum_a \rho_a \underset{\sim}{v}_a$ . The overall equation of motion then becomes the well-known Navier-Stokes equation:

$$\rho (D/Dt) \underset{\sim}{u} \equiv \rho [(\partial/\partial t) + \underset{\sim}{u} \cdot \nabla] \underset{\sim}{u} = \rho \underset{\sim}{F} - \nabla p + \nabla \cdot \underset{\approx}{\pi} \ , \tag{3-8}$$

where $\underset{\sim}{F}$ is the total external force per unit mass, p is the pressure, and $\underset{\approx}{\pi}$ is the total viscous stress tensor. In atmospheric problems it is convenient to choose coordinates rotating with the earth, and to include centrifugal and Coriolis force terms in $\underset{\sim}{F}$:

$$\underset{\sim}{F} = \underset{\sim}{g} - 2\underset{\sim}{\Omega} \times \underset{\sim}{u} - \underset{\sim}{\Omega} \times [\underset{\sim}{\Omega} \times \underset{\sim}{r}] + \underset{\sim}{F}' , \tag{3-9}$$

where $\underset{\sim}{g} = (0, 0, -g)$ is the gravitational force per unit mass, $\underset{\sim}{\Omega}$ is the angular velocity of rotation of the earth, and $\underset{\sim}{r}$ is a position vector measured from the center of the earth. The terms $-2\underset{\sim}{\Omega} \times \underset{\sim}{u}$ and $-\underset{\sim}{\Omega} \times [\underset{\sim}{\Omega} \times \underset{\sim}{r}]$ are the Coriolis and centrifugal forces, respectively, and $\underset{\sim}{F}'$ denotes all other external forces.

The overall energy conservation equation is:

$$(D/Dt)(c_v T) + p\nabla \cdot \underset{\sim}{u} = \nabla \cdot \underset{\sim}{q} + \Phi + Q_R + Q_C , \tag{3-10}$$

where $c_v$ is the specific heat at constant volume per gram; $\underset{\sim}{q}$ is the total heat flux vector:

$$\underset{\sim}{q} = -K\nabla T + \underset{\sim}{D}^T , \tag{3-11}$$

with $K$ the thermal conductivity coefficient and $\underset{\sim}{D}^T$ the thermal diffusion term (which can usually be neglected); $\Phi$ (which contains a proportionality constant equal to the viscosity coefficient $\mu$) is the Rayleigh dissipation function (see, for example, Reference 3-6, p. 347, Eq. (29)); $Q_R$ is the net rate of radiant energy absorption per gram; and $Q_C$ is the net rate of chemical energy evolution per gram.

Finally, the equation of state is the ideal gas law:

$$p = kT\rho/m , \tag{3-12}$$

where $m$ = mean mass of an "air molecule".

### 3.2.4 The Inviscid Approximation to the Hydrodynamic Equations

The hydrodynamic equations as written above are too general and difficult to be useful in describing atmospheric phenomena. Accordingly, it is customary to make a number of approximations. First the effect of viscous dissipation is neglected, which is satisfactory if the Reynolds number is sufficiently large. The Reynolds number Re is defined as the ratio of inertial to frictional force. For motion with speed u in the x-direction, the inertial force per unit volume

is $(\rho u \partial u/\partial x)$ and the frictional force due to shear viscosity is $(\mu \partial^2 u/\partial y^2)$. Thus for motion of length scale d:

$$\mathrm{Re} = \frac{\text{inertial force}}{\text{frictional force}} = \frac{\rho u \partial u/\partial x}{\mu \partial^2 u/\partial y^2} \sim \frac{\rho u^2/d}{\mu u/d^2} \sim \rho u d/\mu \ . \qquad (3\text{-}13)$$

Evidently for $\mathrm{Re} >> 1$ one may ignore the effect of viscous dissipation. Now elementary kinetic theory gives (see, for example, Reference 3-4, chapter 1):

$$\mu = \alpha_v \rho \bar{c} \ell_m \ , \qquad (3\text{-}14)$$

where $\alpha_v$ is a numerical coefficient of the order of unity; $\bar{c}$ is the mean thermal speed which is roughly equal to the sound speed c (~300 m/sec at T ≈ 300 K); while $\ell_m$ is the gas-kinetic mean free path (~$10^{-5}$ cm at sea level, ~10 cm at 100 km altitude). Thus:

$$\mathrm{Re} \sim (u/c)(d/\ell_m) \ , \qquad (3\text{-}15)$$

and for typical meteorological conditions, u ~ 10-100 m/sec, d ~ 1 km, so that $\mathrm{Re} >> 1$ and the neglect of viscous dissipation is a satisfactory approximation; for $\mathrm{Re} \gtrsim 10^3 - 10^6$ the flow becomes turbulent, and turbulence is a major problem in the atmosphere, which is considered in Section 3.5.

When viscous effects are neglected, the equation of motion, Equation (3-8), becomes:

$$\rho \{ D\underset{\sim}{u}/Dt + 2[\underset{\sim}{\Omega} \times \underset{\sim}{u}] \} = -\nabla p + \rho \underset{\sim}{g} + \rho \underset{\sim}{F}' \ , \qquad (3\text{-}16)$$

where the (generally small) centrifugal force term $\underset{\sim}{\Omega} \times [\underset{\sim}{\Omega} \times \underset{\sim}{r}]$ of Equation (3-9) has been discarded, although it can be combined with $\nabla p$ to form an effective pressure since it can be written as $1/2 \nabla [\underset{\sim}{\Omega} \times \underset{\sim}{r}]^2$.

If energy transfer by heat conduction, radiation, and chemical reaction can also be neglected (which is true for sufficiently large scales of motion), the energy equation (3-10) may be replaced by the isentropic equation of state:

$$Dp/Dt = c^2 D\rho/Dt \ , \tag{3-17}$$

with:

$$c^2 = \gamma p/\rho = \gamma \mathcal{R} T/m = \gamma g H \ , \tag{3-18}$$

where c is the sound speed, $\gamma$ is the ratio of principal specific heats, and $H = \mathcal{R}T/mg$ (~7 km) is the atmospheric scale height.

Equations (3-7), (3-16), and (3-17) are sufficient to determine the variables p, $\rho$, and $\underset{\sim}{u}$. The temperature can then be determined from Equation (3-12).

## 3.3 THE DOMINANT FLUID MOTIONS IN THE ATMOSPHERE

### 3.3.1 Elementary Solutions of the Hydrodynamic Equations

In discussing the dominant motions of the atmosphere, it is customary and appropriate to use the inviscid equations of Section 3.2.4. The only simple solutions correspond to the static case:

$$\partial/\partial t \equiv 0 ; \ \underset{\sim}{u} = 0 \ , \tag{3-19}$$

and to the linearized steady-state case with rotation:

$$\partial/\partial t \equiv 0 ; \ 0(u^2) = 0 \ . \tag{3-20}$$

In the static case, the equation of momentum (3-16) reduces to:

$$\partial p/\partial z = -g\rho \ , \tag{3-21}$$

and combining this with the equation of state (3-12), one obtains $\partial p/\partial z = -p/H$, where H is the atmospheric scale height of Equation (3-18). This can be integrated to give:

$$p/p_1 = \exp\left\{ -\int_{z_1}^{z} dz/H \right\} \ , \tag{3-22}$$

where $p_1$ (and $\rho_1$) are values at $z = z_1$. If variations in T, m,

and g are neglected over the integration interval, the scale height H becomes a constant and Equation (3-22) simplifies to:

$$p/p_1 = \rho/\rho_1 = \exp\{-(z-z_1)/H\} . \qquad (3\text{-}23)$$

This is a crude approximation because the actual scale height varies by a factor of two between 50 and 150 km altitude.

In the linearized steady-state case of Equation (3-20), the equation of motion (3-16) gives:

$$\left.\begin{aligned} \partial p/\partial x &= 0 && \text{(a)} \\ \partial p/\partial y &= -2\Omega\rho u_x \sin(\phi) && \text{(b)} \\ \partial p/\partial z &= -g\rho - 2\Omega\rho u_x \sin(\phi)\sin(\theta) && \text{(c)} \end{aligned}\right\} , \qquad (3\text{-}24)$$

where $\phi$ is the latitude and $\theta$ the angle between the wind direction (here called the x-direction) and north, or the axis of rotation of $\underset{\sim}{\Omega}$. Thus as a result of a horizontal pressure gradient $\partial p/\partial y$, there arises a horizontal wind $u_x$ perpendicular to the pressure gradient, and of magnitude given by Equation (3-24b). This is the geostrophic wind, an important feature of the general circulation of the troposphere, although of doubtful importance in the upper atmosphere.

### 3.3.2 The General Circulation of the Middle Atmosphere (Stratosphere and Above)

The sources and sinks of energy in the stratosphere and mesosphere are provided largely by the minor species $CO_2$ and $O_3$, which absorb both sunlight and earthshine and ultimately re-radiate the energy in the infrared, near 15 μm and 9.6 μm, respectively. In the thermosphere, the most important absorbers of radiation are $O_2$ as well as $CO_2$ (insofar as it is not photodissociated), while the important infrared emitters are $CO_2$, OH, and spin-excited atomic oxygen ($O[^3P_{1,0}] \rightarrow O[^3P_2]$) (cf. Chapter 10, Table 10-8).

These radiative energy sources and sinks vary with latitude and height and hence produce pressure gradients and atmospheric motions.

The main motions are indicated in Figure 3-1, which shows the principal atmospheric wind fields between 30 and 100 km altitude, derived primarily from direct measurements using a variety of techniques, e.g., observations of smoke trails, rocket grenades, and chemical releases from rockets; radio observations of meteor trails; tracking of constant-level balloons; etc. (See, for example, Reference 3-7.) The prevailing wind tends to be zonal (i.e., east-west, horizontal) at mid-latitudes, with speeds of 10-100 m/sec; this wind is the so-called jet stream which arises from the temperature gradient associated with the change in altitude of the tropopause (the temperature minimum marking the top of the troposphere) between mid and high latitudes. The position of the jet stream tends to show an oscillation with a 3-7 day period correlated with the changes in the general circulation pattern.

In addition to these zonal, horizontal winds, there are other north-south horizontal winds associated with the general pattern of equatorial heating and polar cooling and the induced convection cells ("Hadley cells") located in a north-south plane; typically there are three such cells between the equator and each pole, so that the horizontal scale of one cell is some 3000 km, while the vertical scale is 10-30 km. Thus the local winds tend to be mainly horizontal, with a vertical component $10^{-3}$ - $10^{-2}$ times the horizontal one.

### 3.3.3 Local Winds and Wind Shears

The examination of actual wind profiles measured over a short time scale, i.e., of periods of the order of minutes, reveals that the general characteristics remain the same. The winds are predominantly horizontal, with speeds up to 100 m/sec, but very significant short-term variations occur in the magnitude and direction of the winds and, in particular, there are strong wind shears. Some typical pictures of these variations are given in Figure 3-2, which shows the vertical structure in the horizontal winds, and indicates gross wind shears $\omega_s$ of the order:

$$\omega_s \equiv \partial u(\text{horiz.})/\partial z \sim 10\text{-}100\ \text{m/sec per 10 km, or } 10^{-2}\text{-}10^{-1}\ \text{sec}^{-1}\ . \tag{3-25}$$

Because of experimental limitations, these values are lower bounds, determined by the resolution limits of the experimental arrangements.

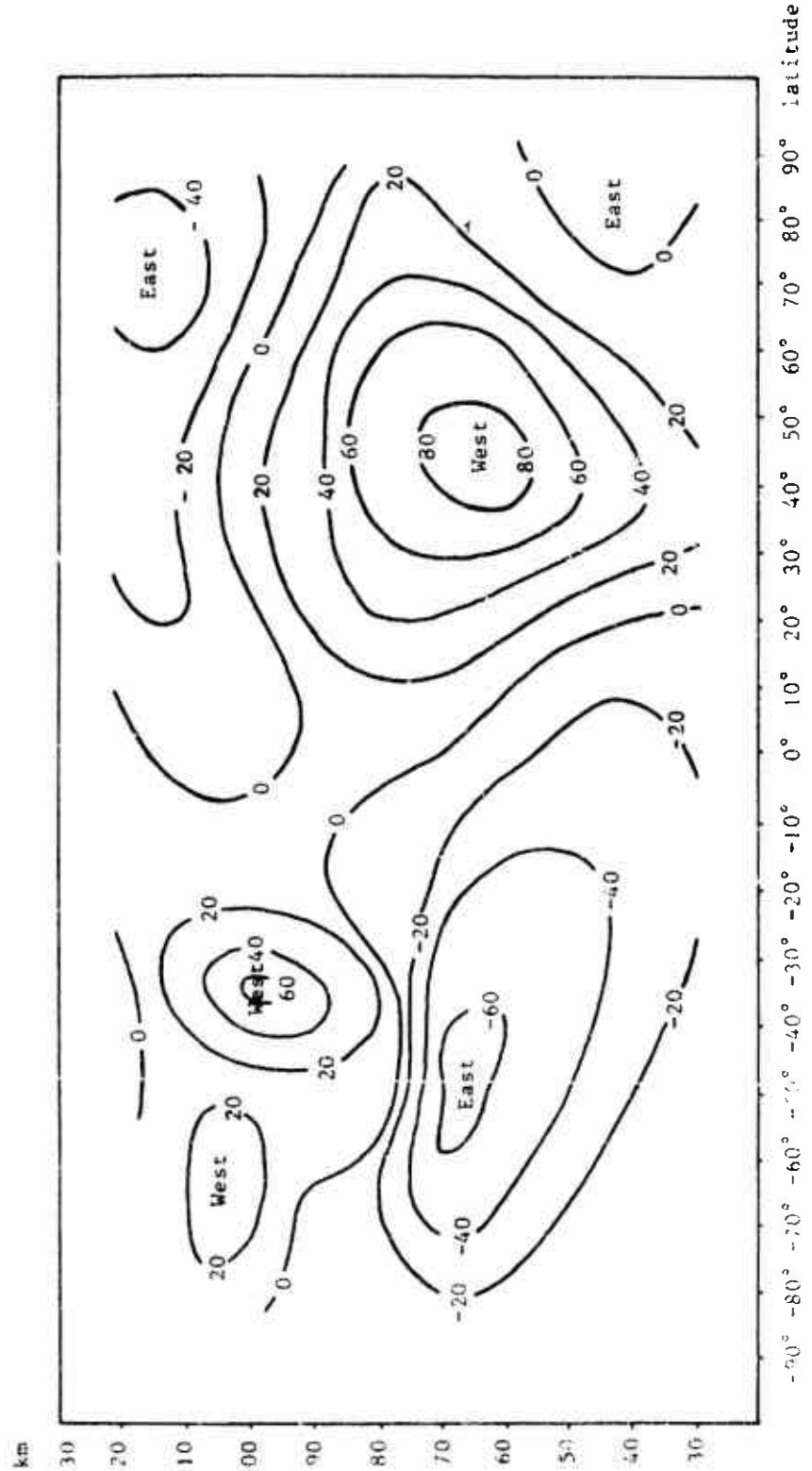


Figure 3-1. Latitudinal cross-section of mean zonal winds ($m\,sec^{-1}$), 30–120 km at the solstices (after Murgatroyd, Reference 3-9).

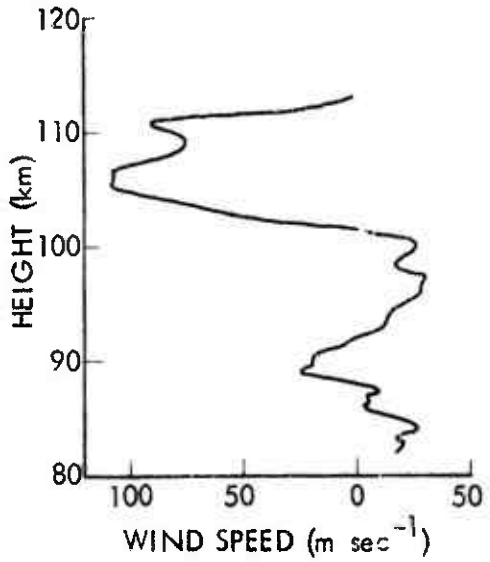


Figure 3-2o. Horizontal wind components in a vertical plane normal to the line of sight, on one representative occasion. Derived by Liller and Whipple (Reference 3-13) from the distortion of a long-enduring meteor trail.

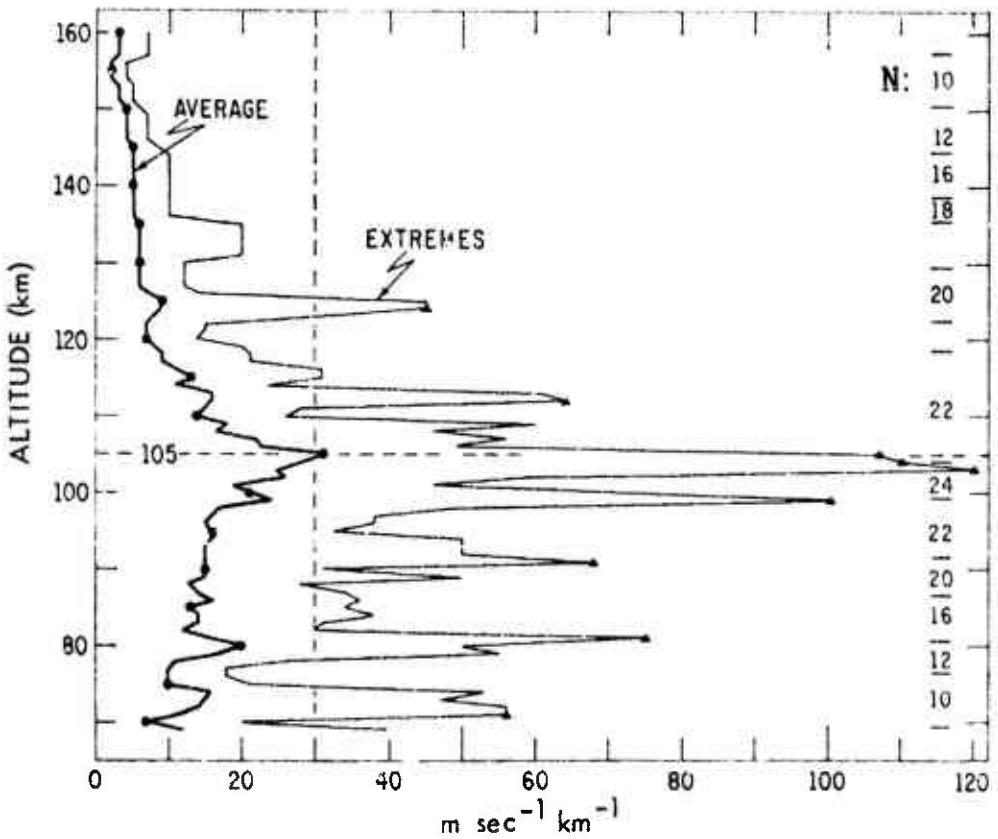


Figure 3-2b. Vertical wind shears based on sodium cloud data from Wallops Island. Vector shears were computed for $\Delta = 1$ km and plotted for each kilometer of elevation. N is number of observations (Reference 3-14).

The small-scale structure in upper atmospheric winds arises from local atmospheric variations in heating and cooling, as well as from the propagation of disturbances from the lower atmosphere. Many of the variations that are seen as weather in the troposphere are damped out or reflected in going up and never pass through the tropopause, but some of these effects do propagate upwards, generally with increasing amplitude associated with the change in density. These phenomena become noticeable in the upper atmosphere as tides, gravity waves, or acoustic waves, on steadily decreasing time scales, and these effects are discussed below in Section 3.4.

Wind shears are important as the primary source of atmospheric turbulence, which is treated in Section 3.5. Moreover, it has been shown that under certain conditions the heating of the thermosphere at altitudes near 100 km by frictional damping of wind shears may be even larger than atmospheric heating by the absorption of solar ultraviolet radiation (References 3-10, 3-11).

A further possible aeronomic significance of wind shears in the lower thermosphere is the production of thin horizontal layers of ionization due to the interaction of wind shears with the geomagnetic field, which has been suggested as a possible cause of mid-latitude sporadic E. (See, for example, Reference 3-12, pp. 201 ff.)

## 3.4 WAVE MOTIONS IN THE ATMOSPHERE

The exploration of the upper atmosphere in the 1950's and 1960's, mainly by rockets and satellites, provided a much more complete understanding of this region than had existed earlier. The U.S. 1962 (Reference 3-15) and CIRA 1965 (Reference 3-16) Standard Atmospheres now provide a satisfactory model for mean conditions in the upper atmosphere. Furthermore, the average deviations about the respective means have been studied. (See the 1966 Supplement to the U.S. 1962 Standard Atmosphere (Reference 3-17), or Chapter 2 on the CIRA 1971 Standard Atmosphere.) The next question concerns the time variation of these deviations, and this leads to the subjects of tides, gravity waves, and acoustic waves.

In discussing smaller-scale wave motions, a number of simplifications are possible. In particular, the waves considered are restricted to those having wavelengths much smaller than the earth's radius, periods much smaller than a day, and the amplitude of the fluctuation of any quantity very much smaller than its mean value.

The first two restrictions permit the rotation and curvature of the earth and the temporal behavior of the tidal generating functions to be neglected, and the third restriction allows the hydrodynamic equations to be linearized. Finally, it is assumed that the effects of viscosity, convective and radiative heat transfer, and chemical reactions may be neglected to the lowest order.

For tidal motions, which have periods that are approximately diurnal (24-hour period), semi-diurnal (12-hour period), or possibly even of higher order, it should be noted that any satisfactory analysis must incorporate both the driving forces (i.e., radiation in the case of solar tides which are produced by the absorption of sunlight by stratospheric ozone and tropospheric water, and lunar gravitational attraction in the case of lunar tides), and also the curvature and rotation of the earth (on account of the large scale of the motions). (For extensive discussions of tides, see Eckart (Reference 3-18), Lindzen and Chapman (Reference 3-19), Siebert (Reference 3-20), Wilkes (Reference 3-21), and references cited therein.)

Small-amplitude atmospheric wave motions are treated by use of the hydrodynamic equations presented above in Section 3.2.4, leading to solutions which consist of an unperturbed background, denoted by a subscript (o), and a small perturbation denoted by a superscript ($'$), so that:

$$\left.\begin{aligned} \rho &= \rho_o + \rho' && \text{(a)} \\ p &= p_o + p' && \text{(b)} \\ \underset{\sim}{u} &= \underset{\sim}{u}' && \text{(c)} \end{aligned}\right\} \quad . \tag{3-26}$$

For simplicity, steady winds and temperature differences are neglected. Then the static solutions of Section 3.3.1 give:

$$p_o,\ \rho_o \sim e^{-z/H}\ ,\quad H = c_o^2/\gamma g\ , \tag{3-27}$$

where:

$$c_o = (\gamma p_o/\rho_o)^{1/2} \tag{3-28}$$

is the sound speed in the unperturbed medium. The equations for

the perturbation term can be linearized by dropping second and higher order terms in $p'$, $\rho'$, $\underset{\sim}{u}$.

This leads in turn to solutions of the form:

$$\rho'/\rho_o\ ,\ p'/p_o\ ,\ \left|\underset{\sim}{u}'/u_c\right| \sim e^{z/2H}.e^{i(\omega t - \underset{\sim}{k}\cdot\underset{\sim}{r})}, \qquad (3\text{-}29)$$

where the frequencies $\omega$ and wave-number vectors $\underset{\sim}{k}$ satisfy the following dispersion relation: *

$$c_o^2 k_z^2 = \omega^2 - \omega_a^2 - c_o^2(k_x^2 + k_y^2)(\omega^2 - N^2)/\omega^2 \ . \qquad (3\text{-}30)$$

Here:

$$\left.\begin{aligned} \omega_a &= c_o/2H = 1/2\gamma^{1/2} g(\rho_o/p_o)^{1/2} \ ; & \text{(a)} \\ N &= [(\gamma-1)^{1/2}/\gamma]\, c_o/H = [(\gamma-1)/\gamma]^{1/2} g(\rho_o/p_o)^{1/2} \ . & \text{(b)} \end{aligned}\right\} \quad (3\text{-}31)$$

The term N is the "Brunt-Väisälä frequency", and $1/N \sim 5$ minutes in the atmosphere. For $\gamma = 1.4$, $\omega_a/N \simeq 1.1$, so that the two characteristic frequencies are fairly close together.

The dispersion relation (3-30) permits different classes of solutions:

(a) Acoustic modes ($\omega >> N$). In the high-frequency limit these waves are the analog of "ordinary" sound waves in an isotropic, compressible medium. Physically they correspond to a vertical wavelength very much less than the scale height H, so that they do not "see" the atmospheric stratification arising from gravity. In the high-frequency limit the dispersion relation (3-30) reduces to:

---

*The dispersion relation (3-30) is obtained by inserting the perturbation ansatz of Equation (3-26) in the dissipationless ("Euler") equations of motion of Section 3.2, in particular Equations (3-7), (3-16), and (3-17). Only terms linear in the small quantities $\rho'$, $p'$, $\underset{\sim}{u}'$ are kept and for these the ansatz (3-29) yields the result (3-30).

$$\omega^2 \sim c_o^2 k^2 + \omega_a^2 \sim c_o^2 k^2 \ , \qquad (3\text{-}32)$$

as in the case of sound waves, so that the group velocity is just the ordinary sound speed $c_o$.

(b) Internal gravity modes ($\omega < \omega_a$). In the low-frequency limit in particular these waves exist also in an incompressible medium, since the restoring force associated with this motion is buoyancy rather than compressibility, as in the case of sound waves, or acoustic modes. The dispersion relation is different; in the low-frequency limit it is:

$$\omega^2 \sim (k_x^2 + k_y^2)\, N^2 / [k^2 + \omega_a^2 / c_o^2] \sim g(k_x^2 + k_y^2) / Ak^2 + B) \ , \qquad (3\text{-}33)$$

where A and B are functions of the medium; it is apparent that this dispersion relation is quite different from that of a sound wave. It may be noted that the vertical wavelength will be of the order of the scale height $H = kT/mg$, i.e., these are fairly large-scale motions which "see" the anisotropy due to gravitational stratification.

(c) Surface waves ($N < \omega < \omega_a$). In this rather narrow frequency range neither acoustic nor gravity waves propagate, but there are different kinds of surface waves ("Lamb modes", etc.) which do not have a phase velocity in the vertical direction. (For a more detailed discussion, see References 3-18, 3-22, or 3-23.)

The earth's atmosphere is not isothermal, and thus both N and $\omega_a$ vary with altitude, which leads to a certain amount of ducting (horizontal propagation) of waves within the atmosphere, frequently guided by an effective surface at about 120-140 km, where N varies rapidly with height. (For a discussion of both the ducting and the surface propagation, see Reference 3-24.)

The presence of wind shear gives rise to a layer in which the speed of propagation equals the wind velocity. Observations have shown peculiar features in this layer, called the critical layer, similar to the critical layer in a boundary layer. The analysis of gravity-wave propagation in the critical layer is inadequately developed.

The single most important characteristic of the atmospheric wave motions is represented by Equation (3-29), which gives:

$$\left|\underset{\sim}{u}\right|, \left|\rho'/p_o\right|, \left|p'/p_o\right| \sim e^{+z/2H} \quad . \tag{3-34}$$

That is, the amplitude of velocity, pressure, and density fluctuations increases with increasing height, but in such a manner that the kinetic energy density $\rho_o u^2$ remains constant because $\rho_o \sim e^{-z/H}$. Thus the importance of wave motions is likely to increase with increasing altitude, at least up to such high altitudes that attenuation mechanisms become important.

Disturbances due to irregularities in atmospheric flow at comparatively low altitudes propagate at a small angle to the local horizontal; study of the energy flow arising from the dispersion equation reveals that this is at an angle $0.1^\circ$ to $1^\circ$ to the horizontal. (See, for example, Reference 3-22, Figure 6.10.) Owing to relation (3-34), the motion in a generally upward direction tends to be more important from the standpoint of energy transfer than that going down. A typical example of this behavior is seen in Figure 3-2a, where a wind pattern observed from radio meteor trails shows a wavelike structure with amplitude increasing with height.

There exist many pieces of evidence for the occurrence of acoustic-gravity waves and tides in the atmosphere; a representative list is shown in Table 3-1. Lists of possible mechanisms for the generation and attenuation of these waves are given in Tables 3-2 and 3-3, respectively; it must be stressed that both the detailed nature and the relative importance of all these mechanisms are not fully understood. It should be noted that in addition to the wave motions considered here, there are also planetary waves with periods of several days (cf. References 3-25, 3-26), and infrasonic waves, which are acoustic modes of periods of order 0.1 to 10 sec (cf. Reference 3-27). These modes have not been observed at high altitudes.

Regarding the energy flux and spectrum of acoustic gravity waves, the information available is incomplete, partly because of the variability of the effects. Some data on the spectrum of waves at sea level are shown in Figure 3-3; at 80-105 km Leovy's (Reference 3-47) estimate is useful, viz., that energy fluxes due to tides (periods of 12 and 24 hours, mainly) and gravity waves (periods of 5 min $\approx 1/N$, the Brunt-Väisälä period, to several hours) are roughly equal when averaged over time and latitude, each being of the order of 5 erg/cm$^2$-sec. However, a later survey (Reference 3-3) stresses

the variability and uncertainty of this energy flux. These rough figures may be compared with the solar radiant energy absorptance, which for 80-105 km is of the order of 15 erg/cm$^2$-sec, so that gravity waves may indeed be important for energy transfer at these and higher altitudes, if mechanisms exist for extracting energy from the wave motions.

Table 3-1. Evidence for the occurrence of gravity waves and tides in the atmosphere.

| Observation | Altitude Range | References |
|---|---|---|
| (a) Gravity Waves | | |
| (a.1) Wave structure on clouds | 0-10 km | |
| (a.2) Pressure variations observed on microbarographs | low altitudes | |
| (a.3) Mountain waves (well known to sailplane pilots) | 0-10 km | |
| (a.4) Rocket grenades | 60-70 km | 3-28 |
| (a.5) Wave patterns on noctilucent clouds | 80-90 km | 3-29 |
| (a.6) Meteor trails and chemical releases show winds with a wave structure | 80-160 km | 3-14 |
| (a.7) Occasional sinusoidal variation in ion temperature observed on satellite-borne instruments | 200-250 km | 3-30 |
| (a.8) Thomson-scatter radar observations of waves | F-region (200-300 km) | 3-31 |
| (a.9) Various ionospheric irregularities, such as Sudden Ionospheric Disturbances (SID's) | 200-300 km | 3-27, 3-32 |
| (a.10) Certain ionospheric disturbances correlate with severe local storms in the troposphere | F2-region | 3-27 (pp. 171-8), 3-33 |
| (b) Tides | | |
| (b.1) Pressure variations observed on microbarographs | low altitudes | |

Toble 3-1. (Cont'd.)

| Observation | Altitude Range | References |
|---|---|---|
| (b) Tides (Cont'd.) | | |
| (b.2) Meteor trails | 80-120 km | 3-22 (Chop.6), 3-34 |
| (b.3) Electron temperature in the E-region | 100-150 km | 3-35 |

Toble 3-2. Possible mechonisms for the generotion of grovity woves in the otmosphere.

(a) Winds blowing transversely over mountain ronges, or equivolent effects on the oir motion produced by worm cities, etc., either directly or by vortices produced by oir flows over non-uniform surfaces (cf. Reference 3-18, p. 120).

(b) Volconic eruptions, thunderstorms, hurricones, typhoons, tornadoes, ond similor di omotic meteorologicol disturbonces.

(c) Temperoture inversions in the lower portion of the otmosphere produce o fluctuoting wind, which correlotes with grovity woves observed on clouds at the lower levels (cf. Reference 3-18, p. 121).

(d) Solar heoting ond photodissociotian with the strotosphere/mesosphere, leoding to locol expansion.

(e) Photochemical "pumping" by either oxygen dissociotion (Reference 3-36) or ozone dissociotion (Reference 3-37).

(f) Auroral currenrs (References 3-38, 3-39).

(g) Turbulent motion in the 55-60 km oltitude region of the otmosphere (Reference 3-40).

Table 3-3. Possible mechanisms for the dissipation of atmospheric grovity waves.

| |
|---|
| (a) Mode coupling, i.e., nonlineor processes in which energy passes from ane wave into others. |
| (b) Frictianal damping, produced by viscosity and thermal conductivity (cf. Reference 3-41). |
| (c) Generation of turbulence (cf. References 3-42, 3-43). |
| (d) Vibrotionol relaxotion (cf. Reference 3-44; see also Item (e) in Table 3-2). |
| (e) Plasmo damping effects (cf. Reference 3-45). |
| (f) Radiotion damping (cf. Reference 3-46). |

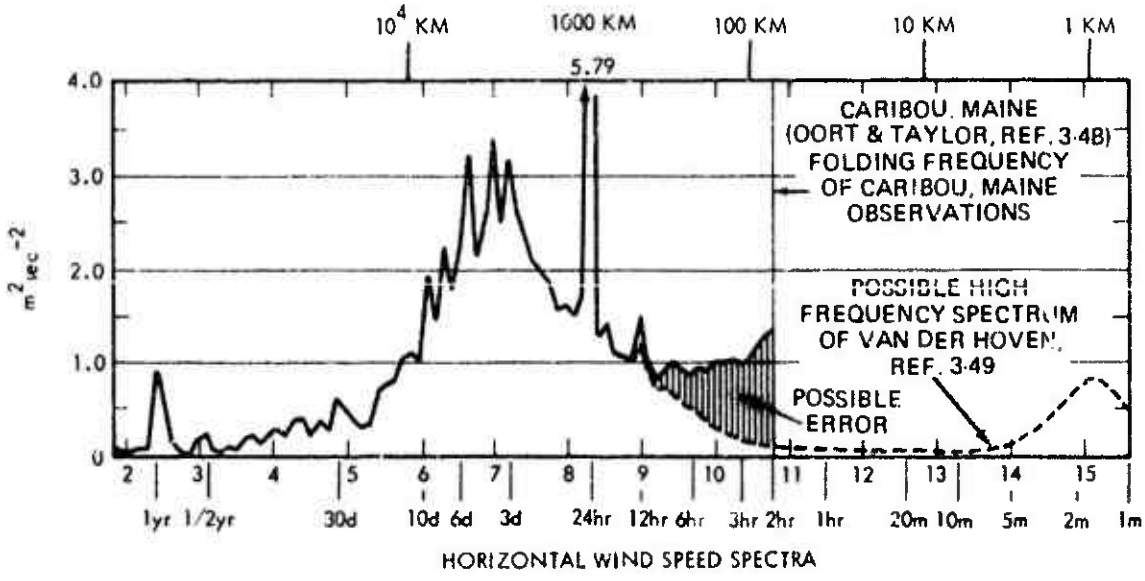


Figure 3-3. Wind speed spectra ot sea level.

There appears to be a significant flux of gravity waves in the F-region, where it drives certain ionospheric wave motions, the "Traveling Ionospheric Disturbances" (TID's). If efficient mechanisms exist for driving these waves, they may originate from higher altitudes, even from the magnetosphere or from auroral bursts, in view of the inversion of electron density with height at a maximum around 300 km. However, it seems more likely that the waves originate at low altitudes and are not all attenuated in passing upward through the 100-200 km altitude range.

The known significant effects of gravity waves may be summarized as follows:

(a) The waves produce high-altitude velocity fluctuations which lead to a number of effects, listed in Table 3-1.

(b) In particular, at altitudes below 90-120 km the gravity waves may be responsible for wind patterns that produce local instabilities which lead to turbulent mixing in the atmosphere. This relatively efficient mixing is the main mechanism for establishing the "homosphere", the coarsely uniformly mixed atmosphere below these altitudes.

(c) For altitudes above 100 km, gravity waves and tides (cf. Reference 3-50) can provide a significant mechanism for vertical energy transfer.

(d) The character of Sporadic-E events is determined partly by wind shears and partly by atmospheric mixing, both of which are clearly related to effects associated with gravity waves.

(e) In the F-region, gravity waves give rise to particular motions of ionization, i.e., the Sudden and Traveling Ionospheric Disturbances, and evidence exists that F-region ionospheric disturbances correlate with severe storms in the troposphere (cf. Reference 3-27, pp. 171-178; and Reference 3-33).

(f) Gravity waves may also influence the vertical transport of minor species (cf. Reference 3-51).

## 3.5 ATMOSPHERIC TURBULENCE

### 3.5.1 Introduction

In general a fluid is considered to be in turbulent motion when its movement is so irregular that the velocity at any given position and time in the fluid is not found to be the same when it is measured several times under seemingly identical conditions; however, the average properties of the motion are determined uniquely by the initial and boundary conditions. These motions may be amenable to description by statistical methods. *

In turbulent motion eddies of varying sizes tend to move about as entities, while simultaneously breaking up and transferring their energy to smaller eddies. Eventually the eddies become so small that viscous dissipation transforms their energy of motion into random thermal motion or heat.

If the velocity $\underset{\sim}{u}$ and pressure p are expressed as the sum of appropriate mean values $\underset{\sim}{\bar{u}}$ and $\bar{p}$ and fluctuations $\underset{\sim}{u}'$, $p'$ :

$$\left.\begin{aligned} \underset{\sim}{u} &= \underset{\sim}{\bar{u}} + \underset{\sim}{u}' \qquad \text{(a)} \\ p &= \bar{p} + p', \qquad \text{(b)} \end{aligned}\right\} \qquad (3\text{-}35)$$

then for an incompressible fluid the equations of continuity for the velocity components $u_i$ (i = x, y, z) are (the summation convention over repeated indices is not used here):

---

*One important but specific problem which is well known to aerodynamicists deals with the onset of turbulence in shear flow. Here turbulence sets in when the magnitude of inertial forces is sufficiently large compared to the viscous dissipative forces. The fluctuations in the motion will be significant if viscous damping is sufficiently small, and the criterion for the onset of shear turbulence is normally expressed in terms of the Reynolds number, Re, (Section 3.2.4), in that $Re > Re_{crit}$ is required for shear turbulence to be established. However, it must be stressed that atmospheric turbulence is a different kind of unstable motion. The criterion for its onset is usually expressed in terms of the Richardson's number, Ri, of Equation (3-46), and this does not involve the viscosity directly.

$$\left.\begin{aligned} &\Sigma_i (\partial \bar{u}_i / \partial x_i) = 0 && \text{(a)} \\ &\partial \bar{u}_i / \partial t + \Sigma_j \bar{u}_j \partial \bar{u}_i / \partial x_j = -(1/\rho)\partial \bar{p} / \partial x_i \\ &\qquad + \Sigma_j (\partial / \partial x_j)[\nu \partial \bar{u}_i / \partial x_j - \overline{u_i' u_j'}] \ ; && \text{(b)} \end{aligned}\right\} \quad (3\text{-}36)$$

$$\left.\begin{aligned} &\Sigma_i (\partial u_i' / \partial x_i) = 0 && \text{(a)} \\ &\partial u_i' / \partial t + \Sigma_j \bar{u}_j \partial u_i' / \partial x_j = -\Sigma_j u_j' \partial \bar{u}_i / \partial x_j \\ &\qquad - (1/\rho)\partial p' / \partial x_i + \nu \nabla^2 u_i' \\ &\qquad - \Sigma_j (\partial / \partial x_j)[u_i' u_j' - \overline{u_i' u_j'}] \ . && \text{(b)} \end{aligned}\right\} \quad (3\text{-}37)$$

Here $\nu \equiv \mu/\rho$ is the kinematic viscosity. The quantity $\{-\rho[\overline{u_i' u_j'}]\}$ is called a "Reynolds stress", and an eddy viscosity K is introduced by the relation:

$$-\overline{u_i' u_j'} \equiv K \partial \bar{u}_i / \partial x_j \ . \quad (3\text{-}38)$$

This eddy viscosity K is somewhat analogous to the kinematic viscosity $\nu$ in determining appropriate stresses and dissipation rates. However, this analogy must not be taken beyond its appropriate limits: molecular viscosity (denoted by terms in $\nu$) applies to arbitrary flows $\bar{u}$, while eddy viscosity (denoted by terms in K) applies only to the appropriately averaged flows $\bar{u}$. Furthermore, K may not be a constant and may depend explicitly on the structure of the turbulence. (See also Reference 3-52.)

Insofar as the fluctuation terms $u'$, $p'$ are not negligibly small, the equations for $\bar{u}_i$ and $u_i'$ are non-linear, and thus extremely difficult to solve. The principal interest, however, lies in statistical quantities, since detailed information with arbitrarily fine space- and time-resolution would not be particularly useful.

Multiplying Equation (3-37b) by $u_i'$, summing over i, transforming, and neglecting terms arising from the inhomogeneity of turbulence such as:

$$(\partial / \partial x_j)\overline{u_i'^2} \ ; \ \Sigma_i (\partial / \partial x_i)\overline{p' u_i'} \ ; \ (\partial / \partial x_j)\overline{u_i'^2 u_j'} \ ,$$

yields an energy equation:

$$(\partial/\partial t)[1/2\Sigma_i \overline{u_i'^2}] = -\Sigma_i\Sigma_j \overline{u_i' u_j'}\, \partial\bar{u}_i/\partial x_j - \nu\Sigma_i\Sigma_j \overline{(\partial u_i'/\partial x_j)^2}, \quad (3\text{-}39)$$

(i) (ii) (iii)

indicating that the time rate of change of turbulent energy (i) is determined by the balance between energy production from wind shear (ii) (which may be written as $[-K\Sigma_i\Sigma_j(\partial\bar{u}_i/\partial x_j)^2]$ from the definition of Equation (3-38)), and the dissipation of energy by molecular viscosity (iii) (which is customarily denoted by $\epsilon_\nu$ (dimension $L^2/T^3$)):

$$\epsilon_\nu = \nu\Sigma_i\Sigma_j \overline{(\partial u_i'/\partial x_j)^2} \; . \quad (3\text{-}40)$$

It is customary to Fourier-analyze the fluctuating velocity component and make a spectral analysis of the turbulent kinetic energy. Let F(k) be the spectrum of the turbulent kinetic energy in wave number (k) space, where:

$$k = 2\pi/\text{wavelength} \; ; \quad (3\text{-}41)$$

$$1/2\Sigma_i \overline{u_i'^2} = \int_0^\infty F(k)\, dk \; . \quad (3\text{-}42)$$

The character of a representative spectrum for homogeneous turbulence is shown in Figure 3-4. If the turbulence is driven by (large-scale) disturbances of length scale $L_o$, then a driving or "non-universal range" of turbulence can be defined for:

$$k < k_o = 2\pi/L_o \; . \quad (3\text{-}43)$$

As the turbulence is dissipated by viscosity, a "viscous subrange" is characterized by:

$$k > k_\nu = (\epsilon_\nu/\nu^3)^{1/4} \; , \quad (3\text{-}44)$$

i.e., the size of the smallest eddies is of the order of $L_\nu = 2\pi/k_\nu$. Between the driving and dissipating ranges lies the "inertial subrange" in which the eddies are downgraded to smaller and smaller sizes in a statistically uniform way. In the case of homogeneous, isotropic turbulence in an incompressible medium, the spectrum in the inertial subrange is characterized by Kolmogoroff's law:

$$F(k)_{Kolm} = A\epsilon_\nu^{2/3} k^{-5/3} , \qquad (3\text{-}45)$$

where A is a universal constant.

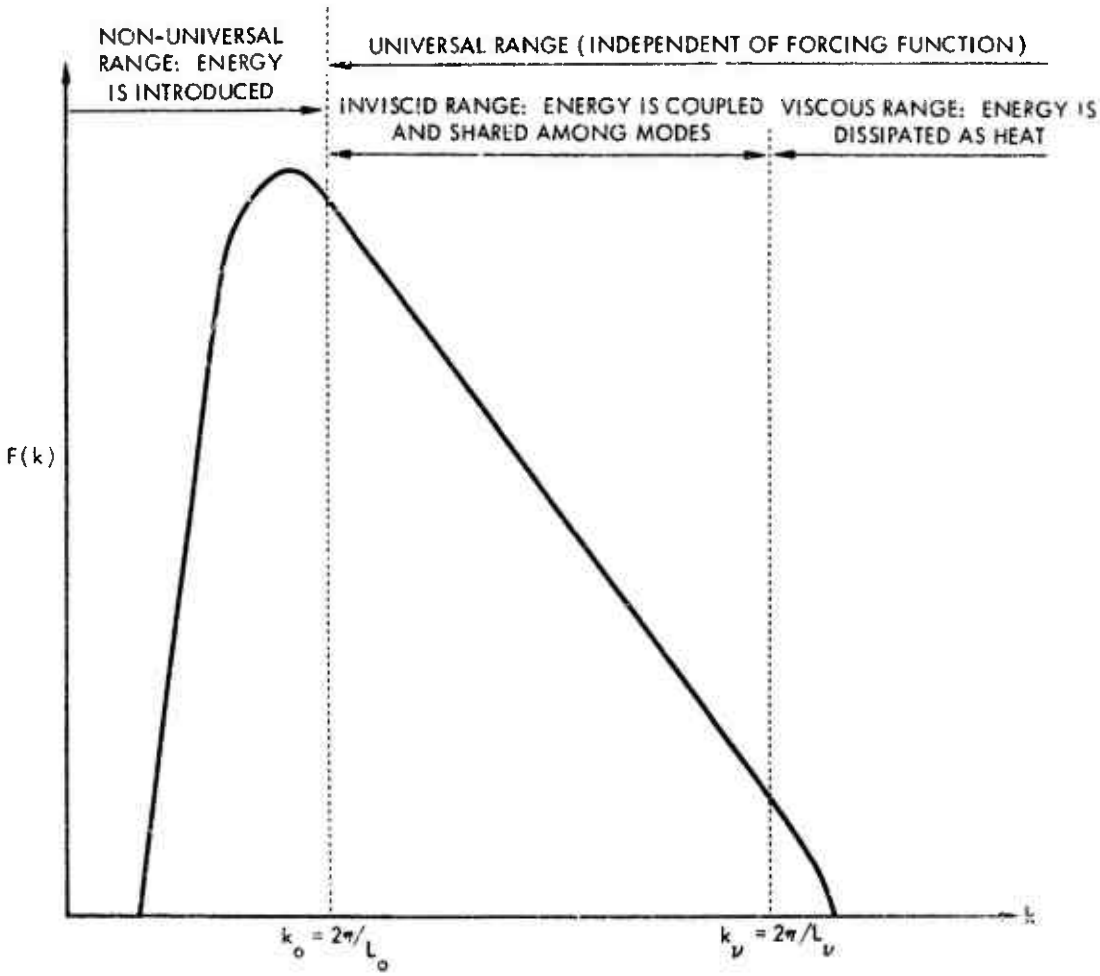


Figure 3-4. General character of the turbulent power spectrum F(k) .

### 3.5.2 Turbulence in the Atmosphere

The earth's atmosphere is not a homogeneous, isotropic, incompressible medium, and therefore the simple model of turbulence presented in the preceding subsection does not suffice to describe the whole problem. Nevertheless, that model does provide a useful starting point for the analysis; and the two characteristic dimensions

of turbulence discussed previously, namely the driving length $L_o$ or the related wave number $k_o = 2\pi/L_o$ of Equation (3-43), and $k_\nu$, the scale of viscous dissipation of Equation (3-44) or the related length $L_\nu = 2\pi/k_\nu$, are still useful concepts. Representative numerical values in the mesosphere are $L_o \sim 100\text{-}1000$m, $L_\nu \sim 0.1\text{-}10$m (cf. Figure 3-2b).

The atmosphere is observed to be usually turbulent below the turbopause which is located at 100-120 km altitude. Above this altitude molecular diffusion becomes so rapid, owing to the low ambient density, that it dominates turbulent mixing on an overall basis. However, it should be noted that small-scale or microturbulence has been observed at higher altitudes, depending on the local generating mechanism: turbulent motions are thus found even in the magnetosphere.

It should be noted that the driving mechanism in atmospheric turbulence is different in different altitude regions. Near the ground there are strong but small-scale wind gradients which produce turbulence, while in the troposphere, where the temperature decreases with altitude, turbulent motions can develop without being damped by thermal stratification. At higher altitudes the wind and gravity waves produce turbulence; thus observations of winds and wind shears from rocket releases indicate the existence of a strongly turbulent region around 85-120 km under most conditions, and to a lesser degree also at 50-55 km (see, for example, Reference 3-40).

The criterion for atmospheric turbulence is normally expressed in terms of the Richardson's number, Ri, which is defined as:

$$\mathrm{Ri} \equiv [(g/\overline{T})(\partial\overline{T}/\partial z) + (\gamma - 1)g^2/c_o^2]/\omega_s^2 \ , \qquad (3\text{-}46)$$

where $\omega_s = \overline{\partial u_{horiz}}/\partial z$ is the wind shear (cf. Equation (3-25)). Experiments show that flows are unstable for:

$$\mathrm{Ri} < \mathrm{Ri}_{crit} \simeq 0.08\text{-}0.25 \ . \qquad (3\text{-}47)$$

The nature of atmospheric turbulence changes significantly at the tropopause. Below this altitude ($\sim$11 km), the temperature falls off rather sharply with increasing height so that typically $\mathrm{Ri} < \mathrm{Ri}_{crit}$, and thus massive atmospheric instability leads to turbulence. Above the tropopause $\langle \mathrm{Ri} \rangle_{av} > \mathrm{Ri}_{crit}$, but turbulence is observed not infrequently at higher altitudes when wind shears and thermal gradients

are appropriate. In particular, this occasional mixing produces the homosphere, or coarsely uniformly mixed atmosphere below the "turbopause" at 100-120 km.

An obvious question arises as to the relation between the Richardson's number criterion (Equation 3-47) and the Reynolds' number criterion (Section 3.2.4) for producing turbulence. Tchen (Reference 3-53) finds that in the atmosphere the energy conservation equation (3-39) can be written as:

$$(\partial/\partial t)[1/2\Sigma_i \overline{u_i'^2}] = \epsilon_s(1 - 4Ri) + \epsilon_\nu(Re - 1) \ . \qquad (3\text{-}48)$$

[term (i) of Equation (3-39)]

Instability clearly occurs when the total energy change is positive, i.e., when term (i) is positive, and this can be achieved under different conditions relating Re , Ri , $\epsilon_s$ , and $\epsilon_\nu$ . (It must be stressed that the model on which this concept of instability is based is still oversimplified, so that turbulence may exist beyond the indicated criterion of stability.)

The spectrum of atmospheric turbulence is not completely characterized by Kolmogoroff's law (3-45), but rather, for $k < k_g$ , is given by:

$$k_g = \epsilon_\nu^{-1/2} N^{3/2} \ . \qquad (3\text{-}49)$$

There is in this case a buoyancy subrange with a spectrum:

$$F_{buoy}(k) \sim N^2 k^{-3} \ , \text{ for } k_o < k < k_g \ , \qquad (3\text{-}50)$$

whereas for $k > k_g$ there is an inertial subrange characterized by a Kolmogoroff spectrum (cf. Reference 3-43). Further complications exist, which are not discussed here. Indeed the overall understanding of this whole field of atmospheric turbulence is undergoing rapid changes.

### 3.5.3 Diffusion of Artificially Released Chemical Clouds: Micro and Macroturbulence

Atmospheric turbulence is of interest because it provides a mixing mechanism which is often much more effective than molecular

diffusion. Thus it is appropriate to study the rate of expansion of a chemical cloud. For example, diffusion in the upper atmosphere is measured most commonly by watching the dispersion of a smoke trail, of a luminous trail resulting from a rocket or grenade release, or of the ionized trail of a meteor.

Consider the diffusion of a test species released at some point. In a uniform atmosphere with no wind and no chemical interaction, the Fickian diffusion equation is commonly used:

$$\partial n/\partial t = \nabla(D\nabla n) \ , \tag{3-51}$$

where n is the species concentration and D the effective diffusion coefficient.

For the simplest possible case of one-dimensional flow with constant diffusivity D , Equation (3-51) reduces to:

$$\partial n/\partial t = D\partial^2 n/\partial x^2 \ . \tag{3-52}$$

For a point source at $x = 0$ , $t = 0$ , this equation has the solution:

$$n = (\text{const})(4\pi Dt)^{-1/2} \exp(-x^2/4Dt) \ , \tag{3-53}$$

giving the mean-square dispersion as:

$$\overline{x^2} = 2Dt \ . \qquad \text{(a)}$$

This result (3-54a) is valid for distances large compared to the turbulent length scale or (for molecular diffusion) to the molecular mean free path. For much shorter distances the particles move in a straight line, so that:

$$\overline{x^2} = v^2t^2 \ . \qquad \text{(b)}$$

(3-54)

where v is the initial velocity.

In the case of molecular diffusion, D in Equation (3-51) is replaced by:

$$D_{mol} = \alpha_d \bar{c} \ell_m \ , \qquad (3\text{-}55)$$

where $\alpha_d$ is a numerical constant of the order of unity, not necessarily equal to $\alpha_v$ of the related Equation (3-14), for which the other quantities were defined above.

For the case of turbulent diffusion, it might appear that the diffusion equation (3-51) could be used, with the diffusivity D equal to the sum of the eddy diffusivity $D_{eddy}$ and of the molecular diffusivity $D_{mol}$. However, this is not universally correct, as may be seen by distinguishing between two cases which depend on whether the effective size of the cloud (or the relevant separation of two test particles) L is greater or smaller than the largest effective scale of turbulence, $L_o$ of Equation (3-43). It is possible to define:

$$\left.\begin{array}{ll} \underline{\text{Microturbulence}} \text{ for } L_o \ll L \ ; & \text{(a)} \\ \underline{\text{Macroturbulence}} \text{ for } L_o \gg L \ . & \text{(o)} \end{array}\right\} \qquad (3\text{-}56)$$

In the case of microturbulence the Fickian diffusion equation (3-51) applies, but with an appropriate larger but constant value of the diffusivity $D = D_{eddy} + D_{mol}$. However, for the case of macroturbulence this is no longer so: while the small scales of turbulence ($k^{-1} < L/2\pi$) will change the separation distance between a pair of particles, the large scales ($k^{-1} > L/2\pi$) will simply transport them without modifying their distance of separation. Thus the diffusion coefficient will vary during the growth of the cloud. Upon introducing a probability $G(\ell, t)$ for the separation distance $\ell$ between a pair of particles, the diffusion equation can be written:

$$\partial G/\partial t = (\partial/\partial t) \{D(\ell) \partial G/\partial \ell\} \ , \qquad (3\text{-}57)$$

in which the effective diffusion coefficient depends on the distance $\ell$.

Since D depends on the spectrum of turbulence, then for a turbulent power spectrum of the type:

$$\left.\begin{array}{ll} F(\kappa) \sim k^{-n} \ , & \text{(a)} \\ \text{dimensional considerations give a diffusion coefficient of the form:} & \\ D(\ell) \sim \ell^{(n+1)/2} \ . & \text{(b)} \end{array}\right\} \qquad (3\text{-}58)$$

Thus the Kolmogoroff spectrum of Equation (3-45) gives:

$$\left.\begin{aligned} D_{Kolm}(\ell) &\sim \epsilon_\nu{}^{1/3}\,\ell^{4/3} \; ; && \text{(a)} \\ \text{hence:} & \\ \overline{\ell^2} &\sim \epsilon_\nu Q t^3 \; , && \text{(b)} \end{aligned}\right\} \quad (3\text{-}59)$$

while the buoyancy spectrum of Equation (3-50) gives:

$$D_{buoy}(\ell) \sim N\ell^2 \; . \qquad (3\text{-}60)$$

Therefore $\overline{\ell^2}$ would increase rather rapidly with t .

It should be noted that experimental data on cloud expansion under different conditions give results ranging from $\overline{\ell^2} \sim t$ to $\overline{\ell^2} \sim t^3$ . (See, for example, Reference 3-54.)

### 3.5.4 The Effective Diffusion Coefficient in the Atmosphere

The actual problem of atmospheric diffusion is not as simple as the idealized problem discussed in Section 3.5.3 because of the stratification of the atmosphere and the presence of (predominantly horizontal) winds.

The effect of horizontal winds should be taken into account, but this is not easy. In particular, in actual measurements there is often a problem of distinguishing between fluctuating winds and turbulent diffusion. This is not a trivial matter because in the actual atmosphere the distinction between gravity waves and turbulence is not always clear-cut.

A model for the diffusion coefficient as a function of altitude is given in Figure 3-5. The results at low altitudes come from meteorological data (e.g., smoke signals, constant-altitude balloons), at intermediate altitudes from smoke trails and rocket grenades, and at higher altitudes (> 70 km) from chemical releases and meteor trails (cf. Reference 3-7). A typical time-scale of observations is of the order of minutes to hours, and the ranges of data are due to the inherent variability of meteorological conditions as well as to errors in measurement and differences in time scales. Curves "A"

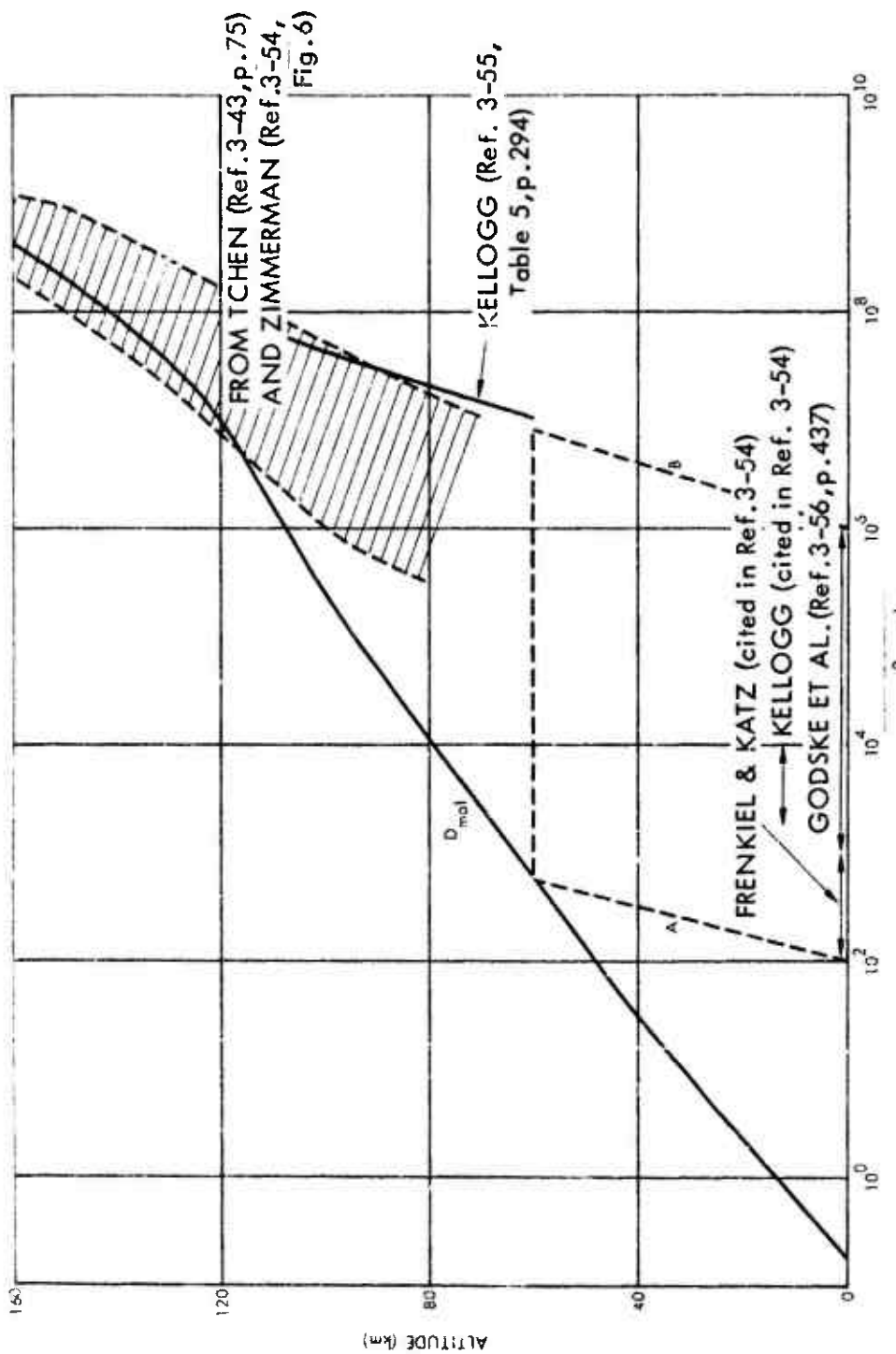


Figure 3-5. Effective atmospheric diffusion coefficient D as a function of altitude.

and "B" of Figure 3-5 indicate plausible minimum and maximum diffusivity values in this altitude range. The variability of the data may reflect in part the difficulty of distinguishing between diffusion and convection induced by variable winds in the meteorological observations.

It must be stressed that the diffusion coefficients of Figure 3-5 (or indeed any such quantity) cannot be applied indiscriminately. Thus in Figure 3-6 some representative data are shown, on the variation of $D_{horiz}$ with time from one to 100 hours; it is of interest to note, in addition to the time variation, the broad scatter of the observations. For shorter time periods, the following simple argument may be considered, in terms of Prandtl's "mixing-length theory":

$$D \sim u\lambda \ , \tag{3-61}$$

where $u \sim 1\text{-}10$ m/sec, and $\lambda$ is the "mixing length". Thus $D \sim 10^6$ cm$^2$/sec implies $\lambda \sim 10\text{-}100$ m, or $\tau = \lambda/u \sim 1\text{-}100$ sec. Then it would take at least this time ($\tau$) for turbulent dispersion to occur, and accordingly the D values of Figure 3-5 or similar sources should not be used for times shorter than the $\tau$ indicated, viz., 1-100 sec.

## 3.6 EFFECT OF TURBULENCE ON CHEMISTRY IN THE UPPER ATMOSPHERE

The simplest possible model for species concentration in the atmosphere assumes that below some turbopause (say, 100-120 km) all chemical species are uniformly mixed, while above this turbopause they all tend towards diffusive equilibrium. Mathematically, the concentration of species j at height z is then:

$$\left.\begin{aligned} n_j(z) &\sim e^{-(z-z_o)/H_{av}}, \quad H_{av} = \mathcal{R}T/m_{av}g \quad \text{(below the turbopause)} \qquad \text{(a)} \\ n_j(z) &\sim e^{-(z-z_o)/H_j}, \quad H_j = \mathcal{R}T_j/m_j g \quad \text{(above the turbopause)}^* \qquad \text{(b)} \end{aligned}\right\} \tag{3-62}$$

*For a non-LTE gas, each component j may have a separate temperature $T_j$ defined as $T_j = p_j m_j/\rho_j \mathcal{R}$.

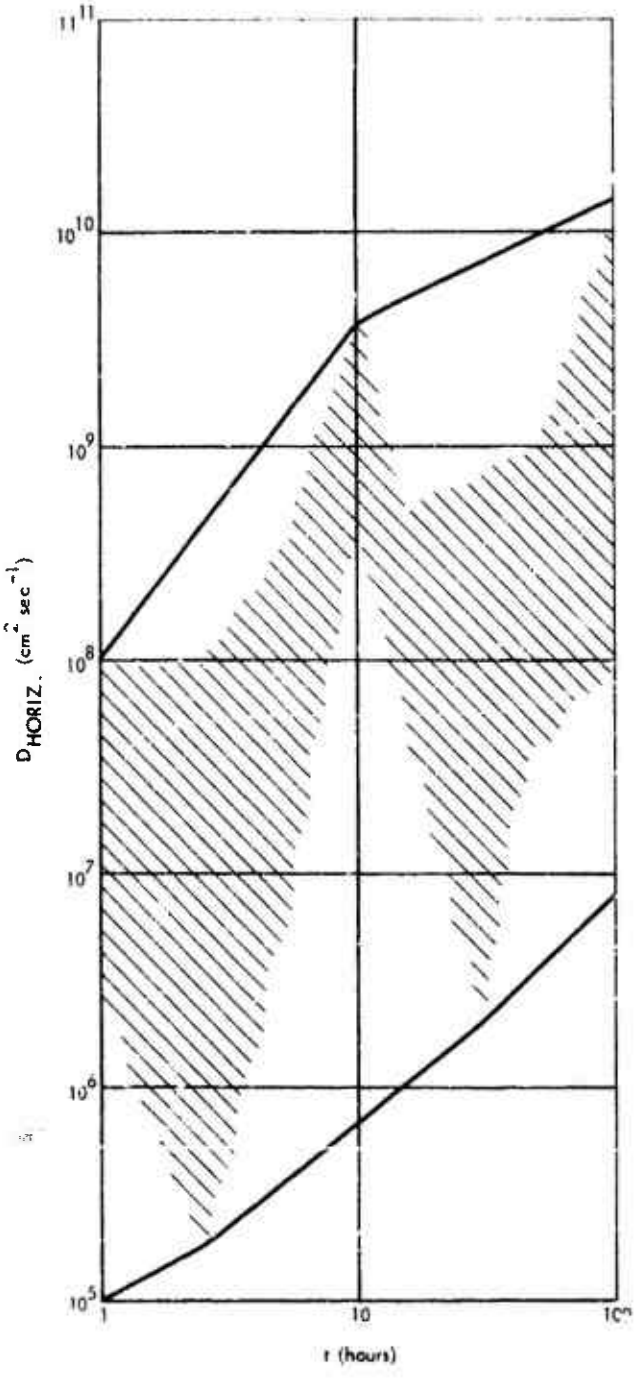


Figure 3-6. Change of horizontal diffusion coefficient with time (replotted from Hefter (Reference 3-57)).

where $m_{av}$ is the mass of an "average air molecule" and $m_j$ is the mass of a molecule of species j ; $z_o$ is some constant reference altitude. Note that while $H_{av} \simeq 7$ km for $T \simeq 250$ K, $H_{He}/H_{Ar} = 10$ because of the mass ratio, so that a significant difference exists between the two limits of Equation (3-62).

The simple models of Equation (3-62) do not represent the actual species concentrations; thus in the present section some of the problems arising from the interaction of diffusion and chemistry will be reviewed for the oxygen photodissociation-recombination process:

$$\left.\begin{aligned} O_2 + h\nu\,(\text{solar}) &\rightarrow O + O \qquad (a) \\ O + O + M &\rightarrow O_2 + M \qquad (b) \end{aligned}\right\}, \tag{3-63}$$

where $h\nu$ (solar) represents all solar flux that photodissociates the oxygen molecule, while M is any third body, atomic or molecular, acting as a recombination catalyst. These two reactions are not only very important in the thermosphere, but they also display the general problems involved in the interaction of diffusion and chemistry in the upper atmosphere.

In the region above 90 km the vertical distribution of $O_2$ and O concentrations, denoted by $n_2$ and $n_1$ respectively, may be written as a solution of the following system:

$$\left.\begin{aligned} \partial n_2/\partial t + (\partial/\partial z)(n_2 u_2) &= -J n_2 + \alpha n_1^{\,2} \qquad (a) \\ \partial n_1/\partial t + (\partial/\partial z)(n_1 u_1) &= 2(J n_2 - \alpha n_1^{\,2}) \qquad (b) \end{aligned}\right\}. \tag{3-64}$$

Here only spatial dependence in the (vertical) z-direction is considered, so that $u_1$ and $u_2$ are the vertical components of the diffusion velocity of O and $O_2$, respectively, which involve the molecular and eddy diffusivities. The molecular diffusivity is calculated according to classical theory (cf. Reference 3-4); J and $\alpha$ are effective rate coefficients (including the solar flux and third-body concentrations) for processes (3-63a) and (3-63b), respectively. The earliest theory of molecular oxygen dissociation in the upper atmosphere was given by Chapman (References 3-58, 3-59). The effects of turbulent diffusion were first included by Colegrove, Hansen, and Johnson (References 3-60, 3-61), who gave a steady-state solution,

considering only the equation of continuity with the chemistry of Equation(3-63), and with an effective eddy diffusivity. Shimazaki (References 3-62, 3-63) treated the time-dependent problem with a diurnal and zenith variation of solar flux, i. e., of $J$, in order to study how a steady state is established. Still later Keneshea and Zimmerman (Reference 3-64) solved Equations (3-64) for the case where the vertical velocity $u_j$ of species $j$ is made up of the sum of laminar and turbulent contributions to the vertical velocity of species $j$, each involving a single effective diffusivity, molecular or eddy.

In Figure 3-7 results are shown from several calculations of the molecular oxygen concentration in the region where process (3-63) is effective. "Photochemical equilibrium" (curve 1 in Figure 3-7) indicates that chemistry is considered, but not diffusion; "diffusive equilibrium" (curve 2) means that chemistry and only molecular diffusion are considered; "total mixing theory" (curve 3) denotes that chemistry and both molecular and turbulent diffusion are included. At the higher altitudes the experimental values (curve 4) are quite different from the photochemical equilibrium theory, and somewhat different from the molecular equilibrium theory, indicating the importance of turbulent mixing. If the atomic oxygen concentration were also shown as a function of height, it would turn out that turbulent mixing is necessary to explain the O-atom concentration at the lower altitudes. Such a plot is omitted here because of major uncertainties in the measured concentrations of atomic oxygen at the lower altitudes (cf. Reference 3-65).

As was pointed out in Section 3.5, the effect of turbulence on transport cannot be represented under all conditions by a constant eddy diffusivity. Not only is the eddy diffusivity itself a function of space or time; the whole concept of an "eddy diffusivity" has severe limitations. Thus Tchen (Reference 3-68) considers the effect of turbulent transport on a chemically reacting system (the oxygen dissociation system of Equation (3-63)) in terms of a correlation of density and velocity fluctuations rather than just an effective eddy diffusivity. (See also Reference 3-2, Section 6.)

In addition to molecular and thermal diffusion coefficients $D_m^j$ and $D_{th}^j$ for species $j$, the corresponding turbulent or eddy diffusivities are introduced:

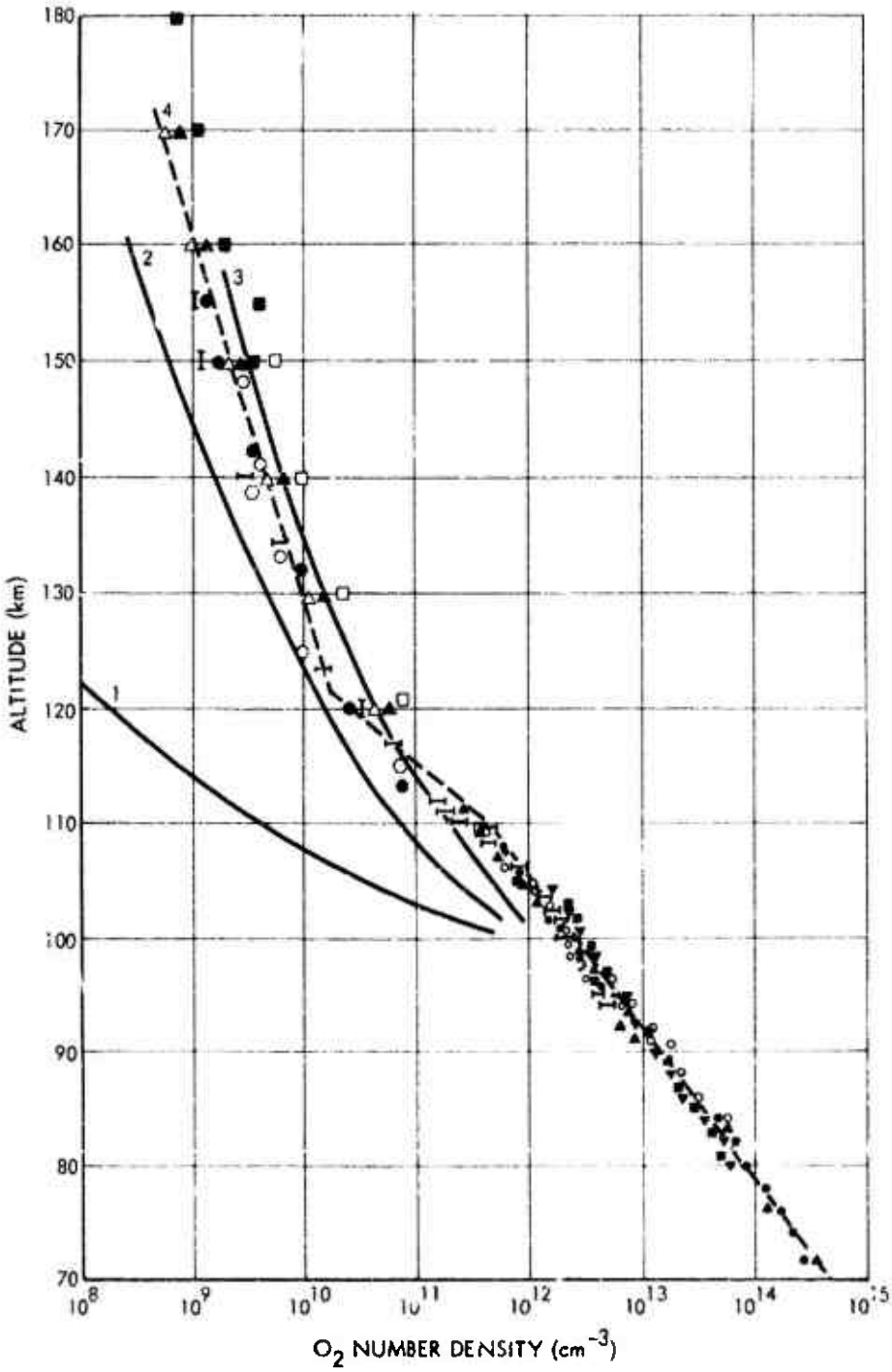


Figure 3-7. Distribution of molecular oxygen: (1) photochemical equilibrium, (2) diffusive equilibrium, (3) total mixing theory (Danilov, Reference 3-66), (4) curve passing through experimental data, based upon data of Keneshea and Zimmerman (Reference 3-64), Weeks and Smith (Reference 3-67).

$$D_{nn}{}^{j} = (\bar{c}_j{}^2/\bar{n}_j{}^2)\int_0^\infty d\tau\, \overline{n_j'(0)n_j'(\tau)} \qquad \text{(a)}$$

$$D_{nT}{}^{j} = (\bar{c}_j{}^2/\bar{n}_j\bar{T}_j)\int_0^\infty d\tau\, \overline{n_j'(0)T_j'(\tau)} \qquad \text{(b)} \qquad \Big\} \quad (3\text{-}65)$$

Here $n_j$ , $T_j$ are the number densities and effective temperatures of species $j$ ; separation (as exemplified in Equation (3-35)) into mean values ($\bar{n}_j$ , $\bar{T}_j$) and fluctuations ($n_j'$, $T_j'$) is made; and $\bar{c}_j$ is the mean thermal speed of species j .

The point is that for a strongly non-uniform (turbulent) flow the molecular and thermal diffusivities as well as their turbulent analogs $D_{nn}{}^{j}$ and $D_{nT}{}^{j}$ of Equation (3-65) become significantly different, a case which Tchen (Reference 3-68) calls non-isomeric. Carrying through the analysis for an atmosphere in a steady state, so that $(\partial/\partial t) \equiv 0$ , with spatial variation only in the vertical (z) direction, integration of the equations analogous to (3-64) yields:

$$-(d/dz)\ln\bar{n}_j = 1/\bar{h}_j + (1+\beta_2{}^{j})/H_j + (1+\beta_1{}^{j}+\beta_2{}^{j})(d\ln T_j/dz) - 1/L_j \ , \qquad (3\text{-}66)$$

where:

$$\overline{h_j}^{-1} = -\bar{x}_j/\bar{n}_j(D_m{}^{j} + D_{nT}{}^{j}) \qquad \text{(a)}$$

$$L_j{}^{-1} = [\underset{\sim}{u} + \bar{c}_j{}^{-1}(\underset{\sim}{D}_{nu}{}^{j}\cdot\nabla)\underset{\sim}{u}]_z/(D_m{}^{j} + D_{nT}{}^{j}) \qquad \text{(b)}$$

$$\beta_1{}^{j} = (D_{th}{}^{j} - D_m{}^{j})/(D_m{}^{j} + D_{nT}{}^{j}) \qquad \text{(c)}$$

$$\beta_2{}^{j} = (D_{nn}{}^{j} - D_{nT}{}^{j})/(D_m{}^{j} + D_{nT}{}^{j}) \qquad \text{(d)} \qquad \Big\} \quad (3\text{-}67)$$

Here:

$$\underset{\sim}{D}_{nu}{}^{j} = (\bar{c}_j{}^2/\bar{n}_j|\underset{\sim}{u}_j|)\int_0^\infty d\tau\, \overline{n_j'(0)\,u_j'(\tau)} \ , \qquad \text{(a)}$$

$$\bar{x}_j \equiv |\underset{\sim}{\bar{x}}_j| \ ; \qquad \text{(b)} \qquad \Big\} \quad (3\text{-}68)$$

where $\underset{\sim}{\bar{x}}_j$ is defined by:

$$\nabla\cdot\underset{\sim}{\bar{x}}_j \equiv \bar{S}_{c;j}/m_j \ , \qquad \text{(c)}$$

in terms of the source function of Equation (3-1) for the oxygen dissociation process. In Equations (3-67a-d), $\bar{h}_j^{-1}$ is a measure of the effect of chemistry, $L_j^{-1}$ the effect of wind shear, $\beta_1^j$ the non-isomeric molecular diffusivity, and $\beta_2^j$ the effect of non-isomeric turbulent diffusivities. The effect of turbulence on the structure of the chemical reaction rate term, $\bar{x}_j$, is discussed below.

Equation (3-66) should be compared with the simple equation:

$$-(d/dz) \ln \bar{n}_j = 1/H_j \; ; \; H_j = \mathcal{R}T_j/m_j g \; , \tag{3-69}$$

(cf. Equations (3-21) and (3-62)) which applies in the absence of:

(1) temperature gradients;

(2) wind shears, the term $L_j^{-1}$;

(3) non-isomeric molecular diffusion ($\beta_1^j = 0$);

(4) non-isomeric turbulent diffusion ($\beta_2^j = 0$); and

(5) chemistry, the term $\bar{h}_j^{-1}$ .

The overall effects of these five factors, as well as of turbulence, are very complicated, and may either reinforce or compensate one another. A detailed discussion of Equation (3-66) is given by Bauer, Selvyn, and Tchen (Reference 3-2); deviations from the predicted fall-off of molecular oxygen concentrations with height, as shown in Figure 3-7, can be explained by appropriate choices of the various parameters.

It was pointed out above that the existence of turbulent mixing can change the effective concentration of chemical reactants, even if there is no change in the chemical reaction rates themselves. However, the presence of turbulence may change the effective rates of chemical reactions. To demonstrate this, consider the definitions in Equations (3-68b, c).

In general, $x_j$ may be a function of all the $n_j$ and $T_i$ so that it may be denoted as $x_j(\{n_i\}, \{T_i\})$. In Equation (3-67a), $\bar{h}_j^{-1}$ was seen to depend on $\bar{x}_j$, the average of $x_j$ taken by the same procedure used to obtain all the $\bar{n}_i$ and $\bar{T}_i$. Ordinarily,

$$\overline{x_j(\{n_i\}, \{T_i\})} \neq x_j(\{\bar{n}_i\}, \{\bar{T}_i\}) \; , \tag{3-70}$$

so that the effect of turbulence on the chemical reaction rate term is to change the form of $\bar{x}_j$ from that given by $x_j$, i.e., to change the effective reaction rates.

Tchen (Reference 3-68) has estimated the magnitude of this effect for the oxygen dissociation problem of Equation (3-63), and finds that:

$$\frac{\left|\overline{x_2(n_2, T_2)} - x_2(\bar{n}_2, \bar{T}_2)\right|}{x_2(\bar{n}_2, \bar{T}_2)} \lesssim 1/2 \frac{\overline{n_2'^2}}{\bar{n}_2^2} \quad , \tag{3-71}$$

which may be of the order of 10 percent or more, depending on the intensity of turbulence; under certain conditions this might produce a non-negligible effect.

## 3.7 CONCLUSIONS

The role of fluid mechanics in aeronomic problems is not very well developed; thus the present chapter coverage should not be considered as definitive. In particular, emphasis has been placed on the identification of important problems in a general discussion which stresses the shorter-period phenomena (turbulence and gravity waves) rather than the longer-time processes (tides and general circulation). Within these limitations, the following conclusions may be drawn:

1. Large-scale motions, principally horizontal winds, do cause a motion and expansion of chemically or otherwise active regions by horizontal convection, at typical speeds of 10-100 m/sec.*

2. The full significance for aeronomic problems of wind shears, tides, and acoustic gravity waves is incompletely established, but three effects are clear:

*An example where this may be important is seen in the problem of stratospheric pollution by the supersonic transport (SST): the main travel routes will be near 40° N latitude across the North Atlantic. Thus there may conceivably be a belt of water or other foreign matter at these latitudes, and even transported around the world by geostrophic winds, but it is most unlikely that the material will be distributed far beyond 30-50° N latitude.

a. These motions provide driving mechanisms for atmospheric turbulence, at least above the troposphere.

b. They provide possible mechanisms for energy transfer into various atmospheric regions, and also possibly into different degrees of freedom. The various processes (cf. Table 3-3) have not all been evaluated adequately, but in the lower thermosphere they may provide the largest single source of energy transfer under some conditions (cf. References 3-10, 3-11).

c. Tides and gravity waves induce motions of ionization in the E- and especially F-regions, i.e., the Sudden and Traveling Ionospheric Disturbances, which affect radio-wave propagation quite significantly. (See, for example, Reference 3-27.)

3. It is known that atmospheric turbulence exists for a significant fraction of the time at all altitudes below a "turbopause" at 100-120 km. Thus, it is responsible for the "homosphere", or uniformly mixed state of the major species below the turbopause, and it also affects the $O\text{-}O_2$ concentration profile in the lower thermosphere. However:

a. Atmospheric turbulence is by no means uniform and isotropic, and its detailed characteristics (intensity, Fourier spectrum, time and space variability) as well as its detailed effects on atmospheric mixing, regarding minor species and variability, are not fully known.

b. The use of a single constant eddy diffusivity $D_{eddy}$, which is very much greater than the molecular diffusivity $D_{mol}$, in the context of a Fickian diffusion equation, is frequently inadequate to describe the effects of turbulent diffusion. First, the effective eddy diffusivity tends to increase with dispersion time, and second, even under equivalent conditions of altitude, time of day, latitude, etc., the value may fluctuate over several orders of magnitude.*

*In particular, it should be noted that the quoted values of eddy diffusivity obtained from meteorological considerations apply for times of an hour or greater, and thus are not applicable to discussions of atmospheric motions associated with nuclear explosions in the atmosphere, during times less than several minutes after the burst.

c. The presence of turbulence can change the effective rate of chemical reactions.

d. Even the best available treatments of atmospheric turbulence with chemistry are incomplete, since the determination of transport coefficients as functions of wind profile and other parameters presents a problem that has not been solved adequately.

4. The effects of fluid mechanical motions should be included in aeronomic calculations. An analysis of the F2-region by Strobel and McElroy (Reference 3-69) indicates their importance, by including the wind shear in the equations of continuity for the different species. Energy transfer by tidal motions should also be included.

## REFERENCES

(N. B.: Papers and books of general interest in the field of coverage of this chapter, i.e., aside from the specific reference to material quoted in the text, are designated by the asterisk, *.)

3-1.* Delcroix, J. L., Plasma Physics, John Wiley, New York (1965).

3-2. Bauer, E., P. A. Selwyn, and C. M. Tchen, Institute for Defense Analyses Report P-756 (1971).

3-3. Moe, O. K., McDonnell-Douglas Report MDC-G2280 (1971).

3-4.* Hirschfelder, J. O., C. F. Curtiss, and R. B. Bird, Molecular Theory of Gases and Liquids, John Wiley, New York (1954).

3-5. Burgers, J. M., Flow Equations for Composite Gases, Academic Press, New York (1969).

3-6. Kuethe, A. M., and J. D. Schetzer, Foundations of Aerodynamics, John Wiley, New York (1950).

3-7.* Fedele, D., p. 34 of Reference 3-8.

3-8.* Rawer, K., Ed., Winds and Turbulence in Stratosphere, Mesosphere and Ionosphere, North-Holland Publishing Co., Amsterdam (1968).

3-9. Murgatroyd, R. J., Proc. Roy. Soc. A288, 575 (1966).

3-10. Rosenberg, N. W., and C. G. Justus, Radio Sci. 1, 149 (1966).

3-11. Zimmerman, S. P., and N. W. Rosenberg, Fourteenth COSPAR Meeting, Seattle, Washington (1971).

3-12.* Rishbeth, H., and O. K. Garriott, Introduction to Ionospheric Physics, Academic Press, New York (1969).

3-13. Liller, W., and F. J. Whipple, J. Atm. Terrestr. Phys., Spec. Suppl. 1, 112 (1954).

3-14. Kochanski, A., J. Geophys. Res. 69, 3651 (1964).

3-15.* Valley, S. L., Ed., Handbook of Geophysics and Space Environments, McGraw-Hill, New York (1965).

3-16.* COSPAR International Reference Atmosphere, North-Holland Publishing Company, Amsterdam (1965).

3-17.* United States Standard Atmosphere Supplement 1966, U. S. Government Printing Office, Washington, D. C. (1966).

3-18.* Eckart, C., Hydrodynamics of Oceans and Atmospheres, Pergamon Press, New York (1960).

3-19.* Lindzen, R. S., and S. Chapman, Space Sci. Revs. 10, 3 (1969).

3-20.* Siebert, M., Adv. Geophys. 7, 105 (1961).

3-21.* Wilkes, M. V., Oscillations of the Earth's Atmosphere, Cambridge University Press, Cambridge (1949).

3-22.* Hines, C. O., et al, Eds., Physics of the Earth's Upper Atmosphere, Prentice-Hall, Englewood Cliffs, N. J. (1965).

3-23. * Gille, J. C., p. 298 of Reference 3-8.

3-24. Gille, J. C., p. 322 of Reference 3-8.

3-25. * Dickinson, R. E., J. Atmos. Sci. 26, 73 (1969).

3-26. * Dickinson, R. E., Revs. Geophys. 7, 483 (1969).

3-27. * Georges, T. M., Ed., Symposium on Acoustic-Gravity Waves in the Atmosphere, Boulder, Colorado, Proceedings, U. S. Government Printing Office, Washington, D. C. (1968).

3-28. Theon, J. C., et al, J. Atmos. Sci. 24, 428 (1967).

3-29. Hines, C. O., "A Jet-Stream Source of Waves in Noctilucent Clouds", in Reference 3-27.

3-30. Harris, K. K., G. W. Sharp, and W. C. Knudsen, J. Geophys. Res. 74, 197 (1969).

3-31. Vasseur, G., and P. Waldteufel, J. Atm. Terrestr. Phys. 31, 885L (1969).

3-32. * Georges, T. M., ESSA Report IER 57-ITSA 54 (1967).

3-33. Baker, D. M., and K. Davies, J. Atm. Terrestr. Phys. 31, 1345 (1969).

3-34. Spizzichino, A., Ann. Geophys. 25, 697, 755, 773 (1969).

3-35. Wand, R. H., J. Geophys. Res. 74, 5688 (1969).

3-36. Leovy, C., J. Atmos. Sci. 23, 223 (1966).

3-37. Shere, K. D., and I. J. Eberstein, Bull. Am. Meteorol. Soc. 51, 387 (1970).

3-38. Blumen, W., and R. G. Handl, J. Atmos. Sci. 26, 210 (1969).

3-39. Chimonas, G., and C. O. Hines, Planet. Space Sci. 18, 565 (1970).

3-40. Murphy, E. A., et al, Trans. Am. Geophys. Union 52, 292 (1971); Abstract SA-17.

3-41. Pitteway, M. L. V., and A. Taylor, Can. J. Phys. 41, 1935 (1963).

3-42. Hodges, R. R., Jr., J. Geophys. Res. 72, 4087 (1967).

3-43. Tchen, C. M., Institute for Defense Analyses Report P-595 (1970).

3-44. Bauer, E., and W. N. Podney, Bull. Am. Meteorol. Soc. 51, 386 (1970).

3-45. Liu, C. H., and K. C. Yeh, J. Geophys. Res. 74, 2248 (1969).

3-46. Gille, J. C., J. Atmos. Sci. 25, 308 (1968).

3-47. Leovy, C., Adv. Geophys. 13, 191 (1969).

3-48. Oort, A. H., and A. Taylor, Monthly Weather Rev. 97, 623 (1969).

3-49. Van der Hoven, J., J. Meteorol. 14, 160 (1957).

3-50. Lindzen, R. S., and D. Blake, J. Geophys. Res. 75, 6868 (1970).

3-51. Hodges, R. R., Jr., J. Geophys. Res. 75, 4842 (1970).

3-52. * Starr, V. P., Physics of Negative Viscosity Phenomena, McGraw-Hill, New York (1968).

3-53. Tchen, C. M., Unpublished Work (1971).

3-54. Zimmerman, S. P., Space Res. 6, 425 (1966).

3-55. Kellogg, W. W., Space Sci. Revs. 3, 275 (1964).

3-56. * Godske, C. L., et al. Dynamical Meteorology and Weather Forecasting, Am. Meteorol. Soc., Boston (1957).

3-57. Heffter, J. L., J. Appl. Meteorol. 4, 153 (1965).

3-58. Chapman, S., Phil. Mag. 10, 345 (1930).

3-59. Chapman, S., Proc. Roy. Soc. A132, 353 (1931).

3-60. Colegrove, D. G., W. B. Hansen, and F. S. Johnson, J. Geophys. Res. 70, 4931 (1965).

3-61. Colegrove, D. G., W. B. Hansen, and F. S. Johnson, J. Geophys. Res. 71, 2227 (1966).

3-62. Shimazaki, T., J. Atm. Terrestr. Phys. 29, 723 (1967).

3-63. Shimazaki, T., J. Atm. Terrestr. Phys. 30, 1279 (1968).

3-64. Keneshea, T. J., and S. P. Zimmerman, J. Atmos. Sci. 27, 831 (1970).

3-65. Von Zahn, U., J. Geophys. Res. 75, 5517 (1970).

3-66. * Danilov, A. D., Chemistry of the Ionosphere, Plenum Press, New York (1970).

3-67. Weeks, L., and L. G. Smith, J. Geophys. Res. 73, 4835 (1968).

3-68. Tchen, C. M., Institute for Defense Analyses Report P-698 (1970).

3-69. Strobel, D. F., and M. B. McElroy, Planet. Space Sci. 18, 1181 (1970).

## SUPPLEMENTARY BIBLIOGRAPHY

(N. B.: As in the preceding list of references, papers and books of general interest are designated by the asterisk, * . Unlike the reference list, however, the works cited here are given in alphabetical order by senior author.)

* Andersen, H. C., in Kinetic Processes in Gases and Plasmas, A. R. Hochstim, Ed., Academic Press, New York (1969); Chapter 2.

* Bortner, M. H., and R. H. Kummler, General Electric Company Report GE-9500-ECS-SRI (1968).

Chasseriaux, J. M., Groupe de Recherches Ionosphériques, Saint-Maur, France, Note Technique GRI/NIP/69 (1970).

* Craig, R. A., The Upper Atmosphere: Meteorology and Physics, Academic Press, New York (1965).

* Eliassen, A., and E. Kleinschmidt, Chapter on "Dynamic Meteorology" in: Handbuch der Physik, Bd. 48, S. Flügge, Ed., Springer-Verlag, Berlin (1957); p. 1.

* Goody, R. M., Atmospheric Radiation. I. Theoretical Basis, Oxford University Press, London (1964).

Hesstvedt, E., Geophys. Publik. 27, No. 4 (1968).

Keneshea, T. J., Air Force Cambridge Research Laboratories Reports AFCRL-63-711 (1963) and AFCRL-67-0221 (1967).

Kuhn, W. R., and J. London, J. Atmos. Sci. 26, 189 (1969).

Lockey, C. W. A., et al, Nature 223, 387 (1969).

Midgley, J. E., and H. G. Liemohn, J. Geophys. Res. 71, 3729 (1966).

Monin, A. S., and A. M. Obukhoff, Tr. Geofiz., Inst. Akad. Nauk SSSR, No. 24 (151), 163 (1954).

* Murgatroyd, R. J., European Space Research Organizati n Report SP-30 (1968).

* Murgatroyd, R. J., "The Physics and Dynamics of the Stratosphere and Mesosphere", Reports Prog. Phys., To be Published (1971).

Murgatroyd, R. J., and R. M. Goody, Quart. J. Roy. Meteorol. Soc. 84, 225 (1958).

Murgatroyd, R. J., and F. Singleton, Quart. J. Roy. Meteorol. Soc. 87, 125 (1961).

Niles, F. E., "Extension of the CHEMION Code", Work in Progress (1971).

Quiroz, R. S., Ed., Meteorological Investigations of the Upper Atmosphere, Meteorol. Monographs 9, No. 31, Am. Meteorol. Soc., Boston (1968).

Rosenberg, N. W., J. Geophys. Res. 73, 4965 (1968).

* Tolstoy, I., Revs. Mod. Phys. 35, 207 (1963).

* Tverskoi, P. N., Physics of the Atmosphere: A Course in Meteorology, Transl. from the Russian, U. S. Dept. of Commerce Clearing House N66-23462 (1965).

* Webb, W. L., Ed., Stratospheric Circulation, Academic Press, New York (1969).

# 4. THE NATURAL ATMOSPHERE: ENERGY BALANCE IN THE UPPER ATMOSPHERE*

E. Bauer, Institute for Defense Analyses
R.H. Kummler, Wayne State University
M.H. Bartner, General Electric Company
(Latest Revision 16 June 1971)

## 4.1 INTRODUCTION

In order to calculate the ionization and radiation properties of the disturbed atmosphere, the density, temperature, and composition (including excited-state populations) of the atmosphere before the disturbance must be known. Many of these parameters are well established by measurements and theory, and the results are summarized in Chapter 2. Others, such as excited-state populations, and electronic and vibrational temperatures in regions where they differ from the kinetic temperature, are still subject to large uncertainties. Since present measurements are insufficient to yield an adequate empirical picture of these, it is desirable to discuss them in a theoretical framework involving the energy transfer and the energy balance of the upper atmosphere. This helps to ensure that conservation laws are satisfied and that the more important processes are emphasized. It also suggests important ways in which the energy deposited by artificial or natural disturbances could affect the upper atmosphere.

## 4.2 CONCENTRATIONS AND POPULATION TEMPERATURES

The fractional concentrations of various chemical species in the atmosphere are shown in Figures 4-1 through 4-3 as functions of altitude (Reference 4-1). Note that below about 100 km (the "turbopause") atmospheric mixing keeps the fractional concentrations of nitrogen, oxygen, argon, and helium constant, while the concentrations of species produced directly or indirectly by photodissociation

* This work was supported by DNA through Contract No. DASA-01-70-C-0082, and by ARPA through Contract No. DAHC-15-67-C-0011.

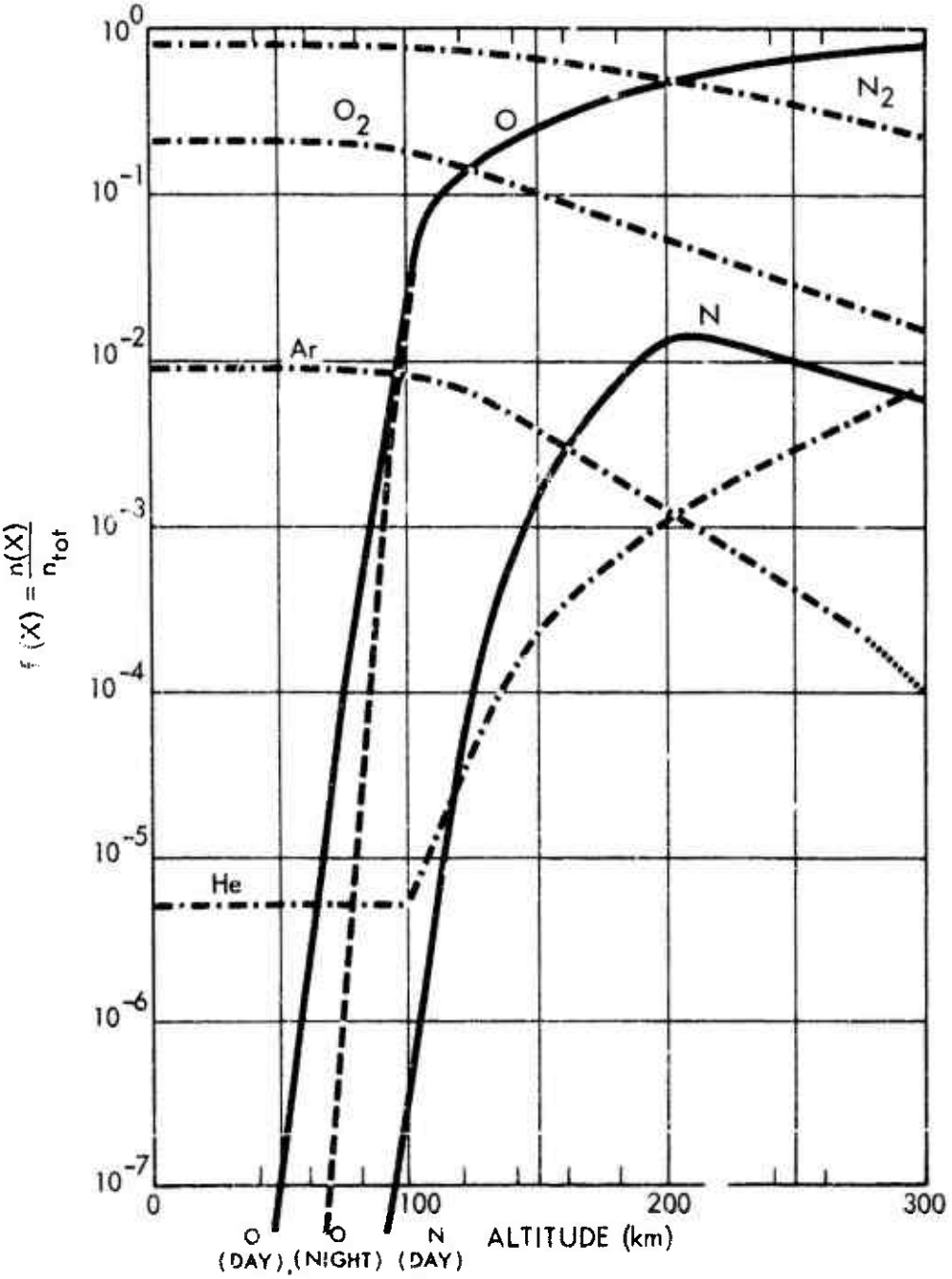


Figure 4-1. Fractional concentrations of the major neutral species in the atmosphere. (N.B.: This graph represents interim data, which may be upgraded upon the completion of Chapter 2. See note at Chapter 2 for further details.)

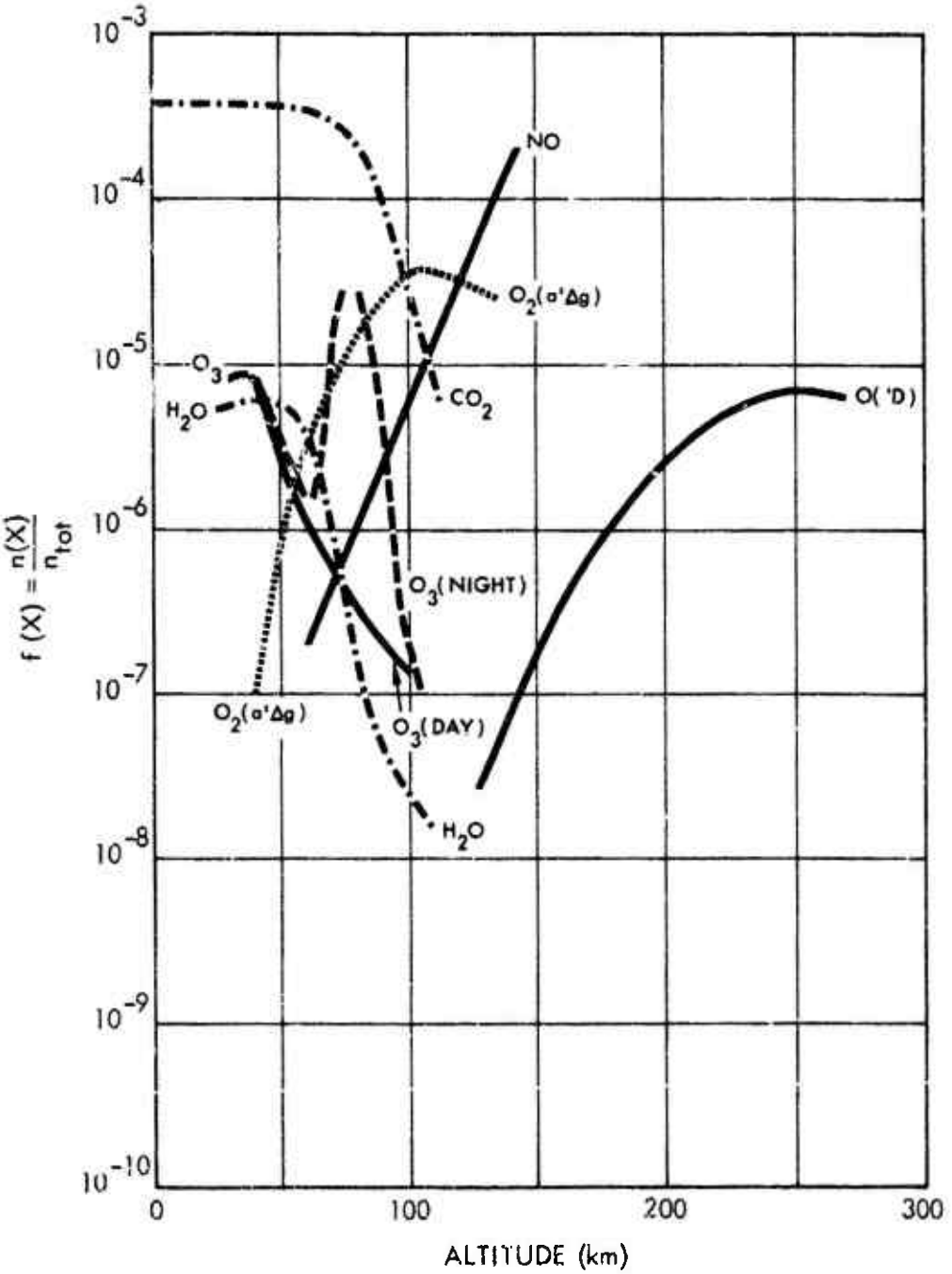


Figure 4-2. Fractional concentrations of the minor neutral species in the atmosphere. (N.B.: This graph represents interim data, which may be upgraded upon the completion of Chapter 2. See note at Chapter 2 for further details.)

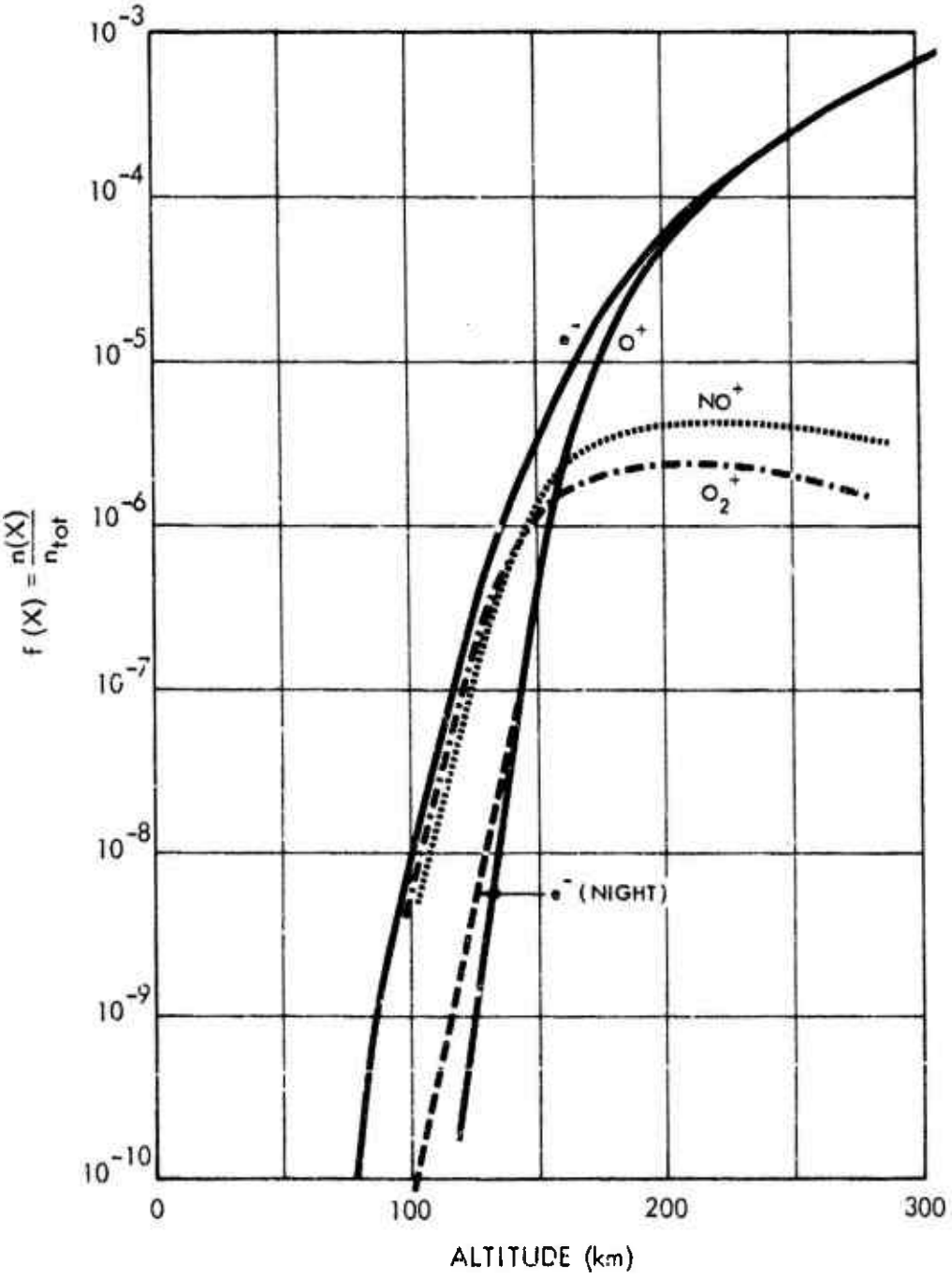


Figure 4-3. Fractional concentrations of the ionic species in the daytime atmosphere. (N.B.: This graph represents interim data, which may be upgraded upon the completion of Chapter 2. See note at Chapter 2 for further details.)

or photoionization vary. Above the turbopause the less reactive species are in separate "diffusive equilibrium", each with its own scale height. Specifically, for species X at altitude h , we have:

$$n(X;h) = n(X;h_o)\exp\{-(h-h_o)/H(X)\}\ ;\ H(X) = kT/M(X)g\ , \quad (4\text{-}1)$$

where M(X) = mass of species X , and H(X) (~5-50 km) is its scale height. Hence at increasing altitudes the concentrations of light species like helium increase relative to those of heavier species like argon or nitrogen. Note also that the degree of ionization is very low: below 200 km, $n_e/n_{tot} \leq 10^{-4}$, which is a representative threshold above which plasma effects become important.

Given these concentrations, population temperatures in terms of the Boltzmann or Saha equation can be defined as follows. For a species A with an electronically excited state $A^*$ of excitation energy $\Delta E$, an excitation temperature $T_{ex}$ may be defined by the Boltzmann relation:

$$n(A^*)/n(A) = \left[g(A^*)/g(A)\right] e^{-\Delta E/kT_{ex}}\ , \quad (4\text{-}2)$$

where the g's are statistical weights of the appropriate states. For an ionization process $AB \rightleftarrows AB^+ + e^-$ with ionization potential I , an "ionization temperature", $T_i$ , can be defined by the Saha equation:

$$\frac{n(e^-)\ n(AB^+)}{n(AB)} = g(e^-)\ \frac{Q(AB^+)}{Q(AB)}\left[\frac{2\pi m_e kT_i}{h^2}\right]^{3/2} e^{-I/kT_i}\ , \quad (4\text{-}3)$$

where

$g(X)$ = electronic statistical weight of species X

$Q(X) = g(X)\ Q_{rot}(X)\ Q_{vib}(X)$ = partition function of (molecular) species X

$Q_{rot}(X)$ = rotational partition function, $kT/hcB$ , for a rigid rotator

$Q_{vib}(X)$ = vibrational partition function, $\left[1 - e^{-hc\omega_e/kT}\right]^{-1}$ , for a harmonic oscillator

$m_e$ = electron mass .

Finally, for a dissociation equilibrium $AB \rightleftarrows A + B$ with dissociation energy D , the Law of Mass Action gives:

$$\frac{n(A)\, n(B)}{n(AB)} = \frac{g(A)\, g(B)}{g(AB)\, Q_{rot}(AB)\, Q_{vib}(AB)} \left[\frac{2\pi \mu_{AB}\, kT_d}{h^2}\right]^{3/2} e^{-D/kT_d} , \qquad (4\text{-}4)$$

where

$\mu_{AB}$ = $M(A)\, M(B)/\{M(A) + M(B)\}$ = reduced mass of AB molecule

$T_d$ = "dissociation temperature" .

The population temperatures for the most important species above 80 km are shown in Figure 4-4. The significant findings are:

(a) The different population temperatures differ by large factors, indicating a large deviation from LTE (local thermodynamic equilibrium) in the upper atmosphere.

(b) The ionization temperatures obtained from the Saha equation for the positive ions $NO^+$ , $O_2^+$ , $O^+$ , do not differ much except when the relative concentration of one of the ions becomes small. One can thus describe the overall state of ionization roughly in terms of a single "ionization temperature".

(c) It is also possible to draw a "dissociation" temperature, largely by following the oxygen dissociation which is of greatest importance from the standpoint of energy content.

(d) There are two translational temperatures, viz., the kinetic temperature of the neutral species, and that of the free electrons; the latter is generally higher (References 4-2, 4-3).

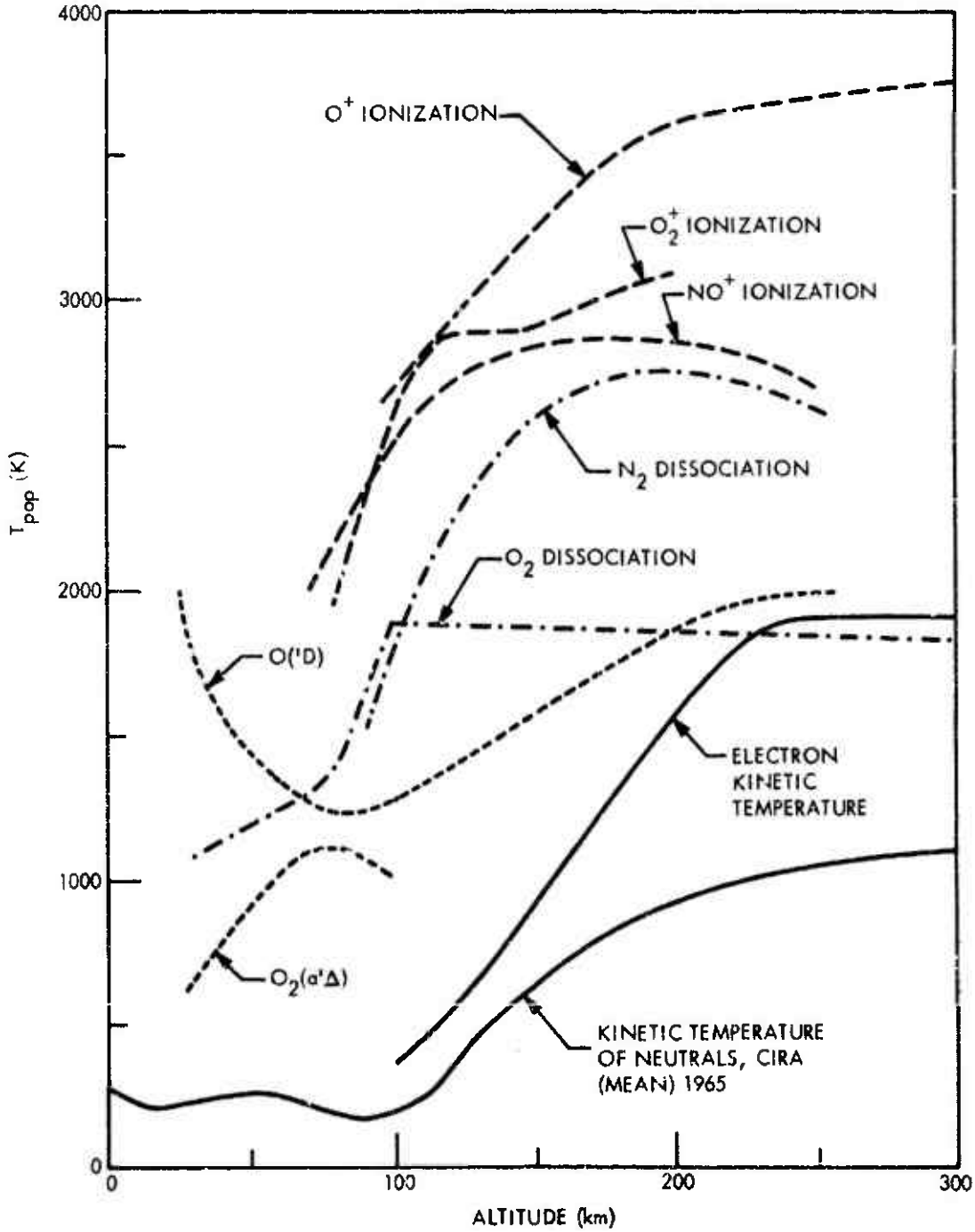


Figure 4-4. Population temperatures of atmospheric species. (N.B.: This graph presents interim computed results, which are subject to revision upon the upgrading of Figures 4-1 through 4-3. See notes thereunto pertaining.)

## 4.3 ENERGY PARTITION

The effective population temperatures shown in Figure 4-4 are simply a restatement of the concentration data of Figures 4-1 through 4-3. The effective temperatures for molecular rotation and vibration are not shown because no direct data exist. It may be assumed for most molecules that the rotational and kinetic temperatures are equal, because in general, translational-rotational energy transfer is very efficient (cf. Reference 4-4). However, vibrational-translational energy transfer is very inefficient when kT is less than the spacing of the vibrational levels. It takes perhaps $10^3$-$10^6$ collisions for nitrogen and oxygen to reach a translational-vibrational steady state. Thus a large uncertainty for the vibrational energy content exists. For infrared-inactive molecules, e.g., nitrogen and oxygen, which do not lose vibrational energy by radiation, the vibrational temperature probably equals or exceeds the kinetic temperature. Since vibrational excitation is produced by electron impact, atom recombination, and quenching of electronic excitation, a "plausible" upper limit to the vibrational temperature is the highest of the three temperatures associated, respectively, with these processes, viz., $T_e$, $T_d$, and $T_{ex}$. Because the effective "temperature" of the photoelectrons exceeds that of the bulk electrons and because the atmosphere is not in LTE, it is theoretically possible for the nitrogen vibrational temperature to exceed $T_e$, $T_d$, and $T_{ex}$, but a more detailed consideration suggests that this is unlikely; hence the "plausible" limit is an empirical and not a theoretical limit.

If the compositions and temperatures of Figure 4-4 are combined with these estimates of the vibrational and rotational temperatures to obtain the partition of energy between different degrees of freedom, Figure 4-5 results. The following points may be made:

(a) The rotational energy generally tracks the kinetic energy or temperature, falling off at high altitudes because of the dissociation.

(b) Above 80-90 km, oxygen dissociation is the single most important contributor to the energy.

(c) The energy of ionization is always very small.

(d) The energy of electronic excitation is very small, but far from LTE defined in terms of the kinetic temperature.

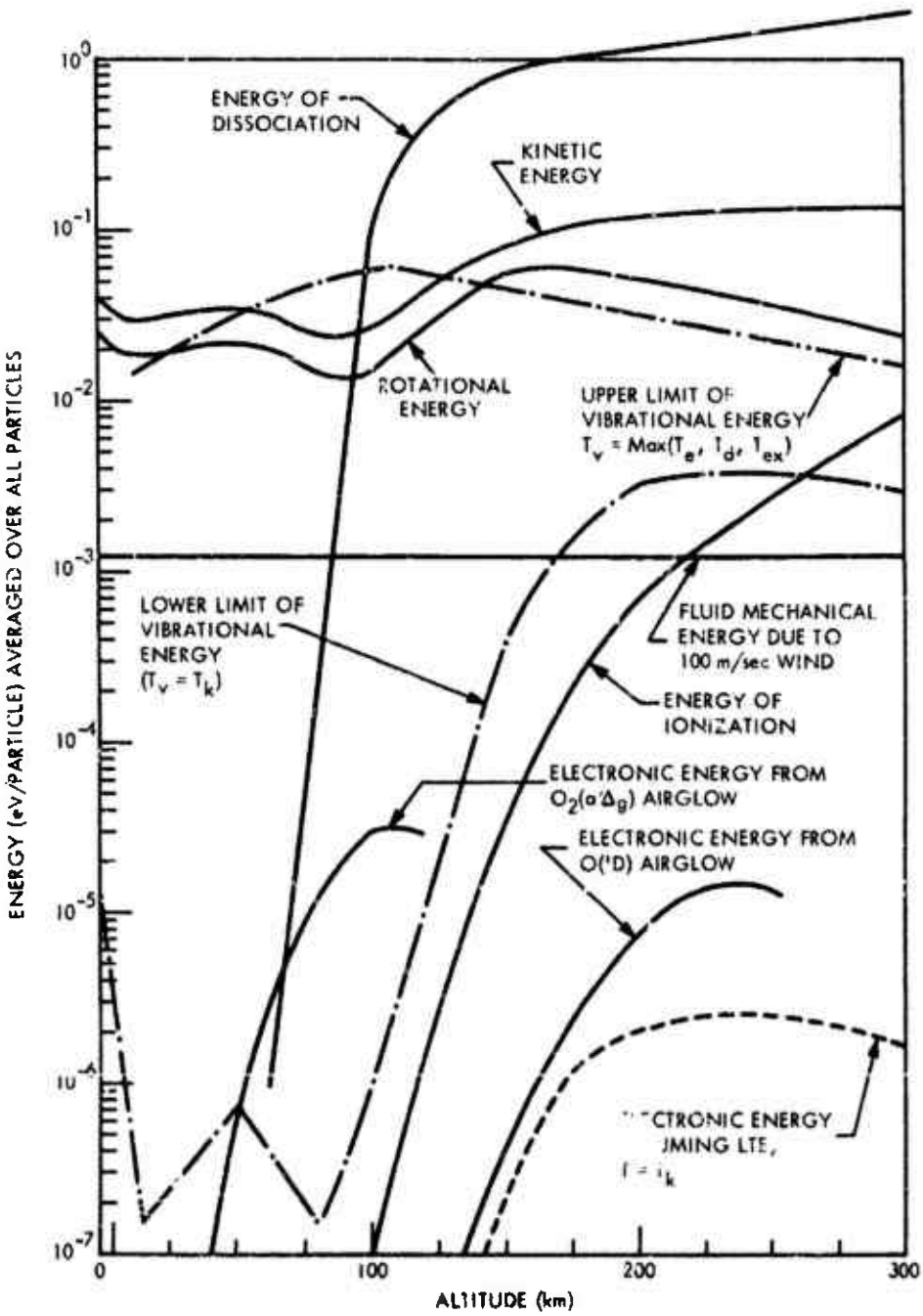


Figure 4-5. Distribution of energy among different degrees of freedom. (N.B.: This graph presents the interim results of calculations based in part upon Figure 4-4 in its interim form. Thus this figure, too, is subject to later revision.)

(e) The curve marked "kinetic energy due to a 100 m/sec wind" corresponds to a typical ionospheric wind. This curve shows that the contribution of overall fluid mechanical motion to the energy content is usually not large. (See Chapter 3 for a fuller discussion of the effects of fluid mechanical motion on energy transfer.)

(f) A major uncertainty exists, regarding the vibrational energy content. The limits of vibrational temperature give a range of vibrational energy of a factor $3 \times 10^4$ at 100 km altitude. This problem is discussed in Section 4.5.

## 4.4 ENERGY TRANSFER AND ENERGY BALANCE

The situation discussed thus far has involved the steady state. This differs very much from LTE, so that the mechanism by which the situation is produced is clearly important. Figure 4-6 shows Leovy's estimates (References 4-5, 4-6) for the energy balance of the 80-105 km region. Figure 4-7 presents curves for the radiative and energy transfer for a wider range of altitudes, based on data from several sources (References 4-7 through 4-11). It is seen that the most important energy source is the solar-ultraviolet radiation, principally in the Schumann-Runge continuum of molecular oxygen, which dissociates the oxygen. The most important sink is the infrared vibration-rotation emission from $CO_2$ (at 15 $\mu$m), below 100-120 km altitude, and the infrared fine-structure emission from atomic oxygen (at 63 $\mu$m), at higher altitudes. Heat conduction and gravity-wave dissipation also play significant roles, although the magnitude of the latter is quite uncertain.

## 4.5 THE VIBRATIONAL POPULATION

As noted previously, the upper atmosphere is far from a LTE condition, i.e., effective or population temperatures for altitudes between 80 and 300 km vary from 180 to 4000 K (cf. Figure 4-4). The vibrational energy content may vary over four to five orders of magnitude depending on the effective vibrational temperature as shown in Figure 4-5. To narrow the range of uncertainty, one must consider the specific processes which lead to vibrational excitation and deexcitation.

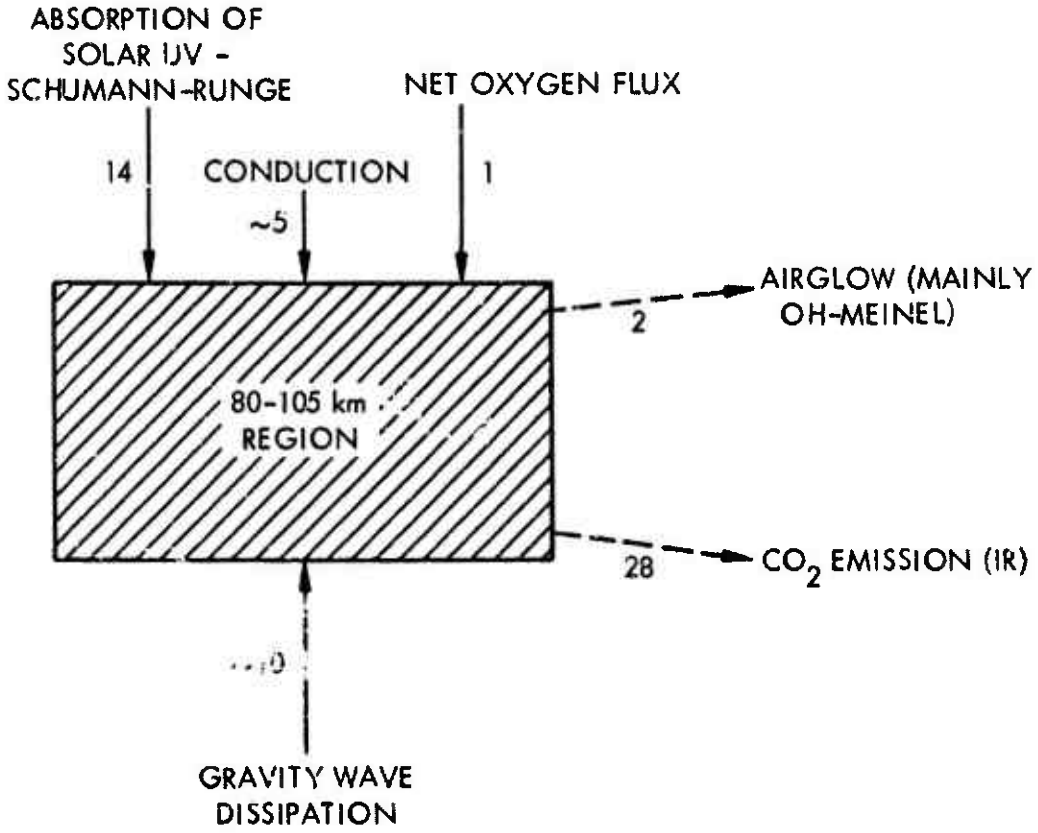


Figure 4-6. Schematic heat budget constituents between 80 and 105 km. (From Reference 4-6.)

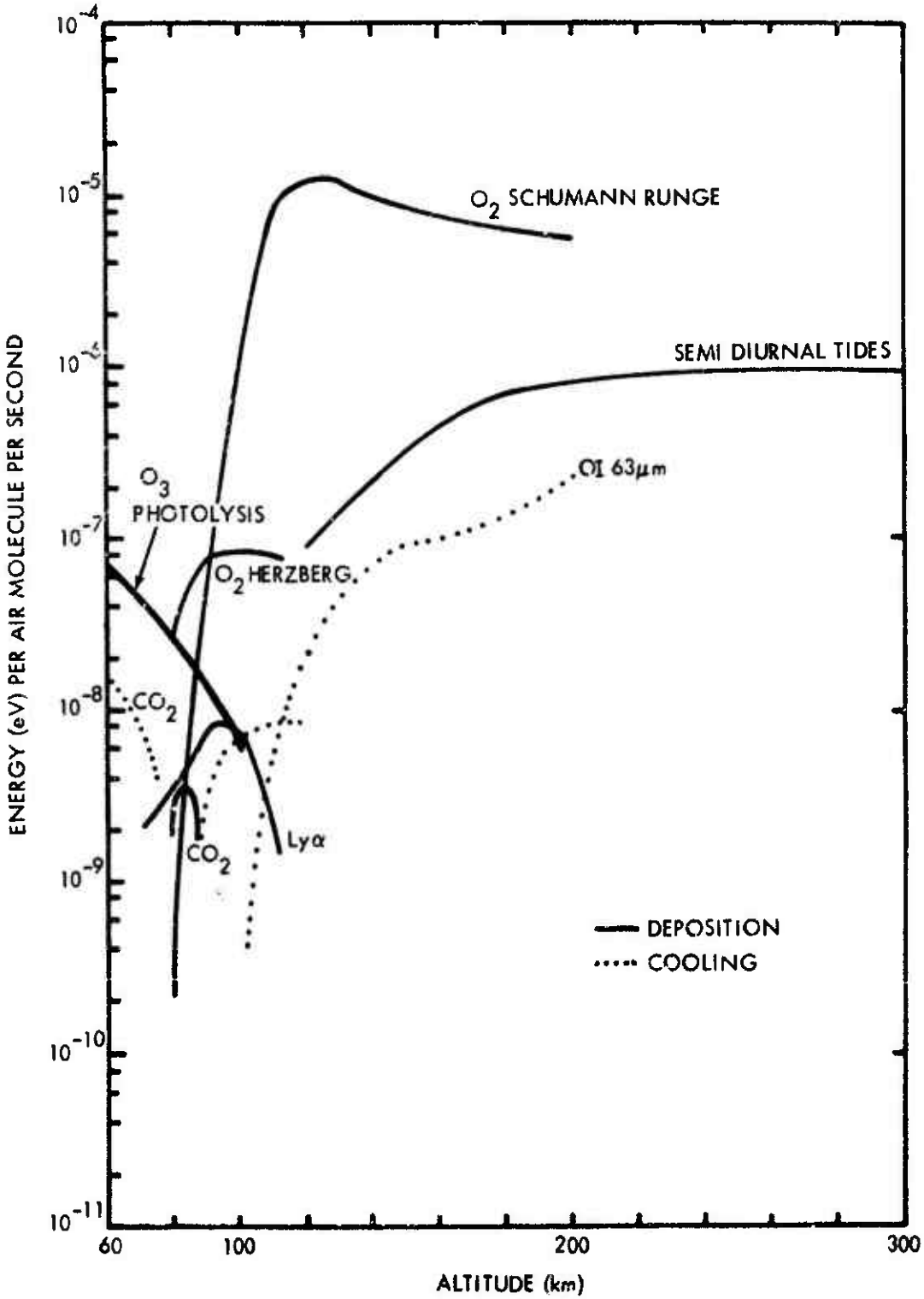


Figure 4-7. Altitude dependence of energy absorption and emission.

Several workers have considered the vibrational state of the nitrogen in the upper atmosphere (References 4-12 through 4-14). The most likely processes for producing vibrationally excited nitrogen ($N_2^\ddagger$) are:

$$O(^1D) + N_2 \rightarrow N_2^\ddagger + O(^3P) \tag{4-5}$$

$$N + NO \rightarrow N_2^\ddagger + O \tag{4-6}$$

$$e^- + N_2 \rightarrow N_2^- \rightarrow N_2^\ddagger(v=1) + e^- \quad . \tag{4-7}$$

Of these reactions, it appears that process (4-5) yields very little vibrational excitation (Reference 4-15). Process (4-6) may yield one-third of its exothermicity in the form of vibrational excitation (Reference 4-16), although this estimate is somewhat controversial (Reference 4-17). Process (4-7) is certainly important under auroral conditions (Reference 4-13), but not in the undisturbed atmosphere below 250 km. Of the three main collisional deexcitation processes, the first:

$$N_2^\ddagger(v=1) + CO_2 \rightarrow CO_2^\ddagger(v_3=1) + N_2 \quad , \tag{4-8}$$

has a relatively large cross section ($\sim 10^{-3}$ gas kinetic); the $CO_2^\ddagger$ then radiates. The second:

$$N_2^\ddagger + O \rightarrow N_2O^* \rightarrow N_2 + O \quad , \tag{4-9}$$

is much faster than most vibrational quenching processes by species other than atomic oxygen (Reference 4-18). The third is:

$$N_2^\ddagger + e \rightarrow N_2 + e \quad , \tag{4-10}$$

which may be important above 300 km. Finally, at high altitudes diffusion is a significant mechanism for the loss of vibrationally excited and many other species.

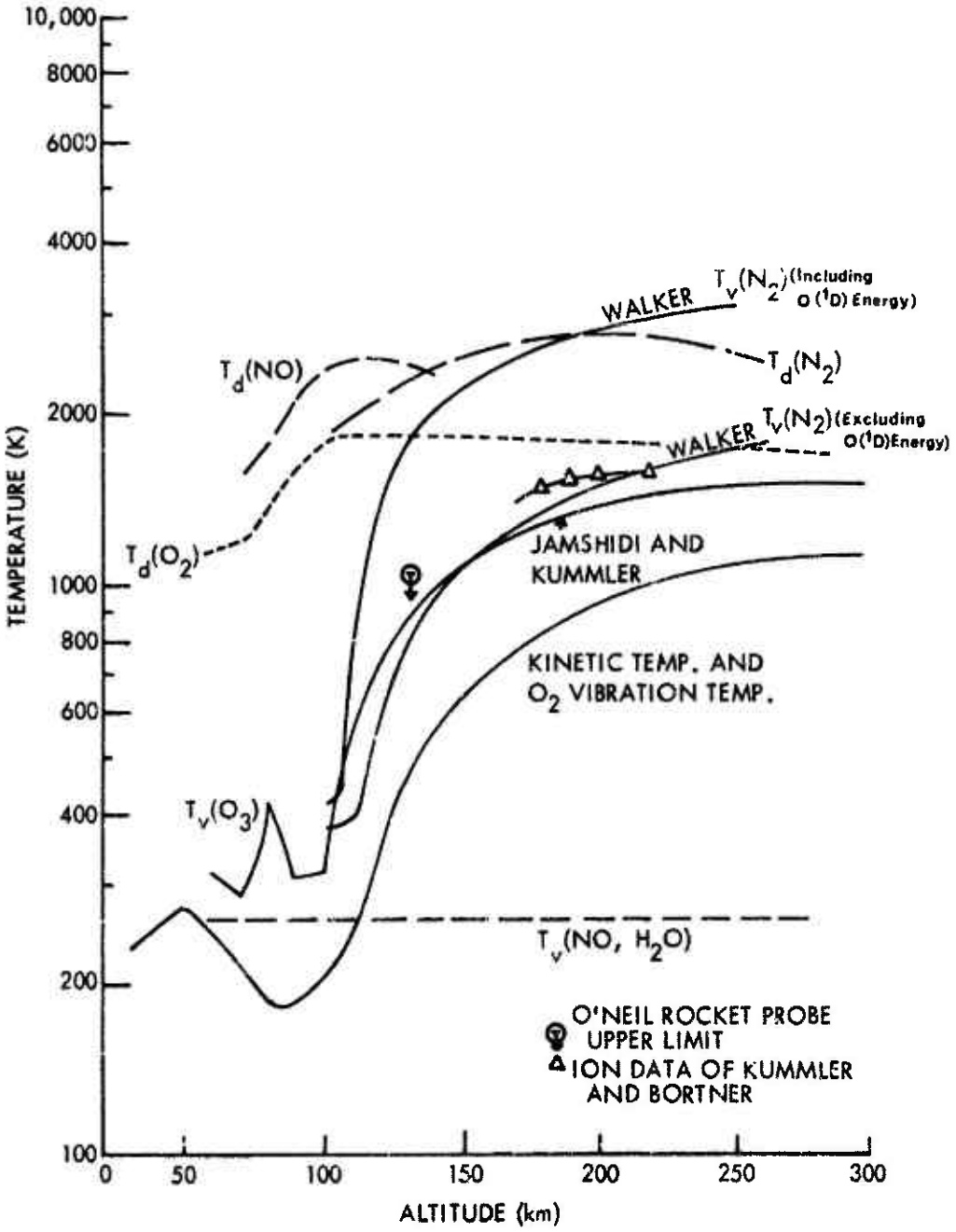


Figure 4-8. Summary af vibrational temperotures in the normal atmosphere, compared ta dissociation and kinetic temperotures. (N.B.: Curves marked "Walker" are from Reference 4-13; curve marked "Jamshidi and Kummler" is from Reference 4-19; paints designated as "O'Neil" and as "Kummler and Bartner" are from References 4-20 and 4-2, respectively.)

The results shown in Figure 4-8 for atmospheric nitrogen are discussed in detail elsewhere (Reference 4-14) and reference should be made as well to Walker et al (Reference 4-13) for the intricate details of the calculation.

For oxygen, the specific excitation-deexcitation processes to be considered are:

$$O + O + M \rightarrow O_2^{\ddagger} + M \tag{4-11}$$

$$O_2^{\ddagger}(v=1) + H_2O \rightleftharpoons O_2 + H_2O^{\ddagger}(v_2=1) \tag{4-12}$$

$$O_2^{\ddagger} + O \rightleftharpoons O_3 \rightleftharpoons O_2 + O \quad , \tag{4-13}$$

and again, diffusion should be mentioned; however, for oxygen, unlike nitrogen, deexcitation by atomic oxygen (Process (4-13)) continues to dominate over diffusion even as high as 300 km. Hence it is plausible to suggest that $T_v(O_2) = T_k$ for all altitudes.

Nevertheless, mention should be made of the analysis of Ferguson et al (Reference 4-21) who from relative concentrations of $Si^+$ in sporadic-E events inferred effective vibrational temperatures of 1000-1900 K for h = 110-120 km. Reid and Withbroe (Reference 4-22) also required an elevated oxygen vibrational temperature to explain solar-ultraviolet absorption.

The NO molecule is infrared-active, and radiative transfer rather than collisions determine the steady-state vibrational excitation at altitudes above about 60 km. The vibrational temperature of NO is expected to be comparable to the effective radiating temperature of the earth's lower atmosphere at the appropriate wavelength (5.4 $\mu$m), but reduced somewhat by the one-sided nature of the radiant flux.

## REFERENCES

4-1. Bortner, M. H., and R. H. Kummler, General Electric Company, Report GE-9500-ECS-SR-1 (1968).

4-2. Kummler, R. H., and M. H. Bortner, Trans. Am. Geophys. Union 52, 310 (1971).

4-3. Evans, J. V., Proc. IEEE 57, 496 (1969).

4-4. Lambert, J. D., in Atomic and Molecular Processes, D. R. Bates, Ed., Academic Press, New York (1962); Chap. 20.

4-5. Leovy, C. B., J. Atmos. Sci. 23, 228 (1966).

4-6. Leovy, C. B., Adv. Geophys. 13, 191 (1969).

4-7. Drayson, S. R., and E. S. Epstein, Space Research IX (North Holland Publishing Co., Amsterdam), 376 (1969).

4-8. Keneshea, T. J., private communication (1970).

4-9. Johnson, F., and B. Gottlieb, Space Research IX (North Holland Publishing Co., Amsterdam), 442 (1969).

4-10. Kockarts, G., and W. Peetermans, Planet. Space Sci. 18, 271 (1970).

4-11. Moe, O. K., McDonnell-Douglas Company, Report MDC G2280 (1971).

4-12. Bortner, M. H., and R. H. Kummler, General Electric Company, Report DASA 2407 (1970).

4-13. Walker, J., R. Stolarski, and R. Nagy, Ann. Geophys. 25, 831 (1969).

4-14. Kummler, R. H., M. H. Bortner, and E. Bauer, Symp. Energetics and Dynamics of Mesosphere and Lower Thermosphere, IAMAP/IAGA/IUGG, Moscow, U. S. S. R. (1971).

4-15. Fisher, E., and E. Bauer, Institute for Defense Analyses, Research Report P-789 (In Press).

4-16. Morgan, J., L. Phillips, and H. Schiff, Disc. Faraday Soc. 33, 118 (1962).

4-17. Wray, K. L., E. Feldman, and P. Lewis, J. Chem. Phys. 53, 4131 (1970).

4-18. Breshears, D., and R. Bird, J. Chem. Phys. 48, 4768 (1968).

4-19. Jamshidi, E., (and R. H. Kummler, preceptor), M. S. Thesis, Wayne State University, Detroit, Mich. (1971).

4-20. O'Neil, R., Space Research (to be published).

4-21. Ferguson, E. E., F. Fehsenfeld, and J. Whitehead, J. Geophys. Res. 75, 7333 (1970).

4-22. Reid, R. H. G., and C. L. Withbroe, Planet. Space Sci. 18, 1255 (1970).

# 5. THE DISTURBED ATMOSPHERE

W. Knapp and D. Archer,* General Electric Company—TEMPO

(Latest Revision 26 October 1971)

## 5.1 THE NATURALLY DISTURBED ATMOSPHERE

Solar flares and magnetic storms may alter the atmospheric density, temperature, pressure, electron and ion densities, and composition. The magnitude of the effects is generally a function of altitude. Air temperature and density are susceptible to change above about 200 km. Electron and ion density changes (due to solar flares) are usually greater below 200 km. Although uncertainties exist with respect to the changes expected for various flare and magnetic storm conditions. the following summarizes some of the pertinent data.

### 5.1.1 Density Variations

Density variations above 200 km have been deduced from satellite drag (References 5-1 through 5-3). Since satellite observations give an average over space and time, it is difficult to obtain information on transient variations.

A correlation exists between the upper atmospheric density and the flux of solar radiation monitored at wavelengths in the 3-30 cm range. Specifically, the density can be expressed as:

$$\rho \propto F^m \quad , \tag{5-1}$$

where F is the solar flux observed at the 10.7-cm wavelength and m is a function of altitude, time of day, and sunspot cycle. For altitudes above 200 km, $m > 0$; thus the greater the solar flux, the greater the atmospheric density.

---

* Present affiliation: Mission Research Corporation.

During intense magnetic storms, the density at any given height may increase significantly within a few hours. The observed data support the relationship:

$$\rho = \rho_o(1+\beta A_p) \quad . \tag{5-2}$$

Here $\rho_o$ is the density before the storm, $A_o$ is the daily geomagnetic index, and $\beta$ is a coefficient that varies with altitude from about $3 \times 10^{-3}$ at 200 km to $1.5 \times 10^{-2}$ at 700 km. The associated uncertainty in the values of $\beta$ is about 30 percent. No detectable variation with latitude has been found. As an example, the normalized density, $\rho/\rho_o$, between 200 and 800 km, has been computed from Equation 5-2 for selected days both prior to and following the magnetic storm of 13 November 1960. The results are shown in Figure 5-1. For this computation, a linear variation of $\beta$ with altitude was assumed, and values of $A_p$ were obtained from Reference 5-3. It is seen that on 13 November 1960, the density at 200 km was almost doubled.

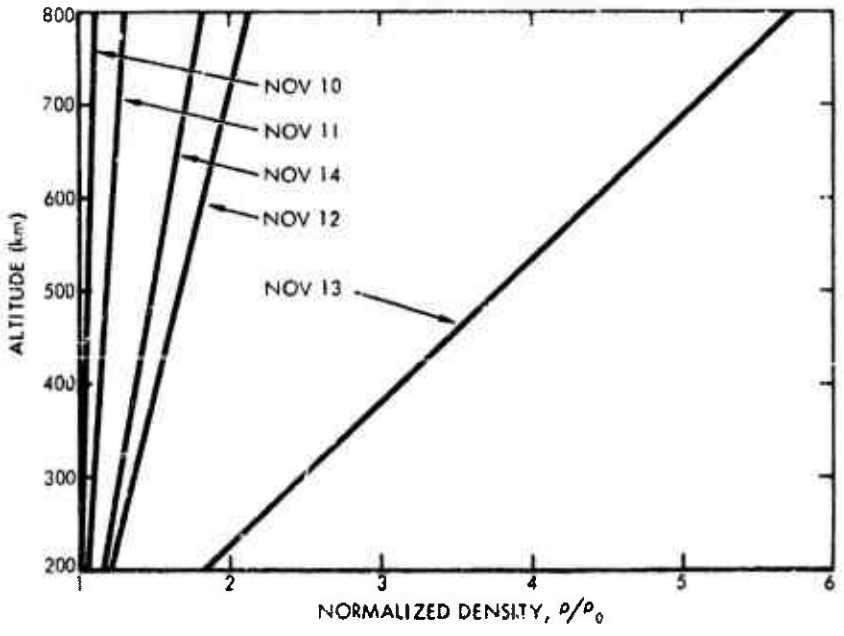


Figure 5-1. Normalized density (from Equation 5-2) as a function of altitude for selected days prior to, during, and following the magnetic storm of 13 November 1960.

### 5.1.2 Temperoture Variations

Satellite observations have also been used (Reference 5-4) to deduce a correlation between the average atmospheric temperature changes (from day to night and over a solar cycle) and the changes in mean flux of solar radiation at 10.7 and 21 cm. It has been deduced (Reference 5-5) that the temperature in the exosphere (above about 300 km) increases during magnetic storms by an amount:

$$\Delta T \approx 1.0\ A_p + 125\ [1 - \exp(-0.08\ A_p)]\ \text{Kelvin}. \qquad (5\text{-}3)$$

Again, $A_p$ is the daily geomagnetic index. As an example, Figure 5-2 shows the temperature increase above 300 km (deduced from Equation 5-3) for 9 through 14 November 1960.

From rocket, satellite, and ground-based (Thompson scatter radars) experiments, it is known that the electron and ion gases above about 150 km are normally substantially hotter than the neutral atmosphere (References 5-6 through 5-8). Figure 5-3 shows electron and ion temperatures versus altitude found by averaging data for

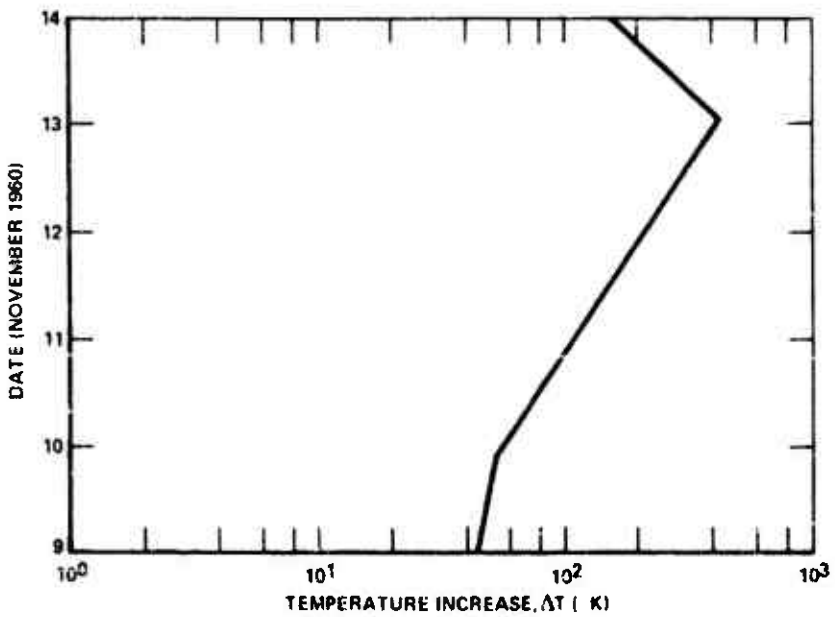


Figure 5-2. Temperature increase (from Equation 5-3) for altitudes above about 300 km for selected days prior to, during, and following the magnetic storm of 13 November 1960.

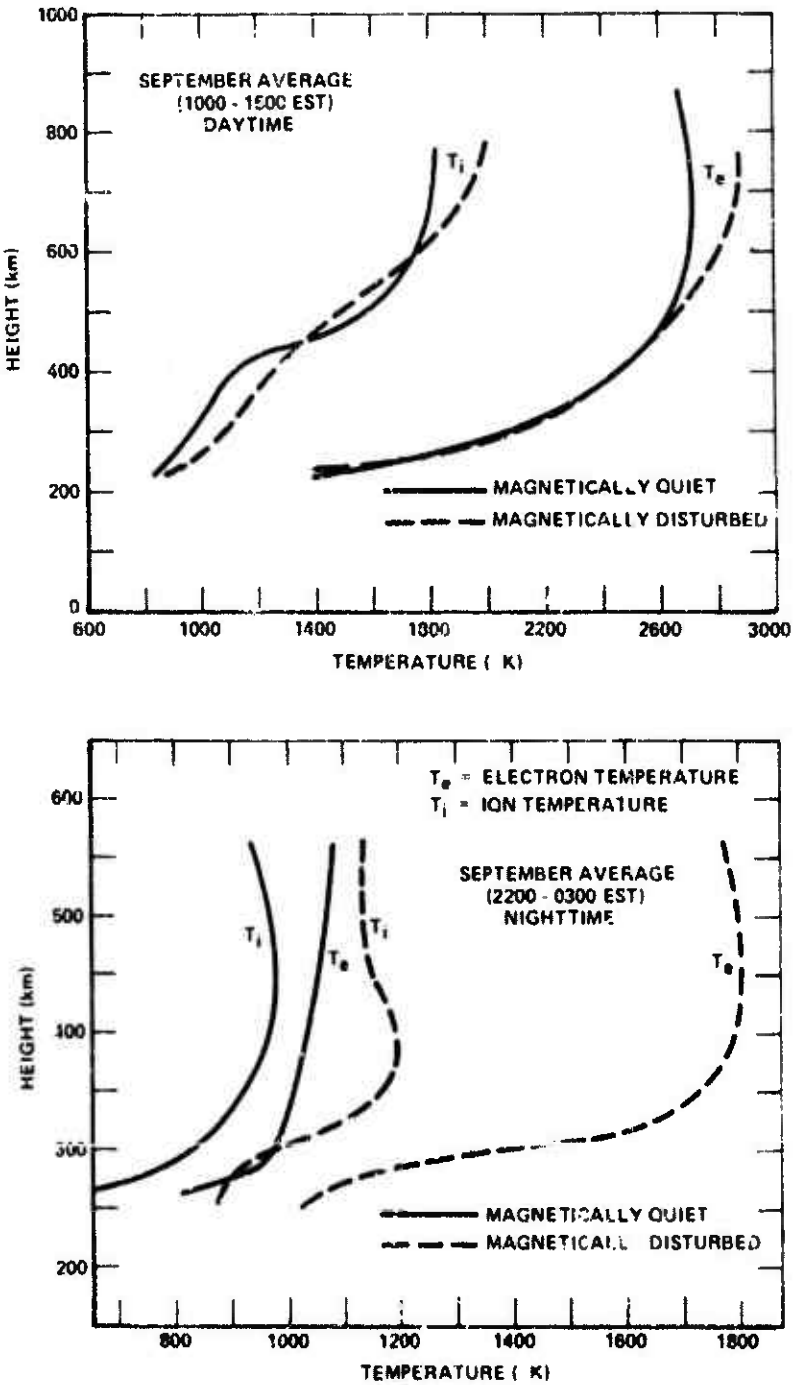


Figure 5-3. A comparison of the average height dependence of $T_e$ and $T_i$ on (a) the magnetically quiet ($A_p \leq 14$) and disturbed ($A_p \geq 19$) days in September, and (b) the magnetically quiet and disturbed nights (J.V. Evans, Reference 5-7).

magnetically quiet days in September 1963 at Milistone Hill radar observatory (71.5°W, 42.6°N). In addition to the diurnal variation, there is considerable variation in the profiles with latitude, longitude, season, and solar cycle.

During intense magnetic storms, the nighttime electron and ion temperatures are increased as illustrated in Figure 5-3. The nighttime electron temperature increase during magnetic storms does not appear to be directly correlated with the magnetic index. Very high (≈4000 K) electron temperatures also occur at high latitudes in auroras.

### 5.1.3 Electron and Ion Density Variations

Ionization rates and electron densities for the quiet daytime D-region are shown in Figures 5-4 and 5-5. These are representative values. Considerable variation exists with respect to location, season, solar cycle, and time of day (cf. Chapters 2 and 13). Measurements with rocket-borne mass spectrometers have shown that the dominant ions in the undisturbed D-region are water-cluster ions (cf. Chapter 2). The dominant negative ions in the D-region appear to be $NO_3^-$ and $NO_3^- \cdot (H_2O)_n$.

During solar flares and magnetic storms, the ionospheric regions behave in different ways depending mainly upon latitude and altitude. At the time of a flare, a sudden ionospheric disturbance (SID) is observed on the sunlit side of the earth, resulting in a sudden increase in radio-wave absorption (Reference 5-11). The SID can last as long as an hour. The absorption increase is attributed to enhanced solar X-rays that penetrate into the D-region and produce additional ionization. Within one to three hours afterwards, upon the arrival of energetic proton streams, a polar cap absorption (PCA) event may be observed at latitudes greater than 65 degrees (Reference 5-12). Twenty-five to forty hours later, an auroral zone absorption (AZA) event (evidently produced by high-energy electrons) may be observed coincident with magnetic storms and changes in the F-region maximum electron density (Reference 5-3). The latter changes are either positive or negative depending on the latitude. Detailed information on solar flares can be found, for example, in Reference 5-13.

Although the exact amount of variation of the electron density from undisturbed to disturbed conditions is a function of latitude,

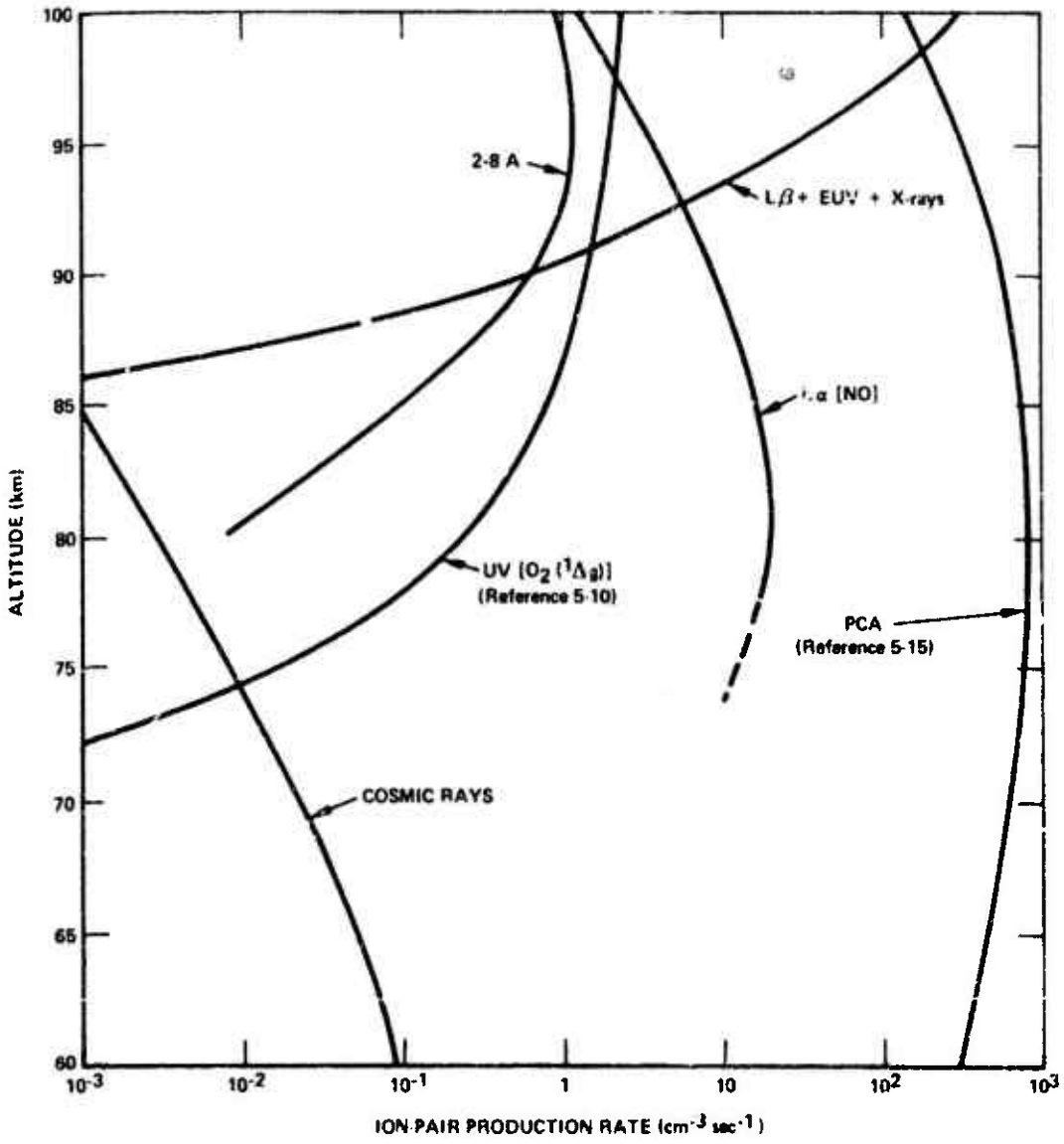


Figure 5-4. Daytime D-region ionization rates (L. Thomas, Reference 5-9).

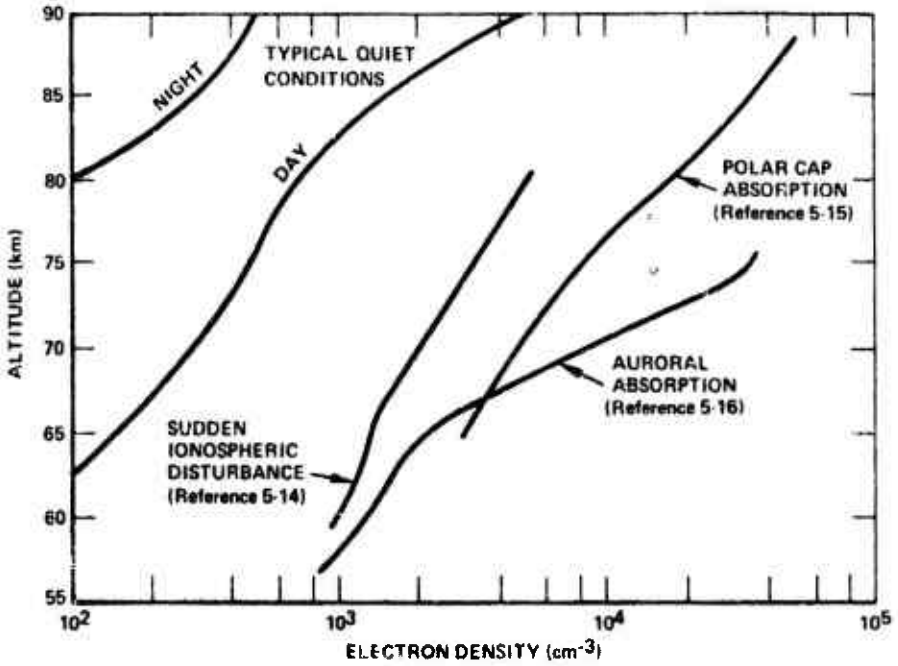


Figure 5-5. Electron density profiles for the D-region of the ionosphere.

time of day, solar flare intensity, etc., fairly typical profiles of D-region electron densities are presented in Figure 5-5 (References 5-14 through 5-16). During the PCA event of 14 April 1969, simultaneous measurements were made of the proton flux and D-region ionization (Reference 5-15). Figure 5-4 shows the ionization rates computed from the proton flux measurements, and Figure 5-5 shows the corresponding electron-density measurements. Mass-spectrometer measurements of positive and negative ion composition were made during the PCA event of 2 November 1969 (References 5-17, 5-18). Results from the nighttime positive-ion measurements between 62 and 139 km showed that water-cluster ions were dominant below 77 km and that $NO^+$ and $O_2^+$ were the major ions from 77 to 139 km. Daytime and sunset measurements of positive ions were made between 73 and 144 km and between 78 and 144 km, respectively. $NO^+$ and $O_2^+$ were the dominant ions down to the lower altitude measurement limits of both flights. The negative-ion measurements showed $O_2^-$ and $O^-$ to be dominant between 72 and 94 km for daytime and nighttime conditions, respectively. The latter two ions were undetectable by the measurement techniques used, during quiet-condition observations.

Rocket- and ground-based measurements have also provided information on the change in electron density and ion composition during a solar eclipse (Reference 5-19). A significant feature of these measurements is that the electron density shows a large decrease near 82 km that does not appear in the positive-ion profile. This indicates an increase in the negative-ion concentration near the maximum of the negative-ion cluster layer.

While atmospheric and laboratory measurements have greatly increased the detailed understanding of the D-region, there still exist a number of unresolved questions concerning specific ionization and loss processes. Changes in the concentrations of minor neutral constituents appear to play an important role in determining changes in ionization. Metastable species such as $O_2(^1\Delta_g)$ and $N(^2D)$ may be important in affecting the ionization rates and the formation of complex hydrated ions.

Increases of electron content of approximately $2 \times 10^{12}$ electrons $m^{-2}$ (about 5 percent of the total ionospheric content) have been observed following solar flares, which appear to be due to increases in F-region ionization owing to enhancement of the solar UV flux (References 5-20, 5-21).

Magnetic storms primarily affect the F-region ionization. In middle and high latitudes, the F-region maximum electron density decreases for approximately three days and then returns to normal. The minimum may be only 6-10 percent of the nominal value (Reference 5-3). In equatorial and low latitudes, the maximum electron density decreases on the initial storm day, and then increases above the normal mean for the next two days before returning to normal. Middle-latitude stations exhibit both types of disturbances (Reference 5-3). Figure 5-6 presents idealized typical electron-density profiles for two types of magnetically disturbed conditions, viz., negative and positive variations of the peak electron density (Reference 5-22).

## 5.2 THE NUCLEAR-PERTURBED ATMOSPHERE

The detonation of a nuclear device in the atmosphere produces effects over a limited volume of space that are much more pronounced than any produced naturally. Each detonation produces changes in the atmosphere that are characteristic of the given weapon yield

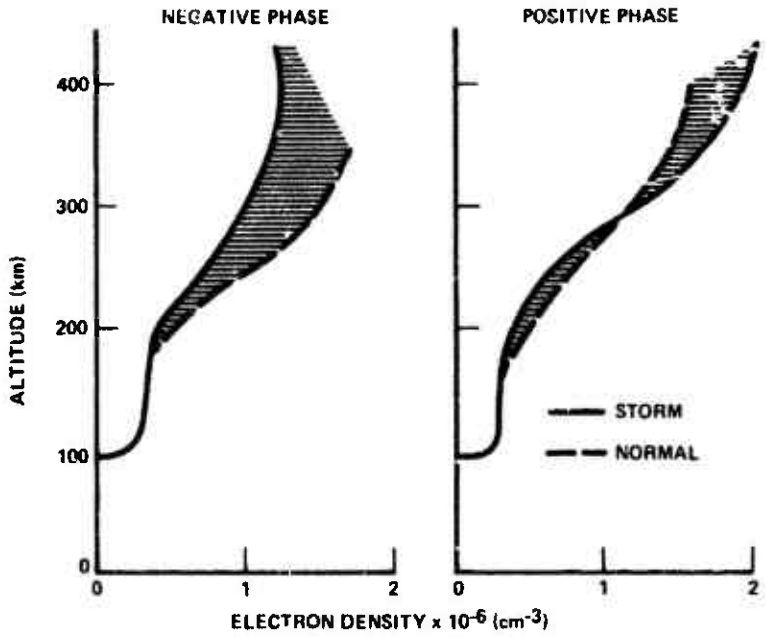


Figure 5-6. Idealized typical $n_e$-h profiles showing negative and positive variations of the peak electron density. (Obayashi, Reference 5-22.)

and altitude. "Typical" curves of changes for an atmospheric explosion are often not very meaningful, and it is usually necessary to state the conditions fairly explicitly. References 5-23 through 5-25 are useful unclassified sources that describe the nuclear-weapon environment.

Detonations below about 300 km produce a fireball, a region of intensely heated air, varying in size from a few tenths of a kilometer to several tens of kilometers. Significant changes in ionization can occur both inside and outside the fireball. Large temperature and density changes occur primarily in and near the fireball.

In addition to changing the properties of the ambient air, a nuclear weapon introduces into the atmosphere a certain amount of foreign material, which may have a profound effect upon the state of ionization within the fireball.

### 5.2.1 Temperoture Chonges

Although the early-time ($\approx 10^{-7}$ sec) temperature of nuclear fireballs is of the order of $10^7$ K, it rapidly drops owing to radiative growth. The subsequent cooling, primarily by fireball expansion and air entrainment, is more gradual, and it may take several hundred seconds to reach ambient values. Fireball temperatures are generally inferred from measurements of the intensity of emitted radiation, both in the radio- and optical-frequency regions. Figure 5-7 represents fairly typical plots of fireball temperatures as a function of time after burst for detonations in three different altitude regions. The time scaling with detonation altitude and yield is complex owing to the interaction of radiative transport and hydrodynamics, which are both altitude- and yield-dependent.

Peak temperatures in shock fronts that propagate outside the fireball within a few seconds after burst are a strongly decreasing function of range from the burst point (propagation into constant density). Typical equilibrium temperatures at low altitudes are a few times ambient, close to the fireball. Shocks running into decreasing den-

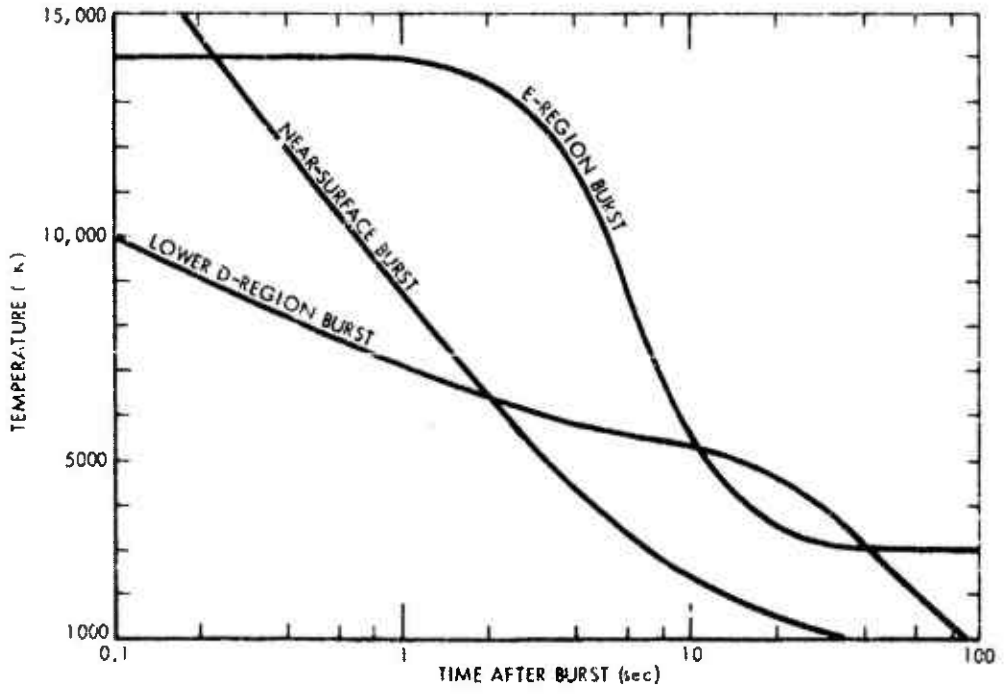


Figure 5-7. Examples of fireboll temperctures for three detonotion regions.

sity increase in strength, and at high altitudes temperatures several times ambient may exist in the shock front over much larger dimensions. Also at high altitudes, large nonequilibrium temperatures, e.g., vibrational, may occur.

For bursts detonated above about 100 km, X-ray energy deposited in the upper D- and lower E-regions can heat the neutral gas sufficiently to cause significant upward air motion in the E- and F-regions. Electron and ion temperatures in the E- and F-regions can be increased by weapon-energy deposition. The increased electron temperature results in increases in electronic temperatures of oxygen and nitrogen atoms and the vibrational temperature of molecular nitrogen.

### 5.2.2 Density Changes

At the elevated temperatures prevailing within fireballs that have expanded so that they are in pressure equilibrium with the surrounding air, the density inside is lower than the ambient density outside by approximately the ratio of the inside to outside (ambient) temperature. Prior to the establishment of pressure equilibrium, the density is intermediate between the two values. For detonations in the D- and E-regions, the fireball may rise rapidly enough that the fireball density becomes larger than that of the surrounding air. Figure 5-8 shows calculations of normalized, average fireball densities for three detonation regions. In general, the difference between fireball density and ambient density at a given altitude is small in comparison to the large change in density that occurs over the altitude region through which a fireball rises.

Higher than ambient density occurs in the air shock front outside the fireball. Typical values for low-altitude bursts are a few times ambient density close to the fireball. At high altitudes, where the shock propagates into decreasing density, the density in the shock front may be several times ambient for radial distances of several hundred kilometers from the fireball. Smaller perturbations in the ambient density can occur over thousands of kilometers as the shock wave degenerates into acoustic and acoustic-gravity waves.

Order-of-magnitude increases in E- and F-region air density can be caused by upward motion of air heated by X-rays.

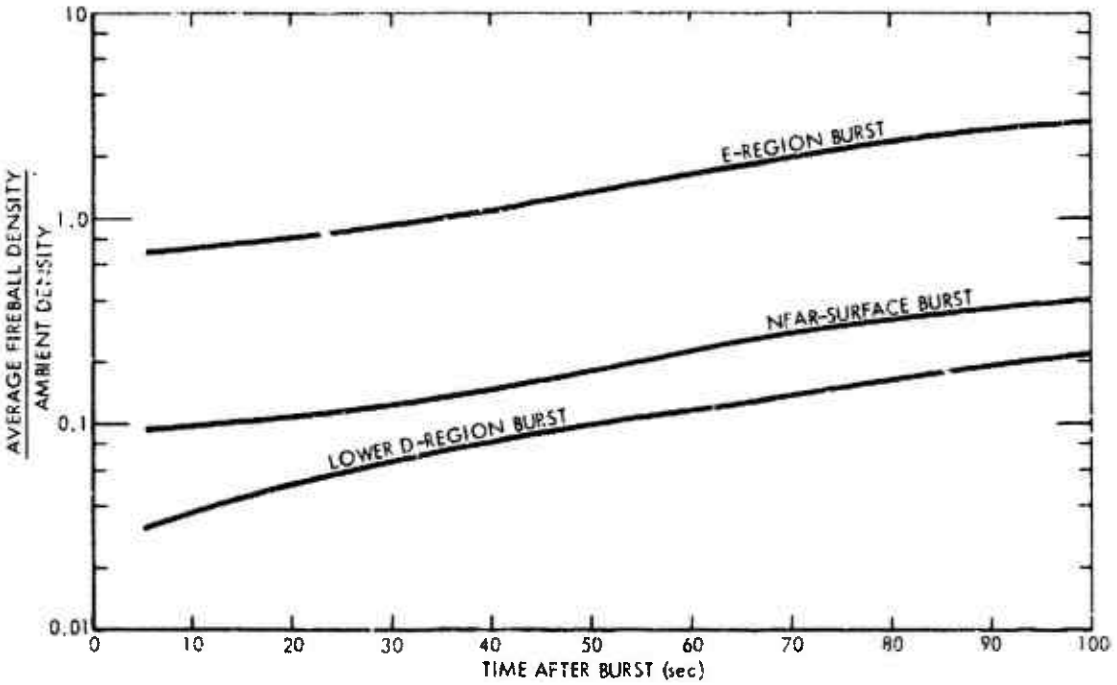


Figure 5-8. Examples of fireball density for three detonation regions.

### 5.2.3 Ionization Changes

The free electrons within fireballs at temperatures above about 3000 K arise primarily by thermal ionization of the contained air and the weapon-case material. At later times when the fireball temperature is lower, the free electrons may arise partly by thermal ionization of the metal atoms and partly by beta-particle ionization of the contained air. In the cooler regions outside the fireball, a prompt radiation pulse produces a large initial enhancement of the ionization. The ionization level subsequently decays to, and is maintained at, above-normal values by delayed beta-particle and gamma-ray emissions from the nuclear-weapon debris. Significant changes in the existing ionization levels can also be caused by shock and acoustic-gravity waves, which may propagate in the ionosphere thousands of kilometers from the burst point.

No direct measurements have been made of ionization inside the fireball regions. Values of the electron density are usually inferred from measurements of radio-wave absorption in the disturbed regions. Examples of inferred electron-density values for various specified conditions are cited below.

### 5.2.3.1 INSIDE FIREBALLS

For detonations in and below the D-region, ionization levels in the fireball are not maintained above single ionization because of radiative effects. At higher detonation altitudes, multiple ionization may be important.

After a few seconds, the electron density within a fireball is determined by either thermal ionization of the air or beta-particle ionization, depending on which is the greater source. At altitudes below about 75 km, reassociation of the initially dissociated air in the fireball occurs rapidly; electrons can recombine dissociatively with the positive molecular ions sufficiently fast that the thermal-equilibrium values of electron density are maintained as the temperature drops. The electron density continues to fall with the temperature until a point is reached, beyond which the subsequent rate of fall-off is determined by beta-particle ionization. For heights above about 75 km, the molecular reassociation process is less rapid, and the electrons tend to recombine with the positive atomic ions by the slower radiative-collisional recombination process. During both the low-altitude equilibrium phase and the high-altitude nonequilibrium phase, the electron density is not a very sensitive function of weapon yield. During the time the ionization is controlled by the beta particles, however, the resulting electron density is approximately proportional to the square root of the weapon yield. In Figure 5-9, curves are shown depicting calculated electron densities within fireballs for the three detonation regions used in the two previous figures to illustrate the temperature and density variations. The results are consistent with deductions from radio-wave absorption data.

The curves of Figure 5-9 are representative of disturbed conditions within nuclear fireballs in which the metallic content is small enough not to influence the degree of ionization to an appreciable extent.

The effect of metallic species within fireballs is highly speculative. However, if metallic ions remain atomic for long periods of time, the electron density in fireballs below about 75 km may be increased significantly at times later than a few seconds after detonation. An example of this effect is shown in Figure 5-10. Plotted here are curves of electron density as a function of time computed for a firehall of a medium-yield weapon detonated at 40 km. The assumed metallic content of 600 pounds of aluminum is considered

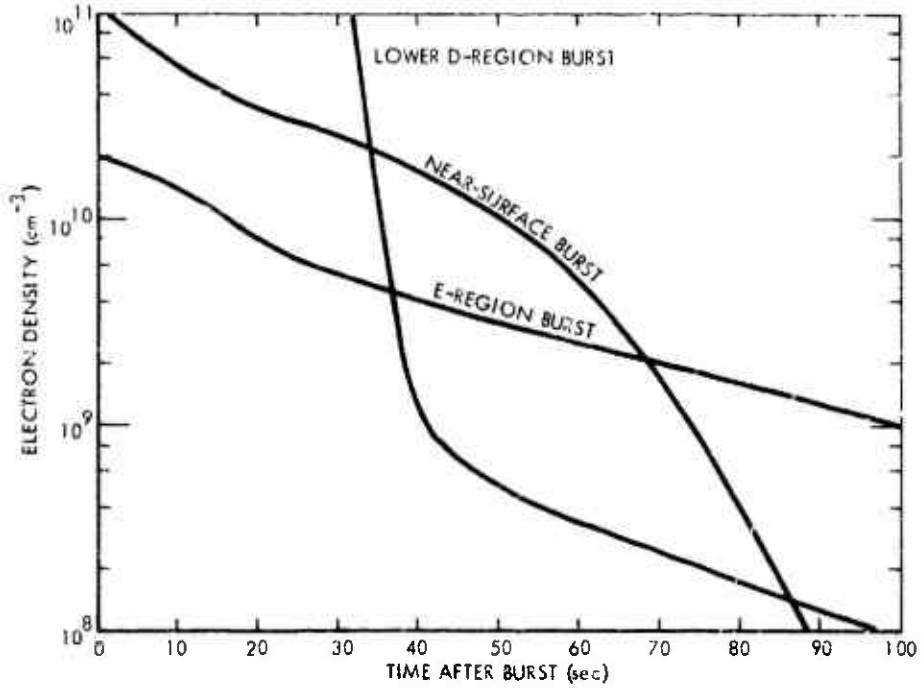


Figure 5-9. Examples of fireball electron density for three detonation regions.

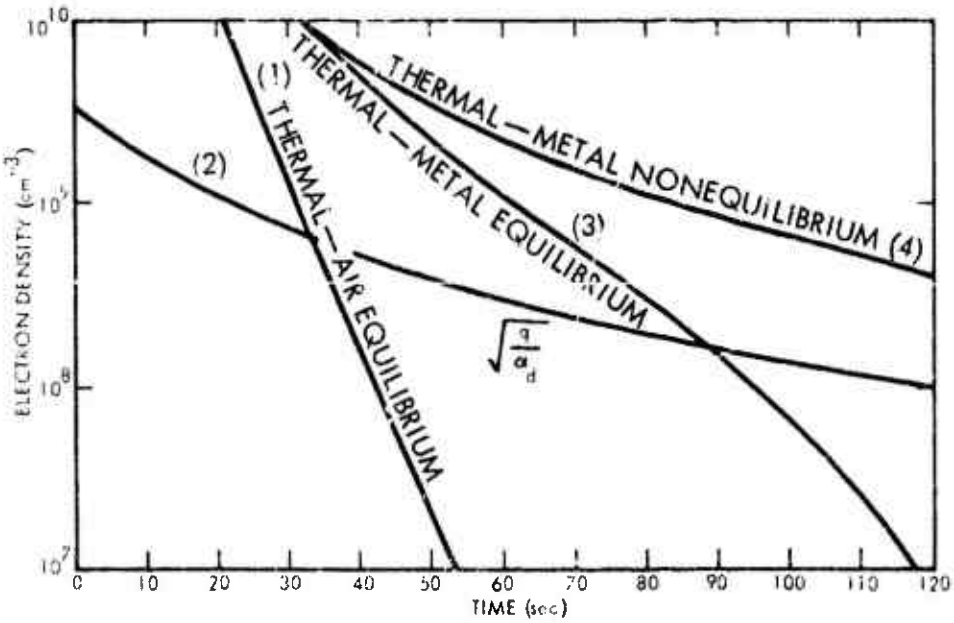


Figure 5-10. Ionization due to a medium-yield weapon (with 600 lb Al) detonated at 40 km.

to be distributed uniformly within the fireball volume. Curve (1) represents the electron density corresponding to thermal ionization of the contained air; curve (2) represents that due to beta-particle ionization of the air; curve (3) represents the ionization that would prevail if the metallic ionization could stay in thermal equilibrium; and curve (4) is based on the assumption that the metallic ions remain atomic so that the ionization cannot diminish fast enough to maintain the thermal equilibrium values. It can be seen that an order-of-magnitude increase in the estimated electron density can result from the presence of an appreciable number of atomic metal ions.

### 5.2.3.2 OUTSIDE FIREBALLS

Most of the total weapon energy is radiated over a very short interval of time and produces an initial pulse of ionization outside the fireball, while a smaller fraction is radiated more slowly in the form of beta particles and gamma rays. Figure 5-11 shows ionization contours representative of the initial pulse for a one-megaton weapon detonated at 120 km. Each contour is labeled by the appropriate horizontal distance in km from the burst, and a "typical"

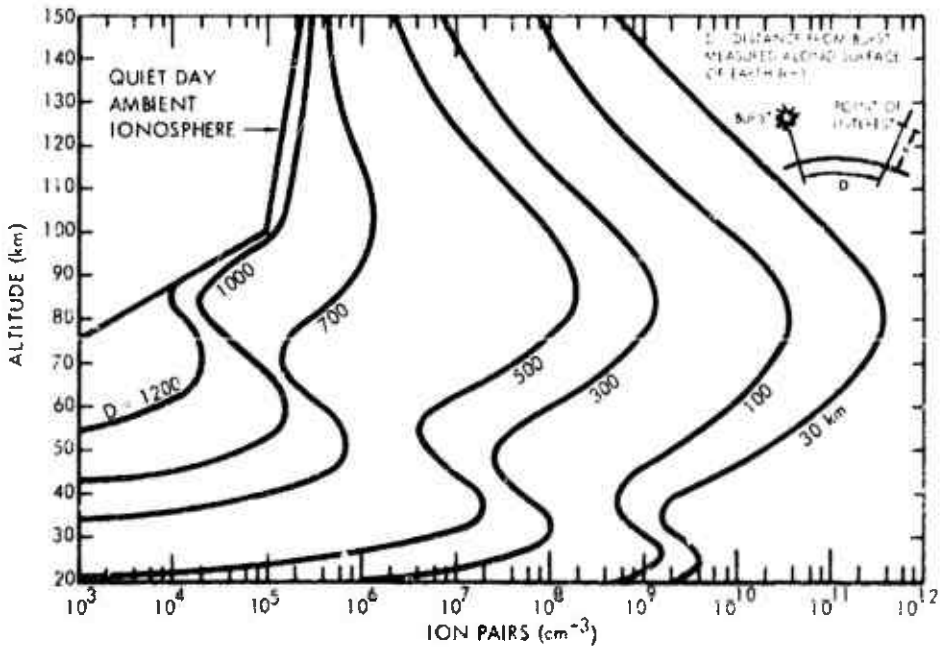


Figure 5-11. Ion-pair density due to prompt radiation from a 1-MT burst detonated at 120 km, t = 0.

quiet day profile of electron density is shown for comparison. The prompt ionization scales directly with the weapon yield. For higher detonation altitudes, the ionization is more widespread but less intense due to divergence. At lower detonation altitudes, absorption of X-rays limits the extent of X-ray ionization.

The D-region ionization level maintained by the delayed beta and gamma radiations, to which the initial ionization soon decays, is dependent upon weapon yield and upon the height and distribution of the fission debris. It is also dependent upon the deionization chemistry. Typical plots of the ion-pair production rates by beta and gamma radiations from a high-fission-yield (1-MT) weapon, at 100 seconds, directly beneath the volume containing the fission debris, are shown in Figure 5-12. The debris is assumed to be at a height of 150 km, and the beta-particle tube is assumed to be perpendicular to the earth's surface beneath the debris region. The production rate scales directly with the fission yield and inversely with $(1+t)^{1.2}$ and the square of the debris radius.

The electron density profiles corresponding to the production rates shown in Figure 5-12 are shown in Figure 5-13. These have

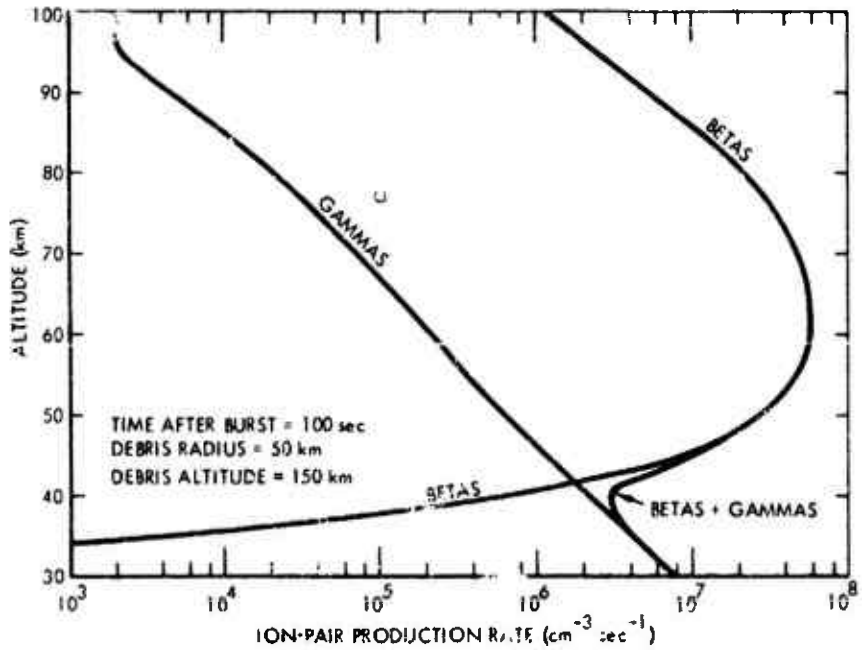


Figure 5-12. Ion-pair production rates from beta and gamma radiation beneath a 1-MT fission debris region.

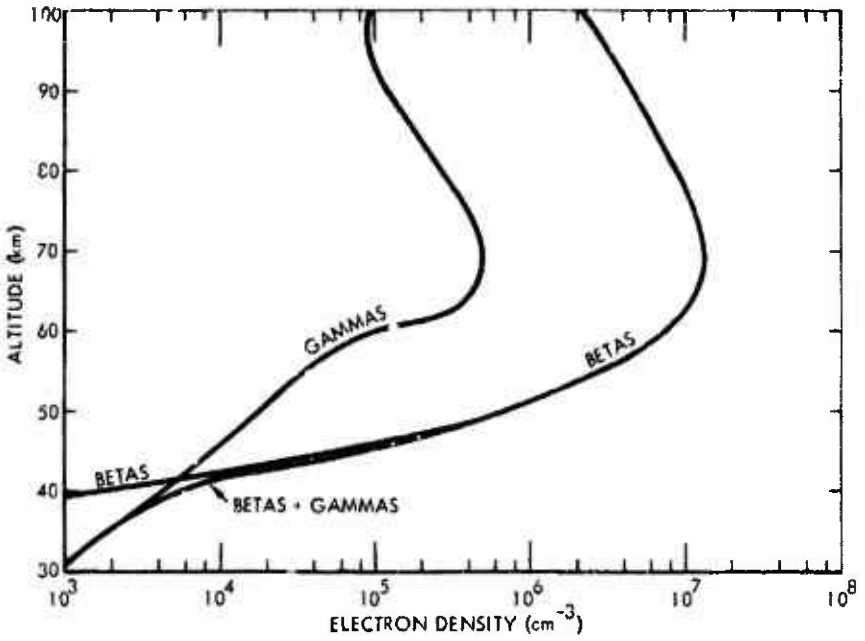


Figure 5-13. Electron density profiles corresponding to the ion-pair production rates shown in Figure 5-12.

been computed using the "lumped-parameter" approach to reaction rates (Reference 5-26), and they are consistent with experimental deductions.

The decay of prompt ionization in the E- and F-regions of the ionosphere is affected by the production of excited states, particularly $O(^1D)$, $N(^2D)$, and vibrationally excited $N_2$. In addition, hydrodynamic motion caused by deposition of prompt radiation can be a significant factor in determining deionization chemistry.

Large-scale traveling disturbances in the E- and F-regions of the ionosphere, e.g., shock waves, acoustic waves, and acoustic gravity waves, can be caused by bursts at low and high altitudes. These traveling disturbances are coupled to the ionization and can cause either positive or negative perturbations to the existing ionization, depending upon height, total energy, wave propagation direction with respect to the geomagnetic field, and other parameters (References 5-27, 5-28).

### 5.2.4 Atmospheric Composition Changes

Atmospheric composition changes following the detonation of nuclear devices undoubtedly occur, at least over limited volumes of space and for limited periods of time. At high temperatures, the air is highly dissociated and ionized by collisional and radiative processes. Unfortunately, no data are available to reach any firm conclusions about the amounts and kinds of new atmospheric species that may be produced. While the amounts and types of contaminants introduced from the weapon case and rocket carrier are known, the subsequent interactions of these materials with the air are not well understood. It is believed, however, that a fireball may carry to a higher altitude concentrations of species (such as NO) that are large relative to those normally present. In addition, when the fractional ionization of the air is large, dissociative recombination of free electrons with positive molecular ions liberates atoms of nitrogen and oxygen. According to calculations by Branscomb and LeLevier (Reference 5-29), the nitrogen atoms oxidize to form nitric oxide on a relatively fast time scale, while at a slower rate the oxygen atoms react to form ozone. Finally, the NO and $O_3$ interact to form nitrogen dioxide. The numerical results are rather dependent upon the fractional ionization and the altitude. For example, a fractional ionization of $5 \times 10^{-5}$ at 70 km produces an ozone concentration more than an order of magnitude greater than that which exists under ambient conditions.

## 5.3 EXCITED SPECIES

Excited species appear to play an important part in determining composition and ionization in both the normal and disturbed atmospheres. The states likely to be of most importance in affecting ionization are the metastable states with relatively long radiative lifetimes. Detailed information concerning excitation and deexcitation processes for excited species is given in Chapter 20.

Some excited states that appear to be important in determining the undisturbed D-region ionization and ion composition are $O_2(a\,^1\Delta_g)$, $O(^1D)$, $O(^1S)$, and $N(^2D)$. In the E- and F-regions, where the electron temperature can be higher than the neutral gas temperature, vibrational excitation of nitrogen molecules affects the loss rate of atomic-oxygen ions (cf. paragraph 20.3.1.1).

The concentration of excited species can be greatly increased during disturbed conditions. Within the fireball, a significant frac-

tion of the metal ions may be excited and rapidly converted to molecular ions (cf. subsection 20.3.3). Outside the fireball, excited states of oxygen may be responsible for preventing the formation of hydrated ions in the upper D-region, with consequent effects on the electron-ion loss rate. As noted above (subsection 5.1.3), the altitude below which hydrated ions are dominant was lowered during a PCA event; a similar phenomenon apparently occurs following nuclear bursts. Very high electron and nitrogen vibrational temperatures can be produced in the E- and F-regions by nuclear bursts. In addition to their effect on reaction rates, excited states are significant in determining the rate at which energy deposited in the upper atmosphere from a nuclear burst is converted to thermal energy.

Excited states are responsible for a variety of optical effects in both the normal and disturbed atmospheres. Radiations from auroras and air glow are used to study atmospheric composition. Analysis of optical radiation is a major tool in the study of regions disturbed by nuclear bursts.

## 5.4 CHEMICAL RELEASES

Spectroscopy of resonant scattering and chemiluminescence from various chemicals released from rockets, either as trails or as point releases, has been used to study atmospheric properties (Reference 5-30). Trails formed by sodium and by trimethyl aluminum have proved valuable in measuring atmospheric winds, diffusion, and turbulence (Reference 5-31). Information on upper-atmospheric composition, temperature, and reaction kinetics is also obtainable from releases of these and other chemicals.

Of particular interest in the study of ionized plasmas is the release of alkali and alkaline-earth metals, which are easily ionized by sunlight. Twilight releases of barium in the ionosphere have proved useful, because both the neutral barium atoms and the barium ions have strong resonance lines in the visible spectrum, and the neutral and ionized clouds produced can be distinguished by color (Reference 5-32). A phenomenon common to most of the releases is the development in the ionized cloud of striations or columns of enhanced ionization aligned with the geomagnetic field (References 5-33, 5-34). In addition to studies of plasma instabilities and field-aligned striations, barium releases have been used to map the ionospheric magnetic and electric fields.

## REFERENCES


5-1. McDermott, D. P., and G. V. Grones, Space Research III: Proc. Third Int'l. Space Sci. Symp., W. Priester, Ed., North Holland Publishing Co., Amsterdam (1963); pp. 19-26.

5-2. Jacchia, L. G., Space Research II: Proc. Second Int'l. Space Sci. Symp., H. C. van den Hulst, C. de Jager, and A. F. Moore, Eds., North Holland Publishing Co., Amsterdam (1961); pp. 747-750.

5-3. Valley, S. L., Ed., Handbook of Geophysics and Space Environments, McGraw-Hill, New York (1965).

5-4. Jacchia, L. G., Space Research III: Proc. Third Int'l. Space Sci. Symp., W. Priester, Ed., North Holland Publishing Co., Amsterdam (1963); pp. 3-18.

5-5. Jacchia, L. G., Smithsonian Astrophys. Obs., Spec. Rep. No. 150 (1964).

5-6. Banks, P. M., Proc. IEEE 57, 258 (1969.

5-7. Evans, J.V., Electron Density Profiles in Ionosphere and Exosphere, J. Frihagen, Ed., North-Holland Publishing Co., Amsterdam (1966); pp. 399-445.

5-8. Evans, J. V., J. Geophys. Res. 75, 4803 (1970).

5-9. Thomas, L., J. Atm. Terrestr. Phys. 33, 157 (1971).

5-10. Huffman, R. E., D. E. Paulsen, and J. S. Larrabee, J. Geophys. Res. 76, 1028 (1971).

5-11. Mitra, S. K., The Upper Atmosphere, The Asiatic Society, Calcutta (1952); pp. 325-330.

5-12. Reid, G. C., in Advances in Upper Atmosphere Research, B. Landmark, Ed., The Macmillan Co., New York (1963); pp. 309-316.

5-13. Ellison, M.A., and J.H. Reid, Res. Geophys. 1, 43 (1964).

5-14. Belrose, J. S., and E. Cetiner, Nature 195, 688 (1962).

5-15. Megill, L. R., et al., J. Geophys. Res. 76, 4587 (1971).

5-16. Jespersen, M., et al., Electron Density Distribution in the Ionosphere and Exosphere, E. Thrane, Ed., North-Holland Publishing Co., Amsterdam (1964); pp. 22-35.

5-17. Narcisi, R. S., et al., "Negative Ion Composition of the D- and E-Regions During a PCA", COSPAR Symposium on November 1969 Solar Particle Event, Boston College, Chestnut Hill, Massachusetts (1971).

5-18. Narcisi, R. S., et al., "Positive Ion Composition of the D- and E-Regions During a PCA", COSPAR Symposium on November 1969 Solar Particle Event, Boston College, Chestnut Hill, Massachusetts (1971).

5-19. Narcisi, R. S., et al., "Ion Composition Measurements in the Lower Ionosphere During the November 1966 and March 1970 Solar Eclipse", COSPAR Eclipse Symposium, Seattle, Washington (1971).

5-20. Windelmann, R. W., and R. B. Dyce, J. Geophys. Res. 69, 3625 (1964).

5-21. Garriott, O. R., et al., J. Geophys. Res. 72, 6099 (1967).

5-22. Obayashi, T., Res. Geophys. 1, 335 (1964).

5-23. Glasstone, S., Ed., The Effects of Nuclear Weapons, U. S. Government Printing Office, Washington, D. C. (1962).

5-24. Pierce, E. T., Proc. IEEE 53, 1944 (1965).

5-25. Latter, R., and R. E. LeLevier, J. Geophys. Res. 68, 1643 (1963).

5-26. Knapp, W. S., et al., General Electric/TEMPO Report 66 TMP-18; DASA 1765 (1966).

5-27. Sears, R. D., "F-Region Electron Loss Rate Dependence Upon Ambient Temperature and Density: Application to Nuclear Burst Shock Wave Effects", DASA-Sponsored Symposium on Physics and Chemistry of the Upper Atmosphere, Waltham, Massachusetts (1968).

5-28. Lomax, J. B., and D. L. Nielson, J. Atm. Terrestr. Phys. 30, 1033 (1968).

5-29. Branscomb, L. M., and R. E. LeLevier, RAND Corporation Report RM-4364-PR (1964).

5-30. Harang, O., in Atmospheric Emissions, B. M. McCormac and A. Omholt, Eds., Reinhold, New York (1969); pp. 489-499.

5-31. Rosenberg, N. W., D. Golomb, and E. F. Allen, Jr., J. Geophys. Res. 68. 5895 (1963).

5-32. Haerendel, G., and R. Lust, Scientific American 219(11), 81 (1968).

5-33. Linson, L. M., and J. B. Workman, J. Geophys. Res. 75, 3211 (1970).

5-34. Haerendel, G. et al., in Atmospheric Emissions, B. M. McCormac and A. Omholt, Eds., Reinhold, New York (1969); pp. 293-303.

# 6. THE CHEMICAL KINETICS OF THE DISTURBED ATMOSPHERE

M.H. Bortner, General Electric Company
T. Baurer, General Electric Company
(Latest Revision 10 June 1971)

## 6.1 INTRODUCTION

The contributory role of chemical rate processes within the phenomenology of the disturbed atmosphere, and the importance of an adequate understanding of the pertinent chemical kinetics as a prerequisite to the simulation and quantitative description of such atmospheres, are summarized very briefly elsewhere in this Handbook (Chapter 1). In the present chapter, the specific types of reaction mechanisms are elaborated in somewhat greater detail. Farther on, in the Group C Chapters of the Handbook, these reaction types are described individually, and the numerical values characterizing the rates of chemical reactions are specified. Finally, in Chapter 24, all relevant chemical rate parameters are tabulated for ready reference, by reaction type.

Referring once again to the brief description in Chapter 1, it will be recalled that three specific environmental regions were defined, relative to the very early post-burst period, viz., the fireball proper, the fireball halo, and the cool disturbed region beyond (Section 1.3). It will be recalled as well that for each of these regions a statement was made as to the relative importance of conventional chemical kinetics, as opposed to the rate processes characterizing very hot plasmas. It was noted also that the latter types of interaction were more typical of the inner regions, while the former pertained more closely to the outermost, which is also the largest. Hence it may be inferred that in the present chapter, the stress is on rate processes typifying the chemical phenomenology of this outermost cool region, with some applicability to the fireball halo as well.

## 6.2 REACTION MECHANISMS

In the complex post-burst chemical kinetics system, the quantities of most interest in the determination of the overall atmospheric

deionization rate include the free electron density, the electron collision frequency, and the rate of decrease of electron density within the region considered, as functions of time and the prevailing environmental parameters. The several direct and ancillary chemical mechanisms which are recognized as important in the normalization of disturbed atmospheres are listed in Table 6-1. The reactions are generally exothermic when read as written, from left to right. In the normal atmosphere, and even in a highly ionized atmosphere which has yet to come to thermal equilibrium but is rather cool, the corresponding endothermic reactions, i.e., as read from right to left, are usually unimportant. The degree to which such reactions may be important is functionally dependent upon the temperature through the inclusion of the exponential term $\exp(-E/\mathcal{R}T)$ in the rate constant. (Cf. Chapter 24.) Certain exothermic interactions also require some energy of activation for reaction to occur. These have a similar temperature dependence and hence a similar exponential term included in their rate constants. All such temperature-dependent reactions tend more readily than elsewhere to occur behind the post-burst shock wave, somewhat as in the case of similar reactions taking place behind a reentry shock (Reference 6-1). Thus while ionization, excitation, and dissociation of ambient species are engendered directly by the radiative flux and high-energy particles emanating from the burst, the same chemical reactions may also be initiated by the thermal effects associated with shock-wave passage.

In regions at ambient temperature, the most important chemical processes are those by which free electrons disappear by entering exothermally into chemical bonding with other species, including both charged and neutral atoms and molecules. For example, electrons are removed by any one of several forms of direct recombination with positive ions, as listed under Reaction Type I in Table 6-1. These direct recombinations include: dissociative recombination, which is very rapid and prevails in the presence of molecular ions; radiative recombination, which is important only in highly dissociated atmospheres; and three-body recombination, which occurs to a significant extent in relatively dense atmospheric media, e.g., at lower altitudes.

Electron removal is accomplished also by attachment to neutral species, especially O, $O_2$, $O_3$, and $NO_2$, according to the processes listed under Reaction Type III of Table 6-1. The resulting negative ions are then removed either by mutual neutralization involving two or three colliding bodies (Reaction Type II of Table 6-1), or

they are destroyed by detachment (Reverse Reaction Type III of Table 6-1), in which case free electrons are returned to the reaction mix. The other Reaction Types listed in Table 6-1 involve either the transfer of charge among atomic and molecular species with no net effect upon the total ion concentration (Type IV), important ancillary reactions of the neutral species (Type V), or the transfer and radiation of quantum-state energy (Type VI).

The definition of chemical systems related to disturbed atmospheres is dependent in part upon an awareness of the possible reaction types listed in Table 6-1, and more specifically upon a knowledge of such reaction rate constants as are tabulated in Chapter 24 and elsewhere. An additional determinative factor is an appreciation of the variability of atmospheric composition, both in time and space, and of the predominant energy currents within the atmosphere. The present state of knowledge, as regards these two concepts, is perhaps best summarized in Reference 6-2, and in Chapter 4 of this Handbook. One final item of input to atmospheric chemical systems definition involves the highly localized thermal climate, which is discussed in the following section.

## 6.3 TEMPERATURE DEPENDENCE

The dependence of all endothermic as well as certain exothermic reactions upon the temperature was noted briefly above. However, in considering extremely localized conditions of interaction, especially at very early post-burst times, it is necessary to recognize the probability of a lack of equilibration among the various available degrees of freedom, and hence the requirement for definitions of "temperature" within the context of each temperature-dependent reaction in the atmospheric system under study.

For example, where such reactions involve the collisional interaction of free electrons, it is the translational temperature of the electrons which is controlling. In the normal atmosphere, the presence of thermal electrons has been reported at altitudes up to at least 120 km (References 6-3, 6-4), and that of electrons having high translational temperatures has been indicated above 200 km (Reference 6-5). But in the early phases of a disturbed atmosphere, when energy relaxation is as yet incomplete, large concentrations of relatively "hot" electrons may exist, especially within the environmental regions surrounding a nuclear fireball.

Table 6-1. Types of reaction.

N.B.: The designation "M" includes any and all catalysts, including neutral species, molecular and atomic ions, and electrons. The letters "W", "X", "Y", and "Z" each may designate any and all reacting species other than the electron, but including atoms (e.g., N, O, H), free radicals (e.g., OH, $NO_3$), and either free or bonded molecules (e.g., NO, $H_2O$). The use of a pair of these letters (e.g., WX, YZ) in designating a species does not in any way reflect on the complexity of the substance so designated; such usage merely facilitates the symbolic representation of particular reaction types. (Cf. Pars. 6.4.1 and 6.4.2.) It should be noted in addition that all reaction types listed in this table are represented by specific cases in the tables of Chapter 24 (where they are classified according to the types here included), except for several which are asterisked (*) below; the latter types have been included here for the sake of completeness of coverage, and to allow for possible future expansion of the table.

I. Ion-Electron Recombination vs. Ionization

A. Radiative Recombination vs. Photoionization ——— $X^+ + e = X + h\nu$

B. Three-Body Recombination vs. Collisional Ionization ——— $X^+ + e + M = X + M$

C. Dissociative Recombination vs. Associative Ionization ——— $XY^+ + e = X + Y$

*D. Ion-Electron Recombination with Dissociation vs. Ionization with Association ——— $X^+ + e + YZ = X + Y + Z$

*E. Ion-Electron Recombination with Rearrangement vs. Ionization with Rearrangement ——— $W + X^+ + e = Y + Z$

II. Ion-Ion Recombination vs. Ion-Pair Formation

A. Mutual Neutralization vs. Ion-Pair Formation $X^+ + Y^- = X + Y$

Table 6-1. (Cont'd)

| | |
|---|---|
| B. Three-Body Associative Ion-Ion Recombination vs. Dissaciative or Three-Body Ion-Pair Formation | $X^+ + Y^- + M = XY + M$ $= X + Y + M$ |
| C. Dissaciative Ion-Ion Recombination vs. Three-Body Assaciative Ion-Pair Farmation | $XY^+ + Z^- = X + Y + Z$ |
| D. Ion-Ion Recombination with Re-orrongement vs. Ion-Pair Formation with Reorrongement | $W^+ + X^- = Y + Z$ |
| **III. Attachment vs. Detochment** | |
| A. Rodiative Attachment vs. Phato-detachment | $X + e = X^- + h\nu$ |
| B. Three-Body Attochment vs. Collisianol Detochment | $X + e + M = X^- + M$ |
| C. Dissociative Attochment vs. Assaciative Detachment | $XY + e = X^- + Y$ |
| *D. Attochment with Reorrangement vs. Detochment with Reorrange-ment | $W + X + e = Y^- + Z$ |
| **IV. Ion-Neutrol Reactions** | |
| A. Positive-Ion Chorge Transfer | $X^+ + Y \rightarrow X + Y^+$ |
| B. Positive-Ian-Atom Interchange | $W^+ + X \rightarrow Y^+ + Z$ |
| C. Negative-Ion Charge Tronsfer | $X^- + Y \rightarrow X + Y^-$ |
| D. Negotive-Ion-Atom Interchange | $W^- + X \rightarrow Y^- + Z$ |
| E. Radiative Pasitive-Ion-Neutral Assaciation vs. Pasitive-Ion Photodissociation | $X^+ + \cdots = XY^+ + h\nu$ |
| F. Three-Body Positive-Ian-Neutrol Associotion vs. Positive-Ion Collisional Dissociotion | $X^+ + Y + M = XY^+ + M$ |

Table 6-1. (Cont'd)

| | |
|---|---|
| G. Radiative Negative-Ion-Neutral Association vs. Negative-Ion Photadissociation | $X^- + Y = XY^- + h\nu$ |
| H. Three-Body Negative-Ian-Neutral Association vs. Negative-Ian Collisional Dissociatian | $X^- + Y + M = XY^- + M$ |
| **V. Neutral Reactions** | |
| A. Radiative Neutral Recombination vs. Neutral Photodissaciation | $X + Y = XY + h\nu$ |
| B. Three-Body Neutral Recombination vs. Neutral Callisional Dissociation | $X + Y + M = XY + M$ |
| C. Rearrangement | $W + X \rightarrow Y + Z$ |
| **VI. Quantum-State Energy Transfer** | |
| A. Radiative Electronic-State De-excitation vs. Electranic-State Photoexcitation | $X^* = X + h\nu$ |
| B. Collisianal Electronic-State Quenching vs. Collisianal Electronic-State Excitation | $X^* + M = X + M$ |
| C. Radiative Vibrational-State De-excitation vs. Vibratianal-State Phatoexcitation | $X^\ddagger = X + h\nu$ |
| D. Collisional Vibrational-State Quenching vs. Callisianal Vibratianal-State Excitatian | $X^\ddagger + M = X + M$ |
| *E. Collisianal Electronic Energy Exchange | $X^* + Y \rightarrow X + Y^*$ |
| F. Collisianal Vibrational Energy Exchange | $X^\ddagger + Y \rightarrow X + Y^\ddagger$ |
| *G. Electronic-Vibrational Energy Transfer vs. Vibrational-Electronic Energy Transfer | $X^* + Y = X + Y^\ddagger$ |

Similarly, other temperature-dependent reactions may be uniquely controlled by the translational temperature of particular collision or interaction partners or classes of partners, e.g., neutrals, ions. In some instances, it has been shown that the vibrational temperature of diatomic reactants, e.g., molecular nitrogen, either partially or totally governs the rates of certain reactions. A dual dependence upon both translational and vibrational temperatures was found to be rate-determining, for instance, in (References 6-6, 6-7):

$$O^+ + N_2^{\ddagger} \rightarrow NO^+ + N \ .$$

A final consideration in this regard is the question as to whether and to what degree the rates of temperature-dependent reactions may be affected by the entry into the process of one or more reactants in a state of electronic excitation. Presumably the energy magnitude involved in the excitation would be expected to contribute to the activation energy requirement. What is not known, however, or even presumed, is whether the probability term inherent in the pre-exponential factor of both endo- and exothermic rate constants is affected significantly by the quantum states of individual reacting species.

## 6.4 ION RECOMBINATION PROCESSES

Although recombination and attachment are the two principal mechanisms for the removal of free electrons, many other reaction types play important roles in support of these processes. The rates of electron disappearance by the above routes depend upon the specific recombining ionic or attaching neutral interaction partner. The identities and concentrations of these reactants are controlled in turn by the output of ion-neutral and neutral-neutral reactions (Types IV and V, respectively, of Table 6-1). This is more readily illustrated by considering the chemical dynamics of the ionic species than of the electrons. However, it must be remembered that, despite any apparent contradiction in emphasis, it is still the free electron which is the critical species in determining the overall electrical balance of the reacting gaseous mixture. In the subsections which follow, the processes relating to molecular ions are treated first; the more complex problem posed by atomic ions is considered thereafter.

### 6.4.1 Molecular Ion Recombination

The principal mechanism by which molecular ions are neutralized

is dissociative recombination:

$$XY^+ + e \rightarrow X + Y \quad , \qquad \text{(I. C)*}$$

where the products X and Y may be atomic (e.g. N, O, or H) or molecular (e.g. $N_2$, $O_2$, NO, or $H_2O$). By extension, this class of reactions may be generalized to a form:

$$X_m Y_n Z_p^+ + e \rightarrow mX + nY + pZ \quad ,$$

whereby a great many complex ions (e.g. mono- and polyhydrates of $NO^+$ and of $H^+$) are included among the possible interacting species.

Alternatively, molecular ions are removed by the three-body process:

$$X^+ + e + M \rightarrow X + M \quad . \qquad \text{(I. B)}$$

which in the general case may be expressed as:

$$X_m Y_n^+ + e + M \rightarrow X_m Y_n + M \quad .$$

In this mechanism, M may represent any neutral or ionic species or an electron, and the ion being neutralized may be atomic or molecular, of any degree of complexity, provided the product X or $X_m Y_n$ is itself a stable species.

Necessary precursors to the above processes of types I. C and I. B sometimes include the association of relatively simple positive ions, i.e., of atomic or diatomic composition, with neutrals to form more complex positive ions, including polyhydrates. This build-up is accomplished either via three-body collision:

$$X^+ + Y + M \rightarrow XY^+ + M \quad , \qquad \text{(IV. F)}$$

or radiatively:

$$X^+ + Y \rightarrow XY^+ + h\nu \quad . \qquad \text{(IV. E)}$$

---

*The numbers given in parentheses are representative of reaction types as listed in Table 6-1.

In the general case, these mechanisms are expressed, respectively, as:

$$X_m Y_n^+ + Z + M \rightarrow X_m Y_n Z^+ + M \ ,$$

and:

$$X_m Y_n^+ + Z \rightarrow X_m Y_n Z^+ + h\nu \ .$$

Finally, molecular as well as atomic ions are neutralized by interaction with negative ions, both atomic and molecular, which have themselves been formed by electron attachment. Neutralizations in this manner may proceed by any of several paths, e.g.:

$$X^+ + Y^- \rightarrow X + Y \qquad \text{(II. A)}$$

$$X^+ + Y^- + M \rightarrow XY + M \text{ (or } X + Y + M) \qquad \text{(II. B)}$$

$$XY^+ + Z^- \rightarrow X + Y + Z \ . \qquad \text{(II. C)}$$

As in the other reaction types mentioned above, each of these is also capable of generalization to include those specific instances in which the positive ion of interest is itself a complex polyatomic species. Furthermore, these reactions are sometimes accompanied by rearrangement among the internal chemical bonds making up the two interacting species:

$$W^+ + X^- \rightarrow Y + Z \ , \qquad \text{(II. D)}$$

in a manner similar to the rearrangement reactions of neutrals.

### 6.4.2 Atomic Ion Recombination

Some of the mechanisms which are important in the neutralization of molecular ions are also important in the removal of atomic ions. Other reaction types, however, play significant roles primarily or solely with respect to the latter. Thus direct radiative recombination:

$$X^+ + e \rightarrow X + h\nu \ , \qquad \text{(I. A)}$$

comes into play to a significant extent only where many atomic ions and few molecules are found, i.e., at high altitudes in a highly ionized

atmosphere. On the other hand, while three-body recombination:

$$X^+ + e + M \rightarrow X + M \qquad \text{(I, B)}$$

is, as noted above, an important means of removing molecular ions, it also relates strongly to the neutralization of atomic ions, primarily in dense regions when many such ions are present, i.e., in highly ionized atmospheres at low altitudes.

Similarly, the two positive-ion-neutral association processes which, according to the discussion above, are responsible for the build-up of polyhydrated and other complex positive ions, also come into play as effective means of removing positively charged atoms, i.e., by converting them into molecular species, either radiatively:

$$X^+ + Y \rightarrow XY^+ + h\nu \,, \qquad \text{(IV, E)}$$

or via three-body interaction:

$$X^+ + Y + M \rightarrow XY^+ + M \,. \qquad \text{(IV, F)}$$

In either event, the ions produced are then subject to the removal mechanisms outlined for molecular ions. This series of reactions tends to be important primarily in very highly dissociated atmospheres in which the total concentration of atoms greatly exceeds that of electrons.

Another means by which atomic ions are removed by transformation to molecular ions, and by far the most common such means, involves charge transfer:

$$X^+ + Y \rightarrow X + Y^+ \,, \qquad \text{(IV, A)}$$

which may be accompanied by atom interchange:

$$W^+ + X \rightarrow Y^+ + Z \,. \qquad \text{(IV, B)}$$

These reaction types usually are characterized by rate constants which are considerably higher than those for other modes of atomic ion removal. Their importance to any given atmospheric chemical system is limited only by the availability within the reaction matrix of neutral molecular concentrations of a magnitude sufficient to ensure an adequate collision frequency. This condition is met, in highly

dissociated atmospheres, by the occurrence as precursor events of neutral atom recombinations taking place either radiatively:

$$X + Y \rightarrow XY + h\nu \ , \qquad (V, A)$$

or through three-body collision:

$$X + Y + M \rightarrow XY + M \ . \qquad (V, B)$$

Since both of these mechanisms are reversible, either through the appropriate form of irradiation in an optically thick medium or through a sufficiently energetic two-body collision, the entry of XY-type products into charge transfer or charged rearrangement interactions with atomic ions is competitive kinetically with their redissociation into neutral atoms. Sometimes, depending upon the particular species involved and the particular atmospheric system under consideration, the odds in this competition may be changed significantly one way or the other by the interim occurrence of neutral rearrangements:

$$W + X \rightarrow Y + Z \ . \qquad (V, C)$$

One final mechanism for the removal of atomic ions, which is important within and in close proximity to the fireball, is called collisional-radiative recombination. This process has not been schematized in Table 6-1, inasmuch as it involves a complex combination of radiative recombination (I. A), three-body recombination (I. B), and collisional excitation and deexcitation (IV. B).

### 6.4.3 Ion Recombination Summary

The recombination mechanisms of atomic ions, including both ambient and contaminant metallic species, are important primarily at high altitudes and in highly dissociated atmospheres. The relative importances of individual mechanisms vary with the conditions prevailing in a given system under consideration. Thus, when the concentration of neutral molecules is at least as great as that of the atomic ions, charge transfer (IV. A, B) tends to dominate. However, there are large zones in which the concentration of atomic ions greatly exceeds that of the neutral molecules. This is especially true in the natural atmosphere at altitudes of 300 km and above, and in disturbed atmospheres appreciably below this level. In such cases, another mechanism must take precedence. Thus for some sets of

conditions, the importance of charge transfer is dependent upon the rate of precursor atom recombination (V, A, B). However, ion-atom association (IV, E, F) is sometimes significantly faster in such circumstances. Furthermore, wherever there is essentially complete dissociation and ionization, as in and near the fireball, only the complex collisional-radiative recombination can occur in the initial stages of deionization. After enough neutral atoms have been formed in ion-electron recombination (I, A, B), other mechanisms including attachment (III, A, B), ion-atom association (IV, E, F), charge transfer (IV, A, C), and mutual neutralization or recombination (II, A, B) all tend to assume increasingly important roles in the overall chain of events. Ultimately the positive molecular ions produced by charge transfer (IV, A, B) and associative processes (IV, E, F) are themselves neutralized primarily by dissociative recombination (I, C), three-body recombination (I, B), and to a lesser degree of importance by any one of several ion-ion recombinations (II, A-D) involving negative ions, both atomic and molecular.

It is imperative, in analyzing perturbed atmospheres and their associated chemical phenomenologies, that all these mechanisms be taken into account. Actual determination of the relative importance of individual deionization mechanisms depends on a knowledge of the values of all the rate constants involved. The high degree, amounting to orders of magnitude, of uncertainty in certain kinetic parameters sometimes adds considerable difficulty to the accurate prediction of the dominant operative processes in the atmospheric chemical systems of greatest concern.

## 6.5 OTHER KINETIC CONSIDERATIONS; THE ROLE OF METASTABLE STATES

Endothermic reactions generally tend to contribute less importantly to the overall deionization phenomenology than exothermic reactions. However, although detachment processes are usually endothermic, as indicated by their presentation in the reverse mode in Table 6-1 (i.e., to be read from right to left), certain associative detachments (III, C) are not. For example, the reaction $O_2 + O^- \rightarrow O_3 + e$ is indeed endothermic, but $O_2^- + O \rightarrow O_3 + e$ and $O^- + O \rightarrow O_2 + e$ are exothermic. The latter pair of interactions play a significant role in atmospheric deionization kinetics under some conditions, insofar as they tend to act in opposition to other processes contributing to the electron density decay. By the same token, the corresponding dissociative attachments, i.e., the reverse of the

last two reactions cited, are endothermic, unlike most attachments, and therefore tend to delay the disappearance of electrons at altitudes below about 80 km in relatively undissociated atmospheres, where the concentration of molecular oxygen is therefore much greater than that of oxygen atoms.

Among other endothermic processes, photoionization (I. A), photodetachment (III. A), and photodissociation (IV. E, G; V. A) require no kinetic energy input, since they derive all their endothermicity from radiative sources. It follows that these become important in systems having an appreciable time scale, and an effective radiating source, e.g., during daylight hours under solar irradiation.

The role played in chemical kinetics by gaseous reactants in excited, as opposed to ground, electronic and vibrational states is an area which has been and continues to be subject to increasingly intensive investigation. This is amply demonstrated by the depth of treatment accorded to the subject elsewhere in this Handbook, viz., Chapter 20. Within the present context, however, certain features relating to excited-state effects are worthy of special emphasis. Thus, while a number of early analyses may be cited (References 6-8 through 6-11) which pertain to excited states in the natural atmosphere, it is in relation to the disturbed environment following a nuclear burst that the greatest interest arises with respect to the populations and interactions of electronically and vibrationally excited species. For it is here that the initial thermal nonequilibrium, combined with the subsequent chemistry, tends to perpetuate a relatively high degree of internal molecular and atomic disequilibrium. As a result, metastable states of the major atmospheric constituents come to develop relatively large concentrations, and therefore intrude directly and significantly into the deionization phenomenology, through direct interaction with charged species as well as through a measure of control of neutral species densities.

It is to be expected, for instance, that the rate constants of individual reactions should be altered by the substitution, for a given reactant in its ground state, of an excited allotrope of the same species, since the spin properties and energetics of excited species generally differ from those of the corresponding unexcited substances. These differences in spin may change a spin-forbidden reaction to an allowed one, or vice versa, and the internal energy associated with electronic or vibrational excitation may be sufficient to convert an otherwise endothermic reaction to an exothermic one, or at least

to reduce the degree of endothermicity. Laboratory results have long since confirmed these expected effects (References 6-12 through 6-18). For example, while collisional detachment from $O_2^-$ is endothermic for reactants in the ground state, it becomes exothermic when the colliding partner is either vibrationally excited nitrogen or electronically excited oxygen, $O_2(a^1\Delta_g)$.

Moreover, beam experiments with species unrelated to atmospheric systems have indicated that in certain instances the translational energy of reactants is ineffective in meeting activation energy requirements of endothermic interactions, but that internal energy of excitation is actually a requirement (Reference 6-19). It would appear to be a matter of the deepest concern that any other reactions of similar requirement but greater pertinence to disturbed atmospheres and to the E and F regions, where the assumption of local thermodynamic equilibrium would be invalid, be identified forthwith. For all such cases, rate constants which have been determined on the basis of equilibrium considerations would simply not be applicable to the environments and time frames of greatest concern. Finally, the reader's attention is redirected to two reactions the kinetics of which have been shown to depend upon vibrational temperature. These are: the charged rearrangement $O^+ + N_2 \rightarrow NO^+ + N$ (discussed in Section 6.3, above), and the dissociative attachment $O_2 + e \rightarrow O^- + O$ (discussed in Chapter 20 of this Handbook), which are controlled by the vibrational temperatures of nitrogen and oxygen, respectively.

In the foregoing paragraphs, specific examples have been cited for which the states of internal electronic or vibrational energy of reacting species are known to affect the deionization rate chemistry. Indeed, whereas the rates of most of the important reactions are so rapid, even with ground-state reactants, that the concentrations of metastables would have to approach parity with those of their unexcited counterparts before they could be expected to affect the overall result of the operative deionization mechanisms to any significant degree, nevertheless this certainly can happen, especially in the warmer and earlier spatial and temporal regions associated with nuclear bursts. In fact, many endothermic reactions, turned exothermic by virtue of the internal excitation of their reactants, may be shown to dominate the deionization phenomenology, even at significantly lower densities than the corresponding ground-state species.

Those electronically and vibrationally excited species which appear to affect the disturbed atmosphere most particularly may be cited here. They include vibrationally excited $N_2$, $O_2$, $O_2^+$, perhaps $N_2^+$, and for those conditions where its presence is acknowledged, CO. The cumulative effect of these metastables directly determines the overall vibrational temperature. The designations and some of the effects of electronically excited species of particular importance are as follows:

$O_2\left(^1\Delta_g\right)$ and $O_2\left(^1\Sigma_g^+\right)$ alter the rate constants of such reactions as $N + O_2 \rightarrow NO + O$ (Reference 6-2).

$O(^1D)$ reverses the endothermicity of the charge exchange between $O_2^+$ and O, and enhances exothermicity in other reactions of this type. Its production rate constant via the dissociative recombination of $NO^+$ is unknown.

$N(^2D)$ similarly affects the direction of energy flow associated with charge exchange, e.g., in $O^+ + N$, and also appears to affect the chemistry of the neutral rearrangement with $O_2$. Its rate of formation in the dissociative recombination of $N_2^+$ is uncertain.

$O^+(^2D)$ also enters into the energetics of charge exchange, especially with N and $N_2$.

$N_2\left(A\ ^3\Sigma_u^+\right)$, $N_2\left(B\ ^3\Pi_g\right)$, $N_2^+\left(A\ ^2\Pi_u\right)$, $N_2^+\left(B\ ^2\Sigma_u^+\right)$, $NO\left(A\ ^2\Sigma^+\right)$, $NO\left(B\ ^2\Pi_r\right)$, $O_2^+\left(A\ ^2\Pi_u\right)$, and $O_2^+\left(b\ ^4\Sigma_g^-\right)$ are all important contributors to the radiative emission of the early post-burst environment, and to some extent may enter into the chemical kinetics as well in media dense enough to provide characteristic collision times comparable with the respective radiative lives.

$O_2^+\left(a\ ^4\Pi_u\right)$ enters into the chemical scheme by way of its participation in charge transfer and charged rearrangement.

A primary concern in evaluating the problems of deionization kinetics in the disturbed atmosphere is that of identifying key reactions in terms of tolerable limits of uncertainty on their respective rate parameters. The value of this aspect of the total analytical treatment has been recognized for some years (Reference 6-20). It continues to be considered among the most central areas for inves-

tigation. Such studies as were reported in Reference 6-20 typically start by assuming a number of candidate reactions and rate parameters within a given system, and then proceed to vary the pertinent numbers both individually and in combinations or groups. Conclusions are drawn from the results of system computations, as to the significance of these variations in determining the overall system dynamics, and hence, as to the real necessity for resolving existing uncertainties. From such studies there eventually issue forth concrete indications as to the most promising directions for further laboratory experimentation.

## 6.6 DATA GATHERING, INTERPRETATION, AND USE

Reaction rate constants comprise primary data necessary for chemical kinetics calculations related to the disturbed atmosphere. These data are obtainable through laboratory experiments, theoretical analyses, and atmospheric observations and measurements, the specific methods for which are described in Chapter Group B of this Handbook.

Rate data derived from any of these sources are usually presented in one of two forms. The first of these is the rate constant itself, which is not always a true constant inasmuch as it is functionally dependent on the temperature. This dependence is most simply expressed in the form: $k = aT^b \exp(-c/T)$, where a, b, and c are characteristic for a given reaction, and the rate "constant", k, reflects the kinetics of the reaction in question under conditions such that the reactants are Boltzmannian with respect to their allowable state distributions. The possibility of departures from Boltzmann statistics in certain cases was treated earlier in this Chapter. However, assuming no such departures exist, i.e., the system under study is adequately describable in Boltzmannian terms, then the use of rate constants which have themselves been determined under equilibrated conditions is quite valid.

If for example, one is dealing with a reversible reaction: A + B = C + D, for which the rate constants in the forward and reverse directions, respectively, are designated as k and k', then the equilibrium constant K (which is discussed in Chapter 10 of this Handbook) is equal to the ratio k/k', always provided that k and k' describe the two reactions for the case where the exact same states of A, B, C, and D are involved. Quite strictly, then, each state of each species

should be considered as a separate species, in order for the generalization $K = k/k'$ to apply in the non-Boltzmann case.

In the tabulations comprising Chapter 24 of this Handbook, the parameters a, b, and c which enter into the formulation of each rate constant are listed in such a manner as to facilitate dimensional treatment of the rate calculations. This is done by normalizing the temperature with respect to 300 K taken as a reference value:

$$k = a(T/300)^b \exp(-c/T) , \qquad (6\text{-}1)$$

where c has the dimensions of a temperature, b is dimensionless, and a has the same units as k, i.e., $sec^{-1}$ for a unimolecular reaction, $cm^3 sec^{-1}$ for a two-body interaction, and $cm^6 sec^{-1}$ for three bodies. The quantity c is in reality the activation energy of the reaction, divided by the Boltzmann constant. Therefore for most, but not all, exothermic reactions it turns out to be zero. Likewise, the quantity b is very often zero for exothermic reactions.

The second form in which the rate chemistry pertaining to individual reactions is presented is as $\sigma$, the cross-section for reaction as a function of the energy of collision. This kind of datum is very specific for the particular interacting states involved, and is therefore convertible to the more familiar rate constant formulation only with utmost care and discretion. As a general rule, the two forms are related to one another through v, the relative velocity of collision:

$$k(cm^3 sec^{-1}) = \sigma(cm^2)\ v(cm\ sec^{-1}) . \qquad (6\text{-}2)$$

It is readily seen that this relationship, and thus the entire validity of cross-section data, pertains only to two-body interactions.

Since this very simple expression is correct only for systems involving the very same reacting states, or distributions of states, as that for which the original cross-sections were obtained, the uses of such information would appear to be rather severely limited. The situation seems even more restrictive when one recalls that a variety of techniques are utilized in the laboratory in order to determine the basic cross-sections. As a result, numerous variations exist on Equation (6-2). These have been compiled in some detail elsewhere (Reference 6-21). A few of the more common of

these variations are presented in the remaining paragraphs of this Chapter.

In the most ordinary instance, it is desired to derive a rate constant $k_T$ for a system having a Maxwellian velocity distribution, from monoenergetic cross-sections $\sigma_E$. This requires integration over the full range of collisional velocities:

$$k_T = \int_0^\infty v \sigma_E f_v \, dv , \tag{6-3}$$

where $f_v$ is the fraction of collisions with relative velocities between v and v + dv. From this can be obtained:

$$k_T = 2.52\mu^{-1/2} T^{-3/2} \int_0^\infty \sigma_E E e^{-E/kT} \, dE , \tag{6-4}$$

which is then solved by graphical integration, and where $\mu$ is the reduced mass of the collision, and $k$ is the Boltzmann constant.

It is often possible, over limited energy ranges, to express the cross-section as a simple function of this energy. This facilitates the conversion of such data to a rate constant which is valid within the corresponding temperature range. In such cases, assuming the available data happen to fall into the most important or interesting energy range, as is often the case, then the need for graphical integration is avoided. For example, the cross-section may be a linear function of the interaction energy. If the corresponding rate constant is intended for application to a Boltzmann system, then the energy range for which cross-sections are available may well be the only part of the total energy spectrum which is of any importance. In this case:

$$\sigma = C(E - E_t) , \tag{6-5}$$

where $E_t$ is the energy threshold for reaction, E is the collision energy, and C is the linear slope. Inserting this relationship into the previous equations, a general expression is obtained for the case in which one particle provides all the interaction energy. Substitution and integration in this manner thus gives:

$$k_T = 1.87 \times 10^{-8} C\mu^{-1/2} T^{1/2} \left(E_t + 1.723 \times 10^{-4} T\right) e^{-E_t/kT} . \tag{6-6}$$

At low or moderate temperatures, this is reduced to

$$k_T = 1.87 \times 10^{-8}\ C\mu^{-1/2}\ E_t\ e^{-E_t/\mathcal{R}T}\ . \qquad (6\text{-}7)$$

For electron collisions:

$$k_T = 6.20 \times 10^{5}\ CT^{1/2} \left(E_t + 1.723 \times 10^{-4}\ T\right) e^{-E_t/\mathcal{R}T}\ ; \qquad (6\text{-}8)$$

and for heavy particle collision processes:

$$k_T = 1.45 \times 10^{4}\ CM^{-1/2}\ T^{1/2} \left(E_t + 1.723 \times 10^{-4}\ T\right) e^{-E_t/\mathcal{R}T}\ , \qquad (6\text{-}9)$$

where M denotes the reduced molecular weight.

As mentioned above, other expressions for $\sigma_E$ as a function of energy are available, and additional details on this entire area may be obtained in comprehensive form elsewhere (Reference 6-21).

## REFERENCES


6-1. Bortner, M. H., General Electric Company Report TIS R63SD63 (1963).

6-2. Bortner, M. H., and R. H. Kummler, General Electric Company Report GE-9500-ECS-SR-1 (1968).

6-3. Dalgarno, A., 15th Gaseous Electronics Conference, Boulder, Colorado (1962).

6-4. Dalgarno, A., and M. B. McElroy, Planet. Space Sci. 13, 143 (1965).

6-5. Evans, J. V., 15th Gaseous Electronics Conference, Boulder, Colorado (1962).

6-6. Schmeltekopf, A. L., E. E. Ferguson, and F. C. Fehsenfeld, J. Chem. Phys. 48, 2966 (1968).

6-7. O'Malley, T. F., J. Chem. Phys. 52, 3269 (1970).

6-8. Hunt, B. G., J. Atmos. Sci. 23, 86 (1966).

6-9. Gattinger, R. L., and A. Vallance-Jones, Planet. Space Sci. 14, 1 (1966).

6-10. Dalgarno, A., DASA Symposium on the Physics and Chemistry of the Lower Atmosphere, Boulder, Colorado (1966).

6-11. Cadle, R., Disc. Faraday Soc. 51, 66 (1964).

6-12. Mathias, A., and H. I. Schiff, Disc. Faraday Soc. 37, 38 (1964).

6-13. Kaufman, F., and J. Kelso, Disc. Faraday Soc. 87, 26 (1964).

6-14. McGee, J., and J. Heicklen, J. Chem. Phys. 41, 2974 (1964).

6-15. Heicklen, J., Aerospace Corporation Report TDR-469 (5250-40)-9 (1965).

6-16. Arnold, J., N. Finlayson, and E. Ogryzlo, J. Chem. Phys. 44, 2529 (1966).

6-17. Snelling, D., V. Baiamonte, and E. Bair, J. Chem. Phys. 44, 4137 (1966).

6-18. Young, R., and G. Black, J. Chem. Phys. 44, 3741 (1966).

6-19. Jaffe, S. B., and J. B. Anderson, J. Chem. Phys. 51, 1057 (1969).

6-20. Bortner, M. H., General Electric Company Report DASA 1667 (1965).

6-21. Bortner, M. H., General Electric Company Report TIS R66SC14 (1966).

## GROUP B

## CHAPTERS ON METHODS OF GATHERING DATA

CHAPTER 7 Data - Gathering Methods Based on Laboratory Experimentation

CHAPTER 8 Data - Gathering Methods Based on Theoratical Analysis

CHAPTER 9 Data - Gathering Methods Based on Atmospharic Measurements

# 7. DATA-GATHERING METHODS BASED ON LABORATORY EXPERIMENTATION*

J.F. Paulsan
Air Force Cambridge Research Laboratories (AFSC)
and
J.K. Layton, R.H. Neynaber, and D.A. Vroom
Gulf Radiation Technology
A Division of Gulf Energy and Environmental Systems Company
(Latest Revision 3 September 1971)

## 7.1 INTRODUCTION

Laboratory methods which have been utilized for the acquisition of collision data pertinent to atmospheric deionization span the whole range of techniques available to the experimental atomic physicist. For the quiescent atmosphere, the interaction energy of the atmospheric species is in the thermal-energy range from about 200 to 2000 kelvins. For a perturbed atmosphere, however, much higher interaction energies are encountered, and the range from thermal levels to several electron volts is appropriate. Indeed, in examining the effects of weapons debris, interaction energies up to several million electron volts must be included.

One of the most widely exploited laboratory systems has been the gas-discharge afterglow, from which data have been obtained at thermal-energy levels on a great variety of two- and three-body collision processes. Rate coefficients for ion-neutral reactions continue to be derived from measurements of secondary ions in mass-spectrometer ion sources. This technique is useful in studying the interaction energy region just above thermal values, i.e., from a fraction of an eV to several eV, but the original method has now been supplanted by several variations and by beam methods. Above about 0.3 eV, ion-neutral reactions are most conveniently studied with the aid of a beam of the charged species passed into a chamber containing the neutral target gas. In the case of chemically unstable

---

* The authors are pleased to acknowledge that Dr. B.R. Turner originally prepared (for the First Edition of the Reaction Rate Handbook) certain material included in this Chapter.

neutral targets, the technique of crossed beams may be employed. Beam techniques have also been applied to a number of other problems of atmospheric interest. Ionization and excitation by electron impact and by photon impact, as well as photodetachment reactions, may be readily investigated using either the collision-chamber or crossed-beam method. Development of the merged-beam technique has provided a method for the study of ion-ion, ion-electron, and ion-neutral reactions over the entire energy range from several hundredths of an electron volt to kiloelectron volts. Finally, success has been achieved in deriving certain rate coefficients from the study of gases contained in a large chamber and irradiated with electrons from a van de Graaff accelerator.

## 7.2 AFTERGLOW STUDIES

Afterglow studies have provided much of the available data for many types of thermal-energy collisions. Among the collision processes which have been investigated are electron-ion (References 7-1 7-2, 7-3), ion-neutral (References 7-4, 7-5), ion-ion (Reference 7-5), neutral-neutral (References 7-6, 7-7), and three-body collisions (Reference 7-6). Most of these measurements were made at or near 300K, except for electron-ion dissociative recombination, which has been investigated for electron temperatures from 80 to 5000 K.

### 7.2.1 Electron-Ion Dissociative Recombination

Electron-ion dissociative recombination has been studied extensively by observation of the free-electron density as a function of time in the stationary afterglows of gas discharges. In a microwave observation technique developed by Biondi et al. (References 7-1, 7-2, 7-3), a pulsed discharge is produced within a microwave cavity. The resonant frequency, a function of the free electron density in the cavity, is measured as a function of time after cessation of the discharge. The identity of the positive ions is determined simultaneously with a mass spectrometer.

An apparatus of Mehr and Biondi (Reference 7-3) is shown in Figure 7-1. This experiment uses two cavity excitation modes in order to produce the plasma and heat the electrons separately. The plasma is produced by a 2-msec pulse from a magnetron. Following the discharge pulse a very low-power probing signal of variable

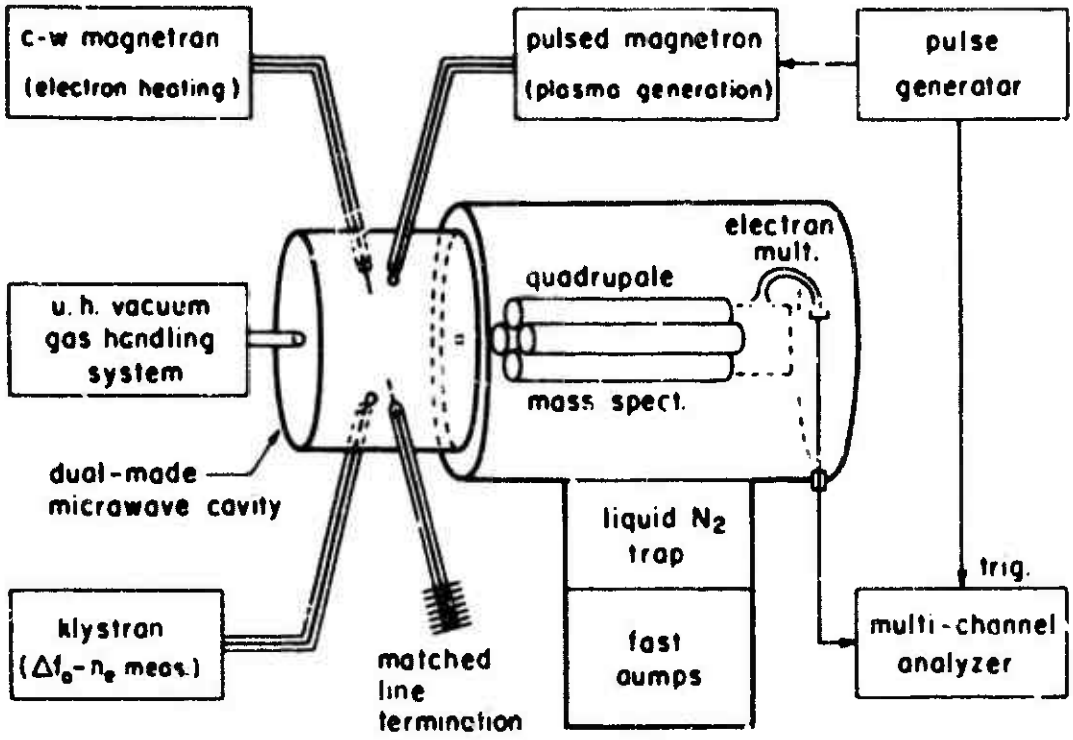


Figure 7-1. Simplified diagram of microwave afterglow mass spectrometer apparatus used by Mehr and Biondi in ion-electron recombination studies (Reference 7-3).

frequency is incident on the cavity. The frequency shifts are determined from measurements of the times of maximum reflections of the probing signals. The frequency measurement range of the microwave system gives reliable numbers for electron densities between $1 \times 10^7$ and $2 \times 10^{10}$ cm$^{-3}$.

To measure electron-temperature dependences of rate coefficients, the electrons are heated by exciting the cavity continuously in a mode different from the excitation producing the discharge. The cavity is loaded for this mode (to lower the Q), so that the small resonant-frequency shift during the afterglow electron decay causes a negligible effect upon the microwave heating field. Thus the electron temperature remains constant throughout the afterglow.

The relative ion densities during the afterglow are monitored with a quadrupole mass spectrometer coupled with an electron multiplier to detect ions effusing through a small hole in a wall of the cavity.

### 7.2.2 Ion-Neutral Interactions

Ion-neutral interactions have been studied extensively with stationary afterglows. In these experiments one observes the time variation of charged-particle densities following an ionizing pulse. Reaction rates can be determined either from afterglow data or from data taken during continuous ionization when the plasma is in equilibrium between production and loss processes. Although the afterglew measurements lead to more accurate rate constants, the twc techniques involve different analyses. Thus, the equilibrium plasma measurements provide a check on the validity of the afterglow data analysis. A detailed discussion of methods of analysis is found in Reference 7-4. A general discussion of afterglows is found in Reference 7-2.

An apparatus used for afterglow experiments at Ballistic Research Laboratories (Reference 7-4) is shown in Figure 7-2. Ionization is produced by photons from a microwave discharge lamp. Photoionization at selected wavelengths is used to provide a minimum of unwanted initial species. The collision processes occurring in the afterglow are studied with time-resolved mass spectrometry.

Some other ion-neutral measurements using stationary afterglows have been performed at the University of Birmingham (Reference 7-5) and at General Atomic (Reference 7-8).

Thermal-energy ion-neutral interactions have also been studied extensively with flowing-afterglow techniques. A diagram of the apparatus used at the National Oceanic and Atmospheric Administration Research Laboratories (Reference 7-9) is shown in Figure 7-3. Unlike the stationary-afterglow experiments, ions are produced in this technique in a rapidly flowing ($\approx 10^4$ cm sec$^{-1}$) carrier gas, commonly helium, and other reacting gases are introduced downstream from the region of primary ionization. The desired ionic reactant may be produced directly by electron impact or by charge transfer or Penning ionization in a gas introduced downstream. Still further downstream the desired neutral reactant is introduced. A quadrupole mass spectrometer is used to sample the ions in the flowing gas mixture through a small effusion orifice.

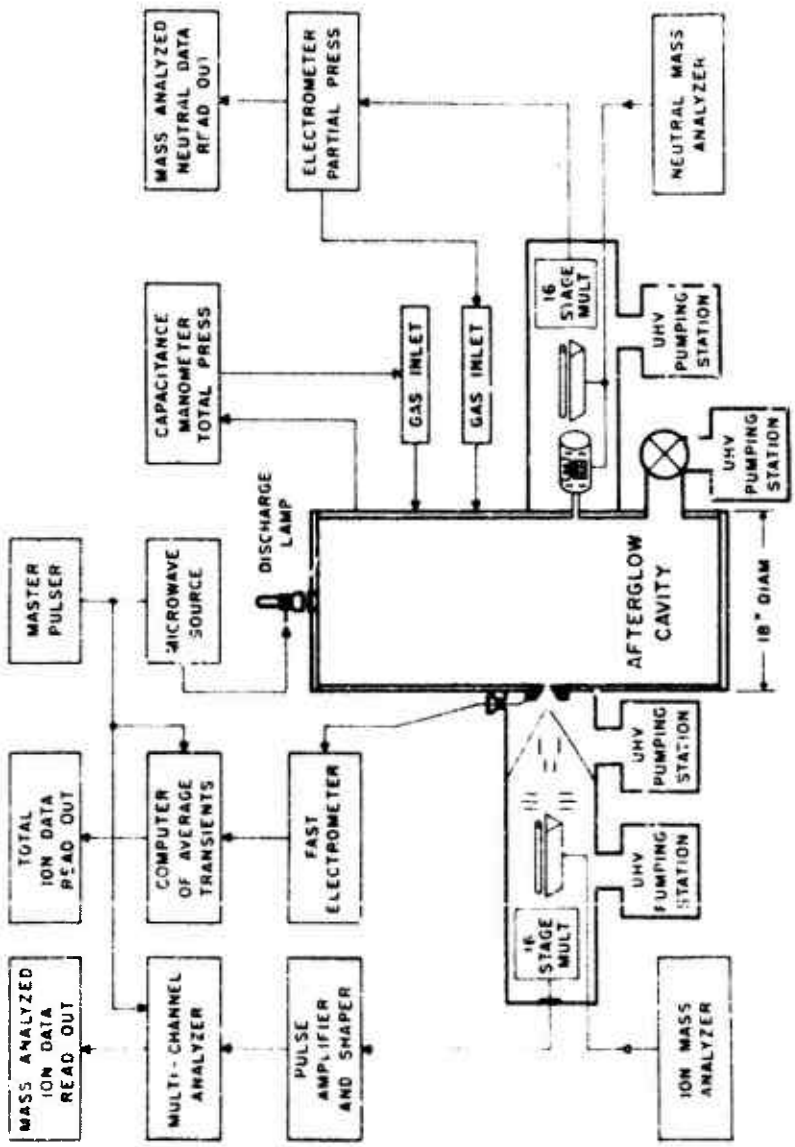


Figure 7-2. Schematic diagram of stationary afterglow apparatus used by Lineberger and Puckett (Reference 7-4).

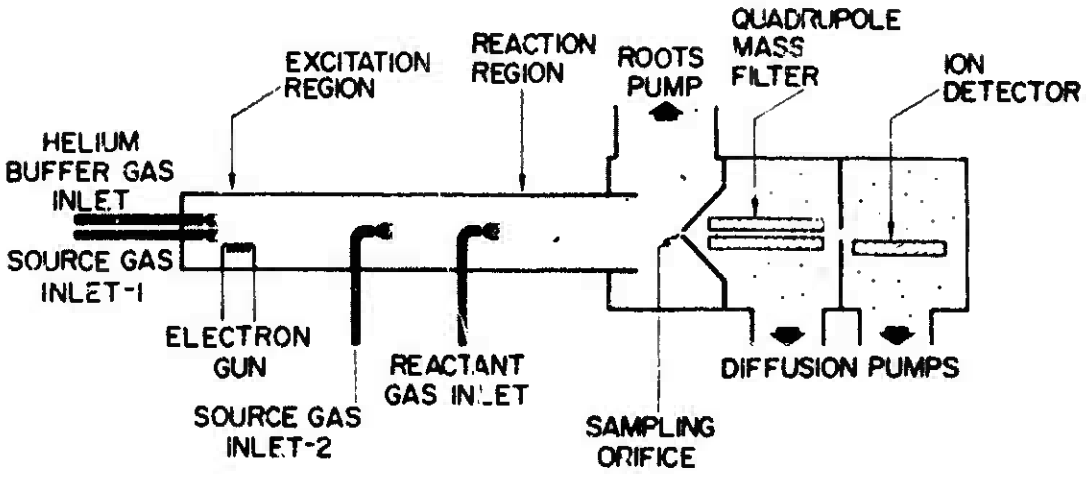


Figure 7-3. Simplified schematic diagram of the flowing-afterglow apparatus of Ferguson, Fehsenfeld, and Schmeltekopf (Reference 7-9).

The parameters measured in the flowing-afterglow experiments are the currents of individual interacting ions, as functions of the variable number densities of neutral reactants. The reaction time is the flow time between the point of introduction of the neutral reactant and the gas-sampling orifice. A plot of the logarithm of the reacting ion current against the number density of neutral reactants yields ideally a straight line whose slope is the product of the reaction rate coefficient and the reaction time.

An important advantage of the flowing-afterglow technique is that the neutral reactants may be unstable species, e.g., oxygen or nitrogen atoms. In addition, the reacting ion is relatively well defined, at least in comparison with stationary-afterglow methods.

Other ion-neutral studies using flowing afterglows have been performed at the University of Pittsburgh (Reference 7-10) and at the University of York (Reference 7-11). A general discussion of flowing-afterglow measurements is found in Reference 7-9.

### 7.2 3 Neutral-Neutral Reactions

Closely related to the flowing-afterglow technique for ion-neutral reactions are the steady-state flow methods used to study neutral-

neutral reactions involving such reactive species as H , O , N , and OH (References 7-6, 7-7). The reactive species are commonly produced either thermally or by electric discharge before mixing with the other reactant in a flow system. By varying either the point of introduction or the flow rate, the course of the reaction can be monitored as a function of time. The available detection systems are numerous and include chemiluminescent light emission, mass spectrometry, optical-absorption spectrometry, electron-spin-resonance (ESR) spectrometry, and hot-wire calorimetry. A detailed discussion, together with a description of several limitations of these techniques, is given in Chapter 19 of this Handbook.

## 7.3 MASS-SPECTROMETER ION-SOURCE MEASUREMENTS

Considerable information concerning low-energy ion-neutral reactions has been derived from measurements using mass-spectrometer ion sources. Reference 7-12 provides a summary of early work in this area. In this technique, primary ions are formed by electron (or photon) impact upon a gas. A weak variable electric repeller field accelerates these ions toward the exit slit of the ion source and into a strong-field low-pressure region where the ions receive their final acceleration before mass analysis. If the number density of neutral molecules in the ion source is sufficiently large, primary ions, in moving toward the exit slit, may suffer collisions with the neutrals and undergo ion-molecule or charge-transfer reactions. The ionic products of these reactive collisions are also subject to the electric repeller field and, unless lost by subsequent collisions, move out of the source and are mass-analyzed and detected.

Several difficulties may arise in the study of ion-neutral reactions by the ion-source technique. The identity of reactant ions is often difficult to determine with certainty. The kinetic energy bandwidth of reactant ions is large and uncertain, and increases with increasing repeller potential. Ion-residence times can be calculated with only fair accuracy; in the case of reactant ions produced by dissociative ionization, the necessary information on initial kinetic energies and angular distributions is rarely available. The pulsed-ion-source technique was developed (References 7-13, 7-14) in order to avoid some of these difficulties.

In the pulsed-source technique, the ionizing electron beam is switched on for about one microsecond; after a (variable) time delay of from zero to ten microseconds the repeller is switched on for about two microseconds in order to drive ions out of the source. This pulsing program is repeated with a frequency of about 10 kHz. Assuming suitable precautions have been taken to eliminate contact potentials and field penetration from the ion-accelerating potential, the ions are in a field-free region during the delay time between the ionizing pulse and the repeller pulse. Reactant ions have only their initial kinetic energy during this time. Rate constants for these conditions, which may be thermal, can be obtained by varying either the delay time or the number density of reactant neutrals in the source. Elegant variations of this technique have been developed in order to provide reactant ions with well-defined kinetic energies in the range from thermal levels up to a few electron volts (References 7-15, 7-16).

An important further modification of the general ion-source technique involves photoionization using monochromatic radiation, in order to produce reactant ions (Reference 7-17). The advantages include the possible production of ions in well-defined electronic and vibrational states and in a reaction chamber free of stray fields emanating from an electron gun and electron beam. The photoionization technique has also been used successfully at relatively high source pressures (0.01 to 0.2 torr) and with a pulsed light source and DC repeller (References 7-18, 7-19). In this case, ion residence times in the source were obtained directly from the arrival times at the detector. At high source pressures, these residence times are related to the ion diffusion coefficients and mobilities and thus finally to the ion temperatures. The method is seen to be closely akin to the drift-tube technique (see Section 7.5). Rate constants measured by the pulsed-source photoionization method for several ion-neutral reactions at thermal energies are in good agreement with results from the afterglow techniques (cf. Subsection 7.2.2).

## 7.4 ION CYCLOTRON RESONANCE

In an ion cyclotron resonance (ICR) spectrometer, ions are formed, usually by electron impact, in a region of uniform static magnetic field, $H$. The subsequent path of these ions is constrained to circular orbits in a plane normal to the magnetic field but is unrestricted in the direction parallel to the field. The angular or cyclotron frequency of the orbital motion, $\omega_c$, is given by:

$$\omega_c = eH/mc \quad . \tag{7-1}$$

In Equation (7-1), m/e is the mass-to-charge ratio of the ion and c is the velocity of light. If an alternating electric field of frequency $\omega$ is applied normal to the direction of H, the ions absorb energy from the electric field when $\omega = \omega_c$ and are accelerated to larger velocities and orbital radii. If the energy absorption is detected, e.g., by the use of a marginal oscillator as the source of the field, a mass spectrum can be generated by fixing $\omega$ and varying H. Finally, if the pressure is high enough so that an ion-neutral reaction occurs, the dependence of the reaction rate upon ion velocity can be studied by irradiating the reactant ion at its cyclotron frequency while observing changes in cyclotron resonance intensity and line shape of the product ion. In addition to this double-resonance experiment (Reference 7-20), numerous other variations of the basic technique (Reference 7-21) have been developed. These include pulsed ionizing beams, pulsed magnetic fields, cells in which ions can be trapped for long times, e.g., seconds, and ion ejection techniques for studying complex reaction schemes. A review of these developments is available (Reference 7-22).

The ICR technique has been most widely used in studying reaction mechanisms and in establishing chemical and thermodynamic relationships, e.g., gas-phase acidities and basicities. More recently, photodetachment spectra of $NH_2^-$ and $PH_2^-$ trapped in the ICR cell have been obtained (Reference 7-23). With the development of pulse methods, some success has been achieved in measuring rate constants for ion-molecule reactions at near-thermal energies. However, only very recently have the essential direct measurements been made of ion residence times and reactant-ion kinetic-energy distributions (Reference 7-24).

## 7.5 DRIFT-TUBE MEASUREMENTS

When a charged particle moves through a gas under the influence of a uniform electric field, it gains energy from the field during the time between collisions and loses energy upon collision subsequently. The mean energy acquired from the field is determined by the parameter E/p, i.e., the ratio of the field intensity to the gas pressure. When E/p is small and constant, the charged-particle motion consists of a slow uniform drift superimposed on the much faster random motion. This particular experimental environment has proved suitable for the study of a variety of thermal-energy collision processes involving either electrons or ions.

In the apparatus developed by McDaniel et al. (Reference 7-25), ions are produced by a magnetically confined beam of electrons inside a drift tube 50 centimeters long containing gas at a pressure up to ten torr. The ions drift down the tube under the influence of an axial electric field, whose strength determines the average ion energy. The drift distance is variable from one to 44 centimeters by varying the position of the ion source. A sample of the ion population at the end of the drift tube is extracted into a quadrupole mass spectrometer. Information concerning the nature and probability of the reactions occurring is revealed by the nature of the resulting ionic mass spectrum.

The drift tube apparatus of Heimerl, Johnsen, and Biondi (Reference 7-26) employs a pulsed-discharge ion source, drift region, and mass-analyzing region interconnected only by small orifices through which ions enter and leave the drift tube. Thus contamination of the gas used in the ion source with the gas admitted to the drift region is minimized. An important innovation in this apparatus provides an additional residence time for the ion bunch in the drift tube by momentary reversal of the drift field. The interaction energy range (0.03 to about 1 eV) can be covered, and several ion-neutral reactions of atmospheric species have been studied using this system (References 7-27, 7-28).

Mass analysis of the reactant ions before injection into the drift tube is provided in the apparatus of Hasted et al (References 7-29, 7-30, 7-31). The system uses a magnetic-sector mass analyzer for this purpose, with the result that ions entering the drift region have initially rather high energies, e.g., 100-400 eV. Successful operation requires that these ions be rapidly thermalized by collisions with the buffer gas, usually helium, before collisions occur with the reactant gas. Various tests of the apparatus indicate that this thermalization does indeed occur. Analysis of the ions leaving the drift tube is carried out using a quadrupole mass filter (Reference 7-30) or a magnetic-sector mass spectrometer (Reference 7-31).

Electron attachment and detachment have also been studied in a drift tube. In the work of Pack and Phelps (Reference 7-32) electrons are ejected from a photocathode by a short pulse of ultraviolet radiation. The electrons then drift through a gas-filled tube under the influence of a uniform electric field, and some of them are captured by the neutral molecules to form negative ions, which continue

down the tube with their own drift velocity. Before arrival at a collector electrode the particles must pass through a grid consisting of a series of fine parallel wires with alternate wires connected together. This grid is made absorbing by applying equal and opposite bias voltages to the alternate wire sets. The grid is then made to permit passage of the charged particles through to the collector during a particular time interval by applying rectangular voltage pulses to the wire sets; this momentarily reduces the fields between the wires to zero. By delaying the application of the latter, or grid-opening, pulse relative to the cathodic photoelectron pulse by various time intervals, it is possible to determine the current reaching the grid as a function of time. From these measurements attachment coefficients and, with a slight variation, detachment coefficients can then be determined.

## 7.6 BEAM TECHNIQUES

The use of beams is an especially versatile technique for the study of two-body reactions. Two beams may he crossed, or one beam may be passed through a stationary target gas. Neutral-neutral, neutral-charged, and charged-charged reactions have been investigated in this way. A general review of many aspects of this field is given in Reference 7-33.

### 7.6.1 Neutral-Neutral Interactions

In this type of experiment either one neutral beam is passed through a stationary neutral gas or two neutral beams are crossed, usually at right angles. Neutral beams can be formed in a number of ways. Thermal-energy beams are generally formed by effusion from a relatively low-pressure source. Somewhat higher energies can be obtained by nozzle-beam techniques, while seeded nozzle beams lead to even higher-energy neutral beams. Nozzle-beam techniques are discussed by Anderson, Andres, and Fenn in Chapter 8 of Reference 7-33. Intermediate energies have heen obtained using sputtering techniques, while high-energy neutral beams are usually formed by charge transfer involving ion beams of the correct energy. The latter mechanism is the most widely applicable, but it suffers from the disadvantage that the resulting neutral beam is generally in an unknown mixture of states. With increasing experience, perhaps more knowledge and control can be achieved with respect to the states of the resulting neutral-beam species.

The major problem associated with neutral-neutral interactions is detection of the reaction products. If fast neutral beams are being studied, then the product may be detected by secondary electron emission from metal surfaces. For thermal beams other techniques may be employed, e.g., surface ionization and the use of universal ionizers.

The neutral-neutral interactions studied can be divided into three general types. First are the studies of elastic scattering of thermal-energy beams and of fast beams produced through electron capture by fast charged beams. Much of the higher-energy work has been concerned with the scattering of rare-gas atoms (Reference 7-34). The thermal-energy experiments on the other hand have generally involved the alkali metals and alkali halides because of their ease of detection by surface-ionization methods (Reference 7-35). However, some work has been done using universal ionizers to detect the collision products (References 7-36, 7-37). Secondly, reactive scattering in neutral-neutral collisions has also been studied at thermal energies, again with considerable emphasis on the alkali metals and alkali halides (Reference 7-38) but with some work reported using universal analyzers (Reference 7-39). The third type of measurement involves the production of an ion pair from relatively low-energy neutral-neutral collisions (References 7-40, 7-41).

Since the systems studied in the above experiments do not, in general, involve atmospheric species, experimental details are not considered further, within the present context. The study of thermal-energy collisions involving species of atmospheric interest appears to be most satisfactorily carried out using other techniques, e.g., the flowing-afterglow system (cf. Subsection 7.2.3), although beam experiments may become more attractive when more efficient neutral-species detectors are developed.

### 7.6.2 Charged-Neutral Reactions

A great deal of information on collisions between ions and neutrals has been derived from measurements involving mass-selected ion beams and neutral targets either in a gas-filled collision chamber or in a neutral beam. Measurements of this general type have been carried out at energies down to about 0.3 eV, and the energy region therefore complements those of afterglows and ion sources. A wide variety of experimental configurations have been employed, of which only a few are mentioned here.

One difficulty which is present in all experiments of this nature is that of the collection efficiency of the products of reaction. When charge-transfer collisions are studied, one can take advantage of the fact that very little momentum is exchanged between the interacting species. Thus a fast ion and a thermal-energy neutral become converted into a fast neutral and a near-thermal-energy ion. When ion-molecule reactions come under study the collection problem is more difficult due to momentum transfer in the collision. The products may both have substantial energies and an angular divergence which may be quite different from that of the reactants. Rapid acceleration of these products after they drift out of the collision region, coupled with the use of strong focusing lenses, have been used to minimize the collection problem.

One of the most versatile techniques employs mass spectrometry to identify both the primary and the secondary ions. An apparatus of this type, used by Giese and Maier (References 7-42, 7-43, 7-44), is illustrated in Figure 7-4. As shown in the diagram, ions produced in either an electron-impact ion source or a surface-ionization source are mass-analyzed and enter a reaction chamber. Ions issuing from the collision region are accelerated in the uniform-field region to about 5 kV and the resulting beam is focused by the quadrupole lens (Reference 7-45) onto the object slit of the secondary mass spectrometer. A differential voltage may be applied across elements of the quadrupole lens to shift the focus in the plane of the object slit. Thus two mass spectrometers are used in tandem. Ions are detected on the first dynode of a 16-stage particle multiplier whose gain is of the order of $10^5$.

The double mass-spectrometer technique has also been used with a modulated neutral beam by Stebbings, Turner, and Rutherford (Reference 7-46). This instrument is illustrated in Figure 7-5. Primary ions are extracted from an electron bombardment source and mass-analyzed at 75 eV in a 180° magnetic mass spectrometer. After mass analysis the ions are retarded or accelerated to the desired collision energy. The ions then pass through a field-free region before intersecting the neutral beam. Collimating apertures ensure that, from purely geometric considerations, all primary ions pass through the modulated neutral beam (modulated at 100 Hz by mechanical chopping). The primary beam intensity is measured in the interaction region by a movable Faraday cup which can be swung into and out of the beam. Secondary ions resulting from collisions between primary ions and neutrals are extracted along the

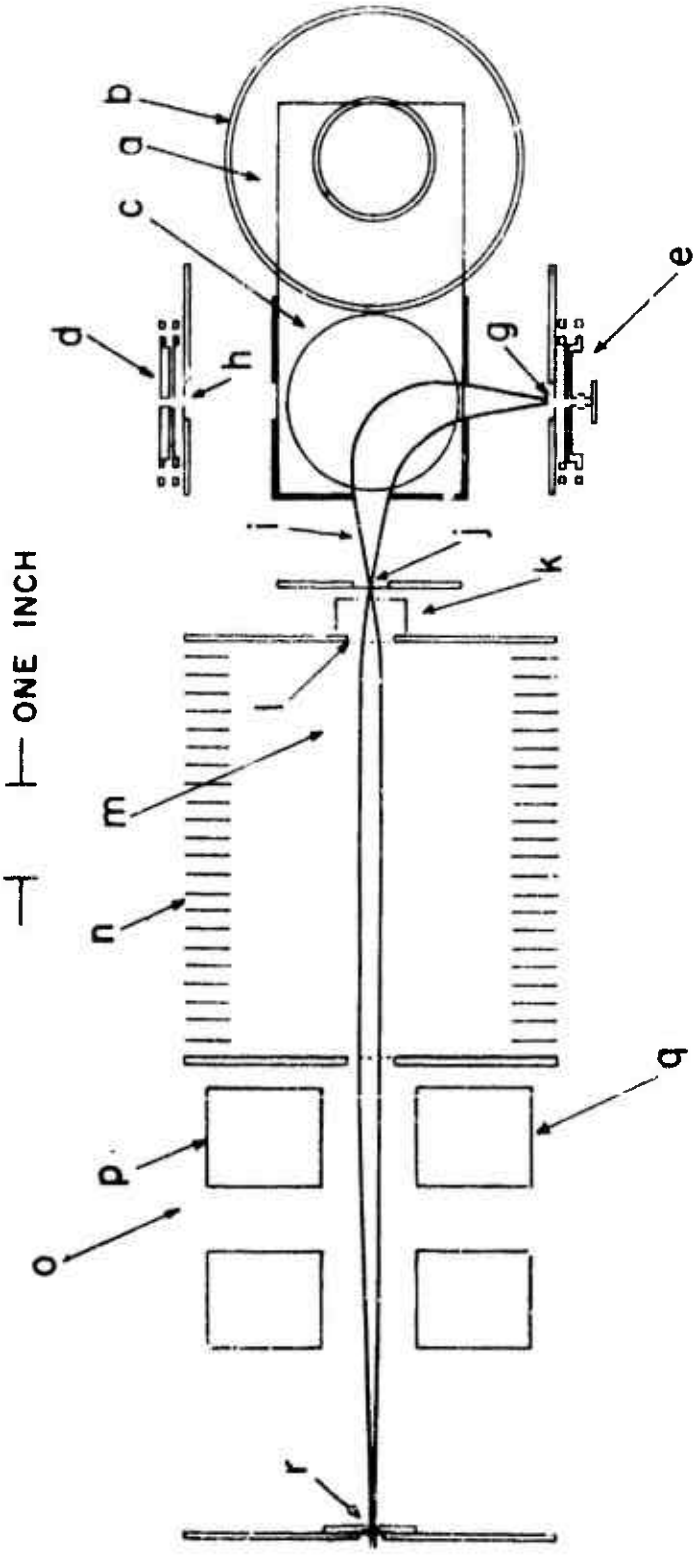


Figure 7-4. Schematic diagram of part of the double mass-spectrometer system of Giese and Maier (References 7-42, 7-43, 7-44).

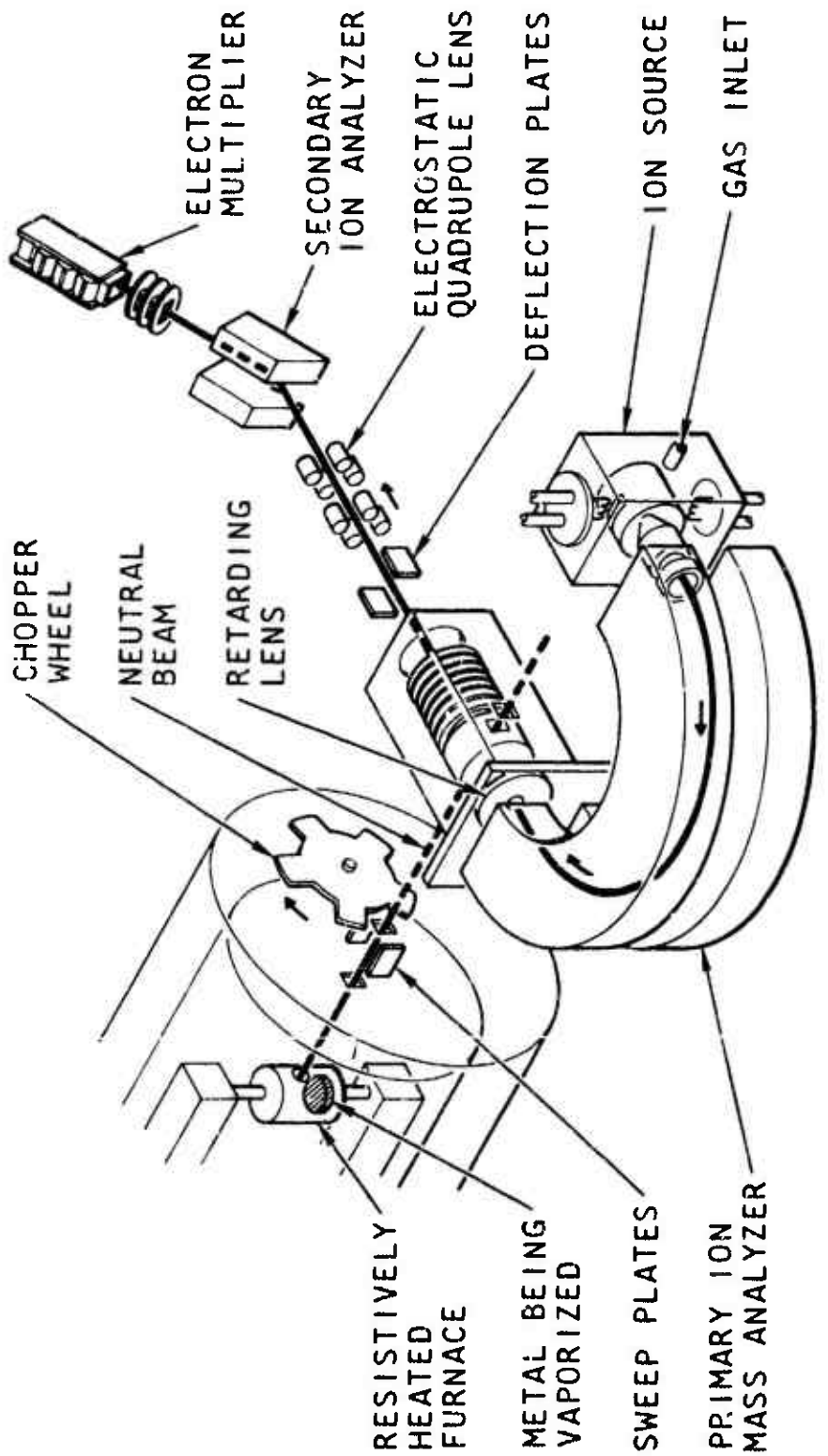


Figure 7-5. Schematic diagram of the apparatus used by Stebbings, Turner, and Rutherford (Reference 7-46).

direction of the primary ion beam by a weak electric field. The ions then enter an electric field where their energy is increased to 1650 eV. After acceleration the ions pass through an electrostatic quadrupole lens which forms the entrance slit for a 60°-sector magnetic mass spectrometer. The selected ions impinge on the first dynode of a 14-stage particle multiplier. The output from the multiplier passes successively through a preamplifier, a 100-Hz narrow-band amplifier, and a phase-sensitive detector, and is then integrated.

The neutral beam employed in the instrument originates in a molecular effusion source. This source may be operated at room temperature when chemically stable gases are being studied, or at an elevated temperature which allows low-vapor-pressure or chemically active species to be studied. The cosine law of molecular effusion is employed to determine the neutral beam density. Apart from the ability to study labile species, an additional advantage in this type of instrument is that the interaction volume is the small region in which the beams cross, approximating a geometric point source for the secondary ions. As such the crossed-beam approach is attractive for the study of differential as well as total cross-sections.

A double mass-spectrometer system employing a quadrupole mass filter for product-ion analysis has been adapted for use in a time-of-flight (TOF) mode by Paulson et al. (Reference 7-47). The particular advantage of this system lies in its ability to perform velocity analyses of slow ions and thereby to study reaction mechanisms and energy-transfer processes in additional ion-neutral collisions. The TOF analysis technique thus complements the retarding-potential and velocity-analyzer methods.

In some experiments interest centers not upon the production of secondary charged particles but on the angular distribution of the scattered primary or secondary ions. One experiment of this type which illustrates the techniques is the elastic differential scattering work of Lorents and Aberth (Reference 7-48). In their instrument, ions are extracted from a source having a low-energy spread and are collimated into a ribbon-shaped beam by a pair of slits. Beam particles are scattered in a gas cell located in the main scattering chamber. The scattered beam, defined by another pair of slits which rotate about the axis of the scattering cell, is electrostatically energy-analyzed and detected with an electron multiplier. The angular range of the system is 1-36° and the primary-beam energy range 20-600 eV. Absolute cross-sections are obtained at small

scattering angles, where intensities are high, by using a Faraday cage in place of the multiplier. The relative data are normalized to the absolute data, yielding cross-sections accurate to about ±25 percent.

Experiments on the angular distributions of charged particles resulting from ion-molecule reactions have been reported by several groups (References 7-49, 7-50). In the work of Wolfgang et al (Reference 7-49), for example, the ion energy range is from one to 100 eV and the angular range from -20 to +50°.

Many of the techniques employed in ion-neutral collision systems are discussed in a book on ion-molecule reactions (Reference 7-51).

### 7.6.3 Charged-Charged Reactions

Crossed-beam techniques have been employed to investigate both ion-electron and ion-ion reactions. Most ion-electron experiments have been designed to study the ionization of positive ions by electron impact (References 7-52, 7-53). Others have been concerned with the excitation of ions (Reference 7-54) and with the dissociation of molecular ions (Reference 7-55) by electron impact. Experiments involving the collision of $H_3^+$ with $H^-$ have also been reported (Reference 7-56).

Other experiments of this type in progress are intended primarily to provide data of astrophysical interest, and are probably unlikely to play any significant part in laboratory studies related to atmospheric deionization. Ionization and excitation of ions are not dominant processes in the latter area of concern while electron-ion recombination is most readily studied by other means.

The principal advantage of beam experiments lies in their versatility. Both positive- and negative-ion reactions are studied with equal ease at energies above about 0.3 eV. Methods are being developed so that the states of both the charged and the neutral species may be determined and varied. Furthermore, the experimental conditions tend to be well defined, thereby imposing little difficulty in interpreting the results of a given experiment.

### 7.6.4 Merging-Beams Techniques

The merging-beams technique is a powerful method for studying

two-body reactions in the low-energy region, i.e., from several hundredths of an electron volt to 10 or 20 eV, with good energy resolution. The technique can also be used to study collisions at energies considerably above the low energy region. Review articles on the subject are available (References 7-57, 7-58). The advantages of this method include: attainability of low relative energies and high energy resolution; easy collection of products for total reaction cross-section measurements; relative ease in detecting these products owing to the large laboratory energies and directed velocities of the primary beams; and applicability to use with labile species.

In a merging-beams apparatus heavy species are generated in ion sources. Neutral beams are obtainable by passing these ions through a charge-transfer cell. The technique requires that two beams be superimposed and travel in the same direction. The laboratory energy of each beam is typically several thousand electron volts, with an energy spread of a few electron volts. By adjusting laboratory energies so that the beam velocities are slightly different, the relative energy of the beams in the center-of-mass system can be made to fall in the low-energy region. For beams of equal masses, for example, the relative energy is considerably less than the difference in laboratory energies of the beams. Furthermore, the spread in relative energy is considerably less than the few electron volts of spread in each individual beam. The use of high laboratory energies minimizes space-charge effects, which create difficulties in the more conventional methods, e.g., crossed beams, used to study two-body reactions in the low-energy region.

Among the limitations of this method is the difficulty of obtaining the angular dependence of cross-sections. This arises because the maximum laboratory solid angle for reaction products is relatively small in merging-beam experiments. Another problem, which is not unique to merging beams, is that of identifying the states of reactants and products. Excited reactants coming from the ion sources can be partially controlled and their abundance studied through the use of electron-bombardment ion sources in which only single collisions between electrons and atoms occur. Excited species in a neutral beam can also be generated in the charge-transfer cell. The effects of some of these species on the measured cross-section can occasionally be studied by a judicious choice of the neutralizing gas. A general technique for detecting excited states and their effects would be highly desirable but has not been developed.

Merging beams can be employed to study a variety of processes, including ion-neutral, neutral-neutral, ion-ion, and electron-ion reactions. Devices which have been used to investigate such processes are described in References 7-59 through 7-65. The apparatus at Gulf Energy and Environmental Systems Company (GEES) has been used to study charge transfer and charge rearrangement between ions and neutrals and to study chemi-ionization processes (Reference 7-59). At Wayne State University (Reference 7-60), charge rearrangement between ions and neutrals has been investigated. Charge transfer between ions and neutrals, and between two ions, have been investigated with merging-beams equipment at the University of Moscow (Reference 7-61), and at the University of Louvain (Reference 7-62), respectively. A facility at Stanford Research Institute (Reference 7-63) and one at the University of Chicago (Reference 7-64) have been used to study mutual neutralization of two ions. Finally, two machines are being developed for conducting dissociative recombination studies between electrons and molecular ions, at GEES and at the University of Western Ontario. Such studies have been conducted previously by merging beams (References 7-65, 7-66). However, because the velocities of the two beams were not made nearly equal, advantage was not taken of the capability of the technique for producing low relative energies with high resolution.

## 7.7 PHOTON MEASUREMENTS

Experiments involving photons are of two types: those in which the interaction of photons with matter is under study, and those in which a given collision process (not necessarily involving reactant photons) is studied by investigation of the resulting photon spectrum. Several methods involving the first type are considered here. Experiments of the second type are also mentioned.

The interaction of ultraviolet radiation with atmospheric constituents is described quantitatively by cross-sections for the various processes involved. The wavelength region of interest here is from 3000 to about 1 A, and the most important processes involved are dissociation, ionization, and excitation. The total absorption cross-section is the sum of the cross-sections for all these processes at any wavelength, when only initial products are considered. At short wavelengths the photoelectron may have sufficient energy to ionize surrounding molecules.

Measurements involving the absorption of photons comprise a direct simulation of atmospheric phenomena. Total absorption cross-

sections can be obtained by measuring the attenuation of a monochromatic photon beam by the gas being studied. Cross-sections for other processes are defined by some other property of the system. For example, ionization cross-sections are defined by the number of ions formed under known conditions. Although some information similar to that obtained in photon absorption processes can be obtained by other methods, such as electron impact, use of the actual radiation of interest is often preferable.

Measurements of photon-particle collisions of interest to the upper atmosphere have been limited primarily by difficulties of working in the vacuum ultraviolet. Because of the structure in the cross-section curves, it is desirable to use continuum background light sources rather than line spectra. Light sources used include: rare-gas continua from mildly high-pressure gas discharges (600-2000 A); rare-gas continua produced by high-current, rapid discharges (best at $\lambda > 1000$ A); the hydrogen continuum ($\lambda > 1650$ A); and synchrotron radiation (most useful in the region 1-600 A). Adequate light sources for all wavelengths are a continuing problem associated with measurements of this nature.

Since many of the measurements require photons of wavelengths where normal optical windows are not available (< 1050 A), it is necessary either to use windowless systems or to employ special filters such as thin metallic films, e.g., aluminum. The problems associated with the available light sources, as well as those related to monochromators, optical gratings, and photon detectors, have been discussed extensively (Reference 7-67).

### 7.7.1 Absorption Measurements

The fundamental measurement in photon-particle collisions is the total absorption cross-section over a given wavelength region. This absorption cross-section $\sigma$ is defined by the equation:

$$I = I_0 e^{-\sigma n x} , \qquad (7\text{-}2)$$

where $I_0$ and $I$ are the photon fluxes before and after transmission through a gas of particle density $n$ and absorption pathlength $x$. The optical density is therefore $\sigma n x$; where this quantity is equal to one, the flux is reduced by $1/e$. The total absorption coefficient $k$ is defined in terms of the total absorption cross-section by the equation:

$$k = n_o \sigma \quad , \tag{7-3}$$

where $n_o$ is Loschmidt's number.

In the usual experiment, the atmospheric gas to be studied is confined in a cell behind the exit slit of the monochromator (or in some cases placed inside the monochromator). The data are obtained by scanning the wavelength region of interest with and without gas in the absorption cell. Using the known pathlength and gas density, the total absorption cross-section can be obtained from the attenuation of the photon beam by the gas at each wavelength. In practice the measurement is often made at a series of pressures to increase the accuracy of the results in regions of very strong and very weak absorption. It should be noted that an absolute measurement of the photon flux is not required for this measurement.

Total absorption cross-sections are frequently reported with an accuracy of ±10 percent. The exponential nature of the absorption law makes more accurate values necessary. Bandwidths used are from about one to 0.05 A. These bandwidths are inadequate only in regions of strong rotational lines, and in such regions they must be reduced to obtain values of the greatest use in atmospheric problems.

Several experimental groups have been active in obtaining total absorption cross-sections for atmospheric species. A general review of the field and the techniques employed is given in the Proceedings of the First International Conference on Vacuum Ultraviolet Radiation Physics (Reference 7-68). Descriptions of the techniques employed by various workers together with discussions of probable experimental errors are given in References 7-69 through 7-73.

### 7.7.2 Photoionization Measurements

The photoionization cross-section $\sigma_i$ may be defined as the absorption cross-section times the ratio of ion-pairs produced per second to the number of photons absorbed per second in a pathlength x, or:

$$\sigma_i = \sigma i_g \left[ e(I_o - I) \right]^{-1} \quad , \tag{7-4}$$

where $i_g$ is the ion current and e the electronic charge. For an

ionization chamber operating in a manner such that all positive ions are collected, $i_g/e$ is equal to the rate of ion-pair production. As in the case of total absorption processes, it is convenient to define a photoionization coefficient $k_i$ where:

$$k_i = n_o \sigma_i \quad . \tag{7-5}$$

The experimental methods used for photoionization studies are generally similar to those used for total absorption measurements. A monochromator is used to isolate a particular wavelength of light which is then directed into a cell located behind the exit slit. The number of ion-pairs formed per second is determined by placing parallel-plate electrodes in the sample cell just outside the photon beam path. A small voltage sufficient to cause current saturation is placed on these plates, and the ion current is measured with a sensitive electrometer. To find the number of photons absorbed per second it is necessary to measure the absolute intensity of the monochromatic photon beam before and after radiation passes through the gas. This difficult measurement can be done in several ways. Two of the more common approaches are to use a calibrated thermopile or, below 1022 A, a xenon ionization cell. The second method utilizes the fact that the ionization yield (ion-pairs formed per photon absorbed) of xenon is unity at wavelengths below 1022 A. Primary standards such as the xenon ionization chamber can be used to standardize detectors such as platinum, tungsten, or other metals with fairly well-known photoelectric efficiencies. Various detectors and calibration methods are discussed in Reference 7-67.

In addition to the determination of accurate first-ionization potentials and cross-sections for ion formation, photoionization has been used to study autoionization processes. The accuracy of photoionization cross-sections is generally less than that for total absorption cross-sections since an absolute value of the photon flux is required.

One variation of the photoionization technique is to use a mass spectrometer to analyze the ion current formed. This technique is more useful for obtaining information on the processes leading to the formation of fragment ions than for obtaining total photoionization cross-sections.

A good standard reference to this general area is a review article by G. L. Weissler (Reference 7-74). Since the appearance of this

review, there have been a number of developments in light sources, detectors, and monochromators, which are summarized in Reference 7-68. Additional descriptions of apparatus and techniques are available (References 7-75, 7-76, 7-77).

### 7.7.3 Photoelectron Spectroscopy

The energies of inner ionization potentials of atoms and molecules are often difficult to obtain in total absorption and photoionization measurements due to masking of the thresholds by autoionization processes. Measurement of the kinetic energy of the electron emitted in the ionization process offers a means of overcoming this problem. Such measurements also give information on the electron temperature after an ionization process has occurred. A useful general reference is available (Reference 7-78).

The basic technique utilizes the fact that when a photon is absorbed, thereby causing an ionization, the excess energy in the system manifests itself as kinetic energy of the ion-electron pair. Conservation of momentum results in virtually all of this energy being given to the electron.

In the usual experiment, a monochromatic beam of radiation obtained either directly from a rare-gas discharge or from a monochromator is directed into the gas under study. The energy of the radiation must be more than sufficient to cause ionization and the gas pressure sufficiently low, such that none of the photoelectrons interact with the gas. The energy of the released electrons is usually measured using retarding-potential techniques (References 7-79, 7-80, 7-81) or by employing electrostatic energy analyzers (Reference 7-82). An illustration of an instrument used by Frost et al (Reference 7-81), in which retarding-potential techniques are used, is shown in Figure 7-6. Here the detector is designed such that there is no discrimination against electrons emitted over a large angular range. Helium-resonance radiation (584 A) from a microwave discharge induces ionization in the spherical grid assembly.

Photoelectron spectroscopy also offers information on the probabilities for forming the various ionic states available for the photon energy used. Since each ionization event releases an electron, and the energy of that electron depends on the particular ionic state formed, measurement of the number of electrons coming from each

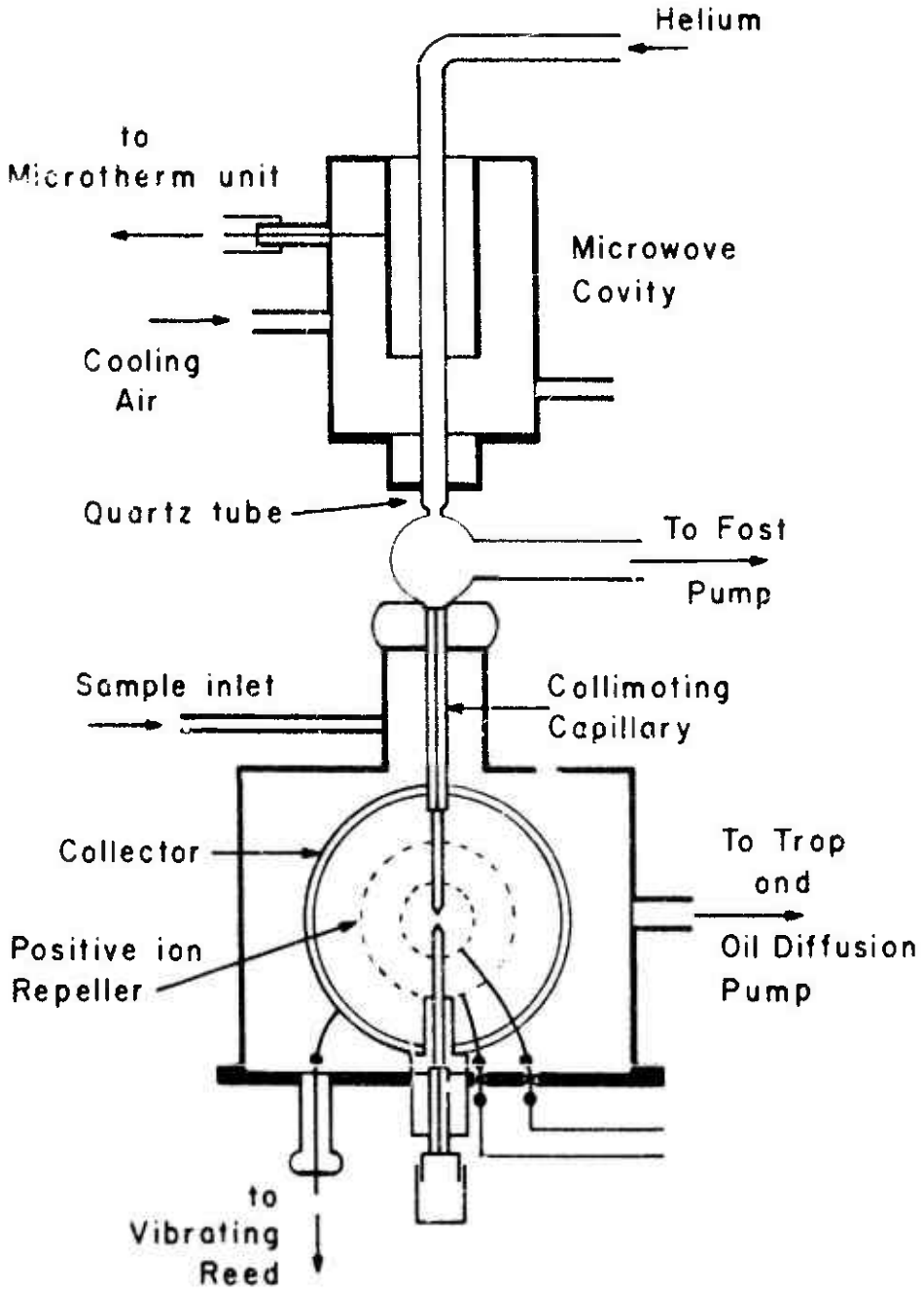


Figure 7-6. System for photoionizotion ond for collection ond retarding-potential onolysis of photoelectrons, used by Frost, McDowell, and Vroom (Reference 7-81).

ionization process yields the relative probability for formation of each state at the photon energy used. Experiments which illustrate how the distribution of the ion states formed changes as a function of wavelength of the ionizing radiation have also been reported (Reference 7-83).

Experimental measurements of the angular distributions of secondary electrons emitted in the photoionization process have been reported (Reference 7-77). Such measurements have been made using the retarding-field method (Reference 7-84), and using a movable electrostatic analyzer (References 7-85, 7-86, 7-87).

### 7.7.4 Photodetachment Measurements

Photodetachment, the removal of electrons from negative ions by photon impact, has been studied experimentally (References 7-88, 7-89, 7-90), using a technique which involves crossing a mass-analyzed negative-ion beam with a modulated photon beam. The slow electrons produced are collected by means of weak magnetic and electric fields and measured using AC amplification and phase-sensitive detection. The experimental scheme is shown in Figure 7-7.

The photon energy is generally much less than that for the photoabsorption or photoionization experiments but the intensities required are much higher. In an earlier method the radiation source was a carbon arc or high-pressure discharge. Specific wavelengths were selected by using optical filters.

In the experiments of Lineberger and Woodward (Reference 7-91) the arc or discharge light source is replaced by a tunable dye laser, thereby increasing both the resolution and the sensitivity of the apparatus and extending the number of systems available for study.

In addition to accurate electron affinities and photodetachment cross-sections, the results of these experiments have led to calculations of the probability of the reverse process, radiative attachment, for which few experimental results are available.

### 7.7.5 Detection of Excited Products Using Optical Spectra

A principal difficulty in the interpretation of collision phenomena lies in the attempt to account for the energy in the system after the

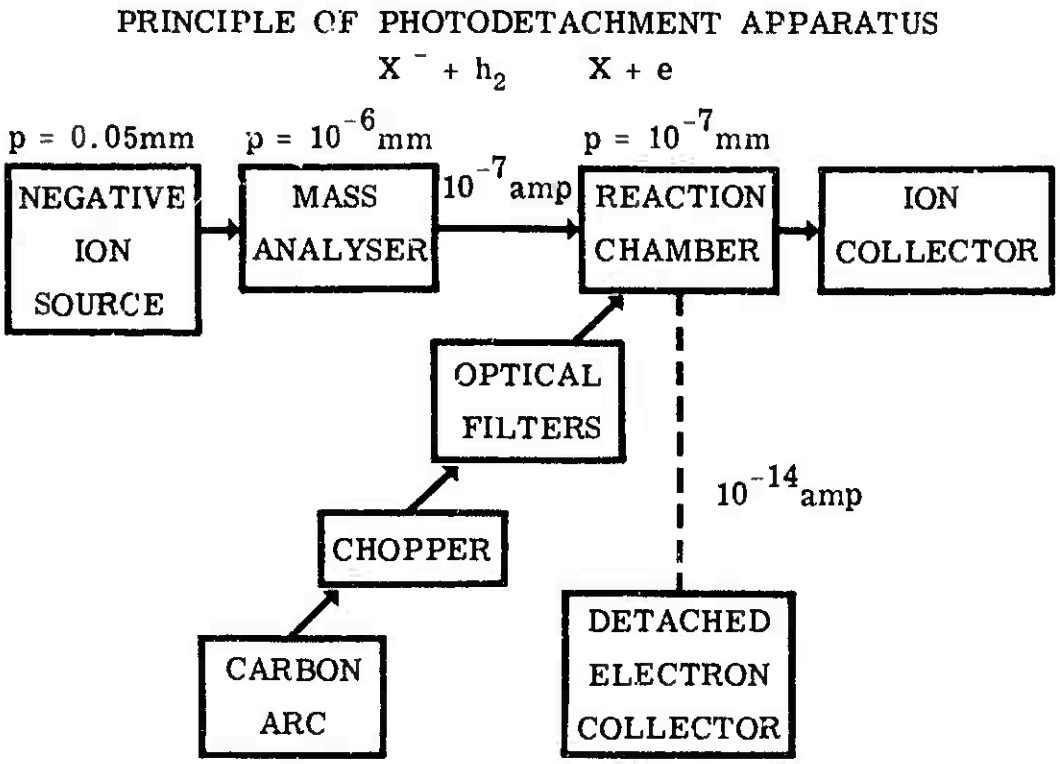


Figure 7-7. Block diagram of photodetachment apparatus of Smith and Branscomb (Reference 7-90).

collision has occurred. One important method of determining whether or not any excess energy goes into translational motion of the products or into internal energy is to search for optical emission from the products. The presence of emission indicates the decay of excited states, and the wavelength allows identification of the state. This method is applicable only in cases where the excited states formed can decay through optical emission.

The experimental technique generally involves passing a beam of charged particles (ions or electrons) through a stationary gas and observing the collision region with a monochromator. Observation of the radiation produced as a function of collision energy leads to information on the relative cross-section for formation of the particular state under consideration. Some care must be taken, however, in interpreting the spectra, since the radiation from the state under consideration may result either totally or partially from popu-

lation of that state through the decay of higher-lying states, i.e., cascade processes. A study of the complete spectrum as a function of impact energy often allows a more reliable interpretation to be made. Accounts of experiments of this nature may be found in Reference 7-92 for electron impact, and Reference 7-93 for ion impact.

## 7.8 STUDIES OF IRRADIATED AIR

This type of experiment attempts to approximate the conditions in the ionosphere as nearly as possible and then to study the electron and ion production and loss mechanisms when the air is subjected to ionizing radiation. Diagnostic techniques used in these studies include UHF measurements of the complex conductivity of the ionized gas, from which densities and collision frequencies of slow secondary electrons can be deduced, as well as mass and optical spectroscopy for the identification and measurement of ionic and neutral species and of excited states, respectively. A schematic diagram of the experimental apparatus used by Hirsh et al (References 7-94, 7-95, 7-96) is shown in Figure 7-8.

A divergent beam of 1.5-MeV electrons from a van de Graaff accelerator traverses the thin foil end of a large (4 feet in diameter, 2 feet long) cylindrical UHF cavity, resonant in the $TE_{011}$ mode at 390 MHz, in which the gas is contained. Over the pressure range employed in these experiments, the gas does not appreciably attenuate the electrons during their traverse of the cavity. This, coupled with the geometry of the divergent beam, provides a source of ionization which is spatially uniform over the gas to within 20 percent.

Two types of experiments are performed. In one, the electron beam irradiates the gas continuously, setting up a steady-state distribution of charged particles and excited neutral species. Densities of ions and slow secondary electrons and intensities of optical emission are measured as functions of the fast electron-beam current and the pressure and chemical composition of the gas. The density of primary-beam electrons is too small to be detected by their contribution to the conductivity, so that only the slow secondaries are measured. In the second type of experiment, the electron beam is pulsed on and off periodically, and time-resolved measurements are made during the approach to in-beam equilibrium and during the radiation afterglow.

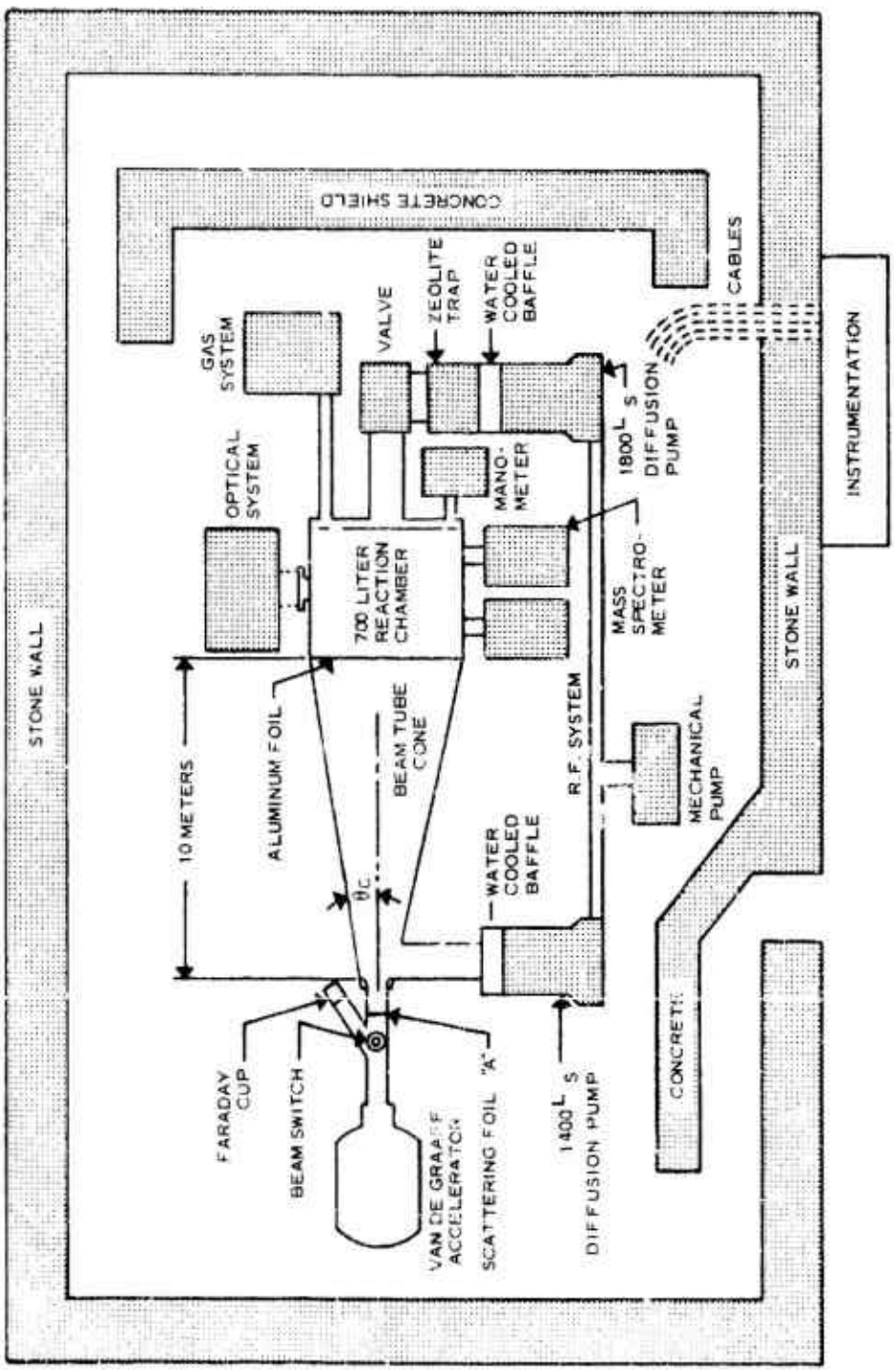


Figure 7-8. Schematic of the apparatus used by Hirsh et al (References 7-94, 7-95, 7-96) for studies of irradiated gases.

The system makes it possible to measure several parameters simultaneously, e.g., electron densities and excited-state densities. These several methods provide complementary information on the inherently multi-parameter ionized gas, thus placing more stringent restrictions on the models used to explain the measurements than could be deduced from a single type of measurement.

van Lint and colleagues (Reference 7-97) have also used the ionization afterglow techniques in air-like mixtures as well as in pure gases. In their experiments the electron-ion pairs are formed by a short pulse of 10- to 30-MeV electrons. A microwave signal is transmitted through this dilute plasma, and the electron density and the electron-atom collision frequency are measured by detecting the amplitude and phase shift with a microwave detector in a bridge configuration. From these results, values of rate coefficients for attachment and electron-ion recombination, as well as the momentum-transfer collision frequency and the energy-transfer collision frequency, for thermal and near-thermal energies, are deduced.

## REFERENCES


7-1. Biondi, M. A., Revs. Sci. Instr. 22, 500 (1951).

7-2. Biondi, M. A., in Methods of Experimental Physics, B. Bederson and W. L. Fite, Eds., Academic Press, New York (1968); vol. 7B, p. 78.

7-3. Mehr, F. J., and M. A. Biondi, Phys. Rev. 181, 264 (1969).

7-4. Lineberger, W. E., and L. J. Puckett, Phys. Rev. 186, 116 (1969).

7-5. Copsey, M. J., D. Smith, and J. Sayers, Planet. Space Sci. 14, 1047 (1966).

7-6. Kaufman, F., Ann. Rev. Phys. Chem. 20, 45 (1969).

7-7. Schiff, H. I., Can. J. Chem. 47, 1903 (1969).

7-8. Fite, W. L., J. A. Rutherford, W. R. Snow, and V. A. J. van Lint, Disc. Far. Soc. 33, 264 (1962).

7-9. Ferguson, E. E., F. C. Fehsenfeld, and A. L. Schmeltekopf, in Advances in Atomic and Molecular Physics, D. R. Bates and I. Estermann, Eds., Academic Press, New York (1969); vol. 5, p. 1.

7-10. Farragher, A. L., J. A. Peden, and W. L. Fite, J. Chem. Phys. 50, 287 (1969).

7-11. Bolden, R. C., R. S. Hemsworth, J. J. Shaw, and N. D. Twiddy, J. Phys. B3, 45 (1970).

7-12. Lampe, F. W., J. L. Franklin, and F. H. Field, in Progress in Reaction Kinetics, G. Porter, Ed., Pergamon Press, New York (1961); vol. 1, p. 67.

7-13. Talroze, V. L., and E. L. Frankevich, Zh. Fiz. Khim. 34, 2709 (1960).

7-14. Ryan, K. R., and J. H. Futrell, J. Chem. Phys. 42, 824 (1965).

7-15. Ryan, K. R., J. H. Futrell, and C. D. Miller, Revs. Sci. Instr. 37, 107 (1966).

7-16. Birkinshaw, K., A. J. Masson, D. Hyatt, L. Matus, I. Cpauszky, and M. J. Henchman, Advan. Mass Spectrom. 4, 379 (1968).

7-17. Chupka, W. A., and M. E. Russell, J. Chem. Phys. 49, 5426 (1968).

7-18. Warneck, P., J. Chem. Phys. 46, 502 (1967).

7-19. Warneck, P., J. Chem. Phys. 46, 513 (1967).

7-20. Beauchamp, J. L., and S. E. Buttrill, J. Chem. Phys. 48, 1783 (1968).

7-21. Bowers, M. T., D. D. Elleman, and J. L. Beauchamp, J. Phys. Chem. 72, 3599 (1968).

7-22. Baldeschwieler, J. D., and S. S. Woodgate, Accts. Chem. Res. 4, 114 (1971).

7-23. Smyth, K. C., R. T. McIver, J. I. Brauman, and R. W. Wallace, J. Chem. Phys. 54, 2758 (1971).

7-24. Futrell, J. H., and R. P. Clow, Intl. J. Mass. Spectrom. Ion Phys. (in press).

7-25. Albritton, D. L., T. M. Miller, D. W. Martin, and E. W. McDaniel, Phys. Rev. 171, 94 (1968).

7-26. Heimerl, J., R. Johnsen, and M. A. Biondi, J. Chem. Phys. 51, 5041 (1969).

7-27. Johnsen, R., H. L. Brown, and M. A. Biondi, J. Chem. Phys. 52, 5080 (1970).

7-28. Johnsen, R., H. L. Brown, and M. A. Biondi, J. Chem. Phys. 55, 186 (1971).

7-29. Kaneko, Y., L. R. Megill, and J. B. Hasted, J. Chem. Phys. 45, 3741 (1966).

7-30. Ong, P., and J. B. Hasted, J. Phys. B2, 91 (1969).

7-31. Kaneko, Y., N. Kobayashi, and I. Kanomata, Mass Spectrosc. 18, 920 (1970).

7-32. Pack, J. L., and A. V. Phelps, J. Chem. Phys. 44, 1870 (1966).

7-33. Ross, J., Ed., Advances in Chemical Physics. X. Molecular Beams, Wiley-Interscience, New York (1966).

7-34. Amdur, I., J. E. Jordan, and S. O. Colgate, J. Chem. Phys. 34, 1525 (1961).

7-35. Ackerman, M., E. F. Greene, A. L. Moursund, and J. Ross, J. Chem. Phys. 41, 1183 (1964).

7-36. Rothe, E. W., L. L. Marino, R. H. Neynaber, P. K. Rol, and S. M. Trujillo, Phys. Rev. 126, 598 (1962).

7-37. Rothe, E. F., R. H. Neynaber, and S. M. Trujillo, J. Chem. Phys. 42, 3310 (1965).

7-38. Birely, J. H., R. R. Herm, K. R. Wilson, and D. R. Herschbach, J. Chem. Phys. 47, 993 (1967).

7-39. Lee, Y. T., J. D. McDonald, P. R. LeBreton, and D. R. Herschbach, Revs. Sci. Instr. 40, 1402 (1969).

7-40. Utterback, N. G., J. Chem. Phys. 44, 2540 (1966).

7-41. Helbing, R. K. B., and E. W. Rothe, J. Chem. Phys. 51, 1607 (1969).

7-42. Giese, C. F., and W. B. Maier, J. Chem. Phys. 39, 197 (1963).

7-43. Maier, W. B., J. Chem. Phys. 41, 2174 (1964).

7-44. Giese, C. F., Advan. Chem. 58, 20 (1966).

7-45. Giese, C. F., Revs. Sci. Instr. 30, 260 (1959).

7-46. Stebbings, R. F., B. R. Turner, and J. A. Rutherford, J. Geophys. Res. 71, 771 (1966).

7-47. Paulson, J. F., F. Dale, and S. A. Studniarz, Intl. J. Mass Spectrom. Ion Phys. 5, 113 (1970).

7-48. Lorents, D. C., and W. H. Aberth, Phys. Rev. 139A, 1017 (1965).

7-49. Herman, Z., J. D. Kerstetter, T. L. Rose, and R. Wolfgang, Revs. Sci. Instr. 40, 538 (1969).

7-50. Gentry, W. R., E. A. Gislason, Y. T. Lee, B. Mahan, and C. W. Tsao, Disc. Far. Soc. 44, 137 (1967).

7-51. McDaniel, E. W., V. Cermack, A. Dalgarno, E. E. Ferguson, and L. Friedman, Ion-Molecule Reactions, Wiley-Interscience New York (1970).

7-52. Dolder, K. T., M. F. A. Harrison, and P. C. Thonemann, Proc. Roy. Soc. A274, 546 (1963).

7-53. Harrison, M. F. A., K. T. Dolder, and P. C. Thonemann, Proc. Phys. Soc. 82, 368 (1963).

7-54. Harrison, M. F. A., A. C. H. Smith, and D. F. Dance, Fourth Intl. Conf. Phys. Electr. Atomic Coll., Quebec, Canada, Science Bookcrafters, Inc., Hastings-on-Hudson, N. Y. (1965); p. 442.

7-55. Dunn, G. H., B. Van Zyl, and R. N. Zare, Phys. Rev. Letts. 15, 610 (1965).

7-56. Rundel, R. D., K. L. Aitken, and M. F. A. Harrison, J. Phys. B2, 954 (1969).

7-57. Neynaber, R. H., in Advances in Atomic and Molecular Physics, D. R. Bates and I. Estermann, Eds., Academic Press, New York (1969); vol. 5, p. 57.

7-58. Dunn, G. H., in Atomic Physics, B. Bederson, V. W. Cohen, and F. M. T. Pichanick, Eds., Plenum Press, New York (1969); p. 417.

7-59. Trujillo, S. M., R. H. Neynaber, and E. W. Rothe, Revs. Sci. Instr. 37, 1655 (1966).

7-60. Rol, P. K. and E. A. Entemann, J. Chem. Phys. 49, 1430 (1968).

7-61. Belyaev, V. A., B. C. Brezhnev, and E. M. Erastov, JETP Letts. 3, 207 (1966).

7-62. Brouillard, F., Ph. D. Thesis, University of Louvain (1968).

7-63. Aberth, W., J. R. Peterson, D. C. Lorents, and C. J. Cook, Phys. Rev. Letts. 20, 979 (1968).

7-64. Weiner, J., W. Peatman, and R. S. Berry, Phys. Rev. Letts. 25, 79 (1970).

7-65. Hagen, G., in Fifth Intl. Conf. Phys. Electr. Atomic Coll., Leningrad, U. S. S. R., Publishing House Nauka (1967); p. 165.

7-66. Hagen, G., University of California at Los Angeles, Report AFCRL-68-0649 (1968).

7-67. Samson, J. A. R., Techniques of Vacuum Ultraviolet Spectroscopy, John Wiley and Sons, Inc., New York (1967).

7-68. Proc. First Intl. Conf. Vac. UV Radn. Phys., J. Quant. Spectry. Radiative Transfer 2, 315 (1962).

7-69. Huffman, R. E., in Handbook of Geophysics and Space Environments, S. L. Valley, Ed., McGraw-Hill, New York (1965); section 6.3.

7-70. Cook, G. R., P. H. Metzger, M. Ogawa, R. A. Becker, and B. K. Ching, Air Force Systems Command, Report No. TDR-469 (9260-01)-4 (1965).

7-71. Marr, G. V., Proc. Roy. Soc. A228, 531 (1965).

7-72. Huffman, R. E., Can. J. Chem. 47, 1823 (1969).

7-73. Hudson, R. D., Revs. Geophys. Space Phys. 9, 305 (1971).

7-74. Weissler, G. L., in Handbuch der Physik, S. Flügge, Ed., Springer-Verlag, Berlin (1956); vol. 21.

7-75. Marr, G. V., Photoionization Processes in Gases, Academic Press, New York (1967).

7-76. Samson, J. A. R., and R. B. Cairns, J. Geophys. Res. 69, 4583 (1964).

7-77. Schoen, R. I., Can. J. Chem. 47, 1879 (1969).

7-78. Turner, D. W., C. Baker, A. D. Baker, and C. R. Brundle, Molecular Photoelectron Spectroscopy, Wiley-Interscience, London (1970).

7-79. Turner, D. W., and M. I. Al-Joboury, J. Chem. Phys. 37, 3007 (1962).

7-80. Al-Joboury, M. I., and D. W. Turner, J. Chem. Soc. 1963, 5141.

7-81. Frost, D. C., C. A. McDowell, and D. A. Vroom, Phys. Rev. Letts. 15, 612 (1965).

7-82. Turner, D. W., and W. C. Price, Proc. Roy. Soc. A307, 15 (1968).

7-83. Schoen, R. I., J. Chem. Phys. 40, 1830 (1964).

7-84. McGowan, J. W., D. A. Vroom, and A. R. Comeaux, J. Chem. Phys. 51, 5626 (1969).

7-85. Berkowitz, J., and H. Ehrhardt, Phys. Letts. 21, 531 (1966).

7-86. Harrison, H., J. Chem. Phys. 52, 901 (1970).

7-87. Hall, J. L., and M. W. Siegel, J. Chem. Phys. 48, 943 (1968).

7-88. Branscomb, L. M., Phys. Rev. 148, 11 (1966).

7-89. Branscomb, L. M., in Atomic and Molecular Processes, D. R. Bates, Ed., Academic Press, New York (1962); p. 100.

7-90. Smith, S. J., and L. M. Branscomb, Revs. Sci. Instr. 31, 733 (1960).

7-91. Lineberger, W. C., and B. W. Woodward, Phys. Rev. Letts. 25, 424 (1970).

7-92. Vroom, D. A., and F. J. deHeer, J. Chem. Phys. 50, 580 (1969).

7-93. Liu, C., and H. P. Broida, Phys. Rev. A2, 1824 (1970).

7-94. Hirsh, M. N., P. N. Eisner, and J. A. Slevin, Revs. Sci. Instr. 39, 1547 (1968).

7-95. Hirsh, M. N., P. N. Eisner, and J. A. Slevin, Phys. Rev. 178, 175 (1969).

7-96. Hirsh, M. N., E. Poss, and P. N. Eisner, Phys. Rev. A1, 1615 (1970).

7-97. van Lint, V. A. J., J. Parez, D. Trueblood, and M. E. Wyatt, Revs. Sci. Instr. 36, 521 (1965).

# 8. DATA-GATHERING METHODS BASED ON THEORETICAL ANALYSIS

A. Dalgarno, Harvard College Observatory and
Smithsonian Astrophysical Observatory

(Latest Revision 15 April 1971)

## 8.1 INTRODUCTION

Quantum mechanics provides a formal description of atomic and molecular processes, but only for a few types of processes is it possible to make accurate quantitative predictions. However, theory may still be useful in providing limits to the efficiencies with which reactions may occur. The basic theory is described in various chapters of References 8-1 and 8-2 where a comprehensive exposition is given of the processes listed in the following summary.

## 8.2 ELECTRON-ION RECOMBINATION PROCESSES

### 8.2. Radiative Recombination

In a low-density plasma, recombination of electrons and positive ions occurs through the radiative recombination process

$$X^+ + e \rightarrow X_b' + h\nu \ , \qquad (8\text{-}1)$$

where the prime indicates that the product atom may be in a bound excited state. For hydrogenic ions, the rate coefficient $\alpha_r$ of Equation (8-1) may be evaluated exactly and numerical values for $H^+$ ions are given in Table 8-1 for a wide range of temperatures. For more complex systems, capture into highly excited levels is similar to capture by protons and capture into low levels may be derived from experimental or theoretical values of the cross-sections for the inverse process of photoionization. Values of $\alpha_r$ at 250 K are presented in Table 8-2 for a number of positive ions. Because of the contributions from capture into the highly excited levels, there is little variation with ionic species. The temperature variations are similar to that illustrated by Table 8-1.

Since process (8-1) is radiative, the calculation of its efficiency reduces to an evaluation of matrix elements of the electric dipole

Table 8-1. Coefficient of radiative recombination of $H^+$ and e .

| T (K) | 250 | 500 | 1000 | 2000 | 4000 | 8000 |
|---|---|---|---|---|---|---|
| $\alpha_r (cm^3 sec^{-1} \times 10^{12})$ | 4.84 | 3.12 | 1.99 | 1.26 | 0.78 | 0.48 |

Table 8-2. Coefficient of radiative recombination of $X^+$ and e at 250K.

| X | H | He | Li | C | N | O | Ne | Na | K |
|---|---|---|---|---|---|---|---|---|---|
| $\alpha_r (cm^3 sec^{-1} \times 10^{12})$ | 4.8 | 4.8 | 3.7 | 4.2 | 3.6 | 3.7 | 3.4 | 3.2 | 3.0 |

operator. The uncertainties in the predicted rate coefficients occur in the wavefunctions of the system X . For most systems, wavefunctions more accurate than hydrogenic are available and more accurate calculations of $\alpha_r$ could be performed. Although the predicted rate of capture into any given level might be significantly altered, a substantial change in the overall recombination coefficient is unlikely because most of the captures occur into highly excited levels for which the hydrogenic approximation provides a valid description.

### 8.2.2 Dielectronic Recombination

At high temperatures, the process of dielectronic recombination must be considered. Dielectronic recombination may also be represented by:

$$X^+ + e \rightarrow X_d' \rightarrow X_b + h\nu \ , \qquad (8\text{-}3)$$

with the difference that $X_d'$ is not in a bound state but is in an excited state which overlaps a continuum. Stabilization is effected by radiative transitions of X to lower excited states. Because of the possibility of a large statistical weight for the final states $X_d'$, dielectronic recombination may be more efficient than radiative recombination in some cases. Burgess (Reference 8-3) has given a simple formula for estimating the rate coefficients $\alpha_d$ for dielectronic recombination. Values as high as $10^{-10}$ $cm^3$ $sec^{-1}$ are possible. However, for the important cases of $N^+$ and $O^+$ ground-state ions, Bates (Reference 8-4) has shown that $\alpha_d$ is smaller than $\alpha_r$ .

Unlike radiative recombination, dielectronic recombination is an electron interaction process. It depends upon the resonance structure of the scattering of electrons by the positive ion. Because of overlapping and interference of resonances and because of changes in the zero-order angular momentum coupling schemes that characterize the resonances (cf. Reference 8-5), the accurate prediction of the efficiency of dielectronic recombination encounters severe difficulties.

### 8.2.3 Collisional Recombination

At high electron densities, stabilization can occur by a collision with a thermal electron:

$$X_d' + e \rightarrow X + e \,, \tag{8-3}$$

and the recombination coefficient becomes proportional to the electron density. Large densities are required before Equation (8-3) has an efficiency comparable to that of Equation (8-2) (Reference 8-6).

#### 8.2.4.1 COLLISIONAL-RADIATIVE RECOMBINATION

In plasmas of moderate and high densities, recombination is complicated by the necessity of taking simultaneous account of radiative and collisional processes and the effective recombination coefficient is a function of the electron density. A detailed study has been carried out by Bates, Kingston, and McWhirter (References 8-6, 8-7). They argue that the populations of the excited states of X are effectively in statistical equilibrium so that the decay of the plasma is controlled by the rate at which the population of the ground state is increased.

Detailed numerical results for an optically thin plasma composed of protons and electrons are reproduced in Table 8-3. Explicit results for a helium-ion plasma are also available (Reference 8-8). The studies of Bates, Kingston, and McWhirter suggest that the recombination coefficient is not very sensitive to the ionic species involved. Results for an optically thick plasma have been given by Bates, Kingston, and McWhirter (Reference 8-9) and by Bates and Kingston (Reference 8-10).

Table 8-3. Coefficient of collisional radiative recombination.

| $n_e(cm^{-3})$ | T(K) | | | |
|---|---|---|---|---|
| | 250 | 500 | 1000 | 2000 |
| $10^8$ | $8.8 \times 10^{-11}$ | $1.4 \times 10^{-11}$ | $4.1 \times 10^{-12}$ | $1.8 \times 10^{-12}$ |
| $10^9$ | $4.0 \times 10^{-10}$ | $3.8 \times 10^{-11}$ | $7.5 \times 10^{-12}$ | $2.5 \times 10^{-12}$ |
| $10^{10}$ | $2.8 \times 10^{-9}$ | $1.6 \times 10^{-10}$ | $1.9 \times 10^{-11}$ | $4.1 \times 10^{-12}$ |
| $10^{11}$ | $2.7 \times 10^{-8}$ | $1.0 \times 10^{-9}$ | $6.9 \times 10^{-11}$ | $9.1 \times 10^{-12}$ |
| $10^{12}$ | $2.6 \times 10^{-7}$ | $9.0 \times 10^{-9}$ | $3.9 \times 10^{-10}$ | $2.9 \times 10^{-11}$ |
| $10^{13}$ | $2.6 \times 10^{-6}$ | $8.9 \times 10^{-8}$ | $3.1 \times 10^{-9}$ | $1.4 \times 10^{-10}$ |
| $10^{14}$ | $2.6 \times 10^{-5}$ | $8.8 \times 10^{-7}$ | $2.9 \times 10^{-8}$ | $9.8 \times 10^{-10}$ |

#### 8.2.4.2 COLLISIONAL-DIELECTRONIC RECOMBINATION

Dielectronic recombination in plasmas of moderate and high densities is also complicated by the effects of collision-induced transitions. Detailed studies for a number of positive ions have been carried out by Burgess and Summers (Reference 8-11).

### 8.2.5 Three-Body Recombination

At high neutral particle densities, the three-body recombination process:

$$X^+ + M + e \rightarrow X + M \quad , \tag{8-4}$$

may be significant. The process is analogous to:

$$X^+ + e + e \rightarrow X + e \quad , \tag{8-5}$$

which contributes to collisional-radiative recombination. Bates and Khare (Reference 8-12) have formulated a statistical theory which incorporates a detailed description of the energy loss processes undergone by the electron. For positive ions moving in helium gas with a number density of $10^{19}$ $cm^{-3}$ at a temperature of 250 K, Bates

and Khare compute rate coefficients of about $10^{-8}$ $cm^3$ $sec^{-1}$. The theory of Bates and Khare, suitably generalized, has been used by Victor, Klein, and Dalgarno and values of high reliability have been obtained for a large number of atomic ions in all the inert gases (Reference 8-13). The rate coefficients are larger for ions moving in molecular gases because of energy losses by rotational and vibrational excitation. Water vapor is particularly efficient as a third body. Detailed calculations (Reference 8-14) have been performed.

### 8.2.6 Dissociative Recombination

Molecular ions may be removed by the process of dissociative recombination:

$$XY^+ + e \rightarrow X' + Y' . \qquad (8\text{-}6)$$

Dissociative recombination proceeds by radiationless transitions which usually occur more rapidly than radiative transitions. The process can be regarded as the formation of a temporary resonance state or molecular complex $(XY)^*$ which stabilizes by dissociation (Reference 8-6). In order for the process to be efficient the interaction potential of the initial state of $XY^+$ must cross that of the resonance state near to the equilibrium separation of $XY^+$. If the time for autoionization of $(XY)^*$ is long compared to the time for the stabilizing dissociation process, the recombination coefficient for $XY^+$ in a particular vibrational level varies approximately with electron temperature $T_e$ as $T_e^{-1/2}$ (Reference 8-15). The recombination coefficient may well be sensitive to the vibrational distribution of the molecular ion. The behavior with vibrational temperature is difficult to predict because it depends upon the detailed nature of the interaction potentials.

Sufficient spectroscopic data are available for the $B\,^2\Pi$ and $B'\,^2\Delta$ states of nitric oxide to permit estimates of the interaction potentials and autoionization lifetimes. Bardsley (Reference 8-15) has calculated a rate coefficient of $2.6 \times 10^{-7}$ $cm^3$ $sec^{-1}$ for their contribution to the dissociative recombination of $NO^+$ at 3 K. Other molecular states may provide paths leading to dissociative recombination and there may occur in addition to the direct processes for dissociative recombination an indirect process in which the electron is captured by transfer of its kinetic energy to the rotational and vibrational modes of the nuclear motion (Reference 8-15). The electron is then moving in a highly excited Rydberg state of the molecule which can dissociate

because of a pseudo-crossing with some non-Rydberg state. Detailed calculations of the properties of Rydberg states (Reference 8-6) may be necessary in order to assess reliably the quantitative significance of the indirect mechanism.

## 8.3 REMOVAL OF NEGATIVE IONS

### 8.3.1 Mutual Neutralization

Positive and negative ions can be converted into neutral species by the process of mutual neutralization:

$$X^+ + Y^- \rightarrow X + Y \,. \qquad (8\text{-}7)$$

Calculations have been carried out by Bates and Lewis (Reference 8-16) and by Bates and Boyd (Reference 8-17), assuming that the process can be regarded as a crossing from the initial to the final potential energy surface, the probability of which is approximated by the Landau-Zener formula. Calculations of a similar kind for more complex systems have been carried out by Olson, Peterson, and Moseley (Reference 8-18). The approximations are very severe and it is not clear that the results have, except by chance, more than qualitative value. The calculations are probably correct in showing that the rate coefficients at a temperature T of 300 K exceed $10^{-7}$ $cm^3$ $sec^{-1}$. Because of the collecting action of the Coulomb force, the rate coefficients vary as $T^{-1/2}$.

### 8.3.2 Associative Detachment

Associative detachment is the process:

$$X^- + Y \rightarrow XY + e \,. \qquad (8\text{-}8)$$

If the process is regarded as occurring through the formation of a quasi-molecular ion which undergoes autodetachment, a rate coefficient of about $10^{-10}$ $cm^3$ $sec^{-1}$ is obtained (Reference 8-19). More elaborate quantal formulations have been advanced (Reference 8-20), which describe the nuclear motion as occurring in a force field derivable from a complex potential. The imaginary part is the inverse of the lifetime towards autodetachment. For H interacting with $H^-$, the potential has been calculated approximately from first principles (Reference 8-21) and also semi-empirically (Reference 8-22) from experimental data on the reverse reaction of dissociative attachment (cf. Section 8.9.1). A semi-classical theory has been used (Refer-

ence 8-23) to calculate the rate coefficient for the associative detachment of H and $H^-$. It is almost constant over a wide range of temperatures with a value of $2 \times 10^{-9}$ $cm^3$ $sec^{-1}$. Calculations have also been reported for O and $O^-$ (Reference 8-24).

### 8.3.3 Collisional Detachment

An approximate description of collisional detachment processes:

$$X^- + Y \rightarrow X + Y + e \,, \tag{8-9}$$

has been presented by Bates and Massey (Reference 8-25) but no quantitative predictions have been made for collisions at thermal velocities.

### 8.3.4 Three-Body Recombination

At high gas densities, the three-body recombination processes:

$$X^+ + Y^- + M \rightarrow X + Y + M \tag{8-10}$$

$$X^+ + Y^- + M \rightarrow XY + M \,,$$

will occur more rapidly than mutual neutralization. Bates, Moffett, and Flannery (Reference 8-26) have formulated an effectively exact statistical theory and have worked out its consequences for ions recombining in various gases. The results agree closely with those of the simple theory introduced by Thomson (Reference 8-27). In air, the predicted value of the recombination coefficient is about $10^{-2}$ $T^{-5/2}$ p $cm^3$ $sec^{-1}$, where p is the pressure in torr and T is the temperature (Reference 8-28).

## 8.4 CHARGE TRANSFER

### 8.4.1 Symmetrical Resonance Charge Transfer

Symmetrical resonance charge transfer:

$$X^+ + X \rightarrow X + X^+ \,, \tag{8-11}$$

does not involve an electronic transition and reliable results can be obtained from a theory which takes account of only the initial and final states. Various simple expressions exist with which estimates can readily be made (References 8-29, 8-30). Detailed calcula-

tions for:

$$O^+ + O \rightarrow O + O^+ ,$$

and: (8-12)

$$N^+ + N \rightarrow N + N^+ ,$$

have been carried out (Reference 8-31) and precise values of the diffusion coefficient of $O^+$ in O have been obtained (References 8-31, 8-32).

### 8.4.2 Accidental Resonance Charge Transfer

Accidental resonance charge transfer, one example of which is:

$$H^+ + O \rightarrow H + O^+ , \quad (8-13)$$

does involve an electronic transition and no reliable procedure has been established for predicting the cross-section. A semi-empirical analysis by Rapp and Francis (Reference 8-29), which yields results in harmony with high-energy measurements, predicts a cross-section of a few times $10^{-15}$ $cm^2$ for Equation (8-13) at thermal velocities.

### 8.4.3 Non-Resonance Charge Transfer

The theoretical studies of non-resonance charge transfer:

$$X^+ + Y \rightarrow X + Y^+ , \quad (8-14)$$

have been reviewed by Bransden (Reference 8-33). In general it appears that non-resonance charge transfer processes proceed slowly at thermal velocities but exceptions are not uncommon, for the colliding particles may form a temporary but long-lived collision complex.

The cross-sections will presumably be sensitive to the detailed structure of the colliding particles. Nevertheless an essentially classical theory (Reference 8-30) has proved remarkably accurate at intermediate velocities.

### 8.4.4 Radiative Charge Transfer

At thermal velocities, radiative charge transfer:

$$X^+ + Y \rightarrow X + Y^+ + h\nu \,, \tag{8-15}$$

may proceed more rapidly than charge transfer for exothermic reactions. The efficiency of Equation (8-15) depends upon the availability of a molecular state which can radiate by an allowed transition. A number of specific calculations have been carried out and a rate coefficient of $10^{-13}$ $cm^3$ $sec^{-1}$ has been obtained in a favorable case (References 8-34, 8-35).

## 8.5 ION-MOLECULE REACTIONS

A summary of the theories of ion-molecule reactions is given in Reference 8-36. If it is assumed that all close collisions lead to reaction, an upper limit of:

$$k = 2.3 \times 10^3 \, (\alpha/M)^{1/2} \; cm^3 \; sec^{-1} \,, \tag{8-16}$$

where $\alpha$ is the molecular polarizability and M is the reduced mass on the chemical scale, is given for the rate coefficient of ion-molecule reactions such as:

$$\begin{aligned} X^+ + XZ &\rightarrow X + YZ^+ \\ &\rightarrow XY^+ + Z \\ &\rightarrow XZ^+ + Y \end{aligned} \tag{8-17}$$

(Reference 8-37). For air molecules, k is of the order of $10^{-9}$ $cm^3$ $sec^{-1}$. The actual rate may be much less but no quantal predictions have been made. Equation (8-16) also provides an upper limit to the coefficient of Equation (8-14). Useful semi-empirical analyses have been carried out by Wolf and Turner (Reference 8-38) and by Bohme, Hasted, and Ong (Reference 8-39).

## 8.6 QUENCHING COLLISIONS

Quenching collisions:

$$X' + Y \rightarrow X + Y' \tag{8-18}$$

can be understood qualitatively in terms of a near approach of mole-

cular potential-energy curves. They are likely to be rapid if the transitions $X' - X$ and $Y' - Y$ are optically allowed (References 8-1, 8-40), especially if the energy defect is small.

The quenching collisions:

$$X' + YZ \rightarrow Y + XZ \qquad (8\text{-}19)$$

$$X' + YZ \rightarrow X + YZ^{\ddagger} , \qquad (8\text{-}20)$$

the double-dagger indicating vibrational excitation, can also occur rapidly provided suitable potential-energy surfaces are available.

Radiative quenching processes:

$$X' + Y \rightarrow X + Y + h\nu , \qquad (8\text{-}21)$$

are usually very slow (Reference 8-41).

## 8.7 VIBRATIONAL DEACTIVATION

The theoretical studies of vibrational deactivation:

$$XY^{\ddagger} + Z \rightarrow XY + Z , \qquad (8\text{-}22)$$

have been comprehensibly reviewed by Takayanagi in Reference 8-42 (see also Reference 8-43). Reliable predictions are prevented in most cases by a lack of knowledge of the interaction potentials.

## 8.8 ELECTRON IMPACT

### 8.8.1 Electronic Excitation

The theory of the excitation of atoms by electron impact has been described by Seaton (Reference 8-44). Reliable cross-sections for the excitation of the metastable levels of atomic oxygen:

$$e + O(^3P) \rightarrow e + O(^1D) \qquad (8\text{-}23)$$

$$e + O(^3P) \rightarrow e + O(^1S) , \qquad (8\text{-}24)$$

have been obtained by Henry, Burke, and Sinfailan (Reference 8-45), by a refinement of the original work of Seaton (Reference 8-46). Reference 8-45 also contains cross-sections for atomic nitrogen and

some positive ions of oxygen and nitrogen. More extensive studies of electron scattering are in progress (Reference 8-47). Cartwright (Reference 8-48) has calculated cross-sections for the electron impact excitation of triplet states of molecular nitrogen using the Ochkur-Rudge approximation.

### 8.8.2 Rotational Excitation

The excitation of rotational levels in molecules has been studied intensively (References 8-49 through 8-55) and accurate predictions are available for the excitation of rotational levels of nitrogen (References 8-53, 8-56). The position regarding molecular oxygen remains obscure but it has been demonstrated that the cross-sections can be larger than those for nitrogen despite the much smaller quadrupole moment (References 8-56, 8-57).

## 8.9 VIBRATIONAL EXCITATION

Model calculations have been performed (References 8-58, 8-59) which reproduce well the cross-sections for vibrational excitation measured by Schulz (Reference 8-60) and the theory has been used to extrapolate the experimental data down to thermal velocities (see in particular References 8-59, 8-61). Purely theoretical predictions have also been made (Reference 8-62). An analysis of the molecular oxygen data has been reported (Reference 8-63).

### 8.9.1 Dissociative Attachment

There have been important developments (Reference 8-64) in the theory of dissociative attachment:

$$e + XY \rightarrow X^- + Y, \qquad (8\text{-}25)$$

and theoretical models (Reference 8-65) have been constructed that are consistent with the data of Henderson, Fite, and Brackmann (Reference 8-66) on the dissociative attachment of vibrationally excited molecular oxygen.

## 8.10 PHOTOIONIZATION

Photoionization cross-section calculations have been summarized by Ditchburn and Opik (Reference 8-67) and by Stewart (Reference 8-68). Hartree-Fock calculations for atomic oxygen have been car-

ried out by Dalgarno, Henry, and Stewart (Reference 8-69), and for atomic nitrogen by Henry (Reference 8-70). Calculations which include the contributions from the resonance associated with the autoionizing levels have been reported also (Reference 8-71). These cross-section data should be reliable. Cross-sections for the photoionization of ions of oxygen and nitrogen have been obtained by Hidalgo (Reference 8-72), by Henry and Williams (Reference 8-73), and by Silk and Brown (Reference 8-74).

The photoionization of molecular nitrogen has been investigated theoretically by Schneider and Berry (Reference 8-75) and Tuckwell (Reference 8-76). The results provide valuable insight into the nature of the end products.

## REFERENCES

8-1. Bates, D. R., Ed., Atomic and Molecular Processes, Academic Press, New York (1962).

8-2. Mott, N. F., and H. S. W. Massey, The Theory of Atomic Collisions, 3rd Edition, Oxford University Press, London (1965).

8-3. Burgess, A., Astrophys. J. 141, 1588 (1965); see also Tucker, W., and R. Gould, Ibid. 144, 244 (1966).

8-4. Bates, D. R., Planet. Space Sci. 9, 77 (1962).

8-5. Trefftz, E., Zeits. Astrophys. 65, 299 (1965); Shore, B. W., Revs. Mod. Phys. 39, 439 (1967); Trefftz, E., J. Phys. B3, 763 (1970).

8-6. Bates, D. R., and A. Dalgarno, in Reference 8-1, pp. 245 ff.

8-7. Bates, D. R., and A. E. Kingston, Proc. Roy. Soc. A279, 10 (1964).

8-8. Bates, D. R., and A. E. Kingston, Proc. Roy. Soc. A279, 32 (1964).

8-9. Bates, D. R., A. E. Kingston, and R. P. McWhirter, Proc. Roy. Soc. A270, 155 (1962).

8-10. Bates, D. R., and A. E. Kingston, Planet. Space Sci. 11, 1 (1963).

8-11. Burgess, A., and H. P. Summers, Astrophys. J. 157, 1007 (1969).

8-12. Bates, D. R., and S. P. Khare, Proc. Phys. Soc. 85, 231 (1965).

8-13. Victor, G. A., and M. Klein, work in preparation (1971).

8-14. Bates, D. R., V. Malaviya, and N. Young, Proc. Roy. Soc. A320, 437 (1971).

8-15. Bardsley, J. N., J. Phys. B1, 349, 365 (1968); O'Malley T. F., Phys. Rev. 185, 101 (1969); Bardsley, J. N., Phys. Rev. A2, 1359 (1970); Bardsley, J. N., and M. A. Biondi, Adv. Atom. Mol. Phys. 6, 1 (1970).

8-16. Bates, D. R., and J. T. Lewis, Proc. Phys. Soc. A68, 173 (1955).

8-17. Bates, D. R., and T. J. M. Boyd, Proc. Phys. Soc. A69, 910 (1956).

8-18. Olson, R. E., J. R. Peterson, and J. Moseley, J. Chem. Phys. 53, 3391 (1970).

8-19. Dalgarno, A., Ann. Geophys. 17, 16 (1961).

8-20. Herzenberg, A., Phys. Rev. 160, 80 (1967); Chen, J. C. Y., Phys. Rev. 156, 12 (1967).

8-21. Bardsley, J. N., A. Herzenberg, and F. Mandl, Proc. Phys. Soc. 89, 305, 321 (1966).

8-22. Chen, J. C. Y., and J. L. Preacher, Phys. Rev. 167, 30 (1968).

8-23. Browne, J. C., and A. Dalgarno, J. Phys. B2, 885 (1969).

8-24. Janev, R. K., and A. R. Tančić, J. Phys. B4, 219 (1971).

8-25. Bates, D. R., and H. S. W. Massey, Phil. Mag. 45, 111 (1954).

8-26. Bates, D. R., and R. J. Moffett, Proc. Roy. Soc. A291, 1 (1966); Bates, D. R., and M. R. Flannery, Proc. Roy. Soc. A302, 367 (1968); Flannery, M. R., J. Phys. B1, 384 (1968); J. Chem. Phys. 50, 546 (1969); Phys. Rev. Letts. 21, 1729 (1968); Ann. Phys., in press (1971). See also Landon, S. A., and J. C. Keck, J. Chem. Phys. 48, 374 (1968); Bates, D. R., and Z. Jundi, J. Phys. B1, 1145 (1968).

8-27. Thomson, J. J., Phil. Mag. 47, 337 (1924).

8-28. Sayers, J. J., Atomic and Molecular Processes, Academic Press, New York (1962).

8-29. Rapp, D., and W. E. Francis, J. Chem. Phys. 37, 2631 (1962).

8-30. Bates, D. R., and R. A. Mapleton, Proc. Phys. Soc. 87, 657 (1966).

8-31. Knopf, H., E. A. Mason, and J. T. Vanderslice, J. Chem. Phys. 40, 3547 (1964).

8-32. Dalgarno, A., J. Atm. Terrestr. Phys. 25, 939 (1964).

8-33. Bransden, B. H., Adv. Atom. Mol. Phys. 1, 45 (1965).

8-34. Arthurs, A. M., and J. Hyslop, Proc. Phys. Soc. A70, 849 (1957).

8-35. Allison, A. C., and A. Dalgarno, Proc. Phys. Soc. 85, 845 (1965).

8-36. McDaniel, E. W., V. Čermák, A. Dalgarno, E. E. Ferguson, and L. Friedman, Ion-Molecule Reactions, John Wiley, New York (1970).

8-37. Gioumousis, G., and D. R. Stevenson, J. Chem. Phys. 29, 294 (1958).

8-38. Wolf, F. A., and B. R. Turner, J. Chem. Phys. 48, 4226 (1960).

8-39. Bohme, D. K., J. B. Hasted, and P. P. Ong, Chem. Phys. Letts. 1, 259 (1967).

8-40. Bykhouvskii, V. K., and E. E. Nikitin, Opt. and Spectrosc. 16, 111 (1964).

8-41. Allison, A. C., J. D. Browne, and A. Dalgarno, Proc. Phys. Soc. 89, 41 (1965).

8-42. Takayanagi, K., Progr. Theoret. Phys. (Suppl.) 25, 1 (1963).

8-43. Marriott, R., Proc. Phys. Soc. 88, 671 (1966).

8-44. Seaton, M. J., Atomic and Molecular Processes, Academic Press, New York (1962).

8-45. Henry, R. J. W., P. G. Burke, and A. L. Sinfailan, Phys. Rev. 176, 218 (1969).

8-46. Seaton, M. J., Phil. Trans. Roy. Soc. A245, 429 (1953).

8-47. Cf. Smith, K., M. J. Conneely, and L. A. Morgan, Phys. Rev. 177, 196 (1969); Reinhardt, W. P., Phys. Rev. A2, 1767 (1970); Burke, P. G., A. Hibbert and W. D. Robb, J. Phys. B4, 219 (1971).

8-48. Cartwright, D. C., Phys. Rev. A2, 1331 (1970).

8-49. Gerjuoy, E., and S. Stein, Phys. Rev. 98, 1848 (1955).

8-50. Dalgarno, A., and R. J. Moffett, Proc. Natl. Acad. Sci. (India) A33, 511 (1964).

8-51. Dalgarno, A., and R. J. W. Henry, Proc. Phys. Soc. 85, 679 (1965).

8-52. Takayanagi, K., and S. Geltman, Phys. Rev. 138, A1003 (1964).

8-53. Sampson, D. H., and R. C. Mjolsness, Phys. Rev. 140, A1466 (1965).

8-54. Chen, J. C. Y., Phys. Rev. 146, 61 (1966).

8-55. Takayanagi, K., and Y. Itikawa, Adv. Atom. Mol. Phys. 6, 109 (1970).

8-56. Takayanagi, K., and S. Geltman, Phys. Rev. 143, 25 (1966).

8-57. Sampson, D. H., and R. C. Mjolsness, Phys. Rev. 144, 116 (1966).

8-58. Herzenberg, A., and F. Mandl, Proc. Roy. Soc. A270, 48 (1962).

8-59. Chen, J. C. Y., J. Chem. Phys. 40, 3507, 3513 (1964).

8-60. Schulz, G. J., Phys. Rev. 135, A988 (1964).

8-61. Bardsley, J. N., A. Herzenberg, and F. Mandl, in Atomic Collision Processes, M. R. C. McDowell, Ed., North-Holland Publishing Co., Amsterdam (1964).

8-62. Krauss, M., and F. H. Mies, Phys. Rev. A1, 1592 (1970); Burke, P. G., and A. L. Sinfailan, J. Phys. B3, 641 (1970).

8-63. Herzenberg, A., J. Chem. Phys. 51, 4942 (1969).

8-64. Cf. Bardsley, J. N., and F. Mandl, Repts. Prog. Phys. 31, 471 (1968).

8-65. Denkov, Yu. N., Phys. Rev. Letts. 15, 235 (1965); O'Malley, T. F., Phys. Rev. 155, 59 (1967); O'Malley, T. F., and H. S. Taylor, Phys. Rev. 176, 207 (1968).

8-66. Henderson, W. R., W. L. Fite, and R. T. Brackmann, Phys. Rev. 183, 157 (1969).

8-67. Ditchburn, R. W. and U. Öpik, in Reference 8-1; pp. 79 ff.

8-68. Stewart, A. L., Adv. Atom. Mol. Phys. 3, 1 (1967).

8-69. Dalgarno, A., R. J. W. Henry, and A. L. Stewart, Planet. Space Sci. 12, 235 (1964).

8-70. Henry, R. J. W., J. Chem. Phys. 44, 4357 (1966).

8-71. Henry, R. J. W., Planet. Space Sci. 16, 1503 (1968).

8-72. Hildalgo, M. B., Astrophys. J. 153, 981 (1968); Ibid. 157, 479 (1969).

8-73. Henry, R. J. W., and R. E. Williams, Pub. Astron. Soc. Pacific 80, 669 (1969).

8-74. Silk, J., and R. L. Brown, Astrophys. J. 163, 495 (1971).

8-75. Schneider, B., and R. S. Berry, Phys. Rev. 182, 141 (1969).

8-76. Tuckwell, H. C., J. Phys. B3, 293 (1970).

# 9. DATA-GATHERING METHODS BASED ON ATMOSPHERIC MEASUREMENTS

I.G. Poppoff
R.C. Whitten
NASA-Ames Reseorch Center

and

R.C. Gunton
J.E. Evons
E.G. Joki
Lockheed Palo Alto Research Laboratory

(Latest Revision 31 July 1971)

## 9.1 INTRODUCTION

The measurement of recombination coefficients and reaction rates in the atmosphere is important even though it is often more accurate and less expensive to measure these parameters in the laboratory. This is because not enough is known about the ionosphere to be certain that the laboratory measurements are valid for ionospheric conditions. The principal deficiencies in desired ionospheric information are a lack of accurate data on ionic species, electron concentrations, and minor neutral species, and an incomplete knowledge of important reactions. These deficiencies are especially severe with regard to the lower D-region although in no region are the excited-state populations well known. Laboratory data and models utilizing or based upon laboratory data must, therefore, be tested against atmospheric data at every opportunity to ensure their relevance. For this purpose, atmospheric measurement techniques must be developed and refined to provide the necessary data.

Historically, it has been the atmospheric measurements (mainly by radio propagation techniques) that have inspired theoretical development and laboratory experiments. Early in the development of radio propagation theory, it was recognized that the ionosphere was sluggish in its response to ionizing radiation. There is a delay in the recovery of the ionosphere after a solar flare, an eclipse of the sun, and after the noontime peak in solar radiation intensity. This delay in recovery is associated with the recombination of ions and electrons or with the attachment of electrons to neutral species. Appleton (Reference 9-1) measured the recovery time $\tau$ and related it to the effective recombination coefficient $\alpha_{eff}$ and to the electron density N:

$$\tau = 1/2\,\alpha_{eff} N .$$

Consideration of the ionospheric recovery problem led to early estimates of the constituents of the ionosphere, the ionizing radiations and reactions, and reaction rates (e.g., Reference 9-2).

The term "effective recombination coefficient", and the more general term "effective rate coefficient", both denote a direct in situ measurement made in a particular environment. An effective coefficient cannot be considered as a constant of nature but must in general be expected to vary as the environment changes.

The accuracy with which reaction rate coefficient measurements can be made using geophysical phenomena involves two major considerations: (1) the precision with which the reactants and reaction products are measured; and (2) the extent to which important influencing factors are known. The latter point has often been crucial in cases where effective rates measured in geophysical phenomena have differed by orders of magnitude from theoretical and laboratory results.

## 9.2 TYPES OF ATMOSPHERIC MEASUREMENTS

The various types of measurements made are summarized in general in Table 9-1. A discussion of measurements in auroras and methods for handling energy deposition are given in References 9-3 to 9-5. Detailed discussions of many instruments and the problems encountered in their use can be found in Reference 9-6. Descriptions are given below of some special type of measurements.

### 9.2.1 Spectral Emission Rates

Emission rates for spectral emission features in aurora are generally expressed as fluorescence efficiencies. These efficiencies are used in accounting for energy loss from the atmosphere. Apparent fluorescence efficiency is the observed rate of energy emission in a spectral feature from a given volume divided by the total observed rate of deposition of energy by energetic particles in the volume. The word "apparent" means that there may be uncertainties: the radiation observed at a distance, because of radiation trapping and absorption effects, may not be a good measure of the radiation emitted in the energy deposition region. Also the energetic particle energy deposition measured simultaneously with the emissions may not represent the true energy source of the emissions in the cases of (1) long-lived metastable states, (2) chemiluminescent reaction

Table 9-1. Types of atmospheric meosurements.

| Meosurement | Plotforms | Techniques | Atmospheric Event* |
|---|---|---|---|
| Electron density | Sotellite<br>Rocket<br>Ground | Electricol probes<br>Rodio propagotion<br>Ionosonde | Aurora<br>Solar proton<br>Eclipse<br>Nuclear<br>Sunrise<br>Sunset |
| Ion densities and composition | Sotellite<br>Rocket | Moss spectrometer<br>Electrical probes | Auroro<br>Solar proton<br>Eclipse |
| Natural species | Rocket<br>Ground | Moss spectrometer<br>Spectroscopic | |
| Rodio propagotion | Satellite<br>Rocket<br>Ground | Reflection<br>Transmission<br>Differentiol Doppler<br>Differential Foradoy rotation | Aurora<br>Solor proton<br>Eclipse<br>SID |
| Porticle precipitation (e, protons, H, $He^+$, He) | Sotellite<br>Rocket | Counters | Aurora<br>Solor proton |
| Spectrol emission rates | Satellite<br>Rocket<br>Ground | Spectroscopic | Aurora<br>Solor proton<br>Eclipse<br>Nuclear<br>Sunrise<br>Sunset<br>Nightglow<br>Dayglow<br>Twilight |

*All meosurements ore oiso mode in the normol ionosphere.

chains with appreciable delays in reaction, and (3) low-energy red and infrared radiation energy sources which may be electric fields and auroral electrojet currents which at present are not directly relatable to energetic particles.

Fluorescence efficiencies in auroras can be measured best by combining vertical (along magnetic field lines from below or from above) photometer measurements from ground, rocket, or satellite platforms with measurements of the flux and energy and angular distributions of the precipitating particles from rockets or satellites. Measurements of the first negative bands of $N_2^+$ at 3914 and 4278 A have been used extensively as an indicator of ion production rate and energy deposition for electrons having energies above 19 eV. Some experimenters prefer the use of the $N_2(0, 0)$ second positive band at 3371 A (11 eV threshold) for total energy deposit measurements from jet aircraft or higher altitude observing platforms (Reference 9-7). The choice between these radiations depends on such factors as atmospheric extinction as well as detector and filter technology. Some of the instruments and experimental techniques used in fluorescence efficiency measurements are described by Johnson et al for satellites (Reference 9-8), Ulwick for rockets (Reference 9-9), Eather and Mende for aircraft (Reference 9-10), and Belon et al for ground observations (Reference 9-11).

Local fluorescence efficiency measurements as a function of altitude have been measured in stable auroras with rocket-borne omnidirectional particle detectors along with magnetic zenith and/or nadir pointing photometers. Ground photographs and scanning photometers with filters are needed (but have been used in only a few experiments) to assure homogeneity over the rocket photometer field of view and the time stability of the precipitation so that altitude derivatives of the particle and luminescence can be evaluated. Ratios of different radiations and vertical profiles are needed to assess the energy spectra of the incident particles. Measurements which have been made with side-looking photometers have not been useful in determining fluorescence efficiencies unless good three-dimensional models of the source luminosity have been constructed and used in analysis.

Once a value has been obtained for the fluorescence efficiency for electrons of keV energies producing 3914 A radiation, $\eta(3914)$, ratio measurements of other radiation intensities such as I(5577), and corresponding measurement of I(3914) made in the magnetic

zenith or nadir will provide apparent fluorescent efficiencies for the other radiations through the relation:

$$\eta(5577) = \eta(3914) \frac{3914\ I(5577)}{5577\ I(3914)} \quad .$$

Hunten (Reference 9-12) has described the techniques used in twilight airglow measurements.

### 9.2.2 Large Scale Coordinated Measurements

In measurements made in situ on large-scale geophysical events, coordinated measurements of several different types have been made simultaneously and from widely separated locations. Störmer (Reference 9-13) first studied the geometry and morphology of auroral arcs. Akasofu et al (Reference 9-14) describe how Elvey and his coworkers in Alaska used all-sky cameras, scanning photometers, patrol spectrographs, riometers, ionosondes, and visual observers during the International Geophysical Year (IGY) 1957-58 to study auroral morphology and emission rates. With the advent of rocket and polar-orbiting-satellite instrument platforms, auroras offered a means of studying effective recombination coefficients and fluorescence efficiencies in the upper atmosphere—in conditions not available to the laboratory. A coordinated input-output experiment (References 9-15, 9-16) to be described briefly in paragraph 9.2.2.2 shows the complex interplay of factors needed to get effective recombination coefficients and fluorescence efficiencies from measurements in the upper atmosphere.

#### 9.2.2.1 COORDINATED MEASUREMENTS IN ECLIPSES

Measurements with satellites, rockets, aircraft, and ground-based instrumentation were made during the 20 July 1963 eclipse over Canada, the 30 May 1965 eclipse in New Zealand, the 20 May 1966 eclipse in Greece, and the 7 March 1970 eclipse over the eastern part of the United States. Papers describing the early results from the 7 March 1970 eclipse have been collected in a single issue of Nature (Reference 9-17).

During the total eclipse over Brazil 12 November 1966 an extensive and carefully coordinated set of rocket, aircraft, and ground-based measurements were made. Instrumented rockets were launched

at short intervals to obtain electron concentrations and temperatures, and ion compositions and temperatures, as functions of altitude and time during the course of the eclipse. The intensities of the solar X-ray and UV ionizing fluxes were measured as a function of time through the eclipse—as well as the residual fluxes and the resulting ion production rates from the uneclipsed corona at totality. The time history of the ionospheric and solar parameters under ambient conditions were measured by several rocket and ground-based instruments during the days just before the eclipse. For papers relating to these measurements, see Bomke et al (Reference 9-18), Narcisi et al (Reference 9-19), and Mechtly and Seino (Reference 9-20).

### 9.2.2.2 COORDINATED MEASUREMENTS IN AURORAS

In a coordinated experiment on auroras (see Meyerott and Evans (References 9-15, 9-21), Evans (Reference 9-16), and Johnson et al (Reference 9-8)) measurements were made of electron-ion recombination coefficients as a function of altitude as well as UV and visible fluorescence efficiencies for electrons and protons of a few keV energy.

The auroral experiment documented the incident particles, luminosities, and electron densities in and near well-behaved homogeneous auroras. The time histories of other environment-influencing factors were also measured. Figure 9-1 shows a typical arrangement and approximate distances involved in the combined polar-orbiting satellite, instrumented aircraft, and ground-station program. The following minimum set of measurements for electron auroras was needed:

1. Electron energy spectra and angular distribution for computation of vertical profiles of ion production rates.

2. Proton energy deposition required to assess proton contamination.

3. Absolute intensity and vertical distribution of selected luminosities to give a direct measurement of ion production rates.

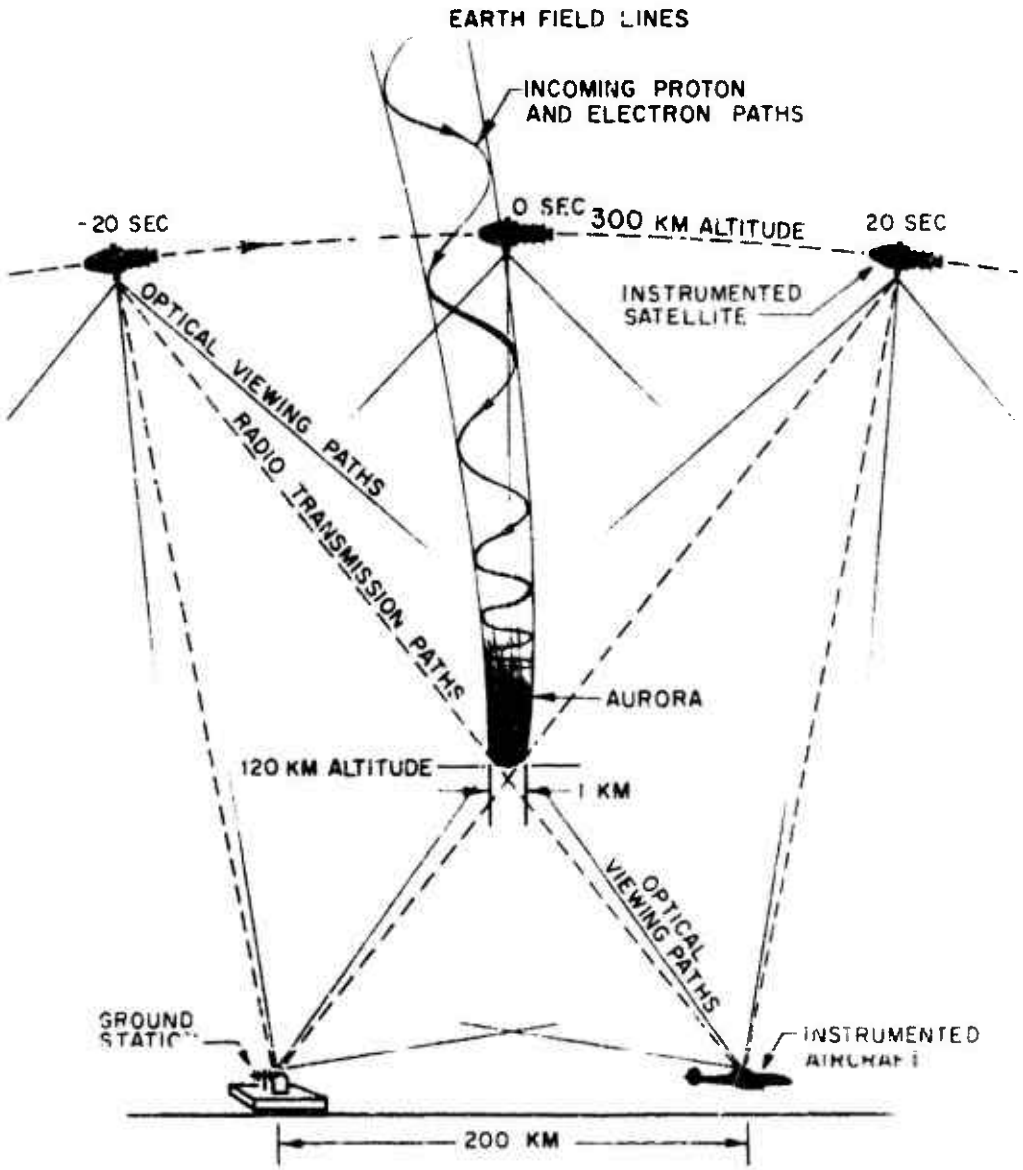


Figure 9-1. Schematic diagram of coordinated experiment.

4. Homogeneity evaluations by photographic measurements from ground or aircraft.

5. Radio phase and attenuation measurements of integrated electron density between the satellite and ground- or aircraft-based receivers.

6. Luminosity distribution time-history measurements for estimation of the ambient atmospheric conditions where the auroral energy deposit was taking place and of the steadiness of the particle precipitation during the observation period.

#### 9.2.2.3 COORDINATED MEASUREMENTS IN PCA EVENTS (SOLAR PROTON EVENTS)

Solar proton (PCA) events occur when the high-energy protons from a solar disturbance are emitted in such a direction that they strike the earth's atmosphere. The protons have sufficient energy to deposit much of their energy in the 50 to 90 km altitude region. This occurs only near the polar cap where the protons can penetrate the earth's magnetic field. A review of measurements made since the discovery and definition of PCA events is given by Bailey (Reference 9-22). More recently a coordinated rocket, satellite, aircraft, and ground measurement program sponsored by DASA and AFCRL, PCA 69, was designed to study the physical chemistry of the ionospheric D-region during a solar proton event. During the event of 2-4 November 1969 a total of 36 rockets were launched at Fort Churchill, Canada, with emphasis on night-to-day variations and on the sunrise and sunset transition periods. Electron and proton flux measurements were made on several satellites. Ground measurements were made with riometer, magnetometer, ionosonde, and partial reflection techniques. Optical measurements were made from aircraft. Rocket instruments included particle detectors, optical photometers, ion mass spectrometers, ion probes, and electron density probes. Rocket measurements were also made of neutral density and the temperatures of neutrals, ions, and electrons.

## 9.3 DETERMINATIONS OF EFFECTIVE RECOMBINATION COEFFICIENTS IN THE D, E, AND F REGIONS

### 9.3.1 General

In the lower ionosphere, where diffusion and magnetic effects are negligible, the electron and ion balance can be described by the fol-

lowing lumped-parameter equations:

$$\frac{dN}{dt} = q - \alpha_D N N^+ - \beta N m + \gamma N^- n + \rho N^- \qquad (9\text{-}1)$$

$$\frac{dN^-}{dt} = -\alpha_i N^- N^+ + \beta N m - \gamma N^- n - \rho N^- \qquad (9\text{-}2)$$

$$N^+ = N + N^- , \qquad (9\text{-}3)$$

where N is the electron concentration, $N^+$ the positive-ion concentration, $N^-$ the negative-ion concentration, m represents the concentration of attaching neutral species, n represents the concentration of detaching neutral species, q the electron production, $\alpha_D$ the ion-electron recombination coefficient, $\alpha_i$ the ion-ion neutralization coefficient, $\beta$ the electron attachment coefficient, $\gamma$ the negative-ion chemical and collisional detachment coefficient, and $\rho$ the negative-ion photodetachment rate.

A negative-ion-to-electron concentration ratio:

$$\lambda = N^-/N , \qquad (9\text{-}4)$$

is often used to write Equations (9-1) to (9-3) in the following form (References 9-23, 9-24):

$$\frac{dN}{dt} = \frac{q}{1+\lambda} - \left(\alpha_D + \lambda\alpha_i\right) N^2 - \frac{N}{(1+\lambda)} \frac{d\lambda}{dt} . \qquad (9\text{-}5)$$

The equation obeyed by $\lambda$ is (Reference 9-25):

$$\frac{1}{(1+\lambda)} \frac{d\lambda}{dt} = \beta m - \lambda \left[ \rho + \gamma n + N\left(\alpha_i - \alpha_D\right) + \frac{q}{N(1+\lambda)} \right] . \qquad (9\text{-}6)$$

The negative-ion-to-electron ratio, $\lambda$, is a very slowly varying function of time; thus Equation (9-5) can be written:

$$\frac{dN}{dt} \cong \frac{q}{(1+\lambda)} - \left(\alpha_D + \lambda\alpha_i\right) N^2 , \qquad (9\text{-}7)$$

and Equation (9-6) can be rewritten:

$$\lambda \cong \frac{\beta m}{\rho + \gamma n} \quad . \tag{9-8}$$

Under some conditions if $\lambda$ is large, e.g., in the lower D-region, the approximate Equation (9-7) may be inappropriate and Equation (9-5) should be used.

During quiescent conditions, $dN/dt \cong 0$ and $dN^-/dt \cong 0$ over much of the sunlit hemisphere and:

$$q \cong (1 + \lambda)\left(\alpha_D + \lambda\alpha_i\right)N^2 = \alpha_{eff}\, N^2 \, . \tag{9-9}$$

Note that $\alpha_{eff}$ is a complex quantity related to a specific recombination coefficient only under rather restricted conditions, since in general it depends on electron-ion and ion-ion recombination, attachment and photodetachment rates, and the neutral species concentrations.

If, as is often the case, $\lambda \ll 1$ in the region of interest, $\alpha_{eff}$ can be considered to be the effective dissociative recombination coefficient, weighted over all ion species (both ground and excited states) in the region.

Two general approaches have been used to measure the effective recombination coefficient. The most common, because of a relative abundance of data, is based on the observation of the effect of a well-defined change in the electron content of the ionosphere. For example, the change in solar radiation production function q during an eclipse causes a change in electron density N at a rate $dN/dt$ controlled by $\alpha_{eff}$. The change can be observed by a variety of ground-based radio propagation techniques. Other examples include the change observed around local noon, the change caused by the pulse of ionizing radiation produced by solar flares, and the radiation pulse produced by high-altitude nuclear bursts. The original papers in which these techniques appear are cited in Section 9.3.2.

The second, and potentially most reliable, approach is to measure electron density, radiation flux, and atmospheric species directly and simultaneously. Such measurements have been attempted for eclipse, PCA, auroral, nuclear test, and quiescent solar condi-

tions. A number of difficulties have plagued these attempts and the data, though interesting, cannot yet be considered definitive. However, future refinements of this approach should yield not only the effective recombination coefficient but also information regarding individual reaction rates, including those that involve excited states.

There is abundant evidence that the dissociative recombination coefficients of diatomic and some triatomic molecular ions (e.g., $O_2^+$, $N_2^+$, $NO^+$, $CO_2^+$) are of approximately the same magnitude (Reference 9-26). If the positive ions present at D-layer altitudes were predominantly these species, one could use an $\alpha_D$ in Equation (9-1) which depended little on ion identity. However, Narcisi and Bailey (Reference 9-27) have shown that the principal species below about 85 km altitude are $H_3O^+$ and its hydrates. Furthermore Biondi (Reference 9-28) has shown that $\alpha_D$ for the hydrates of $H_3O^+$ increases as cluster size increases (by about $1.5 \times 10^{-6}$ $cm^3\ sec^{-1}$ for the first two water molecules added). Their chemistry of formation and loss is such that under quiescent conditions where ion lifetime is very long, the average cluster size is expected to be large. On the other hand, when the ion number density is large (e.g., during PCA events), the mean cluster size is smaller. Hence the effective dissociative recombination coefficient is a function of ionization rate and of other variables, and one must be very careful in interpreting and applying this parameter at altitudes below 85 km.

For the upper part of the E-region and the F-region where a significant number of atomic ions are present, a simple expression for the effective recombination coefficient under quasi-equilibrium conditions with no diffusion becomes:

$$\alpha_{eff} = q/N^2 = \sum_i \alpha_i^D \left(N_{mi}^+/N\right) + \alpha_r \left(N_a^+/N\right) \quad . \tag{9-10}$$

where $\alpha_i^D$ is the electron-ion dissociative recombination coefficient of molecular ion i, $\alpha_r$ is the radiative recombination coefficient for atomic ions, $N_{mi}^+$ is the density of a molecular ion and $N_a^+$ is the density of atomic ions.

It is well known from mass-spectrometric measurements (e.g., Reference 9-29) that the dominant ionic species present in the upper ionosphere is $O^+$. The mechanism of recombination of $O^+$ with electrons is necessarily radiative and is thus very slow

($\alpha_r \approx 10^{-12}$ cm$^3$ sec$^{-1}$). A more rapid means of electron removal is offered by the chain of processes:

$$O^+ + N_2 \rightarrow NO^+ + N \ , \tag{9-11}$$

and:

$$O^+ + O_2 \rightarrow O_2^+ + O \ , \tag{9-12}$$

followed by:

$$NO^+ + e \rightarrow N + O \ , \tag{9-13}$$

and:

$$O_2^+ + e \rightarrow O + O \ . \tag{9-14}$$

The rate constants for reactions (9-11) and (9-12) have been computed from ionospheric observations (see Section 9.4.1), and also measured in the laboratory (References 9-30, 9-31). All such evidence indicates that the rate constants are, respectively, about 2 to 4 x $10^{-12}$ cm$^3$ sec$^{-1}$ and 2 to 4 x $10^{-11}$ cm$^3$ sec$^{-1}$, which yields a rate at 300 km of $\sim 10^{-5}$ to $10^{-4}$ sec$^{-1}$. According to most current models of the upper atmosphere, reaction (9-11) is the more important. This is thought to be much slower than the rate of removal of electrons by processes (9-13) and (9-14); hence reactions (9-11) and (9-12) which control the rate of formation of $NO^+$ and $O_2^+$ also control the rate of electron removal. This assumption is probably valid if $\alpha_D > 10^{-8}$ cm$^{-3}$ for $NO^+$ and $O_2^+$, which seems to be the case (see the temperature dependence suggested by Weller and Biondi, and by Cunton and Shaw (References 9-32, 9-33)). It has, however, been questioned by various investigators, most recently by Awajobi (Reference 9-34) who based his objections on various anomalies in the time development of the F2 region. The recombination term which appears in the continuity equation is a linear one because the recombination rate is independent of the concentration of charged particles:

$$B = k_{11}\left[N_2\right] + k_{12}\left[O_2\right] \ . \tag{9-15}$$

In addition to electron removal, one must include a diffusion term in the continuity equation. Hence, assuming that $O^+$ is the only ionic species present and neglecting electrodynamic drifts, one can write

for the continuity equation (except near equatorial latitudes):

$$\frac{\partial N}{\partial t} = q - BN + D_a \sin I\left[\frac{\partial^2 N}{\partial Z^2} + \frac{3}{2H}\frac{\partial N}{\partial Z} + \frac{1}{2H^2}\right]. \qquad (9\text{-}16)$$

Here N is the $O^+$ (and electron) concentration, $D_a$ is the ambipolar diffusion coefficient for the ions and electrons, H is the scale height of atomic oxygen, and I is the geomagnetic dip angle. The solution of Equation (9-16) is discussed, for example, by Yonezawa in Reference 9-35. Because of diffusion, the electron number density displays a maximum, the well-known F2 peak, at the altitude where $BH^2/D_a = 1$ (Reference 9-36). This relationship offers a way of estimating B if the diffusion coefficient, the scale height, and the number densities of $N_2$ and O at the peak are known. $D_a$ is known quite well (Reference 9-37), but the other parameters can be obtained only from rocket-borne mass-spectrometric measurements.

It would seem to be possible to compute B from observations of the decay of the F2 region at sunset and during eclipses. However, the source term q does not abruptly vanish at any time during such phenomena. Also, the effects of electrodynamic drifts cannot be neglected at these times. Nisbet and Quinn (Reference 9-38) have attempted to measure B by observing the decay of the electron profile along a tube of geomagnetic field lines during the night but there were several limitations to their work.

The rate of reaction (9-11) is much larger if $N_2$ is vibrationally excited (Reference 9-39). Such excitation is present in the quiescent atmosphere and can, for example, be increased by X-rays from a high-altitude nuclear burst. The few observations of the electron density made after the Starfish shot of 1962 suggest that the electron number density in the F2 region may indeed be substantially reduced by this mechanism (Reference 9-40).

### 9.3.2 Effective Recombination Coefficient Data

An extensive search of the literature of the past ten years is summarized in Figure 9-2. The data were obtained from References 9-1, 9-9, 9-21, and 9-41 to 9-72. Some of the values cited in the references were corrected by the present authors when this was known to be necessary.

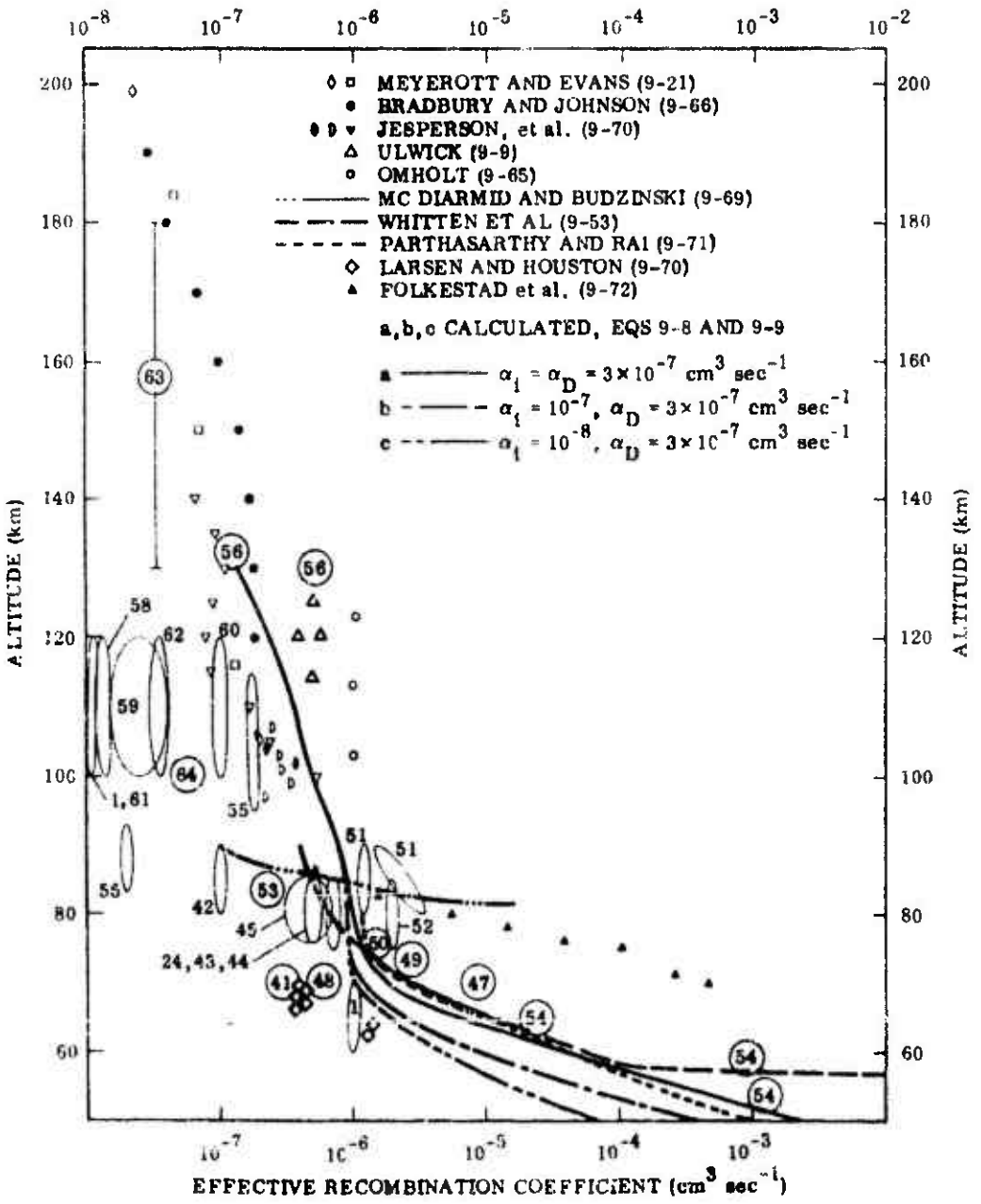


Figure 9-2. Effective recombination rate coefficients measured in the upper atmosphere. Wide avals indicate a range of values for $\alpha_{eff}$ and for altitude. Narrow avals or bars indicate an altitude range. E-region values are plotted at 110 km. (xx) or ()-xx represents a typical value from Reference 9-xx.

In Figure 9-2 curves of $\alpha_{eff}$ calculated from Equation (9-9) are presented for reference. Curves a, b, and c are based on an illustrative $\lambda$ profile (calculated according to Equation 9-8), an assumption that $\alpha_D$ is $3 \times 10^{-7}$ cm$^3$ sec$^{-1}$, and that $\alpha_i = 10^{-8}$, $10^{-7}$, and $3 \times 10^{-7}$ cm$^3$ sec$^{-1}$, respectively. In spite of the many assumptions and errors inherent in these determinations, the values agree to within an order of magnitude. The "equal $\alpha$" curve agrees best with the experimental data.

### 9.3.3 Radiative Recombination

The rate coefficients for reactions of this type are so low that laboratory measurement is very difficult. It may well be that analysis of ionospheric observations is a much better way of determining such coefficients.

Hicks and Chubb (Reference 9-73) have reported the nighttime observation of two longitudinal arcs of weak UV radiation that are rather symmetrically located about the magnetic dip equator. The radiation was identified by Barth and Schaffner (Reference 9-74) as the 1356 and 1340A radiation of OI. Hanson (Reference 9-75) suggested that such radiation would result naturally from radiative recombination below 500 km in the F-region of $O^+$ and electrons with enhancement at the Appleton anomaly peaks where the observed intensity of the radiation is greatest. Knudsen (Reference 9-76) suggested that the neutralization of $O^-$ by $O^+$ with a rate of about $10^{-7}$ cm$^3$ sec$^{-1}$ may provide the necessary excitation, but Hanson (Reference 9-77) notes that the associative detachment reaction $O^- + O \rightarrow O_2 + e$, whose rate is given as $1.4 \times 10^{-10}$ cm$^3$ sec$^{-1}$ by Fehsenfeld et al (Reference 9-78), limits the amount of $O^-$. Hanson (Reference 9-77) shows that the observations are probably accounted for largely by radiative recombination of $O^+$ with a rate of about $5 \times 10^{-13}$ cm$^3$ sec$^{-1}$. Tinsley (Reference 9-79) observed the 4368A OI line whose lower state leads to 1304A OI emission and deduces a radiative recombination coefficient of about $5 \times 10^{-13}$ cm$^3$ sec$^{-1}$ from one observation and about $4 \times 10^{-14}$ cm$^3$ sec$^{-1}$ from another.

## 9.4 MEASUREMENTS AND RESULTS FOR OTHER PARAMETERS

### 9.4.1 Ion-Neutral Reaction Rate Coefficients

Equations (9-1) to (9-3) are, of course, simplified; they assume that the ionosphere acts as if there are only two ionic species—one posi-

tive and one negative. In reality, several atomic and molecular ions are present and therefore several charged rearrangement processes occur simultaneously with the recombination, attachment, and detachment processes. Then Equations (9-1) and (9-2) may be written:

$$\frac{dN}{dt} = \Sigma q_i - \Sigma_i \alpha_i^D N_i^+ N - \Sigma_i \beta_i m_i N - \Sigma_i \gamma_i N_i^- n_i + \Sigma_i \rho_i N_i^- \qquad (9\text{-}16)$$

$$\frac{dN_i^-}{dt} = -\Sigma_{ij} \alpha_{ij}^i N_i^+ N_j^- - \Sigma_{ij} \ell_{ij} N_i^- n_j + \Sigma_{k\ell} \ell_{k\ell} N_k^- n_\ell$$

$$+ \Sigma_i \beta_i m_i N - \Sigma_i \gamma_i N_j^- n_i - \Sigma_i \rho_i N_i^- \quad , \qquad (9\text{-}17)$$

where $\alpha_i^D$ is the ion-electron recombination coefficient, $\alpha^i$ is the ion-ion recombination coefficient, $\ell$ is the charged rearrangement rate constant for negative ions, and the subscripts denote the species. Similar equations can be written for the positive species.

If several ion concentrations, electron concentrations, and radiation fluxes are measured simultaneously at several altitudes then equations like (9-16) and (9-17) can be solved for the reaction rates of the charged rearrangement reactions, as listed in Table 9-2 (References 9-43, 9-44, 9-56, 9-80).

Measurements yielding the rates of some individual ion-neutral reactions are described in Table 9-3 and in the accompanying comments.

### 9.4.2 Rate Coefficients for Ion-Ion Neutralization, Neutral-Neutral Reactions, and Electron Attachment

Values of the ion-ion neutralization coefficient may be derived from analyses of measurements of ion densities and of particle fluxes from which ion production rates may be computed. For D-region altitudes where the electron density is significant, measurements of N should also be made simultaneously and in the analysis a value of the electron-ion recombination rate must be assumed. For altitudes below 60 km where the electron density is small or negligible, analysis of the observations is straightforward. (See Table 9-4.)

Table 9-2. Ian-neutral reactian rate coefficients derived from analysis af ian compasitian measurements.

| Reactian | Rate Coefficients ($cm^3\ sec^{-1}$) | | |
|---|---|---|---|
| | Danahue (Reference 9-56) | Whitten and Poppaff (References 9-43, 9-44) | Matuura (Reference 9-80) |
| $N_2^+ + O \rightarrow NO^+ + N$ | $5 \times 10^{-10}$ | | $(0.9\text{-}1) \times 10^{-10}$ |
| $O^+ + N_2 \rightarrow NO^+ + N$ | $4 \times 10^{-12}$ | $2 \times 10^{-12}$ | $8 \times 10^{-13}$ |
| $N_2^+ + O_2 \rightarrow O_2^+ + N_2$ | $2 \times 10^{-10}$ | $2 \times 10^{-10}$ | $(0.8\text{-}2) \times 10^{-10}$ |
| $N_2^+ + O \rightarrow O^+ + N_2$ | $6 \times 10^{-12}$ | $2 \times 10^{-11}$ | $(4\text{-}6) \times 10^{-11}$ |
| $O^+ + O_2 \rightarrow O_2^+ + O$ | $4 \times 10^{-11}$ | $2 \times 10^{-11}$ | $8 \times 10^{-12}$ |
| $O_2^+ + N_2 \rightarrow NO^+ + NO$ | $<4 \times 10^{-14}$ | | $4 \times 10^{-14}$ |
| $N^+ + O_2 \rightarrow NO^+ + O$ | $5 \times 10^{-10}$ | | |
| $N_2^+ + O_2 \rightarrow NO^+ + NO$ | | | $4 \times 10^{-14}$ |

Table 9-3. Ion-neutrol reoctian rote coefficients—single rote meosurements.

| Reoctian | Altitude (km) | Rate Coefficient ($cm^3\ sec^{-1}$) | References | Comments |
|---|---|---|---|---|
| $Si^+ + O_2^{\ddagger} \rightarrow SiO^+ + O$ | 110 | $1 \times 10^{-9} \exp(-x)$ $x = h\nu/kT_v$ (suggested) | Ferguson et ol (9-81); Fehsenfeld (9-82) | $O_2^{\ddagger}$ - vibrotionolly excited; vibrotionol quontum number $v = 2, 3, 4$. $T_v$ is vibrotionol temperoture. Difficult to reconcile with fost $O_2^{\ddagger}$ relaxa-tian rotes (Chapter 20) |
| $He^+ + N_2 \rightarrow He + N^+ + N$ | 200-400 | $5 \times 10^{-10}$ | Brintan et al (9-83) | Agrees with lab measurement $\sim 1 \times 10^{-9}$ of Fergusan et ol (Reference 9-84). |
| $O^+(^2D) + N_2 \rightarrow N_2^+ + O$ | 300-500 | $2 \times 10^{-9}$ | Dolgorno and McElroy (9-85) | Rundle (Reference 9-86) however infers that the role of this process in doubt. |
| $O^+ + N_2 \rightarrow NO^+ + O$ | 300 | $\sim 6 \times 10^{-13}$ | Smith (9-87) | Smith's loss coefficient of $O^+$ converted to rate agrees with lab measurement of Dunkin et ol (Reference 9-88). |

Table 9-4. Rote coefficients for ion-ian, neutrol-neutral and ottachment.

| Process | Altitude (km) | $\alpha_i$ ($cm^3 sec^{-1}$) | References | Comments |
|---|---|---|---|---|
| Ion-Ion Neutralizatian | | | | |
| 1. $X^+ + Y^- \rightarrow$ Neutrals | 70 | $(1-10) \times 10^{-7}$ | Falkestad et ol (9-72) | Analysis done with Eq.(9-9) but outhors feel model is prabobly too simple. |
| 2. $X^+ + Y^- \rightarrow$ Neutrols | 30-60 | $(1.1-2.8) \times 10^{-8}$ | Guntan (9-89); Bragin (9-90) | Assumptians: Galactic cosmic rays the only saurce; electrons oll attached. |
| Neutral-Neutrol Reactians | | | | |
| NO productian via: | | | | |
| (o) $NO^+ + e \rightarrow N(^2D) + O$ $\rightarrow N(^4S) + O$ | 80-150 | (b) $6 \times 10^{-12}$ | Strobel et al (9-91) | Mare than 50 percent af N praduced by (o) is $N(^2D)$. |
| (b) $N(^2D) + O_2 \rightarrow NO + O$ | 85-150 | (b) $5 \times 10^{-12}$ | Norton ond Borth (9-92) | 70-85 percent af N produced by (o) is $N(^2D)$. |
| | | | Meiro (9-93) | 87 percent af N produced by (a) is $N(^2D)$. Rote of (a) computed far D-regian above 85 km is $7 \times 10^{-7}$ $cm^3 sec^{-1}$. |
| Electron Attachment | | | | |
| $e + X \rightarrow X^-$ | 48-62 | Loss rate ot 60 km | Hadges (9-94) | Detachment induced by radio pulse from racket. Apporent 2-body attachment rate at 60 km 9 times the expected 3-body $O_2^-$ farmatian rote. |

### 9.4.3 Collision Frequency

The determination of collision frequency from the results of radio propagation experiments has been attempted by several investigators. The summary is principally from Belrose and Hewitt (Reference 9-95) with the addition of other results. The data are shown in Figure 9-3.

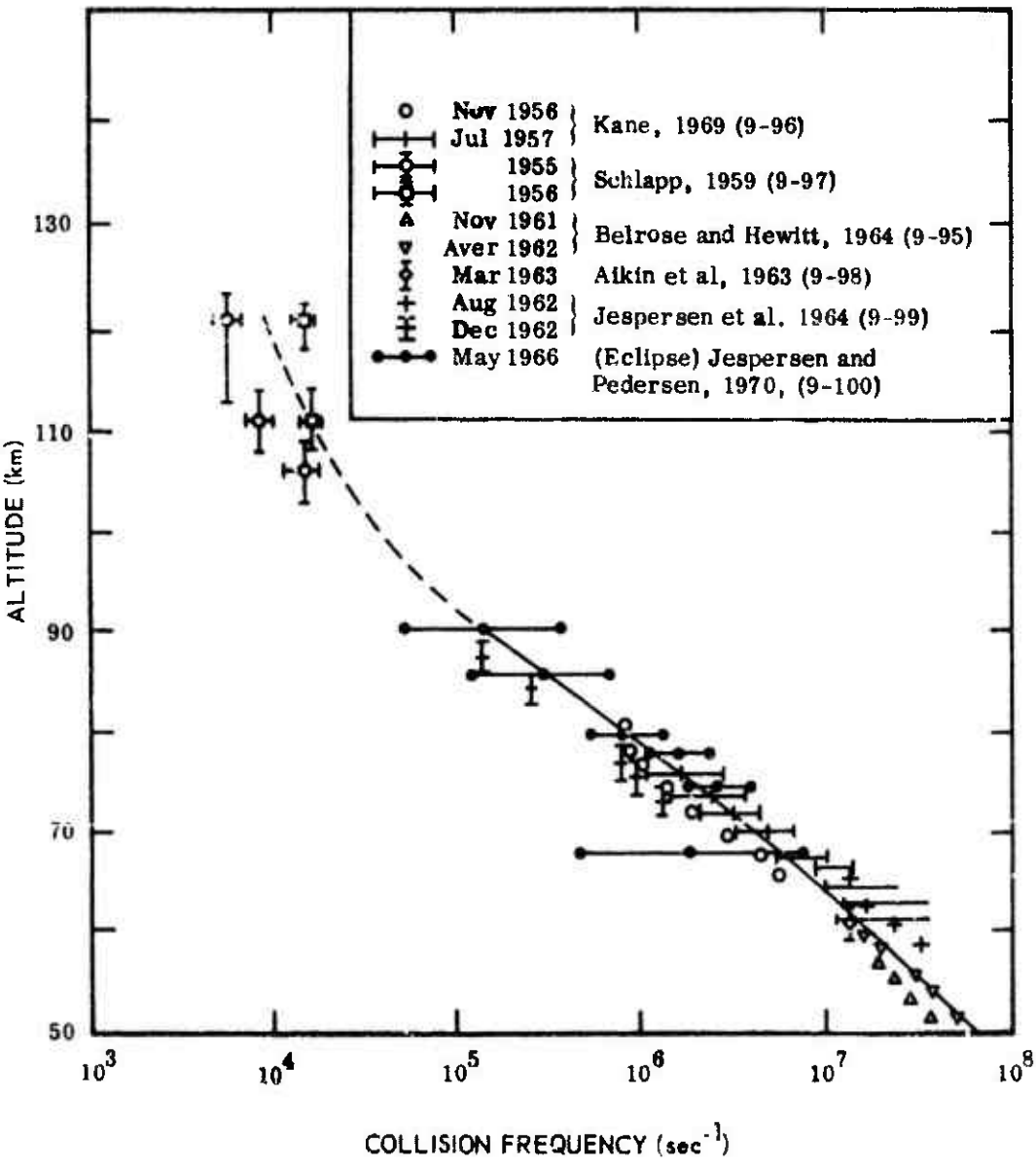


Figure 9-3. Collision frequency measurements.

### 9.4.4 Airglow Emission Rates

The emission rates for known emissions in airglow (day, twilight, and night) have been summarized by Hunten (Reference 9-101) and are presented in Table 9-5. These rates are expressed in 3 ways: (1) as intensities in rayleighs (symbol R); (2) as g-factors which represent the rate of resonance scattering of unattenuated sunlight by a single atom or molecule; and (3) by a factor which represents the rate of fluorescent radiation from a single atom or molecule in unattenuated sunlight. The quenching height $h_q$ is the emission altitude at which quenching equals radiative decay. See also, for example, References 9-12 and 9-102.

### 9.4.5 Fluorescence Efficiencies in Auroras

Many measurements on auroras have led to fluorescence efficiency values for a large number of spectral emissions. An extensive search of the published literature up to 1 October 1970 was made for measurements or combinations of measurements that could be interpreted in terms of fluorescence efficiencies. (See Table 9-6.) Measurements of the intensity ratios of two radiations, in which the fluorescence efficiency of one of the radiations is known, have been very useful in providing many indirectly determined values. Since the $N_2^+$ first negative radiations (3914, 4278, and 4709 A bands) are used most for the indirect values, fluorescence efficiencies derived from careful and extensive laboratory measurements for these radiations are included in Table 9-6.

### 9.4.6 Quenching Coefficients

For this class of reaction rate coefficients, we have included ionospheric measurements of some important metastable species and have made use of the excellent review by Zipf (Reference 9-118). The results are summarized in Table 9-7.

### 9.4.7 Measurements Suggesting New Processes

Some ionospheric experiments after analysis do not yield reaction rate coefficients for specific processes or reactions but do suggest the existence of new processes or indicate the probable importance of processes already known. On the other hand in some cases the results indicate that a known process is not important. Several experiments leading to conclusions of this nature are described below.

Table 9-5. Known airglow emissions for the earth. As explained in Reference 9-101 production processes are: R , resonance scattering; F , fluarescence; C , chemical ossociation; I , ionic reactions; e , phata-electrons; T , excitotion tronsfer. Production rate factars are g ond d; $h_q$ is the quenching height.

| | λ(Å) | Emitter State | DAY | | | TWILIGHT | | NIGHT | | |
|---|---|---|---|---|---|---|---|---|---|---|
| | | | Intensity | Height | Process | Intensity | Height | ntensity | Height | Process |
| 1 | 304 | $He^+$ | Present | | R | | | (4.8) | | R |
| 2 | 584 | He | Present | | R | | | (12) | | |
| 3 | 834 | $O^+$ | Present | | R | | | | | |
| 4 | 1025 | H Ly β | Present | 200-$10^4$ | R | | | 10 R | 200 | R |
| 5 | 1200 | $N(^4P)$ | 400 R | 180 | R? | | | | | |
| 6 | 1216 | H Ly α | 6 kR | 100-$10^5$ | R | | | 2 kR | 100-$10^5$ | R |
| 7 | 1302-4-6 | $O(^3S)$ | 7.5 kR | 190 | eFR | | | | | |
| 8 | 1356 | $O(^5S)$ | 350 R | 140 | e | | | | | |
| 9 | 1300-1500 | $R_2(ang)$ | Present | | e | | | | | |
| 10 | 1493, 1744 | N | Present | | e | | | | | |
| 11 | 2160 etc. | $NO(A^2\Sigma^+)$ | 1 kR | 70-150 | N | | | | | |
| 12 | 3371 etc. | $N_2(C^3\pi_u)$ | 6 kR | 130 up | e | | | | | |
| 13 | 2000-4000 | $N_2(B^3\Sigma_u)$ | | | e | | | | | |
| 14 | 2600-3800 | $O_2(A^3\Sigma_u^+)$ | | | | | | 600 R | 90 | C |
| 15 | 3466 | $N(^2P)$ | Present | | e | | | | | |
| 16 | 3889 | $He(^3P)$ | | | R | 1 R | >400? | | | |
| 17 | 3914 etc. | $N_2^+(B^2\Sigma_u^+)$ | 2.0 kR | 150 | RF | 200-500 R | 300 | <1 R | | |
| 18 | 3933, 68 | $Ca^+(^2P)$, | | | | ≤100 R | 80-200 | | | |
| 19 | 4368 | $O(4^3P)$ | | | | 1 R | | | | |
| 20 | 5200 | $N(^2D)$ | 90 R | ~200 | I | 10 R | | 1 R | ~250 | I |
| 21 | 5000-6500 | $NO_2$? | | | | | | 1 R/Å | ~90 | C |
| 22 | 5577 | $O(^1S)$ | 3.0 kR | 90; 175 | Ce | 400 R | 200? | 250 R | 90; 300 | C, I |
| 23 | 5893 | $Na(^2P)$ | 30 kR | 95 | R | 1-4 kR | 92 | 20-150 R | ~92 | C |
| 24 | 6300, 64 | $O(^1D)$ | 8-20 kR | 250 | FIe | 1 kR | 300 | 100-500 R | 300 | I |
| 25 | 6563 | $N(3^2P)$ | | | | | | 3 R | 200 | F |
| 26 | 6708 | $Li(^2P)$ | | | | 10-1000 R | ~90 | | | |
| 27 | 7619 etc. | $O_2(^1\Sigma)$ | 300 kR | 40-120 | RFT | | | 6 kR | | |
| 28 | 7699 | $K(^2P)$ | | | | 40 R | ~90 | | | |
| 29 | 7774, 8446 | O | 1.6, 1.1 kR | ~150 | e | | | | | |
| 30 | 10510 etc. | $N_2(B^3\pi_g)$ | 900 R | 150 | e | | | | | |
| 31 | 10830 | $He(^3P)$ | | | | 3 kR | 500 | | | |
| 32 | 11036 etc. | $N_2^+(A^2\pi_u)$ | 4 kR | 150 | RF | | | | | |
| 33 | 12700 etc. | $O_2(^1\Delta)$ | 20 MR | 50 | F | 5 MR | 80 | 80 kR | 90? | C? |
| 34 | 24000 | $OH(v \leq 9)$ | 4.5 MR | | C | | | 4.5 MR | 90 | C |

Table 9-5. (Cont'd.)

| | $q$ (photons $cm^{-3}$ $sec^{-1}$) | d(source) | $h_q$ (km) | Remarks |
|---|---|---|---|---|
| 1 | $1.1 \times 10^{-4}$ | | | Nightglow radiation could be either or both. |
| 2 | $1.7 \times 10^{-5}$ | | | |
| 3 | | | | |
| 4 | $2.6 \times 10^{-6}$ | | | |
| 5 | | | | |
| 6 | $2.1 \times 10^{-3}$ | $(4.5 \times 10^{-8}[N_2])$ | | |
| 7 | $1.0 \times 10^{-4}$ | | | |
| 8 | | | | |
| 9 | | | | Lyman-Birge-Hopfield |
| 10 | | | | |
| 11 | $4.0 \times 10^{-6}$ | | | γ bands; g for 1-0 band |
| 12 | | | | 2nd positive |
| 13 | | | | Vegard-Kaplan |
| 14 | | | | Herzberg |
| 15 | | | | |
| 16 | 0.1 | | | Scatterer is $He(^3S)$ |
| 17 | .050 | $10^{-8}[N_2]$ | 46 | 1st negative |
| 18 | 0.3, 0.15 | | | |
| 19 | | | | |
| 20 | $(6 \times 10^{-11})$ | | ~200 | Also quenched by electrons |
| 21 | | | | Continuum |
| 22 | $(1 \times 10^{-11})$ | $3 \times 10^{-4}[O_2]$ | 94 | 2972Å (5%) |
| 23 | 0.80 | | 40 | |
| 24 | $(4.5 \times 10^{-10})$ | $5.8 \times 10^{-6}[O_2]$ | 340 | |
| 25 | $2.6 \times 10^{-6}$ | | | |
| 26 | 16 | | | May be of artificial origin |
| 27 | $6.3 \times 10^{-9}$ | $\leq 5 \times 10^{-3}[O_3]$ | 90 | Atmospheric |
| 28 | 1.67 | | | |
| 29 | | | 37 | 1st positive |
| 30 | | | 37 | 1st positive |
| 31 | 16.8 | | ~400 | Scatterer is $Ne(^3S)$; $h_q$ for its destruction. |
| 32 | .042 | $2.8 \times 10^{-8}$ | | Meinel; g,d for 1-0 band (9200Å) |
| 33 | $(9.4 \times 10^{-11})$ | $9.5 \times 10^{-3}[O_3]$ | 75 | IR Atm; O-1 band 1.58μ; Nomon bands 1.9μ |
| 34 | | | | Meinel; 4.5μ to 3816Å |

Table 9-6. Fluarescence efficiencies measured in auraras.

| Wavelength A | Transition | Fluarescence Efficiency | Comments | Reference | |
|---|---|---|---|---|---|
| 3914 | $N_2^+(0,0)\,B^2\Sigma\text{-}X^2\Sigma$ 1st neg. | $4.1\times10^{-3}$ | Racket phatometer and electran energy detectar | Miller et al. | 9-103 |
| | | $7\times10^{-3}$ | Satellite photometer and particle detectar | Meyeratt and Evans | 9-21 |
| 4278 | $N_2^+(0,0)\,B^2\Sigma\text{-}X^2\Sigma$ 1st neg. | $(11\pm4)\times10^{-4}$ | Graund phatameter, racket electran detectar | Bryant et al. | 9-104 |
| Laboratary derived values used extensively in ratia measurements | | | | | |
| 3914 | $N_2^+(0,0)\,B^2\Sigma\text{-}X^2\Sigma$ 1st neg. | $3.7\times10^{-3}$ | Laboratary value | Dalgarna et al. | 9-105 |
| 4278 | | $1.0\times10^{-3}$ | From 3914 value and branching ratia | Dalgarna et al. | 9-105 |
| 4709 | | $2.2\times10^{-4}$ | From 3914 value and branching ratia | Dalgarno et al. | 9-105 |
| 1180 | $N_2(0,13)\,h\,^1\Sigma\text{-}X\,^1\Sigma$ W-K | $3\times10^{-5}$ | Ratia with 3914 | Miller et al. | 9-103 |
| 1200 | NI $^4P\text{-}^4S$ | $4\times10^{-3}$ | Ratia with 3914 | Theobald and Peek | 9-106 |
| | | $7\times10^{-4}$ | Ratia with 3914 | Miller et al. | 9-103 |
| 1216 | H Lyman $\alpha$ | $5\times10^{-2}$ | Satellite phatometer, estimate af praton flux | Metzger and Clark | 9-107 |
| 1240 | $N_2$ BH(5,11) | $7\times10^{-5}$ | Ratia with 3914 | Miller et al. | 9-103 |
| | $N_2$ BH ar NI | $6\times10^{-4}$ | Ratia with 3914 | Theobald and Peek | 9-106 |
| 1273 | $N_2$ LBH(6,0) $a\,^1\Pi\text{-}X\,^1\Sigma$ | $1.1\times10^{-4}$ | Ratia with 3914 | Miller et al. | 9-103 |
| 1325 | $N_2$ LBH(4,0) | $2.6\times10^{-4}$ | Ratio with 3914 | Miller et al. | 9-103 |
| 1339 | $N_2$ LBH(5,1) | $6\times10^{-5}$ | Ratia with 3914 | Miller et al. | 9-103 |
| 1354 | $N_2$ LBH(3,0) | $5\times10^{-4}$ | Ratia with 3914 | Miller et al. | 9-103 |
| 1356 | OI $^5S\text{-}3p$ | $3\times10^{-4}$ | Ratia with 3914 | Miller et al. | 9-103 |
| | | $3\times10^{-3}$ | Ratio with 3914 | Theobald and Peek | 9-106 |
| 1382 | $N_2$ LBH(5,2) | $7.5\times10^{-5}$ | Ratia with 3914 | Miller, et al. | 9-103 |

Table 9-6. (Cont'd.)

| Wavelength A | Transition | Fluorescence Efficiency | Comments | Reference | |
|---|---|---|---|---|---|
| 1384 | $N_2$ LBH(2,0) | $4\times10^{-4}$ | Ratio with 3914 | Miller et al. | 9-103 |
| | | $1\times10^{-4}$ | Ratio with 3914 | Theobald and Peek | 9-106 |
| 1412 | $N_2$ LBH(4,2) | $2\times10^{-4}$ | Ratio with 3914 | Miller et al. | 9-103 |
| 1416 | $N_2$ LBH(1,0) | $2\times10^{-4}$ | Ratio with 3914 | Miller et al. | 9-103 |
| 1426 | $N_2$ LBH(5,3) | $7\times10^{-5}$ | Ratio with 3914 | Miller et al. | 9-103 |
| 1430 | $N_2$ LBH(2,1) | $3\times10^{-4}$ | Ratio with 3914 | Miller et al. | 9-103 |
| 1446 | $N_2$ LBH(3,2) | $2\times10^{-4}$ | Ratio with 3914 | Miller et al. | 9-103 |
| 1464 | $N_2$ LBH(1,1) | $3\times10^{-4}$ | Ratio with 3914 | Miller et al. | 9-103 |
| | | $8\times10^{-4}$ | Ratio with 3914 | Theobald and Peek | 9-106 |
| 1473 | $N_2$ LBH(5,4) | $8\times10^{-5}$ | Ratio with 3914 | Miller et al. | 9-103 |
| 1493 | $N_2$ LBH(3,3) | $1\times10^{-4}$ | Ratio with 3914 | Miller et al. | 9-103 |
| 1493 | NI $^2P-^2D$ | $3\times10^{-4}$ | Ratio with 3914 | Miller et al. | 9-103 |
| | | $1\times10^{-3}$ | Ratio with 3914 (>110km) | Theobald and Peek | 9-106 |
| 1508 | $N_2$ LBH(4,4) | $4\times10^{-5}$ | Ratio with 3914 | Miller et al. | 9-103 |
| 1515 | $N_2$ LBH(1,2) | $8\times10^{-5}$ | Ratio with 3914 | Miller et al. | 9-103 |
| 1530 | $N_2$ LBH(2,3) | $1\times10^{-4}$ | Ratio with 3914 | Miller et al. | 9-103 |
| | | $5\times10^{-4}$ | Ratio with 3914 | Theobald and Peek | 9-106 |
| 1555 | $N_2$ LBH(0,2) | $5\times10^{-4}$ | Ratio with 3914 | Theobald and Peek | 9-106 |
| Total $N_2$ BH system | | $6\times10^{-3}$ | Ratio with 3914 and BH(5,11) | Miller et al. | 9-103 |
| 1205-2602 ($a^1\Pi-X^1\Sigma$) | Total $N_2$ LBH system | $2\times10^{-2}$ (>110km) | Ratio with 3914 | Theobald and Peek | 9-106 |
| | | $3\times10^{-2}$ (>130km) | Ratio with 3914 | Theobald and Peek | 9-106 |
| | | $7\times10^{-3}$ | Ratio with 3914 | Miller et al. | 9-103 |

Table 9-6. (Cont'd.)

| Wavelength A | Transition | Fluorescence Efficiency | Comments | Reference | |
|---|---|---|---|---|---|
| 2333-5060 | $N_2$ Vegard-Kaplan bands $A^3\Sigma$-$X^1\Sigma$ | $7\times10^{-3}$ | Ratio with $N_2^+$ (first neg.) | Chamberlain | 9-108 |
| | ($v^1 = 0$) $N_2$ Vegard-Kaplan | $1.0\times10^{-3}$ | Ratio with 4278, from 100 km upward | Sharp | 9-109 |
| | ($v^1 = 1$) $N_2$ Vegard-Kaplan | $7\times10^{-4}$ | Ratio with 4278, from 100 km upward | Sharp | 9-109 |
| 2470 | OII $^2P$-$^4S$ | $8\times10^{-5}$ | Branching ratio with 7319-30 | Chamberlain | 9-108 |
| 2972 | OI $^1S$-$^3P$ | $2.2\times10^{-4}$ | Branching ratio with 5577 | Chamberlain | 9-108 |
| 3371 | $N_2$(0, 0) (2nd pos.) | $2.5\times10^{-3}$ | Ratio with 4278 | Sharp | 9-109 |
| 3466 | NI $^2P$-$^4S$ | $8\times10^{-5}$ | Ratio with 6300 OI | Dick | 9-110 |
| 3727 | OII $^2D$-$^4S$ | $2\times10^{-5}$ | Ratio with $N_2^+$ (1st neg.) | Chamberlain | 9-108 |
| 4059 | $N_2$ 2nd pos. C $^3\Pi$-B $^3\Pi$ | $1.6\times10^{-4}$ | Ratio with 3914 | Theobald and Peek | 9-106 |
| 3116-4574 | Total $N_2$ 2nd pos. | $5\times10^{-3}$ | Ratio with 3914 | Theobald and Peek | 9-106 |
| | | $3.5\times10^{-3}$ | Ratio with $N_2^+$ (1st neg.) | Chamberlain | 9-108 |
| 4368 | OI $^3P$-$^3S$ | $1.6\times10^{-5}$ | Ratio with 4278 $N_2^+$ | Dick | 9-110 |
| 4415 | OII $^2D$-$^2P$ | $1.6\times10^{-5}$ | Ratio with 4368 | Chamberlain | 9-108 |
| 4861 | $H_\beta$ | $9\times10^{-5}$ | Protons in past breakup display | Reasoner et al. | 9-111 |
| | | $3.0\times10^{-4}$ | Ratio with 3914 | Eather | 9-112 |
| | | $2.4\times10^{-4}$ | Ratio with 4709 | Eather | 9-112 |
| | | $3.3\times10^{-4}$ | Proton component in aurora | McIlwain | 9-113 |

Toble 9-6. (Cont'd.)

| Wavelength A | Transition | Fluorescence Efficiency | Comments | Reference | |
|---|---|---|---|---|---|
| 5200 | NI $^2D$-$^4S$ | $3.3\times10^{-5}$ | Ratio with 4278 | Eather and Mende | 9-10 |
| | | $6.6\times10^{-4}$ | Ratio with 4278 soft particles | Eather and Mende | 9-10 |
| 5577 | OI $^1S$-$^1D$ | $4.2\times10^{-3}$ | Ratio with 3914 ($K_p$ = 1) | Sandford | 9-114 |
| | | $3.1\times10^{-3}$ | Ratio with 3914 ($K_p$ = 4±2) | Sandford | 9-114 |
| | | $3.9\times10^{-3}$ | Ratio with 4278 | Mende and Eather | 9-115 |
| | | $8.3\times10^{-3}$ | Ratio with 3914 | Theobold and Peek | 9-106 |
| | | $(6\pm2)\times10^{-4}$ | Electrons from rockets, ground-bosed photometer | Bryant et al. | 9-104 |
| | | $2.0\times10^{-3}$ | Ratio with 4861 in proton arc | Eather and Mende | 9-10 |
| 5893 | Na | $2\times10^{-5}$ | Upper limit and applicable only to low-lying displays such as type B ouroras | Chamberlain | 9-108 |
| 6300 | OI $^1D$-$^3P$ | $8\times10^{-4}$ | Ratio with 4278 | Eather ond Mende | 9-10 |
| | | $4\times10^{-4}$ | Ratio with 3914 | Theobald and Peek | 9-106 |
| | | $7\times10^{-3}$ | Ratio with 4278 soft particles | Eather and Mende | 9-10 |
| | | $5.6\times10^{-4}$ | Ratio with 4861 in proton orc | Chamberlain | 9-108 |
| 6364 | OI $^1D$-$^3P$ | $1.2\times10^{-4}$ | Branching ratio with 6300 | Chamberlain | 9-108 |
| 6563 | $H_\alpha$ | $4.5\times10^{-3}$ | Proton and $H_\alpha$ in proton orc | Romick and Sharp | 9-116 |
| 7319-30 | OII $^2P$-$^2D$ | $1.5\times10^{-4}$ | Ratio with 5577 | Chamberlain | 9-108 |
| 7036-15, 748 | $N_2^+$ Meinel bands $A^2\Pi$-$X^2\Sigma$ | $3\times10^{-2}$ | Ratio with $N_2^+$ (1st neg.) | Chamberlain | 9-108 |

Table 9-6. (Cont'd.)

| Wavelength A | Transition | Fluorescence Efficiency | Comments | Reference | |
|---|---|---|---|---|---|
| 7684-8598 | $O_2$ atmospheric bands | | | | |
| | $b\,^1\Sigma - X\,^3\Sigma$ | $5\times10^{-3}$ | Ratio with $N_2^+$ (1st neg.) | Chamberlain | 9-108 |
| | $O_2$ (1, 1) atmospheric | $3\times10^{-4}$ | Ratio with 5577 (17) | Omholt | 9-117 |
| | $O_2$ infrared atmospheric $a\,^1\Delta - X\,^3\Sigma$ | $8\times10^{-4}$ | Ratio with $N_2^+$ (1st neg.) | Chamberlain | 9-108 |
| 5296-6419 | $O_2^+$ (1st neg.) bands $b\,^4\Sigma - a\,^4\Pi$ | $2\times10^{-4}$ | Ratio with $N_2^+$ (1st neg.) | Chamberlain | 9-108 |
| 7774 | OI $^5P - ^5S$ | $2.5\times10^{-4}$ | Ratio with 5577 | Omholt | 9-117 |
| 8446 | OI $^3P - ^3S$ | $3.7\times10^{-4}$ | Ratio with 5577 | Omholt | 9-117 |
| 10400 | NI $^2P - ^2D$ | $2\times10^{-3}$ | Ratio with 5577 | Chamberlain | 9-108 |

Table 9-7. Quenching rate coefficients of impartant atmospheric species.

| Metastable Species | Collisian Partner | Atmaspheric Value ($cm^3$ $sec^{-1}$) | Atmospheric Analysts | Reference | Lab. Value ($cm^3$ $sec^{-1}$) | Experimenters | Reference |
|---|---|---|---|---|---|---|---|
| $O_2(a^1\Delta)$ | M<br>if all $O_2$ | 3(-19)<br>1.5(-18) | Evans et al. | 9-119 | 4(-19)<br>2.2(-18) | Clark and Wayne | 9-120 |
| $O_2(b^1\Sigma)$ | $N_2$ | 1.5(-15) | Wallace and Hunten | 9-121 | 2(-15) | e.g., Yaung and Black | 9-122 |
| $N_2(A)$ | O | 3(-11) | Hunten and McElray | 9-123 | 5(-11) | Yaung | 9-124 |
| $O(^1S)$ | O | 2(-12) | Gadsden and Marovich | 9-125 | for $O_2$ 1-3(-13) | Yaung and Black<br>Stuhl and Welge | 9-126<br>9-127 |
| $O(^1D)$ | $N_2$ | ~9(-11) | Wallace and McElray<br>Parkinsan and Zipf | 9-101<br>9-128 | 2-10(-11) | e.g., Naxan | 9-129 |
| | $O_2$ | ≤1(-14) | Hunten and McElray | 9-123 | 4(-11) | e.g., Yaung et al | 9-130 |

### 9.4.7.1 ASSOCIATIVE DETACHMENT

This process has been considered as important in the D-region for explaining the temporal behavior of PCA events (Whitten and Poppoff, Reference 9-131; Reid, Reference 9-132). The laboratory measurements of Fehsenfeld et al (Reference 9-133) revealed that some chemical detachment reactions of atmospheric interest have high reaction rates $\approx 1 \times 10^{-10}$ cm$^3$ sec$^{-1}$, including $O_2^- + O \rightarrow O_3 + e$ which is likely to be important in maintaining high electron densities where atomic oxygen is abundant.

Reid (Reference 9-134) has presented indirect observational verification of the importance of atomic oxygen based on a comparison of solar proton fluxes measured by a polar-orbiting satellite and a cosmic-noise absorption measurement carried out by high-latitude riometers during the PCA event of September 1966. PCA events show a diurnal variation in absorption; that at night is several times less than the daytime value. If chemical detachment dominates photo-detachment during the daytime, the sunset decrease in electron density is likely to be due mainly to the disappearance of O which takes place rapidly below about 75 km by association with $O_2$. Above this level the lifetime of O atoms is longer and only small changes occur from day to night. Then the absorption produced by low-energy solar protons which ionize mainly at heights above 75 km should show little change from day to night. On the other hand the absorption produced by energetic protons should show a change accompanying the change in O below 75 km. The analysis by Reid lends support to these ideas and indirectly supports the importance of chemical detachment by O atoms.

Doherty (Reference 9-135), has analyzed the propagation of an LF signal along a path through the path of the solar eclipse of July 1963. The phase change of the signal increased to a maximum three minutes after maximum obscuration and may be interpreted as due to a change of the apparent reflection height from about 67 to 74 km. The change in height was temporally very nearly the same as the increase in ozone content computed by Hunt (Reference 9-136), for altitudes just above and below reflection height range. The increase in reflection height is considered to be due to reduced chemical detachment because of reduction of the O atom density and/or to increased dissociative attachment to ozone by the reaction $e + O_3 \rightarrow O_2 + O^-$.

### 9.4.7.2 PROCESS CONVERTING $O_2^+$ RAPIDLY TO $NO^+$

Donahue et al (Reference 9-137) have made ion composition measurements with a rocket-borne mass spectrometer flown during an aurora. Near 115 km the $NO^+$ density was larger and the $O_2^+$ density much smaller than expected from existing ionospheric models. The ratio $NO^+/O_2^+$ was so large that a new mechanism must be found to convert $O_2^+$ to $NO^+$, one which does not exist in the normal mid-latitude daytime ionosphere. Among the possibilities are large densities of NO and/or $N_2$ reacting with $O_2^+$ or large vibrational excitation of $N_2$ which might increase the rate constant for the reaction $O_2^+ + N_2 \rightarrow NO^+ + NO$ two orders of magnitude above its 300 K value.

### 9.4.7.3 DISSOCIATIVE RECOMBINATION OF $O_2^+$ AS SOURCE OF $O(^1S)$

Dalgarno and Khare (Reference 9-138) and Rees et al (Reference 9-139) suggested that $O(^1S)$ produced in the dissociative recombination of $O_2$ and electrons is the source of the green line 5577A. Omholt (Reference 9-68) argues against this view from observations of rapidly varying auroras. This proposed source would cause an additional time lag between the $N_2^+$ emission which is in phase with the ionization and the portion of the green line excited by recombination, since $O_2^+$ ions have lifetimes of some seconds against recombination. No reports exist of such a lag in addition to that caused by the natural lifetime (0.75 sec) of $O(^1S)$ and the observations of Omholt support his own argument.

Parkinson et al (Reference 9-140), in a rocket investigation of the origin of the auroral green line (5577A), have made measurements with rocket-borne photometers, electron-energy analyzers, and ion mass spectrometers. The results show that direct excitation of atomic oxygen to $O(^1S)$ by auroral electrons can excite only a small fraction of the auroral green line observed. From measured ion distributions in the altitude range 100-150 km dissociative recombination is shown to contribute only weakly to the excitation of $O(^1S)$ except at high altitudes. The authors propose that dissociative excitation of $O_2$ can account for the major portion of the production of $O(^1S)$ if the cross-section for the process is of order $10^{-16}$ $cm^2$. Dissociative recombination may provide 10 percent of the total emission at the higher altitudes.

## REFERENCES


9-1. Appleton, E. V., J. Atm. Terrestr. Phys. 3, 228 (1953).

9-2. Piddington, J. H., J. Geophys. Res. 56, 409 (1951).

9-3. Walt, M., in Aurora and Airglow, B. M. McCormac, Ed., Reinhold, New York (1967); p. 287.

9-4. Davidson, G. T., J. Geophys. Res. 70, 1061 (1965).

9-5. McNeal, R. J., and J. H. Birely, in The Radiating Atmosphere, B. M. McCormac, Ed., Reidel, Dordrecht, Holland (1971); in press.

9-6. Defense Atomic Support Agency, Ionospheric Measurement Instrumentation: A Survey, DASIAC SR32; DASA 1583 (1965).

9-7. Fastie, W., private communication (1970).

9-8. Johnson, R. G., R. E. Meyerott, and J. E. Evans, in Aurora and Airglow, B. M. McCormac, Ed., Reinhold, New York (1967); p. 169.

9-9. Ulwick, J. C., in Aurora and Airglow, B. M. McCormac, Ed., Reinhold, New York (1967); p. 225.

9-10. Bather, R. H., and S. B. Mende, J. Geophys. Res. 76, 1746 (1971).

9-11. Belon, A. E., C. J. Romick, and M. H. Rees, Planet. Space Sci. 14, 597 (1966).

9-12. Hunten, D. M., Space Sci. Rev. 6, 493 (1967).

9-13. Stormer, C., The Polar Aurora, Oxford Univ. Press, London (1955).

9-14. Akasofu, S. I., S. Chapman, and A. B. Meinel, Handbuch der Physik, S. Flügge, Ed., Springer-Verlag, Berlin (1966); Vol. 49/1.

9-15. Meyerott, R. E., and J. E. Evans, Trans. Am. Geophys. Union 43, 436 (1962).

9-16. Evans, J. E., in Auroral Phenomena—Experiments and Theory, M. Walt, Ed., Stanford University Press, Stanford, Calif. (1965); p. 130.

9-17. Rishbeth, H., Nature 226, 1099 (1970).

9-18. Bomke, H. A., H. A. Blake, A. K. Harris, and D. J. Sheppard, J. Geophys. Res. 75, 6980 (1970).

9-19. Narcisi, R. S., C. R. Philbrick, A. D. Bailey, and L. Della Lucca, Aeronomy Report No. 32, University of Illinois (1969); p. 355.

9-20. Mechtly, E. A., and K. Seino, Radio Sci. 4, 371 (1969).

9-21. Meyerott, R. E., and J. E. Evans, in Atmospheric Emissions, B. M. McCormac and A. Omholt, Eds., Van Nostrand-Reinhold, New York (1969); p. 119.

9-22. Bailey, D. K., Planet. Space Sci. 12, 495 (1964).

9-23. Mitra, S. K., The Upper Atmosphere, 2nd ed., The Asiatic Society, Calcutta (1952).

9-24. Whitten, R. C., and A. Dalgarno, Stanford Research Institute, DASA 1827-1; AD801953L (1966).

9-25. Bates, D. R., and H. S. W. Massey, Proc. Roy. Soc. A187, 261 (1946).

9-26. Biondi, M. A., Can. J. Chem. 47, 1711 (1969).

9-27. Narcisi, R. S., and A. D. Bailey, J. Geophys. Res. 70, 3687 (1965).

9-28. Biondi, M. A., private communication (1970).

9-29. Taylor, H. A., and H. C. Brinton, J. Geophys. Res. 66, 2587 (1961).

9-30. Ferguson, E. E., F. C. Fehsenfeld, P. D. Goldan, A. L. Schmeltekopf, and H. I. Schiff, Planet. Space Sci. 13, 828 (1965).

9-31. Dickinson, P. H. G., and J. Sayers, Proc. Phys. Soc. 26, 137 (1960).

9-32. Weller, C. S., and M. A. Biondi, Phys. Rev. 172, 198 (1968).

9-33. Gunton, R. C., and T. M. Shaw, Phys. Rev. 140A, 756 (1965).

9-34. Awajobi, O. A., J. Atm. Terrestr. Phys. 28, 375 (1966).

9-35. Yonezawa, T., Space Sci. Rev. 5, 49 (1966).

9-36. Rishbeth, H., and O. K. Garriott, Stanford University Tech. Rept. 8 (SU-SEL-64-111) (1964).

9-37. Dalgarno, A., J. Atm. Terrestr. Phys. 26, 939 (1964).

9-38. Nisbet, J. S., and T. P. Quinn, J. Geophys. Res. 68, 1031 (1963).

9-39. Thomas, L., and R. B. Norton, J. Geophys. Res. 71, 227 (1966).

9-40. Whitten, R. C., and A. Dalgarno, Planet. Space Sci. 15, 1419 (1967).

9-41. Nestorov, G., Geomagn. Aeron. 5, 650 (1965).

9-42. Mitra, A. P., in Advances in Upper Atmosphere Research, B. Landmark, Ed., Pergamon Press and the MacMillan Co., New York and London (1963). For recent general review of D-region processes by the same author, see J. Atm. Terrestr. Phys. 30, 1065 (1968).

9-43. Whitten, R. C., and I. G. Poppoff, J. Atmos. Sci. 21, 117 (1964).

9-44. Whitten, R. C., and I. G. Poppoff, Disc. Faraday Soc. 37, 185 (1964).

9-45. LeLevier, R. E., J. Geophys. Res. 69, 481 (1964).

9-46. Kozlov, S. I., and Yu. P. Raizer, Cosmic Res. 4, 509 (1966).

9-47. Volland, H., J. Atm. Terrestr. Phys. 26, 695 (1964).

9-48. Lerfald, G. M., J. K. Hargreaves, and J. M. Watts, Radio Sci. 69D, 939 (1961).

9-49. Swift, D. W., J. Atm. Terrestr. Phys. 23, 29 (1961).

9-50. Nestorov, G., and J. Taubenheim, Izv. Geofiz. Inst. Bolgarsk, AN 7, 37 (1965).

9-51. Smith, L. C., C. A. Accardo, L. H. Weeks, and P. J. McKinnon, J. Atm. Terrestr. Phys. 27, 803 (1965).

9-52. Gustafsson, C., Planet. Space Sci. 12, 195 (1964).

9-53. Whitten, R. C., I. G. Popp[illegible], R. S. Edmonds, and W. W. Berning, J. Geophys. Res. 70, 1737 (1965).

9-54. Chilton, C. J., J. P. Conner, and F. K. Steele, Proc. IEEE 53, 2018 (1965).

9-55. Bourdeau, R. E., A. C. Aikin, and J. L. Donley, J. Geophys. Res. 71, 727 (1966).

9-56. Donahue, T. M., Planet. Space Sci. 14, 33 (1966).

9-57. Nestorov, G., and J. Taubenheim, J. Atm. Terrestr. Phys. 24, 633 (1962).

9-58. Minnis, C. M., in Solar Eclipses and the Ionosphere, W. J. G. Beynon and G. M. Brown, Eds., Pergamon Press, New York (1956).

9-59. McElhinny, M. W., J. Atm. Terrestr. Phys. 14, 273 (1959).

9-60. Bowhill, S. A., J. Atm. Terrestr. Phys. 20, 19 (1961).

9-61. Mitra, A. P., J. Geophys. Res. 69, 4067 (1964).

9-62. Landmark, B., in Solar Eclipses and the Ionosphere, W. J. G. Beynon and G. M. Brown, Eds., Pergamon Press, New York (1956).

9-63. Oya, H., and T. Obayashi, Repts. Ionosph. Space Res. Japan 21, 9 (1967).

9-64. Bomke, H. A., H. A. Blake, A. K. Harris, W. H. Hulse, D. J. Sheppard, A. A. Giesecke, and A. Pantoja, J. Geophys. Res. 72, 5913 (1967).

9-65. Omholt, A., J. Atm. Terrestr. Phys. 7, 73 (1955).

9-66. Johnson, R. G., and J. N. Bradbury, Trans. Am. Geophys. Union 49, 735 (1968).

9-67. Jeperson, N., B. Landmark, and K. Maseide, J. Atm. Terrestr. Phys. 31, 1251 (1969).

9-68. Omholt, A., Ann. Geophys. 24 215 (1968).

9-69. McDiarmid, I. B., and E E. Budzinski, Can. J. Phys. 42, 2048 (1964).

9-70. Larson, L. E., and R. E. Houston, J. Geophys. Res. 74, 2402 (1969).

9-71. Parthasarathy, R., and D. B. Rai, Radio Sci. 1, 1397 (1966).

9-72. Folkestad, K., B. Landmark, G. Slovli, and J. A. Kane, J. Atm. Terrestr. Phys. 31, 835 (1969).

9-73. Hicks, G. T., and T. A. Chubb, J. Geophys. Res. 75, 6233 (1970).

9-74. Barth, C. A., and S. Schaffner, J. Geophys. Res. 75, 7299 (1970).

9-75. Hanson, W. B., J. Geophys. Res. 74, 3720 (1969).

9-76. Knudsen, W. C., J. Geophys. Res. 75, 3862 (1970).

9-77. Hanson, W. B., J. Geophys. Res. 75, 4343 (1970).

9-78. Fehsenfeld, F. C., A. L. Schmeltekopf, D. B. Dunkin, and E. E. Ferguson, ESSA Tech. Rept. ERL 135-AL 3 (1969).

9-79. Tinsley, B. A., J. Geophys. Res. 75, 3932 (1970).

9-80. Matuura, N., Repts. Ionosph. Space Res. Japan 20, 289 (1966).

9-81. Ferguson, E. E., F. C. Fehsenfeld, and J. D. Whitehead, J. Geophys. Res. 75, 4366 (1970).

9-82. Fehsenfeld, F. C., Can. J. Chem. 47, 1808 (1969).

9-83. Brinton, H. C., M. W. Pharo, III, H. G. Mayr, and J. A. Findlay, J. Geophys. Res. 74, 2941 (1969).

9-84. Ferguson, E. E., F. C. Fehsenfeld, D. B. Dunkin, A. L. Schmeltekopf, and H. I. Schiff, Planet. Space Sci. 12, 1169 (1964).

9-85. Dalgarno, A., and M. B. McElroy, Planet. Space Sci. 14, 1321 (1966).

9-86. Rundle, H. N., in The Radiating Atmosphere, B. M. McCormac, Ed., Reidel, Dordrecht, Holland (1971); in press.

9-87. Smith, F. L., III, J. Geophys. Res. 73, 7385 (1968).

9-88. Dunkin, D. B., F. C. Fehsenfeld, A. L. Schmeltekopf, and E. E. Ferguson, J. Chem. Phys. 49, 1365 (1968).

9-89. Gunton, R. C., unpublished work (1970).

9-90. Bragin, Yu. A., Cosmic Res. 5, 413 (1967).

9-91. Strobel, D. F., D. M. Hunten, and M. B. McElroy, J. Geophys. Res. 75, 4307 (1970).

9-92. Norton, R. B., and C. A. Barth, J. Geophys. Res. 75, 3903 (1970).

9-93. Meira, L. G., Jr., J. Geophys. Res. 76, 202 (1971).

9-94. Hodges, R.R., J. Geophys. Res. 70, 185 (1965).

9-95. Belrose, J.S., and L.W. Hewitt, Nature 202, 267 (1964).

9-96. Kane, J.A., J. Atm. Terrestr. Phys. 23, 338 (1961).

9-97. Schlapp, D.M., J. Atm. Terrestr. Phys. 16, 340 (1959).

9-98. Aikin, A.C., J.A. Kane, and J. Troim, J. Geophys. Res. 69, 4621 (1964).

9-99. Jesperson, M., O. Petersen, J. Rybner, B. Bjelland, O. Holt, B. Landmark, and J.A. Kane, Planet. Space Sci. 12, 543 (1964).

9-100. Jesperson, M., and B.M. Pederson, J. Atm. Terrestr. Phys. 32, 1859 (1970).

9-101. Hunten, D.M., in The Radiating Atmosphere, B.M. McCormac, Ed., Reidel, Dordrecht, Holland (1971); in press.

9-102. Dalgarno, A., M.B. McElroy, and A.I. Stewart, J. Atmos. Sci. 26, 753 (1969).

9-103. Miller, R.E., W.G. Fastie, and R.C. Isler, J. Geophys. Res. 73, 3353 (1968).

9-104. Bryant, D.A., G.M. Courtier, G. Skovli, H.R. Lindalen, K. Aarsnes, and K. Maseide, J. Atm. Terrestr. Phys. 32, 1695 (1970).

9-105. Dalgarno, A., I.D. Latimer, and J.W. McConkey, Planet. Space Sci. 13, 1008 (1965).

9-106. Theobald, K., and M. Peek, Los Alamos Scientific Laboratory Report LA-3929 (1969).

9-107. Metzger, P.H., and M.A. Clark, J. Geophys. Res. 76, 1756 (1971).

9-108. Chamberlain, J.W., Physics of the Aurora and Airglow, Academic Press, New York (1961).

9-109. Sharp, W. E., J. Geophys. Res. 76, 987 (1971).

9-110. Dick, K. A., J. Geophys. Res. 75, 5605 (1970).

9-111. Reasoner, D. L., R. H. Eather, and B. J. O'Brien, J. Geophys. Res. 73, 4185 (1969).

9-112. Eather, R. H., J. Geophys. Res. 73, 119 (1968).

9-113. McIlwain, C. E., J. Geophys. Res. 65, 2727 (1960).

9-114. Sanford, B. P., in Aurora and Airglow, B. M. McCormac, Ed., Reinhold, New York (1967); p. 443.

9-115. Mende, S. B., and R. H. Eather, Planet. Space Sci. 19, 49 (1971).

9-116. Romick, G. J., and R. D. Sharp, J. Geophys. Res. 72, 4791 (1967).

9-117. Omholt, A., J. Atm. Terrestr. Phys. 10, 320 (1957).

9-118. Zipf, E. C., Jr., Can. J. Chem. 47, 1863 (1969).

9-119. Evans, W. F. J., D. M. Hunten, E. J Llewellyn, and A. Vallance Jones, J. Geophys. Res. 73, 2885 (1968).

9-120. Clark, I. D., and R. P. Wayne, Chem. Phys. Letts. 3, 93 (1969).

9-121. Wallace, L., and D. M. Hunten, J. Geophys. Res. 73, 4813 (1968).

9-122. Young, R. A., and G. Black, J. Chem. Phys. 47, 2311 (1967).

9-123. Hunten, D. M., and N. B. McElroy, Revs. Geophys. 4, 303 (1966).

9-124 Young, R. A., private communication (1969).

9-125. Gadsden, M., and E. Marovich, J. Atm. Terrestr. Phys. 31, 817 (1969).

9-126. Young, R. A., and G. Black, J. Chem. Phys. 44, 3741 (1966).

9-127. Stuhl, F., and K. H. Welge, Can. J. Chem. 47, 1870 (1969).

9-128. Parkinson, T. M., and E. C. Zipf, Jr., Planet. Space Sci. 19, 267 (1971).

9-129. Noxon, J. F., J. Chem. Phys. 52, 1852 (1970).

9-130. Young, R. A., G. Black, and T. G. Slanger, J. Chem. Phys. 49, 4758 (1968).

9-131. Whitten, R. C., and I. G. Poppoff, J. Geophys. Res. 67, 1183 (1962).

9-132. Reid, G. C., in Electron Density Profiles in Ionosphere and Exosphere, J. Frihagen, Ed., North-Holland, Amsterdam (1966); p. 17.

9-133. Fehsenfeld, F. C., A. L. Schmeltekopf, H. I. Schiff, and E. E. Ferguson, Planet. Space Sci. 15, 373 (1967).

9-134. Reid, G. C., Planet. Space Sci. 17, 731 (1969).

9-135. Doherty, R. H., J. Geophys. Res. 73, 2429 (1968).

9-136. Hunt, B. G., Tellus 17, 516 (1965).

9-137. Donahue, T. M., E. C. Zipf, Jr., and T. D. Parkinson, Planet. Space Sci. 18, 171 (1970).

9-138. Dalgarno, A., and S. P. Khare, Planet. Space Sci. 15, 938 (1967).

9-139. Rees, M. H., J. C. G. Walker, and A. Dalgarno, Planet Space Sci. 15, 1097 (1967).

9-140. Parkinson, T. D., E. C. Zipf, Jr., and T. M. Donahue, Planet. Space Sci. 18, 187 (1970).

## GROUP C

## CHAPTERS ON PERTINENT RATE DATA


CHAPTER 10 Basic Energy - Level and Equilibrium Date

CHAPTER 11 The Kinetics of Atmospheric Radietive Processes in the Infrered

CHAPTER 12 Photochemical Processes: Cross - Section Data

CHAPTER 13 Photochemical Processes: Solar Photoionization Rate Constants and Ultraviolet Intensities

CHAPTER 14 Kinetics of Low - Energy Electron Collision Processes

CHAPTER 15 Kinetics of High - Energy Heavy - Particle Collisional Processes

CHAPTER 16 Cherged - Particle Recombination Processes

CHAPTER 17 Electron Attachment and Detechment Processes

CHAPTER 18 Ion - Neutral Reactions

CHAPTER 19 Neutral Reactions

CHAPTER 20 Excitation and Deexcitation Processes

CHAPTER 21 Electron Collision Frequencies and Radio - Frequency Absorption

# 10. BASIC ENERGY-LEVEL AND EQUILIBRIUM DATA

F.R. Gilmore, R&D Associates
(Latest Revision 28 October 1971)

## 10.1 INTRODUCTION

An important property of any reaction is its reaction energy, i.e., the amount of energy taken up or given off when unit amounts of the reactants are converted to the products. Heats of formation, dissociation energies, ionization energies, etc., represent specific types of reaction energies. When a reaction is exothermic, the reaction energy represents the energy available for excitation or heating of the products of the reaction. When a reaction is endothermic, the reaction energy must be supplied by the thermal or excitational energy of the reactants. Consequently, endothermic reactions will be very slow when the mean thermal energy is much less than the reaction energy, unless the reactants have above-thermal excitational energy. (The converse, however, is not true; reactions are not necessarily fast just because sufficient energy is available.)

An understanding of reactions involving excited states also requires a knowledge of the excited energy levels of the reacting or product species. Moreover, for the case of thermal equilibrium (i.e., for a Boltzmann distribution of excited-state populations), such energy levels can be used to calculate "equilibrium constants" which relate the forward to the backward rates of reactions (see section 10.4 on Equilibrium Constants). Finally, since most reaction energies and energy levels can be determined, by spectroscopic, calorimetric, or other methods, with an accuracy far surpassing that attainable in reaction-rate measurements, such data form a firm though limited foundation on which to build the often crude and speculative edifices of reaction mechanisms and rates. This chapter presents such data for atoms and simple molecules involving hydrogen, carbon, nitrogen, oxygen, and argon.

## 10.2 REACTION ENERGIES

The energy of a reaction may be defined as the net gain or loss of energy accompanying the interaction of reactants, in molecular

or molar quantities (corresponding to a balanced chemical equation), to form products. Unless otherwise stated in the equation of reaction, reactants and products are always assumed to be in their ground rotational, vibrational, and electronic levels, i.e., with no excitation. Such a reaction energy is equivalent to what chemists call "the heat of reaction at 0 K", since at absolute zero (in thermal equilibrium) all species are defined as being in their lowest energy levels. Moreover, for gases at absolute zero no distinction needs to be made between the reaction enthalpy (or heat) and the reaction energy, since $\Delta H_0^o = \Delta E_0^o = \Delta(pV)_0^o = 0$, where by convention the subscript "0" designates 0 K and the superscript "o" the reference or standard state. (A similar relation holds for the free energy: $\Delta F_0^o = \Delta A_0^o = \Delta E_0^o$.)

Chemists usually consider the reaction energy as variable with temperature, because of the varying thermal energy of the reactants and products. However, only the zero-temperature reaction energy is tabulated here, for two reasons: First, the variation with temperature is usually relatively small except at high temperatures, and can be readily estimated if necessary. Second, and more important in the present context, the products of a reaction are highly unlikely to be produced with an initial energy distribution corresponding to the gas temperature. Hence, the temperature-dependent reaction energy is not really pertinent to the reaction-rate problem, but only to the question of the net heating after the products have been thermalized by subsequent collisions.

The algebraic sign of the reaction energy depends upon whether it is defined as the energy absorbed or the energy released on reaction. For the cases considered here (formation, dissociation, and ionization), it is conventional to define a positive reaction energy as the energy absorbed during formation, dissociation, or ionization, or equivalently the excess of the internal energy of the products over that of the reactants. Conversely, a negative reaction energy designates energy emitted during the corresponding reverse processes, i.e., excess of the internal energy of the reactants over that of the products.

Before standard heats of formation can be determined, it is also necessary to establish "reference states" which are the standard descriptions of substances, from which other species are presumed to have been formed. For the species of present interest the conventional reference or standard states are $H_2$, $N_2$, $O_2$, and Ar in the ideal-gas (or isolated-molecule) state, and C in the form of graphite.

Table 10-1 gives the molecular weight, energy of formation, dissociation energy, and ionization energy for each of the (gaseous) atoms and small molecules of present interest, together with relevant references. All energies are given in three different units: physical (electron volts per particle), spectroscopic, i.e., reciprocal of the wavelength of photons having the same energy ($10^3$ $cm^{-1}$, also known as kilokaysers), and thermochemical (kilocalories per mole). Conversion factors are taken from the standard NAS-NRC list (Reference 10-1). The accuracy of each value is indicated approximately by the number of decimal places shown (see notes accompanying Table 10-1). The energy of any reaction involving these species is calculated by adding together the formation energies of the products and subtracting those of the reactants.

## 10.3 ENERGY LEVELS AND POTENTIAL CURVES

The energy levels of atoms and atomic ions depend upon the arrangement of their orbital electrons. The lower energy levels of the atoms and ions of present interest are listed in Tables 10-2 through 10-11, together with their respective electronic-state designations and statistical weights. (For an explanation of the latter terms see References 10-2 and 10-3.) The ions $H^-$, $H^+$, and $C^-$ have only one bound state each, so they are not tabulated here. All of the listed species except $O^-$ actually have an infinite number of highly excited states. However, the present tables list only those states for which all the bound electrons have principal quantum numbers less than five. In most physical situations higher states are not expected to be important, but if needed they can he obtained from the more extensive tabulations of Moore (Reference 10-3), or calculated from the Rydberg formula (Reference 10-2).

Also included in Tables 10-2 through 10-11 are the equilibrium fractional populations of the different electronic states, for various temperatures up to 10,000 K. These results are often useful in problems concerning equilibrium gases. However, in many situations involving low-density gases, or transient processes even at high densities, equilibrium is not attained and these tahulated populations are therefore inapplicable.

For several atoms, some of the electronic states listed in Tables 10-2 through 10-11 are shown graphically in the Grotrian diagrams

in Figures 10-1 through 10-4. These figures show a number of the energy levels of H , N , O , and $O^+$ , and some of the radiative transitions between them as well as the wavelengths of these transitions. Grotrian diagrams of many atoms are available elsewhere (References 10-2, 10-4, 10-5). Partial energy-level diagrams for some other atoms are given in Chapter 20.

Molecules, because of their additional rotational and vibrational degrees of freedom, have so many individual energy levels that it is rather impractical to tabulate them all. Fortunately, however, for each degree of electronic excitation the rotational and vibrational levels are usually quite regular and can be represented by simple formulas, only the coefficients of which therefore need to be tabulated (see Reference 10-6). For present purposes it is probably sufficient to note that the vibrational levels of each electronic state are fairly evenly spaced, only slowly converging near the dissociation limit. The rotational levels are not evenly spaced, but vary approximately quadratically with the rotational quantum number; however, the spacing is generally so close ($10^{-3}$ to $10^{-2}$ eV) that for most reaction-rate purposes the rotational energy levels can be treated as if they formed a continuum.

Tables 10-12 through 10-18 present the electronic energy, lowest vibrational interval, and fractional population for each of the lower electronic states of several diatomic molecules and ions of present interest. Similar values for other diatomic molecules, but without the fractional population numbers, are given in Table 10-19. Again, the reader is cautioned against use of the equilibrium population values in nonequilibrium situations.

For triatomic molecules, existing knowledge of the lower excited electronic states is quite incomplete. Consequently, just the ground state and its lowest vibrational intervals, for the three normal vibrational modes, are listed in Table 10-20.

In vibrating, the atoms in a molecule move within the force field produced by the bound electrons. For each electronic state a potential curve or surface can be drawn, representing the effective potential energy as a function of the internuclear distance(s) and angle(s). Figures 10-5 through 10-7 present such curves for $N_2$ , NO , $O_2$ , and the corresponding molecular ions, including marks indicating the observed vibrational levels available within each electronic state. Such curves are useful not only in depicting molecular-energy levels, but also in understanding electronic transitions, since

the Franck-Condon principle states that energy-level transitions caused by photon absorption or emission, or by collisions with electrons or fast heavy particles, are most likely to take place when accompanied by zero change in the internuclear distance (Reference 10-6).

## 10.4 EQUILIBRIUM CONSTANTS

In any ideal gas mixture in complete thermal and chemical equilibrium, containing three or more interacting species related by a balanced chemical equation, e.g., $XY \rightleftarrows X+Y$ or $W+X \rightleftarrows Y+Z$, the corresponding product:reactant concentration ratio, e.g., $[X][Y]/[XY]$ or $[Y][Z]/[W][X]$, respectively, can be shown to depend only on the temperature (Reference 10-7). Since all such ratios are independent of the individual species concentrations, and are thus characteristic of chemical systems in the equilibrium condition, they are called equilibrium constants.

A reacting gas mixture initially out of chemical equilibrium tends to approach equilibrium, and the corresponding concentration ratio as defined above tends to approach its equilibrium value as well. As equilibrium is approached the various reaction rates do not actually diminish; instead the rate of each forward reaction comes into balance with that of its reverse counterpart. Consequently, it is not difficult to show that in equilibrium the ratio of the forward to the backward rate coefficients for each reversible reaction is equal to the equilibrium constant.

Unfortunately, a rate coefficient is measureable and has practical significance only in nonequilibrium situations. Furthermore, for each species in a reacting mixture there are always individual members whose velocities, i.e., kinetic energies, form some statistical distribution about the value which might be deduced from the kinetic temperature of the mix. Usually a characteristic range of rotational, vibrational, and electronic energy levels of the species exists as well, and generally some of these levels tend to be more reactive than others, especially in endothermic interactions, by virtue of their greater internal energies. In nonequilibrium situations the more reactive levels will thus be removed (by reaction) more rapidly than the others, resulting in an internal distribution of levels in each reacting species such as to make it less reactive than if the distribution were in equilibrium (Reference 10-8).

Molecular dissociation calculations based on a simple model show that when the mean thermal energy is much less than the dissociation energy the dissociation and association coefficients are only slightly smaller than their equilibrium values. Moreover, both coefficients are decreased by the same fraction, so that their ratio still equals the equilibrium constant (Reference 10-9). However, other reactions may not have such a convenient behavior.

In the present work, equilibrium constants have been calculated for several pertinent dissociation and ionization reactions. Results up to 10,000 K are presented graphically in Figures 10-8 through 10-11.

## REFERENCES

10-1. National Academy of Sciences-National Research Council Committee on Fundamental Constants, Physics Today 17, No. 48 (1964).

10-2. Herzberg, G., Atomic Spectra and Atomic Structure, Dover Publications, New York (1944).

10-3. Moore, C. E., Atomic Energy Levels, vol I, National Bureau of Standards, Circular 467 (1949). (See also the additions and corrections in the back of vols II and III.)

10-4. Grotrian, W., Graphische Darstellung der Spektren von Atomen und Ionen mit Ein, Zwei, und Drei Valenzelektronen, Springer-Verlag, Berlin (1928).

10-5. Moore, C. E., and P. W. Merrill, Partial Grotrian Diagrams of Astrophysical Interest, NSRDS-NBS 23, (1968).

10-6. Herzberg, G., Spectra of Diatomic Molecules, 2nd edition, Van Nostrand Company, New York (1950).

10-7. Mayer, J. E., and M. G. Mayer, Statistical Mechanics, John Wiley and Sons. New York (1940).

10-8. Widom, B., Advs. Chem. Phys. 5, 353 (1963).

10-9. Keck, J., and G. Carrier, J. Chem. Phys. 43, 2284 (1965).

10-10. Pekeris, C. L., Phys. Rev. 112, 1649 (1958).

10-11. Lagergren, C. R., Ph. D. Thesis, University of Minnesota (1955).

10-12. Branscomb, L. M., Adv. Electronics Electron Phys. 9, 43 (1957).

10-13. McConkey, J. W., and J. A. Kenahan, Phys. Letts. 27A, 82 (1968).

10-14. Berry, R. S., J. C. Mackie, R. L. Taylor, and R. Lynch, J. Chem. Phys. 43, 3067 (1965).

10-15. Herzberg, G., Phys. Rev. Letts. 23, 1081 (1969).

10-16. Joint Army-Navy-Air Force Thermochemical Panel, JANAF Thermochemical Tables, Dow Chemical Company (1960) (with later revisions).

10-17. Douglas, A. E., and C. K. Moller, Can. J. Phys. 33, 125 (1955).

10-18. Brewer, L., and A. W. Searcy, Ann. Rev. Phys. Chem. 7, 259 (1956).

10-19. Takamine, T., Y. Tanaka, and M. Iwata, Sci. Pap. Inst. Phys. Chem. Res. (Tokyo) 40, 371 (1943).

10-20. Dorman, F. H., and J. D. Morrison, J. Chem. Phys. 35, 575 (1961).

10-21. Tilford, S. G., and P. G. Wilkinson, J. Mol. Spectry. 12, 347 (1964).

10-22. Ogawa, M., and Y. Tanaka, Can. J. Phys. 40, 1593 (1962).

10-23. Dorman, F. H., and J. D. Morrison, J. Chem. Phys. 39, 1906 (1963).

10-24. Seigel, M. W., et al., Phys. Rev. A (to be published).

10-25. Huber, K. P., Helv. Phys. Acta 34, 929 (1961).

10-26. Dressler, K., and E. Miescher, Astrophys. J. 141, 1266 (1965).

10-27. Celotta, R. J., et al., Phys. Rev. A (to be published).

10-28. Brix, P., and G. Herzberg, Can. J. Phys. 32, 110 (1954).

10-29. McNeal, R. J., and G. R. Cook, J. Chem. Phys. 45, 3469 (1966).

10-30. Asundi, R. K., Curr. Sci. 37, 160 (1968).

10-31. Branscomb, L. M., Phys. Rev. 148, 11 (1966).

10-32. Barrow, R. F., Ark. Fys. 11, 281 (1956).

10-33. Dibeler, V. H., J. A. Walker, and H. M. Rosenstock, J. Res. Natl. Bur. Stds. 70A, 459 (1966).

10-34. Herzberg, G., Electronic Spectra and Electronic Structure of Polyatomic Molecules, Van Nostrand Company, Princeton, New Jersey (1966).

10-35. Dibeler, V. H., J. A. Walker, and S. K. Liston, J. Res. Natl. Bur. Stds. 71A, 371 (1967).

10-36. Byerly, R., and E. C. Beaty, J. Geophys. Res. 76, 4596 (1971).

10-37. Herron, J. T., and H. I. Schiff, J. Chem. Phys. 24, 1266 (1956).

10-38. Minnhagen, L., Ark. Fys. 7, 413 (1954); Ibid. 14, 481 (1959).

10-39. Glad, S., Ark. Fys. 7, 7 (1954).

10-40. Eriksson, K. B. S., Ark. Fys. 13, 429 (1958).

10-41. Eriksson, K. B. S., and I. Johansson, Ark. Fys. 19, 235 (1961).

10-42. Eriksson, K. B. S., Ark. Fys. 13, 303 (1958).

10-43. Berry, R. S., J. C. Mackie, R. L. Taylor, and R. Lynch, J. Chem. Phys. 43, 3067 (1965).

10-44. Bowen, I. S., Astrophys. J. 121, 306 (1955).

10-45. Eriksson, K. B. S., Ark. Fys. 19, 229 (1961).

10-46. Burns, K., and K. B. Adams, J. Opt. Soc. Am. 43, 1020 (1953).

10-47. Humphreys, C. J., and E. Paul, Jr., J. Opt. Soc. Am. 49, 1[illegible] (1959).

10-48. Minnhagen, L., Ark. Fys. 14, 123 (1958); Ibid. 18, 97 (1960).

10-49. Krupenie, P. H., National Bureau of Standards, Report NSRDS-NBS 5 (1966).

10-50. Herzberg, G., et al., Can. J. Phys. 44, 3039 (1966).

10-51. Gilmore, F. R., The Rand Corporation, Research Memorandum RM-4034-1-PR (1966); J. Quant. Spectry. Radiative Transfer 5, 369 (1965).

10-52. Benesch, W., and K. A. Saum, J. Phys. B4, 732 (1971).

10-53. Edqvist, O., et al., Ark. Fys. 40, 439 (1970).

10-54. Degen, V., Can. J. Phys. 46, 783 (1968).

10-55. Albritton, D. L., A. L. Schmeltekopf, and R. N. Zare, Diatomic Franck-Condon Factors, Harper and Row, New York (to be published).

10-56. Stoicheff, B. P., Can. J. Phys. 25, 730 (1957).

10-57. Wallace, L., Astrophys. J. Suppl. 7, 165 (1962).

10-58. Spence, D., and G. J. Schulz, Phys. Rev. A3, 1968 (1971).

10-59. Boness, M. J. W., and G. J. Schulz, Phys. Rev. A2, 2182 (1970).

10-60. Narayanamurti, V., D. Seward, and R. D. Pohl, Phys. Rev. 148, 481 (1966).

10-61. Holzer, W., et al., J. Mol. Spectry. 26, 543 (1968).

10-62. Nobgen, J. W., A. D. McElroy, and H. F. Klodowski, Inorg. Chem. 4, 1796 (1965).

10-63. Herman, K., and P. A. Giguère, Can. J. Chem. 43, 1746 (1965).

Table 10-1. Molecular weights and energies of formotian, dissociation, and ianization for selected atoms and molecules.

| Species | Molec. Weight* | Ener·gy (or Heat) of Formation** | Dissaciation Energy | Ianizatian Energy** | References*** |
|---|---|---|---|---|---|
| $H^-$ | 1.00852 | 1.485 eV<br>$11.974 \times 10^3\ cm^{-1}$<br>34.235 kcol/mole | — | 0.754<br>6.083<br>17.392 | 10-10 |
| H | 1.00797 | 2.239<br>18.057<br>51.627 | — | 13.598<br>109.679<br>313.585 | 10-3 |
| $H^+$ | 1.00742 | 15.837<br>127.736<br>365.213 | — | — | — |
| $C^-$ | 12.01170 | 6.24<br>50.4<br>144.0 | — | 1.13<br>9.1<br>26.0 | 10-11, 10-12 |
| C | 12.01115 | 7.371<br>59.452<br>169.979 | — | 11.259<br>90.814<br>259.648 | 10-3 |
| $C^+$ | 12.001060 | 18.630<br>150.265<br>429.627 | — | 24.382<br>196.659<br>562.272 | 10-3 |

Table 10-1. (Cont'd.)

| Species | Molec. Weight* | Energy (or Heat) of Formation** | Dissociation Energy | Ionization Energy** | References*** |
|---|---|---|---|---|---|
| N | 14.0067 | 4.880 eV<br>$39.359 \times 10^3$ cm$^{-1}$<br>112.532 kcal/mole | — | 14.534<br>117.225<br>335.160 | 10-13 |
| $N^+$ | 14.0062 | 19.414<br>156.584<br>447.692 | — | 29.601<br>238.751<br>682.618 | 10-3 |
| $O^-$ | 15.9999 | 1.079<br>8.705<br>24.89 | — | 1.478<br>11.925<br>34.10 | 10-14 |
| O | 15.9994 | 2.558<br>20.630<br>58.984 | -- | 13.618<br>109.837<br>314.037 | 10-3 |
| $O^+$ | 15.9989 | 16.175<br>130.467<br>373.021 | — | 35.117<br>283.244<br>809.829 | 10-3 |
| Ar | 39.948 | 0<br>0<br>0 | — | 15.759<br>127.110<br>363.423 | 10-3 |

Table 10-1. (Cont'd.)

| Species | Molec. Weight* | Energy (or Heat) of Formation** | Dissociation Energy | Ionization Energy** | References*** |
|---|---|---|---|---|---|
| $Ar^+$ | 39.947 | 15.759 eV<br>$127.110 \times 10^3$ cm$^{-1}$<br>363.423 kcal/mole | — | 27.629<br>222.848<br>637.149 | 10-3 |
| $H_2$ | 2.01594 | 0<br>0<br>0 | 4.478<br>36.118<br>103.266 | 15.426<br>124.418<br>355.727 | 10-15 |
| $H_2^+$ | 2.01539 | 15.426<br>124.418<br>355.727 | 2.651<br>21.379<br>61.125 | — | 10-15 |
| CO | 28.0106 | -1.179<br>-9.513<br>-27.200 | 11.108<br>89.595<br>256.163 | 14.013<br>113.029<br>323.163 | 10-16 through 10-19 |
| $CO^+$ | 28.0100 | 12.834<br>103.516<br>295.963 | 8.354($C^+$–O)<br>67.380<br>192.648 | 27.8<br>224<br>640 | 10-20<br><br>10-18, 10-21 |
| $N_2$ | 28.0134 | 0<br>0<br>0 | 9.759<br>78.717<br>225.061 | 15.580<br>125.667<br>359.297 | 10-22 |

Table 10-1. (Cont'd.)

| Species | Molec. Weight* | Energy (or Heat) of Formation** | Dissociation Energy | Ionization Energy** | References*** |
|---|---|---|---|---|---|
| $N_2^+$ | 28.0129 | 15.580 eV<br>$125.667 \times 10^3$ cm$^{-1}$<br>359.297 kcal/mole | 8.711<br>70.264<br>200.893 | 27.1<br>219<br>626 | 10-23 |
| $NO^-$ | 30.0066 | 0.911<br>7.35<br>21.00 | 5.049($N-O^-$)<br>40.72<br>116.42 | 0.020<br>0.16<br>0.46 | 10-24 |
| NO | 30.0061 | 0.931<br>7.506<br>21.46 | 6.507<br>52.483<br>150.055 | 9.267<br>74.747<br>213.711 | 10-16, 10-25, 10-26 |
| $NO^+$ | 30.0056 | 10.198<br>82.253<br>235.17 | 10.857($N-O^+$)<br>87.573<br>250.382 | 30.5<br>246<br>703 | 10-20 |
| $O_2^-$ | 31.9993 | -0.429<br>-3.46<br>-9.89 | 4.066<br>32.80<br>93.76 | 0.429<br>3.46<br>9.89 | 10-27 |
| $O_2$ | 31.9988 | 0<br>0<br>0 | 5.115<br>41.260<br>117.967 | 12.063<br>97.295<br>278.178 | 10-28 through 10-30 |

Table 10-1. (Cont'd.)

| Species | Molec. Weight* | Energy (or Heat) of Formation** | Dissociation Energy | Ionization Energy** | References*** |
|---|---|---|---|---|---|
| $O_2^+$ | 31.9983 | 12.063 eV<br>$97.295 \times 10^3$ cm$^{-1}$<br>278.78 kcal/mole | 6.670<br>53.802<br>153.826 | 24.2<br>195<br>558 | 10-23 |
| $OH^-$ | 17.0079 | -1.43<br>-11.51<br>-32.9 | 4.75 ($O^-$ - H)<br>38.27<br>109.4 | 1.83<br>14.75<br>42.2 | 10-31 |
| OH | 17.0074 | 0.401<br>3.24<br>9.26 | 4.395 (O - H)<br>35.45<br>101.33 | 12.94<br>104.4<br>298.4 | 10-32, 10-33 |
| $OH^+$ | 17.0068 | 13.34<br>107.6<br>307.7 | 5.05 (O - $H^+$)<br>40.7<br>116.5 | — | — |
| $H_2O$ | 18.0153 | -2.476<br>-19.972<br>-57.103 | 5.116 (H - OH)<br>41.27<br>117.98 | 12.619<br>101.78<br>291.0 | 10-16, 10-34 |
| $H_2O^+$ | 18.0148 | 10.143<br>81.81<br>233.9 | 5.84 (H - $OH^+$)<br>47.1<br>134.7 | — | — |

Table 10-1. (Cont'd.)

| Species | Molec. Weight* | Energy (or Heat) of Formation ** | Dissociation Energy | Ionization Energy** | References*** |
|---|---|---|---|---|---|
| $CO_2$ | 44.0100 | -4.075 eV<br>$-32.865 \times 10^3$ cm$^{-1}$<br>-93.965 kcal/mole | 5.453 (CO - O)<br>43.982<br>125.750 | 13.769<br>111.06<br>317.5 | 10-16, 10-34 |
| $CO_2^+$ | 44.0094 | 9.694<br>78.19<br>223.5 | 5.179 ($CO - O^+$)<br>41.77<br>119.4 | 22.6<br>182<br>521 | 10-20 |
| $NO_2^-$ | 46.0060 | -2.1<br>-17<br>-49 | 4.1 ($NO - O^-$)<br>33<br>94 | 2.5<br>20<br>58 | Chap. 17 |
| $NO_2$ | 46.0055 | 0.372<br>3.00<br>8.59 | 3.116 (NO - O)<br>25.13<br>71.86 | 9.78<br>78.9<br>225.6 | 10-16, 10-35 |
| $NO_2^+$ | 46.0050 | 10.15<br>81.9<br>234.2 | 2.60 ($NO^+ - O$)<br>21.0<br>60.0 | — | — |
| $N_2O$ | 44.0128 | 0.881<br>7.107<br>20.32 | 1.677 ($N_2 - O$)<br>13.523<br>38.66 | 12.894<br>104.00<br>297.35 | 10-16, 10-34 |

Table 10-1. (Cont'd.)

| Species | Malec. Weight* | Energy (ar Heat) af Farmatian** | Dissaciutian Energy | Ianizatian Energy** | References*** |
|---|---|---|---|---|---|
| $N_2O^+$ | 44.0123 | 13.775 eV<br>111.11 x $10^3$ $cm^{-1}$<br>317.67 kcal/male | 1.302 (N - $NO^+$)<br>10.50<br>30.02 | — | — |
| $O_3^-$ | 47.9987 | -0.6<br>-5<br>-13 | 1.7 ($O_2$ - $O^-$)<br>14<br>38 | 2.1<br>17<br>48 | 10-36 |
| $O_3$ | 47.9982 | 1.506<br>12.15<br>34.74 | 1.051 ($O_2$ - O)<br>8.48<br>24.25 | 12.80<br>103.2<br>295.2 | 10-16, 10-37 |
| $O_3^+$ | 47.9977 | 14.31<br>115.4<br>329.9 | 0.32 ($O_2^+$ - O)<br>2.5<br>7.3 | — | — |

* Molecular weights are far the normal isatopic mixture, based an $C^{12}$ = 12.00000.

** All reactian energies are far isolated particles in their lawest ratatianal, vibratianal, and electranic state (microscopic descriptian), ar far ideal gases at 0K (equivalent macrascopic descriptian). All energies are given in three units: physical (electran valts), spectrascopic ($10^3$ $cm^{-1}$ ar kilakaysers), and thermachemical (kilacalaries per male).

*** Ta avaid unnecessary duplicatian, references are indicated anly where they give directly a farmatian, dissociatian, ar ianization energy. Where a dissaciatian energy is calculated fram the farmatian energies af the malecule and its dissaciatian products, references ta the latter are given anly oppasite the praducts. Similarly, na direct references are given far farmatian energies calculated fram measured dissaciatian ar ionizatian energies.

Table 10-2. Energy levels and equilibrium fractional electronic populations of H .

| State | Level (CM-1) | Level (EV) | Stat. Wt. | Temperature (K) 200 | 250 | 300 | 400 | 500 | 600 | 800 | 1000 | 1500 |
|---|---|---|---|---|---|---|---|---|---|---|---|---|
| 1s | 0 | 0.0000 | 2 | 1.00E 00 | 1.00E 00 | 1.00E 00 | 1.00E 00 | 1.00E 00 | 1.00E 00 | 1.00E 00 | 1.00E 00 | 1.00E 00 |
| 2s | 82259 | 10.1986 | 2 | 0. | 0. | 0. | 0. | 0. | 0. | 0. | 0. | 5.41E-35 |
| 2p | 82259 | 10.1986 | 6 | 0. | 0. | 0. | 0. | 0. | 0. | 0. | 0. | 1.62E-34 |
| 3s | 97492 | 12.0872 | 2 | 0. | 0. | 0. | 0. | 0. | 0. | 0. | 0. | 0. |
| 3p | 97492 | 12.0872 | 6 | 0. | 0. | 0. | 0. | 0. | 0. | 0. | 0. | 0. |
| 3d | 97492 | 12.0872 | 10 | 0. | 0. | 0. | 0. | 0. | 0. | 0. | 0. | 0. |
| 4s | 102824 | 12.7482 | 2 | 0. | 0. | 0. | 0. | 0. | 0. | 0. | 0. | 0. |
| 4p | 102824 | 12.7482 | 6 | 0. | 0. | 0. | 0. | 0. | 0. | 0. | 0. | 0. |
| 4d | 102824 | 12.7482 | 10 | 0. | 0. | 0. | 0. | 0. | 0. | 0. | 0. | 0. |
| 4f | 102824 | 12.7482 | 14 | 0. | 0. | 0. | 0. | 0. | 0. | 0. | 0. | 0. |

Energy levels from reference 10-3.

| Level | Temperature (K) 2000 | 2500 | 3000 | 3500 | 4000 | 4500 | 5000 | 6000 | 7000 | 8000 | 9000 | 10000 |
|---|---|---|---|---|---|---|---|---|---|---|---|---|
| (CM-1) | | | | | | | | | | | | |
| 0 | 1.00E 00 | 1.00E 00 | 1.00E 00 | 1.00E 00 | 1.00E 00 | 1.00E 00 | 1.00E 00 | 1.00E 00 | 1.00E 00 | 1.00E 00 | 1.00E 00 | 1.00E 00 |
| 82259 | 1.99E-26 | 2.75E-21 | 7.36E-18 | 2.06E-15 | 1.41E-13 | 3.78E-12 | 5.25E-11 | 2.71E-09 | 4.54E-08 | 3.76E-07 | 1.94E-06 | 7.24E-06 |
| 82259 | 5.98E-26 | 8.26E-21 | 2.21E-17 | 6.18E-15 | 4.24E-13 | 1.13E-11 | 1.57E-10 | 8.14E-09 | 1.36E-07 | 1.13E-06 | 5.83E-06 | 2.17E-05 |
| 97492 | 3.47E-31 | 4.29E-25 | 4.94E-21 | 3.93E-18 | 5.89E-16 | 2.90E-14 | 6.55E-13 | 7.03E-11 | 1.98E-09 | 2.43E-08 | 1.70E-07 | 8.09E-07 |
| 97492 | 1.04E-30 | 1.29E-24 | 1.48E-20 | 1.18E-17 | 1.77E-15 | 8.70E-14 | 1.97E-12 | 2.11E-10 | 5.95E-09 | 7.28E-08 | 5.11E-07 | 2.43E-06 |
| 97492 | 1.74E-30 | 2.15E-24 | 2.47E-20 | 1.97E-17 | 2.95E-15 | 1.45E-13 | 3.28E-12 | 3.51E-10 | 9.92E-09 | 1.21E-07 | 8.52E-07 | 4.05E-06 |
| 102824 | 7.40E-33 | 1.99E-26 | 3.83E-22 | 4.39E-19 | 8.66E-17 | 5.27E-15 | 1.41E-13 | 1.96E-11 | 6.63E-10 | 9.30E-09 | 7.26E-08 | 3.76E-07 |
| 102824 | 2.25E-32 | 5.98E-26 | 1.15E-21 | 1.32E-18 | 2.60E-16 | 1.58E-14 | 4.24E-13 | 5.87E-11 | 1.99E-09 | 2.79E-08 | 2.18E-07 | 1.13E-06 |
| 102824 | 3.75E-32 | 9.97E-26 | 1.91E-21 | 2.20E-18 | 4.33E-16 | 2.64E-14 | 7.06E-13 | 9.78E-11 | 3.31E-09 | 4.65E-08 | 3.63E-07 | 1.88E-06 |
| 102824 | 5.25E-32 | 1.40E-25 | 2.68E-21 | 3.07E-18 | 6.06E-16 | 3.69E-14 | 9.89E-13 | 1.37E-10 | 4.64E-09 | 6.51E-08 | 5.08E-07 | 2.63E-06 |

Table 10-3. Energy levels and equilibrium fractional electron population of C .

| State | Level (CM-1) | Level (EV) | Stat. Wt. | Temperature (K) 200 | 250 | 300 | 400 | 500 | 600 | 800 | 1000 | 1500 |
|---|---|---|---|---|---|---|---|---|---|---|---|---|
| $2s^1\,2p^3\ {}^5P_e$ | 0 | 0.0000 | 1 | 1.57E-01 | 1.31E-01 | 1.28E-01 | 1.23E-01 | 1.21E-01 | 1.19E-01 | 1.17E-01 | 1.16E-01 | 1.14E-01 |
| ${}^5P_o$ | 16.4 | 0.0020 | 3 | 3.64E-01 | 3.58E-01 | 3.54E-01 | 3.49E-01 | 3.46E-01 | 3.44E-01 | 3.41E-01 | 3.40E-01 | 3.38E-01 |
| ${}^5P_e$ | ~43.5 | 0.0054 | 5 | 4.99E-01 | 5.11E-01 | 5.18E-01 | 5.28E-01 | 5.33E-01 | 5.37E-01 | 5.42E-01 | 5.44E-01 | 5.48E-01 |
| ${}^3D$ | 10194 | 1.2639 | 5 | 9.67E-33 | 2.18E-26 | 3.74E-22 | 7.34E-17 | 1.10E-13 | 1.44E-11 | 6.39E-09 | 2.47E-07 | 9.24E-05 |
| ${}^1S$ | 21648 | 2.6839 | 1 | 0. | 0. | 0. | 1.88E-35 | 1.07E-28 | 3.40E-24 | 1.45E-18 | 3.45E-15 | 1.10E-10 |
| $2s\ 2p^3\ {}^5S^o$ | 33735 | 4.1825 | 5 | 0. | 0. | 0. | 0. | 0. | 4.39E-36 | 2.62E-27 | 4.83E-22 | 5.06E-15 |
| ${}^3D^o$ | 64491 | 7.9461 | 15 | 0. | 0. | 0. | 0. | 0. | 0. | 0. | 0. | 3.43E-21 |
| ${}^3P^o$ | 75256 | 9.3303 | 9 | 0. | 0. | 0. | 0. | 0. | 0. | 0. | 0. | 4.60E-32 |
| ${}^1S^o$ | 105801 | 13.1173 | 3 | 0. | 0. | 0. | 0. | 0. | 0. | 0. | 0. | 0. |
| ${}^1D^o$ | 97878* | 12.1350 | 5 | 0. | 0. | 0. | 0. | 0. | 0. | 0. | 0. | 0. |
| ${}^1P^o$ | 1196784 | 14.8626 | 3 | 0. | 0. | 0. | 0. | 0. | 0. | 0. | 0. | 0. |
| $2s^2$ ${}^3P$ | 150000* | 18.5972 | 9 | 0. | 0. | 0. | 0. | 0. | 0. | 0. | 0. | 0. |
| ${}^1D$ | 148000* | 19.5890 | 5 | 0. | 0. | 0. | 0. | 0. | 0. | 0. | 0. | 0. |
| ${}^1S$ | 181000* | 22.4406 | 1 | 0. | 0. | 0. | 0. | 0. | 0. | 0. | 0. | 0. |
| $2s^2\,2p\ ({}^2P^o)\ 3s$ | 60776 | 7.5351 | 3 | 0. | 0. | 0. | 0. | 0. | 0. | 0. | 1.47E-38 | 6.60E-26 |
| 3p | 66722 | 8.6442 | 36 | 0. | 0. | 0. | 0. | 0. | 0. | 0. | 0. | 3.70E-29 |
| 3d | 78426 | 9.7233 | 40 | 0. | 0. | 0. | 0. | 0. | 0. | 0. | 0. | 1.47E-32 |
| 4s | 78184 | 9.6933 | 12 | 0. | 0. | 0. | 0. | 0. | 0. | 0. | 0. | 3.70E-33 |
| 4p | 80865 | 10.0258 | 36 | 0. | 0. | 0. | 0. | 0. | 0. | 0. | 0. | 8.47E-34 |
| 4d | 83853** | 10.3958 | 60 | 0. | 0. | 0. | 0. | 0. | 0. | 0. | 0. | 8.06E-35 |
| 4f | 84000* | 10.4144 | 84 | 0. | 0. | 0. | 0. | 0. | 0. | 0. | 0. | 9.78E-35 |
| $2s\ 2p^2\ ({}^4P)\ 3s$ | 116000** | 14.3818 | 24 | 0. | 0. | 0. | 0. | 0. | 0. | 0. | 0. | 0. |
| 3p | 125000* | 15.4978 | 72 | 0. | 0. | 0. | 0. | 0. | 0. | 0. | 0. | 0. |
| 3d | 132000* | 16.3655 | 120 | 0. | 0. | 0. | 0. | 0. | 0. | 0. | 0. | 0. |
| 4 | 136169* | 16.8824 | 24 | 0. | 0. | 0. | 0. | 0. | 0. | 0. | 0. | 0. |
| $2s\ 2p^2\ ({}^2D)\ 3s$ | 138000* | 17.1094 | 20 | 0. | 0. | 0. | 0. | 0. | 0. | 0. | 0. | 0. |
| 3p | 145000* | 17.9772 | 60 | 0. | 0. | 0. | 0. | 0. | 0. | 0. | 0. | 0. |
| 3d | 154000* | 19.0952 | 100 | 0. | 0. | 0. | 0. | 0. | 0. | 0. | 0. | 0. |
| 4 | 158000* | 19.5890 | 320 | 0. | 0. | 0. | 0. | 0. | 0. | 0. | 0. | 0. |
| $({}^2P)\ 3$ | 184000* | 22.8125 | 108 | 0. | 0. | 0. | 0. | 0. | 0. | 0. | 0. | 0. |
| 4 | 194000* | 24.0523 | 192 | 0. | 0. | 0. | 0. | 0. | 0. | 0. | 0. | 0. |
| $({}^2S)\ 3$ | 170000* | 21.0748 | 36 | 0. | 0. | 0. | 0. | 0. | 0. | 0. | 0. | 0. |
| 4 | 179000* | 22.1928 | 96 | 0. | 0. | 0. | 0. | 0. | 0. | 0. | 0. | 0. |
| $2p^3\ ({}^4S^o)\ 3$ | 216000* | 26.7779 | 72 | 0. | 0. | 0. | 0. | 0. | 0. | 0. | 0. | 0. |
| 4 | 225000* | 27.8957 | 128 | 0. | 0. | 0. | 0. | 0. | 0. | 0. | 0. | 0. |
| $({}^2D^o)\ 3$ | 224000* | 27.7717 | 150 | 0. | 0. | 0. | 0. | 0. | 0. | 0. | 0. | 0. |
| 4 | 233000* | 28.8876 | 320 | 0. | 0. | 0. | 0. | 0. | 0. | 0. | 0. | 0. |
| $({}^2P)\ 3$ | 243000* | 30.1274 | 108 | 0. | 0. | 0. | 0. | 0. | 0. | 0. | 0. | 0. |
| 4 | 252000* | 31.2432 | 192 | 0. | 0. | 0. | 0. | 0. | 0. | 0. | 0. | 0. |

*Estimated. **Includes estimated sublevels.

Nonstarred energy levels from References 10-3, 10-38.

Table 10-3. (Cont'd.)

| State | | Level (CM-1) | Temperature (K) 2000 | 2500 | 3000 | 3500 | 4000 | 4500 | 5000 | 6000 | 7000 | 8000 | 9000 | 10000 |
|---|---|---|---|---|---|---|---|---|---|---|---|---|---|---|
| $2s^2\,2p^4$ | $^3P_2$ | 0 | 1.13E-01 | 1.13E-01 | 1.12E-01 | 1.12E-01 | 1.11E-01 | 1.10E-01 | 1.09E-01 | 1.07E-01 | 1.04E-01 | 1.02E-01 | 1.00E-01 | 9.80E-02 |
| | $^3P_1$ | 16 | 3.36E-01 | 3.35E-01 | 3.34E-01 | 3.32E-01 | 3.30E-01 | 3.28E-01 | 3.25E-01 | 3.19E-01 | 3.12E-01 | 3.06E-01 | 2.99E-01 | 2.93E-01 |
| | $^3P_0$ | 43 | 5.50E-01 | 5.50E-01 | 5.50E-01 | 5.49E-01 | 5.45E-01 | 5.41E-01 | 5.37E-01 | 5.28E-01 | 5.17E-01 | 5.07E-01 | 4.97E-01 | 4.87E-01 |
| | $^1D$ | 10194 | 3.71E-04 | 1.60E-03 | 4.22E-03 | 8.44E-03 | 1.41E-02 | 2.11E-02 | 2.89E-02 | 4.63E-02 | 6.42E-02 | 8.17E-02 | 9.81E-02 | 1.13E-01 |
| | $^1S$ | 21648 | 1.96E-08 | 4.38E-07 | 3.48E-06 | 1.52E-05 | 4.60E-05 | 1.08E-04 | 2.14E-04 | 5.94E-04 | 1.22E-03 | 2.08E-03 | 3.14E-03 | 4.35E-03 |
| $2s\ 2p^3$ | $^5S^o$ | 33735 | 1.64E-11 | 2.09E-09 | 5.28E-08 | 5.29E-07 | 2.97E-06 | 1.14E-05 | 3.31E-05 | 1.64E-04 | 5.09E-04 | 1.18E-03 | 2.28E-03 | 3.82E-03 |
| | $^3D^o$ | 64091 | 1.61E-20 | 1.62E-16 | 7.53E-14 | 6.04E-12 | 1.62E-10 | 2.08E-09 | 1.60E-08 | 3.38E-07 | 2.98E-06 | 1.51E-05 | 5.33E-05 | 1.45E-04 |
| | $^3P^o$ | 75256 | 3.14E-24 | 1.57E-19 | 2.14E-16 | 3.66E-14 | 1.75E-12 | 3.51E-11 | 3.85E-10 | 1.40E-08 | 1.80E-07 | 1.22E-06 | 5.37E-06 | 1.75E-05 |
| | $^1S^o$ | 105801 | 3.00E-34 | 1.22E-27 | 3.09E-21 | 4.32E-20 | 9.85E-18 | 6.71E-16 | 1.96E-14 | 3.07E-12 | 1.13E-10 | 1.67E-09 | 1.35E-08 | 7.20E-08 |
| | $^1D^o$ | 97878 | 1.49E-31 | 1.94E-25 | 2.30E-21 | 1.87E-18 | 2.64E-16 | 1.41E-14 | 3.19E-13 | 3.42E-11 | 9.56E-10 | 1.16E-08 | 8.01E-08 | 3.75E-07 |
| | $^1P^o$ | 119876 | 1.20E-38 | 3.69E-31 | 3.62E-26 | 1.33E-22 | 6.23E-20 | 7.44E-18 | 3.41E-16 | 1.05E-13 | 6.24E-12 | 1.33E-10 | 1.43E-09 | 9.50E-09 |
| $2p^4$ | $^3P$ | 150000 | 0. | 3.27E-38 | 9.77E-32 | 1.67E-27 | 3.68E-24 | 1.47E-21 | 1.76E-19 | 2.29E-16 | 3.83E-14 | 1.77E-12 | 3.47E-11 | 3.74E-10 |
| | $^1D$ | 158000 | 0. | 0. | 6.92E-34 | 3.45E-29 | 1.15E-25 | 6.31E-23 | 7.77E-21 | 1.87E-17 | 4.11E-15 | 2.33E-13 | 5.36E-12 | 6.57E-11 |
| | $^1S$ | 181000 | 0. | 0. | 2.24E-39 | 5.41E-34 | 5.88E-30 | 8.08E-27 | 2.61E-24 | 1.51E-20 | 7.27E-18 | 7.45E-16 | 2.71E-14 | 4.80E-13 |
| $2s^2\,2p\ (^2P^o)$ | 3s | 80774 | 1.40E-19 | 8.73E-16 | 2.93E-13 | 1.89E-11 | 4.26E-10 | 4.79E-09 | 3.32E-08 | 5.99E-07 | 4.72E-06 | 2.20E-05 | 7.24E-05 | 1.87E-04 |
| | 3p | 69722 | 6.73E-22 | 1.52E-17 | 1.21E-14 | 1.43E-12 | 5.12E-11 | 8.23E-10 | 7.58E-09 | 2.10E-07 | 2.25E-06 | 1.32E-05 | 5.20E-05 | 1.55E-04 |
| | 3d | 78426 | 2.14E-24 | 1.69E-19 | 2.11E-16 | 6.67E-14 | 3.72E-12 | 8.49E-11 | 1.03E-09 | 4.35E-08 | 6.25E-07 | 4.59E-06 | 2.15E-05 | 7.39E-05 |
| | 4s | 78184 | 5.09E-25 | 3.89E-20 | 6.99E-17 | 1.47E-14 | 8.13E-13 | 1.83E-11 | 2.21E-10 | 9.22E-09 | 1.31E-07 | 9.59E-07 | 4.48E-06 | 1.53E-05 |
| | 4p | 80866 | 2.22E-25 | 2.49E-20 | 5.80E-17 | 1.47E-14 | 9.29E-13 | 2.33E-11 | 3.07E-10 | 1.45E-08 | 2.27E-07 | 1.78E-06 | 8.75E-06 | 3.12E-05 |
| | 4d | 83850 | 4.32E-26 | 7.46E-21 | 2.31E-17 | 7.17E-15 | 5.29E-13 | 1.50E-11 | 2.17E-10 | 1.18E-08 | 2.05E-07 | 1.73E-06 | 9.05E-06 | 3.30E-05 |
| | 4f | 84000 | 5.43E-26 | 9.58E-21 | 3.01E-17 | 9.44E-15 | 7.02E-13 | 2.00E-11 | 2.91E-10 | 1.60E-08 | 2.78E-07 | 2.36E-06 | 1.24E-05 | 4.64E-05 |
| $2s\ 2p^4\ (^4P)$ | 3s | 116000 | 1.56E-36 | 2.75E-29 | 1.86E-24 | 9.22E-21 | 2.01E-18 | 2.06E-16 | 8.32E-15 | 2.13E-12 | 1.11E-10 | 2.13E-09 | 2.12E-08 | 1.33E-07 |
| | 3p | 121000 | 0. | 4.64E-31 | 3.44E-26 | 3.88E-22 | 2.37E-19 | 3.47E-17 | 1.87E-15 | 7.37E-13 | 5.22E-11 | 1.27E-09 | 1.51E-08 | 1.09E-07 |
| | 3d | 132000 | 0. | 1.38E-32 | 4.32E-27 | 3.63E-23 | 3.18E-20 | 6.17E-18 | 4.16E-16 | 2.29E-13 | 2.06E-11 | 6.00E-10 | 8.22E-09 | 6.64E-08 |
| | 4 | 136169 | 0. | 2.50E-34 | 1.17E-28 | 1.31E-24 | 1.42E-21 | 3.26E-19 | 2.51E-17 | 1.69E-14 | 1.75E-12 | 5.67E-11 | 8.44E-10 | 7.29E-09 |
| $2s\ 2p^4\ (^2D)$ | 3s | 138000 | 0. | 7.27E-35 | 4.05E-29 | 5.14E-25 | 6.13E-22 | 1.51E-19 | 1.23E-17 | 9.06E-15 | 1.00E-12 | 3.40E-11 | 5.25E-10 | 4.67E-09 |
| | 3p | 145000 | 0. | 3.89E-36 | 4.23E-30 | 8.68E-26 | 1.48E-22 | 4.83E-20 | 4.94E-18 | 5.07E-15 | 7.14E-13 | 2.90E-11 | 5.14E-10 | 5.12E-09 |
| | 3d | 154000 | 0. | 3.64E-38 | 9.42E-32 | 3.58E-27 | 9.71E-24 | 4.53E-21 | 6.18E-19 | 9.77E-16 | 1.87E-13 | 9.57E-12 | 2.03E-10 | 2.34E-09 |
| | 4 | 158000 | 0. | 0. | 4.43E-32 | 2.21E-27 | 7.37E-24 | 4.04E-21 | 6.25E-19 | 1.20E-15 | 2.63E-13 | 1.49E-11 | 3.43E-10 | 4.20E-09 |
| | $(^2P)$ 3 | 184000 | 0. | 0. | 5.74E-38 | 1.70E-32 | 2.16E-28 | 3.34E-25 | 1.19E-22 | 7.93E-19 | 4.24E-16 | 4.69E-14 | 1.81E-12 | 3.37E-11 |
| | 4 | 194000 | 0. | 0. | 0. | 4.96E-34 | 1.05E-29 | 2.43E-26 | 1.19E-23 | 1.28E-19 | 9.65E-17 | 1.38E-14 | 6.52E-13 | 1.42E-11 |
| | $(^2S)$ 3 | 170000 | 0. | 0. | 1.58E-35 | 1.79E-30 | 1.11E-26 | 9.80E-24 | 2.23E-21 | 7.58E-18 | 2.51E-15 | 1.94E-13 | 5.67E-12 | 8.41E-11 |
| | 4 | 179000 | 0. | 0. | 3.74E-37 | 7.88E-32 | 7.73E-28 | 9.80E-25 | 2.97E-22 | 1.56E-18 | 7.02E-16 | 6.83E-14 | 2.39E-12 | 4.10E-11 |
| $2p^3\ (^4S^o)$ | 3 | 216000 | 0. | 0. | 0. | 2.20E-38 | 1.44E-33 | 8.03E-30 | 7.94E-27 | 2.46E-22 | 3.93E-19 | 9.90E-17 | 7.26E-15 | 2.25E-13 |
| | 4 | 225000 | 0. | 0. | 0. | 0. | 1.01E-34 | 8.03E-31 | 1.06E-27 | 5.05E-23 | 1.10E-19 | 3.49E-17 | 3.06E-15 | 1.09E-13 |
| | $(^2D^o)$ 3 | 224000 | 0. | 0. | 0. | 0. | 2.03E-34 | 1.56E-30 | 1.99E-27 | 9.02E-23 | 1.90E-19 | 5.87E-17 | 5.05E-15 | 1.78E-13 |
| | 4 | 233000 | 0. | 0. | 0. | 0. | 1.42E-35 | 1.56E-31 | 2.65E-28 | 1.80E-23 | 5.31E-20 | 2.07E-17 | 2.13E-15 | 8.65E-14 |
| | $(^2P^o)$ 3 | 243000 | 0. | 0. | 0. | 0. | 1.31E-37 | 2.15E-33 | 5.03E-30 | 5.68E-25 | 2.29E-21 | 1.16E-18 | 1.45E-16 | 6.93E-15 |
| | 4 | 257000 | 0. | 0. | 0. | 0. | 0. | 2.15E-34 | 6.71E-31 | 1.17E-25 | 6.41E-22 | 4.07E-19 | 6.13E-17 | 3.37E-15 |

Table 10-4. Energy levels and equilibrium fractional electronic populations of $C^+$.

| State | Level (CM-1) | Level (EV) | Stat. Wt. | Temperature (K) 200 | 250 | 300 | 400 | 500 | 600 | 800 | 1000 | 1500 |
|---|---|---|---|---|---|---|---|---|---|---|---|---|
| $2s^2\ 2p\ ^2P^o_{1/2}$ | 0 | 0.0000 | 2 | 4.42E-01 | 4.20E-01 | 4.05E-01 | 3.86E-01 | 3.75E-01 | 3.68E-01 | 3.59E-01 | 3.54E-01 | 3.47E-01 |
| $^2P^o_{3/2}$ | 64.0 | 0.0079 | 4 | 5.58E-01 | 5.80E-01 | 5.95E-01 | 6.14E-01 | 6.25E-01 | 6.32E-01 | 6.41E-01 | 6.46E-01 | 6.53E-01 |
| $2s\ 2p^3\ ^4P$ | 43033 | 5.3353 | 12 | 0. | 0. | 0. | 0. | 0. | 0. | 5.27E-34 | 2.74E-27 | 2.47E-18 |
| $^2D$ | 74932 | 9.2901 | 10 | 0. | 0. | 0. | 0. | 0. | 0. | 0. | 0. | 1.06E-31 |
| $^2S$ | 96494 | 11.9634 | 2 | 0. | 0. | 0. | 0. | 0. | 0. | 0. | 0. | 0. |
| $^2P$ | 110653 | 13.7189 | 6 | 0. | 0. | 0. | 0. | 0. | 0. | 0. | 0. | 0. |
| $2p^3\ ^4S^o$ | 142024 | 17.6083 | 4 | 0. | 0. | 0. | 0. | 0. | 0. | 0. | 0. | 0. |
| $^2D^o$ | 150465 | 18.6548 | 10 | 0. | 0. | 0. | 0. | 0. | 0. | 0. | 0. | 0. |
| $^2P^o$ | 168744 | 20.9210 | 6 | 0. | 0. | 0. | 0. | 0. | 0. | 0. | 0. | 0. |
| $2s^2(^1S)\ 3s$ | 116538 | 14.4485 | 2 | 0. | 0. | 0. | 0. | 0. | 0. | 0. | 0. | 0. |
| 3p | 131725 | 16.3314 | 6 | 0. | 0. | 0. | 0. | 0. | 0. | 0. | 0. | 0. |
| 3d | 145550 | 18.0454 | 10 | 0. | 0. | 0. | 0. | 0. | 0. | 0. | 0. | 0. |
| 4s | 157235 | 19.4942 | 2 | 0. | 0. | 0. | 0. | 0. | 0. | 0. | 0. | 0. |
| 4p | 162523 | 20.1498 | 6 | 0. | 0. | 0. | 0. | 0. | 0. | 0. | 0. | 0. |
| 4d | 168125 | 20.8443 | 10 | 0. | 0. | 0. | 0. | 0. | 0. | 0. | 0. | 0. |
| 4f | 168979 | 20.9502 | 14 | 0. | 0. | 0. | 0. | 0. | 0. | 0. | 0. | 0. |
| $2s\ 2p\ (^3P^o)\ 3s$ | 170643 | 21.1565 | 18 | 0. | 0. | 0. | 0. | 0. | 0. | 0. | 0. | 0. |
| 3p | 184786 | 22.9100 | 54 | 0. | 0. | 0. | 0. | 0. | 0. | 0. | 0. | 0. |
| 3d | 197842 | 24.5163 | 90 | 0. | 0. | 0. | 0. | 0. | 0. | 0. | 0. | 0. |
| 4s | 210000** | 26.0360 | 18 | 0. | 0. | 0. | 0. | 0. | 0. | 0. | 0. | 0. |
| 4p | 215730** | 26.7464 | 54 | 0. | 0. | 0. | 0. | 0. | 0. | 0. | 0. | 0. |
| 4d | 220465 | 27.3335 | 90 | 0. | 0. | 0. | 0. | 0. | 0. | 0. | 0. | 0. |
| 4f | 221458 | 27.4566 | 126 | 0. | 0. | 0. | 0. | 0. | 0. | 0. | 0. | 0. |
| $(^3P^o)\ ?$ | 219000* | 27.1518 | 6 | 0. | 0. | 0. | 0. | 0. | 0. | 0. | 0. | 0. |
| 3p | 234000* | 29.0116 | 18 | 0. | 0. | 0. | 0. | 0. | 0. | 0. | 0. | 0. |
| 3d | 246000* | 30.4993 | 30 | 0. | 0. | 0. | 0. | 0. | 0. | 0. | 0. | 0. |
| 4s | 260000* | 32.2351 | 6 | 0. | 0. | 0. | 0. | 0. | 0. | 0. | 0. | 0. |
| 4p | 265000* | 32.8550 | 18 | 0. | 0. | 0. | 0. | 0. | 0. | 0. | 0. | 0. |
| 4d | 270500* | 33.5369 | 30 | 0. | 0. | 0. | 0. | 0. | 0. | 0. | 0. | 0. |
| 4f | 271400* | 33.6484 | 42 | 0. | 0. | 0. | 0. | 0. | 0. | 0. | 0. | 0. |
| $2p^2\ (^3P)\ 3s$ | 257000* | 31.8631 | 18 | 0. | 0. | 0. | 0. | 0. | 0. | 0. | 0. | 0. |
| 3p | 271000* | 33.5989 | 54 | 0. | 0. | 0. | 0. | 0. | 0. | 0. | 0. | 0. |
| 3d | 283000* | 35.0866 | 90 | 0. | 0. | 0. | 0. | 0. | 0. | 0. | 0. | 0. |
| 4 | 304500* | 37.7522 | 298 | 0. | 0. | 0. | 0. | 0. | 0. | 0. | 0. | 0. |
| $(^1D)\ 3s$ | 267000* | 33.1029 | 10 | 0. | 0. | 0. | 0. | 0. | 0. | 0. | 0. | 0. |
| 3p | 281000* | 34.8387 | 30 | 0. | 0. | 0. | 0. | 0. | 0. | 0. | 0. | 0. |
| 3d | 292000* | 36.2025 | 50 | 0. | 0. | 0. | 0. | 0. | 0. | 0. | 0. | 0. |
| 4 | 313000* | 38.8061 | 160 | 0. | 0. | 0. | 0. | 0. | 0. | 0. | 0. | 0. |
| $(^1S)\ 3$ | 319000* | 39.5499 | 18 | 0. | 0. | 0. | 0. | 0. | 0. | 0. | 0. | 0. |
| 4 | 349000* | 43.2694 | 32 | 0. | 0. | 0. | 0. | 0. | 0. | 0. | 0. | 0. |

*Estimated. **Includes estimated sublevels.

Nonstarred energy levels from References 10-3, 10-39.

Table 10-4. (Cont'd.)

| State | Level | Temperature (K) | | | | | | | | | | | |
|---|---|---|---|---|---|---|---|---|---|---|---|---|---|
| | (CM-1) | 2000 | 2500 | 3000 | 3500 | 4000 | 4500 | 5000 | 6000 | 7000 | 8000 | 9000 | 10000 |
| $2s^2\,2p\ ^2P^o_{3/2}$ | 0 | 3.44E-01 | 3.42E-01 | 3.40E-01 | 3.39E-01 | 3.38E-01 | 3.38E-01 | 3.37E-01 | 3.37E-01 | 3.36E-01 | 3.36E-01 | 3.35E-01 | 3.34E-01 |
| $^2P^o_{1/2}$ | 64 | 6.56E-01 | 6.58E-01 | 6.60E-01 | 6.61E-01 | 6.62E-01 | 6.62E-01 | 6.63E-01 | 6.63E-01 | 6.64E-01 | 6.64E-01 | 6.63E-01 | 6.62E-01 |
| $2s\ 2p^3\ ^4S^o$ | 43033 | 7.40E-14 | 3.60E-11 | 2.22E-09 | 4.23E-08 | 3.95E-07 | 2.15E-06 | 8.48E-06 | 6.67E-05 | 2.91E-04 | 8.77E-04 | 2.07E-03 | 4.10E-03 |
| $^2D^o$ | 74932 | 6.67E-24 | 3.19E-19 | 4.20E-16 | 7.11E-14 | 3.33E-12 | 6.65E-11 | 7.29E-10 | 2.65E-08 | 3.44E-07 | 2.36E-06 | 1.05E-05 | 3.47E-05 |
| $^2P^o$ | 86494 | 2.45E-31 | 2.60E-25 | 2.71E-21 | 2.01E-18 | 2.86E-16 | 1.35E-14 | 2.95E-13 | 3.01E-11 | 8.18E-10 | 9.75E-09 | 6.69E-08 | 3.12E-07 |
| $2p^3\ ^4S^o$ | 110653 | 2.77E-35 | 2.26E-28 | 9.15E-24 | 1.79E-20 | 5.26E-18 | 4.37E-16 | 1.50E-14 | 3.02E-12 | 1.34E-10 | 2.29E-09 | 2.09E-08 | 1.22E-07 |
| $^2D^o$ | 142024 | 0. | 2.17E-36 | 1.78E-30 | 2.99E-26 | 4.41E-23 | 1.28E-20 | 1.20E-18 | 1.09E-15 | 1.41E-13 | 5.42E-12 | 9.23E-11 | 8.92E-10 |
| $^2P^o$ | 150465 | 0. | 4.21E-38 | 7.78E-32 | 2.33E-27 | 5.29E-24 | 2.16E-21 | 2.65E-19 | 3.60E-16 | 6.23E-14 | 2.97E-12 | 5.99E-11 | 6.62E-10 |
| | 168744 | 0. | 0. | 7.27E-36 | 7.61E-31 | 4.43E-27 | 3.75E-24 | 8.26E-22 | 2.70E-18 | 8.72E-16 | 6.65E-14 | 1.93E-12 | 2.86E-11 |
| $2s^1\ ^1S$ 3s | 116518 | 1.34E-37 | 2.54E-30 | 1.81E-25 | 5.31E-22 | 2.11E-19 | 2.22E-17 | 9.21E-16 | 2.46E-13 | 1.33E-11 | 2.65E-10 | 2.72E-09 | 1.74E-08 |
| 3p | 131725 | 0. | 1.22E-33 | 3.74E-28 | 3.09E-24 | 2.69E-21 | 5.19E-19 | 3.49E-17 | 3.93E-14 | 1.76E-12 | 5.18E-11 | 7.19E-10 | 5.89E-09 |
| 3d | 145550 | 0. | 7.13E-37 | 8.22E-31 | 1.75E-26 | 3.10E-23 | 1.04E-20 | 1.09E-18 | 1.17E-15 | 1.71E-13 | 7.18E-12 | 1.31E-10 | 1.34E-09 |
| 4s | 157235 | 0. | 0. | 6.05E-34 | 2.80E-29 | 9.27E-26 | 4.96E-23 | 7.56E-21 | 1.42E-17 | 3.10E-15 | 1.76E-13 | 4.06E-12 | 5.00E-11 |
| 4p | 162523 | 0. | 0. | 1.44E-34 | 9.82E-30 | 4.15E-26 | 2.74E-23 | 4.95E-21 | 1.20E-17 | 3.13E-15 | 2.04E-13 | 5.23E-12 | 7.01E-11 |
| 4d | 168125 | 0. | 0. | 1.63E-35 | 1.64E-30 | 9.22E-27 | 7.63E-24 | 1.65E-21 | 5.21E-18 | 1.65E-15 | 1.24E-13 | 3.56E-12 | 5.22E-11 |
| 4f | 168979 | 0. | 0. | 1.52E-35 | 1.61E-30 | 9.50E-27 | 8.13E-24 | 1.80E-21 | 5.95E-18 | 1.94E-15 | 1.49E-13 | 4.35E-12 | 6.46E-11 |
| $2s\ 2p\ (^3P^o)\ 2s$ | 170643 | 0. | 0. | 8.78E-36 | 1.05E-30 | 6.71E-27 | 6.14E-24 | 1.44E-21 | 5.13E-18 | 1.77E-15 | 1.42E-13 | 4.28E-12 | 6.53E-11 |
| 3p | 184786 | 0. | 0. | 2.96E-38 | 9.37E-33 | 1.24E-28 | 2.00E-25 | 7.35E-23 | 4.18E-19 | 2.90E-16 | 3.34E-14 | 1.34E-12 | 2.56E-11 |
| 3d | 197742 | 0. | 0. | 0. | 7.60E-35 | 1.96E-30 | 5.30E-27 | 2.95E-24 | 3.86E-20 | 3.37E-17 | 5.42E-15 | 2.81E-13 | 6.62E-12 |
| 4s | 210000 | 0. | 0. | 0. | 9.84E-38 | 4.77E-33 | 2.10E-29 | 1.73E-26 | 4.09E-22 | 5.43E-19 | 1.20E-16 | 7.93E-15 | 2.27E-13 |
| 4p | 215730 | 0. | 0. | 0. | 2.80E-38 | 1.82E-33 | 1.01E-29 | 9.99E-27 | 3.10E-22 | 5.02E-19 | 1.28E-16 | 9.52E-15 | 2.99E-13 |
| 4d | 220465 | 0. | 0. | 0. | 0. | 5.53E-34 | 3.70E-30 | 4.26E-27 | 1.66E-22 | 3.16E-19 | 9.10E-17 | 7.44E-15 | 2.52E-13 |
| 4f | 221458 | 0. | 0. | 0. | 0. | 5.42E-34 | 3.78E-30 | 4.48E-27 | 1.83E-22 | 3.61E-19 | 1.07E-16 | 8.89E-15 | 3.06E-13 |
| $(^3P^o)\ 3s$ | 219000 | 0. | 0. | 0. | 0. | 6.25E-35 | 3.95E-31 | 4.33E-28 | 1.57E-23 | 2.85E-20 | 7.90E-18 | 6.27E-16 | 2.07E-14 |
| 3p | 234000 | 0. | 0. | 0. | 0. | 8.50E-37 | 9.78E-33 | 1.73E-29 | 1.29E-24 | 3.91E-21 | 1.60E-18 | 1.71E-16 | 7.18E-15 |
| 3d | 246000 | 0. | 0. | 0. | 0. | 1.89E-38 | 3.52E-34 | 9.15E-31 | 1.21E-25 | 5.54E-22 | 3.07E-19 | 4.18E-17 | 2.13E-15 |
| 4s | 260000 | 0. | 0. | 0. | 0. | 0. | 8.00E-37 | 3.26E-33 | 8.46E-28 | 6.23E-24 | 4.95E-21 | 8.92E-19 | 5.66E-17 |
| 4p | 265000 | 0. | 0. | 0. | 0. | 0. | 4.85E-37 | 2.32E-33 | 7.65E-28 | 6.69E-24 | 6.35E-21 | 1.20E-18 | 8.30E-17 |
| 4d | 270500 | 0. | 0. | 0. | 0. | 0. | 1.39E-37 | 7.93E-34 | 3.41E-28 | 3.60E-24 | 3.75E-21 | 8.33E-19 | 6.27E-17 |
| 4f | 271400 | 0. | 0. | 0. | 0. | 0. | 1.46E-37 | 8.57E-34 | 3.85E-28 | 4.19E-24 | 4.46E-21 | 1.01E-18 | 7.71E-17 |
| $4p^1\ ^3P\ 3s$ | 257000 | 0. | 0. | 0. | 0. | 0. | 0. | 6.26E-36 | 2.32E-32 | 5.21E-27 | 3.46E-23 | 2.55E-20 | 4.33E-18 | 2.62E-16 |
| 3p | 271000 | 0. | 0. | 0. | 0. | 0. | 2.14E-37 | 1.24E-33 | 5.44E-28 | 5.85E-24 | 6.17E-21 | 1.38E-18 | 1.05E-16 |
| 3d | 283000 | 0. | 0. | 0. | 0. | 0. | 0. | 6.52E-35 | 5.11E-29 | 8.27E-25 | 1.19E-21 | 3.39E-19 | 3.11E-17 |
| 4 | 304500 | 0. | 0. | 0. | 0. | 0. | 0. | 4.29E-37 | 9.42E-31 | 3.19E-26 | 7.95E-23 | 3.49E-20 | 4.52E-18 |
| $^1D\ 3s$ | 267000 | 0. | 0. | 0. | 0. | 0. | 1.42E-37 | 7.24E-34 | 2.63E-28 | 2.46E-24 | 2.34E-21 | 4.86E-19 | 3.46E-17 |
| 3p | 281000 | 0. | 0. | 0. | 0. | 0. | 0. | 3.87E-35 | 2.75E-29 | 4.16E-25 | 5.67E-22 | 1.55E-19 | 1.38E-17 |
| 3d | 292000 | 0. | 0. | 0. | 0. | 0. | 0. | 2.72E-36 | 3.28E-30 | 7.23E-26 | 1.31E-22 | 4.46E-20 | 4.74E-18 |
| 4 | 313000 | 0. | 0. | 0. | 0. | 0. | 0. | 0. | 6.82E-32 | 3.09E-27 | 9.58E-24 | 4.98E-21 | 7.39E-19 |
| $^3S\ 3$ | 319000 | 0. | 0. | 0. | 0. | 0. | 0. | 0. | 1.82E-33 | 1.01E-28 | 3.66E-25 | 2.14E-22 | 3.51E-20 |
| 4 | 349000 | 0. | 0. | 0. | 0. | 0. | 0. | 0. | 2.43E-36 | 3.78E-31 | 2.95E-27 | 3.15E-24 | 8.32E-22 |

Table 10-5. Energy levels and equilibrium fractional electronic populations of N .

| State | Level (cm⁻¹) | Level (eV) | Stat. Wt. | Temperature (K) 400 | 500 | 600 | 800 | 1000 | 1500 | 2000 | 2500 | 3000 |
|---|---|---|---|---|---|---|---|---|---|---|---|---|
| $2s^2 2p^3$ $^4S^o$ | 0 | 0.00000 | 4 | 1.00E 00 | 1.00E 00 | 1.00E 00 | 1.00E 00 | 1.00E 00 | 1.00E 00 | 1.00E 00 | 1.00E 00 | 1.00E 00 |
| $^2D^o$ | 19224 | 2.38439 | 10 | 2.10E-30 | 2.34E-24 | 2.30E-20 | 2.40E-15 | 2.42E-12 | 2.44E-08 | 2.46E-06 | 3.91E-05 | 2.47E-04 |
| $^2P^o$ | 28839 | 3.57555 | 6 | 0. | 1.37E-36 | 1.39E-30 | 4.47E-23 | 1.43E-18 | 1.45E-12 | 1.47E-09 | 9.29E-08 | 1.48E-06 |
| $2s\ 2p^4$ $^4P$ | 86132 | 10.68267 | 12 | 0. | 0. | 0. | 0. | 0. | 5.80E-37 | 8.75E-28 | 2.81E-22 | 1.32E-18 |

| State | Level (cm⁻¹) | Level (eV) | Stat. Wt. | Temperature (K) 3500 | 4000 | 4500 | 5000 | 6000 | 7000 | 8000 | 9000 | 10000 |
|---|---|---|---|---|---|---|---|---|---|---|---|---|
| $2s^2 2p^3$ $^4S^o$ | 0 | 0.00000 | 4 | 9.99E-01 | 9.97E-01 | 9.95E-01 | 9.90E-01 | 9.74E-01 | 9.51E-01 | 9.20E-01 | 8.85E-01 | 8.47E-01 |
| $^2D^o$ | 19224 | 2.38439 | 10 | 9.22E-04 | 2.47E-03 | 5.32E-03 | 9.78E-03 | 2.42E-02 | 4.57E-02 | 7.24E-02 | 1.02E-01 | 1.33E-01 |
| $^2P^o$ | 28839 | 3.57555 | 6 | 1.06E-05 | 4.68E-05 | 1.48E-04 | 3.69E-04 | 1.46E-03 | 3.80E-03 | 7.71E-03 | 1.32E-02 | 2.00E-02 |
| $2s\ 2p^4$ $^4P$ | 86132 | 10.68267 | 12 | 5.53E-16 | 5.11E-14 | 1.73E-12 | 2.88E-11 | 1.94E-09 | 3.87E-08 | 3.61E-07 | 2.02E-06 | 7.50E-06 |
| $^2D$ | 121000* | 15.00117 | 10 | 6.24E-22 | 3.13E-19 | 3.92E-17 | 1.67E-15 | 6.10E-13 | 3.76E-11 | 8.14E-10 | 8.79E-09 | 5.82E-08 |
| $^2S$ | 142110* | 17.61899 | 2 | 2.13E-26 | 3.15E-23 | 9.70E-21 | 8.61E-19 | 9.73E-16 | 9.80E-14 | 3.65E-12 | 6.01E-11 | 5.58E-10 |
| $^2P$ | 158200* | 19.62138 | 6 | 8.55E-29 | 2.90E-25 | 1.61E-22 | 2.52E-20 | 4.89E-17 | 1.08E-14 | 6.07E-13 | 1.38E-11 | 1.65E-10 |
| $2p^4$ $^4P^o$ | 232000* | 28.77952 | 6 | 0. | 6.20E-37 | 6.82E-33 | 1.16E-29 | 8.13E-25 | 2.31E-21 | 8.88E-19 | 8.97E-17 | 3.56E-15 |
| $2s^2 2p^3$ $^4P^o$ 3s | 842?? | 10.45?61 | 14 | 4.03E-15 | 3.00E-13 | 8.85E-12 | 1.30E-10 | 7.31E-09 | 1.28E-07 | 1.08E-06 | 5.60E-06 | 2.06E-05 |
| 3p | 95?40 | 11.8?749 | 54 | 1.07E-16 | 1.47E-14 | 6.73E-13 | 1.43E-11 | 1.39E-09 | 3.62E-08 | 4.10E-07 | 2.67E-06 | 1.18E-05 |
| 3d | 104961 | 13.00008 | 90 | 4.27E-18 | 9.34E-16 | 8.15E-14 | 1.75E-12 | 2.63E-10 | 9.33E-09 | 1.34E-07 | 1.04E-06 | 5.34E-06 |
| 4s | 105861 | 13.11768 | 18 | 1.29E-18 | 2.68E-16 | 1.69E-14 | 4.67E-13 | 6.69E-11 | 2.29E-09 | 3.20E-08 | 2.45E-07 | 1.23E-06 |
| 4p | 107420** | 13.31800 | 54 | 8.96E-19 | 2.23E-16 | 1.63E-14 | 5.03E-13 | 8.55E-11 | 3.31E-09 | 5.06E-08 | 4.16E-07 | 2.22E-06 |
| 4d | 110315 | 13.67770 | 90 | 4.54E-19 | 1.31E-16 | 1.08E-14 | 3.64E-13 | 7.12E-11 | 3.04E-09 | 5.01E-08 | 4.36E-07 | 2.44E-06 |
| 4f | 110441 | 13.69326 | 126 | 6.04E-19 | 1.76E-16 | 1.45E-14 | 4.92E-13 | 9.67E-11 | 4.15E-09 | 6.85E-08 | 5.99E-07 | 3.35E-06 |
| $(^2D^o)$ 3s | 96664 | 12.32664 | 10 | 4.02E-18 | 6.73E-16 | 3.60E-14 | 8.68E-13 | 1.02E-10 | 3.02E-09 | 3.78E-08 | 2.66E-07 | 1.25E-06 |
| 3p | 110973 | 13.75895 | 30 | 1.15E-19 | 3.45E-17 | 2.91E-15 | 1.00E-13 | 2.03E-11 | 8.85E-10 | 1.48E-08 | 1.31E-07 | 7.39E-07 |
| 3d | 121000** | 15.00117 | 50 | 3.12E-21 | 1.56E-18 | 1.96E-16 | 9.35E-15 | 3.05E-12 | 1.88E-10 | 4.07E-09 | 4.39E-08 | 2.91E-07 |
| 4 | 124600** | 15.44480 | 140 | 2.27E-21 | 1.37E-18 | 1.99E-16 | 1.06E-14 | 4.12E-13 | 2.87E-10 | 6.82E-09 | 7.91E-08 | 5.55E-07 |
| $(^2S)$ 3s | 116279 | 14.41664 | 2 | 8.69E-22 | 3.42E-19 | 3.55E-17 | 1.46E-15 | 3.78E-13 | 1.98E-11 | 3.81E-10 | 3.74E-09 | 2.30E-08 |
| 3p | 126400* | 15.68102 | 6 | 1.79E-23 | 1.31E-20 | 2.21E-18 | 1.33E-16 | 6.21E-14 | 4.52E-12 | 1.29E-10 | 1.61E-09 | 1.20E-08 |
| 3d | 133500* | 17.0474 | 10 | 7.07E-25 | 8.27E-22 | 2.01E-19 | 1.62E-17 | 1.17E-14 | 1.26E-12 | 4.19E-11 | 6.28E-10 | 5.42E-09 |
| 4 | 142000* | 17.60553 | 32 | 3.56E-25 | 5.24E-22 | 1.52E-19 | 1.42E-17 | 1.27E-14 | 1.60E-12 | 5.68E-11 | 9.79E-10 | 9.08E-09 |
| $2s\ 2p^4$ $(^2S^e)$ 3 | 153500* | 19.0603 | 90 | 1.09E-26 | 2.82E-23 | 1.27E-20 | 1.69E-18 | 2.55E-15 | 4.70E-13 | 2.32E-11 | 4.75E-10 | 5.24E-09 |
| 4 | 156000* | 19.3410 | 260 | 5.63E-27 | 1.70E-23 | 8.67E-21 | 1.26E-18 | 2.21E-15 | 4.51E-13 | 2.40E-11 | 5.22E-10 | 6.05E-09 |
| $(^2D^o)$ 3 | 152000* | 23.0044 | 270 | 3.56E-33 | 6.84E-29 | 1.47E-25 | 6.77E-23 | 6.65E-19 | 4.66E-16 | 6.26E-14 | 2.79E-12 | 5.75E-11 |
| 4 | 202000* | 25.0442 | 450 | 1.04E-34 | 3.33E-30 | 1.07E-26 | 6.77E-24 | 1.07E-19 | 1.06E-16 | 1.84E-14 | 1.00E-12 | 2.43E-11 |
| $(^4P^o)$ 3-4 | 215000* | 26.6459 | 450 | 4.64E-37 | 2.91E-32 | 1.56E-28 | 1.51E-25 | 4.46E-21 | 6.87E-18 | 1.67E-15 | 1.18E-13 | 3.50E-12 |
| $(^4S^o/^2D,^2P^o)$ 3-4 | 244000* | 32.1111 | 450 | 0. | 0. | 1.49E-34 | 5.84E-31 | 1.43E-25 | 5.92E-22 | 7.45E-19 | 1.27E-16 | 7.63E-15 |
| $2p^3(^4P,^2D,^2S)$ 3-4 | 331000* | 41.0377 | 450 | 0. | 0. | 0. | 0. | 6.17E-33 | 5.06E-28 | 2.42E-24 | 1.73E-21 | 3.30E-19 |

*Estimated. **Includes estimated sublevels.

Nonstarred energy levels from References 10-3, 10-40, 10-41.

Note: States involving electrons with principal quantum numbers above N = 4 are not included.

All levels above 117214 $cm^{-1}$ are subject to autoionization.

Table 10-6. Energy levels and equilibrium fractional electronic papulations of $N^+$ .

| State | | Level (CM-1) | Level (EV) | Stat. Wt. | Temperature (K) 200 | 250 | 300 | 400 | 500 | 600 | 800 | 1000 | 1500 |
|---|---|---|---|---|---|---|---|---|---|---|---|---|---|
| $2s^2\ 2p^2\ ^3P_0$ | | 0 | 0.0000 | 1 | 1.97E-01 | 1.78E-01 | 1.65E-01 | 1.51E-01 | 1.42E-01 | 1.37E-01 | 1.30E-01 | 1.26E-01 | 1.21E-01 |
| $^3P_1$ | | 48.7 | 0.0060 | 3 | 4.17E-01 | 4.03E-01 | 3.93E-01 | 3.79E-01 | 3.70E-01 | 3.65E-01 | 3.57E-01 | 3.52E-01 | 3.46E-01 |
| $^3P_2$ | | 130.8 | 0.0162 | 5 | 3.85E-01 | 4.19E-01 | 4.42E-01 | 4.70E-01 | 4.87E-01 | 4.99E-01 | 5.13E-01 | 5.22E-01 | 5.33E-01 |
| $^1D$ | | 15316 | 1.8989 | 5 | 0. | 4.65E-39 | 1.04E-32 | 8.93E-25 | 5.14E-20 | 7.65E-17 | 7.07E-13 | 1.69E-10 | 2.52E-07 |
| $^1S$ | | 32689 | 4.0528 | 1 | 0. | 0. | 0. | 0. | 0. | 1.24E-35 | 3.81E-27 | 4.72E-22 | 2.92E-15 |
| $2s\ 2p^3\ ^5S^o$ | | 46785 | 5.8005 | 5 | 0. | 0. | 0. | 0. | 0. | 0. | 1.86E-37 | 3.67E-30 | 1.96E-20 |
| $^3D^o$ | | 92245 | 11.4366 | 15 | 0. | 0. | 0. | 0. | 0. | 0. | 0. | 0. | 6.79E-39 |
| $^3P^o$ | | 109218 | 13.5410 | 9 | 0. | 0. | 0. | 0. | 0. | 0. | 0. | 0. | 0. |
| $^1S^o$ | | 155127 | 19.2328 | 3 | 0. | 0. | 0. | 0. | 0. | 0. | 0. | 0. | 0. |
| $^1D^o$ | | 164188 | 17.8766 | 5 | 0. | 0. | 0. | 0. | 0. | 0. | 0. | 0. | 0. |
| $^1P^o$ | | 166766 | 20.6758 | 3 | 0. | 0. | 0. | 0. | 0. | 0. | 0. | 0. | 0. |
| $2p^4$ | $^3P$ | 218000* | 27.0279 | 9 | 0. | 0. | 0. | 0. | 0. | 0. | 0. | 0. | 0. |
| | $^1D$ | 229000* | 28.3916 | 5 | 0. | 0. | 0. | 0. | 0. | 0. | 0. | 0. | 0. |
| | $^1S$ | 264000* | 32.7310 | 1 | 0. | 0. | 0. | 0. | 0. | 0. | 0. | 0. | 0. |
| $2s^2\ 2p\ (^3P^o)\ 3s$ | | 149056 | 18.4801 | 12 | 0. | 0. | 0. | 0. | 0. | 0. | 0. | 0. | 0. |
| | 3p | 169022 | 20.9555 | 36 | 0. | 0. | 0. | 0. | 0. | 0. | 0. | 0. | 0. |
| | 3d | 187693 | 23.2704 | 60 | 0. | 0. | 0. | 0. | 0. | 0. | 0. | 0. | 0. |
| | 4s | 196955 | 24.4187 | 12 | 0. | 0. | 0. | 0. | 0. | 0. | 0. | 0. | 0. |
| | 4p | 203384 | 25.2158 | 36 | 0. | 0. | 0. | 0. | 0. | 0. | 0. | 0. | 0. |
| | 4d | 210284 | 26.0712 | 60 | 0. | 0. | 0. | 0. | 0. | 0. | 0. | 0. | 0. |
| | 4f | 211271 | 26.1936 | 84 | 0. | 0. | 0. | 0. | 0. | 0. | 0. | 0. | 0. |
| $2s\ 2p^2\ (^4P)\ 3s$ | | 207974 | 25.7848 | 24 | 0. | 0. | 0. | 0. | 0. | 0. | 0. | 0. | 0. |
| | 3p | 226455 | 28.0761 | 72 | 0. | 0. | 0. | 0. | 0. | 0. | 0. | 0. | 0. |
| | 3d | 244500 | 30.3134 | 120 | 0. | 0. | 0. | 0. | 0. | 0. | 0. | 0. | 0. |
| | 4 | 266100 | 32.9913 | 384 | 0. | 0. | 0. | 0. | 0. | 0. | 0. | 0. | 0. |
| $2s\ 2p^2\ (^2D)\ 3s$ | | 252000 | 31.2432 | 20 | 0. | 0. | 0. | 0. | 0. | 0. | 0. | 0. | 0. |
| | 3p | 270000 | 33.4749 | 60 | 0. | 0. | 0. | 0. | 0. | 0. | 0. | 0. | 0. |
| | 3d | 288000 | 35.7065 | 100 | 0. | 0. | 0. | 0. | 0. | 0. | 0. | 0. | 0. |
| | 4 | 309800 | 38.4093 | 320 | 0. | 0. | 0. | 0. | 0. | 0. | 0. | 0. | 0. |
| $(^2P)\ 3$ | | 323100 | 40.0583 | 108 | 0. | 0. | 0. | 0. | 0. | 0. | 0. | 0. | 0. |
| | 4 | 354800 | 43.9885 | 192 | 0. | 0. | 0. | 0. | 0. | 0. | 0. | 0. | 0. |
| $(^2S)\ 3$ | | 308100 | 38.1985 | 36 | 0. | 0. | 0. | 0. | 0. | 0. | 0. | 0. | 0. |
| | 4 | 339800 | 42.1287 | 64 | 0. | 0. | 0. | 0. | 0. | 0. | 0. | 0. | 0. |
| $2p^3\ (^4S^o)\ 3$ | | 364000 | 45.1291 | 72 | 0. | 0. | 0. | 0. | 0. | 0. | 0. | 0. | 0. |
| | 4 | 396000 | 49.0965 | 128 | 0. | 0. | 0. | 0. | 0. | 0. | 0. | 0. | 0. |
| $(^2D^o)\ 3$ | | 380000 | 47.1128 | 180 | 0. | 0. | 0. | 0. | 0. | 0. | 0. | 0. | 0. |
| | 4 | 412000 | 51.0802 | 320 | 0. | 0. | 0. | 0. | 0. | 0. | 0. | 0. | 0. |
| $(^2P^o)\ 3$ | | 408000 | 50.5842 | 108 | 0. | 0. | 0. | 0. | 0. | 0. | 0. | 0. | 0. |
| | 4 | 439000 | 54.4277 | 192 | 0. | 0. | 0. | 0. | 0. | 0. | 0. | 0. | 0. |

*Estimated.

Nonstarred energy levels from References 10-3, 10-42.

Table 10-6. (Cont'd.)

| State | Level | Temperature (K) | | | | | | | | | | | |
|---|---|---|---|---|---|---|---|---|---|---|---|---|---|
| | (CM-1) | 2000 | 2500 | 3000 | 3500 | 4000 | 4500 | 5000 | 6000 | 7000 | 8000 | 9000 | 10000 |
| $2s^2\ 2p^2\ ^3P_2$ | 0 | 1.18E-01 | 1.17E-01 | 1.16E-01 | 1.15E-01 | 1.14E-01 | 1.14E-01 | 1.13E-01 | 1.12E-01 | 1.10E-01 | 1.09E-01 | 1.07E-01 | 1.06E-01 |
| $^3P_1$ | 48 | 3.43E-01 | 3.41E-01 | 3.40E-01 | 3.38E-01 | 3.37E-01 | 3.36E-01 | 3.35E-01 | 3.32E-01 | 3.28E-01 | 3.24E-01 | 3.20E-01 | 3.15E-01 |
| $^3P_0$ | 130 | 5.39E-01 | 5.42E-01 | 5.44E-01 | 5.45E-01 | 5.46E-01 | 5.46E-01 | 5.45E-01 | 5.42E-01 | 5.38E-01 | 5.32E-01 | 5.26E-01 | 5.19E-01 |
| $^1D$ | 15316 | 9.71E-06 | 8.68E-05 | 3.74E-04 | 1.06E-03 | 2.32E-03 | 4.25E-03 | 6.90E-03 | 1.42E-02 | 2.37E-02 | 3.47E-02 | 4.66E-02 | 5.84E-02 |
| $^1S$ | 32689 | 7.25E-12 | 7.90E-10 | 1.80E-08 | 1.68E-07 | 8.96E-07 | 3.29E-06 | 9.30E-06 | 4.41E-05 | 1.33E-04 | 3.05E-04 | 5.77E-04 | 9.59E-04 |
| $2s\ 2p^3\ ^5S^o$ | 46785 | 1.43E-15 | 1.18E-12 | 1.04E-10 | 2.56E-09 | 2.81E-08 | 1.81E-07 | 8.05E-07 | 7.51E-06 | 3.68E-05 | 1.21E-04 | 3.03E-04 | 6.31E-04 |
| $^3D^o$ | 92245 | 2.69E-29 | 1.54E-23 | 1.06E-19 | 5.87E-17 | 6.68E-15 | 2.65E-13 | 5.03E-12 | 4.15E-10 | 9.66E-09 | 1.02E-07 | 6.35E-07 | 2.73E-06 |
| $^3P^o$ | 109218 | 8.03E-35 | 5.29E-28 | 1.86E-23 | 3.28E-20 | 8.94E-18 | 6.99E-16 | 2.29E-14 | 4.25E-12 | 1.77E-10 | 2.89E-09 | 2.52E-08 | 1.43E-07 |
| $^5S^o$ | 155127 | 0. | 0. | 1.70E-33 | 6.97E-29 | 2.01E-25 | 9.84E-23 | 1.39E-20 | 2.35E-17 | 4.71E-15 | 2.50E-13 | 5.47E-12 | 6.43E-11 |
| $^1D^o$ | 144188 | 0. | 5.34E-37 | 5.38E-31 | 1.04E-26 | 1.71E-23 | 5.41E-21 | 5.41E-19 | 5.39E-16 | 7.43E-14 | 2.98E-12 | 5.24E-11 | 5.17E-10 |
| $^1P^o$ | 166766 | 0. | 0. | 6.40E-36 | 5.83E-31 | 3.05E-27 | 2.38E-24 | 4.90E-22 | 1.44E-18 | 4.30E-16 | 3.08E-14 | 8.50E-13 | 1.21E-11 |
| $2s^2$ $^1P$ | 218000 | 0. | 0. | 0. | 0. | 9.08E-35 | 5.49E-31 | 5.81E-28 | 1.99E-23 | 3.45E-20 | 9.20E-18 | 7.07E-16 | 2.27E-14 |
| $^1D$ | 229000 | 0. | 0. | 0. | 0. | 9.65E-37 | 9.05E-33 | 1.36E-29 | 7.92E-25 | 2.00E-21 | 7.07E-19 | 6.77E-17 | 2.60E-15 |
| $^1S$ | 264000 | 0. | 0. | 0. | 0. | 0. | 2.50E-38 | 1.15E-34 | 3.59E-29 | 3.00E-25 | 2.61E-22 | 5.03E-20 | 3.37E-18 |
| $2s^2\ 2p\ (^2P^o)\ 3s$ | 149056 | 0. | 7.79E-38 | 1.25E-31 | 3.38E-27 | 7.13E-24 | 2.74E-21 | 3.20E-19 | 4.03E-16 | 6.56E-14 | 2.98E-12 | 5.77E-11 | 6.16E-10 |
| $3p$ | 169022 | 0. | 0. | 2.60E-35 | 2.77E-30 | 1.63E-26 | 1.39E-23 | 3.07E-21 | 1.01E-17 | 3.25E-15 | 2.46E-13 | 7.12E-12 | 1.05E-10 |
| $3d$ | 187693 | 0. | 0. | 0. | 2.14E-33 | 3.28E-29 | 5.91E-26 | 2.37E-23 | 1.91E-19 | 1.17E-16 | 1.43E-14 | 5.99E-13 | 1.19E-11 |
| $4s$ | 196953 | 0. | 0. | 0. | 9.50E-36 | 2.35E-31 | 6.12E-28 | 3.31E-25 | 4.13E-21 | 3.48E-18 | 5.40E-16 | 2.73E-14 | 6.26E-13 |
| $4p$ | 203384 | 0. | 0. | 0. | 2.03E-36 | 6.97E-32 | 2.35E-28 | 1.56E-25 | 2.65E-21 | 2.78E-18 | 5.10E-16 | 2.93E-14 | 7.45E-13 |
| $4d$ | 210284 | 0. | 0. | 0. | 1.98E-37 | 9.71E-33 | 4.31E-29 | 3.57E-26 | 8.46E-22 | 1.12E-18 | 2.46E-16 | 1.62E-14 | 4.60E-13 |
| $4f$ | 211271 | 0. | 0. | 0. | 1.85E-37 | 9.53E-33 | 4.40E-29 | 3.76E-26 | 9.35E-22 | 1.28E-18 | 2.88E-16 | 1.94E-14 | 5.59E-13 |
| $2s\ 2p^2\ (^1D)\ 3s$ | 207974 | 0. | 0. | 0. | 2.05E-37 | 8.92E-33 | 3.61E-29 | 2.77E-26 | 5.89E-22 | 7.22E-19 | 1.49E-16 | 9.37E-15 | 2.57E-13 |
| $3p$ | 226455 | 0. | 0. | 0. | 0. | 3.47E-35 | 2.94E-31 | 4.08E-28 | 2.10E-23 | 4.85E-20 | 1.61E-17 | 1.46E-15 | 5.39E-14 |
| $3d$ | 244500 | 0. | 0. | 0. | 0. | 8.78E-38 | 1.53E-33 | 3.78E-30 | 4.62E-25 | 1.98E-21 | 1.04E-18 | 1.36E-16 | 6.70E-15 |
| $4$ | 266100 | 0. | 0. | 0. | 0. | 0. | 4.90E-36 | 2.42E-32 | 8.33E-27 | 7.48E-23 | 6.87E-20 | 1.38E-17 | 9.58E-16 |
| $2s\ 2p^2\ (^1D)\ 3s$ | 252000 | 0. | 0. | 0. | 0. | 0. | 2.32E-35 | 7.28E-32 | 1.28E-26 | 2.07E-23 | 4.52E-20 | 6.85E-18 | 3.79E-16 |
| $3p$ | 270000 | 0. | 0. | 0. | 0. | 0. | 2.20E-37 | 1.23E-33 | 5.11E-28 | 5.24E-24 | 5.33E-21 | 1.16E-18 | 8.56E-17 |
| $3d$ | 288000 | 0 | 0. | 0. | 0. | 0. | 0. | 1.15E-35 | 1.14E-29 | 2.16E-25 | 3.49E-22 | 1.08E-19 | 1.07E-17 |
| $4$ | 309800 | 0. | 0. | 0. | 0. | 0. | 0. | 6.96E-38 | 1.95E-31 | 7.83E-27 | 2.21E-23 | 1.06E-20 | 1.48E-18 |
| $^2P$ 3 | 323100 | 0. | 0. | 0. | 0. | 0. | 0. | 0. | 2.71E-33 | 1.72E-28 | 6.83E-25 | 4.28E-22 | 7.39E-20 |
| 4 | 344800 | 0. | 0. | 0. | 0. | 0. | 0. | 0. | 2.41E-36 | 4.52E-31 | 4.06E-27 | 4.80E-24 | 1.37E-21 |
| $^2S$ 3 | 308100 | 0. | 0. | 0. | 0. | 0. | 0. | 1.28E-38 | 3.30E-32 | 1.25E-27 | 3.38E-24 | 1.57E-21 | 2.13E-19 |
| 4 | 396600 | 0. | 0. | 0. | 0. | 0. | 0. | 0. | 2.93E-35 | 3.29E-30 | 2.01E-26 | 1.76E-23 | 3.96E-21 |
| $2p^3\ ^5S^o$ 3 | 364000 | 0. | 0. | 0. | 0. | 0. | 0. | 0. | 9.95E-38 | 2.56E-32 | 2.91E-28 | 4.13E-25 | 1.37E-22 |
| 4 | 395000 | 0. | 0. | 0. | 0. | 0. | 0. | 0. | 0. | 6.33E-35 | 1.64E-30 | 4.41E-27 | 2.44E-24 |
| $^3D^o$ 3 | 380000 | 0. | 0. | 0. | 0. | 0. | 0. | 0. | 0. | 2.39E-33 | 4.09E-29 | 8.00E-26 | 3.43E-23 |
| 4 | 412000 | 0. | 0. | 0. | 0. | 0. | 0. | 0. | 0. | 5.90E-36 | 2.30E-31 | 8.56E-28 | 6.10E-25 |
| $^3P^o$ 3 | 408000 | 0. | 0. | 0. | 0. | 0. | 0. | 0. | 0. | 4.53E-36 | 1.60E-31 | 5.46E-28 | 3.66E-25 |
| 4 | 439000 | 0 | 0. | 0. | 0. | 0. | 0. | 0. | 0. | 0. | 1.07E-33 | 6.84E-30 | 7.52E-27 |

Table 10-7. Energy levels and equilibrium fractional electronic populations of $O^-$.

| State | Level (CM-1) | Level (EV) | Stat. Wt. | Temperature (K) 200 | 250 | 300 | 400 | 500 | 600 | 800 | 1000 | 1500 |
|---|---|---|---|---|---|---|---|---|---|---|---|---|
| $2s^2 2p^5\ ^2P_{3/2}$ | 0 | 0.0000 | 4 | 9.40E-01 | 9.12E-01 | 8.87E-01 | 8.48E-01 | 8.20E-01 | 7.98E-01 | 7.70E-01 | 7.51E-01 | 7.24E-01 |
| $^2P_{1/2}$ | 285 | 0.0353 | 2 | 6.05E-02 | 8.84E-02 | 1.13E-01 | 1.52E-01 | 1.80E-01 | 2.02E-01 | 2.30E-01 | 2.49E-01 | 2.76E-01 |

Energy levels from Reference 10-43.

| Level | Temperature (K) 2000 | 2500 | 3000 | 3500 | 4000 | 4500 | 5000 | 6000 | 7000 | 8000 | 9000 | 10000 |
|---|---|---|---|---|---|---|---|---|---|---|---|---|
| (CM-1) | | | | | | | | | | | | |
| 0 | 7.11E-01 | 7.02E-01 | 6.96E-01 | 6.92E-01 | 6.89E-01 | 6.87E-01 | 6.85E-01 | 6.82E-01 | 6.80E-01 | 6.78E-01 | 6.77E-01 | 6.76E-01 |
| 285 | 2.89E-01 | 2.98E-01 | 3.04E-01 | 3.08E-01 | 3.11E-01 | 3.13E-01 | 3.15E-01 | 3.18E-01 | 3.20E-01 | 3.22E-01 | 3.23E-01 | 3.24E-01 |

Table 10-8. Energy levels and equilibrium fractianal electronic populotians of O .

| State | | Level (CM-1) | Level (EV) | Stat. Wt. | Temperature (K) 200 | 250 | 300 | 400 | 500 | 600 | 800 | 1000 | 1500 |
|---|---|---|---|---|---|---|---|---|---|---|---|---|---|
| $2s^2\ 2p^4\ {}^3P_2$ | | 0 | 0.0000 | 5 | 8.12E-01 | 7.72E-01 | 7.42E-01 | 7.00E-01 | 6.74E-01 | 6.55E-01 | 6.31E-01 | 6.16E-01 | 5.97E-01 |
| | $^3P_1$ | 158.4 | 0.0196 | 3 | 1.56E-01 | 1.86E-01 | 2.08E-01 | 2.38E-01 | 2.56E-01 | 2.69E-01 | 2.85E-01 | 2.95E-01 | 3.07E-01 |
| | $^3P_0$ | 226.5 | 0.0281 | 1 | 3.18E-02 | 4.19E-02 | 5.01E-02 | 6.20E-02 | 7.02E-02 | 7.61E-02 | 8.40E-02 | 8.90E-02 | 9.60E-02 |
| | $^1D$ | 15868 | 1.9673 | 5 | 0. | 0. | 6.60E-34 | 1.14E-25 | 9.95E-21 | 1.95E-17 | 2.55E-13 | 7.49E-11 | 1.46E-07 |
| | $^1S$ | 33792 | 4.1896 | 1 | 0. | 0. | 0. | 0. | 0. | 8.42E-37 | 5.10E-28 | 9.46E-23 | 1.00E-15 |
| $2s\ 2p^3\ {}^5P^o$ | | 126304 | 15.6593 | 9 | 0. | 0. | 0. | 0. | 0. | 0. | 0. | 0. | 0. |
| | $^3P^o$ | 189837 | 23.5362 | 3 | 0. | 0. | 0. | 0. | 0. | 0. | 0. | 0. | 0. |
| $2p^4\ {}^3S$ | | 277000* | 34.3427 | 1 | 0. | 0. | 0. | 0. | 0. | 0. | 0. | 0. | 0. |
| $2s^2\ 2p^3\ (^4S^o)$ | 3s | 74903 | 9.2865 | 8 | 0. | 0. | 0. | 0. | 0. | 0. | 0. | 0. | 5.99E-32 |
| | 3p | 87379 | 10.8333 | 24 | 0. | 0. | 0. | 0. | 0. | 0. | 0. | 0. | 1.14E-36 |
| | 3d | 97443 | 12.0811 | 40 | 0. | 0. | 0. | 0. | 0. | 0. | 0. | 0. | 0. |
| | 4s | 95757 | 11.8720 | 8 | 0. | 0. | 0. | 0. | 0. | 0. | 0. | 0. | 0. |
| | 4p | 99314 | 12.3130 | 24 | 0. | 0. | 0. | 0. | 0. | 0. | 0. | 0. | 0. |
| | 4df | 102900** | 12.7576 | 116 | 0. | 0. | 0. | 0. | 0. | 0. | 0. | 0. | 0. |
| | $(^2D^o)$ 3s | 101527 | 12.5869 | 20 | 0. | 0. | 0. | 0. | 0. | 0. | 0. | 0. | 0. |
| | 3p | 113600** | 14.0842 | 60 | 0. | 0. | 0. | 0. | 0. | 0. | 0. | 0. | 0. |
| | 3d | 123940** | 15.3662 | 100 | 0. | 0. | 0. | 0. | 0. | 0. | 0. | 0. | 0. |
| | 4 | 128700** | 15.9564 | 320 | 0. | 0. | 0. | 0. | 0. | 0. | 0. | 0. | 0. |
| | $(^2P^o)$ 3s | 114416 | 14.1854 | 12 | 0. | 0. | 0. | 0. | 0. | 0. | 0. | 0. | 0. |
| | 3p | 127900** | 15.8572 | 36 | 0. | 0. | 0. | 0. | 0. | 0. | 0. | 0. | 0. |
| | 3d | 138000* | 17.1094 | 60 | 0. | 0. | 0. | 0. | 0. | 0. | 0. | 0. | 0. |
| | 4 | 142100* | 17.6177 | 192 | 0. | 0. | 0. | 0. | 0. | 0. | 0. | 0. | 0. |
| $2s\ 2p^4\ (^4P\ )$ | 3 | 212000* | 26.2840 | 216 | 0. | 0. | 0. | 0. | 0. | 0. | 0. | 0. | 0. |
| | 4 | 222000* | 27.5238 | 384 | 0. | 0. | 0. | 0. | 0. | 0. | 0. | 0. | 0. |
| $(^2D\ )$ | 3 | 258000* | 31.9871 | 180 | 0. | 0. | 0. | 0. | 0. | 0. | 0. | 0. | 0. |
| | 4 | 268000* | 33.2269 | 320 | 0. | 0. | 0. | 0. | 0. | 0. | 0. | 0. | 0. |
| $(^2S\ )$ | 3 | 287000* | 35.5825 | 36 | 0. | 0. | 0. | 0. | 0. | 0. | 0. | 0. | 0. |
| | 4 | 298000* | 36.9469 | 64 | 0. | 0. | 0. | 0. | 0. | 0. | 0. | 0. | 0. |
| $(^2P\ )$ | 3 | 304000* | 37.6902 | 108 | 0. | 0. | 0. | 0. | 0. | 0. | 0. | 0. | 0. |
| | 4 | 314000* | 38.9300 | 192 | 0. | 0. | 0. | 0. | 0. | 0. | 0. | 0. | 0. |
| $2p^5\ (^3P^o)$ | 3 | 409000* | 50.7082 | 108 | 0. | 0. | 0. | 0. | 0. | 0. | 0. | 0. | 0. |
| | 4 | 419000* | 51.9480 | 192 | 0. | 0. | 0. | 0. | 0. | 0. | 0. | 0. | 0. |

*Estimated. **Includes estimated sublevels.
Nanstarred energy levels from References 10-3, 10-44.

Table 10-8. (Cont'd.)

| State | | Level | Temperature (K) | | | | | | | | | | |
|---|---|---|---|---|---|---|---|---|---|---|---|---|---|
| | | (CM-1) | 2000 | 2500 | 3000 | 3500 | 4000 | 4500 | 5000 | 6000 | 7000 | 8000 | 9000 | 10000 |
| $2s^2\,2p^4\ {}^3P_2$ | | 0 | 5.86E-01 | 5.80E-01 | 5.76E-01 | 5.73E-01 | 5.70E-01 | 5.67E-01 | 5.65E-01 | 5.59E-01 | 5.52E-01 | 5.45E-01 | 5.38E-01 | 5.31E-01 |
| $^3P_1$ | | 158 | 3.14E-01 | 3.18E-01 | 3.20E-01 | 3.22E-01 | 3.23E-01 | 3.24E-01 | 3.24E-01 | 3.23E-01 | 3.21E-01 | 3.18E-01 | 3.15E-01 | 3.11E-01 |
| $^3P_0$ | | 226 | 9.96E-02 | 1.02E-01 | 1.03E-01 | 1.04E-01 | 1.05E-01 | 1.06E-01 | 1.06E-01 | 1.06E-01 | 1.06E-01 | 1.05E-01 | 1.05E-01 | 1.03E-01 |
| $^1D$ | | 15868 | 6.46E-06 | 6.27E-05 | 2.85E-04 | 8.42E-04 | 1.89E-03 | 3.55E-03 | 5.87E-03 | 1.24E-02 | 2.12E-02 | 3.14E-02 | 4.26E-02 | 5.41E-02 |
| $^1S$ | | 33792 | 3.25E-12 | 4.15E-10 | 1.05E-08 | 1.06E-07 | 6.00E-07 | 2.30E-06 | 6.76E-06 | 3.38E-05 | 1.06E-04 | 2.50E-04 | 4.85E-04 | 8.21E-04 |
| $2s\ 2p^5\ {}^3P^o$ | | 126304 | 0. | 2.82E-32 | 5.11E-27 | 2.91E-23 | 1.91E-20 | 2.96E-18 | 1.67E-16 | 7.06E-14 | 5.28E-12 | 1.34E-10 | 1.65E-09 | 1.22E-08 |
| $^1P^o$ | | 189837 | 0. | 0. | 0. | 4.41E-35 | 7.56E-31 | 1.48E-27 | 6.39E-25 | 5.69E-21 | 3.75E-18 | 4.87E-16 | 2.13E-14 | 4.38E-13 |
| $2p^6\ {}^1S$ | | 277000 | 0. | 0. | 0. | 0. | 0. | 0. | 2.73E-36 | 1.59E-30 | 2.07E-26 | 2.52E-23 | 6.31E-21 | 5.22E-19 |
| $2s^2\,2p^3\ (^4S^o)$ | 3s | 74903 | 3.72E-24 | 1.76E-19 | 2.31E-16 | 3.89E-14 | 1.82E-12 | 3.61E-11 | 3.94E-10 | 1.42E-08 | 1.82E-07 | 1.23E-06 | 5.43E-06 | 1.77E-05 |
| | 3p | 87379 | 1.41E-27 | 4.03E-22 | 1.75E-18 | 6.91E-16 | 6.13E-14 | 2.00E-12 | 3.26E-11 | 2.13E-09 | 4.20E-08 | 3.92E-07 | 2.22E-06 | 8.84E-06 |
| | 3d | 97443 | 1.69E-30 | 2.05E-24 | 2.33E-20 | 1.84E-17 | 2.73E-15 | 1.34E-13 | 3.00E-12 | 3.16E-10 | 8.85E-09 | 1.07E-07 | 7.39E-07 | 3.46E-06 |
| | 4s | 95757 | 1.14E-30 | 1.08E-24 | 1.05E-20 | 7.35E-18 | 1.00E-15 | 4.59E-14 | 9.75E-13 | 9.53E-11 | 2.50E-09 | 2.89E-08 | 1.94E-07 | 8.82E-07 |
| | 4p | 99314 | 2.64E-31 | 4.19E-25 | 5.70E-21 | 5.11E-18 | 8.37E-16 | 4.41E-14 | 1.05E-12 | 1.22E-10 | 3.62E-09 | 4.58E-08 | 3.29E-07 | 1.59E-06 |
| | 4df | 102900 | 9.55E-32 | 2.57E-25 | 4.93E-21 | 5.66E-18 | 1.11E-15 | 6.77E-14 | 1.81E-12 | 2.49E-10 | 8.36E-09 | 1.16E-07 | 8.96E-07 | 4.58E-06 |
| $(^2D^o)$ | 3s | 101523 | 4.48E-32 | 9.79E-26 | 1.65E-21 | 1.72E-18 | 3.15E-16 | 1.81E-14 | 4.64E-13 | 5.98E-11 | 1.91E-09 | 2.57E-08 | 1.92E-07 | 9.62E-07 |
| | 3p | 113600 | 2.27E-35 | 2.61E-28 | 1.51E-23 | 9.60E-20 | 1.23E-17 | 1.14E-15 | 4.31E-14 | 9.90E-12 | 4.80E-10 | 8.77E-09 | 8.38E-08 | 5.08E-07 |
| | 3d | 123940 | 2.22E-38 | 1.22E-30 | 1.76E-25 | 8.55E-22 | 4.96E-19 | 7.00E-17 | 3.66E-15 | 1.38E-12 | 9.54E-11 | 2.28E-09 | 2.67E-08 | 1.91E-07 |
| | 4 | 128700 | 0. | 2.52E-31 | 5.76E-26 | 3.87E-22 | 2.87E-19 | 4.89E-17 | 2.98E-15 | 1.41E-12 | 1.15E-10 | 3.09E-09 | 4.00E-08 | 3.08E-07 |
| $(^2P^o)$ | 3s | 114416 | 2.52E-36 | 3.52E-29 | 2.04E-24 | 5.15E-21 | 1.83E-18 | 1.76E-16 | 6.01E-15 | 1.63E-12 | 8.11E-11 | 1.51E-09 | 1.47E-08 | 9.03E-08 |
| | 3p | 127900 | 0. | 4.50E-32 | 9.51E-27 | 6.04E-23 | 4.30E-20 | 7.10E-18 | 4.22E-16 | 1.93E-13 | 1.52E-11 | 4.02E-10 | 5.11E-09 | 3.89E-08 |
| | 3d | 138000 | 0. | 2.24E-34 | 1.25E-28 | 1.58E-24 | 1.89E-21 | 4.68E-19 | 3.84E-17 | 2.85E-14 | 3.18E-12 | 1.09E-10 | 1.69E-09 | 1.52E-08 |
| | 4 | 142100 | 0. | 6.78E-35 | 5.59E-29 | 9.40E-25 | 1.39E-21 | 4.04E-19 | 3.78E-17 | 3.41E-14 | 4.39E-12 | 1.67E-10 | 2.82E-09 | 2.69E-08 |
| $2s\ 2p^4\ (^3P\ )$ | 3 | 212000 | 0. | 0. | 0. | 3.51E-37 | 1.88E-32 | 8.94E-29 | 7.82E-26 | 2.02E-21 | 2.84E-18 | 6.51E-16 | 4.44E-14 | 1.30E-12 |
| | 4 | 222000 | 0. | 0. | 0. | 0. | 9.15E-34 | 6.50E-30 | 7.82E-27 | 3.26E-22 | 6.47E-19 | 1.92E-16 | 1.60E-14 | 5.48E-13 |
| $(^1D\ )$ | 3 | 258000 | 0. | 0. | 0. | 0. | 0. | 3.05E-35 | 1.16E-31 | 2.72E-26 | 1.85E-22 | 1.38E-19 | 2.37E-17 | 1.45E-15 |
| | 4 | 268000 | 0. | 0. | 0. | 0. | 0. | 2.22E-36 | 1.16E-32 | 4.40E-27 | 4.22E-23 | 4.08E-20 | 8.52E-18 | 6.09E-16 |
| $(^1S\ )$ | 3 | 287000 | 0. | 0. | 0. | 0. | 0. | 0. | 5.52E-36 | 5.19E-30 | 9.56E-26 | 1.50E-22 | 4.59E-20 | 4.46E-18 |
| | 4 | 298000 | 0. | 0. | 0. | 0. | 0. | 0. | 4.14E-37 | 6.60E-31 | 1.77E-26 | 3.70E-23 | 1.41E-20 | 1.63E-18 |
| $(^3P\ )$ | 3 | 304000 | 0. | 0. | 0. | 0. | 0. | 0. | 1.24E-37 | 2.64E-31 | 8.71E-27 | 2.12E-23 | 9.10E-21 | 1.16E-18 |
| | 4 | 314000 | 0. | 0. | 0. | 0. | 0. | 0. | 0. | 4.27E-32 | 1.98E-27 | 6.24E-24 | 3.27E-21 | 4.88E-19 |
| $2p^3\ (^2P^o)$ | 3 | 409000 | 0. | 0. | 0. | 0. | 0. | 0. | 0. | 0. | 3.69E-36 | 1.33E-31 | 4.67E-28 | 3.18E-25 |
| | 4 | 419000 | 0. | 0. | 0. | 0. | 0. | 0. | 0. | 0. | 8.40E-37 | 3.93E-32 | 1.68E-28 | 1.34E-25 |

Table 10-9. Energy levels and equilibrium fractional electronic populations of $O^+$.

| State | Level (CM-1) | Level (eV) | Stat. Wt. | Temperature (K) 400 | 500 | 600 | 800 | 1000 | 1500 | 2000 | 2500 | 3000 |
|---|---|---|---|---|---|---|---|---|---|---|---|---|
| $2s^2\ 2p^3\ {}^4S^o$ | 0 | 0.0000 | 4 | 1.00E 00 | 1.00E 00 | 1.00E 00 | 1.00E 00 | 1.00E 00 | 1.00E 00 | 1.00E 00 | 1.00E 00 | 1.00E 00 |
| $^2D^o$ | 26819 | 3.3250 | 10 | 0. | 7.62E-34 | 2.94E-28 | 2.82E-21 | 4.36E-17 | 1.68E-11 | 1.04E-08 | 4.95E-07 | 6.44E-06 |
| $^2P^o$ | 40447 | 5.0171 | 6 | 0. | 0. | 0. | 3.70E-32 | 7.76E-26 | 2.08E-17 | 3.41E-13 | 1.15E-10 | 5.53E-09 |

| State | Level (CM-1) | Level (eV) | Stat. Wt. | Temperature (K) 3500 | 4000 | 4500 | 5000 | 6000 | 7000 | 8000 | 9000 | 10000 |
|---|---|---|---|---|---|---|---|---|---|---|---|---|
| $2s^2\ 2p^3\ {}^4S^o$ | 0 | 0.0000 | 4 | 1.00E 00 | 1.00E 00 | 1.00E 00 | 9.99E-01 | 9.96E-01 | 9.90E-01 | 9.79E-01 | 9.65E-01 | 9.46E-01 |
| $^2D^o$ | 26815 | 3.3250 | 10 | 4.07E-05 | 1.62E-04 | 4.72E-04 | 1.11E-03 | 4.01E-03 | 9.99E-03 | 1.97E-02 | 3.21E-02 | 4.99E-02 |
| $^2P^o$ | 40467 | 5.0171 | 6 | 8.94E-08 | 7.15E-07 | 3.60E-06 | 1.31E-05 | 9.12E-05 | 3.62E-04 | 1.01E-03 | 2.24E-03 | 4.27E-03 |
| $2s\ 2p^4\ {}^4P$ | 110433 | 14.8604 | 12 | 1.16E-21 | 5.52E-19 | 6.66E-17 | 3.08E-15 | 9.66E-13 | 5.84E-11 | 1.26E-09 | 1.36E-08 | 9.10E-08 |
| $^2D$ | 163591 | 20.5797 | 10 | 5.80E-30 | 2.94E-26 | 2.23E-23 | 4.50E-21 | 1.29E-17 | 3.77E-15 | 2.65E-13 | 7.21E-12 | 1.03E-10 |
| $^2S$ | 195710 | 24.2443 | 2 | 5.79E-36 | 1.34E-31 | 3.33E-28 | 1.74E-25 | 2.07E-21 | 1.68E-18 | 2.53E-16 | 1.25E-14 | 2.77E-13 |
| $^2P$ | 212690 | 26.3646 | 6 | 1.63E-38 | 9.06E-34 | 4.44E-30 | 3.98E-27 | 1.07E-22 | 1.55E-19 | 3.61E-17 | 2.49E-15 | 7.32E-14 |
| $2p^5\ {}^2P^o$ | 311400* | 38.3516 | 6 | 0. | 0. | 0. | 0. | 1.32E-33 | 6.50E-29 | 2.38E-25 | 1.33E-22 | 2.09E-20 |
| $2s^2\ 2p^3\ ({}^4P)\ 3s$ | 198604 | 23.1354 | 12 | 2.18E-33 | 3.18E-29 | 5.52E-26 | 2.15E-23 | 1.65E-19 | 9.80E-17 | 1.17E-14 | 4.81E-13 | 9.31E-12 |
| $3p$ | 220204 | 25.9278 | 36 | 6.03E-37 | 2.81E-32 | 1.20E-28 | 9.66E-26 | 2.19E-21 | 2.82E-18 | 6.03E-16 | 3.89E-14 | 1.04E-12 |
| $3d$ | 232563 | 28.8334 | 30 | 0. | 1.05E-35 | 1.15E-31 | 1.94E-28 | 1.35E-23 | 3.87E-20 | 1.31E-17 | 1.55E-15 | 6.25E-14 |
| $4s$ | 239348 | 29.6766 | 12 | 0. | 1.83E-37 | 2.62E-33 | 5.51E-30 | 5.31E-25 | 1.52E-21 | 8.90E-19 | 1.05E-16 | 4.71E-15 |
| $4p$ | 246860** | 30.6089 | 36 | 0. | 3.69E-38 | 7.11E-34 | 1.90E-30 | 2.63E-25 | 1.23E-21 | 6.91E-19 | 9.45E-17 | 4.80E-15 |
| $4d$ | 255006 | 31.6159 | 30 | 0. | 0. | 8.76E-35 | 3.04E-31 | 6.21E-26 | 3.84E-22 | 2.66E-19 | 4.28E-17 | 2.68E-15 |
| $4f$ | 255932 | 31.7307 | 28 | 0. | 0. | 9.12E-35 | 3.26E-31 | 6.97E-26 | 4.45E-22 | 3.16E-19 | 5.17E-17 | 3.03E-15 |
| $({}^2D)\ 3s$ | 284372 | 35.2606 | 10 | 2.80E-37 | 1.16E-32 | 4.55E-29 | 3.40E-26 | 6.94E-22 | 8.28E-19 | 1.67E-16 | 1.03E-14 | 2.76E-13 |
| $3p$ | 289888 | 35.9430 | 30 | 0. | 9.15E-36 | 8.95E-32 | 1.39E-28 | 8.53E-24 | 2.23E-20 | 8.11E-18 | 7.90E-16 | 3.06E-14 |
| $3d$ | 292571 | 36.3140 | 50 | 0. | 0. | 1.06E-34 | 3.41E-31 | 6.19E-26 | 3.52E-22 | 2.25E-19 | 3.51E-17 | 1.95E-15 |
| $4$ | 297230** | 36.8381 | 150 | 0. | 0. | 5.05E-37 | 3.11E-33 | 1.50E-27 | 1.72E-23 | 1.48E-20 | 4.34E-18 | 3.34E-16 |
| $({}^2S)\ 3s$ | 298951* | 37.0252 | 2 | 0. | 1.83E-36 | 1.58E-32 | 2.23E-29 | 1.18E-24 | 2.78E-21 | 9.36E-19 | 8.58E-17 | 3.16E-15 |
| $3p$ | 302751* | 37.5264 | 6 | 0. | 0. | 2.67E-35 | 7.97E-32 | 1.30E-26 | 6.80E-23 | 4.17E-20 | 6.11E-18 | 3.27E-16 |
| $3d$ | 305451* | 37.8727 | 10 | 0. | 0. | 1.20E-38 | 8.15E-35 | 4.55E-29 | 5.76E-25 | 6.84E-22 | 1.67E-19 | 1.39E-17 |
| $4$ | 306500* | 38.0084 | 32 | 0. | 0. | 0. | 8.15E-37 | 1.19E-30 | 2.59E-26 | 5.95E-23 | 2.17E-20 | 2.42E-18 |
| $2s\ 2p^3\ ({}^4S^o)\ 3$ | 291000** | 36.0847 | 30 | 0. | 0. | 0. | 1.72E-34 | 1.22E-28 | 1.34E-24 | 2.48E-21 | 6.72E-19 | 5.88E-17 |
| $4$ | 313000** | 38.8041 | 150 | 0. | 0. | 0. | 0. | 1.01E-31 | 4.54E-27 | 1.40E-23 | 7.17E-21 | 1.09E-18 |
| $({}^2D^o)\ 3$ | 340000* | 42.1549 | 270 | 0. | 0. | 0. | 0. | 2.62E-34 | 2.58E-29 | 1.84E-25 | 1.61E-22 | 3.63E-20 |
| $4$ | 373000* | 46.2449 | 440 | 0. | 0. | 0. | 0. | 0. | 6.01E-32 | 9.63E-28 | 1.47E-24 | 5.60E-22 |
| $({}^2P^o)\ 3-4$ | 383000* | 47.4947 | 450 | 0. | 0. | 0. | 0. | 0. | 7.21E-33 | 1.34E-28 | 2.78E-25 | 1.24E-22 |
| $({}^3S^o, {}^1D^o, {}^3P^o)\ 3-4$ | 417000* | 54.1797 | 550 | 0. | 0. | 0. | 0. | 0. | 0. | 5.92E-33 | 6.06E-29 | 6.42E-26 |
| $2p^4({}^3P, {}^1D, {}^1S)\ 3-4$ | 534000* | 66.2059 | 750 | 0. | 0. | 0. | 0. | 0. | 0. | 0. | 1.52E-35 | 7.61E-32 |

*Estimated. **Includes estimated sublevels.

Nonstarred energy levels from References 10-3, 10-45.

Note: States involving electrons with principal quantum numbers above N = 4 are not included.

All levels above 283244 $cm^{-1}$ are subject to autoionization.

Table 10-10. Energy levels and equilibrium fractional electronic populations of Ar .

| State | | Level (cm⁻¹) | Level (eV) | Stat. Wt. | Temperature (K) 400 | 500 | 600 | 800 | 1000 | 1500 | 2000 | 2500 | 3000 |
|---|---|---|---|---|---|---|---|---|---|---|---|---|---|
| $3s^2 3p^6\ ^1S$ | | 0 | 0.0000 | 1 | 1.00E 00 | 1.00E 00 | 1.00E 00 | 1.00E 00 | 1.00E 00 | 1.00E 00 | 1.00E 00 | 1.00E 00 | 1.00E 00 |
| | | | | | Temperature (K) 3500 | 4000 | 4500 | 5000 | 6000 | 7000 | 8000 | 9000 | 10000 |
| $3s^2 3p^6\ ^1S$ | | 0 | 0.0000 | 1 | 1.00E 00 | 1.00E 00 | 1.00E 00 | 1.00E 00 | 1.00E 00 | 1.00E 00 | 1.00E 00 | 1.00E 00 | 1.00E 00 |
| $3s^2 3p^5\ ^2P^o_{3/2}$ | 3d | 114854 | 14.2397 | 20 | 6.25E-20 | 2.29E-17 | 2.25E-15 | 8.86E-14 | 2.19E-11 | 1.12E-09 | 2.14E-08 | 2.12E-07 | 1.33E-06 |
| | 4s | 95129 | 11.8015 | 4 | 4.06E-17 | 5.40E-15 | 2.42E-13 | 5.08E-12 | 4.89E-10 | 1.27E-08 | 1.47E-07 | 9.85E-07 | 4.51E-06 |
| | 4p | 107421 | 13.3182 | 12 | 7.97E-19 | 1.99E-16 | 1.46E-14 | 4.51E-13 | 7.86E-11 | 3.05E-09 | 4.88E-08 | 4.18E-07 | 2.33E-06 |
| | 4d | 120721 | 14.9671 | 20 | 5.61E-21 | 2.77E-18 | 3.45E-16 | 1.64E-14 | 5.36E-12 | 3.35E-10 | 7.44E-09 | 8.31E-08 | 5.72E-07 |
| | 4f | 121854 | 15.0828 | 28 | 5.35E-21 | 2.77E-18 | 3.59E-16 | 1.75E-14 | 5.99E-12 | 3.87E-10 | 8.81E-09 | 1.00E-07 | 7.01E-07 |
| $3s^2 3p^5\ ^2P^o_{1/2}$ | 3d | 112948 | 14.0036 | 40 | 2.74E-19 | 9.08E-17 | 9.24E-15 | 3.07E-13 | 6.91E-11 | 2.31E-09 | 6.03E-08 | 5.76E-07 | 3.50E-06 |
| | 4s | 93371 | 11.5762 | 8 | 1.71E-16 | 2.08E-14 | 8.67E-13 | 1.72E-11 | 1.51E-09 | 3.70E-08 | 4.08E-07 | 2.63E-06 | 1.17E-05 |
| | 4p | 105681 | 13.0962 | 24 | 9.33E-18 | 7.57E-16 | 5.16E-14 | 1.51E-12 | 2.40E-10 | 8.93E-09 | 1.35E-07 | 1.11E-06 | 6.02E-06 |
| | 4d | 119211 | 14.7769 | 40 | 2.09E-20 | 9.54E-18 | 1.17E-15 | 5.06E-14 | 1.54E-11 | 9.13E-10 | 1.95E-08 | 2.12E-07 | 1.42E-06 |
| | 4f | 120222 | 14.9052 | 56 | 1.93E-20 | 9.28E-18 | 1.13E-15 | 5.29E-14 | 1.65E-11 | 1.04E-09 | 2.38E-08 | 2.52E-07 | 1.72E-06 |
| $3s^2 3p^4\ ^1S$ | 3d | 222000* | 27.5238 | 10 | 0. | 4.18E-34 | 2.98E-30 | 3.51E-27 | 1.52E-22 | 3.05E-19 | 9.15E-17 | 7.72E-15 | 2.69E-13 |
| | 4s | 203000* | 25.1681 | 4 | 2.29E-36 | 7.77E-32 | 2.59E-28 | 1.71E-25 | 2.89E-21 | 3.03E-18 | 5.48E-16 | 3.22E-14 | 8.27E-13 |
| | 4p | 215000* | 26.6559 | 12 | 4.95E-38 | 3.11E-33 | 1.68E-29 | 1.62E-26 | 4.98E-22 | 7.71E-19 | 1.93E-16 | 1.42E-14 | 4.41E-13 |
| | 4d | 227000* | 28.2553 | 20 | 0. | 5.01E-35 | 4.52E-31 | 6.61E-28 | 3.65E-23 | 9.07E-20 | 3.16E-17 | 3.01E-15 | 1.15E-13 |
| | 4f | 228000* | 28.3793 | 28 | 0. | 4.85E-35 | 4.60E-31 | 6.94E-28 | 4.06E-23 | 1.03E-19 | 3.70E-17 | 3.59E-15 | 1.39E-13 |

*Estimated. **Includes estimated sublevels.

Nonstarred energy levels from References 10-3, 10-46, 10-47.

Note: States involving electrons with principal quantum numbers above N = 4 are not included.

All levels above 127110 $cm^{-1}$ are subject to autoionization.

Table 10-11. Energy levels and equilibrium fractional electranic populatians of $Ar^+$.

| State | Level (CM-1) | Level (EV) | Stat. Wt. | Temperature (K) 200 | 250 | 300 | 400 | 500 | 600 | 800 | 1000 | 1500 |
|---|---|---|---|---|---|---|---|---|---|---|---|---|
| $3s^2 3p^5\ ^2P_{3/2}$ | 0 | 0.0000 | 4 | 1.00E 00 | 1.00E 00 | 9.99E-01 | 9.97E-01 | 9.92E-01 | 9.84E-01 | 9.63E-01 | 9.40E-01 | 8.88E-01 |
| $^2P_{1/2}$ | 1432.0 | 0.1775 | 2 | 1.68E-05 | 1.32E-04 | 5.20E-04 | 2.89E-03 | 8.05E-03 | 1.59E-02 | 3.67E-02 | 5.99E-02 | 1.12E-01 |
| $3s\ 3p^6\ ^2S$ | 108723 | 13.4796 | 2 | 0. | 0. | 0. | 0. | 0. | 0. | 0. | 0. | 0. |
| $3s^2 3p^4(^3P)3d\ ^4D$ | 132476 | 16.4245 | 20 | 0. | 0. | 0. | 0. | 0. | 0. | 0. | 0. | 0. |
| 3d other | 146319 | 18.1408 | 70 | 0. | 0. | 0. | 0. | 0. | 0. | 0. | 0. | 0. |
| 4s | 136028 | 16.8649 | 18 | 0. | 0. | 0. | 0. | 0. | 0. | 0. | 0. | 0. |
| 4p | 158023 | 19.5918 | 54 | 0. | 0. | 0. | 0. | 0. | 0. | 0. | 0. | 0. |
| 4d | 186693 | 23.1464 | 90 | 0. | 0. | 0. | 0. | 0. | 0. | 0. | 0. | 0. |
| 4f | 195557 | 24.2466 | 126 | 0. | 0. | 0. | 0. | 0. | 0. | 0. | 0. | 0. |
| $(^1D)3d$ | 164082 | 20.3431 | 50 | 0. | 0. | 0. | 0. | 0. | 0. | 0. | 0. | 0. |
| 4s | 148754 | 18.4427 | 10 | 0. | 0. | 0. | 0. | 0. | 0. | 0. | 0. | 0. |
| 4p | 171831 | 21.3018 | 30 | 0. | 0. | 0. | 0. | 0. | 0. | 0. | 0. | 0. |
| 4d | 199657 | 24.7537 | 50 | 0. | 0. | 0. | 0. | 0. | 0. | 0. | 0. | 0. |
| 4f | 209029 | 25.9156 | 70 | 0. | 0. | 0. | 0. | 0. | 0. | 0. | 0. | 0. |
| $(^1S)3d$ | 179728 | 22.2829 | 10 | 0. | 0. | 0. | 0. | 0. | 0. | 0. | 0. | 0. |
| 4s | 167309 | 20.7432 | 2 | 0. | 0. | 0. | 0. | 0. | 0. | 0. | 0. | 0. |
| 4p | 192095 | 23.8161 | 6 | 0. | 0. | 0. | 0. | 0. | 0. | 0. | 0. | 0. |
| 4d | 220000* | 27.2758 | 10 | 0. | 0. | 0. | 0. | 0. | 0. | 0. | 0. | 0. |
| 4f | 228000* | 28.2677 | 14 | 0. | 0. | 0. | 0. | 0. | 0. | 0. | 0. | 0. |
| $3s\ 3p^5(^2P^*)3d$ | 269000* | 33.3509 | 90 | 0. | 0. | 0. | 0. | 0. | 0. | 0. | 0. | 0. |
| 4s | 249000* | 30.8713 | 18 | 0. | 0. | 0. | 0. | 0. | 0. | 0. | 0. | 0. |
| 4p | 273000* | 33.8468 | 54 | 0. | 0. | 0. | 0. | 0. | 0. | 0. | 0. | 0. |
| 4d | 301000* | 37.3183 | 90 | 0. | 0. | 0. | 0. | 0. | 0. | 0. | 0. | 0. |
| 4f | 309000* | 38.3101 | 126 | 0. | 0. | 0. | 0. | 0. | 0. | 0. | 0. | 0. |

*Estimated.

Nonstarred energy levels from References 10-3, 10-48.

Table 10-11. (Cont'd.)

| State | Level | Temperature (K) | | | | | | | | | | | |
|---|---|---|---|---|---|---|---|---|---|---|---|---|---|
| | (CM-1) | 2000 | 2500 | 3000 | 3500 | 4000 | 4500 | 5000 | 6000 | 7000 | 8000 | 9000 | 10000 |
| $3s^2 3p^4\ ^3P_{3/2}$ | 0 | 8.49E-01 | 8.20E-01 | 7.99E-01 | 7.83E-01 | 7.70E-01 | 7.60E-01 | 7.51E-01 | 7.38E-01 | 7.29E-01 | 7.21E-01 | 7.15E-01 | 7.11E-01 |
| $^3P_{1/2}$ | 1432 | 1.51E-01 | 1.80E-01 | 2.01E-01 | 2.17E-01 | 2.30E-01 | 2.40E-01 | 2.49E-01 | 2.62E-01 | 2.71E-01 | 2.79E-01 | 2.85E-01 | 2.89E-01 |
| $3s\ 3p^5\ ^1S$ | 108723 | 4.56E-35 | 2.74E-28 | 9.04E-24 | 1.52E-20 | 3.99E-18 | 3.04E-16 | 9.72E-15 | 1.76E-12 | 7.18E-11 | 1.16E-09 | 1.01E-08 | 5.72E-08 |
| $3s^1 3p^4\ (^1P)3d\ ^2D$ | 132476 | 0. | 3.17E-33 | 1.02E-27 | 8.74E-24 | 7.78E-21 | 1.53E-18 | 1.04E-16 | 5.90E-14 | 5.44E-12 | 1.62E-10 | 2.27E-09 | 1.87E-08 |
| 3d other | 146319 | 0. | 3.85E-34 | 4.67E-30 | 1.03E-25 | 1.87E-22 | 6.40E-20 | 6.81E-18 | 7.47E-15 | 1.11E-12 | 4.70E-11 | 8.69E-10 | 8.95E-09 |
| 4s | 136028 | 0. | 3.70E-34 | 1.67E-28 | 1.83E-24 | 1.95E-21 | 4.42E-19 | 3.38E-17 | 2.26E-14 | 2.36E-12 | 7.70E-11 | 1.16E-09 | 1.01E-08 |
| 4p | 158023 | 0. | 0. | 1.31E-32 | 6.49E-28 | 2.14E-24 | 1.17E-21 | 1.81E-19 | 3.48E-16 | 7.71E-14 | 4.42E-12 | 1.03E-10 | 1.28E-09 |
| 4d | 186693 | 0. | 0. | 0. | 8.23E-33 | 1.19E-28 | 2.04E-25 | 7.88E-23 | 5.99E-19 | 3.54E-16 | 4.25E-14 | 1.76E-12 | 3.45E-11 |
| 4f | 195567 | 0. | 0. | 0. | 3.00E-34 | 6.83E-30 | 1.67E-26 | 8.59E-24 | 9.99E-20 | 8.01E-17 | 1.21E-14 | 5.96E-13 | 1.35E-11 |
| ($^1D$)3d | 164082 | 0. | 0. | 6.66E-34 | 4.98E-29 | 2.25E-25 | 1.56E-22 | 2.93E-20 | 7.53E-17 | 2.05E-14 | 1.38E-12 | 3.63E-11 | 4.96E-10 |
| 4s | 148754 | 0. | 1.35E-37 | 2.08E-31 | 5.42E-27 | 1.11E-23 | 4.20E-21 | 4.83E-19 | 5.95E-16 | 9.59E-14 | 4.34E-12 | 8.41E-11 | 9.01E-10 |
| 4p | 171831 | 0. | 0. | 9.72E-36 | 1.23E-30 | 8.30E-27 | 7.86E-24 | 1.89E-21 | 7.05E-18 | 2.51E-15 | 2.05E-13 | 6.30E-12 | 9.77E-11 |
| 4d | 199657 | 0. | 0. | 0. | 2.22E-35 | 6.22E-31 | 1.79E-27 | 1.05E-24 | 1.49E-20 | 1.37E-17 | 2.29E-15 | 1.23E-13 | 2.97E-12 |
| 4f | 209029 | 0. | 0. | 0. | 6.58E-37 | 2.99E-32 | 1.25E-28 | 9.91E-26 | 2.20E-21 | 2.80E-18 | 5.95E-16 | 3.85E-14 | 1.08E-12 |
| ($^1S$)3d | 179728 | 0. | 0. | 7.34E-38 | 1.60E-32 | 1.62E-28 | 2.10E-25 | 6.50E-23 | 3.54E-19 | 1.65E-16 | 1.65E-14 | 5.95E-13 | 1.05E-11 |
| 4s | 167309 | 0. | 0. | 5.67E-36 | 5.28E-31 | 2.81E-27 | 2.23E-24 | 4.63E-22 | 1.39E-18 | 4.23E-16 | 3.08E-14 | 8.66E-13 | 1.25E-11 |
| 4p | 192095 | 0. | 0. | 0. | 5.95E-35 | 1.13E-30 | 2.41E-27 | 1.11E-24 | 1.09E-20 | 7.78E-18 | 1.07E-15 | 4.94E-14 | 1.06E-12 |
| 4d | 220000 | 0. | 0. | 0. | 0. | 8.26E-35 | 5.37E-31 | 5.02E-28 | 2.26E-23 | 4.19E-20 | 1.18E-17 | 9.51E-16 | 3.18E-14 |
| 4f | 228000 | 0. | 0. | 0. | 0. | 6.51E-36 | 5.82E-32 | 8.44E-29 | 4.65E-24 | 1.13E-20 | 3.92E-18 | 3.71E-16 | 1.41E-14 |
| $3s\ 3p^3(^3P^o)3d$ | 269000 | 0. | 0. | 0. | 0. | 0. | 7.59E-37 | 4.08E-33 | 1.61E-27 | 1.59E-23 | 1.58E-20 | 3.39E-18 | 2.48E-16 |
| 4s | 249000 | 0. | 0. | 0. | 0. | 0. | 9.09E-35 | 2.58E-31 | 3.89E-26 | 1.94E-22 | 1.15E-19 | 1.66E-17 | 8.83E-16 |
| 4p | 273000 | 0. | 0. | 0. | 0. | 0. | 1.27E-37 | 7.74E-34 | 3.69E-28 | 4.20E-24 | 4.63E-21 | 1.07E-18 | 8.38E-17 |
| 4d | 301000 | 0. | 0. | 0. | 0. | 0. | 0. | 4.09E-37 | 7.47E-31 | 2.22E-26 | 5.01E-23 | 2.04E-20 | 2.49E-18 |
| 4f | 303000 | 0. | 0. | 0. | 0. | 0. | 0. | 5.73E-38 | 1.54E-31 | 5.99E-27 | 1.66E-23 | 7.93E-21 | 1.10E-18 |

Toble 10-12. Energy levels and equilibrium fractionol electronic populotions of CO .

| | | STATE | | | | | | |
|---|---|---|---|---|---|---|---|---|
| | | $X^1\Sigma^+$ | $a^3\Pi$ | $a'^3\Sigma^+$ | $d^3\Delta$ | $e^3\Sigma^-$ | $I^1\Sigma^-$ | $A^1\Pi$ |
| ENERGY | (CM-1) | 0 | 48474 | 55354 | 60647 | 63709 | 64547 | 64747 |
| | (EV) | 0.0000 | 6.0099 | 6.8628 | 7.5191 | 7.8987 | 8.0026 | 8.0273 |
| VIB. | (CM-1) | 2143 | 715 | 1209 | 1138 | 1094 | 1071 | 1481 |
| INT. | (EV) | 0.2657 | 0.2126 | 0.1499 | 0.1410 | 0.1357 | 0.1328 | 0.1836 |

| Temp. (K) | FRACTIONAL POPULATION | | | | | | |
|---|---|---|---|---|---|---|---|
| 200 | 1.00E 00 | 0. | 0. | 0. | 0. | 0. | 0. |
| 250 | 1.00E 00 | 0. | 0. | 0. | 0. | 0. | 0. |
| 300 | 1.00E 00 | 0. | 0. | 0. | 0. | 0. | 0. |
| 400 | 1.00E 00 | 0. | 0. | 0. | 0. | 0. | 0. |
| 500 | 1.00E 00 | 0. | 0. | 0. | 0. | 0. | 0. |
| 600 | 1.00E 00 | 0. | 0. | 0. | 0. | 0. | 0. |
| 800 | 1.00E 00 | 0. | 0. | 0. | 0. | 0. | 0. |
| 1000 | 1.00E 00 | 3.68E-30 | 1.30E-34 | 0. | 0. | 0. | 0. |
| 1500 | 1.00E 00 | 4.77E-20 | 4.85E-23 | 6.43E-25 | 1.79E-26 | 2.73E-27 | 2.98E-27 |
| 2000 | 1.00E 00 | 5.49E-15 | 3.03E-17 | 1.44E-18 | 8.34E-20 | 1.57E-20 | 1.73E-20 |
| 2500 | 1.00E 00 | 5.99E-12 | 9.17E-14 | 9.35E-15 | 8.48E-16 | 1.80E-16 | 1.99E-16 |
| 3000 | 1.00E 00 | 6.37E-10 | 1.93E-11 | 3.28E-12 | 4.01E-13 | 9.20E-14 | 1.02E-13 |
| 3500 | 1.00E 00 | 1.79E-08 | 8.85E-10 | 2.17E-10 | 3.29E-11 | 7.94E-12 | 8.83E-12 |
| 4000 | 1.00E 00 | 2.19E-07 | 1.56E-08 | 5.04E-09 | 8.96E-10 | 2.25E-10 | 2.51E-10 |
| 4500 | 1.00E 00 | 1.53E-06 | 1.46E-07 | 5.84E-08 | 1.18E-08 | 3.03E-09 | 3.40E-09 |
| 5000 | 1.00E 00 | 7.29E-06 | 8.77E-07 | 4.15E-07 | 9.26E-08 | 2.42E-08 | 2.73E-08 |
| 6000 | 1.00E 00 | 7.58E-05 | 1.29E-05 | 7.91E-06 | 2.04E-06 | 5.45E-07 | 6.21E-07 |
| 7000 | 9.99E-01 | 4.05E-04 | 8.82E-05 | 6.48E-05 | 1.86E-05 | 4.97E-06 | 5.73E-06 |
| 8000 | 9.98E-01 | 1.42E-03 | 3.74E-04 | 3.12E-04 | 9.60E-05 | 2.57E-05 | 2.99E-05 |
| 9000 | 9.94E-01 | 3.77E-03 | 1.14E-03 | 1.05E-03 | 3.40E-04 | 9.08E-05 | 1.07E-04 |
| 10000 | 9.85E-01 | 8.15E-03 | 2.75E-03 | 2.71E-03 | 9.17E-04 | 2.45E-04 | 2.89E-04 |

Bosed on energy-level dato from References 10-49, 10-50.

Table 10-13. Energy levels and equilibrium fractional electronic populations of $N_2$.

| | | STATE | | | | | | | |
|---|---|---|---|---|---|---|---|---|---|
| | | $X\ ^1\Sigma_g^+$ | $A\ ^3\Sigma_u^+$ | $B\ ^3\Pi_g$ | $W\ ^3\Delta_u$ | $B'\ ^3\Sigma_u^-$ | $a'\ ^1\Sigma_u^-$ | $a\ ^1\Pi_g$ | $w\ ^1\Delta_u$ |
| ENERGY | (CM-1) | 0 | 49756 | 59310 | 59329 | 65852 | 67739 | 68951 | 71698 |
| | (EV) | 0.0000 | 6.1688 | 7.3533 | 7.3557 | 8.1644 | 8.3984 | 8.5486 | 8.8892 |
| VIB. | (CM-1) | 2330 | 1433 | 1705 | 1505 | 1493 | 1506 | 1666 | 1536 |
| INT. | (EV) | .2888 | .1777 | .2114 | .1866 | .1851 | .1867 | .2066 | .1904 |
| Temp. (K) | | FRACTIONAL POPULATION | | | | | | | |
| 200 | | 1.00E+00 | 0. | 0. | 0. | 0. | 0. | 0. | 0. |
| 250 | | 1.00E+00 | 0. | 0. | 0. | 0. | 0. | 0. | 0. |
| 300 | | 1.00E+00 | 0. | 0. | 0. | 0 | 0. | 0. | 0. |
| 400 | | 1.00E+00 | 0. | 0. | 0. | 0. | 0. | 0. | 0. |
| 500 | | 1.00E+00 | 0. | 0. | 0. | 0. | 0. | 0. | 0. |
| 600 | | 1.00E+00 | 0. | 0. | 0. | 0. | 0. | 0. | 0. |
| 800 | | 1.00E+00 | 0. | 0. | 0. | 0. | 0. | 0. | 0. |
| 1000 | | 1.00E+00 | 0. | 0. | 0. | 0. | 0. | 0. | 0. |
| 1500 | | 1.00E+00 | 0. | 0. | 0. | 0. | 0. | 0. | 0. |
| 2000 | | 1.00E+00 | 1.51E-15 | 2.51E-18 | 3.02E-18 | 1.36E-20 | 0. | 0. | 0. |
| 2500 | | 1.00E+00 | 2.03E-12 | 1.31E-14 | 1.61E-14 | 1.84E-16 | 2.05E-17 | 1.75E-17 | 4.09E-18 |
| 3000 | | 1.00E+00 | 2.49E-10 | 3.97E-12 | 4.92E-12 | 1.05E-13 | 1.40E-14 | 1.34E-14 | 4.09E-15 |
| 3500 | | 1.00E+00 | 7.75E-09 | 2.35E-10 | 2.94E-10 | 9.83E-12 | 1.49E-12 | 1.54E-12 | 5.69E-13 |
| 4000 | | 1.00E+00 | 1.02E-07 | 5.04E-09 | 6.35E-09 | 2.96E-10 | 4.94E-11 | 5.40E-11 | 2.31E-11 |
| 4500 | | 1.00E+00 | 7.64E-07 | 5.47E-08 | 6.93E-08 | 4.19E-09 | 7.54E-10 | 8.62E-10 | 4.13E-10 |
| 5000 | | 1.00E+00 | 3.82E-06 | 3.69E-07 | 4.70E-07 | 3.50E-08 | 6.68E-09 | 7.92E-09 | 4.15E-09 |
| 6000 | | 1.00E+00 | 4.28E-05 | 6.47E-06 | 8.32E-06 | 8.48E-07 | 1.77E-07 | 2.21E-07 | 1.33E-07 |
| 7000 | | 1.00E+00 | 2.40E-04 | 5.02E-05 | 6.48E-05 | 8.29E-06 | 1.84E-06 | 2.39E-06 | 1.59E-06 |
| 8000 | | 9.99E-01 | 8.67E-04 | 2.33E-04 | 3.02E-04 | 4.59E-05 | 1.07E-05 | 1.43E-05 | 1.02E-05 |
| 9000 | | 9.96E-01 | 2.33E-03 | 7.64E-04 | 9.94E-04 | 1.74E-04 | 4.19E-05 | 5.76E-05 | 4.34E-05 |
| 10000 | | 9.89E-01 | 5.08E-03 | 1.96E-03 | 2.56E-03 | 5.00E-04 | 1.25E-04 | 1.75E-04 | 1.38E-04 |

Based on energy-level data from References 10-51, 10-52.

Table 10-14. Energy levels and equilibrium fractianal electronic populations of $N_2^+$.

| | | STATE | | | | | | | |
|---|---|---|---|---|---|---|---|---|---|
| | | $X^2\Sigma_g^+$ | $A^2\Pi_u$ | $B^2\Sigma_u^+$ | $4\Sigma_u^+$ | $4\Delta_u$ | $D^2\Pi_g$ | $4\Sigma_u^-$ | $C^2\Sigma_u^+$ |
| ENERGY | (CM-1) | 0 | 3068 | 25566 | 44328 | 51328 | 51203 | 60328 | 64542 |
| | (EV) | 0.0000 | 1.0003 | 3.1697 | 5.4958 | 6.3637 | 6.3482 | 7.4795 | 8.0020 |
| VIB. | (CM-1) | 2175 | 1873 | 2371 | 1668 | 1572 | 889 | 1472 | 2051 |
| INT. | (EV) | 0.2696 | 0.2323 | 0.2940 | 0.2068 | 0.1949 | 0.1102 | 0.1825 | 0.2543 |
| Temp. (K) | | FRACTIONAL POPULATION | | | | | | | |
| 200 | | 1.00E 00 | 1.37E-25 | 0. | 0. | 0. | 0. | 0. | 0. |
| 250 | | 1.00E 00 | 1.51E-20 | 0. | 0. | 0. | 0. | 0. | 0. |
| 300 | | 1.00E 00 | 3.46E-17 | 0. | 0. | 0. | 0. | 0. | 0. |
| 400 | | 1.00E 00 | 5.50E-13 | 0. | 0. | 0. | 0. | 0. | 0. |
| 500 | | 1.00E 00 | 1.83E-10 | 1.04E-32 | 0. | 0. | 0. | 0. | 0. |
| 600 | | 1.00E 00 | 8.79E-09 | 2.19E-27 | 0. | 0. | 0. | 0. | 0. |
| 800 | | 1.00E 00 | 1.12E-06 | 9.87E-21 | 5.92E-35 | 0. | 0. | 0. | 0. |
| 1000 | | 1.00E 00 | 2.06E-05 | 9.68E-17 | 5.08E-28 | 4.37E-32 | 4.75E-32 | 0. | 0. |
| 1500 | | 9.99E-01 | 1.01E-03 | 2.02E-11 | 9.09E-19 | 2.26E-21 | 2.57E-21 | 2.37E-25 | 1.67E-27 |
| 2000 | | 9.93E-01 | 7.08E-03 | 9.13E-09 | 3.86E-14 | 5.19E-16 | 6.16E-16 | 4.74E-19 | 8.81E-21 |
| 2500 | | 9.77E-01 | 2.26E-02 | 3.53E-07 | 2.29E-11 | 8.49E-13 | 1.04E-12 | 2.85E-15 | 9.40E-17 |
| 3000 | | 9.52E-01 | 4.82E-02 | 3.97E-06 | 1.30E-09 | 1.16E-10 | 1.48E-10 | 9.29E-13 | 4.48E-14 |
| 3500 | | 9.18E-01 | 8.16E-02 | 2.20E-05 | 3.26E-08 | 3.85E-09 | 5.02E-09 | 5.71E-11 | 3.61E-12 |
| 4000 | | 8.81E-01 | 1.19E-01 | 7.85E-05 | 3.07E-07 | 5.24E-08 | 6.99E-08 | 1.24E-09 | 9.54E-11 |
| 4500 | | 8.41E-01 | 1.58E-01 | 2.08E-04 | 1.73E-06 | 3.94E-07 | 5.34E-07 | 1.34E-08 | 1.20E-09 |
| 5000 | | 8.03E-01 | 1.97E-01 | 4.50E-04 | 6.84E-06 | 1.96E-06 | 2.69E-06 | 3.90E-08 | 9.02E-09 |
| 6000 | | 7.32E-01 | 2.67E-01 | 1.41E-03 | 5.19E-05 | 2.13E-05 | 2.93E-05 | 1.49E-06 | 1.80E-07 |
| 7000 | | 6.71E-01 | 3.25E-01 | 3.13E-03 | 2.14E-04 | 1.14E-04 | 1.55E-04 | 1.09E-05 | 1.48E-06 |
| 8000 | | 6.21E-01 | 3.72E-01 | 5.66E-03 | 6.00E-04 | 3.96E-04 | 5.23E-04 | 4.71E-05 | 6.97E-06 |
| 9000 | | 5.78E-01 | 4.09E-01 | 8.92E-03 | 1.31E-03 | 1.02E-03 | 1.31E-03 | 1.44E-04 | 2.27E-05 |
| 10000 | | 5.41E-01 | 4.38E-01 | 1.28E-02 | 2.38E-03 | 2.16E-03 | 2.65E-03 | 3.45E-04 | 5.72E-05 |

Table 10-15. Energy levels and equilibrium fractional electronic populations of NO .

| | | STATE | | | | | | |
|---|---|---|---|---|---|---|---|---|
| | | $X^2\Pi$ | $a^4\Pi$ | $A^2\Sigma^+$ | $B^2\Pi$ | $b^4\Sigma^-$ | $C^2\Pi$ | $D^2\Sigma^+$ |
| ENERGY | (CM-1) | 67* | ~37965 | 44199 | 45505 | ~47092 | 52380† | 53291 |
| | (EV) | 0.0077* | ~4.7069 | 5.4799 | 5.6418 | ~5.8385 | 6.4941† | 6.6071 |
| VIB. | (CM-1) | 1876 | 995 | 2342 | 1023 | ~1203 | 2365† | 2279 |
| INT. | (EV) | 0.2326 | 0.1234 | 0.2903 | 0.1268 | ~0.1491 | 0.2932† | 0.2826 |

| Temp. (K) | FRACTIONAL POPULATION | | | | | | |
|---|---|---|---|---|---|---|---|
| 200 | 1.00E 00 | 0. | 0. | 0. | 0. | 0. | 0. |
| 250 | 1.00E 00 | 0. | 0. | 0. | 0. | 0. | 0. |
| 300 | 1.00E 00 | 0. | 0. | 0. | 0. | 0. | 0. |
| 400 | 1.00E 00 | 0. | 0. | 0. | 0. | 0. | 0. |
| 500 | 1.00E 00 | 0. | 0. | 0. | 0. | 0. | 0. |
| 600 | 1.00E 00 | 0. | 0. | 0. | 0. | 0. | 0. |
| 800 | 1.00E 00 | 8.47E-30 | 1.40E-35 | 0. | 0. | 0. | 0. |
| 1000 | 1.00E 00 | 7.49E-24 | 1.08E-28 | 7.45E-29 | 5.89E-30 | 1.67E-33 | 2.26E-34 |
| 1500 | 1.00E 00 | 6.58E-16 | 1.63E-19 | 2.41E-19 | 3.99E-20 | 1.27E-22 | 2.68E-23 |
| 2000 | 1.00E 00 | 6.31E-12 | 6.26E-15 | 1.40E-14 | 3.34E-15 | 3.48E-17 | 9.07E-18 |
| 2500 | 1.00E 00 | 1.56E-09 | 3.49E-12 | 1.01E-11 | 3.04E-12 | 6.30E-14 | 1.85E-14 |
| 3000 | 1.00E 00 | 6.20E-08 | 2.34E-10 | 8.24E-10 | 2.87E-10 | 9.31E-12 | 2.93E-12 |
| 3500 | 1.00E 00 | 8.61E-07 | 4.65E-09 | 1.91E-08 | 7.43E-09 | 3.26E-10 | 1.06E-10 |
| 4000 | 1.00E 00 | 6.17E-06 | 4.32E-08 | 2.02E-07 | 8.56E-08 | 4.65E-09 | 1.54E-09 |
| 4500 | 1.00E 00 | 2.83E-05 | 2.41E-07 | 1.27E-06 | 5.74E-07 | 3.63E-08 | 1.21E-08 |
| 5000 | 1.00E 00 | 9.52E-05 | 9.40E-07 | 5.51E-06 | 2.63E-06 | 1.86E-07 | 6.20E-08 |
| 6000 | 9.99E-01 | 5.73E-04 | 7.00E-06 | 4.98E-05 | 2.57E-05 | 2.09E-06 | 6.89E-07 |
| 7000 | 9.98E-01 | 2.00E-03 | 2.82E-05 | 2.37E-04 | 1.29E-04 | 1.13E-05 | 3.68E-06 |
| 8000 | 9.94E-01 | 4.94E-03 | 7.75E-05 | 7.56E-04 | 4.22E-04 | 3.88E-05 | 1.24E-05 |
| 9000 | 9.87E-01 | 9.73E-03 | 1.65E-04 | 1.83E-03 | 1.04E-03 | 9.85E-05 | 3.11E-05 |
| 10000 | 9.77E-01 | 1.63E-02 | 2.94E-04 | 3.65E-03 | 2.11E-03 | 2.02E-04 | 6.29E-05 |

*Average energy of the two spin components, above that of the lower component ($^2\Pi_{1/2}$) .

†"Deperturbed" values.

Based on data from Reference 10-7.

Table 10-16. Energy levels and equilibrium fractional electronic populations of $NO^+$.

| | | STATE | | | | | | | |
|---|---|---|---|---|---|---|---|---|---|
| | | $X\ ^1\Sigma^+$ | $a\ ^3\Sigma^+$ | $b\ ^3\Pi$ | $w\ ^3\Delta$ | $b'\ ^3\Sigma^-$ | $A'\ ^1\Sigma^-$ | $w\ ^1\Delta$ | $A\ ^1\Pi$ |
| ENERGY | (CM-1) | 0 | 51470 | 58810 | 61250 | 67090 | 68910 | 70850 | 73084 |
| | (EV) | 0.0000 | 6.3813 | 7.2913 | 7.5938 | 8.3179 | 8.5435 | 8.7841 | 9.0610 |
| VIB. | (CM-1) | 2344 | 1258 | 1698 | 1306 | 1290 | 1253 | 1216 | 1561 |
| INT. | (EV) | .2907 | .1560 | .2105 | .1619 | .1599 | .1553 | .1508 | .1935 |
| Temp. (K) | | FRACTIONAL POPULATION | | | | | | | |
| 200 | | 1.00E+00 | 0. | 0. | 0. | 0. | 0. | 0. | 0. |
| 250 | | 1.00E+00 | 0. | 0. | 0. | 0. | 0. | 0. | 0. |
| 300 | | 1.00E+00 | 0. | 0. | 0. | 0. | 0. | 0. | 0. |
| 400 | | 1.00E+00 | 0. | 0. | 0. | 0. | 0. | 0. | 0. |
| 500 | | 1.00E+00 | 0. | 0. | 0. | 0. | 0. | 0. | 0. |
| 600 | | 1.00E+00 | 0. | 0. | 0. | 0. | 0. | 0. | 0. |
| 800 | | 1.00E+00 | 0. | 0. | 0. | 0. | 0. | 0. | 0. |
| 1000 | | 1.00E+00 | 0. | 0. | 0. | 0. | 0. | 0. | 0. |
| 1500 | | 1.00E+00 | 0. | 0. | 0. | 0. | 0. | 0. | 0. |
| 2000 | | 1.00E+00 | 5.21E-16 | 3.61E-18 | 8.95E-19 | 0. | 0. | 0. | 0. |
| 2500 | | 1.00E+00 | 9.06E-13 | 1.76E-14 | 6.34E-15 | 1.11E-16 | 1.33E-17 | 8.90E-18 | 1.75E-18 |
| 3000 | | 1.00E+00 | 1.32E-10 | 5.08E-12 | 2.35E-12 | 7.24E-14 | 1.03E-14 | 8.33E-15 | 2.01E-15 |
| 3500 | | 1.00E+00 | 4.64E-09 | 2.92E-10 | 1.62E-10 | 7.44E-12 | 1.22E-12 | 1.11E-12 | 3.10E-13 |
| 4000 | | 1.00E+00 | 6.73E-08 | 6.09E-09 | 3.87E-09 | 2.41E-10 | 4.37E-11 | 4.36E-11 | 1.36E-11 |
| 4500 | | 1.00E+00 | 5.40E-07 | 6.48E-08 | 4.58E-08 | 3.62E-09 | 7.12E-10 | 7.59E-10 | 2.59E-10 |
| 5000 | | 1.00E+00 | 2.86E-06 | 4.30E-07 | 3.32E-07 | 3.16E-08 | 6.67E-09 | 7.47E-09 | 2.73E-09 |
| 6000 | | 1.00E+00 | 3.49E-05 | 7.36E-06 | 6.48E-06 | 8.19E-07 | 1.92E-07 | 2.30E-07 | 9.30E-08 |
| 7000 | | 1.00E+00 | 2.09E-04 | 5.60E-05 | 5.42E-05 | 8.35E-06 | 2.12E-06 | 2.63E-06 | 1.14E-06 |
| 8000 | | 9.99E-01 | 7.98E-04 | 2.56E-04 | 2.66E-04 | 4.72E-05 | 1.27E-05 | 1.62E-05 | 7.41E-06 |
| 9000 | | 9.96E-01 | 2.25E-03 | 8.29E-04 | 9.10E-04 | 1.80E-04 | 5.04E-05 | 6.53E-05 | 3.11E-05 |
| 10000 | | 9.89E-01 | 5.09E-03 | 2.10E-03 | 2.41E-03 | 5.15E-04 | 1.49E-04 | 1.96E-04 | 9.62E-05 |

Based on energy-level data from Reference 10-53.

Table 10-17 Energy levels and equilibrium fractional electronic populations of $O_2$.

| | | STATE | | | | | | |
|---|---|---|---|---|---|---|---|---|
| | | $X\ ^3\Sigma_g^-$ | $a\ ^1\Delta_g$ | $b\ ^1\Sigma_g^+$ | $c\ ^1\Sigma_u^-$ | $C\ ^3\Delta_u$ | $A\ ^3\Sigma_u^+$ | $B\ ^3\Sigma_u^-$ |
| ENERGY | (CM-1) | 0 | 7882 | 13121 | 32664 | 34329 | 35009 | 49358 |
| | (EV) | 0.0000 | .9773 | 1.6267 | 4.0497 | 4.2561 | 4.3404 | 6.1194 |
| VIB. | (CM-1) | 1556 | 1483 | 1405 | 768 | 820 | 771 | 688 |
| INT. | (EV) | .1930 | .1839 | .1742 | .0952 | .1017 | .0956 | .0853 |

| Temp. (K) | FRACTIONAL POPULATION | | | | | | |
|---|---|---|---|---|---|---|---|
| 200 | 1.00E+00 | 0. | 0. | 0. | 0. | 0. | 0. |
| 250 | 1.00E+00 | 1.34E-20 | 0. | 0. | 0. | 0. | 0. |
| 300 | 1.00E+00 | 2.58E-17 | 0. | 0. | 0. | 0. | 0. |
| 400 | 1.00E+00 | 3.29E-13 | 0. | 0. | 0. | 0. | 0. |
| 500 | 1.00E+00 | 9.56E-11 | 1.39E-17 | 0. | 0. | 0. | 0. |
| 600 | 1.00E+00 | 4.20E-09 | 7.54E-15 | 0. | 0. | 0. | 0. |
| 800 | 1.00E+00 | 4.76E-07 | 1.99E-11 | 0. | 0. | 0. | 0. |
| 1000 | 1.00E+00 | 8.14E-06 | 2.25E-09 | 0. | 0. | 0. | 0. |
| 1500 | 1.00E+00 | 3.60E-04 | 1.24E-06 | 2.04E-14 | 2.30E-14 | 6.28E-15 | 0. |
| 2000 | 9.98E-01 | 2.39E-03 | 2.91E-05 | 5.58E-11 | 9.29E-11 | 2.88E-11 | 1.25E-15 |
| 2500 | 9.92E-01 | 7.44E-03 | 1.94E-04 | 6.39E-09 | 1.32E-08 | 4.36E-09 | 1.57E-12 |
| 3000 | 9.84E-01 | 1.58E-02 | 6.81E-04 | 1.47E-07 | 3.47E-07 | 1.19E-07 | 1.78E-10 |
| 3500 | 9.72E-01 | 2.66E-02 | 1.87E-03 | 1.35E-06 | 3.46E-06 | 1.21E-06 | 5.07E-09 |
| 4000 | 9.57E-01 | 3.97E-02 | 3.25E-03 | 6.91E-06 | 1.88E-05 | 6.67E-06 | 6.07E-08 |
| 4500 | 9.41E-01 | 5.37E-02 | 5.43E-03 | 2.40E-05 | 6.82E-05 | 2.44E-05 | 4.07E-07 |
| 5000 | 9.23E-01 | 6.81E-02 | 8.16E-03 | 6.37E-05 | 1.86E-04 | 6.73E-05 | 1.82E-06 |
| 6000 | 8.88E-01 | 9.60E-02 | 1.48E-02 | 2.60E-04 | 7.95E-04 | 2.90E-04 | 1.63E-05 |
| 7000 | 8.53E-01 | 1.21E-01 | 2.24E-02 | 6.72E-04 | 2.11E-03 | 7.74E-04 | 7.38E-05 |
| 8000 | 8.20E-01 | 1.43E-01 | 3.00E-02 | 1.31E-03 | 4.20E-03 | 1.54E-03 | 2.19E-04 |
| 9000 | 7.90E-01 | 1.60E-01 | 3.71E-02 | 2.13E-03 | 6.93E-03 | 2.56E-03 | 4.92E-04 |
| 10000 | 7.64E-01 | 1.75E-01 | 4.35E-02 | 3.07E-03 | 1.01E-02 | 3.73E-03 | 9.19E-04 |

Based on energy-level data from References 10-51, 10-54.

Toble 10-18. Energy levels and equilibrium fractianal electronic populations of $O_2^+$ .

| | | STATE | | | |
|---|---|---|---|---|---|
| | | $X\ ^2\Pi_g$ | $a\ ^4\Pi_u$ | $A\ ^2\Pi_u$ | $b\ ^4\Sigma_g^-$ |
| ENERGY | (CM-1) | 100 | 32624 | 40170 | 49291 |
| | (EV) | .0124 | 4.0448 | 4.9803 | 6.1111 |
| VIB. | (CM-1) | 1873 | 1015 | 871 | 1163 |
| INT. | (EV) | .2322 | .1258 | .1080 | .1441 |

| Temp. (K) | FRACTIONAL POPULATION | | | |
|---|---|---|---|---|
| 200 | 1.00E+00 | 0. | 0. | 0. |
| 250 | 1.00E+00 | 0. | 0. | 0. |
| 300 | 1.00E+00 | 0. | 0. | 0. |
| 400 | 1.00E+00 | 0. | 0. | 0. |
| 500 | 1.00E+00 | 0. | 0. | 0. |
| 600 | 1.00E+00 | 0. | 0. | 0. |
| 800 | 1.00E+00 | 0. | 0. | 0. |
| 1000 | 1.00E+00 | 1.78E-20 | 0. | 0. |
| 1500 | 1.00E+00 | 1.18E-13 | 4.97E-17 | 0. |
| 2000 | 1.00E+00 | 3.10E-10 | 8.23E-13 | 7.57E-16 |
| 2500 | 1.00E+00 | 3.53E-08 | 2.85E-10 | 9.42E-13 |
| 3000 | 1.00E+00 | 8.35E-07 | 1.42E-08 | 1.10E-10 |
| 3500 | 1.00E+00 | 8.04E-06 | 2.32E-07 | 3.31E-09 |
| 4000 | 1.00E+00 | 4.41E-05 | 1.88E-06 | 4.27E-08 |
| 4500 | 1.00E+00 | 1.66E-04 | 9.46E-06 | 3.13E-07 |
| 5000 | 9.99E-01 | 4.78E-04 | 3.42E-05 | 1.54E-06 |
| 6000 | 9.97E-01 | 2.32E-03 | 2.28E-04 | 1.66E-05 |
| 7000 | 9.92E-01 | 7.03E-03 | 8.47E-04 | 8.87E-05 |
| 8000 | 9.82E-01 | 1.57E-02 | 2.19E-03 | 3.04E-04 |
| 9000 | 9.66E-01 | 2.87E-02 | 4.42E-03 | 7.73E-04 |
| 10000 | 9.46E-01 | 4.53E-02 | 7.53E-03 | 1.59E-03 |

* Average energy of the two spin components, abave that of the lawer component ($^2\Pi_{1/2}$) .
Based on energy-level data from Reference 10-55.

Table 10-19. Lower electronic and vibrational energy levels of selected diatomic molecules. Units: $cm^{-1}$ and eV.

| Molecule | State | Electronic Energy | Lowest Vibrational Interval | References |
|---|---|---|---|---|
| $H_2$ | $X^1\Sigma_g^+$ | 0 $cm^{-1}$<br>0 eV | 4161 $cm^{-1}$<br>0.516 eV | 10-56 |
| $H_2^+$ | $X^2\Sigma_g^+$ | 0<br>0 | 2191<br>0.272 | 10-15 |
| $CO^+$ | $X^2\Sigma^+$ | 0<br>0 | 2184<br>0.271 | 10-57 |
| | $A^2\Pi$ | 20408<br>2.530 | 1535<br>0.190 | |
| | $B^2\Sigma^+$ | 45633<br>5.658 | 1679<br>0.208 | |
| $NO^-$ | $X^3\Sigma^-$ | 0<br>0 | (1355)<br>(0.168) | 10-58 |
| $O_2^-$ | $X^2\Pi_g$ | 0<br>0 | (1065)<br>(0.132) | 10-59 |
| $OH^-$ | $X^1\Sigma^+$ | 0<br>0 | (3600)<br>(0.446) | 10-31 |
| OH | $X^2\Pi$ | 0<br>0 | 3570<br>0.443 | 10-57 |
| | $A^2\Sigma^+$ | 32402<br>4.017 | 2989<br>0.371 | |
| $OH^+$ | $X^3\Sigma^-$ | 0<br>0 | 2967<br>0.368 | 10-57 |
| | $A^3\Pi$ | 27952<br>3.466 | 1986<br>0.246 | |

Table 10-20. Vibrotionol spocing of triotomic molecules.

| Molecule | Ground State | Vibrotionol Intervals ($cm^{-1}$; eV) | | | References |
|---|---|---|---|---|---|
| | | $\nu_1$ | $\nu_2$ | $\nu_3$ | |
| $H_2O$ | $^1A_1$ | 3657 $cm^{-1}$<br>0.453 eV | 1595 $cm^{-1}$<br>0.198 eV | 3756 $cm^{-1}$<br>0.466 eV | 10-34 |
| $H_2O^+$ | $(^2B_1)$ | (~3200)<br>(~0.40) | (~1500)<br>(~0.19) | (~3300)<br>(~0.41) | * |
| $CO_2$ | $1\Sigma_g^+$ | 1388<br>0.172 | 667<br>0.083 | 2349<br>0.291 | 10-34 |
| $CO_2^+$ | $^2\Pi_g$ | 1280<br>0.159 | (~400)<br>(~0.05) | (1469)<br>(0.182) | 10-34 |
| $NO_2^-$ | $^1A_1$ | (1280)<br>(0.159) | (790)<br>(0.098) | (1210)<br>(0.150) | 10-60** |
| $NO_2$ | $^2A_1$ | (1320)<br>(0.164) | 750<br>0.093 | 1618<br>0.201 | 10-34 |
| $NO_2^+$ | $(1\Sigma_g^+)$ | (1396)<br>(0.173) | (571)<br>(0.071) | (2360)<br>(0.293) | 10-62 |
| $N_2O$ | $1\Sigma^+$ | 2224<br>0.276 | 589<br>0.073 | 1285<br>0.159 | 10-34 |
| $N_2O^+$ | $^2\Pi$ | 1737<br>0.215 | 461<br>0.057 | 1126<br>0.140 | 10-34 |
| $O_3^-$ | $(^2B_1)$ | (1260)<br>(0.156) | (800)<br>(0.099) | (1140)<br>(0.141) | 10-63 |
| $O_3$ | $^1A_1$ | 1110<br>0.138 | 705<br>0.087 | 1042<br>0.129 | 10-34 |
| $O_3^+$ | $(^2A_1)$ | (~1300)<br>(~0.16) | (~700)<br>(~0.09) | (~1600)<br>(~0.20) | *** |

* Vibrationol intervols estimated from Rydberg states of $H_2O$ .

** Values measured in potassium halide crystals extrapolated to the isolated ion in the manner of Holzer et ol (Reference 10-61).

*** Vibrational intervals estimated from $NO_2$.

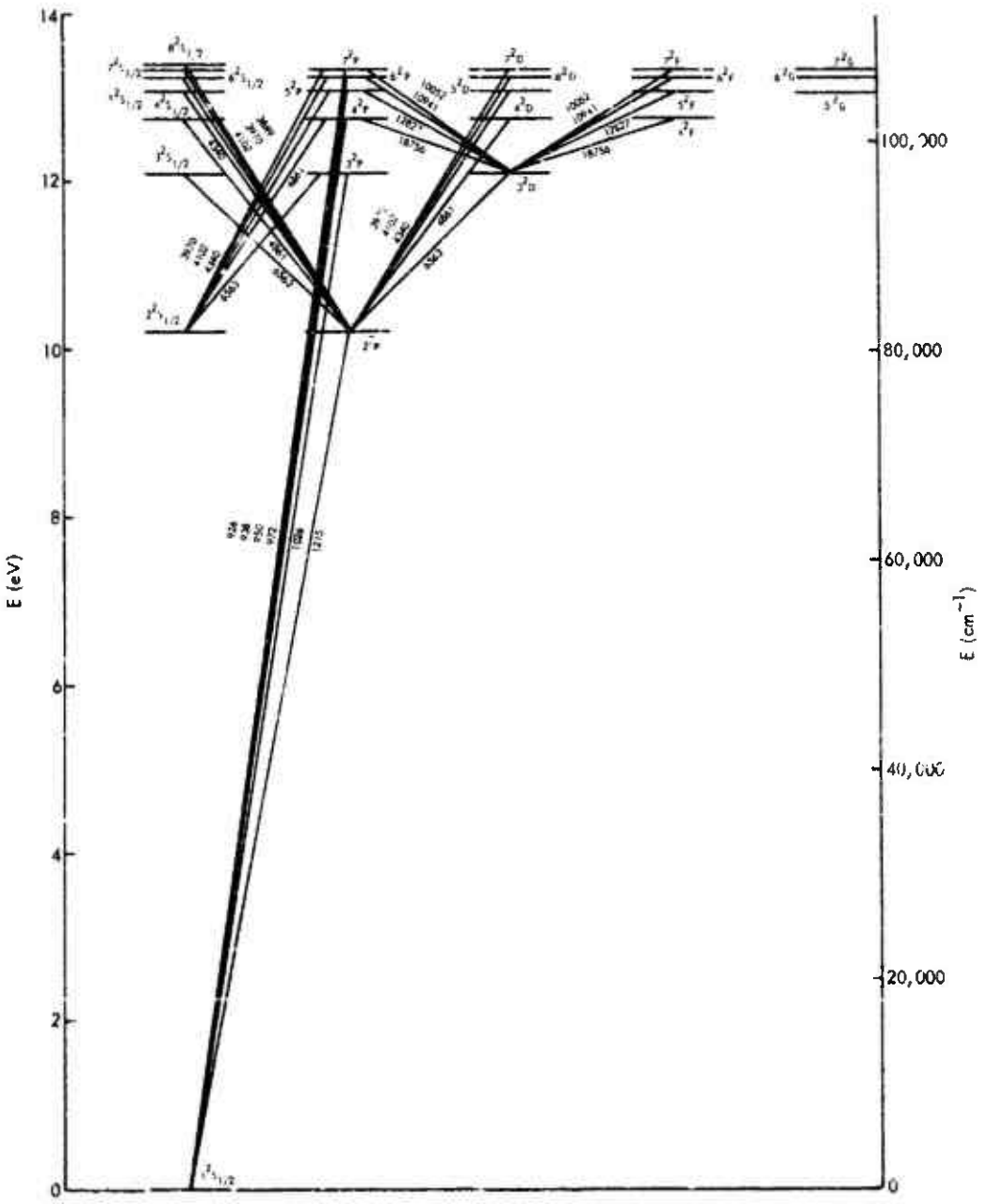


Figure 10-1. Partial Grotrian diagram of hydrogen atom.

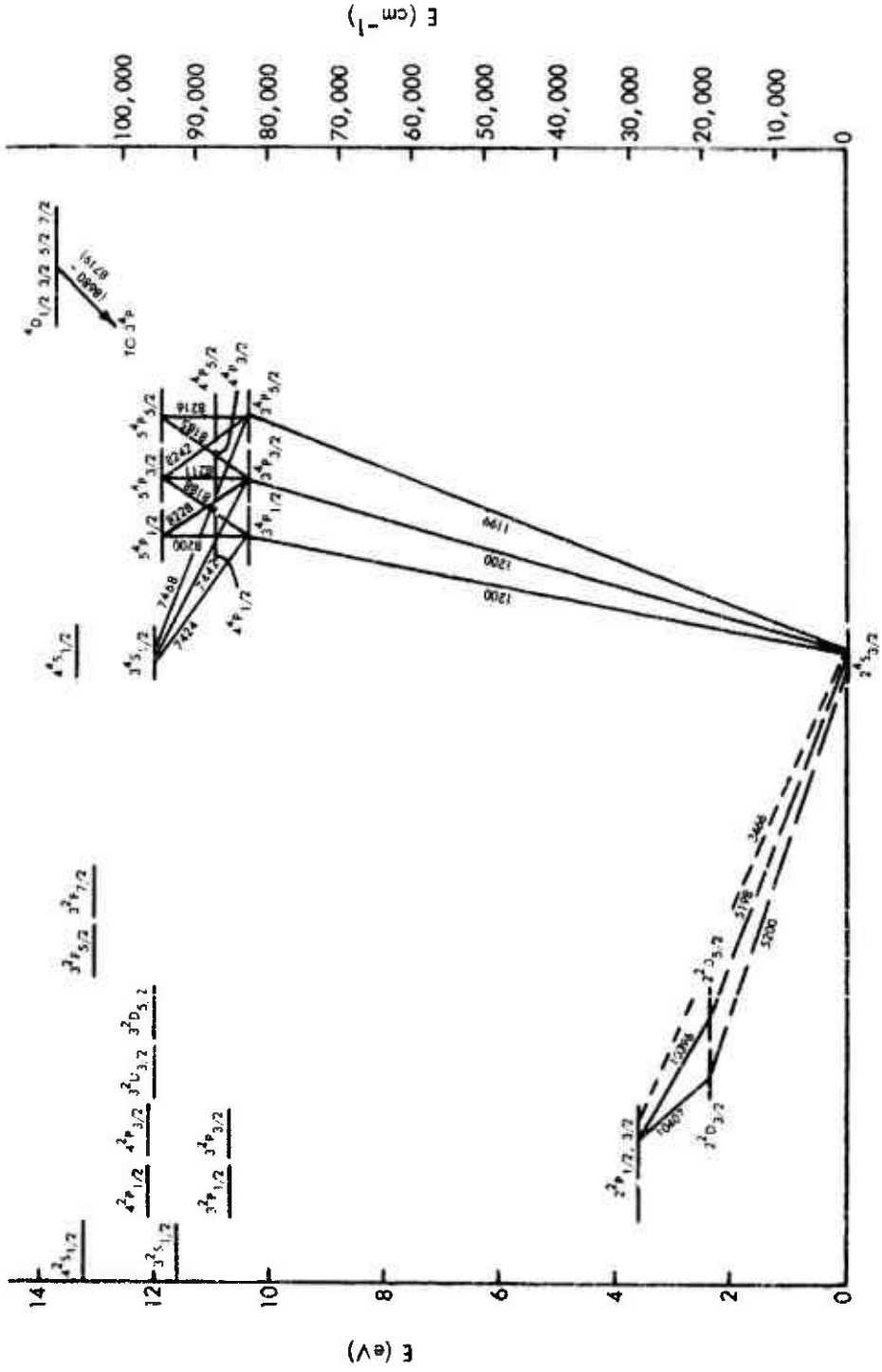


Figure 10-2. Partial Gratrian diagram of atomic nitrogen.

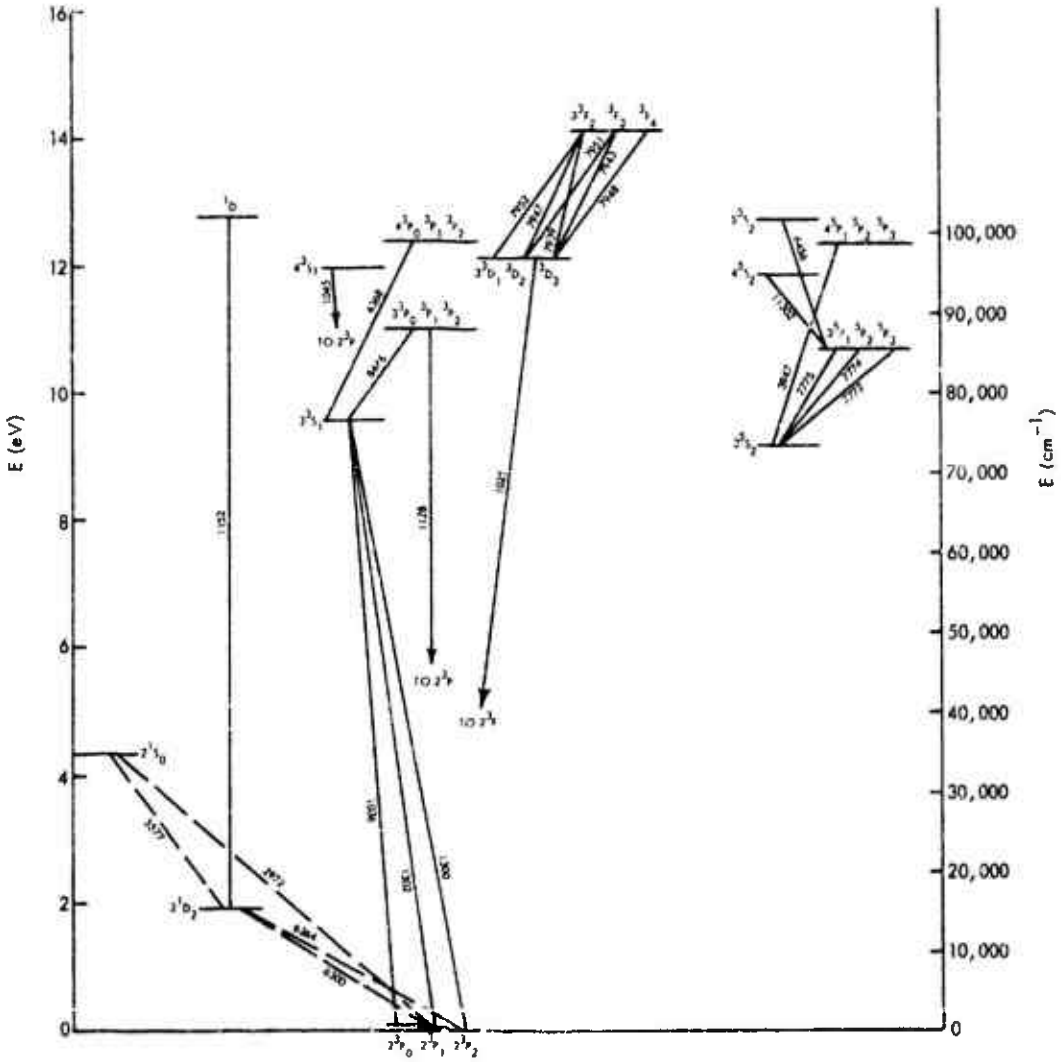


Figure 10-3. Partial Grotrian diagram of atomic oxygen.

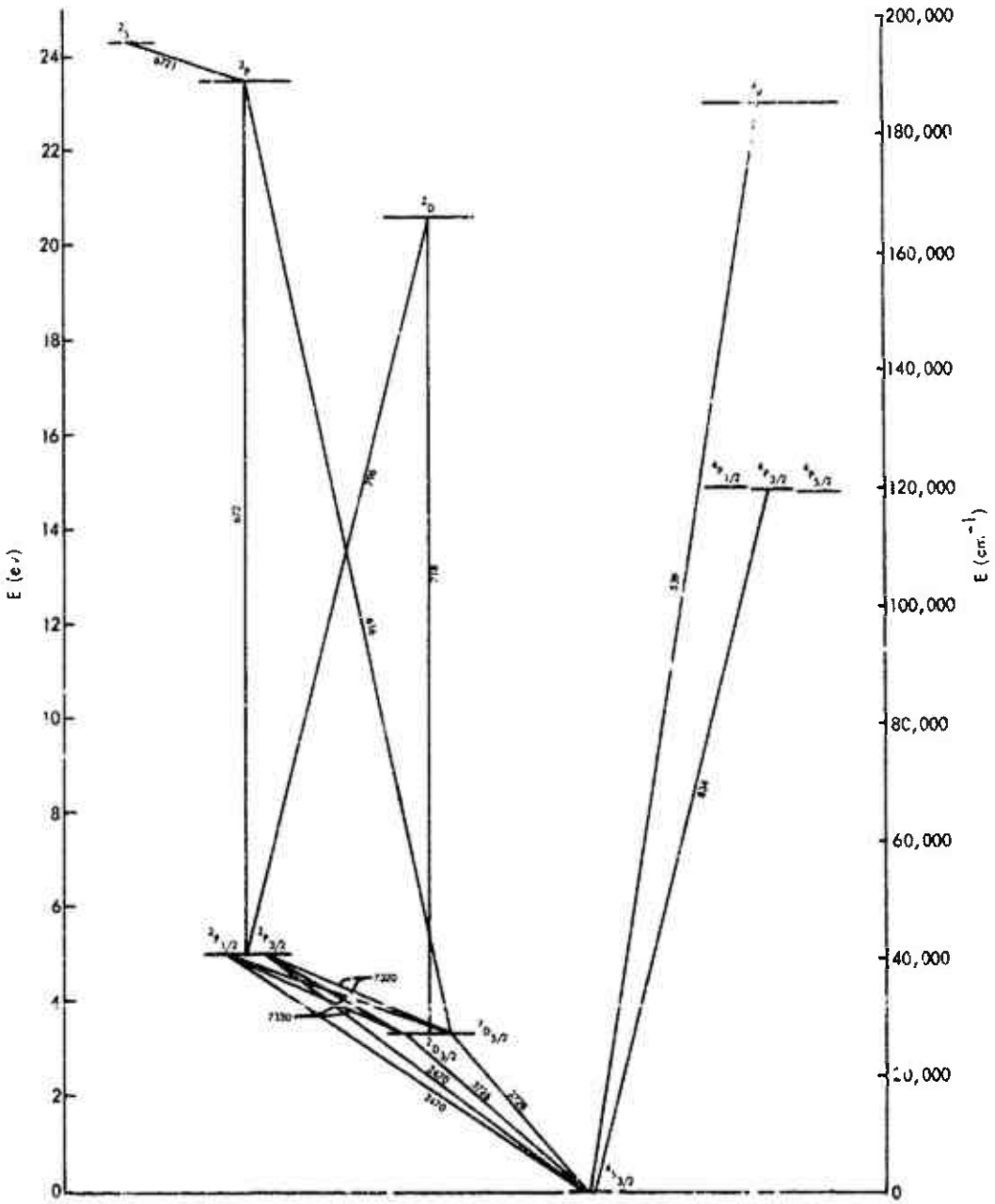


Figure 10-4. Partial Gratrian diagram of $O^+$ .

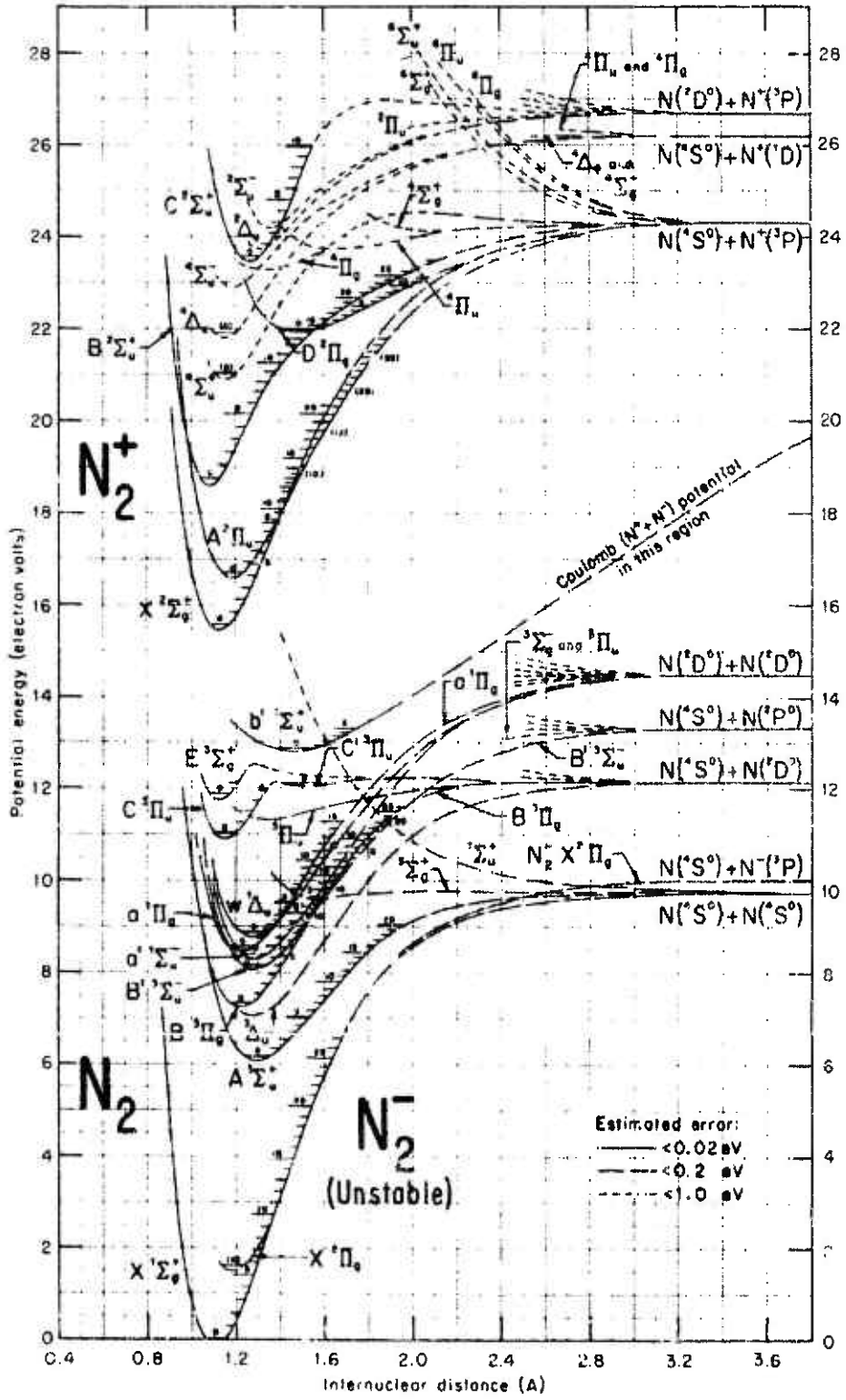


Figure 10-5. Potential-energy curves for $N_2^-$ (unstable), $N_2$, and $N_2^+$.

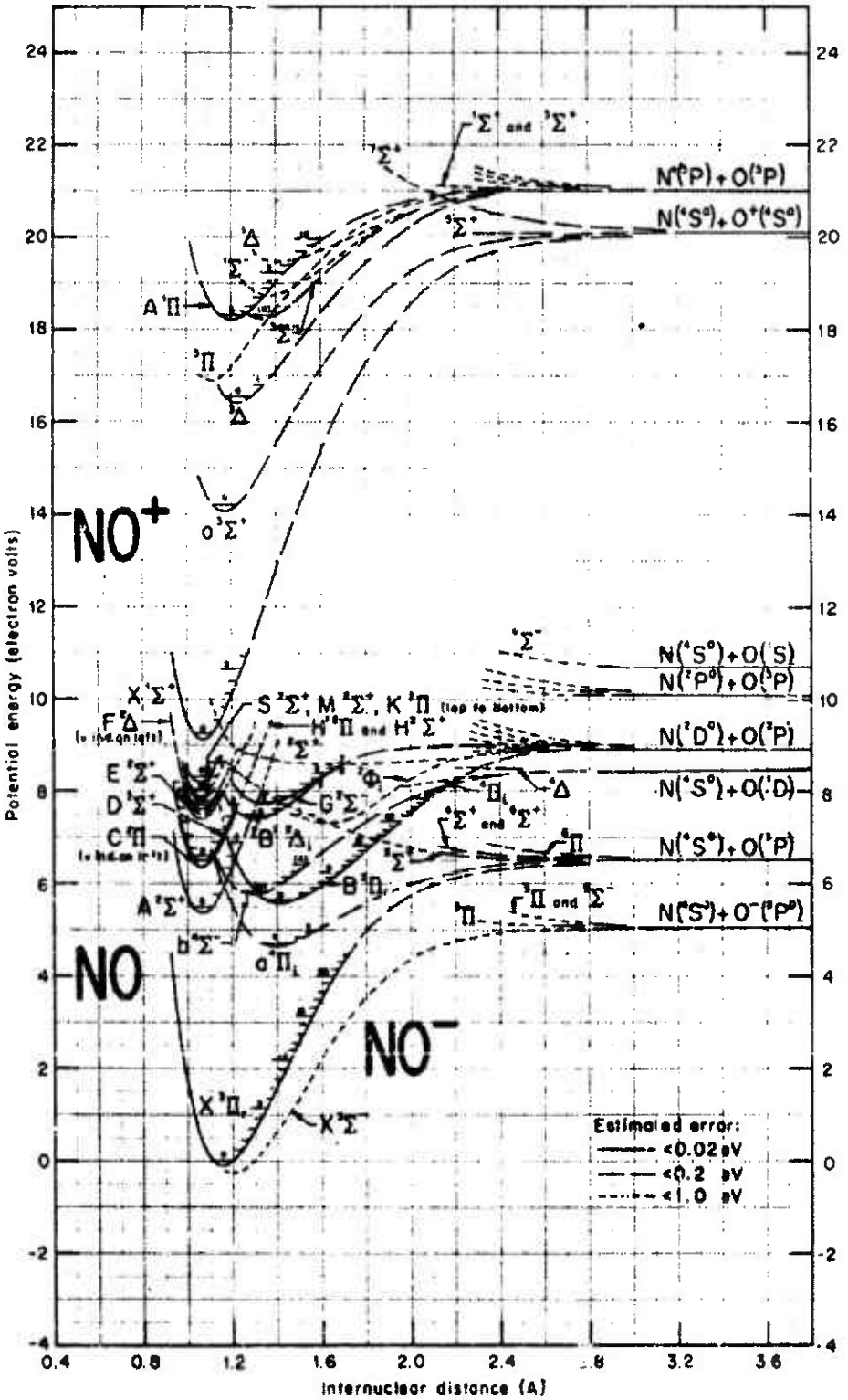


Figure 10-6. Potential-energy curves for $NO^-$, NO, and $NO^+$.

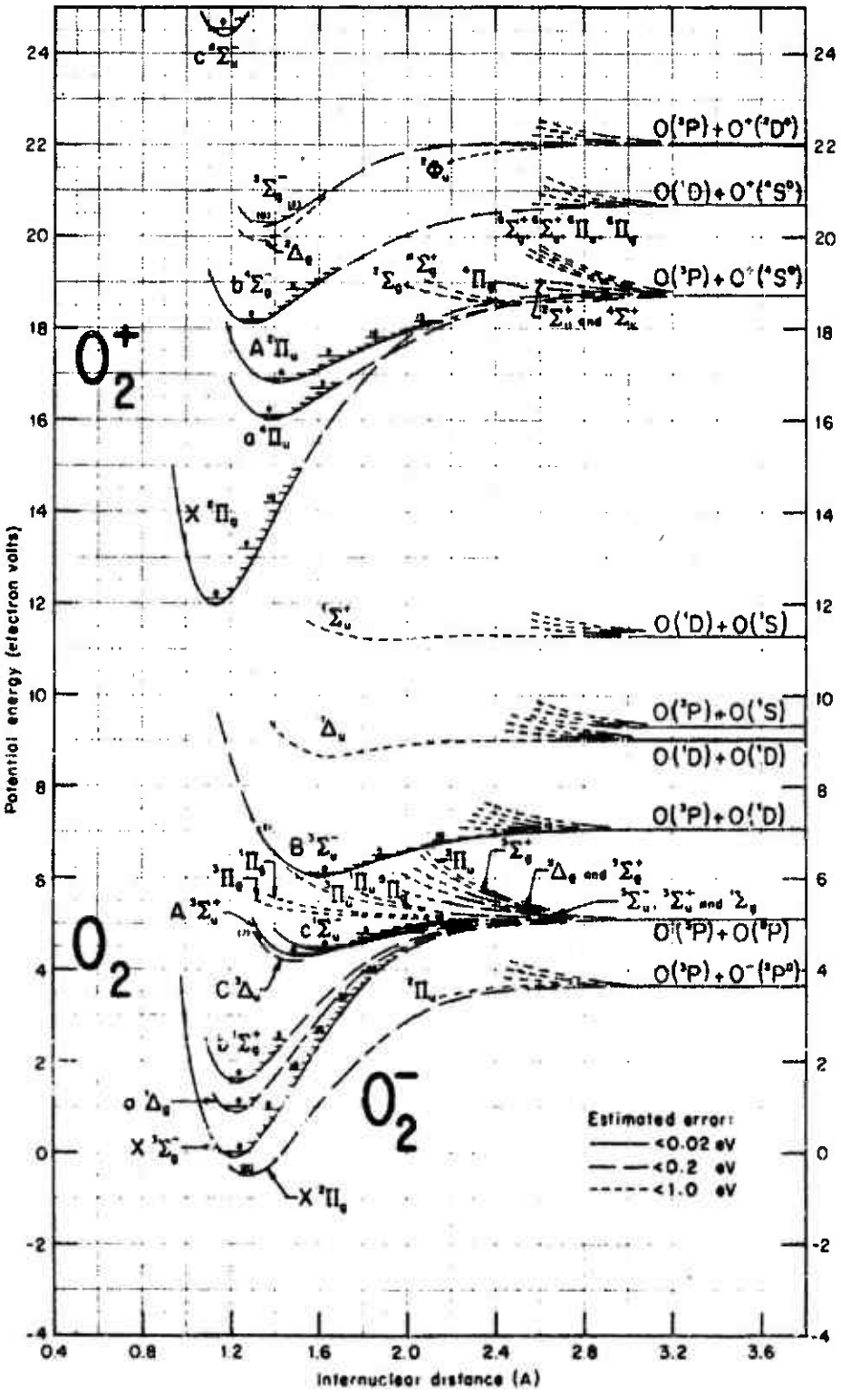


Figure 10-7. Potential-energy curves for $O_2^-$, $O_2$, and $O_2^+$.

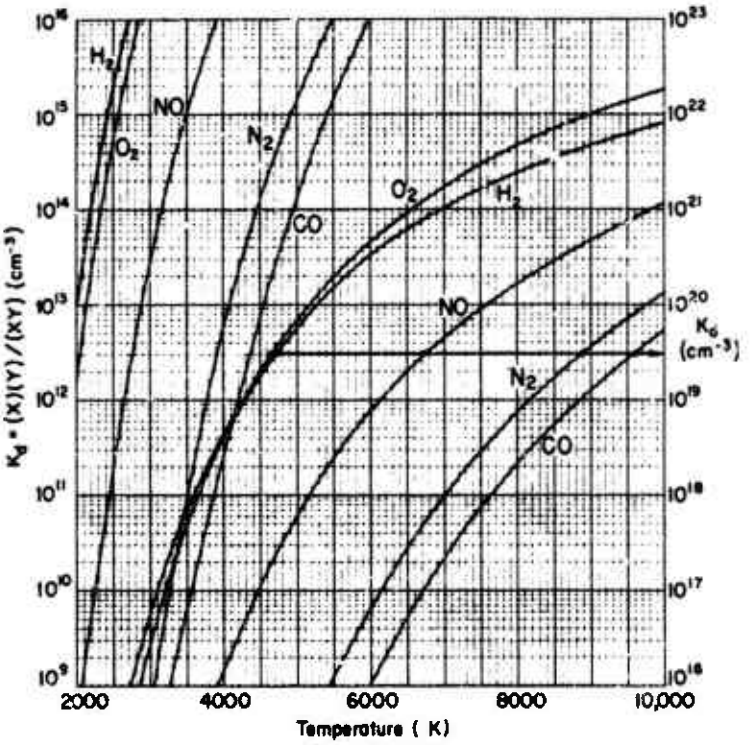


Figure 10-8. Equilibrium constants for dissociation.

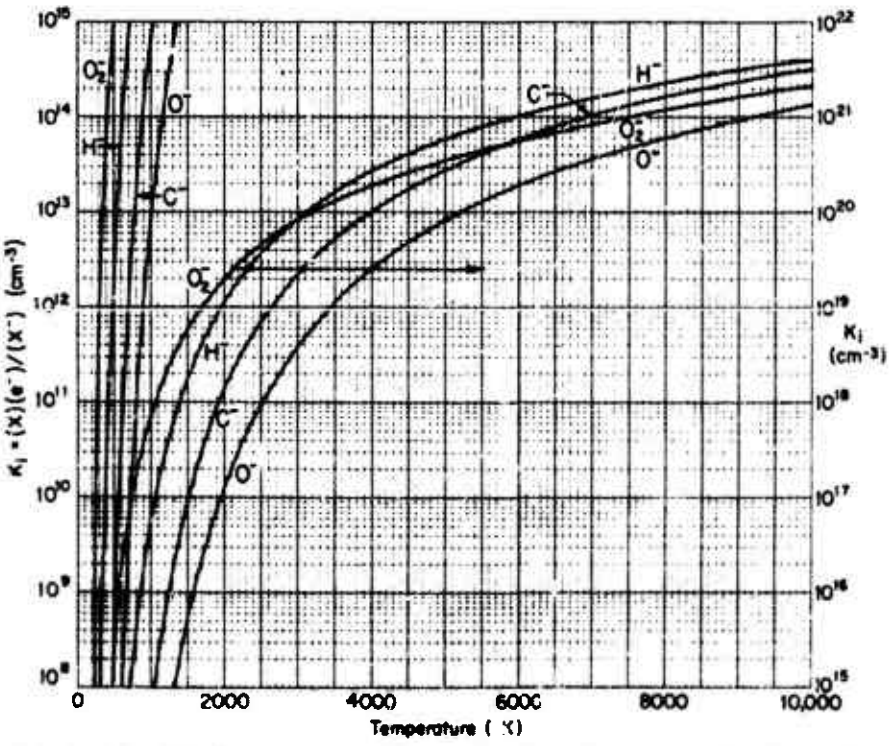


Figure 10-9. Equilibrium constants for ionization (detachment) of negative ions.

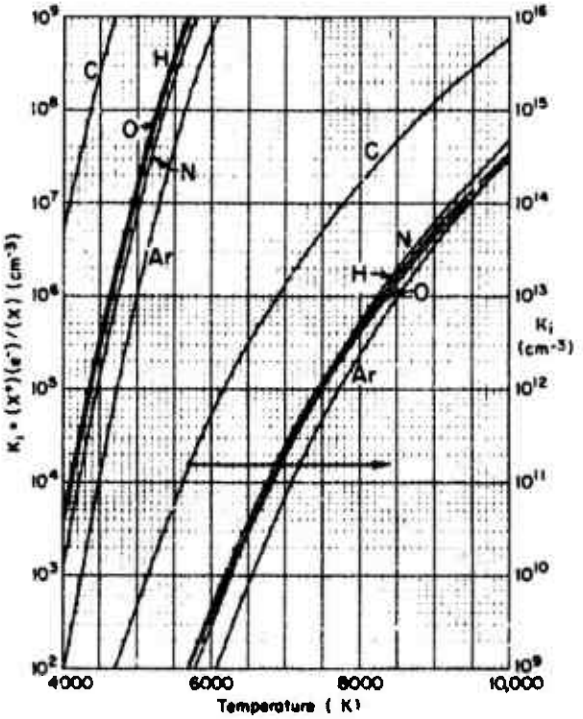


Figure 10-10. Equilibrium canstonts for ianizotion of atoms.

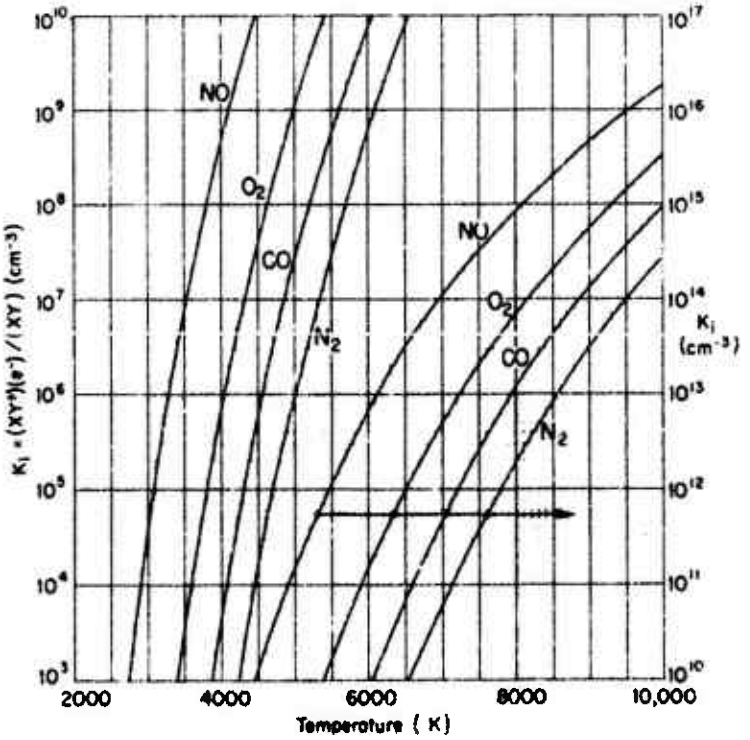


Figure 10-11. Equilibrium constants far ionization af diatomic molecules.

# 11. THE KINETICS OF ATMOSPHERIC RADIATIVE PROCESSES IN THE INFRARED

J.P. Kennealy and F.P. Del Greco
Air Force Cambridge Research Laboratories
(Latest Revision 1 February 1972)

## 11.1 INTRODUCTION

In the normal or unperturbed atmosphere such species as ozone, water vapor, carbon dioxide, and the hydroxyl radical are recognized radiative sources in the infrared. The contributions of these sources to the normal atmosphere are illustrated in Figures 11-1 and 11-2 for the 4-8 $\mu$m and 8-16 $\mu$m bands, respectively (References 11-1, 11-2). In disturbed atmospheres wide-ranging and persistent perturbations of the infrared radiation from naturally occurring species are to be expected. If the perturbing source is a nuclear detonation, the new species introduced by debris interactions may also give rise to radiative perturbations, as shown for the 1.5-3 $\mu$m and 3-6 $\mu$m bands in Figures 11-3 and 11-4, respectively (Reference 11-3).

Even in the normal atmosphere, and certainly in perturbed atmospheres, an observer may encounter a radiation background which reduces contrast along the line of sight. Certain computer codes have been designed to calculate the background radiance for arbitrary sight lines and atmospheric conditions. Table 11-1 presents selected data on species for which potential contributions to the atmospheric infrared radiation should be considered in such codes. Most of the infrared-active species listed in Table 11-1 are minor constituents in either a normal or a disturbed atmosphere. An exception is the case (Reference 11-4) in which NO appears to have achieved relatively very large concentrations in an aurorai disturbance. Although infrared radiation comprises a major energy sink in some portions of the atmosphere, infrared radiative rates capable of generating a background radiance problem need not imply an important drain on the energy sources available in a disturbed atmosphere.

Subsequent sections of this chapter will discuss the important mechanisms of vibrational excitation, viz., collisional excitation

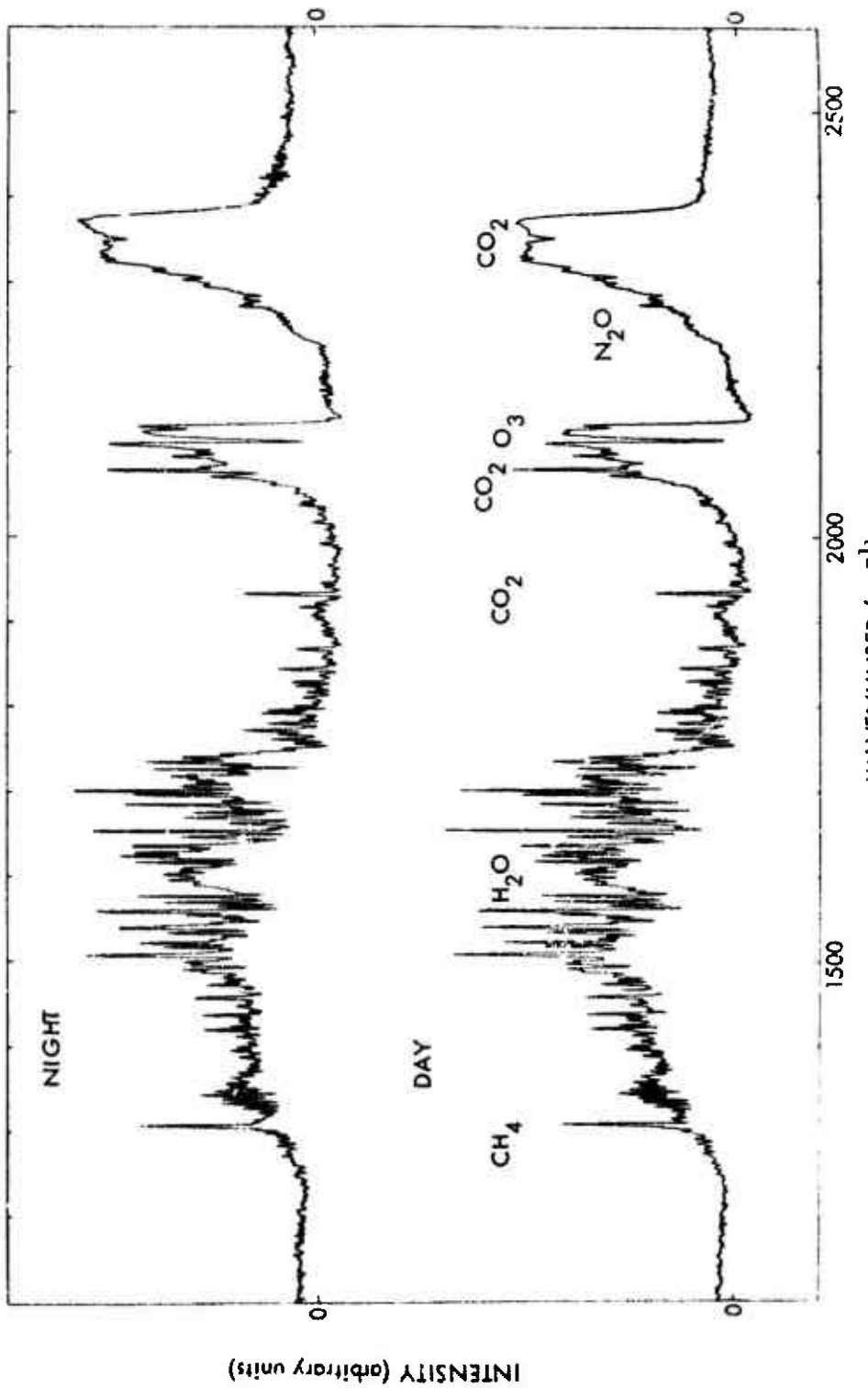


Figure 11-1. Spectrum of the airglow between 4 and 8 μm (Reference 11-1).

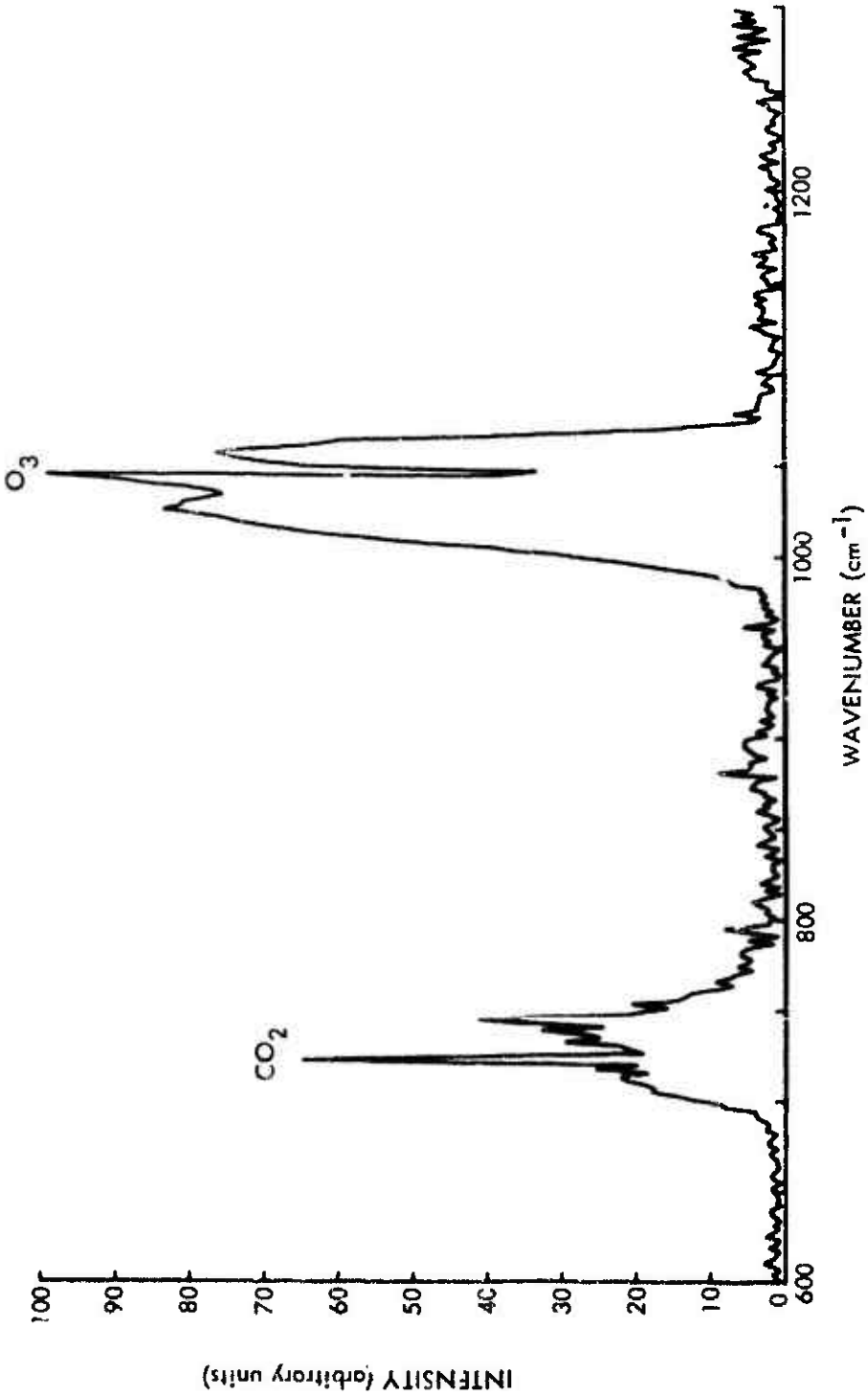


Figure 11-2. Atmospheric emission spectrum between 8 and 16 μm (altitude ≈ 12 km) (Reference 11-2).

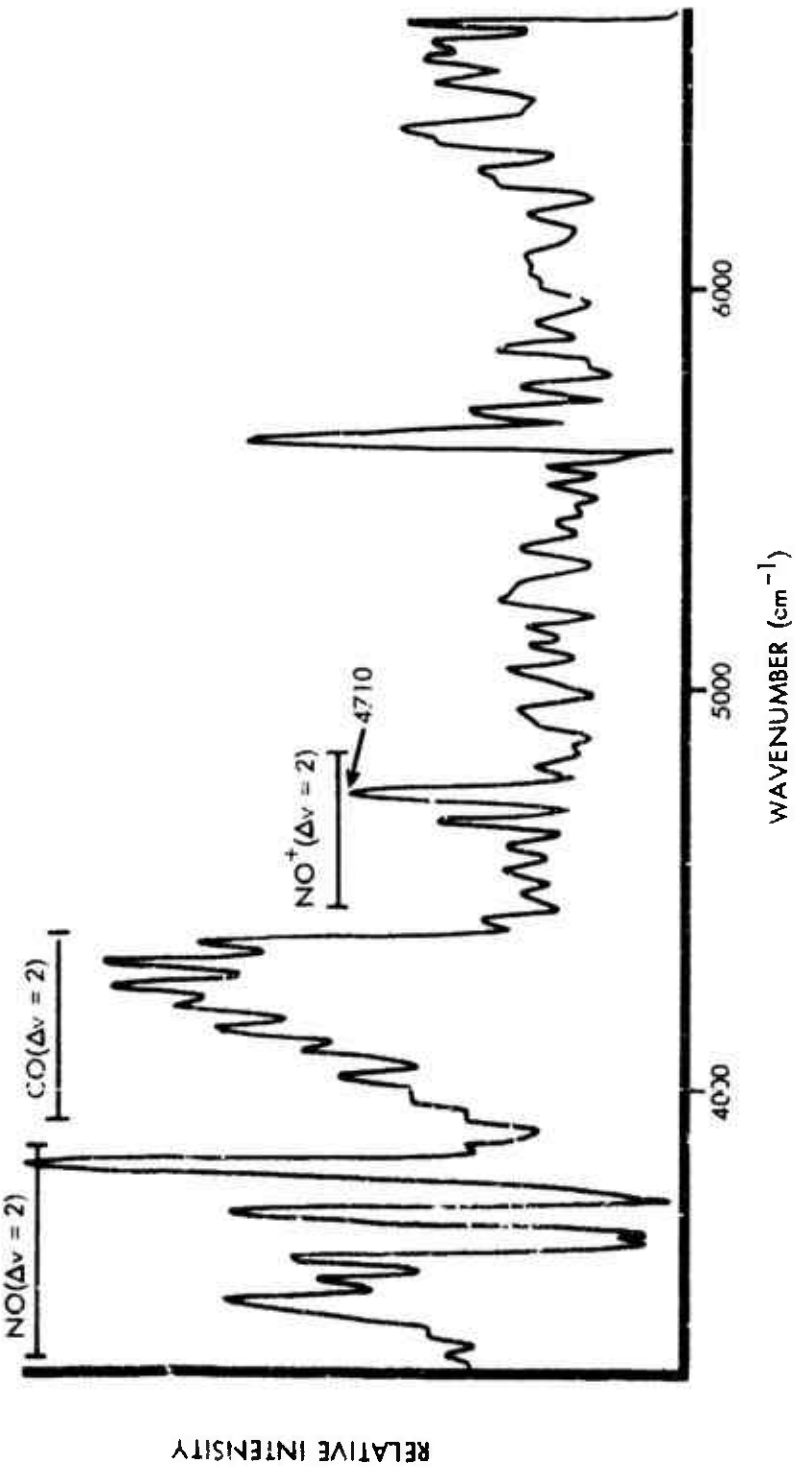


Figure 11-3. Infrared spectrum of a high-altitude nuclear detonation in the 1.5-3 μm region (Reference 11-3).

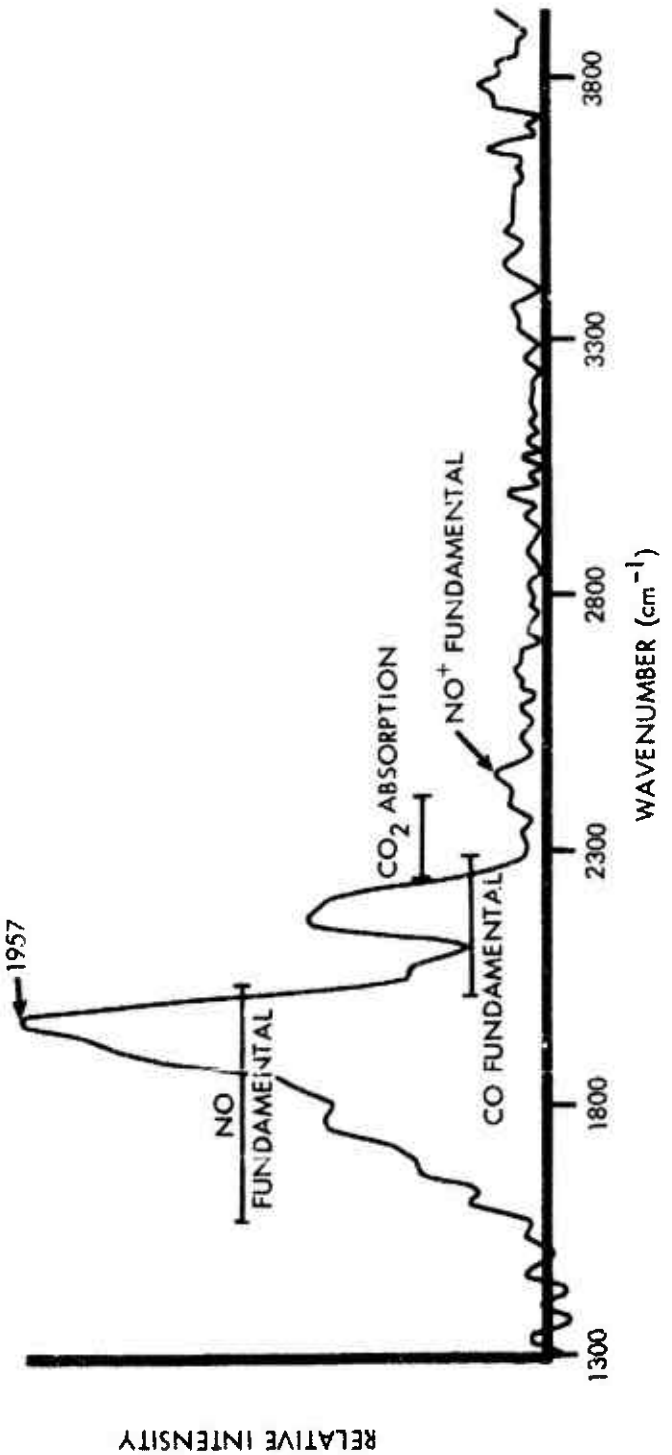


Figure 11-4. Infrared spectrum of a high-altitude nuclear detonation in the 3-6 μm region (Reference 11-3).

Table 11-1. Data on infrared bands of atmospheric interest.

| Species | Ratatianal Constant, B | Transition | Band Origin | | Band Strength, S | Einstein Coefficient, A | References |
|---|---|---|---|---|---|---|---|
| | | | Wave Number, $\nu_o$ ($cm^{-1}$) | Wovelength, $\lambda_a$ ($\mu m$) | ($cm^{-2}$ $atm^{-1}$) | ($sec^{-1}$) | |
| $CO_2$ | 0.390 | 100-000 | 1388 | | Inactive | | 11-5 |
| | | 010-000 | 667 | 15.0 | 223 | 2.77 | 11-5 |
| | | 001-000 | 2349 | 4.26 | 2590 | 400. | 11-5 |
| | | 101-000 | 3715 | 2.69 | 45.4 | 17.6 | 11-5 |
| | | 201-000 | 4978 | 2.01 | .95 | .659 | 11-5 |
| | | 001-100 | 961 | 10.4 | a | .2 | 11-5 |
| $H_2O$ | 27.877 | 100-000 | 3652 | 2.74 | 21.9 | 8.17 | 11-5 |
| | | 010-000 | 1595 | 6.27 | 316 | 22.5 | 11-5 |
| | | 001-000 | 3755 | 2.66 | 213 | 84.3 | 11-5 |
| | | 011-000 | 5331 | 1.88 | 24.5 | 19.4 | 11-5 |
| $N_2O$ | 0.419 | 001-000 | 2224 | 4.49 | 1858 | 258. | 11-5 |
| | | 010-000 | 589 | 17.0 | 33.2 | .322 | 11-5 |
| | | 100-000 | 1285 | 7.78 | 235 | 10.9 | 11-5 |

Table 11-1. (Cont'd.)

| Species | Rotational Constant, B | Transition | Band Origin | | Band Strength, S | Einstein Coefficient, A | References |
|---|---|---|---|---|---|---|---|
| | | | Wave Number, $\nu_o$ ($cm^{-1}$) | Wavelength, $\lambda_o$ ($\mu m$) | ($cm^{-2}$ $otm^{-1}$) | ($sec^{-1}$) | |
| $O_3$ | 3.553 | 100-000 | 1103 | 9.01 | 3.59 | .124 | 11-5 |
| | | 010-000 | 705 | 14.2 | 19.6 | .272 | 11-5 |
| | | 001-000 | 1042 | 9.60 | 356 | 10.8 | 11-5 |
| $HO_2$ | | 100-000 | 1101 | 9.09 | — | — | 11-6 |
| | | 010-000 | 1389 | 7.2 | — | — | |
| | | 001-000 | 3414 | 2.93 | — | — | |
| $NO_2$ | 8.000 | 100-000 | 1320 | 7.57 | | | |
| | | 010-000 | 750 | 13.3 | | | |
| | | 001-000 | 1618 | 6.19 | 2060 | 150.6 | 11-7 |
| | | 101-000 | | 3.4 | 57 | 13.8 | 11-7 |
| $CH_4$ | 5.241 | $\nu_1$ (1-0) | 2916 | 3.43 | Inoctive | | 11-5 |
| | | $\nu_2$ (1-0) | 1534 | 6.51 | 2.03 | .13 | 11-5 |
| | | $\nu_3$ (1-0) | 3020 | 3.31 | 324 | 83. | 11-5 |
| | | $\nu_4$ (1-0) | 1306 | 7.66 | 190 | 9.1 | 11-5 |

Table 11-1. (Cont'd.)

| Species | Rotational Constant, B | Transition | Band Origin | | Band Strength, S | Einstein Coefficient, A | References |
|---|---|---|---|---|---|---|---|
| | | | Wave Number, $\nu_o$ ($cm^{-1}$) | Wavelength, $\lambda_o$ ($\mu m$) | ($cm^{-2}$ $atm^{-1}$) | ($sec^{-1}$) | |
| $HNO_3$ | 9.405 | $\nu_5$ ($\Delta v=1$) | 879 | 11.38 | 600 | 13.0 | 11-8 |
| $NH_3$ | 9.444 | $\nu_2$ (1,0) | | 10.5 | 190 | 4.83 | 11-5 |
| | | $\nu_4$ (1,0) | | 6.1 | 150 | 11.3 | 11-5 |
| CO | 1.931 | 1-0 | 2143 | 4.6 | 262 | 34.7 | 11-9 |
| | | 2-0 | 4260 | 2.35 | 1.89 | .96 | 11-9 |
| NO | 1.705 | 1-0 | 1876 | 5.32 | 120 | 12.1 | 11-10, 11-11 |
| | | 2-0 | 3724 | 2.68 | 2 | .78 | 11-10, 11-11 |
| OH | 18.871 | 1-0 | 3568 | 2.80 | ~34 | 12.1 | 11-12 |
| | | 2-0 | 6971 | 1.43 | 4 | 5.5 | 11-13 |
| $NO^+$ | 2.002 | 1-0 | 2344 | 4.26 | 500 | 77 | 11-3 |
| | | 2-0 | 4655 | 2.15 | 3 | 1.8 | 11-3 |

Table 11-1. (Cont'd.)

| Species | Rotational Constant, B | Transition | Band Origin | | Bond Strength, S | Einstein Coefficient, A | References |
|---|---|---|---|---|---|---|---|
| | | | Wave Number, $\nu_o$ ($cm^{-1}$) | Wavelength, $\lambda_o$ ($\mu m$) | ($cm^{-2}$ $otm^{-1}$) | ($sec^{-1}$) | |
| UO | | 1-0 | 776[b] | 12.88[b] | — | — | 11-14 |
| FeO | 0.418 | $\Delta v=1$ | 870 | 11.49 | 450 | 9.5 | 11-15 |
| AlO | 0.641 | 1-0 | 965 | 10.36 | 190 | 5 | 11-16 |

Notes:

[a] Temperature-dependent, since the lower level is not the ground state.

[b] In a rare-gas matrix.

(Section 11.2), radiative excitation (Section 11.3), and in a special section for which we are indebted to J. W. Cooper of the National Bureau of Standards, radiative processes in low-density plasmas (Section 11.4). Two appendices to the chapter describe technical aspects of the subject, viz., band widths and shapes, and definitions and equations pertaining to resonance fluorescence, respectively.

## 11.2 COLLISIONAL EXCITATION PROCESSES

### 11.2.1 Translational-Vibrational Energy Transfer

A system is said to be in local thermodynamic equilibrium (LTE) if a single temperature characterizes the distribution, throughout all the available degrees of freedom, of the total energy contained in the system. Emission or absorption of infrared radiation may cause a system to depart from LTE. The system remains in LTE so long as the collisional processes holding the infrared-active modes to the LTE condition continue to dominate all other source and sink terms for these modes. In general, the numbers of collisions required for translational, rotational, and vibrational relaxation are of the order of $<10$, $<100$, and $10^3$-$10^6$, respectively (References 11-17, 11-18). For polyatomic species having more than one vibrational mode, the effective mechanism for translational-vibrational (T-V) coupling into the molecule is thought to involve the mode of lowest frequency, which then couples intramolecularly with the other modes. T-V excitation of infrared-active modes, and their subsequent radiative emission, comprise an important cooling mechanism in the lower atmosphere (Reference 11-19).

For a vibrational mode of species X, simplifying to a two-level model and neglecting absorption of radiation:

$$\frac{d[X(1)]}{dt} = K'_{01}[X(0)] - \left(K'_{10} + A_{10}\right)[X(1)] \quad , \tag{11-1}$$

and in the steady state:

$$\frac{[X(1)]}{[X(0)]} = \frac{K'_{01}}{\left(K'_{10} + A_{10}\right)} \quad . \tag{11-2}$$

Here, $K'_{01}$ ($sec^{-1}$) and $K'_{10}$ ($sec^{-1}$) are the collisional excitation and deexcitation rates, respectively, $[X(i)]$ is the number density ($cm^{-3}$) of species X in vibrational state i, and $A_{10}$ ($sec^{-1}$) is the Einstein coefficient for the transition (cf. Table 11-1). If $Z_{ij}$ is the number of collisions required to bring about one transition from state i to state j, and N is the number of collisions per second experienced by a molecule at a given altitude, then $K'_{ij} \equiv N/Z_{ij}$. For the example given, $K'_{10} \equiv N/Z \gg A_{10}$ is the condition to be met if radiative loss is not to disrupt LTE. In that case $[X(1)]/[X(0)]$ is given by the Boltzmann factor, $\exp[-\theta/T]$, where T is the kinetic temperature and $\theta$ is the characteristic temperature $h\nu_o/k$ of the mode. When $T << \theta$, the reciprocal of $K'_{10}$ is a good approximation to the relaxation time for the system; it applies about as well for a system of many harmonic oscillators (Reference 11-17).

Failure of $K'_{10}$ to dominate $A_{10}$ implies $[X(1)]/[X(0)] < \exp[-\theta/T]$, $T_{vib} < T_{kinetic}$, and therefore a condition where the volume emission rate in an optically thin atmosphere is subject to one variety of collision-limiting. For most species this condition has its onset somewhere above 70 km, the actual altitude depending on where in the atmosphere $N/Z_{10} \sim A_{10}$. Values of $Z_{10}$ for $CO_2$ and $H_2O$ are listed in Table 11-2.

The emission features of the spectra shown in Figures 11-1 and 11-2 are attributable to thermal radiation from chemically stable species in the atmosphere. For important minor species like $O_3$ at 9.6 μm and $CO_2$ at 15 μm, the atmosphere is optically thick to the radiation. The surface brightness of the atmosphere at these wavelengths approaches that of a blackbody at the local kinetic temperature. To calculate the brightness of thermally excited transitions for which the atmosphere is not optically thick, given a specific slant path, requires a knowledge of the number-density profile of the emitting species along the line of sight, as well as the atmospheric temperature in each volume element along the optical path. Then within each such volume element, again using the 1, 0 transition of species X as an example:

$$l_{vol} = \frac{[X]\, A_{10} \exp[-\theta/T]}{Q_V} \text{ photons cm}^{-3} \text{ sec}^{-1} , \qquad (11\text{-}3)$$

where $l_{vol}$ is the volume emission rate, $Q_V$ is the vibrational partition function for species X, and $[X]$ is the concentration of species

Table 11-2. Callisianal Excitatian Parameters.

| Originally Excited Species | Band Origin Wave Number, $\nu_a$ ($cm^{-1}$) | Characteristic Temperature, $\theta = \frac{h\nu_a}{k}$ (K) | No. of Callisians Required to Bring Abaut V-V Exchange: | | No. of Callisians Required to Bring Abaut T-V Exchange: | | Reference[b] |
|---|---|---|---|---|---|---|---|
| | | | $Z_{01}^{10}$[a] | With Callisian Partner | $Z_{10}$[a] | With Callision Partner | |
| $CO_2$ | 667 | 959 | — | — | $4 \times 10^5$ | $N_2$ | 11-20 |
| $CO_2$ | 2349 | 3380 | $7 \times 10^2$ | $N_2$ | — | -- | 11-20 |
| $H_2O$ | 1595 | 2295 | $\sim 5 \times 10^3$ | $O_2$ | $\sim 2 \times 19^4$ | Air | 11-20 |
| NO | 1876 | 2700 | $5 \times 10^5$ | $N_2$ | — | — | 11-18 |
| NO(A) | 2341 | 3371 | $7.9 \times 10^2$ | $N_2$ | — | — | 11-18 |
| CO | 2143 | 3080 | $4.5 \times 10^6$ | $O_2$ | — | — | 11-18 |
| $O_2$ | 1556 | 2228 | — | — | — | — | 11-18 |
| $N_2$ | 2331 | 3336 | — | — | — | — | 11-17 |

Notes:

[a] The Z-values relate ta ~300 K.

[b] Reference 11-17 derives the thearetical basis far calculating relaxatian rates at ather temperatures and References 11-18 and 11-20 compile much af the pertinent data.

X in the volume element. The line-of-sight emission rate $I_{col}$ (photons $cm^{-2}$ $sec^{-1}$) is the line integral of the volume rate. For moderate temperatures ($T << \theta$), $Q_V$ approximates unity and $[X] \sim [X(0)]$. Usually the profiles of species density and temperature along a given line of sight tend to be more difficult to determine than the species column density $[X]_{col}$ ($cm^{-2}$) and some average kinetic temperature. Allowing these simplifying substitutions:

$$I_{col} \approx \frac{[X]_{col} A_{10} \exp[-\theta/T_{av}]}{Q_V} \text{ photons cm}^{-2} \text{ sec}^{-1} . \quad (11\text{-}4)$$

While the spectra obtained by aircraft- and balloon-borne instruments have yielded such unforeseen results as the observation of emission from methane (Reference 11-1), and confirmation of the presence of nitric acid (Reference 11-21), no anomalies attributable to LTE breakdown at high altitudes—which would be indicative of insufficient amounts of thermal molecules—have been detected. It is certain that in the normal atmosphere any such effect is nearly impossible to demonstrate unequivocally, for two reasons. First, the column density of stable infrared-active species above about 70 km is likely to be small. In addition, the kinetic temperature is so low in the D- and lower E-regions that detection of a thermally equilibrated radiative contribution from the second vibrationally excited level of a molecule, even assuming no further complication, would still be difficult.

Oxygen atoms have been shown to accelerate the vibrational relaxation of both molecular nitrogen (Reference 11-22) and molecular oxygen (Reference 11-23). In the E-region and above, O atoms are a major species and could in principle aid in the relaxation of radiative species in the atmosphere. As pointed out earlier, unless the kinetic temperature has been greatly increased by some perturbation, the practical importance of any such relaxation as a means of aiding the T-V energy-transfer process is likely to be minimal. It may, however, be effective in quenching vibrators excited by alternative mechanisms. The impact on each potential radiator must be assessed as additional pertinent data become available.

### 11.2.2 Vibrational-Vibrational Energy Transfer

The exchange of vibrational quanta between molecules (V-V), in the fashion:

$$X(v=1) + Y(v=0) \rightarrow X(v=0) + Y(v=1) \quad , \qquad (11\text{-}5)$$

is a process which in some disturbed atmospheric situations may play an important role in the emission of infrared radiation. This possibility exists because homonuclear diatomic species, such as $N_2$ and $O_2$, are both infrared-inactive and generally resistant to V-T deexcitation. Vibrationally excited nitrogen is particularly likely to remain excited and so to provide a persistent energy reservoir. (See Chapter 20 for a much fuller discussion of the dynamics of vibrationally excited nitrogen.) In addition, an important quenching process for vibrationally excited NO may be V-V energy transfer to $O_2$.

The energy-transfer process of Equation (11-5) is known to be most efficient when species X and Y have nearly equal vibrational frequencies. Even in the normal atmosphere, the effective nitrogen vibrational temperature in the E-region is believed to be greater than the local kinetic temperature, i.e., $T_{vib} > T_{kin}$, but the altitude profile of $T_{vib}$ and its response to auroral or other perturbations remain controversial (References 11-24, 11-25). At altitudes below 125 km the principal sink for nitrogen vibrational energy is probably the near-resonant transfer to $CO_2$, with an energy deficiency of only 19 $cm^{-1}$ (cf. Chapter 10):

$$N_2(1) + CO_2(000) \overset{k}{\rightarrow} N_2(0) + CO_2(001) \quad , \qquad (11\text{-}6)$$

where $k \sim 7 \times 10^{-13}$ $cm^3$ $sec^{-1}$. The process of Equation (11-6) is followed by radiation in the infrared of the energy just transferred, i.e.:

$$CO_2(001) \overset{A}{\rightarrow} CO_2(000) + h\nu(2349\ cm^{-1}) \quad , \qquad (11\text{-}7)$$

for which $A = 400\ sec^{-1}$ (Table 11-1).

Hence, if $T_{vib} \sim 1000$ K at an altitude of 120 km, $[N_2(1)] \sim 1.4 \times 10^{10}$ $cm^{-3}$, the rate of excitation of $CO_2$ is of the order of $10^{-2}$ $sec^{-1}$. Even for this quite efficient process excitation is collision-limited, i.e., the radiation and excitation rates are approximately equal.

The actual importance of V-V exchange in generating infrared backgrounds in a disturbed atmosphere depends primarily upon the effective vibrational temperature achieved by the excited nitrogen, and also upon the mixing ratio of emitter species introduced into the same region. Furthermore, the form of the temperature dependence of V-V exchange processes is rather uncertain, especially at low kinetic temperatures (Reference 11-20). No direct experimental measurements of atmospheric infrared radiation for which V-V exchange is required as an excitation mechanism appear to be available.

Values of $Z_{01}^{10}$, the number of collisions required to bring about V-V exchange, are listed for several pairs of interacting partners in Table 11-2.

### 11.2.3 Chemiexcitation Processes

Part or all of the energy output of exothermic interactions may be distributed into the available vibrational degrees of freedom of one or more reaction products. The number of reactions for which this is known to be true is large and growing, with special impetus in this area coming from the field of chemical lasers. Following a nuclear or other disturbance, chemical reactions take place for prolonged periods of time over large volumes of the atmosphere. It is thus inherently plausible that chemiexcitation should be an important source of infrared background radiation. In the paragraphs which follow, some of the chemiexcitation reaction products which are known or thought to be important within this context are discussed specifically.

#### 11.2.3.1 VIBRATIONALLY EXCITED HYDROXYL ($OH^{\ddagger}$)*

One of the best-known examples of chemiexcitation involves the reaction:

$$H + O_3 \rightarrow O_2 + OH^{\ddagger} \quad , \tag{11-8}$$

which is mainly responsible for the $OH^{\ddagger}$ component of atmospheric

---

* Throughout these discussions, vibrationally excited forms of any species X are designated by $X^{\ddagger}$.

radiation peaking near 90-100 km, among the brightest features of the airglow (Reference 11-26). Polanyi et al (References 11-27, 11-28) have shown that most of the OH produced in Reaction (11-8) is channeled into the v=9 level with progressively smaller rates of formation in the lower (v<9) levels. Shefov (Reference 11-29) has summarized and collated the observed data on atmospheric hydroxyl emission and its dependence on geophysical variables. From this work it is concluded that at least one secondary source of $OH^{\ddagger}$ must be postulated in order to account for an apparent diurnal variation in the vibrational temperature of $OH^{\ddagger}$ from approximately 6000 K in the daytime to about 12,000 K at night, as well as an accompanying intensity variation. Breig (Reference 11-30) has suggested that the process:

$$O + HO_2 \rightarrow O_2 + OH^{\ddagger}(v_{max} = 6) \qquad (11\text{-}9)$$

may play a more important relative role in the daytime, thereby accounting for the lower daytime vibrational temperature (inasmuch as Reaction (11-9) tends to enhance the populations of the lower vibrational levels ($v \leq 6$) by contrast with the effect of Reaction (11-8) in preferentially populating the v=9, 8, 7 levels in that order, as noted above).

The problem of analyzing the important chemical systems underlying $OH^{\ddagger}$ radiation in the atmosphere is so complex as readily to justify continuing efforts involving multi-wavelength measurements in the atmosphere (References 11-31, 11-32), as well as further laboratory attempts at detailed elucidation of the Reaction (11-9) mechanism. A simplified sample analysis involving Reaction (11-8) will serve to demonstrate some of the complexities of the problem. For each vibrational level v of the product $OH^{\ddagger}$, and considering the radiative and collisional transitions only between nearest-neighbor levels:

$$\frac{d[OH(v)]}{dt} = k(v)[H][O_3] + K_Q(v+1)[OH(v+1)] + A(v+1)[OH(v+1)] - K_Q(v)[OH(v)] - A(v)[OH(v)] - K_R(v)[OH(v)] \; . \qquad (11\text{-}10)$$

Here, k(v) is the rate constant for formation of $OH^{\ddagger}$ in vibrational level v, $K_Q(v)$ is the quenching rate for level v at a given total density and composition of quenching species, A(v) is the Einstein

coefficient for the vibrational transition $v \rightarrow v-1$, and $K_R(v)$ is the chemical destruction rate. Thus from the OH loss mechanism:

$$O + OH \xrightarrow{k_{11}} O_2 + H \quad , \tag{11-11}$$

the destruction rate for OH is $K_R(OH) = k_{11}[O] \sim 10\ sec^{-1}$ at 100 km.

For the two highest levels of $OH^{\ddagger}$ (v=9, 8), the steady-state solutions are:

$$[OH(9)]_{ss} = \frac{k(9)[H][O_3]}{K_Q(9) + K_R(9) + A(9)} \tag{11-12}$$

and:

$$[OH(8)]_{ss} = \frac{k(8)[H][O_3] + \left(K_Q(9) + A(9)\right)[OH(9)]}{K_Q(8) + K_R(8) + A(8)} \quad , \tag{11-13}$$

respectively. As indicated above, the rate constants k(9), k(8), etc., are such that the several vibrational states of $OH^{\ddagger}$ can be thought of as being populated inversely, i.e., from the top down (References 11-27, 11-28). For altitudes above about 70 km the collisional vibrational relaxation process represented by $K_Q$ is probably inefficient for OH, which tends to preserve the initial distribution, aside from radiative cascade effects. Therefore $T_{vib} > T_{kin}$ for $OH^{\ddagger}$ in the steady state, in agreement with the observed brightness of this feature of the airglow at 90-100 km, as noted above (Reference 11-26).

Furthermore, since A and $K_R$ are of the same order of magnitude for OH, e.g., $K_R(OH) \sim 10\ sec^{-1}$ at 100 km by Reaction (11-11), and $A(1) \sim 34\ sec^{-1}$, the actual values of individual densities $[OH(v)]$ at each altitude, time of day, etc., are dependent upon the relationships among $[H]$, $[O_3]$, $K_R(v)$, and $A(v)$, in accordance with Equations (11-12), (11-13), and their counterparts for the lower vibrational levels.

### 11.2.3.2 VIBRATIONALLY EXCITED NITRIC OXIDE ($NO^{\ddagger}$)

Emissions from both $NO^{\ddagger}$ and $NO^{+\ddagger}$ have been observed in the spectrum of hot air resulting from an atmospheric nuclear detonation (Reference 11-3). Following atmospheric disturbances, both species play important roles in the complex chain of deionization reactions, and act in addition as potential sources of infrared radiation from chemiluminescent reactions.

Hushfar, Rogers, and Stair (Reference 11-33) have measured the infrared emission from the reaction:

$$N(^4S) + O_2 \rightarrow NO^{\ddagger} + O \quad , \tag{11-14}$$

under conditions such that the product $NO^{\ddagger}$ was deexcited more rapidly by subsequent interaction with N :

$$N + NO^{\ddagger} \rightarrow N_2 + O \quad , \tag{11-15}$$

than by radiation. Assuming the rate of Reaction (11-15) is independent of vibrational excitation, it can then be shown (Reference 11-34) that for most atmospheric situations of interest, where radiative deexcitation dominates, the total number of infrared photons emitted around 2.7 $\mu$m, i.e., in the $\Delta v=2$ (first overtone) band, is 0.012 per occurence of Reaction (11-14). On the other hand, if the rate of Reaction (11-15) increases with vibrational excitation of the $NO^{\ddagger}$ , the photon yield may be much higher (Reference 11-34). Additional experimental results are anticipated (Reference 11-33), with improved spectral resolution, in an attempt to determine the individual vibrational-level rate constants k(v) for Reaction (11-14). An additional source of $NO^{\ddagger}$ which may be important in disturbed atmospheres is the fast reaction:

$$N(^2D) + O_2 \rightarrow NO^{\ddagger} + O \quad , \tag{11-16}$$

for which a value of the chemiluminescent yield is needed.

The previously mentioned (cf. Section 11.1) anomalously high density of NO detected in an auroral arc (Reference 11-4) is especially significant. The reactions leading to its formation in the

aurora have not yet been identified, but unusually high production rates are required to account, during the auroral time scale, for the observed NO density, viz., $3.8 \times 10^{10}$ $cm^{-3}$ at 120 km, as compared with approximately $10^7$ $cm^{-3}$ at the same altitude in the undisturbed atmosphere. The reactions producing NO are necessarily fast, therefore exothermic, and consequently likely to be chemiluminescent.

### 11.2.3.3 VIBRATIONALLY EXCITED OZONE ($O_3^{\ddagger}$)

Another potentially important source of chemiluminescent infrared radiation in a disturbed atmosphere is $O_3^{\ddagger}$. The probable formation reaction is the three-body recombination process:

$$O + O_2 + M \rightarrow O_3^{\ddagger} + M \quad . \qquad (11\text{-}17)$$

No information has yet come to light as to the distribution of the exothermicity (1.04 eV) of Reaction (11-17) among the three available vibrational modes (cf. Table 11-1). Degges (Reference 11-35) has argued qualitatively that perhaps one $v_3$ quantum per recombination may be emitted.

Further with regard to the role of ozone chemistry in the atmosphere, certain interesting speculations have centered upon the identity of an "ozone precursor", identified by ultraviolet absorption at ~3000 A in the spectrum of oxygen which had been subjected to pulse radiolysis (References 11-36, 11-37). The evidence is at least partially consistent with the unknown precursor's being $O_3^{\ddagger}$. Adding further to the interest of this possibility is the observation by Krueger (Reference 11-38) of otherwise unexplained atmospheric solar attenuation in broadly the same wavelength region at altitudes above 40 km. Noxon's contention (Reference 11-39) that none of the species $O_2(b\,^1\Sigma_g^+$, $a\,^1\Delta_g$, $X\,^3\Sigma_g^-$ $(v \sim 11))$ is acceptable as a possible cause of the anomalous absorption lends further credence to the idea that $O_3^{\ddagger}$ may be responsible.

### 11.2.3.4 VIBRATIONALLY EXCITED METAL OXIDES ($MeO_x^{\ddagger}$)

The debris of nuclear detonations includes metallic matter which originates in the structures of both the nuclear devices and their carriers. If exothermic reactions take place between such metallic

substances and ambient atmospheric species, then the likelihood of chemiluminescent processes is enhanced. Assuming the debris species to be primarily atomic metals (Me), reactions of two types:

$$Me + O_2 \rightarrow MeO + O \ , \qquad (11\text{-}18)$$

and:

$$Me + O_2 + M \rightarrow MeO_2 + M \ , \qquad (11\text{-}19)$$

are expected to participate in the formation of metal monoxides and dioxides, respectively. These oxides may be formed with vibrational excitation, to a degree depending partially on the exothermicity of Reactions (11-18) and (11-19) for specific metals. It is noteworthy that even the endothermic oxide-forming reaction:

$$Fe + O_2 \rightarrow FeO + O \ , \qquad (11\text{-}20)$$

the only such case for which data are available, evidently has a pre-exponential factor close to the gas-kinetic cross-section, and an activation energy approximating the endothermicity of the reaction (References 11-15, 11-40). This tends to reinforce the a priori assumption that Reaction (11-18), at least, may be fast for many metals, and therefore of interest to the overall atmospheric radiation problem.

## 11.3 RADIATIVE EXCITATION

### 11.3.1 Direct Infrared Excitation: Earthshine and Sunshine

In order that the earth be in radiative equilibrium with the sun it must emit radiation at the same rate as a 250 K blackbody. The spectra shown in Figures 11-5 and 11-6 indicate that, as sensed at high altitude, it is more nearly a graybody with valleys in its spectral emission pattern wherever the stronger absorption bands of infrared-active atmospheric gases occur. The spectral distribution of blackbody isothermals between 200 and 300 K are also indicated in Figures 11-5 and 11-6. Figure 11-7 compares the irradiance of the quiet sun at the top of the atmosphere with that of 250 and 300 K blackbodies. It will be noted that from approximately the vicinity of 5 μm to longer wavelengths the earthshine appears to be the more important source of vibrational excitation.

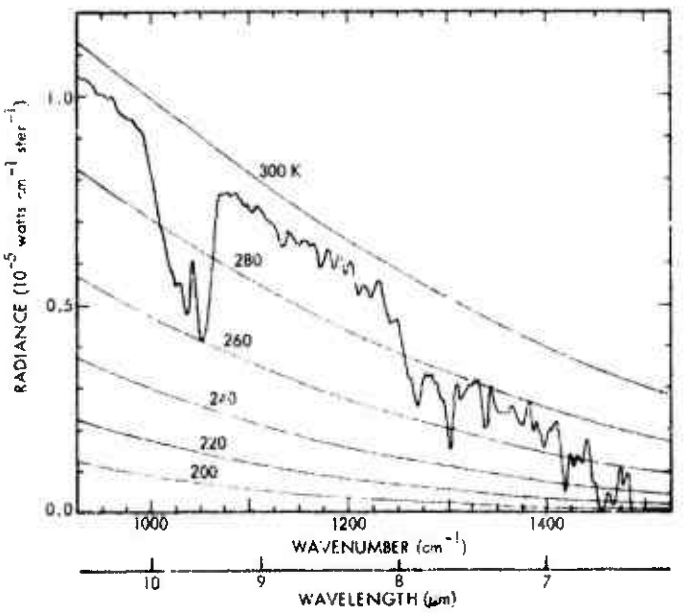


Figure 11-5. Earthshine in the 1000-1450 $cm^{-1}$ region (Reference 11-41).

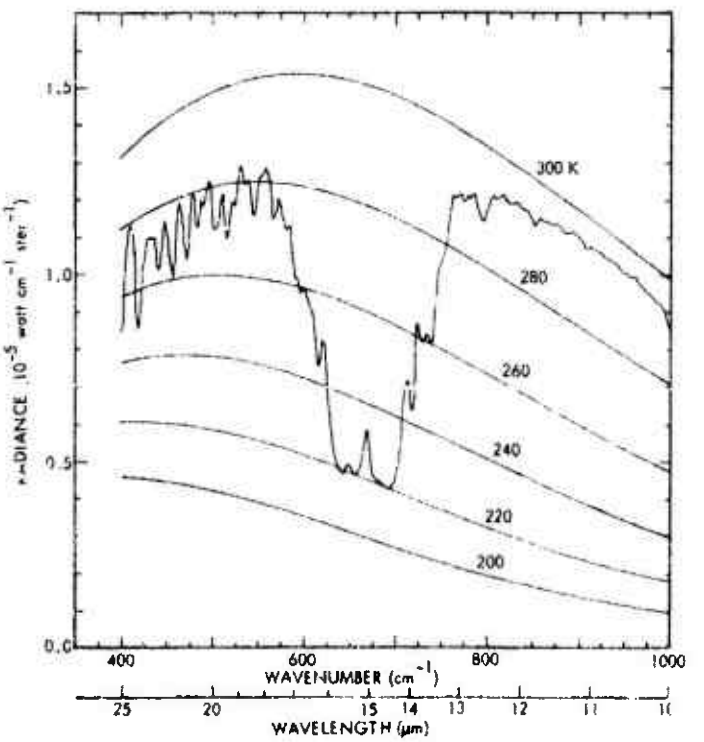


Figure 11-6. Earthshine in the 400-1000 $cm^{-1}$ region (Reference 11-41).

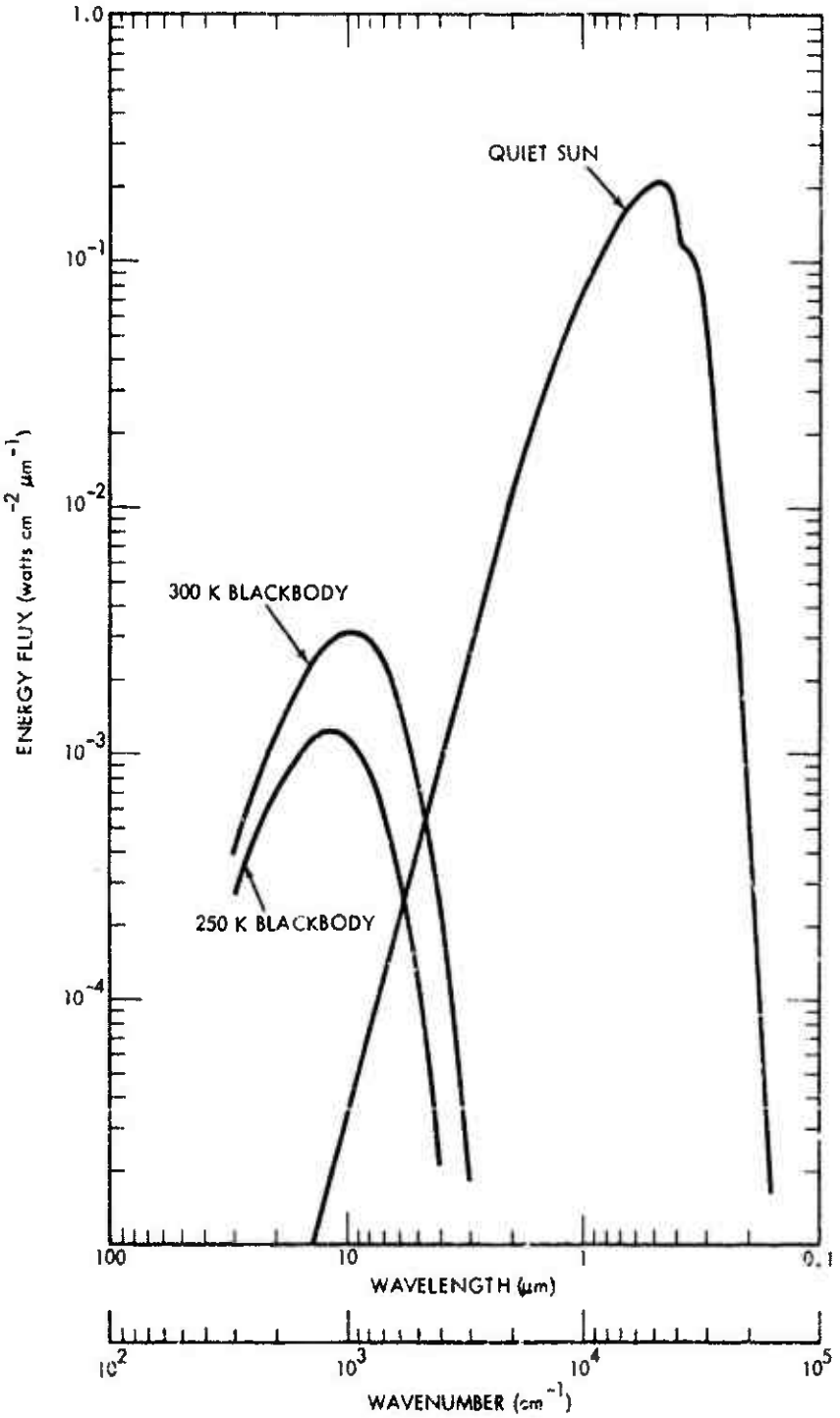


Figure 11-7. Irrodiance at the top of the otmosphere, for quiet sun and two blackbody sources.

Among the entries in Table 11-1 the metal oxides are most susceptible to this source of excitation, since their fundamentals tend to fall near the peak of the earthshine irradiance spectrum. For each volume element in the atmosphere, the fraction of optically active molecules under irradiation, which are excited per second, can be shown to be (Reference 11-13):

$$F = \frac{N_{ex}}{N} \cong 1.87 \times 10^{-5} \lambda_{\mu}^{3} R_{\lambda\mu} S \ , \qquad (11\text{-}21)$$

where $\lambda_{\mu}$ is the wavelength ($\mu$m), $R_{\lambda\mu}$ is the irradiance (watts $cm^{-2}$ $\mu m^{-1}$) incident upon the volume element from the source considered (viz., in this instance, earthshine), and S is the integrated band strength of the transition ($cm^{-2}$ $atm^{-1}$).

Assuming the entire volume to be optically thin to the incident radiation, the excitation rate along a line of sight through an atmospheric volume is $F \times N_{col}$ excitations $sec^{-1}$ $cm^{-2}$, where $N_{col}$ = column density ($cm^{-2}$) of molecules under excitation. Inasmuch as the Einstein coefficient A of typical metal oxides is of the order of 5-10 $sec^{-1}$ (Table 11-1), the rate constant for a quenching process such as:

$$MeO(v=1) + M \rightarrow MeO(v=0) + M \qquad (11\text{-}22)$$

would have to be of the order of $10^{-12}$ $cm^{3}$ $sec^{-1}$ in order for collisional quenching to be competitive with spontaneous radiation at altitudes above 100 km. However, quenching rate constants of this magnitude are not expected; therefore the radiative excitation rate is generally likely to be the emitted radiation rate. Thus for example, for AlO in the 10.4-$\mu$m band the result is that:

$$\frac{d[h\nu(10.4\ \mu m)]/dt}{[AlO]_{col}} \cong 0.01 - 0.02\ sec^{-1} \qquad (11\text{-}23)$$

### 11.3.2 Electronic-Transition Cascode Excitation

It appears that for many metal monoxides significant rates of vibrational excitation can be achieved by solar-induced fluorescence.

The typical MeO has an accessible upper electronic state MeO(A), such that the wavelengths of the $\Delta v=0, +1, +2$ sequence in the MeO(A) → MeO(X) transition occur at or near the broad maximum of the solar continuum, viz., 3500-7500 A. Groups of transitions of the following types:

$$MeO(X, v''=0) + h\nu_{solar} \rightarrow MeO(A, v') \quad ; \tag{11-24}$$

$$MeO(A, v') \rightarrow MeO(X, v''>1) + h\nu_f, \ (\nu_f<\nu_s) \quad ; \tag{11-25}$$

are effective in populating upper vibrational levels in the ground electronic state MeO(X). The normalized rate of MeO(X) → MeO(A) transitions in this case is:

$$\frac{d[MeO(A)]/dt}{[MeO]} \sim 1.87 \times 10^{-5} R_{\lambda\mu e} S_e \lambda_e^3 \ sec^{-1} \ , \tag{11-26}$$

where $\lambda_e$ is the "center wavelength" ($\mu$m) of the MeO(A) ↔ MeO(X) transition, $S_e$ is the integrated intensity ($cm^{-2}$ $atm^{-1}$) of the same transition, and $R_{\lambda\mu e}$ is the solar irradiance (watts $cm^{-2}$ $\mu m^{-1}$) upon the atmosphere at $\lambda_e$. Relationship (11-26) is an approximate one because, for simplicity, all $v'' \rightarrow v'$ transitions are treated together in this calculation. In reality $\lambda_e$, $S_e$, and $R_{\lambda\mu e}$ all depend to some extent on the exact vibrational transition involved. Actually, with a careful choice of $\lambda_e$ the above calculation is good to better than a factor of two.

In order for this process to be important, MeO(A) → MeO(X) must be an allowed transition; then the radiative lifetime of MeO(A) is small enough that collisional quenching can be ignored at the altitudes of interest.

To a first approximation, the mean number of vibrational quanta excited in MeO(X) by the fluorescence process is simply a function of the Franck-Condon factors governing the electronic transition:

$$\overline{v''} = \sum_{v'} q_{v'0} \sum_{v''} q_{v'v''} \, v'' \quad . \tag{11-27}$$

Neglecting collisional quenching, the normalized rate of infrared emission, due to solar fluorescence, is:

$$\frac{d[h\nu(1,0)]/dt}{[MeO]} = 1.87 \times 10^{-5} \lambda_e^3 S_e R_{\lambda\mu e} \left( \sum_{v'} q_{v'0} \sum_{v''} q_{v'v''v''} \right) , \quad (11\text{-}28)$$

and in the case of AℓO:

$$\frac{d[h\nu(10.4\ \mu m)]/dt}{[AlO]} \cong 0.06\ sec^{-1} . \quad (11\text{-}29)$$

The numerical result, (11-29), is based on an f-value of 0.014 for the AℓO(A) → AℓO(X) transition, consistent with theoretical calculations of Michels (Reference 11-42).

Metal oxides are not the only species of interest which can achieve significant excitation rates through fluorescence mechanisms. Bortner et al (Reference 11-43) have compared various radiative and collisional excitation mechanisms involving atmospheric nitric oxide, and have described in detail the calculation of solar infrared, solar electronic, and earthshine infrared radiation rates for that species.

## 11.4 RADIATIVE PROCESSES IN LOW-DENSITY PLASMAS*

For atmospheric plasmas of low density ($< 10^{11}$ cm$^{-3}$) and moderate temperature (<10,000 K), there exist basically four processes which need to be considered in computing the emissivity for wavelengths comparable to or longer than those in the visible region of the spectrum, viz., ion and neutral Bremsstrahlung, and radiative and collisional-radiative recombination. The present discussion is limited to theoretical techniques used to evaluate the emissivities due to these processes.

Although omitted from consideration here, certain other processes may be important in specific instances. For example, in an oxygen plasma, electron attachment to the neutral atom to form $O^-$ must be taken into consideration for wavelengths of the order of 7500 A or shorter.

---

* For the writing of this section, the authors are indebted to J. W. Cooper, of the National Bureau of Standards.

### 11.4.1 Ionic Bremsstrahlung and Radiative Recombination (Free-Free and Free-Bound Emission

The rate of emission for both of these processes may be calculated exactly for electrons scattered by or recombining with hydrogenic ions (Reference 11-44). For practical calculations it is convenient to use the semi-classical expressions due to Kramers (Reference 11-45) for the emission rates for both processes, and to express deviations from the semi-classical results in terms of Gaunt factors which depend on the frequency of emission. A full treatment of the problem along these lines has been given by Griem (Reference 11-46) and the frequency dependence of the Gaunt factors has been studied by Karzas and Latter (Reference 11-47). In the spectral range considered here the Gaunt factors can be taken as unity. With this assumption and a Maxwellian distribution of electron velocities the emission rate per unit frequency range for both processes is given by the simple frequency-independent expression (Reference 11-48):

$$\epsilon_\nu = \frac{32\pi^2 e^6}{c^3 (6\pi m)^{1.5}} \frac{n_e n_i}{(kT)^{0.5}} , \qquad (11\text{-}30)$$

or in practical units by:

$$\epsilon_\lambda = \frac{1.63 \times 10^{-31} n_e n_i}{\lambda^2 T^{0.5}} \text{ watts cm}^{-3}\,\text{ster}^{-1}\,\mu\text{m}^{-1} , \qquad (11\text{-}31)$$

where the wavelength $\lambda$ is expressed in $\mu$m, the electron and ion densities $n_e$ and $n_i$ in $cm^{-3}$, and the temperature in K.

Despite the simplicity of these relationships, they are expected to provide an adequate first-order treatment of emissivity for most plasmas in the range of wavelengths, temperatures, and electron densities considered here. Deviations from Equation (11-31) owing to the use of unit Gaunt factors are not expected to lead to serious errors for wavelengths longer than those in the visible region. For example, Anderson and Griem (Reference 11-49) have investigated the deviations to be expected for helium plasmas at 20,000 K and find less than ten percent discrepancies for wavelengths longer than

5000 A. Equation (11-31), or the more complicated expressions including Gaunt factors given by Griem (Reference 11-46), can be corrected in the case of non-hydrogenic plasmas, by multiplying by a temperature- and wavelength-dependent factor (Reference 11-50). Such computations have been carried out for rare-gas plasmas and for oxygen and nitrogen (References 11-51, 11-52). The results for argon (Reference 11-51) at 8000 and 16,000 K show deviations of greater than a factor of two in the visible region of the spectrum and deviations of the order of ten percent or less for one-$\mu$m wavelengths.

At shorter wavelengths and/or at lower temperatures, Equation (11-31) may not be adequate if the detailed wavelength dependence is needed, since in these circumstances the equation smooths out the variations—actually somewhat jagged—caused by the discrete nature of the bound levels. In such cases the contribution of free-free transitions and of recombination to each bound level must be estimated separately (Reference 11-52). A systematic procedure for carrying out calculations of this type has been described by Griem (Reference 11-46). The emissivity for recombination into a particular level $n\ell$ at frequency $\nu$ ($sec^{-1}$) is expressed as:

$$\epsilon_\nu = \frac{4\pi^{1.5}\hbar^5\nu^3\sigma_{n\ell}(\nu)}{(mec)^2}\,\frac{g_{n\ell}}{g_{ion}}\,n_e n_i\,\frac{(E_{n\ell}-h\nu)}{(kT)^{2.5}}\,,\quad (h\nu > E_{n\ell})\,, \tag{11-32}$$

where $g_{n\ell}$ and $g_{ion}$ are the statistical weights of the recombining level $n\ell$ and the ionic ground state, respectively, and $E_{n\ell}$ is the binding energy of level $n\ell$. The quantity $\sigma_{n\ell}(\nu)$ is the cross-section for photoabsorption for an initial state $n\ell$, the inverse process of recombination. These cross-sections may be estimated by quantum-defect methods (Reference 11-53). For most purposes it is adequate to do this for only the lowest excited states to which recombination is allowed and to use the relationship pertaining to hydrogenic species:

$$\sigma_{n\ell} = \frac{64\,e^2}{3^{1.5}\hbar c}\left(\frac{E_{Ryd}}{h\nu}\right)^3\frac{\pi a_o^2\,g_n(\nu)}{n^5} \tag{11-33}$$

for higher levels.

If Equation (11-32) is used for the free-bound emissivity, the free-free emissivity must be estimated separately. This is given by the Kramers relation (Reference 11-54):

$$\epsilon_{ff} = \frac{32\pi^2 e^6 n_e n_i \exp(-h\nu/\kappa T)}{c^3 (6\pi m)^{1.5} (kT)^{0.5}} \quad , \tag{11-34}$$

or alternatively in practical units as:

$$\epsilon_{ff} = \frac{1.63 \times 10^{-31} n_e n_i \exp(-1.44 \times 10^4/\lambda T)}{\lambda^2 T^{0.5}}$$

$$\text{watts cm}^{-3} \text{ ster}^{-1} \mu\text{m}^{-1} \quad , \tag{11-35}$$

by analogy with Equations (11-30) and (11-31), respectively. Detailed calculations of the emissivities of oxygen plasmas have been carried out using this approach, by Sappenfield (Reference 11-53). Some of his results, at three different temperatures, are presented in Figures 11-8 through 11-10. For wavelengths longer than one μm Equation (11-31) is probably adequate for most practical applications.* For example, Sappenfield's results (Reference 11-53) deviate no more than ten percent from those calculated using Equation (11-31), for wavelengths of 10 μm in the 500-6000 K temperature range.

### 11.4.2 Neutral Bremsstrahlung

Calculations of neutral Bremsstrahlung are generally more difficult to perform than the analogous calculations for ions, for two reasons. First, the simplest case, viz.:

$$e + H \rightarrow e + H + h\nu \quad , \tag{11-36}$$

involves a two-electron problem, so that an accurate analytic theory cannot be given as in the case of positive-ion Bremsstrahlung.

---

* Equations (11-30) and (11-31) are only valid for frequencies well above the plasma frequency. For a discussion of the problem for extremely long wavelengths, see Reference 11-44, pp. 121 ff.

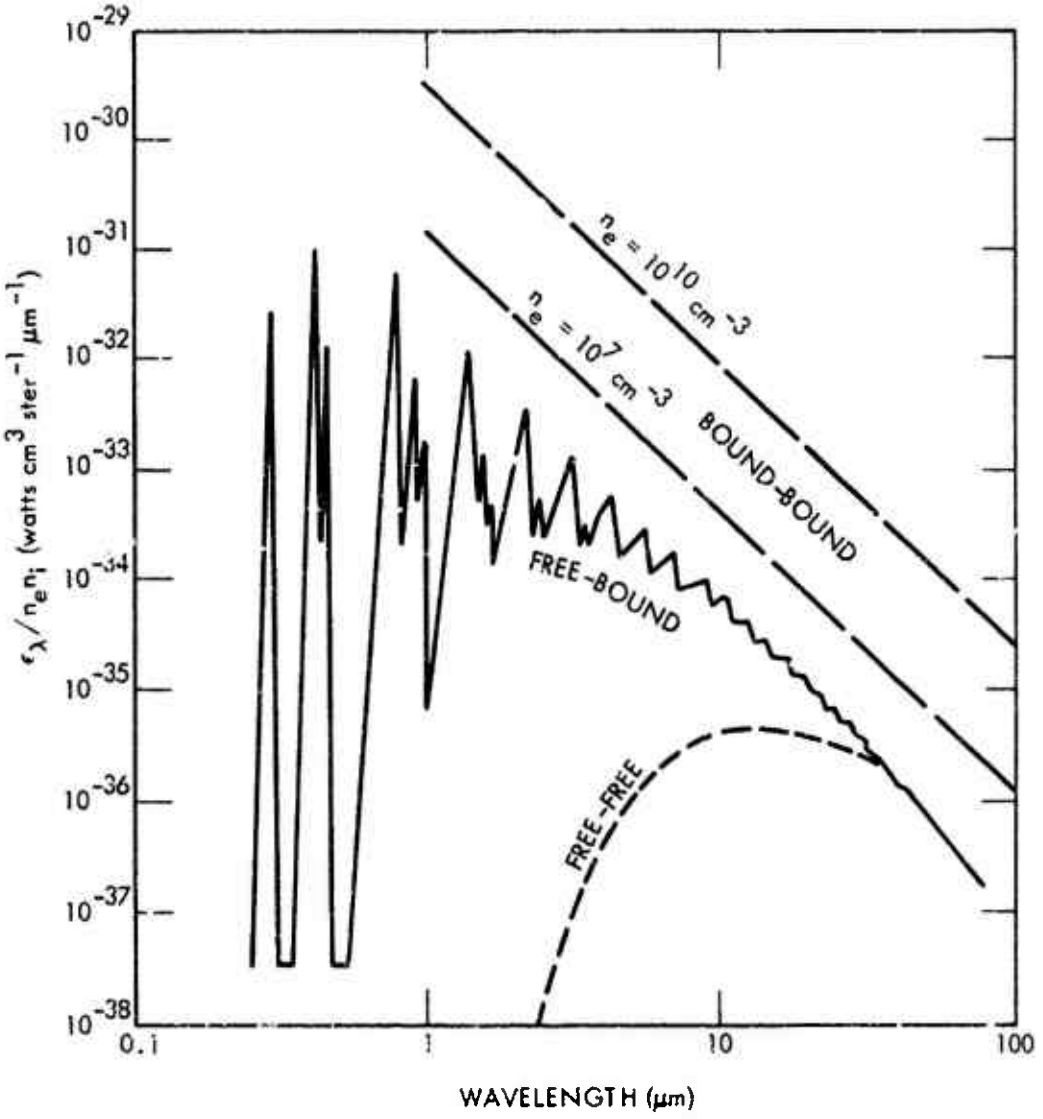


Figure 11-8. Calculated emissivities of oxygen plasma at 500 K (Reference 11-53).

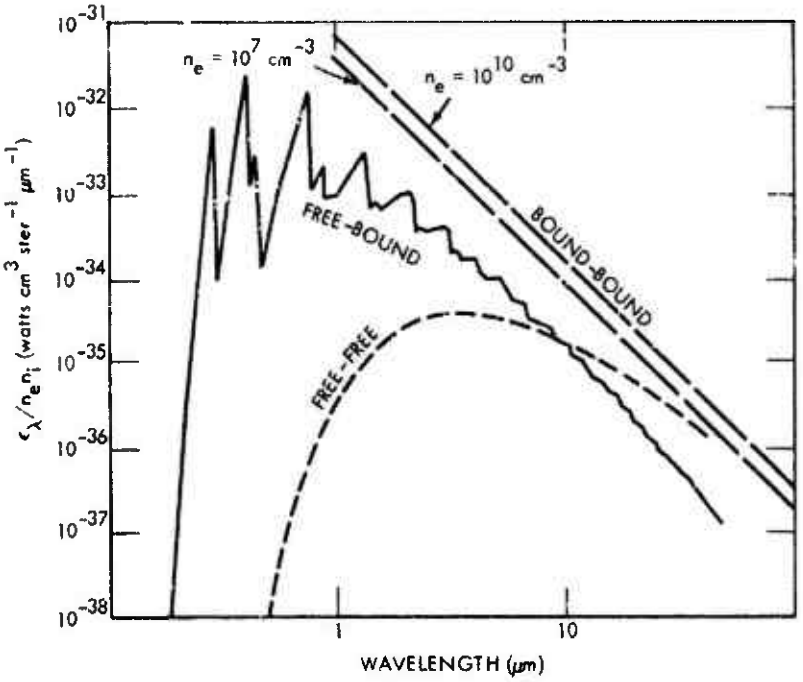


Figure 11-9. Calculated emissivities of oxygen plasma at 2000 K (Reference 11-53).

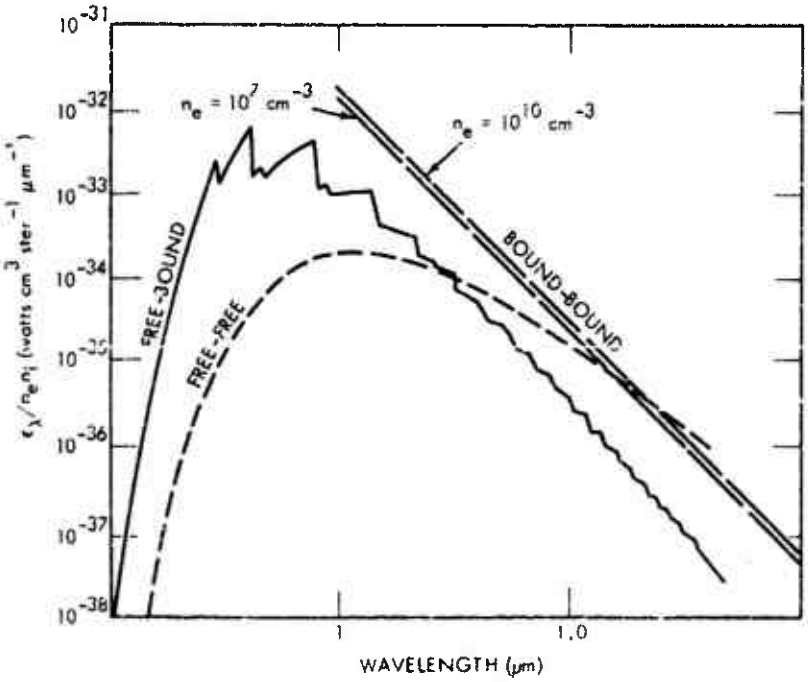


Figure 11-10. Calculated emissivities of oxygen plasma at 6000 K (Reference 11-53).

Second, since negative ions possess at most a few bound states, quantum-defect methods cannot be used to compute the recombination emissivity if negative-ion formation is possible. *

Quantum-mechanical calculations of neutral Bremsstrahlung or the related free-free absorption process for hydrogen have been carried out (References 11-55 through 11-57), and the results are reported in a study of the emissivity of LTE hydrogen plasma (Reference 11-58). Among the species important in air chemistry, detailed calculations have been carried for atomic nitrogen and oxygen by Mjolsness and Ruppel (Reference 11-59). Using the assumption that the emission rate is proportional to the final electron velocity, they derive an equation for the emissivity:

$$\epsilon_\lambda = 2.402 \times 10^{-31} \sigma_o n_e n_i \theta^{-3.5} (u+2) u^2 \exp(-u)$$

$$\text{watts cm}^{-3} \text{ ster}^{-1} \mu\text{m}^{-1} , \qquad (11\text{-}37)$$

where $\theta = 5040/T$, $u = 2.855\theta/\lambda$, and $\sigma_o$ is a constant which for atomic oxygen and nitrogen has values of $7.1 \times 10^{-7}$ and $8.0 \times 10^{-7}$, respectively. The accuracy of Equation (11-37) is difficult to assess since little work of comparable sophistication has been done for neutral low-energy Bremsstrahlung (see, however, Reference 11-60). Equation (11-37) is probably accurate to better than a factor of three for wavelengths shorter than one $\mu$m within the electron-energy and temperature ranges considered here, and should be more accurate at longer wavelengths. It should provide only order-of-magnitude estimates at shorter wavelengths and lower temperatures.

No calculations starting from first principles have been carried out for free-free emission involving molecules. A simplified expression relating the emission rate to the product of momentum-transfer cross-section times the initial electron energy has been derived semi-classically by Zel'dovich and Raizer (Reference 11-61) and has been used in the computation of emission from both atoms and molecules (References 11-59, 11-62, 11-63). The same result can be obtained through a consideration of the asymptotic representation of the quantum-mechanical expression for the Bremsstrahlung rate (References 11-64, 11-65). Such asymptotic representation

* Recombination to form negative ions is not considered here.

shows further that the correct form for the Bremsstrahlung rate is:

$$\frac{dq}{d\nu} = \frac{4e^2}{3c^3}\left[E_i\sigma_m(E_f) + E_f\sigma_m(E_i)\right] , \qquad (11\text{-}38)$$

(which reduces to Zel'dovich and Raizer's result (Reference 11-61) when $E_i \cong E_f$) where $E_i$ and $E_f$ are, respectively, the initial and final electron energies, and $\sigma_m$ is the momentum-transfer cross-section. Provided the Bremsstrahlung rate is not seriously affected by resonant effects,* the emissivity for all air species may be calculated using Equation (11-38), or its long-wavelength limit, from measured or calculated momentum-transfer cross-sections. This has been done by Kivel (Reference 11-63) for both atomic and molecular oxygen and nitrogen. The accuracy of this procedure was investigated experimentally by Taylor and Caledonia (Reference 11-67), who found agreement within a factor of about ten.

### 11.4.3 Collisional-Radiative Recombination

In a recombining plasma the rate of recombination is determined by radiative recombination (free-bound processes) only if the electron density is sufficiently low that electron-atom collision processes can be neglected. In the range of temperatures and electron densities considered here the rate of recombination is considerably enhanced owing to the effect of such collisions. The emissivity of a recombining plasma is also enhanced since in the recombination process a quasi-equilibrium distribution of excited atomic states occurs which emits via decay to lower states (bound-bound emission). Calculations of the emissivity due to this process therefore depend on estimates of the population of excited states in the recombining plasma. A procedure for estimating the excited-state population has been given by Bates, Kingston, and McWhirter (References 11-68, 11-69). This procedure consists of setting up rate equations to describe the population changes among neutral atomic levels which occur as a result of electron excitation or deexcitation and radiative decay. Three assumptions are made in the solution of these equa-

---

* Resonance effects greatly enhance the probability of vibrational excitation by electron impact at electron energies below three electron volts for both $N_2$ and $O_2$. See Reference 11-66. The effect on emissivities has not been explored.

tions, viz.: the populations of highly excited levels above some large principal quantum number are assumed to be in Saha equilibrium with the plasma; either all the radiation emitted in the decay process is assumed to escape from the plasma or it is assumed optically thick in strong (resonance-line) transitions; and neutral collision processes are neglected.

Detailed calculations of emissivities due to bound-bound transitions in recombining plasmas have been carried out only for hydrogen (Reference 11-53), oxygen (Reference 11-53), and helium plasmas (Reference 11-70). The results for oxygen, illustrated in Figures 11-8 through 11-10, indicate that at low temperatures (<6000 K) the bound-bound emission is probably the most intense type of radiation in a recombining plasma.

The accuracy of calculations of bound-bound emissivities cannot be estimated easily since the coefficients of the rate equations which determine the excited neutral populations are obtained from theoretical calculations of uncertain accuracy. Indirect evidence of the validity of the calculations for oxygen and helium plasmas has been obtained by comparing the results with experimentally determined level populations. Sappenfield (Reference 11-71) has compared level populations computed for an oxygen plasma with those obtained from visible observations of a nuclear event. He finds good agreement in the relative populations obtained by both methods. Johnson and Hinnov (Reference 11-70) have applied the same procedure to a helium plasma and compared calculated results with the observed level populations obtained by emission of light in a helium afterglow. They find it necessary to modify considerably the classical electron collision cross-sections in order to obtain agreement with the level populations determined experimentally.

Among the three assumptions noted above, that relating to Saha equilibrium was checked by varying the quantum-number level above which it was assumed that Saha equilibrium prevails. No appreciable error was noted thereby. In addition, alternative calculations were carried out, assuming the plasma to be either transparent or opaque to resonance radiation (References 11-68, 11-69). Considerable deviations in the populations of low-lying states occurred as a result of these alternative treatments. Finally, the effect of neutral collisions on emissivity has been studied theoretically by Collins (Reference 11-72), but has not been investigated experimentally.

## 11.5 CONCLUSIONS

Atmospheric radiative processes are directly related to the overall chemistry, in both the normal and disturbed atmospheres. At low altitudes the mechanism of T-V energy transfer is fast enough to maintain LTE vibrational populations of ambient infrared-active species, and therefore thermal radiation is dominant. Thus for any given emitter the important unknown is the profile of its mixing ratio. Somewhere above 70 km the collision frequency drops to a value low enough that LTE is no longer preserved. At about the same altitude, other excitation processes besides T-V energy transfer become important. These include: V-V processes such as the excitation of $CO_2$ by $N_2^{\ddagger}$ (Equation 11-6); a wide variety of possible chemiluminescent reactions; and fluorescence due to sunshine or earthshine.

In low-density plasmas, the important processes include neutral and ionic Bremsstrahlung (free-free emission), radiative recombination (free-bound emission), and line emission (bound-bound emission) due to collisional-radiative recombination. In atmospheric plasmas below 6000 K the bound-bound emission probably dominates.

Much remains to be done, both to understand the phenomenology of normal and perturbed atmospheric radiative processes, and to develop soundly based and accurate methods for calculating the emissivity of low-density plasmas.

## APPENDIX I: BAND SHAPES AND BAND WIDTHS

The shape and width of a given band depend on its rotational temperature, which is usually related in turn to the local kinetic temperature. The number of bands contributing radiation depends on the effective vibrational temperature. These points are illustrated in Figures 11-11 through 11-14, for the spectrum of CO, in the range 4.30-5.30 $\mu$m. A rough approximation to the width of a particular emission band may be taken as the distance between the peaks of the P and R branches. It can be shown that the width thus defined is:

$$\Delta\nu \approx 2.35(BT_{rot})^{0.5} \text{ cm}^{-1} , \qquad (11\text{-}39)$$

where B is the rotational constant of the emitting state and $T_{rot}$ the rotational temperature. The band origin of the (1-0) transition as given in Table 11-1 is at:

$$\nu_o = \omega_e - 2\omega_e x_e \text{ cm}^{-1} , \qquad (11\text{-}40)$$

where $\omega_e$ and $\omega_e x_e$ are, respectively, the vibrational constant and the first anharmonic correction term. Succeeding band origins of (2-1), (3-2), etc., are displaced by $v(2\omega_e x_e)$ cm$^{-1}$ where v is the vibrational quantum number of the lower state. The $\nu_o$ and B data in Table 11-1 are adequate for rough calculations of both band location and band width. For polyatomic species, which have more than one rotational constant, the one given in Table 11-1 is the largest value for the species.

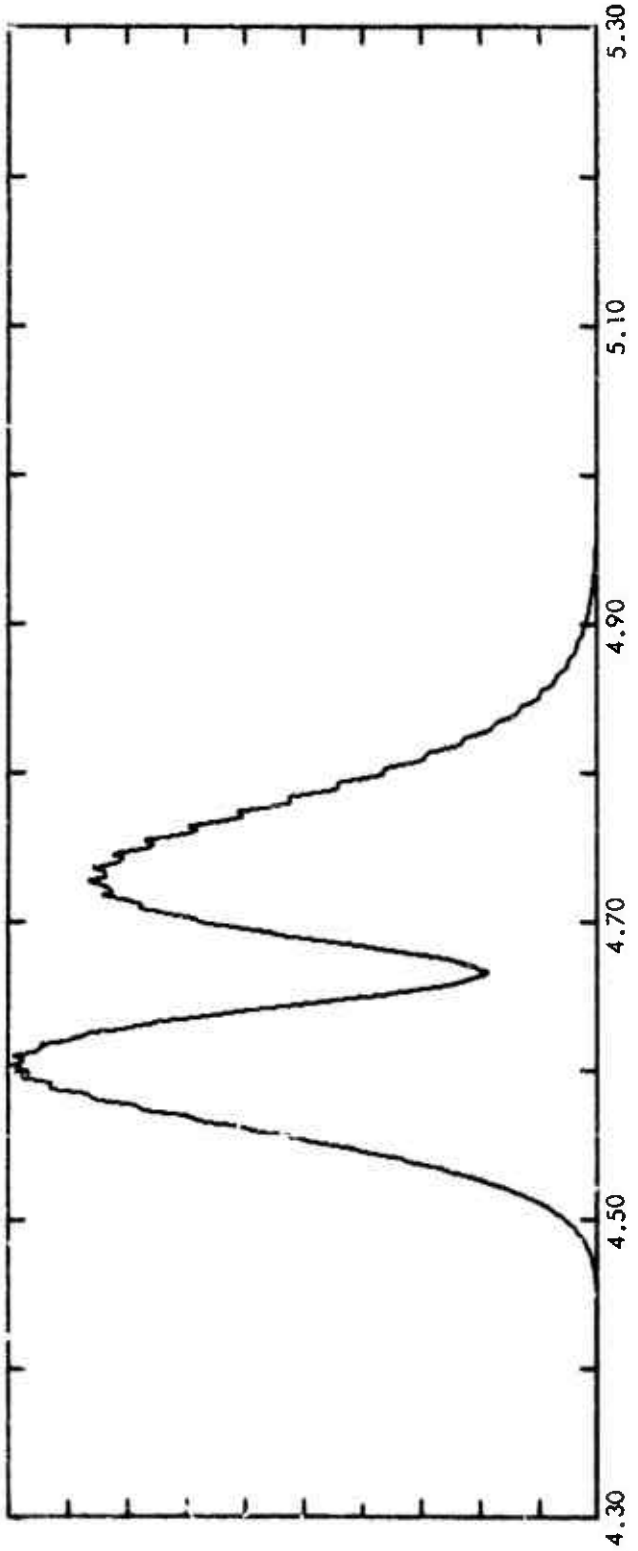


Figure 11-11. CO spectral band shapes in the 4.30-5.30 μm range (vibrational temperature = 300 K; rotational temperature = 300 K).

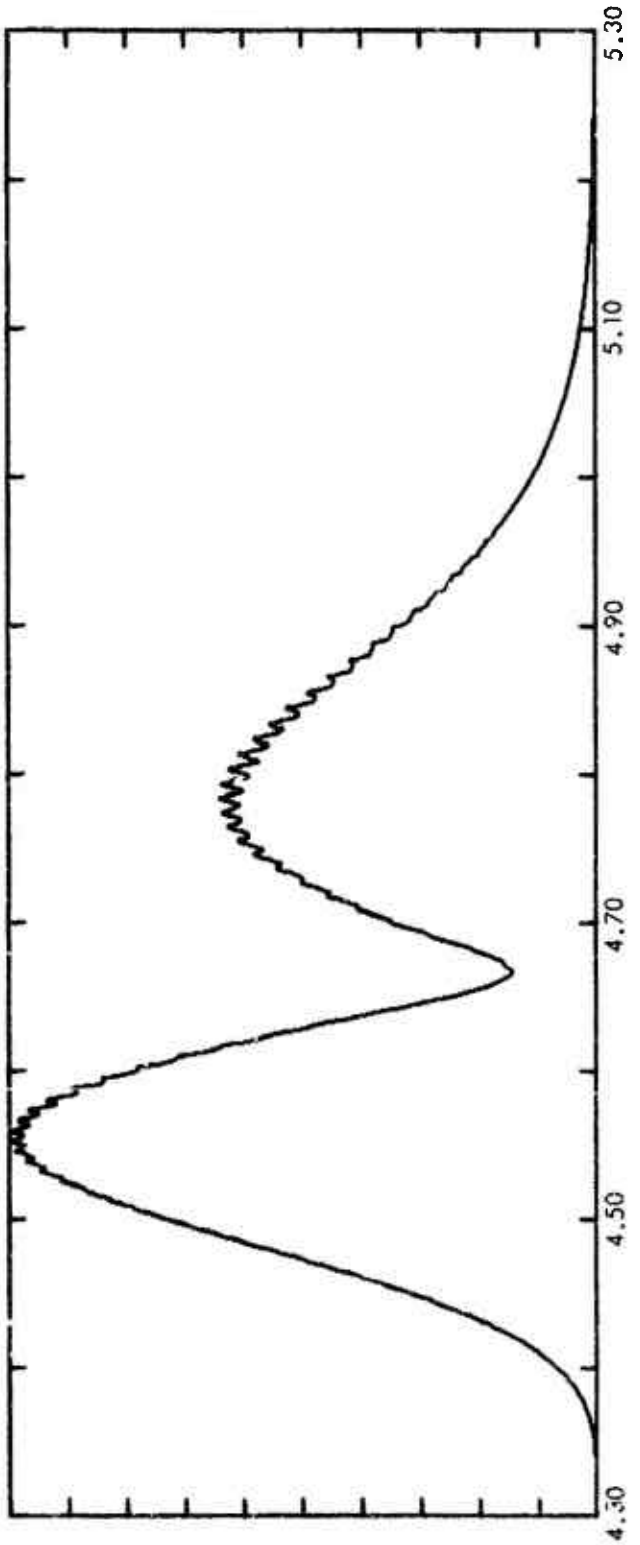


Figure 11-12. CO spectral band shapes in the 4.30-5.30 μm range (vibrational temperature = 1000 K; rotational temperature = 1000 K).

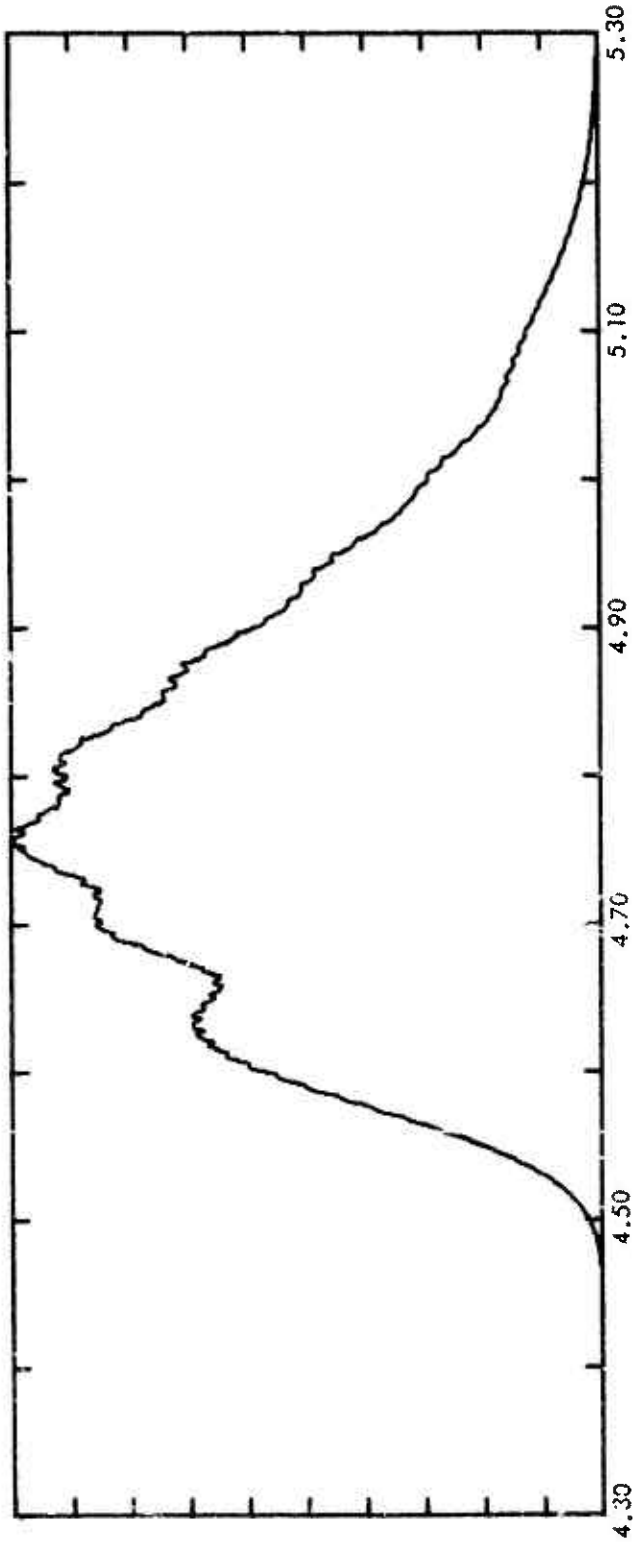


Figure 11-18. CO spectral band shapes in the 4.30–5.30 μm range (vibrational temperature = 5000 K; rotational temperature = 300 K).

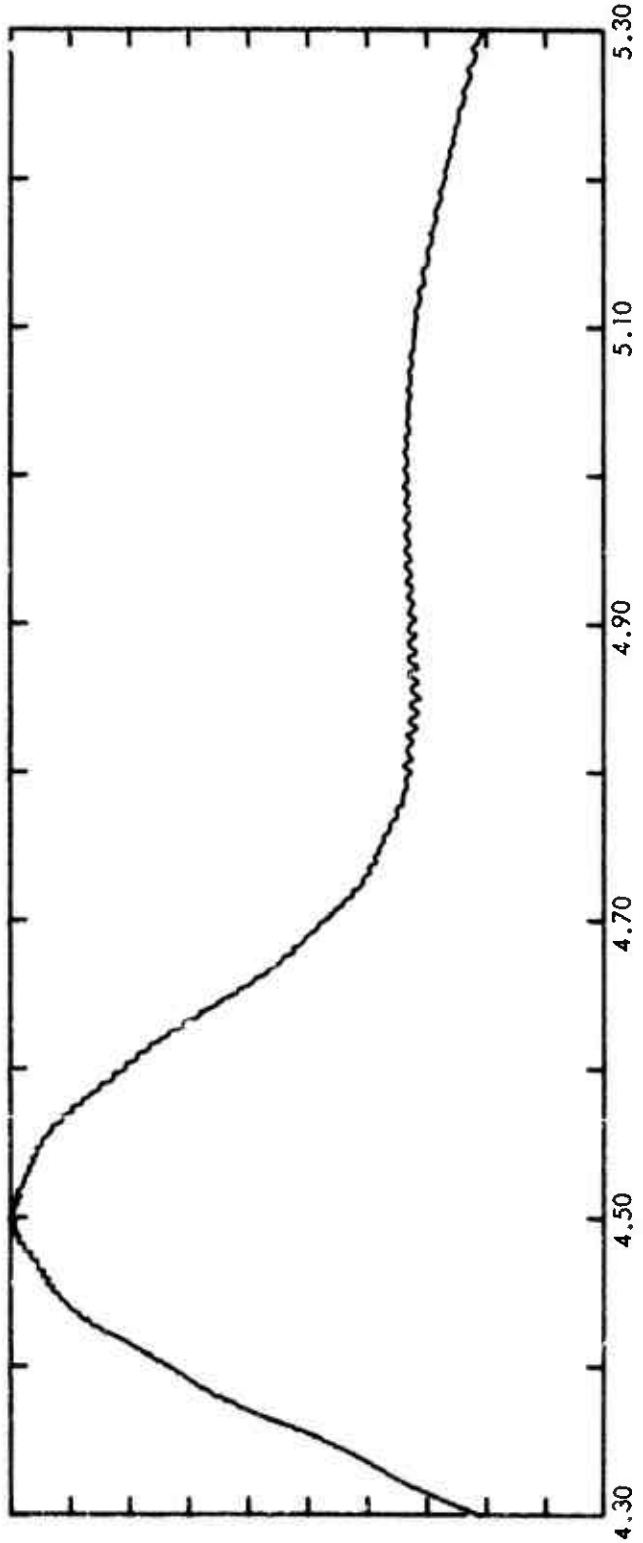


Figure 11-14. CO spectral band shapes in the 4.30–5.30 μm range (vibrational temperature = 5000 K; rotational temperature = 5000 K).

## APPENDIX II: RESONANCE FLUORESCENCE EXCITATION RELATIONSHIPS

Following are a group of definitions and equations which are useful in calculating infrared emission rates of gases:

### A. Definitions

| | |
|---|---|
| $S$ ($cm^{-2}$ $atm^{-1}$) | Integrated bandstrength of a transition |
| $S_e$ ($cm^{-2}$ $atm^{-1}$) | Bandstrength of an electronic transition |
| $f$ | Oscillator strength or "f-value" of a transition |
| $N_{col}$ ($cm^{-2}$) | Column density of a radiating species |
| $\lambda_\mu$ ($\mu m$) | Wavelength of a transition |
| $A$ ($sec^{-1}$) | Einstein spontaneous radiative transition probability |
| $B$ (watts $cm^{-2}$ $ster^{-1}$ $\mu m^{-1}$) | Surface brightness of a radiating volume |
| $R_{\lambda\mu}$ or $R_{\lambda\mu e}$ (watts $cm^{-2}$ $\mu m^{-1}$) | Irradiance falling upon a surface from either earthshine or sunshine, respectively. |
| $F$ | Fraction of molecules in an irradiated column excited per second under the influence of sunshine irradiance |

### B. Equations

$$S = 0.357 \lambda_\mu^2 A = 2.38 \times 10^7 f$$

$$h\nu = 1.98 \times 10^{-19} \lambda_\mu^{-1} \text{ watt-sec photon}^{-1}$$

$$F = 1.87 \times 10^{-5} \lambda_\mu^3 R_{\lambda\mu e} S$$

$F \times N_{col}$ = excitation rate along a line of sight

$$B = F\, N_{col}\, h\nu/4\pi = 2.94 \times 10^{-25}\, \lambda_{\mu}^{2}\, R_{\lambda\mu e}\, S\, N_{col} \ ,$$

in the absence of quenching

## REFERENCES


11-1. Bunn, F. E., and H. P. Gush, Can. J. Phys. 48, 98 (1970).

11-2. Huppi, E. R., and A. T. Stair, Jr., Air Force Cambridge Research Laboratories, private communication.

11-3. Stair, A. T., Jr., and H. P. Gauvin, in Aurora and Airglow, B. M. McCormac, Ed., Reinhold, New York (1967); p.365.

11-4. Zipf, E. C., Jr., W. L. Borst, and T. M. Donahue, J. Geophys. Res. 75, 6371 (1970).

11-5. Abstracted from AFCRL-OPI transmission program compilation (1972).

11-6. Milligan, D. E., and M. Jacox, J. Chem. Phys. 38, 2627 (1963).

11-7. Guttman, A., J. Quant. Spectry. Radiative Transfer 2, 1 (1962).

11-8. Goldman, A., T. G. Kyle, and F. S. Bonomo, Appl. Optics 10, 65 (1971).

11-9. Young, L. A., J. Quant. Spectry. Radiative Transfer 8, 693 (1968).

11-10. Feinberg, R. M., and M. Camac, J. Quant. Spectry. Radiative Transfer 7, 581 (1967).

11-11. Schurin, B., and S. A. Clough, J. Chem. Phys. 38, 1855 (1963).

11-12. Murphy, R. E., Air Force Cambridge Research Laboratories, private communication.

11-13. Penner, S. S., Quantitative Molecular Spectroscopy and Gas Emissivities, Addison-Wesley Publishing Co., Reading, Mass. (1959).

11-14. Abramowitz, S., N. Acquista, and K.R. Thompson, J. Phys. Chem. 75, 2283 (1971); also private communication.

11-15. Von Rosenberg, C. W., Jr., and K. L. Wray, Avco Aerospace Research Laboratory, Report AFCRL-70-0597 (AD 716493) (1970).

11-16. Kennealy, J. P., Air Force Cambridge Research Laboratories, unpublished estimate.

11-17. Herzfeld, K.F., and T. A. Litovitz, Absorption and Dispersion of Ultrasonic Waves, Academic Press, New York (1959).

11-18. Callear, A. B., and J. D. Lambert, in Comprehensive Chemical Kinetics III, C. H. Bamford and C. F. H. Tipper, Eds., Elsevier, New York (1969).

11-19. Kuhn, W. R., and J. London, J. Atm. Sci. 26, 189 (1969).

11-20. Taylor, R. L., and S. Bitterman, Revs. Mod. Phys. 41, 26 (1969).

11-21. Murcray, D. G., W. J. Williams, and J. N. Brooks, University of Denver, private communication.

11-22. Breshears, W. D., and R. Bird, J. Chem. Phys. 48, 4768 (1968).

11-23. Kieffer, J. H., and R. W. Lutz, in Eleventh Symp. (Int'l.) on Combustion, Berkeley, Calif., 1966, The Combustion Institute, Pittsburgh, Pa. (1967); p. 67.

11-24. Walker, J. C. G., R. S. Stolarski, and A. F. Nagy, Ann. Geophys. 25, 831 (1969).

11-25. O'Neil, R., Air Force Cambridge Research Laboratories, unpublished results.

11-26. Chamberlain, J. W., Physics of the Aurora and the Airglow, Academic Press, New York (1961).

11-27. Anlauf, K. G., R. G. MacDonald, and J. C. Polanyi, Chem. Phys. Letts. 1, 619 (1968).

11-28. Charters, P. E., R. G. MacDonald, and J. C. Polanyi, Appl. Optics 10, 1747 (1971).

11-29. Shefov, N. N., Planet. Space Sci. 17, 797, 1629 (1969); Ibid. 19, 129 (1971).

11-30. Breig, E. L., Planet. Space Sci. 18, 1271 (1970).

11-31. Stair, A. T., Jr., Air Force Cambridge Research Laboratories, private communication.

11-32. Good, R. E., Air Force Cambridge Research Laboratories, private communication.

11-33. Hushfar, F., J. W. Rogers, and A. T. Stair, Jr., Appl. Optics 10, 1843 (1971).

11-34. Hamlin, D. A., and B. F. Myers, Science Applications, Inc., private communication.

11-35. Degges, T., Visidyne, Inc., private communication.

11-36. Hochanadel, C. J., J. A. Ghormley, and J. W. Boyle, J. Chem. Phys. 48, 2416 (1968).

11-37. Riley, J. F., and R. W. Cahill, J. Chem. Phys. 52, 3297 (1970).

11-38. Kreuger, A. J., Science 166, 998 (1969).

11-39. Noxon, J. F., Science 168, 1120 (1970).

11-40. Fontijn, A., and S. Kurzius, AeroChem Research Laboratories, Report DNA 2735 1 (1971).

11-41. Conrath, B. J., R. A. Hanel, V. G. Kunde, and C. Prabhakara, J. Geophys. Res. 75, 5831 (1970).

11-42. Michels, H. H., J. Chem. Phys. 56, 665 (1972).

11-43. Bortner, M. H., R. A. Carabetta, and R. H. Kummler, General Electric Co., Report DASA 2560 (1970).

11-44. Bethe, H. A., and E. E. Salpeter, Quantum Mechanics of One and Two Electron Systems, Academic Press, New York (1957); Section 78.

11-45. Kramers, H. A., Phil. Mag. 46, 836 (1923).

11-46. Griem, H. R., Plasma Spectroscopy, McGraw-Hill, New York (1964); Chapter 5, especially Equations 5 through 26.

11-47. Karzas, W. J., and R. Latter, Astrophys. J., Suppl. 55, 167 (1961).

11-48. Finkelnberg, W., and T. Peters, in Handbuch der Physik 28, S. Flügge, Ed., Springer-Verlag, Berlin (1957); p. 97.

11-49. Anderson, A. D., and H. R. Griem, Proc. Sixth Int'l. Conf. Ionization Phenomena Gases, North Holland Publishing Co., Amsterdam (1963); Vol. 3, p. 293.

11-50. Biberman, L. M., and G. E. Norman, Opt. i Spektrosk. 8, 230 (1960).

11-51. Richter, J., in Plasma Diagnostics, W. Lochte-Holtgreven, Ed., North Holland Publishing Co., Amsterdam (1968); pp. 36 ff.

11-52. Schlüter, D. Z., Z. Astrophys. 61, 67 (1964).

11-53. Sappenfield, D., private communication.

11-54. Burgess, A., and M. J. Seaton, Monthly Notices Roy. Astron. Soc. 120, 121 (1961).

11-55. Geltman, S., Astrophys. J. 141, 376 (1965).

11-56. Doughty, N. A., P. A. Frazier, and R. P. McEachron, Monthly Notices Roy. Astron. Soc. 132, 255 (1966).

11-57. John, T. L., Monthly Notices Roy. Astron. Soc. 131, 315 (1966).

11-58. Roberts, J. R., and P. A. Voigt, J. Res. Natl. Bur. Stds. 75A, 89 (1971).

11-59. Mjolsness, R. C., and H. M. Ruppel, Phys. Rev. 154, 98 (1967).

11-60. Kivel, B., J. Quant. Spectry. Radiative Transfer 7, 27 (1967).

11-61. Zel'dovich, Y. B., and Yu. P. Raizer, Physics of Shock Waves and High Temperature Hydrodynamic Phenomena, Academic Press, New York (1966); Vol. 1, pp. 255 ff.

11-62. Holland, D. H., M. Scheibe, C. H. Humphrey, D. R. Churchill, G. Gioumousis, and L. M. Tannenwald, private communication.

11-63. Kivel, B., J. Quant. Spectry. Radiative Transfer 7, 51 (1967).

11-64. Frisov, O. B., and M. I. Chibisov, Sov. Phys. - JETP 12, 2235 (1961).

11-65. Geltman, S., Joint Institute for Laboratory Astrophysics, Private communication.

11-66. Bardsley, J. N., and F. Mandl, Repts. Prog. Phys. 31, 471 (1968).

11-67. Taylor, R. L., and G. Caledonia, J. Quant. Spectry. Radiative Transfer 9, 681 (1969).

11-68. Bates, D. R., E. Kingston, and R. W. P. McWhirter, Proc. Phys. Soc. A267, 297 (1962); Ibid A270, 155 (1962).

11-69. Bates, D. R., and E. Kingston, Planet. Space Sci. 11, 1 (1963).

11-70. Johnson, L. C., and E. Hinnov, Phys. Rev. 187, 143 (1969).

11-71. Peek, M., and D. Sappenfield, private communication.

11.72. Collins, C. B., Phys. Rev. 177, 254 (1969); Ibid. 186, 113 (1969).

# 12. PHOTOCHEMICAL PROCESSES: CROSS-SECTION DATA

Robert E. Huffman, Air Force Cambridge Research Laboratories
(Latest Revision 8 June 1971)

## 12.1 INTRODUCTION

The ultraviolet photon absorption processes are an important production mechanism for electrons, ions, and atoms in the atmosphere. These products serve as the reactants in ion-molecule, recombination, chemiluminescent, and other reactions discussed in this Handbook. Under normal atmospheric conditions, the ultraviolet photon absorption processes are the major energy deposition mechanism for solar energy in the upper atmosphere, although x-ray and particle reactions may be more important under special conditions. Following a nuclear detonation, energy in the form of ultraviolet photons is deposited by absorption in the atmosphere and leads to the production of ions and electrons.

In this chapter, the most important photon absorption processes related to the interests of DNA have been selected, and data from spectroscopic research on cross-sections, ionization thresholds, etc., are given. The wavelength region considered is approximately 3500 to 10 A. (Data to 1 A are found in Chapter 13.) The upper wavelength is approximately the ultraviolet limit of solar radiation absorbed by some constituent of the atmosphere. Wavelengths less than 2900 A are completely absorbed in the upper atmosphere. Since the shorter wavelengths in the range given are generally absorbed high in the atmosphere and are not available at lower altitudes, a further selection has been made of wavelength regions where especially important atmospheric absorption is known to occur.

This general research area is also of importance to reaction rate studies in other ways. Ultraviolet spectroscopy measures energy levels, characterizes excited states, and yields potential curves. Dissociation energies, transition probabilities, and ionization thresholds may be obtained. All of this information is intimately related to the study of reaction rates. In addition, the highly specific nature

of ultraviolet spectroscopy has led to its use as a tool in detecting transient species and measuring reaction rates.

## 12.2 TYPES OF ABSORPTION PROCESSES

When an ultraviolet photon is absorbed by a molecule, several processes may occur, as shown in Table 12-1. Generally speaking, the minimum energy required for these processes increases as one proceeds down the list of reactions in the table; however, the relative importance of the various processes and the threshold wavelength depend on the detailed electronic structure of the molecule. For example, a dissociation process may not occur even when energetically permissible because of the absence of a suitable repulsive state. The processes in Table 12-1 also may occur when the absorber is an atom, with the obvious exceptions of dissociation, ion-pair formation, and dissociative ionization. Although usually not specifically indicated or known, the products may be in excited states (electronic, vibrational, rotational) or possess excess kinetic energy. Processes resulting in ionization of the gas are particularly important, and the ionization thresholds of atmospheric gases are given in Table 12-2.

Scattering cross-sections are much smaller than the cross-sections of the processes considered here. The final state of the scattering species is identical with the initial state, as well, and for these reasons scattering is not considered.

As shown in Table 12-1, several general categories of absorption spectra may occur. Discrete absorption in the ultraviolet region consists of molecular vibration-rotation bands, or atomic line multiplets, of various electronic states. Continuum absorption indicates dissociation or ionization processes, which can occur over a wide range of photon energies, since kinetic energy can be imparted to the products. Diffuse spectra represent an intermediate case and are primarily associated with processes such as autoionization or predissociation for the species of interest here. Since a number of these processes may occur over the same wavelength regions, the spectrum may become rather complex. High resolution coupled with information about the products is generally required to find the types of processes. It is usually possible to restrict somewhat the number of processes likely to be important by considering energy limitations and the appearance of the spectrum.

Table 12-1. Photon absorption processes. (In general, energy required increases or threshold wavelength decreases from top to bottom of the table. Although not usually shown here, the products may be in excited states. The examples are meant to be illustrative and do not include all possible combinations.)

| Process | Example | Absorption Spectrum |
|---|---|---|
| Excitation | $O_2 + h\nu \rightarrow O_2^*$ | Discrete |
| Predissociation | $O_2 + h\nu \rightarrow O_2^* \rightarrow O + O$ | Diffuse |
| Dissociation | $O_2 + h\nu \rightarrow O + O$ | Continuum |
| Ionization | $O_2 + h\nu \rightarrow O_2^+ + e$ | Continuum |
| Autoionization | $O_2 + h\nu \rightarrow O_2^* \rightarrow O_2^+ + e$ | Diffuse |
| Ion-Pair Formation | $O_2 + h\nu \rightarrow O^+ + O^-$ | Continuum |
| Dissociative ionization | $O_2 + h\nu \rightarrow O^+ + O + e$ | Continuum |
| Multiple ionization | $O + h\nu \rightarrow O^{++} + 2e$ | Continuum |

Table 12-2. First ionization threshalds

| Gas | Wavelength (A) | Energy (eV) | Method | Reference |
|---|---|---|---|---|
| $O_2$ | 1027.8 | 12.063 | Photoionization | 12-80,81 |
| $N_2$ | 795.8 | 15.580 | Rydberg Series | 12-82 |
| O | 910.4 | 13.617 | Rydberg Series | 12-83 |
| $O_3$ | 986.6 | 12.80 | Electron Impact | 12-84 |
| NO | 1340.3 | 9.25 | Photoionization | 12-85 |
| N | 853.1 | 14.53 | Rydberg Series | 12-86 |
| $NO_2$ | 1267.7 | 9.78 | Photoionization | 12-81 |
| $N_2O$ | 961.1 | 12.90 | Photoionization | 12-81 |
| $CO_2$ | 900.4 | 13.769 | Rydberg Series | 12-79 |
| $H_2O$ | 982.6 | 12.618 | Rydberg Series | 12-79 |
| H | 911.8 | 13.598 | Rydberg Series | 12-87 |
| He | 504.3 | 24.587 | Rydberg Series | 12-87 |
| $O_2(o\,^1\Delta_g)$ | 1118.9 | 11.081 | Emission Spectro and Photoionization | 12-80,88 |

The total loss of photons by absorption for all processes at a given wavelength is given by the total absorption cross-section $\sigma_T$, with units of $cm^2$. It is defined through the absorption law:

$$I(\lambda) = I_o(\lambda) \exp[-\sigma_T(\lambda)\, n\ell] \quad , \tag{12-1}$$

where I and $I_o$ are the transmitted and incident light intensities, n is the density of the absorbing gas in $cm^{-3}$, and $\ell$ is the light path in cm. A commonly used unit is the Megabarn (Mb), which is equal to $10^{-18}$ $cm^2$. The absorption coefficient $k_T$, which is proportional to the cross-section, is frequently used in the literature. It has units of $cm^{-1}$ and is equal to $\sigma_T n_o$. Loschmidt's number, $n_o$, is equal to $2.69 \times 10^{19}$ $cm^{-3}$. Note that the absorption law equation is strictly applicable only when the bandwidth of the measuring instrument is small compared with the spectral feature measured. This is generally the case in continuum and diffuse spectra, but the possibility of error of this type should be kept in mind, especially with discrete spectra.

The ionization cross-section describes all the processes at a given wavelength which produce ions. It is the product of the ionization yield and the total absorption cross-section. The ionization yield is the fraction of the absorption which leads to ionization, and throughout most of the wavelength region considered here, the yield is generally less than one, since the emitted electron does not have sufficient energy for further ionization. When the excess kinetic energy of the electron can be greater than the ionization potential, the emitted electron may collide with an unionized gas molecule and produce additional ionization. The total yield would then be greater than unity. A rough value of about 30 eV kinetic energy per ion-electron pair, based on electron impact yields, has been used, but no experimental values for photoionization have been measured directly.

Cross-sections for the formation of specific products by the various processes in Table 12-1 can also be defined based on the yield of any product, in a manner similar to the ionization cross-section. Only the total absorption and ionization cross-sections are generally available. However, product cross-sections are required for many purposes, and the results of some measurements are given here.

A number of techniques are available with which to study the detailed interaction of photons with gases. These include photoelectron

spectroscopy, high-resolution photoionization mass spectrometry, ion energy analysis. fluorescence from excited products, and angular distribution studies. This information is included here where it appears to be important for aeronomic applications.

## 12.3 PHOTON CROSS-SECTION DATA

### 12.3.1 General

In this section photon cross-sections for the atmospheric gases $O_2$, $N_2$, O, N, NO, $O_3$, $CO_2$, $H_2O$, and $O_2(^1\Delta_g)$ are given in wavelength regions of importance to atmospheric studies. The cross-sections are given by a number of curves and by several tables covering absorption at emission lines found in the solar spectrum or predicted to result from nuclear detonations. Additionai tables covering the solar continua and shorter wavelengths are given in Chapter 13.

The data recommended here are the most reliable at this time in the judgment of the author. No attempt at a critical review of every measurement has been made. In fact, as has been pointed out several times in related scientific fields, the necessary information to form judgments about systematic and other errors is frequently lacking. There is, however, a general convergence of cross-section values for important atmospheric gases. For more details on all available measurements, leading references are given for guidance to the original literature. There are reviews primarily on photoionization (References 12-1, 12-2, 12-3), absorption of atmospheric gases (Reference 12-4), and absorption cross-sections (References 12-5, 12-6, 12-7).

### 12.3.2 Limitations of Data

The measurement of photon absorption cross-sections in the laboratory for use in atmospheric problems generally does not involve the uncertainties regarding pressure extrapolation, wall effects, or kinetic energy of reactants that are frequently a problem with the other reactions covered in this Handbook. The process studied is a relatively good simulation of the atmospheric event.

The density in the laboratory measurements is usually much higher than that of the atmosphere at altitudes of interest here. However, the measurements are invariably made over a range of densities, and

if the absorption law (Equation 12-1) is found to be valid at these densities, there is no reason to doubt that the cross-section is suitable for use at lower densities. Equation (12-1) may not be followed because of dimerization or pressure broadening, but these effects are generally not a problem at laboratory densities.

The temperature of the laboratory measurements is generally room temperature (about 300 K), and no indication of large changes in most cross-sections are predicted in the 200-300 K range of primary interest here, with the exception of the oxygen Schumann-Runge bands. A change in temperature will affect the cross-section by shifting the vibrational distribution in the ground state of the molecule or the sub-level distribution in a multiplet atomic state. For the atmospheric gases, there will be little change in these distributions over the temperature range quoted. However, there has been little research on temperature effects, and one cannot generalize. It is thought that the largest effect will probably be found in dissociation continua.

The cross-sections are generally known to about ±20 percent, although this is a very general figure and there are many measurements of better accuracy. Because of the exponential nature of the absorption law, considerably higher accuracies would be desirable.

The bandwidth or resolution used for cross-section measurements is generally inadequate in regions of discrete absorption due to molecular bands or atomic lines. In these cases, each absorption line has a Doppler half-width of less than .001 A at room temperature, which is much less than the laboratory bandwidth of from perhaps 0.05 to 1 A. For measureable changes in transmitted light, there is generally complete absorption at the peak of the line. Thus, the observed cross-section generally increases as the pressure or density decreases, and the reported cross-sections in these regions are typically the values at the lowest pressures used. These resolution-limited cross-sections have some application for atmospheric problems using similar bandwidths involving approximately the same number of molecules in the light path. In some cases, absorption data in regions of discrete structure can be used to obtain oscillator strengths by extrapolating to zero pressure.

There is virtually no information available on the photon cross-sections for atmospheric gases in excited electronic states, except for the $O_2(a^1\Delta_g)$ data given here. Emission spectra involving the

excited state can be used to find ionization thresholds and energy levels, which define generally the wavelength regions of absorption. Photon absorption processes may be the source of excited states formed by dissociation and ionization processes, but little quantitative information is available.

### 12.3.3 Data Summary

#### 12.3.3.1 MOLECULAR OXYGEN $O_2$

The weak Herzberg continuum in the 2600-1850 A region is usually considered as the primary source of oxygen atoms from $O_2$ photodissociation below 80 km. In this dissociation process two ground state ($^3P$) oxygen atoms are formed. There are two measurements in fairly good agreement (References 12-8, 12-9). The cross-sections are very small ($\sim 10^{-23}$ cm$^2$), and the high pressures necessary result in some dimerization, so extrapolation to zero pressure is necessary. The cross-section curve is given in Figure 12-1.

The Schumann-Runge bands ($^3\Sigma_u^- \leftarrow {}^3\Sigma_g^-$) between 1750 and 2010 A are discrete transitions requiring high resolution to obtain accurate cross-sections (References 12-4, 12-9 through 12-12). It is also difficult to separate the Herzberg continuum and the Schumann-Runge bands in the 1900-2030 A region. Absorption data (Reference

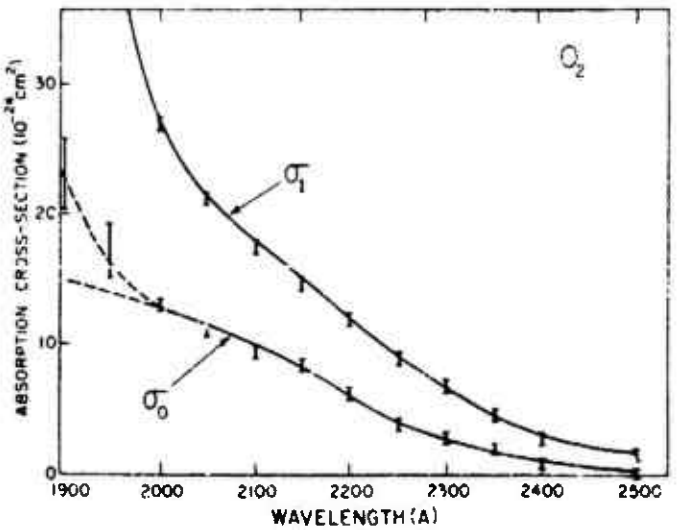


Figure 12-1. Oxygen absorption cross-sections in the Herzberg continuum. The one-atmosphere cross-section is denoted by $\sigma_1$ and the extrapolated zero-pressure cross-section by $\sigma_0$. Data of Ditchburn and Young, Reference 12-8

12-8) are given in Figures 12-2 and 12-3; however, these curves were taken with low resolution and serve to indicate only the principal absorption regions. The more recent work has partially resolved the rotational structure (Reference 12-13). For rotational line wavelengths, high-resolution spectra are available (Reference 12-14). Oscillator strengths have been obtained using pressure broadening (Reference 12-15), weak line absorption (Reference 12-12), and high-temperature absorption (Reference 12-11).

The strong Schumann-Runge continuum (1250-1750 A) is very important, since it is the primary source of oxygen atoms at altitudes greater than 80 km. The cross-section has been measured repeatedly with generally good agreement (References 12-9, 12-16 through 12-19), and a representative curve (Reference 12-9) is given in Figure 12-4. Absorption in the principal continuum produces one ground state ($^3P$) and one metastable ($^1D$) oxygen atom (References 12-20, 12-21, 12-22). A temperature effect has been discussed (Reference 12-23), and other measurements (Reference 12-24) have found an increase in cross-section with temperature in the 1580-1950 A region.

In the region from the hydrogen Lyman-alpha line (1215.7 A) to approximately 304 A, cross-sections are given at important solar

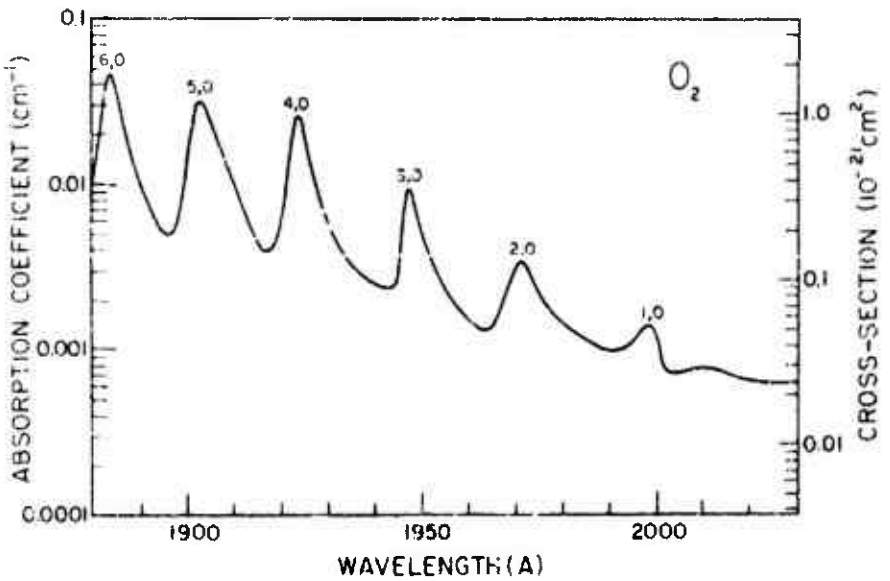


Figure 12-2. Oxygen absorption cross-sections, Schumann-Runge bands (1, 0 to 6, 0). Data of Blake, Carver, and Haddad, Reference 12-9.

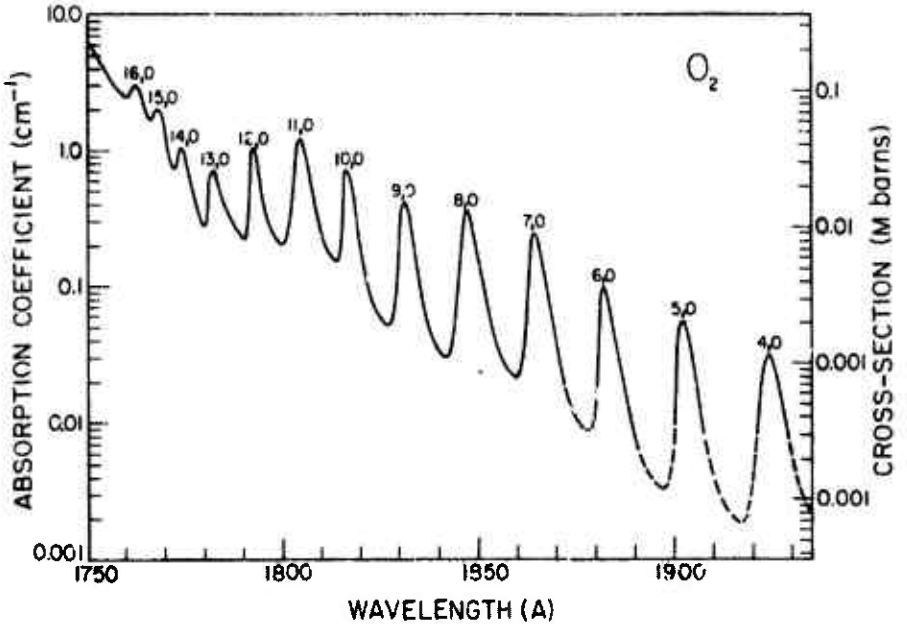


Figure 12-3. Oxygen absorption cross-sections, Schumonn-Runge bands (4, 0 to 16, 0). Dato of Bloke, Carver, ond Haddad, Reference 12-9.

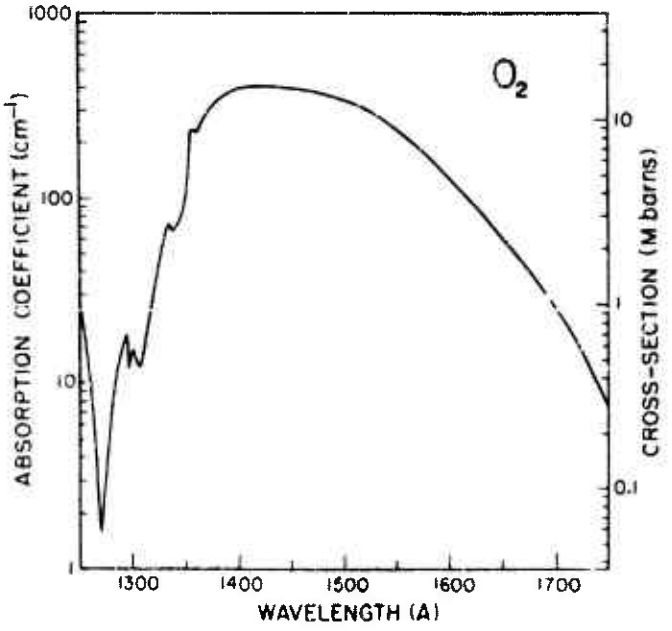


Figure 12-4. Oxygen absorptian cross-sectians ir. the Schumonn-Runge continuum. Data af Bloke, Carver, and Haddod, Reference 12-9.

emission lines in Table 12-3. Values at wavelengths less than 304 A are presented in Table 12-4. From 1250 A to the ionization threshold (1027.8 A) the spectrum is complex with several regions of low absorption (References 12-4, 12-9, 12-17, 12-25, 12-26), such as the important H Ly α window (Table 12-3). In the ionization region, Table 12-3 includes both total absorption and ionization cross-sections, and is based on several measurements (References 12-18, 12-27 through 12-30), which are in general agreement with earlier work (Reference 12-4). The cross-section curves are available in the references.

Table 12-3. Absorption and ionization cross-sections of $O_2$, $N_2$, and O at solar lines. Cross-sections in Megabarns ($10^{-18}cm^2$). Values based on data in References 12-4, 12-18, 12-27, 12-28, 12-29, 12-31, 12-36, 12-37, 12-43, and 12-47. Table prepared in collaboration with R.I. Schoen and based on Reference 12-5.

| Solar Line λ(A) | Class. | $O_2$ | | $N_2$ | | O |
|---|---|---|---|---|---|---|
| | | σ | $\sigma_i$ | σ | $\sigma_i$ | $\sigma = \sigma_i$ |
| 1215.7 | HLy α | 0.010 | 0 | $<6\times10^{-5}$ | 0 | 0 |
| 1206.5 | SiIII | 15 | 0 | ~0 | 0 | 0 |
| 1175.5[a] | CIII | 1.3 | 0 | - | 0 | 0 |
| 1085.7[d] | N II | 2[b] | 0 | - | 0 | 0 |
| 1037.6[a] | OVI | 0.78 | 0 | $<7\times10^{-4}$ | 0 | 0 |
| 1031.9 | OVI | 1.04 | 0 | $<7\times10^{-4}$ | 0 | 0 |
| 1025.7 | HLy β | 1.58 | .98 | $<10^{-3}$ | 0 | e |
| 991.6[c] | N III | 1.75 | 1.21 | 1.9[b,c] | 0 | 0 |
| 989.8[a] | N III | 1.4 | 0.95[b,c] | 1.1[c] | 0 | e |
| 977.0 | CIII | 4.0 | 2.5 | 0.7[c] | 0 | 0 |
| 972.5 | HLy γ | 32 | 25[b] | 360[b,c] | 0 | 0 |
| 949.7 | H Ly | 6.3 | 4[b] | 5.2[b] | 0 | 0 |
| 937.8 | H Ly | 5.0 | 3 | 10[b] | 0 | e |
| 930.7 | H Ly | 26 | 17[b] | 4.8[b] | 0 | e |
| 904 | CII | 11 | 6.3[b] | 6.3 | 0 | 3.0 |

Table 12-3. (Cont'd.)

| Solar Line λ(A) | Class. | $O_2$ | | $N_2$ | | O |
|---|---|---|---|---|---|---|
| | | σ | $\sigma_i$ | σ | $\sigma_i$ | $\sigma = \sigma_i$ |
| 835.3 | O III | 10 | 3.7 | 20[b] | 0 | 2.6[f] |
| 835.1 | O III | 10 | 3.7 | 41[b] | 0 | 2.6 |
| 834.5 | O II | 11 | 4.0 | 7.5[b] | 0 | 2.6[f] |
| 833.7 | O III | 13 | 5.1 | 6[b] | 0 | 2.6 |
| 833.3 | O II | 13 | 5 | 2.3 | 0 | 2.6 |
| 832.9 | O III | 26 | 10 | 7[b] | 0 | 2.6[f] |
| 832.8 | O II | 26 | 10 | 2.1 | 0 | 2.6 |
| 790.2 | O IV | 28 | 10[b] | 22[c] | 10[b,c] | 2.9 |
| 790.1 | O IV | 28 | 10[b] | 28[c] | 11[b,c] | 2.9 |
| 787.7 | O IV | 24 | 13[b] | 10[c] | 8[c] | 2.9[f] |
| 780.3 | Ne VIII | 28 | 11[b] | 19 | - | 2.9 |
| 770.4 | Ne VIII | 18 | 11 | 15 | - | 7[e] |
| 765.1 | N IV | 23 | 12[b] | 67[c] | 51[b,c] | 3.0 |
| 760.4 | O V | 20 | 10 | 40 | 22 | 2.9[f] |
| 703.8 | O III | 26 | 23 | 22 | 20 | 6.5 |
| 702.3 | O III | 24 | 21 | 24 | 22 | 6.5 |
| 686.3 | N III | 22 | 22 | 25[c] | 24[c] | 6.5[e] |
| 685.8 | N III | 18 | 18 | 26[c] | 25[c] | 6.5 |
| 685.5 | N III | 18 | 18 | 25[c] | 24[c] | 6.5[e] |
| 685.0 | N III | 26 | 26 | 25[c] | 24[c] | 6.5 |
| 629.7 | O V | 30 | 29 | 23[c] | 23[c] | 9.0 |
| 625 | Mg X | 25 | 24 | 24 | 23 | 9.0 |
| 610 | Mg X | 27 | 25 | 24 | 24 | 9.0 |
| 599.6 | O III | 28 | 27 | 23 | 22 | 9.0 |
| 584.3 | He I | 23 | 23 | 23 | 23 | 9.5 |
| 555.3 | O IV | 26 | 25 | 25 | 24 | 9.5 |

Table 12-3. (Cont'd.)

| Solar Line λ(A) | Class. | $O_2$ | | $N_2$ | | O |
|---|---|---|---|---|---|---|
| | | σ | $\sigma_i$ | σ | $\sigma_i$ | $\sigma = \sigma_i$ |
| 554.5 | CIV | 26 | 26 | 25 | 23 | 9.5 |
| 554.1 | OIV | 26 | 25 | 25 | 24 | 9.5 |
| 553.3 | OIV | 26 | 24 | 25 | 24 | 9.5 |
| 537.0 | He I | 21 | 21 | 25 | 24 | 9.3 |
| 525.8 | OIII | 25 | 24 | 26 | 26 | 9.3 |
| 522.2 | HeI | 21 | 21 | 24 | 23 | 9.3 |
| 508.2 | OIII | 24 | 23 | 22 | 22 | 9.3 |
| 507.7[d] 507.4 | OIII | 23 | 22 | 24 | 24 | 9.3 |
| 435.0 | O III | 21 | 21 | 24 | 24 | 9 |
| 430.2[d] 430.0 429.9 | O II | 18 | 18 | 21 | 21 | 9 |
| 303.8 | HeI | 17 | 17 | 12 | 12 | 8.5 |

Notes:

[a] Blend of severol lines observed in salar spectrum.

[b] The absarbing gas has discrete structure at this wavelength ond thus the cross-sectian presently measureable given in the table may nat be applicable. See text and references.

[c] Canside rable variation among measurements.

[d] These lines nat resolved in loboratory cross-section measurement.

[e] Passible averlap with atomic axygen graund-state ($^3P$) absorptian line.

[f] Possible overlap with otomic axygen metastable-stote ($^1D$) absorption line.

Table 12-4. Absorption cross-sections[a] at wavelengths less than 304 A. Data primarily from References 12-47, 12-89, 12-90. Cross-sections in Megabarns ($10^{-18}cm^2$).

| Wovelength[b] (A) | $O_2$ | $N_2$ | O |
|---|---|---|---|
| 247.2 | 12.3 | 9.8 | 6 |
| 209.3 | 9.0 | 6.5 | 4 |
| 100 | 1.9 | .84 | 0.8 |
| 68.0 | .9 | .50 | .2 |
| 44.6 | .31 | .18 | .1 |
| 13.4 | .29 | .089 | .14[c] |
| 9.9 | .14 | .042 | .071[c] |

Notes:

[a] These cross-sections ore ossumed to be equal to the ionization cross-section at ieast to 100 A, although there are no yield measurements.

[b] There are a number of solar lines in this region, but there have been few meosurements, and also the cross-section curve appears to be relatively smooth. The wavelengths used should allow a reasonable estimate to be made.

[c] This value is one-half the $O_2$ cross-section.

The dissociative ionization process giving $O^+$ and O begins at 662 A, and the yield appears to be less than 10 percent of the total ionization yield in the region down to about 450 A, with a conventional magnetic mass spectrometer (Reference 12-31). However, excess kinetic energy has been found in the product ions, and a more recent estimate is 15 percent dissociative ionization at the 584 A line (Reference 12-32). The cross-sections for excitation to various specific molecular ions over a range of wavelengths (Reference 12-33) are given in Figures 12-5 and 12-6. These were obtained by energy analysis of the emitted electrons.

Appreciable quantities of the metastable oxygen $O_2(a\,^1\Delta_g)$ molecule appear to be present in the upper atmosphere (References 12-34, 12-35). It is conceivable that absorption by this molecule may be

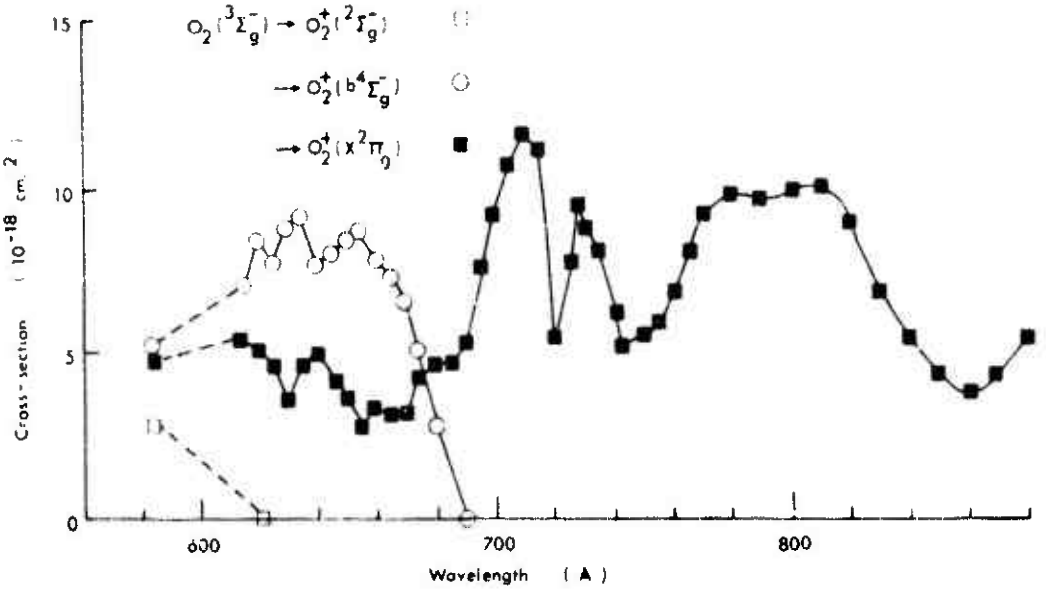


Figure 12-5. Oxygen partial cross-sections for molecular ions. Data of Blake and Carver, Reference 12-33.

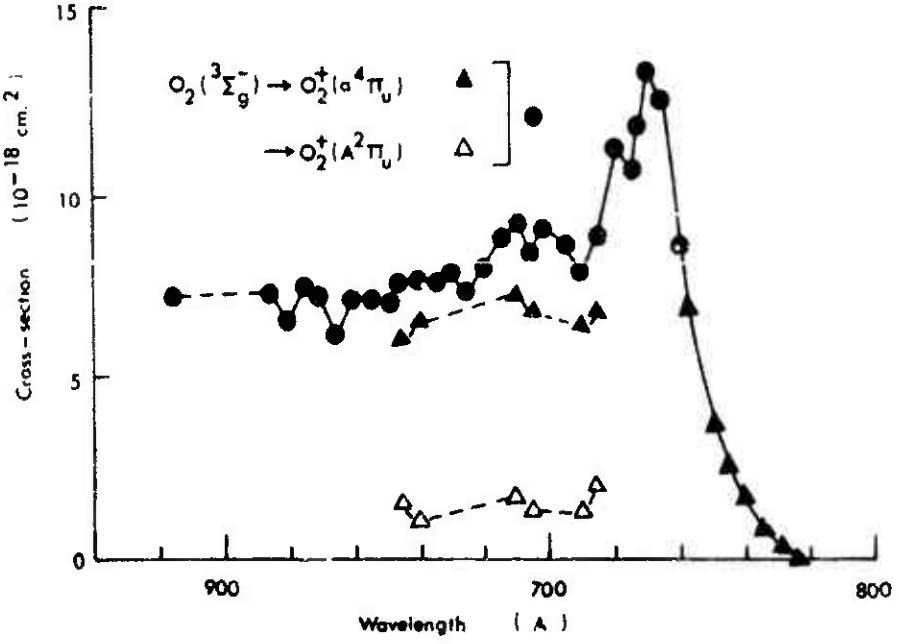


Figure 12-6. Oxygen partial cross-sections for molecular ions. Data of Blake and Carver, Reference 12-33.

more significant than is generally realized. Some intense bands attributed to absorption by the (a $^1\Delta_g$), or less likely the (b $^1\Sigma_g^+$), state have been observed in the 830-900 A region (References 12-36, 12-37), and high-resolution work has found absorption bands of both the (a $^1\Delta_g$) and the (b $^1\Sigma_g^+$) states in the 1200-1600 A region (Reference 12-38).

The ionization threshold of $O_2$(a $^1\Delta_g$) is at 1118.9 A. Measurements are available of the photoionization cross-section (References 12-26, 12-39) between this wavelength and the ionization threshold for ground-state $O_2$ at 1027.8 A. This wavelength region is important (Reference 12-40) in D-region ionization because some of these wavelengths penetrate to lower altitudes in $O_2$ absorption "windows". However, absorption by the trace amounts of carbon dioxide present at these altitudes considerably reduces the solar flux (Reference 12-26).

### 12.3.3.2 MOLECULAR NITROGEN $N_2$

The absorption spectrum of nitrogen begins at about 1450 A with the weak Lyman-Birge-Hopfield bands, but in the region to approximately 1000 A the cross-sections are very small (less than $10^{-21}$ $cm^2$). This absorption is insignificant compared with $O_2$ absorption in the same region. High-temperature absorption (Reference 12-41) and oscillator strengths (Reference 12-42) have been measured in this region. Between 1000 and 660 A there are many strong bands. One band coincides with the strong H Ly $\alpha$ solar emission line at 972.5 A. In the ionization region at wavelengths less than 795.8 A, most of the $N_2$ bands are autoionized.

There are no strong dissociation continua for nitrogen as there are for oxygen, although predissociation has been predicted (Reference 12-43). There are strong ionization continua at wavelengths less than 795.8 A, the ionization threshold. Absorption in this region is an important electron source in the F-region.

Table 12-3 gives absorption and ionization cross-sections for nitrogen at important solar lines based on several investigations (References 12-18, 12-27, 12-29, 12-44, 12-45). Absorption cross-sections below 304 A are included in Table 12-4. Earlier work has been summarized (References 12-4, 12-5). In Table 12-3, there are a number of wavelengths at $N_2$ absorption bands where reliable cross-sections could not be obtained, as indicated in the table. Cross-section curves using continuum background light sources are available in the references (References 12-18, 12-28, 12-29, 12-44).

Dissociative ionization begins at 510 A; however, the yield is only about one percent of the molecular ion yield in the one measurement available (Reference 12-31). Cross-sections for production of excited molecular ions (Reference 12-33) are given in Figure 12-7.

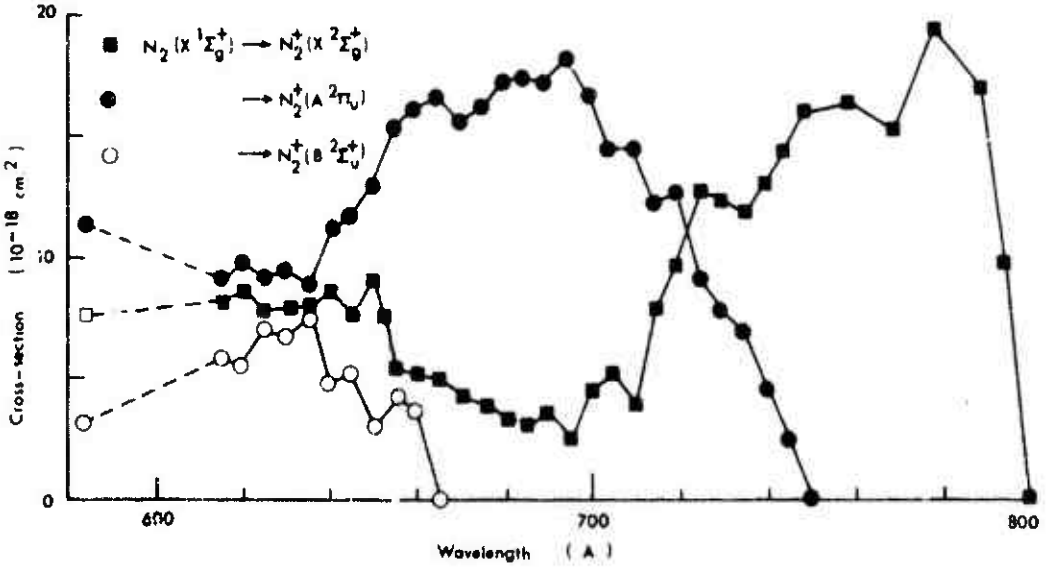


Figure 12-7. Nitrogen partial cross-sections for molecular ions. Data of Blake and Carver, Reference 12-33.

### 12.3.3.3 ATOMIC OXYGEN O

The absorption spectrum of ground-state atomic oxygen $2p^4\,{}^3P_{2,1,0}$ consists of a number of resonance line series beginning with the triplet at 1302, 1305, 1306 A and the ionization continuum at wavelengths shorter than 910.4 A, the first ionization threshold.

The available data concerning absorption in the ionization continuum region are given in Figures 12-8 through 12-10. Theoretical calculations (Reference 12-46) of the continuum cross-section are also given in the figures. The curves are similar to previous, more approximate calculations (Reference 12-47). The experimental values are much more recent, since there are many difficulties in working with atomic oxygen. The first measurements (Reference 12-48) used

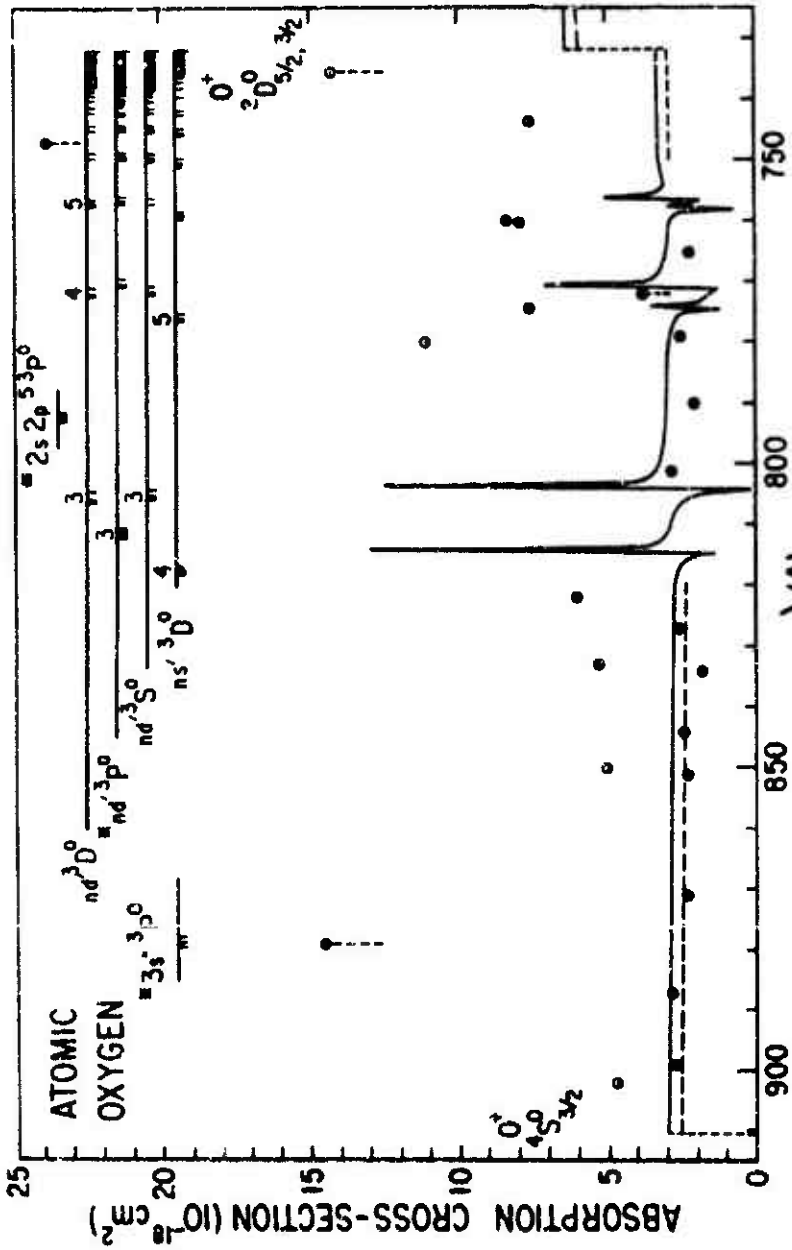
ATOMIC
OXYGEN
ABSORPTION CROSS-SECTION ($10^{-18}$ cm$^2$)
λ (A)
0
5
10
15
20
25
900
850
800
750
$^4S^0_{3/2}$
$^2D^0_{5/2, 3/2}$
$^3P^0$
$^3S^0$
$^3D^0$
$^3P^0

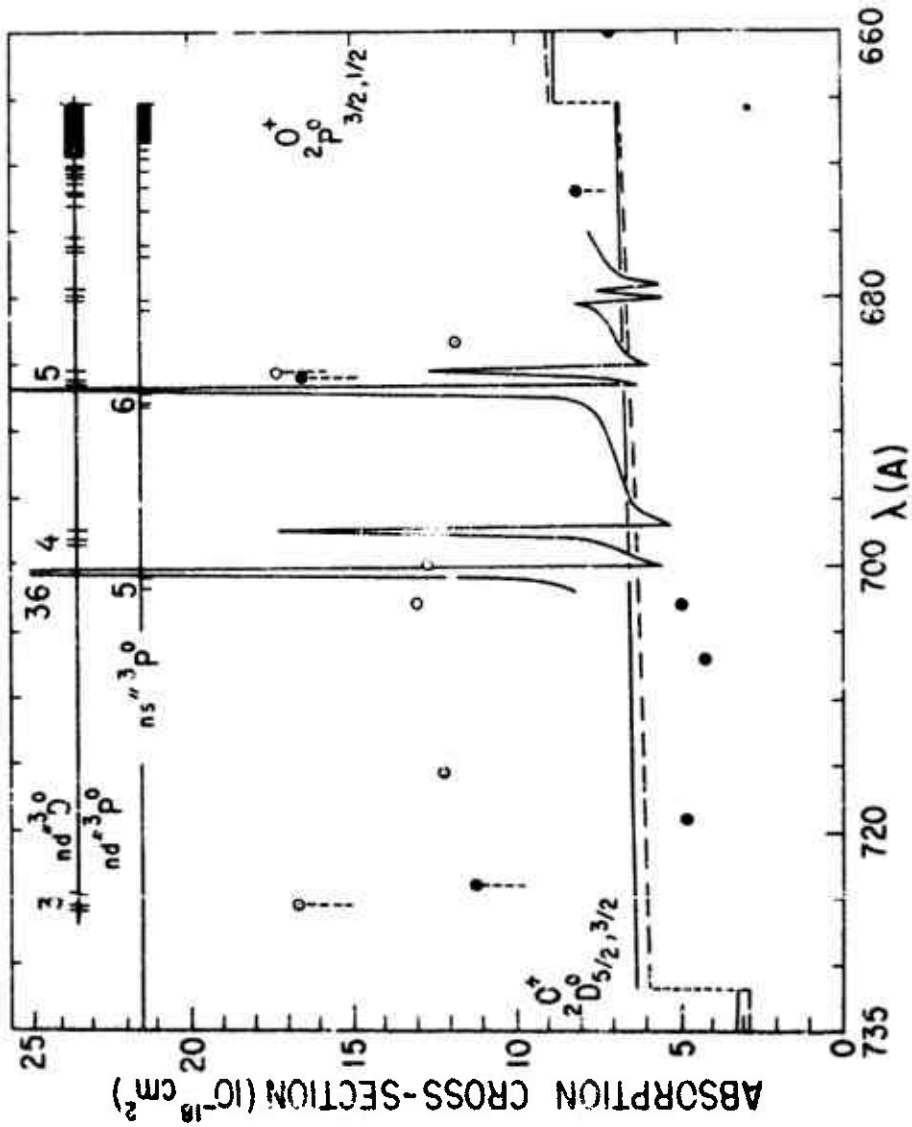


Figure 12-9. Atomic oxygen cross-sections: $^2D$ threshold to $^2P$ limit. See Figure 12-8 caption for references.

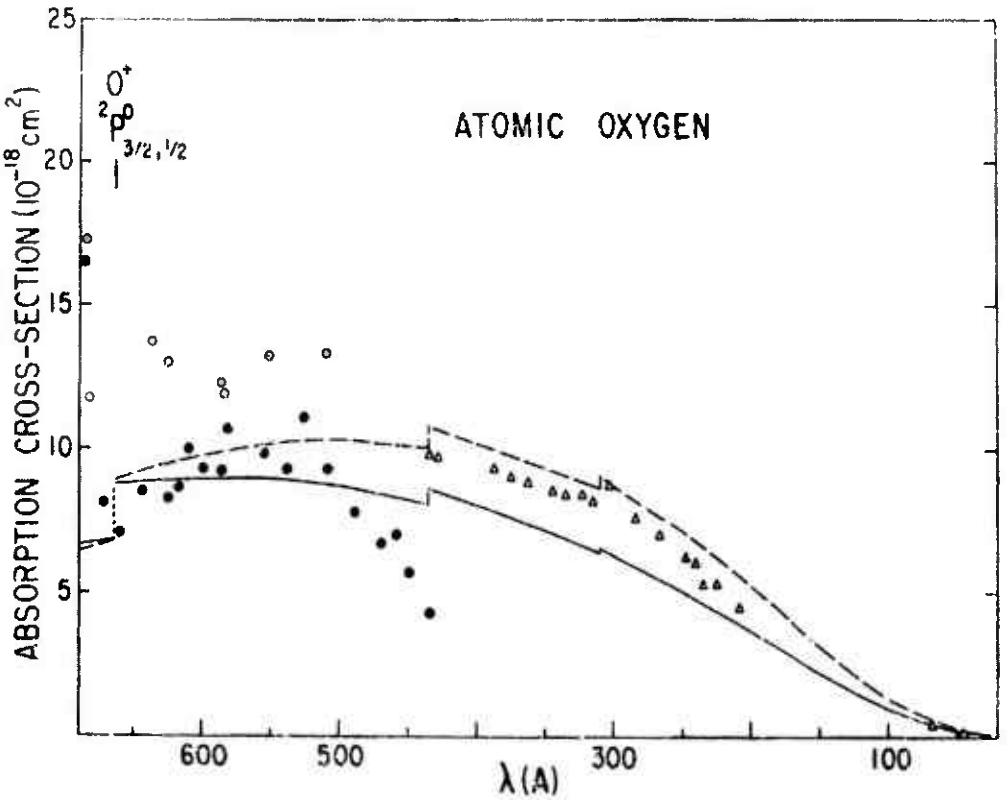


Figure 12-10. Atomic oxygen cross-sections: $^2P$ threshold to shorter wavelengths. See Figure 12-8 caption for references. Open triangles are one-holf of molecular oxygen cross-section (Reference 12-46).

discharged oxygen, which required a difficult correction for metastable $O_2$ molecules also present in the absorption cell. More recent measurements have used a beam technique (Reference 12-49) which required calibration based on the very accurate calculations possible for a hydrogen-atom beam. The theoretical values and the beam data are in best agreement, except at wavelengths shorter than 500 A, where the beam results become much lower than theoretical. The theoretical curve is preferred in the continuum absorption regions. The values in Table 12-3 are from these curves. Additional values are listed in Table 12-4. By analogy with the rare gases, the absorption and ionization continuum cross-sections are identical.

The ionization continuum region is complicated by the presence of series converging to the excited oxygen ion states $2p^3\ ^2D^o$ and

$2p^3\ ^2P^o$. These lines have been classified and measured in absorption (Reference 12-36), which enables the previously unknown autoionized lines to be observed. The lower members of these series are shown in Figures 12-8 and 12-9, with the unautoionized levels indicated by an asterisk. Accidental line absorption (References 12-48, 12-50) has led to cross-section measurements that are larger than nearby points, as shown by the dashed lines beneath some points in Figures 12-8 and 12-9.

There has been a theoretical calculation of some autoionized line profiles (Reference 12-51). The published calculations used a bandwidth corresponding to 1 A. Since the measurements used atomic lines, this bandwidth is considerably too large to use in a meaningful comparison with experimental values. Further calculations using a 0.1 A bandwidth (Reference 12-52) are shown in Figures 12-8 and 12-9. These profiles and maxima are in much better agreement with the available cross-sections and with estimates of absorption line maxima (Reference 12-53). Some maxima are not shown because the calculated points were too widely spaced in wavelength.

Both the $2p^4\ ^1D_2$ and $2p^4\ ^1S_o$ metastable states of atomic oxygen are known to be present in the atmosphere. Measurements of absorption series of these metastables have been reported (Reference 12-37). There also exist calculations of their ionization cross-sections (Reference 12-46) and a review of $O(^1D)$ formation and reactions (Reference 12-54).

It is possible that atmospheric spectrophotometric measurements may be influenced by the accidental overlap of a solar emission line and an atomic oxygen line (Reference 12-53). An abridged version of the possible solar lines involved is given in Table 12-5.

For a number of atmospheric problems, the cross-sections for ionization between specific electronic states of the atom and the ion are required. These are given for all $2p^4 \rightarrow 2p^3$ transitions in Figure 12-11 (Reference 12-55), which is based on an interpolation formula developed following close-coupling calculations (Reference 12-56). This formula does not include the autoionization structure apparent in Figures 12-8 and 12-9, which is based on experiment and on more detailed calculations. Therefore, Figures 12-8 through 12-10 are more useful for total attenuation calculations and Figure 12-11 is necessary to calculate the products.

Table 12-5. Atomic oxygen lines which may absorb solar lines. Atomic oxygen resonance lines (1302, 1305, 1306 A) not included. References 12-36, 12-37, 12-53 give details.

| Solar Line (A) | OI Line (A) | Classification | Remarks |
|---|---|---|---|
| 1025.7 | 1025.7 | $^3P_2 - 3d\,^3D^o$ | a |
| 939.8 | 990.13 | $^3P_1 - 3s'\,^3D^o$ | |
| 937.8 | 937.84 | $^3P_2 - 7s'\,^3S^o$ | |
| 930.7 | 930.89 | $^3P_1 - 7d\,^3D^o$ | |
| 835.3 | 835.44 | $^1D_2 - 10d'\,^1F^o,\ ^1D^o$ | |
| 834.5 | 834.34 | $^1D_2 - 12s'\,^1D^o$ | |
| 832.9 | 833.10 | $^1D_2 - 12d'\,^1F^o,\ ^1D^o$ | |
| 787.7 | 788.18 | $^1D_2 - 5s''\,^1P^o$ | b |
| 770.4 | 770.35 | $^3P_1 - 4d'\,^3P_2{}^o$ | |
| 761.1 | 761.26 | $^1D_2 - 6d''\,^1F^o,\ ^1D^o$ | b |
| 686.3 | 686.28 | $^3P_1 - 5d''\,^3P^o,\ ^3D^o$ | b, c |
| 685.5 | 685.54 | $^3P_2 - 5d''\,^3P^o\,^3D^o$ | b, c |

Notes:

a Solar line known to be broad.

b Atomic oxygen line broadened by autoionization.

c These lines known to overlap. See References 12-25 and 12-27.

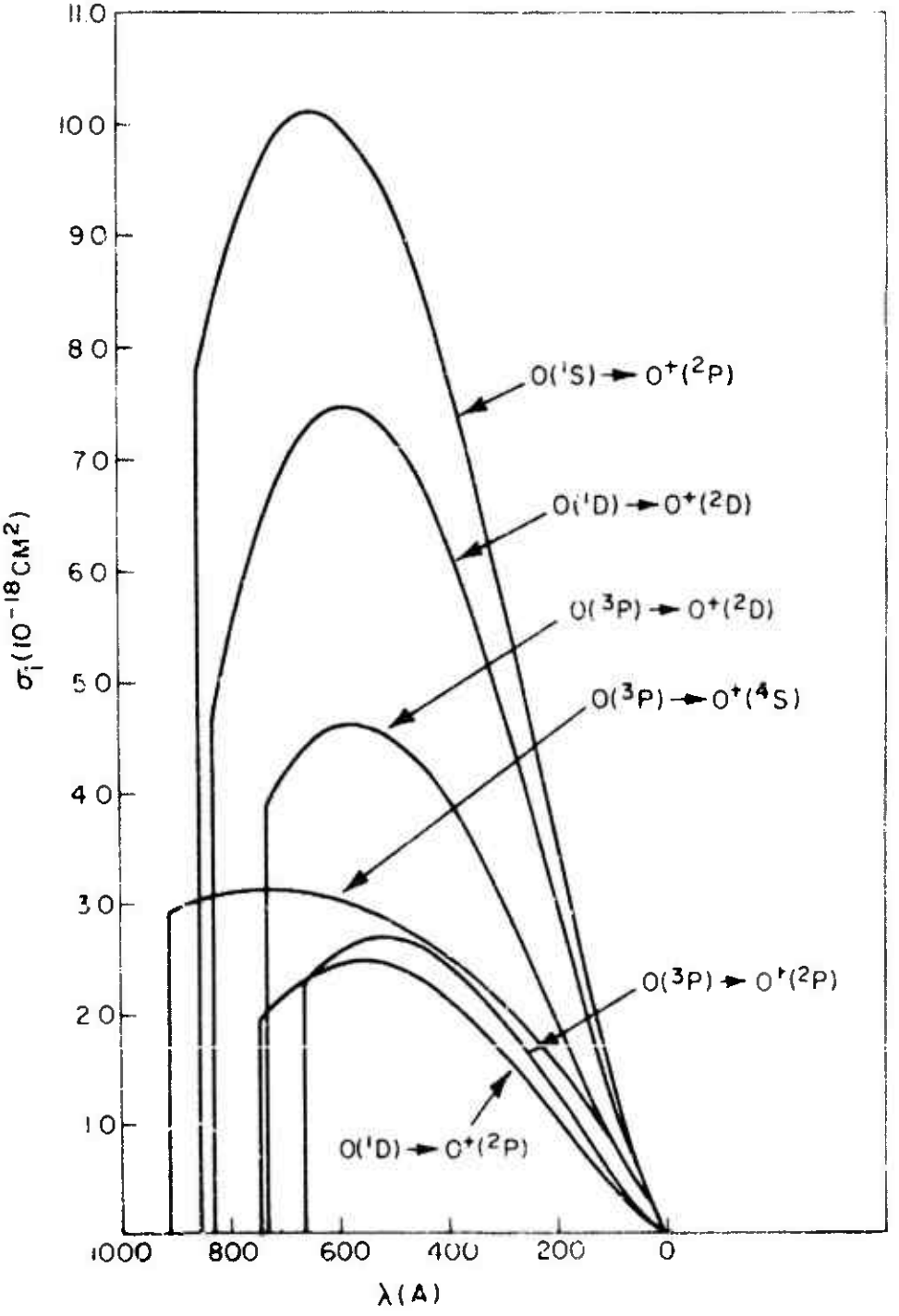


Figure 12-11. Atomic oxygen photoionization cross-sections for specific initial and final states. References 12-55, 12-56.

### 12.3.3.4 ATOMIC NITROGEN N

The absorption spectrum of ground-state atomic nitrogen $2p^3\ ^4S^o_{3/2}$ consists of resonance line series beginning with a triplet at 1199.5, 1200.2, and 1200.7 A and converging to the ionization continuum at wavelengths less than 853.1 A, the first ionization threshold.

Cross-sections in the ionization continuum region are given in Figure 12-12, which is based on curves (Reference 12-55) drawn from close-coupling calculations (Reference 12-56). Also included in the figure are experimental points (Reference 12-57) for absorption by the atomic ground state. They are in reasonably good agreement with the approximate calculation shown in Figure 12-12 and with more detailed calculations (Reference 12-58). In addition, Figure 12-12 gives the cross-sections for production of excited atomic ions due to absorption by excited neutrals for all transitions $2p^3 \rightarrow 2p^2$. The autoionized lines known to exist (References 12-57, 12-59) in some portions of the wavelength region shown are not reflected in the calculated curves.

### 12.3.3.5 NITRIC OXIDE NO

The ionization of nitric oxide by the hydrogen Lyman alpha line (1215.7 A) is an important process in the D-region. At other wavelengths, the NO absorption is not as important. The total and ionization cross-section curves (Reference 12-60) are given in Figure 12-13 for the 1100-1350 A region. The ionization cross-section (References 12-2, 12-61) at hydrogen Lyman alpha is $1.97 \times 10^{-18}$ $cm^2$.

### 12.3.3.6 OZONE $O_3$

Ozone absorption becomes important in the upper atmosphere at wavelengths less than about 3500 A. The region from about 3000 to 3500 A contains the weak Huggins bands; however, the relatively more intense solar radiation of these wavelengths makes absorption by ozone important here (Reference 12-62) as well as at wavelengths less than 3000 A. The absorption curve (Reference 12-63) is shown in Figure 12-14. New data in this region have been published (Reference 12-64). The weak Chappuis bands in the visible (maximum wavelength near 6000 A; maximum cross-section about 0.004 Mb) is an important dissociation mechanism in the stratosphere (Reference 12-65).

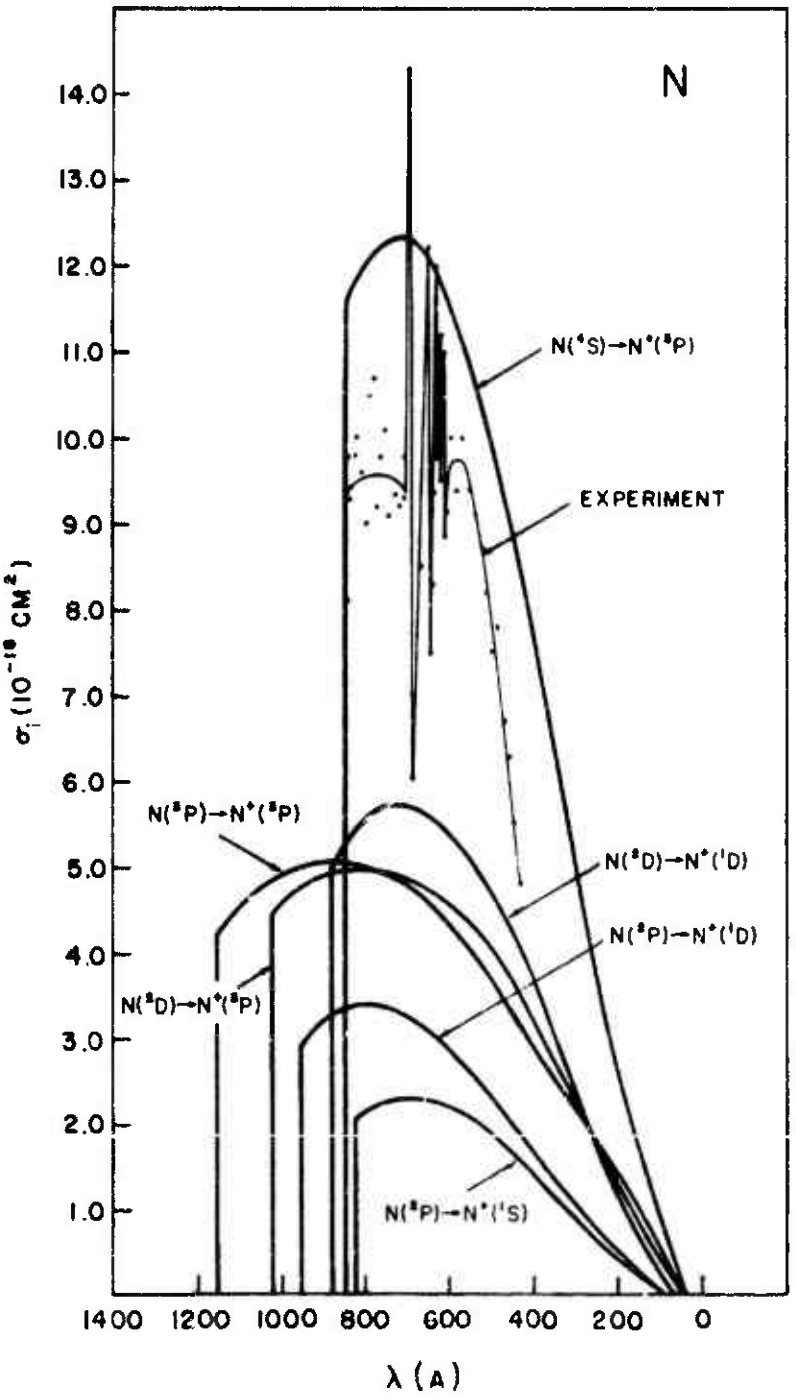


Figure 12-12. Atomic nitrogen photoionization cross-sections for specific initial and final states. Curves, References 12-55, 12-56; points, Reference 12-57.

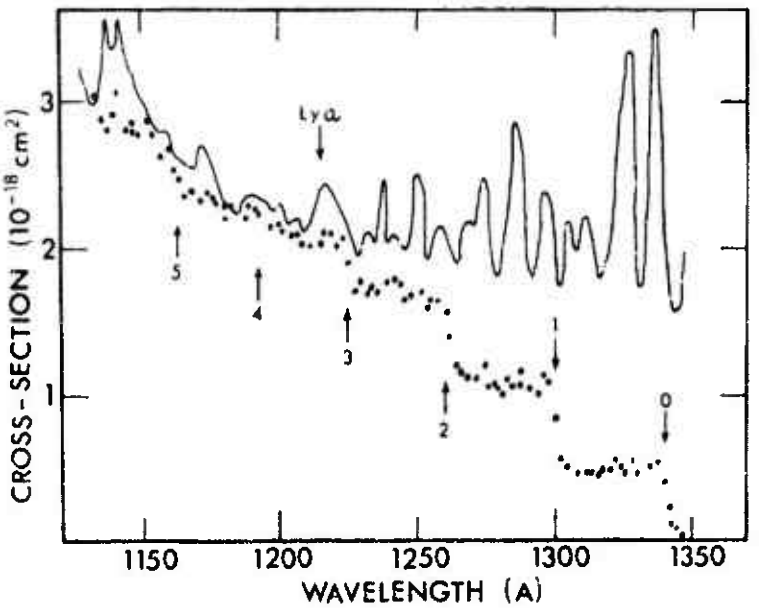


Figure 12-13. Nitric oxide crass-sections. Solid curve is obsorption cross-section; points are ionization crass-section. Data af Watanabe and Marmo, Reference 12-60.

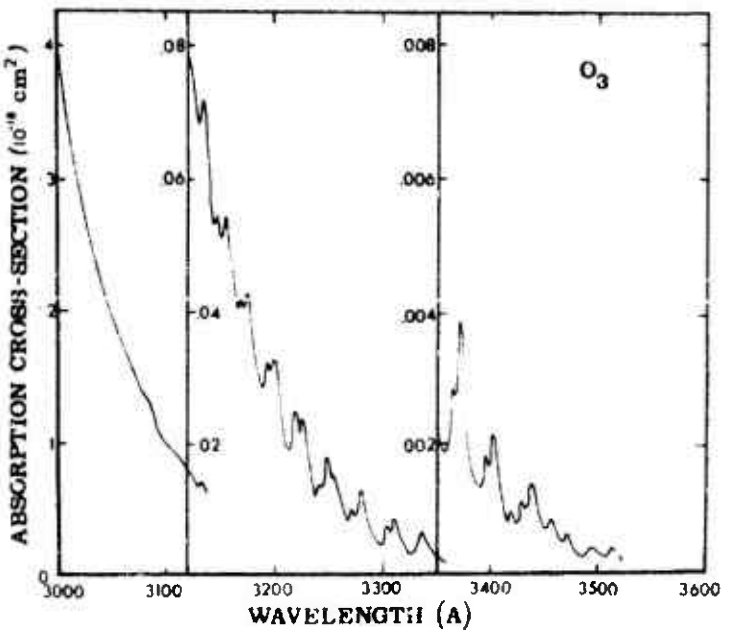


Figure 12-14. Ozone cross-sections. Wavelength 3000-3600 A. Data of Inn and Tanaka, Reference 12-63.

The Hartley continuum cross-sections (Reference 12-63) between 2000 and 3000 A are shown in Figure 12-15. There is general agreement on the cross-section in this region (References 12-65, 12-66). Toward lower wavelengths, ozone absorption is not as important in the atmosphere as oxygen molecule absorption.

Photodissociation in the Hartley continuum is probably the primary source of $O_2$ ($a\ ^1\Delta_g$) which may be important in D-region photoionization (Reference 12-67). It is believed that the initial photolysis products in the Hartley continuum are $O_2$ ($a\ ^1\Delta_g$) and $O(^1D)$, which are spin-allowed and energetically permissible at wavelengths less than 3100 A (Reference 12-68). However, the laboratory evidence is not complete. Flash and steady-state photolysis (References 12-69, 12-70) give better evidence for the presence of $O(^1D)$ than for $O_2$ ($a\ ^1\Delta_g$). Evidence from the emission of photolysis products indicates that the $O_2$ ($a\ ^1\Delta_g$) is probably formed in secondary reactions (Reference 12-71), which is consistent with the absorption spectra of the photolysis products (Reference 12-72). Further work is clearly needed.

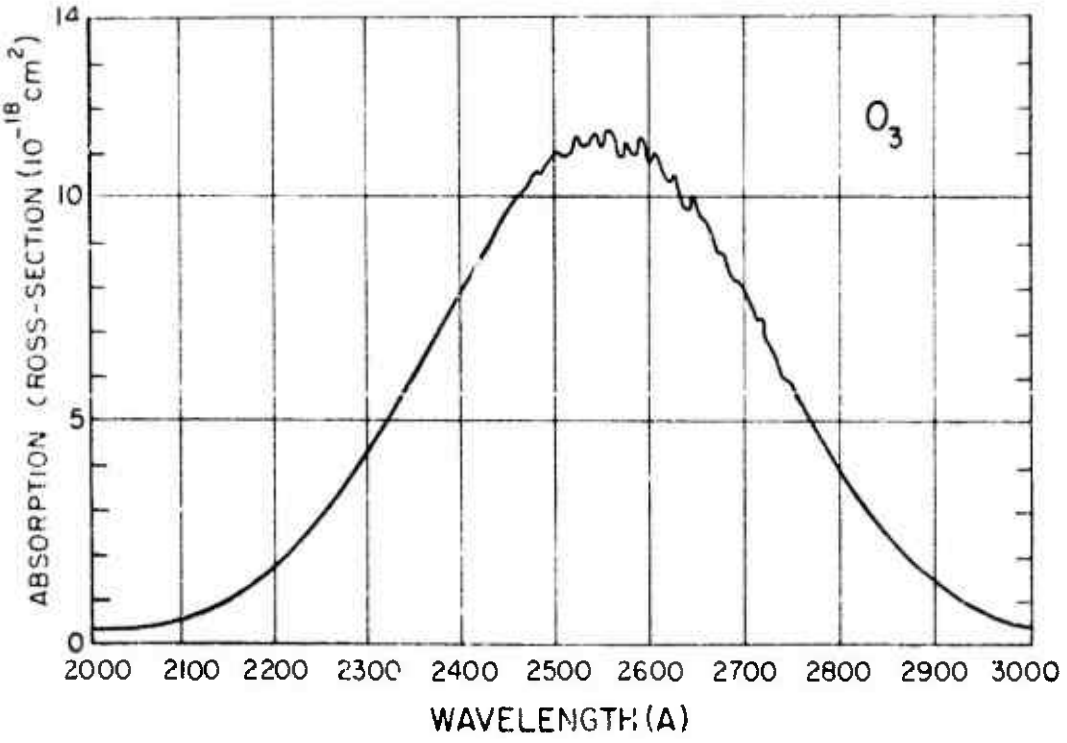


Figure 12-15. Ozone cross-sections. Wavelength 2000-3000 A. Data of Inn and Tanaka, Reference 12-63.

### 12.3.3.7 CARBON DIOXIDE, $CO_2$

Carbon dioxide absorption has been measured from about 1950 A to shorter wavelengths. Perhaps the most important wavelength region is the dissociation continuum in the region to 1200 A, shown in Figure 12-16 (References 12-9, 12-10, 12-73). The figure is simplified by not including a number of diffuse absorption bands. The continuum appears to be related to the threshold for $O(^1D)$ production, as supported by several investigations indicating the presence of this atom (Reference 12-74). The photodissociation efficiency is not known, but the data of Figure 12-16 can be considered an upper limit to the dissociation cross-section.

There are additional strong continua and lines toward shorter wavelengths (References 12-73, 12-75), and especially at wavelengths shorter than the first ionization threshold at 900.4 A. The absorption cross-sections in the regions of small $O_2$ cross-sections ("windows") have become important in connection with D-region photoionization of $O_2(a\ ^1\Delta_g)$. Relative cross-sections (Reference 12-26) resolve an apparent accidental shift in wavelength scale and favor the data of Reference 12-73.

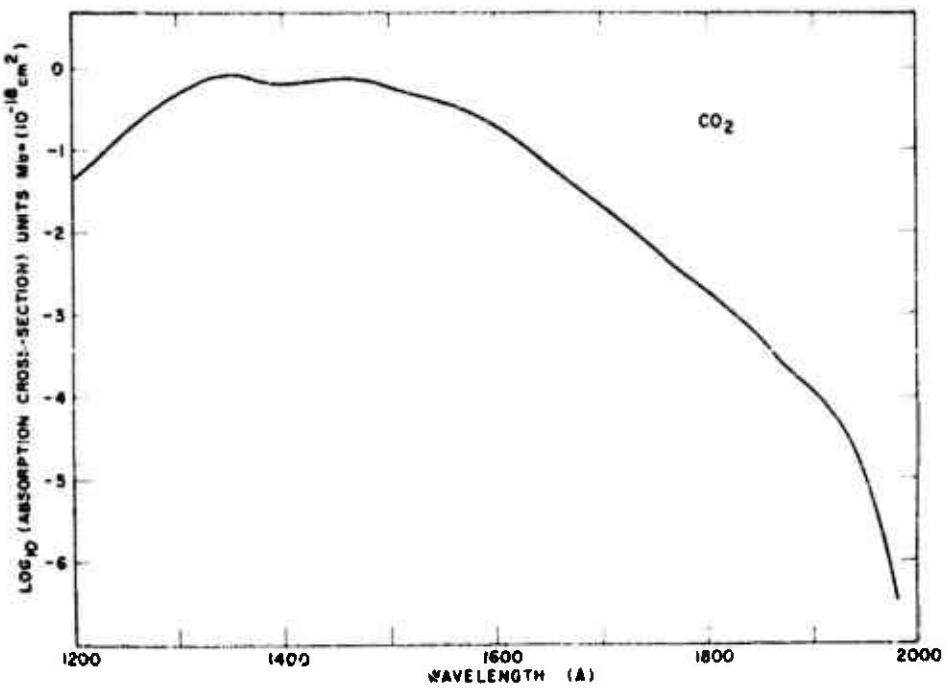


Figure 12-16. Carbon dioxide cross-sections. Adapted from Reference 12-10.

### 12.3.3.8 WATER VAPOR $H_2O$

Water vapor absorption extends from about 1850 A to shorter wavelengths. The relatively structureless continuum region ending about 1250 A is shown (Reference 12-76) in Figure 12-17. Absorption and ionization cross-sections to shorter wavelengths are also available (References 12-77, 12-78). The ionization threshold is at 982.6 A (Reference 12-79).

The dissociation products of $H_2O$ have not been well characterized (Reference 12-68). It is however known from fluorescence measurements that excited OH radicals are formed in the second continuum (1250-1430 A) shown in Figure 12-17.

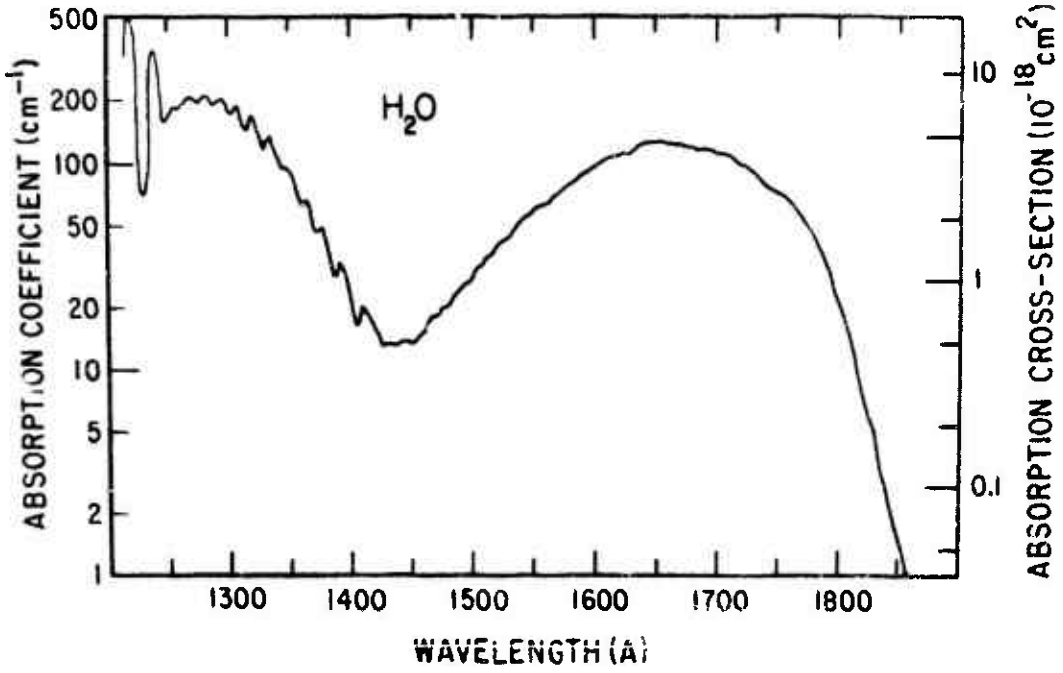


Figure 12-17. Water vapor cross-sections. Data of Watanabe and Zelikoff, Reference 12-76.

## 12.4 PHOTON CROSS-SECTIONS FOR ULTRAVIOLET DEPOSITION CODES

Cross-sections for photon absorption processes are given in Tables 12-6 through 12-9, which are available for studies of the disturbed ionosphere, and in other studies which determine the atmospheric characteristics resulting from ultraviolet radiation deposi-

tion. For such studies, it is sometimes necessary to know the total absorption cross-section, in order to evaluate the total energy deposition, and the product cross-sections such as the total photoionization cross-section and ion and atom production cross-sections, in order to obtain the electron density and to find the initial species involved in the reactions which return the atmosphere to its original condition.

These tables result from a recommendation by Dr. F. R. Gilmore, R&D Associates, who also specified the atomic emission line multiplets.

The emission line multiplets have been found in previous computer code studies, and they consist of the more intense atomic transitions of multiply ionized oxygen and nitrogen. These transitions are almost entirely in the vacuum-ultraviolet wavelength region. Many of these emission lines are not found in the solar spectrum and therefore previous solar line cross-section tables are not completely applicable. Also, the line widths and shapes will be different in the two cases. It is likely that the line widths of emission lines from the nuclear burst will be large enough in some cases that an effective cross-section different from the value given here will be necessary because the line will overlap several rotational lines of the atmospheric gas. These cases can be handled later as they are identified. In addition, there are a number of other multiplets predicted to be less intense, and it is planned to prepare cross-section tables for these lines, or others that become important, in the future.

The atmospheric species included in these tables are molecular nitrogen, $N_2$; molecular oxygen, $O_2$; atomic oxygen, O; atomic nitrogen, N; and nitric oxide, NO. It is possible that vibrationally excited gases and minor species should be included in future tables.

Experimental and, for atomic gases, theoretical total absorption and photoionization cross-sections are available for all wavelengths considered here. However, improved resolution and additional measurements are needed in many cases. Ion product cross-sections are becoming available using photoelectron spectroscopy, and they are included in the tables, as is dissociative ionization. However, excitation cross-sections and atom production cross-sections resulting

from photodissociation are not generally known. The values in the tables are predictions based on energy levels and an interpretation of the observed spectrum rather than from detection of products. Therefore, they are subject to change based on future work.

For the total absorption and photoionization cross-sections, the values in the tables are selected after considering all published data and in some cases additional unpublished results from this laboratory. Consideration is given to the author's estimated uncertainty, experimental method, region of spectrum (i.e., generally continuum or vibration-rotation band), and agreement between different measurements. References used are given. Individual multiplets are not discussed. No estimated errors are shown; however, unless there is evidence of structure in the region, they are probably accurate to ±25 percent. No energy-level tables are given, since they are readily available elsewhere, e.g. Chapter 10. In the tables, a zero indicates that there is insufficient energy from the photon for the process indicated.

Table 12-6a. Molecular nitrogen, $N_2$: photon cross-sections for very strong emission lines in megobarns ($10^{-18}$ cm$^2$). References: 12-4, 12-5, 12-27, 12-29, 12-33, 12-42, 12-44, 12-45.

| Emission Lines (A) | Total $\sigma_T$ | Ionization $\sigma_i$ | Ion products[a] | | | Neutral[b] $\sigma_N$ | Neutral Product | Remarks |
|---|---|---|---|---|---|---|---|---|
| | | | $\sigma_{i_X}$ | $\sigma_{i_A}$ | $\sigma_{i_B}$ | | | |
| $N_{II}$ #1 | | | | | | | | |
| 1085.70 | <0.1 | 0 | 0 | 0 | 0 | <0.1 | Excitation | c |
| 1084.57 | <0.1 | 0 | 0 | 0 | 0 | <0.1 | Excitation | |
| 1083.98 | <0.1 | 0 | 0 | 0 | 0 | <0.1 | Excitation | |
| 1085.54 | <0.1 | 0 | 0 | 0 | 0 | <0.1 | Excitation | |
| $O_{II}$ #1 | | | | | | | | |
| 834.467 | 7.5 | 0 | 0 | 0 | 0 | 7.5 | Excitation | d,e |
| 833.332 | 2.3 | 0 | 0 | 0 | 0 | 2.3 | Dissoc. | |
| 832.762 | 2.1 | 0 | 0 | 0 | 0 | 2.1 | Dissoc. | |
| $N_{III}$ #1 | | | | | | | | |
| 991.579 | 2 | 0 | 0 | 0 | 0 | 2 | Excitation | f,d |
| 989.790 | 1 | 0 | 0 | 0 | 0 | 1 | Excitation | |
| 991.514 | 2 | 0 | 0 | 0 | 0 | 2 | Excitation | |
| $N_{III}$ #3 | | | | | | | | |
| 685.816 | 23 | 22 | 4 | 18 | 0 | 1 | Dissoc. | g |
| 685.513 | 24 | 23 | 4 | 19 | 0 | 1 | Dissoc. | |
| 686.335 | 25 | 23 | 4 | 19 | 0 | 2 | Dissoc. | |

Toble 12-6a. (Cont'd.)

| Emission Lines (A) | Totol $\sigma_T$ | Ionizotion $\sigma_i$ | Ion Products[c] $\sigma_{i_x}$ | $\sigma_{i_A}$ | $\sigma_{i_B}$ | Neutrol[b] $\sigma_N$ | Neutrol Product | Remorks |
|---|---|---|---|---|---|---|---|---|
| $N_{III}$ #3 (Cant'd.) | | | | | | | | |
| 684.996 | 23 | 21 | 3 | 18 | 0 | 2 | Dissoc. | |
| $O_{III}$ #1 | | | | | | | | |
| 835.292 | 20 | 0 | 0 | 0 | 0 | 20 | Excitotion | h |
| 833.742 | 6 | 0 | 0 | 0 | 0 | 6 | Dissac. | |
| 832.927 | 7 | 0 | 0 | 0 | 0 | 7 | Dissoc. | |
| 835.096 | 41 | 0 | 0 | 0 | 0 | 41 | Excitotion | |
| $N_{IV}$ #1 | | | | | | | | |
| 765.140 | 67 | 51 | 51 | 0 | 0 | 16 | Dissac. | i |
| $N_V$ #1 | | | | | | | | |
| 1238.81 | <0.1 | 0 | 0 | 0 | 0 | <0.1 | Excitotion | j |
| 1242.80 | <0.1 | 0 | 0 | 0 | 0 | <0.1 | Excitotion | |

Table 12-6b. Moleculor nitrogen, $N_2$: photon cross-sections for strong emissian lines in megaborns ($10^{-18}$ cm$^2$). References: 12-4 12-5, 12-27, 12-29, 12-33, 12-42, 12-44, 12-45.

| Emission Lines (A) | Totol $\sigma_T$ | Ionizatian $\sigma_i$ | Ion Products[a] $\sigma_{i_x}$ | $\sigma_{i_A}$ | $\sigma_{i_B}$ | Neutral[b] $\sigma_N$ | Neutral Product | Remarks |
|---|---|---|---|---|---|---|---|---|
| $N_{II}$ #2 | | | | | | | | |
| 916.700 | 14-32 | 0 | 0 | 0 | 0 | 14-32 | Excitotion | k |
| 916.004 | .4-2.8 | 0 | 0 | 0 | 0 | .4-2.8 | Dissoc. | |
| 915.955 | .4-2.8 | 0 | 0 | 0 | 0 | .4-2.3 | Dissoc. | |
| 915.603 | .8-1.7 | 0 | 0 | 0 | 0 | .8-1.7 | Excitotion | |
| $N_{III}$ #2 | | | | | | | | |
| 764.357 | 13 | 10 | 10 | 0 | 0 | 3 | Dissoc. | i |
| 763.340 | 28 | 19 | 19 | 0 | 0 | 9 | Dissoc. | |
| $O_{III}$ #2 | | | | | | | | |
| 703.850 | 22 | 20 | 4 | 16 | 0 | 2 | Dissoc. | g |
| 702.899 | 23 | 21 | 4 | 17 | 0 | 2 | Dissoc. | |
| 702.822 | 23 | 21 | 4 | 17 | 0 | 2 | Dissac. | |
| 702.332 | 24 | 22 | 5 | 17 | 0 | 2 | Dissoc. | |
| $O_{IV}$ #1 | | | | | | | | |
| 790.203 | 22 | 10 | 10 | 0 | 0 | 12 | Dissoc. | i, l |
| 787.710 | 10 | 8 | 8 | 0 | 0 | 2 | Dissoc. | |
| 790.103 | 28 | 11 | 11 | 0 | 0 | 17 | Dissoc. | |

Table 12-6b. (Cont'd.)

| Emission Lines (A) | Total $\sigma_T$ | Ionization $\sigma_i$ | Ion Products[a] $\sigma_{i_X}$ | $\sigma_{i_A}$ | $\sigma_{i_B}$ | Neutral[b] $\sigma_N$ | Neutral Product | Remarks |
|---|---|---|---|---|---|---|---|---|
| O V #1 629.732 | 23 | 23 | 8 | 9 | 6 | 0 | - | - |

Notes:

a Ion product cross-sections: $\sigma_{ix}$, $(X\ ^2\Sigma_g^+)$ ; $\sigma_{iA}$ , $(A\ ^2\Pi_u)$ ; $\sigma_{iB}$ , $(B\ ^2\Sigma_u^+)$ .

b Neutral, or non-ionized product, cross-section, $\sigma_N = \sigma_T - \sigma_i$ .

c No dissociation cantinuum identified in this region. Near forbidden bands w - X (15, 0) and a - X (16, 0), Reference 12-42.

d In region where there are sharp electronic vibration-rotation bands making it difficult to predict the effective cross-sectians.

e The line 834.467 should largely excite b'(25) $(^1\Sigma_u^+)$ R(0, 1,2) at 834.470 (sharp band-head). Other lines should lead to dissociatian with all products except two $^2P$ otoms possible. Nearby lines will lead to excitation if emission line is braadened. Closest lines: 833.332 - $c_6'(o)$ $(^1\Sigma_u^+)$ R(14) at .346; 832.762 - $c_5'(2)$ $(^1\Sigma_u^+)$ P(9) at .660, and P(10) at .786 (Reference 12-87).

f Excitation predicted because lines near a number of weak, high-rotational-quantum-number lines. These are interim values. There is large disagreement between different measurements. Large variation of cross-section with number density, which indicates line absorption.

g Predict dissociation, any pair of $^4S$, $^2D$, and $^2P$ atoms energetically possible.

h For 835.292, $c_5(o)$ $(^1\Pi_u)$ P(3) at .304 (sharp line) excited; for 835.096, $c_5(o)$ $(^1\Pi_u)$ R(1) at .097 (shorp line) excited; predict photodissociation other lines, all products except two $^2P$ atoms possible. There are nearby $N_2$ lines thot will lead to excitation also, if emission lines broadened. Closest are 833.742 - $c_6'(o)$ $(^1\Sigma_u^+)$R(0) at .717 and P(1) at .772; 832.927 - appears to be a very weak band in this region (Reference 12-87)

i Predict photodissociation, any combination except two $^2P$ atoms.

j No accurate measurements at these lines. No continuum observable. In weak forbidden band region. Nearest band is w - X (6,0).

Table 12-6. (Cont'd.)

Notes (Cont'd.)

k In region with many bands having sharp rotation lines. For 916.700, predict excitation of b(11)($^1\Pi_u$) Q(5) at .710; for 915.603, predict excitation of b' (8)($^1\Sigma^+$) P(18), R(21) at .592. The other two lines appear to be in continuum region and predict dissociation giving one $^4S$ plus $^4S$, $^2D$, or $^2P$ atom. Range of values found at different column densities due to inadequate resolution (Reference 87).

ℓ Dissociation predicted, since in a diffuse rotational line region. Some variation with column density; it is possible that 787.710 might have an effective cross-section up to 20 in some cases.

Table 12-7a. Molecular oxygen, $O_2$: photon cross-sections for very strong emission lines in megabarns ($10^{-18}$ cm$^2$). References: 12-4, 12-5, 12-27 through 12-30, 12-33.

| Emission Lines (A) | Total $\sigma_T$ | Ionization $\sigma_i$ | Ion Products[a] $\sigma_{ix}$ | $\sigma_{iaA}$ | $\sigma_{ib}$ | Neutral[b] $\sigma_N$ | Neutral Product | Remarks |
|---|---|---|---|---|---|---|---|---|
| NII #1 | | | | | | | | |
| 1085.70 | 2.4 | 0 | 0 | 0 | 0 | 2.4 | Dissoc. | c |
| 1084.57 | 1.4 | 0 | 0 | 0 | 0 | 1.4 | Dissoc. | |
| 1083.98 | 1.1 | 0 | 0 | 0 | 0 | 1.1 | Dissoc. | |
| 1085.54 | 2.2 | 0 | 0 | 0 | 0 | 2.2 | Dissoc. | |
| OII #1 | | | | | | | | |
| 834.467 | 11 | 4 | 4 | 0 | 0 | 7 | Dissoc. | d |
| 833.332 | 15 | 6 | 6 | 0 | 0 | 9 | Dissoc. | |
| 832.762 | 26 | 10 | 10 | 0 | 0 | 16 | Dissoc. | |
| NIII #1 | | | | | | | | |
| 991.579 | 1.8 | 1.2 | 1.2 | 0 | 0 | 0.6 | Dissoc. | d |
| 989.790 | 1.4 | 1.0 | 1.0 | 0 | 0 | 0.4 | Dissoc. | |
| 991.514 | 1.8 | 1.2 | 1.2 | 0 | 0 | 0.6 | Dissoc. | |
| NIII #3 | | | | | | | | |
| 685.816 | 18 | 18 | 6 | 10 | 2 | 0 | - | |
| 685.513 | 18 | 18 | 6 | 10 | 2 | 0 | - | |
| 686.335 | 22 | 22 | 7 | 13 | 2 | 0 | - | |
| 684.996 | 26 | 26 | 9 | 15 | 2 | 0 | - | |

Table 12-7a. (Cont'd.)

| Emission Lines (A) | Total $\sigma_T$ | Ionizatian $\sigma_i$ | Ion Products[a] $\sigma_{ix}$ | $\sigma_{ioA}$ | $\sigma_{ib}$ | Neutral[b] $\sigma_N$ | Neutral Product | Remarks |
|---|---|---|---|---|---|---|---|---|
| $O_{III}$ #1 | | | | | | | | |
| 835.292 | 10 | 4 | 4 | 0 | 0 | 6 | Dissoc. | d |
| 833.742 | 13 | 5 | 5 | 0 | 0 | 8 | Dissoc. | |
| 832.927 | 26 | 10 | 10 | 0 | 0 | 16 | Dissac. | |
| 835.096 | 10 | 4 | 4 | 0 | 0 | 6 | Dissoc. | |
| $N_{IV}$ #1 | | | | | | | | |
| 765.140 | 23 | 12 | 11 | 1 | 0 | 11 | Dissoc. | e |
| $N_V$ #1 | | | | | | | | |
| 1238.81 | 0.3 | 0 | 0 | 0 | 0 | 0.3 | Dissoc. | f |
| 1242.80 | 4±2 | 0 | 0 | 0 | 0 | 4 ± 2 | Dissoc. | |

Toble 12-7b. Muleculor oxygen, $O_2$: photan crass-sections for strong emission lines in megobarns ($10^{-18}$ $cm^2$). Refe\ences: 12-4, 12-5, 12-27 through 12-30, 12-33, 12-49.

| Emission Lines (A) | Total $\sigma_i$ | Ionizotion $\sigma_i$ | Ion Products[a] $\sigma_{ix}$ | $\sigma_{iaA}$ | $\sigma_{ib}$ | Neutral[b] $\sigma_N$ | Neutral Praduct | Remarks |
|---|---|---|---|---|---|---|---|---|
| $N_{II}$ #2 | | | | | | | | |
| 916.700 | 16 | 10 | 10 | 0 | 0 | 6 | Dissoc. | c,g |
| 916.004 | 5 | 3 | 3 | 0 | 0 | 2 | Dissoc. | |
| 915.955 | 5 | 3 | 3 | 0 | 0 | 2 | Dissoc. | |
| 915.603 | 5 | 3 | 3 | 0 | 0 | 2 | | |
| $N_{III}$ #2 | | | | | | | | |
| 764.357 | 18 | 10 | 9 | 1 | 0 | 8 | Dissoc. | e,d |
| 763.340 | 22 | 12 | 11 | 1 | 0 | 10 | Dissoc. | |
| $O_{III}$ #2 | | | | | | | | |
| 703.850 | 28 | 25 | 13 | 12 | 0 | 3 | Dissoc. | d |
| 702.899 | 30 | 26 | 14 | 12 | 0 | 4 | Dissoc. | |
| 702.822 | 30 | 26 | 14 | 12 | 0 | 4 | Dissoc. | |
| 702.332 | 21 | 18 | 10 | 8 | 0 | 3 | Dissoc. | |
| $O_{IV}$ #1 | | | | | | | | |
| 790.203 | 28 | 10 | 10 | 0 | 0 | 18 | Dissoc. | d |
| 787.710 | 24 | 13 | 13 | 0 | 0 | 11 | Dissoc. | |
| 790.103 | 28 | 10 | 10 | 0 | 0 | 18 | Dissoc. | |

Table 12-7b. (Cont'd.)

| Emission Lines (A) | Total $\sigma_T$ | Ionization $\sigma_i$ | Ion Products[a] $\sigma_{ix}$ | $\sigma_{iaA}$ | $\sigma_{ib}$ | Neutral[b] $\sigma_N$ | Neutral Product | Remarks |
|---|---|---|---|---|---|---|---|---|
| $O_V$ #1 629.732 | 30 | 29[h] | 6 | 10 | 12 | 1 | Dissac. | d,h |

Notes:

a Ion product cross-sections: $\sigma_{ix}$, ($X\ ^2\Pi_g$) ; $\sigma_{iaA}$ , ($a\ ^4\Pi_u$) and ($A\ ^2\Pi_u$) ; $\sigma_{ib}$, ($b\ ^4\Sigma_g^-$) .

b Neutral, or nonionized product, cross-section, $\sigma_N = \sigma_T - \sigma_i$ .

c Dissociation products can be any combination of the atomic states $^3P$, $^1D$, $^1S$, except two $^1S$ atoms.

d Dissociation products can be any combination of the atomic states $^3P$, $^1D$, and $^1S$.

e The value in $\sigma_{iaA}$ column refers only to the ($a\ ^4\Pi_u$) state.

f Dissociation products can be any combination of the atomic states $^3P$, $^1D$, $^1S$, except $^1S + {}^1D$ and two $^1S$ atoms.

g There is structure in this region, especially at 916.700, but the bands appear to be diffuse indicating dissociation.

h Dissociative ionization cross-section is 1 Mb with products $O(^3P)$ and $O^+(^4S)$ (Reference 12-49).

Table 12-8a. Atomic oxygen O , and atomic nitrogen, N: photon cross-sections for very strong emission lines in megabarns ($10^{-18}cm^2$).
References: O: 12-5, 12-36, 12-37, 12-46, 12-48, 12-49, 12-51
N: 12-57, 12-58

| Emission Lines (A) | ATOMIC OXYGEN | | | | ATOMIC NITROGEN |
|---|---|---|---|---|---|
| | Total[a] $\sigma_i$ | Ion Products[e] $\sigma_{iS}$ | $\sigma_{iD}$ | $\sigma_{iP}$ | Total[c,b] $\sigma_i$ |
| $N_{II}$ #1 | | | | | |
| 1085.70 | 0 | 0 | 0 | 0 | 0 |
| 1084.57 | 0 | 0 | 0 | 0 | 0 |
| 1083.98 | 0 | 0 | 0 | 0 | 0 |
| 1085.54 | 0 | 0 | 0 | 0 | 0 |

Toble 12-8a. (Cont'd.)

| Emission Lines (A) | ATOMIC OXYGEN | | | | ATOMIC NITROGEN |
|---|---|---|---|---|---|
| | Total[o] $\sigma_i$ | Ion Products[e] | | | Totol[o,b] $\sigma_i$ |
| | | $\sigma_{iS}$ | $\sigma_{iD}$ | $\sigma_{iP}$ | |
| $O_{II}$ #1 | | | | | |
| 834.467 | 2.6 | 2.6 | 0 | 0 | 10 |
| 833.332 | 2.6 | 2.6 | 0 | 0 | 10 |
| 832.762 | 2.6 | 2.6 | 0 | 0 | 10 |
| $N_{III}$ #1 | | | | | |
| 991.579 | 0 | 0 | 0 | 0 | 0 |
| 989.790 | 0[c] | 0 | 0 | 0 | 0 |
| 991.514 | 0 | 0 | 0 | 0 | 0 |
| $N_{III}$ #3 | | | | | |
| 685.816 | 6.5 | 3.0 | 3.5 | 0 | 6 |
| 685.513 | 6.5 | 3.0 | 3.5 | 0 | 6 |
| 686.335 | 6.5 | 3.0 | 3.5 | 0 | 6 |
| 684.996 | 6.5 | 3.0 | 3.5 | 0 | 6 |
| $O_{III}$ #1 | | | | | |
| 835.292 | 2.6 | 2.6 | 0 | 0 | 10 |
| 833.742 | 2.6 | 2.6 | 0 | 0 | 10 |
| 832.927 | 2.6 | 2.6 | 0 | 0 | 10 |
| 835.096 | 2.6 | 2.6 | 0 | 0 | 10 |
| $N_{IV}$ #1 | | | | | |
| 765.140 | 3.0 | 3.0 | 0 | 0 | 10 |
| $N_{V}$ #1 | | | | | |
| 1238.81 | 0 | 0 | 0 | 0 | 0 |
| 1242.80 | 0 | 0 | 0 | 0 | 0 |

Table 12-8b. Atomic oxygen, O , ond atomic nitrogen, N: photon cross-sections for strong emission lines in megobarns ($10^{-18}$ $cm^2$).
References: O: 12-5, 12-36, 12-37, 12-46, 12-48, 12-49, 12-51
N: 12-57, 12-58

| Emission Lines (A) | ATOMIC OXYGEN | | | | ATOMIC NITROGEN |
|---|---|---|---|---|---|
| | Totol[o] $\sigma_i$ | Ion Products[e] | | | Totol[o,b] $\sigma_i$ |
| | | $\sigma_{iS}$ | $\sigma_{iD}$ | $\sigma_{iP}$ | |
| $N_{II}$ #2 | | | | | |
| 916.700 | 0[d] | 0 | 0 | 0 | 0 |
| 916.004 | 0[d] | 0 | 0 | 0 | 0 |

Table 12-8b. (Cont'd.)

| Emission Lines (A) | ATOMIC OXYGEN | | | | ATOMIC NITROGEN |
|---|---|---|---|---|---|
| | Total[a] $\sigma_i$ | ion Products[e] | | | Total[a,b] $\sigma_i$ |
| | | $\sigma_{iS}$ | $\sigma_{iD}$ | $\sigma_{iP}$ | |
| $N_{II}$ #2 (Cont'd.) | | | | | |
| 915.955 | 0[d] | 0 | 0 | 0 | 0 |
| 915.603 | 0[d] | 0 | 0 | 0 | 0 |
| $N_{III}$ #2 | | | | | |
| 764.357 | 3.0 | 3.0 | 0 | 0 | 10 |
| 763.340 | 3.0 | 3.0 | 0 | 0 | 10 |
| $O_{III}$ #2 | | | | | |
| 703.850 | 6.5 | 3.0 | 3.5 | 0 | 9 |
| 702.899 | 6.5 | 3.0 | 3.5 | 0 | 9 |
| 702.822 | 6.5 | 3.0 | 3.5 | 0 | 9 |
| 702.332 | 6.5 | 3.0 | 3.5 | 0 | 9 |
| $O_{IV}$ #1 | | | | | |
| 790.203 | 2.9 | 2.9 | 0 | 0 | 10 |
| 787.710 | 2.9 | 2.9 | 0 | 0 | 10 |
| 790.103 | 2.9 | 2.9 | 0 | 0 | 10 |
| $O_V$ #1 | | | | | |
| 629.732 | 9.0 | 2.7 | 4.0 | 2.3 | 12 |

Notes:

a The total absorption cross-section is equal to the total photoionization cross-section in the continuum regions, except where overlap with atomic lines occurs as referenced in footnotes.

b The only ion product will be the $^3P$ state of $N^+$, due to photon energy.

c This line may overlap an atomic oxygen absorption line at 990.13 A giving an effective cross-section of up to 10.

d These lines probably overlap several atomic oxygen lines of series converging to the first ionization threshold. Effective $\sigma$ large (possibly 100 Mb) and dependent on emission line width. This absorption does not lead to ionization. The interval to nearest line is .116, .013, .036, and .104 A, respectively.

e The subscripts iS, iD, and iP refer to the atomic oxygen ion states $^4S$, $^2D$, and $^2P$, respectively.

Toble 12-9a. Nitric oxide, NO: photon cross-sections for very strong emission lines in megobarns ($10^{-18}$ $cm^2$). References: 12-4, 12-5, 12-61, 12-88.

| Emission Lines (A) | Totol $\sigma_T$ | Ionizotion $\sigma_i$ | Ion Products[a] | | | Neutrol[b] $\sigma_N$ |
|---|---|---|---|---|---|---|
| | | | $\sigma_{iX}$ | $\sigma_{iA}$ | $\sigma_{i8}$ | |
| $N_{III}$ #1 | | | | | | |
| 1085.70 | 9 | 7 | 7 | 0 | 0 | 2 |
| 1084.57 | 8 | 6 | 6 | 0 | 0 | 2 |
| 1083.98 | 8 | 6 | 6 | 0 | 0 | 2 |
| 1085.54 | 9 | 7 | 7 | 0 | 0 | 2 |
| $O_{II}$ #1 | | | | | | |
| 834.467 | 21 | 11 | 11 | 0 | 0 | 10 |
| 833.332 | 20 | 10 | 10 | 0 | 0 | 10 |
| 832.762 | 16 | 9 | 9 | 0 | 0 | 7 |
| $N_{III}$ #1 | | | | | | |
| 991.579 | 17 | 8 | 8 | 0 | 0 | 9 |
| 989.790 | 18 | 9 | 9 | 0 | 0 | 9 |
| 991.514 | 17 | 8 | 8 | 0 | 0 | 9 |
| $N_{III}$ #3 | | | | | | |
| 685.816 | 18 | 17 | 5 | 7 | 5 | 1 |
| 685.513 | 18 | 17 | 5 | 7 | 5 | 1 |
| 686.335 | 21 | 19 | 6 | 7 | 6 | 2 |
| 684.996 | 19 | 17 | 5 | 7 | 5 | 2 |
| $O_{III}$ #1 | | | | | | |
| 835.292 | 21 | 9 | 9 | 0 | 0 | 12 |
| 833.742 | 18 | 9 | 9 | 0 | 0 | 9 |
| 832.927 | 17 | 10 | 10 | 0 | 0 | 7 |
| 835.096 | 22 | 10 | 10 | 0 | 0 | 12 |
| $N_{IV}$ #1 | | | | | | |
| 765.140 | 15 | 9 | 6 | 3 | 0 | 6 |
| $N_V$ #1 | | | | | | |
| 1238.81 | 2.1 | 1.6 | 1.6 | 0 | 0 | 0.5 |
| 1242.80 | 2.1 | 1.7 | 1.7 | 0 | 0 | 0.4 |

Table 12-9b. Nitric oxide, NO: photon cross-sections for strong emission lines in megobarns ($10^{-18}$ $cm^2$). References: 12-4, 12-5, 12-51, 12-88.

| Emission Lines (A) | Total $\sigma_T$ | Ionization $\sigma_i$ | Ion Products[a] | | | Neutral[b] $\sigma_N$ |
|---|---|---|---|---|---|---|
| | | | $\sigma_{iX}$ | $\sigma_{iA}$ | $\sigma_{iB}$ | |
| $N_{II}$ #2 | | | | | | |
| 916.700 | 31 | 9 | 9 | 0 | 0 | 22 |
| 916.004 | 30 | 10 | 10 | 0 | 0 | 20 |
| 915.955 | 30 | 10 | 10 | 0 | 0 | 20 |
| 915.603 | 29 | 10 | 10 | 0 | 0 | 19 |
| $N_{III}$ #2 | | | | | | |
| 764.357 | 34 | 19 | 13 | 6 | 0 | 15 |
| 763.340 | 13 | 6 | 4 | 2 | 0 | 7 |
| $O_{III}$ #2 | | | | | | |
| 703.850 | 21 | 18 | 7 | 8 | 3 | 3 |
| 702.899 | 20 | 18 | 7 | 8 | 3 | 2 |
| 702.822 | 20 | 18 | 7 | 8 | 3 | 2 |
| 702.332 | 19 | 18 | 7 | 8 | 3 | 1 |
| $O_{IV}$ #1 | | | | | | |
| 790.203 | 18 | 10 | 9 | 1 | 0 | 8 |
| 787.710 | 17 | 11 | 10 | 1 | 0 | 6 |
| 790.103 | 17 | 10 | 9 | 1 | 0 | 7 |
| $O_V$ #1 | | | | | | |
| 629.732 | 21 | 21 | 5 | 8 | 8 | 0 |

Notes:

[a] Ion product cross-sections: $\sigma_{iX}$ ($X\ ^1\Sigma^+$); $\sigma_{iA}$, includes ($a\ ^3\Sigma^+$) and ($b\ ^3\Pi$); $\sigma_{iB}$, includes ($w\ ^3\Delta$), ($b'\ ^3\Sigma^-$), ($A'\ ^1\Sigma^-$), ($W\ ^1\Delta$), and ($A\ ^1\Pi$) (see Ref. 12-88).

[b] Neutral, or non-ionized product, cross-section, $\sigma_N = \sigma_T - \sigma_i$. It is predicted that all absorption will lead to photodissociation, either directly or through predissociation; however, further data are necessary.

## REFERENCES


12-1. Weissler, G. L., in Handbuch der Physik, S. Flügge, Ed., Springer-Verlag, Berlin (1966); Vol. 21.

12-2. Marr, G. V., Photoionization Processes in Gases, Academic Press, New York (1967); Proc. Roy. Soc. A228, 531 (1965).

12-3. Schoen, R. I., Proc. IAGA Symp. Lab. Aeronomy, York Univ., Toronto, Canada (1968); Can. J. Chem. 47, 1879 (1969).

12-4. Watanabe, K., Adv. Geophys. 5, 153 (1958).

12-5. Huffman, R. E., Proc. IAGA Symp. Lab. Aeronomy, York Univ., Toronto, Canada (1968); Can. J. Chem. 47, 1823 (1969); in Handbook of Geophysics and Space Environments, S. L. Valley, Ed., McGraw-Hill, New York (1965).

12-6. Kieffer, L. J., Univ. of Colorado, JILA Information Center Report No. 5 (1968).

12-7. Hudson, R. D., Revs. Geophys. Space Phys. 9, 305 (1971).

12-8. Ditchburn, R. W., and P. A. Young, J. Atm. Terrestr. Phys. 24, 127 (1962).

12-9. Blake, A. J., J. H. Carver, and G. H. Haddad, J. Quant. Spectry. Radiative Transfer 6, 451 (1966).

12-10. Thompson, B. A., P. Harteck, and R. R. Reeves, J. Geophys. Res. 68, 6431 (1963).

12-11. Hudson, R. D., and V. L. Carter, J. Opt. Soc. Am. 58, 1621 (1968).

12-12. Farmer, A. J. D., W. Fabian, B. R. Lewis, K. H. Lokan, and G. N. Haddad, J. Quant. Spectry. Radiative Transfer 8, 1739 (1968).

12-13. Ackerman, M., F. Biaume, and G. Kockarts, Planet. Space Sci. 18, 1639 (1970).

12-14. Carroll, P. K., Astrophys. J. 129, 794 (1959); references cited therein.

12-15. Bethke, G. W., J. Chem. Phys. 31, 669 (1959).

12-16. See reference 12-4 for earlier work in this region.

12-17. Metzger, P. H., and G. R. Cook, J. Quant. Spectry. Radiative Transfer 4, 107 (1964).

12-18. Huffman, R. E., Y. Tanaka, and J. C. Larrabee, Disc. Faraday Soc. 37, 154 (1964).

12-19. Goldstein, R., and F. N. Mastrup, J. Opt. Soc. Am. 56, 765 (1966).

12-20. Noxon, J. F., private communication.

12-21. Sullivan, J. O., and P. Warneck, J. Chem. Phys. 46, 953 (1967).

12-22. Young, R. A., and G. Black, J. Chem. Phys. 47, 2311 (1967).

12-23. Evans, J. S., and C. J. Schexnayder, NASA Tech. Rept. R-92 (1961).

12-24. Hudson, R. D., V. L. Carter, and J. A. Stein, J. Geophys. Res. 71, 2295 (1966).

12-25. Ogawa, M., J. Geophys. Res. 73, 6759 (1968).

12-26. Huffman, R. E., D. E. Paulsen, J. C. Larrabee, and R. B. Cairns, J. Geophys. Res. 76, 1028 (1971).

12-27. Samson, J. A. R., and R. B. Cairns, J. Geophys. Res. 69, 4583 (1964).

12-28. Huffman, R. E., J. C. Larrabee, and Y. Tanaka, J. Chem. Phys. 40, 356 (1964).

12-29. Cook, G. R., and P. H. Metzger, J. Chem. Phys. 41, 321 (1964).

12-30. Matsunaga, F. M., and K. Watanabe, Science of Light 16, 31 (1967).

12-31. Weissler, G. L., J. A. R. Samson, M. Ogawa, and G. R. Cook, J. Opt. Soc. Am. 49, 338 (1959).

12-32. Doolittle, P. H., R. I. Schoen, and K. E. Schubert, J Chem. Phys. 49, 5108 (1968).

12-33. Blake, A. J., and J. H. Carver, Phys. Letts. 19, 387 (1965); J. Chem. Phys. 47, 1038 (1967).

12-34. Evans, W. F. J., D. M. Hunter, E. J. Llewellyn, and A. Vallance Jones, J. Geophys. Res. 73, 2885 (1968).

12-35. Wayne, R. P., Quart. J. Roy. Meteorol. Soc. 43, 69 (1967).

12-36. Huffman, R. E., J. C. Larrabee, and Y. Tanaka, J. Chem. Phys. 46, 2213 (1967).

12-37. Huffman, R. E., J. C. Larrabee, and Y. Tanaka, J. Chem. Phys. 47, 4462 (1967).

12-38. Alberti, F., K. A. Ashby, and A. E. Douglas, Can. J. Phys. 46, 337 (1968).

12-39. Clark, I. D., and R. P. Wayne, J. Geophys. Res. 75, 699 (1970); Mol. Phys. 18, 523 (1970).

12-40. Hunten, D. M., and M. B. McElroy, J. Geophys. Res. 73, 2421 (1968).

12-41. Appleton, J. A., and M. Steinberg, J. Chem. Phys. 46, 1521 (1967).

12-42. Ching, B. K., G. R. Cook, and R. A. Becker, J. Quant. Spectry. Radiative Transfer 7, 323 (1967).

12-43. Hudson, R. D., and V. L. Carter, J. Geophys. Res. 74, 393 (1969).

12-44. Huffman, R. E., Y. Tanaka, and J. C. Larrabee, J. Chem. Phys. 39, 910 (1963).

12-45. Unpublished data, this laboratory (AFCRL).

12-46. Henry, R. J. W., Planet. Space Sci. 15, 1747 (1967).

12-47. Dalgarno, A., R. J. W. Henry, and A. L. Stewart, Planet. Space Sci. 12, 235 (1964); references cited therein.

12-48. Cairns, R. B., and J. A. R. Samson, Phys. Rev. 5, A1403 (1965).

12-49. Comes, F. J., F. Speier, and A. Elzer, Z. Naturforsch. 23a, 114 (1968).

12-50. Huffman, R. E., J. C. Larrabee, and Y. Tanaka, Phys. Rev. Letts. 16, 1033 (1966).

12-51. Henry, R. J. W., Planet. Space Sci. 16, 1503 (1968).

12-52. Henry, R. J. W., private communication.

12-53. Huffman, R. E., and J. C. Larrabee, J. Geophys. Res. 73, 7419 (1968).

12-54. McGrath, W. D., and J. J. McGarvey, Planet. Space Sci. 15, 427 (1967).

12-55. Ali, A. W., U. S. Naval Research Laboratory, Plasma Dynamics Technical Note No. 32 (1971).

12-56. Henry, R. J. W., Astrophysical J. 161, 1153 (1970).

12-57. Comes, F. J., and A. Elzer, Z. Naturforsch. 23a, 133 (1968).

12-58. Henry, R. J. W., J. Chem. Phys. 48, 3635 (1968).

12-59. Carroll, P. K., R. E. Huffman, J. C. Larrabee, and Y. Tanaka, Astrophys. J. 146, 553 (1966).

12-60. Watanabe, K., J. Chem. Phys. 22, 1564 (1954); Marmo, F. F., J. Opt. Soc. Am. 43, 1186 (1953).

12-61. Watanabe, K., F. M. Matsunaga, and H. Sokai, Appl. Optics 6, 391 (1967).

12-62. Leighton, P. A., Photochemistry of Air Pollution, Academic Press, New York (1961); p. 48.

12-63. Inn, E. C. Y., and Y. Tanaka, J. Opt. Soc. Am. 43, 870 (1953).

12-64. Vigroux, E., Ann. Phys. (France) 2, 209 (1967).

12-65. Dütsch, H. U., Quart. J. Roy. Meteorol. Soc. 94, 483 (1968).

12-66. Vigroux, E., Ann. Phys. (Paris) 8, 709 (1953).

12-67. Hunten, D. M., and M. B. McElroy, J. Geophys. Res. 73, 2431 (1968).

12-68 McNesby, J. R., and H. Okabe, Adv. Photochem. 3, 157 (1964).

12-69. Wayne, R. P., Quart. J. Roy. Meteorol. Soc. 93, 69 (1967).

12-70. De More, W. B., and O. Raper, J. Chem. Phys. 44, 1780 (1966).

12-71. Izod, T. P. J., and R. P. Wayne, Nature 217, 947 (1968).

12-72 Huffman, R. E., J. C. Larrabee, and V. C. Baisley, J. Chem. Phys. 50, 4594 (1969).

12-73. Nakata, R. S., K. Watanabe, and F. M. Matsunaga, Science of Light 14, 54 (1965).

12-74. Young, R. A., and A. Y. M. Ung, J. Chem. Phys. 44, 3038 (1966); Slanger, T. G., Ibid. 45, 4127 (1966); Warneck, P., Ibid. 41, 3435 (1964).

12-75. Cairns, R. B., and J. A. R. Samson, J. Geophys. Res. 70, 99 (1965).

12-76. Watanabe, K., and M. Zelikoff, J. Opt. Soc. Am. 43, 753 (1953).

12-77. Watanabe, K., and A. S. Jursa, J. Chem. Phys. 41, 1650 (1964).

12-78. Katayama, D. J., C. L. O'Bryan, and R. E. Huffman, unpublished data, AFCRL.

12-79. Herzberg, G., Electronic Spectra of Polyatomic Molecules, Van Nostrand, New York (1966).

12-80. Samson, J. A. R., and R. B. Cairns, J. Opt. Soc. Am. 56, 769 (1966).

12-81. Watanabe, K., T. Nakayama, and J. Mottl, J. Quant. Spectry. Radiativ. Transfer 2, 369 (1962).

12-82. Worley, R. E., and F. A. Jenkins, Phys. Rev. 54, 305 (1938).

12-83. Eriksson, K. B. S., and H. B. S. Isberg, Ark. Fys. 24, 549 (1963).

12-84. Herron, J. T., and H. I. Schiff, J. Chem. Phys. 24, 1266 (1956).

12-85. Watanabe, K., J. Chem. Phys. 22, 1564 (1954).

12-86. Bowen, I. S., Astrophys. J. 121, 306 (1955).

12-87. Yoshino, K., AFCRL, private communication (to be published). (Wavelengths and classifications from 6.8 meter spectrograph plates.)

12-88. Bahr, J. L., A. J. Blake, J. H. Carver, J. L. Gardner, and V. Kumar, Dept. Physics, Univ. Adelaide, Australia, Rept. No. ADP 84 (1970).

12-89. Samson, J. A. R., and R. B. Cairns, J. Opt. Soc. Am. 55, 1035 (1965).

12-90. Samson, J. A. R., Adv. Atom. Mol. Phys. 2, 177 (1966).

# 13. PHOTOCHEMICAL PROCESSES: SOLAR PHOTOIONIZATION RATE CONSTANTS AND ULTRAVIOLET INTENSITIES

T.J. Kenesheo, R.E. Huffman, and J.D. George
Air Force Cambridge Research Laboratories (AFSC)
(Latest Revision 7 December 1971)

## 13.1 FIRST-ORDER RATE CONSTANTS

In ionospheric computations, it is often necessary to have some knowledge of the ionization produced by incident solar radiation. The intensity of this radiation arriving at a specific altitude depends upon several factors including its intensity at the top of the atmosphere, the absorption cross-sections over the wavelength region that produces the ionization, and the neutral ambient atmosphere that absorbs the radiation as it penetrates to this altitude. Since it is convenient in most chemical computer codes to include the ionization of neutral atmospheric species as specific chemical reactions, e.g.:

$$N_2 + h\nu \rightarrow N_2^+ + e \ ,$$

typical calculations of first-order rate constants for solar photoionization are presented in this chapter. In order to obtain ion-pair production rates, these rate constants are simply multiplied by the local neutral species concentrations. It should be pointed out that the tables presented here are for a specific neutral atmosphere; a different ambient atmosphere would yield other rate constants.

The solar flux and cross-section values used in these calculations are presented in Table 13-1. The wavelengths are restricted to the region which primarily contributes to photoionization. This region includes the hydrogen Lyman-$\alpha$ line at 1215.7 A and all wavelengths from the molecular oxygen photoionization threshold (1027.8 A) to 1 A. The latter region effectively begins at the hydrogen Lyman-$\beta$ line at 1025.7 A. The atmospheric gases included are $O_2$, $N_2$, O, and NO. Further discussion of the cross-sections is given in Chapter 12 of this Handbook. The cross-sections given here are for the lines and wavelength ranges of solar flux as reported, and therefore include averages not given in Chapter 12.

In Table 13-1, the solar-flux intensities incident on the earth's atmosphere from 1215.7 to 270 A are taken from Hall and Hinteregger (Reference 13-1). For shorter wavelengths, values and references given by Hinteregger (Reference 13-2) and by Swider (Reference 13-3) are used. The contribution from the region 33.6-10 A is generally considered small and is not included. Further discussion of the solar-flux measurements is given in Section 13.2 of this Chapter.

The cross-sections for total absorption and for total photoionization are obtained by consideration of all reported experimental and theoretical values. References, definitions, and a discussion of the absorption spectra are given in Chapter 12 for values to 304 A. At shorter wavelengths, absorption values are taken from Swider (Reference 13-3).

The problem of calculating absorption in a region of sharp lines is encountered here, especially for molecular nitrogen. Cases exist for which strong solar lines overlap sharp rotational structure and where the solar flux is reported over a wavelength range. The present calculation does not solve these problems accurately. A more satisfactory solution must await an improved knowledge of both the solar flux and the cross-sections. For wavelength regions having little structure or broad, diffuse bands, an average value is used. For several regions in nitrogen, a technique similar to earlier calculations (Reference 13-4) is used, wherein an average cross-section is assigned to a fractional part of the flux in the range considered. This procedure is considered adequate, except perhaps for the case of nitrogen in the solar Lyman continuum. For short-wavelength regions, averages have been found from enlarged plots of the original data.

The total photoionization cross-sections presented in Table 13-1 refer to ionization products in any state of excitation. For shorter wavelengths, they also include multiple ionization caused by collisions of energetic photoelectrons with other atmospheric gases. The energy per ion-pair is assumed to be typical, viz., 35 eV.

The photoionization of NO is only important at the hydrogen Ly$\alpha$ line, and the cross-section (Reference 13-5) used here is $2.02 \times 10^{-18}$ $cm^2$. The photoionization of the $O_2(a\ ^1\Delta_g)$ metastable state between 1118 and 1027 A has not been included because of indications (Reference 13-6) of decreased rates due to $CO_2$ absorption.

The first-order rate constants for photoionization are computed in Tables 13-2 through 13-7 for a latitude of 30°N and a solar declination of 0°. Each of the three pairs of tables in this group is computed for a given solar zenith angle viz., 30°, 60°, 75°. The first or even-numbered table in each pair lists the model atmosphere and the integrated column densities. Each succeeding odd-numbered table then gives the first-order rate constants for $N_2^+$, $O_2^+$, $O^+$, and $NO^+$ production appropriate to that model. The rate constants are computed over the altitude range 60-200 km. The lower limit is chosen because cosmic-ray ionization generally exceeds the EUV ionization below this altitude. The upper limit is arbitrary.

The number-density profiles of $O_2$, $N_2$, and O from zero altitude to 520 km are from Chapter 2 of the Handbook. Only the portions of these profiles between 60 and 200 km are considered in Tables 13-2 through 13-7. The column densities are computed by performing a numerical integration along the ray path, assuming a spherical earth from the given altitude to the top of the atmosphere (520 km) at the indicated solar zenith angle. This maximum altitude is chosen because, for ray paths that extend down to the D- and E-regions, species concentrations above 520 km do not contribute significantly to the absorption integrals. The integration is carried out using Simpson's rule, with 1-km increments along the ray path for $O_2$ and $N_2$ and with 0.5-km increments for O.

Let $\Phi_\infty(\Delta\lambda)$ be the photon flux incident on the top of the atmosphere and $\Phi_z(\Delta\lambda)$ be the local photon flux at some altitude z in the wavelength range $\Delta\lambda$. Then:

$$\Phi_z(\Delta\lambda) = \Phi_\infty(\Delta\lambda)\, e^{-\tau(\Delta\lambda)} \quad , \tag{13-1}$$

where $\tau(\Delta\lambda)$ is the optical depth for the wavelengths in the range $\Delta\lambda$. The optical depth can be written as:

$$\tau(\Delta\lambda) = \tau_{O_2}(\Delta\lambda) + \tau_{N_2}(\Delta\lambda) + \tau_O(\Delta\lambda) \quad . \tag{13-2}$$

The optical depth for each constituent is defined as:

$$\tau_{O_2}(\Delta\lambda) = \sigma_{O_2}(\Delta\lambda) \cdot \int_z^\infty [O_2]\, dL \quad , \tag{13-3}$$

$$\tau_{N_2}(\Delta\lambda) = \sigma_{N_2}(\Delta\lambda) \cdot \int_z^\infty [N_2]\, dL \quad . \tag{13-4}$$

and

$$\tau_O(\Delta\lambda) = \sigma_O(\Delta\lambda) \cdot \int_z^\infty [O]dL \ , \qquad (13\text{-}5)$$

where $\sigma(\Delta\lambda)$ is the absorption cross-section at $\Delta\lambda$ and the integrals represent the total number of particles in a sq cm column extending from $z$ to the top of the atmosphere along the path $L$.

The first-order rate constant for photoionization of $O_2$, $N_2$, and O at altitude $z$ in the wavelength range given in Table 13-1 is:

$$k_j(z) = \sum_\lambda \sigma_j'(\lambda)\, \Phi_\infty(\lambda) \exp\left(-\sum_{j=1}^{3} \sigma_j(\lambda) \cdot \int_z^\infty [N_j]dL\right) \ , \qquad (13\text{-}6)$$

where $\sigma_j'(\lambda)$ is the ionization cross-section at wavelength $\lambda$ for species $j$.

The tables list the rate constants $k_j(z)$ of $O_2^+$, $N_2^+$, and $O^+$ at the specified altitudes for the given solar conditions. Also given are the rate coefficients for the production of $NO^+$ by Lyman alpha. That is:

$$k(NO^+) = \sigma'(L_\alpha) \cdot \Phi_\infty(L_\alpha) \exp\left(-\sigma_{O_2}(L_\alpha) \cdot \int_z^\infty [O_2]dL\right) \ . \qquad (13\text{-}7)$$

## 13.2 SOLAR ULTRAVIOLET INTENSITIES

Solar ultraviolet radiation at wavelengths less than about 2900 A is absorbed in the earth's atmosphere and therefore does not penetrate to ground level. The total range of interest here (4000-1 A) has been studied from rockets, satellites, and balloons, and the general characteristics of the radiation have been described in several reviews (References 13-7 through 13-9). Uncertainties exist in the flux values, because of the limited number of measurements and because of variations in emission over the solar cycle.

The solar spectrum from 4000 to 2085 A appears to be a continuation of the visible spectrum with an emission continuum containing superimposed Fraunhofer absorption lines. At wavelengths less than 2085 A, there is a gradual change to a spectrum consisting largely of emission lines with some emission continua superimposed. Toward shorter wavelengths, the emission lines tend to be due to

higher ionization states present in the corona. These lines also tend to increase more during solar flares.

The solar flux incident on the earth's atmosphere in the wavelength range 4000-1750 A is given in Figure 13-1. The intensities were obtained from References 13-9 and 13-10. The region 3000-1100 A has been investigated further (References 13-11 through 13-14), and most results support the measurements (Reference 13-15) given in Figure 13-1. The solar flux intensities at wavelengths shorter than hydrogen Lyman-$\alpha$ (1215.7 A) have been measured and discussed (References 13-1 through 13-3, 13-7, 13-9, 13-10). The values used for the calculations of this chapter are given in Table 13-1.

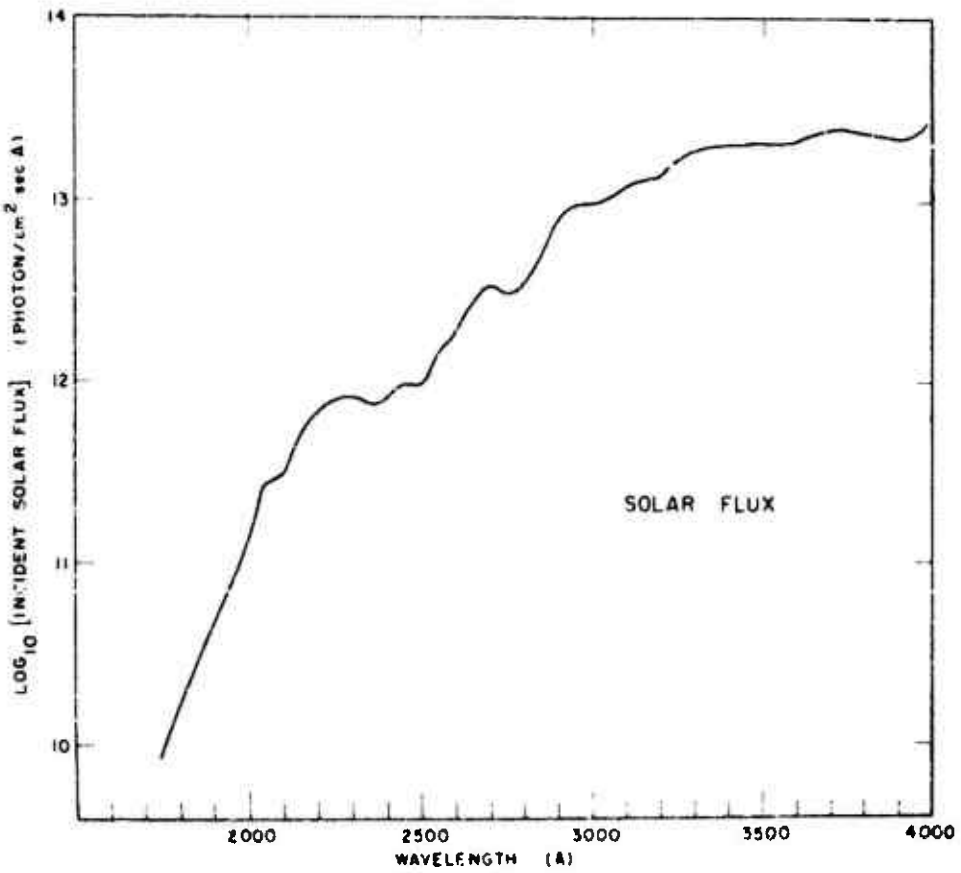


Figure 13-1. Solar flux incident on upper atmosphere. Values from References 13-9 and 13-10. Averaged over 50 A (4000-2650 A); 25 A (2600-2000 A); unaveraged (1950-1750 A).

## REFERENCES

13-1. Hall, L. A., and H. E. Hinteregger, J. Geophys. Res. 75, 6959 (1970).

13-2. Hinteregger, H. E., Ann. Geophys. 26, 547 (1970).

13-3. Swider, W., Jr., Revs. Geophys. 7, 573 (1969).

13-4. Keneshea, T. J., Air Force Cambridge Research Laboratories Report AFCRL-67-0221 (1967).

13-5. Watanabe, K., F. M. Matsunaga, and H. Sakai, Appl. Optics. 6, 391 (1967).

13-6. Huffman, R. E., D. E. Paulsen, J. C. Larrabee, and R. B. Cairns, J. Geophys. Res. 76, 1028 (1971).

13-7 Hinteregger, H. E., L. A. Hall, and G. Schmidtke, Space Research 5, 1175 (1965).

13-8. Goldberg, L., Ann. Rev. Astron. Astrophys. 5, 279 (1967).

13-9. Tousey, R., Space Sci. Revs. 2, 3 (1963); Astrophys. J. 149, 239 (1967).

13-10. Detwiler, C. R., D. L. Garrett, J. D. Purcell, and R. Tousey, Ann. Geophys. 17, 9 (1961).

13-11. Parkinson, W. H., and E. M. Reeves, Solar Phys. 10, 342 (1969).

13-12. Bonnet, R. M., Space Research 8, 458 (1968).

13-13. Ackerman, M., D. Frimout, and R. Pastiels, Ciel et Terre 84, 408 (1968).

13-14. Widing, K. G., J. D. Purcell, and G. D. Sandlin, Solar Phys. 12, 52 (1970).

13-15. Ackerman, M., "Ultraviolet Solar Radiation Related to Mesospheric Processes", Proceedings Fourth ESRIN-ESLAB Symposium, 1970, Dordrecht, Holland (1971).

Table 13-1.*

| WAVELENGTH (A) | FLUX PH/CM2/SEC | SIGMAT C2 (CM2) | SIGMAT N2 (CM2) | SIGMAT O (CM2) | SIGMAI O2 (CM2) | SIGMAI N2 (CM2) | SIGMAI O (CM2) |
|---|---|---|---|---|---|---|---|
| 1225.7 | 3.[illegible]E+11 | 1.300000E-20 | 0. | 0. | 0. | 0. | 0. |
| 1025.7 | 3.50800E+09 | 1.5[illegible]E-18 | 5.000000E-22 | 0. | 9.80000E-19 | 0. | 0. |
| [illegible] | 6.[illegible]E+10 | 1.6[illegible]E-18 | 1.5[illegible]E-18 | 0. | 1.10000E-18 | 0. | 0. |
| 977.0 | 4.40000E+09 | 4.00000E-18 | 7.000000E-19 | 0. | 2.50000E-18 | 0. | 0. |
| 972.5 | 8.[illegible]E+10 | 3.2[illegible]E-17 | 2.6[illegible]E-18 | 0. | 2.5[illegible]E-17 | 0. | 0. |
| [illegible]9.7 | 3.[illegible]E+11 | 6.306[illegible]E-18 | 5.206[illegible]E-18 | 0. | 4.[illegible]E-18 | 0. | 0. |
| [illegible]4.5 | 1.[illegible]E+10 | 3.2[illegible]E-18 | 1.000000E-18 | 0. | 2.60000E-18 | 0. | 0. |
| 937.8 | 2.20000E+08 | 5.[illegible]E-18 | 1.600000E-17 | 0. | 3.00000E-18 | 0. | 0. |
| 933.4 | 1.[illegible]E+10 | 1.[illegible]E-17 | 2.[illegible]E-18 | 0. | 6.[illegible]E-18 | 0. | 0. |
| 930.7 | 1.39[illegible]E+08 | 2.60[illegible]E-17 | 4.80[illegible]E-18 | 0. | 1.70[illegible]E-17 | 0. | 0. |
| 926.2 | 1.38[illegible]E+10 | 6.70[illegible]E-18 | 2.[illegible]E-18 | 0. | 6.70[illegible]E-18 | 0. | 0. |
| | 2.42[illegible]E+11 | 7.46[illegible]E-18 | 1.38[illegible]E-17 | 0. | 3.30[illegible]E-18 | 0. | 0. |
| | 9.68[illegible]E+07 | 7.40[illegible]E-18 | 5.[illegible]E-17 | 0. | 3.30[illegible]E-18 | 0. | 0. |
| 1027-911 | 3.[illegible]E+10 | 7.40[illegible]E-18 | 1.[illegible]E-17 | 0. | 3.30[illegible]E-18 | 0. | 0. |
| | 4.63[illegible]E+08 | 7.42[illegible]E-18 | 2.[illegible]E-18 | 0. | 3.30[illegible]E-18 | 0. | 0. |
| | 2.48[illegible]E+08 | 7.46[illegible]E-18 | 2.[illegible]E-18 | 0. | 3.36[illegible]E-18 | 0. | 0. |
| 911-849 | 9.68[illegible]E+08 | 9.3[illegible]E-18 | 1.30[illegible]E-17 | 3.[illegible]E-18 | 4.46[illegible]E-18 | 0. | 3.[illegible]E-18 |
| | 2.24[illegible]E+09 | 9.30[illegible]E-18 | 2.[illegible]E-18 | 7.[illegible]E-18 | 4.50[illegible]E-18 | 0. | 3.[illegible]E-18 |
| 904 | 1.38[illegible]E+08 | 1.1[illegible]E-17 | 6.30[illegible]E-18 | 3.[illegible]E-18 | 6.30[illegible]E-18 | 0. | 3.[illegible]E-18 |
| 898-860 | 1.04[illegible]E+09 | 7.[illegible]E-18 | 1.[illegible]E-17 | 2.[illegible]E-18 | 4.[illegible]E-18 | 0. | 2.[illegible]E-18 |
| | 1.67[illegible]E+09 | 7.[illegible]E-18 | 2.[illegible]E-18 | 2.[illegible]E-18 | 4.[illegible]E-18 | 0. | 2.[illegible]E-18 |
| 860-830 | 6.[illegible]E+09 | 9.[illegible]E-18 | 1.[illegible]E-17 | 2.[illegible]E-18 | 4.[illegible]E-18 | 0. | 2.[illegible]E-18 |
| | 9.[illegible]E+08 | 9.[illegible]E-18 | 2.[illegible]E-18 | 2.[illegible]E-18 | 4.[illegible]E-18 | 0 | 2.[illegible]E-18 |
| 835.3 | 7.43[illegible]E+07 | 1.[illegible]E-17 | 2.[illegible]E-17 | 2.[illegible]E-18 | 3.70[illegible]E-18 | 0. | 2.[illegible]E-18 |
| 835.1 | 7.47[illegible]E+07 | 1.[illegible]E-17 | 4.[illegible]E-17 | 2.[illegible]E-18 | 3.70[illegible]E-18 | 0. | 2.[illegible]E-18 |
| 834.5 | 7.43[illegible]E+07 | 1.[illegible]E-17 | 7.50[illegible]E-18 | 2.[illegible]E-18 | 4.[illegible]E-18 | 0. | 2.[illegible]E-18 |
| 833.7 | 7.43[illegible]E+07 | 1.3[illegible]E-17 | 6.[illegible]E-18 | 2.[illegible]E-18 | 5.[illegible]E-18 | 0. | 2.[illegible]E-18 |
| 833.3 | 7.43[illegible]E+07 | 1.50[illegible]E-17 | 2.30[illegible]E-18 | 2.[illegible]E-18 | 6.[illegible]E-18 | 0. | 2.[illegible]E-18 |
| 832.5 | 7.43[illegible]E+07 | 2.68[illegible]E-17 | 7.46[illegible]E-18 | 2.[illegible]E-18 | 1.68[illegible]E-17 | 0. | 2.[illegible]E-18 |
| 832.8 | 7.43[illegible]E+07 | 2.60[illegible]E-17 | 2.10[illegible]E-18 | 2.[illegible]E-18 | 1.[illegible]E-17 | 0. | 2.[illegible]E-18 |
| | 7.[illegible]E+07 | 1.90[illegible]E-17 | 5.[illegible]E-17 | 2.[illegible]E-18 | 7.[illegible]E-18 | 0. | 2.[illegible]E-18 |
| 830-800 | 2.34[illegible]E+08 | 1.96[illegible]E-17 | 1.[illegible]E-17 | 2.[illegible]E-18 | 7.[illegible]E-18 | 0. | 2.[illegible]E-18 |
| | 4.68[illegible]E+08 | 1.9[illegible]E-17 | 2.[illegible]E-18 | 2.[illegible]E-18 | 7.[illegible]E-18 | 0. | 2.[illegible]E-18 |
| | 3.98[illegible]E+08 | 2.60[illegible]E-17 | 1.[illegible]E-18 | 3.[illegible]E-18 | 1.[illegible]E-17 | 6.[illegible]E-17 | 3.[illegible]E-18 |
| 800-770 | 7.80[illegible]E+07 | 2.60[illegible]E-17 | 5.[illegible]E-17 | 3.[illegible]E-18 | 1.30[illegible]E-17 | 2.30[illegible]E-17 | 3.[illegible]E-18 |
| | 1.16[illegible]E+08 | 2.66[illegible]E-17 | 2.50[illegible]E-17 | 3.[illegible]E-18 | 1.[illegible]E-17 | 1.60[illegible]E-17 | 3.[illegible]E-18 |
| 790.1 | 2.68[illegible]E+08 | 2.90[illegible]E-17 | 2.50[illegible]E-17 | 2.[illegible]E-18 | 1.[illegible]E-17 | 1.10[illegible]E-17 | 2.[illegible]E-18 |
| 787.7 | 1.30[illegible]E+08 | 2.40[illegible]E-17 | 1.[illegible]E-17 | 2.[illegible]E-18 | 1.30[illegible]E-17 | 8.[illegible]E-18 | 2.[illegible]E-18 |
| 786.5 | 8.[illegible]E+07 | 2.30[illegible]E-17 | 4.40[illegible]E-17 | 2.[illegible]E-18 | 7.[illegible]E-18 | 3.30[illegible]E-17 | 2.[illegible]E-18 |
| 780.3 | 1.20[illegible]E+09 | 2.90[illegible]E-17 | 3.[illegible]E-17 | 2.[illegible]E-18 | 1.10[illegible]E-17 | 1.70[illegible]E-17 | 2.[illegible]E-18 |
| 770.4 | 2.70[illegible]E+09 | 1.90[illegible]E-17 | 1.20[illegible]E-17 | 2.[illegible]E-18 | 1.10[illegible]E-17 | 7.[illegible]E-18 | 2.[illegible]E-18 |
| 770-740 | 1.37[illegible]E+07 | 1.90[illegible]E-17 | 5.[illegible]E-17 | 3.30[illegible]E-18 | 1.[illegible]E-17 | 3.[illegible]E-17 | 3.30[illegible]E-18 |
| | 1.76[illegible]E+08 | 1.90[illegible]E-17 | 2.40[illegible]E-17 | 3.30[illegible]E-18 | 1.[illegible]E-17 | 1.70[illegible]E-17 | 3.30[illegible]E-18 |

* SIGMAT = Total absorption cross-section. SIGMAI = Total ionization cross-section.

Table 13-1. (Cont'd.)

| WAVELENGTH (Å) | FLUX (PH/CM²/SEC) | SIGMA (2 (CM²) | SIGMA N2 (CM²) | SIGMA O (CM²) | SIGMA O2 (CM²) | SIGMA N2 (CM²) | SIGMA O (CM²) |
|---|---|---|---|---|---|---|---|
| 765.1 | 1.460000E+07 | 2.300000E-17 | 1.700000E-17 | 3.050000E-18 | 1.200000E-17 | 5.100000E-17 | 3.050000E-18 |
| 760.4 | 8.000000E+07 | 2.900000E-17 | 1.800000E-17 | 2.950000E-18 | 1.600000E-17 | 2.200000E-17 | 2.950000E-18 |
| 748-710 | 9.000000E+07 | 3.050000E-17 | 2.200000E-17 | 5.250000E-18 | 3.200000E-17 | 2.100000E-17 | 5.500000E-18 |
| 710-688 | 4.000000E+07 | 2.400000E-17 | 2.300000E-17 | 6.500000E-18 | 2.300000E-17 | 2.100000E-17 | 6.500000E-18 |
| 703 | 2.700000E+08 | 2.600000E-17 | 2.350000E-17 | 6.500000E-18 | 2.300000E-17 | 2.100000E-17 | 6.500000E-18 |
| 688-656 | 2.600000E+08 | 2.750000E-17 | 2.400000E-17 | 6.000000E-18 | 1.900000E-17 | 2.500000E-17 | 6.000000E-18 |
| | 7.500000E+08 | 2.200000E-17 | 2.400000E-17 | 6.000000E-18 | 1.900000E-17 | 2.400000E-17 | 6.000000E-18 |
| 629.7 | 9.250000E+08 | 1.900000E-17 | 2.300000E-17 | 5.000000E-18 | 2.500000E-17 | 2.300000E-17 | 5.000000E-18 |
| 625.1 | 7.500000E+07 | 2.500000E-17 | 2.400000E-17 | 6.000000E-18 | 2.400000E-17 | 2.300000E-17 | 6.000000E-18 |
| 609.8 | 5.000000E+08 | 2.700000E-17 | 2.500000E-17 | 6.000000E-18 | 2.500000E-17 | 2.400000E-17 | 6.000000E-18 |
| 599.6 | 8.000000E+07 | 2.800000E-17 | 2.300000E-17 | 5.800000E-18 | 2.700000E-17 | 2.500000E-17 | 5.800000E-18 |
| 596.1 | 1.900000E+08 | 2.300000E-17 | 2.300000E-17 | 5.400000E-18 | 2.300000E-17 | 2.300000E-17 | 5.500000E-18 |
| 584 | 1.100000E+08 | 2.600000E-17 | 2.500000E-17 | 5.500000E-18 | 2.500000E-17 | 2.400000E-17 | 5.500000E-18 |
| 521.0 | 1.900000E+08 | 2.100000E-17 | 2.400000E-17 | 5.300000E-18 | 2.100000E-17 | 2.300000E-17 | 5.300000E-18 |
| 508 | 8.000000E+07 | 2.300000E-17 | 2.300000E-17 | 5.300000E-18 | 2.200000E-17 | 2.300000E-17 | 5.300000E-18 |
| 504-497 | 5.000000E+08 | 2.500000E-17 | 2.300000E-17 | 5.500000E-18 | 2.200000E-17 | 2.300000E-17 | 5.500000E-18 |
| 497.3 | 7.400000E+08 | 2.200000E-17 | 2.300000E-17 | 5.500000E-18 | 2.200000E-17 | 2.300000E-17 | 5.500000E-18 |
| 485.9 | 1.600000E+08 | 2.100000E-17 | 2.300000E-17 | 1.000000E-17 | 2.100000E-17 | 2.300000E-17 | 1.000000E-17 |
| 830-460 | 4.400000E+07 | 2.300000E-17 | 2.300000E-17 | 5.400000E-18 | 2.300000E-17 | 2.300000E-17 | 5.400000E-18 |
| 461.7 | 1.000000E+08 | 2.000000E-17 | 2.100000E-17 | 1.050000E-17 | 2.000000E-17 | 2.100000E-17 | 1.050000E-17 |
| 460-371 | 5.100000E+08 | 2.200000E-17 | 2.000000E-17 | 1.000000E-17 | 2.000000E-17 | 2.000000E-17 | 1.000000E-17 |
| 368.1 | 5.600000E+08 | 1.800000E-17 | 1.700000E-17 | 9.500000E-18 | 1.800000E-17 | 1.700000E-17 | 9.500000E-18 |
| 365 | 1.700000E+08 | 1.800000E-17 | 1.600000E-17 | 9.500000E-18 | 1.800000E-17 | 1.600000E-17 | 9.500000E-18 |
| 362.7 | 3.600000E+08 | 1.700000E-17 | 1.600000E-17 | 9.500000E-18 | 1.700000E-17 | 1.600000E-17 | 9.500000E-18 |
| 335.4 | 7.200000E+08 | 1.700000E-17 | 1.400000E-17 | 8.800000E-18 | 1.700000E-17 | 1.400000E-17 | 8.800000E-18 |
| 303.8 | 5.400000E+08 | 1.700000E-17 | 1.300000E-17 | 8.500000E-18 | 1.700000E-17 | 1.200000E-17 | 8.500000E-18 |
| 296.1 | 1.100000E+08 | 1.500000E-17 | 1.100000E-17 | 8.500000E-18 | 1.500000E-17 | 1.100000E-17 | 8.500000E-18 |
| 294-288 | 2.400000E+08 | 1.600000E-17 | 1.300000E-17 | 8.500000E-18 | 1.600000E-17 | 1.300000E-17 | 8.500000E-18 |
| 288-231 | 3.100000E+08 | 1.700000E-17 | 1.000000E-17 | 7.500000E-18 | 2.200000E-17 | 1.300000E-17 | 1.500000E-17 |
| 231-206 | 1.400000E+08 | 1.000000E-17 | 7.000000E-18 | 6.500000E-18 | 2.100000E-17 | 1.400000E-17 | 1.300000E-17 |
| 206-175 | 3.700000E+08 | 5.400000E-18 | 5.600000E-18 | 4.600000E-18 | 1.200000E-17 | 1.100000E-17 | 8.000000E-18 |
| 175-151 | 4.000000E+08 | 5.200000E-18 | 4.400000E-18 | 3.600000E-18 | 1.040000E-17 | 9.000000E-18 | 6.000000E-18 |
| 151-101 | 4.000000E+09 | 3.060000E-18 | 2.700000E-18 | 1.700000E-18 | 7.500000E-18 | 5.400000E-18 | 5.100000E-18 |
| 94.8-88.1 | 1.600000E+09 | 2.000000E-18 | 1.200000E-18 | 1.000000E-18 | 6.000000E-18 | 3.600000E-18 | 3.060000E-18 |
| 101-90 | 9.500000E+07 | 2.000000E-18 | 1.200000E-18 | 1.500000E-18 | 6.000000E-18 | 3.600000E-18 | 3.060000E-18 |
| 88.5-86.7 | 1.000000E+09 | 1.400000E-18 | 9.500000E-19 | 7.000000E-19 | 4.200000E-18 | 2.800000E-18 | 2.100000E-18 |
| 90-80 | 1.200000E+08 | 1.500000E-18 | 8.900000E-19 | 7.500000E-19 | 4.500000E-18 | 2.700000E-18 | 2.300000E-18 |
| 76.8 | 4.000000E+08 | 1.130000E-18 | 6.750000E-19 | 5.650000E-19 | 4.400000E-18 | 2.700000E-18 | 2.300000E-18 |
| 80-70 | 9.400000E+07 | 1.100000E-18 | 6.500000E-19 | 5.500000E-19 | 4.400000E-18 | 2.600000E-18 | 2.300000E-18 |
| 66.3 | 7.000000E+08 | 8.300000E-19 | 4.900000E-19 | 4.100000E-19 | 4.600000E-18 | 2.600000E-18 | 1.600000E-18 |
| 70-66 | 1.600000E+08 | 8.000000E-19 | 4.500000E-19 | 3.900000E-19 | 4.000000E-18 | 1.600000E-18 | 2.000000E-18 |
| 60.4 | 2.400000E+07 | 4.500000E-19 | 2.500000E-19 | 2.300000E-19 | 2.700000E-18 | 1.500000E-18 | 1.400000E-18 |
| 60-50 | 8.300000E+07 | 5.100000E-19 | 3.000000E-19 | 2.500000E-19 | 3.100000E-18 | 1.800000E-18 | 1.500000E-18 |
| 44.1 | 6.400000E+08 | 3.000000E-19 | 1.600000E-19 | 1.400000E-19 | 2.100000E-18 | 1.200000E-18 | 1.200000E-18 |
| 50-40 | 4.700000E+07 | 3.100000E-19 | 1.800000E-19 | 1.600000E-19 | 2.200000E-18 | 1.400000E-18 | 1.100000E-18 |
| 33.8 | 4.800000E+06 | 1.500000E-19 | 9.000000E-20 | 8.000000E-20 | 1.500000E-18 | 8.000000E-19 | 8.000000E-19 |
| 8 | 1.400000E+05 | 1.000000E-19 | 6.500000E-20 | 5.000000E-20 | 3.900000E-19 | 2.500000E-19 | 2.000000E-19 |
| 7 | 2.800000E+04 | 5.200000E-20 | 3.000000E-20 | 2.600000E-20 | 2.600000E-19 | 1.500000E-19 | 1.300000E-19 |
| 5 | 2.500000E+03 | 2.000000E-20 | 1.200000E-20 | 1.000000E-20 | 1.400000E-19 | 8.400000E-19 | 7.100000E-19 |
| 3 | 3.000000E+01 | 4.600000E-21 | 2.600000E-21 | 2.300000E-21 | 5.400000E-19 | 3.300000E-19 | 2.700000E-19 |
| 1 | 1.900000E-01 | 1.700000E-22 | 1.000000E-22 | 8.600000E-23 | 9.900000E-19 | 3.500000E-20 | 2.300000E-19 |

## Table 13-2

LATITUDE = 3.00000E+01 DEGREES.
SOLAR DECLINATION = 0. DEGREES.
SOLAR ZENITH ANGLE = 3.00000E+01 DEGREES.

| ALT KM | N2 N/CC | N2 COLUMN N/SQ CM | O2 N/CC | O2 COLUMN N/SQ CM | O N/CC | O COLUMN N/SQ CM | ALT KM | N2 N/CC | N2 COLUMN N/SQ CM | O2 N/CC | O2 COLUMN N/SQ CM | O N/CC | O COLUMN N/SQ CM |
|---|---|---|---|---|---|---|---|---|---|---|---|---|---|
| 60 | 5.21E+15 | 4.49E+21 | 1.40E+15 | 1.20E+21 | 1.64E+10 | 1.51E+18 | 130 | 1.25E+11 | 2.65E+17 | 1.59E+10 | 2.20E+16 | 6.69E+10 | 1.90E+17 |
| 62 | 4.86E+15 | 3.42E+21 | 1.09E+15 | 9.14E+20 | 1.64E+10 | 1.50E+18 | 132 | 1.04E+11 | 1.78E+17 | 1.30E+10 | 1.94E+16 | 5.69E+10 | 1.75E+17 |
| 64 | 3.17E+15 | 2.59E+21 | 8.53E+14 | 6.91E+20 | 1.64E+10 | 1.50E+18 | 134 | 8.72E+10 | 1.56E+17 | 1.07E+10 | 1.67E+16 | 5.22E+10 | 1.63E+17 |
| 66 | 2.45E+15 | 1.96E+21 | 6.57E+14 | 5.10E+20 | 1.64E+10 | 1.50E+18 | 136 | 7.37E+10 | 1.30E+17 | 8.85E+09 | 1.45E+16 | 4.66E+10 | 1.52E+17 |
| 68 | 1.88E+15 | 1.45E+21 | 5.04E+14 | 3.85E+20 | 1.64E+10 | 1.49E+18 | 138 | 6.27E+10 | 1.22E+17 | 7.41E+09 | 1.26E+16 | 4.10E+10 | 1.42E+17 |
| 70 | 1.42E+15 | 1.07E+21 | 3.82E+14 | 2.83E+20 | 1.64E+10 | 1.49E+18 | 140 | 5.38E+10 | 1.09E+17 | 6.29E+09 | 1.10E+16 | 3.77E+10 | 1.33E+17 |
| 72 | 1.07E+15 | 7.81E+20 | 2.86E+14 | 2.07E+20 | 1.64E+10 | 1.49E+18 | 142 | 4.65E+10 | 9.71E+16 | 5.31E+09 | 9.70E+15 | 3.42E+10 | 1.24E+17 |
| 74 | 7.91E+14 | 5.68E+20 | 2.12E+14 | 1.49E+20 | 1.64E+10 | 1.46E+18 | 144 | 4.04E+10 | 8.71E+16 | 4.54E+09 | 8.57E+15 | 3.11E+10 | 1.17E+17 |
| 76 | 5.83E+14 | 4.18E+20 | 1.55E+14 | 1.07E+20 | 2.01E+10 | 1.48E+18 | 146 | 3.53E+10 | 7.84E+16 | 3.91E+09 | 7.60E+15 | 2.65E+10 | 1.10E+17 |
| 78 | 4.27E+14 | 2.95E+20 | 1.13E+14 | 7.64E+19 | 3.53E+10 | 1.47E+18 | 148 | 3.10E+10 | 7.07E+16 | 3.38E+09 | 6.76E+15 | 2.61E+10 | 1.04E+17 |
| 80 | 3.11E+14 | 2.10E+20 | 8.21E+13 | 5.41E+19 | 6.20E+10 | 1.46E+18 | 150 | 2.73E+10 | 6.40E+16 | 2.94E+09 | 6.03E+15 | 2.41E+10 | 9.63E+16 |
| 82 | 2.25E+14 | 1.49E+20 | 5.90E+13 | 3.79E+19 | 9.64E+10 | 1.44E+18 | 152 | 2.42E+10 | 5.81E+16 | 2.57E+09 | 5.39E+15 | 2.22E+10 | 9.38E+16 |
| 84 | 1.61E+14 | 1.05E+20 | 4.21E+13 | 2.63E+19 | 1.27E+11 | 1.42E+18 | 154 | 2.15E+10 | 5.20E+16 | 2.25E+09 | 4.64E+15 | 2.06E+10 | 6.62E+16 |
| 86 | 1.14E+14 | 7.32E+19 | 2.96E+13 | 1.81E+19 | 1.50E+11 | 1.39E+18 | 156 | 1.92E+10 | 4.81E+16 | 1.90E+09 | 4.35E+15 | 1.91E+10 | 6.36E+16 |
| 88 | 7.99E+13 | 5.11E+19 | 2.05E+13 | 1.24E+19 | 1.62E+11 | 1.35E+18 | 158 | 1.72E+10 | 4.39E+16 | 1.75E+09 | 3.92E+15 | 1.76E+10 | 7.94E+16 |
| 90 | 5.58E+13 | 3.55E+19 | 1.42E+13 | 8.45E+18 | 1.67E+11 | 1.31E+18 | 160 | 1.54E+10 | 4.02E+16 | 1.55E+09 | 3.54E+15 | 1.66E+10 | 7.55E+16 |
| 92 | 3.87E+13 | 2.40E+19 | 9.74E+12 | 5.72E+18 | 1.69E+11 | 1.27E+18 | 162 | 1.39E+10 | 3.68E+16 | 1.30E+09 | 3.20E+15 | 1.55E+10 | 7.16E+16 |
| 94 | 2.67E+13 | 1.75E+19 | 6.65E+12 | 3.85E+18 | 1.79E+11 | 1.23E+18 | 164 | 1.25E+10 | 3.38E+16 | 1.23E+09 | 2.98E+15 | 1.46E+10 | 6.84E+16 |
| 96 | 1.85E+13 | 1.22E+19 | 4.53E+12 | 2.57E+18 | 2.16E+11 | 1.19E+18 | 166 | 1.13E+10 | 3.10E+16 | 1.10E+09 | 2.63E+15 | 1.37E+10 | 6.52E+16 |
| 98 | 1.28E+13 | 8.50E+18 | 3.04E+12 | 1.71E+18 | 3.09E+11 | 1.13E+18 | 168 | 1.03E+10 | 2.85E+16 | 9.86E+08 | 2.39E+15 | 1.28E+10 | 6.22E+16 |
| 100 | 8.71E+12 | 6.11E+16 | 1.99E+12 | 1.14E+18 | 4.15E+11 | 1.05E+18 | 170 | 9.34E+09 | 2.63E+16 | 8.85E+06 | 2.18E+15 | 1.21E+10 | 5.93E+16 |
| 102 | 6.00E+12 | 4.45E+18 | 1.27E+12 | 7.66E+17 | 4.66E+11 | 9.43E+17 | 172 | 8.50E+09 | 2.42E+16 | 7.96E+08 | 1.98E+15 | 1.14E+10 | 5.66E+16 |
| 104 | 4.27E+12 | 3.20E+18 | 8.25E+11 | 5.26E+17 | 4.59E+11 | 6.20E+17 | 174 | 7.75E+09 | 2.23E+16 | 7.17E+08 | 1.81E+15 | 1.06E+10 | 5.41E+16 |
| 106 | 3.04E+12 | 2.44E+18 | 5.43E+11 | 3.73E+17 | 4.22E+11 | 7.20E+17 | 176 | 7.08E+09 | 2.06E+16 | 6.47E+08 | 1.65E+15 | 1.02E+10 | 5.17E+16 |
| 108 | 2.19E+12 | 1.84E+18 | 3.65E+11 | 2.69E+17 | 3.74E+11 | 6.30E+17 | 178 | 6.47E+09 | 1.91E+16 | 5.85E+08 | 1.51E+15 | 9.62E+09 | 4.94E+16 |
| 110 | 1.59E+12 | 1.41E+18 | 2.51E+11 | 1.99E+17 | 3.23E+11 | 5.51E+17 | 180 | 5.92E+09 | 1.76E+16 | 5.30E+08 | 1.30E+15 | 9.11E+09 | 4.73E+16 |
| 112 | 1.16E+12 | 1.10E+18 | 1.76E+11 | 1.51E+17 | 2.75E+11 | 4.84E+17 | 182 | 5.43E+09 | 1.63E+16 | 4.80E+08 | 1.26E+15 | 8.64E+09 | 4.53E+16 |
| 114 | 8.61E+11 | 8.66E+17 | 1.27E+11 | 1.16E+17 | 2.33E+11 | 4.27E+17 | 184 | 4.98E+09 | 1.51E+16 | 4.36E+08 | 1.16E+15 | 8.19E+09 | 4.33E+16 |
| 116 | 6.46E+11 | 6.93E+17 | 9.35E+10 | 9.09E+16 | 1.97E+11 | 3.70E+17 | 186 | 4.58E+09 | 1.40E+16 | 3.96E+08 | 1.06E+15 | 7.70E+09 | 4.15E+16 |
| 118 | 4.92E+11 | 5.63E+17 | 7.04E+10 | 7.21E+16 | 1.87E+11 | 3.35E+17 | 188 | 4.21E+09 | 1.30E+16 | 3.61E+08 | 9.74E+14 | 7.39E+09 | 3.96E+16 |
| 120 | 3.79E+11 | 4.63E+17 | 5.42E+10 | 5.78E+16 | 1.42E+11 | 3.00E+17 | 190 | 3.00E+09 | 1.21E+16 | 3.29E+08 | 8.94E+14 | 7.03E+09 | 3.81E+16 |
| 122 | 2.96E+11 | 3.85E+17 | 4.12E+10 | 4.49E+16 | 1.20E+11 | 2.71E+17 | 192 | 3.57E+09 | 1.12E+16 | 3.00E+08 | 8.22E+14 | 6.69E+09 | 3.66E+16 |
| 124 | 2.35E+11 | 3.24E+17 | 3.18E+10 | 3.85E+16 | 1.03E+11 | 2.46E+17 | 194 | 3.30E+09 | 1.04E+16 | 2.74E+08 | 7.56E+14 | 6.37E+09 | 3.51E+16 |
| 126 | 1.88E+11 | 2.76E+17 | 2.50E+10 | 3.20E+16 | 8.82E+10 | 2.24E+17 | 196 | 3.04E+09 | 9.68E+15 | 2.50E+08 | 6.95E+14 | 6.07E+09 | 3.37E+16 |
| 128 | 1.53E+11 | 2.37E+17 | 1.98E+10 | 2.69E+16 | 7.65E+10 | 2.06E+17 | 198 | 2.81E+09 | 9.01E+15 | 2.29E+08 | 6.40E+14 | 5.78E+09 | 3.23E+16 |
| 130 | 1.25E+11 | 2.05E+17 | 1.59E+10 | 2.28E+16 | 6.69E+10 | 1.93E+17 | 200 | 2.60E+09 | 8.39E+15 | 2.09E+08 | 5.90E+14 | 5.52E+09 | 3.10E+16 |

Table 13-3.

LATITUDE = 3.00000E+01 DEGREES.
SOLAR DECLINATION = 0. DEGREES.
SOLAR ZENITH ANGLE = 3.00000E+01 DEGREES.

| ALT KM | K(O2+) /SEC | K(N2+) /SEC | K(O+) /SEC | K(NO+) /SEC |
|---|---|---|---|---|
| 60 | 2.603E-16 | 1.822E-21 | 1.197E-20 | 3.702E-12 |
| 62 | 3.040E-16 | 2.130E-21 | 1.399E-20 | 6.477E-11 |
| 64 | 3.432E-16 | 2.695E-21 | 1.683E-20 | 6.039E-10 |
| 66 | 3.770E-16 | 6.595E-21 | 2.059E-20 | 3.407E-09 |
| 68 | 4.053E-16 | 3.223E-20 | 4.269E-20 | 1.293E-08 |
| 70 | 4.285E-16 | 1.366E-19 | 1.386E-19 | 3.571E-08 |
| 72 | 4.472E-16 | 4.347E-19 | 3.737E-19 | 7.679E-08 |
| 74 | 4.624E-16 | 1.130E-18 | 9.459E-19 | 1.359E-07 |
| 76 | 4.772E-16 | 3.673E-18 | 3.072E-18 | 2.073E-07 |
| 78 | 5.061E-16 | 1.622E-17 | 1.365E-17 | 2.821E-07 |
| 80 | 5.936E-16 | 6.503E-17 | 5.496E-17 | 3.529E-07 |
| 82 | 8.016E-16 | 2.329E-16 | 1.961E-16 | 4.148E-07 |
| 84 | 1.910E-15 | 8.352E-16 | 7.140E-16 | 4.656E-07 |
| 86 | 5.944E-15 | 3.237E-15 | 2.768E-15 | 5.055E-07 |
| 88 | 2.552E-14 | 1.511E-14 | 1.289E-14 | 5.353E-07 |
| 90 | 1.271E-13 | 7.388E-14 | 6.324E-14 | 5.569E-07 |
| 92 | 1.823E-12 | 3.769E-13 | 3.200E-13 | 5.723E-07 |
| 94 | 1.157E-11 | 2.271E-12 | 1.903E-12 | 5.831E-07 |
| 96 | 7.933E-11 | 1.235E-11 | 1.032E-11 | 5.906E-07 |
| 98 | 3.100E-10 | 4.736E-11 | 3.966E-11 | 5.957E-07 |
| 100 | 7.884E-10 | 1.274E-10 | 1.072E-10 | 5.991E-07 |
| 102 | 1.489E-09 | 2.567E-10 | 2.169E-10 | 6.014E-07 |
| 104 | 2.382E-09 | 4.281E-10 | 3.659E-10 | 6.028E-07 |
| 106 | 3.504E-09 | 6.307E-10 | 5.377E-10 | 6.037E-07 |
| 108 | 4.901E-09 | 8.468E-10 | 7.284E-10 | 6.044E-07 |
| 110 | 6.564E-09 | 1.068E-09 | 9.462E-10 | 6.040E-07 |
| 112 | 8.461E-09 | 1.302E-09 | 1.225E-09 | 6.051E-07 |
| 114 | 1.059E-08 | 1.572E-09 | 1.622E-09 | 6.053E-07 |
| 116 | 1.298E-08 | 1.932E-09 | 2.205E-09 | 6.054E-07 |
| 118 | 1.571E-08 | 2.462E-09 | 3.049E-09 | 6.056E-07 |
| 120 | 1.886E-08 | 3.247E-09 | 4.210E-09 | 6.056E-07 |
| 122 | 2.251E-08 | 4.371E-09 | 5.739E-09 | 6.057E-07 |
| 124 | 2.672E-08 | 5.911E-09 | 7.677E-09 | 6.058E-07 |
| 126 | 3.158E-08 | 7.934E-09 | 1.006E-08 | 6.058E-07 |
| 128 | 3.715E-08 | 1.050E-08 | 1.292E-08 | 6.059E-07 |
| 130 | 4.349E-08 | 1.367E-08 | 1.626E-08 | 6.059E-07 |

| ALT KM | K(O2+) /SEC | K(N2+) /SEC | K(O+) /SEC | K(NO+) /SEC |
|---|---|---|---|---|
| 130 | 4.349E-08 | 1.367E-08 | 1.626E-08 | 6.059E-07 |
| 132 | 5.064E-08 | 1.740E-08 | 2.009E-08 | 6.059E-07 |
| 134 | 5.861E-08 | 2.196E-08 | 2.448E-08 | 6.059E-07 |
| 136 | 6.737E-08 | 2.712E-08 | 2.915E-08 | 6.059E-07 |
| 138 | 7.691E-08 | 3.296E-08 | 3.432E-08 | 6.059E-07 |
| 140 | 8.717E-08 | 3.945E-08 | 3.988E-08 | 6.059E-07 |
| 142 | 9.807E-08 | 4.656E-08 | 4.571E-08 | 6.059E-07 |
| 144 | 1.095E-07 | 5.423E-08 | 5.184E-08 | 6.059E-07 |
| 146 | 1.215E-07 | 6.241E-08 | 5.818E-08 | 6.060E-07 |
| 148 | 1.336E-07 | 7.102E-08 | 6.468E-08 | 6.060E-07 |
| 150 | 1.464E-07 | 8.001E-08 | 7.130E-08 | 6.060E-07 |
| 152 | 1.593E-07 | 8.929E-08 | 7.799E-08 | 6.060E-07 |
| 154 | 1.723E-07 | 9.888E-08 | 8.471E-08 | 6.060E-07 |
| 156 | 1.853E-07 | 1.085E-07 | 9.142E-08 | 6.060E-07 |
| 158 | 1.983E-07 | 1.183E-07 | 9.809E-08 | 6.060E-07 |
| 160 | 2.112E-07 | 1.281E-07 | 1.047E-07 | 6.060E-07 |
| 162 | 2.240E-07 | 1.379E-07 | 1.112E-07 | 6.060E-07 |
| 164 | 2.367E-07 | 1.477E-07 | 1.176E-07 | 6.060E-07 |
| 166 | 2.491E-07 | 1.574E-07 | 1.239E-07 | 6.060E-07 |
| 168 | 2.612E-07 | 1.669E-07 | 1.300E-07 | 6.060E-07 |
| 170 | 2.731E-07 | 1.763E-07 | 1.359E-07 | 6.060E-07 |
| 172 | 2.647E-07 | 1.855E-07 | 1.417E-07 | 6.060E-07 |
| 174 | 2.959E-07 | 1.946E-07 | 1.473E-07 | 6.060E-07 |
| 176 | 3.069E-07 | 2.034E-07 | 1.528E-07 | 6.060E-07 |
| 178 | 3.175E-07 | 2.119E-07 | 1.580E-07 | 6.060E-07 |
| 180 | 3.277E-07 | 2.202E-07 | 1.631E-07 | 6.060E-07 |
| 182 | 3.376E-07 | 2.283E-07 | 1.680E-07 | 6.060E-07 |
| 184 | 3.472E-07 | 2.361E-07 | 1.727E-07 | 6.060E-07 |
| 186 | 3.564E-07 | 2.436E-07 | 1.773E-07 | 6.060E-07 |
| 188 | 3.653E-07 | 2.509E-07 | 1.816E-07 | 6.060E-07 |
| 190 | 3.739E-07 | 2.579E-07 | 1.858E-07 | 6.060E-07 |
| 192 | 3.822E-07 | 2.647E-07 | 1.899E-07 | 6.060E-07 |
| 194 | 3.902E-07 | 2.712E-07 | 1.937E-07 | 6.060E-07 |
| 196 | 3.979E-07 | 2.775E-07 | 1.974E-07 | 6.060E-07 |
| 198 | 4.052E-07 | 2.835E-07 | 2.010E-07 | 6.060E-07 |
| 200 | 4.124E-07 | 2.892E-07 | 2.044E-07 | 6.060E-07 |

Table 13-4.

LATITUDE = 3.00000E+01 DEGREES.
SOLAR DECLINATION = 0. DEGREES.
SOLAR ZENITH ANGLE = 6.00000E+01 DEGREES.

| ALT KM | N2 N/CC | N2 COLUMN N/SQ CM | O2 N/CC | O2 COLUMN N/SQ CM | O N/CC | O COLUMN N/SQ CM | ALT KM | N2 N/CC | N2 COLUMN N/SQ CM | O2 N/CC | O2 COLUMN N/SQ CM | O N/CC | O COLUMN N/SQ CM |
|---|---|---|---|---|---|---|---|---|---|---|---|---|---|
| 60 | 5.21E+15 | 7.79E+21 | 1.48E+15 | 2.07E+21 | 1.64E+10 | 2.56E+18 | 130 | 1.25E+11 | 3.52E+17 | 1.59E+10 | 3.92E+16 | 6.69E+18 | 3.25E+17 |
| 62 | 4.88E+15 | 5.91E+21 | 1.09E+15 | 1.58E+21 | 1.84E+10 | 2.56E+18 | 132 | 1.04E+11 | 3.06E+17 | 1.30E+10 | 3.34E+16 | 5.89E+10 | 3.01E+17 |
| 64 | 3.17E+15 | 4.47E+21 | 8.50E+14 | 1.15E+21 | 1.64E+10 | 2.55E+18 | 134 | 8.72E+10 | 2.68E+17 | 1.07E+10 | 2.68E+16 | 5.22E+10 | 2.79E+17 |
| 66 | 2.45E+15 | 3.36E+21 | 6.57E+14 | 8.95E+20 | 1.64E+10 | 2.55E+18 | 136 | 7.37E+10 | 2.37E+17 | 8.85E+09 | 2.49E+16 | 4.66E+10 | 2.60E+17 |
| 68 | 1.88E+15 | 2.58E+21 | 5.84E+14 | 6.65E+20 | 1.64E+10 | 2.54E+18 | 138 | 6.27E+10 | 2.10E+17 | 7.41E+09 | 2.17E+16 | 4.18E+10 | 2.42E+17 |
| 70 | 1.42E+15 | 1.84E+21 | 3.82E+14 | 4.89E+20 | 1.64E+10 | 2.54E+18 | 140 | 5.38E+10 | 1.87E+17 | 6.25E+09 | 1.90E+16 | 3.77E+10 | 2.27E+17 |
| 72 | 1.07E+15 | 1.35E+21 | 2.86E+14 | 3.57E+20 | 1.64E+10 | 2.53E+18 | 142 | 4.65E+10 | 1.67E+17 | 5.31E+09 | 1.67E+16 | 3.42E+10 | 2.13E+17 |
| 74 | 7.91E+14 | 9.81E+20 | 2.12E+14 | 2.58E+20 | 1.64E+10 | 2.53E+18 | 144 | 4.04E+10 | 1.49E+17 | 4.54E+09 | 1.47E+16 | 3.11E+10 | 2.00E+17 |
| 76 | 5.83E+14 | 7.09E+20 | 1.56E+14 | 1.85E+20 | 2.01E+10 | 2.53E+18 | 146 | 3.53E+10 | 1.35E+17 | 3.91E+09 | 1.31E+16 | 2.85E+10 | 1.88E+17 |
| 78 | 4.27E+14 | 5.09E+20 | 1.13E+14 | 1.32E+20 | 3.53E+10 | 2.52E+18 | 148 | 3.18E+10 | 1.21E+17 | 3.38E+09 | 1.15E+16 | 2.61E+10 | 1.78E+17 |
| 80 | 3.11E+14 | 3.83E+20 | 8.21E+13 | 9.34E+19 | 6.28E+10 | 2.50E+18 | 150 | 2.73E+10 | 1.10E+17 | 2.94E+09 | 1.04E+16 | 2.41E+10 | 1.68E+17 |
| 82 | 2.25E+14 | 2.57E+20 | 5.90E+13 | 6.55E+19 | 9.64E+10 | 2.47E+18 | 152 | 2.42E+10 | 9.97E+16 | 2.57E+09 | 9.27E+15 | 2.22E+10 | 1.59E+17 |
| 84 | 1.61E+14 | 1.81E+20 | 4.21E+13 | 4.55E+19 | 1.27E+11 | 2.43E+18 | 154 | 2.15E+10 | 9.06E+16 | 2.25E+09 | 8.31E+15 | 2.86E+10 | 1.51E+17 |
| 86 | 1.14E+14 | 1.27E+20 | 2.96E+13 | 3.13E+19 | 1.50E+11 | 2.37E+18 | 156 | 1.92E+10 | 8.26E+16 | 1.98E+09 | 7.47E+15 | 1.91E+10 | 1.43E+17 |
| 88 | 7.99E+13 | 8.82E+19 | 2.05E+13 | 2.15E+19 | 1.62E+11 | 2.31E+18 | 158 | 1.72E+10 | 7.54E+16 | 1.75E+09 | 6.73E+15 | 1.78E+10 | 1.36E+17 |
| 90 | 5.58E+13 | 6.14E+19 | 1.42E+13 | 1.46E+19 | 1.67E+11 | 2.25E+18 | 160 | 1.54E+10 | 6.89E+16 | 1.55E+09 | 6.08E+15 | 1.66E+10 | 1.29E+17 |
| 92 | 3.87E+13 | 4.28E+19 | 9.74E+12 | 9.88E+18 | 1.69E+11 | 2.19E+18 | 162 | 1.39E+10 | 6.31E+16 | 1.38E+09 | 5.50E+15 | 1.55E+10 | 1.23E+17 |
| 94 | 2.67E+13 | 2.99E+19 | 6.65E+12 | 6.65E+18 | 1.79E+11 | 2.12E+18 | 164 | 1.25E+10 | 5.79E+16 | 1.23E+09 | 4.98E+15 | 1.46E+10 | 1.17E+17 |
| 96 | 1.85E+13 | 2.10E+19 | 4.53E+12 | 4.45E+18 | 2.16E+11 | 2.04E+18 | 166 | 1.13E+10 | 5.31E+16 | 1.10E+09 | 4.52E+15 | 1.37E+10 | 1.11E+17 |
| 98 | 1.28E+13 | 1.40E+19 | 3.04E+12 | 2.96E+18 | 3.09E+11 | 1.94E+18 | 168 | 1.03E+10 | 4.89E+16 | 9.86E+08 | 4.10E+15 | 1.28E+10 | 1.06E+17 |
| 100 | 8.71E+12 | 1.06E+19 | 1.99E+12 | 1.98E+18 | 4.15E+11 | 1.88E+18 | 170 | 9.34E+09 | 4.50E+16 | 8.85E+08 | 3.73E+15 | 1.21E+10 | 1.81E+17 |
| 102 | 6.00E+12 | 7.68E+18 | 1.27E+12 | 1.32E+18 | 4.66E+11 | 1.62E+18 | 172 | 5.58E+09 | 4.15E+16 | 7.96E+08 | 3.40E+15 | 1.14E+10 | 9.65E+16 |
| 104 | 4.27E+12 | 5.66E+18 | 8.25E+11 | 9.12E+17 | 4.59E+11 | 1.42E+18 | 174 | 7.75E+09 | 3.82E+16 | 7.17E+08 | 3.10E+15 | 1.08E+10 | 9.22E+16 |
| 106 | 3.04E+12 | 4.21E+18 | 5.43E+11 | 6.44E+17 | 4.22E+11 | 1.25E+18 | 176 | 7.08E+09 | 3.53E+16 | 6.47E+08 | 2.83E+15 | 1.02E+10 | 8.81E+16 |
| 108 | 2.19E+12 | 3.18E+18 | 3.65E+11 | 4.65E+17 | 3.74E+11 | 1.09E+18 | 178 | 6.47E+09 | 3.26E+16 | 5.85E+08 | 2.59E+15 | 9.62E+09 | 8.42E+16 |
| 110 | 1.59E+12 | 2.43E+18 | 2.51E+11 | 3.44E+17 | 3.23E+11 | 9.53E+17 | 180 | 5.92E+09 | 3.02E+16 | 5.38E+08 | 2.37E+15 | 9.11E+09 | 8.06E+16 |
| 112 | 1.16E+12 | 1.89E+18 | 1.76E+11 | 2.60E+17 | 2.75E+11 | 8.36E+17 | 182 | 5.43E+09 | 2.79E+16 | 4.80E+08 | 2.17E+15 | 8.64E+09 | 7.71E+16 |
| 114 | 8.61E+11 | 1.49E+18 | 1.27E+11 | 2.00E+17 | 2.33E+11 | 7.37E+17 | 184 | 4.98E+09 | 2.59E+16 | 4.36E+08 | 1.98E+15 | 8.19E+09 | 7.38E+16 |
| 116 | 6.46E+11 | 1.19E+18 | 9.35E+10 | 1.57E+17 | 1.97E+11 | 6.53E+17 | 186 | 4.58E+09 | 2.40E+16 | 3.96E+08 | 1.82E+15 | 7.78E+09 | 7.07E+16 |
| 118 | 4.92E+11 | 9.69E+17 | 7.84E+10 | 1.24E+17 | 1.67E+11 | 5.79E+17 | 188 | 4.21E+09 | 2.23E+16 | 3.61E+08 | 1.67E+15 | 7.39E+09 | 6.78E+16 |
| 120 | 3.79E+11 | 7.97E+17 | 5.42E+10 | 9.97E+16 | 1.42E+11 | 5.17E+17 | 190 | 3.88E+09 | 2.07E+16 | 3.29E+08 | 1.53E+15 | 7.03E+09 | 8.50E+18 |
| 122 | 2.96E+11 | 6.63E+17 | 4.12E+10 | 8.08E+16 | 1.20E+11 | 4.66E+17 | 192 | 3.57E+09 | 1.92E+16 | 3.00E+08 | 1.41E+15 | 6.69E+09 | 6.23E+16 |
| 124 | 2.35E+11 | 5.58E+17 | 3.18E+10 | 6.64E+16 | 1.03E+11 | 4.23E+17 | 194 | 3.30E+09 | 1.78E+16 | 2.74E+08 | 1.30E+15 | 6.37E+09 | 5.97E+16 |
| 126 | 1.88E+11 | 4.74E+17 | 2.50E+10 | 5.51E+16 | 8.82E+10 | 3.85E+17 | 196 | 3.04E+09 | 1.66E+16 | 2.58E+08 | 1.19E+15 | 6.07E+09 | 5.73E+16 |
| 128 | 1.53E+11 | 4.07E+17 | 1.98E+10 | 4.62E+16 | 7.65E+10 | 3.53E+17 | 198 | 2.81E+09 | 1.54E+16 | 2.29E+08 | 1.10E+15 | 5.78E+09 | 5.58E+16 |
| 130 | 1.25E+11 | 3.52E+17 | 1.59E+10 | 3.92E+16 | 6.69E+10 | 3.25E+17 | 200 | 2.60E+09 | 1.44E+16 | 2.09E+08 | 1.01E+15 | 5.52E+09 | 5.28E+16 |

Table 13-5.

LATITUDE = 3.00000E+01 DEGREES.
SOLAR DECLINATION = 0. DEGREES.
SOLAR ZENITH ANGLE = 6.00000E+01 DEGREES.

| ALT KM | K(O2+) /SEC | K(N2+) /SEC | K(O+) /SEC | K(NO+) /SEC |
|---|---|---|---|---|
| 60 | 1.619E-16 | 1.133E-21 | 7.467E-21 | 5.981E-16 |
| 62 | 2.117E-16 | 1.482E-21 | 9.739E-21 | 8.376E-14 |
| 64 | 2.618E-16 | 1.627E-21 | 1.231E-20 | 3.957E-12 |
| 66 | 3.070E-16 | 2.162E-21 | 1.413E-20 | 7.658E-11 |
| 68 | 3.479E-16 | 2.861E-21 | 1.635E-20 | 7.662E-10 |
| 70 | 3.827E-16 | 8.643E-21 | 2.249E-20 | 4.549E-09 |
| 72 | 4.112E-16 | 4.653E-20 | 5.482E-20 | 1.707E-08 |
| 74 | 4.341E-16 | 1.956E-19 | 1.775E-19 | 4.579E-08 |
| 76 | 4.522E-16 | 5.895E-19 | 5.838E-19 | 9.499E-08 |
| 78 | 4.672E-16 | 1.615E-18 | 1.349E-18 | 1.617E-07 |
| 80 | 4.850E-16 | 6.366E-18 | 5.337E-18 | 2.381E-07 |
| 82 | 5.306E-16 | 2.926E-17 | 2.459E-17 | 3.147E-07 |
| 84 | 6.795E-16 | 1.148E-16 | 9.720E-17 | 3.644E-07 |
| 86 | 1.210E-15 | 4.246E-16 | 3.623E-16 | 4.430E-07 |
| 88 | 3.177E-15 | 1.563E-15 | 1.353E-15 | 4.898E-07 |
| 90 | 1.175E-14 | 6.748E-15 | 5.747E-15 | 5.237E-07 |
| 92 | 5.507E-14 | 3.278E-14 | 2.815E-14 | 5.490E-07 |
| 94 | 3.459E-13 | 1.564E-13 | 1.337E-13 | 5.678E-07 |
| 96 | 4.382E-12 | 8.386E-13 | 7.883E-13 | 5.796E-07 |
| 98 | 3.991E-11 | 4.756E-12 | 3.977E-12 | 5.884E-07 |
| 100 | 1.843E-10 | 2.129E-11 | 1.781E-11 | 5.942E-07 |
| 102 | 5.338E-10 | 6.507E-11 | 5.458E-11 | 5.960E-07 |
| 104 | 1.071E-09 | 1.484E-10 | 1.250E-10 | 6.005E-07 |
| 106 | 1.757E-09 | 2.718E-10 | 2.298E-10 | 6.021E-07 |
| 108 | 2.590E-09 | 4.270E-10 | 3.623E-10 | 6.032E-07 |
| 110 | 3.618E-09 | 6.028E-10 | 5.120E-10 | 6.039E-07 |
| 112 | 4.835E-09 | 7.862E-10 | 6.741E-10 | 6.044E-07 |
| 114 | 6.247E-09 | 9.736E-10 | 8.482E-10 | 6.048E-07 |
| 116 | 7.814E-09 | 1.164E-09 | 1.049E-09 | 6.051E-07 |
| 118 | 9.513E-09 | 1.366E-09 | 1.305E-09 | 6.052E-07 |
| 120 | 1.135E-08 | 1.599E-09 | 1.649E-09 | 6.054E-07 |
| 122 | 1.332E-08 | 1.898E-09 | 2.113E-09 | 6.055E-07 |
| 124 | 1.547E-08 | 2.277E-09 | 2.729E-09 | 6.056E-07 |
| 126 | 1.782E-08 | 2.802E-09 | 3.524E-09 | 6.057E-07 |
| 128 | 2.042E-08 | 3.503E-09 | 4.523E-09 | 6.057E-07 |
| 130 | 2.331E-08 | 4.418E-09 | 5.747E-09 | 6.058E-07 |
| 132 | 2.654E-08 | 5.582E-09 | 7.217E-09 | 6.058E-07 |
| 134 | 3.014E-08 | 7.028E-09 | 8.952E-09 | 6.058E-07 |
| 136 | 3.416E-08 | 8.791E-09 | 1.097E-08 | 6.058E-07 |
| 138 | 3.864E-08 | 1.090E-08 | 1.328E-08 | 6.059E-07 |
| 140 | 4.361E-08 | 1.339E-08 | 1.589E-08 | 6.059E-07 |
| 142 | 4.909E-08 | 1.629E-08 | 1.882E-08 | 6.059E-07 |
| 144 | 5.511E-08 | 1.963E-08 | 2.206E-08 | 6.059E-07 |
| 146 | 6.166E-08 | 2.341E-08 | 2.560E-08 | 6.059E-07 |
| 148 | 6.876E-08 | 2.766E-08 | 2.944E-08 | 6.059E-07 |
| 150 | 7.640E-08 | 3.238E-08 | 3.356E-08 | 6.059E-07 |
| 152 | 8.455E-08 | 3.756E-08 | 3.796E-08 | 6.059E-07 |
| 154 | 9.320E-08 | 4.320E-08 | 4.259E-08 | 6.059E-07 |
| 156 | 1.023E-07 | 4.927E-08 | 4.745E-08 | 6.060E-07 |
| 158 | 1.118E-07 | 5.574E-08 | 5.251E-08 | 6.060E-07 |
| 160 | 1.217E-07 | 6.260E-08 | 5.774E-08 | 6.060E-07 |
| 162 | 1.319E-07 | 6.980E-08 | 6.311E-08 | 6.060E-07 |
| 164 | 1.424E-07 | 7.730E-08 | 6.860E-08 | 6.060E-07 |
| 166 | 1.531E-07 | 8.507E-08 | 7.417E-08 | 6.060E-07 |
| 168 | 1.640E-07 | 9.307E-08 | 7.982E-08 | 6.060E-07 |
| 170 | 1.750E-07 | 1.013E-07 | 8.550E-08 | 6.060E-07 |
| 172 | 1.861E-07 | 1.096E-07 | 9.120E-08 | 6.060E-07 |
| 174 | 1.972E-07 | 1.180E-07 | 9.689E-08 | 6.060E-07 |
| 176 | 2.083E-07 | 1.265E-07 | 1.026E-07 | 6.060E-07 |
| 178 | 2.194E-07 | 1.351E-07 | 1.082E-07 | 6.060E-07 |
| 180 | 2.304E-07 | 1.436E-07 | 1.139E-07 | 6.060E-07 |
| 182 | 2.413E-07 | 1.521E-07 | 1.193E-07 | 6.060E-07 |
| 184 | 2.520E-07 | 1.605E-07 | 1.247E-07 | 6.060E-07 |
| 186 | 2.626E-07 | 1.689E-07 | 1.300E-07 | 6.060E-07 |
| 188 | 2.730E-07 | 1.772E-07 | 1.352E-07 | 6.060E-07 |
| 190 | 2.831E-07 | 1.853E-07 | 1.403E-07 | 6.060E-07 |
| 192 | 2.931E-07 | 1.933E-07 | 1.453E-07 | 6.060E-07 |
| 194 | 3.029E-07 | 2.012E-07 | 1.502E-07 | 6.060E-07 |
| 196 | 3.124E-07 | 2.089E-07 | 1.549E-07 | 6.060E-07 |
| 198 | 3.216E-07 | 2.164E-07 | 1.595E-07 | 6.060E-07 |
| 200 | 3.307E-07 | 2.237E-07 | 1.640E-07 | 6.060E-07 |

Table 13-6.

LATITUDE = 3.00000E+01 DEGREES.
SOLAR DECLINATION = 0. DEGREES.
SOLAR ZENITH ANGLE = 7.50000E+01 DEGREES.

| ALT KM | N2 N/CC | N2 COLUMN N/SQ CM | O2 N/CC | O2 COLUMN N/SQ CM | O N/CC | O COLUMN N/SQ CM | ALT KM | N2 N/CC | N2 COLUMN N/SQ CM | O2 N/CC | O2 COLUMN N/SQ CM | O N/CC | O COLUMN N/SQ CM |
|---|---|---|---|---|---|---|---|---|---|---|---|---|---|
| 60 | 5.21E+15 | 1.48E+22 | 1.40E+15 | 3.98E+21 | 1.64E+10 | 4.68E+16 | 130 | 1.25E+11 | 6.61E+17 | 1.59E+09 | 7.39E+16 | 6.69E+10 | 6.86E+17 |
| 62 | 4.88E+15 | 1.13E+22 | 1.39E+15 | 3.02E+21 | 1.64E+10 | 4.68E+16 | 132 | 1.84E+11 | 5.75E+17 | 1.38E+09 | 6.30E+16 | 5.89E+10 | 5.56E+17 |
| 64 | 3.17E+15 | 8.54E+21 | 8.50E+14 | 2.28E+21 | 1.64E+10 | 4.61E+16 | 134 | 8.72E+10 | 5.04E+17 | 1.07E+09 | 5.42E+16 | 5.22E+10 | 5.13E+17 |
| 66 | 2.45E+15 | 6.41E+21 | 6.57E+14 | 1.71E+21 | 1.64E+10 | 4.61E+16 | 136 | 7.37E+10 | 4.43E+17 | 8.85E+08 | 4.68E+16 | 4.66E+10 | 4.77E+17 |
| 68 | 1.88E+15 | 4.77E+21 | 5.04E+14 | 1.27E+21 | 1.64E+10 | 4.61E+16 | 138 | 6.27E+10 | 3.93E+17 | 7.41E+08 | 4.08E+16 | 4.18E+10 | 4.45E+17 |
| 70 | 1.42E+15 | 3.52E+21 | 3.82E+14 | 9.36E+20 | 1.64E+10 | 4.62E+16 | 140 | 5.38E+10 | 3.49E+17 | 6.25E+08 | 3.56E+16 | 3.77E+10 | 4.16E+17 |
| 72 | 1.07E+15 | 2.58E+21 | 2.86E+14 | 6.83E+20 | 1.64E+10 | 4.62E+16 | 142 | 4.65E+10 | 3.12E+17 | 5.31E+08 | 3.13E+16 | 3.42E+10 | 3.90E+17 |
| 74 | 7.91E+14 | 1.88E+21 | 2.12E+14 | 4.94E+20 | 1.64E+10 | 4.63E+16 | 144 | 4.04E+10 | 2.79E+17 | 4.54E+08 | 2.76E+16 | 3.11E+10 | 3.66E+17 |
| 76 | 5.83E+14 | 1.36E+21 | 1.56E+14 | 3.55E+20 | 2.81E+10 | 4.63E+16 | 146 | 3.53E+10 | 2.51E+17 | 3.91E+08 | 2.45E+16 | 2.85E+10 | 3.45E+17 |
| 78 | 4.27E+14 | 9.75E+20 | 1.13E+14 | 2.53E+20 | 3.53E+10 | 4.63E+16 | 148 | 3.10E+10 | 2.27E+17 | 3.38E+08 | 2.19E+16 | 2.61E+10 | 3.25E+17 |
| 80 | 3.11E+14 | 6.95E+20 | 8.21E+13 | 1.79E+20 | 6.28E+10 | 4.61E+16 | 150 | 2.73E+10 | 2.05E+17 | 2.94E+08 | 1.94E+16 | 2.41E+10 | 3.07E+17 |
| 82 | 2.25E+14 | 4.93E+20 | 5.90E+13 | 1.25E+20 | 9.84E+10 | 4.56E+16 | 152 | 2.42E+10 | 1.86E+17 | 2.57E+08 | 1.74E+16 | 2.22E+10 | 2.98E+17 |
| 84 | 1.61E+14 | 3.47E+20 | 4.21E+13 | 8.72E+19 | 1.27E+11 | 4.49E+16 | 154 | 2.15E+10 | 1.69E+17 | 2.25E+08 | 1.56E+16 | 2.06E+10 | 2.75E+17 |
| 86 | 1.14E+14 | 2.42E+20 | 2.96E+13 | 6.08E+19 | 1.58E+11 | 4.40E+16 | 156 | 1.92E+10 | 1.54E+17 | 1.98E+08 | 1.40E+16 | 1.91E+10 | 2.60E+17 |
| 88 | 7.99E+13 | 1.69E+20 | 2.05E+13 | 4.11E+19 | 1.62E+11 | 4.38E+16 | 158 | 1.72E+10 | 1.40E+17 | 1.75E+08 | 1.26E+16 | 1.70E+10 | 2.47E+17 |
| 90 | 5.58E+13 | 1.18E+20 | 1.42E+13 | 2.88E+19 | 1.67E+11 | 4.19E+16 | 160 | 1.54E+10 | 1.28E+17 | 1.55E+08 | 1.14E+16 | 1.66E+10 | 2.35E+17 |
| 92 | 3.87E+13 | 8.18E+19 | 9.74E+12 | 1.89E+19 | 1.69E+11 | 4.08E+16 | 162 | 1.39E+10 | 1.17E+17 | 1.38E+08 | 1.03E+16 | 1.55E+10 | 2.23E+17 |
| 94 | 2.67E+13 | 5.72E+19 | 6.65E+12 | 1.27E+19 | 1.79E+11 | 3.96E+16 | 164 | 1.25E+10 | 1.08E+17 | 1.23E+08 | 9.38E+15 | 1.46E+10 | 2.12E+17 |
| 96 | 1.85E+13 | 4.01E+19 | 4.53E+12 | 8.52E+18 | 2.16E+11 | 3.82E+16 | 166 | 1.13E+10 | 9.89E+16 | 1.10E+08 | 8.44E+15 | 1.37E+10 | 2.02E+17 |
| 98 | 1.28E+13 | 2.83E+19 | 3.04E+12 | 5.66E+18 | 3.89E+11 | 3.64E+16 | 168 | 1.03E+10 | 9.89E+16 | 9.86E+08 | 7.66E+15 | 1.23E+10 | 1.93E+17 |
| 100 | 8.71E+12 | 2.02E+19 | 1.90E+12 | 3.76E+18 | 4.15E+11 | 3.37E+16 | 170 | 9.34E+09 | 8.36E+16 | 8.85E+07 | 6.97E+15 | 1.21E+10 | 1.84E+17 |
| 102 | 6.00E+12 | 1.47E+19 | 1.27E+12 | 2.53E+18 | 4.66E+11 | 3.04E+16 | 172 | 8.50E+09 | 7.71E+16 | 7.98E+08 | 6.35E+15 | 1.14E+10 | 1.75E+17 |
| 104 | 4.27E+12 | 1.08E+19 | 8.25E+11 | 1.74E+18 | 4.59E+11 | 2.68E+16 | 174 | 7.73E+09 | 7.11E+16 | 7.17E+08 | 5.79E+15 | 1.08E+10 | 1.67E+17 |
| 106 | 3.04E+12 | 8.02E+18 | 5.43E+11 | 1.23E+18 | 4.22E+11 | 2.35E+16 | 176 | 7.08E+09 | 6.55E+16 | 6.47E+08 | 5.26E+15 | 1.02E+10 | 1.60E+17 |
| 108 | 2.19E+12 | 6.85E+18 | 3.65E+11 | 9.67E+17 | 3.74E+11 | 2.85E+16 | 178 | 6.47E+09 | 6.06E+16 | 5.85E+08 | 4.78E+15 | 9.62E+09 | 1.53E+17 |
| 110 | 1.59E+12 | 4.63E+18 | 2.51E+11 | 6.55E+17 | 3.23E+11 | 1.79E+16 | 180 | 5.92E+09 | 5.61E+16 | 5.30E+08 | 4.41E+15 | 9.11E+09 | 1.46E+17 |
| 112 | 1.16E+12 | 3.59E+18 | 1.76E+11 | 4.95E+17 | 2.75E+11 | 1.57E+16 | 182 | 5.43E+09 | 5.19E+16 | 4.88E+08 | 4.04E+15 | 6.64E+09 | 1.40E+17 |
| 114 | 8.61E+11 | 2.83E+18 | 1.27E+11 | 3.81E+17 | 2.33E+11 | 1.38E+16 | 184 | 4.98E+09 | 4.81E+16 | 4.36E+08 | 3.78E+15 | 8.19E+09 | 1.34E+17 |
| 116 | 6.46E+11 | 2.26E+18 | 9.35E+10 | 2.98E+17 | 1.97E+11 | 1.22E+16 | 186 | 4.58E+09 | 4.45E+16 | 3.96E+08 | 3.39E+15 | 7.58E+09 | 1.28E+17 |
| 118 | 4.92E+11 | 1.83E+18 | 7.04E+10 | 2.36E+17 | 1.67E+11 | 1.08E+16 | 188 | 4.21E+09 | 4.13E+16 | 3.61E+08 | 3.11E+15 | 7.03E+09 | 1.23E+17 |
| 120 | 3.79E+11 | 1.58E+18 | 5.42E+10 | 1.89E+17 | 1.42E+11 | 9.62E+15 | 190 | 3.88E+09 | 3.83E+16 | 3.29E+08 | 2.86E+15 | 7.08E+09 | 1.18E+17 |
| 122 | 2.96E+11 | 1.25E+18 | 4.12E+10 | 1.57E+17 | 1.20E+11 | 8.66E+17 | 192 | 3.57E+09 | 3.56E+16 | 3.00E+08 | 2.63E+15 | 6.69E+09 | 1.13E+17 |
| 124 | 2.35E+11 | 1.05E+18 | 3.10E+10 | 1.28E+17 | 1.03E+11 | 7.83E+17 | 194 | 3.30E+09 | 3.31E+16 | 2.74E+08 | 2.41E+15 | 6.37E+09 | 1.08E+17 |
| 126 | 1.88E+11 | 8.93E+17 | 2.50E+10 | 1.04E+17 | 8.82E+10 | 7.12E+17 | 196 | 3.04E+09 | 3.07E+16 | 2.50E+08 | 2.22E+15 | 6.07E+09 | 1.04E+17 |
| 128 | 1.53E+11 | 7.65E+17 | 1.98E+10 | 8.73E+16 | 7.65E+10 | 6.53E+17 | 198 | 2.81E+09 | 2.86E+16 | 2.29E+08 | 2.04E+15 | 5.78E+09 | 9.96E+16 |
| 130 | 1.25E+11 | 6.61E+17 | 1.59E+10 | 7.39E+16 | 6.69E+10 | 6.88E+17 | 200 | 2.68E+09 | 2.66E+16 | 2.09E+08 | 1.88E+15 | 5.52E+09 | 9.56E+16 |

Table 13-7.

LATITUDE = 3.00000E+01 DEGREES.
SOLAR DECLINATION = 0. DEGREES.
SOLAR ZENITH ANGLE = 7.50000E+01 DEGREES.

| ALT KM | K(O2+) /SEC | K(N2+) /SEC | K(O+) /SEC | K(NO+) /SEC |
|---|---|---|---|---|
| 60 | 9.799E-17 | 4.059E-22 | 2.66?E-21 | 3.769E-24 |
| 62 | 9.677E-17 | 6.774E-22 | 4.45?E-21 | 4.712E-20 |
| 64 | 1.443E-16 | 1.010E-21 | 6.63?E-21 | 7.419E-17 |
| 66 | 1.967E-16 | 1.377E-21 | 9.05?E-21 | 2.237E-14 |
| 68 | 2.498E-16 | 1.749E-21 | 1.149E-20 | 1.123E-12 |
| 70 | 2.998E-16 | 2.185E-21 | 1.379E-20 | 9.223E-11 |
| 72 | 3.439E-16 | 2.715E-21 | 1.601E-20 | 6.552E-10 |
| 74 | 3.809E-16 | 7.933E-21 | 2.183E-20 | 4.322E-09 |
| 76 | 4.110E-16 | 4.576E-20 | 5.399E-20 | 1.742E-08 |
| 78 | 4.347E-16 | 2.838E-19 | 1.836E-19 | 4.833E-08 |
| 80 | 4.533E-16 | 6.303E-19 | 5.343E-19 | 1.013E-07 |
| 82 | 4.688E-16 | 1.828E-18 | 1.52?E-18 | 1.728E-07 |
| 84 | 4.898E-16 | 7.979E-18 | 6.696E-18 | 2.534E-07 |
| 86 | 5.462E-16 | 3.799E-17 | 3.205E-17 | 3.325E-07 |
| 88 | 7.393E-16 | 1.497E-16 | 1.273E-16 | 4.018E-07 |
| 90 | 1.437E-15 | 5.576E-16 | 4.761E-16 | 4.561E-07 |
| 92 | 4.051E-15 | 2.193E-15 | 1.793E-15 | 5.015E-07 |
| 94 | 1.568E-14 | 9.126E-15 | 7.774E-15 | 5.335E-07 |
| 96 | 7.524E-14 | 4.249E-14 | 3.633E-14 | 5.565E-07 |
| 98 | 7.601E-13 | 1.924E-13 | 1.642E-13 | 5.727E-07 |
| 100 | 1.055E-11 | 9.604E-13 | 8.087E-13 | 5.837E-07 |
| 102 | 7.040E-11 | 4.705E-12 | 3.934E-12 | 5.909E-07 |
| 104 | 2.481E-10 | 1.827E-11 | 1.527E-11 | 5.955E-07 |
| 106 | 5.885E-10 | 5.222E-11 | 4.375E-11 | 5.986E-07 |
| 108 | 1.044E-09 | 1.151E-10 | 9.673E-11 | 6.007E-07 |
| 110 | 1.610E-09 | 2.083E-10 | 1.753E-10 | 6.020E-07 |
| 112 | 2.272E-09 | 3.267E-10 | 2.766E-10 | 6.030E-07 |
| 114 | 3.056E-09 | 4.624E-10 | 3.926E-10 | 6.037E-07 |
| 116 | 3.985E-09 | 6.078E-10 | 5.177E-10 | 6.042E-07 |
| 118 | 5.058E-09 | 7.580E-10 | 6.489E-10 | 6.046E-07 |
| 120 | 6.256E-09 | 9.091E-10 | 7.856E-10 | 6.049E-07 |
| 122 | 7.541E-09 | 1.059E-09 | 9.323E-10 | 6.051E-07 |
| 124 | 8.888E-09 | 1.210E-09 | 1.099E-09 | 6.052E-07 |
| 126 | 1.026E-08 | 1.367E-09 | 1.293E-09 | 6.054E-07 |
| 128 | 1.169E-08 | 1.540E-09 | 1.544E-09 | 6.055E-07 |
| 130 | 1.316E-08 | 1.741E-09 | 1.851E-09 | 6.056E-07 |

| ALT KM | K(O2+) /SEC | K(N2+) /SEC | K(O+) /SEC | K(NO+) /SEC |
|---|---|---|---|---|
| 130 | 1.316E-08 | 1.741E-09 | 1.851E-09 | 6.056E-07 |
| 132 | 1.471E-08 | 1.985E-09 | 2.235E-09 | 6.056E-07 |
| 134 | 1.634E-08 | 2.290E-09 | 2.707E-09 | 6.057E-07 |
| 136 | 1.809E-08 | 2.672E-09 | 3.281E-09 | 6.057E-07 |
| 138 | 1.998E-08 | 3.149E-09 | 3.968E-09 | 6.058E-07 |
| 140 | 2.202E-08 | 3.739E-09 | 4.780E-09 | 6.058E-07 |
| 142 | 2.424E-08 | 4.458E-09 | 5.728E-09 | 6.058E-07 |
| 144 | 2.667E-08 | 5.324E-09 | 6.824E-09 | 6.059E-07 |
| 146 | 2.932E-08 | 6.356E-09 | 8.079E-09 | 6.059E-07 |
| 148 | 3.223E-08 | 7.572E-09 | 9.504E-09 | 6.059E-07 |
| 150 | 3.541E-08 | 8.994E-09 | 1.111E-08 | 6.059E-07 |
| 152 | 3.890E-08 | 1.064E-08 | 1.291E-08 | 6.059E-07 |
| 154 | 4.270E-08 | 1.254E-08 | 1.490E-08 | 6.059E-07 |
| 156 | 4.686E-08 | 1.470E-08 | 1.710E-08 | 6.059E-07 |
| 158 | 5.137E-08 | 1.716E-08 | 1.952E-08 | 6.059E-07 |
| 160 | 5.627E-08 | 1.992E-08 | 2.215E-08 | 6.059E-07 |
| 162 | 6.155E-08 | 2.300E-08 | 2.500E-08 | 6.059E-07 |
| 164 | 6.724E-08 | 2.643E-08 | 2.806E-08 | 6.059E-07 |
| 166 | 7.332E-08 | 3.019E-08 | 3.134E-08 | 6.059E-07 |
| 168 | 7.981E-08 | 3.430E-08 | 3.483E-08 | 6.060E-07 |
| 170 | 8.668E-08 | 3.877E-08 | 3.851E-08 | 6.060E-07 |
| 172 | 9.393E-08 | 4.357E-08 | 4.238E-08 | 6.060E-07 |
| 174 | 1.015E-07 | 4.871E-08 | 4.643E-08 | 6.060E-07 |
| 176 | 1.095E-07 | 5.418E-08 | 5.065E-08 | 6.060E-07 |
| 178 | 1.177E-07 | 5.995E-08 | 5.501E-08 | 6.060E-07 |
| 180 | 1.263E-07 | 6.601E-08 | 5.950E-08 | 6.060E-07 |
| 182 | 1.351E-07 | 7.234E-08 | 6.411E-08 | 6.060E-07 |
| 184 | 1.441E-07 | 7.891E-08 | 6.884E-08 | 6.060E-07 |
| 186 | 1.534E-07 | 8.570E-08 | 7.362E-08 | 6.060E-07 |
| 188 | 1.628E-07 | 9.268E-08 | 7.844E-08 | 6.060E-07 |
| 190 | 1.723E-07 | 9.982E-08 | 8.329E-08 | 6.060E-07 |
| 192 | 1.819E-07 | 1.071E-07 | 8.814E-08 | 6.060E-07 |
| 194 | 1.916E-07 | 1.145E-07 | 9.330E-08 | 6.060E-07 |
| 196 | 2.013E-07 | 1.220E-07 | 9.827E-08 | 6.060E-07 |
| 198 | 2.111E-07 | 1.295E-07 | 1.032E-07 | 6.060E-07 |
| 200 | 2.208E-07 | 1.371E-07 | 1.082E-07 | 6.060E-07 |

# 14. KINETICS OF LOW-ENERGY ELECTRON COLLISION PROCESSES*

L.J. Kieffer and G.E. Chamberlain
Joint Institute for Laboratory Astrophysics
University of Colorado
(Latest Revision 5 August 1971)

## 14.1 INTRODUCTION

The calculation of rates for low-energy electron collisional processes, e.g., ionization, detachment, dissociation, dissociative attachment, and vibrational and rotational excitation, when the electron energy distribution is non-Boltzmann requires the direct use of cross-section data. Experimental information for several atomic and molecular species of atmospheric interest are given in Figures 14-1 through 14-90, and in Tables 14-1 through 14-3 interspersed therewith. The data given in each graph are considered to be of comparable reliability (see References 14-1 and 14-2 for a discussion of the criteria used in selection of the data). The observed differences among independent measurements are probably a reasonable measure of the range of systematic errors and hence the accuracy of the data.

In the particular case of production of $N_2^+$ 3914 A radiation from $N_2$ the experimental results are seen to divide into two curves nearly a factor of three different in magnitude. Although all measurements since 1968 are close to the excitation curve of larger magnitude, there is, as yet, no objective reason for eliminating the smaller magnitude results.

For species that are stable at room temperature, i.e., $\approx$ 300 K, it is assumed, since the data were taken at room temperature under equilibrium conditions, that the initial state of the atom or molecule can probably be characterized by a Boltzmann distribution for T = 300 K. Unstable species that were generated in high-temperature ovens or discharges are assumed to be in the ground electronic state initially. Data for these species were selected on the basis of evidence indicating that this was indeed the case.

---

*This research was supported by the Advanced Research Projects Agency of the Department of Defense and was monitored by Army Research Office—Durham under Contract No. DA-31-124 ARO-D-139.

Data in the literature on dissociative ionization plus excitation are quite new. The uniqueness of the data precludes an assessment of reliability by comparison. These data are selected in part on the basis of evidence that the author has accounted for systematic effects due to the kinetic energy of the dissociating fragments.

Information on the state of the ion immediately after electron collision with the neutral parent atom or molecule is extremely scarce and is usually indirect. For example, the cross-sections given in Figures 14-35 and 14-47 are for production of the radiation of the wavelength indicated, and branching ratios must be known in order to determine the population of the state radiating that wavelength.

One could say then that the most reliable data are those for electron production, i.e., total cross-sections, and that data on the final states of the ions after electron impact are sketchy and mostly unreliable.

In regions where the electron energy distribution is Boltzmann, a rate constant can be obtained by using equations for $k_T$ for electron collisions given in Chapter 6. For the purpose of estimating rates for ionization by electron impact, the ionization threshold region is most important. Unfortunately, in this region the cross-section data are least reliable and theoretical calculations appear to be undependable. Therefore, the threshold behaviors of ionization cross-sections remain in doubt. Ionization thresholds necessary for calculation of rates for a Boltzmann distribution are tabulated in Chapter 10.

An extensive tabulation of ionization rates for atomic species and their ions for high electron temperatures (> 1.0 eV) has been prepared by W. Lotz (Reference 14-3). The rates given, however, are likely to be quite unreliable.

## 14.2 FIGURE LABELS

A set of labels has been devised to permit presentation of the data in a compact form and to indicate the process which has been measured. These labels appear in the upper right corners of the figures and on the ordinates of the graphs. The impacting electron energy is given on the abscissas in electron volts.

Since the laboratory conditions almost never allow a precise statement of the initial and final states of the systems the labels were chosen

to reflect this uncertainty. For atoms and atomic ions the presumption is that the system initially is in its ground electronic state. For sources of ions and atoms such as discharges, high-temperature ovens and charge-exchange cells, positive evidence that the target was in its ground electronic state was used as a criterion for selecting the data. For molecules, the initial condition is presumed to be that of a gas in equilibrium at room temperature, except where otherwise noted.

The Greek lower case sigma ($\sigma$) is used to indicate the cross-section for the process per atom or molecule of the original species. X and Y represent a particular atomic or molecular species. If the cross-section is normalized the units are indicated on the ordinate label. Specific comments about the labels follow.

$\boxed{\sigma_T(X)}$

This label indicates a total ionization cross-section measurement for species X. A total ionization cross-section is equivalent to the cross-section for electron production and is defined as:

$$\sigma_T = \sigma_1 + 2\sigma_2 + 3\sigma_3 + \ldots , \qquad (14\text{-}1)$$

where the subscripts refer to the positive charge state of the ion produced.

$\boxed{X^+/X}$

This label indicates that the cross-section measured is for the production of $X^+$ from X. This implies that the numbers of $X^+$'s and X's were measured. The charge state of the species can be positive, negative, or neutral.

$\boxed{Y^+/X\ 3914\ A\ (\nu',\ \nu''\ \text{band};\ B^2\Sigma \rightarrow X^2\Sigma)}$

The cross-section in this case is for the production from a target species X of photons of wavelength 391.4 nm which is a characteristic wavelength of the positive ion $Y^+$ in the exit channel. For molecules, wavelengths of prominent bandheads are used. The radiation is classified in brackets by the vibrational (molecules) and electronic

states involved in the transition. Vibrational states are represented by ($\nu'$, $\nu''$) , where $\nu'$ and $\nu''$ are the vibrational quantum numbers, respectively, of the upper and lower electronic states. In some cases the classification of radiation is incomplete.

X (K shell ejection)

This label indicates that the cross-section for the ejection of a single electron from the K-shell of the atom X has been measured.

+ Ions KE > 0.25 eV/X

This label indicates the production of positive ions from species X with the positive ions produced with a kinetic energy of more than 0.25 eV. In this case most of the ions are produced by a dissociative ionization process.

Neg. Ions/X

This label indicates that the total negative-ion current was measured and that the cross-section reported is for the production of a singly-charged negative ion per molecule of the target species. This includes processes such as dissociative attachment where the products are a negative ion and a neutral fragment, as well as ion-pair formation where the products are a negative ion and a positive ion.

X

In cases where only the species is given in the label, additional information is given on the ordinate and in the body of the graph. v indicates the vibrational state of the molecule indicated and unless specified, the molecule is in the ground electronic state.

The processes are arranged in the following order. All processes for a given parent species are arranged together in order:

negatively charged atoms
neutral atoms
neutral molecules
positively charged atoms
positively charged molecules

Each of these is arranged in order of increasing molecular weight. For any parent species the processes are arranged in the order:

total ionization
single ionization
single ionization with electronic excitation
multiple ionization
K-shell ejection
dissociative ionization
dissociative ionization with electronic excitation
negative-ion formation
detachment
dissociation
vibrational excitation
rotational excitation

## 14.3 DATA SOURCES

The figures and tables contain abbreviated information about the data sources. Each experiment is identified by the name of the first author, followed by a number in parentheses referring to the bibliographic section in which the full citation may be found. When necessary, the captions and footnotes also contain specific information about the experiments or about how the data were handled.

## 14.4 BIBLIOGRAPHY

Following the figures is a Bibliography, listing all the publications from which data were taken. This list is ordered by the JILA Information Center citation numbers which appear in the figure captions as mentioned above, and which should be used in any pertinent correspondence with JILA or with the authors of this chapter.

The authors of papers thus cited in the Bibliography are included in Appendix G of the Handbook, where their contributions are listed specifically according to the same JILA numbers.

## 14.5 PREPARATION OF FIGURES

Once the digital data are obtained, they are permanently stored on magnetic tapes. The figures are photocomposed from these tapes on a DD250 Cathode Ray Tube at the National Oceanic and Atmospheric Administration Boulder Laboratories computing facility. Because the CRT is a very high speed device, the possibility exists for plotting error. Errors due to digitizing and plotting amount to less than 0.5 percent near the peak values and are somewhat larger where the cross-section is small (<10 percent of the peak). However, handling this volume of data entirely by computer, from input to final display, minimizes the possibility of transcribing errors, thus bypassing one of the most difficult problems in preserving the integrity of the data.

The computer programs used in preparing these graphs were written by Patricia Ruttenberg; the graphs were prepared by Lois Spangenberg.

## REFERENCES

14-1. Kieffer, L. J., and G. H. Dunn, Revs. Mod. Phys. 38, 1 (1966).

14-2. Moiseiwitsch, B. L., and S. J. Smith, Revs. Mod. Phys. 40, 238 (1968).

14-3. Lotz, W., Astrophys. J., Suppl. Ser. 14, 207 (1967).

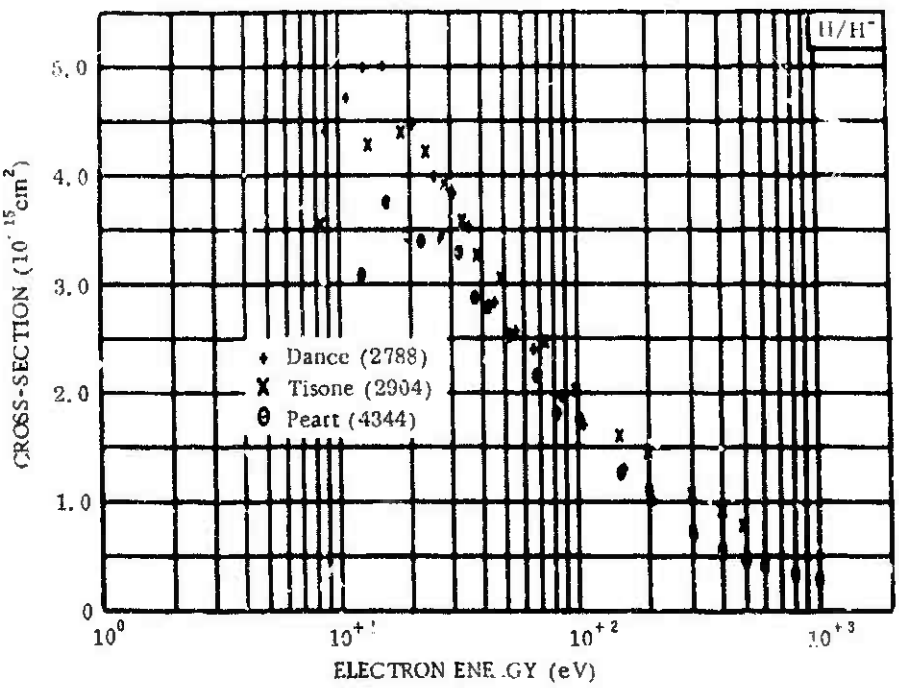


Figure 14-1.

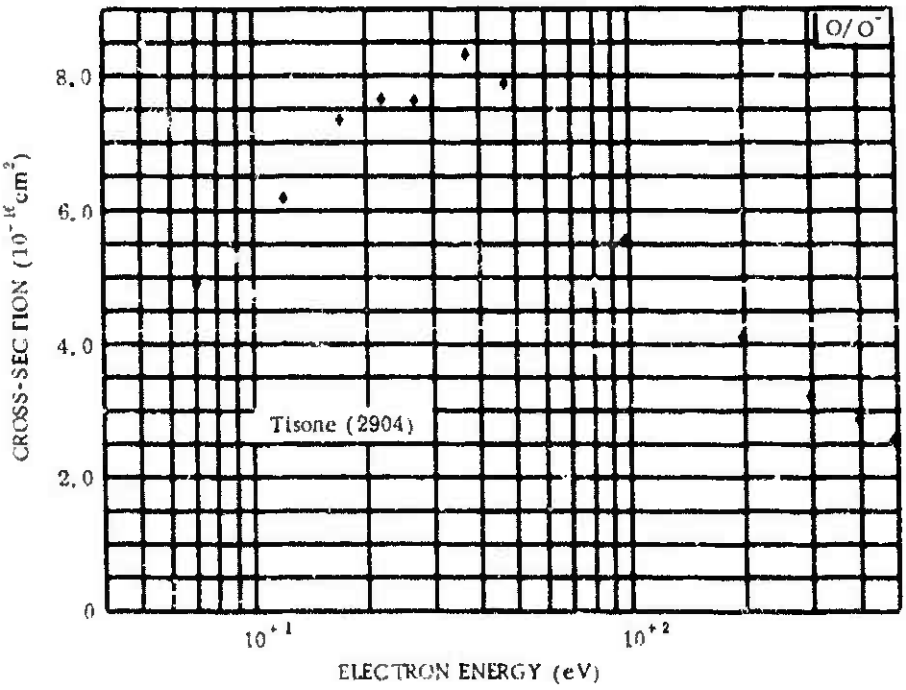


Figure 14-2.

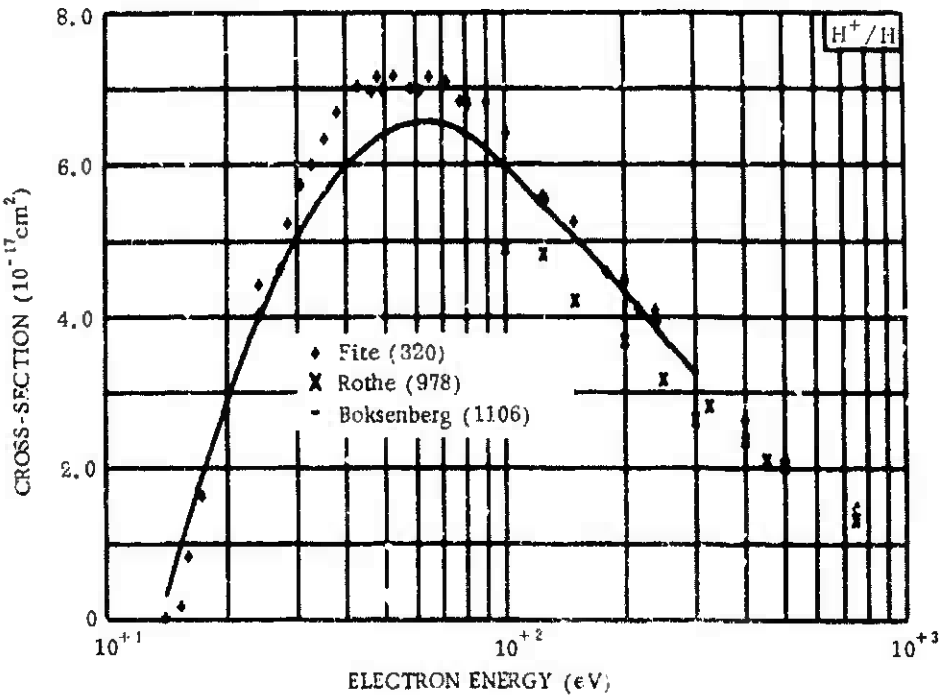


Figure 14-3.

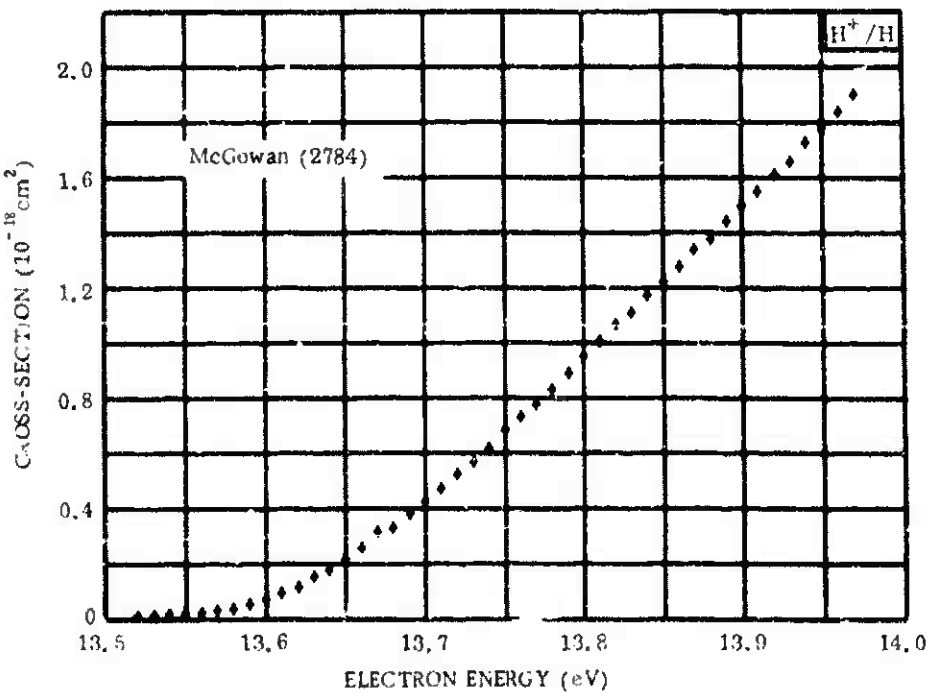


Figure 14-4.

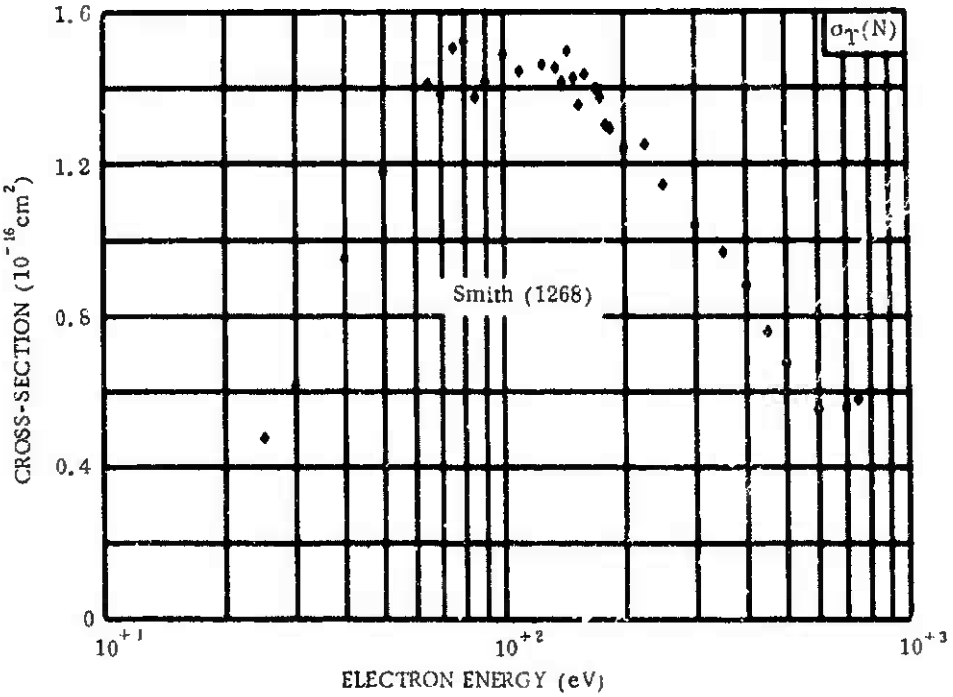


Figure 14-5.

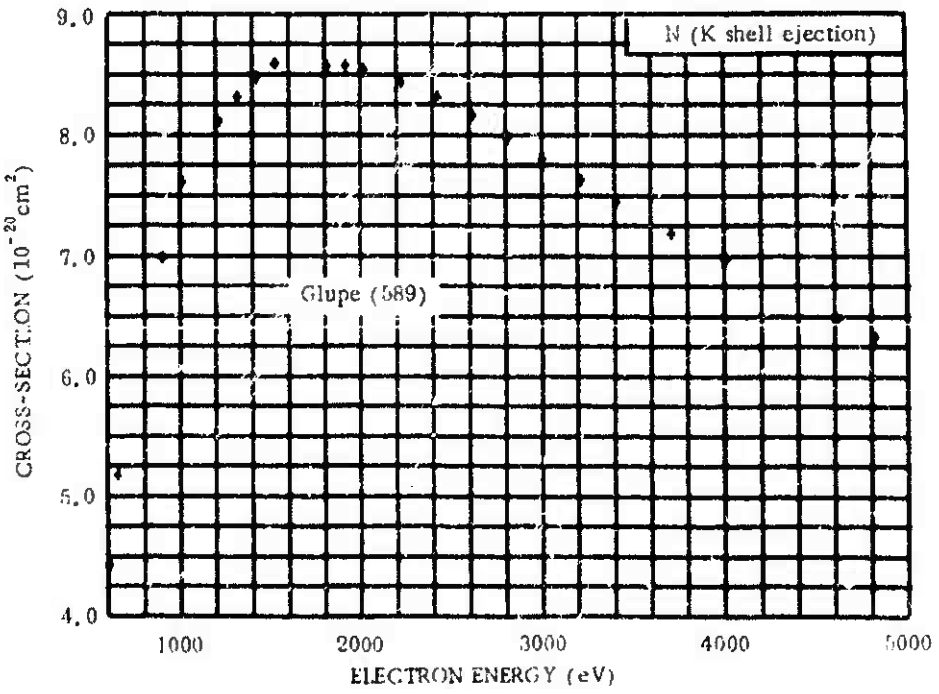


Figure 14-6.

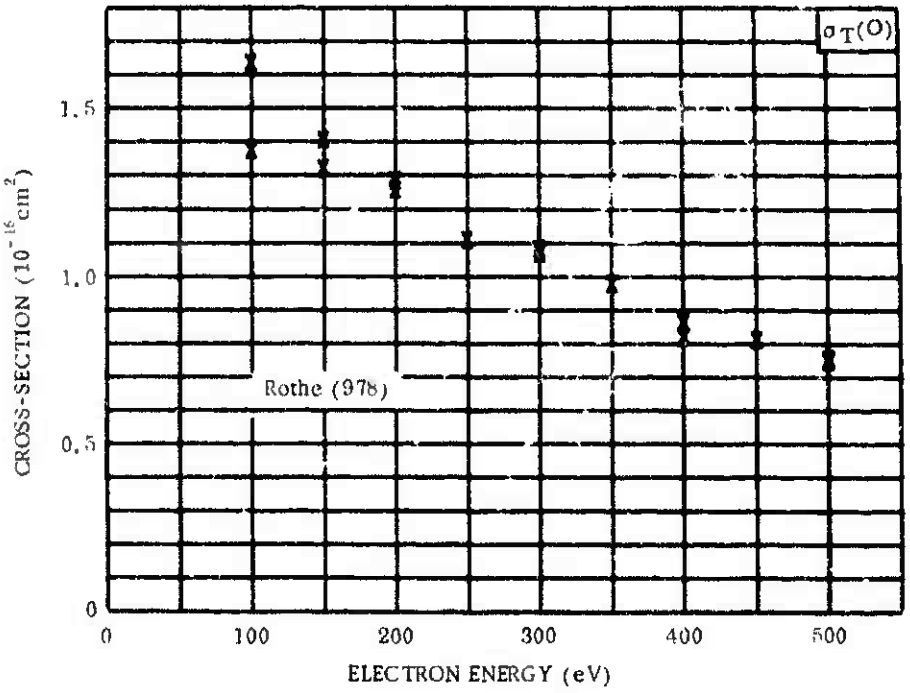


Figure 14-7.

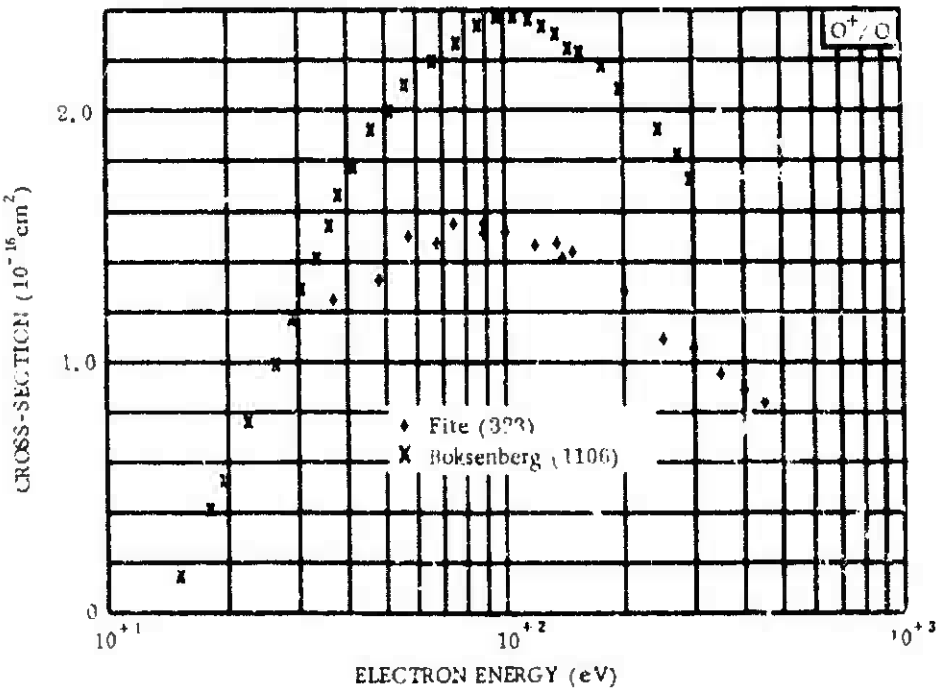


Figure 14-8.

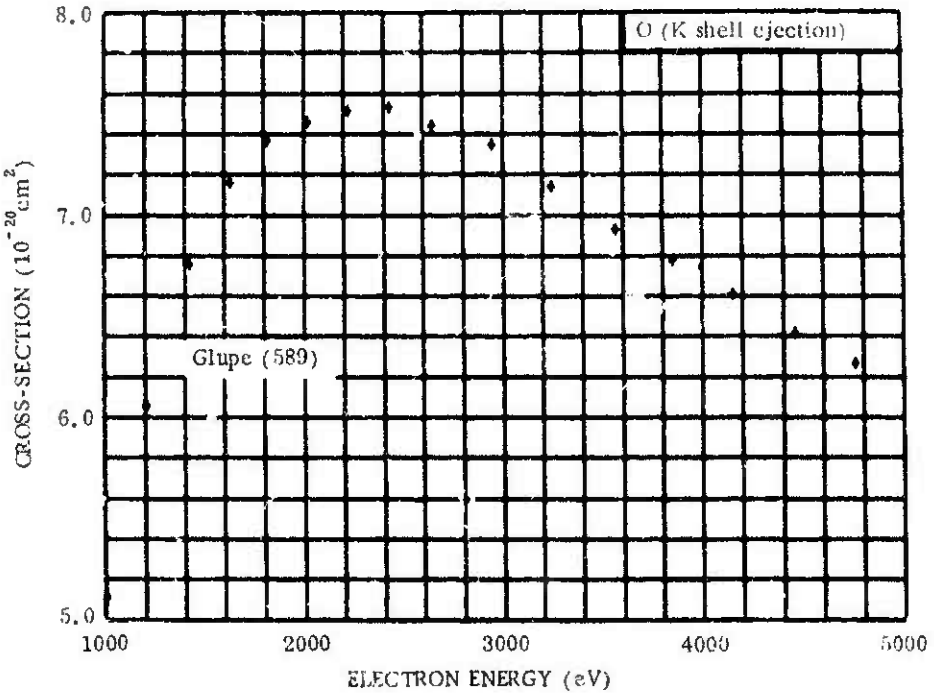


Figure 14-9.

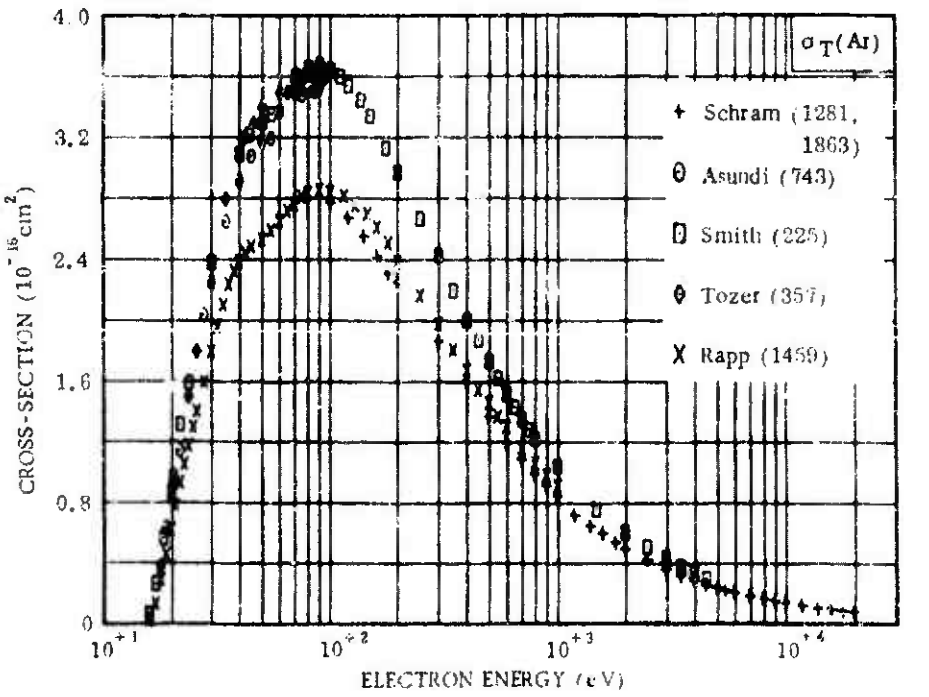


Figure 14-10.

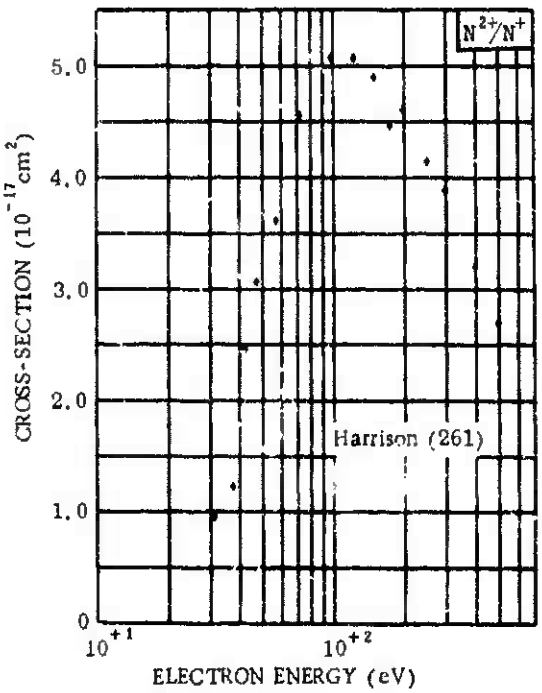


Figure 14-11.

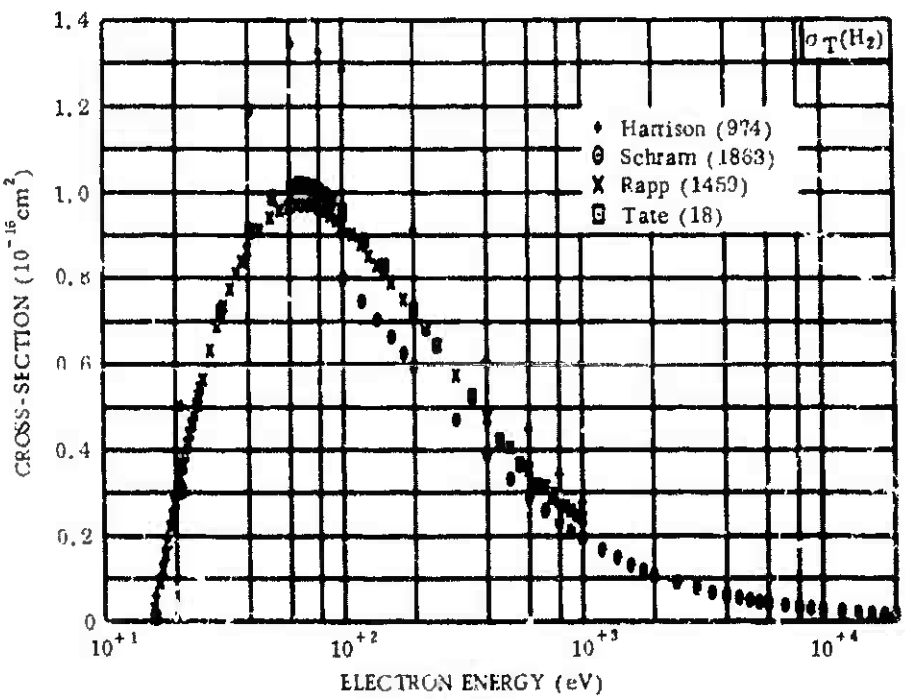


Figure 14-12.

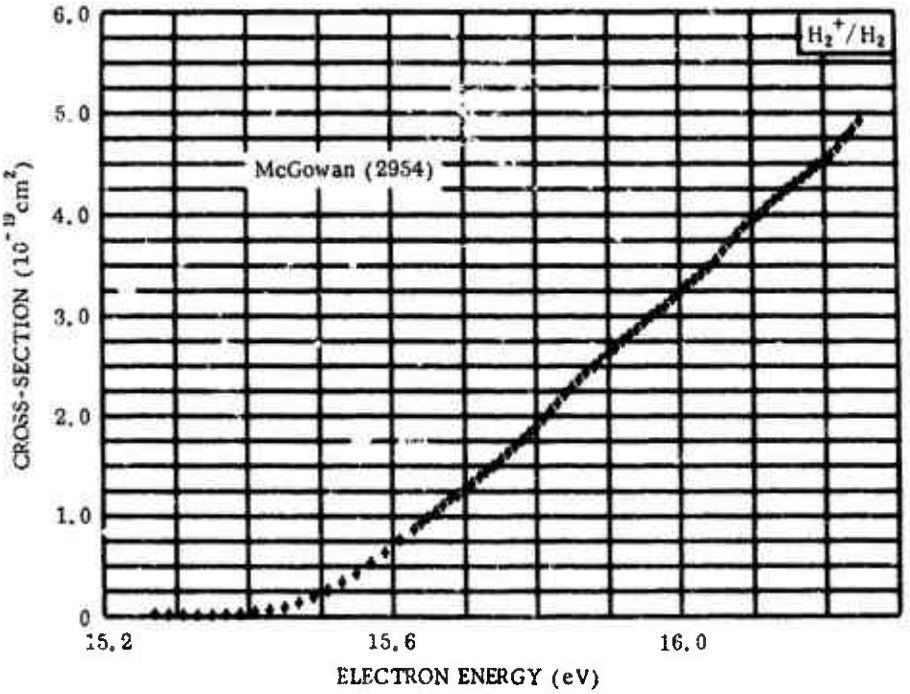


Figure 14-13.

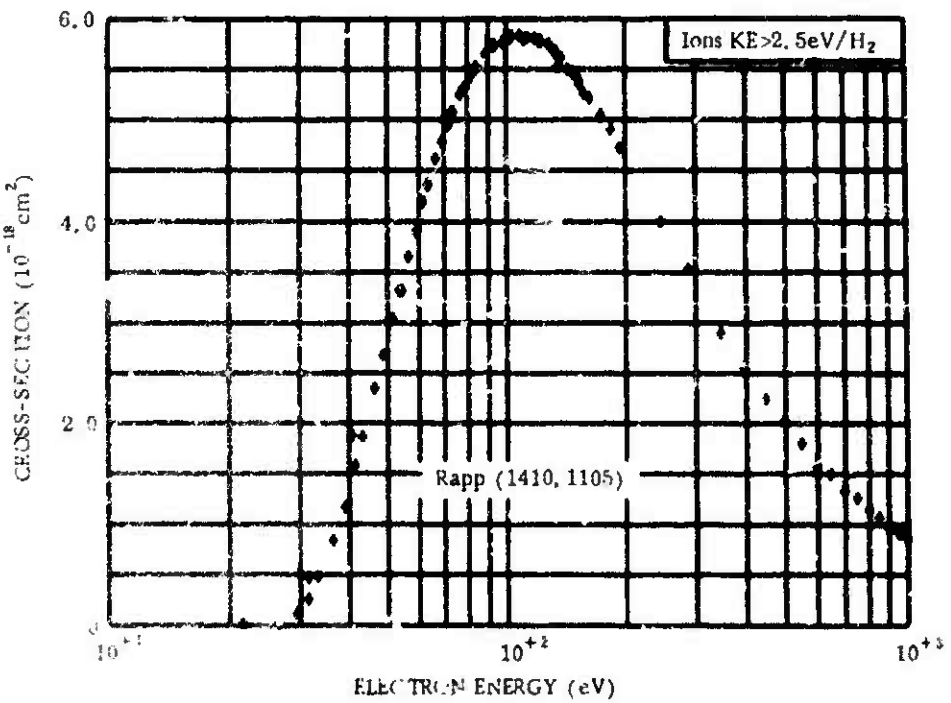


Figure 14-14.

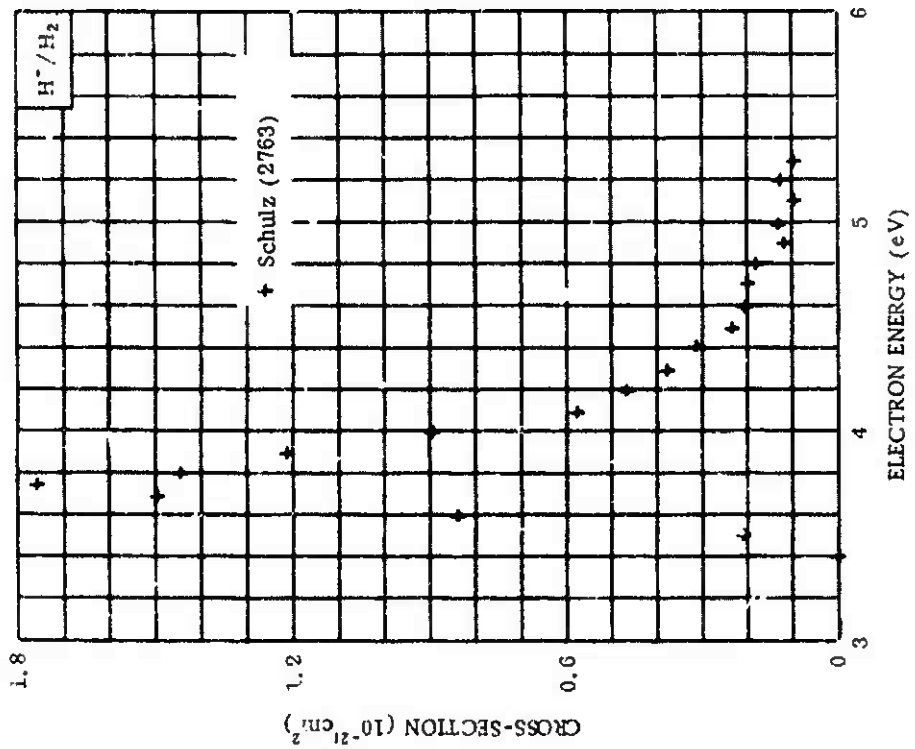


Figure 14-16.

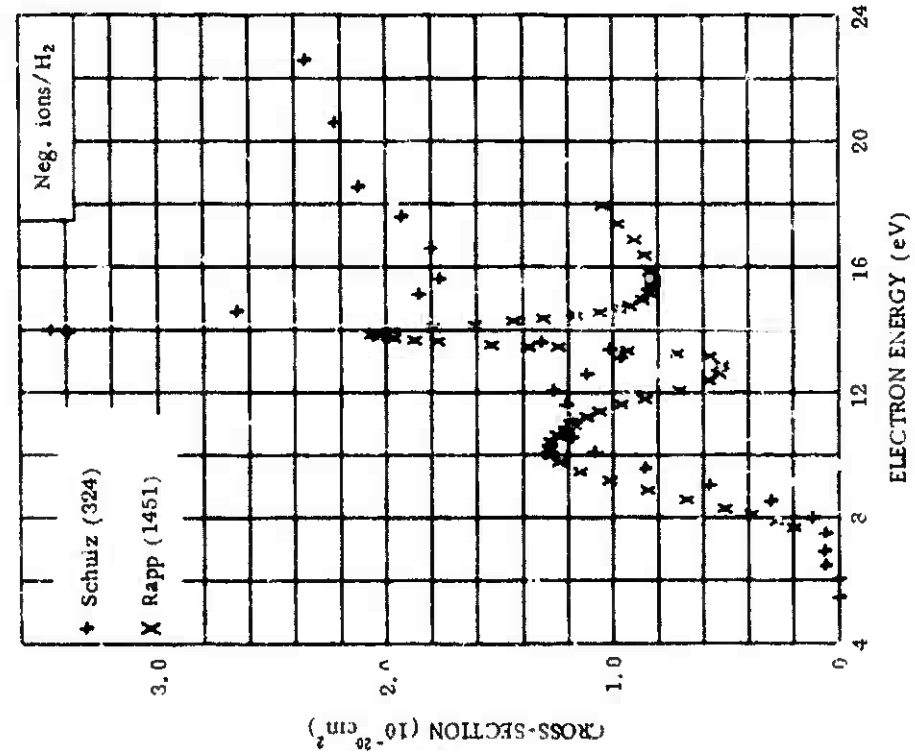


Figure 14-15.

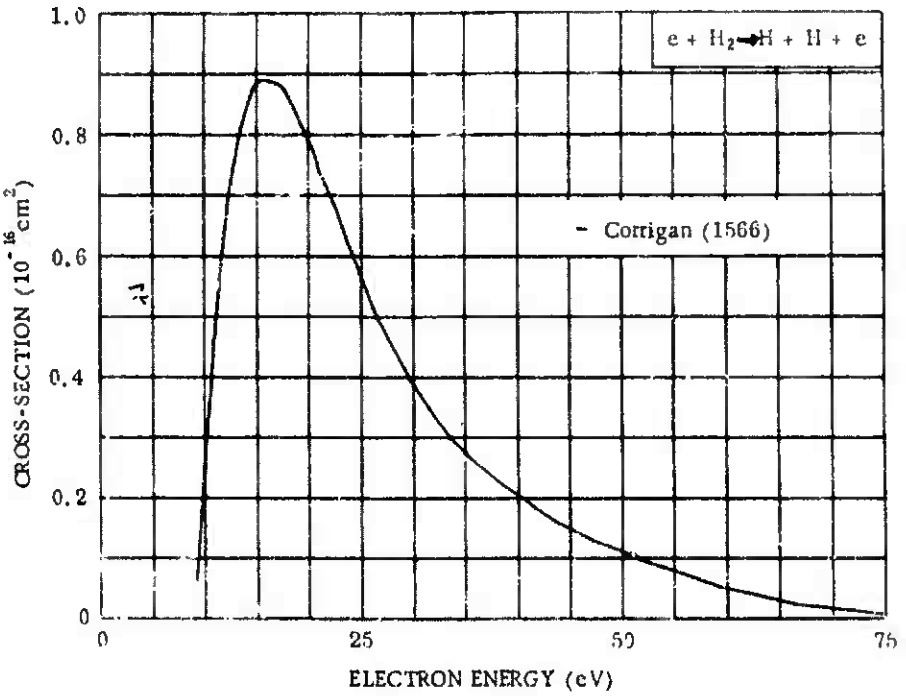


Figure 14-17.

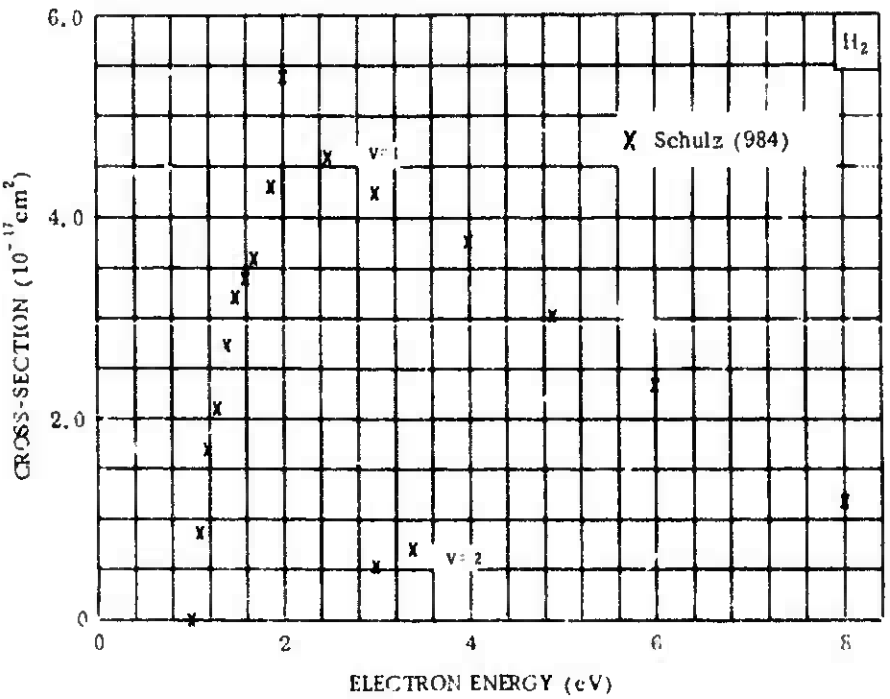


Figure 14-18.

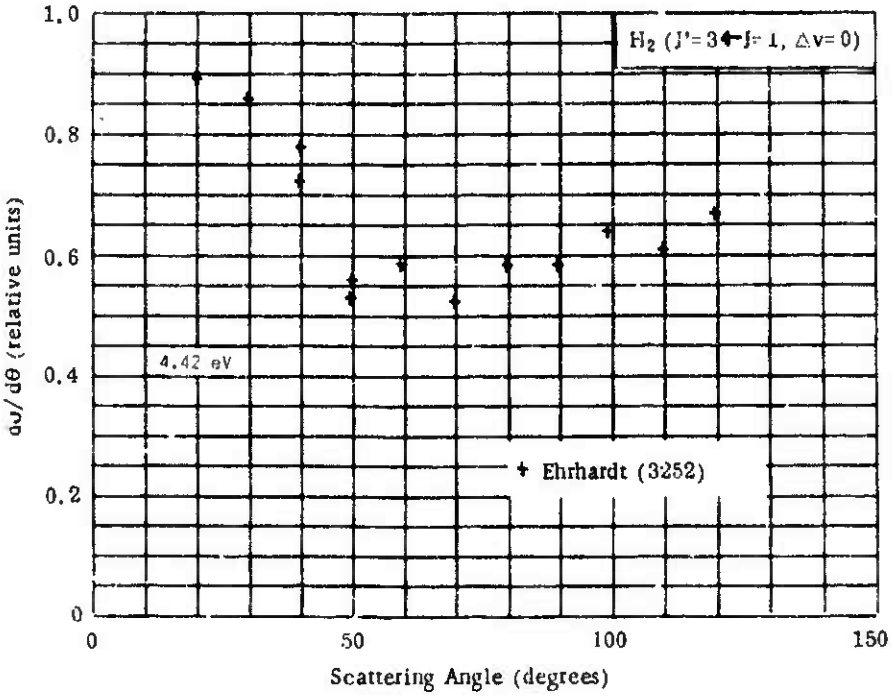


Figure 14-19.

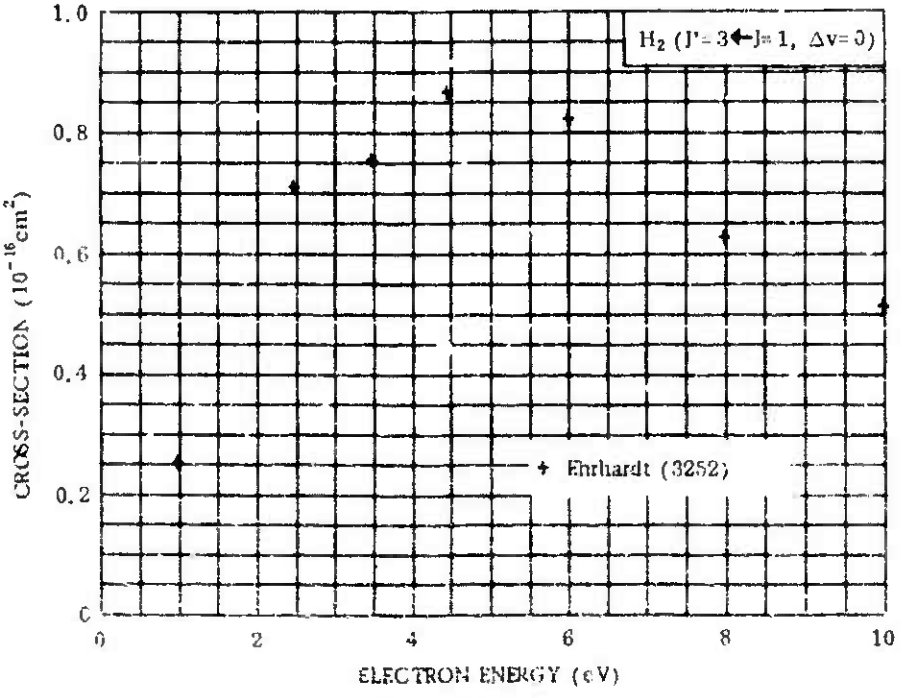


Figure 14-20.

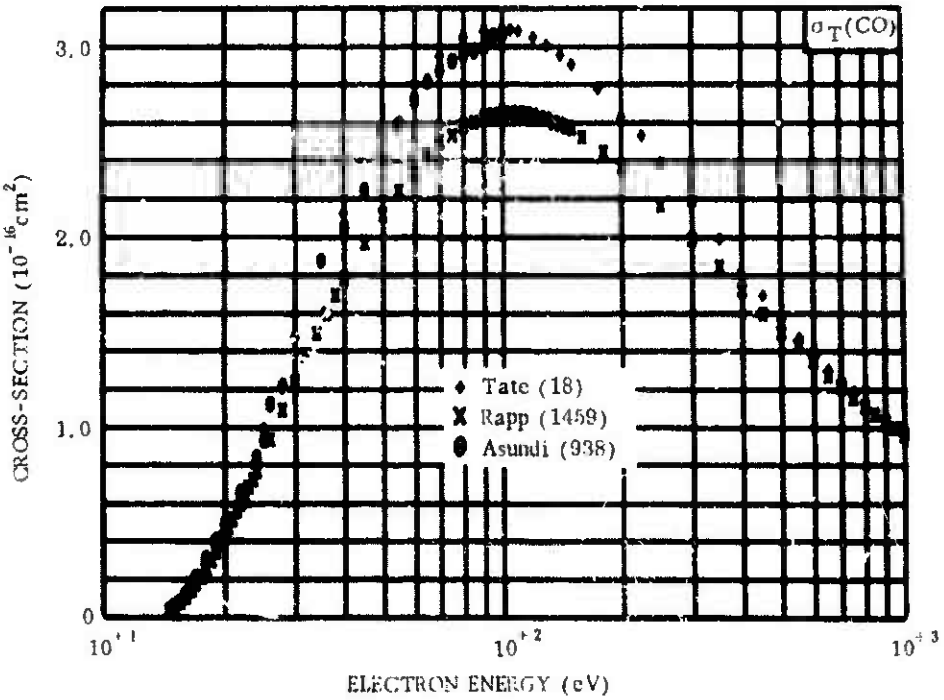


Figure 14-21.

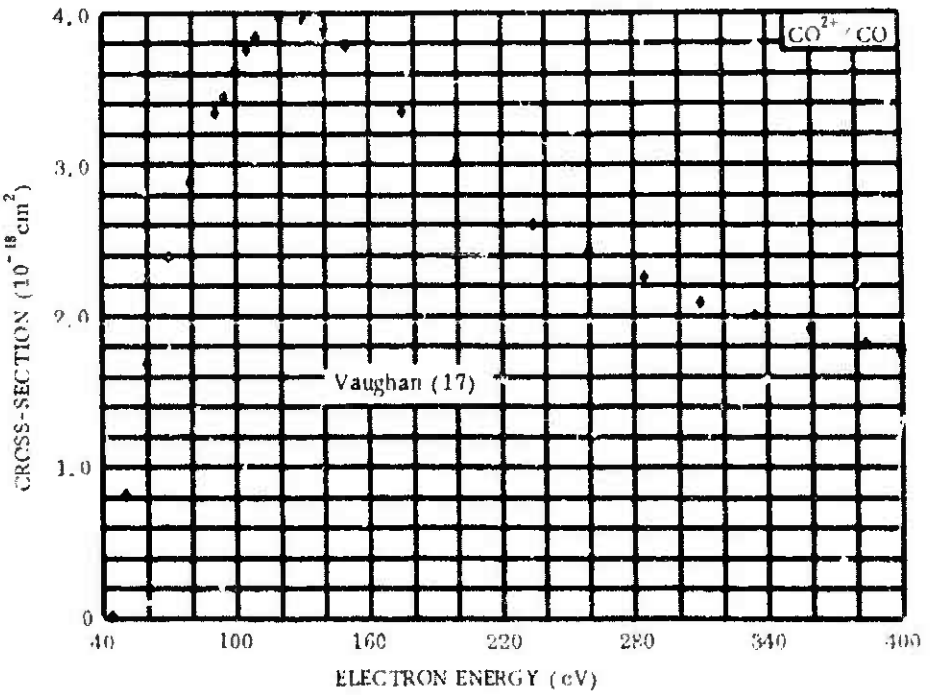


Figure 14-22.

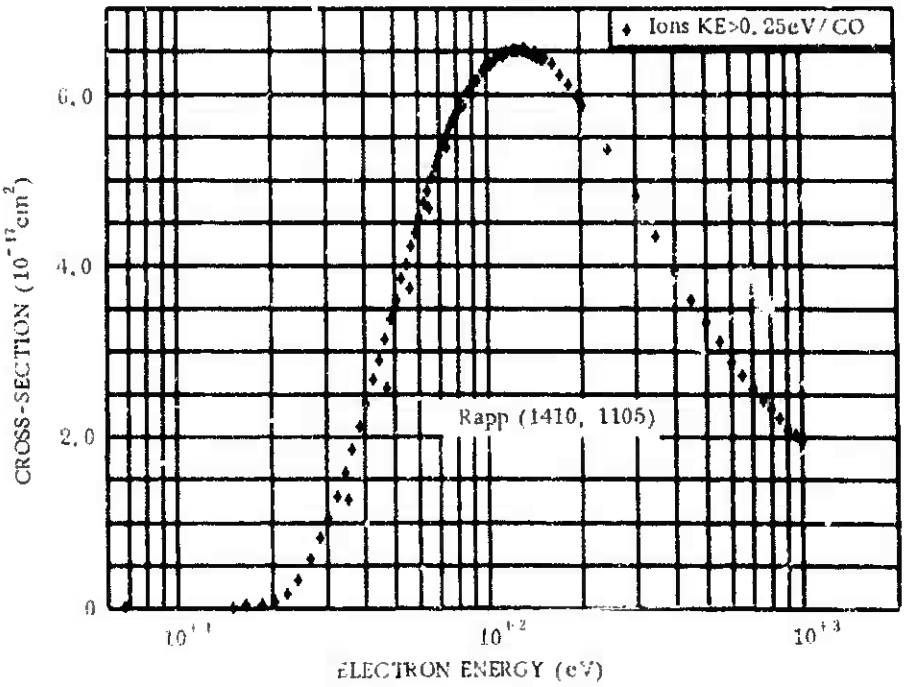


Figure 14-23.

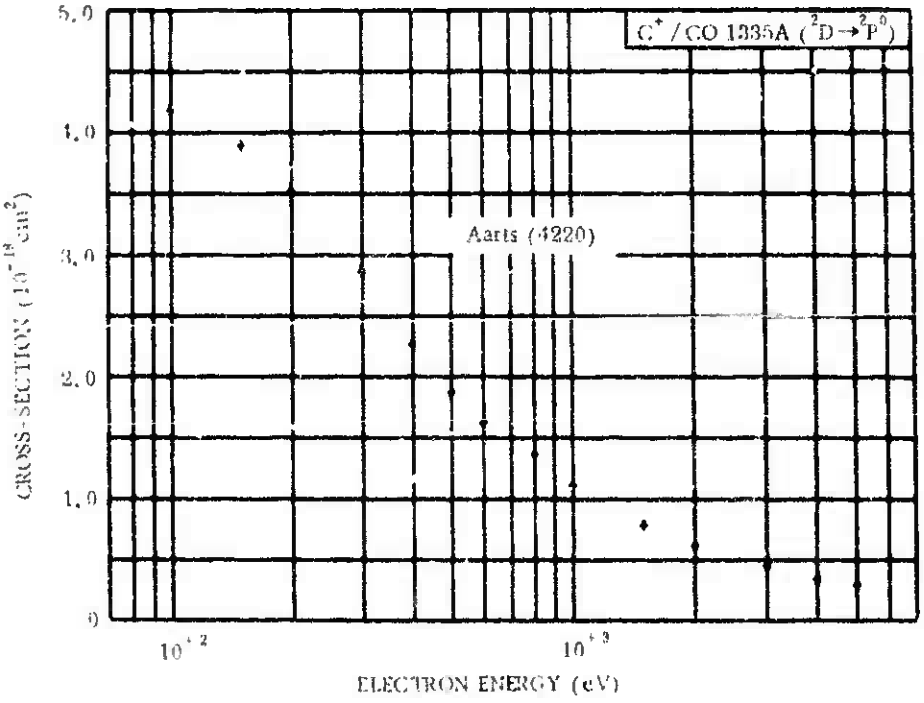


Figure 14-24.

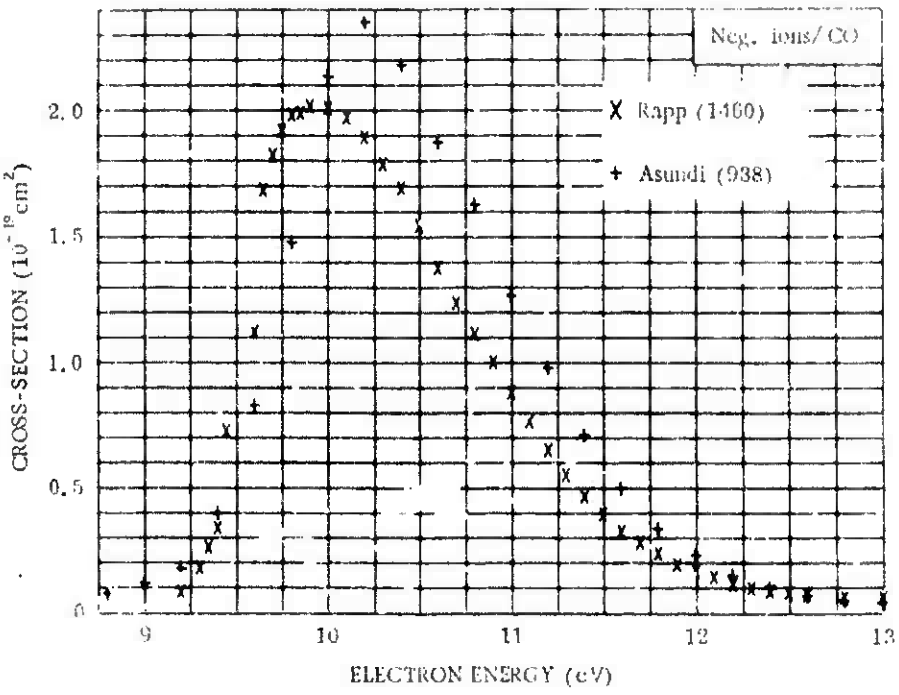


Figure 14-25.

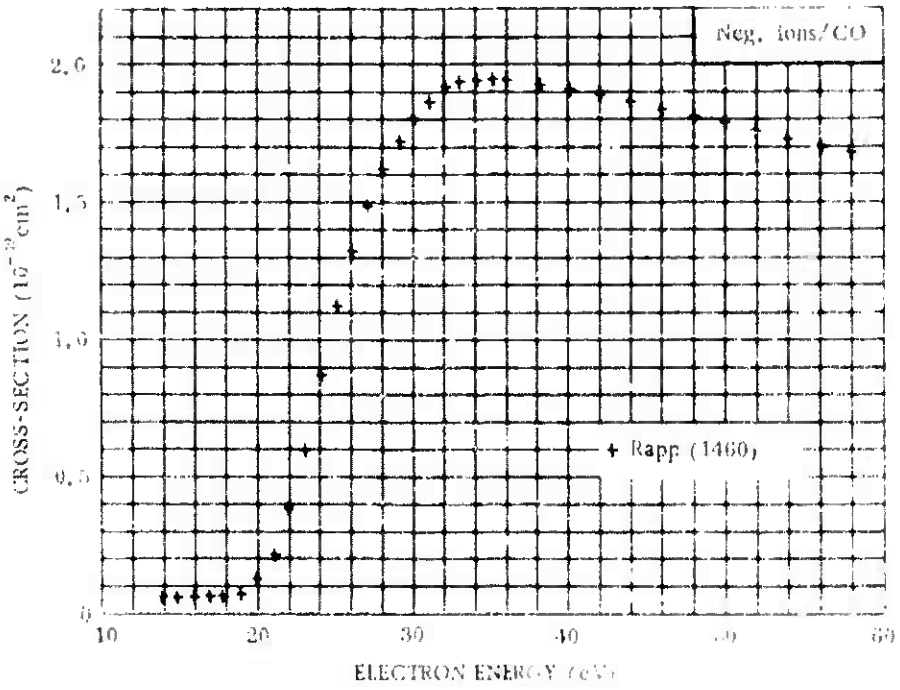


Figure 14-26.

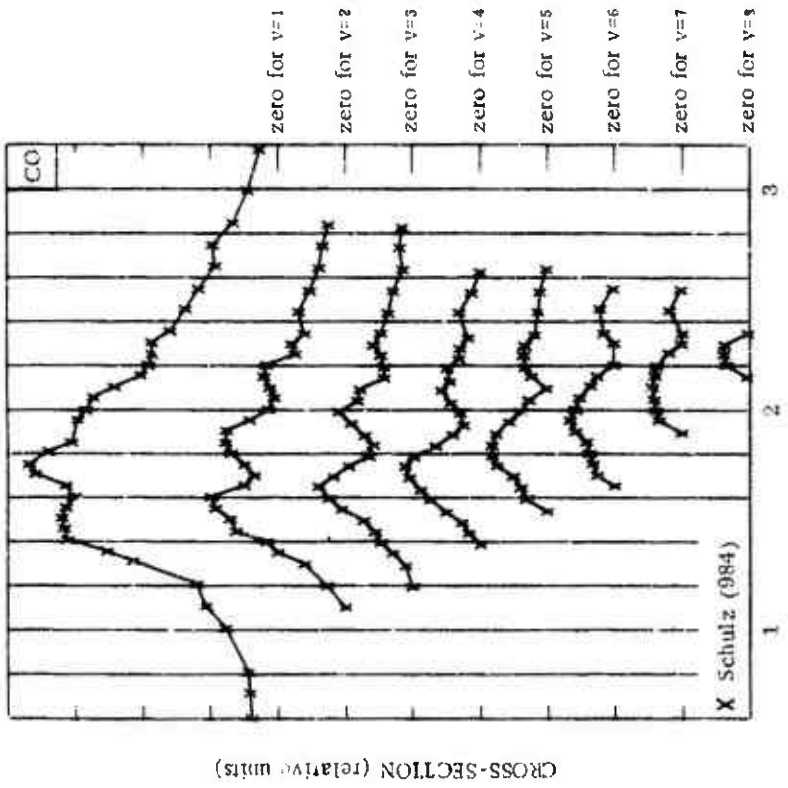


Figure 14-28.

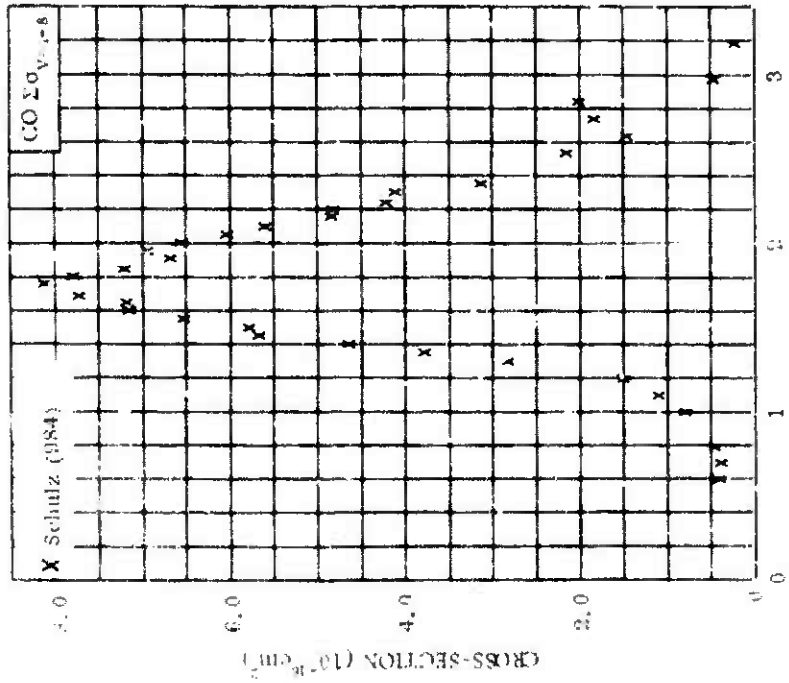


Figure 14-27.

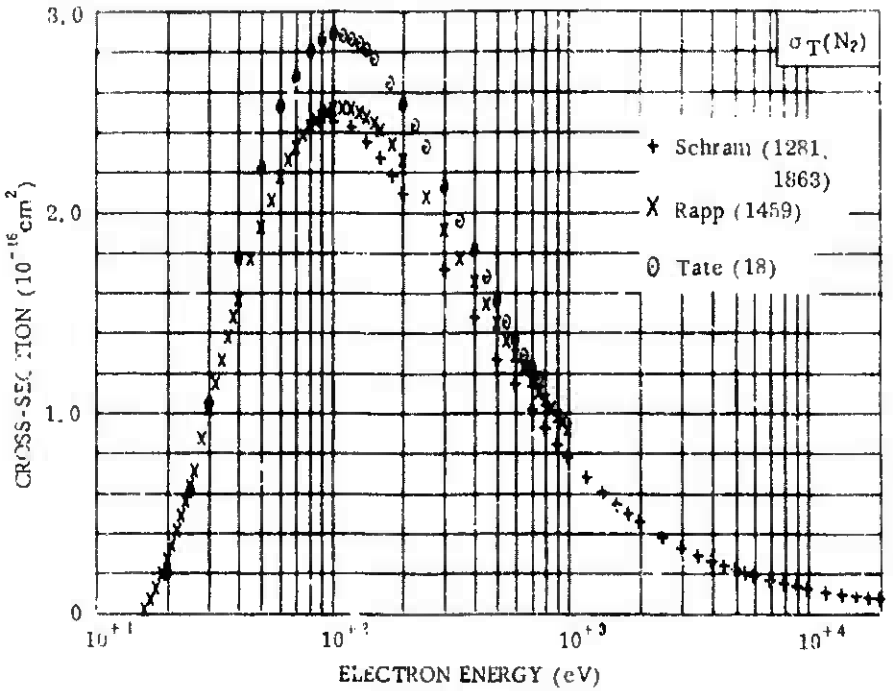


Figure 14-29.

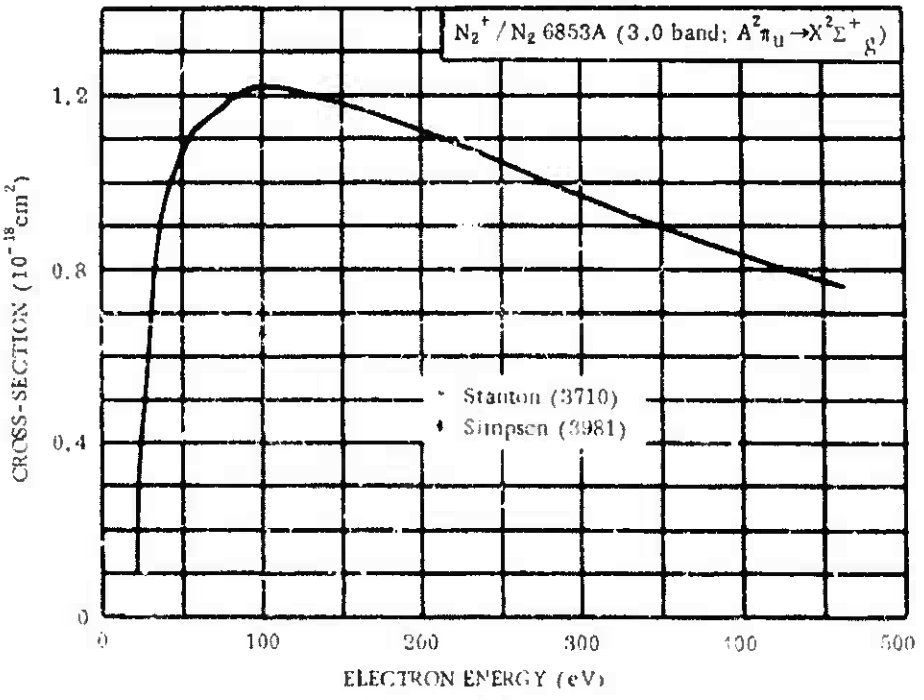


Figure 14-30.

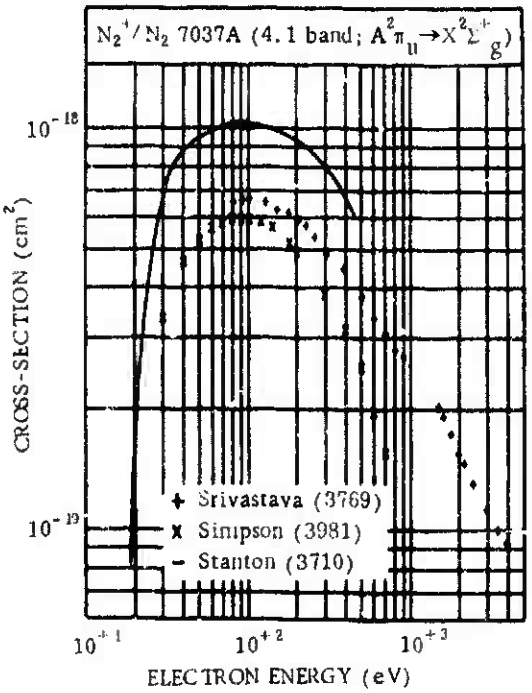


Figure 14-31.

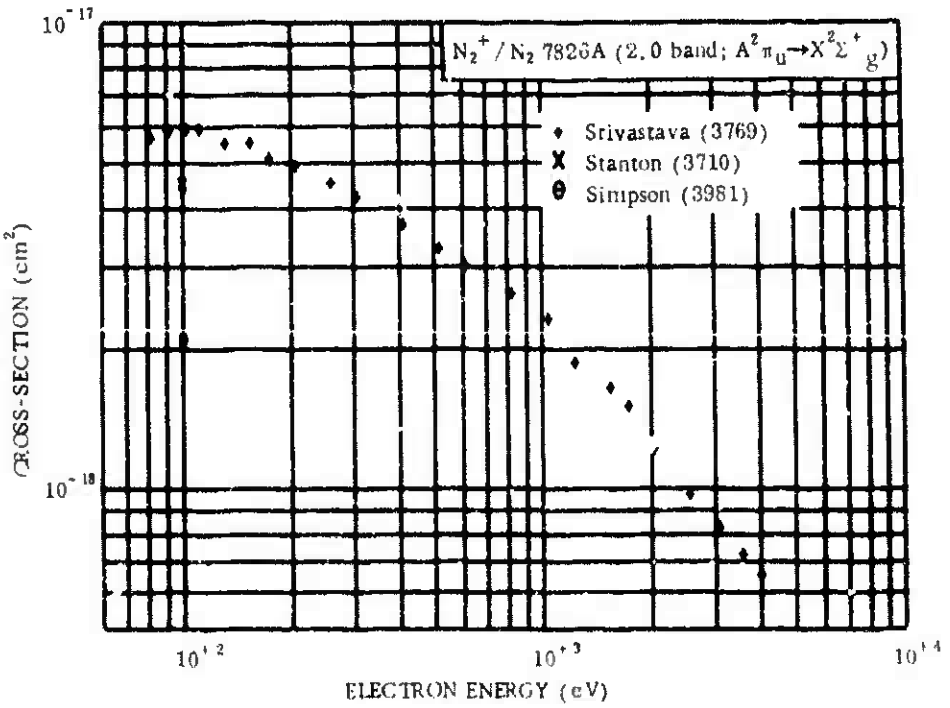


Figure 14-32.

Table 14-1. Effective line excitation crass-sectians af the Meinel bands of $N_2^+$.

$N_2^+/N_2$

| Wavelength[1] (A) | v', v'' | E (eV) | σ ($10^{-19}$ $cm^2$) |
|---|---|---|---|
| 6106 | 4,0 | 100. | 2.4[a] / 1.4[b] |
| 6268 | 5,1 | 100. | 2.7[a] |
| 7240 | 5,2 | 100. | 0.6[a] / 1.3[b] |
| 9145 | 1,0 | 100. | 110.[a] |
| 9431 | 2,1 | 100. | 58.[a] |
| 11036 | 0,0 | 100. | 80.[a] |

Nates:

[1] The electranic transitian far this system is $A^2\Pi_u \rightarrow X^2\Sigma_g^+$ .

[a] The data were taken from Stantan (3710).

[b] The data were taken from Simpsan (3981).

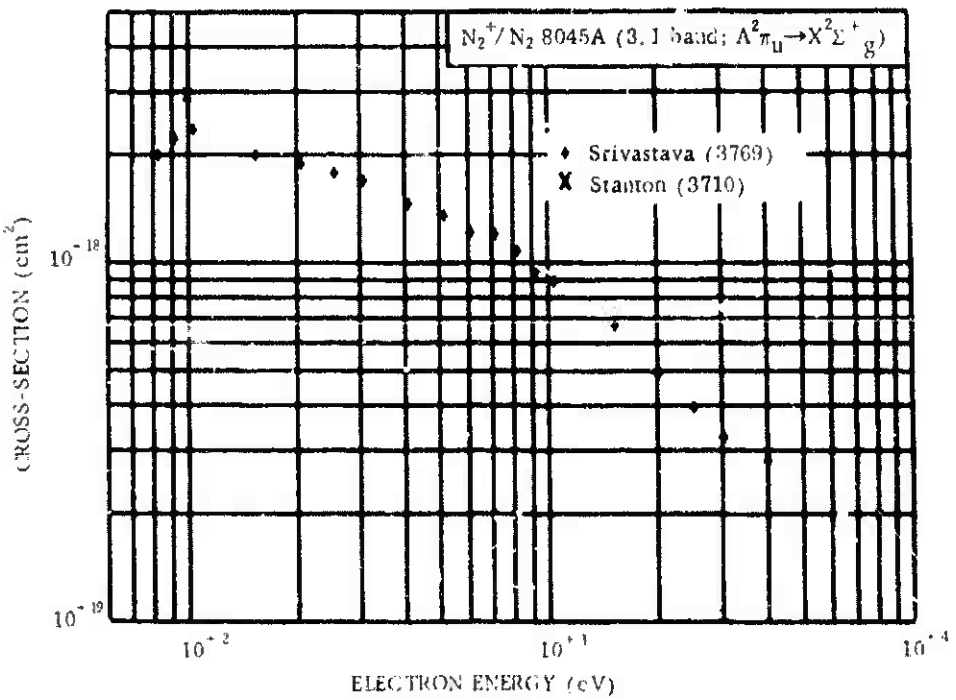


Figure 14-33.

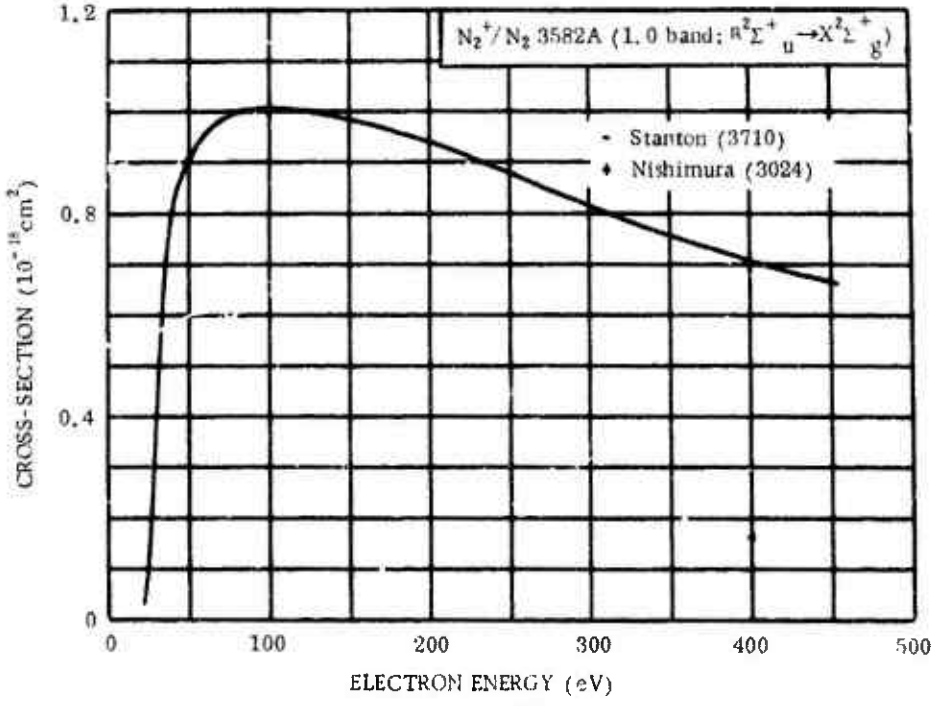


Figure 14-34.

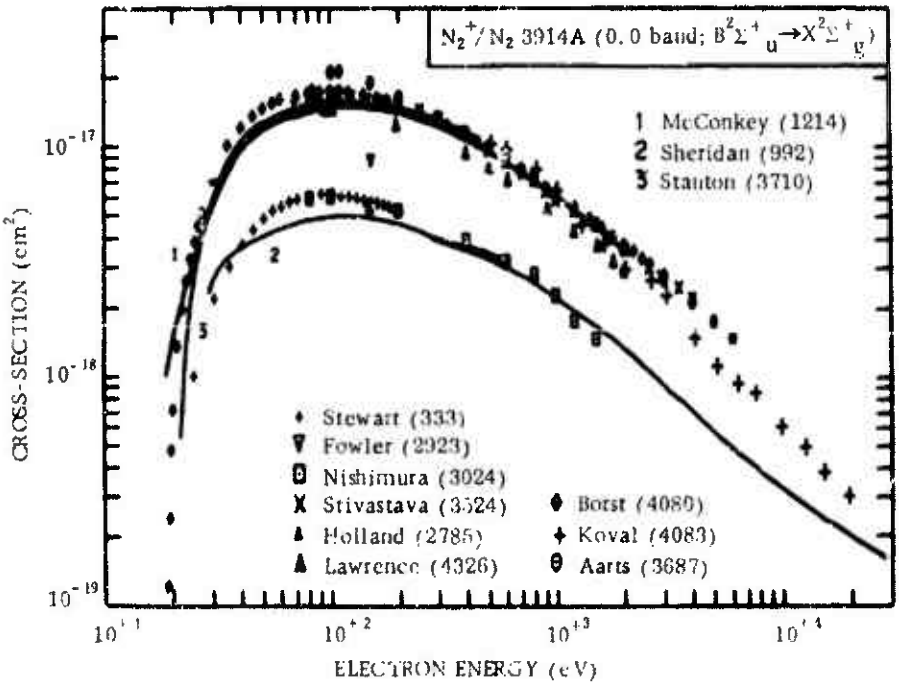


Figure 14-35.

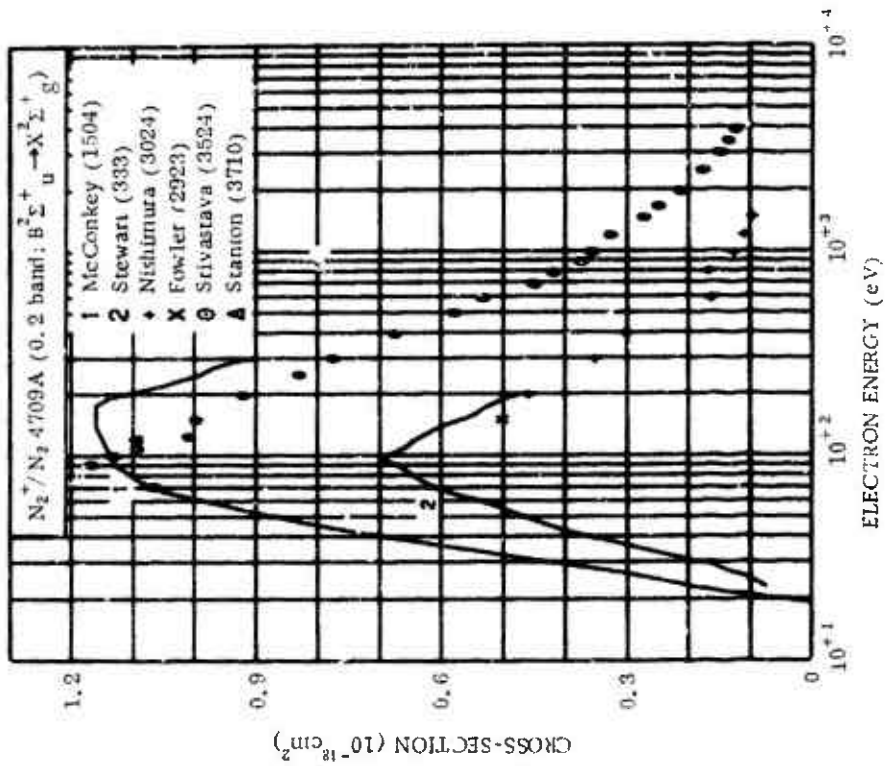


Figure 14-37.

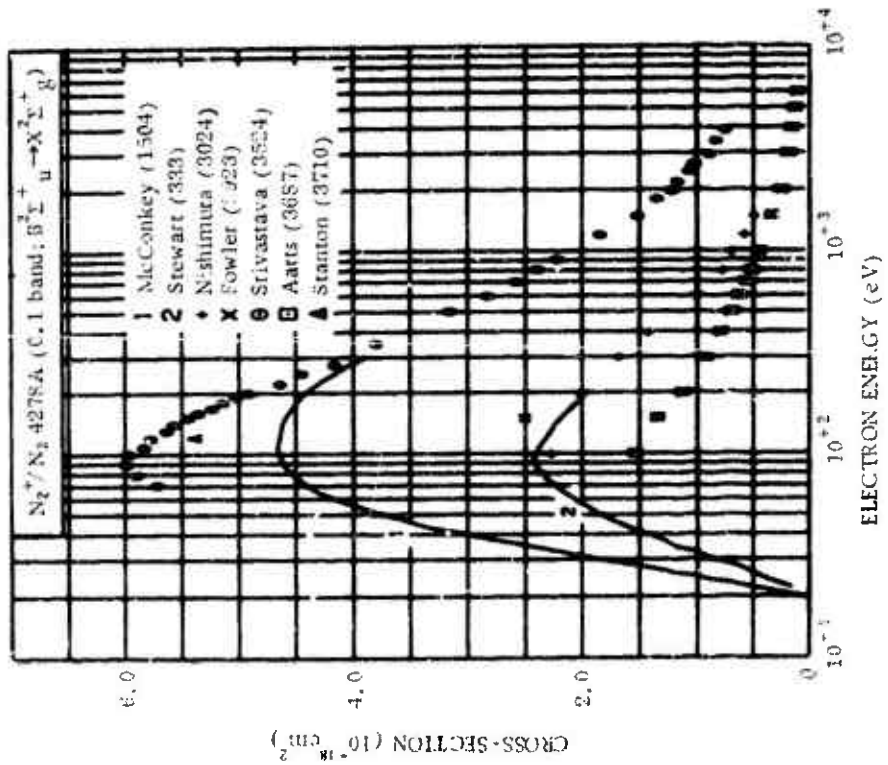


Figure 14-36.

Table 14-2. Effective line excitation cross-sections of the 1st negative bands of $N_2^+$.

$N_2^+/N_2$

| Wavelength[1] (A) | v', v" | E (eV) | $\sigma(10^{-19}\ cm^2)$ [2] |
|---|---|---|---|
| 3549 | 3,2 | 120. | 0.50 |
| 3564 | 2,1 | 120. | 1.1 |
| 3884 | 1,1 | 120. | 6.1 |
| | | 400. | 1.5 |
| 4199 | 2,3 | 120. | 0.45 |
| 4236 | 1,2 | 120. | 6.9 |
| | | 400. | 1.5 |
| 4652 | 1,3 | 120. | 2.7 |
| | | 400. | 0.3 |
| 5149 | 1,4 | 120. | 0.65 |
| 5228 | 0,3 | 120. | 2.1 |
| | | 400. | 0.5 |

Notes:

[1] The electranic transitian for this system is $B^2\Sigma_u^+ \rightarrow X^2\Sigma_g^+$.

[2] Cross-sectians at 120 eV were measured by Stanton (3710); cross-sections at 400 eV were measured by Nishimura (3024).

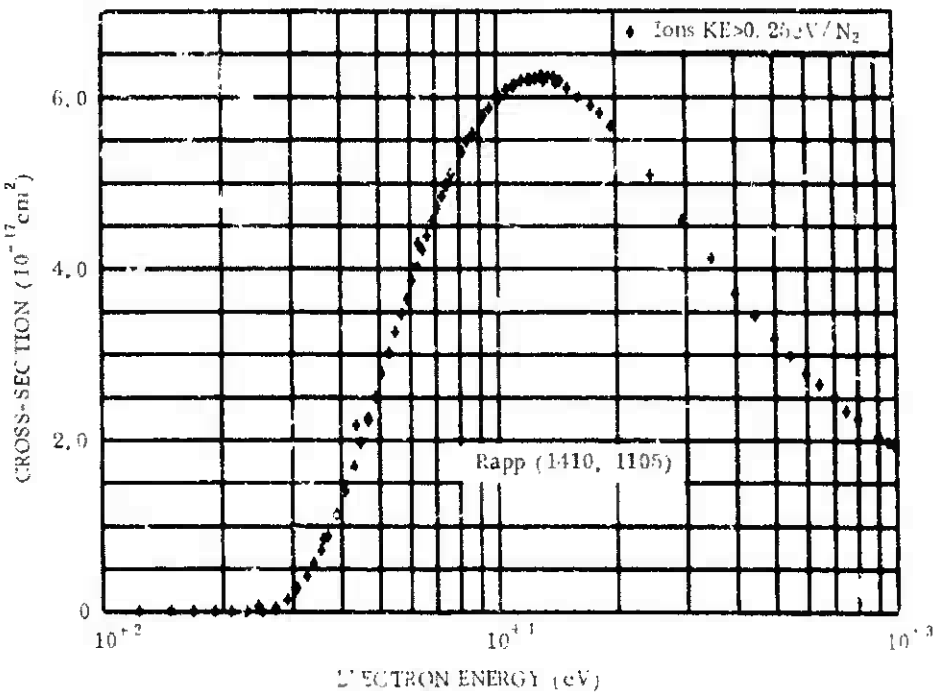


Figure 14-38.

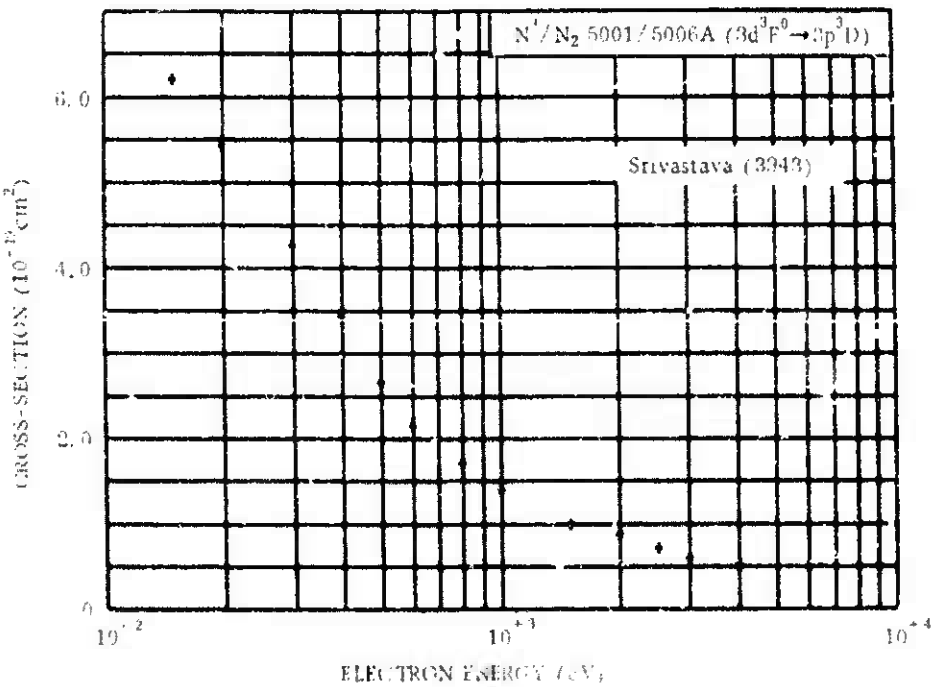


Figure 14-39.

Table 14-3. Effective dissociative ionization cross-sections of $N_2$.

$N^+/N_2$

| Wavelength (A) | Transition | E (eV) | $\sigma(10^{-18}\ cm^2)$ [1] |
|---|---|---|---|
| 623.9 | $3s'\ ^5P \rightarrow 2p'\ ^5S$ | 100. | 0.23 |
| 645.6 | $2p'\ ^3S \rightarrow 2p\ ^3P$ | 100. | 0.25 |
| 671.4 | $2s\ ^3P \rightarrow 2p\ ^3P$ | 100. | 4.5 |
| 746.4 | $3s'\ ^1P \rightarrow 2p\ ^1D$ | 100. | 3.2 |
| 746.4 | $2p'\ ^1P \rightarrow 2p\ ^1S$ | 100. | 3.2 |
| 775.1 | $2p'\ ^1D \rightarrow 2p\ ^1D$ | 100. | 2.3 |
| 918 | $2p'\ ^3P \rightarrow 2p\ ^3P$ | 100. | 11.9 |
| 1084.4 | $2p'\ ^3D \rightarrow 2p\ ^3P$ | 100. | 20.4 |
| 5667 | $3p\ ^3D_2 \rightarrow 3s\ ^3P_1$ | 500. | 0.0886 |
| 5680 | $3p\ ^3D_3 \rightarrow 3s\ ^3P_2$ | 500. | 0.231 |

Note:

[1] Cross-sections at 100 eV were measured by Sroka (3833); cross-sections at 500 eV were measured by Srivastava (3943).

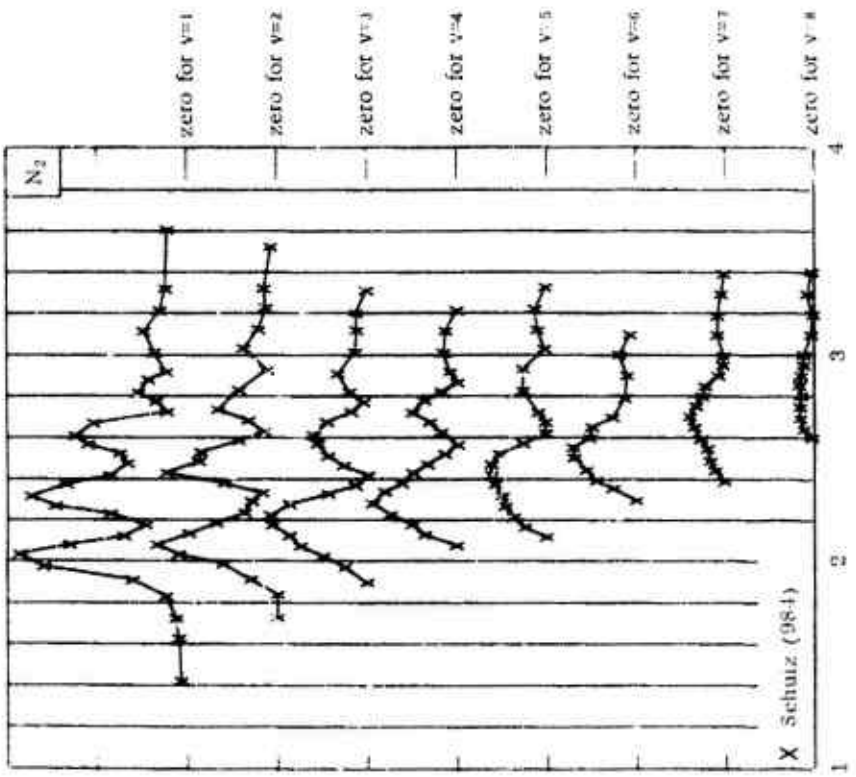


Figure 14-41.

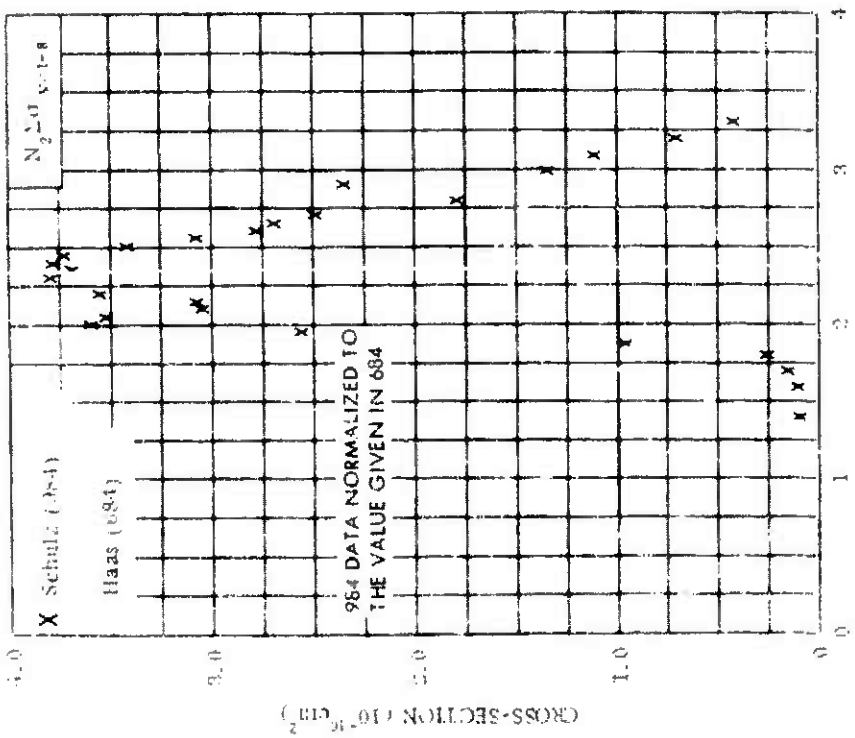


Figure 14-40.

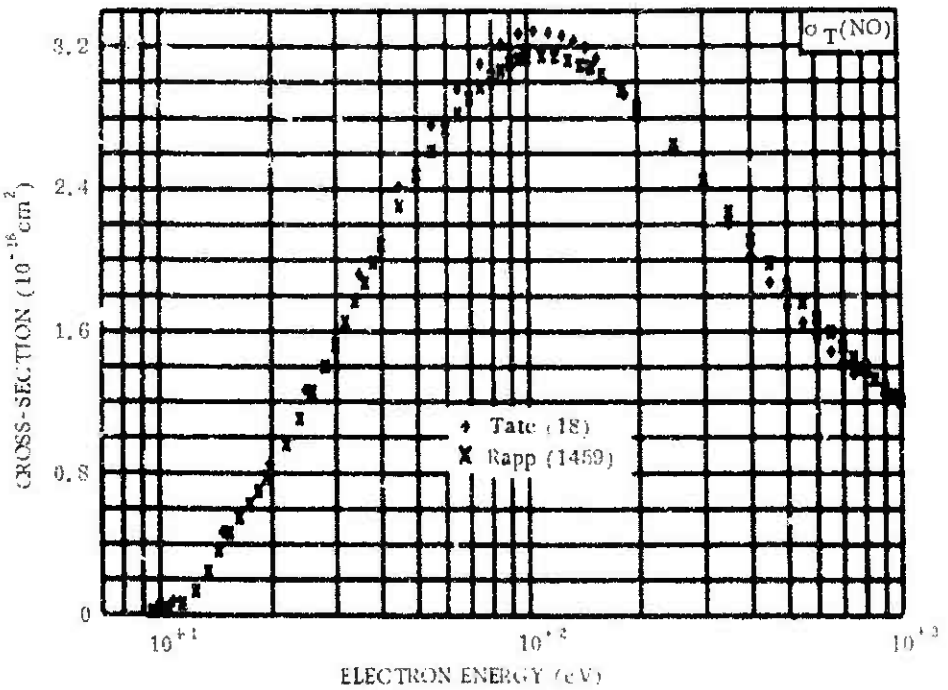


Figure 14-42.

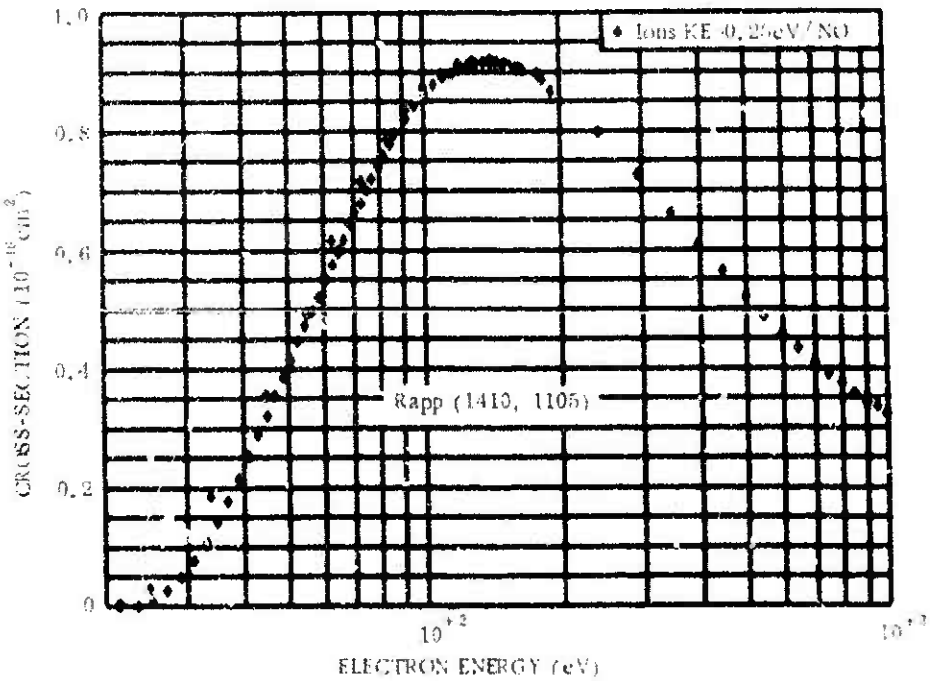


Figure 14-43.

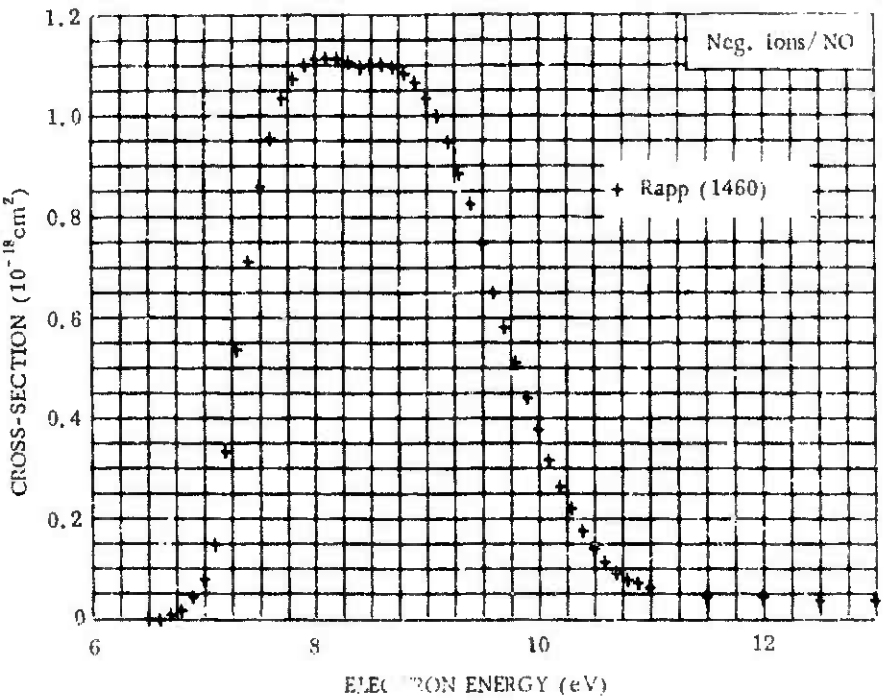


Figure 14-44.

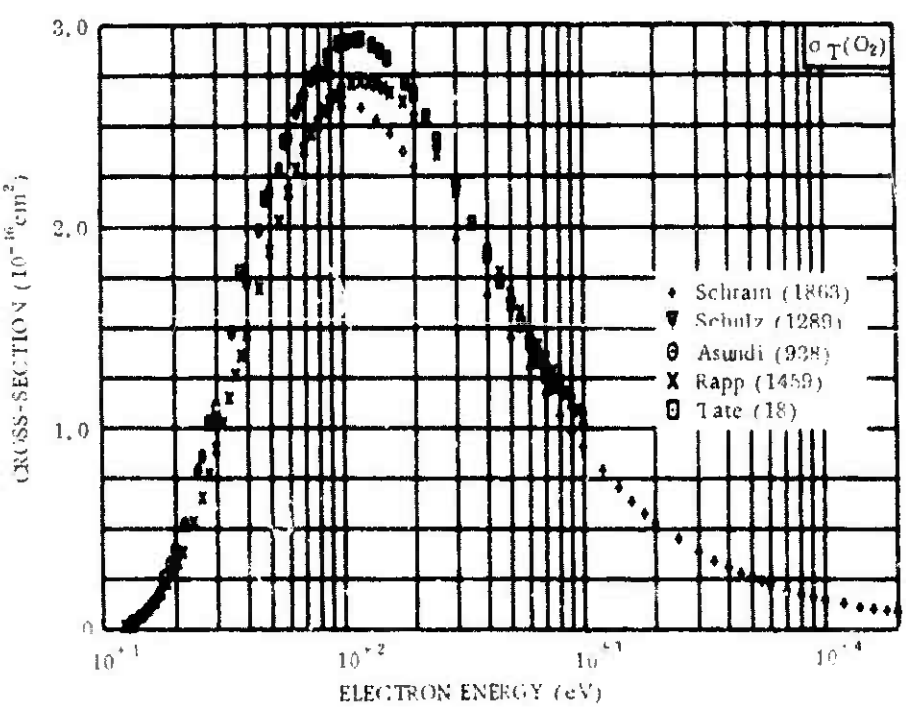


Figure 14-45.

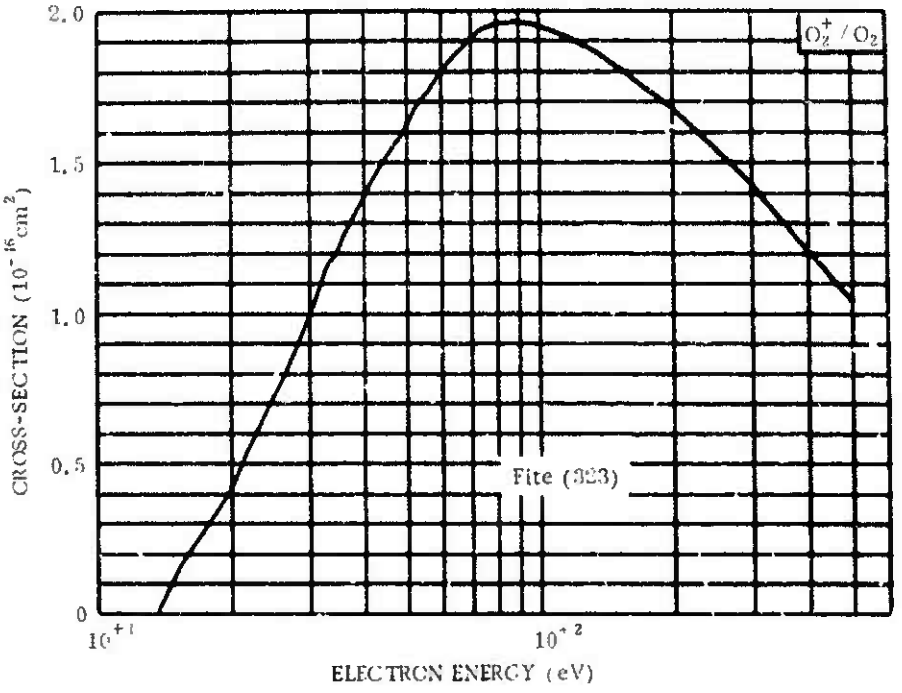


Figure 14-46.

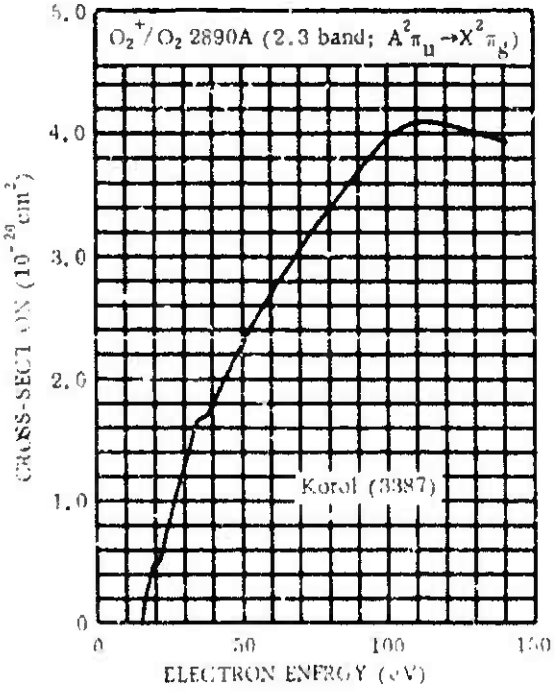


Figure 14-47.

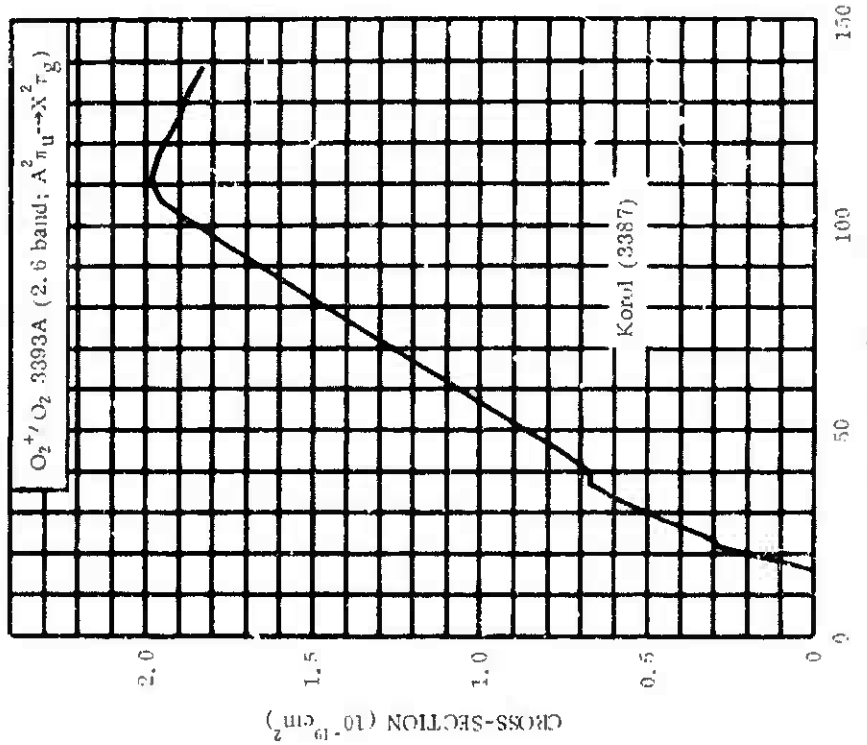


Figure 14-49.

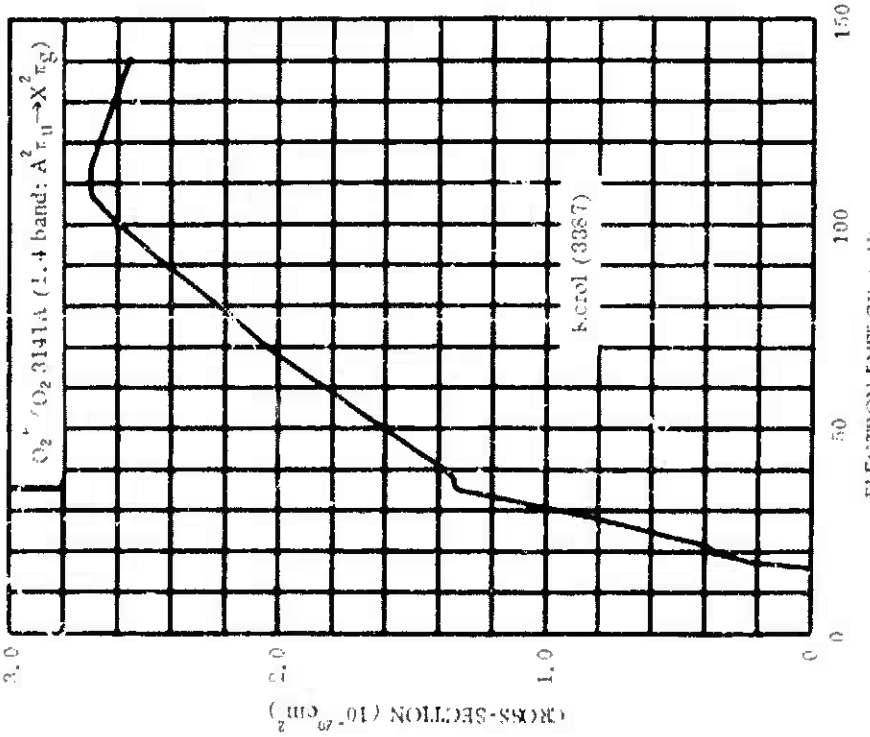


Figure 14-48.

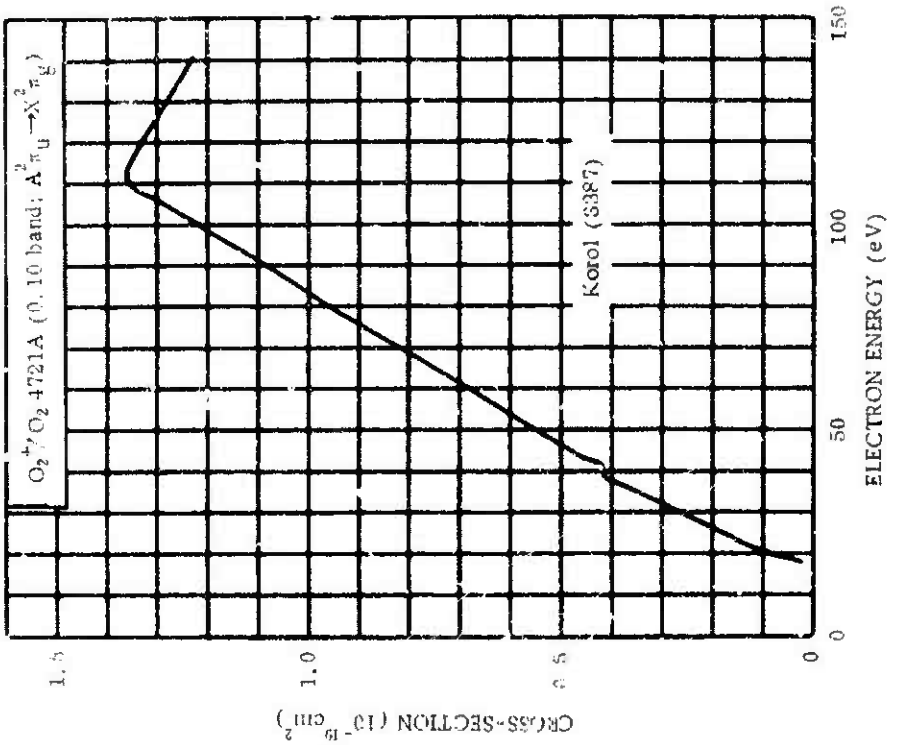


Figure 14-51.

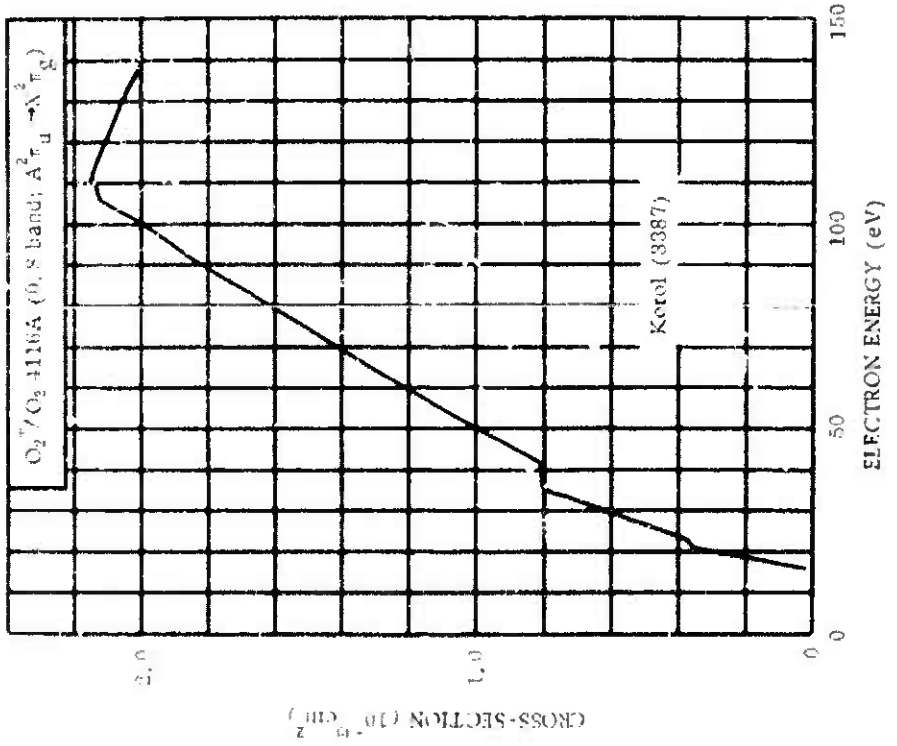


Figure 14-52.

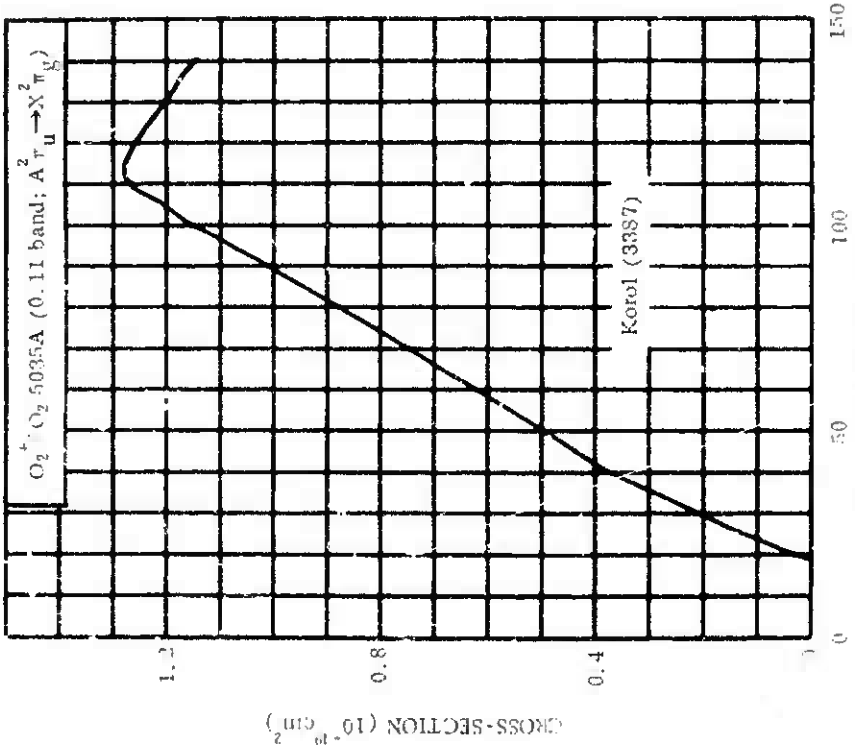


Figure 14-53.

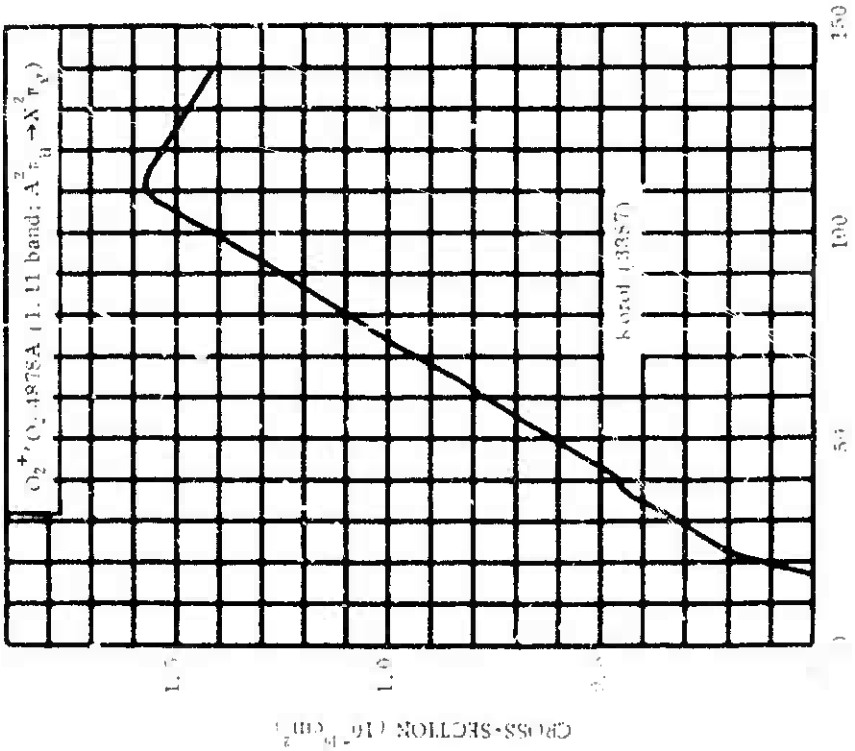


Figure 14-52.

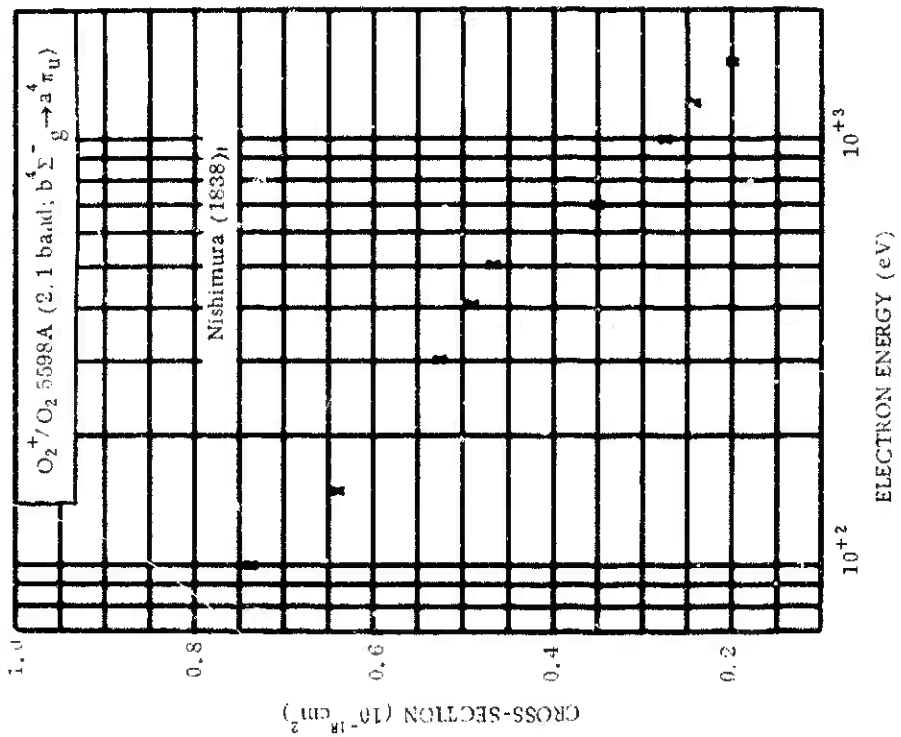


Figure 14-55.

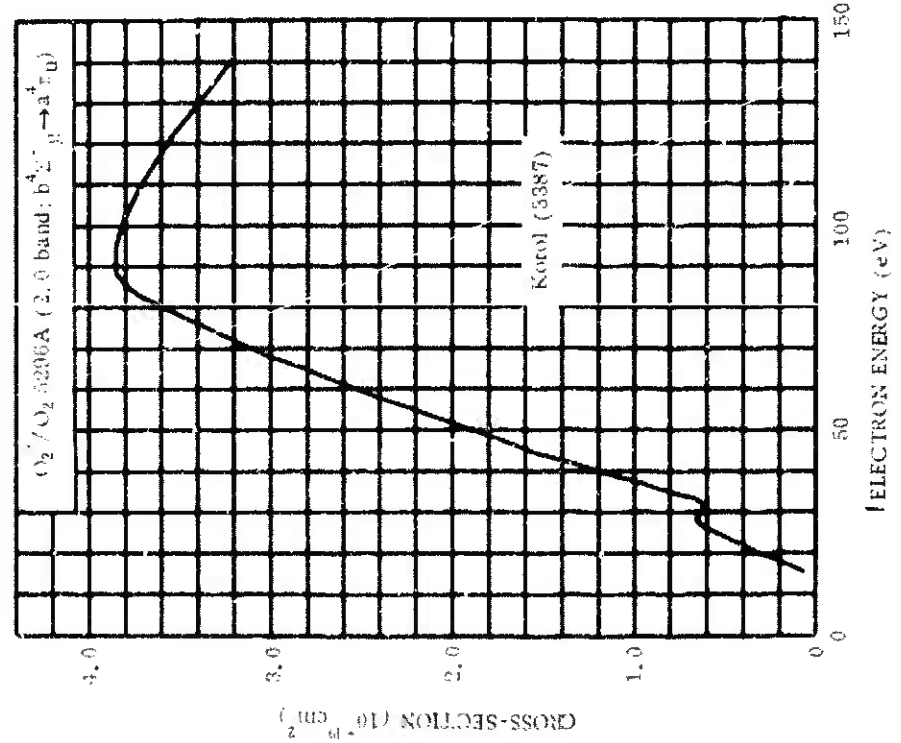


Figure 14-54.

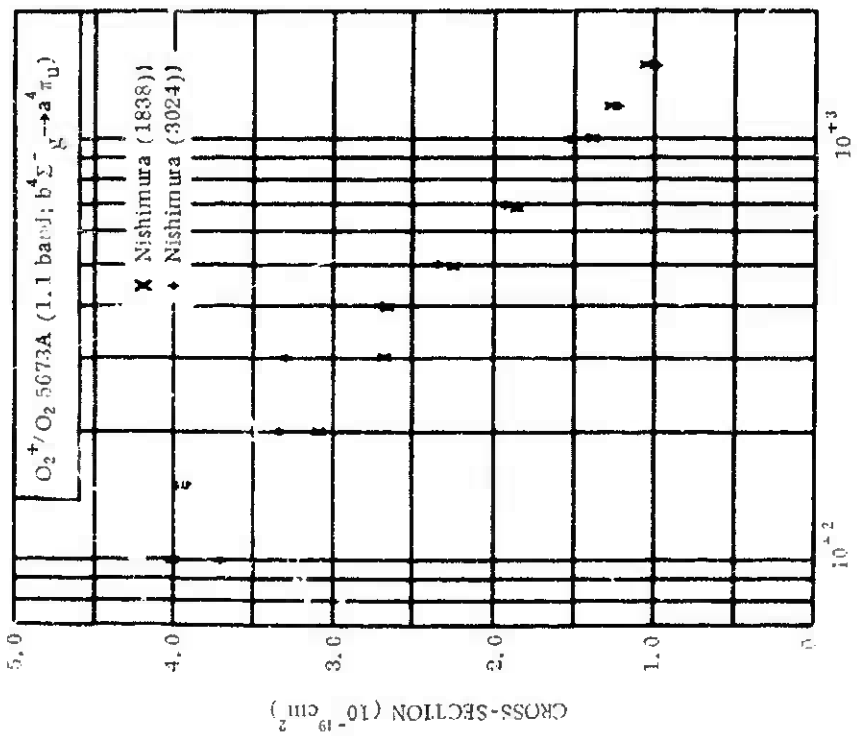


Figure 14-57.

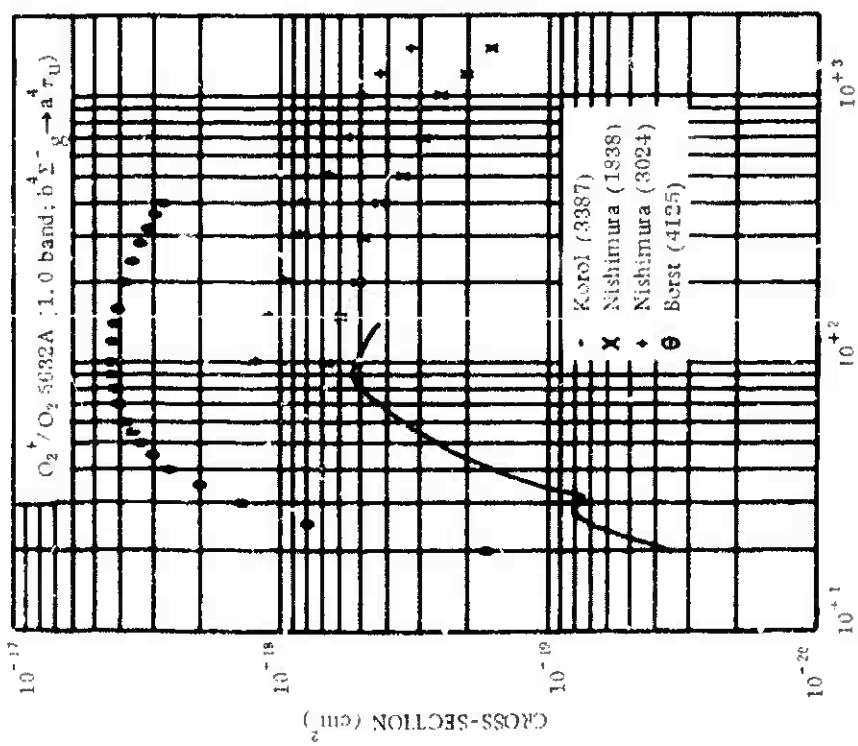


Figure 14-56.

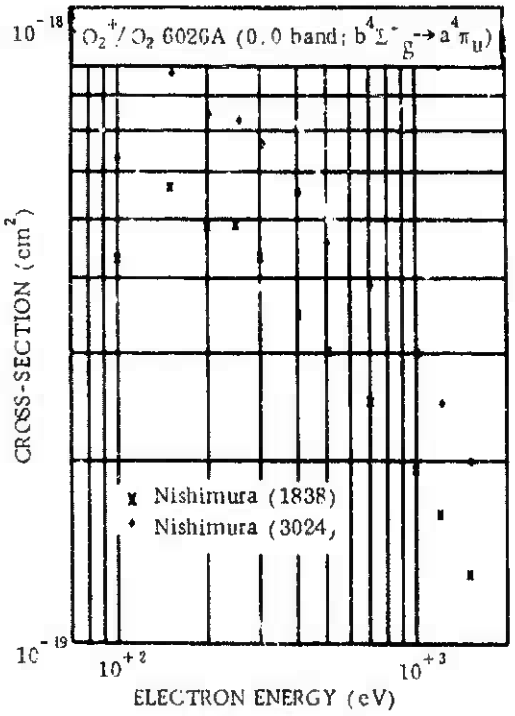


Figure 14-58.

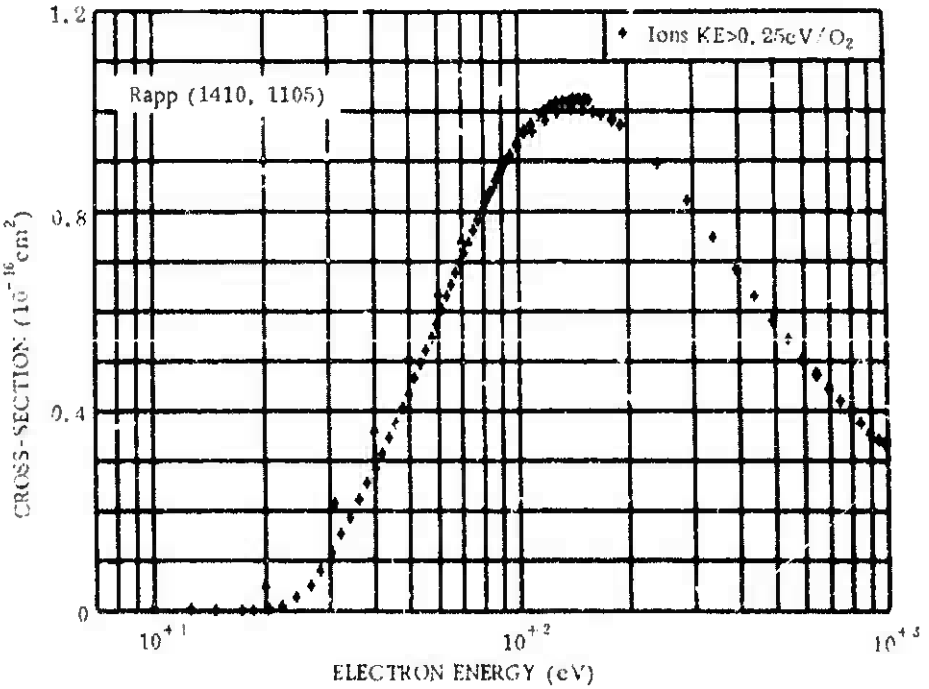


Figure 14-59.

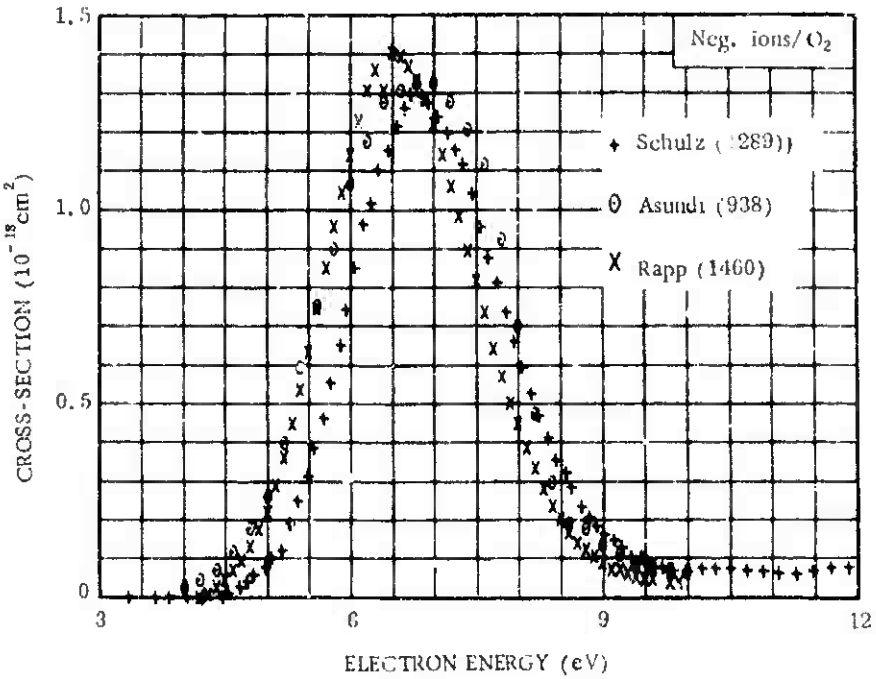


Figure 14-60.

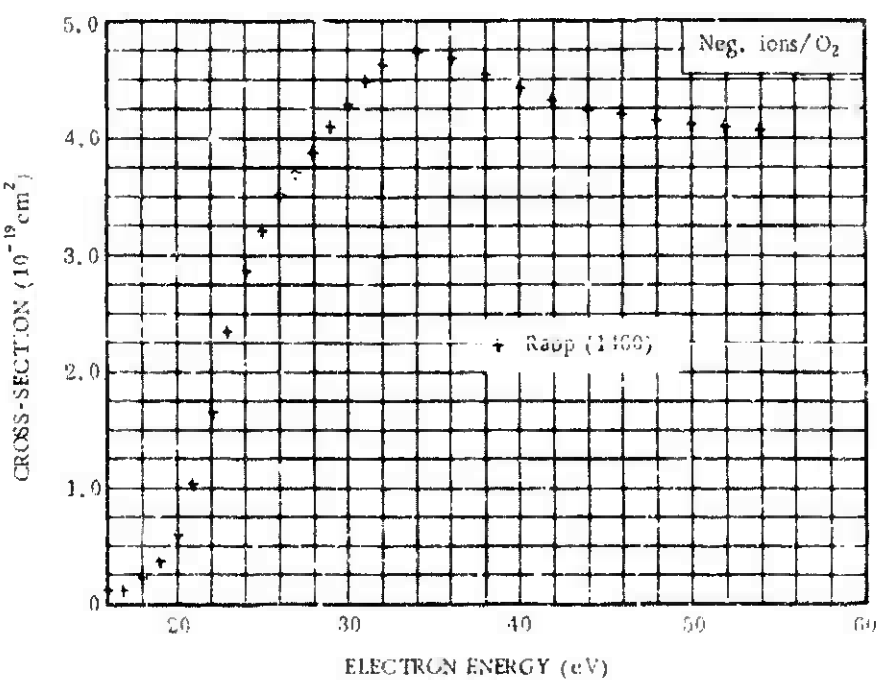


Figure 14-61.

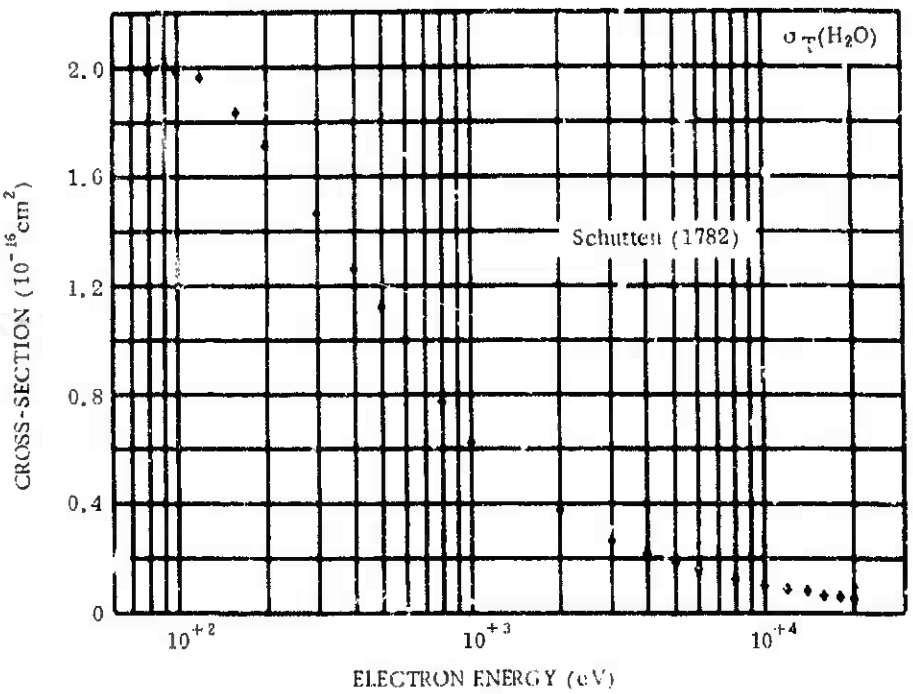


Figure 14-62.

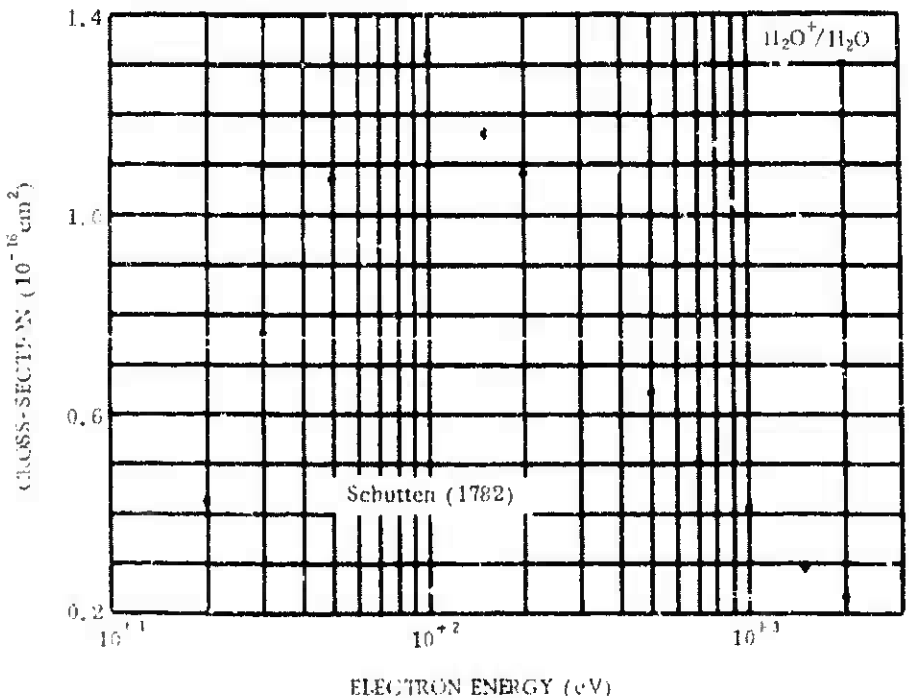


Figure 14-63.

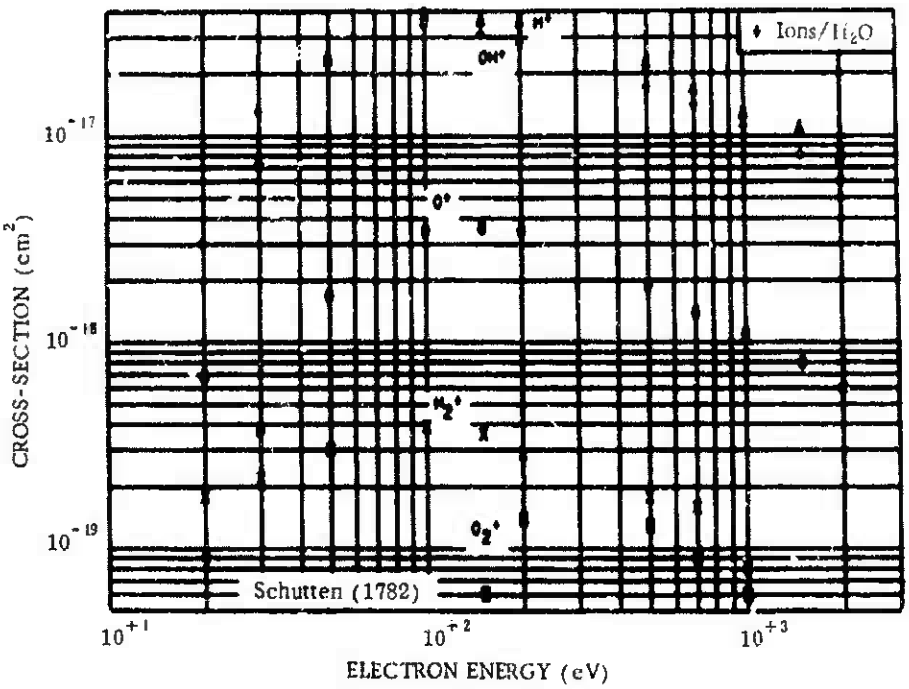


Figure 14-64.

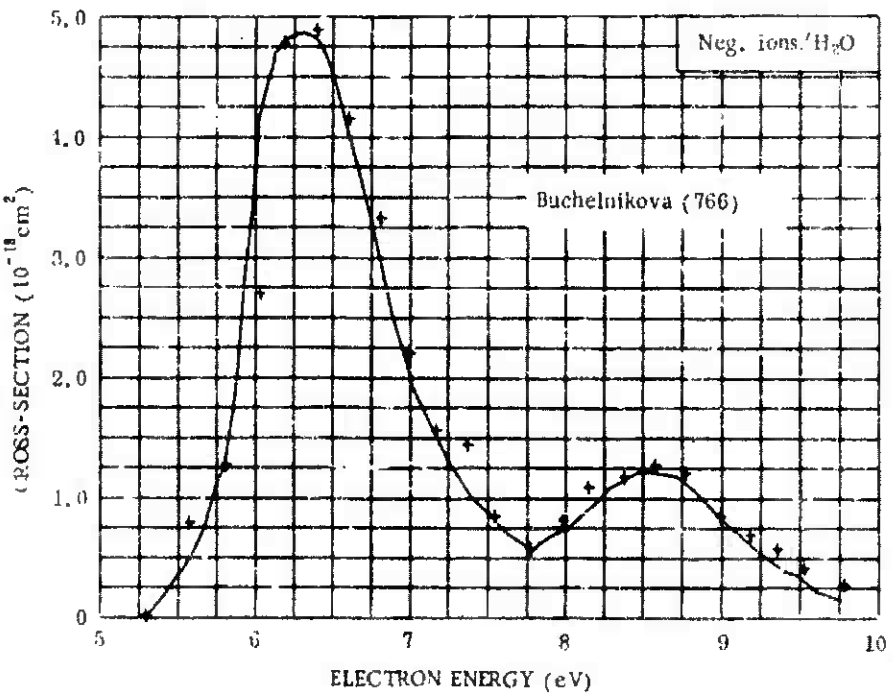


Figure 14-65.

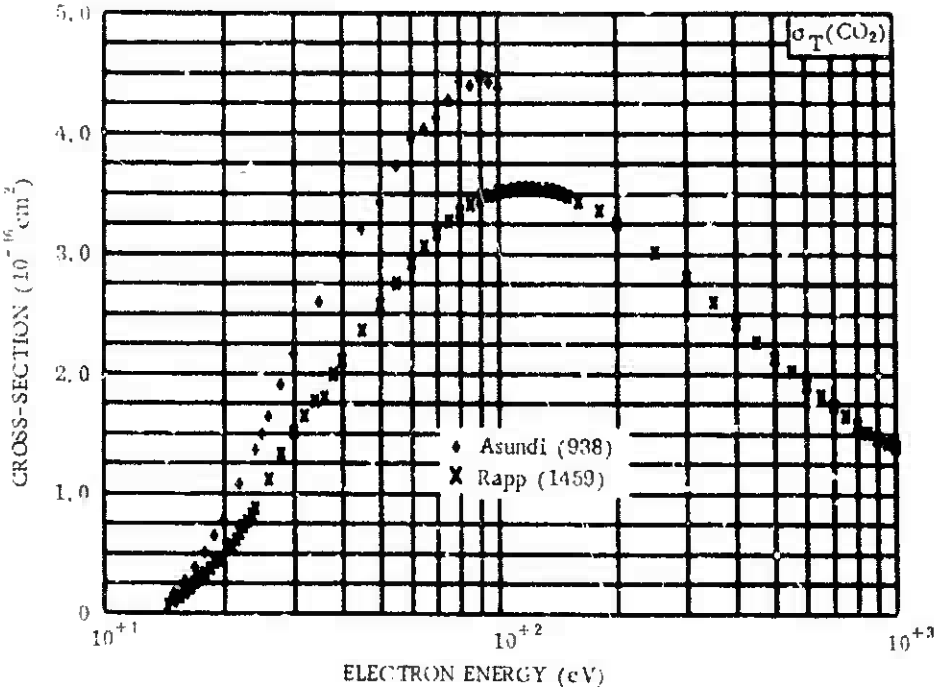


Figure 14-66.

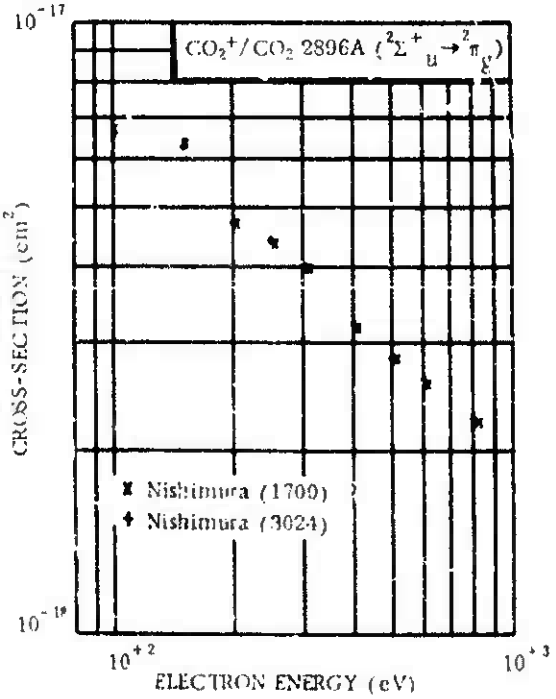


Figure 14-67.

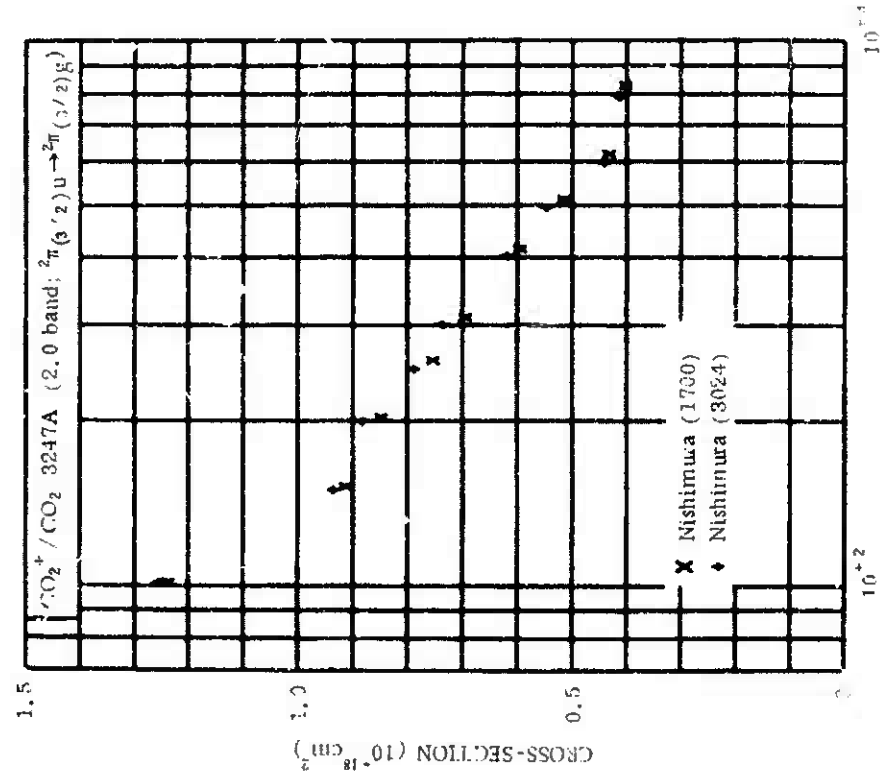


Figure 14-69.

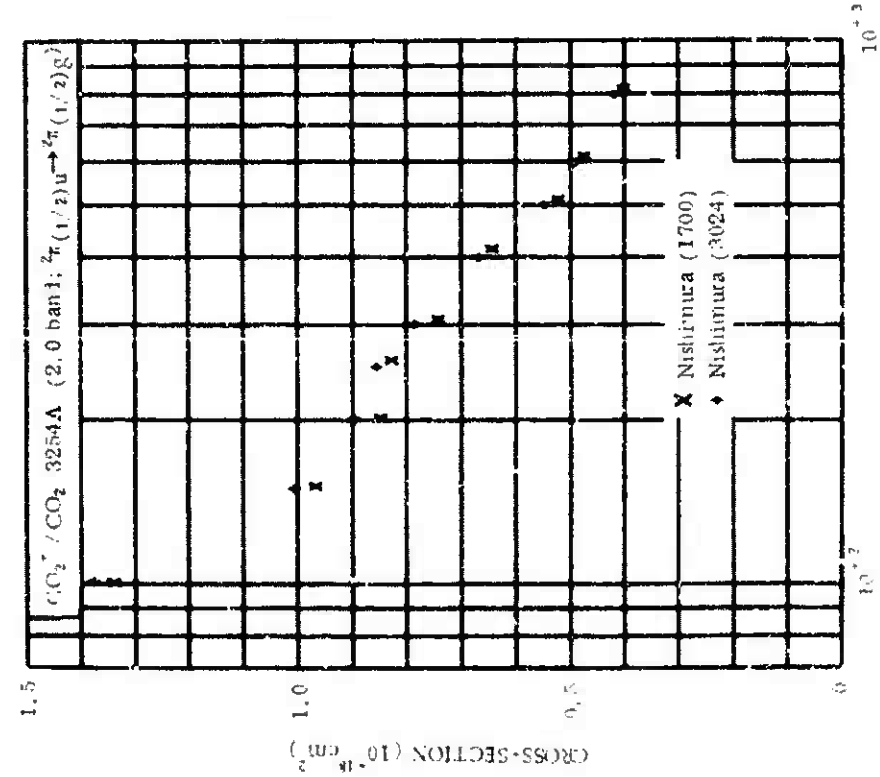


Figure 14-68.

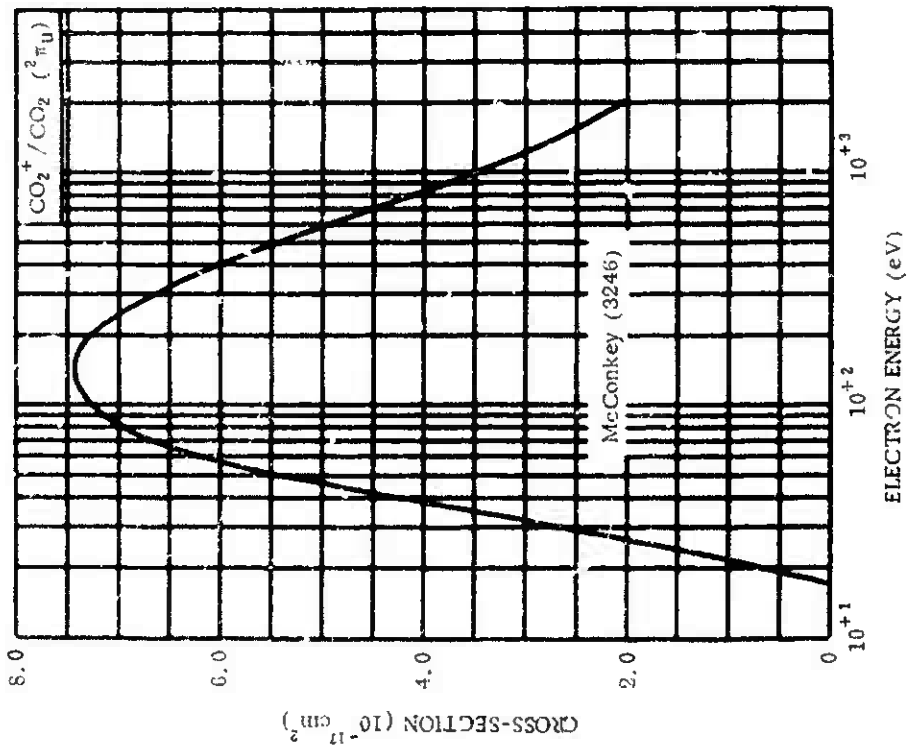


Figure 14-71.

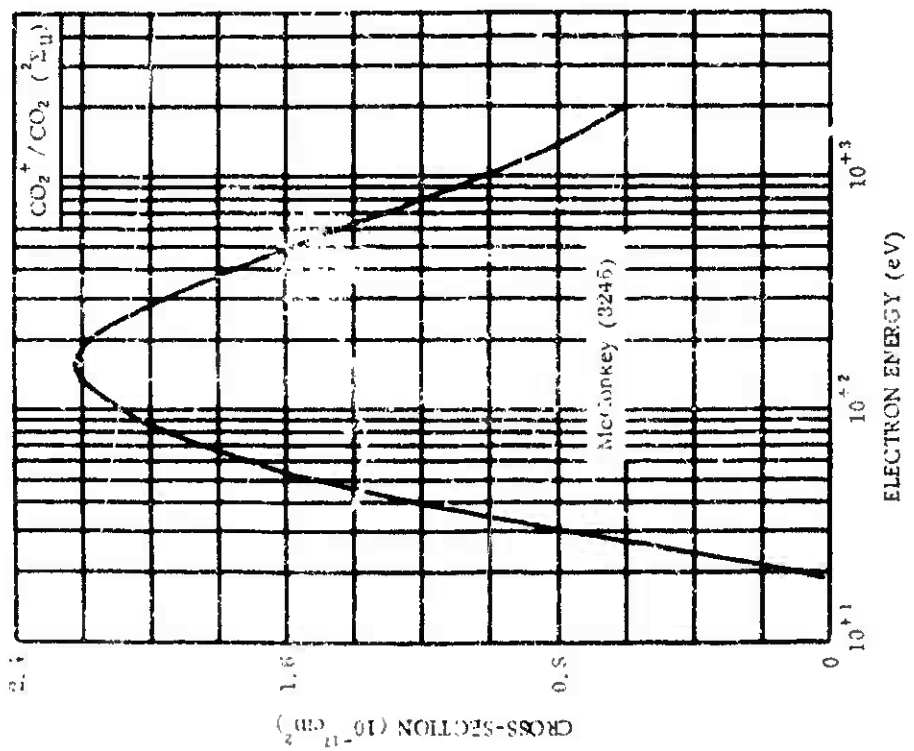


Figure 14-70.

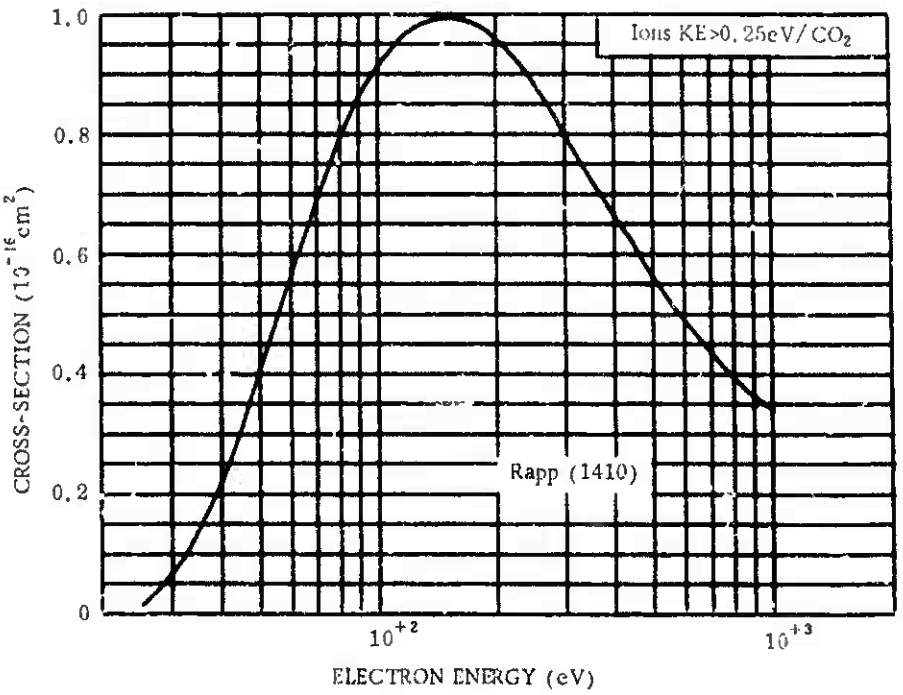


Figure 14-72.

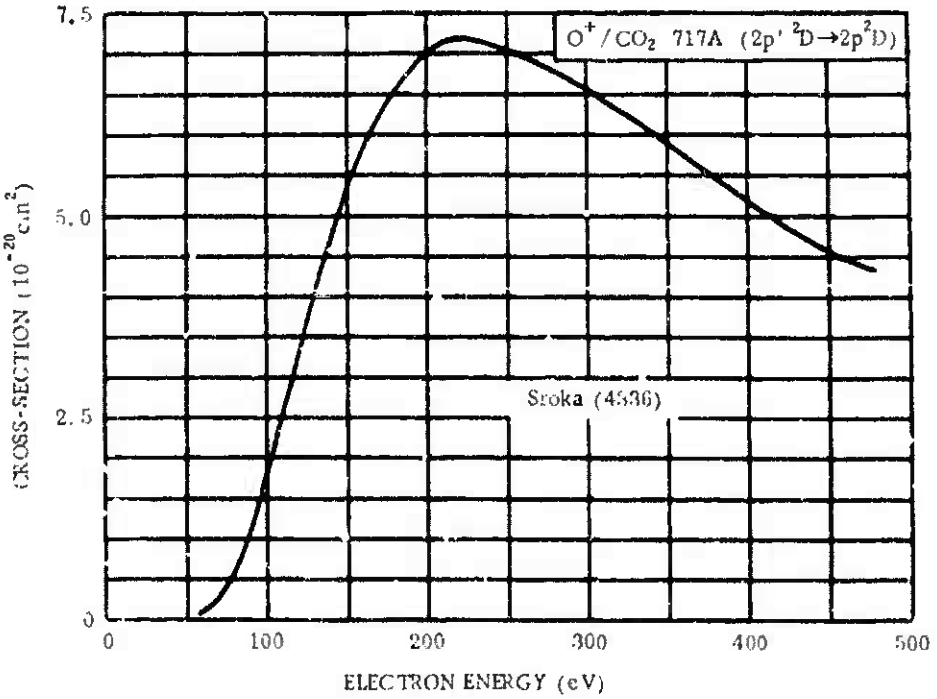


Figure 14-73.

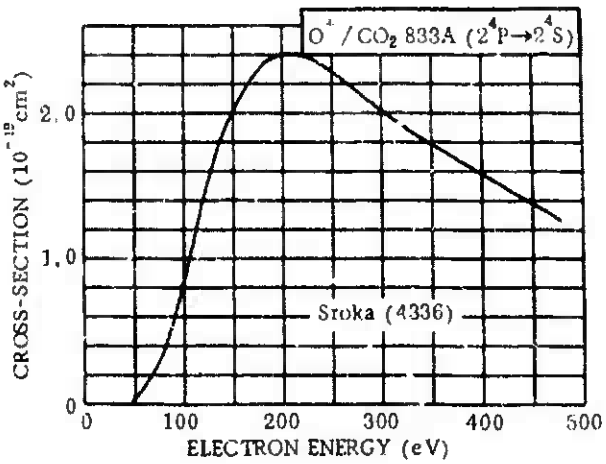


Figure 14-74.

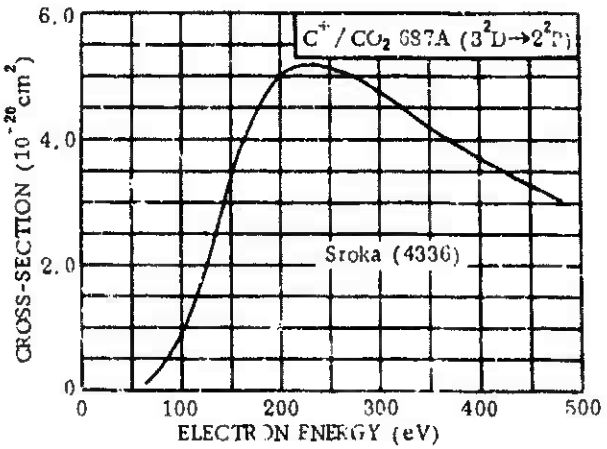


Figure 14-75.

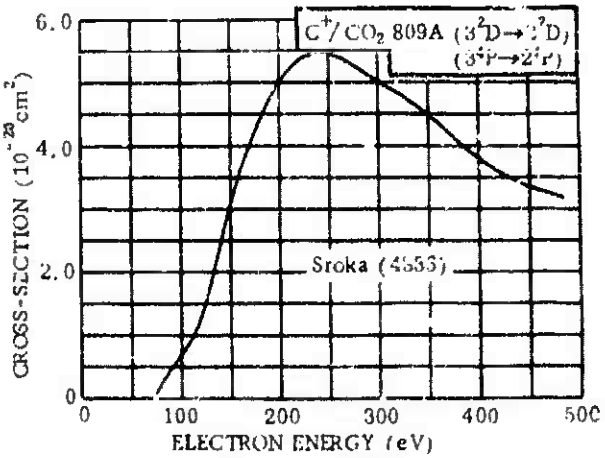


Figure 14-76.

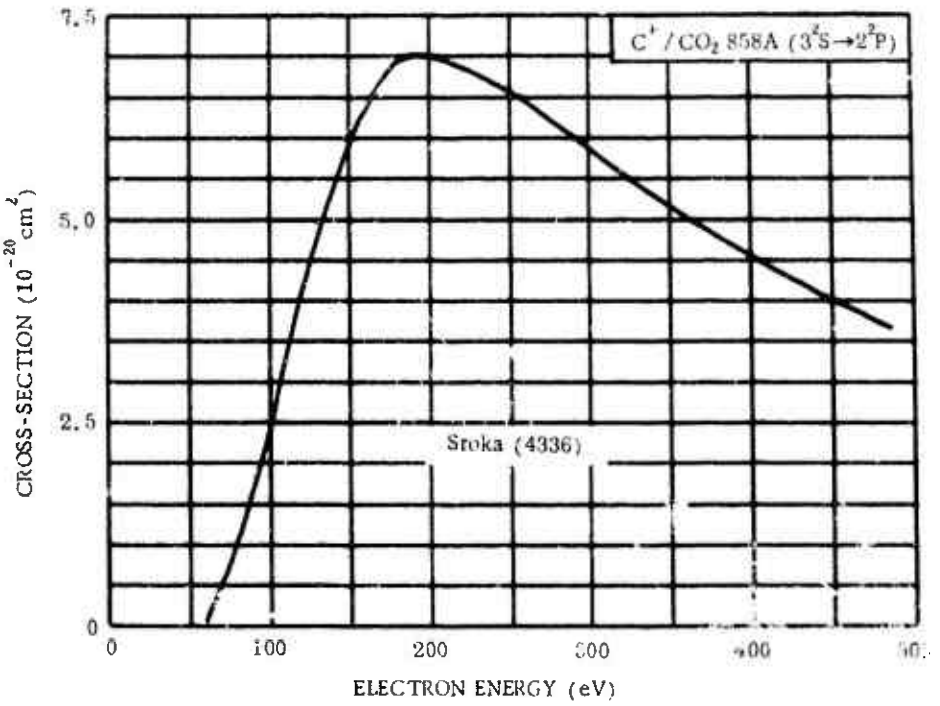


Figure 14-77.

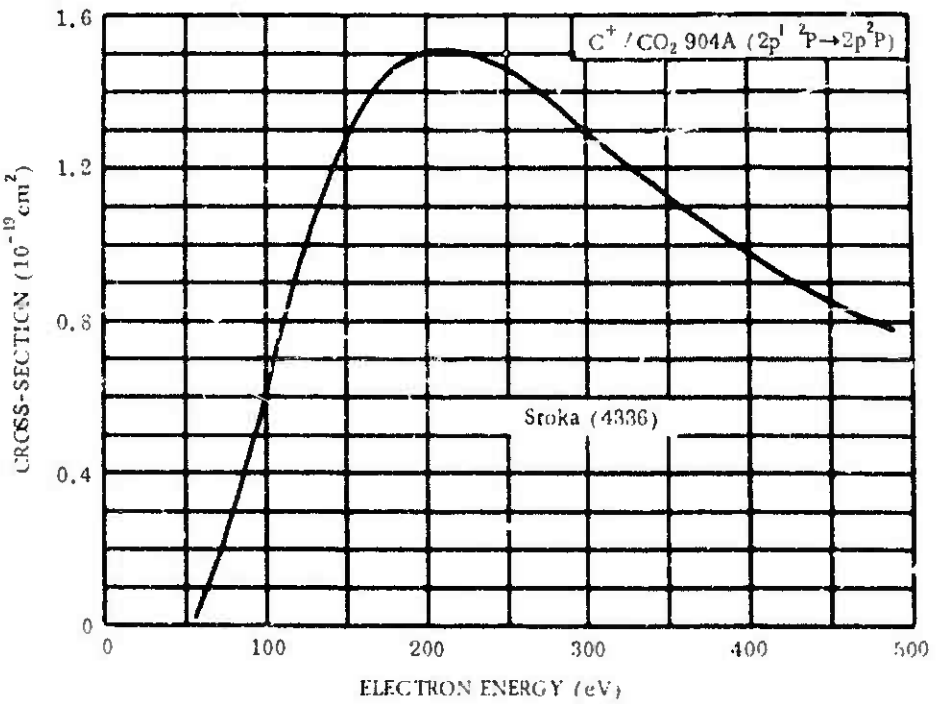


Figure 14-78.

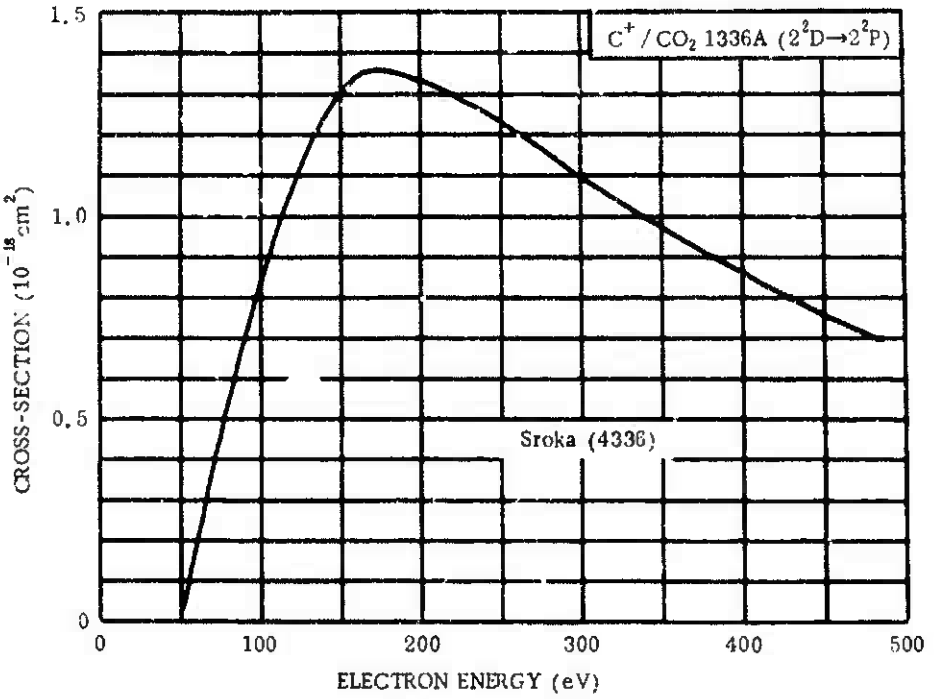


Figure 14-79.

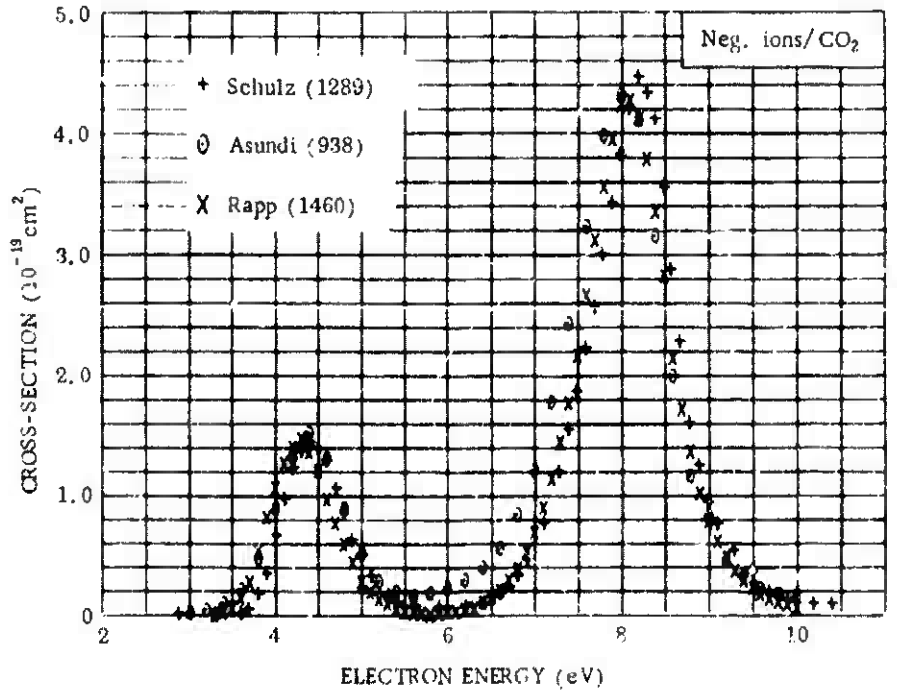


Figure 14-80.

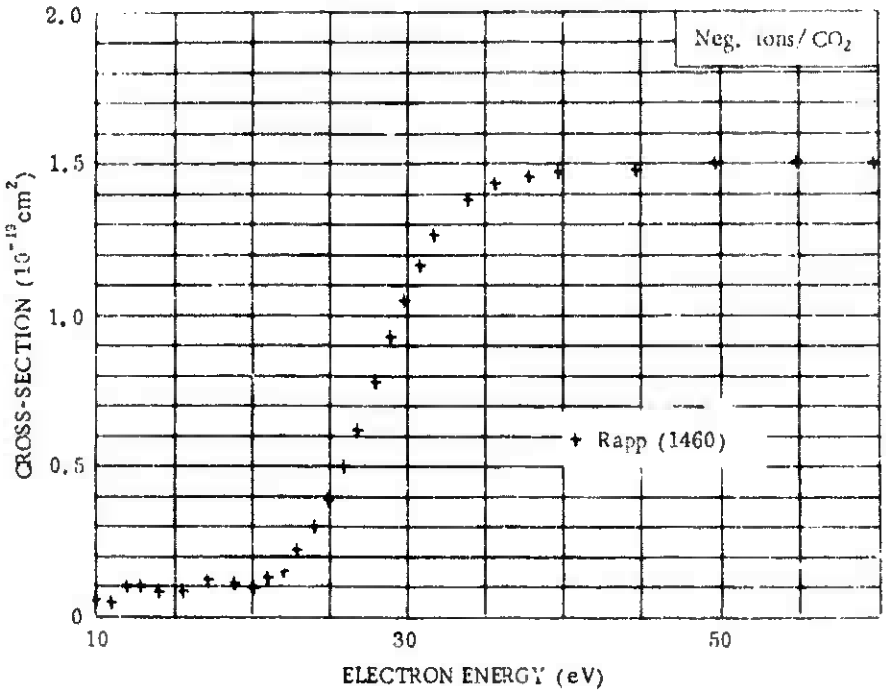


Figure 14-81.

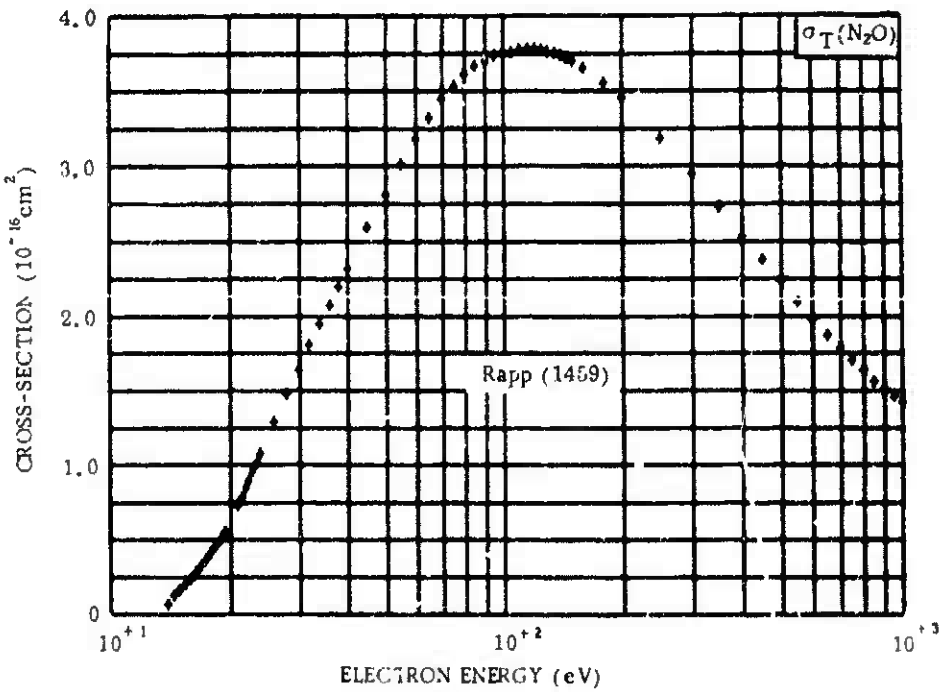


Figure 14-82.

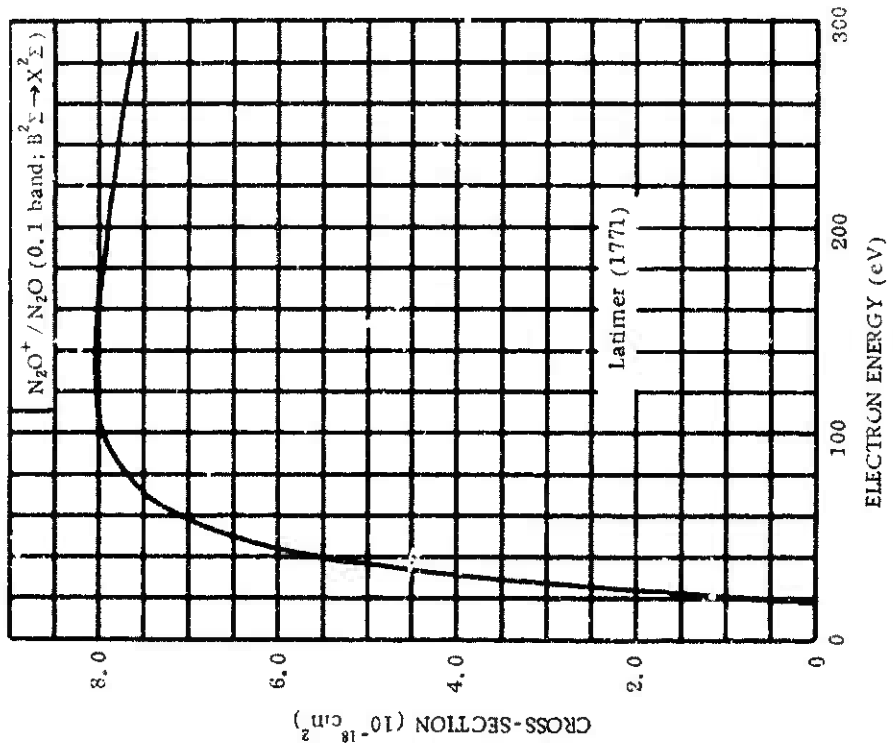


Figure 14-84.

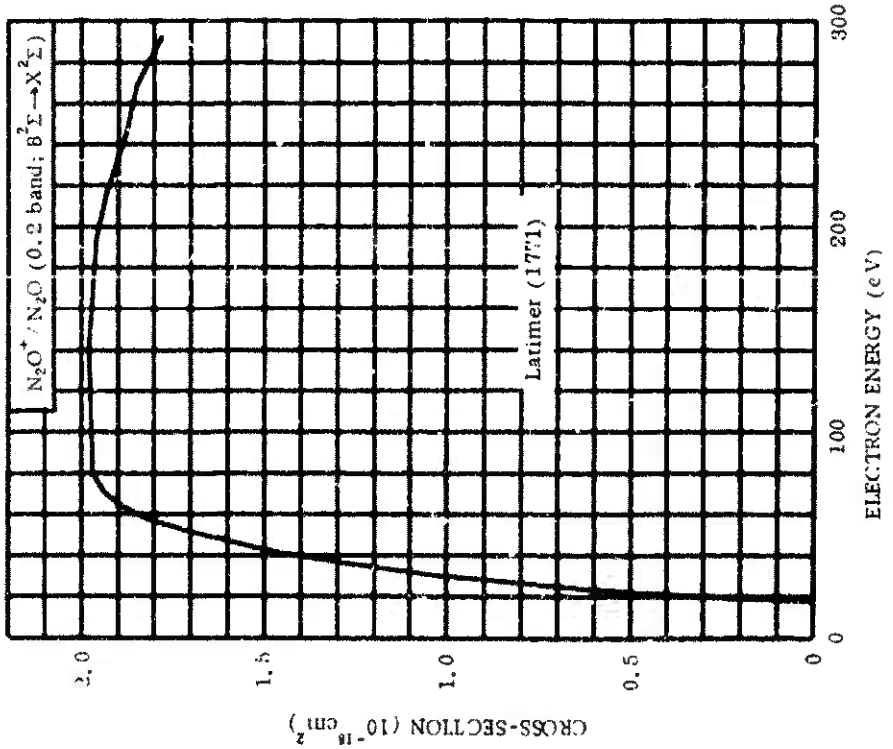


Figure 14-83.

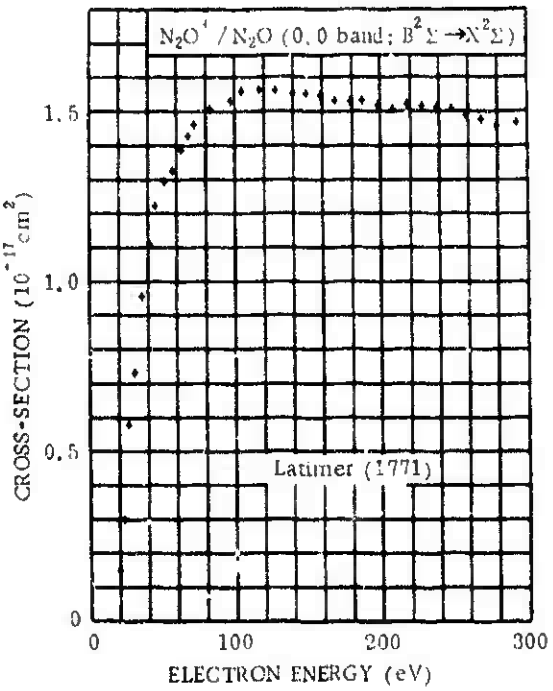


Figure 14-85.

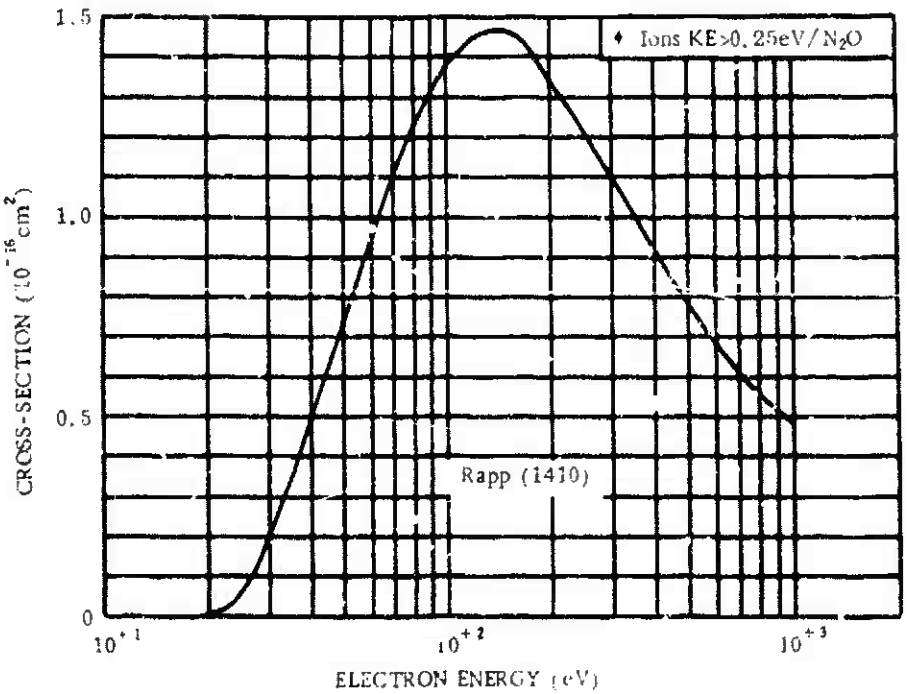


Figure 14-86.

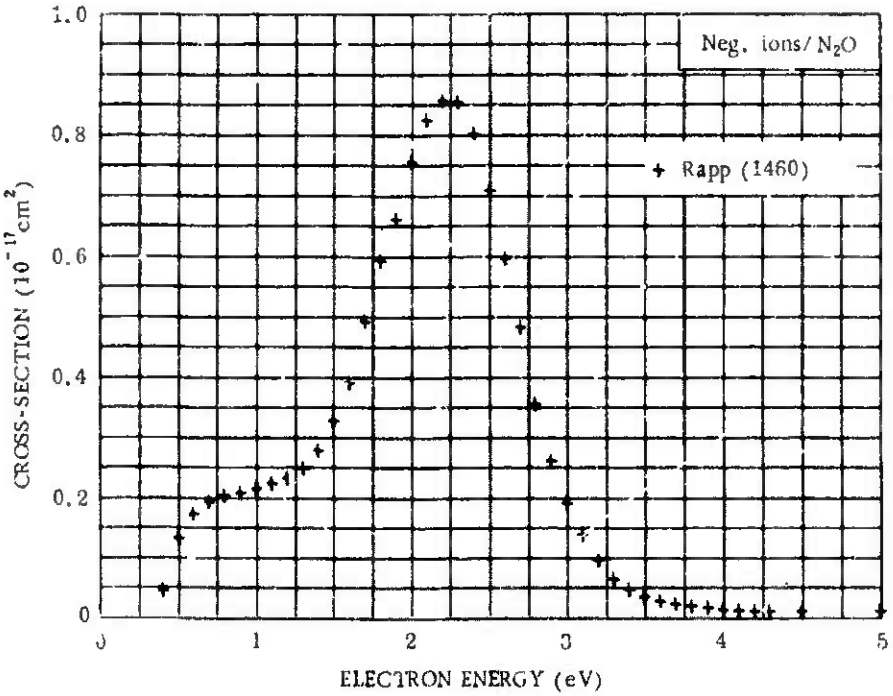


Figure 14-87.

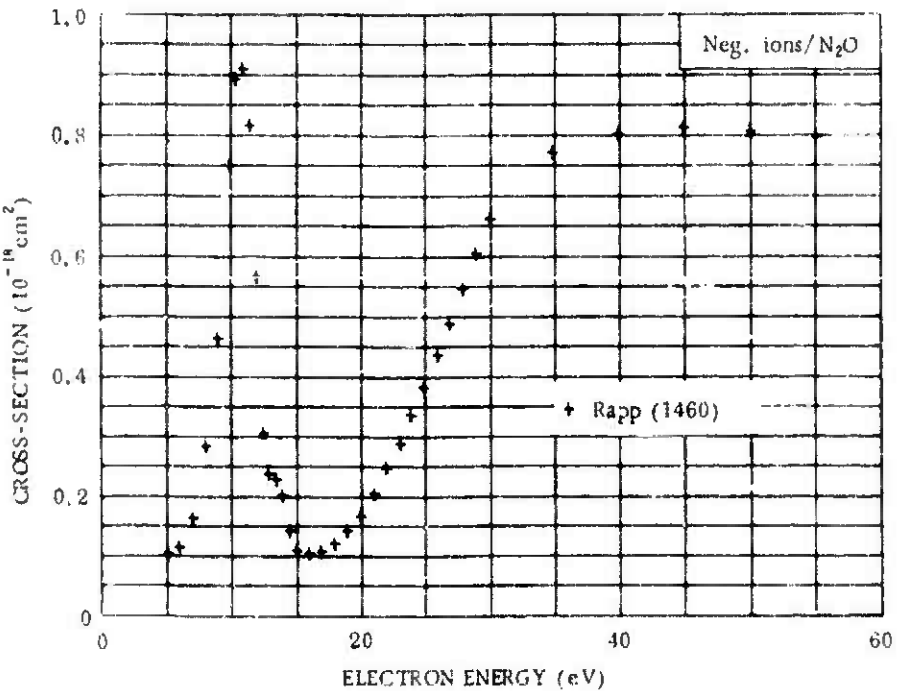


Figure 14-88.

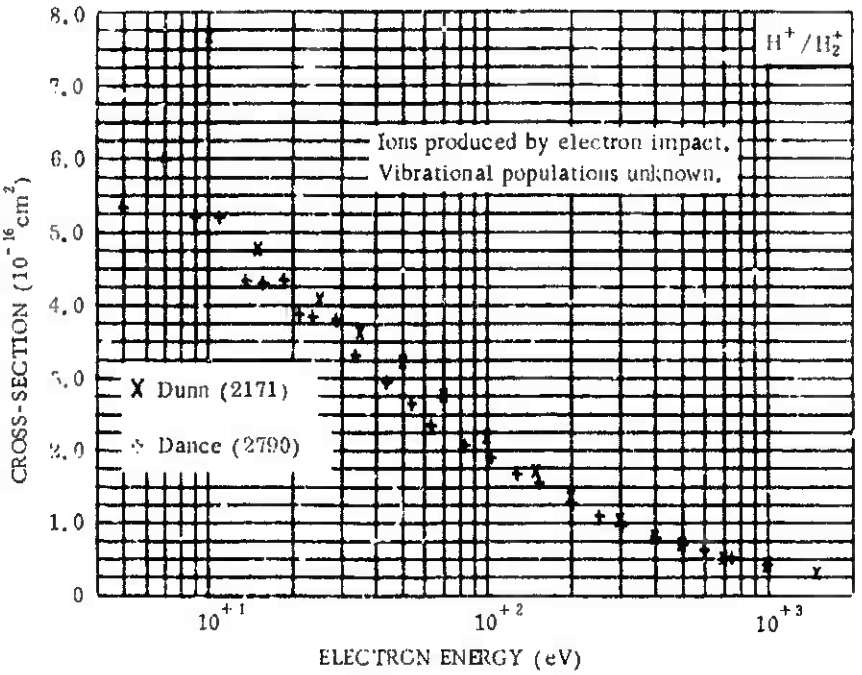


Figure 14-89.

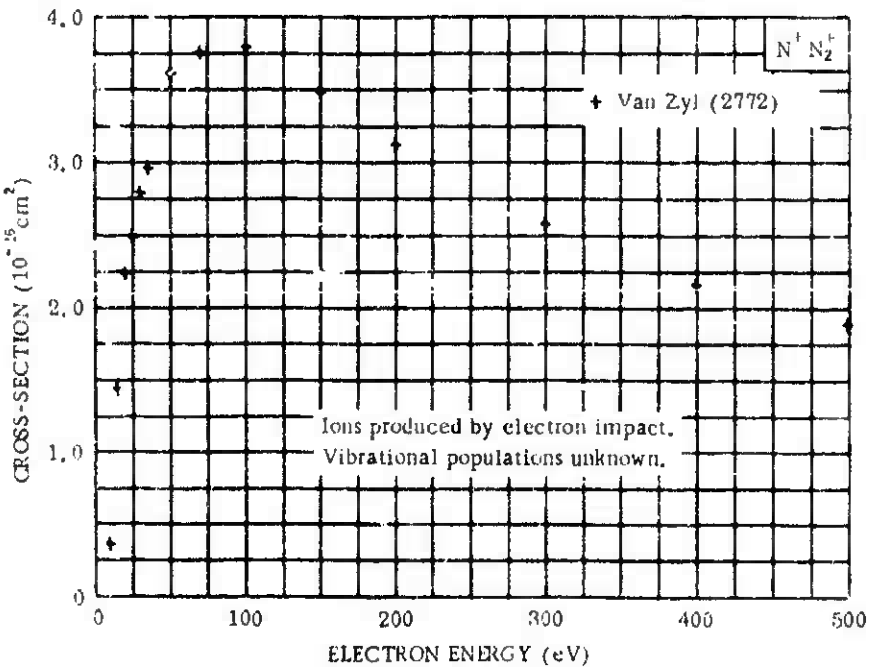


Figure 14-90.

## BIBLIOGRAPHY*

(17) Vaughan, A. L., Phys. Rev. 38, 1687 (1931).

(18) Tate, J. T., and P. T. Smith, Phys. Rev. 39, 270 (1932).

(225) Smith, P. T., Phys. Rev. 36, 1293 (1930).

(261) Harrison, M. F. A., K. T. Dolder, and P. C. Thonemann, Proc. Phys. Soc. 82, 368 (1963).

(320) Fite, W. L., and R. T. Brackmann, Phys. Rev. 112, 1141 (1958).

(323) Fite, W. L., and R. T. Brackmann, Phys. Rev. 113, 815 (1959).

(324)[b] Schulz, G. J., Phys. Rev. 113, 816 (1959).

(333) Stewart, D. T., Proc. Phys. Soc. A69, 437 (1956).

(357) Tozer, B. A., and J. D. Craggs, J. Elec. Control 8, 103 (1960).

(589) Glupe, G., and W. Mehlhorn, Phys. Letts. 25A, 274 (1967).

(684)[a] Haas, R., Z. Physik 148, 177 (1957).

(743) Asundi, R. K., and M. V. Kurepa, J. Elec. Control 15, 41 (1963).

(766)[b] Buchelnikova, N. S., Sov. Phys.-JETP 8, 783 (1959).

(938)[b] Asundi, R. K., J. D. Craggs, and M. V. Kurepa, Proc. Phys. Soc. 82, 967 (1963).

---

* The citation number listed to the left of each entry refers to its JILA Information Center citation number, and should be used in any pertinent correspondence with JILA or with the authors of this chapter.

[a] Vibrational and rotational excitation.

[b] Dissociation processes.

(974) Harrison, H., Thesis, Catholic Univ. of America, Washington, D. C. (1956).

(978) Rothe, E. W., R. Neynaber, L. L. Marino, and S. M. Trujillo, Phys. Rev. 125, 582 (1962).

(984)[a] Schulz, G. J , Phys. Rev. 135, A988 (1964).

(992) Sheridan, W. F., O. Oldenberg, and N. P. Carleton Second Intl. Conf. Phys. Electronic Atomic Collisions, Boulder, Colo., June 1961, W. A. Benjamin, Inc., New York (1961); p. 159.

(1105) Englander-Golden, P., and D. Rapp, Lockheed Missiles and Space Co., Rept. LMSC-6-74-64-12 (1964).

(1106) Boksenberg, A., Thesis, Univ. of London (1961).

(1214) McConkey, J. W., J. M. Woolsey, and D. J. Burns, Planet. Space Sci. 15, 1332 (1967).

(1268) Smith, A. C. H., E. W. Rothe, E. Caplinger, R. Neynaber, and S. M. Trujillo, Phys. Rev. 127, 1647 (1962).

(1281) Schram, B. L., F. J. DeHeer, M. J. van der Wiel, and J. Kistemaker, Physica 31, 94 (1965).

(1289)[b] Schulz, G. J., Phys. Rev. 128, 178 (1962).

(1410) Rapp, D., D. D. Briglia, and P. Englander-Golden, J. Chem. Phys. 42, 4081 (1965).

(1451)[b] Rapp, D., D. D. Briglia, and T. E. Sharp, Phys. Rev. Letts. 14, 533 (1965).

(1459) Rapp, D., and P. Englander-Golden, J. Chem. Phys. 43, 1464 (1965).

(1460)[b] Rapp D., and D. D. Briglia, J. Chem. Phys. 43, 1480 (1965).

(1504) McConkey, J. W., and I. D. Latimer, Proc. Phys. Soc. 86, 463 (1965).

(1566)[b] Corrigan, S. J. B., J. Chem. Phys. 43, 4381 (1965).

(1700) Nishimura, H., J. Phys. Soc. Japan 21, 564 (1966).

(1771) Latimer, I. D., and J. W. McConkey, Proc. Phys. Soc. 86, 745 (1965).

(1782) Schutten, J., F. J. De Heer, H. R. Moustafa, A. J. H. Boerboom, and J. Kistemaker, J. Chem. Phys. 44, 3924 (1966).

(1838) Nishimura, H., J. Phys. Soc. Japan 21, 1018 (1966).

(1863) Schram, B. L., Thesis, Univ. of Amsterdam (1966).

(2171)[b] Dunn, G. H., and B. van Zyl, Phys. Rev. 154, 40 (1967).

(2763)[b] Schulz, G. J., and R. K. Asundi, Phys. Rev. 158, 25 (1967).

(2772)[b] van Zyl, B., and G. H. Dunn, Phys. Rev. 163, 43 (1967).

(2784) McGowan, J. W., M. A. Fineman, E. M. Clarke, and H. P. Hanson, General Atomic, Preprint GA-7387. Pt. 1 (1967).

(2785) Holland, R. F., Los Alamos Scientific Lab. Rept. LA-3783 (1967).

(2788) Dance, D. F., M. F. A. Harrison, and R. D. Rundel, Proc. Roy. Soc. A299, 525 (1967).

(2790)[b] Dance, D. F., M. F. A. Harrison, R. D. Rundel, and A. C. H. Smith, Proc. Phys. Soc. 92, 577 (1967).

(2904) Tisone, G. C., and L. M. Branscomb, Phys. Rev. 170, 169 (1968).

(2923) Fowler, R. G., C. C. Lin, and R. M. St. John, Air Force Weapons Lab., Report AFWL-TR-66-132 (1967).

(2954) McGowan, J. W., M. A. Fineman, E. M. Clarke, and H. P. Hanson, Phys. Rev. 167, 52 (1968).

(3024) Nishimura, H., J. Phys. Soc. Japan 24, 130 (1968).

(3246) McConkey, J. W., D. J. Burns, and J. M. Woolsey, J. Phys. B1, 71 (1968).

(3252)[a] Ehrhardt, H., and F. Linder, Phys. Rev. Letts. 21, 419 (1968).

(3387) Korol, V. I., S. M. Kishko, and V. V. Skubenich, Ukr. Fiz. Zh. 13, 1225 (1968).

(3524) Srivastava, B. N., and I. M. Mirza, Phys. Rev. 176, 137 (1968).

(3687) Aarts, J. F. M., F. J. De Heer, and D. A. Vroom, Physica 40, 197 (1968).

(3710) Stanton, P. N., and R. M. St. John, J. Opt. Soc. Am. 59, 252 (1969).

(3769) Srivastava, B. N., and I. M. Mirza, Can. J. Phys. 47, 475 (1969).

(3833) Sroka, W., Z. Naturforsch. 24a, 398 (1969).

(3943) Srivastava, B. N., J. Quant. Spectry. Radiative Transfer 9, 1639 (1969).

(3981) Simpson, F. R., and J. W. McConkey, Planet. Space Sci. 17, 1941 (1969).

(4080) Borst, W. L., and E. C. Zipf, Jr., Phys. Rev. A1, 834 (1970).

(4083) Koval, A. G., V. T. Koppe L. I. Proshchak, and Ya. M. Fogel. Opt. and Spectry. 27, 198 (1969).

(4125) Borst, W. L., and E. C. Zipf, Jr., Phys. Rev. A1, 1410 (1970).

(4220) Aarts, J. F. M., and F. J. De Heer, J. Chem. Phys. 52, 5354 (1970)

(4326) Lawrence, G. M., Phys. Rev. A2, 397 (1970).

(4336) Sroka, W., Z. Naturforsch. 25a, 1434 (1970).

(4344) Peart, B., D. S. Walton, and K. T. Dolder, J. Phys. B3, 1346 (1970).

# 15. KINETICS OF HIGH-ENERGY HEAVY-PARTICLE COLLISIONAL PROCESSES

W.L. Fite, University of Pittsburgh
J.S. Greene, Jr., Air Force Weapons Laboratory
A.W. Ali, Naval Research Laboratory
I.M. Pikus, General Electric Company

(Latest Revision 28 September 1971)

## 15.1 INTRODUCTION

High-energy particle and photon interactions are of fundamental importance for auroral geophysics, planetary and stellar atmospheres, thermonuclear experiments, and nuclear-weapon debris-air interactions, to name a few. In comparison to the low-energy regime, relatively little exists in the way of any comprehensive review or compilation of work on extrathermal-particle interactions. Historically the study of high-energy heavy-particle processes has differed in an operational way from the studies of thermal and low-energy interactions. Interest has generally been directed toward securing specific cross-sections for application to specific physical and engineering problems. Extensive, but quite clean, experimental techniques are available and occasionally simplified theoretical approximations are valid. The objective of this chapter is to provide a limited collection of results and methods of obtaining results for certain high-energy heavy-particle collision processes of particular interest in the early-time interaction of nuclear-weapon debris with the atmosphere above an altitude of about 100 km. The projectiles of interest are weapon materials such as Fe, Al, and U, fission fragments, and atmospheric species (mainly O and N). The projectiles may be singly and sometimes doubly charged. The targets considered are O, $N_2$, and $O_2$, with considerable emphasis on O. An enormous body of information has been published on collisions involving light particles (H, He, and Li) and the inert gas atoms. The work has been covered by a number of reviews (References 15-1 through 15-6) and for the most part is not discussed here. The heavy-particle interaction processes of electron capture and loss, slow-ion production, and electron production are

considered. Other processes which are known to be, or may prove to be important to high-altitude nuclear-debris motion and effects, such as inner-shell excitation, photon processes, electron collisions, and nonequilibrium chemical kinetics are not considered. There is a recognized need (Reference 15-7) for these subjects to be expanded into a separate handbook on extrathermal collision processes.

## 15.2 CROSS-SECTION DEFINITIONS

The type of process of interest involves the collision of a fast primary particle with i positive electronic charges (including i = 0), $A^{i+}$, and a stationary neutral target particle B, and can be represented by:

$$A^{i+} + B \rightarrow A^{j+} + B^{n+} + (j + n - i)e \quad . \tag{15-1}$$

The cross-section, $Q_{ij}^{0n}$, is defined in terms of the number of secondary particles produced per unit time according to the equation:

$$\frac{dA^{j+}}{dt} = \frac{dB^{n+}}{dt} = Q_{ij}^{0n} \cdot n_B I_1 \cdot dx \quad . \tag{15-2}$$

where $n_B$ is the number density (particles per unit volume) of target particles B, $I_1$ is the total number of primary particles $A^{i+}$ passing through the target per unit time, and dx is the distance of the primary particle beam through the target.

The "electron capture-and-loss cross-sections" are defined by:

$$\sigma_{ij} = \sum_n Q_{ij}^{0n} \quad , \tag{15-3}$$

and represent the total cross-section for the fast particle changing from i+ to j+, irrespective of the change of charge of the originally neutral target particle. Measurements of $\sigma_{ij}$ are performed by examination of the charge state j of fast particles after a beam with initial charge i traverses a gas target.

When slow charged particles are collected, as with a parallel-plate condenser method of detection, and total currents are mea-

sured, the "total slow positive-charge-production cross-sections":

$$Q_+ = \sum_j \sum_n n\, Q_{ij}^{0n} \quad , \tag{15-4}$$

are determined. These are weighted sums of the cross-sections for raising the target particle to all charge states, irrespective of the change of charge on the initially fast particle.

When electrons are collected at a condenser plate, the "electron production cross-section":

$$Q_- = \sum_j \sum_n (j + n - i)\, Q_{ij}^{0n} \quad , \tag{15-5}$$

is obtained.

The "charge-transfer cross-section" is, strictly speaking, $Q_{ij}^{0n}$ where $i = n + j$. Most commonly, the term is used when $i = 1$, i.e., to describe the cross section $Q_{10}^{01}$. It is evident that at sufficiently low energies, production of free fast electrons from either the fast or the slow particles does not occur, so that in the limit of low energies $\sigma_{10} = Q_{10}^{01}$ also.

When the slow ions are separated by a mass-spectrometric detector the "specific slow-ion-production cross-sections" are measured. These are:

$$Q_n = \sum_j Q_{ij}^{0n} \quad . \tag{15-6}$$

The slow ions include products of dissociative ionization in the case of molecular target gases as well as multiply charged ions of the target species itself. Because of the difficulty of ensuring total collection of slow ions into a mass-spectrometric device, it is common to measure $Q_+$ and then in a separate experiment using mass-spectrometric detection to measure ratios of the various slow ions formed.

"Electron stripping cross-sections from neutrals" $\sigma_{0j}$ defined from Equation (15-3) by $\sigma_{0j} = \sum_n Q_{0j}^{0n}$, experimentally require the production of initially fast particle beams of neutrals. A cross-

section (unnamed), designated by:

$$q_0 = \sum_j \sigma_{0j} \quad , \tag{15-7}$$

which at low energies approximates $\sigma_{01}$ , can be obtained using initially singly-charged ion beams and thickened targets. (See Reference 15-8, pages 3 and 4, for details.)

The term "ionization cross-section" is ambiguous in heavy-particle collisions. Analogy with electron-impact collisions would require that ionization cross-sections be given by $Q_{ii}^{0n}$ . Only in very rare cases can this one cross-section be isolated from concurrent processes in which j is not equal to i , i.e., electron capture by and loss (stripping) from the initial fast particle.

## 15.3 EXPERIMENTAL METHODS

Experiments on fast heavy-particle collisions are designed very closely in accordance with the cross-section definition (Equation 15-2). Ions produced in an appropriate ion source are accelerated, mass-selected to obtain the single desired species or charge state, and then passed through a collision chamber containing the target gas. For fast-particle detection, the emerging fast particles are separated by a transverse electric or magnetic field and the currents of the separately dispersed beams are measured. In slow-particle detection, the basic technique is to use two parallel plates on opposite sides of the collision chamber and by means of an electric field between the plates to draw the ions to one plate and the electrons to the other, where their respective electric currents are measured. Determination of the species of slow ions formed is made by drawing a sample of ions from the collision chamber into a mass spectrometer to determine charge-to-mass ratio.

When the initial fast particle is to be neutral, an initial ion beam is passed through either a gas or solid foil, where some of the ions become neutralized through electron-capture processes. A transverse field then removes the charged species leaving only the neutral component to enter the collision chamber. A variation of this technique is used to produce initial beams of charge state higher than can be easily formed in the ion source.

In most cases little care is taken with regard to the internal energy state of the fast ion beam, although it has been found, in experi-

ments using sources with controlled electron-impact ionization of vapors, that some cross-sections vary significantly with internal energy states of the reactants.

The subject of energy states of the final products in high-energy heavy-particle collisions has received very little attention to date, a major activity being the observation of characteristic radiation, e.g., excitation of the first-negative bands of $N_2^+$ (References 15-9, 15-10).

## 15.4 THEORETICAL METHODS

The theory of high-energy heavy-particle collisions is complicated by two features. First, the colliding particles are many-electron systems. Second, although the energies are high, the massiveness of the particles places the relative velocities in the awkward range of being neither "high" nor "low", where certain simplifications can be generated. Theoretical treatment has to a great extent depended upon the generation of what D. R. Bates has called "bold approximations", several of which are summarized in this section.

While the failure of experiment has generally been that only sums of cross-sections, involving both single and multiple electron exchanges, are measured, theory has been almost completely limited to electron capture and loss processes in which a single electron is involved, and has rarely treated the multiple processes which experiments indicate become important at the higher energy ranges of interest. Because of the limitations of both theory and experiment, it is often difficult to compare predictions and experimental results. Nonetheless, it is evident from such comparisons as are illustrated in this section, that for some processes and collision partners, certain approximations appear to give better reliability than others. Because it is extremely difficult to measure experimental cross-sections with certain collision partners, e.g., whenever atomic nitrogen is the target gas, it is important to have reliable, and preferably simple, methods to obtain theoretical cross-section values.

### 15.4.1 Classical

The simple classical models for charge-transfer collisions at high energies developed by Bohr and Lindhard (References 15-11, 15-12), Bell (Reference 15-13), Gluckstern (Reference 15-14), and

Thomas (Reference 15-15), have been reviewed by Dalgarno et al (Reference 15-16), and Florance (Reference 15-17). These models predict a slower variation of cross-section with velocity than observed and do not provide any insight into the observed dependence on the projectile charge. Since these reviews, two significant classical calculations of charge-exchange cross-sections using classical methods have appeared in the literature (Reference 15-18).

Bates and Mapleton Model: In the original Thomas theory (Reference 15-15) the charge-exchange cross-section was proportional to a quantity C which was taken to be a constant ($\cong 3.49$) at high velocities. Bates and Mapleton (Reference 15-19) generalized the Thomas model to include the velocity dependence of C in which C is principally a function of the ratio of the impact velocity to the escape velocity of the active electron from the target atom. The Bates-Mapleton prediction of $Q_{10}^{01}$ cross-sections for $Al^+ + O$ and $Fe^+ + O$ near MeV energies are compared with experimental data (Reference 15-10) in subsection 15.4.3.1, below.

Binary Encounter Theory: The validity of the classical approach derives from the correspondence principle and the Rutherford scattering identity (Reference 15-20). The correspondence principle, well known from the foundation of quantum mechanics, was discussed in its application to inelastic scattering by Garcia (Reference 15-21). He showed explicitly that, as expected, in the limit of large principal quantum numbers, the Born approximation to the cross-section for the ionization of hydrogen by electrons approaches the classical expression. The Rutherford identity concerns the fact that scattering of particles by an inverse-square-law force is described classically and quantum-mechanically with identical cross-sections (Reference 15-20). Neither factor explains the success of classical theory in cross-section prediction for complex atomic collisions, i.e., those for which many excitable degrees of freedom exist.

Application of the classical approach to complex systems was spurred on by the works of Gryzinski (References 15-22 through 15-25). In this method, the cross-section is determined by first computing the differential cross-section for energy exchange between the incoming projectile and the general bound electron of the target atom, then summing over all the bound electrons, and finally integrating over the energy range involved. The calculation assumes that no significant interactions occur among the bound electrons during the collision. This implies the invalidity of collisions so slow

that rearrangement among the atomic electrons can occur during the collision process.

Consider an incident ion of mass $m_1$, charge $Z_1 e$, and velocity $v_1$, and a target atom whose general bound electron has mass $m_e$, charge $-e$, and velocity $v_e$. The incident ion has a kinetic energy $E_2$ and the bound electron has kinetic energy $E_e$ and potential energy $U_e$. During the collision an energy in the amount $\Delta E$ is transferred from the projectile to the target electron. The cross-section for the transfer of energy $\Delta E$ is given by (Reference 15-26):

$$\frac{3v_1^2 v_e}{\pi e^4} \int_{\Delta E} \sigma_{\Delta E}^{eff} \, d(\Delta E) = -\left[\frac{2v_e^3}{(\Delta E)^2} + \frac{6v_e}{m_e(\Delta E)}\right] \text{ if } 0 < \Delta E < b$$

$$= \left[3\left(\frac{v_1 m_e - v_e m_1}{\Delta E m_1 m_e}\right) + \frac{\left(v_e'^3 - v_e^3\right) - \left(v_1'^3 + v_1^3\right)}{(\Delta E)^2}\right] \text{ if } b < \Delta E < a \qquad (15\text{-}8)$$

$$= -\frac{2v_1}{(\Delta E)^2} \text{ if } \Delta E > a \text{ and } m_e v_e > (m_1 - m_e)v_1$$

$$= 0 \text{ if } \Delta E > a \text{ and } m_e v_e < (m_1 - m_e)v_1 \ ,$$

where:

$$a = \frac{4 m_1 m_e}{(m_1 + m_e)^2}\left[E_1 - E_2 + \frac{v_1 v_e}{2}(m_1 - m_e)\right] \ ; \qquad (15\text{-}9)$$

$$b = \frac{4 m_1 m_e}{(m_1 + m_e)^2}\left[E_1 - E_2 - \frac{v_1 v_e}{2}(m_1 - m_e)\right] \ ; \qquad (15\text{-}10)$$

$$v_1' = \left[v_1^2 - 2(\Delta E)/m_1\right]^{1/2}; \ v_e' = \left[v_e^2 + 2(\Delta E)/m_e\right]^{1/2} . \qquad (15\text{-}11)$$

Making the classical assumption that for bound electrons:

$$U_e = m_e v_e^2 \quad , \tag{15-12}$$

allows the averaging over velocities to be replaced by an averaging over the potential distribution in the atom. These relationships have been explored numerically in several specific cases for ionization of neutrals and ions and charge transfer by proton impact (Reference 15-27).

The classical model has been applied to the case of ion-atom charge transfer (Reference 15-28). The results of a comparison with experimental data are summarized in Table 15-1.

Table 15-1. Comparison of classical theoretical predictions with experimental data for ion-atom charge transfer. (See Reference 15-28 for more detail.)

| System | Velocity Range Considered (cm/sec) | Range for Good Agreement (cm/sec) | Remarks |
|---|---|---|---|
| $Be^+$ on Ar | $(5 - 8) \times 10^7$ | None | Predicted value exceeds by a factor of 2. |
| $I^+$ on Ar | $(2 - 4) \times 10^7$ | $(2 - 2.5) \times 10^7$ | Predicted exceeds by as much as a factor of 4. |
| $Sr^+$ on Ar | $(0.2 - 2) \times 10^8$ | $(0.5 - 1) \times 10^8$ | Predicted is lower at lower speeds and at higher speeds. |
| $K^+$ on Ar | $(0.6 - 3) \times 10^8$ | $(0.8 - 2) \times 10^8$ | Predicted is low at low speeds and high at high speeds. |
| $U^+$ on Ar | $(0.3 - 1.2) \times 10^8$ | At $4 \times 10^7$ and $1.1 \times 10^8$ only. | Predicted is too low at low speeds, too high at high speeds, and too high in between. |
| $N^+$ on Ar | $(2 - 4.2) \times 10^8$ | $(3 - 4.2) \times 10^8$ | Predicted is too high at low speeds. |

Table 15-1. (Cant d.)

| System | Velocity Range Considered (cm/sec) | Range for Gaad Agreement (cm/sec) | Remorks |
|---|---|---|---|
| $U^+$ on Ne | $(0.6 - 1.2) \times 10^8$ | $\sim 1.2 \times 10^8$ | Predicted is high by obout o foctor of 4 over most af the range. |
| $N^+$ an Ne | $(1.8 - 4.2) \times 10^8$ | $(2 - 4.2) \times 10^8$ | Predicted is slightly higher. |
| $U^+$ on $N_2$ | $(0.2 - 1.2) \times 10^8$ | At $4 \times 10^7$ and at $1.2 \times 10^7$ only. | Predicted is too high over mast af the range but too low at end of ronge. |
| $U^+$ on $N_2$ | $(0.2 - 1.2) \times 10^8$ | At $3 \times 10^7$ only. | Predicted is high over most of range but becomes too low at law end. |
| $N^+$ on $O_2$ | $(0.? - 1.2) \times 10^8$ | $(3 - 4) \times 10^8$ | Predicted is too high ot low speed ond becomes tao low ot high speed. |
| $N^+$ on $N_2$ | $(1.8 - 4) \times 10^8$ | $(3 - 4) \times 10^8$ | Predicted is too high at low speed. |

### 15.4.2 Semiempiricol

Fleischmann, Dohmel, and Lee (References 15-29, 15-30) propose a semiempirical scaling law, including the scaling of absolute cross-section values as well as beam energies, which adequately describes direct transitions of an electron between the bound and continuum states. The scaling law uses a general energy parameter $\epsilon = E/E_1$ (where E = beam energy, $E_1 = MR^2(E_i/13.6)^2$, M = projectile mass, $E_i$ = ionization energy of the projectile, and R = "interaction distance" ≈ radius of target atom) and a scaling of the absolute cross-section values proportional to $(Z_p^{2/3} + Z_t^{2/3})(13.6/E_i)^{1/2}$. The model succeeds in reducing a rather wide variety of single-electron-loss cross-sections to a general cross-section curve according to:

$$\sigma(E)_{i,\,i+1} = n_{eff}\left(Z_p^{2/3} + Z_t^{2/3}\right)\left(\frac{13.6}{E_i}\right)^{1/2}\sigma(E/E_1)_{TM}\ , \quad (15\text{-}13)$$

where $n_{eff}$ is the number of electrons available for ionization in the outer shell of the projectile.

Equation (15-13) originally was derived solely from an empirical analysis of a wide range of published experimental data, in which it appeared that the total cross-sections increased with the atomic numbers of projectile and target and with the number of electrons in the outer shell of the projectile, and decreased approximately as the root of the ionization energy $E_i$. The functional dependence on these parameters given in Equation (15-13) appears to give the best overall fit of the experimental data. The scaling law was found to reduce a large majority of published data to within a factor of two of a general cross-section curve.

The resulting plots of the normalized cross-section curve $\sigma(E/E_1)_{TM}$ from over 80 published experimental data on single-electron stripping in neutral-neutral collisions are shown in Figures 15-1 and 15-2. Major deviations occur only for low-energy stripping of some of the rare-gas atoms on rare gases (see Figure 15-1). It is noteworthy that most of these collisions are much better described by the Firsov model (subsection 15.4.3.2, below).

### 15.4.3 Quantum-Mechanical

The simplest quantum theoretical treatments, the Born-Bethe (Reference 15-34) approximations, have not provided useful estimates of cross-sections in the velocity range of interest. This is understandable from the formal theory viewpoint, in that heavy-particle collisions in this velocity range have a great variety of channels open. The probability of ending in a given final state directly, as assumed by the Born approximation, is often smaller than the probability of reaching it via some intermediate state. It is also likely that several such intermediate states play equivalently large roles in the transition. Choosing a limited number of these certainly is preferable to a Born approximation. However, the cost in time and effort of including more than a few channels is generally prohibitive.

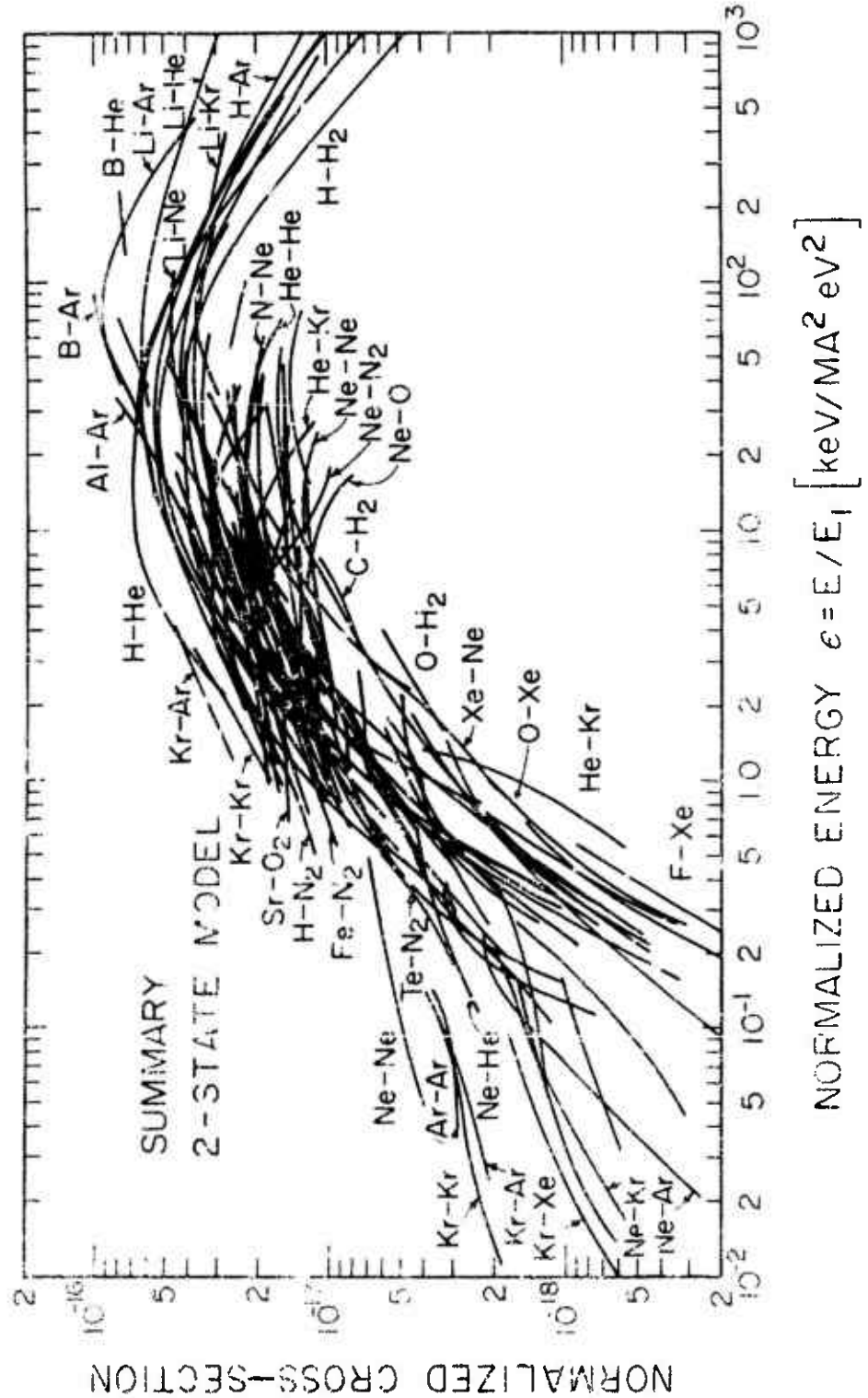


Figure 15-1. Result of published data scaled according to Equation (15-13) to give a normalized universal curve.

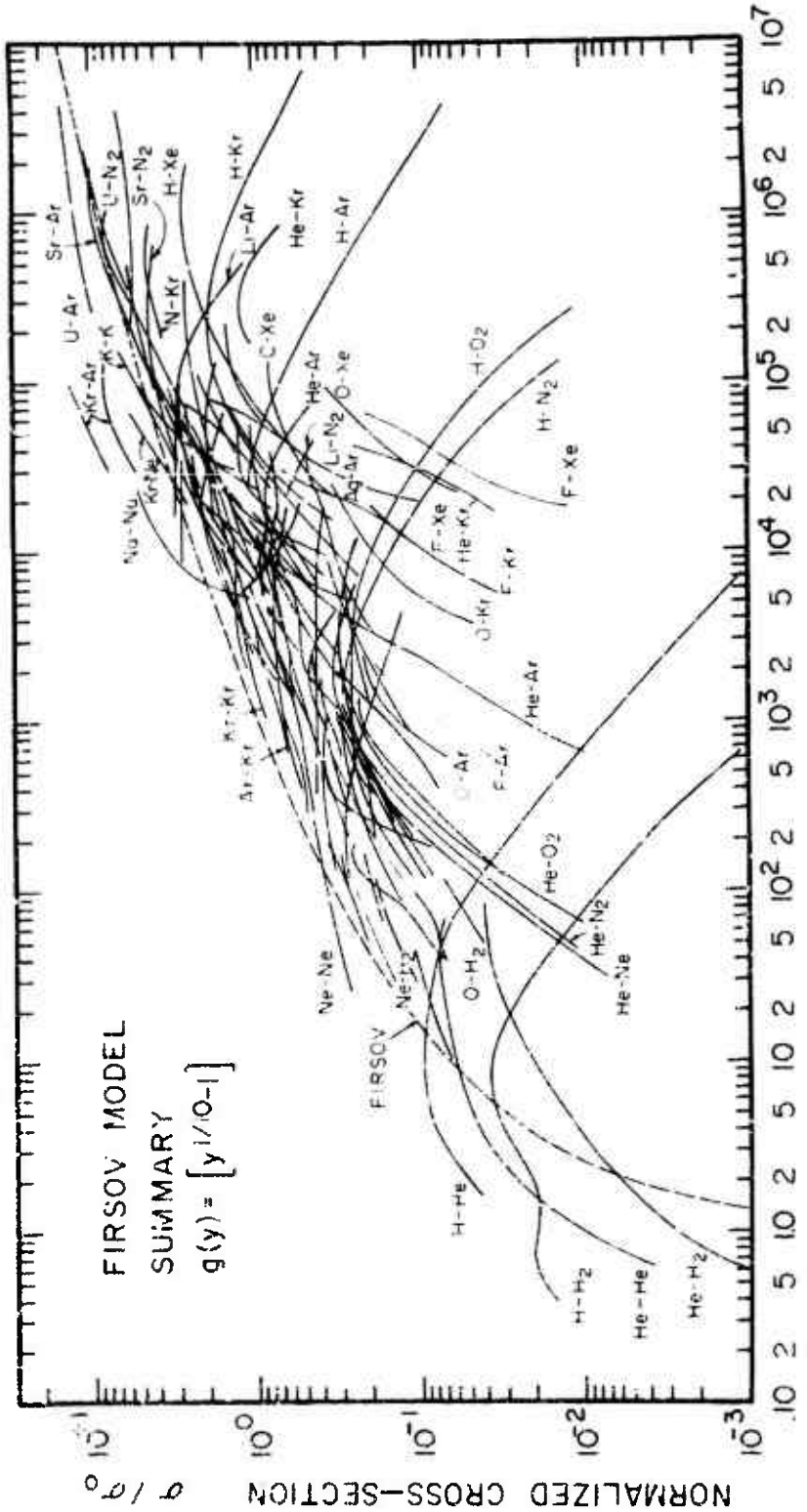


Figure 15-2. Experimental data scaled according to Equation (15-13) and compared with the statistical theory of Firsov (Subsection 15.4.3.2).

### 15.4.3.1 QUANTAL TWO-STATE MODELS

The details of the method of calculation and computed numerical values of the differential and total charge-transfer cross-sections using the Brinkman-Kramers (BK) approximation are reported in Reference 15-16. In order to reduce the discrepancy between computed BK cross-sections and experimental data and to remove unphysical capture probabilities, Dalgarno et al (Reference 15-18) transformed the BK results to the impact-parameter formulation. The modified BK method overestimated the cross-section by almost an order of magnitude at the velocity of maximum cross-section; however, the cross-section curves were generally qualitatively reasonable. It was concluded (Reference 15-18) that a more accurate quantal method was necessary. Another quantal approach is to attempt to solve the exact equation of motion of the system to which that BK approximation is a first-order solution.

Dalgarno et al (Reference 15-31) have applied the Bates and McCarroll theory (Reference 15-32) of fast collisions to the calculation of charge-exchange cross-sections for collisions between heavy ions and atmospheric ions and molecules. A brief review is presented here, of the theory applied to a two-state one-electron system; cf. Dalgarno et al (Reference 15-33). Atomic units are employed throughout.

Consider point A to move past point B at a constant velocity $\vec{v}$, i.e., a rectilinear trajectory characterized by an impact parameter $\rho$. Let a single electron have position vectors $\underset{\sim}{r}_a$, $\underset{\sim}{r}_b$, and $\underset{\sim}{r}$ with respect to A, B, and midpoint of AB, respectively. Let the electron see potentials $V_a(r_a)$ and $V_b(r_b)$ centered on the appropriate points, and let there exist bound-state wavefunctions:

$$\left[T + V_a(r_a) - i\frac{\partial}{\partial t}\right] \phi_i(\underset{\sim}{r}_a) \exp(-iE_i t) = 0 \qquad (15\text{-}14)$$

considering A to be at rest, and:

$$\left[T + V_b(r_b) - i\frac{\partial}{\partial t}\right] \phi_j(\underset{\sim}{r}_b) \exp(-iE_j t) = 0 \qquad (15\text{-}15)$$

considering B to be at rest, where T is the kinetic energy operator, ; the midpoint of AB is taken to be at rest, wavefunctions simply

derived from $\phi_i$ and $\phi_j$ are solutions of the time-dependent Schrödinger equation; thus:

$$\left[T + V_a(r_a) - i\frac{\partial}{\partial t}\right] \phi_i(\underset{\sim}{r}_a, \underset{\sim}{r}) \exp\left[-i\left(E_i + \frac{1}{8}v^2\right)t\right] = 0 , \qquad (15\text{-}16)$$

and:

$$\left[T + V_b(r_b) - i\frac{\partial}{\partial t}\right] \phi_j(\underset{\sim}{r}_b, \underset{\sim}{r}) \exp\left[-i\left(E_j + \frac{1}{8}v^2\right)t\right] = 0 , \qquad (15\text{-}17)$$

where:

$$\phi_i(\underset{\sim}{r}_a\ \underset{\sim}{r}) = \phi_i(\underset{\sim}{r}_a) \exp\left(-\frac{1}{2} i\ \underset{\sim}{v} \cdot \underset{\sim}{r}\right) , \qquad (15\text{-}18)$$

and:

$$\phi_j(\underset{\sim}{r}_b, \underset{\sim}{r}) = \phi_j(\underset{\sim}{r}_b) \exp\left(\frac{1}{2} i\ \underset{\sim}{v} \cdot \underset{\sim}{r}\right) . \qquad (15\text{-}19)$$

The total wavefunction $\psi$ in this approximation is then expanded as:

$$\psi = a_i\phi_i \exp\left[-i\left(E_i + \frac{1}{8}v^2\right)t\right] + b_j\phi_j \exp\left[-i\left(E_j + \frac{1}{8}v^2\right)t\right] , \qquad (15\text{-}20)$$

and substituted into the conditions:

$$\left[\phi_i, \left(H - i\frac{\partial}{\partial t}\right)\psi\right] \exp\left[i\left(E_i + \frac{1}{8}v^2\right)t\right] = 0 , \qquad (15\text{-}21)$$

and:

$$\left[\phi_j, \left(H - i\frac{\partial}{\partial t}\right)\psi\right] \exp\left[i\left(E_j - \frac{1}{8}v^2\right)t\right] = 0 , \qquad (15\text{-}22)$$

where $H = T + V_a + V_b$ is the total Hamiltonian. The equations of the two-state model then follow:

$$\left.\begin{aligned} i\dot{a}_i + i\,S_{ij}\exp\left[i(E_i-E_j)t\right]\dot{b}_j &= n_{ii}a_i + h_{ij}\exp\left[i(E_i-E_j)t\right]b_j \\ iS_{ji}\exp\left[i(E_j-E_i)t\right]\dot{a}_i + i\dot{b}_j &= h_{ji}\exp\left[i(E_j-E_i)t\right]a_i + h_{jj}b_j \end{aligned}\right\} \quad (15\text{-}23)$$

where $S_{ij} = (\phi_i, \phi_j)$, $h_{ij} = (\phi_i, V_a\phi_j)$, and $h_{ji} = (\phi_j, V_b\phi_i)$. The initial conditions are that, say, $a_i = 1$, $b_j = 0$. At the end of the trajectory $|b_j|^2$ will be the capture probability for that impact parameter:

$$c(\rho) = \left|b_j(+\infty)\right|^2 , \quad (15\text{-}24)$$

and the cross-section is:

$$Q = 2\pi \int_0^\infty c(\rho)\rho\, d\rho \quad . \quad (15\text{-}25)$$

Sample calculations for $Fe^+ + O$ and $Al^+ + O$ are shown, respectively, in Figures 15-3 and 15-4 and compared with the experimental data of Brackmann et al (Reference 15-10). The maximum value of the $Q_{10}^{01}$ cross-sections computed by Dalgarno are within a factor of two of the experimental $\sigma_{10}$ cross-section. They fall off more rapidly at higher energies as one would expect, since the $\sigma_{10}$ cross-section includes several possible processes $Q_{10}^{0n}$.

Rosen and Zener (Reference 15-37) give an approximate solution of the equations of motion (Equation 15-23) in analytic form. This approximation consistently underestimates and overestimates the cross sections arising from a numerical integration at velocities respectively below and above the velocity of maximum cross-section (Reference 15-31).

Rapp and Francis (Reference 15-35) have introduced a model of non-resonant charge transfer based on resonant charge-transfer theory and on the Rosen-Zener approximation to the two-state equations. Their method is based on the fact that the probability for resonant charge transfer is a rapidly oscillating function of impact parameter (b) out to a certain radius beyond which the probability falls to zero. This probability function is approximated by a constant value (equal to the average value) out to an effective cut-off

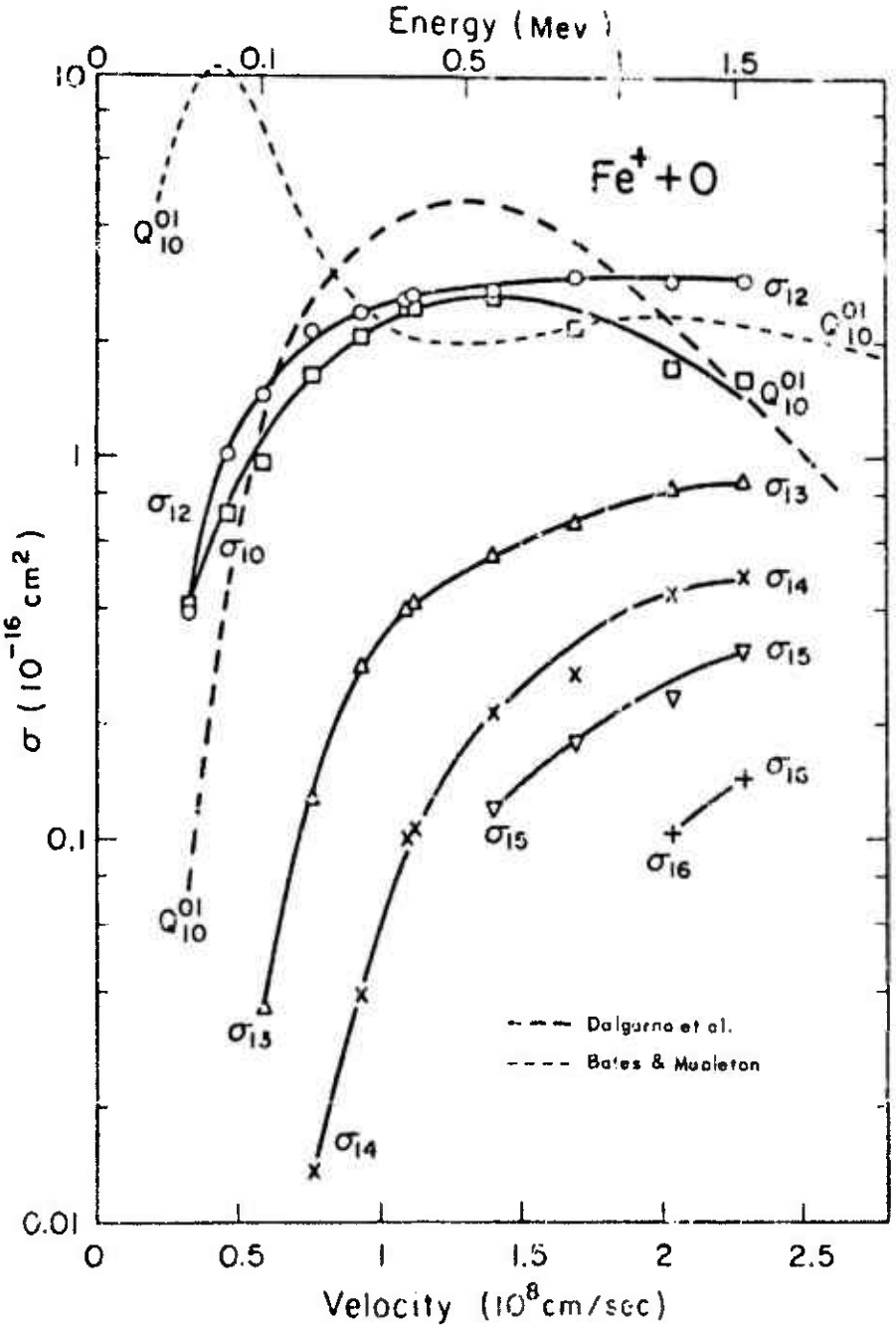


Figure 15-3. Electron capture and loss cross-sections of $Fe^+$ on O. (The Dalgarno et al curve is from Reference 15-31 and the Bates and Mapleton curve is from Reference 15-19.)

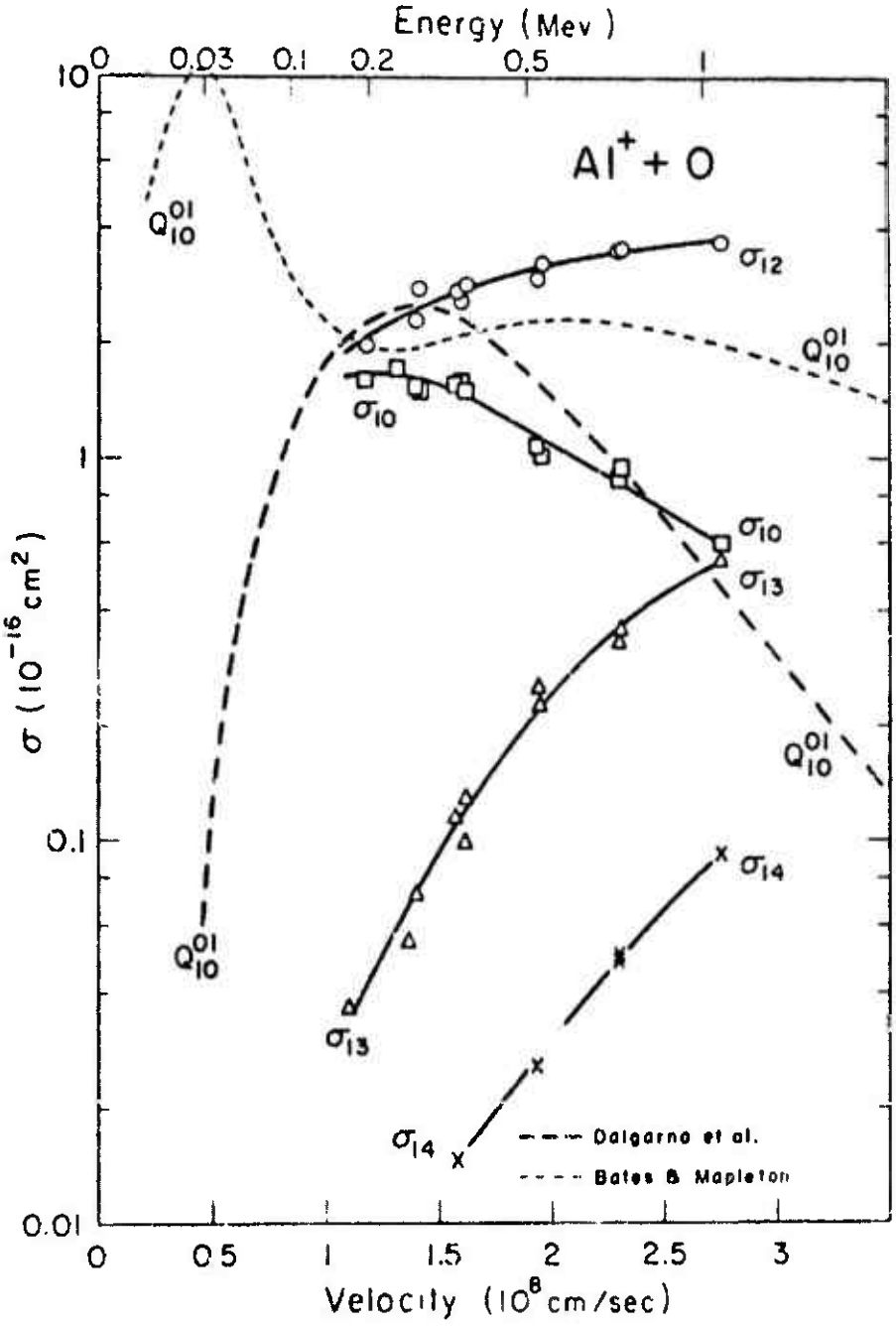


Figure 15-4. Electron capture and loss cross-sections of $Al^+$ on O. (The Dalgarno et al curve is from Reference 15-31 and the Bates and Mapleton curve is from Reference 15-19.)

radius ($b_1$) beyond which it is zero. The probability of symmetric charge transfer as calculated in time-dependent perturbation theory is a function of the energy difference between symmetric and antisymmetric molecular energy states as the internuclear separation (R) changes. Expressions for these energies are found by using linear combinations of semiempirical atomic orbitals in which the ionization energy is an adjustable parameter. The wave functions can be written as (Reference 15-28):

$$\psi(r) = (1/\pi a_o^3)^{1/2} (I/I_H)^{3/4} \exp\left[-(I/I_H)^{1/2} (r/a_o)\right] , \qquad (15\text{-}26)$$

where I is the ionization potential of the state, $I_H$ is the ionization potential of ground-state hydrogen (13.6 eV), and $a_o$ is the radius of the first Bohr orbit. From these wavefunctions the energy difference between antisymmetric and symmetric states for a nuclear separation of R is determined to be:

$$E_a - E_s = 2I(R/a_o) \exp\left[-(I/I_H)^{1/2} (R/a_o)\right] . \qquad (15\text{-}27)$$

For separations large with respect to $a_o$ or for large ionization energy, the probability for charge transfer in a collision at relative velocity u and impact parameter b is found to be:

$$P(b, u) = \sin^2\left[\left(\frac{2\pi}{\gamma a_o}\right)\left(\frac{I}{\hbar u}\right) b^{3/2} \left(1 + \frac{a_o}{\gamma b}\right) \exp\left(-\frac{\gamma b}{a_o}\right)\right] , \qquad (15\text{-}28)$$

where $\gamma = (I/I_H)^{1/2}$. Rapp and Francis approximate this rapidly varying function of impact parameter b by the value 0.5 for $b \leq b_1$ and by 0 for $b > b_1$ where $b_1$ is chosen to be the largest value of b for which the argument in the above equation is $\pi/6$. Defining $x_o$ as:

$$x_o = (b_1/a_o)(I/I_H)^{1/2} , \qquad (15\text{-}29)$$

the equation for $b_1$ can be written in terms of $x_o$ as:

$$x_o^3(1 + 1/x_o)^2 \exp(-2x_o) = \pi u^2 \hbar^2/e^4 . \qquad (15\text{-}30)$$

In this form $x_o$ can be seen to be a function of u only; therefore the cross-section for the charge transfer $\sigma = \pi b_1^2/2$ can be rewritten as:

$$\sigma(I, u) = \pi a_o^2 x_o^2 I_H/2I \quad . \tag{15-31}$$

This equation states that the cross-section can be scaled. If the cross-section $\sigma(I_1, u)$, involving atoms with an ionization potential $I_1$, is known, then that for any other atom with ionization potential $I_2$ can be found.

Rapp and Francis (Reference 15-35) calculated the cross-section for resonant charge transfer in hydrogen by their method and compared the results with experimental values. For velocities between $\sim 5 \times 10^6$ and $\sim 2 \times 10^8$ cm/sec their calculations agreed to within about a factor of two with experiment. Assessment of this method in the case of non-resonant charge transfer is somewhat less satisfying. There are, in that case, two ionization potentials involved, that of the target and that of the projectile. It seems most reasonable to consider the charge transfer as being governed by the lower of these. This leads to fairly good agreement, viz., by a factor of two to four with experiment, for many combinations of target and projectile species, but poor agreement for collisions of metal ions with atmospheric species. In the latter case, better agreement is obtained by using the higher of the two ionization potentials.

### 15.4.3.2 STATISTICAL MODELS

The Firsov model (References 15-36 through 15-38) provides an estimate of the average energy of excitation of two colliding atomic systems based on momentum transfer due to electrons passing between the colliding atoms. Momentum transfer arises from the relative motion of the collision partners. The calculation is made by computing the net rate at which electrons from the projectile system carry momentum across a plane normal to and bisecting the line joining the colliding nuclei. The electron density is found in the Thomas-Fermi method. The electron excitation energy found from the momentum transfer is (Reference 15-39):

$$\epsilon = \frac{0.35(Z_a+Z_b)^{5/3}\,(\hbar u/a_o)}{\left[1 + 0.16(Z_a+Z_b)^{1/3}\,(R_o/a_o)\right]^5} \quad , \tag{15-32}$$

where $Z_a$ and $Z_b$ are the respective nuclear charges, $R_o$ the impact parameter (cm), $a_o$ the Bohr radius (cm), and $u$ the radial component of relative velocity of the collision partners.

The cross-section for ionization is computed as that area corresponding to the impact parameter for which $\epsilon$ is equal to the ionization energy. Thus if $\epsilon_o$ is the ionization energy in eV then:

$$\sigma = \pi R_I^2 = (3.3 \times 10^{-15})(Z_a+Z_b)^{-2/3}\left[\left((Z_a+Z_b)^{5/3}\right.\right.$$
$$\left.\left.(4.3 \times 10^{-8}\, u/\epsilon_o)\right)^{1/5} - 1\right]^2 \text{ cm}^2 \quad , \qquad (15\text{-}33)$$

which can be written in the form:

$$\sigma = \sigma_o \left[(u/u_o)^{1/5} - 1\right]^2 \text{ cm}^2 \quad , \qquad (15\text{-}34)$$

where:

$$u_o = \left[2.3 \times 10^7\, \epsilon/(Z_a+Z_b)^{5/3}\right] \text{ cm/sec} \quad , \qquad (15\text{-}35)$$

and:

$$\sigma_o = \left[3.3 \times 10^{-15}/(Z_a+Z_b)^{3/2}\right] \text{ cm}^2 \quad . \qquad (15\text{-}36)$$

This method is expected to be reasonably valid at velocities not so high as to be comparable to electron orbital velocities ($\sim 2 \times 10^8$ cm/sec) or so low that a molecular eigenstate description is appropriate. The lower limit can be determined as in an argument presented by Garcia and Gerjuoy (Reference 15-28). From the uncertainty relation, $\Delta E \Delta t \approx \hbar$ but $\Delta t \sim R_o/u$. For the Firsov model to be valid it is then expected that $\Delta E$ must be of the order of at least 1 eV and $R_o$ no less than about $10^{-8}$ cm. This requires that $u$ must be approximately $1.5 \times 10^7$ cm/sec.

Garcia and Gerjuoy (Reference 15-28) presented a comparison between electron-removal cross-sections as calculated by the Firsov

model, and the corresponding experimental cross-sections. The velocity range considered was of the order of $10^7$ - $10^8$ cm/sec. When argon was the target, the agreement with experiment was good when the projectiles were aluminum, strontium, and uranium atoms, moderately good (within a factor of two), for iron and nitrogen atoms, and poor for iodine and potassium atoms (cf. Figure 15-5).

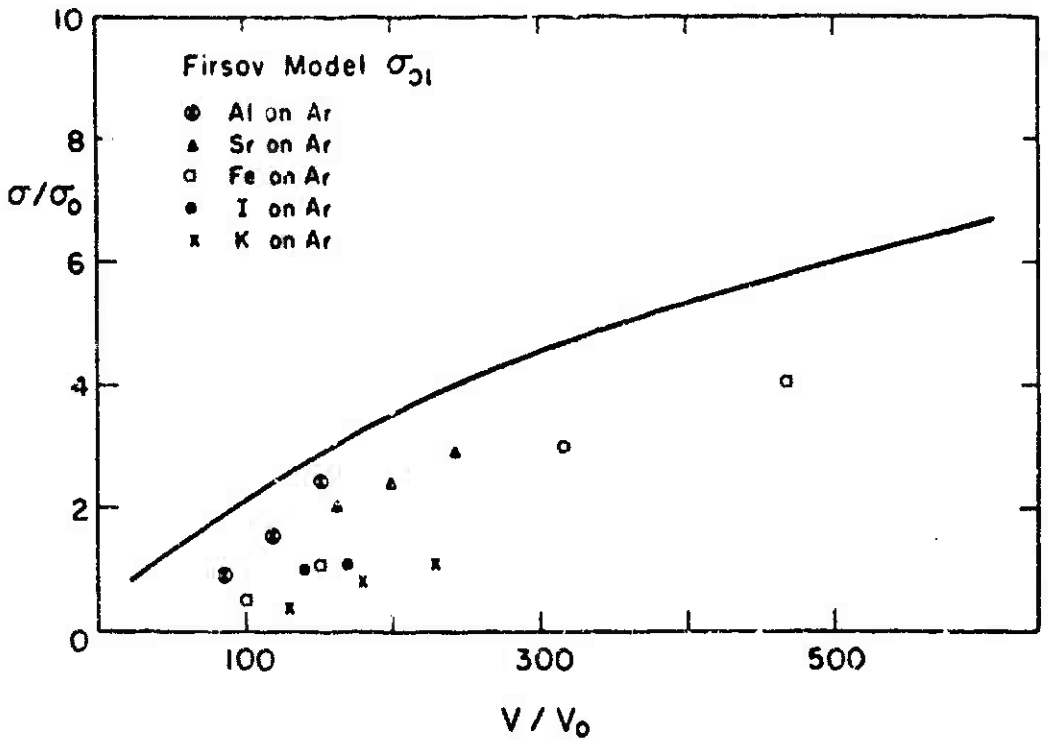


Figure 15-5. Stripping cross sections for various projectile atoms on argon. The solid curve is the Firsov model prediction. Experimental data are from Layton and Fite (Reference 15-47).

Comparisons have also been made for several species incident upon molecular nitrogen and molecular oxygen (cf. Figures 15-6 through 15-8). In addition to Figure 15-2, further comparisons of Firsov's model with scaled experimental data are contained in Reference 15-30. Among the shortcomings of the Firsov formula are its failure to account for the charge states of colliding particles and the general decrease of the cross-section for velocities above the orbital-electron velocities. An indication of the effect of the charge

state for $N^+$ and $N^{2+}$ colliding with $N_2$ in the velocity range (2-5) x $10^8$ cm/sec is given in a paper by Pivovar et al (Reference 15-39). Landshoff (Reference 15-40) suggested a modification to the Firsov formula to take account of the decrease of the cross-section at sufficiently high velocities.

Russek Model: A theory of ionization produced in the collision of heavy atoms or ions is given by Russek (Reference 15-42). This theory is based on the assumptions that: (a) during an energetic atomic collision the energy transferred from projectile to target is determined solely by the collision parameters; and (b) the excitation energy becomes distributed among the atomic electrons in a statistical fashion. It is assumed that these two stages in the process are essentially uncoupled. In order to determine the probability that an atom, having received a given quantity of energy, will release a certain number of electrons, it is necessary to model the ionization process to the point where ionization energies are determined. There is, in Russek's theory, some question as to whether the ionization

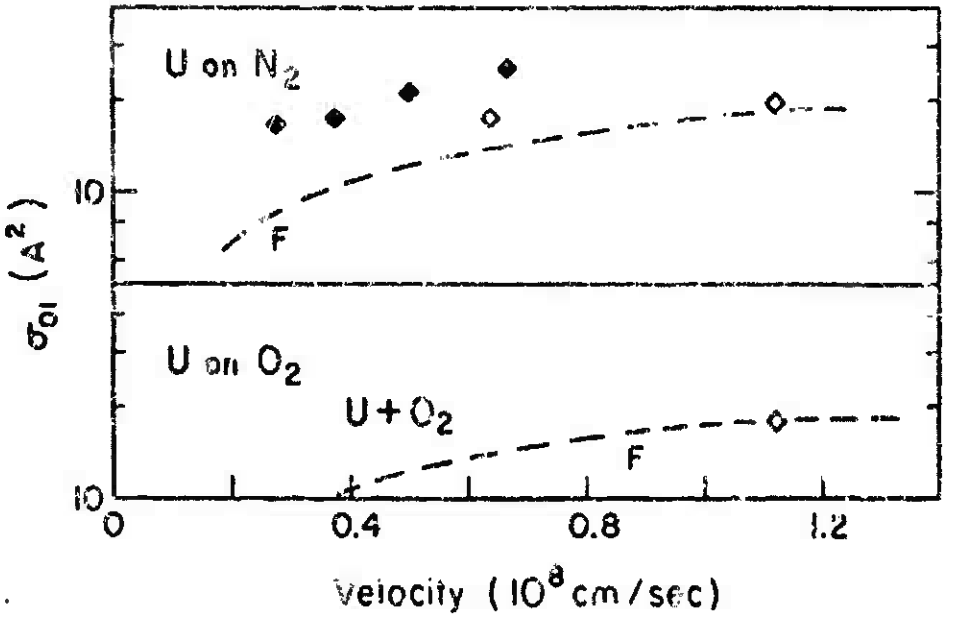


Figure 15-6 Stripping cross-sections for uranium on nitrogen and oxygen. The dashed curves are the Firsov model predictions. All experimental data are from Lotton and Fite (Reference 15-47).

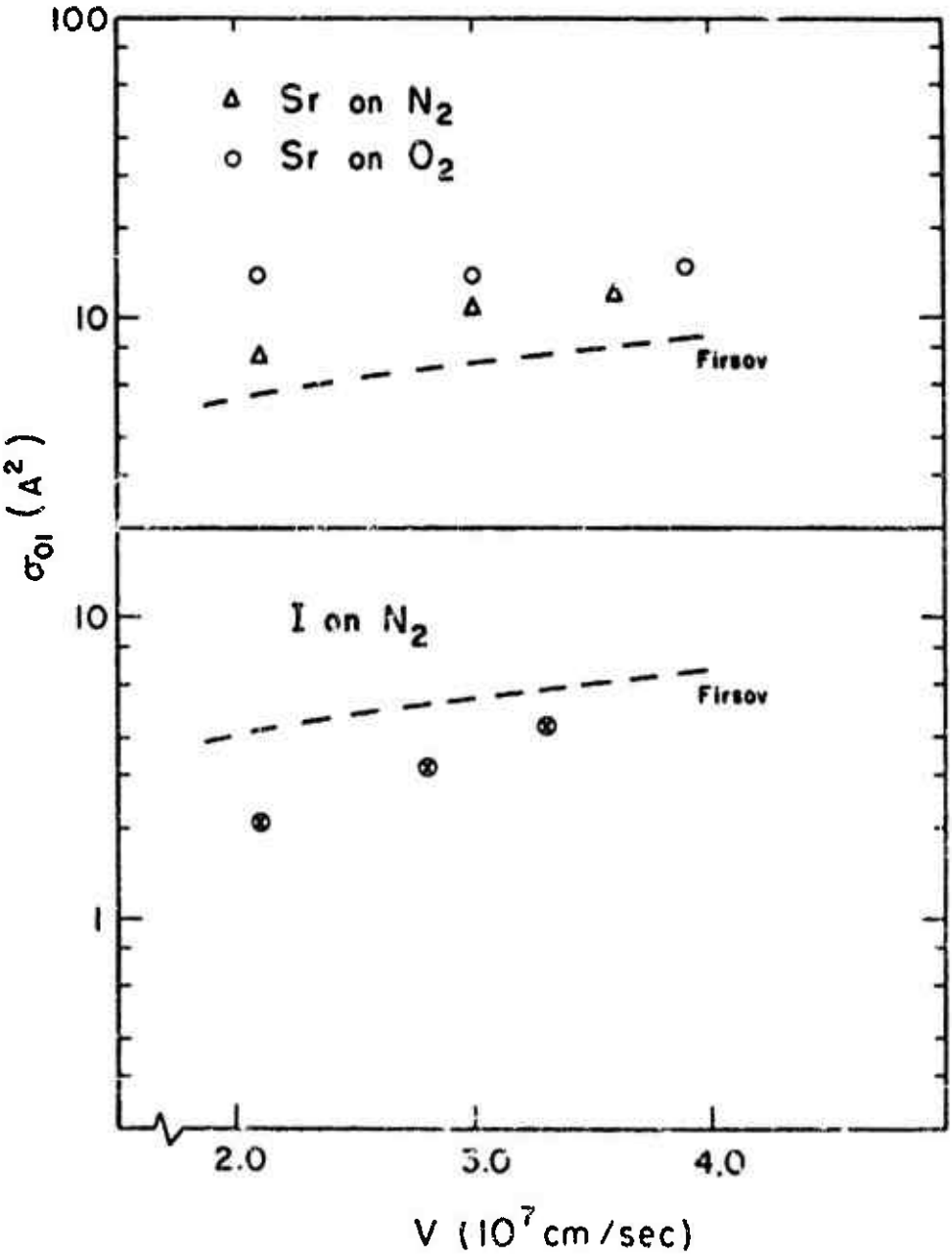


Figure 15-7. Stripping crass-sections as indicated. The dashed curves are the Firsov model predictions. Experimental data for strantium an nitrogen (triangles) and for iodine on nitragen (crossed circles) are from Laytan and Fite (Reference 15-47); for strantium an oxygen (open circles), data are from Garcia, Gerjuoy, and Welker (Reference 15-27).

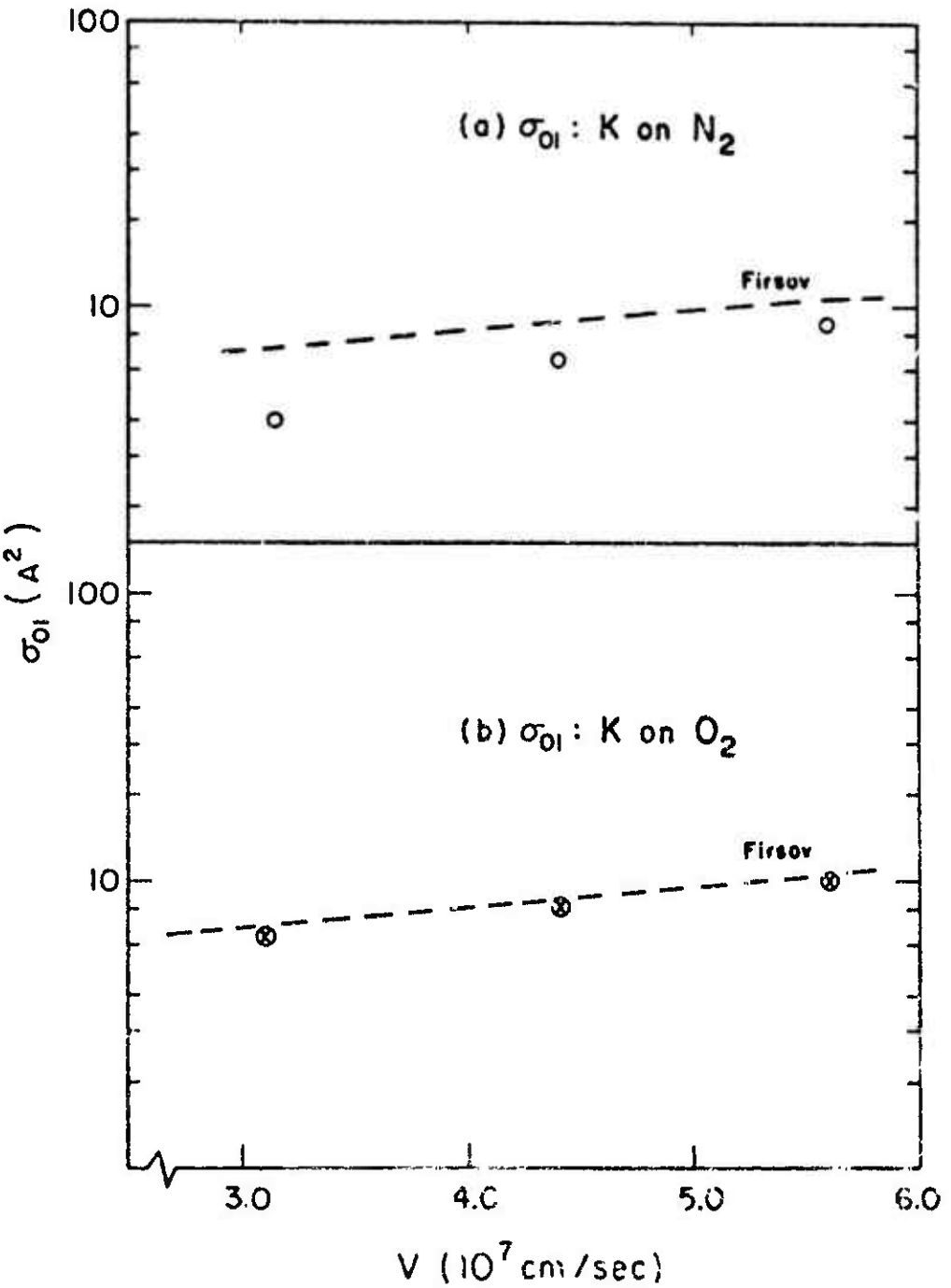


Figure 15-8. Stripping cross-sections for potassium atoms on nitrogen and on oxygen. The dashed curves are the respective Firsov model predictions. Experimental data are from Layton and Fite (Reference 15-47).

energy should be independent of the number of electrons released or whether this energy is itself a function of that number. There is a further question as to the numerical values to be assigned as ionization energies.

It should be noted that Russek's approach has not yet yielded ionization cross-sections but has been used successfully to calculate the angular distribution of ions scattered in different ionization states (Reference 15-42, page 398).

Garcia and Gerjuoy (Reference 15-28) compared Russek model predictions of the probability of multiple ionizations with experimental data for three systems, viz., uranium on neon, uranium on argon, and atomic nitrogen on molecular nitrogen. They found only moderate agreement with experiment and observed that the choice of ionization energy independent of the number of electrons released provides better agreement than the self-consistent ionization energy. The calculation required predetermination of the average charge state. The uncertainties involved in this determination tended to overshadow any apparent agreement with experiment.

A second application of the Russek model, using the approximation of Firsov to determine the excitation energy as a function of impact parameter, was carried out by Garcia and Gerjuoy (Reference 15-28). The Firsov approximation was modified by the assumption that the electron density of interest is that arising from the superposition of the densities of the two atoms. Despite several sources of uncertainty, the agreement between prediction and experiment was within a factor of approximately two or better. The systems considered were: $N^+$ on $N_2$ stripping 2, 3, or 4 electrons at an impact velocity between $2 \times 10^8$ and $4.5 \times 10^8$ cm/sec; and $U^+$ on Ne stripping 2, 3, or 4 electrons at an impact velocity between $4 \times 10^7$ and $1.2 \times 10^8$ cm/sec. The results for $N^+$ on $N_2$ are shown in Figure 15-9.

## 15.5 SAMPLE EXPERIMENTAL DATA

This compilation summarizes data on: species of slow ions formed; electron and slow positive-charge production; and electron capture and loss cross-sections for heavy fast particles passing through O, $N_2$, and Ne. The types of experimental techniques and detection methods used to obtain the data are summarized in Table 15-2. The symbols used to identify the various measured cross-section

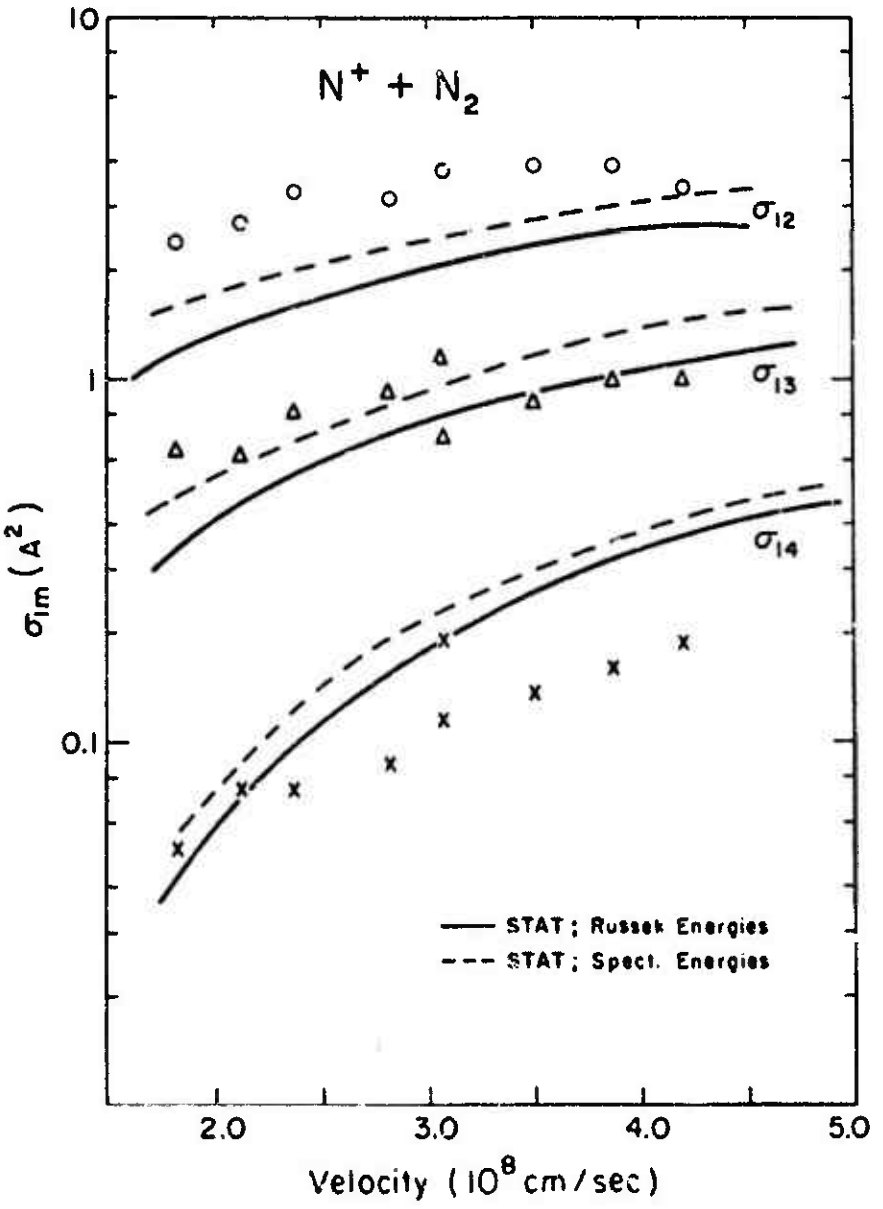


Figure 15-9. Comparison of the combined Russek-Firsov models for $N^+$ on $N_2$. The solid curves represent the model with energies determined as a function of the impact parameter. The dashed curves represent the model with spectroscopic energies. Circles, triangles, and crosses indicate data points for the stripping of 2, 3, and 4 electrons, respectively. From the work of Garcia and Gerjuoy (Reference 15-28).

values summarized in Subsection 15.5.1 are defined in Table 15-3. The data reported in the first subsection are based largely upon the literature search of Lo and Fite (Reference 15-49), which was completed in October 1969. Subsections 15.5.2 and 15.5.3 present data obtained more recently, under Air Force Weapons Laboratory Contract No. F29601-70-C-0057, DNA Project 5710, at the University of Pittsburgh.

Table 15-2. Summary of experimental techniques and detection methods used by various authors.

| Author (and References) | Velocity or Energy Range | Technique | Detection | Experimental Uncertainty (percent) |
|---|---|---|---|---|
| Brackmann (15-8, 15-43, 15-44) | 30-2000 keV | A | C | 15 for $\sigma_{ij}$, $j-i \leq 2$<br>22 for $\sigma_{ij}$, $j-i \geq 3$ |
| Dmitriev (15-50, 15-51) | $(2.6-12) \times 10^8$ cm/sec | A | C | 15-20 for $\sigma_{ij}$, $j-i \leq 3$<br>30 for $\sigma_{ij}$, $j-i \geq 4$ |
| Fagel (15-52) | 10-65 keV | A | C | 15 |
| Jones (15-53) | 25-100 keV | A | C | |
| Laytan (15-45, 15-46, 15-47, 15-54, 15-55) | 4-70 keV<br>200-2500 keV | A | C, D<br>C | See Brackmann & Fite (Reference 15-8) |
| Nikolaev (15-56) | $(2.6-12) \times 10^8$ cm/sec | | | See Dmitriev (References 15-50, 15-51) |
| Ryding (15-57) | 400-4000 keV | A | C | 10 |
| Stebbings (15-58, 15-59, 15-60) | 30 eV - 10 keV | B | D | 15<br>25 for atomic oxygen as target gas |
| Wittkower (15-61) | 60-450 keV | A | C | 12 |

A, beam-in-static-gas technique; B, crossed-beam technique; C, fast-particle detection; D, slow-particle detection.

Table 15-3. Symbols for measured cross-section values (as used in Section 15.5).

| Authors (References) | Cross-Sections | | | | | | | | |
|---|---|---|---|---|---|---|---|---|---|
| | $\sigma_{01}$ $q_0$ | $\sigma_{10}$ | $\sigma_{12}$ $\sigma_{21}$ | $\sigma_{13}$ $\sigma_{23}$ | $\sigma_{14}$ $\sigma_{24}$ | $\sigma_{15}$ $\sigma_{25}$ | $\sigma_{16}$ $\sigma_{26}$ | $\sigma_{17}$ | $\sigma_{18}$ |
| Brackmann, Fite (15-8, 15-43, 15-44) | ◇ | □ | ○ | △ | × | ▽ | + | ▷ | ○ |
| Dmitriev et al (15-50, 15-51) | ◆ | | ● | ▲ | ⊗ | | | | |
| Fogel et al (15-52) | ◈ | ■ | ◉ | | | | | | |
| Janes et al (15-53) | | ◪ | ◒ | △ | ⊗ | ▼ | | | |
| Laytan et al (15-45, 15-46, 15-47, 15-54, 15-55) | ◈ | ◪ | ◒ | △ | ◉ | | | | |
| Nikolaev et al (15-56) | | ■ | | | | | | | |
| Ryding (15-57) | | ▪ | • | | | | | | |
| Stebbings et al (15-58, 15-59, 15-60) | | ●●● | | | | | | | |
| Wittkower et al (15-61) | | ◪ | | | | | | | |

N.B.: All other single-electron capture and loss cross-sections are denoted by a small dot (•).

## 15.5.1 Electron Capture and Loss Cross-Sections

### 15.5.1.1 NEUTRAL PROJECTILES ON ATOMIC OXYGEN

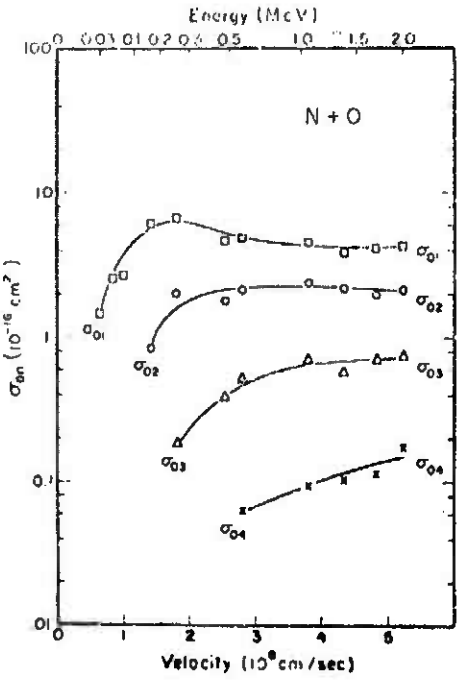


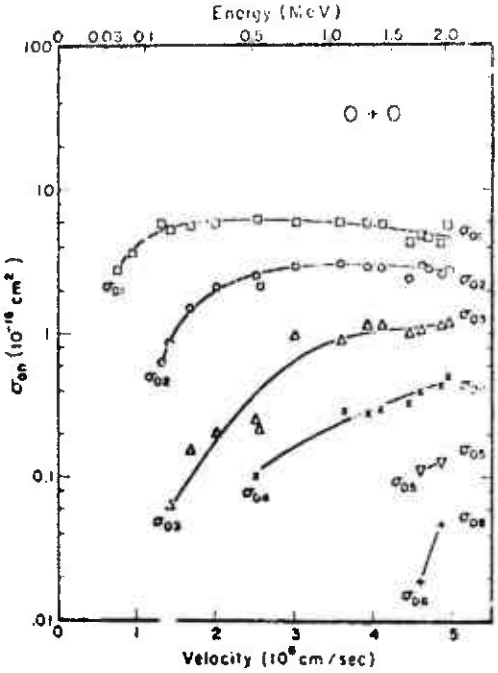


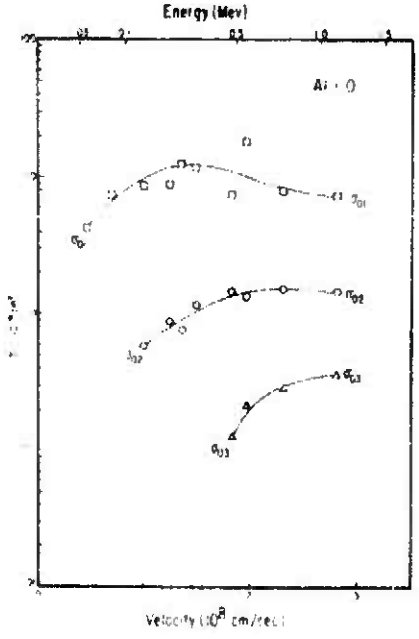


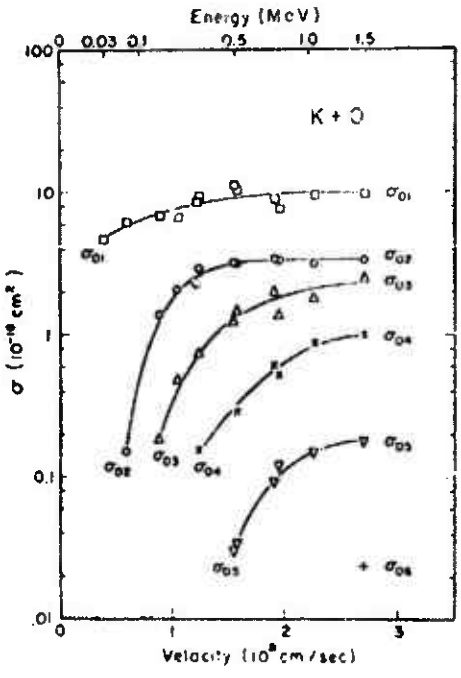

## 15.5.1.1 NEUTRAL PROJECTILES ON ATOMIC OXYGEN (Cont'd.)

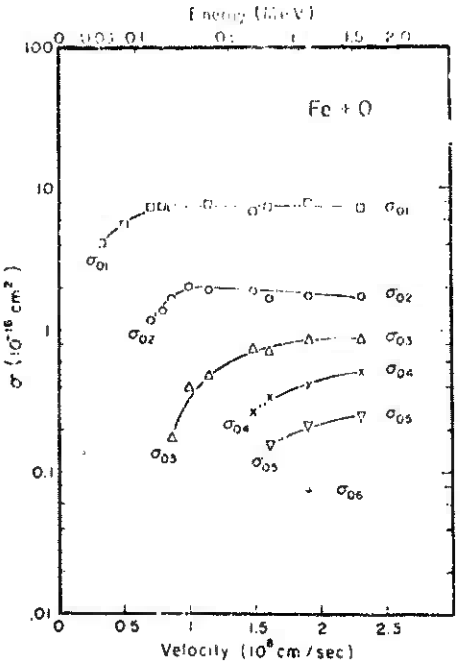


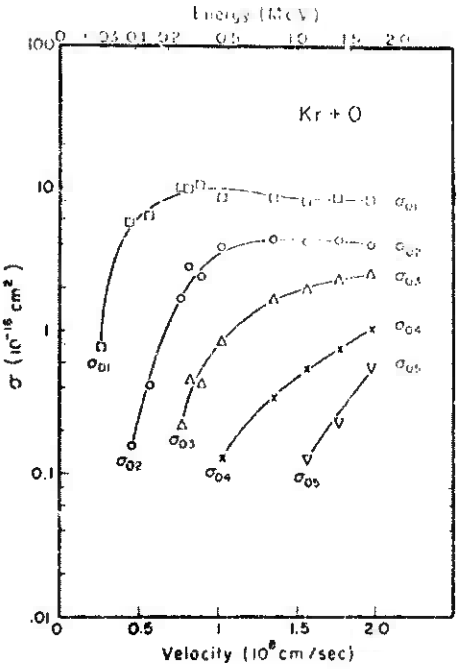


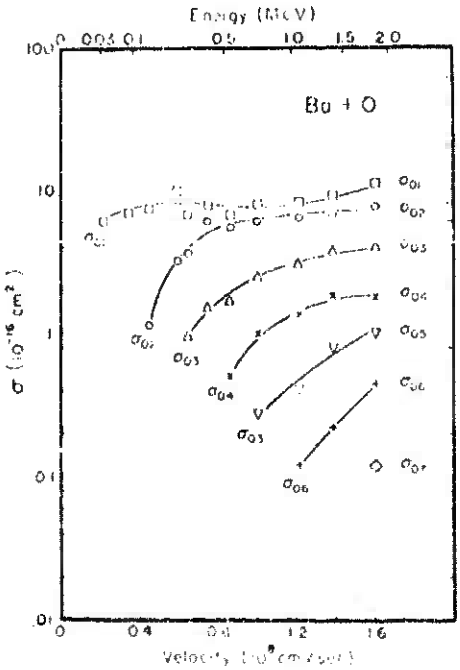


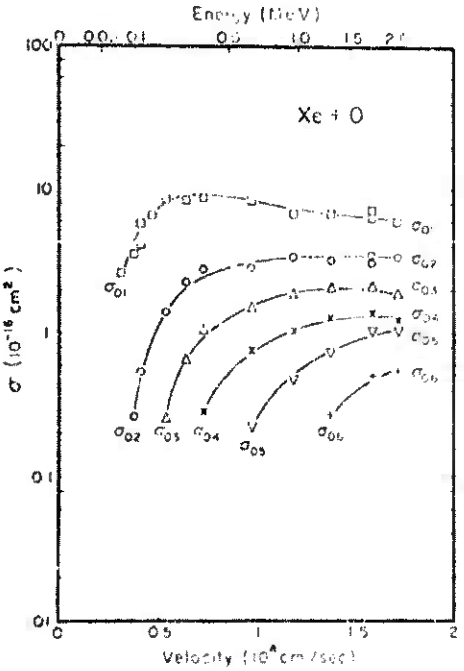

## 15.5.1.2 ION PROJECTILES ON ATOMIC OXYGEN

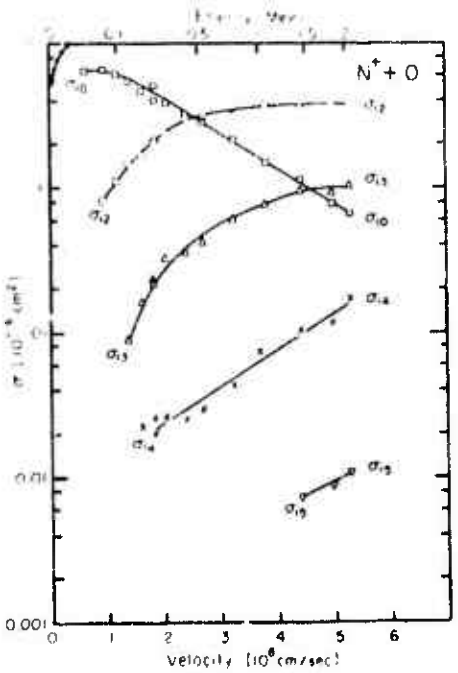


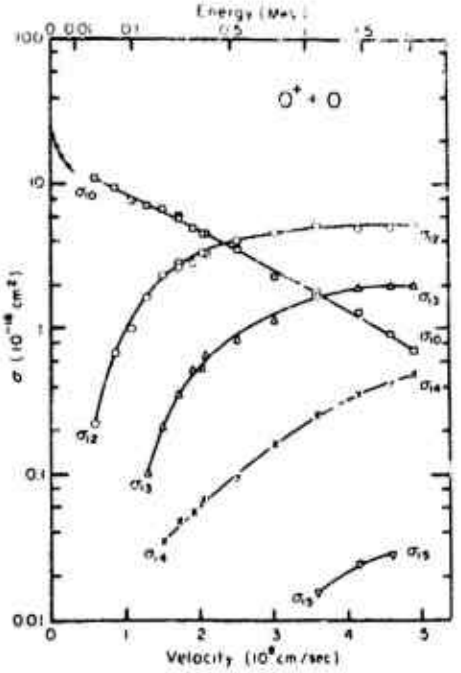


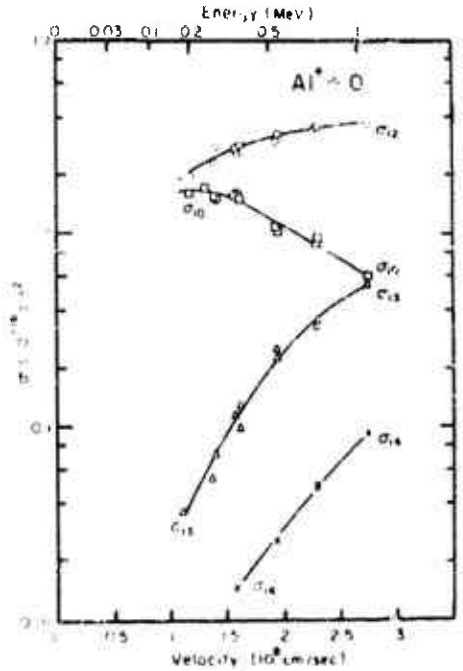


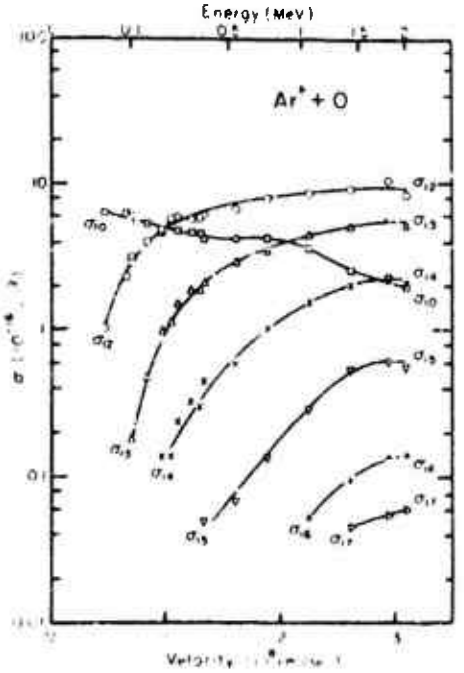

## 15.5.1.2 ION PROJECTILES ON ATOMIC OXYGEN (Cont'd.)

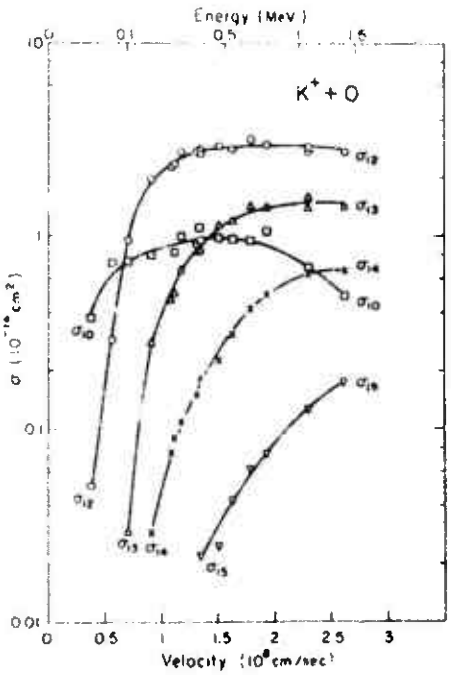


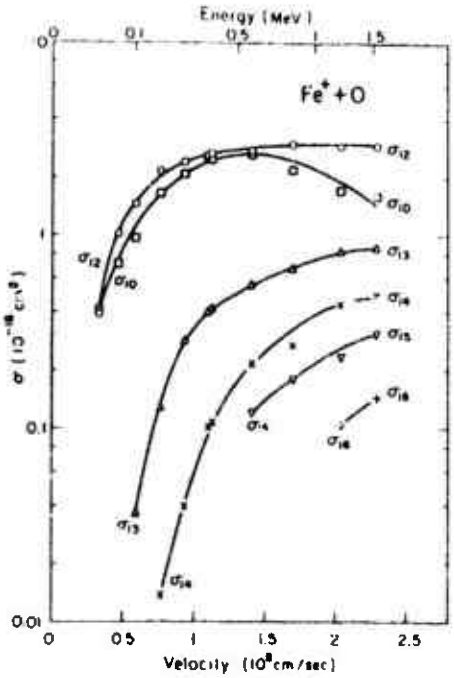


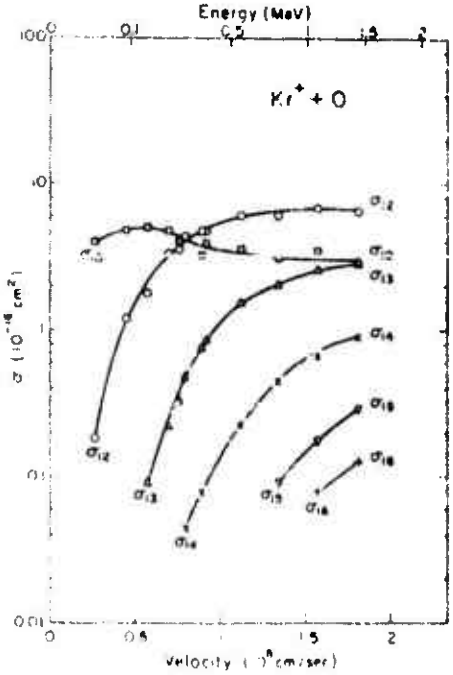


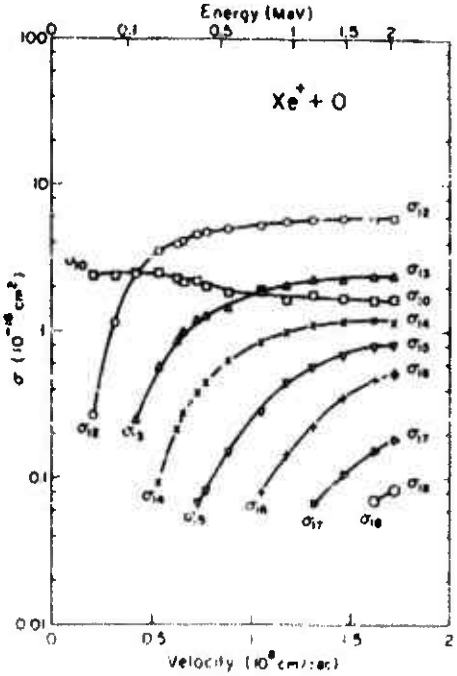

## 15.5.1.2 ION PROJECTILES ON ATOMIC OXYGEN (Cont'd.)

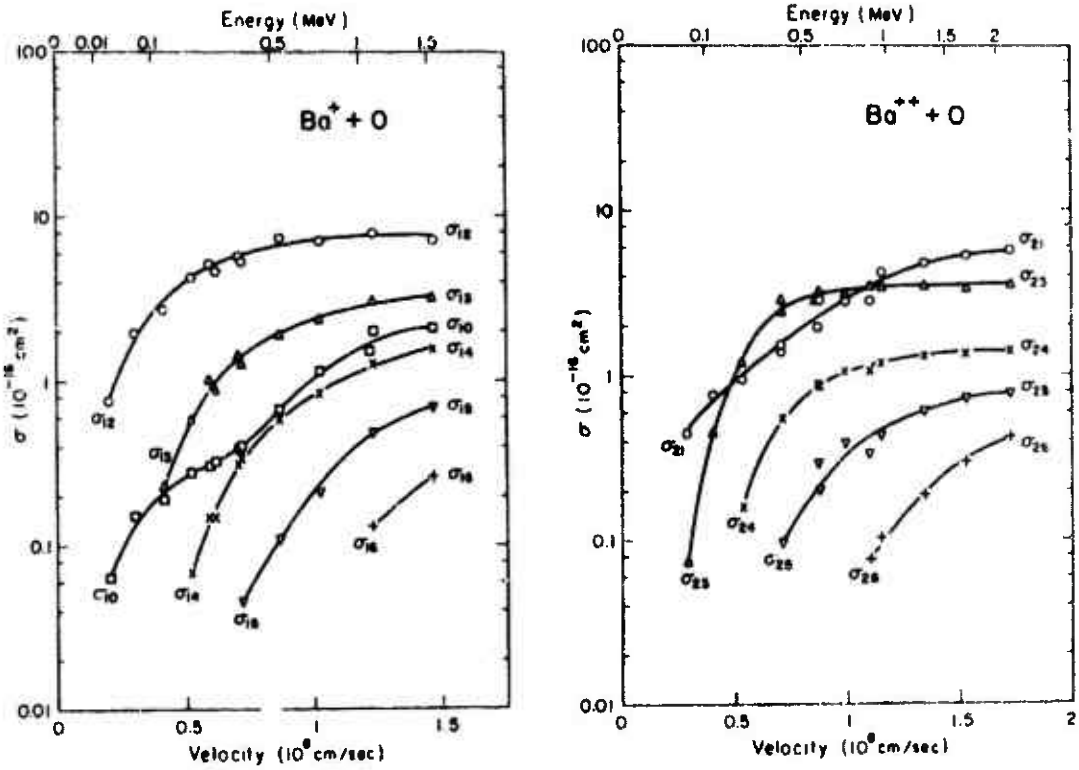

## 15.5.1.3 ION PROJECTILES ON MOLECULAR NITROGEN

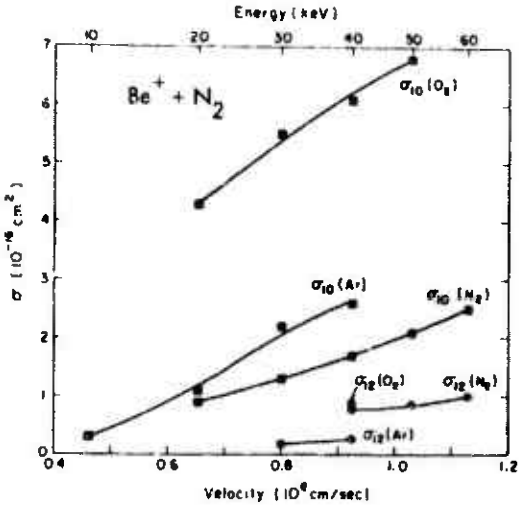


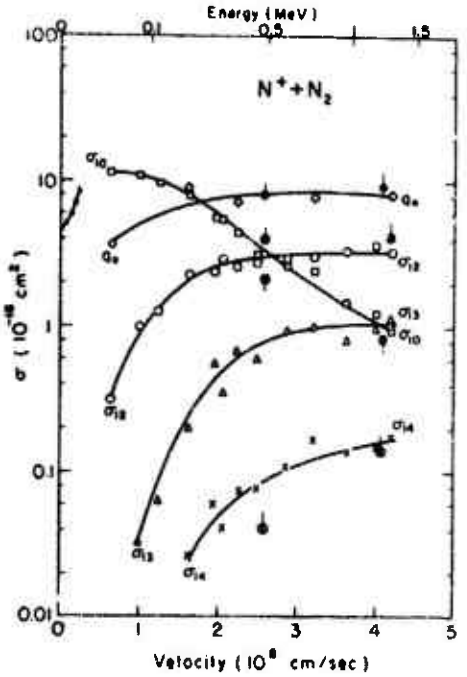


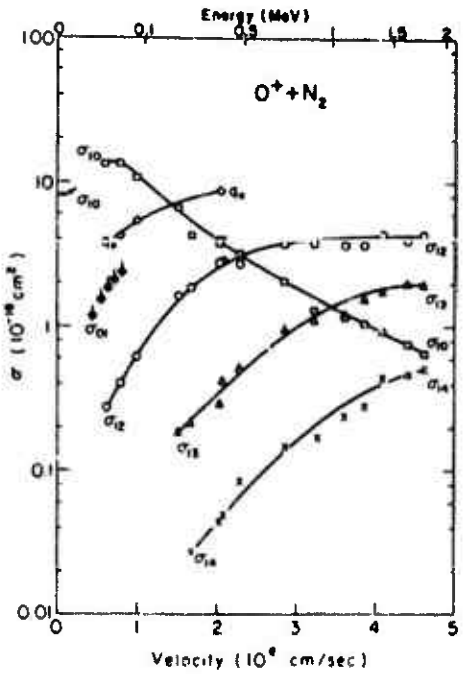


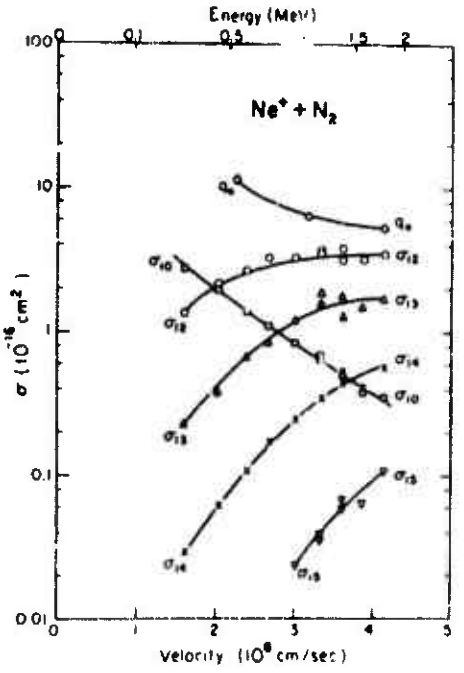

## 15.5.1.3 ION PROJECTILES ON MOLECULAR NITROGEN (Cont'd.)

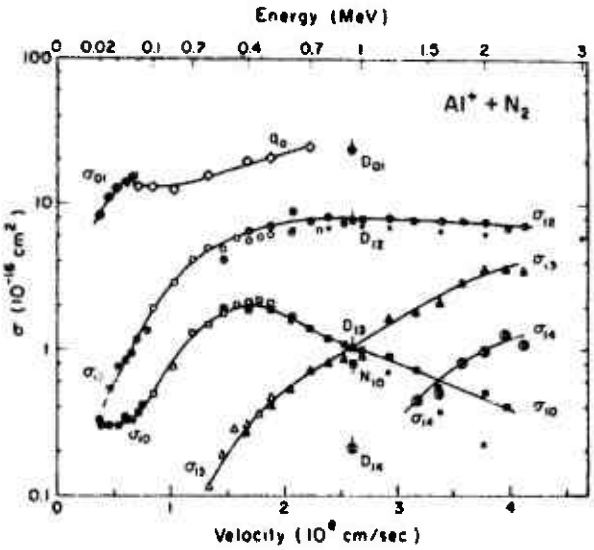


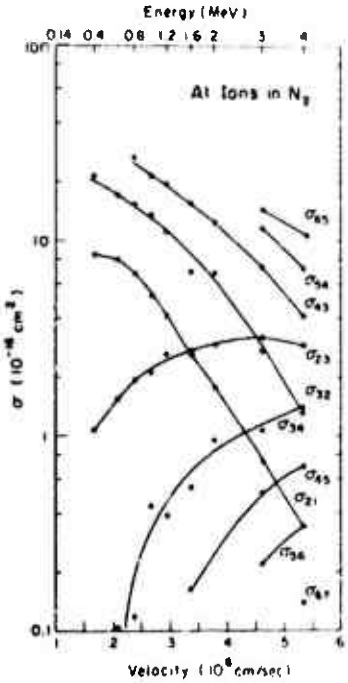


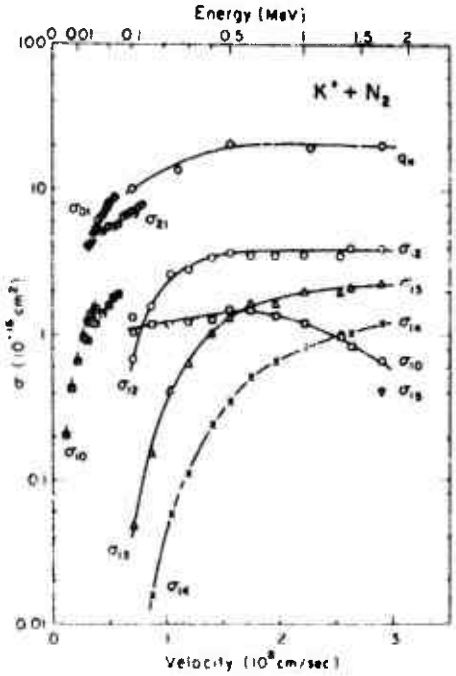


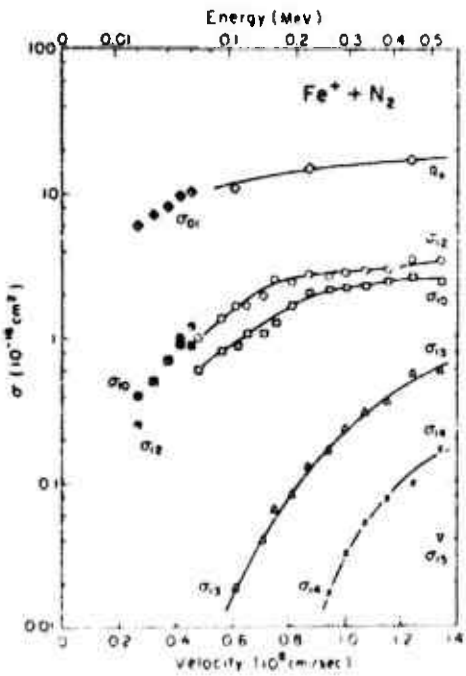

## 15.5.1.3 ION PROJECTILES ON MOLECULAR NITROGEN (Cont'd.)

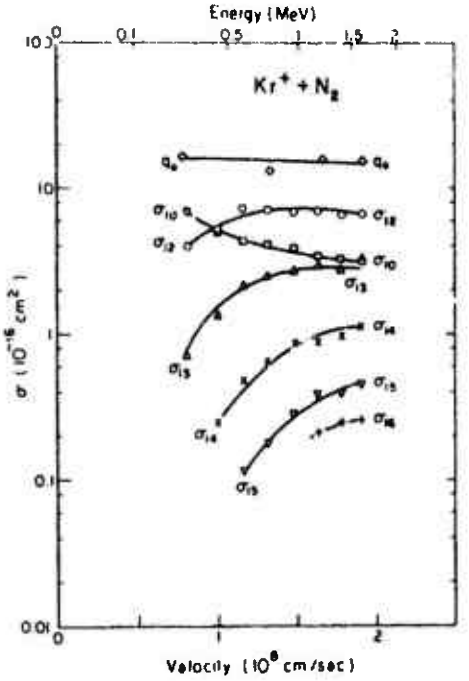


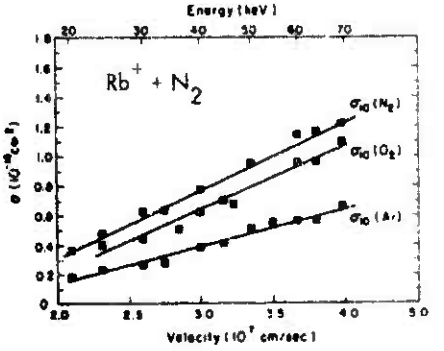


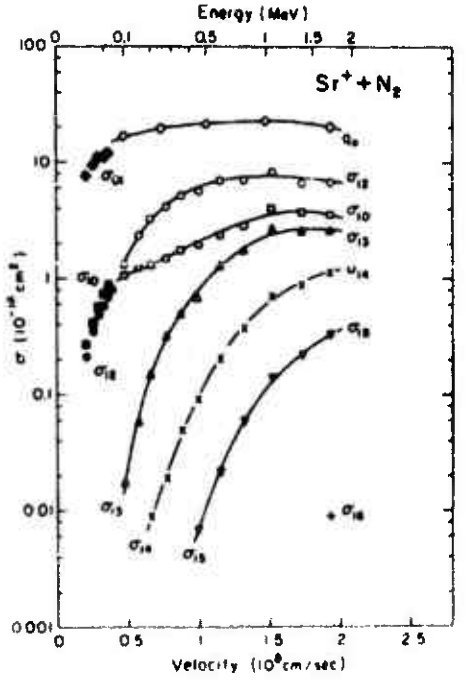


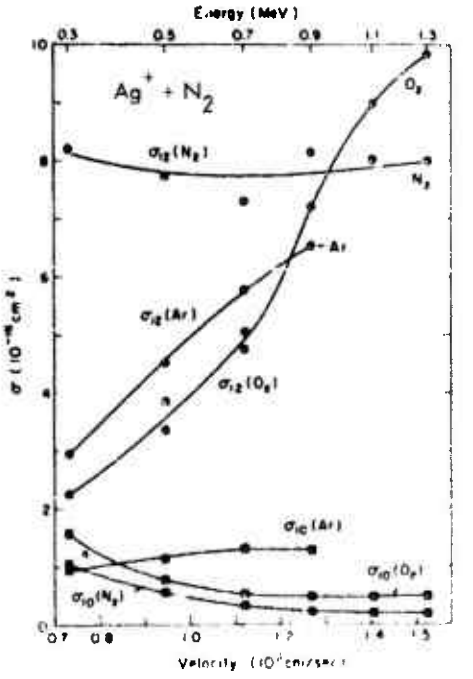

## 15.5.1.3 ION PROJECTILES ON MOLECULAR NITROGEN (Cont'd.)

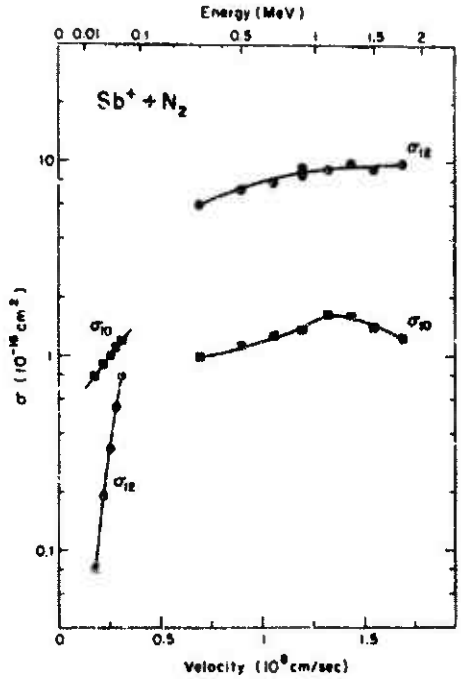


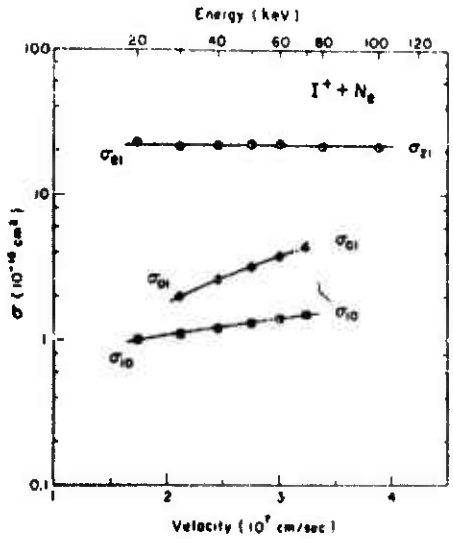


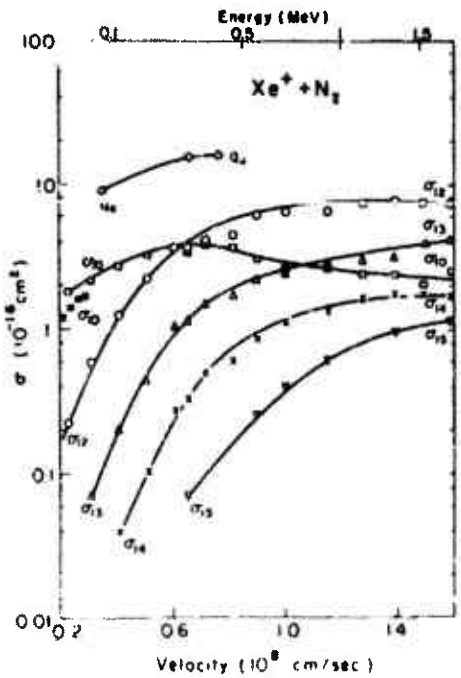


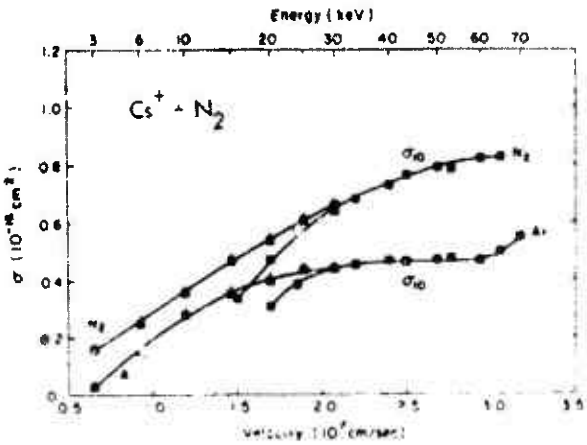

## 15.5.1.3 ION PROJECTILES ON MOLECULAR NITROGEN (Cont'd.)

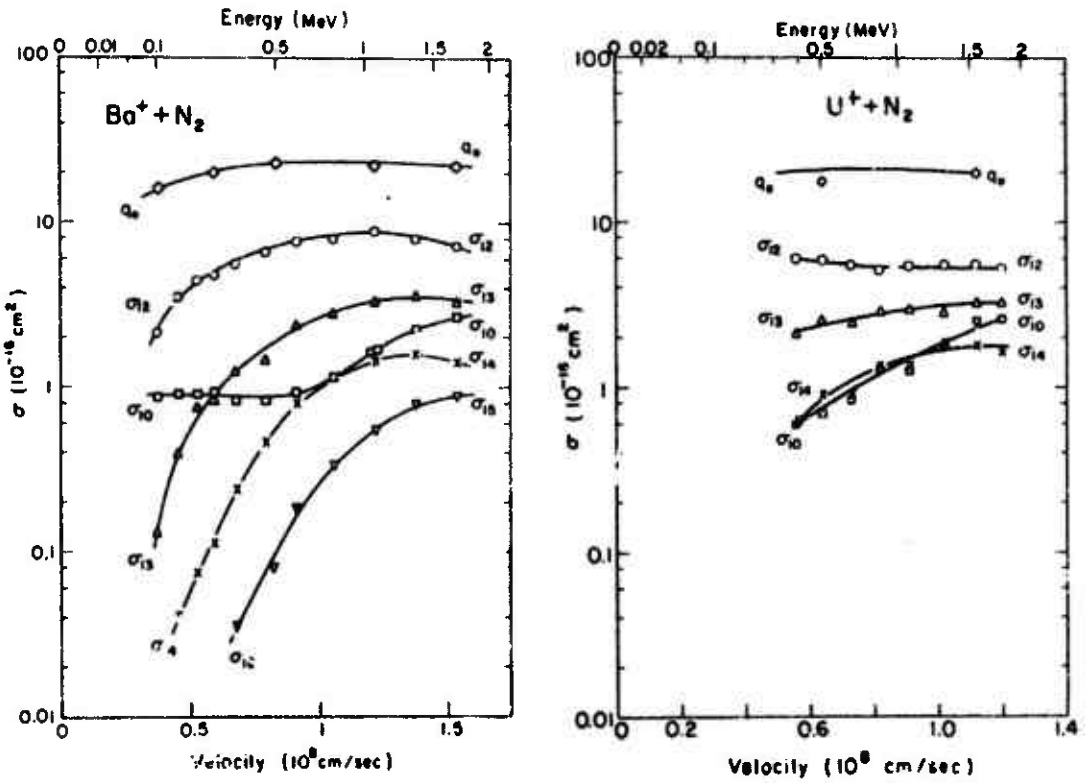

## 15.5.1.4 ION PROJECTILES ON MOLECULAR OXYGEN

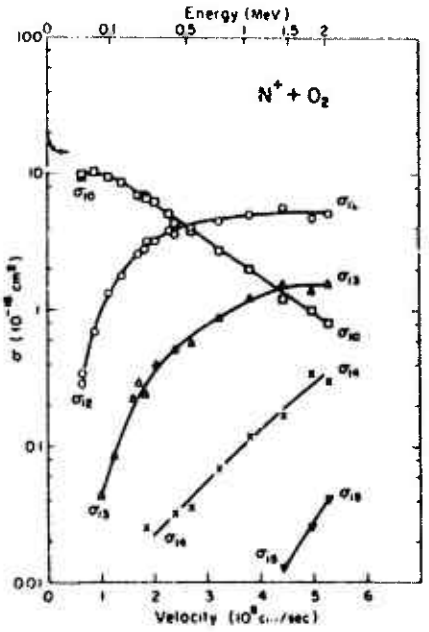


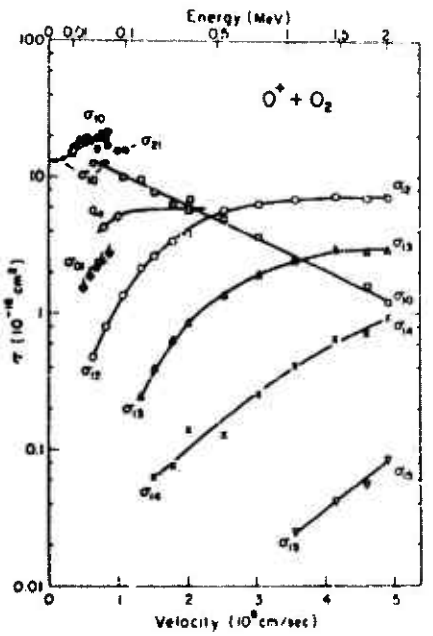


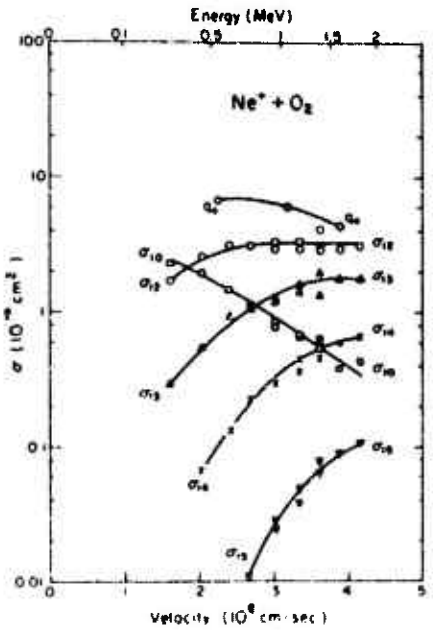


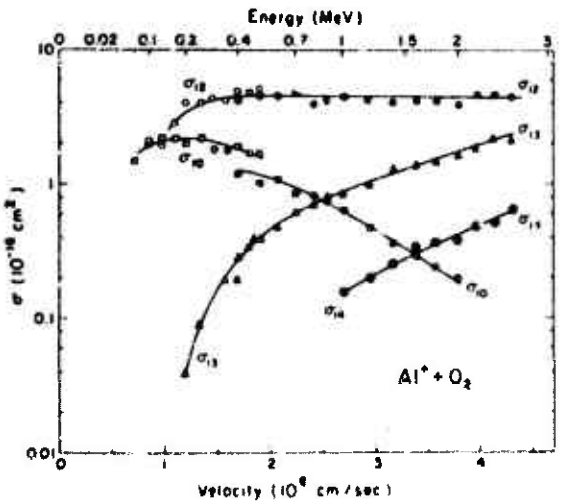

## 15.5.1.4 ION PROJECTILES ON MOLECULAR OXYGEN (Cont'd.)

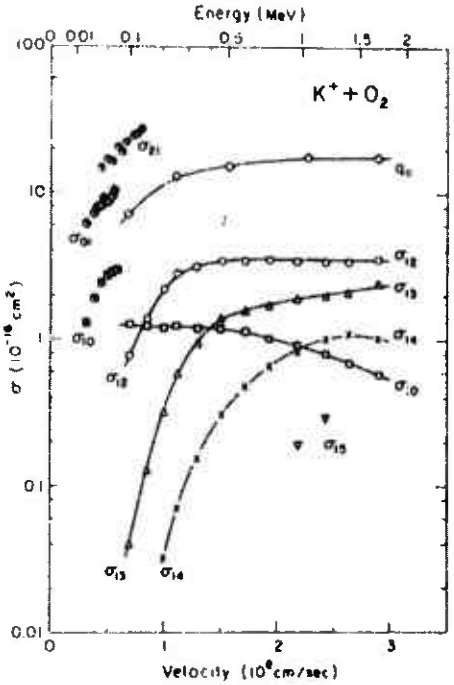


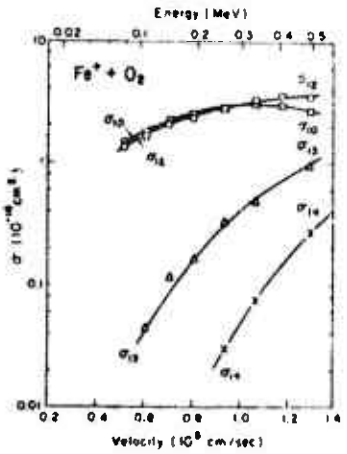


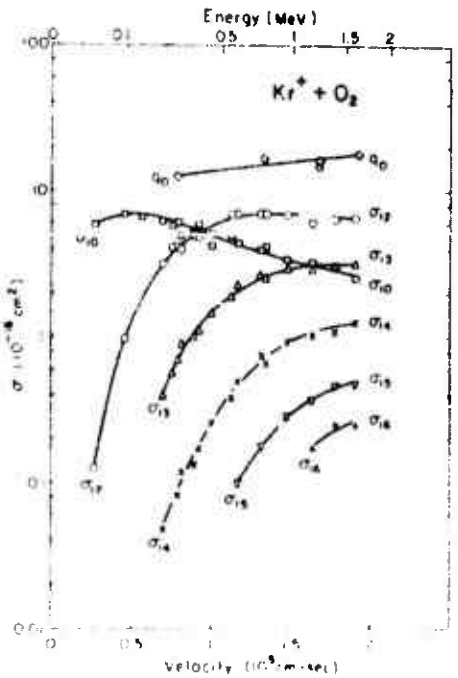


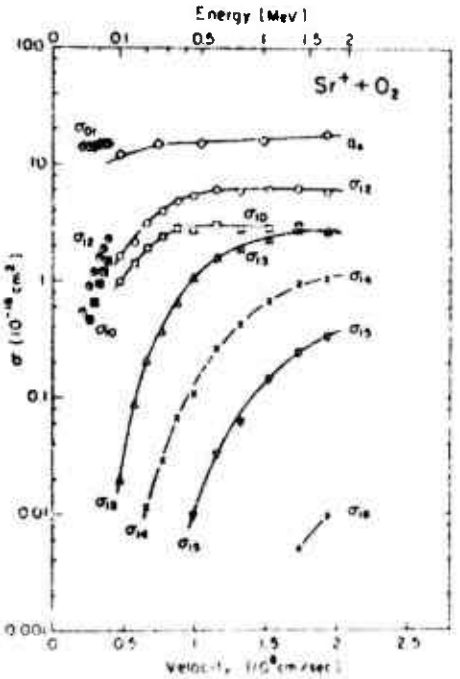

## 15.5.1.4 ION PROJECTILES ON MOLECULAR OXYGEN (Cont'd.)

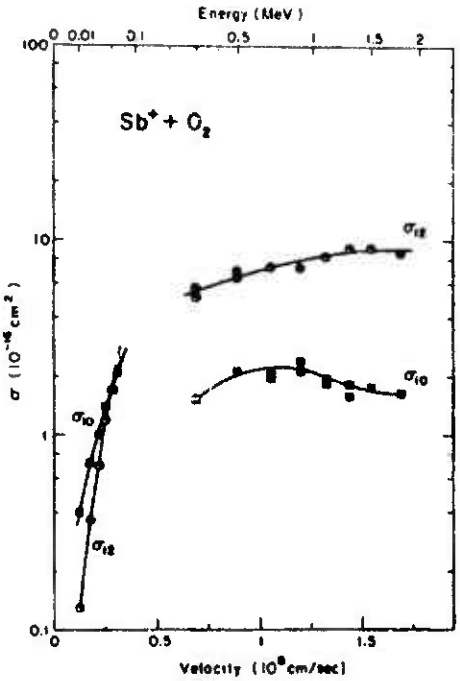


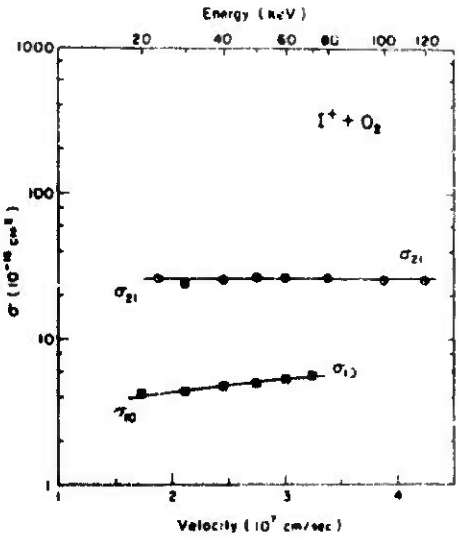


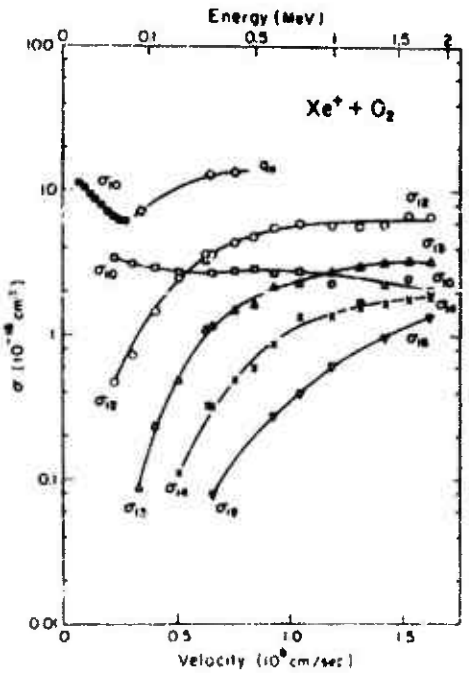


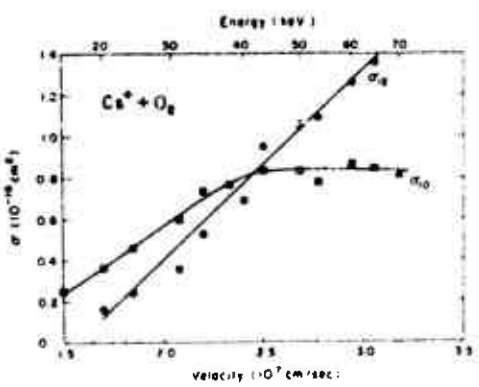

## 15.5.1.4 ION PROJECTILES ON MOLECULAR OXYGEN (Cont'd.)

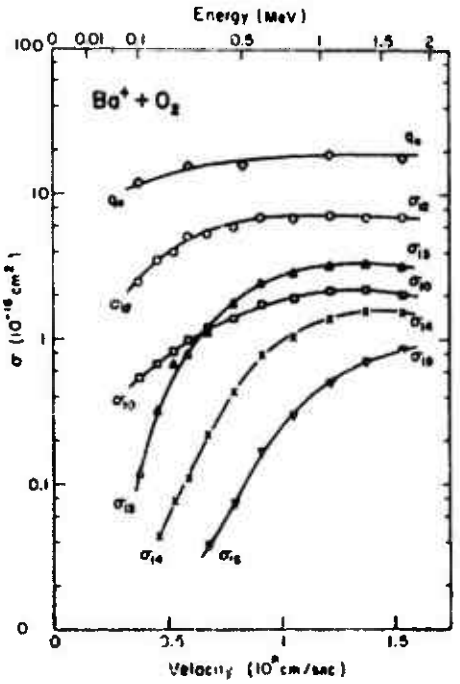


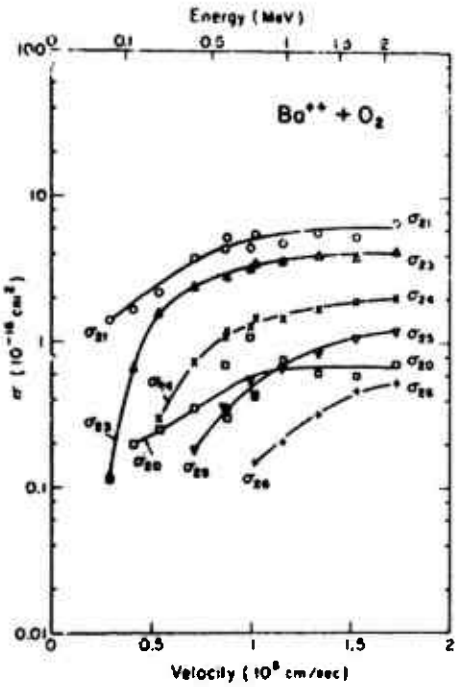


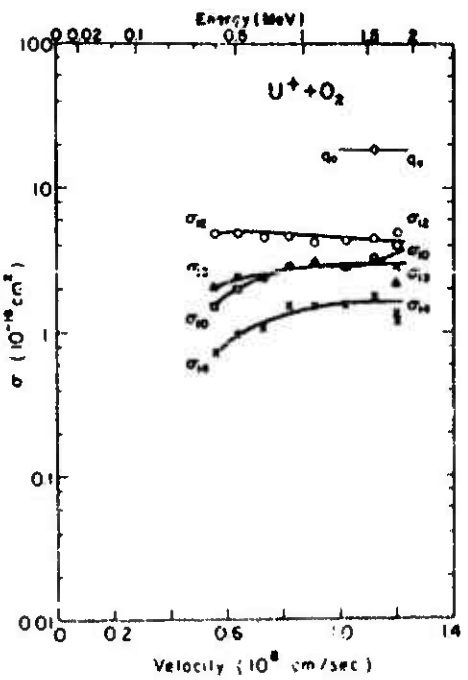

## 15.5.2 Species of Slow Ions Formed

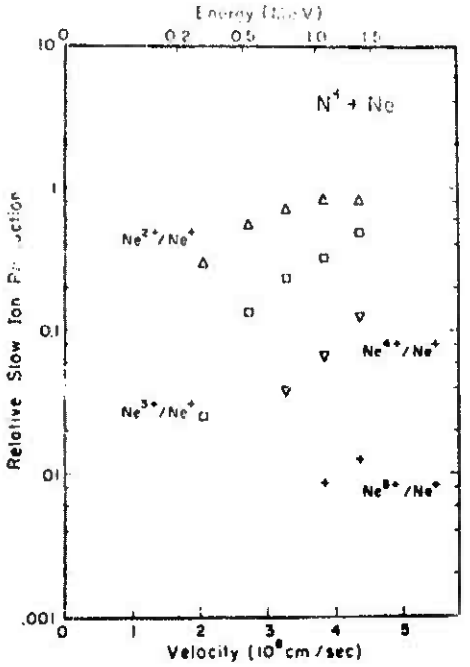


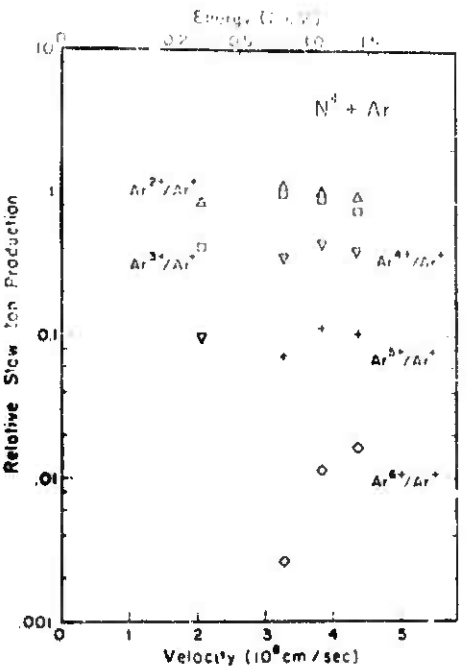


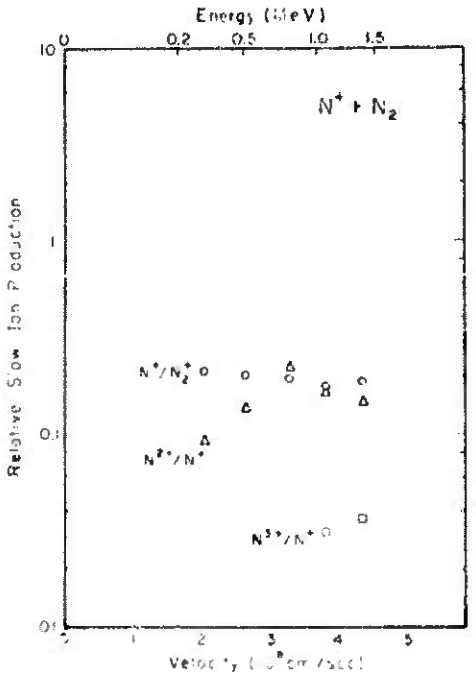


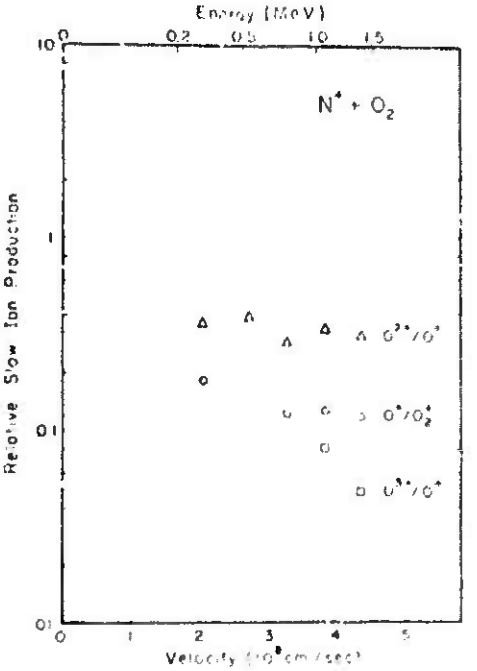

## 15.5.3 Electron and Slow Positive-Charge Production Cross-Sections ($Q_-$, $Q_+$)

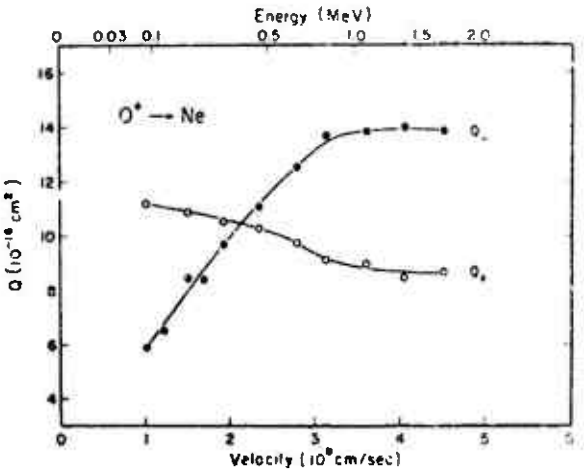


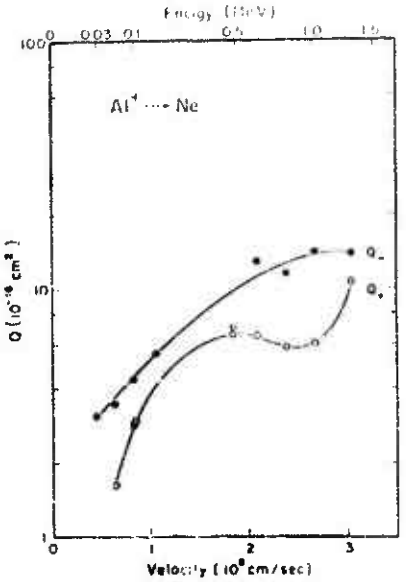


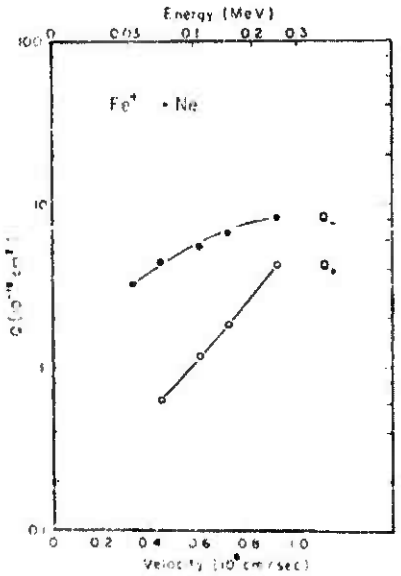


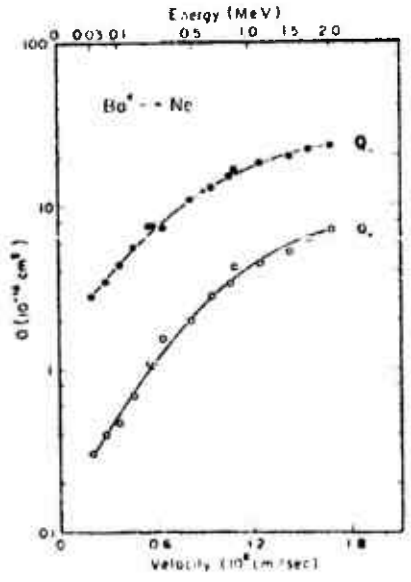

## 15.5.3 Electron and Slow Positive-Charge Production Cross-Sections ($Q_-$, $Q_+$) (Cont'd.)

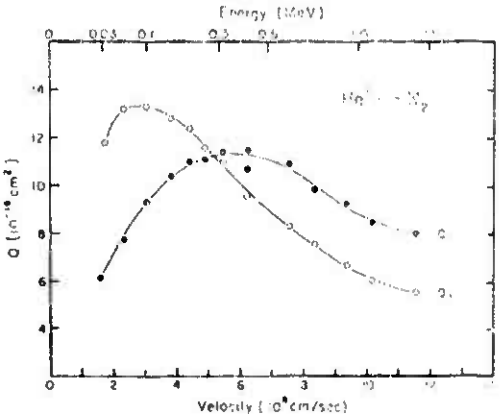


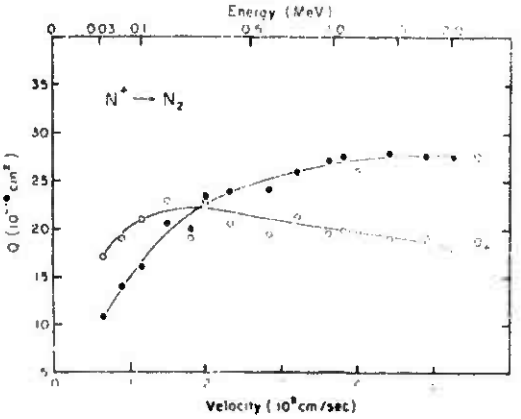


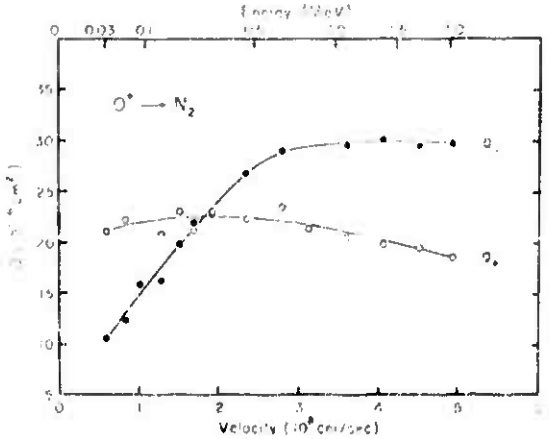


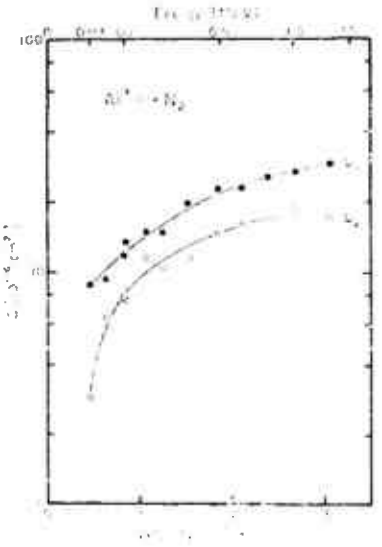

## 15.5.3 Electron and Slow Positive-Charge Production Cross-Sections ($Q_-$, $Q_+$) (Cont'd.)

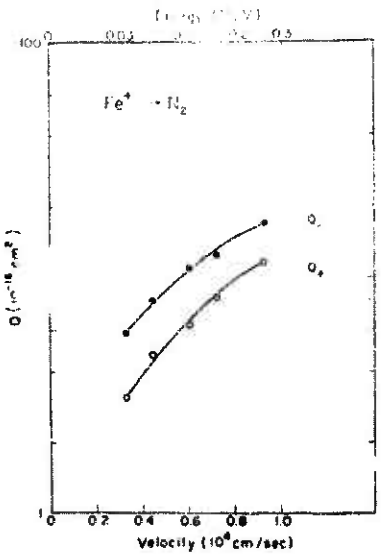


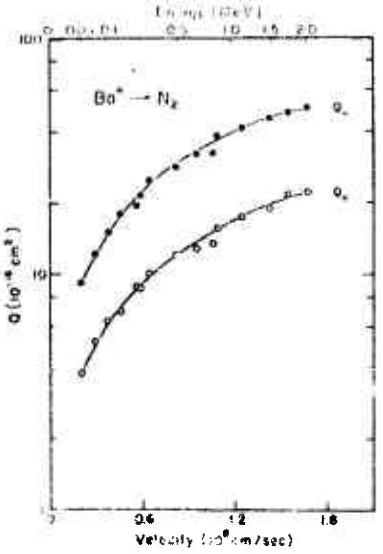


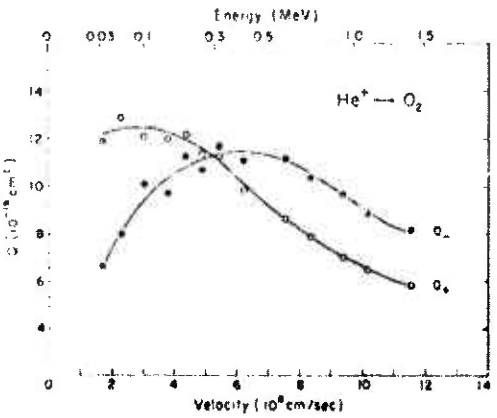


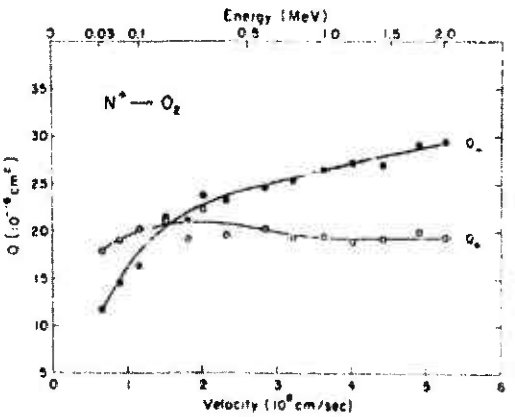

## 15.5.3 Electron and Slow Positive-Charge Production Cross-Sections ($Q_-$, $Q_+$) (Cont'd.)

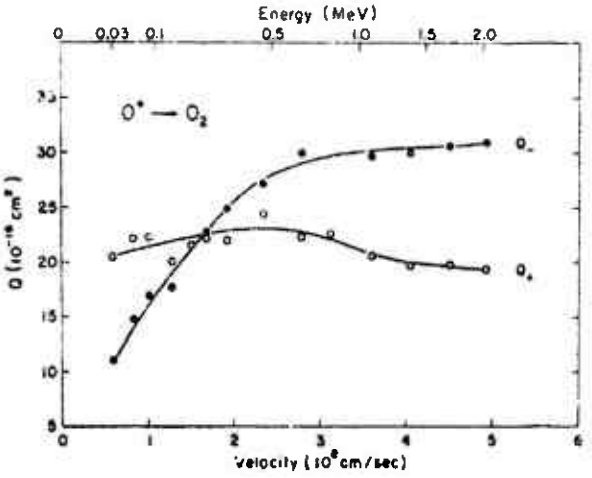


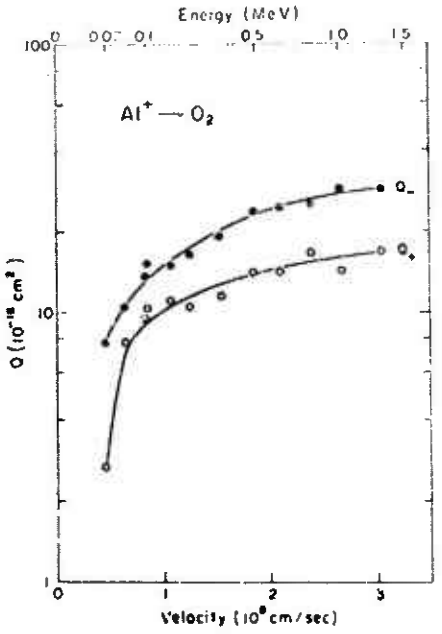


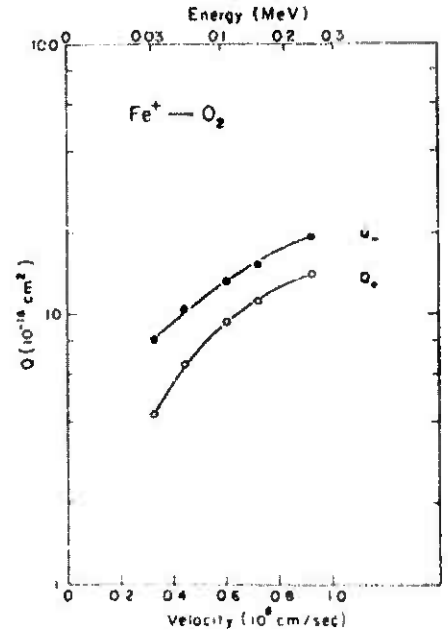


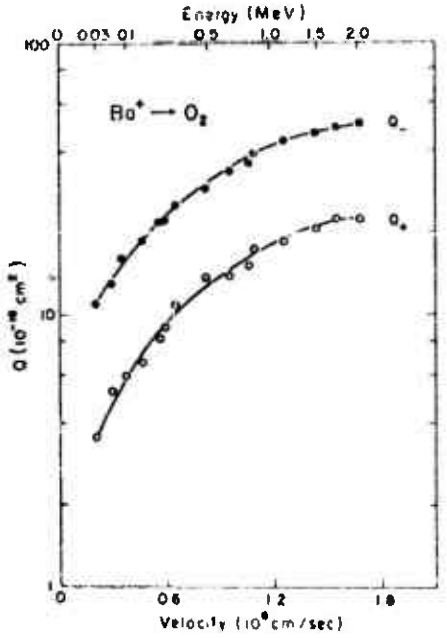

## REFERENCES

15-1. Allison, S. K., Revs. Mod. Phys. 30, 1137 (1958).

15-2. Allison, S. K., and M. Garcia-Munoz, in Atomic and Molecular Processes, D. R. Bates, Ed., Academic Press, New York (1962); p. 721.

15-3. Hasted, J. B., in Advances in Electronics and Electron Physics, L. L. Marton, Ed., Academic Press, New York (1960); Vol. 13, p. 1.

15-4. Bates, D. R., and A. E. Kingston, in Advances in Atomic and Molecular Physics, D. R. Bates, Ed., Academic Press, London, England (1970); Vol. 6, p. 269.

15-5. Fedorenko, N. V., Usp. Fiz. Nauk 68, 431 (1959).

15-6. Fedorenko, N. V., Sov. Phys.-Tech. Phys. 15, 1947 (1971).

15-7. Whitaker, W. A., and J. S. Greene, Jr., AFWL Handbook of Extrathermal Collision Processes (Draft), Handbook No. AFWL-HB-69-1, Air Force Weapons Laboratory, Kirtland AFB, New Mexico (1969). The draft was distributed in limited numbers to prospective contributing authors as a basis for coordinating contemplated inputs.

15-8. Brackmann, R. T., and W. L. Fite, Air Force Weapons Lab., Tech. Rept. AFWL-TR-68-96 (1968).

15-9. Kurzweg, L., H. H. Lo, R. T. Brackmann, and W. L. Fite, Phys. Rev. 179, 55 (1969).

15-10. Brackmann, R. T., W. L. Fite, and H. H. Lo, Air Force Weapons Lab., Tech. Rept. AFWL-TR-70-9 (1970).

15-11. Bohr, N., Kel Danske Videnskab Selskab, Mat. Fys. Medd. 18, No. 8 (1948).

15-12. Bohr, N., and Lindhard, Kel Danske Videnskab Selskab, Mat. Fys. Medd. 28, No. 7 (1954).

15-13. Bell, G., Phys. Rev. 90, 548 (1953).

15-14. Gluckstern, R., Phys. Rev. 98, 1817 (1955).

15-15. Thomas, H., Proc. Roy. Soc. A114, 561 (1927).

15-16. Dalgarno, A., T. C. Degges, E. T. Florance, G. A. Victor, and T. G. Webb, Air Force Weapons Lab., Tech Rept. AFWL-TR-64-110 (1965).

15-17. Florance, E. T., Geophysical Corporation of America, Tech. Rept. 64-2-A (1964).

15-18. Dalgarno, A., E. T. Florance, H. K. McComber, and T. G. Webb, Air Force Weapons Lab., Tech. Rept. AFWL-TR-65-203 (1966).

15-19. Bates, D. R., and R. A. Mapleton, Proc. Phys. Soc. 87, 657 (1966).

15-20. Burgess, A., and I. C. Percival, in Advances in Atomic and Molecular Physics, D. R. Bates and I. Estermann, Eds., Academic Press, New York (1968); Vol. 4, p. 109.

15-21. Garcia, J. D., Phys. Rev. 159, 39 (1967).

15-22. Gryzinski, M., Phys. Rev. 115, 374 (1959).

15-23. Gryzinski, M., Phys. Rev. 138, A305 (1965).

15-24. Gryzinski, M., Phys. Rev. 138, A322 (1965).

15-25. Gryzinski, M., Phys. Rev. 138, A336 (1965).

15-26. Garcia, J. D., E. Gerjuoy, and J. Welker, Phys. Rev. 165, 72 (1968).

15-27. Garcia, J. D., E. Gerjuoy, and J. Welker, Phys. Rev. 165, 66 (1968).

15-28. Fite, W. L., E. Gerjuoy, J. D. Garcia, and J. A. Peden, Air Force Weapons Lab., Tech. Rept. AFWL-TR-69-26 (1969).

15-29. Fleischmann, H. H., and R. C. Dehmel, Seventh Intl. Conf. Phys. Electronic Atomic Collisions, Amsterdam, Netherlands (1971).

15-30. Fleischmann, H. H., R. C. Dehmel, and S. K. Lee, "Direct Transition Features in Stripping Collisions of Heavy Neutral Atoms and Ions", Submitted to Phys. Rev. (1971).

15-31. Dalgarno, A., E. J. Florance, H. K. Macomber, and T. G. Webb, Air Force Weapons Lab., Tech. Rept. AFWL-TR-67-1 (1967).

15-32. Bates, D. R., and R. McCarroll, Adv. Phys. 11, 39 (1962).

15-33. Dalgarno, A., T. G. Webb, and G. A. Victor, Air Force Weapons Lab., Tech. Rept. AFWL-TR-68-114 (1969).

15-34. Rosen, N., and C. Zener, Phys. Rev. 40, 502 (1932).

15-35. Rapp, D., and W. E. Francis, J. Chem. Phys. 37, 2631 (1962).

15-36. Firsov, O. B., Sov. Phys.-JETP 5, 1192 (1957).

15-37. Firsov, O. B., Sov. Phys.-JETP 6, 534 (1968).

15-38. Firsov, O. B., Sov. Phys.-JETP 9, 1076 (1959).

15-39. Pivovar, L. I., Yu Z. Levchenko, A. N. Grigor'ev, and S. M. Khazan, Sov. Phys.-JETP 29, 399 (1969).

15-40. Landshoff, R. K., and J. K. Magee, Lockheed Missiles and Space Co., Rept. LMSC-3-27-67-1, Vol. 4 (1967).

15-41. Russek, A., Phys. Rev. 132, 246 (1963).

15-42. Hasted, J. B., Physics of Atomic Collision, Butterworths, Washington, D. C. (1964).

15-43. Brackmann, R. T., et al., Fourth Intl. Conf. Phys. Electronic Atomic Collisions, Quebec, Canada, 1965, Science Bookcrafters, Inc., Hastings-on-Hudson, N. Y. (1965); p. 326.

15-44. Brackmann, R. T., H. H. Lo, and W. L. Fite, Fifth Intl. Conf. Phys. Electronic Atomic Collisions, Leningrad, USSR, 1967, Nauka Publishing House, Leningrad (1967); p. 422.

15-45. Fite, W. L., J. K. Layton, and R. F. Stebbings, Air Force Weapons Lab., Tech. Rept. AFWL-TR-65-181 (1966).

15-46. Layton, J. K., R. F. Stebbings, R. T. Brackmann, W. L. Fite, W. R. Otto, C. E. Carlston, A. R. Comeaux, G. D. Magnuso, and P. Mahadevan, Phys. Rev. 161, 73 (1967).

15-47. Layton, J. K., and W. L. Fite, Air Force Weapons Lab., Tech. Rept. AFWL-TR-67-2 (1967).

15-48. Lo, H. H., PhD. Thesis, Univ. of Pittsburgh (1969).

15-49. Lo, H. H., and W. L. Fite, Atomic Data 1, 305 (1970).

15-50. Dmitriev, I. S., V. S. Nikolaev, L. N. Fateeva, and Ya. A. Teplova, Sov. Phys.-JETP 15, 11 (1962).

15-51. Dmitriev, I. S., V. S. Nikolaev, L. N. Fateeva, and Ya. A. Teplova, Sov. Phys.-JETP 16, 259 (1963).

15-52. Fogel, Ya. M., V. A. Ankudinov, and D. V. Filipenko, Sov. Phys.-JETP 8, 601 (1959).

15-53. Jones, P. R., F. P. Ziemba, H. A. Moses, and E. Everhart, Phys. Rev. 113, 182 (1959).

15-54. Layton, J. K., Fifth Intl. Conf. Phys. Electronic Atomic Collisions, Leningrad, USSR, 1967, Nauka Publishing House, Leningrad (1967); p. 412.

15-55. Turner, B. R., General Atomic, Rept. DASA 2227 (1969).

15-56. Nikolaev, V. S., I. S. Dmitriev, L. N. Fateeva, and Ya. A. Teplova, Sov. Phys.-JETP 13, 695 (1961).

15-57. Ryding, G., A. B. Wittkower, G. H. Nussbaum, A. C. Saxman, and P. H. Rose, Sixth Intl. Conf. Phys. Electronic Atomic Collisions, Cambridge, Mass., 1969, MIT Press, Cambridge, Mass. (1969), p. 696.

15-58. Stebbings, R. F., A. C. H. Smith, and H. B. Gilbody, J. Chem. Phys. 38, 2280 (1963).

15-59. Stebbings, R. F., A. C. H. Smith, and H. Ehrhardt, in Atomic Collision Processes, M. R. C. McDowell, Ed., North Holland Publishing Co., Amsterdam (1964); p. 814.

15-60. Stebbings, R. F., B. R. Turner, and A. C. H. Smith, J. Chem. Phys. 38, 2277 (1963).

15-61. Wittkower, A. B., and H. B. Gilbody, Proc. Phys. Soc. 90, 353 (1967).

# 16. CHARGED-PARTICLE RECOMBINATION PROCESSES

Manfred A. Biondi, University of Pittsburgh
(Latest Revision 10 August 1971)

## 16.1 INTRODUCTION

Recombination between electrons and positive ions or between positive and negative ions may proceed as a direct two-body interaction or may require the assistance of a third body, such as a neutral molecule or perhaps another electron. (Processes in which a positive or negative ion acts as the third body have not been studied; however, under circumstances of interest one expects such processes to be of lesser importance.) As we shall see, much of our quantitative information concerning recombination rates has been obtained from experiment; however, in a number of cases theoretical estimates are all we have for the rate of a particular recombination process. Probably the most extensive experimental work has been devoted to studies of two-body recombination processes, especially dissociative electron-ion recombination, with substantial work on collisional-radiative electron-ion recombination. (At moderate to high plasma densities, electrons act as third bodies in the latter reaction.) Three-body, neutral-stabilized electron-ion recombination has been studied experimentally and little more than estimates of the rate of such recombination have been made theoretically. In the case of ion ion recombination there are some experimental data concerning both two-body (mutual neutralization) and neutral stabilized, three-body recombination. However, only a few cases of interest have been studied; thus appeal will also be made to theoretical calculations for estimated rates. A discussion of electron-ion and ion-ion recombination processes of importance in the upper atmosphere has been given in a review (Reference 16-1).

The principal recombination reactions we shall deal with may be placed in the following simplified classifications:

A. Electron-Ion

1. Two-Body

a. Dissociative $XY^+ + e \rightarrow X + Y$ (16-1)

1. Two-Body (Cont'd.)

   b. Radiative† $X^+ + e \rightarrow X^* + h\nu$ (16-2)

2. Three-Body

   a. Electron-Stabilized† $X^+ + e + e \rightarrow X^* + e$ (16-3)

   b. Neutral-Stabilized $X^+ + e + M \rightarrow X^* + M$ (16-4)

B. Ion-Ion

1. Two-Body

   a. Mutual Neutralization $X^+ + Y^- \rightarrow X + Y$ (16-5)

2. Three-Body

   a. Thomson (neutral-stabilized) $X^+ + Y^- + M \rightarrow X + Y + M$ (16-6)

In following sections the rates of specific reactions of interest are presented and pertinent factors relating to the reliability of the measurements and/or theoretical calculations are discussed.

## 16.2 METHODS OF MEASUREMENT AND ANALYSIS

With the possible exception of merged-beam and certain shock-tube measurements, determinations of recombination coefficients start with the appropriate continuity equation for the electrons or ions under study.†† Using electrons as an example, we have, at a given point in space:

$$\partial n_e/\partial t = \sum_i P_i - \sum_j L_j - \nabla \cdot \vec{\Gamma}_e , \quad (16\text{-}7)$$

where $P_i$ represents the rates of various processes leading to electron production (e.g., photoionization), $L_j$ represents the rates of

† These two reactions taken together comprise the "Collisional-Radiative" recombination process, i.e., A.1.b and A.2.a.

†† In the case of varying electron or ion "temperature" during the measurements, it is necessary to use the full Boltzmann Transport Equation in the analysis.

volume electron destruction processes (e.g., attachment to neutral molecules and recombination with positive ions), and $\vec{\Gamma}_e$ represents the particle current density (e.g., the diffusion of electrons to the boundaries of the container holding the ionized gas). With the possibility of so many processes contributing to the growth or decay of electron density it is necessary to achieve conditions under which one, or at most a few, processes are of importance in order to obtain reliable, quantitative determinations of the desired recombination coefficients.

The rates of two- and three-body electron-ion recombinations may be represented in the forms:

$$L_{2r} = \alpha_{2r} n_e n_+ , \tag{16-8}$$

and:

$$L_{3r} = k_{3r} n_e n_+ n_s , \tag{16-9}$$

where $\alpha_{2r}$ is the two-body recombination coefficient, $k_{3r}$ the three-body rate coefficient, and $n_e$ , $n_+$ , and $n_s$ are electron, positive-ion, and stabilizing agent (electron or neutral molecule) concentrations, respectively. Analogous equations, involving substitution of the negative-ion concentration $n_-$ for $n_e$ , describe ion-ion recombination coefficients. It can be seen that, in order to obtain an absolute rate determination, an absolute determination of the electron or ion concentration is required; therefore, it is important to have reliable techniques for such absolute determinations.

Four principal methods have been used in the recombination coefficient studies: (1) measurements of rate of growth of ionization; (2) measurements of stationary ionization density reached when a steady ionization source is turned on at time zero; (3) measurements of the rate of decay of ionization when the ionizing source is suddenly turned off (afterglow measurements); and (4) determinations of the production of neutral atoms by the merging of an electron and an ion beam. In some experiments more than one of these methods have been used to cross-check the rate determinations.

The apparatuses used fall roughly into microwave afterglow, ionization chamber, shock tube, and merged beam categories. Several ionizing sources have been used in the studies; pulsed dc discharges, microwave discharges, photoionization, chemionization, and pulsed

high-energy (MeV) electron beams are the principal ones. Absolute determinations of average electron and ion densities have been provided by microwave and radio-frequency techniques (good accuracy), by ionization chamber charge collection (good accuracy), and by Langmuir probes (questionable accuracy). In the merged-beam studies, the currents of electrons and of ions to a collecting electrode, together with probing of the beam profiles, are used to infer the ion and/or electron concentrations in the merged region.

As examples of the measurement procedures, consider the afterglow and the stationary-state analyses. The afterglow method involves establishment of an ionized gas by application of some external ionizing agent, followed by its abrupt termination. By careful choice of experimental parameters it is possible to assure that delayed ionization sources (e.g., metastable atoms) are negligible. When attachment is unimportant and only one type of positive ion is present in the afterglow, so that we may set $n_e \approx n_+$ (quasi-neutrality). Equation (16-7) reduces to:

$$\partial n_e(\vec{r}, t)/\partial t = -\alpha_{2r} n_e^2(\vec{r}, t) - \nabla \cdot \vec{\Gamma}_e(\vec{r}, t) , \qquad (16\text{-}10)$$

if electron-ion recombination proceeds via the two-body process. Inasmuch as the measuring techniques provide volume-averaged electron densities, it is necessary to integrate Equation (16-10) over the volume of the container. Since it is often possible to neglect the diffusive flow of electrons to the boundary in comparison to the volume loss by recombination, one obtains the simplified result:

$$d\left\langle n_e(t)\right\rangle/dt = -\alpha_{2r}\left\langle n_e^2(t)\right\rangle , \qquad (16\text{-}11)$$

where the brackets refer to space averages of the electron density. Solution of Equation (16-11) following separation of variables (Reference 16-2) yields the "recombination solution":

$$\left\langle n_e(t)\right\rangle^{-1} - \left\langle n_e(0)\right\rangle^{-1} = S\alpha_{2r} t , \qquad (16\text{-}12)$$

where $S = \left\langle n_e^2(r)\right\rangle \left\langle n_e(r)\right\rangle^{-2}$ is the electron density "shape factor" resulting from diffusion to the boundaries. Thus, <u>absolute</u> determinations of $\alpha$ require not only absolute values of average electron density but also knowledge of the <u>form</u> of the spatial distribution of the electrons and ions in the bounding container. Gray and Kerr (Reference 16-3) have obtained computer solutions of Equation (16-10)

for the infinite cylinder and the sphere; Frommhold and Biondi (Reference 16-4) present a computer-code solution applicable to finite cylinders, rectangular parallelepipeds, and certain one-dimensional geometries. These solutions permit correction of the data to obtain $\alpha$ from the ($S\alpha$) determinations.

In the stationary-state method, a known, constant rate of ionization is maintained for a long time. Then, if attachment processes are unimportant and electron-ion recombination proceeds via a two-body process with only one type of positive ion present, Equation (16-7) leads to the condition:

$$\partial n_e/\partial t = 0 = P_i - \alpha_{2r} n_e^2 + D_a \nabla^2 n_e \ , \qquad (16\text{-}13)$$

where $D_a$ is the ambipolar diffusion coefficient of the electrons and positive ions. Efforts are made to achieve conditions in which the recombination greatly outweighs ambipolar diffusion. In this special case:

$$\alpha_{2r} = P_i / n_e^2(\infty) \ , \qquad (16\text{-}14)$$

where $n_e(\infty)$ is the stationary electron density reached a long time after the ionizing source is turned on. This method has been used by Doering and Mahan (Reference 16-5) and by Young and St. John (Reference 16-6) in their studies of dissociative recombination of $NO^+$ ions with electrons. As in the afterglow analysis it is necessary to consider the spatial distribution of the ionizing source and of the electron density in order to obtain absolute values of $\alpha$.

It should be noted that in this stationary method it is important to know the electron and ion energies during the measurement. By use of either photoionization, chemionization, or high-energy (MeV) electron beams (no applied fields), even though the electrons are produced with initial kinetic energy, they quickly decay to ambient gas temperature and may, therefore, be regarded as essentially thermal during the recombination events.

Two of the more troublesome problems encountered in the recombination studies are: (1) establishing the identity and the state of the ion under investigation; and (2) in the case of electron-ion recombination measurements in electronegative gases, minimizing attachment/negative-ion effects. The former problem has been solved

reasonably well in plasma-afterglow studies by adding a differentially pumped mass spectrometer to the side of the ionized-gas container and, simultaneously with electron or ion density measurements in the volume, monitoring the ion currents reaching the wall and effusing through a small hole into the mass spectrometer (References 16-2, 16-7 through 16-9). With positive ions it has sometimes been possible to identify the electronic and vibrational states in which they exist by knowledge of the ionizing source properties (e.g., Penning ionization by metastable atoms and photoionization with line radiation).

In the case of negative-ion effects in electron-ion recombination studies, it is not sufficient to make sure that the rate of electron attachment is small compared to recombination in a cycled afterglow or in a stationary-state measurement. Negative ions are essentially trapped in a plasma until the ambipolar space-charge field collapses (due to decreasing electron density); they therefore build up with time until enhanced ambipolar diffusion loss of electrons (References 16-10, 16-11) and positive-ion-negative-ion recombination become important, severely complicating the electron-ion recombination analysis. Here, at least in afterglow measurements, it has been possible to minimize these effects by using a "single-pulse" technique in which the gas is ionized for a brief period and the electron density decay is determined from a single afterglow. By starting with a small attachment rate, negative-ion buildup never becomes important during the recombination-controlled portion of the decay. However, in the stationary density measurements it is quite possible that negative-ion accumulation increases the electron loss by enhanced ambipolar diffusion to give an excessive apparent $\alpha$ value.

In determinations of positive-ion-negative-ion recombination rates, the techniques in many cases parallel those just described for the electron-ion recombination studies. For example, resonant-cavity techniques at radio frequencies provide determinations of ion density decays during the afterglow, as dc ionization chamber measurements. Merging beams of positive ions and negative ions have been used in recombination studies. In general, the problems with identification of the ions, specification of their spatial distributions, etc., discussed in the electron-ion case, must also be considered.

## 16.3 RESULTS

In this section, recombination rates for various ions and processes are discussed. Instead of guessing at such values for

ions which have been studied neither experimentally nor theoretically, the reader is asked to infer the likely rate for an uninvestigated ion by noting the results for the investigated ion most closely resembling the ion in question. In addition, although most of the relevant measurements are discussed in the text, only the most reliable data points and theoretical predictions are plotted in the accompanying figures.

### 16.3.1 Electron-Ion Recombination— Two Body Processes

#### 16.3.1.1 DISSOCIATIVE RECOMBINATION

It has been possible to show that the large two-body recombination rates ($\alpha_{2r} \gtrsim 10^{-7}$ cm$^3$/sec) observed in laboratory studies of noble gases such as neon and argon are the result of the dissociative recombination process (Equation 16-1) by demonstrating the required presence of molecular ions (References 16-12, 16-13) and by detecting the dissociation kinetic energy of the excited atoms produced by the recombination process (References 16-14, 16-15). It is reasonable to infer that similar laboratory studies of recombination involving ions of ionospheric interest (e.g., $N_2^+$, $O_2^+$, $NO^+$) also involve the dissociative recombination process.

$N_2^+$, $N_3^+$, $N_4^+$

Although there have been a number of studies of recombination in nitrogen afterglows (References 16-2, 16-16 through 16-21), lack of ion identification in most of the studies relegates them to a supporting role in establishing the desired rate coefficients. Simultaneous microwave and mass-spectrometric studies of nitrogen-neon afterglows permitted Kasner and Biondi (Reference 16-2) to establish the rate of recombination of $N_2^+$ ions with electrons under conditions where $T_e = T_+ = T_{gas} = 300$ K should obtain. The $N_2^+$ ion current to the walls accurately followed the recombination-controlled volume electron-density decay during much of the afterglow. The value, $\alpha(N_2^+) = (2.9 \pm 0.3) \times 10^{-7}$ cm$^3$/sec at 300 K was obtained from electron-density decay curves which obeyed the recombination law, Equation (16-13), over a density range $13 \leq f \leq 22$.*

*The quantity f is defined as range of reciprocal electron densities over which a linear variation with time (to within 1 percent) is obtained.

The Penning ionization of $N_2$ by neon $^3P_2$ metastables assured that the $N_2^+$ ions were in their ground electronic, and a low ($v \leq 4$, possibly $v = 0$) vibrational state. The error quoted is much larger than any random errors or any variation with experimental parameters such as nitrogen or neon pressure; it reflects uncertainty concerning the precise form of the electron spatial distribution within the cavity resulting from diffusion to the walls.

Kasner (Reference 16-20) has measured the variation of $\alpha(N_2^+)$ with gas temperature, again under conditions where it is expected that $T_e = T_+ = T_{gas}$, over the range 200 to 480 K. In these studies the cavity walls enclosing the ionized gas under investigation were heated or cooled. Over this range very little variation in $\alpha$ was found; a $T^{-0.62}$ power law variation provided the best fit to the data, starting from a value $\alpha(N_2^+) = (2.7 \pm 0.3) \times 10^{-7}$ cm$^3$/sec at 300 K (see Figure 16-1). Mehr and Biondi (Reference 16-21), using a multi-mode microwave afterglow apparatus to provide microwave electron heating while leaving $T_+ = T_{gas} = 300$ K, have determined the variation of $\alpha(N_2^+)$ with $T_e$ by comparison of the measured electron density decays from recombination-controlled afterglows with computer solutions of the continuity equation, Equation (16-10). The apparatus makes use of a differentially-pumped quadrupole mass spectrometer to sample the ions under study. Although conditions were achieved where ions other than $N_2^+$ (e.g., $N_3^+$) were a small minority throughout the recombination-controlled portion of the afterglow, ion "tracking" of the electron-density decays was imperfect, raising some question as to whether these values of $\alpha(N_2^+)$ are accurate to ± 10 percent, as should normally be the case. Mehr and Biondi found that over the range 300 K ≤ $T_e$ ≤ 5000 K, $\alpha(N_2^+)$ displayed a variation as $T_e^{-0.39}$, starting from a value $(1.8^{+0.4}_{-0.2}) \times 10^{-7}$ cm$^3$/sec at $T_e$ = 300 K. These data are also displayed in Figure 16-1. The rather different temperature dependencies of $\alpha(N_2^+)$ when $T_e$ alone is varied and when $T_e$ and $T_i$ are covaried is, in principle, explicable in terms of differing recombination coefficients for molecular ions in different vibrational states. However, the known large vibrational spacing of $N_2^+$ suggests that even at 480 K almost all of the ions in Kasner's study are in the $v = 0$ vibrational state and hence the two types of measurements should have given the same energy dependence over the common temperature range. No explanation is available for the difference, but it is suggested that, at higher electron temperatures (> 500 K), the $T_e^{-0.39}$ variation be used.

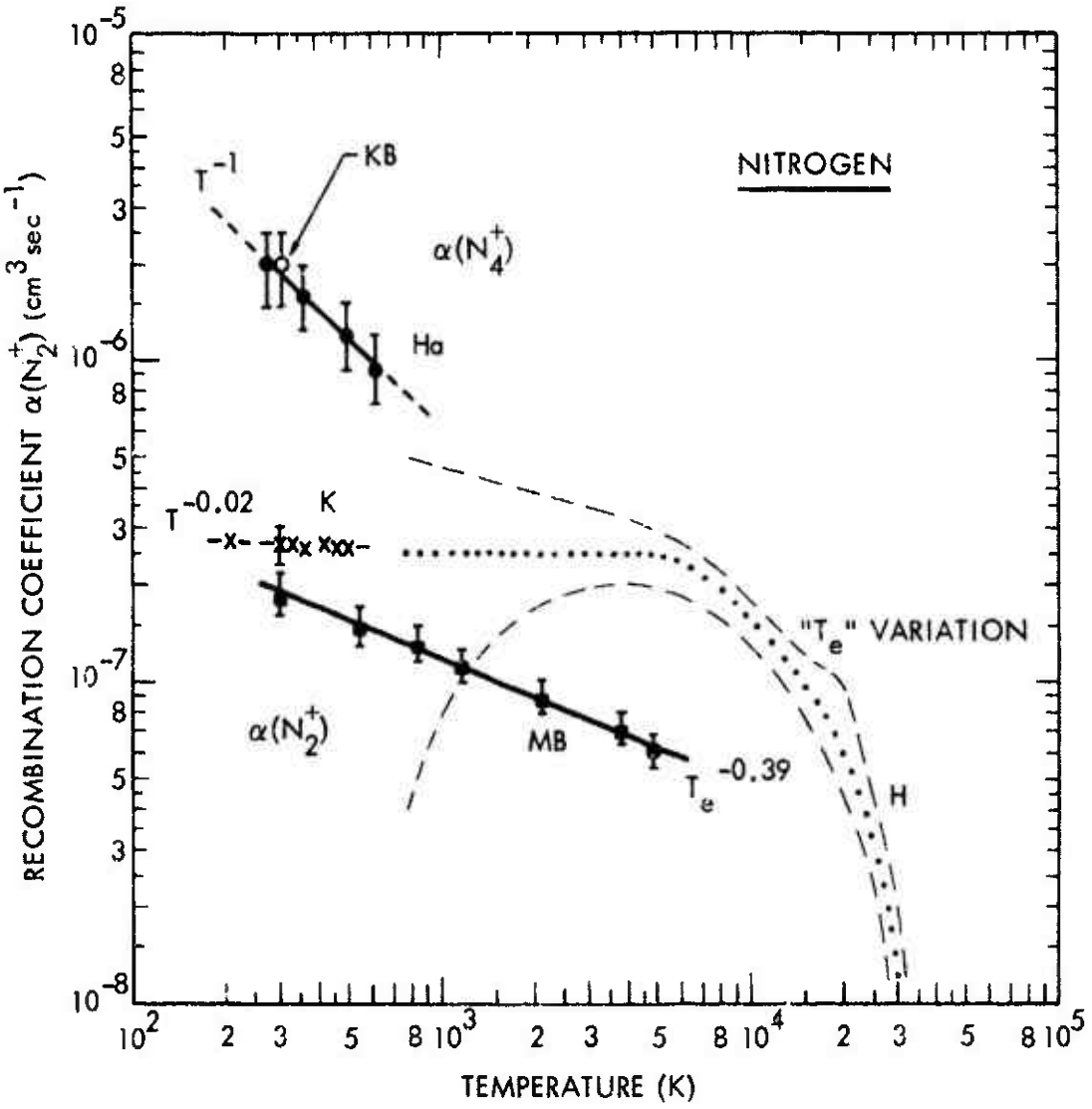


Figure 16-1. Two-body electron-ion recombination coefficients, $\alpha(N_2^+)$ and $\alpha(N_4^+)$. The symbol T refers to conditions such that $T_e = T_+ = T_{gas}$ and the symbol $T_e$ to the condition $T_+ = T_{gas} = 300\,K$, with $T_e$ variable. Results shown are from Kasner and Biondi (KB) (Reference 16-2), Hockam (Ho) (Reference 16-19), Kasner (K) (Reference 16-20), Mehr and Biondi (MB) (Reference 16-21), and Hagen (H) (Reference 16-22).

Kasner and Biondi (Reference 16-2) were able to study the recombination of the dimer ion $N_4^+$ by increasing the amount of nitrogen in their nitrogen-neon mixtures. At higher nitrogen partial pressures ($> 10^{-2}$ torr), $N_4^+$ and to a lesser extent $N_3^+$ are the important afterglow ions. A coefficient $\alpha(N_4^+) \simeq 2 \times 10^{-6}$ cm$^3$/sec was obtained at 300 K and the inference from the data appears to be that $\alpha(N_3^+)$ is appreciably smaller.

It is not possible to reconcile these results with the data of Mentzoni (Reference 16-18), who obtains a strong pressure dependence for $\alpha$ in nitrogen at much higher pressures (2 to 6 torr) than should lead to predominance of $N_2^+$ ions. In addition, his values at 300 K are too small to agree with the $N_4^+$ results of Kasner and Biondi. By way of contrast, Hackam (Reference 16-19) obtains very good agreement at 300 K and high nitrogen pressures ($> 10$ torr) between his recombination coefficient and the $\alpha(N_4^+)$ value of Kasner and Biondi. Over the temperature range 300 to 700 K he finds a variation of $\alpha$ approximately as $T^{-1}$. Thus, it is tentatively concluded that $\alpha(N_4^+)$ exhibits this variation for $T_e = T_+ = T_{gas}$ over the quoted range.

Before leaving the discussion of nitrogen, it should be noted that merging-beam determinations of $\alpha(N_2^+)$ have been the subject of preliminary reports (References 16-22, 16-23). Hagen (Reference 16-22) finds that $\alpha(N_2^+)$ starts from a value $(2.5^{+2}_{-2.0})\times 10^{-7}$ cm$^3$/sec at 0.1 eV relative energy between ions and electrons, varies little with energy to ~0.7 eV, and then falls more and more rapidly with increasing energy to ~5 eV. Theard (Reference 16-23), on the other hand, finds that the relative values of $\alpha(N_2^+)$ decrease approximately inversely with the first power of the relative energy between ~0.2 and 1 eV and then fall more and more rapidly up to the maximum relative energy (3eV) studied. These techniques, when made more quantitative, may prove useful for extending recombination-rate determinations to much higher electron energies than can be studied by plasma-afterflow techniques.

## $NO^+$, $(NO \cdot NO^+)$

There have been a number of investigations of recombination of $NO^+$ ions produced by photoionization of NO (References 16-5, 16-7, 16-24), by chemionization in mixtures of N and O atoms (Reference 16-6), and by fast (MeV) electron bombardment of NO gas (Reference 16-25). In only two of these studies (Reference 16-7

16-24) has a differentially-pumped mass spectrometer been used to identify the ions present, although in one the mass spectrometer could only be operated at pressures lower than those used in the actual recombination studies (Reference 16-7).

Weller and Biondi (Reference 16-24) determined the values of $\alpha(NO^+)$ at gas temperatures of 200, 300, and 450 K from "single-pulse-afterglow" studies of electron-density decays in photoionized NO-Ne mixtures. At all temperatures conditions were achieved where $NO^+$ was the only significant afterglow ion, and ion "tracking" of the electron-density decays was satisfactory. Good fits of the electron decays to computer solutions of Equation (16-10) suggested very good ($\lesssim \pm 10$ percent) accuracy in the determinations. The values obtained were $(7.4 \pm 0.7)$, $(4.1^{+0.3}_{-0.2})$ and $(3.1 \pm 0.2) \times 10^{-7}$ cm$^3$/sec at 200, 300, and 450 K, respectively.

Except at low temperatures, where Weller and Biondi found that it required considerable care to achieve conditions which limited the concentration of the dimer ion ($NO \cdot NO^+$), the results were in good agreement with those of Gunton and Shaw (Reference 16-7), whose earlier studies using similar photoionization and microwave techniques had not involved mass-spectrometer operation under recombination-controlled (high-pressure) conditions. Their values were $(10^{+2}_{-4})$, $(4.6^{+0.5}_{-1.3})$, and $(3.5^{+0.2}_{-0.5}) \times 10^{-7}$ cm$^3$/sec at 196, 298, and 358 K, respectively. The 196 K value is almost certainly high owing to the interference of the dimer ion, whose recombination rate is discussed below.

Earlier studies by Doering and Mahan (Reference 16-5) of photoionized NO using Langmuir probes to determine the positive ion densities had led to estimates of the recombination coefficient at 300 K lying between $2 \times 10^{-6}$ cm$^3$/sec, from the stationary-ion-density method, Equation (16-14), and $4 \times 10^{-7}$ cm$^3$/sec, from analysis of repetitive-afterglow decay data, using Equation (16-12), with $f \leq 4$.

Much better success in obtaining consistent results between the stationary-ion-density method and a time-variation method (in this case, rate of growth measurements) has been obtained by Young and St. John (Reference 16-6), who employed chemionization in N and O atom mixtures to produce $NO^+$ ions. Using ionization-chamber charge-collection techniques to determine ion densities, they obtained $\alpha = (5 \pm 2) \times 10^{-7}$ cm$^3$/sec at 300 K. in satisfactory agreement

with the results of Weller and Biondi, and of Gunton and Shaw. At the present time, negative-ion accumulation effects in the stationary-state method have not been evaluated.

Van Lint and Wyatt (Reference 16-25) reported microwave afterglow measurements on He-NO mixtures (1000:1), ionized by a pulse of energetic (Mev) electrons. Over the mixture pressure range ~10 to 100 torr they obtained $\alpha \approx 5 \times 10^{-7}$ cm$^3$/sec, independent of pressure at 300 K. Rather impure NO samples were used in these studies, as evidenced by anomalously large attachment losses.

The several room-temperature measurements appear to support the value $\alpha(NO^+) = (4.1 \pm 0.3) \times 10^{-7}$ cm$^3$/sec, independent of the means of generating the $NO^+$.

The available knowledge of the temperature dependence of $\alpha(NO^+)$ is contained in Figure 16-2. The relevant data between 200 and 450 K of Weller and Biondi and of Gunton and Shaw are included. Also shown on the figure are microwave electron-density decay measurements of shock-heated air by Stein et al (Reference 16-26), which presumably refer to $NO^+$ ions in the gas at ≈2900 K. In addition, Lin and Teare (Reference 16-27), from a complicated analysis of ionization behind shock waves in air, concluded that a value of $\alpha \approx 2 \times 10^{-8}$ cm$^3$/sec at 5000 K was consistent with their electron-density measurements. The two latter results are very uncertain but represent the only experimental high-temperature $\alpha$-value estimates available.

Bardsley (Reference 16-28) has calculated the recombination coefficient $\alpha(NO^+)$ via the direct dissociative capture process for $NO^+$ ions in their ground vibrational state. Using available spectroscopic data concerning vibrational spacing and estimates of the shapes of the potential curves involved in the process, he finds, for direct capture into two of the four accessible repulsive states, a value $\alpha_d(NO^+) = 2.6 \times 10^{-7}$ cm$^3$/sec at 300 K. In addition he has calculated the variation of $\alpha_d(NO^+)$ under conditions where $T_e$ alone is varied, leaving $T_i = T_n = 300$ K, and where $T_e$ and $T_i$ are covaried. His predicted variations of $\alpha_d(NO^+)$ for each case are shown by the dashed line in Figure 16-2. It will be seen that Bardsley's values of $\alpha_d(NO^+)$ for two of the four possible repulsive states, which should represent a lower bound on the total coefficient $\alpha(NO^+)$, lie above the high-temperature values of Stein et al, and of Lin and Teare. In view of the great uncertainty in the high-temperature measurements,

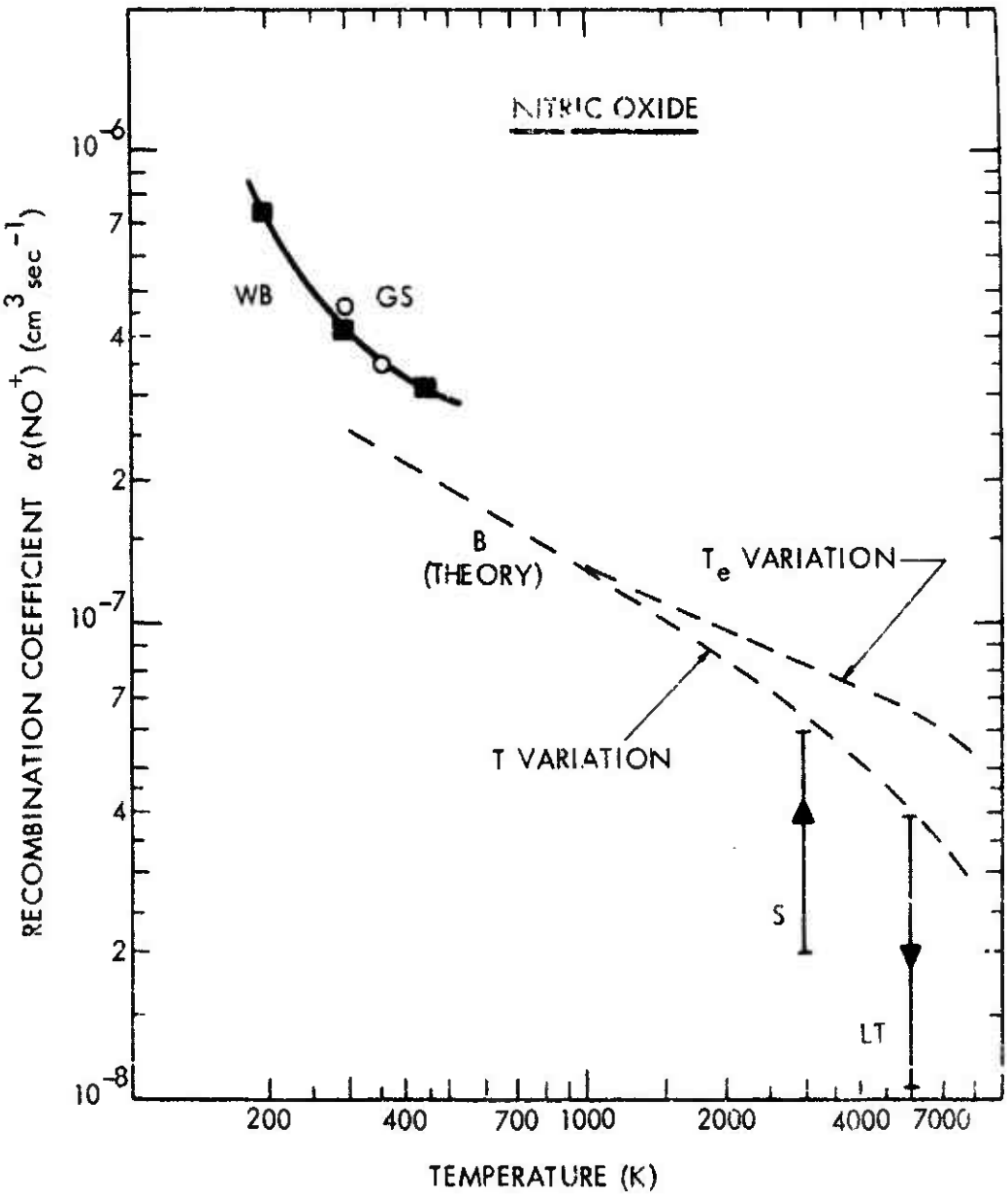


Figure 16-2. Two-body electron-ion recombination coefficient $\alpha(NO^+)$ as a function of temperature. Experimental results for $T_e = T_+ = T_{gas}$ are from Gunton and Shaw (GS-open circles) (Reference 16-7), Weller and Biandi (WB-solid squares) (Reference 16-24), Stein et al. (S) (Reference 16-26), and Lin and Teare (LT) (Reference 16-27). The theoretical calculations of Bardsley (B) (Reference 16-28) are also shown.

the theoretically predicted energy variation of $\alpha_d(NO^+)$ probably provides the best available estimate of the high-temperature values.

Finally, as in the case of nitrogen it has been possible to obtain a value for the recombination of the dimer ion $(NO \cdot NO^+)$ by increasing the partial pressure of NO to $\sim 0.2$ torr in the NO-Ne mixtures. From such studies Weller and Biondi (Reference 16-24) find $\alpha(NO \cdot NO^+) = (1.7 \pm 0.4) \times 10^{-6}$ cm$^3$/sec at T = 300 K.

$O_2^+$, $O_4^+$

Simultaneous microwave and mass-spectroscopic measurements of electron and positive-ion decays in oxygen-neon mixtures have been used by Kasner and Biondi (Reference 16-29) to determine $\alpha(O_2^+)$. A "single-pulse-afterglow" method was used to avoid negative-ion accumulation effects and it was found that, in contrast to earlier repetitive pulse-afterglow studies (Reference 16-30), the $O_2^+$ ion wall current accurately "tracked" the recombination-controlled electron-density decay. At 300 K, a value $\alpha(O_2^+) = (2.2 \pm 0.5) \times 10^{-7}$ cm$^3$/sec was found from $1/\langle n_e \rangle$ versus t plots exhibiting linear regions, $f \geq 10$ over the ranges $3 \times 10^{-4} < p(O_2) < 10^{-2}$ torr and $p(Ne) \approx 20$ torr. In these studies it is possible that the $^3P_2$ neon metastables produce $O_2^+$ ions in their ground electronic state and a high vibrational state ($v \leq 20$) or even in the first excited electronic state ($a\,^4\Pi_u$). In triple mixture ($Ne:Ar:O_2$) studies, attempts were made to limit the $O_2^+$ ions to the ground electronic and lower ($v \leq 5$) vibrational states.

Mehr and Biondi (Reference 16-21) have used a microwave afterglow/mass-spectrometer apparatus employing microwave electron heating to determine $\alpha(O_2^+)$ in oxygen-neon mixtures. Good $O_2^+$ ion tracking of the electron-density decays was obtained and accurate values of $\alpha(O_2^+)$ were determined from comparison of the experimental data with computer solutions of Equation (16-10). At $T_e = 300$ K a value $\alpha(O_2^+) = (1.95 \pm 0.2) \times 10^{-7}$ cm$^3$/sec was obtained, in good agreement with Kasner and Biondi's results.

Previous microwave afterglow work without mass identification of the ions by Biondi and Brown (Reference 16-16) and by Mentzoni (Reference 16-31) led to values of $\alpha \approx 3 \times 10^{-7}$ and $2 \times 10^{-7}$ cm$^3$/sec, respectively, at low pressures ($\approx 2$ torr) of pure oxygen. However, at even lower oxygen pressures in oxygen-helium mixtures Kasner, Rogers, and Biondi (Reference 16-30) found substantial $O_3^+$ ion concentrations, so that the afterglow ionic compositions in the studies without mass analysis are in doubt.

In temperature-dependence studies Kasner and Biondi (Reference 16-29) find that, over the range 205 to 690 K, $\alpha(O_2^+)$ for ions in the $(X^2\Pi_g)$ ground state decreases from the value $3.0 \times 10^{-7}$ to $1.0 \times 10^{-7}$ $cm^3/sec$. These results are shown by the X-symbols and dashed line in Figure 16-3. Similarly, Smith and Goodall (Reference 16-32) have used a Langmuir probe to determine electron-density decays in oxygen-helium afterglows; however, although mass analysis of the ions had been employed in related ion-molecule reaction studies, they omitted such analysis in the recombination work. (They

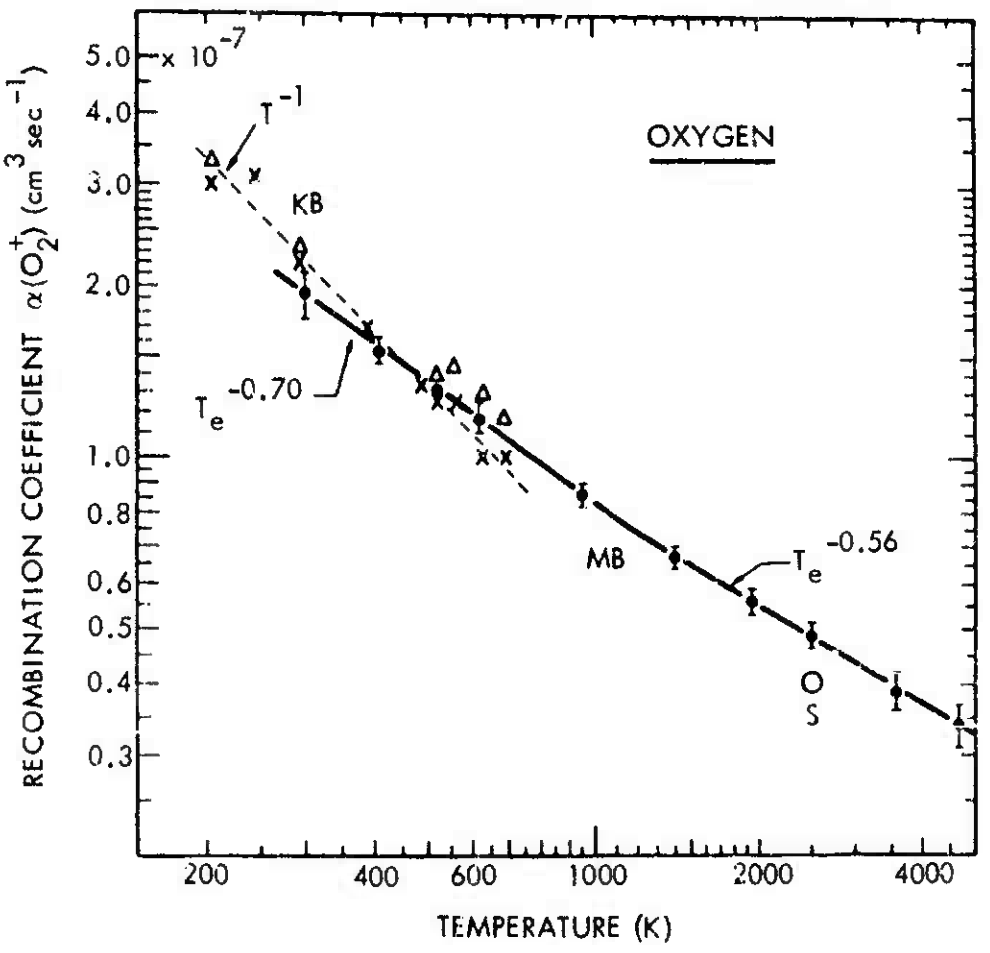


Figure 16-3. Two-body electron-ion recombination coefficient $\alpha(O_2^+)$ as a function of temperature. The experimental results are from Kasner and Biondi (KB) (Reference 16-29), Mehr and Biondi (MB) (Reference 16-21), and Soyers (S) (Reference 16-33).

are remedying this deficiency). While their value at 300 K is in good agreement with the data of Kasner and Biondi, the variation with gas temperature is less rapid. Similarly Mentzoni's data (Reference 16-31), taken over the range 300-900 K, fall consistently higher than Kasner and Biondi's results at the higher temperatures. As a result of lack of ion identification in the studies of Smith and Goodall and of Mentzoni, their inferred temperature variation of $\alpha(O_2^+)$ is probably less reliable.

Mehr and Biondi (Reference 16-21) determined $\alpha(O_2^+)$ over the range $300\,K \leq T_e \leq 5000\,K$ (with $T_+ = T_{gas} = 300\,K$) and found that the recombination coefficient varies approximately as $T_e^{-0.70}$ between 300 and 1200 K, and as $T_e^{-0.56}$ between 1200 and 5000 K. Sayers (Reference 16-33), using a Langmuir-probe/mass-spectrometer apparatus to study oxygen-helium afterglows, reported the value $\alpha(O_2^+) = 4 \times 10^{-8}$ cm$^3$/sec at $T_e = 2500\,K$, in fair agreement with the results of Mehr and Biondi. The various data are given in Figure 16-3 and it will be seen that, over the common temperature range, $\alpha(O_2^+)$ exhibits roughly the same energy variation when $T_e$ alone and when $T_e$ and $T_i$ together are increased above room temperature, provided binary mixture ($O_2$:Ne) data are compared. In this case, there may be some effect of excited ($a\,^4\Pi_u$) $O_2^+$ ions on the recombination determinations. Only in the triple-mixture studies (Ne:Ar:$O_2$) of Kasner and Biondi (X-symbols in Figure 16-3) can one assume that the $O_2^+$ ions are in their ground electronic state.

Finally, at low temperatures Kasner and Biondi (Reference 16-29) were able to separate the effects of $O_2^+$ and $O_4^+$ on the recombination loss of electrons, and found a value $\alpha(O_4^+) \sim 2.3 \times 10^{-6}$ cm$^3$/sec at 205 K for the dimer ion.

Zipf (Reference 16-34) has measured the branching ratios for production of various O-atom states. For each $O_2^+$ ion recombined, two O atoms are produced in the ratios $1.0(^3P) : 0.9(^1D) : 0.1(^1S)$.

## Hydronium Series and Other Ions

Although measurements have been carried out in other gases of possible ionospheric interest (e.g., $NO_2$), lack of ion identification makes reporting the deduced recombination coefficients speculative. In general, at 300 K the "lighter" diatomic molecular ions (including $Ne_2^+$) yield $\alpha$ values in the range $(2\text{-}5) \times 10^{-7}$ cm$^3$/sec, while the more complex ions, judging by the behavior of $N_4^+$, ($NO \cdot NO^+$), and $O_4^+$, may exhibit substantially larger values, i.e., $\alpha > 10^{-6}$ cm$^3$/sec.

Of particular importance, in view of its discovery in D-region rocket sounding, is the hydronium-ion series, $H_3O^+ \cdot (H_2O)_n$, where n = 0, 1, 2, ... . A considerable amount of activity has focussed upon laboratory determination of the corresponding recombination rates. In earlier studies, Green and Sugden (Reference 16-35) used a mass spectrometer to measure the decay of $H_3O^+$ ions from a hydrogen-oxygen-acetylene flame at approximately 2100 K, and found a value $\alpha(H_3O^+) \simeq 2 \times 10^{-7}$ cm$^3$/sec. Wilson and Evans (Reference 16-36) used microwave techniques to measure the decay of electron density behind shock fronts in argon containing small amounts of oxygen and hydrocarbon (e.g., acetylene). Presumably the ion in these recombination-controlled decays is $H_3O^+$. They found that $\alpha$ varied approximately as $T^{-2}$ over the range 2400 K < T < 5600 K, with a value $\alpha \simeq 1.5 \times 10^{-7}$ cm$^3$/sec at 3000 K. With the usual inverse temperature dependences encountered for dissociative recombination, a value in excess of $10^{-6}$ cm$^3$/sec at 300 K is implied.

Biondi, Leu, and Johnsen (Reference 16-37) have reported preliminary measurements of hydronium-series ion coefficients using their microwave-afterglow/mass-spectrometer apparatus. Using varying amounts of water vapor in helium buffer gas and varying the gas temperature to control the members of the hydronium-series ions present in the afterglow, they were able to study one or two of the ion types at a time. They find recombination coefficients ranging from $\alpha(19^+) = (1.1 \pm 0.2) \times 10^{-6}$ cm$^3$/sec at T = 540 K to $\alpha(109^+) = (10 \pm 2) \times 10^{-6}$ cm$^3$/sec at 205 K. In addition, only a weak temperature dependence is seen in the studies of $\alpha(55^+)$ at 540, 415, and 300 K. The inferred temperature dependence, $\sim T^{-0.2}$, is weaker than that found for dissociative recombination, suggesting that for these complex ions, the very large recombination coefficients may result from excitation of internal modes (e.g., rotation) in the initial capture step, thus lengthening the autoionization time and assuring stabilization by dissociation.

## Theoretical Calculations

Substantial progress in theoretical calculations of dissociative recombination coefficients has been achieved in the past few years. In addition to the previously mentioned calculations by Bardsley of $\alpha(NO^+)$ (Reference 16-28) and its variation with $T_e$ and with $T_i$,

there are calculations by Wilkins and by Warke of $\alpha(N_2^+)$ and $\alpha(O_2^+)$ for ions in their ground vibrational states (References 16-38, 16-39), which yield values in qualitative agreement with the experimental data at 300 K. All of these calculations either make assumptions or use spectroscopic data in an effort to characterize the potential curve crossings in the direct dissociative process and are not, therefore, ab initio theoretical calculations.

Nielsen and Berry (Reference 16-40) have carried out ab initio calculations of the potential curves of the Rydberg states of the $H_2$ molecule which may contribute to a special form of the "indirect" dissociative recombination process, and have found that, to reach the vibration continuum of one of the Rydberg states so that dissociation can occur, the $H_2^+$ ions must be in their $v = 7$ vibrational state. Thus it appears that this mechanism does not provide a significant contribution to the overall dissociative recombination process.

A difficulty with ab initio calculations of the direct dissociative process appears to be lack of a suitable technique for calculation of the repulsive potential curves of the excited molecule in the region where they cross the molecular-ion state.

### 16.3.1.2 RADIATIVE RECOMBINATION

Most of the available information concerning rates of radiative capture of electrons by positive ions comes from theory (References 16-41, 16-42). The radiative process (Equation 16-2) will only be of importance when the molecular-ion/atomic-ion ratio is small ($\leq 10^{-4}$) and when charged-particle densities are low ($< 10^8$ cm$^{-3}$). Theory indicates that for capture into the lower levels of the excited atom, the partial recombination coefficient varies as $T_e^{-0.5}$, while for capture into the highly excited states lying within $\approx kT_e$ of the continuum, it varies approximately as $T_e^{-1.5}$. The overall recombination coefficient varies approximately as $T_e^{-0.7}$. The calculated recombination coefficients for various positive ions appear to be quite similar in magnitude, varying by less than a factor of two in going from $H^+$ to $K^+$. The dependence of the radiative recombination coefficient on electron temperature for $He^+$ or $H^+$ ions is shown in Figure 16-4 by the intercepts at the low-electron-density end of the scale, illustrating the $\approx T_e^{-0.7}$ dependence. The little experimental evidence relating to radiative recombination supports the calculated magnitudes of the coefficients.

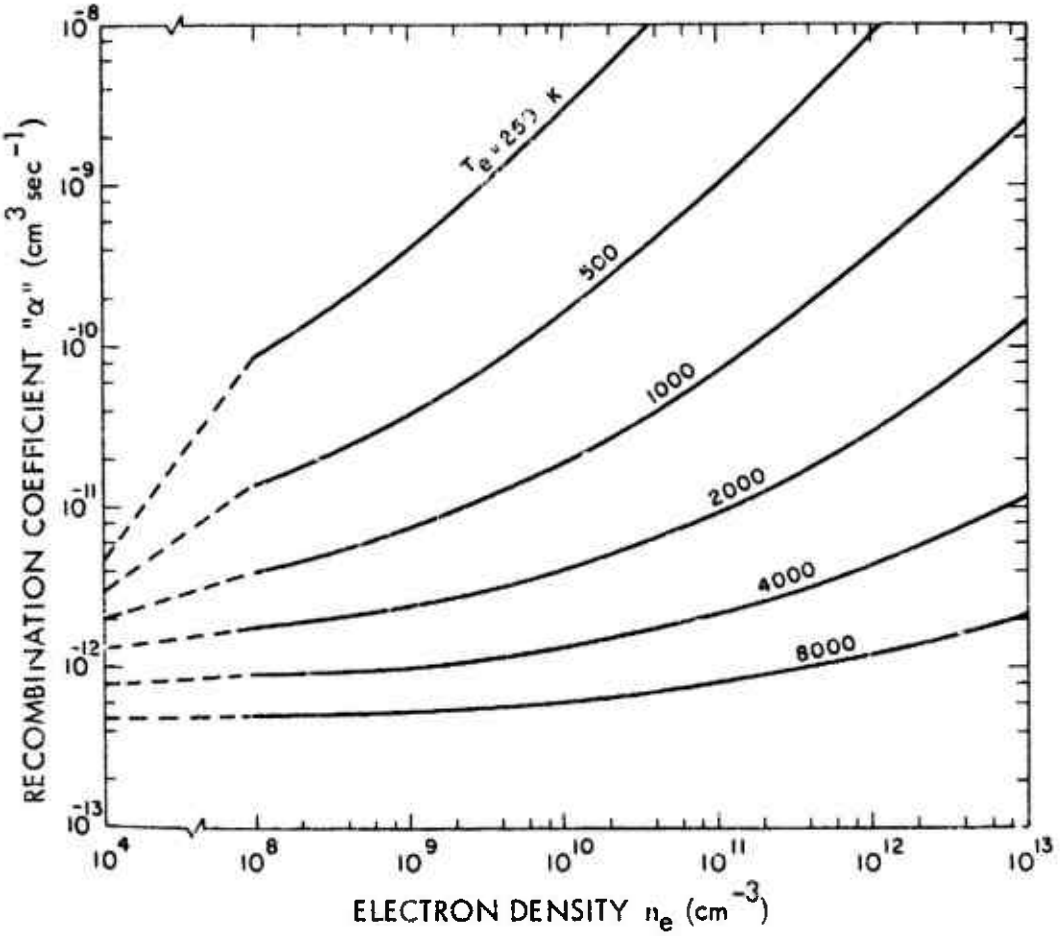


Figure 16-4. Effective two-body recombination coefficient for collisianol-radiative recombinotian of electrons and $H^+$ ions as a function of electron density, over a range of electron temperatures.

### 16.3.2 Electron-Ion Recombination — Three-Body Processes

#### 16.3.2.1 ELECTRON-STABILIZED RECOMBINATION

Under circumstances where a relatively large electron density ($\geq 10^6$ cm$^{-3}$) is present, capture of an electron by an atomic ion is assisted by a second electron (Equation 16-3), leading to the "collisional" part of collisional-radiative recombination. Here again, more is known about the process from theoretical calculations such as those of Bates, Kingston, and McWhirter (Reference 16-43), based

on the use of certain measured collision cross-section data, than from experiment. It appears that the recombination coefficient is not particularly sensitive to the identity of the singly-charged ions, and available experimental results (References 16-44, 16-45) are consistent with the calculated values.

Essentially the same three-body coefficient $k_{3e}$ is obtained for $He^+$ and $H^+$ ions; at "low" electron temperatures, $T_e < 2000$ K, one has a variation of $k_{3e}$ approximately as $T_e^{-4.5}$. In comparing this three-body rate to two-body rates it is useful to note that at 300 K the equivalent two-body rate for this process is "$\alpha_{3e}$" $\approx (10^{-19} n_e)$ cm$^3$/sec, where $n_e$ is expressed in electrons/cm$^3$. The results of the calculations of the electron-stabilized recombination coefficients are shown by the lines which approach a 45-degree slope in Figure 16-4.

### 16.3.2.2 NEUTRAL-STABILIZED RECOMBINATION

In the lower atmosphere, where neutral-molecule concentrations are large, Reaction (16-4) may raise recombination rates above the dissociative value. There is a limited amount of experimental information concerning the rate of neutral-stabilized, three-body recombination, and available theory yields little better than a crude estimate of the possible rates. Deloche et al, and Berlande et al (References 16-46, 16-47), have studied electron loss by recombination as a function of neutral concentration in a high-pressure helium-plasma-afterglow. They used microwave interferometry techniques to determine the electron-density decay but did not employ a mass spectrometer to analyze the ions. At low-to-moderate electron densities they find the rate coefficient to be two-body in character with respect to electrons and ions and to vary directly with the neutral helium concentration, suggesting that the process under study is:

$$He_2^+ + e + He \rightarrow \text{neutral products} . \qquad (16\text{-}15)$$

They obtain a three-body rate coefficient $k = (2.0 \pm 0.5) \times 10^{-27}$ cm$^6$/sec at 300 K.

On the theoretical side, Massey and Burhop (Reference 16-48) used an argument paralleling Thomson's theory for ions to suggest that for "air" ions at 300 K the coefficient may be of the order

$k_{3n} \approx 6 \times 10^{-27}$ cm$^6$/sec. There is no information which can be used to set error limits on this estimate; however, a distinction has been made between atoms and molecules acting as third bodies in stabilizing the recombination, owing to the fact that the molecule is more effective than the atom in removing kinetic energy at a collision with an electron as a result of the large number of low-energy vibrational and rotational states which may be excited. This factor was taken into account in the estimate of $k_{3n}$ for "air" ions and neutral stabilizing molecules. If for some reason only atoms are present, $k_{3n}$ may be substantially smaller. This theoretical prediction is in accord with the experimental determinations for helium, which reveal a rather smaller value of $k_{3n}$ when atoms (helium) are the stabilizing agent.

The modified Thomson theory suggests an energy variation approximately as $T_e^{-5/2}$ for the neutral stabilized process. This leads to the general rate coefficient for any positive ion of:

$$k_{3n} \approx 1 \times 10^{-(26\pm1)} (T_e/300)^{-5/2} \text{ cm}^6/\text{sec}, \qquad (16\text{-}16)$$

where the order of magnitude of the quoted uncertainty is in doubt.

### 16.3.3 Ion-Ion Recombination— Two-Body Processes

#### 16.3.3.1 MUTUAL NEUTRALIZATION*

Several studies of ion-ion mutual neutralization, Equation (16-5), have been carried out at near-thermal energies. Greaves (Reference 16-9) and Sayers (Reference 16-49) have investigated halogen ions such as $I_2^+$ and $I^-$. An afterglow technique was employed, making use of radio-frequency ($\approx$ 10 MHz) determinations of the dielectric coefficient of the ions to determine ion concentrations. Ion identification was supplied by a small, differentially-pumped mass spectrometer appended to the experimental tube (Reference 16-9). In iodine (Reference 16-9) and bromine (Reference 16-49) vapor, a coefficient $\alpha_{mn} \approx 1 \times 10^{-7}$ cm$^3$/sec was found at $T \approx 300$ K from curves having f values between 2 and 6. With increasing temperature from 300 to 340 K, $\alpha$ decreased from $1.2 \times 10^{-7}$ to $1.0 \times 10^{-7}$ cm$^3$/sec in iodine, leading to an approximate $T^{-3/2}$ dependence over this extremely limited range.

*The author wishes to thank J. R. Peterson of Stanford Research Institute for his contributions to the writing of this subsection on mutual neutralization.

Hirsh et al (References 16-50, 16-51) have carried out afterglow studies of ion-ion recombination using an r-f impedance probe to determine the ion concentrations in air-like $N_2$-$O_2$ mixtures following ionization by a pulse of MeV electrons. A differentially-pumped mass spectrometer identified the principal ions undergoing recombination as $NO^+$, $NO_2^-$, and $NO_3^-$. Their earlier value (Reference 16-50), $\alpha_{mn} = (4\pm1) \times 10^{-8}$ cm$^3$/sec at 300 K, was later redetermined (Reference 16-51) as $(3.4\pm1.2) \times 10^{-8}$ cm$^3$/sec, and was also indicated as referring specifically to the reaction of $NO^+ + NO_3^-$. A value of $(17.5\pm6) \times 10^{-8}$ cm$^3$/sec was obtained for $NO^+ + NO_2^-$ (Reference 16-51)

Mahan and Person (Reference 16-52) studied ionic recombination in photoionized NO-$NO_2$-noble gas mixtures using an apparatus which did not employ mass analysis of the ions. They argued that the ions under study were probably $NO^+$ and $NO_2^-$. A parallel-plate ionization chamber employing pulsed charge collection was used to determine ion densities in the afterglow. At low pressures, a two-body coefficient $\alpha_{mn} \simeq (2\pm0.5) \times 10^{-7}$ cm$^3$/sec was obtained at 300 K from decay curves exhibiting substantial f values, i.e., > 15. Thus, the quoted error limit has more to do with uncertainties concerning the exact form of the ions' spatial distribution than with slope measurement errors.

More recently, a merged-beam apparatus has been used by a group at Stanford Research Institute to obtain mutual-neutralization cross-sections between a variety of mass-analyzed positive and negative ions over a range of center-of-mass energies from 0.1 to about 300 eV. Systems that have been investigated include $H^+ + H^-$, $N^+ + O^-$, $O^+ + O^-$, $He^+ + D^-$, $N_2^+ + O_2^-$, $O_2^+ + O_2^-$, $O_2^+ + NO_2^-$, $NO^+ + NO_2^-$, $O_2^+ + NO_3^-$, and $NO^+ + NO_3^-$ (References 16-53 through 16-61). Generally, all of the measured values of $\alpha_{mn}$ lie between 0.5 and $3.0 \times 10^{-7}$ cm$^3$/sec, and all rates increase toward lower energy.

A low-energy expansion of the Landau-Zener formula for these reactions (Reference 16-56) was used to extrapolate the results to thermal energies. After Boltzmann averaging, thermal rate coefficients were obtained and reported (e.g., in Reference 16-56) in the form:

$$\alpha_{mn}(T) = A\,T^{-1/2} + B + C\,T^{1/2} + D\,T\,, \qquad (16\text{-}17)$$

where the constants A , B , C, and D were derived from a least-squares fit to the measurements, and T is in K. At energies near 300K, only the first two terms are significant.

Measurements by the same group (Reference 16-61) on $Na^+ + O^-$ yielded reaction rates similar to those of $O^+ + O^-$, in contradiction to the much larger values reported by Weiner, Peatman, and Berry (Reference 16-62). On the other hand, their results on the systems $H^+ + H^-$ , $He^+ + H^-$ , and $He^+ + D^-$ (Reference 16-57) agreed well with those of Harrison et al (References 16-63, 16-64), who used colliding beams inclined at 20°, over an energy range from 125 to 10, 000 eV.

A multistate Landau-Zener method has been used for the calculation of neutralization cross-sections between atomic ions (Reference 16-57). The agreement with experimental data is usually within a factor of two. Values for $\alpha_{min}$ (300 K) were also calculated, and exceeded $1 \times 10^{-7}$ $cm^3/sec$ in every case. Calculations of this type provide information concerning the final neutral states of the products of the reaction, which can assist in the interpretation of ionospheric phenomena (Reference 16-58). It is not clear whether these calculations can be extended to include molecular systems.

#### 16.3.3.2 OTHER TWO-BODY PROCESSES

Other processes, such as neutralization with rearrangement of the atoms in the molecules, may well offer (Reference 16-65) recombination coefficients orders of magnitude smaller than for the mutual neutralization process; these are omitted from consideration here.

### 16.3.4 Ion-Ion Recombination— Three-Body Processes

#### 16.3.4.1 THOMSON RECOMBINATION

For the case of neutral-molecule-stabilized, positive-ion-negative-ion recombination, there exist measurements of recombination rates for "air" ions, whose identity, however, has not been established. Gardner (Reference 16-66) and Sayers (Reference 16-67) have measured the coefficients of Thomson recombination, $k_{3n}^1$, in pure oxygen and in air, respectively, over the pressure range ≈ 0.1 to 1 atmosphere at ≈ 300 K and verified the linear dependence of k on neutral gas density predicted by Thomson's theory (Reference 16-68).

A value $k_{3n}^{i} \simeq 3 \times 10^{-25}$ cm$^6$/sec was obtained. Thus at pressures in excess of 10 torr, Thomson recombination should outweigh two-body mutual neutralization.

Similar results were obtained by McGowan (Reference 16-69) in oxygen-nitrogen mixtures; however, this was without benefit of mass identification. Mahan and Person (Reference 16-52), using the method described earlier, have carried out a systematic study of three-body ionic recombination which is thought to involve the following ionic reactions:

$$NO^+ + NO_2^- + M \rightarrow \text{neutrals}, \qquad (16\text{-}18)$$

$$NO^+ + SF_6^- + M \rightarrow \text{neutrals}, \qquad (16\text{-}19)$$

and:

$$C_6H_6^+ + SF_6^- + M \rightarrow \text{neutrals}, \qquad (16\text{-}20)$$

where the third-body M includes He, Ne, Ar, Kr, Xe, $H_2$, $D_2$, and $N_2$. Of greatest interest is the system, $NO^+ + NO_2^- + N_2$, where a rate constant $k_{3n}^{i} \simeq 2 \times 10^{-25}$ cm6/sec was obtained at 300 K. The variation of k with choice of M lay between $k = 4 \times 10^{-26}$ for He and $k = 3 \times 10^{-25}$ for Xe.

There are no experimental measurements of the temperature dependence of Thomson recombination; however, Thomson's (Reference 16-68) and Natason's (Reference 16-70) treatments lead to a predicted $T_i^{-5/2}$ variation. Thus, for atmospheric ions it may be estimated that:

$$k_{3n}^{i} \simeq 2 \times 10^{-(25 \pm 0.5)} (T_i/300)^{-5/2} \text{ cm}^6/\text{sec} \quad . \qquad (16\text{-}21)$$

### 16.3.4.2 OTHER THREE-BODY PROCESSES

Fueno et al (Reference 16-71) considered a two-step ion recombination process, i.e.:

$$X^+ + N \rightleftarrows (XN)^+ \quad , \qquad (16\text{-}22)$$

followed by:

$$(XN)^+ + Y^- \rightleftarrows XY + N \ , \qquad (16\text{-}23)$$

the rate constant of which was calculated to be $k \approx 1 \times 10^{-26}$ $cm^6/sec$ at 300 K, and therefore should be of lesser importance than Thomson recombination.

Finally, the associative ion-ion recombination process, that is:

$$X^+ + Y^- + N \rightarrow XY + N \ , \qquad (16\text{-}24)$$

appears (Reference 16-65) to offer a much smaller coefficient, $k \approx 10^{-27}$ $cm^6/sec$ at 300 K, than Thomson recombination; this mechanism is neglected in the present discussion, since its importance seems highly questionable.

## 16.4 SUMMARY

Values for the appropriate recombination coefficients for all processes where there is either sufficient experimental and/or theoretical information, or where there is a critical need for an estimate, are contained in Table 16-1. In general, those values with larger quoted uncertainties reveal a greater degree of guesswork which has taken place in attempting to evaluate the kinetics of the process.

Table 16-1. Recombination coefficient tabulation according to the form $k = (a \pm \Delta a)\,(T/T_r)^{(b \pm \Delta b)}$ for the case $T_r = 300$ K. The notation [-x] signifies $10^{-x}$. The symbol {T} indicates the dependence for simultaneous variation of $T_{gas}$, $T_i$, and $T_e$, while the symbol $\{T_e\}$ indicates the dependence for variation of $T_e$ alone. Units are $cm^3\ sec^{-1}$ for all two-body, and $cm^6\ sec^{-1}$ for all three-body interactions.

| Process | Reactants | $a \pm \Delta a$ | $b \pm \Delta b$ | Remarks |
|---|---|---|---|---|
| 1. Electron-Ion | | | | |
| a. Dissociative | $N_2^+ + e$ | $(2.7 \pm 0.3)[-7]$<br>$\left(1.8^{+0.4}_{-0.2}\right)[-7]$ | $-(0.2 \pm 0.2)\{T\}$<br>$-(0.39)\{T_e\}$ | See Figure 16-1 for range of validity. |
| [simple ions] | $NO^+ + e$ | $(4 \pm 0.3)[-7]$ | $-(1.0 \pm 0.2)\{T\}$<br>$-(0.5 \pm 0.1)\{T\}$ | 200-300 K<br>300-4000 K<br>See Figure 16-2. |
| | $O_2^+ + e$ | $(2.1 \pm 0.2)[-7]$ | $-(0.7 \pm 0.3)\{T\}$<br>$-(0.6 \pm 0.1)\{T_e\}$ | See Figure 16-3. |
| [dimer ions] | $N_4^+ + e$ | $(2 \pm 1)[-6]$ | $-(1 \pm ?)\{T\}$ | See Figure 16-1. |
| | $(NO^+ \cdot NO) + e$ | $(1.7 \pm 0.5)[-6]$ | $-(1 \pm ?)\{T\}$ | No temp. dependence has been determined. |
| | $O_4^+ + e$ | $(2 \pm 0.5)[-6]$ | $-(1 \pm ?)\{T\}$ | Measurement at 205 K. |

Table 16-1. (Cont'd.)

| Process | Reactants | $a \pm \Delta a$ | $b \pm \Delta b$ | Remarks |
|---|---|---|---|---|
| a. Dissociative (Cont'd.) [$H_3O^+ \cdot (H_2O)_n$ series ions] N.B.: These are designated by their respective mass numbers, i.e., as $(M)^+$. | $(19)^+ + e$ | $(1.3 \pm 0.3)[-6]$ | $-\left(0.2^{+0.4}_{-0.1}\right)[T]$ | $(19)^+$, $(37)^+$ and $(55)^+$ measured at 540 K. $(37)^+$ and $(55)^+$ also measured at 415 K. $(55)^+$ and $(73)^+$ measured at 300 K. $(91)^+$ and $(109)^+$ measured at 205 K. |
| | $(37)^+ + e$ | $(2.8 \pm 0.4)[-6]$ | | |
| | $(55)^+ + e$ | $(5.1 \pm 0.7)[-6]$ | | |
| | $(73)^+ + e$ | $(6.1 \pm 1.2)[-6]$ | | |
| | $(91)^+ + e$ | $(7.4 \pm 1.5)[-6]$ | | |
| | $(109)^+ + e$ | $(9.3 \pm 2)[-6]$ | | |
| b. Radiative | $H^+$ thru $K^+ + e$ | $(3.5 \pm 1)[-12]$ | $-(0.7 \pm 0.1)$ | See Figure 16-4. |
| c. Electron-stabilized | $H^+ + 2e$ and $He^+ + 2e$ | $(1 \pm ?)[-19]$ | $-(4.5 \pm ?)$ | Valid for $T_e < 2000$ K. |
| d. Neutral-stabilized | "Air" ions + neutrals + e | $(1)[-26 \pm 1]$ | $-(2.5 \pm ?)$ | Rough estimate. |
| | $He_2^+ + e + He$ | $(2 \pm 0.5)[-27]$ | - | Measured at 300 K. |

Table 16-1. (Cont'd.)

| Process | Reactants | a ±Δa | b ±Δb | Remarks |
|---|---|---|---|---|
| 2. Ion-Ion | | | | |
| a. Mutual neutralization | $I_2^+ + I^-$<br>$Br_2^+ + Br^-$ | (1)[-7±0.5] | -(1.5±0.1) | 300<T<340 K |
| | $H^+ + H^-$ | (3.9±2.1)[-7] | -(0.45±0.05) | See Refs. 16-55, 16-57. |
| | $H_2^+ + D^-$ | (4.7±0.7)[-7] | -(0.45±0.05) | See Ref. 16-60. |
| | $O^+ + O^-$ | (2.7±1.3)[-7] | -(0.45±0.05) | See Refs. 16-57, 16-58. |
| | $O_2^+ + O^-$ | (9.6±3.0)[-8] | -(0.45±0.05) | Unpublished work of J.R. Peterson. |
| | $O_2^+ + O_2^-$ | (4.2±1.3)[-7] | -(0.45±0.05) | See Refs. 16-54, 16-56. |
| | $O_2^+ + NO_2^-$ | (4.1±1.3)[-7] | -(0.45±0.05) | See Ref. 16-56. |
| | $O_2^+ + NO_3^-$ | (1.3±0.5)[-7] | -(0.45±0.05) | See Ref. 16-59. |
| | $N_2^+ + O_2^-$ | (1.6±0.5)[-7] | -(0.45±0.05) | See Ref. 16-54. |
| | $NO^+ + O^-$ | (4.9±1.5)[-7] | -(0.45±0.05) | Unpublished work of J.R. Peterson. |

Table 16-1. (Cont'd.)

| Process | Reactants | a ±Δa | b ±Δb | Remarks |
|---|---|---|---|---|
| a. Mutual neutralization (Cont'd.) | $NO^+ + NO_2^-$ | (5.1±1.5)[-7] | -(0.45±0.05) | See Ref. 16-56. |
| | | (1.75±0.6)[-7] | -(0.45±0.05) | See Ref. 16-51. |
| | $NO^+ + NO_3^-$ | (8.0±3.0)[-7] | -(0.45±0.05) | See Ref. 16-59. |
| | | (3.4±1.2)[-8] | -(0.45±0.05) | See Ref. 16-51. |
| | $N^+ + O^-$ | (2.6±0.8)[-7] | -(0.45±0.05) | See Refs. 16-53, 16-54, 16-57. |
| b. Neutral-stabilized | "Air" | (3±1)[-25] | -(2.5±?) | M=$N_2$, $O_2$ . |
| | $NO^+ + NO_2^- + M$ | (2±?)[-25] | -(2.5±?) | M=$N_2$ |
| | | (4±?)[-26] | -(2.5±?) | M=He |
| | | (3±?)[-25] | -(2.5±?) | M=Xe |

## REFERENCES

16-1. Biondi, M. A., Can. J. Chem. 47, 1711 (1969).

16-2. Kasner, W. H., and M. A. Biondi, Phys. Rev. 137, A317 (1965).

16-3. Gray, E. P., and D. E. Kerr, Ann. Phys. (New York) 17, 276 (1962).

16-4. Frommhold, L., and M. A. Biondi, Ann. Phys. (New York) 48, 407 (1968).

16-5. Doering, J. P., and B. H. Mahan, J. Chem. Phys. 36, 669 (1962).

16-6. Young, R. A., and G. St. John, Phys. Rev. 152, 25 (1966).

16-7. Gunton, R. C., and T. M. Shaw, Phys. Rev. 140, A748, A756 (1965).

16-8. Weller, C. S., and M. A. Biondi, Phys. Rev. Letts. 19, 59 (1967).

16-9. Greaves, C., J. Electron. Control 17, 171 (1964).

16-10. Biondi, M. A., Phys. Rev. 109, 2005 (1958).

16-11. Oskam, H., Phillips Res. Repts. 13, 335 (1968).

16-12. Biondi, M. A., Phys. Rev. 129, 1181 (1963).

16-13. Kasner, W. H., Phys. Rev. 167, 148 (1968).

16-14. Conner, T. R., and M. A. Biondi, Phys. Rev. 140, A778 (1965).

16-15. Frommhold, L., and M. A. Biondi, Phys. Rev. 185, 244 (1969).

16-16. Biondi, M. A., and S. C. Brown, Phys. Rev. 76, 1697 (1949).

16-17. Faire, A. C., and K. S. W. Champion, Phys. Rev. 113, 1 (1959).

16-18. Mentzoni, M. H., J. Geophys. Res. 68, 4181 (1963).

16-19. Hackam, R., Planet. Space Sci. 13, 667 (1965).

16-20. Kasner, W. H., Phys. Rev. 164, 194 (1967).

16-21. Mehr, F. J., and M. A. Biondi, Phys. Rev. 181, 264 (1969).

16-22. Hagen, G., Air Force Cambridge Research Laboratories, Rept. AFCRL-68-0649 (1968).

16-23. Theard, L. P., Sixth Intl. Conf. Phys. Electronic Atomic Collisions, Cambridge, Mass. (1969); p. 1042.

16-24. Weller, C. S., and M. A. Biondi, Phys. Rev. 172, 198 (1968).

16-25. van Lint, V. A. J., and M. E. Wyatt, General Atomics, Rept. DASA-GA-5615, Part II (1964).

16-26. Stein, R. P., M. Schiebe, M. W. Syverson, T. M. Shaw, and R. C. Gunton, Phys. Fluids 7, 1641 (1964).

16-27. Lin, S. C., and J. D. Teare, Phys. Fluids 6, 355 (1963).

16-28. Bardsley, J. N., J. Phys. B1, 365 (1968); also private communication.

16-29. Kasner, W. H., and M. A. Biondi, Phys. Rev. 174, 139 (1968).

16-30. Kasner, W. H., W. A. Rogers, and M. A. Biondi, Phys. Rev. Letts. 7, 321 (1961).

16-31. Mentzoni, M. H., J. Appl. Phys. 36, 57 (1965).

16-32. Smith, D., and C. V. Goodall, Planet. Space Sci. 16, 1177 (1968).

16-33. Sayers, J., J. Atm. Terrestr. Phys. 6, Spec. Suppl., 212 (1956).

16-34. Zipf, E. C., Jr., Bull. Am. Phys. Soc. 15, 418 (1970).

16-35. Green, J. A., and T. M. Sugden, Ninth Symp. (Intl.) on Combustion, The Combustion Institute, Pittsburgh, Pa. (1963); p. 607.

16-36. Wilson, L. N., and E. W. Evans, J. Chem. Phys. 46, 859 (1967).

16-37. Biondi, M. A., M. T. Leu, and R. Johnsen, Proc. COSPAR Symp. D and E Region Ion Chem., Urbana, Ill. (1971).

16-38. Wilkins, R. L., J. Chem. Phys. 44, 1884 (1966).

16-39. Warke, C. S., Phys. Rev. 144, 120 (1966).

16-40. Nielsen, S. E., and R. E. Berry, Sixth Intl. Conf. Phys. Electronic Atomic Collisions, Cambridge, Mass. (1969); p. 1047.

16-41. Seaton, M. J., Monthly Not. Roy. Astron. Soc. 119, 81 (1959).

16-42. Bates, D. R., and A. Dalgarno, in Atomic and Molecular Processes, D. R. Bates, Ed., Academic Press, New York and London (1962); Chapter 7.

16-43. Bates, D. R., A. E. Kingston, and R. W. P. McWhirter, Proc. Roy. Soc. A267, 297 (1962).

16-44. Kuckes, A. F., R. W. Motley, E. Hinnov, and J. G. Hirschberg, Phys. Rev. Letts. 6, 337 (1961).

16-45. Born, G. H., Phys. Rev. 169, 155 (1968).

16-46. Deloche, R., A. Gonfalone, and M. Cheret, Compt. Rend. Acad. Sci. Paris 267, 934 (1968).

16-47. Berlande, J., M. Cheret, R. Deloche, A. Gonfalone, and C. Manus, Phys. Rev. A1, 887 (1970).

16-48. Massey, H. S. W., and E. H. S. Burhop, Electronic and Ionic Impact Phenomena, Oxford Univ. Press, London and New York (1952).

16-49. Sayers, J., in Atomic and Molecular Processes, D. R. Bates, Ed., Academic Press, New York and London (1962); Chapter 8.

16-50. Hirsch, M. N., G. M. Halpern, and N. S. Wolf, Bull. Am. Phys. Soc. 13, 199 (1968).

16-51. Eisner, P. M., and M. N. Hirsch, Phys. Rev. Letts. 26, 874 (1971).

16-52. Mahan, B. H., and J. C. Person, J. Chem. Phys. 40, 392, 3683 (1964).

16-53. Aberth, W., J. R. Peterson, D. C. Lorents, and C. J. Cook, Phys. Rev. Letts. 20, 979 (1968).

16-54. Aberth, W. H., and J. R. Peterson, Phys. Rev. A1, 158 (1970).

16-55. Moseley, J. T., W. H. Aberth, and J. R. Peterson, Phys. Rev. Letts. 24, 435 (1970).

16-56. Peterson, J. R., W. H. Aberth, J. T. Moseley, and J. R. Sheridan, Phys. Rev. A3, 1651 (1971).

16-57. Olson, R. E., J. R. Peterson, and J. T. Moseley, J. Chem. Phys. 53, 3391 (1970).

16-58. Olson, R. E., J. R. Peterson, and J. T. Moseley, J. Geophys. Res., Space Phys. 76, 2516 (1971).

16-59. Moseley, J. T., W. H. Aberth, and J. R. Peterson, Bull. Am. Phys. Soc. 16, 208 (1971).

16-60. Peterson, J. R., J. T. Moseley, and W. H. Aberth, Bull. Am. Phys. Soc. 15, 1510 (1970).

16-61. Moseley, J. T., W. H. Aberth, and J. R. Peterson, Seventh Intl. Conf. Phys. Electronic Atomic Collisions, Amsterdam, Holland (1971).

16-62. Weiner, J., W. B. Peatman, and R. S. Berry, Phys. Rev. Letts. 25, 79 (1970).

16-63. Rundel, R. D., K. L. Aitken, and M. F. A. Harrison, J. Phys. B2, 954 (1969).

16-64. Gaily, T. D., and M. F. A. Harrison, J. Phys. B3, 1098 (1970).

16-65. Bortner, M. H., General Electric Company, Rept. AFCRL-65-392 (1965).

16-66. Gardner, M. E., Phys. Rev. 53, 75 (1938).

16-67. Sayers, J. Proc. Roy. Soc. A169, 83 (1938).

16-68. Thomson, J. J., Phil. Mag. 6, 377 (1924).

16-69. McGowan, S., Can. J. Phys. 45, 429, 439 (1967).

16-70. Natason, G. L., Zhur. Tekh. Fiz. 29, 1373 (1959).

16-71. Fueno, T., H. Eyring, and T. Ree, Can. J. Chem. 38, 1693 (1960).

# 17. ELECTRON ATTACHMENT AND DETACHMENT PROCESSES*

A.V. Phelps, Joint Institute for Laboratory Astrophysics
(Latest Revision 6 July 1971)

## 17.1 INTRODUCTION

The purpose of this chapter is to review the available data regarding the rates of electron attachment and detachment processes involving atmospheric gases. The various types of attachment-detachment processes are considered and the recommended values for the rate coefficients are listed. Next an attempt is made to estimate the stability of the various negative ions of ionospheric interest. Finally, the ionospheric significance of these processes is discussed briefly. The suggested rate coefficients are tabulated in Tables 17-1 through 17-6.

## 17.2 TYPES OF ATTACHMENT-DETACHMENT PROCESSES

Electron attachment and detachment processes of significance in the normal and disturbed atmosphere are: radiative attachment and its inverse, photodetachment; dissociative attachment and its inverse, associative detachment; and three-body attachment, with a ground-state molecule or an electron as the third body, and its inverse, collisional detachment.

### 17.2.1 Photodetachment and Radiative Attachment: $e + X \rightleftarrows X^- + h\nu$

Radiative detachment and attachment rates involving negative ions of atmospheric gases have been determined from measurements of the cross-sections for the photodetachment of electrons from negative ions. Measurements (References 17-1 through 17-6) of photodetachment cross-sections of possible interest (References 17-7

*Based on work done at the Westinghouse Research Laboratories, and supported in part by the U. S. Army Research Office—Durham.

through 17-9) include $O^-$, $H^-$, $OH^-$, $O_2^-$, $H_2O_3^-$, $NO^-$, $O_3^-$, $NO_3^-$, and $NO_2^-$. Other ions of possible atmospheric interest (References 17-1, 17-7 through 17-9) which have not been studied are $CO_3^-$, $CO_4^-$, $HO_2^-$, and the hydrates of the ions listed. Mass-spectrometric studies (Reference 17-10) in the atmosphere have shown the presence of negative ions such as $O^-$, $O_2^-$, $NO_3^-(H_2O)_n$, and $CO_4^-$. The simpler ions are observed at higher altitudes and during periods of ionospheric disturbance.

The measured photodetachment cross-sections for $O^-$ and $O_2^-$ as a function of wavelength have been integrated (Reference 17-1) over the incident solar flux to give daytime photodetachment cross-sections. Also, measurements of photodetachment rates under white light illumination have been made (Reference 17-5) for $O_2^-$ formed by the three-body attachment process and for $O_3^-$. Photodetachment cross-sections have been measured (References 17-1, 17-6) for $NO_2^-$, $NO_3^-$, and $NO^-$. The angular dependence of the photodetachment cross-sections for $O^-$ and $H^-$ has been shown to agree with theory (Reference 17-11).

Theoretical calculations (Reference 17-12) of photodetachment rates for complex systems are not available because of uncertainties as to the range of energies over which threshold laws are valid and because of the difficulties of accurate calculations. Attempts (Reference 17-13) have been made to relate elastic scattering cross-sections and photodetachment cross-sections.

Radiative attachment is expected to be of significance only when an electronegative neutral species is present in appreciable concentrations, e.g., atomic oxygen. The rate coefficient (Reference 17-1) for radiative attachment to O is $(1.3 \pm 0.1) \times 10^{-15}$ cm$^3$/sec for electron energies below 1 eV. Because of differences between the apparent electron affinity derived from photodetachment experiments (References 17-1, 17-2) using theoretical "threshold laws" and from attachment-detachment equilibrium experiments (Reference 17-14), there is considerable uncertainty as to the radiative attachment coefficient for $O_2$. It is probably (References 17-1, 17-14) less than $2 \times 10^{-18}$ cm$^3$/sec for electrons at 230 K. Photodetachment measurements (Reference 17-4) have been made for $OH^-$, but because of the effects of rotational structure on the cross-section it has not been possible to calculate the radiative attachment rate coefficient for low-energy electrons to OH. Radiative attachment coefficients for $O_3$ and NO are unknown. The other major components of the atmosphere,

i.e., $N_2$, $CO_2$, Ar, and $H_2O$, do not form stable negative ions by the attachment of low-energy electrons. Recommended photodetachment and radiative detachment rate coefficients are given in Tables 17-1 and 17-2.

Table 17-1. Radiative attachment.

| Reaction | Rate Coefficient ($cm^3/sec$) | Reference |
|---|---|---|
| 1. $e + O \rightarrow O^- + h\nu$ | $(1.3 \pm 0.1) \times 10^{-15}$ | 17-1 |
| 2. $e + O_2 \rightarrow O_2^- + h\nu$ | $2 \times 10^{-(19\pm1)}$ | 17-1, 17-14 |
| 3. $e + OH \rightarrow OH^- + h\nu$ | $10^{-(15\pm1)}$ | 17-4 |
| 4. $e + O_3 \rightarrow O_3^- + h\nu$ | unknown | |
| All others should be unimportant | | |

Table 17-2. Photodetachment.[a]

| Reaction | Destruction Frequency ($sec^{-1}$) | Reference |
|---|---|---|
| 1. $h\nu + O^- \rightarrow O + e$ | 1.4 | 17-2 |
| 2. $h\nu + O_2^- \rightarrow O_2 + e$ | $0.3 \pm 0.1$ | 17-2, 17-5 |
| 3. $h\nu + O_3^- \rightarrow O_3 + e$ | $0.2 \pm 0.1$ | 17-44 |
| 4. $h\nu + NO_2^- \rightarrow NO_2 + e$ | $10^{-(2\pm1)}$[b] | 17-1, 17-55 |
| 5. $h\nu + OH^- \rightarrow OH + e$ | $\sim 1$[b] | 17-4 |
| 6. $h\nu + CO_3^- \rightarrow CO + O_2 + e$ | unknown | |
| 7. $h\nu + NO_3^- \rightarrow ? + e$ | unknown | |

Notes:

[a] Values given (Reference 17-1) are integrated cross-sections for solar radiation without corrections for atmospheric absorption, back-scattering, etc.

[b] The available photodetachment cross section data do not appear to have been folded into the solar flux distribution. The values quoted are very rough estimates based on the cross-sections and photon energy dependences given in the references cited.

### 17.2.2 Dissociative Attachment and Associative Detachment: $e + XY \rightleftarrows X^- + Y$

The process of dissociative attachment has been studied extensively in atmospheric gases for many years. Energy-dependent cross-sections are available (Reference 17-15) for dissociative attachment by electron impact for $O_2$, NO, $H_2$, $CO_2$, and $H_2O$ at room temperature. In each case the electron energy must exceed some threshold value in order for attachment to occur. Past attempts to predict the temperature dependence of the dissociative attachment reaction have used the room-temperature determination of the threshold as the activation energy. However, recent measurements for $O_2$ (Reference 17-16) and for $N_2O$ (Reference 17-17) have shown that the attachment cross-section at low electron energies increases rapidly with temperature. Theory is now capable of describing the dependence of dissociative attachment cross-sections on temperature in the case of $O_2$ (Reference 17-18). In the lower ionosphere it appears that the only dissociative attachment process of probable significance is the attachment of low energy electrons to $O_3$. Recent measurements (Reference 17-19) yield rate coefficients varying from $5 \times 10^{-12}$ cm$^3$/sec at 200 K to $9 \times 10^{-12}$ cm$^3$/sec at 300 K. In this case the negative ion formed is expected to be $O^-$ (Reference 17-20).

The process of associative detachment was predicted theoretically (Reference 17-21) many years ago as the logical inverse of dissociative attachment. However, experimental studies of this process have been reported (References 17-7, 17-22, 17-23) only recently. In many cases the observed rate coefficients are a large fraction of the ion-scattering cross-section due to the induced polarization interaction between the negative ion and the neutral atom or molecule (References 17-7, 17-21 through 17-24), i.e., $(2 - 10) \times 10^{-10}$ cm$^3$/sec. Associative detachment reactions involving atomic oxygen (Reference 17-22) are of particular importance in the ionosphere (References 17-7 through 17-9). There is not much information available as to the temperature dependence of the rate coefficient for associative detachment. In many cases, the associative detachment rate coefficient is essentially independent of ion energy (Reference 17-23), e.g., for $O^-$ + CO and $O^-$ + $H_2$ at ion energies below 0.15 eV. However, for $O^-$ + NO the rate coefficient decreases (Reference 17-23) by approximately an order of magnitude as the average ion energy increases from 0.04 to 0.26 eV. In the case of the detachment of electrons in collisions of energetic $O^-$ ions with $O_2$, it appears that associative detachment is less important than collisional detachment (Reference 17-25) and conversion to $O_2^-$ (References 17-5, 17-23, 17-26). Associative

detachment in collisions of thermal $O^-$ ions with $N_2$ has not been observed (Reference 17-27) although energetic $O^-$ ions appear (Reference 17-25) to undergo detachment collisions with $N_2$. The neutral molecule formed by associative detachment is usually in a highly excited state (Reference 17-24) so that the detailed-balance relations are not expected to be useful for relating the associative detachment and dissociative attachment coefficients. Recommended dissociative attachment and associative detachment rate coefficients are given in Tables 17-3 and 17-4.

Table 17-3. Dissociative attachment.*

| Reaction | Rate Coefficient ($cm^3/sec$) | Reference |
|---|---|---|
| 1. $e + O_3 \rightarrow O^- + O_2$ | $9 \times 10^{-12} (T/300)^{3/2}$ $(200 < T < 300\,K)$ | 17-19 |
| 2. $e + O_2 \rightarrow O^- + O$ | $< 10^{-16}$ $(T < 2000\,K)$ | 17-16 |
| 3. $e + H_2O \rightarrow H^- + OH$ | very small | 17-15 |

*No temperature-dependent rate coefficients are given for $O_2$ and $H_2O$ since the values will be critically dependent upon cross-section at energies below 1 eV and no experimental data are available for that region.

Table 17-4. Associative detachment.

| Reaction | Rate Coefficient ($cm^3/sec$) | Reference |
|---|---|---|
| 1. $O^- + O \rightarrow O_2 + e$ | $2 \times 10^{-10}$ | 17-22, 17-36 |
| 2. $O^- + O_2(^1\Delta_g) \rightarrow O_3 + e$ | $\sim 3 \times 10^{-10}$ | 17-36 |
| 3. $O^- + N \rightarrow NO + e$ | $2.2 \times 10^{-10}$ | 17-7, 17-36 |
| 4. $O^- + H_2 \rightarrow H_2O + e$ | $7.5 \times 10^{-10}$ | 17-22, 17-23 |
| 5. $O^- + NO \rightarrow NO_2 + e$ | $3 \times 10^{-10}(T_{ion}/300)^{-1}$ $(300 < T_{ion} < 2000\,K)$ | 17-22, 17-23 |
| 6. $O^- + N_2 \rightarrow N_2O + e$ | $< 1 \times 10^{-12}(T_{ion} \sim 300\,K)$ | 17-22 |
| | $< 4 \times 10^{-9} \exp(-26,000/T_{ion})$ $(4000 < T_{ion} < 20,000\,K)$ | 17-25 |

Table 17-4. (Cont'd.)

| Reaction | Rate Coefficient ($cm^3$/sec) | Reference |
|---|---|---|
| 7. $O^- + O_2 \rightarrow O_3 + e$ | $<5 \times 10^{-15}$ $(300 < T_{ion} < 10,000\ K)$ | 17-23 |
| | $<2.3 \times 10^{-9} \exp(-26,000/T_{ion})$ $(4000 < T_{ion} < 20,000\ K)$ | 17-25 |
| 8. $O_2^- + O \rightarrow O_3 + e$ | $3 \times 10^{-10}$ | 17-22, 17-36 |
| 9. $CO_3^- + O \rightarrow O_2 + CO_2 + e$ | slow | 17-7 |
| 10. $O_2^- + N \rightarrow NO_2 + e$ | $5 \times 10^{-10}$ | 17-22 |
| 11. $O_3^- + O \rightarrow 2O_2 + e$ | unknown | |

### 17.2.3 Three-Body Attachment and Collisional Detachment with a Neutral Third Body: $e + X + M \rightleftarrows X^- + M$

An apparent three-body attachment process has been found (References 17-14, 17-28 through 17-34) to be important in $O_2$, NO, $N_2O$, and $NO_2$, and in mixtures (References 17-14, 17-28, 17-33, 17-34) of these gases with other gases. The rate coefficients for three-body attachment processes in $O_2$ and NO are found (References 17-28, 17-30, 17-31) to be a maximum at electron energies of about 0.1 eV. In general it has not been possible to distinguish between a three-body process involving an intermediate excited negative ion which is stabilized by collision (Bloch-Bradbury model) and an apparent three-body process involving the dissociative attachment of an electron in a collision with a temporary neutral complex composed of two molecules. A theoretical study (Reference 17-35) of the Bloch-Bradbury model for electron attachment in $O_2$ predicts a three-body attachment coefficient approximately equal to the observed value. Because of uncertainties as to the proper model, as well as questions of excited states, the dependence of the apparent three-body attachment coefficient on electron energy cannot be assumed to be the same as the temperature dependence of the rate coefficient. The available experimental data are shown in Table 17-5. In view of the large rate coefficients for associative detachment in the presence of atomic nitrogen or oxygen discussed above there is no need to guess at the effectiveness of N or O atoms as third bodies in the attachment process. As pointed out in a review (Reference 17-29), measurements of the room-temperature attachment coefficient

Table 17-5. Three-body attachment.

| Reaction | Rate Coefficient ($cm^6$/sec) | Reference |
|---|---|---|
| 1. $e + O_2 + O_2 \rightarrow O_2^- + O_2$ | $(1.4 \pm 0.2) \times 10^{-29} \times (300/T)\exp(-600/T)$ $(195 < T < 600\,K)$ | 17-14, 17-29 |
| 2. $e + O_2 + N_2 \rightarrow O_2^- + N_2$ | $(1 \pm 0.5) \times 10^{-31}$ | 17-14, 17-29 |
| 3. $e + O_2 + CO_2 \rightarrow O_2^- + CO_2$ | $(3.3 \pm 0.7) \times 10^{-30}$ $(300 < T < 525\,K)$ | 17-14, 17-29 |
| 4.[a] $e + O_2 + H_2O \rightarrow O_2^- + H_2O$ | $(1.4 \pm 0.2) \times 10^{-29}$ $(300 < T < 400\,K)$ | 17-14 |
| 5.[a] $e + NO + NO \rightarrow NO^- + NO$ | $8 \times 10^{-31}$ | 17-30 |
| 6.[a] $e + NO_2 + N_2 \rightarrow NO_2^- + N_2$ | $4 \times 10^{-11}$[b] | 17-56, 17-57 |
| 7. $e + 2CO_2 \rightarrow X^- + ?$ | $< 2 \times 10^{-36}$ $(T_e = 300\,K)$ | 17-14 |

[a] Products uncertain.

[b] In $cm^3$/sec units since observed to be a saturated three-body process.

for thermal electrons in $O_2$ and in air at pressures below 100 torr which differ significantly from the presently accepted values of $2 \times 10^{-30}$ and $1 \times 10^{-31}$ $cm^6$/sec, respectively, should be regarded as highly suspect. At sufficiently high pressures of $O_2$ or dry air, the apparent attachment rate coefficient is lowered because attachment occurs before the electrons thermalize (Reference 17-34).

The inverse of the three-body attachment process is the collisional detachment process in which a negative ion collides with an atom or molecule and an electron is released. In the case of ground-state molecules this process has an activation energy in the center-of-mass coordinates equal to or greater than the electron affinity of the negative ion. This is observed (Reference 17-14) to be the case for $O_2^-$ ions in $O_2$ at temperatures between 375 and 580 K. There is now evidence (Reference 17-30) for collisional detachment in NO but there are questions (Reference 17-31) as to the identity of the ions present in some experiments. We have recommended attachment coefficients obtained in experiments which take into account that the

collisional detachment rate coefficients are much larger than for $O_2$. Collisional detachment has been observed (Reference 17-25) as the result of collisions of energetic $O^-$ ions with $O_2$, $N_2$, and $H_2O$. Collisional detachment caused by excited molecules has been observed (Reference 17-36) to occur with a large rate coefficient in the case of $O_2(^1\Delta_g) + O_2^-$. Recommended collisional detachment rate coefficients are given in Table 17-6.

Table 17-6. Collisional detachment.

| Reaction | Rate Coefficient ($cm^3$/sec) | Reference |
|---|---|---|
| 1. $O_2^- + O_2 \rightarrow O_2 + O_2 + e$ | $(2.7 \pm 0.3) \times 10^{-10} \times (T/300)^{1/2} \exp(-5590/T)$ $(375 < T < 600\,K)$ | 17-14 |
| 2. $O_2^- + N_2 \rightarrow N_2 + O_2 + e$ | $(1.9 \pm 0.4) \times 10^{-12} \times (T/300)^{3/2} \exp(-4990/T)$ $(375 < T < 600\,K)$ | 17-14 |
| 3. $O^- + O_2 \rightarrow O + O_2 + e$ | $2.3 \times 10^{-9} \exp(-26,000/T_{ion})$ $(T_i < 20000\,K)$ | 17-25 |
| 4. $O^- + N_2 \rightarrow O + N_2 + e$ | $2.3 \times 10^{-9} \exp(-26,000/T_{ion})$ $(T_i < 20000\,K)$ | assumed (see 17-25) |
| 5. $O_2^- + O_2(^1\Delta_g) \rightarrow 2O_2 + e$ | $2 \times 10^{-10}$ | 17-36 |

### 17.2.4 Three-Body Attachment and Detachment with an Electron as the Third Body: $e + e + X \rightleftarrows e + X^-$

The only experimental data concerning the role of an electron as an agent for the attachment and detachment reactions are the measurements (Reference 17-37) of the cross-sections for the collisional detachment of electrons from $H^-$ and $O^-$ by electrons at electron energies between 9 and 500 eV. As a result one is forced to rely on theory for estimates of rate coefficients for low-energy electrons. Although more recent theory (Reference 17-38) yields considerably larger values for low-energy electrons than previous theories, it is unlikely that these processes will have a significant effect on the negative-ion density in the earth's atmosphere.

## 17.3 STABILITY OF NEGATIVE IONS

Table 17-7 contains a list of negative ions of interest in approximate order of increasing stability, i.e., electron affinity. The values are based on a variety of experiments and theory (References 17-39 through 17-61). It may be noted that $N_2^-$, $H_2^-$, and $H_2O^-$ are not stable, i.e., if they are formed they have a very short lifetime (Reference 17-39). The $CO_2^-$ ion has been produced in negative ion-molecule reactions (Reference 17-59), but consistency with electron-beam excitation experiments and molecular structure theory (Reference 17-60) seems to require that the $CO_2^-$ ions be in a metastable state with a negative adiabatic electron affinity.

Many of the values cited in Table 17-7 are subject to significant uncertainties because of the preliminary nature of the data and because of incomplete analysis of the equilibrium-constant data. The analysis of equilibrium-constant data in terms of dissociation energies is made difficult by apparent differences in the internal structure of the complex negative ions. Thus, the data for $CO_4^-$ have been interpreted (Reference 17-14) as showing that there is a large freedom of internal motion whereas the data for $O_4^-$ appear to indicate a rather rigid structure (Reference 17-45). A further complication is the apparent existence of at least two forms of $NO_3^-$. Presumably at least one of these forms is in an excited metastable electronic state with a rather different molecular structure than that of the lower energy state. At present the only information available regarding these states is the differences in their reactivity (References 17-43, 17-54) with, for example, NO and $CO_2$. Some simplifications in the classification of negative-ion complexes have been pointed out (Reference 17-43); it appears that complexes formed from $O_2^-$ in the order of increasing stability are: $(O_2^- \cdot O_2)$, $(O_2^- \cdot H_2O)$, $(O_2^- \cdot CO_2)$, and $(O_2^- \cdot NO)$. Similarly for $O^-$, the order of stability of known ions is (Reference 17-43): $(O^- \cdot N_2)$, $(O^- \cdot O_2)$, $(O^- \cdot CO_2)$, $(O^- \cdot NO)$, and $(O^- \cdot NO_2)$. There are not sufficient data available to say whether similar series exist for other negative ions such as $NO^-$ and $OH^-$. The relative concentrations of the various ions in the atmosphere will depend upon competing detachment reactions as well as on the concentrations of the minor neutral constituents. Furthermore these ions can form hydrates and so effectively become more stable. An important area of future investigation is the study of the reactivity of the larger and more stable negative-ion hydrates with species such as O, $O_3$, and $NO_2$ (Reference 17-67).

Table 17-7. Stability of negative ions of possible ionospheric interest.[a]

| Ion | Adiabatic Electron Affinity (eV) | Dissociation Energy [c] (eV) | | Vertical Detachment Energy (eV) |
|---|---|---|---|---|
| $NO^-$ | 0.024 (17-30, 17-40) | $(O^- \cdot N)$ | 5.2 | < 1.0 (17-6) |
| $O_2^-$ | 0.43 ± 0.03 (17-14, 17-52) | $(O^- \cdot O)$ | 4.08 | ≤0.5 (17-2) |
| $O_4^-$ | 1.0 [b] | $(O_2^- \cdot O_2)$ | 0.54 (17-45) | ≥ 1.0 [b] |
| $O_2^-(H_2O)$ | 1.2 [b] | $(O_2^- \cdot H_2O)$ | 0.8 (17-42, 17-46) | ≥ 1.2 [b] |
| $CO_4^-$ | 1.2 ± 0.1 (17-14) | $(O_2^- \cdot CO_2)$ | 0.8 ± 0.08 | ≥ 1.2 [b] |
| $H_3O_2^-$ | ≤ 1.2 [b] | $(OH^- \cdot H_2O)$ | ≤ 1.2 | 2.95 (17-6) |
| $SF_6^-$ | ~1.4 (17-47, 17-48) $EA(O_2) < EA(SF_6) < EA(O)$ (17-49) | $(SF_5^- \cdot F)$ | ≤ 1.4 (17-61) | |
| $O^-$ | 1.47 ± 0.01 (17-1, 17-2, 17-50) | | | 1.47 ± 0.1 (17-1, 17-2) |
| $O_2^-(H_2O)_2$ | 1.95 [b] | $(O_2^-(H_2O) \cdot H_2O)$ | 0.75 (17-42) | ≥ 1.95 [b] |
| $O_3^-$ | 1.9 (17-41, 17-58) | $(O^- \cdot O_2)$<br>$(O_2^- \cdot O)$ | 1.4<br>2.5 | 2.1 (17-44) |
| $O_2^-(H_2O)_3$ | 2.6 [b] | $(O_2^-(H_2O)_2 \cdot H_2O)$ | 0.67 (17-42) | > 2.6 [b] |

Table 17-7. (Cont'd.)

| Ion | Adiabatic Electron Affinity (eV) | Dissociation Energy [c] (eV) | | Vertical Detachment Energy (eV) |
|---|---|---|---|---|
| $CO_3^-$ | | $(O^- \cdot CO_2)$ | Unknown (17-43) | |
| $NO_2^-$ | 2.5 ± 0.2 (17-51, 17-65, 17-66) | $(O^- \cdot NO)$ | 4.1 | 2.75 (17-1)<br>≥2.74 (17-55) |
| $O_2^-(H_2O)_4$ | 3.2 [b] | $(O_2^-(H_2O)_3 \cdot H_2O)$ | 0.6 (17-42) | >3.2 |
| $O_2^-(H_2O)_5$ | 3.7 [b] | $(O_2^-(H_2O)_4 \cdot H_2O)$ | 0.5 (17-42) | >3.7 |
| $NO_3^-$ [d] | Unknown | $(O_2^- \cdot NO)$ | $>D_o(O_2^- \cdot O) = 2.5$ (17-7) | |
| | 3.6 ± 0.2 (17-51, 17-66) | $(O^- \cdot NO_2)$ | 4.3 (17-51, 17-68) | |

[a] References given in parentheses. When no reference is given, the values cited are our calculations based on other entries for the same species.

[b] Calculated assuming that the neutral complex has a negligibly small dissociation energy for separation into the stable neutral fragment molecules, e.g., $O_2$, $H_2O$, and $CO_2$. For a discussion of the interaction of $O_2$ with $CO_2$, $H_2O$, and CO see Reference 17-63. For $O_2$ with $O_2$ see Reference 17-64.

[c] This dissociation energy is for the bond indicated by the dot in the formula for the negative ion. The dot is not intended to indicate the structure of the complex. The dissociation energies for NO and $O_2$ are from Reference 17-52 and that for the $O_2 \cdot O$ bond from Reference 17-55.

[d] Recent evidence (Reference 17-43) suggests that there is a metastable form of this ion with a sufficient lifetime so as to lead to different reaction sequences.

## 17.4 IONOSPHERIC SIGNIFICANCE

It is convenient to divide a discussion (References 17-1, 17-8, 17-9, 17-29) of the dominant attachment and detachment reactions in the earth's atmosphere into three categories: (1) the initial attachment of the free electrons to neutral species to form negative ions; (2) the ion-molecule reactions which convert the initial negative ions into more stable species; and (3) the detachment process.

The important attachment processes in undisturbed, dry air are:

$$e + 2O_2 \rightarrow O_2^- + O_2 ,$$

and:

$$e + O \rightarrow O^- + h\nu .$$

The relative importance of these processes varies with altitude and time because of the varying concentrations of O and $O_2$ . When the moisture content is high or when the gas temperature is high and the air composition is altered, other processes may be important, e.g., $e + O_2 + H_2O \rightarrow O_2^- + H_2O$ in moist air. At present it appears that the reaction:

$$e + O_3 \rightarrow O^- + O_2 ,$$

can be important only under highly disturbed conditions.

The negative-ion-molecule reactions of importance in the atmosphere are discussed in Chapter 18A so that it need merely be noted that the initial $O_2^-$ and $O^-$ ions can react (References 17-7 through 17-9, 17-22, 17-36, 17-43, 17-54) with minor constituents of the normal atmosphere, i.e., $O_3$ , $CO_2$, and NO , to form ions such as $O_3^-$ , $CO_3^-$ , $NO_2^-$ , and $NO_3^-$ . The relative concentrations of the various ions will depend upon competing detachment reactions as well as on the ion conversion processes. Furthermore these ions can form hydrates and so effectively become more stable.

Associative detachment reactions have been shown (References 17-7 through 17-9) to play an important role in determining the concentrations of free electrons and negative ions. Ionospheric model studies (References 17-8, 17-9) have not been able to identify the detachment reactions controlling the changes in electron density which occur at sunrise and sunset. It seems certain that $O^-$ and $O_2^-$ are not the dominant negative ions. The identity of the dominant ions as determined by rocket-borne mass spectrometers

varies with altitude and with the degree of ionospheric disturbance. The negative ions observed (Reference 17-10) include $O^-$, $O_2^-$, $NO_3^-$, and $NO_3^- \cdot (H_2O)_n$.

## REFERENCES


17-1. For a review of relevant photodetachment data prior to 1964, see Branscomb, L.M., Ann. Geophys. 20, 88 (1964).

17-2. Burch, D.S., S.J. Smith, and L.M. Branscomb, Phys. Rev. 112, 171 (1958); Ibid. 114, 1652 (1959).

17-3. Branscomb, L.M., S.J. Smith, and G. Tisone, J. Chem. Phys. 43, 2906 (1965).

17-4. Branscomb, L.M., Phys. Rev. 148, 11 (1966).

17-5. Woo, S.B., L.M. Branscomb, and E.C. Beaty, J. Geophys. Res. 74, 2933 (1969).

17-6. Golub, S., and B. Steiner, J. Chem. Phys. 49, 5191 (1968); DASA Symposium on Physics and Chemistry of the Upper Atmosphere, Stanford Research Institute (1969).

17-7. Fehsenfeld, F.C., A.L. Schmeltekopf, H.I. Schiff, and E.E. Ferguson, Planet. Space Sci. 15, 373 (1967).

17-8. LeLevier, R., and L.M. Branscomb, J. Geophys. Res. 73, 271 (1968).

17-9. Niles, F.E., DASA Symposium on Physics and Chemistry of the Upper Atmosphere, Stanford Research Institute (1969), Ballistic Research Laboratories, Rept. 1458 (1969).

17-10. Narcisi, R.S., A.D. Bailey, L. Della Lucca, C. Sherman, and D.M. Thomas, J. Atm. Terrestr. Phys. 33, 1147 (1971); Narcisi, R.S., A.D. Bailey, L.E. Wlodyka, and C.R. Philbrick, Ibid. (accepted for publication); Arnold, F., and D. Krankowsky, Ibid. 33, 1693 (1971).

17-11. Siegel, M.W., and J.L. Hall, J. Chem. Phys. 48, 943 (1968); Cooper, J., and R.N. Zare, Ibid. 942.

17-12. Geltman, S., Phys. Rev. 112, 176 (1958); O'Malley, T.F., Ibid. 137, A1688 (1965).

17-13. See, for example, Klein, M.M., and K.A. Brueckner, Phys. Rev. 111, 1115 (1958). Note, however, that the data discussed for O in Chapter 21 of this Handbook show that consistency of theoretical and experimental photodetachment cross-sections does not guarantee an accurate calculation of total (elastic) scattering cross-sections.

17-14. Pack, J.L., and A.V. Phelps, J. Chem. Phys. 44, 1870 (1966); Ibid. 45, 4316 (1966). The electron affinity for $O_2$ from this paper has been raised from 0.43 to 0.44 eV on the basis of a reanalysis of the original data taking into account the different vibrational constants for $O_2$ and $O_2^-$ and the shift in the equilibrium caused by small concentrations of $O_4^-$ at the lower temperatures.

17-15. Bucel'nikova, N.S., Fortschr. Physik 8, 626 (1960); Rapp, D., and D.D. Briglia, J. Chem. Phys. 43, 1480 (1965).

17-16. Henderson, W.R., W.L. Fite, and R.T. Brackmann, Phys. Rev. 183, 157 (1969).

17-17. Chantry, P.J., J. Chem. Phys. 51, 3369 (1969).

17-18. O'Malley, T.F., Phys. Rev. 155, 59 (1967).

17-19. Stelman, D., and A.V. Phelps, DASA Symposium on Physics and Chemistry of the Upper Atmosphere, Stanford Research Institute (1969); J. Chem. Phys. (submitted 1971).

17-20. Curran, R.K., J. Chem. Phys. 35, 1849 (1961). In view of the temperature dependence of the appearance potentials observed using electron-beam techniques in $CO_2$, for example, the low-energy attachment cross-section and the threshold for $O_2^-$ formation from this experiment should not be considered as final. See Schulz, G.J., and D. Spence, Phys. Rev. Letts. 22, 47 (1969).

17-21. Bates, D.R., and H.W.S. Massey, Proc. Roy. Soc. A239, 269 (1943). The large cross-sections found for favorable cases of associative detachment were first predicted by Dalgarno, A., Ann. Geophys. 17, 16 (1961).

17-22. Fehsenfeld, F.C., E.E. Ferguson, and A.L. Schmeltekopf, J. Chem. Phys. 45, 1884 (1966); McDaniel, E.W., et al, Ion-Molecule Reactions, John Wiley and Sons, Inc., New York (1970); Chap. 6.

17-23. Moruzzi, J.L., and A.V. Phelps, J. Chem. Phys. 45, 4316 (1966); Moruzzi, J.L., J.W. Ekin, Jr., and A.V. Phelps, Ibid. 48, 3070 (1968).

17-24. Chen, J.C.Y., Phys. Rev. 156, 12 (1967); Herzenberg, A., Ibid 160, 80 (1967).

17-25. Frommhold, L., Fortschr. Physik 12, 597 (1964); Muschlitz, E.E., Proc. Fourth Intl. Conf. Ionization Phenomena Gases, Uppsala, Sweden (1959); Hasted, J.B., and R.A. Smith, Proc. Roy. Soc. A235, 349 (1956); Compton, R.N., and T.L. Bailey, J. Chem. Phys. 53, 454 (1970).

17-26. Burch, D.S., and R. Geballe, Phys. Rev. 106, 188 (1957).

17-27. Ferguson, E.E., F.C. Fehsenfeld, and A.L. Schmeltekopf, J. Chem. Phys. 47, 3085 (1967).

17-28. Chanin, L.M., A.V. Phelps, and M.A. Biondi, Phys. Rev. 128, 219 (1962); Hirsch, M.N., P.N. Eisner, and J. Selvin, Ibid. 178, 175 (1969).

17-29. A recent review of these and other attachment and detachment processes is given in Phelps, A.V., Can. J. Chem. 47, 1783 (1969).

17-30. Parkes, D.A., and T.M. Sugden, Trans. Faraday Soc. (submitted 1971).

17-31. Gunton, R.C., and T.M. Shaw, Phys. Rev. 140, A748 (1965); Weller, C.S., and M.A. Biondi, Ibid. 172, 198 (1968); Puckett, L.J., M.D. Kregel, and M.W. Teague, Ibid. A4, 1659 (1971).

17-32. Phelps, A.V., and R.E. Voshall, J. Chem. Phys. 49, 3246 (1968); Warman, J.M., and R.W. Fessenden, Ibid. 49, 4718 (1968).

17-33. van Lint, V.A.J., E.G. Wikner, and D.L. Trueblood, Bull. Am. Phys. Soc. 5, 122 (1960); General Atomic, Report TR59-43 (1959).

17-34. See Grünberg, R., Naturforsch. 24a, 1039 (1969) for $O_2$ data and Hessenaur, H., Z. Physik 204, 142 (1967) for air data obtained at electron energies somewhat above thermal.

17-35. Herzenberg, A., J. Chem. Phys. 51, 4942 (1969).

17-36. Fehsenfeld, F.C., D.L. Albritton, J.A. Burt, and H.I. Schiff, Can. J. Chem. 47, 1793 (1969).

17-37. Dance, D.F., M.F.A. Harrison, and R.D. Rundel, Proc. Roy. Soc. A299, 525 (1967); Tisone, G., and L.M. Branscomb, Phys. Rev. 170, 169 (1968).

17-38. Smirnov, B.M., and M.I. Chibisov, J. Exptl. Theoret. Phys. (USSR) 49, 841 (1965); [Translation: Sov. Phys.-JETP 22, 585 (1966)].

17-39. Bardsley, J.N., and F. Mandl. Repts. Prog. Phys. 31, 471 (1968).

17-40. Siegel, M.W., R. Celotta, J. Levine, J.L. Hall and R.A. Bennett, Phys. Rev. A (submitted 1971).

17-41. Wood, R.H., and L.A. D'Orazio, J. Phys. Chem. 69, 2562 (1965).

17-42. Kebarle, P., M. Arshadi, and J. Scarborough, J. Chem. Phys. 49, 817 (1969); Arshadi, M., and P. Kebarle, J. Phys. Chem. 74, 1483 (1970). The dissociation energies given in Table 17-7 for the $(O_2 \cdot (H_2O)_n)$ complexes, $n > 3$, are calculated from the equilibrium constants given in these references assuming the molecules of the complex to have complete freedom of internal rotation. See Reference 17-14.

17-43. Adams, N. G., D. K. Bohme, D. B. Dunkin, F. C. Fehsenfeld, and E. E. Ferguson, J. Chem. Phys. 52, 3133 (1970); Fehsenfeld, F. C., E. E. Ferguson, and D. K. Bohme, Planet. Space Sci. 17, 1759 (1969).

17-44. Byerly, R., Jr., and E. C. Beaty, J. Geophys. Res. 76, 4596 (1971); Vorburger, T. V., and S. B. Woo, Bull. Am. Phys. Soc. 16, 213 (1971).

17-45. This value is calculated from the data of Conway, D. C., and L. E. Nesbit, J. Chem. Phys. 48, 509 (1968) using the type of analysis outlined by Voshall, R. E., J. L. Pack, and A. V. Phelps, Ibid. 43, 1990 (1965). Our value for $D_o$ is somewhat smaller than the value of $\Delta H$ given by Conway and Nesbit. The limiting equilibrium constant for a rigid nonlinear $O_4^-$ structure given by Voshall et al has been corrected so as to include the third rotational degree of freedom. The results of Conway and Nesbit are most consistent with a rigid $O_4^-$ structure with perhaps one active vibrational or internal rotational mode. A similar value for $O_2$ has been obtained by C. Shafer and E. C. Beaty (private communication).

17-46. Limits for the dissociation energy of $O_2^- \cdot H_2O$ are the value for $O_2^- \cdot O_2$ and $O_2^- \cdot CO_2$ since the data of Reference 17-43 show the order of stability to be: $O_2^- \cdot O_2$, $O_2^- \cdot H_2O$, and $O_2^- \cdot CO_2$.

17-47. Kay, J., and F. M. Page, Trans. Faraday Soc. 60, 1042 (1964).

17-48. Compton, R. N., L. G. Christophorou, G. S. Hurst, and P. W. Reinhardt, J. Chem. Phys. 45, 4634 (1966). The value of EA for $SF_6$ calculated from the data of this reference is too low because of too low an attachment coefficient.

17-49. Fehsenfeld, F. C., J. Chem. Phys. 54, 438 (1971).

17-50. Elder, F.A., D. Villarjo, and M.G. Inghram, J. Chem. Phys. 43, 758 (1965); Chantry, P.J., and G.J. Schulz, Phys. Rev. 156, 134 (1967).

17-51. Ferguson, E.E., D.B. Dunkin, and F.C. Fehsenfeld, J. Chem. Phys. (submitted 1971).

17-52. Gilmore, F.R., J. Quant. Spectry. Radiative Transfer 5, 369 (1965).

17-53. Herzberg, G., Electronic Spectra of Polyatomic Molecules, Van Nostrand Co., Inc., Princeton, New Jersey (1966).

17-54. Ferguson, E.E., Can. J. Chem. 47, 1815 (1969).

17-55. Warneck, P., Chem. Phys. Letts. 3, 532 (1969).

17-56. Mahan, B.H., and I.C. Walker, J. Chem. Phys. 47, 3780 (1967). The interpretation of the experiments has been questioned. See Reference 17-57.

17-57. Klots, C.E., J. Chem. Phys. 53, 1616 (1970).

17-58. Berkowitz, J., W. A. Chupka, and D. Gutman, J. Chem. Phys. 55, 2733 (1951).

17-59. Paulson, J.F., J. Chem. Phys. 52, 963 (1970).

17-60. Clayton, C.R., G.A. Segal, and H.S. Taylor, J. Chem. Phys. 52, 3387 (1970); see also Bardsley, J.N., Ibid. 51, 3384 (1969).

17-61. Chen, C.L., and P.J. Chantry, Bull. Am. Phys. Soc. 15, 418 (1970). These authors find that there is a resonance cross-section at near-zero electron energy for $SF_5^-$ production as well as for $SF_6^-$ production. This means that the $SF_5 \cdot F$ bond energy is less than the electron affinity of $SF_6$.

17-62. Celotta, R., R. Bennett, J. Hall, M.W. Siegel, and J. Levine, Bull. Am. Phys. Soc. 15, 1515 (1970); Phys. Rev. A (submitted 1971).

17-63. Walker, R.E., and A.A. Westenberg, J. Chem. Phys. 32, 436 (1960).

17-64. Blickensderfer, R.P., and G.E. Ewing, J. Chem. Phys. 47, 331 (1967); Ibid. 51, 873 (1969).

17-65. Lifshitz, C., B.M. Hughes, and T.O. Tiernan, Chem. Phys. Letts. 7, 469 (1970).

17-66. Payzant, J.D., R. Yamdagni, and P. Kebarle, Can. J. Chem. 49, 3308 (1971).

17-67. Ferguson, E.E., Revs. Geophys. Space Phys. 9, 997 (1971).

17-68. Vedeneyev, V.I., et al., Bond Energies, Ionization Potentials, and Electron Affinities, St. Martin's Press, New York (1966); p. 80.

# 18. ION-NEUTRAL REACTIONS
# A. THERMAL PROCESSES

Eldan Ferguson
Aeranomy Labaratory
Natianal Oceanic and Atmaspheric Administratian
Research Labaratories
(Latest Revisian 21 Navember 1971)

## 18A.1 INTRODUCTION

Pragress in the field af ion-neutral reactions has been very rapid in the few years since the first edition of the Reaction Rate Handbook was prepared. The number of atmospherically relevant rate constants known has multiplied greatly and most of those previously known have been improved so that an almost complete rewriting of this chapter (prepared by Wade L. Fite in the first edition of the Handbook) was called for. The convenient format of Fite is retained. The emphasis of this chapter is on data tabulation. The reactions reported are positive- and negative-ion charge-transfer (electron transfer) with neutrals, ion-atom-interchange reactions (chemical rearrangement), and three-body association reactions. Associative-detachment reactions af negative ions are cavered in Chapter 17. The survey is restricted largely to low (near-thermal) energies.

Some useful general references and review articles are:

(a) Sinnott, G. A., Bibliography of Ion-Molecule Reaction Rate Data, JILA Information Center Report No. 9, University of Colorado, Boulder, Colorado (1969).

(b) McDaniel, E. W., V. Cermak, A. Dalgarno, E. E. Ferguson, and L. Friedman, Ion-Molecule Reactions, John Wiley, New York (1970).

(c) Hochstim, A. R., Ed., Bibliography of Chemical Kinetics and Collision Processes, Plenum Press, New York (1969).

(d) Franklin, J. L., J. G. Dillard, H. M. Rosenstock, T. J. Herron, K. Draxl, and F. H. Field, Ionization Potentials, Appear-

ance Potentials, and Heats of Formation of Gaseous Ions, NSRDS-NBS 26, U. S. Gov't. Printing Office, Washington (1969).

(e) Schiff, H. I., Ed., Proceedings of The Symposium on Laboratory Measurements of Aeronomic Interest, Can. J. Chem. 47, No. 10 (1969).

(f) Ferguson, E. E., Ann. Geophys. 25, 819 (1969).

(g) Ferguson, E. E., Ann. Geophys. 26, 589 (1970).

(h) Franklin, J. L., Ed., Ion-Molecule Reactions, Plenum Press, New York, to be published (1972).

(i) Ferguson, E. E., Accts. Chem. Res. 3, 402 (1970).

(j) Ferguson, E. E., Laboratory Measurements of D-Region Ion-Molecule Reactions, ESRIN-ESLAB Symposium on "Upper Atmospheric Models and Related Experiments", Frascati, Italy, July 1970, to be published in Conference Proceedings.

(k) Bibliography of Atomic and Molecular Processes, compiled by Atomic and Molecular Processes Information Center, Oak Ridge National Laboratory, on a continuing basis.

## 18A.2 TECHNIQUES

The experimental techniques in use are described in detail in Chapter 7, in reference item (b) above, and elsewhere. Only brief reference is made here to recent advances which have led to new reaction-rate data.

### 18A.2.1 Stationary Afterglows

The use of stationary afterglows for ion-neutral reaction studies is described in Chapter 7. Important studies (Reference 18A-1) in the complex nitric oxide system have been carried out with and without added water vapor, looking at both positive- and negative-ion processes. Other work (References 18A-2, 18A-3) has concentrated on the ionospheric reactions, varying the gas temperature from 185 to 576 K in some cases.

### 18A.2.2 Flowing Afterglow

The flowing-afterglow technique, a versatile method for ion-neutral reaction studies in the sense of being applicable to a wide range of ion and neutral reactants, has been extended to cover the temperature range 80-600 K for some reactions (References 18A-4, 18A-5). It has been applied to metal-ion reactions (Reference 18A-6) and to three-body ion reactions (References 18A-7 through 18A-9). The method has been applied to measurements of atmospheric-ion charge-transfer with sodium (Reference 18A-10) and ion reactions with water (References 18A-11, 18A-12). The NOAA system discussed in Chapter 7 has been extended to study $O^-$ and $O_2^-$ reactions with electronically excited $O_2(a\,^1\Delta_g)$ (Reference 18A-13), and to study product states formed by an ion-neutral reaction spectroscopically in the charge transfer of $He^+$ with $N_2$ (Reference 18A-14).

### 18A.2.3 Secondary Ions in Mass Spectrometers

The mass-spectrometer ion-source technique, long the standard tool for radiation chemistry, has made important contributions to ionospheric reaction-rate data. The photoionization source method of Warneck (References 18A-15, 18A-16) has allowed the measurement of a large number of ionospheric reactions, generally corroborating earlier afterglow results. The isotope studies of Paulson (Reference 18A-17) have allowed some mechanisms of ionospheric reactions to be determined. In addition Paulson has obtained data on the energy dependence of certain reactions, and has also extended the mass spectrometer to the study of ionospheric negative ions (Reference 18A-18). Kebarle (References 18A-19, 18A-20) has made important measurements of two- and three-body reactions involving water, which are difficult to do otherwise. Kebarle and also Conway have measured equilibrium constants in high-pressure mass-spectrometer ion sources, adding greatly to our knowledge of the important ionospheric-ion chemistry.

### 18A.2.4 Crossed-Beam Experiments

The method of Turner and Rutherford (cf. Chapter 7) continues to produce large amounts of valuable ionospheric information on charge-transfer processes, both for positive and negative ions, at energies down to a few electron volts (Reference 18A-21). The relative constancy of charge-transfer rate constants from thermal levels to several electron volts allows a reasonable extrapolation of the low-energy crossed-beam data in many cases. Important

data on the reactions of excited-state ions, which are almost unavailable by any other technique, have also been obtained (Reference 18A-22). The crossed-beam studies have shown great versatility in the kinds of reactants studied.

### 18A.2.5 Drift-Tube Techniques

A very promising new development is the use of drift tubes to study ionospheric ion-neutral reactions over a range of energies, from thermal levels to several electron volts, not otherwise readily accessible. The works of Biondi (References 18A-23, 18A-24), Varney (Reference 18A-25), Hasted (References 18A-26, 18A-27), McDaniel (Reference 18A-28), and Kaneko (Reference 18A-29) are especially noteworthy.

## 18A.3 EXAMPLES OF IMPORTANT IONOSPHERIC REACTIONS

Several of the more important ionospheric reactions are discussed in some detail in this section. A variety of different types of reactions are discussed in order to point out different kinds of problems which arise. Reviews are available by Fite (Reference 18A-30) for aeronomic positive-ion reactions, and by Ferguson (Reference 18A-31) for aeronomic negative-ion reactions.

### 18A.3.1 $He^+ + N_2 \rightarrow N^+ + N + He$
$\rightarrow N_2^+ + He$

This is an example of one of the simplest ionospheric reactions to be measured, involving an ion of a stable neutral reacting with a stable neutral. Consequently a number of measurements in a variety of experiments support a value $k = (1.2 \pm 0.3) \times 10^{-9}$ cm$^3$/sec. The rate constant is insensitive to temperature variation and to vibrational excitation of the nitrogen. The branching ratio, i.e., $N^+/N_2^+$ product ratio, is less certain than the rate-constant measurement, since it involves a knowledge of the sampling efficiency (as a function of mass) for the mass spectrometer, which is unnecessary for the rate-constant measurement alone in certain techniques. The $N^+/N_2^+$ ratio lies between one and two, and depends on the nitrogen vibrational temperature. This reaction is near resonant charge transfer into the $N_2^+(C)$ state, which then radiates the second-negative system to give ground-state $N_2^+$, or predissociates to give $N^+$ (Reference 18A-14). This is one of the few reactions for

which the product states are well known. There is evidence that the $N_2^+$ produced is rotationally excited.

### 18A.3.2 $O^+ \quad O_2 \rightarrow O_2^+ + O$

This reaction has been measured by several workers; all results are consistent with $k = 2.0 \times 10^{-11} (T/300)^{-1/2}$ cm$^3$/sec for the temperature range 80-600 K (References 18A-3 through 18A-5).

### 18A.3.3 $O^+ + N_2 \rightarrow NO^+ + N$

This reaction has been studied in great detail, often with conflicting results. The rate constant is $1.2 \times 10^{-12}$ cm$^3$/sec at 300 K, and decreases to about $5 \times 10^{-13}$ cm$^3$/sec at 600 K (Reference 18A-4). The reaction-rate constant is extremely sensitive to the nitrogen vibrational temperature, increasing sharply for $T_{vib} > 1200$ K (Reference 18A-32). At higher energies, where the $O^+$ kinetic energy exceeds 0.5 eV, the rate constant also increases sharply. It seems likely that in the important ionospheric temperature range 600-2500 K the effect of nitrogen vibrational-temperature increase will dominate the effect of kinetic-energy increase. Kaneko et al (Reference 18A-29) have obtained cross-section data for ion kinetic energies from thermal levels to about one electron volt. O'Malley has developed a theory for this reaction which yields some extrapolation tables (Reference 18A-33).

### 18A.3.4 $N_2^+ + O_2 \rightarrow O_2^+ + N_2$

Johnsen et al (Reference 18A-24) find the rate constant to be about $6 \times 10^{-11}$ cm$^3$/sec at 300 K and to decrease regularly to about $10^{-14}$ cm$^3$/sec at $N_2^+$ kinetic energy equal to one electron volt. This agrees very well with the flowing-afterglow data (Reference 18A-4) in the region of overlap, 300-600 K.

### 18A.3.5 $SiO^+ + O \rightarrow Si^+ + O_2$

This reaction has been found to have a rate constant of approximately $2 \times 10^{-10}$ cm$^3$/sec (Reference 18A-34). A reaction such as this is very difficult to measure, since the reactant ion is not readily produced, and since the neutral reactant is unstable. No experimental methods exist in which the temperature dependence of reactions involving unstable neutrals can be measured.

18A.3.6 $Mg^+ + O_3 \rightarrow MgO^+ + O_2$

This reaction has a rate constant equal to $2.3 \times 10^{-10}$ $cm^3/sec$ (Reference 18A-6), and represents a kind of reaction which is difficult to measure because of problems in handling both the ion and neutral reactants. The measurements are correspondingly less accurate than for experimentally simpler reactions, and such details as the energy dependence of the rate constant are not available.

18A.3.7 $O_2^+ + Na \rightarrow Na^+ + O_2$

This reaction and the analogous $N_2^+$ and $NO^+$ charge-transfer reactions have been measured in a flowing-afterglow system (Reference 18A-10), the rate constant for the $O_2^+$ reaction being $6.7 \times 10^{-10}$ $cm^3/sec$ at 300 K. Reactions of ions with neutral metals pose problems in measurement because of the difficulty of handling and measuring the neutral reactant. However, such reactions are being treated in crossed-beam experiments, down to a few electron volts of ion energy (see Table 18A-6). Because of the difficulties enumerated above, crossed-beam measurements will probably supply the bulk of useful information of this kind for some years. In the case of charge-transfer reactions generally, the rate-constant dependence on energy is usually relatively slight, so that the long extrapolation from a few electron volts to atmospheric temperatures is not so hazardous as would be the case for ion-atom interchange. However, for $O_2^+ + Na$ the extrapolation gives about twice as large a rate constant as the flowing-afterglow measurement, and for $N_2^+ + Na$ the discrepancy is a factor of four, the extrapolated beam result again being larger. An important detail about reactions such as this which remains undetermined is the chemical state of the products, i.e., either $O_2$ or $O + O$ could be produced in the present instance.

18A.3.8 $O_2^+ + O_2 + M \rightarrow O_4^+ + M$

This reaction is particularly important with respect to the D-region chemistry (Reference 18A-35). Reactions such as this one are difficult to measure in the laboratory and good rate data are correspondingly sparse. The problem is compounded by the fact that several third bodies (M) are of potential importance in the atmosphere, and by the additional fact that three-body rate constants are markedly temperature-dependent. Much of the atmospheric interest is in the D-region where $T < 300$ K, which is not a readily accessible range in most laboratory experiments. For $M = O_2$ and $T = 298$ K, Durden et al (Reference 18A-19) find $k = 2.8 \times 10^{-30}$ $cm^6/sec$ for

the above reaction. For M = He and T = 80 K, Bohme et al (Reference 18A-8) find $k = 3.1 \times 10^{-29}$ cm$^6$/sec. This illustrates the marked increase in rate constant with decreasing temperature, a very general finding. It is unlikely that helium is as effective a third body as molecular oxygen at any temperature. In the analogous $N_2^+$ reaction at 300 K, molecular nitrogen is 2.5 times as effective as helium, for example (Reference 18A-8). This reaction ($N_2^+ + 2N_2 \rightarrow N_4^+ + N_2$) is about 18 times faster than the corresponding $O_2^+$ reaction cited above, which is attributable to a larger $N_4^+$ dissociation energy. Three-body-association rate constants are expected to increase markedly, both with the dissociation energy of the complex formed and with the sizes of the molecules involved, as well as with a decrease in temperature.

### 18A.3.9 $O_2^- + O_2 + M \rightarrow O_4^- + M$

It is recognized that $O_4^-$ formation may be of great importance in D-region negative-ion chemistry (Reference 18A-36), owing to a number of rapid $O_4^-$ reactions, e.g., $O_4^- + NO \rightarrow NO_3^- + O_2$, which lead to stable (non-electron-detaching) products. This reaction appears to be quite slow; McKnight and Sawina (Reference 18A-37) report $k = 3 \times 10^{-31}$ cm$^6$/sec at 310 K, from drift-tube studies. This is an order of magnitude slower than the analogous $O_2^+$ positive-ion association at room temperature, suggesting a definite anomaly inasmuch as the $O_4^-$ dissociation energy is thought to be greater (0.59 eV) than the $O_4^+$ bond energy (0.42 eV).

### 18A.3.10 $NO_2^- + NO_2 \rightarrow NO_3^- + NO$

This reaction is observed to take place with a rate constant of approximately $4 \times 10^{-12}$ cm$^3$/sec (Reference 18A-36), indicating that $EA(NO_3) > EA(NO_2) + 0.9$ eV, or that $EA(NO_3) > 2.7$ eV at least, and probably > 3.1 eV. Additionally, these data seem to establish that the reverse reaction ($NO_3^- + NO$) is endothermic. However, it has also been found (Reference 18A-38) that a form of $NO_3^-$ can be produced which reacts readily with NO in the laboratory. Presumably this $NO_3$ is a different stable geometrical form of the same empirical formula $NO_3^-$. Polyatomic ions are known to exist in different isomeric forms, e.g., O-N-O-O$^-$ and O-N-O (with O$^-$) in the present instance. This suggests a potential source of error in certain laboratory observations, as well as a considerable additional complexity of the D-region chemistry, where such factors may have an important influence upon the ion chemistry in particular.

### 18A.3.11 The $O_2^+$ - $H_2O$ Sequence

A reaction scheme which proceeds sequentially from $O_2^+$ to $H_3O^+ \cdot H_2O$ and higher hydrated clusters, is known to be very significant in the D-region. The three-body association of $O_2^+$ to $O_4^+$, discussed in subsection 18A.3.8, is efficient at approximately 200 K in the D-region. Following this initial step, the sequence proceeds via:

| | K* | F** |
|---|---|---|
| (a) $O_4^+ + H_2O \rightarrow O_2^+ \cdot H_2O + O_2$ | $1.3 \times 10^{-9}$ | $2.2 \times 10^{-9}$ |
| (b) $O_2^+ \cdot H_2O + H_2O \rightarrow H_3O^+ \cdot OH + O_2$ | $9 \times 10^{-10}$ | $1.9 \times 10^{-9}$ |
| (c) $\rightarrow H_3O^+ + OH + O_2$ | $3 \times 10^{-10}$ | $3.0 \times 10^{-10}$ |
| (d) $H_3O^+ \cdot OH + H_2O \rightarrow H_3O^+ \cdot H_2O + OH$ | $\geq 1 \times 10^{-9}$ | $3.2 \times 10^{-9}$ |

These are followed in turn by further three-body clustering of water molecules to the hydrated cluster-ions. Reaction (c) (producing $H_3O^+$) is almost certainly endothermic and presumably occurs as a consequence of vibrational excitation of the reactant $O_2^+ \cdot H_2O$. This may account for reported variations in the branching ratio represented by reactions (b) and (c), with different experimental conditions. Fehsenfeld (Reference 18A-39) has found that the reaction:

(e) $O_4^+ + O \rightarrow O_2^+ + O_3$

has a large rate constant, i.e., $k = (3 \pm 2) \times 10^{-10}$ cm$^3$/sec. This plays an important role in the $O_2^+$ - $H_2O$ reaction scheme in the D-region.

In addition to $O_2^+ \cdot H_2O$ production from $O_4^+$, direct $O_2^+$ hydration can occur:

(f) $O_2^+ + H_2O + M \rightarrow O_2^+ \cdot H_2O + M$ .

* Rate constants from Kebarle (Reference 18A-20), in cm$^3$/sec.

** Rate constants from Ferguson (Reference 18A-9), in cm$^3$/sec.

Howard, Rundle, and Kaufman have found the rate constant to be $1.9 \times 10^{-28}$ $cm^6/sec$ for $M = O_2$ at 296 K (Reference 18A-12), and Good et al (Reference 18A-20) and Fehsenfeld et al (Reference 18A-9) have obtained similar results.

### 18A.3.12 The $NO^+ - H_2O$ Sequence

The sequence of events involved in $NO^+$ hydration in the D-region have been shown (References 18A-1, 18A-12, 18A-35, 18A-40, 18A-41) to include:*

| | | F | H | P |
|---|---|---|---|---|
| (a) | $NO^+ + H_2O + M \rightarrow NO^+ \cdot H_2O + M$ ; | $k = 1.6 \times 10^{-28}$ | $1.4 \times 10^{-28}$ | $1.6 \times 10^{-28}$ $cm^6/sec.$ |
| (b) | $NO^+ \cdot H_2O + H_2O + M \rightleftarrows NO^+(H_2O)_2 + M$ ; | $k = 1.0 \times 10^{-27}$ | $1.2 \times 10^{-27}$ | $1.1 \times 10^{-27}$ $cm^6/sec.$ |
| | | $k_r = < 1 \times 10^{-13}$ | $1.7 \times 10^{-14}$ | $1.4 \times 10^{-14}$ $cm^3/sec.$ |
| (c) | $NO^+(H_2O)_2 + H_2O + M \rightleftarrows NO^+(H_2O)_3 + M$ ; | $k = 2.0 \times 10^{-27}$ | $1.4 \times 10^{-27}$ | $1.9 \times 10^{-27}$ $cm^6/sec.$ |
| | | $k_r = 1.3 \times 10^{-12}$ | $1.4 \times 10^{-12}$ | $1.9 \times 10^{-12}$ $cm^3/sec.$ |
| (d) | $NO^+(H_2O)_3 + H_2O \rightarrow H_3O^+(H_2O)_2 + HNO_2$; | $k = 8 \times 10^{-11}$ | $7 \times 10^{-11}$ | $7 \times 10^{-11}$ $cm^3/sec.$ |

The results presented above agree remarkably well in view of the complexity of the coupled reaction sequence.

### 18A.3.13 $NO_2^+ + NO \rightarrow NO^+ + NO_2$

This reaction has been found to be very rapid; $k = 2.9 \times 10^{-10}$ $cm^3/sec$ (Reference 18A-42), which is important insofar as it confirms that $IP(NO_2) > IP(NO)$.

### 18A.3.14 $NO^+ + CO_2 + M \rightarrow NO^+ \cdot CO_2 + M$

The reaction, where $M = N_2$, has been found to have a rate constant of $3 \times 10^{-29}$ $cm^6/sec$ at 197 K in the afterglow (Reference

* Rate constants under "F" (via flowing afterglow, where $M = N_2$) are from Fehsenfeld et al (Reference 18A-40), who also report data for M = He, Ar. Rate constants under "H" (via flowing afterglow, where $M = N_2$) are from Howard et al (Reference 18A-12), who also report data for M = He, Ar, $O_2$. Rate constants under "P" (via stationary afterglow, where M = NO) are from Puckett and Teague (Reference 18A-41). All data pertain to room-temperature measurements.

18A-43). Furthermore, the reaction $NO^+ \cdot CO_2 + H_2O \rightarrow NO^+ \cdot H_2O + CO_2$ is very fast, i.e., $k \sim 10^{-9}$ cm$^3$/sec. These combined results are important in that the $CO_2$ association with $NO^+$, followed by the rapid "switching" of $CO_2$ and $H_2O$, appears to be a more rapid means of hydrating $NO^+$ in the D-region than the direct three-body association of $NO^+$ and $H_2O$.

## 18A.4 SUMMARY OF REACTION RATE CONSTANTS

Following are several tables of reaction-rate constants of atmospheric interest: Table 18A-1, positive-ion charge-transfer reactions; Table 18A-2, negative-ion charge-transfer reactions; Table 18A-3, positive-ion atom-interchange reactions: Table 18A-4, negative-ion atom-interchange reactions; Table 18A-5, three-body positive-ion reactions; Table 18A-6, three-body negative-ion reactions; and Table 18A-7, the Gulf General Atomic charge-transfer reactions of positive ions with metallic neutrals. The latter are kept separate because they form a cohesive set of data and because of the special extrapolation methods used to estimate the thermal-energy rate constants. Throughout all tables except the last (18A-7), the rate constants are reported in the form m(-n), which designates $m \times 10^{-n}$.

Unless otherwise specified, rate constants were obtained at room temperature. For some older measurements, review papers are referenced rather than the original papers.

Table 18A-1. Positive-ion charge-transfer.

| Reaction | k ($cm^3$/sec) | References | Comments |
|---|---|---|---|
| 1.a. $He^+ + N_2 \rightarrow He + N + N^+$ | 1.2(-9) | 18A-30, 44 | See par. 18A.3.1. |
| b. $\rightarrow He + N_2^+$ | | | |
| 2. $He^+ + O_2 \rightarrow He + O + O^+$ | 1.1(-9) | 18A-30, 44 | Also produces $O_2^+$. |
| 3. $He_2^+ + N_2 \rightarrow 2He + N_2^+$ | 1.2(-9) | 18A-45 | 200 K |
| 4. $O^+ + H \rightarrow O + H^+$ | 6.8(-10) | 18A-46, 47 | $\sigma$ = 20-40 $A^2$ |
| 5. $O^+ + O_2 \rightarrow O + O_2^+$ | 2.0(-11) | 18A-3, 4 | See par. 18A.3.2. |
| 6. $O^+ + NO \rightarrow O + NO^+$ | < 1.3(-12) | 18A-48 | |
| 7. $O^+ + NO_2 \rightarrow NO_2^+ + O$ | 1.6(-9) | 18A-48 | 393 K |
| 8. $O^+ + N_2O \rightarrow N_2O^+ + O$ | 6.3(-10) | 18A-48 | 393 K |
| 9. $O^+ + H_2O \rightarrow H_2O^+ + O$ | 2.33(-9) | 18A-11 | |
| 10. $N^+ + O_2 \rightarrow N + O_2^+$ | 3.0(-10) | 18A-4, 24 | Also produces $NO^+$ with approximately same rate const. |

Table 18A-1. (Cont'd.)

| Reaction | k ($cm^3$/sec) | References | Comments |
|---|---|---|---|
| 11. $N^+ + NO \rightarrow N + NO^+$ | 8.0(-10) | 18A-49 | |
| 12. $N^+ + H_2O \rightarrow H_2O^+ + N$ | 2.57(-9) | 18A-11 | |
| 13. $O_2^+ + NO \rightarrow O_2 + NO^+$ | 6.3(-10) | 18A-24,50 | Cf. Ref. 18A-24 for energy dependence. |
| 14. $O_2^+ + Na \rightarrow O_2 + Na^+$ | 6.7(-10) | 18A-10 | See par. 18A.3.7. |
| 15. $O_2^+(a^4\Pi_u) + N_2 \rightarrow N_2^+ + O_2$ | 5(-10) | 18A-51 | |
| 16. $N_2^+ + O \rightarrow N_2 + O^+$ | < 1.0(-11) | 18A-49,52 | Not observed. |
| 17. $N_2^+ + N \rightarrow N_2 + N^+$ | < 1.0(-11) | 18A-52 | Not observed. |
| 18. $N_2^+ + O_2 \rightarrow N_2 + O_2^+$ | 5.0(-11) | 18A-24,30,44 | See par. 18A.3.4. |
| 19. $N_2^+ + NO \rightarrow N_2 + NO^+$ | 3.3(-10) | 18A-50 | |
| 20.a. $N_2^+ + H_2O \rightarrow H_2O^+ + N_2$ | 2.19(-9) | 18A-11 | |
| b. $\rightarrow N_2H^+ + OH$ | | | |

Table 18A-1. (Cont'd.)

| Reaction | k ($cm^3$/sec) | References | Comments |
|---|---|---|---|
| 21. $N_2^+ + Na \rightarrow N_2 + Na^+$ | 5.8(-10) | 18A-10 | $N_2$ may dissaciate. |
| 22. $N_4^+ + O_2 \rightarrow O_2^+ + 2N_2$ | 4(-10) | 18A-43 | |
| 23. $NO^+ + Na \rightarrow NO + Na^+$ | 7.0(-11) | 18A-10 | |
| 24. $NO_2^+ + NO \rightarrow NO_2 + NO^+$ | 2.9(-10) | 18A-42 | See par. 18A.3.12. |
| 25. $H^+ + O \rightarrow O^+ + H$ | 3.8(-10) | 18A-47 | |
| 26. $H^+ + NO \rightarrow NO^+ + H$ | 1.9(-9) | 18A-47 | |
| 27. $OH^+ + O_2 \rightarrow OH + O_2^+$ | ~ 2.0(-10) | 18A-53 | |
| 28. $H_2O^+ + O_2 \rightarrow H_2O + O_2^+$ | ~ 2.0(-10) | 18A-44,53 | |
| 29. $CO^+ + O \rightarrow O^+ + CO$ | 1.4(-10) | 18A-47 | |
| 30. $CO^+ + NO \rightarrow NO^+ + CO$ | 3.3(-10) | 18A-47 | |

Table 18A-1. (Cont'd.)

| Reaction | k ($cm^3$/sec) | References | Comments |
|---|---|---|---|
| 31. $CO_2^+ + H \rightarrow H^+ + CO_2$ | ~1(-10) | 18A-54 | Produces mostly $HCO^+$ (See Table 18A-3). |
| 32. $CO_2^+ + O \rightarrow CO_2 + O^+$ | ~1(-10) | 18A-50 | Also produces $O_2^+$ (See Table 18A-3). |
| 33. $CO_2^+ + O_2 \rightarrow CO_2 + O_2^+$ | 5.0(-11) | 18A-50 | |
| 34. $CO_2^+ + NO \rightarrow CO_2 + NO^+$ | 1.2(-10) | 18A-50 | |

Table 18A-2. Negative-ion charge-transfer.

| Reaction | k ($cm^3$/sec) | References | Comments |
|---|---|---|---|
| 1. $O^- + O_3 \rightarrow O + O_3^-$ | 5.3(-10) | 18A-31 | |
| 2. $O^- + NO_2 \rightarrow O + NO_2^-$ | 1.2(-9) | 18A-31 | |
| 3. $O_2^- + O_3 \rightarrow O_2 + O_3^-$ | 4.0(-10) | 18A-31 | |
| 4. $O_2^- + NO_2 \rightarrow O_2 + NO_2^-$ | 8.0(-10) | 18A-31 | |
| 5. $O_3^- + NO_2 \rightarrow NO_2^- + O_3$ | 1.9(-11) | 18A-39 | Products uncertain, may be $NO_3^- + O_2$. |
| 6. $H^- + NO_2 \rightarrow H + NO_2^-$ | 2.9(-9) | 18A-31 | |
| 7. $Cl^- + NO_2 \rightarrow Cl + NO_2^-$ | <6.0(-12) | 18A-31,55 | Not observed. |
| 8. $Br^- + NO_2 \rightarrow NO_2^- + Br$ | <3.0(-11) | 18A-55 | Not observed. |
| 9. $I^- + NO_2 \rightarrow NO_2^- + I$ | <3.0(-11) | 18A-55 | Not observed. |
| 10. $NO^- + O_2 \rightarrow O_2^- + NO$ | 5.0(-10) | 18A-56 | |

Table 18A-2. (Cont'd.)

| Reaction | $k$ ($cm^3/sec$) | References | Comments |
|---|---|---|---|
| 11. $OH^- + NO_2 \rightarrow OH + NO_2^-$ | 1.0(-9) | 18A-31 | |
| 12. $HS^- + NO_2 \rightarrow NO_2^- + HS$ | 4.8(-10) | 18A-55 | |

Table 18A-3. Positive-ion atom-interchange.

| Reaction | $k$ ($cm^3/sec$) | References | Comments |
|---|---|---|---|
| 1. $O^+ + N_2 \rightarrow N + NO^+$ | 1.2(-12) | 18A-30,44 | See par. 18A.3.3. |
| 2. $O^+ + H_2 \rightarrow H + OH^+$ | 2.0(-9) | 18A-53 | |
| 3. $O^+ + CO_2 \rightarrow CO + O_2^+$ | 1.1(-9) | 18A-24,30,44 | Cf. Ref. 18A-24 for energy dependence. |
| 4. $N^+ + O_2 \rightarrow O + NO^+$ | 3.0(-10) | 18A-4,24 | Also gives $O_2^+$ with approximately same rate constant. |
| 5. $N^+ + H_2 \rightarrow H + NH^+$ | 5.6(-10) | 18A-53 | |
| 6. $O_2^+ + N \rightarrow O + NO^+$ | 1.8(-10) | 18A-30,44 | |

Table 18A-3. (Cont'd.)

| Reaction | k ($cm^3$/sec) | References | Comments |
|---|---|---|---|
| 7. $O_2^+ + N_2 \rightarrow NO + NO^+$ | <1.0(-15) | 18A-30, 44 | Nat observed; rate constant limitation shown here is applicable ot 300 and 600 K. |
| 8. $O_2^+ + H_2 \rightarrow$ Products | <1.0(-11) | 18A-53 | |
| 9. $O_2^+ + Na \rightarrow O + NaO^+$ | 7.7(-11) | 18A-57 | |
| 10. $N_2^+ + O \rightarrow N + NO^+$ | 1.4(-10) | 18A-50 | |
| 11. $N_2^+ + H_2 \rightarrow H + N_2H^+$ | 1.7(-9) | 18A-53 | |
| 12. $N_3^+ + O_2 \rightarrow$ Products | 1.0±0.3(-10) | 18A-43 | 200 K |
| 13. $O_4^+ + O \rightarrow O_2^+ + O_3$ | ~ 3(-10) | 18A-39 | |
| 14. $O_4^+ + H_2O \rightarrow O_2 + O_2^+ \cdot H_2O$ | 2.2(-9) | 18A-9 | See por. 18A.3.11. |
| 15. $N_4^+ + O_2 \rightarrow O_2^+ + N_2 + N_2$ | 4±1(-10) | 18A-43 | 200 K |
| 16. $H^+ + CO_2 \rightarrow HCO^+ + O$ | 3(-9) | 18A-54 | |

Table 18A-3. (Cont'd.)

| Reaction | k ($cm^3$/sec) | References | Comments |
|---|---|---|---|
| 17. $H_2O^+ + H_2O \rightarrow H_3O^+ + OH$ | 1.8(-9) | 18A-20,30 | |
| 18. $CO_2^+ + H \rightarrow HCO^+ + O$ | 6(-10) | 18A-54 | |
| 19. $CO_2^+ + O \rightarrow CO + O_2^+$ | ~ 1.6(-10) | 18A-50 | Also produces $O^+$. (See Table 18A-1.) |
| 20. $O_2^+ \cdot N_2 + O_2 \rightarrow N_2 + O_4^+$ | >5.0(-11) | 18A-38 | 80 K |
| 21.a. $O_2^+ \cdot H_2O + H_2O \rightarrow O_2 + OH + H_3O^+$ | ≤3(-10) | 18A-9 | See par. 18A.3.11. |
| b. $\rightarrow O_2 + H_3O^+ \cdot OH$ | 1.9(-9) | 18A-9 | |
| 22. $NO^+ \cdot NO + H_2O \rightarrow NO^+ \cdot H_2O + NO$ | 1.4(-9) | 18A-41 | |
| 23. $NO^+ \cdot H_2O + NO \rightarrow NO^+ \cdot NO + H_2O$ | 9(-14) | 18A-41 | 296 K |
| 24. $NO^+ \cdot H_2O + H \rightarrow H_3O^+ + NO$ | <1(-11) | 18A-58,59 | Not observed. |
| 25. $NO^+(H_2O)_3 + H_2O \rightarrow H_3O^+(H_2O)_2 + HNO_2$ | 7(-11) | 18A-12,40,41 | See par. 18A.3.12. |
| 26. $NO^+ \cdot CO_2 + H_2O \rightarrow NO^+ \cdot H_2O + CO_2$ | ~ 1(-9) | 18A-43 | See par. 18A.3.14. |

Table 18A-3. (Cont'd.)

| Reaction | $k$ ($cm^3$/sec) | References | Comments |
|---|---|---|---|
| 27. $H_3O^+ \cdot OH + H_2O \rightarrow H_3O^+ \cdot H_2O + OH$ | 3.2(-9) | 18A-9 | |
| 28. $Na^+ + O_3 \rightarrow O_2 + NaO^+$ | < 1.0(-11) | 18A-6 | Not observed. |
| 29. $K^+ + O_3 \rightarrow O_2 + KO^+$ | < 1.0(-11) | 18A-6 | Not observed. |
| 30. $Mg^+ + O_3 \rightarrow O_2 + MgO^+$ | 2.3(-10) | 18A-6 | |
| 31. $Co^+ + O_3 \rightarrow O_2 + CoO^+$ | 1.6(-10) | 18A-6 | |
| 32. $Fe^+ + O_3 \rightarrow O_2 + FeO^+$ | 1.5(-10) | 18A-6 | |
| 33. $MgO^+ + O \rightarrow O_2 + Mg^+$ | ~ 1.0(-11) | 18A-6 | |
| 34. $SiO^+ + O \rightarrow O_2 + Si^+$ | ~ 2.0(-10) | 18A-34 | See par. 18A.3.5. |

Table 18A-4. Negative-ion atom-interchange.

| Reaction | $k$ ($cm^3$/sec) | References | Comments |
|---|---|---|---|
| 1. $O^- + N_2O \rightarrow NO + NO^-$ | 2.0(-11) | 18A-60 | |
| 2. $O_3^- + N_2 \rightarrow O_2 + N_2O^-$ | < 1.0(-15) | 18A-31 | Not observed. |

Table 18A-4. (Cont'd.)

| Reaction | k ($cm^3$/sec) | References | Comments |
|---|---|---|---|
| 3. $O_3^- + NO \rightarrow O_2 + NO_2^-$ | 1.0(-11) | 18A-31 | Product identificotion ($NO_3^-$ + O) given in Ref. 18A-31 is probobly incorrecr |
| 4. $O_3^- + CO_2 \rightarrow O_2 + CO_3^-$ | 4.0(-10) | 18A-31 | |
| 5. $O_4^- + O \rightarrow O_2 + O_3^-$ | 4.0(-10) | 18A-36 | $2O_2 + O^-$ moy be o minor product chonnel. |
| 6. $O_4^- + NO \rightarrow O_2 + NO_3^-$ | 2.5(-10) | 18A-36 | |
| 7. $O_4^- + H_2O \rightarrow O_2^- \cdot H_2O - O_2$ | 1.4(-9) | 18A-61 | |
| 8. $O_4^- + CO_2 \rightarrow O_2 + CO_4^-$ | 4.3(-10) | 18A-36 | |
| 9. $NO_2^- + O \rightarrow$ Products | $<1.0(-11)$ | 18A-39 | Not observed. |
| 10. $NO_2^- + N \rightarrow$ Products | $<1.0(-11)$ | 18A-39 | Not observed. |
| 11.o. $NO_2^- + H \rightarrow OH^- + NO$<br>b. $\rightarrow HNO_2 + e$ | 3(-10) | 18A-62 | $k_{11o} \geq 0.5\, k_{11}$;<br>$0 \leq k_{11b} \leq k_{11}$ |

Table 18A-4. (Cont'd.)

| Reaction | k ($cm^3$/sec) | References | Comments |
|---|---|---|---|
| 12. $NO_2^- + O_3 \rightarrow O_2 + NO_3^-$ | 1.8(-11) | 18A-31 | |
| 13. $NO_2^- + NO_2 \rightarrow NO + NO_3^-$ | ~ 4.0(-12) | 18A-36 | See par. 18A.3.10. |
| 14. $NO_3^- + O \rightarrow$ Products | < 1.0(-11) | 18A-36 | Not observed. |
| 15. $NO_3^- + N \rightarrow$ Products | < 1.0(-11) | 18A-36 | Not observed. |
| 16. $NO_3^- + NO \rightarrow NO_2 + NO_2^-$ | < 1.0(-12) | 18A-36 | See par. 18A.3.10. |
| 17. $OONO^- + NO \rightarrow NO_2 + NO_2^-$ | ~ 1.5(-11) | 18A-38 | |
| 18. $CO_3^- + O \rightarrow CO_2 + O_2^-$ | 8.0(-11) | 18A-31 | |
| 19. $CO_3^- + NO \rightarrow CO_2 + NO_2^-$ | 9.0(-12) | 18A-31 | |
| 20. $CO_3^- + NO_2 \rightarrow CO_2 + NO_3^-$ | 8.0(-11) | 18A-31 | |
| 21. $CO_4^- + O \rightarrow O_2 + CO_3^-$ | 1.5(-10) | 18A-36 | $CO_2 + O_3^-$ may be a minar praduct chonnel. |

Table 18A-4. (Cont'd.)

| Reaction | k ($cm^3$/sec) | References | Comments |
|---|---|---|---|
| 22. $CO_4^- + NO \rightarrow CO_2 + NO_3^-$ | 4.8(-11) | 18A-36 | |
| 23. $O_2^- \cdot H_2O + NO \rightarrow H_2O + NO_3^-$ | 3.1(-10) | 18A-38 | |
| 24. $O_2^- \cdot H_2O + CO_2 \rightarrow H_2O + CO_4^-$ | 5.8(-10) | 18A-38 | |

Table 18A-5. Three-body positive-ion reactions.

| Reaction | k ($cm^6$/sec) | References | Comments |
|---|---|---|---|
| 1. $O^+ + N_2 + He \rightarrow NO^+ + N + He$ | 5.1(-29) | 18A-8 | 82 K; $N_2O^+$ appears to form at first and then predissociate. |
| 2. $O_2^+ + 2O_2 \rightarrow O_4^+ + O_2$ | 2.8(-30) | 18A-19 | 307 K; see par. 18A.3.8. |
| 3. $O_2^+ + N_2 + He \rightarrow O_2^+ \cdot N_2 + He$ | 1.9(-29) | 18A-38 | 200 K |
| 4. $O_2^+ + N_2O + He \rightarrow O_2^+ \cdot N_2O + He$ | 5.2(-29) | 18A-38 | 200 K |
| 5. $O_2^+ + H_2O + O_2 \rightarrow O_2^+ \cdot H_2O + O_2$ | 1.9(-28) | 18A-12 | 296 K; see par. 18A.3.11. |

Table 18A-5. (Cont'd.)

| Reaction | k ($cm^6$/sec) | References | Comments |
|---|---|---|---|
| 6. $O_2^+ + CO_2 + He \rightarrow O_2^+ \cdot CO_2 + He$ | 2.3(-29) | 18A-38 | 200 K |
| 7.a. $N_2^+ + N_2 + He \rightarrow N_4^+ + He$ | 1.2(-28) | 18A-8 | 82 K |
| | 1.9(-29) | 18A-8 | 280 K |
| b. $N_2^+ + 2N_2 \rightarrow N_4^+ + N_2$ | 5.0(-29) | 18A-28 | 300 K |
| 8. $NO^+ + O_2 + He \rightarrow NO^+ \cdot O_2 + He$ | <6(-34) | 18A-43 | 200 K |
| 9.a. $NO^+ + N_2 + He \rightarrow NO^+ \cdot N_2 + He$ | <5(-33) | 18A-43 | 200 K |
| b. $NO^+ + N_2 + N_2 \rightarrow NO^+ \cdot N_2 + N_2$ | 2(-31) | 18A-63 | 300 K |
| 10. $NO^+ + 2NO \rightleftarrows NO^+ \cdot NO + NO$ | 5.0(-30) | 18A-1 | 300 K; reverse rate constant = 9(-16) $cm^3$/sec. |
| 11. $NO^+ + H_2O + N_2 \rightarrow NO^+ \cdot H_2O + N_2$ | 1.5(-28) | 18A-12,40 | 300 K; see par. 18A.3.12. |
| 12.a. $NO^+ + CO_2 + He \rightarrow NO^+ \cdot CO_2 + He$ | 1.0(-29) | 18A-43 | 200 K |
| b. $NO^+ + CO_2 + N_2 \rightarrow NO^+ \cdot CO_2 + N_2$ | 3(-29) | 18A-43 | 200 K |
| c. $NO^+ + CO_2 + CO_2 \rightarrow NO^+ \cdot CO_2 + CO_2$ | 2(-29) | 18A-64 | 300 K |
| 13.a. $H_3O^+ + H_2O + O_2 \rightarrow H_3O^+(H_2O) + O_2$ | 3.7(-27) | 18A-20 | 307 K; Reverse rate constant = 7(-26) $cm^3$/sec. |
| b. $H_3O^+ + H_2O + N_2 \rightarrow H_3O^+(H_2O) + N_2$ | 3.4(-27) | 18A-20 | 300 K; Reverse rate constant = 7(-26) $cm^3$/sec. |

Table 18A-5. (Cont'd.)

| Reaction | k ($cm^6$/sec) | References | Comments |
|---|---|---|---|
| 14.a. $H_3O^+(H_2O) + H_2O + O_2 \rightleftarrows H_3O^+(H_2O)_2 + O_2$ | 2.0(-27) | 18A-20 | 307 K; Reverse rate constant = 7(-18) $cm^3$/sec. |
| b. $H_3O^+(H_2O) + H_2O + N_2 \rightleftarrows H_3O^+(H_2O)_2 + N_2$ | 2.3(-27) | 18A-20 | 300 K; Reverse rate constant = 7(-18) $cm^3$/sec. |
| 15.a. $H_3O^+(H_2O)_2 + H_2O + O_2 \rightleftarrows H_3O^+(H_2O)_3 + O_2$ | 2.0(-27) | 18A-20 | 307 K; Reverse rate constant = 4.0(-14) $cm^3$/sec. |
| b. $H_3O^+(H_2O)_2 + H_2O + N_2 \rightleftarrows H_3O^+(H_2O)_3 + N_2$ | 2.4(-27) | 18A-20 | 300 K; Reverse rate constant = 4.0(-14) $cm^3$/sec. |
| 16. $H_3O^+(H_2O)_3 + H_2O + O_2 \rightleftarrows H_3O^+(H_2O)_4 + O_2$ | 9.0(-28) | 18A-20 | 307 K; reverse rate constant = 6.0(-12) $cm^3$/sec. |
| 17. $NO^+ \cdot H_2O + H_2O + N_2 \rightarrow NO^+(H_2O)_2 + N_2$ | 1.1(-27) | 18A-12,40 | 300 K; see par. 18A.3.12. |
| 18. $NO^+(H_2O)_2 + H_2O + N_2 \rightarrow NO^+(H_2O)_3 + N_2$ | 1.6(-27) | 18A-12,40 | 300 K; see par. 18A.3.12. |
| 19. $Mg^+ + O_2 + Ar \rightarrow MgO_2^+ + Ar$ | ~ 2.5(-30) | 18A-6 | 300 K |
| 20. $Ca^+ + O_2 + Ar \rightarrow CaO_2^+ + Ar$ | ~ 6.6(-30) | 18A-6 | 300 K |
| 21. $Fe^+ + O_2 + Ar \rightarrow FeO_2^+ + Ar$ | ~ 1.0(-30) | 18A-6 | 300 K |
| 22. $K^+ + CO_2 + CO_2 \rightleftarrows K^+ \cdot CO_2 + CO_2$ | $4^{+4}_{-2}$(-30) | 18A-65 | Reverse rate constant = $2.5^{+2.5}_{-1.3}$(-13) $cm^3$/sec. |

Table 18A-5. (Cont'd.)

| Reaction | k ($cm^6$/sec) | References | Comments |
|---|---|---|---|
| 23. $Na^+ + CO_2 + CO_2 \rightleftarrows Na^+ \cdot CO_2 + CO_2$ | 2(-29±0.5) | 18A-66 | Reverse rate constant = 1(-14±0.5) $cm^3$/sec. |
| 24. $Na^+ \cdot CO_2 + CO_2 + CO_2 \rightleftarrows Na^+ (CO_2)_2 + CO_2$ | 2(-29±0.5) | 18A-66 | Reverse rate constant = 5(-13±0.5) $cm^3$/sec. |

Table 18A-6. Three-body negative-ian reactions.

| Reaction | k ($cm^6$/cm) | References | Comments |
|---|---|---|---|
| 1. $O^- + 2O_2 \rightarrow O_3^- + O_2$ | 1.2(-30)<br>1.05(-30) | 18A-61<br>18A-67 | 300 K<br>298 K |
| 2. $O^- + N_2 + He \rightarrow N_2O^- + He$ | 1.3(-30)<br>~ 4.0(-31) | 18A-31<br>18A-38 | 80 K<br>200 K |
| 3. $O^- + H_2O + O_2 \rightarrow O^- \cdot H_2O + O$ | 1.0(-28) | 18A-61 | 300 K |
| 4. $O^- + CO_2 + CO_2 \rightarrow CO_3^- + CO_2$ | 8.0(-29) | 18A-68 | 300 K |
| 5. $O_2^- + O_2 + O_2 \rightleftarrows O_4^- + O_2$ | 3.0(-31)<br>4.0(-31)<br>3.0(-31) | 18A-37<br>18A-61<br>18A-67 | 310 K; see par. 18A.3.9.<br>300 K; reverse rate constant = 2.7(-14) $cm^3$/sec.<br>298 K |

Table 18A-6. (Cont'd.)

| Reaction | k ($cm^6/cm$) | References | Comments |
|---|---|---|---|
| 6. $O_2^- + N_2 + He \rightarrow O_2^- \cdot N_2 + He$ | ~ 4.0(-32) | 18A-38 | 200 K |
| 7. $O_2^- + H_2O + O_2 \rightarrow O_2^- \cdot H_2O + O_2$ | 3(-28) | 18A-61 | 300 K |
| 8.a. $O_2^- + CO_2 + O_2 \rightarrow CO_4^- + O_2$ | 2.0(-29) | 18A-68 | 300 K |
| b. $O_2^- + CO_2 + CO_2 \rightarrow CO_4^- + CO_2$ | 9.0(-30) | 18A-68 | 300 K |
| 9. $O_3^- + H_2O + O_2 \rightarrow O_3^- \cdot H_2O + O_2$ | 2.1(-28) | 18A-61 | 300 K |
| 10. $NO_2^- + H_2O + NO \rightarrow NO_2^- \cdot H_2O + NO$ | 1.3(-28) | 18A-1 | 300 K |
| 11. $O_2^- \cdot H_2O + H_2O + O_2 \rightarrow O_2^-(H_2O)_2 + O_2$ | 4(-28) | 18A-61 | 300 K |

Table 18A-7. Charge transfer to neutral metals.[a]

| Reaction | Measured cross-section for ions of 1 eV (at the center of mass) ($cm^2$) | Extrapolated value of thermal-energy rate constant ($cm^3/sec$)[b] |
|---|---|---|
| $N^+ + Na \rightarrow N + Na^+$ | small | |
| $O^+ + Na \rightarrow O + Na^+$ | small | |
| $N_2^+ + Na \rightarrow N_2 + Na^+$ | $3.0 \times 10^{-15}$ | $1.9 \times 10^{-9}$ |
| $O_2^+ + Na \rightarrow O_2 + Na^+$ | $5.5 \times 10^{-15}$ | $1.4 \times 10^{-9}$ |
| $NO^+ + Na \rightarrow NO + Na^+$ | $1.2 \times 10^{-15}$ | |
| $H_2O^+ + Na \rightarrow H_2O + Na^+$ | $2.8 \times 10^{-14}$ | $2.7 \times 10^{-9}$ |
| $H_3O^+ + Na \rightarrow H_3O + Na^+$ | $2.4 \times 10^{-14}$ | |
| $N_2O^+ + Na \rightarrow N_2O + Na^+$ | $2.7 \times 10^{-14}$ | $2.0 \times 10^{-9}$ |
| $Na^+ + Na \rightarrow Na + Na^+$ | $2.3 \times 10^{-14}$ | $2.8 \times 10^{-9}$ |
| $N^+ + Mg \rightarrow N + Mg^+$ | $1.1 \times 10^{-14}$ | $1.2 \times 10^{-9}$ |
| $O^+ + Mg \rightarrow O + Mg^+$ | small | |
| $N_2^+ + Mg \rightarrow N_2 + Mg^+$ | $1.8 \times 10^{-14}$ | |
| $O_2^+ + Mg \rightarrow O_2 + Mg^+$ | $7.6 \times 10^{-15}$ | $1.2 \times 10^{-9}$ |
| $NO^+ + Mg \rightarrow NO + Mg^+$ | $1.4 \times 10^{-14}$ | $1.0 \times 10^{-9}$ |
| $H_2O^+ + Mg \rightarrow H_2O + Mg^+$ | $1.8 \times 10^{-14}$ | $2.2 \times 10^{-9}$ |
| $H_3O^+ + Mg \rightarrow H_3O + Mg^+$ | $8.8 \times 10^{-15}$ | |
| $N_2O^+ + Mg \rightarrow N_2O + Mg^+$ | $2.6 \times 10^{-14}$ | $2.1 \times 10^{-9}$ |
| $Mg^+ + Mg \rightarrow Mg + Mg^+$ | $3.0 \times 10^{-14}$ | $4.7 \times 10^{-9}$ |
| $N^+ + Ca \rightarrow N + Ca^+$ | $5.3 \times 10^{-15}$ | $1.1 \times 10^{-9}$ |

Table 18A-7. (Cont'd.)

| Reaction | Measured cross-section for ions of 1 eV (at the center of mass) ($cm^2$) | Extrapolated value of thermal-energy rate constant ($cm^3/sec$) [b] |
|---|---|---|
| $O^+ + Ca \rightarrow O + Ca^+$ | $1.1 \times 10^{-14}$ | $7.5 \times 10^{-10}$ |
| $N_2^+ + Ca \rightarrow N_2 + Ca^+$ | $3.0 \times 10^{-14}$ | $1.7 \times 10^{-9}$ |
| $O_2^+ + Ca \rightarrow O_2 + Ca^+$ | $1.5 \times 10^{-14}$ | $4.1 \times 10^{-9}$ |
| $NO^+ + Ca \rightarrow NO + Ca^+$ | $2.2 \times 10^{-14}$ | $4.0 \times 10^{-9}$ |
| $H_2O^+ + Ca \rightarrow H_2O + Ca^+$ | $5.5 \times 10^{-14}$ | $4.0 \times 10^{-9}$ |
| $H_3O^+ + Ca \rightarrow H_3O + Ca^+$ | $3.4 \times 10^{-14}$ | $4.4 \times 10^{-9}$ |
| $N_2O^+ + Ca \rightarrow N_2O + Ca^+$ | $4.5 \times 10^{-14}$ | $3.7 \times 10^{-9}$ |
| $Ca^+ + Ca \rightarrow Ca + Ca^+$ | $6.0 \times 10^{-14}$ | |
| | Measured cross-section for ions of 3 eV (at the center of mass) ($cm^2$) | |
| $H^+ + Fe \rightarrow H + Fe^+$ | $9.5 \times 10^{-16}$ | |
| $N^+ + Fe \rightarrow N + Fe^+$ | $1.6 \times 10^{-16}$ | $1.5 \times 10^{-9}$ |
| $O^+ + Fe \rightarrow O + Fe^+$ | $1.3 \times 10^{-15}$ | $2.9 \times 10^{-9}$ |
| $N_2^+ + Fe \rightarrow N_2 + Fe^+$ | $2.9 \times 10^{-15}$ | $4.3 \times 10^{-10}$ |
| $NO^+ + Fe \rightarrow NO + Fe^+$ | $2.4 \times 10^{-15}$ | $9.1 \times 10^{-10}$ |
| $O_2^+ + Fe \rightarrow O_2 + Fe^+$ | $2.0 \times 10^{-15}$ | $1.2 \times 10^{-9}$ |
| $H_2O^+ + Fe \rightarrow H_2O + Fe^+$ | $3.3 \times 10^{-15}$ | $1.5 \times 10^{-9}$ |

Notes:

[a] Table kindly supplied by J.A. Rutherford (Reference 18A-69).

b Extrapolation scheme described in Reference 18A-70.

## REFERENCES


18A-1. Lineberger, W. C., and L. J. Puckett, Phys. Rev. 186, 116 (1969); Ibid. 187, 286 (1969); Ibid. A1, 1635 (1970).

18A-2. Copsey, M. J., D. Smith, and J. Sayers, Planet. Space Sci. 14, 1047 (1966).

18A-3. Smith, D., and R. A. Fouracre, Planet. Space Sci. 16, 243 (1968).

18A-4. Dunkin, D. B., F. C. Fehsenfeld, A. L. Schmeltekopf, and E. E. Ferguson, J. Chem. Phys. 49, 1365 (1968).

18A-5. Ferguson, E. E., D. K. Bohme, F. C. Fehsenfeld, and D. B. Dunkin, J. Chem. Phys. 50, 5039 (1969).

18A-6. Ferguson, E. E., and F. C. Fehsenfeld, J. Geophys. Res. 73, 6215 (1968).

18A-7. Bohme, D. K., D. B. Dunkin, F. C. Fehsenfeld, and E. E. Ferguson, J. Chem. Phys. 49, 5201 (1968).

18A-8. Bohme, D. K., D. B. Dunkin, F. C. Fehsenfeld, and E. E. Ferguson, J. Chem. Phys. 51, 863 (1969).

18A-9. Fehsenfeld, F. C., M. Mosesman, and E. E. Ferguson, J. Chem. Phys. 55, 2115 (1971).

18A-10. Farragher, A. L., J. A. Peden, and W. L. Fite, J. Chem. Phys. 50, 287 (1969).

18A-11. Howard, C. J., H. W. Rundle, and F. Kaufman, J. Chem. Phys. 53, 3745 (1970).

18A-12. Howard, C. J., H. W. Rundle, and F. Kaufman, Bull. Am. Phys. Soc. 16, 213 (1971).

18A-13. Fehsenfeld, F. C., D. L. Albritton, J. A. Burt, and H. I. Schiff, Can. J. Chem. 47, 1793 (1969).

18A-14. Albritton, D. L., A. L. Schmeltekopf, and E. E. Ferguson, Bull. Am. Phys. Soc. 13, 212 (1968).

18A-15. Warneck, P., J. Chem. Phys. 47, 4279 (1967).

18A-16. Warneck, P., Planet. Space Sci. 15, 1349 (1967).

18A-17. Paulson, J. F., R. L. Mosher, and F. Dale, J. Chem. Phys. 44, 3025 (1966).

18A-18. Paulson, J. F., Adv. Chem. 58, 28 (1966).

18A-19. Durden, D. A., P. Kebarle, and A. Good, J. Chem. Phys. 50, 805 (1969).

18A-20. Good, A., D. A. Durden, and P. Kebarle, J. Chem. Phys. 52, 212, 222 (1970).

18A-21. Turner, B. R., and J. A. Rutherford, J. Geophys. Res. 73, 6751 (1968).

18A-22. Turner, B. R., J. A. Rutherford, and D. M. J. Compton, J. Chem. Phys. 48, 1602 (1968).

18A-23. Heimerl, J., R. Johnsen, and M. A. Biondi, J. Chem. Phys. 51, 5041 (1969).

18A-24. Johnsen, R., H. L. Brown, and M. A. Biondi, J. Chem. Phys. 52, 5080 (1970).

18A-25. Golden, D. E., G. Sinnott, and R. N. Varney, Phys. Rev. Letts. 20, 239 (1968).

18A-26. Bohme, D. K., P. P. Ong, J. B. Hasted, and L. R. Megill, Planet. Space Sci. 15, 1777 (1967).

18A-27. Ong, P. P., and J. B. Hasted, J. Phys. B2, 91 (1969).

18A-28. Miller, T. M., J. T. Moseley, D. W. Martin, and E. W. McDaniel, Phys. Rev. Letts. 21, A3 (1968).

18A-29. Kaneko, Y., N. Kobayashi, and I. Kanomata, Mass Spectrosc. 18, 920 (1970).

18A-30. Fite, W. L., Can. J. Chem. 47, 1797 (1969).

18A-31. Ferguson, E. E., Can. J. Chem. 47, 1815 (1969).

18A-32. Schmeltekopf, A. L., E. E. Ferguson, and F. C. Fehsenfeld, J. Chem. Phys. 48, 2966 (1968).

18A-33. O'Malley, T. F., J. Chem. Phys. 52, 3269 (1970).

18A-34. Fehsenfeld, F. C., Can. J. Chem. 47, 1808 (1969).

18A-35. Fehsenfeld, F. C., and E. E. Ferguson, J. Geophys. Res. 74, 2217 (1969).

18A-36. Fehsenfeld, F. C., E. E. Ferguson, and D. K. Bohme, Planet. Space Sci. 17, 1759 (1969).

18A-37. McKnight, L. G., and J. M. Sawina, DASA Symposium on Physics and Chemistry of the Upper Atmosphere, Stanford Research Institute (1969).

18A-38. Adams, N. G., D. K. Bohme, D. B. Dunkin, F. C. Fehsenfeld, and E. E. Ferguson, J. Chem. Phys. 52, 5133 (1970).

18A-39. Fehsenfeld, F. C., private communication.

18A-40. Fensenfeld, F. C., M. Mosesman, and E. E. Ferguson, J. Chem. Phys. 55, 2120 (1971).

18A-41. Puckett, L. J., and M. W. Teague, J. Chem. Phys. 54, 2564 (1971).

18A-42. Fehsenfeld, F. C., E. E. Ferguson, and M. Mosesman, Chem. Phys. Letts. 4, 73 (1969).

18A-43. Dunkin, D. B., F. C. Fehsenfeld, A. L. Schmeltekopf, and E. E. Ferguson, J. Chem. Phys. 54, 3817 (1971).

18A-44. Ferguson, E. E., Revs. Geophys. 5, 305 (1967).

18A-45. Bohme, D. K., N. G. Adams, M. Mosesman, D. B. Dunkin, and E. E. Ferguson, J. Chem. Phys. 52, 5094 (1970).

18A-46. Stebbings, R. F., and J. A. Rutherford, J. Geophys. Res. 73, 1035 (1968).

18A-47. Fehscnfeld, F. C., and E. E. Ferguson, J. Chem. Phys. (in press).

18A-48. Dunkin, D. B., M. McFarland, F. C. Fehsenfeld, and E. E. Ferguson, J. Geophys. Res. 76, 3820 (1971).

18A-49. Ferguson, E. E., F. C. Fehsenfeld, P. D. Goldan, and A. L. Schmeltekopf, J. Geophys. Res. 70, 4323 (1965).

18A-50. Fehsenfeld, F. C., D. B. Dunkin, and E. E. Ferguson, Planet. Space Sci. 18, 1267 (1970).

18A-51. Ryan, K. R., J. Chem. Phys. 51, 4136 (1969).

18A-52. Ferguson, E. E., F. C. Fehsenfeld, P. D. Goldan, A. L. Schmeltekopf, and H. I. Schiff, Planet. Space Sci. 13, 823 (1965).

18A-53. Fehsenfeld, F. C., A. L. Schmeltekopf, and E. E. Ferguson, J. Chem. Phys. 46, 2802 (1967).

18A-54. Fehsenfeld, F. C., and E. E. Ferguson, J. Geophys. Res. (in press).

18A-55. Paulson, J., F. Dale, and J. Welsh, DASA Symposium on Physics and Chemistry of the Upper Atmosphere, Waltham, Mass. (1968).

18A-56. McFarland, M., D. B. Dunkin, F. C. Fehsenfeld, A. L. Schmeltekopf, and E. E. Ferguson, J. Chem. Phys. (in press).

18A-57. Rol, P. K., and E. A. Entemann, J. Chem. Phys. 49, 1430 (1968).

18A-58. Fehsenfeld, F. C., and E. E. Ferguson, COSPAR Symposium, Urbana, Illinois (1971).

18A-59. Fehsenfeld, F. C., and E. E. Ferguson, Radio Sci. (in press).

18A-60. Paulson, J. F., J. Chem. Phys. 52, 959 (1970).

18A-61. Pack, J. L., and A. V. Phelps, Bull. Am. Phys. Soc. 16, 214 (1971).

18A-62. Fehsenfeld, F. C., and E. E. Ferguson, Planet. Space Sci. (in press).

18A-63. Heimerl, J. M., and J. A. Vanderhoff, American Geophysical Union Meeting, San Francisco, California (1971).

18A-64. Heimerl, J., and L. J. Puckett, Trans. Am. Geophys. Union 52, 303 (1971).

18A-65. Keller, G. E., and R. A. Beyer, Bull. Am. Phys. Soc. 16, 214 (1971).

18A-66. Keller, G. E., and R. A. Beyer, J. Geophys. Res. 76, 289 (1971).

18A-67. Parkes, D. A., Trans. Faraday Soc. 67, 711 (1971).

18A-68. Moruzzi, J. L., and A. V. Phelps, J. Chem. Phys. 45, 4617 (1966).

18A-69. Turner, B. R., and J. A. Rutherford, Gulf General Atomic, Report GA-9827 (1970).

18A-70. Wolf, F. A., and B. R. Turner, J. Chem. Phys. 48, 4226 (1968).

# 18. ION-NEUTRAL REACTIONS
# B. NON-THERMAL PROCESSES

A chapter on this subject will be prepared and distributed to authorized recipients of the Handbook at an early date.

The Editors

# 19. NEUTRAL REACTIONS

Frederick Kaufman, University of Pittsburgh
(Latest Revision 29 June 1971)

## 19.1 INTRODUCTION

Much chemical information on the reactions of neutral species is required for an understanding of the normal and perturbed upper atmosphere. In general, such information, in the form of reaction rate constants as functions of temperature, represents a very small fraction of the vast field of chemical reaction kinetics, and might be expected to be found scattered throughout the literature on chemical rate processes. This does not turn out to be the case, because some of the reactants in most of the interesting steps are atomic species which are not normally present in chemical reactions except under extreme thermal or photochemical conditions. Thus, the quantitative studies of the reaction rates, to be described in the following sections and to be summarized in Chapter 24, are mostly less than ten years old, use special experimental techniques to prepare the reactants at controlled temperature and in specific quantum states, and owe their existence to the recent impetus of acronomy and to the renaissance in the field of atom reaction theory. The study of neutral reactions is both harder and easier than that of charged species which makes up most of this Handbook: harder because the rate constants span a much wider range in magnitude due to the frequent existence of energy barriers (energies of activation) whose a priori prediction is difficult; easier because most systems are thermally homogeneous, i.e., do not require the difficult experimental and theoretical extrapolation to thermal conditions inherent in beam or swarm experiments involving charged particles and applied electric fields.

In the following sections of this chapter some of the principal experimental methods will be described briefly and their strengths and weaknesses pointed out; five important reactions will then be discussed in some detail, followed by briefer expositions of some coupled reaction systems. In conclusion, some important gaps in our knowledge will be mentioned and suggestions made for future work.

## 19.2 EXPERIMENTAL METHODS

The data for the neutral reactions listed in Chapter 24 come from an astonishing variety of experimental techniques. These include classical gas reaction kinetics (thermal decomposition of ozone); shock tube studies (O and N—recombination); photochemical decomposition; and low-pressure flow reactor methods with or without discharges to produce atomic species. This last method has been the most widely used and will be described in greater detail than the others.

Classical kinetic studies are particularly welcome in the few instances where they can be applied. Rate constants can be measured far more accurately in static, homogeneous systems than in shock tubes or discharge-flow systems because of better temperature control, absence of diffusion or convection effects, and more accurate analyses for changes in pressure or chemical composition. Their principal shortcoming for the purpose of the present survey is that they often deal with overall changes more complex than a single reaction, i.e., that the multi-step mechanism must be known, so that the increased experimental accuracy is lost in the apportioning of errors to the various elementary steps.

The shock-tube method has been by far the most productive technique for the study of dissociation and recombination reactions at high temperatures. Its accuracy is fairly low, both for aerodynamic reasons (boundary layer effects, shock instabilities) and for their instrumental and chemical counterparts (low signal-to-noise ratio, large uncertainty in kinetic temperature, vibrational relaxation effects).

Photochemical studies under static conditions share the advantage of easy temperature and composition control as well as good chemical analysis with other static methods, but they suffer from several shortcomings such as the experimental difficulty of accurate actinometry, spatial inhomogeneity due to strong absorption, uncertainty in the nature of the electronically excited states, and hot-atom or radical effects in photolytic bond dissociation. There is an increasing and very welcome emphasis on the measurement of fundamental quantities such as radiative lifetimes, specific quenching cross-sections, fluorescence spectra, etc., rather than the less

specific measurements of quantum yield as a function of time, pressure, and composition. Flash-photolysis methods have been applied most successfully to iodine-atom recombination studies.

Steady-state flow methods in which the desired reactant species are produced thermally or in a gas discharge, mixed with other reactants, and the progress of reaction measured as a function of a space coordinate have found increasing use during the past ten years. Their principal advantages include: the wide range of energetic reactant species such as H, O, N, and OH which can be produced and measured quantitatively; the simple expedient of transforming a rapid time variation into a space variation in a cylindrical flow tube; and the great wealth of detection methods such as chemiluminescent light emission, mass spectrometry, optical absorption spectrometry, electron spin resonance spectrometry, or hot-wire calorimetry. These techniques also have an appealing experimental simplicity. They have produced measurements of rate constants ranging from near-gas-kinetic collision frequency (and larger as in their direct application to ion-molecule reactions) to much lower values for reactions which have appreciable energy barriers.

The disadvantages or limitations of these methods fall into four categories:

1. Characterization of the flow. Proper account must be taken of the viscous pressure drop along the tube; of radial diffusion which should be fast enough to justify one-dimensional analysis; of axial diffusion which should be slow enough to make it a small correction to the measured spatial decay; and of the onset of turbulence at large flow velocities and high pressures. Some of these and other effects are discussed in various references (References 19-1 through 19-3). In the case of very fast reactions, rapid mixing of reactants becomes a major problem.

2. Detector interference. Although closely related to (1), this requires special consideration, particularly in the case of catalytic probe detectors where the convective flow may be disturbed well upstream of the probe if diffusion is fast, or in the case of scavenger (titration) methods where another reactant is introduced which greatly reduces the atom concentration by rapid reaction.

3. Surface recombination. This is often a principal limitation. Gas reactions of reactive species can only be studied if the rate at which these species are removed at the wall is a small fraction of their total rate of disappearance. Thus, the surface recombination coefficient (the ratio of atom-removing to total number of wall collisions) must be smaller than $10^{-3}$ (or preferably smaller than $10^{-4}$) and walls must, therefore, be kept sufficiently clean or suitably poisoned. At the large throughputs of gases in fast-flow experiments it is often not possible to keep surfaces clean. In most studies, surface coatings of strong acids ($H_3PO_4$, $H_2SO_4$), teflon, or organic silicon compounds have been used on glass or silica flow tubes.

4. Metastable states. Insofar as flow discharges are used to produce the desired atomic or other reactant species, the presence and reactions of undesirable metastables may interfere grossly with the processes under study. This interference is particularly severe in the case of $N_2$ or $O_2$ discharges, and has led to serious errors in measurements of rate constants. There are, of course, no general remedies against it except the use of more nearly thermal sources (ozone decomposition for O-atoms, thermal dissociation of $H_2$ or $O_2$), or the removal of metastables in discharge-flow systems. When the latter cannot be achieved, the harmlessness of these metastables to the particular process under investigation must be clearly established.

## 19.3 DETAILED DISCUSSION OF SOME IMPORTANT REACTIONS*

### 19.3.1 $O + O_3 \rightarrow 2O_2$ ($\Delta E^o = -93.7$ kcal $= -4.06$ eV)

Although this reaction has been studied by all of the methods described in the preceding section, a substantial uncertainty in its

*Reaction energies are here given in both kcal and eV units. It is understood that the proper units are kcal/g mole and eV/molecule and that 1 eV/molecule equals 23.06 kcal/g mole. The symbol $\Delta E^o$ stands for the change in energy at T = 0 K and therefore also for the

energy of activation has been resolved only recently. The thermal work summarized by Benson and Axworthy (Reference 19-4) and the shock tube study of Jones and Davidson (Reference 19-5) suffer from the unavoidable limitation that in the mechanism:

$$O_3 + M \underset{2}{\overset{1}{\rightleftharpoons}} O_2 + O + M; \quad O + O_3 \xrightarrow{3} 2\,O_2,$$

experiments in dilute ozone under steady-state conditions only determine $(k_1/k_2) \times k_3$. The large temperature coefficient of this expression is mostly due to the equilibrium constant of the first step ($\Delta E^o$ = 24.2 kcal = 1.05 eV) and, therefore, needs to be measured with unattainable accuracy in order to determine the desired activation energy $E_3$ (known to be in the range of 3 to 6 kcal) to within ±0.2 kcal. In shock tube experiments where steady state is not reached because reaction 1 is very fast and reaction 2 is negligible, the situation is equally bad because the large activation energy of reaction 1 overshadows that of reaction 3. The reported values of $k_3$ are $5.6 \times 10^{-11} \exp(-5.7/RT)$, c = 2900 (Reference 19-4, from data in the range 340 to 390 K) and $(4.0 \pm 0.8) \times 10^{-11} \exp[-(5.6 \pm 0.5)/RT]$, c = 2800 ± 300 (Reference 19-5, T = 700 to 900 K). Results of measurements in which O-atoms (from a glow discharge) and $O_3$ (ozonized $O_2$) were mixed in a flowtube experiment gave $8.2 \times 10^{-12} \exp[-(3.3 \pm 1.0)/RT]$, c = 1700 ± 500, as recalculated by Campbell and Nudelman (Reference 19-6) from data by Leighton et al (Reference 19-7), but this result as well as others based on the measured steady-state ozone concentration in afterflows of oxygen discharges are suspect due to the known presence of sizable concentrations of metastable $O_2(a\,^1\Delta_g$ and, to a lesser extent, $b\,^1\Sigma_g^+)$, which react rapidly with $O_3$.

---

change in enthalpy, $\Delta H^o$, at T = 0 K, per g mole of reaction proceeding as written. Rate constants k are in units of $cm^3\ sec^{-1}$ for two-body, and $cm^6\ sec^{-1}$ for three-body processes. These are presented in two forms, viz; $k = A(T/T_r)^B \exp(-E/RT)$, corresponding to the form of expression of most of the published data, where the reference temperature ($T_r$) is usually 300 K but may be designated otherwise, E is the activation energy in kcal/g mole/K, and R = $1.987 \times 10^{-3}$ kcal/g mole; and $k = a(T/300)^b \exp(-c/T)$, corresponding to the practice used and explained elsewhere in the Handbook and in Table 19-1 of this chapter, i.e., c = E/R, b = B, and a = A unless $T_r \neq 300$ K.

The photochemical study by Castellano and Schumacher (Reference 19-8), in which $O_3$ was photolyzed by red light (which can produce $O_2$ + O only in their electronic ground states), obviates the above difficulties by measuring the ratio $k_2/k_3$ whose temperature coefficient is mainly determined by $E_3$. Unfortunately, the experiments were carried out at only three temperatures from 278 to 298 K. Combining these ratios with a value of $6.5 \times 10^{-34}(T/300)^{-2.6}$, which is further discussed later, and putting $k_3 = A_3 \exp[-E_3/RT]$, one obtains $(1.4 \pm 0.3) \times 10^{-12} \exp[-(3.0 \pm 0.4)/RT]$, $c = 1500 \pm 200$. This gives rate constants in excellent agreement with the expression of Reference 19-4 near 400 K, but is a factor of 6 lower than Reference 19-5 near 800 K. The situation is further complicated by the fact that shock-tube work (Reference 19-9) on ozone in the temperature range 1600 to 3300 K suggests a larger value of $k_3/k_1$ than that given by Jones and Davidson whose $k_3$ is 20 to 30 times larger than the present one at those temperatures.

In a review by Schiff (Reference 19-10), two experimental studies of the reaction were cited: one by Kondratiev and Intezarova (Reference 19-11) who reported $k = (4.8 \pm 1.5) \times 10^{-12} \exp(-3\ 7/RT)$, $c = 1900$, and another by Lundell, Ketcheson, and Schiff (Reference 19-12), $k = 3.2 \times 10^{-11} \exp(-4.5/RT)$, $c = 2300$. Two additional investigations have further clarified this problem: Krezenski (Reference 19-13) measured the competitive reactions of O with OCS and $O_3$ from 197 to 299 K and obtained $1.1 \times 10^{-12} \exp(-4.33/RT)$, $c = 2180$, for the rate constant of the $O + O_3$ reaction, and McCrumb and Kaufman (Reference 19-14) found $k = 1.8 \times 10^{-11} \exp(-4.46/RT)$, $c = 2240$. Johnston's (Reference 19-15) critical review analyzed data up to 1967 and therefore did not include the four later studies. He recommended $2.0 \times 10^{-11} \exp(-4.79/RT)$, $c = 2400$. The reaction-kinetic problem may be considered resolved, and the present author recommends $k = 1.4 \times 10^{-11} \exp(-4.4/RT)$, $c = 2200$.

### 19.3.2 $N + O_2 \rightarrow NO + O$ ($\Delta E^\circ = -32.07$ kcal $= -1.39$ eV)

There have been four studies of this reaction, three by flow methods in the forward direction, at temperatures from 400 to 750 K, and one by static methods in the reverse direction, at temperatures from 1500 to 1700 K. There is substantial agreement that the forward reaction has a small activation energy whose magnitude lies in the range from 5.9 to 7.5 kcal. As the most direct investigation over the largest temperature range, the work of Clyne and Thrush

(Reference 19-16) is preferred. Their forward rate constant of $(1.4 \pm 0.2) \times 10^{-11} \exp[-(7.1 \pm 0.4)/RT]$, $c = 3600 \pm 200$ is in good agreement with one calculated from the reverse step and the equilibrium constant as reported by Kaufman and Decker (Reference 19-17). It is unlikely that this rate constant is substantially in error, although a larger value would help explain the relatively large densities of NO which have been measured in the upper atmosphere.

A new measurement by Wilson (Reference 19-18) over the large temperature range 300-910 K yields $2.4 \times 10^{-11} \exp(-7.9/RT)$, $c = 4000$, which differs only slightly from the earlier recommendation, and may be preferable.

### 19.3.3 $N + NO \rightarrow N_2 + O$ ($\Delta E^\circ = -74.99$ kcal $= -3.25$ eV)

This very fast reaction was first studied by Kistiakowsky and Volpi (Reference 19-19) by mass spectrometry in a "stirred reactor", low-pressure flow system and by Kaufman and Kelso (Reference 19-20) who explained the sequence of visible afterglows when increasing amounts of NO are added to "active nitrogen", in terms of radiation originating from electronically excited products of N + N, N + O, and O + NO recombinations. The N + NO reaction represents the key to the understanding of these phenomena by the rapid, quantitative formation of O from N, and makes possible the "titration" of N by NO with a clearly observable "endpoint" in low-pressure flow systems. Its rate constant was indirectly determined by Clyne and Thrush (Reference 19-16) to be $4 \times 10^{-11}$, independent of temperature over the range 475 to 755 K, and directly by Phillips and Schiff (Reference 19-21), in a low-pressure flow system with mass-spectrometric detection, who reported $(2.2 \pm 0.6) \times 10^{-11}$ at 300 K. As there should be some steric requirements for a reactive collision of N and NO, the above value of one-tenth the gas-kinetic collision frequency indicates a very small (< 0.5 kcal) or zero energy barrier. In the absence of any experimental temperature dependence this value of $(2.2 \pm 0.6) \times 10^{-11}$ will be adopted here.

The reaction has been shown to yield $N_2$ with extensive vibrational excitation (References 19-22, 19-23), the average energy of $N_2^\ddagger$ being 21 ± 5 kcal, corresponding to 3 to 4 vibrational quanta, and $N_2^\ddagger$ was found to decompose $O_3$ [$k = (5.4 \pm 1.1) \times 10^{-13}$ near 300 K]. The latter behavior appears to be in contrast to that of $O_2^\ddagger$ formed in the $O + O_3$ reaction, with the possible explanation that O deactivates $O_2^\ddagger$ much more efficiently (Reference 19-9b) than N does $N_2^\ddagger$.

19.3.4 $O + O_2 + M \rightarrow O_3 + M$ ($\Delta E^\circ$ = -24.25 kcal = -1.05 eV)

Some of the above discussion is applicable here, since the recombination step is the reverse of the decomposition of ozone as studied by static (Reference 19-4) or shock-tube (References 19-5, 19-9) methods. From the measured decomposition rate constant and the equilibrium constant, Benson and Axworthy report $k = 8.2 \times 10^{-35} \exp(+0.89/RT)$, $c = 450$, near 360 K for $M = O_2$. Jones and Davidson report $(2.6 \pm 0.3) \times 10^{-35} \exp[+(1.7 \pm 0.3)/RT]$, $c = -860 \pm 150$ or $4.1 \times 10^{-34} (T/300)^{-1.66}$ to represent the combined shock-tube and lower temperature data for $M = N_2$, which should be multiplied by $1.5 \pm 0.05$ for $M = O_2$. There are further, direct measurements by Kaufman and Kelso (Reference 19-24) at 300 K for various M, and Clyne, McKenney, and Thrush (Reference 19-25) for M = Ar from 188 to 373 K. The former authors find $k = 7.5 \times 10^{-34}$ for $M = O_2$ and $5.5 \times 10^{-34}$ for $M = N_2$; the latter report $2.5 \times 10^{-35} \exp[+(1.8 \pm 0.4)/RT]$, $c = -910 \pm 200$, or $5.6 \times 10^{-34} (T/300)^{-3.4 \pm 0.8}$ from their own data, and $9.1 \times 10^{-36} \exp[+2.3/RT]$, $c = -120$ or $5.0 \times 10^{-34} (T/300)^{-2.6}$ from a combination of all data, for M = Ar. By pulse radiolysis of Ar - $O_2$ mixtures with great excess of Ar, Sauer and Dorfman (Reference 19-26) were able to measure the ozone recombination rate at pressures up to 100 atmospheres, and reported $(2.3 \pm 0.2) \times 10^{-34}$ at 296 K for M = Ar, in good agreement with other results. The relative efficiencies of $N_2$ and Ar were found to be $1.54 \pm 0.17$ in the shock-tube work (Reference 19-5) near 800 K, $1.56 \pm 0.2$ in photolysis (Reference 19-8), and $1.4 \pm 0.2$ in direct-flow-tube experiments (Reference 19-24), and one would calculate $(7.5 \pm 2) \times 10^{-34} (T/300)^{-2.6}$ for $M = N_2$, somewhat higher than the direct results of $5.5 \times 10^{-34}$ and $3.5 \times 10^{-34}$ of References 19-24 and 19-26, respectively (the latter value representing the reported datum multiplied by the 1.5 efficiency ratio for $N_2$:Ar).

Three other investigations are available. Mulcahy and Williams (Reference 19-27) report $4.7 \times 10^{-35} \exp(+1.7/RT)$, $c = -860$, for M = Ar, 1.5 to 2 times larger than the best earlier values. Two pulse-radiolysis studies (References 19-28, 19-29) near 295 K support a lower rate constant, and are in satisfactory agreement with earlier results on relative M-effects. This author's original recommendation of $5.5 \times 10^{-34} (T/300)^{-2.6}$ or an equivalent exponential expression, $3.2 \times 10^{-35} \exp(+1.7/RT)$, $c = -860$, where $M = N_2$, still seems satisfactory.

19.3.5 $O + O + M \rightarrow O_2 + M$ ($\Delta E^o = -117.98$ kcal $= -5.11$ eV)

Although the gap between low-temperature extrapolations of shocktube data and flow-tube experiments has been narrowed, particularly for M = Ar, several discrepancies remain.

Among the latter studies, there is excellent agreement between Morgan and Schiff's (Reference 19-30) rate constant of $2.8 \times 10^{-33}$ at 294 K for $M = N_2$ and Campbell and Thrush's (Reference 19-31) $3.2 \times 10^{-33}$ for the same conditions. (The recombination rate constant is here defined by $d[O_2]/dt = k[O]^2[M]$.) These authors do not agree, however, on the relative efficiency of $N_2$ and Ar, the former claiming a ratio >3.3, finding no measurable increase in rate for an addition of 40 percent Ar; the latter reporting a ratio of 1.9. This is of particular importance for comparison with shocktube work, much of which was done for M = Ar. Much shocktube work was also done for $M = O_2$, a case which is difficult to do in flowtubes because of the interfering ozone recombination. No shocktube work was done for $M = N_2$. Earlier flowtube results may have been in error due to the presence of metastables or hydrogenous impurities. Campbell and Thrush (Reference 19-31) also measured the temperature dependence from 190 to 350 K.

The shocktube studies show very large ratios of relative efficiencies for different M such as 1:18:50 for $Ar:O_2:O$. Extrapolated values at 300 K (Reference 19-32) of $1.3 \times 10^{-31}$ for $M = O_2$ using a $T^{-2.5}$ dependence and of $2.5 \times 10^{-30}$ for M = O using a $T^{-3}$ dependence seem impossibly high. Yet, most temperature dependence studies of recombination reactions near 300 K have given a $T^{-n}$ dependence with n from 2 to 3.5, in qualitative agreement with the n's found for the most efficient third-body species at high temperatures. To bring these data into agreement there would have to be a temperature range within the 500 to 2000 K interval where n decreases greatly. Careful studies are needed which overlap the lower part of this temperature interval. For the present, Campbell and Thrush's (Reference 19-31) $3.0 \times 10^{-33}(T/300)^{-2.9\pm0.4}$ or $2.8 \times 10^{-34} \exp(+1.4/RT)$, $c = -700$, will be adopted for $M = N_2$ for the range 190 to 400 K and $3.9 \times 10^{-34}(T/3000)^{-2.5\pm0.5}$ (Reference 19-32) for $M = O_2$ (and $N_2$) for the range 2500 to 5000 K.

## 19.4 BRIEF DISCUSSION OF OTHER REACTIONS

### 19.4.1 The O + NO System

In the presence of NO , O-atoms undergo three reactions: the overall three-body recombination $O + NO + M \rightarrow NO_2 + M$ ; the concurrent chemiluminescent recombination $O + NO \rightarrow NO_2 + h\nu$ ; and the reaction with the product, $NO_2$ , of the first two reactions, $O + NO_2 \rightarrow NO + O_2$ . The chemical equations are not meant to imply that the processes occur in single kinetic steps as there is good experimental evidence that they do not. Nevertheless, the equations properly represent the kinetic orders of the first and third reactions over the pressure range 0 to 10 torr and that of the second at least from 0.1 to 10 torr. The behavior of the chemiluminescent reaction below 0.1 torr is still in some doubt, although recent work favors a fall-off in the second-order rate constant below about 0.05 torr and a possible return to second-order behavior below $10^{-3}$ torr.

For $O + NO + M \rightarrow NO_2 + M$($\Delta E^o$ = -71.76 kcal = -3.11 eV) there is very good agreement on the rate constant among several studies. For M = $N_2$ at 300 K, Klein and Herron (Reference 19-33) find $(1.03 \pm 0.04) \times 10^{-31}$, Kaufman and Kelso (Reference 19-34) find $(0.93 \pm 0.13) \times 10^{-31}$, and Ford and Endow (Reference 19-35) find $0.83 \times 10^{-31}$. For its temperature dependence, Reference 19-33 reports a negative activation energy of $1.93 \pm 0.1$ kcal which corresponds to a $T^{-2.4 \pm 0.1}$ dependence. Clyne and Thrush (Reference 19-36) report an $\exp[+(1.8 \pm 0.4)/RT]$, $c = -910 \pm 200$, dependence for M = $O_2$ corresponding to $T^{-3.3 \pm 0.8}$. An estimate of $(1.0 \pm 0.1) \times 10^{-31}(T/300)^{-2.5 \pm 0.3}$ for M = $N_2$ , and $(7 \pm 2) \times 10^{-32}(T/300)^{-2.5 \pm 0.3}$ for M = $O_2$ is made, but further work on the temperature dependence is in progress.

The third reaction, $O + NO_2 \rightarrow NO + O_2$( $\Delta E^o$ = -46.22 Kcal = -2.00 eV ) is very fast (though considerably slower than the N + NO reaction in the previous section) and is often used to "titrate" O-atoms in flow systems. Its much greater speed than the three-body O + NO + M reaction in the 1-torr pressure range tends to keep the NO concentration constant and thereby makes the chemiluminescent intensity emitted by the second reaction depend on the O-atom concentration in a single experiment (Reference 19-2). Its rate constant at 298 K was reported as $(2.5 \pm 0.7) \times 10^{-12}$ by Phillips and Schiff (Reference 19-23), and as $(5.5 \pm 0.6) \times 10^{-12}$ by Klein and Herron (Reference 19-33). The latter authors also measured its temperature dependence between 278 and 374 K, finding an activation energy of $1.1 \pm 0.2$ kcal. The reaction leads to appreciable vibrational excitation of the product $O_2$ molecule, but its quantitative extent is still in doubt.

The temperature dependence of the rate constant has been measured by two more groups. Smith (Reference 19-37) reports $k = 1.8 \times 10^{-11} [(-0.7 \pm 0.45)/RT]$, $c = 350 \pm 230$, and Westenberg and deHaas (Reference 19-38) find $1.6 \times 10^{-11} \exp(-0.6/RT)$, $c = 300$. The latter expression is now preferred although it differs only slightly from the earlier recommendation of $2.8 \times 10^{-11} \exp(-1.1/RT)$, $c = 550$.

The spectrum, rate constant, and temperature dependence of the chemiluminescent recombination are reasonably well known. The spectrum extends from 3975A, corresponding to the full energy of the reaction, to about 14,000 A, and has maximum intensity near 6000 A. It appears to be continuous, but has small-intensity fluctuations which correspond to the strongest features of the complex absorption spectrum of $NO_2$. There is thus little doubt that the same electronically excited state is involved in the O + NO emission and in $NO_2$ absorption (and fluorescence), as is further indicated by similar, slight spectral shifts with pressure of the two emissions (References 19-39, 19-40). The rate constant, integrated over all wavelengths, was found to be $6.4 \times 10^{-17}$ ($M = O_2$, $T = 296$ K) by Fontijn, Meyer, and Schiff (Reference 19-41), and its temperature dependence was variously found to be: $T^{-2.8 \pm 0.8}$ by Clyne and Thrush (Reference 19-36); $T^{-1.55 \pm 0.3}$ by Hartunian, Thompson, and Hewitt (Reference 19-42) at $T = 500$ to 1100 K; and $T^{-2.0 \pm 0.3}$ by Parkes and Kaufman (Reference 19-43) at $T = 140$ to 380 K. A total chemiluminescent rate constant of $[(6.2 \pm 1.0) \times 10^{-17}] (T/300)^{-2.0 \pm 0.5}$ is recommended. Further work on the effect of different M and of the behavior at low pressure ($10^{-4}$ to $10^{-1}$ torr) is needed to settle the question whether the radiation comes mostly from the initial, unstabilized collision complex (which would lead to second-order pressure dependence if the collisional quenching of the electronically excited state is much faster than vibrational de-excitation within that state) or from collisionally stabilized excited $NO_2$.

The question of the pressure dependence and detailed mechanism of the chemiluminescent recombination of O and NO is nearing solution. Various studies have confirmed the fall-off of its rate constant at low pressures; and work by Keyser, Kaufman, and Zipf (Reference 19-44) suggests that vibrational relaxation of electronically excited $NO_2$ is of major importance in the chemiluminescence. This leads to the prediction of an irreducible, second-order component of the rate constant at low pressure due to radiation from unstabilized $NO_2$.

### 19.4.2 The $H + O_2$ System

Although H is not a major constituent of the normal or slightly perturbed upper atmosphere, the following reactions are included here because they represent an efficient path for the recombination of O-atoms, due mainly to the much larger recombination rate constant of $H + O_2 + M$ than of $O + O_2 + M$. Thus, the first step, $H + O_2 + M \rightarrow HO_2 + M$ ($\Delta E^o = -46 \pm 2$ kcal $= -2.0 \pm 0.1$ eV), is followed by the fast bimolecular steps, $HO_2 + O \rightarrow OH + O_2$ ($\Delta E^o = -55.4 \pm 2$ kcal $= -2.4 + 0.1$ eV), and $OH + O \rightarrow O_2 + H$ ($\Delta E^o = -16.6 \pm 0.5$ kcal $= -0.72 \pm 0.02$ eV) which result in the regeneration of H and the overall recombination of two O-atoms.

The first reaction was studied by Clyne and Thrush (Reference 19-45) who reported a rate constant of $(2.2 \pm 0.2) \times 10^{-32}$ for M = Ar and He, and $(5 \pm 2) \times 10^{-31}$ for $M = H_2O$. For $M = N_2$ one can estimate $(5 \pm 2) \times 10^{-32}$ on the basis of several studies of $H_2 - O_2$ explosion limits (Reference 19-46) on the doubtful assumption that different gaseous M affect the rate constant but not its temperature dependence. It is also surprising that He and Ar were equally efficient in Reference 19-45, whereas most explosion studies find He about 1.8 to 2 times more efficient than Ar. Combining all reported data from 250 to 800 K, Reference 19-45 finds a $T^{-1.8 \pm 0.7}$ dependence. A value of $(5 \pm 2) \times 10^{-32} (T/300)^{-2.0 \pm 0.5}$ is recommended for $M = N_2$.

Indirect evidence is cited in Reference 19-47 that the $O + HO_2$ reaction is fast and second-order, and a rate constant of $>10^{-11}$ can be estimated.

The last of the three steps, $OH + O \rightarrow H + O_2$, is also discussed in Reference 19-47. It is a very fast, second-order reaction with a rate constant of $(5 \pm 2) \times 10^{-11}$ near 300 K. It cannot have an appreciable activation energy ($E < 0.5$ kcal), but may have a $T^{0.5}$ dependence.

Recent work on $H + O_2 + M$ is reviewed by Baulch, Drysdale, and Lloyd (Reference 19-48) and by Kaufman (Reference 19-49). The former reviewers recommend $4.4 \times 10^{-33} \exp(+1.0/RT)$, c = -500, for M = Ar and about twice that for $M = N_2$.

### 19.4.3 Other Neutral Reactions (List in Chapter 24)

Among the atom recombination reactions there is still a surprising lack of agreement on the rate constant ($d[N_2]/dt = k[N]^2[M]$) of $N + N + M \rightarrow N_2 + M$ where values from 7 to 17 x $10^{-33}$ are cited in a review by Barth (Reference 19-50). Two additional values are (11.3 ± 1.0) x $10^{-33}$ (Reference 19-51) and 3.6 x $10^{-33}$ (Reference 19-31) for M = $N_2$, T = 300 K. The latter authors also report a $T^{-2.0\pm0.4}$ dependence.

A summary of all available high-temperature shocktube work by Baurer (Reference 19-52) suggested a value of $4.6 \times 10^{-33}(T/3000)^{-1.7}$ for M = $N_2$. This again points up the discrepancy with low temperature work as it would provide a rate constant at 300 K which is one to two orders of magnitude too large.

In the temperature range 90-600 K, Clyne and Stedman (Reference 19-53) report 7 x $10^{-34}$ exp(+1.0/RT), c = -500, and Campbell and Thrush (Reference 19-54) find 8.3 x $10^{-34}$ exp(+1.0/RT), c = -500, for $N + N + N_2 \rightarrow 2N_2$. An average of the two, $7.6 \times 10^{-34}$exp(+1.0/RT), c = -500, is recommended.

For $N + O + M \rightarrow NO + M$, older work (Reference 19-50) gives 5 to 16 x $10^{-33}$ at T = 300 K for M = $N_2$, whereas Reference 19-31 reports 11 x $10^{-33}(T/300)^{-0.5\pm0.2}$ or 6.9 x $10^{-33}$ exp(+0.3/RT), c = -150.

The reactions $O + NO \rightarrow O_2 + N$ and $O + N_2 \rightarrow NO + N$ are the reverse of previous reactions and they are therefore highly endothermic and unlikely to be important except at high temperatures. For this reason, the forward reaction rates previously mentioned have been combined with simple expressions for the equilibrium constants, K = A exp(B/RT), which represent least-squares fits to the JANAF Thermochemical Values for the range T = 1000 to 5000 K. The resulting expressions are (5.3 ± 1.1) x $10^{-12}$ exp[-(40.1 ±0.4)/RT], c = 20,200 ± 200, for $O + NO \rightarrow O_2 + N$, and (1.0 ± 0.3) x $10^{-10}$ exp[-(75.3 ± 0.5)/RT], c = 37,800 ± 300 for $O + N_2 \rightarrow NO + N$.

The two reactions of O with $N_2O$ which produce 2 NO or $N_2 + O_2$ are known to have large activation energies and are unlikely to be important except at high temperatures. Some of the experimental evidence is reviewed in Reference 19-2. The expression for the first reaction by Fenimore and Jones (Reference 19-55) of (1.5 ± 0.5) x $10^{-10}$ exp[-(28 ±3)/RT], c = 14,000 ± 1500, ($d[NO]/dt = 2k[O][N_2O]$, seems to be correct even though its pre-exponential factor is unusually large. The formation of $N_2 + O_2$ appears to be

about a factor of 3 slower, but its rate constant is more uncertain. A value of $(5 \pm 2) \times 10^{-11} \exp[-(29 \pm 3)/RT]$, $c = 15,000 \pm 1500$, is suggested.

The reaction of N with $NO_2$ can apparently give four sets of products: (1) $N_2O + O$ ; (2) $2\,NO$ ; (3) $N_2 + O_2$ ; and (4) $N_2 + 2\,O$ . Phillips and Schiff (Reference 19-56) have found the relative rates of (1) to (4) to be $(0.43 + 0.04)$: $(.33 \pm 0.07)$: $(0.10 \pm 0.12)$: $(0.13 \pm 0.11)$, and they report a total rate constant of $(1.8 \pm 0.2) \times 10^{-11}$ at 300 K.

The reaction $NO + O_3 \rightarrow NO_2 + O_2$ ($\Delta E^\circ = -47.5$ kcal $= -2.1$ eV) was investigated by Clyne, Thrush, and Wayne (Reference 19-57), who reported a rate constant of $9.5 \times 10^{-13} \exp[-(2.45 \pm 0.15)/RT]$, $c = 1230 \pm 80$, in good agreement with earlier results.

Finally, the reaction $NO_2 + O_3 \rightarrow 2\,NO + O_2$ (or $NO_3 + O_2$) may be important at low altitude under highly perturbed conditions. Johnston and Yost's (Reference 19-58) value of $9.8 \times 10^{-12}$ $(-7.0/RT)$, $c = 3500$, is recommended.

## 19.5 CONCLUSIONS

Rate constants for some of the reactions discussed are listed in Table 19-1. Several conclusions can be reached from the preceding sections: (1) The general field is a very active one, most of the relevant work dating back only a few years, on the average. (2) For most of the principal neutral reactions of aeronomic interest, rate constants are fairly well known, especially near 300 K. (3) Greatly increased experimental effort appears to be needed, however, in two distinct areas: (a) Many of the important steps, especially simple recombination processes, must be studied over wider temperature ranges, i.e., from about 100 to 1000 K, where possible, in order to clearly establish the functional form of the temperature dependence, resolve the existing discrepancies with shocktube work, and accurately measure activation energies where they exist; and (b) in many of the reactions, the role of internal excitation in the reactants or products must be established, i.e., steps should be taken to proceed from studies of overall rates to those of detailed molecular dynamics. Excellent beginnings have been made in these fields, and one may hope that the near future will bring solutions to such problems as the formation, quenching, and reactions of $O(^1D$ and $^1S)$, $O_2(b\,^1\Sigma_g^+$ and $a\,^1\Delta_g)$, vibrationally excited $O_2$ or $N_2$, and the like.

While some of these species and their reactions are discussed separately in Chapter 20, their intimate relationship with the overall field of neutral reactions should not be overlooked.

The general field of elementary reactions which are of interest to DNA has remained a very active one. A welcome by-product of this activity has been the considerable effort which has gone into the preparation of thorough reviews, some of them on a major continuing basis. These include the NSRDS-NBS series, the British series by Baulch and co-workers at Leeds, the review by Schofield (Reference 19-59), the proceedings of I. A. G. A. Symposium No. 8 (Can. J. Chem. 47, No. 10 (1969)) and its precursor, and many specific reviews in series such as Annual Reviews of Physical Chemistry, Progress in Reaction Kinetics, Advances in Chemical Physics, and others.

Table 19-1. Neutral reaction rate constants.*

$$k = (a \pm \Delta a)(T/T_r)^{b \pm \Delta b} \exp[-(c \pm \Delta c)/T]$$

| Reaction | $a \pm \Delta a$ | $b \pm \Delta b$ | $c \pm \Delta c$ | Remarks | Cf. Par. No. |
|---|---|---|---|---|---|
| Rearrangement | | | | | |
| $O + O_3 \rightarrow 2O_2$ | $(1.4 \pm 0.3)[-11]$ | | $(2.22 \pm 0.2)[3]$ | | 19.3.1 |
| $O + NO_2 \rightarrow NO + O_2$ | $(1.6 \pm 0.5)[-11]$ | | $(3.0 \pm 1.5)[2]$ | | 19.4.1 |
| $O + NO \rightarrow O_2 + N$ | $(5.3 \pm 1.1)[-12]$ | | $(2.02 \pm 0.02)[4]$ | | 19.4.3 |
| $O + N_2 \rightarrow NO + N$ | $(1.0 \pm 0.3)[-10]$ | | $(3.79 \pm 0.03)[4]$ | | 19.4.3 |
| $O + N_2O \rightarrow 2NO$ | $(1.5 \pm 0.5)[-10]$ | | $(1.4 \pm 0.2)[4]$ | | 19.4.3 |
| $O + N_2O \rightarrow N_2 + O_2$ | $(5 \pm 2)[-11]$ | | $(1.4 \pm 0.2)[4]$ | | 19.4.3 |
| $O + OH \rightarrow O_2 + H$ | $(5 \pm 2)[-11]$ | | | | 19.4.2 |
| $O + HO_2 \rightarrow OH + O_2$ | $1[-11]$ | | | | 19.4.2 |
| $N + O_2 \rightarrow NO + O$ | $(2.4 \pm 0.3)[-11]$ | | $(4.0 \pm 0.2)[3]$ | | 19.3.2 |
| $N + NO \rightarrow N_2 + O$ | $(2.2 \pm 0.6)[-11]$ | | | | 19.3.3 |
| $N + NO_2 \rightarrow$ Products | $(1.8 \pm 0.2)[-11]$ | | | | 19.4.3 |

Table 19-1. (Cant'd.)

| Reaction | a ± Δa | b ± Δb | c ± Δc | Remarks | Cf. Par. No. |
|---|---|---|---|---|---|
| Rearrangement (Cont'd.) | | | | | |
| $NO + O_3 \rightarrow NO_2 + O_2$ | 9.5[-13] | | (1.3 ± 0.1)[3] | | 19.4.3 |
| $NO_2 + O_3 \rightarrow \begin{cases} NO_3 + O_2 \\ NO + 2O_2 \end{cases}$ | (9.8 ± 1.5)[-12] | | (3.5 ± 0.2)[3] | | 19.4.3 |
| Three-Body Recombination | | | | | |
| $O + O_2 + M \rightarrow O_3 + M$ | (5.5 ± 2)[-34]<br>(3.2)[-35] | -(2.6 ± 0.4) | -(8.5 ± 2)[2] | M = $N_2$ | 19.3.4 |
| $O + NO + M \rightarrow NO_2 + M$ | (1.0 ± 0.1)[-31] | -(2.5 ± 0.3) | | M = $N_2$ | 19.4.1 |
| $O + O + M \rightarrow O_2 + M$ | 3.0[-33] | -(2.9 ± 0.4) | | | |
| | 2.8[-34] | | -(7 ± 2)[2] | M = $N_2$, T = 200-500 K | 19.3.5 |
| | 3.9[-34] | -(2.5 ± 0.5) | | $T_r$ = 3000 K, M = $N_2$ | |
| $N + N + M \rightarrow N_2 + M$ | (7.6 ± 2)[-34] | | -(5.0 ± 2.0)[2] | M = $N_2$ | 19.4.3 |
| | 4.6[-33] | -1.7 | | $T_r$ = 3000 K, M = $N_2$ | |

Table 19-1. (Cont'd.)

| Reaction | $a \pm \Delta a$ | $b \pm \Delta b$ | $c \pm \Delta c$ | Remarks | Cf. Par. No. |
|---|---|---|---|---|---|
| Three-Body Recombination (Cont'd.) | | | | | |
| $N + O + M \rightarrow NO + M$ | $(6.9 \pm 2)[-33]$<br>$(1.1 \pm 0.3)[-32]$ | $-(0.5 \pm 0.2)$ | $-(1.5 \pm 1)[2]$ | $T = 200\text{–}400\,K$<br>$M = N_2$ | 19.4.3 |
| $H + O_2 + M \rightarrow HO_2 + M$ | $(9 \pm 2)[-33]$ | | $-(5.0 \pm 3.0)[2]$ | $M = N_2$ | 19.4.2 |
| Radiative Recombination | | | | | |
| $O + NO \rightarrow NO_2 + h\nu$ | $(6.2 \pm 1)[-17]$ | $-(2.0 \pm 0.5)$ | | | 19.4.1 |

*In this table, $T_r = 300\,K$ except where noted. The notation [-p] signifies $10^{-p}$. When the space under one or more of the parameters is left blank this does not imply that the parameter is zero but that it is either unknown or that the data do not warrant the use of a three-parameter expression. The units are $cm^3 molecule^{-1} sec^{-1}$ for all reactions of the type $A + B \rightarrow$, and $cm^6 molecule^{-2} sec^{-1}$ for all reactions of the type $A + B + C \rightarrow$.

## REFERENCES


19-1. Rosner, D. E., AeroChem Research Laboratories, Rept. AFOSR TN-60-887 (1960).

19-2. Kaufman, F., in Progress in Reaction Kinetics, G. Porter, Ed., Pergamon, New York (1961); pp. 1-39.

19-3. Rony, P. R., University of California, Rept. UCRL-16050 (1965).

19-4. Benson, S. W., and A. E. Axworthy, Jr., J. Chem. Phys. 42, 2614 (1965).

19-5. Jones, W. M., and N. Davidson, J. Am. Chem. Soc. 84, 2868 (1962).

19-6. Campbell, E. S., and C. Nudelman, New York Univ., Rept. AFOSR TN-60-502 (1960).

19-7. Leighton, F., H. B. Urback, J. A. Wojtowicz, and J. A. Zaslowsky, 136th Meeting, Am. Chem. Soc. (1959); Papers 46-S, 47-S.

19-8. Castellano, E., and H. J. Schumacher, Z. Physik. Chem. 34, 198 (1962).

19-9. (a) Wray, K. L., J. Chem. Phys. 38, 1518 (1963); (b) Kiefer, J. H., and R. W. Lutz, Eleventh Symp. (Intl.) on Combustion, The Combustion Inst., Pittsburgh, Pa. (1967); p. 67.

19-10. Schiff, H. I., Can. J. Chem. 47, 1903 (1969).

19-11. Intezarova, E. I., and V. N. Kondratiev, Izv. Akad. Nauk SSSR, Ser. Khim. 1967, No. 11, 2440.

19-12. Lundell, O. R., R. D. Ketcheson, and H. I. Schiff, Twelfth Symp. (Intl.) on Combustion, The Combustion Inst., Pittsburgh, Pa. (1969); p. 307; also unpublished work.

19-13. Krezenski, D. C., Pennsylvania State Univ. Ionosphere Research Rept. 368 (1971).

19-14. McCrumb, J. L., and F. Kaufman, submitted for publication, J. Chem. Phys.

19-15. Johnston, H. S., Univ. of Calif., Rept. NSRDS-NBS 20 (1968).

19-16. Clyne, M. A. A., and B. A. Thrush. Proc. Roy. Soc. A261, 259 (1961).

19-17. Kaufman, F., and L. J. Decker, Seventh Symp. (Intl.) on Combustion, Butterworths, London (1959); p. 57.

19-18. Wilson, W. E., J. Chem. Phys. 46, 2017 (1967).

19-19. Kistiakowsky, G. B., and G. G. Volpi, J. Chem. Phys. 27, 1141 (1957).

19-20. Kaufman, F., and J. R. Kelso, J. Chem. Phys. 27, 1209 (1957); Seventh Symp. (Intl.) on Combustion, Butterworths, London (1959); p. 53.

19-21. Phillips, L. F., and H. I. Schiff, J. Chem. Phys. 36, 1509 (1962).

19-22. Kaufman, F., and J. R. Kelso, J. Chem. Phys. 28, 510 (1958).

19-23. Phillips, L. F., and H. I. Schiff, J. Chem. Phys. 36, 1509, 3283 (1962); Morgan, J. E., L. F. Phillips, and H. I. Schiff, Disc. Faraday Soc. 33, 118 (1962).

19-24. Kaufman, F., and J. R. Kelso, Disc. Faraday Soc. 37, 26 (1964); J. Chem. Phys. 46, 4541 (1967).

19-25. Clyne, M. A. A., D. J. McKenney, and B. A. Thrush, Trans. Faraday Soc. 61, 2701 (1965).

19-26. Sauer, M. C., Jr., and L. M. Dorfman, J. Am. Chem. Soc. 87, 3801 (1965).

19-27. Mulcahy, M. F. R., and D. J. Williams, Trans. Faraday Soc. 64, 59 (1968).

19-28. Sauer, M. C., Jr., J. Phys. Chem. 71, 3311 (1967).

19-29. Meaburn, G. M., D. Perner, J. LeCalve, and M. Bourene, J. Phys. Chem. 72, 3920 (1968).

19-30. Morgan, J. E., and H. I. Schiff, J. Chem. Phys. 38, 1495 (1963).

19-31. Campbell, I. M., and B. A. Thrush, Proc. Roy. Soc. A296, 222 (1967).

19-32. Wray, K. L., Tenth Symp. (Intl.) on Combustion, The Combustion Institute, Pittsburgh, Pa. (1965); p. 523.

19-33. Klein, F. S., and J. T. Herron, J. Chem. Phys. 41, 1285 (1964).

19-34. Kaufman, F., and J. R. Kelso, submitted for publication, J. Chem. Phys.

19-35. Ford, H. W., and N. Endow, J. Chem. Phys. 27, 1156 (1957).

19-36. Clyne, M. A. A., and B. A. Thrush, Proc. Roy. Soc. A259, 404 (1962).

19-37. Smith, I. W. M., Trans. Faraday Soc. 64, 378 (1968).

19-38. Westenberg, A. A., and N. DeHaas, J. Chem. Phys. 50, 707 (1969).

19-39. Meyers, G. H., D. M. Silver, and F. Kaufman, J. Chem. Phys. 44, 718 (1966).

19-40. Freedman, E., and J. R. Kelso, Bull. Am. Phys. Soc. 11, 453 (1966).

19-41. Fontijn, A., C. B. Meyer, and H. I. Schiff, J. Chem. Phys. 40, 64 (1964).

19-42. Hartunian, R. A., W. P. Thompson, and E. W. Hewitt, J. Chem. Phys. 44, 1765 (1966).

19-43. Parkes, D. A., and F. Kaufman, submitted for publication, J. Chem. Phys.

19-44. Keyser, L., F. Kaufman, and E. C. Zipf, Jr., Chem. Phys. Letts. 2, 523 (1968).

19-45. Clyne, M. A. A., and B. A. Thrush, Proc. Roy. Soc. A275, 559 (1963).

19-46. Linnett, J. W., and N. J. Selley, Z. Physik. Chem. 37, 402 (1963); Baldwin, R. R., and C. T. Brooks, Trans. Faraday Soc. 58, 1782 (1962); Ashmore, P. G., and B. J. Tyler, Ibid. 1108.

19-47. Kaufman, F., Ann. Geophys. 20, 77 (1964).

19-48. Baulch, D. L., D. D. Drysdale, and A. C. Lloyd, The University, Leeds, England, High Temperature Reaction Rate Data Rept. 3 (1969).

19-49. Kaufman, F., Can. J. Chem. 47, 1917 (1969).

19-50. Barth, C. A., Ann. Geophys. 20, 137 (1964).

19-51. Evenson, K. M., and D. S. Burch, J. Chem. Phys. 45, 2450 (1966).

19-52. Baurer, T., S. Ciolkowski, M. S. Wecker, and D. Attwood, General Applied Science Laboratories, Report DASA 1834 (1966).

19-53. Clyne, M. A. A., and D. H. Stedman, J. Phys. Chem. 71, 3071 (1967).

19-54. Campbell, I. M., and B. A. Thrush, Proc. Roy. Soc. A296, 201 (1967).

19-55. Fenimore, C. P., and G. W. Jones, Eighth Symp. (Intl.) on Combustion, Williams and Wilkins, Baltimore (1962); p. 127.

19-56. Phillips, L. F., and H. I. Schiff, J. Chem. Phys. 42, 3171 (1965).

19-57. Clyne, M. A. A., B. A. Thrush, and R. P. Wayne, Trans. Faraday Soc. 60, 359 (1964).

19-58. Johnston, H. S., and D. M. Yost, J. Chem. Phys. 71, 386 (1949).

19-59. Schofield, K., Planet. Space Sci. 15, 643 (1967).

# 20. EXCITATION AND DEEXCITATION PROCESSES

J. William McGowan*, General Atomic**
Ralph H. Kummler, Wayne State University
Forrest R. Gilmore, R&D Associates
(Latest Revision 8 October 1971)

## 20.1 GENERAL CONSIDERATIONS

This chapter discusses the internal degrees of freedom of atoms, ions, and molecules, including the mechanisms of production of excited species and the ways in which the energy is contained in excitation and distributed through collision. Emphasis is placed on the description and interrelation of such interactions in all areas which involve atoms, ions, and molecules in those excited states likely to be important in atmospheric processes. In the laboratory, as well as in the quiescent and disturbed atmospheres, it is often difficult to recognize and separate the effects of excited species, and for a long time it was expedient to assume that the excited-state reactions were subsidiary to ground-state reactions. However, it is now recognized that in both the laboratory and the atmosphere small numbers of excited species can have large effects on total reaction rates and upon steady-state conditions.

The experimental methods used in excited-state studies are not described specifically within this chapter. Some of these techniques are discussed in Chapter 7 and additional information is given in Table 2 of Reference 20-1. Special mention should be made of material contained in a review on excited nitrogen by Wright and Winkler (Reference 20-2). Elsewhere in the present chapter, section 20.2 examines the lifetimes and energies contained in the various excited atmospheric species, and in section 20.3 some excitation and deexcitation results for the more important atmospheric species are presented. In section 20.4 a more complete list of pertinent rate constants and cross-sections is given. Throughout this chapter,

---

* Present address: University of Western Ontario, London, Ontario.

** Now Gulf Energy and Environmental Systems Company.

an asterisk (*) is used to refer to electronically excited species, which for molecules may also include vibrational and rotational excitation. Vibrational excitation (including possible rotational excitation) as opposed to electronic excitation, is denoted by ‡ .

## 20.2 LIFETIMES OF, AND ENERGY STORED IN, EXCITED STATES

It is necessary to distinguish between the effective lifetime, $\tau_c$ , which allows for collisional deexcitation, and the collision-free radiative lifetime of the excited species, $\tau_o$. These two lifetimes are simply related through the reactive collision frequency (kn):

$$\frac{1}{\tau_c} = \frac{1}{\tau_o} + \Sigma_i k_i n_i \,, \qquad (20\text{-}1)$$

where $k_i$ is the rate constant ($cm^3\ sec^{-1}$) by which the excited atom, ion, or molecule inelastically scatters from another atom, ion, electron, or molecule of number density $n_i$ ($cm^{-3}$).

Much of what is known about the radiative lifetimes of the longer-lived species is summarized in Table 20-1. These values are believed to be the best presently available, although some are controversial.

Figures 20-1 and 20-2 comprise energy-level diagrams for those levels of interest in upper atmospheric chemistry. In energy-transfer reactions, energy resonance or near resonance may play some part depending upon the details of the potential-energy surface associated with the interaction considered (References 20-3 through 20-7).

## 20.3 THE EXCITATION AND DEEXCITATION OF SPECIFIC STATES

In this section some of the literature is considered, which is relevant to an understanding of the role played by specific excited atoms, ions, and molecules in the quiescent and disturbed atmospheres and in the laboratory. This subject is also covered, at least in part, in papers by Hunter and McElroy (Reference 20-42), Bates (Reference 20-43), Muschlitz (Reference 20-44), Gilmore, Bauer, and McGowan (Reference 20-6), and Donovan and Hudson (Reference 20-45) in review

articles included in a special supplement on chemical lasers (Reference 20-46); in the aforementioned review of active nitrogen (Reference 20-2); and in books by Chamberlain (Reference 20-47) and others (References 20-10, 20-48 through 20-52).

### 20.3.1 Nitrogen

#### 20.3.1.1 VIBRATIONAL EXCITATION AND DEEXCITATION OF THE GROUND ELECTRONIC STATE

An appreciable fraction of the energy deposited in the atmosphere finally comes to rest in vibrational excitation of nitrogen, either through radiative decay of higher-lying excited states (Reference 20-37), e.g.:

$$N_2(A\,^3\Sigma_u,\ v') \rightarrow N_2(X\,^1\Sigma_g^+,\ v'') + h\nu\ , \qquad (20\text{-}2)$$

chemical reaction (References 20-53, 20-54), e.g.:

$$NO(X\,^2\Pi) + N(^4S^o) \rightarrow N_2(\ ^1\Sigma_g^+,\ v > 0) + O(^3P)\ , \qquad (20\text{-}3)$$

energy transfer (References 20-42, 20-55 through 20-58), e.g.:

$$O(^1D) + N_2(X\,^1\Sigma_g^+,\ v = 0) \rightarrow O(^3P) + N_2(X\,^1\Sigma_g^+,\ v \leq 1)\ , \qquad (20\text{-}4)$$

or resonance excitation under electron impact (References 20-59, 20-60), e.g.:

$$N_2(X\,^1\Sigma_g^+,\ v) + e \rightarrow N_2^-(^2\Pi,\ v') \rightarrow N_2(X\,^1\Sigma_g^+,\ v'') + e\ . \qquad (20\text{-}5)$$

The latter process is very efficient, with a cross-section approaching $6 \times 10^{-16}$ cm$^2$ at its maximum (Reference 20-61). These cross-sections have been integrated over a Boltzmann distribution by Abraham and Fisher (References 20-62, 20-63), and the results are presented in Figure 20-3 (from Fisher). (See also Ali, Reference 20-64, for similar results.)

A number of chemical reactions have been reported in which vibrationally excited products have been identified (References 20-6, 20-65 through 20-67), but reaction (20-3) is the only one thus far studied in detail (References 20-53, 20-54) which gives $N_2^{\ddagger}$ as a product.

The quenching of $O(^1D)$ by $N_2$, reaction (20-4), can be a very efficient source of vibrationally excited nitrogen even though the curve-crossing mechanism does not permit more than one or two quanta of $N_2$ vibrational energy per $O(^1D)$ quench. Hunten and McElroy (Reference 20-42) have pointed out that whereas $O(^1D)$ is readily quenched by energy transfer to $N_2$, $O(^1S)$ is not, even though it is nearly resonant with $v = 16$.

The vibrational excitation of nitrogen through inelastic resonance collisions of electrons has been examined experimentally by Schulz (Reference 20-59), by Golden (Reference 20-68), and by others. The cross-section for this reaction has been measured and calculated with good agreement, but the reverse quenching cross-sections have been obtained only from the theoretical study by Chen (Reference 20-60). Green et al (References 20-69, 20-70) have used these and similar excitation data to calculate in detail the fractions of the energy from 30-kev incident electrons going into vibrational and into electronic excitation. (Note an error in the vibrational excitation in the latter work.) Quenching has also been observed experimentally (Reference 20-71).

The quenching of vibrationally excited molecules through energy transfer to the vibrational levels of other molecules (Vibration-Vibration, VV) or to kinetic energy (Vibration-Translation, VT) is thought to be well understood (References 20-72 through 20-75). The $N_2$ $(1 \rightarrow 0)$ transition at room temperature requires nearly $10^{10}$ collisions to transfer the one quantum of vibrational energy to kinetic energy (Reference 20-73). For relaxation by atom exchange (References 20-76 through 20-79):

$$N—N^{\pm} + N \rightarrow N + N—N \quad , \tag{20-6}$$

or by resonance energy transfer (Reference 20-73), the number of required collisions is considerably less. The probability of vibrational energy transfer increases with increasing temperature or decreasing vibrational energy difference. Usually the process of deactivating higher levels is a step-by-step, ladder-descending process, so that a molecule put in a high-lying vibrational level may react before all its energy is equipartitioned. For most conditions $\Delta v = \pm 1$ but for very high levels and/or high kinetic temperatures it is likely that $\Delta v > 1$ (References 20-80, 20-81). Taylor and Bitterman have reviewed those VT and VV processes relevant to $CO_2$ laser action (Reference 20-82). For many more molecules, the VT data are summarized by Millikan and White (Reference 20-83).

The near-resonant transfer of nitrogen vibrational energy to the electronic states of atoms and molecules depends quite sensitively on the potential-energy surfaces. Hunten (Reference 20-84) has argued that excitation of the sodium D-line in low aurorae (< 100 km) is likely to be the result of energy transfer from vibrationally excited nitrogen. This reaction has been observed in the laboratory (Reference 20-85) and the cross-section has been measured as $10^{-15}$ $cm^2$ (Reference 20-86), altnough it is doubtful that vibrationally excited nitrogen exists below the turbopause (Reference 20-56). The cross-sections for energy transfer from excited alkali metal atoms to the vibrational modes of nitrogen have been calculated by Fisher and Smith (Reference 20-87).

The degree of vibrational excitation significantly affects certain reaction rates, the most important of which probably is the exothermic reaction:

$$N_2^{\ddagger}(X\ {}^1\Sigma_g^+,\ v) + O^+({}^4S) \rightarrow NO^+(X) + N({}^4S)\ , \qquad (20\text{-}7)$$

which depends sensitively upon the vibrational level of the nitrogen molecule (References 20-88, 20-89). From the work of Schmeltekopf et al (Reference 20-89), Thomas and Norton (Reference 20-90), O'Malley (Reference 20-91), and Walker et al (References 20-57, 20-58), one can infer that: (1) The electron density in the F-region is affected by the nitrogen vibrational temperature through the conversion of atomic ions with low electron-ion recombination coefficients to molecular ions with large recombination coefficients, mainly by reaction (20-7). (2) A decrease in electron density for a highly disturbed atmosphere is to be expected when the effective vibrational temperature is high. This probably occurs, for example, in the red arc associated with the sunspot maximum, in some aurorae, and in the atmosphere disturbed by a nuclear burst (References 20-92, 20-93).

In Table 20-2, some of the energy-transfer rate constants of interest to this chapter are listed. The values quoted are usually for bulk reaction coefficients and are normally related to the specific value of $v = 1$, except for the reaction $N_2^{\ddagger} + O^+$, treated separately in Table 20-3.

Data for vibrational-translational energy transfer are usually presented as a relaxation-time-pressure product $p\tau$, where $\tau$ refers to the e-folding time of the vibrational energy, $\epsilon$, according

to the classical equation:

$$d\epsilon/dt = \frac{1}{\tau} [\epsilon(\text{equil}) - \epsilon] , \qquad (20\text{-}8)$$

at constant translational temperature in the absence of sources. The rate constant for deactivation of the first vibrational level $k_{10}$ is related to $\tau$ by (see Reference 20-97, for example):

$$k_{10} M = [\tau(1 - e^{-h\nu/kT})]^{-1} , \qquad (20\text{-}9)$$

where M = number density of collision partner (at pressure p ), and $h\nu$ is the vibrational-energy-level spacing. The data of Table 20-2 have been used in conjunction with the CIRA 1965 Atmosphere (Reference 20-98) to calculate the loss rates for $N_2^+$ pertinent to the atmosphere, as presented in Figure 20-4.

### 20.3.1.2 EXCITATION AND DEEXCITATION OF THE ($A\ ^3\Sigma_u^+$) STATE

The ($A\ ^3\Sigma_u^+$) state at 6.1 eV is the lowest electronic metastable state of the nitrogen molecule, and as yet no significant reactions in the upper atmosphere have been ascribed to it, even though it is found to have a lifetime near two seconds (Reference 20-15). It can be populated through electron impact (References 20-99 through 20-103) and by cascade from the higher-lying triplet states such as the ($B\ ^3\Pi_g$) at 7.3 eV and the ($C\ ^3\Pi_u$) at 11.1 eV.

Repeated measurements of the rotational temperature of the Vegard-Kaplan bands ($A \rightarrow X$) of nitrogen in aurorae have indicated a rotational temperature of this diffuse radiation to be 800 K (Reference 20-104) or higher (References 20-105, 20-106). To be consistent with these measurements, it was argued on the basis of the older 13-second lifetime (Reference 20-107) that the radiation had to be emitted from an altitude in excess of 220 km, i.e., where kinetic temperature is 800 K. It was also postulated that there was no radiation from the A-state at lower altitudes because the A-state was effectively quenched by either atomic or molecular oxygen, which would consequently have to have large quenching rates. However, for the same auroral displays, measurements of the rotational temperatures of the $N_2^+$ First Negative System ($B \rightarrow A$) invariably gave temperatures between 200 and 600 K, implying that the aurora was considerably lower in the atmosphere. Broadfoot and Hunten (Refer-

ence 20-104) observed that the distribution of vibrational levels of the A-state was not consistent with that obtained either from direct electron-impact excitation of the state or from cascade. It is now known (Reference 20-10) from rocket experiments that the (A → X) emission comes from 120-170 km, consistent with the new data for both radiative lifetimes and quenching coefficients. Hence, the altitude profile is resolved but the source remains in doubt. One reaction which should be considered is the near-resonant charge-transfer interaction:

$$N_2^+ (X) + NO \rightarrow N_2 (A) + NO^+ , \qquad (20\text{-}10)$$

which has a reaction rate constant in excess of $10^{-10}$ $cm^3$ $sec^{-1}$ (References 20-108, 20-109). Although the concentrations of the reactants are known to be small in the undisturbed atmosphere, they will be increased in an auroral display. Furthermore, it has been observed (References 20-110, 20-111) that some charge-transfer reactions which proceed through an intermediate complex lead to molecular products which have a high (or poorly defined) rotational temperature.

Cross-sections for electron-impact excitation to the A, B, W, B', C, E, and D states of nitrogen have been obtained by Cartwright et al (References 20-112 through 20-115) and were used to predict absolute photon fluxes in eleven band systems of nitrogen under night-time auroral conditions. Significant radiation was found in the 1-10$\mu$m region. The strongest radiation was found at 2.75, 3.33, and 4.23 $\mu$m.

Noxon (Reference 20-116), in agreement with Zipf (Reference 20-117), has shown that the deexcitation rate constant of $N_2$ ($A\,^3\Sigma_u^+$) in collision with ground-state nitrogen is small. It has also been observed (Reference 20-118) that nitrogen atoms effectively quench $N_2$ (A) through atom exchange:

$$N + N_2 (A) \rightarrow N_2 (X) + N . \qquad (20\text{-}11)$$

Hunten and McElroy (Reference 20-42) found that only oxygen atoms could provide the necessary quenching in the atmosphere. A summary of the available quenching data is presented in Table 20-4. Metallic species like Na, Fe, Hg, Ba, etc., are also effective quenchers through Penning ionization (References 20-44, 20-119, 20-120):

$$N_2 (A) + M \rightarrow N_2 (X) + M^+ + e . \qquad (20\text{-}12)$$

### 20.3.1.3 HIGHER-LYING STATES OF NITROGEN

No attempt is made here to review in detail information on metastable states of nitrogen above the ($A\ ^3\Sigma_u^+$) state, except to note that a metastable state at approximately 8.5 eV which was observed by Cermak (Reference 20-126) may lead to associative ionization:

$$N_2^* + NO \rightarrow N_2NO^+ + e \ . \qquad (20\text{-}13)$$

The product $N_2NO^+$ has not been identified specifically in recent D-region mass-spectral studies, but may be important as an intermediate.

### 20.3.1.4 EXCITATION AND DEEXCITATION OF $N_2^+$ STATES, PARTICULARLY ($A\ ^2\Pi_u$), ($B\ ^2\Sigma_u^+$), ($^4\Sigma_u^+$), AND ($^4\Delta_u$)

The 3914A band associated with the ($0 \rightarrow 0$) ($B \rightarrow X$) transition in $N_2^+$ is one of the strongest in the aurora, twilight glow, and dayglow. The primary sources of the $N_2^+(B)$ state are photoionization by solar radiation, e.g.:

$$N_2 + h\nu(>18.7\ eV) \rightarrow N_2^+(B\ ^2\Sigma_u^+) + e \ , \qquad (20\text{-}14)$$

ionization by energetic electrons, e.g.:

$$N_2 + e \rightarrow N_2^+(B\ ^2\Sigma_u^+) + 2e \ , \qquad (20\text{-}15)$$

excitation by slow electrons, (Reference 20-127), e.g.:

$$N_2^+ + e \rightarrow N_2^+(B\ ^2\Sigma_u^+) + e \ , \qquad (20\text{-}16)$$

and resonance scattering of sunlight by ground-state ions, e.g.:

$$N_2^+(X) + h\nu(>3.2\ eV) \rightleftarrows N_2^+(B\ ^2\Sigma_u^+) \ . \qquad (20\text{-}17)$$

Only the second of these (20-15) is likely to be active in aurorae, where the secondary electrons are produced by heavy-particle bombardment of the atmosphere. Similar mechanisms can produce the ($A\ ^2\Pi_u$) state of the ion, although (as is shown later) charge transfer from $O^+(^2D)$ with $N_2$ also leads to A-state ions and possibly an asymmetry in the subsequent Meinel radiation.

Wallace and McElroy (Reference 20-128) have discussed the relative importance of the above reactions in producing excited $N_2^+$. They show that above 100 to 150 km, resonance scattering is the major source of 3914A radiation. At low densities, reactive collisions involving either the A or B states of $N_2^+$ are slower than the loss of excitation by radiation. However, at higher densities reactions such as:

$$N_2^+(B\ ^2\Sigma_u^+) + O_2(X\ ^3\Sigma_g^-) = N_2(X\ ^1\Sigma_g^+) + O_2^+(b\ ^4\Sigma_g^-)\ , \qquad (20\text{-}18)$$

and:

$$N_2^+(A\ ^2\Pi_u) + O_2(X\ ^3\Sigma_g^-) = N_2(X\ ^1\Sigma_g^+) + O_2^+(a\ ^4\Pi_u)\ , \qquad (20\text{-}19)$$

may be significant. Both reactions are nearly energy-resonant and conserve spin. However, even these reactions cannot greatly affect electron density in laboratory afterglows or the upper atmosphere, since both parent and product ions are diatomic with similar recombination rates. The major results of the above charge-transfer reactions would be to produce additional $O_2^+(b \rightarrow a)$ first-negative radiation and metastable $O_2^+(a\ ^4\Pi_u)$ ions. Laboratory experiments (References 20-129, 20-130) have demonstrated that reaction (20-19) and perhaps reaction (20-18) have cross-sections well in excess of the corresponding process for ground-state ions. However, the charge transfer of excited $N_2^+$ ions with $N_2$ has a smaller cross-section than do ground-state ions (References 20-130, 20-131). This reflects the fact that some $(N_2^+)^*$ ions formed under electron impact around the equilibrium internuclear distance of the neutral molecule relax to larger internuclear distances, so that charge transfer is no longer energy-resonant.

The study of collision-induced dissociation of $(N_2^+)^*$ has proved to be an effective means of studying highly excited molecular ions. In particular, McGowan and Kerwin (Reference 20-131) have identified the metastable $(^4\Sigma_u^+)$ and $(^4\Delta)$ states of $N_2^+$ which form $N_3^+$ by:

$$N_2^+(^4\Sigma_u \text{ or } ^4\Delta) + N_2(X\ ^1\Sigma_g^+) = N_3^+ + N\ . \qquad (20\text{-}20)$$

Higher excited states of $N_2^+$ (and $O_2^+$) have been identified in some laboratory experiments (Reference 20-131) where the reaction time was near 3 $\mu$sec. In other experiments (Reference 20-129) where the time between formation and collision was nearer 10 $\mu$sec,

these states were not observed. Therefore, the higher states may decay with a lifetime of less than $10^{-5}$ sec and be of less importance in the atmosphere.

Studies of electron-impact ionization of molecular nitrogen and oxygen near threshold (References 20-132, 20-133) have demonstrated that a Franck-Condon distribution of vibrational levels is not obtained because many ions are formed indirectly, via autoionizing states. The importance of autoionization can be seen in the case of $N_2^+(X)$, where the Franck-Condon factors for transitions from $N_2(X, v'' = 0)$ to $N_2^+(X, v')$ decrease by nearly an order of magnitude for each successive vibrational level of the ion, while for electrons with energy not far above the ionization potential, Fineman et al (Reference 20-134) have demonstrated that the populations of the $v' = 0$ and $v' = 1$ levels are nearly equal.

### 20.3.1.5 EXCITATION AND DEEXCITATION OF $N(^2D)$

The $(^2D)$ states of atomic nitrogen, which are the upper states of the 5200A dayglow, are probably excited (Reference 20-128) by dissociative recombination:

$$N_2^+(X\ ^2\Sigma_g^+) + e \rightarrow N(^2D) + N \qquad (20\text{-}21)$$

$$NO^+(X\ ^1\Sigma^+) + e \rightarrow N(^2D) + O\ , \qquad (20\text{-}22)$$

and by ion-atom interchange:

$$N_2^+(B^2\Sigma^+) + O(^3P) \rightarrow NO^+(X\ ^1\Sigma^+) + N(^2D)\ . \qquad (20\text{-}23)$$

$N(^2D)$ may play a vital role in the NO balance of the D region via its major loss reaction (Reference 20-135):

$$N(^2D) + O_2 \rightarrow NO + O\ . \qquad (20\text{-}24)$$

which has a rate constant $k = 6 \times 10^{-12}$ cm$^3$ sec$^{-1}$. By comparison, the quenching of $N(^2D)$ by molecular nitrogen is slow; $k = (3 \pm 3) \times 10^{-15}$ cm$^3$ sec$^{-1}$ (Reference 20-136).

Henryet al (Reference 20-14) have calculated electron impact excitation cross-sections for $N(^2D)$ and $N(^2P)$. Ali (Reference 20-64) has integrated these cross-sections over a Boltzmann distribution to obtain the rate constants illustrated in Figure 20-5.

## 20.3.2 Oxygen

### 20.3.2.1 THE VIBRATIONALLY EXCITED GROUND STATE, $O_2$ ($X^3\Sigma_g^-$)

The cross-section for dissociative attachment of electrons to oxygen:

$$O_2 + e \rightarrow O^- + O \,, \tag{20-25}$$

is strongly dependent upon the molecular oxygen temperature (References 20-133, 20-137, 20-138). As the equilibrium oxygen temperature is increased from 300 to 2100 K, both the energy at maximum cross-section and the threshold are shifted downward. O'Malley (Reference 20-139), through a multiparameter data fit, interpreted the results as being due to vibrational excitation of the molecule. Chen, however, demonstrated theoretically that rotational excitation must also be important (Reference 20-140).

Other methods for the production and destruction of the higher vibrational levels of $O_2(X\ ^3\Sigma_g^-)$ have been reviewed by Dalgarno (Reference 20-77), by Hunten and McElroy (Reference 20-42), and by Dalgarno and McElroy (Reference 20-111).

Rate constants for molecular oxygen deactivation are given in Table 20-5; these data are then employed, in conjunction with the CIRA 1965 atmosphere (Reference 20-98), to calculate the effective first-order rate constants for vibrationally excited $O_2(v = 1)$ deactivation, illustrated in Figure 20-6. At high energies (10-20 eV), vibrational excitation by ion-molecule collision, e.g.:

$$O^+ + O_2 \rightarrow O^+ + O_2^{\ddagger}\ (v \geq 1) \,, \tag{20-26}$$

has been observed (Reference 20-141).

As shown by Schulz (References 20-144, 20-145), $O_2^{\ddagger}$ may also be excited by electron impact. The cross-sections of Schulz have been integrated over a Boltzmann distribution by Ali (Reference 20-64), whose results are displayed in Figure 20-7.

### 20.3.2.2 $O_2(a\ ^1\Delta_g)$ AND $(b\ ^1\Sigma_g^+)$

Perhaps the most abundant metastable state in the upper atmosphere is the $(a\ ^1\Delta_g)$ state of oxygen, which is produced in the D-region by the photodissociation of ozone (Reference 20-146):

$$O_3 + h\nu\ (\text{Hartley continuum}) \rightarrow O_2(a\ ^1\Delta_g) + O(^1D) \ . \qquad (20\text{-}27)$$

This produces a density of approximately $10^{10}$ $(a\ ^1\Delta_g)$ molecules $cm^{-3}$ in the normal atmosphere at altitudes in the vicinity of 50 km (References 20-147, 20-148). Another mechanism which may contribute, particularly in the disturbed atmosphere, is (Reference 20-149):

$$O(^3P) + O_3 \rightarrow O_2 + O_2(a\ ^1\Delta_g) \ , \qquad (20\text{-}28)$$

with a reported rate constant $k \approx 4.5 \times 10^{-15}\ cm^3\ sec^{-1}$. Collisional energy transfer from $O(^1D)$ may produce the $(b\ ^1\Sigma_g^+)$ state of oxygen (References 20-150, 20-151):

$$O(^1D) + O_2(X\ ^3\Sigma_g^-) \rightarrow O(^3P) + O_2(b\ ^1\Sigma_g^+,\ v \leq 2) \ . \qquad (20\text{-}29)$$

Noxon (Reference 20-151) observed the decay of 6300Å radiation and the rise of 7618Å radiation, thereby measuring the rate constant $k = 9 \times 10^{-11}\ cm^3\ sec^{-1}$. This reaction is probably important in aurorae (Reference 20-152). Electronically excited oxygen may also be produced efficiently by the impact of relatively low-energy electrons. Cartwright et al (Reference 20-113) have measured $(a\ ^1\Delta_g)$, $(b\ ^1\Sigma_g^+)$, $(c\ ^1\Sigma_u^-)$, $(A\ ^3\Sigma_u^+)$, and $(B\ ^3\Sigma_u^-)$ electron excitation cross-sections. They find that excitation of the $(c\ ^1\Sigma_u^-)$ and of the $(B\ ^3\Sigma_u^-)$ states yields dissociation into two $O(^3P)$ atoms and $O(^3P) + O(^1D)$, respectively, but produces little direct radiation. The cross-sections for excitation of $(a\ ^1\Delta_g)$ and $(b\ ^1\Sigma_g^+)$ are shown in Figure 20-8.

The $O_2(a\ ^1\Delta_g)$ state is quite stable. Its behavior is documented in a monograph (Reference 20-153). Data on $O_2(^1\Delta_g)$ quenching have shown excellent agreement, according to the review of Clark and Wayne (Reference 20-154). The most reliable values (excluding the data of Reference 20-155) are given in Table 20-6. It is obvious from these data that molecular oxygen is the dominant quenching partner in the atmosphere, a fact confirmed by Evans' interpretation of $O_2(^1\Delta_g)$ emission at 1.27μm in the atmosphere (Reference 20-148).

It was suggested by Megill and Hasted (Reference 20-161) in relation to polar-cap absorption events, and by Kummler and Bortner (Reference 20-162) with respect to disturbed atmospheres, that $O_2(a\ ^1\Delta_g)$ might be effective in detaching electrons from $O_2^-$ by:

$$O_2^- + O_2(a\ ^1\Delta_g) \rightarrow 2O_2 + e\ , \qquad (20\text{-}30)$$

in a deexcitation-detachment reaction analogous to a Penning ionization reaction. Subsequent investigations have verified the rapidity of the reaction (References 20-163, 20-164), which has a rate constant $k \approx 2 \times 10^{-10}$ cm$^3$ sec$^{-1}$, and have indicated that:

$$O^- + O_2(^1\Delta_g) \rightarrow O_3 + e \qquad (20\text{-}31)$$

is rapid as well; $k \approx 3 \times 10^{-10}$ cm$^3$ sec$^{-1}$.

Deexcitation-detachment reactions are particularly significant for the disturbed atmosphere, in which anomalously high 1.27$\mu$m intensities are found, presumably due to $O_2(^1\Delta_g)$ (References 20-165 through 20-167), in some aurorae.

Another channel through which high concentrations of $O_2(a\ ^1\Delta_g)$ may be quenched is radiative $O_2$ dimer formation (References 20-153, 20-168):

$$2O_2(a\ ^1\Delta_g) \rightleftarrows O_4^* \rightarrow 2O_2(X\ ^3\Sigma_g^-) + h\nu\ (6340,\ 7030\text{A})\ . \qquad (20\text{-}32)$$

The same collision leads also to the excitation of the $(b\ ^1\Sigma_g^+)$ state (References 20-168, 20-169):

$$2O_2(a\ ^1\Delta_g) \rightarrow O_2(b\ ^1\Sigma_g^+) + O_2(X\ ^3\Sigma_g^-)\ . \qquad (20\text{-}33)$$

Reaction (20-29) is the dominant source of $O_2(b\ ^1\Sigma_g^+)$ in the atmosphere, and molecular nitrogen is the major quenching agent. There is good agreement between laboratory results ($k_{N_2} = 1.5\text{-}2.5 \times 10^{-15}$ cm$^3$ sec$^{-1}$) and the study of Wallace and Hunten (References 20-10, 20-170) in the upper atmosphere ($k_{N_2} = 1.5 \times 10^{-15}$ cm$^3$ sec$^{-1}$). There is still considerable disagreement over the relative effectiveness of other quenchants, but molecular oxygen appears to

be an order of magnitude less effective than nitrogen ($k_{O_2} \leq 10^{-16}$ $cm^3$ $sec^{-1}$) (Reference 20-10), although the results of Welge (Reference 20-171) ($k_{O_2} \approx 4.5 \times 10^{-16}$ $cm^3$ $sec^{-1}$) indicate that data taken at high pressure may be suspect.

### 20.3.2.3 PRODUCTION AND DESTRUCTION OF THE ($^1S$) AND ($^1D$) STATES OF ATOMIC OXYGEN

The ($^1D$) state of atomic oxygen yields the forbidden red-line radiations (6300 and 6364A) which are prominent in the aurora and dayglow, twilight, and nightglow. In the dayglow, the major source of $O(^1D)$ is photodissociation in the Schumann-Runge continuum (Reference 20-172):

$$O_2 + h\nu\ (> 7.1\ eV) \rightarrow O(^3P) + O(^1D)\ . \qquad (20\text{-}34)$$

Evidence suggests that dissociative recombination may be the dominant source of $O(^1D)$ at night; a recombination rate constant $k = 2.2 \times 10^{-7}$ $cm^3$ $sec^{-1}$ at 300 K is consistent with other available data (Reference 20-128). Zipf (References 20-173, 20-174) studied excited-state formation from the dissociative recombination of $O_2^+$ in afterglows. His results are given in Table 20-7. Note that the sum total of $\alpha$ is equal to twice the rate constant since each recombination electron leads to two product atoms.

In 1931 Chapman (Reference 20-175) suggested that $O(^1S)$ may be formed in the nightglow by the reaction:

$$3\,O(^3P) \rightarrow O_2 + O(^1S)\ . \qquad (20\text{-}35)$$

Young and Black (Reference 20-176) found the three-body rate constant $k = 1.5 \times 10^{-34}$ $cm^6$ $sec^{-1}$, which is consistent with the value required by Chapman's theory. They also found the rate constant $k = 3 \times 10^{-33}$ $cm^6$ $sec^{-1}$ for the reaction:

$$N(^4S) + 2\,O(^3P) \rightarrow NO + O(^1S)\ . \qquad (20\text{-}36)$$

The production and destruction of both $O(^1D)$ and $O(^1S)$ through electron collisions:

$$O(^3P) + e \rightleftharpoons O(^1D \text{ or } ^1S) + e\ , \qquad (20\text{-}37)$$

have been studied extensively by Seaton (Reference 20-177) and applied to atmospheric problems by Hunten and McElroy (Reference 20-42). The latter authors conclude that below 100 km neither excitation nor quenching through electron impact is important in comparison with other excitation and quenching mechanisms. This is not true, however, for the lowest excited states of N, $N^+$, and $O^+$. For these cases superelastic quenching is likely to remain important even below 100 km. In studies of higher density plasma afterglows in helium, Ingraham and Brown (Reference 20-178) showed that superelastic collisions play an important role in heating the electrons in the afterglow. Metastable-metastable collisions leading to Penning ionization are also active. Additional atomic excitation cross-sections have been calculated by Henry et al (Reference 20-179). Henry's values have been integrated over a Boltzmann distribution of electron energies by Ali (Reference 20-54) and these results are illustrated in Figure 20-9.

Data from the flowing-afterglow experiments of Young and Black (Reference 20-176) suggest that the deactivation process:

$$O(^1S) + O(^3P) \rightarrow 2\,O(^1D) \text{ or } O(^1D) + O(^3P)\,, \qquad (20\text{-}38)$$

has a rate coefficient $k = 1.8 \times 10^{-13}$ cm$^3$ sec$^{-1}$, which would make it important in the nightglow (Reference 20-42). Evans and Vallance Jones (Reference 20-180) found in auroral measurements that the effective lifetime for the green line ($^1S \rightarrow {}^1D$) transition was shorter than the predicted lifetime. This decrease in the effective lifetime is confirmed by the decreased intensity of the green line relative to that of the 3914A line of $N_2^+$. It seems unlikely that Reaction (20-38) could account for the observed decrease in lifetime, nor does the stimulated ($^1S \rightarrow {}^1D$) emission reported at high pressures (>100 torr) (Reference 20-181).

From the data gathered by Zipf (Reference 20-10), as well as References 20-136, 20-182, 20-183, it appears that $O(^1S)$ is quenched primarily by molecular oxygen, whenever the density ratio $n_{O_2}/n_O$ is large ($k_{O_2} = (2 - 3) \times 10^{-13}$ cm$^3$ sec$^{-1}$). Quenching by molecular nitrogen is slow ($k_{N_2} < 10^{-16}$ cm$^3$ sec$^{-1}$) (Reference 20-182); and the only other possible atmospheric quenchers are water vapor ($k_{H_2O} \approx 3 \times 10^{-10}$ cm$^3$ sec$^{-1}$) (References 20-184, 20-185) and carbon dioxide ($k_{CO_2} = 3 \times 10^{-13}$ cm$^3$ sec$^{-1}$) (References 20-136, 20-183).

Considerable controversy has centered upon the rates at which $O(^1D)$ is quenched by collisions with various atoms and molecules. Much of the older data and results are discussed in detail by Hunten and McElroy (Reference 20-42), who conclude that molecular nitrogen is the most efficient quencher, with a rate constant $k \approx 8 \times 10^{-11}$ $cm^3\ sec^{-1}$. This value is supported by the work of Carleton et al (Reference 20-186) and by that of McGrath and McGarvey (Reference 20-187), who found that the rate for nitrogen as a quencher exceeds that for oxygen. This subject has been reviewed by Zipf (Reference 20-10), who concurs in the view that nitrogen is the major atmospheric quenchant. Relevant quenching data are summarized in Table 20-8, together with the recommended quenching constant for nitrogen. Clearly the contribution to $O(^1D)$ quenching by oxygen is not negligible.

Hunt (Reference 20-197) and Hampson (Reference 20-198) have demonstrated how very small concentrations of $O(^1D)$ can greatly affect the lower D-region. Hampson, for example, showed that in the stratosphere the free radicals OH and $HO_2$ are present only because of the action of $O(^1D)$ on water vapor. Hunt showed that an ozone concentration in agreement with measured values could be derived only if several $O(^1D)$ reactions involving hydrogen and water were taken into consideration, e.g.:

$$O(^1D) + H_2 \rightarrow OH + H \text{ (assumed } k = 10^{-11}\ cm^3\ sec^{-1}) \quad . \quad (20\text{-}39)$$

Hunt (Reference 20-197) concluded that the concentration of $O(^1D)$ from 40 to 100 km lies between $10^3$ and $10^4$ $cm^{-3}$. This value is probably too large because his assumed rate constants are wrong, but the general conclusion that even small concentrations of $O(^1D)$ are extremely important persists, even when turbulent transport is taken into account (References 20-199, 20-200).

### 20.3.2.4 PRODUCTION AND DESTRUCTION OF $O^+(^2D)$ AND $O^+(^2P)$

The production of both $O^+(^2D)$ and $O^+(^2P)$ occurs in the dayglow through direct photoionization:

$$O(^3P) + h\nu \rightarrow O^+(^4S,\ ^2D,\ \text{or}\ ^2P) + e \quad , \quad (20\text{-}40)$$

and through ionization by photoelectrons:

$$O(^3P) + e \rightarrow O^+(^4S,\ ^2D,\ \text{or}\ ^2P) + 2e \quad . \quad (20\text{-}41)$$

Both excited states can be destroyed through superelastic collisions with electrons, or through superelastic, energy-transfer, or reactive collisions with neutral particles. The rate for deactivation of ions through superelastic electron collision is large (Reference 20-177), giving a quenching frequency in the dayglow of 0.1 $sec^{-1}$, while the transition probabilities for such states are much smaller.

In aurora the $N_2^+$ Meinel radiation is probably affected by the near-resonant reaction (References 20-201, 20-202):

$$O^+(^2D) + N_2(X\,^1\Sigma_g, v=0) \rightarrow O(^3P) + N_2^+(A\,^2\Pi_u, v=1) \quad . \qquad (20\text{-}42)$$

Similarly, the cross-section for the near-resonant reactions:

$$O^+(^2D) + O_2(X\,^3\Sigma_g^-) \rightarrow O(^3P) + O_2^+(a\,^4\Pi_u, v=7) \qquad (20\text{-}43)$$

$$\rightarrow O(^3P) + O_2^+(A\,^2\Pi_u, v=0) \quad , \qquad (20\text{-}44)$$

are large ($k \approx 3 \times 10^{-10}$ $cm^3$ $sec^{-1}$) (References 20-129, 20-131).

Wallace and McElroy (Reference 20-128) tried to match theoretically the observed dayglow emission of the 3914A (B → X) transition of $N_2^+$. Using the excitation mechanisms discussed above, as well as reactions (20-14), (20-15), and (20-17), and the loss reactions:

$$N_2^+ + e = N + N \quad , \qquad (20\text{-}45)$$

$$N_2^+ + O = NO^+ + N \quad . \qquad (20\text{-}46)$$

and

$$N_2^+ + O_2 = N_2 + O_2^+ \quad , \qquad (20\text{-}47)$$

a fit of the data gives the values of $k_{45}$, $k_{46}$, and $k_{47}$ shown in the second column of Table 20-9.

At twilight the first negative bands have a high rotational temperature, suggesting a source of $N_2^+(B)$ which gives high rotational temperatures, such as the charge transfer of $O^+(^2D)$ with $N_2$ might provide. If the rate coefficient for this charge-transfer reaction is

taken as $k = 2 \times 10^{-9}$ cm$^3$ sec$^{-1}$, Dalgarno and McElroy (Reference 20-111) found that the reaction rate constants $k_{46}$ and $k_{47}$ are not greatly changed, but that $k_{45}$ must be increased by a factor of six to give the measured 3914A emission data (see Table 20-9, column 3). It is interesting to note that this change is brought about by $O^+(^2D)$ ion densities as low as 100 cm$^{-3}$.

### 20.3.3 Metallic Ions

It has been deomonstrated (Reference 20-203) that metallic ions are present in the D-region. Since these species are atomic and will tend therefore to recombine slowly with electrons (though faster with negative ions), it is important to study their reaction rates with the various molecular atmospheric species. Ground-state metallic ions, owing to their low energy, will not readily enter into charge-transfer or ion-molecule reactions. However, ions which are in excited states may quickly be converted to molecular ions through ion-molecular reactions, or transfer their charge directly to molecular species. In atmospheric detonations of nuclear devices, where tremendous energy and much metallic debris are deposited in the atmosphere, a large fraction of the metallic ions which are formed may be excited. For $Na^+$, $Fe^+$, $Al^+$, and a few other metallic ions, Fogel (Reference 20-204) and Layton (Reference 20-205) have shown that excitation has a marked effect upon the cross-sections measured at kilovolt energies. As the ionizing electron energy is increased in the ion source, so that excited ions are added to the beam, the total measured cross-section varies markedly.

Observation of metallic ion populations have also led to speculation about vibrational temperatures. Without an elevated oxygen vibrational temperature at 110 km, Ferguson et al (Reference 20-206) could not explain the observed atmospheric $Si^+/SiO^+$ ratio. However, as noted by Bauer et al (Reference 20-56), it is difficult to reconcile an elevated oxygen vibrational temperature with known $O_2^*$ deactivation rates by atomic oxygen.

## 20.4 REACTION RATES FOR REACTIONS INVOLVING EXCITED SPECIES

The reaction rates and cross-sections listed in Table 20-10 represent a considerable portion of the information available on excited-state production and destruction processes involving atmospheric species. The format of Chapters 16 through 19 of this Handbook has not been followed in the presentation of these data, since their accuracy

and the incompleteness of most studies do not permit it. The temperature dependence of most reaction coefficients is not given; the temperature at which the measurements were made is given instead. Also included are the general types of experiments used, with appropriate references, in obtaining the data quoted.

During the compilation of Table 20-10, it became clear that most of the information on energy transfer and the excitation of long-lived excited atoms, ions, and molecules is limited to reactions where the products are only inferred and for which temperature dependences are as yet unmeasured. Clearly, the detailed study of both reaction products and energy dependences is essential to future progress in this field.

Table 20-1. Radiative lifetimes and transitions for principal atmospheric species.

| Species and State | Mean Radiative Lifetime (sec) | Principal Transition; λ (in A); Name of Transition | Approx. $\Delta E_{if}$ (eV) | References |
|---|---|---|---|---|
| ATOMS AND ATOMIC IONS | | | | |
| $C(^3P)$ | Ground State | | | |
| $(^1D)$ | $3.2 \times 10^3$ | $^3P - {}^1D$ ; 9823, 9850 | 1.26 | 20-8 |
| $(^1S)$ | 2.0 | $^1D - {}^1S$ ; 8727 | 1.42 | 20-8 |
| $(2p^3\ {}^5S^o)$ | 0.03 | $^3P - {}^5S$ ; 2965, 2967 | 4.18 | 20-8 |
| $C^+(^2P^o)$ | Ground State | | | |
| $(^4P)$ | Mod. long | $^2P^o - {}^4P$ ; ~2330 | 5.35 | 20-9 |
| $N(^4S^o)$ | Ground State | | | |
| $(^2D^o_{3/2})$ | $6.1 \times 10^4$ | $^4S^o - {}^2D^o_{3/2}$ ; 5200 (nebular) | 2.38 | 20-8, 20-10 |
| $(^2D^o_{1/2})$ | $1.4 \times 10^5$ | $^4S^o - {}^2D^o_{5/2}$ ; 5201 | 2.38 | 20-8, 20-10 |
| $(^2P^o)$ | 13 | $^2D^o - {}^2P^o$ ; 10,396; 10,404 | 1.19 | 20-8, 20-10 |
| $(3s\ {}^4P)$ | $2.5 \times 10^{-9}$ | $^4S^o - {}^4P$ ; 1200, 1201 | 10.31 | 20-11 |
| $N^+(^3P)$ | Ground State | | | |

Table 20-1. (Cont'd.)

| Species and State | Mean Rociative Lifetime (sec) | Principal Transition; λ (in A); Name of Transition | Approx. $\Delta E_{if}$ (eV) | References |
|---|---|---|---|---|
| ATOMS AND ATOMIC IONS (Cont'd.) | | | | |
| $N^+(^1D)$ | 250 | $^3P \leftarrow {}^1D$ ; 6584, 6548 | 1.89 | 20-8, 20-10 |
| $(^1S)$ | 0.90 | $^1D \leftarrow {}^1S$ ; 5755 | 2.15 | 20-8 |
| $O(^3P)$ | Ground State | | | |
| $(^1D)$ | 148 | $^3P \leftarrow {}^1D$ ; 6300, 6364 (red lines) | 1.96 | 20-8, 20-12, 20-13 |
| $(^1S)$ | 0.80 | $^1D \leftarrow {}^1S$ ; 5577 (green line) | 2.22 | 20-239 |
| $(3s\ ^5S^o)$ | 0.0006 | $^3P \leftarrow {}^5S^o$ ; 1356, 1359 | 9.13 | 20-8 |
| $(3s\ ^3S^o)$ | $1.8 \times 10^{-9}$ | $^3P \leftarrow 3S^o$ ; 1302, 1305, 1306 | 9.51 | 20-14 |
| $O^+(^4S^o)$ | Ground State | | | |
| $(^2D^o_{3/2})$ | $5.9 \times 10^3$ | $^4S^o \leftarrow {}^2D^o_{3/2}$ ; 3726 (nebular) | 3.33 | 20-8, 20-10 |
| $(^2D^o_{5/2})$ | $2.1 \times 10^4$ | $^4S^o \leftarrow {}^2D^o_{5/2}$ ; 3729 | 3.32 | 20-8, 20-10 |
| $(^2P^o_{1/2})$ | 5.4 | $^2D^o \leftarrow {}^2P^o_{1/2}$ ; 7319, 7330 (auroral) | 1.69 | 20-8, 20-10 |

Table 20-1. (Cant'd.)

| Species and State | Mean Radiative Lifetime (sec) | Principal Transitian; λ (in A); Name af Transitian | Approx. $\Delta E_{if}$ (eV) | References |
|---|---|---|---|---|
| ATOMS AND ATOMIC IONS (Cant'd.) | | | | |
| $O^+(^2p^a{}_{3/2})$ | 4.2 | $^2D^a \leftarrow {}^2p^a{}_{3/2}$ ; 7319, 7330 | 1.69 | 20-8, 20-10 |
| DIATOMIC MOLECULES AND MOLECULAR IONS[a] | | | | |
| $N_2(X\,^1\Sigma_g^+)$ | Ground State | | | |
| $(A\,^3\Sigma_u^+)$ | 1.3 ($F_2$); 2.7 ($F_1$, $F_3$) | A → X (Vegard-Kaplan) | 6.2 | 20-10, 20-15, 20-16 |
| $(B\,^3\Pi_g)$ | $8.0 \times 10^{-6}$ | B → A; 10,510 (first positive) | 1.2 | 20-17, 20-18 |
| $(W\,^3\Delta_u)$ | Lang | W → X<br>W → B | 7.4<br>0.003 | 20-19 |
| $(B'\,^3\Sigma_u^-)$ | $10^{-5}$ est. | B' → B (Y bands) | 0.8 | 20-9 |
| $(a'\,^1\Sigma_u^-)$ | ≥0.04 | a' → X (Wilkinsan) | 8.4 | |
| $(a\,^1\Pi_g)$ | $1.4 \times 10^{-4}$ | a → X; 1450 (Lyman-Birge-Hapfield)[c] | 8.6 | 20-20 |
| $(w\,^1\Delta_u)$ | $10^{-4}$ est. | w → a; 36,400 | 0.3 | 20-9 |
| $N_2^+(X\,^2\Sigma_g^+)$ | Ground State | | | |

Table 20-1. (Cont'd.)

| Species and Stote | Mean Rod ative Lifetime (sec) | Principal Transition; λ (in A); Nome of Tronsition | Approx. $\Delta E_{if}$ (eV) | References |
|---|---|---|---|---|
| DIATOMIC MOLECULES AND MOLECULAR IONS (Cont'd.) | | | | |
| $N_2^+(A\ ^2\Pi_u)$ | $1.2 \times 10^{-5}$ (v = 3) | A → X; 11,036 (Meinel) | 1.0 | 20-18 |
| $(B\ ^2\Sigma_u^+)$ | $5.9 \times 10^{-8}$ | B → X; 3914 (first negotive) | 3.2 | 20-21 through 20-23 |
| $(^4\Sigma_u^+)$ | Mod. Long | $^4\Sigma_u^+ \rightarrow X$ | ~6 | 20-9 |
| $NO(X\ ^2\Pi)$ | Ground State | | | |
| $(a\ ^4\Pi)$ | ~0.16 | a → X | 4.7 | 20-24, 20-25 |
| $(A\ ^2\Sigma^+)$ | $2.0 \times 10^{-7}$ | A → X; 2265 (γ bands) | 5.5 | 20-26, 20-27 |
| $(B\ ^2\Pi)$ | $3.6 \times 10^{-6}$ | B → X; (β bonds) | 5.6 | 20-26 |
| $NO^+(X\ ^1\Sigma^+)$ | Ground State | | | |
| $(a\ ^3\Sigma^+)$ | Long | o → X | 6.4 | 20-28 |
| $(b\ ^3\Pi)$ | $1.4 \times 10^{-4}$ | b → a | 0.9 | 20-29 |
| $(w\ ^3\Delta)$ | $\sim 10^{-4}$ est. | w → b | 0.3 | 20-9 |

Table 20-1. (Cont'd.)

| Species and State | Mean Radiative Lifetime (sec) | Principal Transition; λ (in A); Name of Transition | Approx. $\Delta E_{if}$ (eV) | References |
|---|---|---|---|---|
| DIATOMIC MOLECULES AND MOLECULAR IONS (Cont'd.) | | | | |
| $NO_2(^2B_1)$ [d] | $5.5 \times 10^{-5}$ to $9.0 \times 10^{-5}$ | $A\ ^2B_1 \rightarrow X\ ^2A_1$ | | 20-30, 20-31 |
| $O_2(X\ ^3\Sigma_g^-)$ | Ground State | | | |
| $(a\ ^1\Delta_g)$ | $3.9 \times 10^3$ | a → X; 12,680 (infrared atmospheric) | 0.98 | 20-12, 20-13, 20-32 |
| $(b\ ^1\Sigma_g^+)$ | 12 | b → X; 7619 (atmospheric) | 1.63 | 20-12, 20-33, 20-34 |
| $(c\ ^1\Sigma_u^-)$ | Long | c → X; 2856 (Herzberg II) | 4.0 | 20-35 |
| $(C\ ^3\Delta_u)$ | Long | C → X (Herzberg III)<br>C → a | ~4.2 | 20-9 |
| $(A\ ^3\Sigma_u^+)$ | 0.03 | A → X; 2856 (Herzberg I)<br>A → b; 4586 (Broida-Goydon) | 4.3 | 20-36 |
| $(B\ ^3\Sigma_u^-)$ | $4.2 \times 10^{-6}$ | B → X; 2030 (Schumann-Runge) | 6.1 | 20-37 |
| $O_2^+(X\ ^2\Pi_g)$ | Ground | | | |
| $(a\ ^4\Pi_u)$ | Long | a → X; 6026 | 4.0 | 20-9 |

Table 20-1. (Cant'd.)

| Species and State | Mean Radiative Lifetime (sec) | Principal Transitian; λ(in A); Name af Transitian | Approx. $\Delta E_{if}$ (eV) | References |
|---|---|---|---|---|
| DIATOMIC MOLECULES AND MOLECULAR ICNS (Cant'd.) | | | | |
| $O_2^+(A\ ^2\Pi_u)$ | $7 \times 10^{-7}$ | A – X (secand negative)[b] | 5.0 | 20-38, 20-39 |
| $(b\ ^4\Sigma_g^-)$ | $1.1 \times 10^{-6}$ | b → a; 6026 (first negative) | 2.1 | 20-38, 20-39 |

Nates

[a] The quated lifetime is far the v = 0 level, and the wavelength and energy are far the (0,0) transitian.

[b] The much shorter lifetime measured by Copeland (Reference 20-40) has been disregarded since it would give an unreasanably large transitian moment (Reference 20-9).

[c] It is passible that the quoted lifetime is actually that af the w state, which cascades ta the a state, while the true lifetime af the a state is about $1 \times 10^{-5}$ sec, as obtained by Jeunehomme (Reference 20-41).

[d] This triatomic malecule is included at this paint far the sake af cantinuity with the NO and $NO^+$ species preceding.

Table 20-2. Energy transfer from $N_2^{\ddagger}$.

| Level, v | Collision Partner | Probable Product | Rate Constant ($cm^3\ sec^{-1}$) | Temp. Range (K) | References |
|---|---|---|---|---|---|
| 1 | $N_2$ | Kinetic Energy | $1.3 \times 10^{-11}\ Te^{-220/T^{1/3}}$ | 300-5000 | 20-94 |
| | | $N_2^{\ddagger}$ (Resonant VV) | $3 \times 10^{-13}$ | 300 | |
| 1 | $O_2$ | Kinetic Energy | $\frac{2.5 \times 10^{-7}\ e^{-263T^{-1/3}}}{(1 - e^{-3390/T})}$ | 1000-10,000 | 20-82* |
| | | $O_2^{\ddagger}$ (Non-Resonant VV) | | | |
| 1 | O | Kinetic Energy | $\frac{6.21 \times 10^{-14}\ Te^{-51.5/T^{1/3}}}{(1 - e^{-3990/T})}$ or $\frac{3.43 \times 10^{-12}\ Te^{-152/T^{1/3}}}{(1 - e^{-3990/T})}$ | 3000-4500 | 20-95, 20-96 |
| 1 | $CO_2$ | $CO_2^{\ddagger}$ (Near Resonant VV) | $6 \times 10^{-13}\left(\frac{T}{300}\right)^{-1/2}$ | 300-1200 | 20-82 |
| ≥4 | $N_2O$ | $N_2O^{\ddagger}$ | $2.5 \times 10^{-14}$ | 300 | 20-54 |
| ≥1 | Ar | Kinetic Energy | $2.5 \times 10^{-16}$ | 300 | 20-54 |
| 1 | NO | $NO^{\ddagger}$ (Non-Resonant VV) | $1.5 \times 10^{-16}$ | 300 | 20-94 |

*Note that the rate constants for VT from Reference 20-82 must be divided by $(1-e^{-\theta_v/T})$ to obtain rate equations of the conventional form.

Table 20-3. Rate constants (units of $10^{-12}$ $cm^3$ $sec^{-1}$) for the reaction $N_2^{\ddagger} + O^+ \rightarrow NO^+ + N$ for a range of vibrational and translation temperatures (Reference 20-91).

| Translation Temperature, $T_{tr}$ (K) | Vibrational Temperature, $T_v$ (K) | | | | | | | | | | |
|---|---|---|---|---|---|---|---|---|---|---|---|
| | 300 | 1000 | 1500 | 2000 | 2500 | 3000 | 3500 | 4000 | 5000 | 6000 | 7000 |
| 300 | 1.3[a] | 1.4[a] | 2.1[a] | 4.2 | 7.8 | 12.6 | 18.2 | 24.0 | 35.7 | 46.2 | 55.1 |
| 1000 | 0.7[a] | 0.9 | 2.0 | 4.9 | 9.5 | 15.4 | 22.1 | 29.0 | 42.5 | 54.3 | 64.2 |
| 1500 | 0.6 | 0.9 | 2.3 | 5.5 | 10.6 | 16.9 | 24.0 | 31.2 | 45.0 | 57.0 | 67.0 |
| 2000 | 0.6 | 1.0 | 2.7 | 6.4 | 11.9 | 18.6 | 26.0 | 33.4 | 47.4 | 59.5 | 69.4 |
| 2500 | 0.8 | 1.3 | 3.1 | 7.6 | 13.6 | 20.7 | 28.3 | 36.0 | 50.2 | 62.3 | 72.1 |
| 3000 | 1.1 | 1.8 | 4.3 | 9.0 | 15.5 | 23.1 | 31.0 | 38.9 | 53.4 | 65.5 | 75.2 |
| 3500 | 1.6 | 2.5 | 5.4 | 10.7 | 17.7 | 25.7 | 34.0 | 42.1 | 56.7 | 68.9 | 78.5 |
| 4000 | 2.3 | 3.4 | 6.8 | 12.6 | 20.2 | 28.6 | 37.2 | 45.4 | 60.3 | 72.4 | 82.0 |
| 5000 | 4.4 | 6.0 | 10.4 | 17.3 | 25.8 | 35.0 | 44.0 | 52.6 | 67.7 | 79.7 | 89.1 |
| 6000 | 7.5 | 9.6 | 14.9 | 22.9 | 32.3 | 42.1 | 51.5 | 60.3 | 75.4 | 87.3 | 96.3 |
| 7000 | 11.7 | 14.2 | 20.5 | 29.5 | 39.6 | 49.8 | 59.5 | 68.3 | 83.3 | 94.8 | 103.5 |

[a]For these values, the dominant contribution comes from a low-energy mechanism.

Table 20-4. Quenching data for $N_2(A^3\Sigma_u^+)$.

| Quenchant | Rate Constant ($cm^3\ sec^{-1}$) | References |
|---|---|---|
| $N_2$ | $< 3 \times 10^{-19}$ | 20-116 |
| | $< 1.2 \times 10^{-18}$ | 20-117 |
| $O_2$ | $< 4 \times 10^{-10}$ | 20-42 |
| | $3.8 \times 10^{-12}$ | 20-121 |
| O | $\leq 3 \times 10^{-11}$ | 20-42 |
| N | $5 \times 10^{-11}$ | 20-122 |
| | $5 \times 10^{-12}$ | 20-123 |
| | $5 \times 10^{-11}$ | 20-124 |
| NO | $7 \times 10^{-11}$ | 20-125 |

Table 20-5. Deactivation of $O_2^{\ddagger}$ (v = 1).

| Reaction | Rate Constant, $k_{10}$ ($cm^3\ sec^{-1}$) | T Range (K) | References |
|---|---|---|---|
| $O_2^{\ddagger} + M \rightarrow O_2 + M$ <br> $M = N_2$ or $O_2$ | $\frac{2.5 \times 10^{-12}\ T \exp[-(2.95 \times 10^6/T)]^{1/3}}{(1 - e^{-2270/T})}$ | 800-3200 | 20-82 |
| $O_2^{\ddagger} + O \rightarrow O_2 + O$ | $3.3 \times 10^{-13}\ T^{1/2} \exp(-483/T)$ | 300-1700 | 20-79*, 20-142 |
| | $1.7 \times 10^{-10} \exp(-4000/T)$ | 2000-4000 | 20-143 |
| $O_2^{\ddagger} + H_2O \rightarrow O_2 + H_2O^{\ddagger}$ | $10^{-(12\pm1)}(T/300)^{-1/2}$ | | 20-82 |

*Assuming that reaction occurs as fast as isotopic exchange.

Table 20-6. Quenching data for $O_2(^1\Delta_g)$.

| Quenching Species | Rate Constant ($cm^3\ sec^{-1}$) | References |
|---|---|---|
| $O_2$ | $2.4 \times 10^{-18}$ | 20-154 |
| | $2.2 \times 10^{-18}$ | 20-156 |
| | $2.2 \times 10^{-18}$ | 20-157 |
| | $2.0 \times 10^{-18}$ | 20-158 |
| $N_2$ | $< 1.1 \times 10^{-19}$ | 20-148 |
| $CO_2$ | $3.9 \times 10^{-18}$ | 20-154 |
| $H_2O$ | $1.5 \times 10^{-17}$ | 20-154 |
| Ar | $\leq 2.1 \times 10^{-19}$ | 20-154 |
| O | $\leq 1.3 \times 10^{-16}$ | 20-159 |
| N | $(2.8 \pm 2) \times 10^{-15}$ | 20-159 |
| $O_3$ | $3 \times 10^{-15}$ | 20-160 |

Table 20-7. Dissociative recombination of $O_2^+$ with electrons (Reference 20-174).

| $O_2^+ + e \rightarrow O^* + O^{**}$ | Product Ratio | Rate constant[a] ($cm^3\ sec^{-1}$) for Production at 300 K |
|---|---|---|
| Total $O^*(^1S)$ | 0.1 | $2.1 \times 10^{-8}$ |
| Total $O^*(^1D)$ | 0.9 | $1.9 \times 10^{-7}$ |
| Total $O(^3P)$ | 1 | $2.1 \times 10^{-7}$ |

[a] The rate constant is defined here in terms of the individual species production and not in terms of $O_2^+$ disappearance.

Table 20-8. Quenching of $O(^1D)$ by various gases, relative to molecular nitrogen. ($k_{N_2} \approx 8 \times 10^{-11}$ cm$^3$ sec$^{-1}$)[o]

| Quencher | Source of Data (Reference No.) | | | | | | | | | |
|---|---|---|---|---|---|---|---|---|---|---|
| | 20-121 | 20-188 | 20-189, 20-190 | 20-150 | 20-151 | 20-191 | 20-192, 20-193 | 20-194 | 20-195 | 20-196 |
| He | | | 0.077 | | | | | | | |
| Ar | | 0.046 | | <0.036 | | | | | <0.002 | |
| Kr | | 0.25 | 0.35 | | | | | | | |
| Xe | 2.5 | 3.2 | 0.32 | | | | | | | |
| $N_2$ | 1.00 | 1.00 | 1.00 | 1.00 | 1.00 | 1.00 | 1.00 | 1.00 | 1.00 | 1.00 |
| $CO_2$ | | 4.20 | 3.50 | 4.7 | 0.3 | 15. | | | 4.35 | 0.038 |
| $H_2O$ | | 4.25 | 9.2 | 3.6 | | 28. | | | 5.0 | |
| $NO_2$ | | 6.75 | | | | | | | | |
| $O_2$ | 7.5 | | | 0.82 | 0.60 | 2.1 | 1.0 | 0.25 | 1.0 | |

[o] References 20-10, 20-42, 20-186, 20-187.

Table 20-9. Calculated reaction coefficients.

| | With No $O^+(^2D)$ Source ($cm^3$ $sec^{-1}$) | With $O^+(^2D)$ Reaction Included ($cm^3$ $sec^{-1}$) |
|---|---|---|
| $k_{45}$ | $6 \times 10^{-8}$ | $3.5 \times 10^{-7}$ |
| $k_{46}$ | $7 \times 10^{-11}$ | $1 \times 10^{-10}$ |
| $k_{47}$ | $9 \times 10^{-11}$ | $5 \times 10^{-11}$ |

Table 20-10. Excitation and deexcitation rate coefficients or cross sections.[a]

| Reaction | (1) Reaction Coefficient ($cm^3\ sec^{-1}$) or (2) Cross-Section ($cm^2$) | Temperature or Energy | Type of Experiment | References |
|---|---|---|---|---|
| ELECTRON-IMPACT EXCITATION AND DEEXCITATION | | | | |
| A major review of electron-impact excitation rates is being performed under the sponsorship of the Data Center at the Joint Institute for Laboratory Astrophysics. For application to the atmosphere see Reference 20-207. | | | Beams and Fast-flowing System[b] | 20-208 |
| $e + H(1S) \rightarrow e + H(^2P)$ | (2) $6 \times 10^{-17}$ (max) | 30-50 eV | b | 20-209 |
| $\rightarrow e + H(^2S)$ | (2) $1.0 \times 10^{-17}$ (max) | 12 eV | b | 20-210 |
| $e + Na(3^2S) \rightarrow e + Na(3^2P)$ | (2) $2 \times 10^{-15}$ (max) | 10 eV | b | 20-211 |
| $e + He(1^1S) \rightarrow e + He^*(2^3S)$ | (2) $3 \times 10^{-18}$ (max) | 20.6 eV | b | 20-212 |
| $e + He^*(2^1S) \rightarrow e + He^*(2^3S)$ | (2) $3 \times 10^{-14}$ | 0.025 eV | Static afterglow | 20-178, 20-213 |
| $e + N^*(^2D) \rightarrow e + N(^4S)$ | (1) $5 \times 10^{-10}$ | 1000 K | Theary | 20-177 |
| $e + N^*(^2P) \rightarrow e + N(^4S)$ | (1) $2 \times 10^{-9}$ | 1000 K | Theary | 20-177 |

Table 20-10. (Cont'd.)

| Reaction | (1) Reaction Coefficient ($cm^3\ sec^{-1}$) or (2) Cross-Section ($cm^2$) | Temperature or Energy | Type of Experiment | References |
|---|---|---|---|---|
| ELECTRON-IMPACT EXCITATION AND DEEXCITATION (Cont'd.) | | | | |
| $e + O^*(^1D) \rightarrow e + O(^3P)$ | (1) $1.5 \times 10^{-9}$ | 1000 K | Theory | 20-177 |
| $e + O^*(^1S) \rightarrow e + O(^3P)$ | (1) $1.8 \times 10^{-9}$ | 1000 K | Theory | 20-177 |
| $e + N_2 \rightarrow e + N_2^{\ddagger}$ | (2) $6 \times 10^{-16}$ | 2.3 eV | b, Theory | 20-59, 20-61 |
| $e + N_2 \rightarrow e + N_2^*(C, v=0)$ | (2) $1.6 \times 10^{-17}$ (max) | 17 eV | b | 20-214 |
| $e + CO \rightarrow e + CO^{\ddagger}$ | (2) $8 \times 10^{-16}$ (max) | 1.75 eV | b | 20-59 |
| $e + H_2 \rightarrow e + H_2^{\ddagger}$ | (2) $6 \times 10^{-17}$ (max) | 2 eV | b | 20-59 |
| $e + N_2 \rightarrow 2e + N_2^+(B)$ | (2) $9.5 \times 10^{-18}$ (max) | 90 eV | b | 20-215 |
| $e + N_2O^{\ddagger} \rightarrow N_2 + O^-$ | (2) $8.3 \times 10^{-18}$ | 2.3 eV | b | 20-216 |

Table 20-10. (Cont'd.)

| Reaction | (1) Reaction Coefficient ($cm^3\ sec^{-1}$) or (2) Cross-Section ($cm^2$) | Temperature or Energy | Type of Experiment | References |
|---|---|---|---|---|
| TWO-BODY REACTIONS | | | | |
| $O^*(^1S) + O(^3P) \rightarrow O(^1D) + O(^1D \text{ or } ^3P)$ | (1) $1.8 \times 10^{-13}$ | 300 K | Flowing afterglow | 20-176 |
| $O^*(^1S) + N_2O \rightarrow O + N_2O$ | (1) $6 \times 10^{-13}$ | 300 K | Flowing afterglow | 20-176 |
| $O^*(^1S) + O_2 \rightarrow O + O_2$ | (1) $1 \times 10^{-13}$ | 300 K | Flowing afterglow | 20-176 |
| $O^*(^1S) + CO_2 \rightarrow O + CO_2$ or $O_2 + CO$ | (1) $2.5 \times 10^{-14}$ | 300 K | Flowing afterglow | 20-176 |
| $O^*(^1S) + N_2 \rightarrow O + N_2$ | (1) $< 10^{-17}$ | 300 K | Flowing afterglow | 20-176 |
| $O^*(^1D) + N_2 \rightarrow O(^3P) + N_2$ | (1) $8 \times 10^{-11}$ | 300 K | Atmospheric, Flowing afterglow | Table 20-8 |
| $O^*(^1D) + O_2 \rightarrow O(^3P) + O_2$ | (1) $9 \times 10^{-11}$ | 300 K | Atmospheric, Flowing afterglow | Table 20-8 |
| $O^+(^2D) + N_2 \rightarrow O(^3P) + N_2^+$ | (1) $\sim 3 \times 10^{-10}$ | | b | 20-129 |
| $O^+(^2D) + O_2 \rightarrow O(^3P) + O_2^+$ | (1) $\sim 3 \times 10^{-10}$ | | b | 20-129 |

Table 20-10. (Cont'd.)

| Reaction | (1) Reaction Coefficient ($cm^3$ $sec^{-1}$) or (2) Cross-Section ($cm^2$) | Temperature or Energy | Type of Experiment | References |
|---|---|---|---|---|
| TWO-BODY REACTIONS (Cont'd.) | | | | |
| $O + O_3 \rightarrow O_2 + O_2(o\ ^1\Delta_g)$ | (1) $4.5 \times 10^{(-15\pm2)}$ | 300 K | Flowing afterglow | 20-149 |
| $O_2^{\ddagger}(X,\ v \geq 17) + O_3 \rightarrow 2O_2 + O^*(^1D)$ | (1) Large | 300 K | Flosh photolysis | 20-217 |
| $O_2^*(a\ ^1\Delta_g) + O_2 \rightarrow O_2(X) + O_2$ | (1) $2.4 \times 10^{-18}$ | 300 K | Flowing afterglow | 20-153, 20-154 |
| $O_2^*(a\ ^1\Lambda_g) + O_2^- \rightarrow 2O_2 + e$ | (1) $2 \times 10^{-10}$ | 300 K | Flowing afterglow | 20-161, 20-163 |
| $O_2^*(a\ ^1\Delta_g) + O^- \rightarrow O_3 + e$ | (1) $3 \times 10^{-10}$ | 300 K | Flowing afterglow | 20-163 |
| $O_2^*(a\ ^1\Delta_g) + N \rightarrow NO + O$ | (1) $(2.8\pm2) \times 10^{-15}$ | 300 K | Flowing afterglow | 20-159 |
| $O_2^*(b\ ^1\Sigma_g^+) + O_3 \rightarrow 2O_2 + O$ | (1) $6 \times 10^{-13}$ | 300 K | Flowing afterglow | 20-218 |
| $O_2^+ + e \rightarrow O^* + O^{**}$ | (1) See Table 20-7 | 300 K | Flowing afterglow | 20-173 |
| $N^*(^2D) + O_2 \rightarrow NO + O$ | (1) $4 \times 10^{-13}\ T^{1/2}$ | 236-365 K | Flash photolysis | 20-219 |

Table 20-10. (Cont'd.)

| Reaction | (1) Reaction Coefficient ($cm^3\ sec^{-1}$) or (2) Cross-Section ($cm^2$) | Temperature or Energy | Type of Experiment | References |
|---|---|---|---|---|
| TWO-BODY REACTIONS (Cnnt'd.) | | | | |
| $N + NO \rightarrow N_2^{\ddagger}(X,\ v \approx 8) + O(^3P)$ | (1) $2.2 \times 10^{-11}$ | 300 K | Flowing ofterglow | 20-116 |
| $N + N_2(X) \rightarrow N + N_2^*(A)$ | (1) $1.9 \times 10^{-6} T^{-3/2} \exp(-E_{XA}/kT)$ | | Shocks | 20-124 |
| $N_2 + N_2(X) \rightarrow N_2^* + N_2(A)$ | (1) $k(N_2) \leq 0.01\, k(N)$ | | Active discharge, Shocks | 20-124 |
| $A^{\ddagger} + B \rightarrow A + B^{\ddagger}$ | Consideroble literoture is ovoiloble on this type of reoction. The generol agreement of vibrotionol energy transfer assaciated with lower vibrational levels is encouroging. | | Flomes, Flosh photolysis, Shocks, Theory | 20-73, 20-75 20-82 |
| $A + BC^{\ddagger} \rightarrow AB + C$ | Consideroble literoture on this subject of o non-atmospheric noture hos been generoted by Polonyi ot the University of Toronto. (Cf. the listed references.) | | | 20-220, 20-221 |
| $NO^*(A, v=x) + N_2(X, v=0) \rightarrow NO^*(A, v=x-1) + N_2^{\ddagger}(X, v=1)$ | (1) Very lorge | 300 K | Flosh photolysis, Theory | 20-73, 20-75 |

Table 20-10. (Cont'd.)

| Reaction | (1) Reaction Coefficient ($cm^3\ sec^{-1}$) or (2) Cross-Section ($cm^2$) | Temperature or Energy | Type of Experiment | References |
|---|---|---|---|---|
| TWO-BODY REACTIONS (Cont'd.) | | | | |
| $N_2^{\pm}(X,v) + O^- \rightarrow NO^+ + N$ | (1) See Table 20-3 | 300 K | Flowing afterglow | 20-88 |
| $N_2^{\pm}(X,v \geq 7) + Na(3^2S) \rightarrow N_2 + Na^+$ | (1) $\sim 10^{-10}$ | 300 K | Flowing afterglow | 20-86 |
| $N_2^{\pm}(X,v \geq 4) + M = N_2(X,v < 4) + M$ | (1) See Table 20-2 | ~300 K | Flowing afterglow | 20-42, 20-54, 20-85, 20-86, 20-88 |
| $N_2^*(A) + N_2 \rightarrow N_2(X) + N_2$ | (1) $< 3 \times 10^{-19}$ | 300 K | High pressure chemical reactions | 20-116 |
| $N_2^*(A) + O_2 \rightarrow N_2 + (O_2 \text{ or } 2O)$ | (1) Large | ~300 K | Atmospheric | 20-42 |
| $N_2^*(A) + O \rightarrow N_2 + O \text{ or } NO + N$ | (1) Large | ~300 K | Atmospheric | 20-42 |
| $N_2^*(A) + N \rightarrow N + N_2^{\pm}(X)$ | (1) $\geq 2 \times 10^{-10}$ | ~300 K | Flowing afterglow | 20-118 |

Table 20-10. (Cont'd.)

| Reaction | (1) Reaction Coefficient ($cm^3\ sec^{-1}$) or (2) Cross-Section ($cm^2$) | Temperature or Energy | Type of Experiment | References |
|---|---|---|---|---|
| TWO-BODY REACTIONS (Cont'd.) | | | | |
| $N_2^*(a,v) + N_2 \rightarrow N_2^*(a,v'<v) + N_2$ | (1) Large | 1000 K | Theory | 20-222 |
| $N_2^* + Ba \rightarrow N_2(X) + Ba^{+*}(6\ ^2P_{3/2}) + e$ | (1) Large | 300 K | b, Static afterglow | 20-119, 20-223, 20-224 |
| $OH^{\ddagger}(X,v') + OH^{\ddagger}(X,v) \rightarrow OH^*(A) + OH(X)$ | (1) $\sim 10^{-10}$ | ~340 K | Flames | 20-225 |
| $N_2^{+*}(A\ ^2\Pi_u) + O_2 \rightarrow N_2 + O_2^+$ | (1) Large | | b | 20-110 |
| $N_2^{+*}(A) + N_2 \rightarrow N_2^+ + N_2$ | (1) $1 \times 10^{-9}$ | 300 K | b | 20-226 |
| $N_2^{+*}(B) + N_2 \rightarrow N_2^+ + N_2$ | (1) $6 \times 10^{-10}$ | 300 K | Stotic ofterglow | 20-227 |
| $N_2^{+*}(B) + O_2 \rightarrow N_2^+ + O_2$ | (1) $2 \times 10^{-9}$ | 300 K | Static ofterglow | 20-227 |
| $N_2^+ + CO \rightarrow N_2 + CO^{+*}(A)$ | (2) $\sim 10^{-16}$ | 8 eV | b | 20-106 |

Table 20-10. (Cont'd.)

| Reaction | (1) Reaction Coefficient ($cm^3\ sec^{-1}$) or (2) Cross-Section ($cm^2$) or (3) Reaction Coefficient ($cm^6\ sec^{-1}$) | Temperature or Energy | Type of Experiment | References |
|---|---|---|---|---|
| TWO-BODY REACTIONS (Cont'd.) | | | | |
| $He^*(2\ ^3S) + N_2 \rightarrow He(^1S) + N_2^{+*}(B) + e$ | (1) $1.4 \times 10^{-10}$ | 300 K | b | 20-85, 20-228 |
| $He^*(2\ ^3S) + O_2 \rightarrow He(^1S) + O_2^{-*} + e$ | (1) $5.0 \times 10^{-10}$ | | Flowing afterglow | 20-228 |
| $He^+ + N_2(X) \rightarrow He + N_2^*(C, v=3)$ | (2) Large | $2\text{-}10^3$ eV | b | 20-229 |
| $H^+ + Cs \rightarrow H^*(2p) + Cs^+$ | (2) $38 \times 10^{-16}$ | 200 eV | b | 20-230 |
| THREE-BODY REACTIONS | | | | |
| $N + N + N_2 \rightarrow N_2^*(B) + N_2$ | (3) $1.4 \times 10^{-33}$ | 300 K | Flowing afterglow | 20-231 |
| $N + O + N_2 \rightarrow NO^*(B) + N_2$ | (3) $1 \times 10^{-34}$ | 300 K | Flowing afterglow | 20-176 |
| $O + O + N_2 \rightarrow O_2^*(A) + N_2$ | (3) $2.1 \times 10^{-37}$ | 300 K | Flowing afterglow | 20-176 |

Table 20-10. (Cont'd.)

| Reaction | (1) Reaction Coefficient ($cm^3\ sec^{-1}$) or (2) Cross-Section ($cm^2$) or (3) Reaction Coefficient ($cm^6\ sec^{-1}$) | Temperature or Energy | Type of Experiment | References |
|---|---|---|---|---|
| THREE-BODY REACTIONS (Cont'd.) | | | | |
| $O + O + N_2 \rightarrow O_2^*(b) + N_2$ | (3) $1.7 \times 10^{-37}$ | 300 K | Flowing afterglow | 20-176 |
| $O + O + O_2 \rightarrow O_2^*(A, v=9, 10) + O_2$ | (3) $1 \times 10^{-33}$ (v=9) | 1000 K | Theory | 20-232 |
| | (3) $5.5 \times 10^{-33}$ (v=10) | 1000 K | Theory | 20-233 |
| $O + O + CN \rightarrow O_2 + CN^*(A)$ | (3) $10^{-31}$-$10^{-30}$ | 300 K | Flash photolysis | 20-234 |
| $O + O + Na \rightarrow O_2 + Na^*(^2P)$ | (3) $1.5 \times 10^{-29}$ | 1250-1500 K | Flames | 20-235 |
| $H + H + Na \rightarrow H_2 + Na^*(^2P)$ | (3) $5 \times 10^{-31}$ | 1250-1500 K | Flames | 20-235 |
| $N + N + O \rightarrow N_2 + O^*(^1S)$ | (3) $10^{-33}+(5\times10^{-33})p_{N_2}$ ($p_{N_2}$ in torr) | ~300 K | Flowing afterglow | 20-176 |
| $N + O + O \rightarrow NO + O^*(^1S)$ | (3) $3 \times 10^{-33}$ | 300 K | Flowing afterglow | 20-176 |

Table 20-15. (Cont'd.)

| Reaction | (1) Reaction Coefficient ($cm^3\ sec^{-1}$) or (2) Cross-Section ($cm^2$) or (3) Reaction Coefficient ($cm^6\ sec^{-1}$) | Temperature or Energy | Type of Experiment | References |
|---|---|---|---|---|
| THREE BODY REACTIONS (Cont'd.) | | | | |
| $O + O + O \rightarrow O_2 + O^*(^1S)$ | (3) $1.5 \times 10^{-34}$ | 300 K | Flowing afterglow | 20-176 |
| $O + O + O \rightarrow O_2 + O^*(^1D)$ | (3) Large | 300 K | Theary | 20-236 |
| $H + H_2 + O_2 \rightarrow H_2O + OH^*(A)$ | (3) $5 \times 10^{-37}$ | 1000-1900 K | Static afterglow | 20-237 |
| $H^+ + e + e \rightarrow H^*(n) + e$ | Cross-sections for recombination into the higher values of n are very large and can be estimated from detailed balance from the calculations for Ionization. | | Theory | 20-238 |

Notes:

[a] This list, which was revised last in December 1970, is believed to include the major portion of all simple atomic and diatomic chemical excitation and energy transfer reaction rates of interest for the quiescent and disturbed atmosphere.

[b] Including electron, ion, and neutral inelastic and reactive scattering.

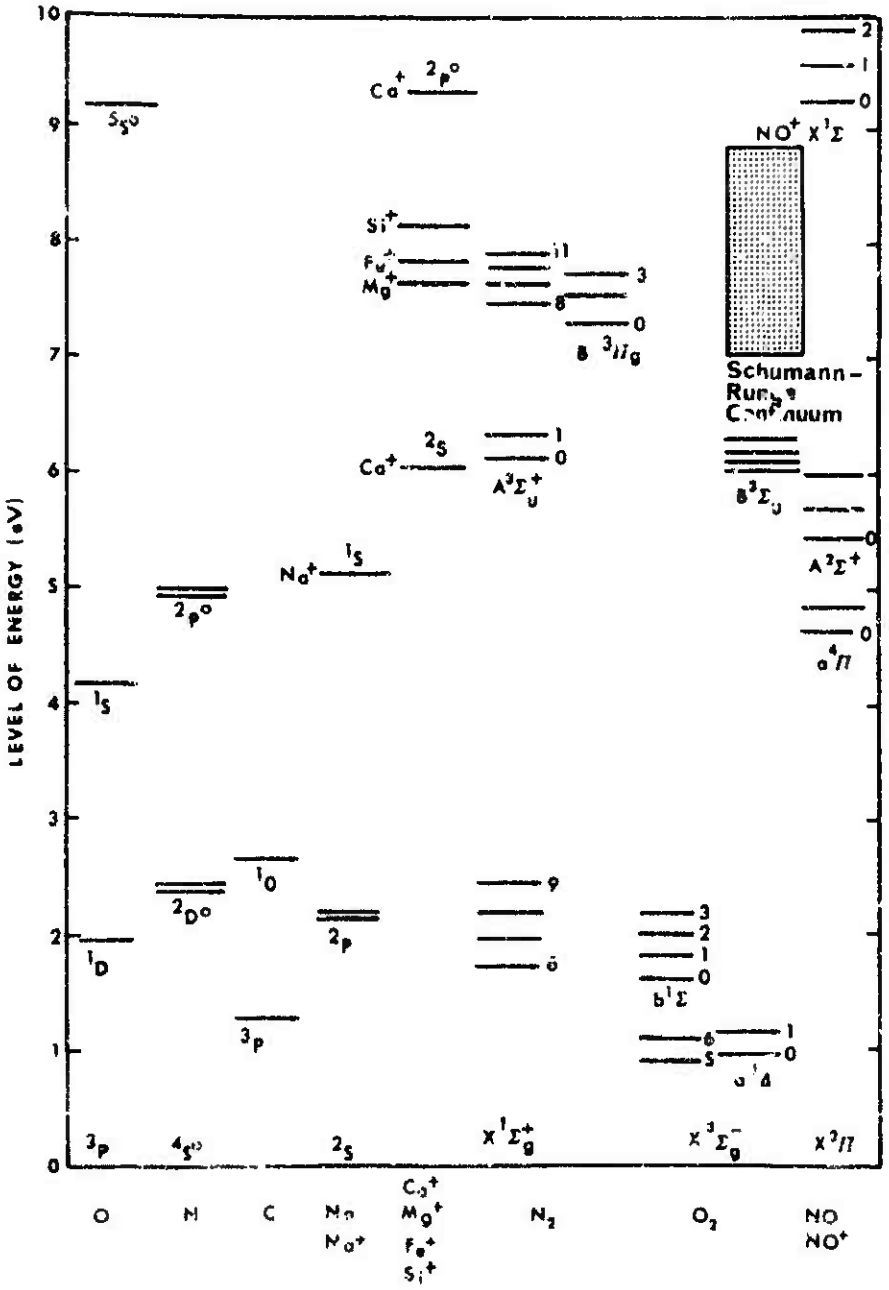


Figure 20-1. Energ, levels of pertinent atoms, molecules, and metallic ions.

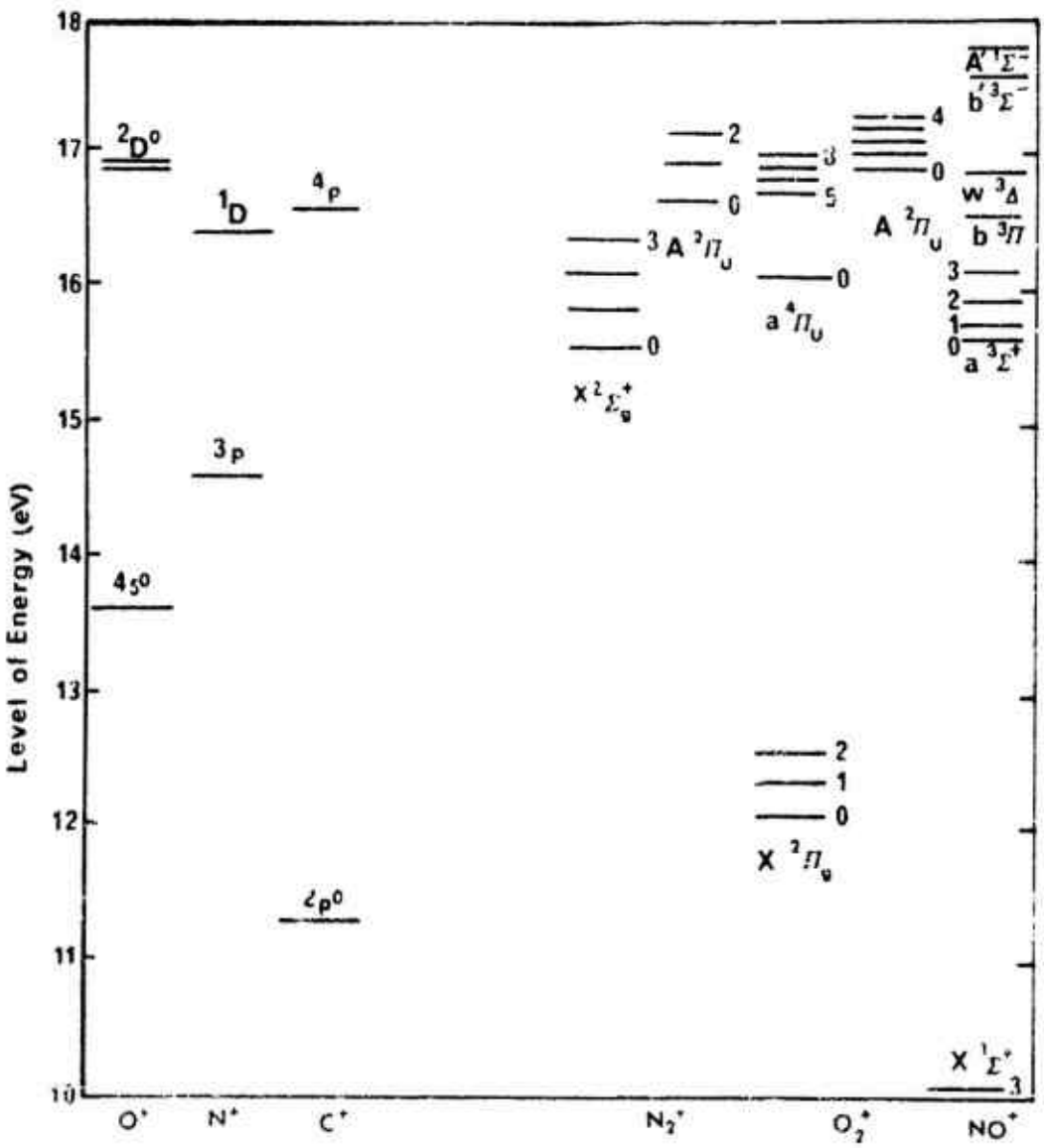


Figure 20-2. Energy levels of pertinent ions above those of corresponding ground-state neutral species.

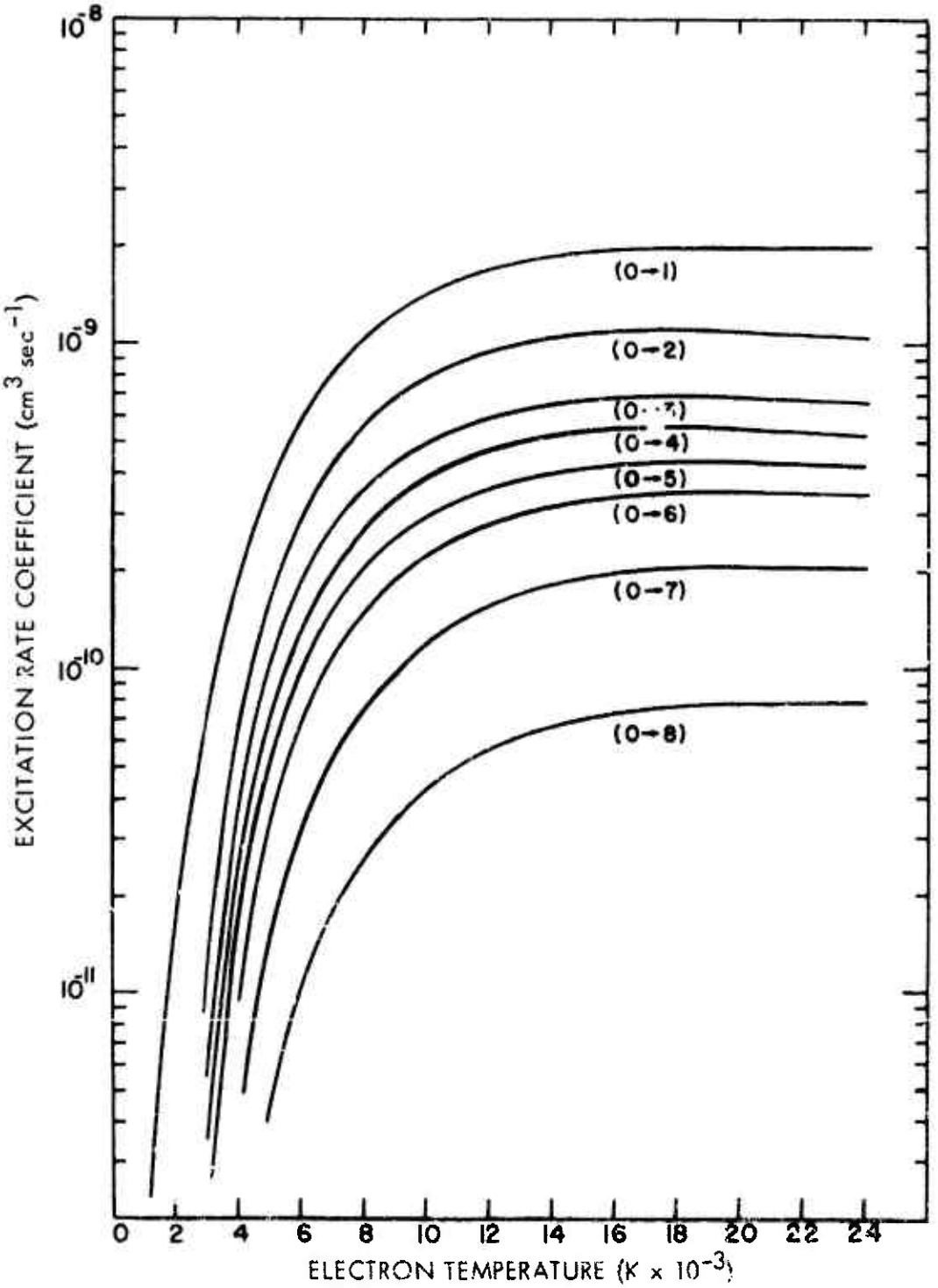


Figure 20-3. Nitrogen vibrotional excitation rate constants as a function of the electran kinetic temperature for 300 K $N_2$ kinetic temperature (References 20-62, 20-63).

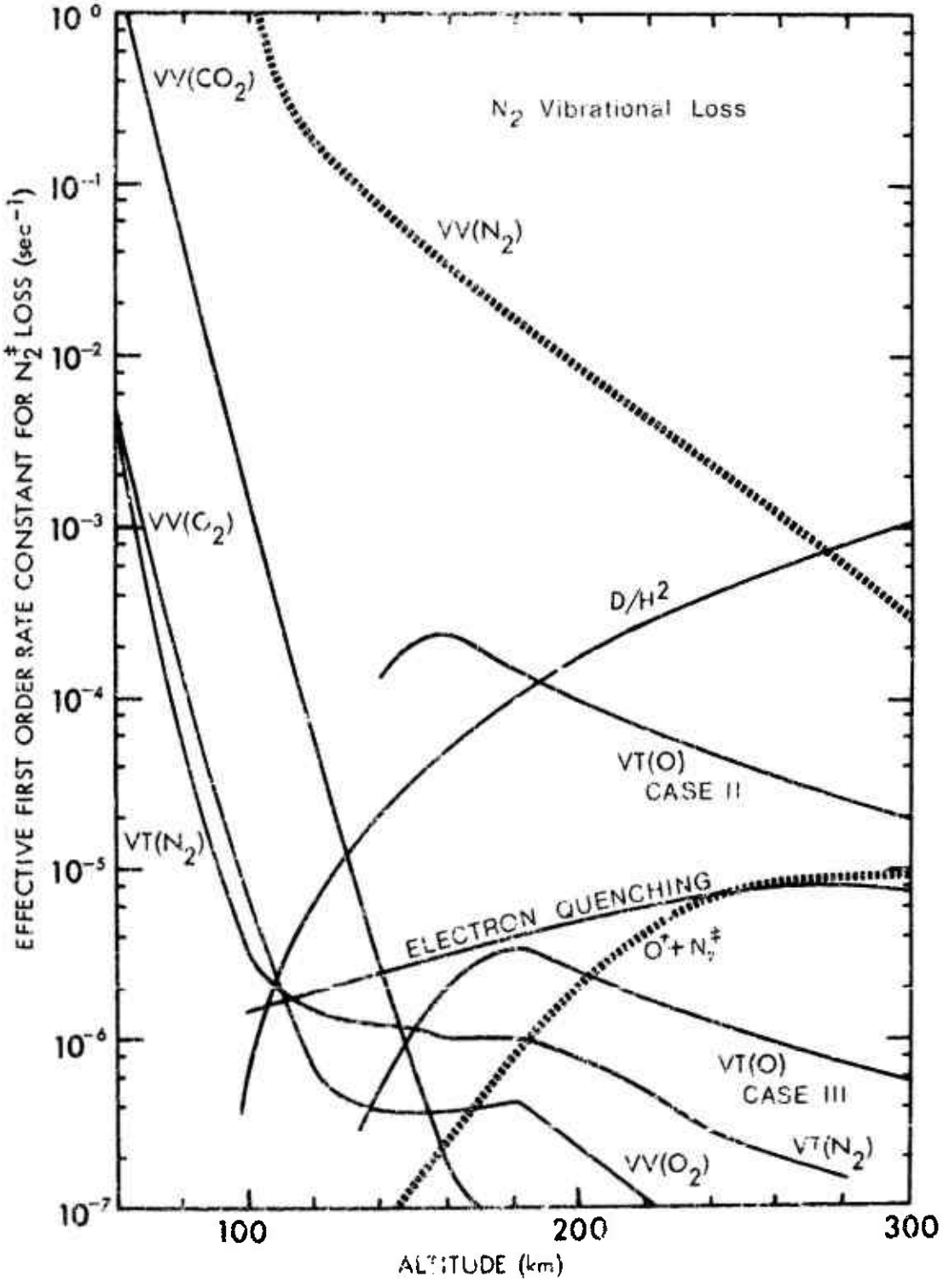


Figure 20-4. Loss frequencies ($sec^{-1}$) for $N_2$ vibration as a function of altitude.

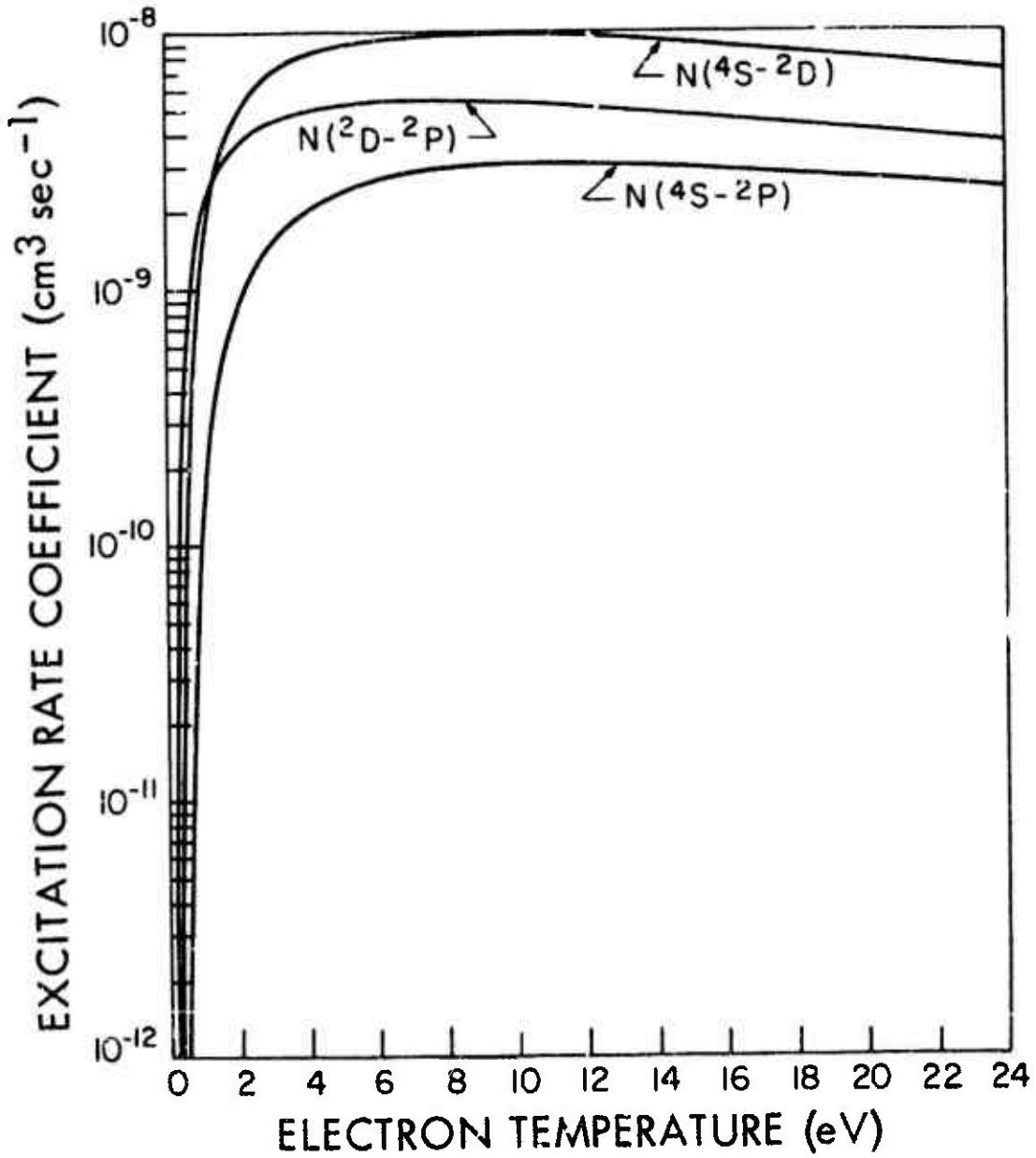


Figure 20-5. Excitation of atomic nitrogen by electron impact.

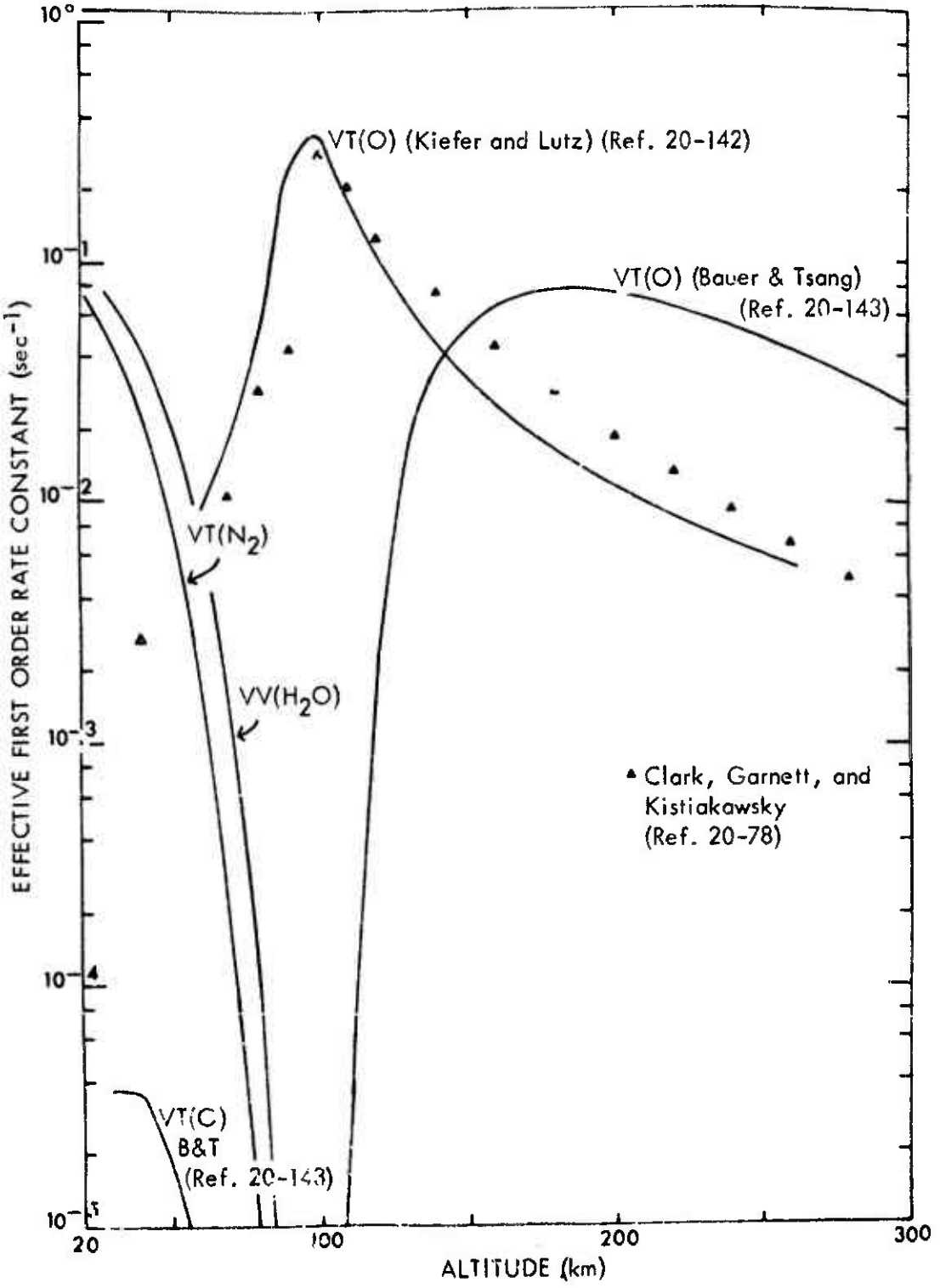


Figure 20-6. Decctivation of $O_2^{\ddagger}$ (v = 1).

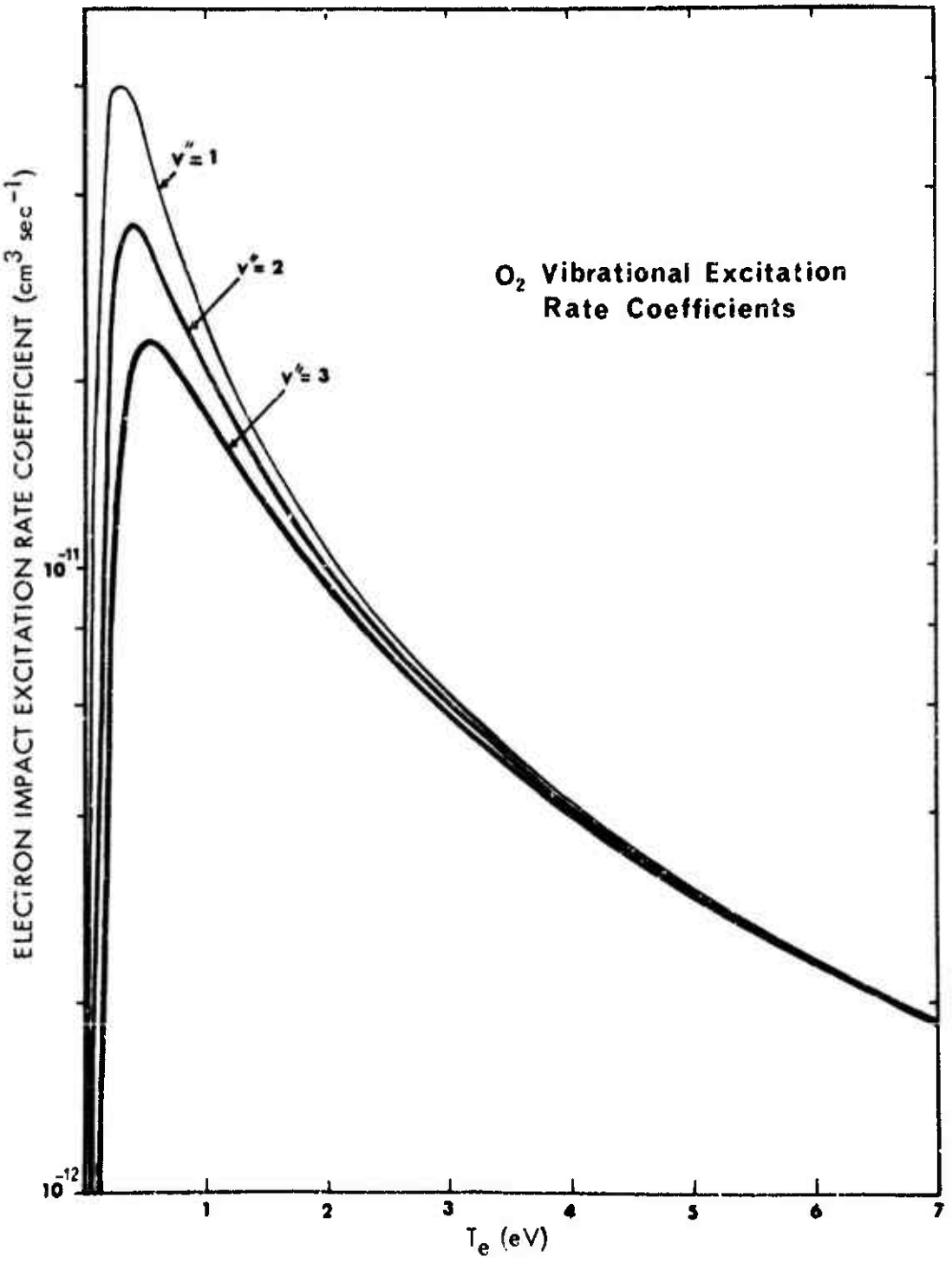


Figure 20-7. The rate coefficient for $O_2$ vibrational excitation by electron impact as reported by A.W. Ali (Reference 20-64).

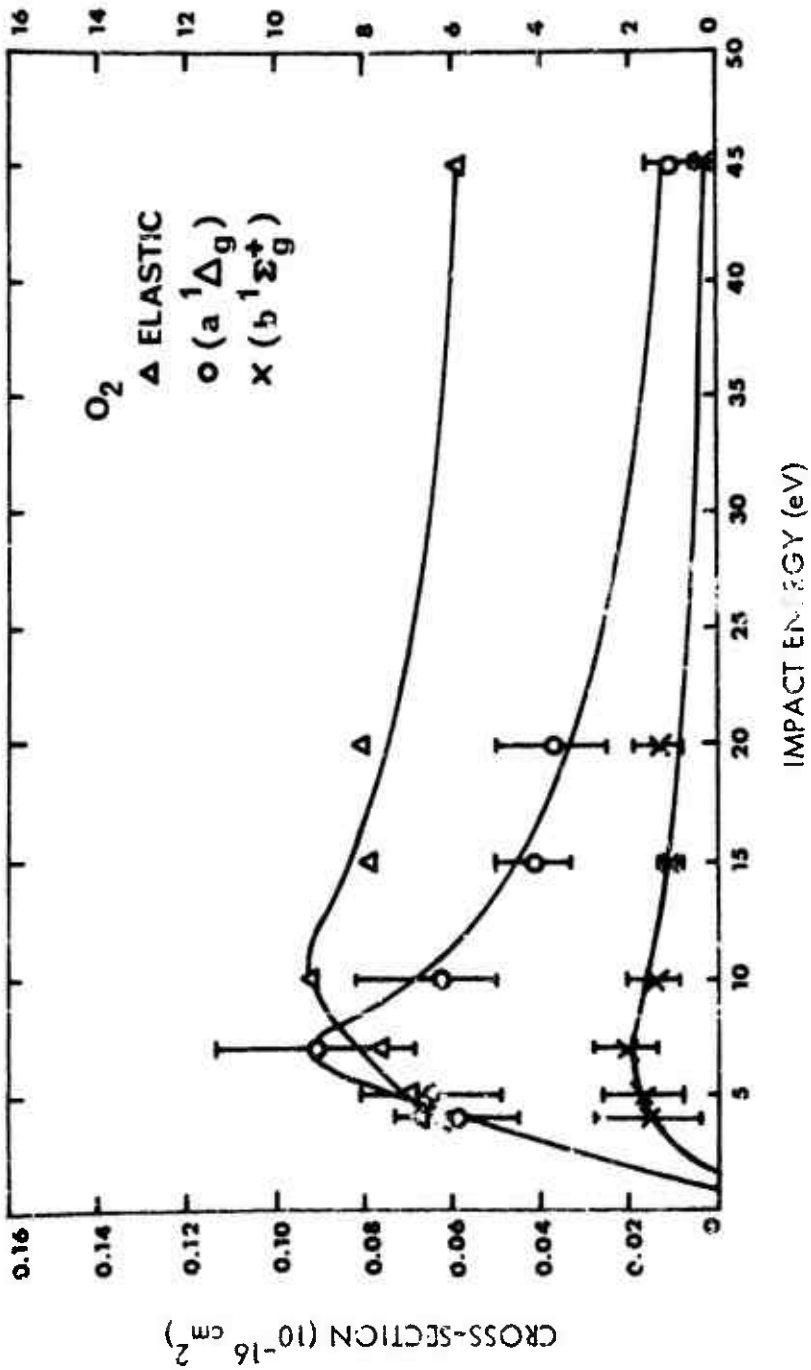


Figure 20-8. Cross-section for electron-impact excitation of $O_2$ (from Cartwright, Reference 20-113).

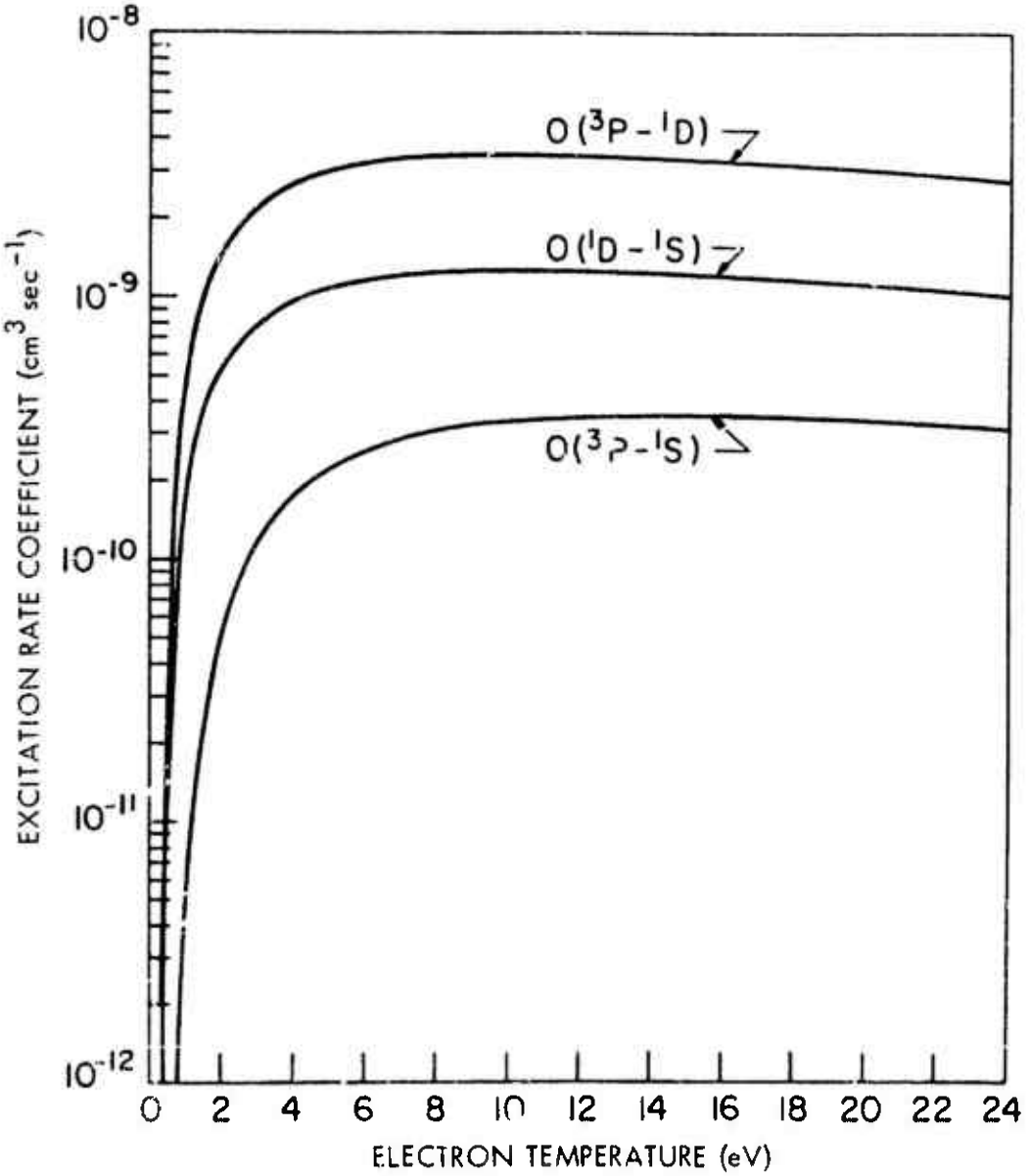


Figure 20-9. Electron-impact excitation of atomic oxygen (Reference 20-64).

## REFERENCES


20-1. McGowan, J. W., General Atomic Division (of General Dynamics Corporation) Report GA-7590 (1967).

20-2. Wright, A., and C. Winkler, Active Nitrogen, Academic Press, New York (1968).

20-3. Laidler, K. J., Chemical Kinetics of the Excited States, Oxford University Press, London (1955).

20-4. Bates, D. R., Ed., Atomic and Molecular Processes, Academic Press, New York (1962).

20-5. Fano, U., and W. Lichten, Phys Rev. Letts. 14, 627 (1965).

20-6. Gilmore, F. R., E. Bauer, and J. W. McGowan, J. Quant. Spectry. Radiative Transfer 9, 157 (1969).

20-7. Bauer, E., E. R. Fisher, and F. R. Gilmore, J. Chem. Phys. 51, 4173 (1969).

20-8. Wiese, W. L., M. Smith, and B. M. Glennon, "Atomic Transition Probabilities", Vol. I, National Standard Reference Data System Report NSRDS-NBS-4 (1966).

20-9. Gilmore, F. R., Unpublished Work (1971).

20-10. Zipf, E. C., Jr., Can. J. Chem. 47, 1863 (1969).

20-11. Lawrence, G. M., and B. D. Savage, Phys. Rev. 141, 67 (1966).

20-12. Nicholls, R., Ann. Geophys. 20, 144 (1964).

20-13. Garstang, R. H., Mon. Not. Roy. Astron. Sci. 111, 115 (1951).

20-14. Lawrence, G. M., Can. J. Chem. 47, 1856 (1969); Phys. Rev. 2A, 397 (1970).

20-15. Shemansky, D., J. Chem. Phys. 51, 689 (1969).

20-16. Shemansky, D., and N. P. Carleton, J. Chem. Phys. 51, 682 (1969).

20-17. Jeunehomme, M., J. Chem. Phys. 45, 1805 (1966).

20-18. Hollstein, M., D. C. Lorents, R. Peterson, and J. R. Sheridan, Can. J. Chem. 47, 1858 (1969).

20-19. Wu, H. L., and W. Benesch, Phys. Rev. 172, 31 (1968).

20-20. Shemansky, D. E., J. Chem. Phys. 51, 5487 (1969).

20-21. Head, C. E., Phys. Letts. 34A, 92 (1971).

20-22. Hesser, J. E., J. Chem. Phys. 48, 2518 (1968).

20-23. Johnson, A. W., and R. G. Fowler, J. Chem. Phys. 53, 65 (1970).

20-24. Frosch, R., and G. Robinson, J. Chem. Phys. 41, 367 (1964).

20-25. Lefebvre-Brion, H., and F. Guerin, J. Chem. Phys. 49, 1446 (1968).

20-26. Jeunehomme, M., J. Chem. Phys. 45, 4433 (1966).

20-27. Bubert, H., and F. W. Froben, Chem. Phys. Letts. 8, 242 (1971).

20-28. Edqvist, O. et al, Ark. Fys. 40, 439 (1970).

20-29. Maier, W. B., and R. F. Holland, J. Chem. Phys. 54, 2693 (1971).

20-30. Schwartz, S., and H. Johnston. J. Chem. Phys. 51, 1286 (1969).

20-31. Keyser, L., S. Levine, and F. Kaufman, J. Chem. Phys. 54, 355 (1971).

20-32. Badger, R. M., A. C. Wright, and R. F. Whitlock, J. Chem. Phys. 43, 4345 (1965).

20-33. Miller, J. H., R. W. Boese, and L. P. Giver, J. Quant. Spectry. Radiative Transfer 9, 1507 (1969).

20-34. Childs, W., and R. Mecke, Zeits. Phys. 68, 344 (1931).

20-35. Degen, V., Can. J. Phys. 46, 783 (1968).

20-36. Jarmain, W. R., and R. W. Nicholls, Proc. Phys. Soc. 90, 545 (1967).

20-37. Nicholls, R. W., Ann. Geophys. 20, 144 (1964).

20-38. Jeunehomme, M., J. Chem. Phys. 44, 4253 (1966).

20-39. Fink, E. H., and K. H. Welge, Z. Naturforsch. 23a, 358 (1968).

20-40. Copeland, G. E., J. Chem. Phys. 54, 3482 (1971).

20-41. Jeunehomme, M., Air Force Weapons Laboratory, Rept. AFWL-TR-66-143 (1967).

20-42. Hunten, D. M., and M. B. McElroy, Revs. Geophys. 4, 303 (1966).

20-43. Bates, D. R., Disc. Faraday Soc. 37, 21 (1964).

20-44. Muschlitz, E. E., in Molecular Beams, J. Ross, Ed., Interscience Publishers, New York (1966); p. 171.

20-45. Donovan, R. J., and D. Husain, Chem. Revs. 70, 489 (1970).

20-46. Shuler, K. E., and W. R. Bennett, Eds., Appl. Opt., Suppl. 2: Chem. Lasers, Vol. 4 (1965).

20-47. Chamberlain, J. W., Physics of the Aurora and Airglow, Academic Press, New York (1961).

20-48. Armstrong, E. B., and A. Dalgarno, Eds., The Airglow and Aurorae, Pergamon Press, London (1956).

20-49. Ratcliffe, J. A., Ed., Physics of the Upper Atmosphere, Academic Press, New York (1960).

20-50. Zelikoff, M., Ed., The Threshold of Space, Pergamon Press, New York (1957).

20-51. Cadle, R. D., Ed., Chemical Reactions in the Lower and Upper Atmosphere, Interscience Publishers, New York (1961).

20-52. Hines, C. O. et al, Eds., Physics of the Earth's Upper Atmosphere, Prentice-Hall, Englewood Cliffs, New Jersey (1965).

20-53. Phillips, L. F., and H. I. Schiff, J. Chem. Phys. 36, 1509, 3283 (1962).

20-54. Morgan, J. E., L. F. Phillips, and H. I. Schiff, Disc. Faraday Soc. 33, 118 (1962).

20-55. Bauer, E., and E. R. Fisher, Private Communication (1970).

20-56. Bauer, E., R. H. Kummler, and M. H. Bortner, Appl. Optics 10, 1861 (1971).

20-57. Walker, J., Planet. Space Sci. 16, 321 (1968).

20-58. Walker, J. C., R. S. Stolarski, and A. F. Nagy, Ann. Geophys. 25, 831 (1969).

20-59. Schulz, G. J., Phys. Rev. 125, 229 (1962); Ibid. 135, A988 (1964).

20-60. Chen, J. C. Y., J. Chem. Phys. 40, 3513 (1964); Phys. Rev. 146, 61 (1966).

20-61. Engelhardt, A. G., A. V. Phelps, and C. G. Risk, Phys. Rev. 135, A1566 (1964).

20-62. Abraham, G., and E. R. Fisher, Wayne State University Report RIES 70-01 (1970).

20-63. Fisher, E. R., and R. H. Kummler, Spring Symposium on Quantum Electronics, Sun Valley, Idaho (1971).

20-64. Ali, A. W., U. S. Naval Research Laboratory, Plasma Dynamics Technical Note 24 (1970).

20-65. Shuler, K. E., T. Carrington, and J. C. Light, p. 81 of Reference 20-46.

20-66. Polanyi, J. C., J. Quant. Spectry. Radiative Transfer 3, 471 (1963).

20-67. Herschbach, D., p. 128 of Reference 20-46.

20-68. Golden, D. E., Bull. Am. Phys. Soc. 12, 222 (1967).

20-69. Green, A. E. S., and C. A. Barth, J. Geophys. Res. 70, 1083 (1965).

20-70. Green, A. E. S., Ed., The Middle Ultraviolet, John Wiley and Sons, New York (1966); p. 165.

20-71. Burrow, P. D., and P. Davidovitz, Phys. Rev. Letts. 21, 1789 (1968).

20-72. Rapp, D., and T. E. Sharp, J. Chem. Phys. 38, 2641 (1963).

20-73. Callear, A. B., p. 145 of Reference 20-46.

20-74. Herzfeld, K. F., and T. A. Litovitz, Absorption and Dispersion of Ultrasonic Waves, Academic Press, New York (1959).

20-75. Takayanagi, K., in Advances in Atomic and Molecular Physics, D. R. Bates and I. Estermann, Eds., Academic Press, New York (1965); Vol. 1, p. 149.

20-76. Bates, D. R., J. Atm. Terrestr. Phys. 6, 171 (1955).

20-77. Dalgarno, A., Planet. Space Sci. 1 19 (1963).

20-78. Clark, T. C., S. H. Garnett, and G. B. Kistiakowsky, J. Chem. Phys. 52, 4694 (1970).

20-79. Garnett, S. H., G. B. Kistiakowsky, and B. V. O'Grady. J. Chem. Phys. 51, 84 (1969).

20-80. Bauer, E., and F. W. Cummings, J. Chem. Phys. 36, 618 (1962).

20-81. Treanor, C. E., J. Chem. Phys. 43, 532 (1965).

20-82. Taylor, R., and S. Bitterman, Revs. Mod. Phys. 41, 26 (1969).

20-83. Millikan, R., and D. White, J. Chem. Phys. 39, 3209 (1963).

20-84. Hunten, D. M., J. Atm. Terrestr. Phys. 27, 583 (1965).

20-85. Starr, W. L., J. Chem. Phys. 43, 73 (1965).

20-86. Fite, W. L., W. R. Henderson, H. F. Krause, and J. E. Mentall, Fifth Intl. Conf. Phys. Electronic Atomic Collisions, Leningrad, USSR (1967).

20-87. Fisher, E. R., and G. Smith, Appl. Optics 10, 1803 (1971).

20-88. Schmeltekopf, A. L. et al, Planet. Space Sci. 15, 401 (1967).

20-89. Schmeltekopf, A. L., E. E. Ferguson, and F. C. Fehsenfeld, J. Chem. Phys. 48, 2966 (1968).

20-90. Thomas, L., and R. B. Norton, J. Geophys. Res. 15, 401 (1967).

20-91. O'Malley, T. F., J. Chem. Phys. 52, 3269 (1970).

20-92. Whitten, R., and A. Dalgarno, Planet. Space Sci. 15, 1419 (1967).

20-93. Sears, R. D., Private Communication (1968).

20-94. Fisher, E. R., and R. H. Kummler, J. Chem. Phys. 49, 1075 (1968).

20-95. Bortner, M. H., and R. H. Kummler, General Electric Company, Report DASA 2407 (1970).

20-96. Breshears, D., and R. Bird, J. Chem. Phys. 48, 4768 (1968).

20-97. Vincenti, W. G., and C. H. Kruger, Physical Gas Dynamics, John Wiley, New York (1965); p. 202.

20-98. COSPAR International Reference Atmosphere, North-Holland Publishing Company, Amsterdam (1965).

20-99. Lichten, W., Phys. Rev. 120, 848 (1960).

20-100. Olmsted, J., A. S. Norton, and K. Street, J. Chem. Phys. 42, 2321 (1965).

20-101. Winters, H. F., J. Chem. Phys. 43, 926 (1965).

20-102. Schulz, G. J., Phys. Rev. 116, 1141 (1959).

20-103. Foner, S. N., and R. L. Hudson, J. Chem. Phys. 37, 1662 (1962).

20-104. Broadfoot, A. L., and D. M. Hunten, Can. J. Phys. 42, 1212 (1964).

20-105. Wallace, L., J. Atm. Terrestr. Phys. 17, 46 (1959).

20-106. Petrie, W., Phys. Rev. 86, 790 (1952).

20-107. Wentink, T., and L. Isaacson, J. Chem. Phys. 46, 822 (1967).

20-108. Turner, B. R., J. A. Rutherford, and R. F. Stebbings, J. Geophys. Res. 71, 4521 (1966).

20-109. Coldan, P. C. et al, J. Chem. Phys. 44, 4095 (1966).

20-110. Peterson, J., and D. C. Lorents, Private Communication (n. d.).

20-111. Dalgarno, A., and M. B. McElroy, Planet. Space Sci. 14, 1321 (1966).

20-112. Cartwright, D. C., W. Williams, and S. Trajmar, I. U. G. G. Meeting, Moscow, USSR (1971).

20-113. Cartwright, D. C., S. Trajmar, and W. Williams, I. U. G. G. Meeting, Moscow, USSR (1971).

20-114. Cartwright, D. C., Aerospace Corp., Rept. TR-0059 (9260-01)-6 (1970).

20-115. Cartwright, D. C., Phys. Rev. A2, 1331 (1970).

20-116. Noxon, J. F., J. Chem. Phys. 36, 926 (1962).

20-117. Zipf, E. C., Jr., Bull. Am. Phys. Soc. 9, 185 (1964).

20-118. Young, R. A., Can. J. Chem. 44, 1171 (1966).

20-119. Kenty, C., J. Chem. Phys. 23, 1555 (1955).

20-120. Cermak, V., J. Chem. Phys. 44, 1318 (1966).

20-121. Young, R. A., G. Black, and T. G. Slanger, J. Chem. Phys. 50, 303 (1969).

20-122. Young, R. A., and G. A. St. John, J. Chem. Phys. 48, 895 (1968).

20-123. Thrush, B. A., J. Chem. Phys. 47, 3691 (1967).

20-124. Wray, K., J. Chem. Phys. 44, 623 (1966).

20-125. Young, R. A., and G. A. St. John, J. Chem. Phys. 48, 898 (1968).

20-126. Cermak, V., J. Chem. Phys. 43, 4527 (1965).

20-127. Lee, A. R. and N. P. Carleton, Phys. Letts. 27A, 195 (1968).

20-128. Wallace, L., and M. B. McElroy, Planet. Space Sci. 14, 677 (1966).

20-129. Stebbings, R. F., B. R. Turner, and J. Rutherford, J. Geophys. Res. 71, 771 (1966).

20-130. Ammie, R. C., and N. G. Utterback, in Atomic Collision Processes, M. R. C. McDowell, Ed., North-Holland Publishing Company, Amsterdam (1964); p. 847.

20-131. McGowan, J. W., and L. Kerwin, Can. J. Phys. 42, 2086 (1964).

20-132. McGowan, J. W. et al, Phys. Rev. Letts. 14, 620 (1964).

20-133. Fite, W. L., and R. T. Brackmann, Proc. Sixth Intl. Conf. Ionization Gases, North-Holland Publishing Company, New York (1963); Vol. 1. p. 21.

20-134. Vineman, M. A. et al, Proc. Fourth Intl. Conf. Phys. Electronic Atomic Collisions, Science Bookcrafters, Inc., New York (1965); p. 425.

20-135. Kaufman, F., Private Communication (1970).

20-136. Black, G., T. G. Slanger, G. St. John, and R. A. Young, J. Chem. Phys. 51, 116 (1969).

20-137. Stebbings, R. F. et al., General Atomic Division (of General Dynamics Corporation) Report DASA 1708 (1965).

20-138. Fite, W. L., R. T. Brackmann, and W. R. Henderson, Proc. Fourth Intl. Conf. Phys. Electronic Atomic Collisions, Science Bookcrafters, Inc., New York (1965); p. 100.

20-139. O'Malley, T. F., Phys. Rev. 155, 59 (1967).

20-140. Chen, J. C. Y., and J. L. Preacher, Phys. Rev. 163, 103 (1967).

20-141. Cosby, P., and T. Moran, J. Chem. Phys. 52, 6157 (1970).

20-142. Kiefer, J. H., and R. W. Lutz, Eleventh Symp. (Intl.) on Combustion, The Combustion Institute, Pittsburgh, Pa. (1967); p. 67.

20-143. Bauer, S. H., and S. C. Tsang, Phys. Fluids 6, 182 (1963).

20-144. Schulz, G., and J. T. Dowell, Phys. Rev. 128, 174 (1962).

20-145. Spence, D., and G. Schulz, Phys. Rev. A2, 1802 (1970).

20-146. Jones, I. T. N., and R. P. Wayne, J. Chem. Phys. 51 3617 (1969).

20-147. Vallance Jones, A., and R. L. Gattinger, Planet. Space Sci. 11, 961 (1963).

20-148. Evans, W. F., D. M. Hunten, E. J. Llewellyn, and A. Vallance Jones, J. Geophys. Res. 73, 2885 (1968).

20-149. Flugge, R., and D. Headrick, Cornell Aeronautical Laboratory, Rept. DASA 2551 (1970).

20-150. Young, R. A., G. Black, and T. G. Slanger, J. Chem. Phys. 49, 4758 (1968).

20-151. Noxon, J., J. Chem. Phys. 52, 1852 (1970).

20-152. Wallace, L., and J. W. Chamberlain, Planet. Space Sci. 2, 60 (1959).

20-153. Trozzolo, A. M., Ed., Intl. Conf. Singlet Molecular Oxygen and Its Role in Environmental Sciences, Ann. N. Y. Acad. Sci. 171, Art. 1 (1970).

20-154. Clark, I. D., and R. P. Wayne, Proc. Roy. Soc. A314, 111 (1969).

20-155. Winer, A., and K. Bayes, J. Phys. Chem. 70, 302 (1966).

20-156. Clark, I. D., and R. P. Wayne, Chem. Phys. Letts. 3, 93 (1969).

20-157. Findlay, F., C. Fortin, and D. Snelling, Chem. Phys. Letts. 3, 204 (1969).

20-158. Steer, R. P., R. A. Ackerman, and J. N. Pitts, Jr., J. Chem. Phys. 51, 843 (1969).

20-159. Clark, I. D., and R. P. Wayne, Chem. Phys. Letts. 3, 405 (1969).

20-160. McNeal, R. J., and G. R. Cook, J. Chem. Phys. 47, 5385 (1967).

20-161. Megill, L. R., and J. B. Hasted, Planet. Space Sci. 13, 339 (1965).

20-162. Kummler, R. H., and M. H. Bortner, General Electric Company TIS Report R67SD20 (1967).

20-163. Fehsenfeld, F. C., D. L. Albritton, J. A. Burt, and H. I. Schiff, Can. J. Chem. 47, 1793 (1969).

20-164. Kummler, R. H., and M. H. Bortner, p. 237 of Reference 20-153.

20-165. Noxon, J., J. Geophys. Res. 75, 1879 (1970).

20-166. Megill, L., A. Despain, D. Baker, and K. Baker. J. Geophys. Res. 75, 4775 (1970).

20-167. Schiff, H. I., J. Haslett, and L. Megill, J. Geophys. Res. 75, 4363 (1970).

20-168. Arnold, S. T., N. Finlayson, and E. A. Ogryzlo, J. Chem. Phys. 44, 2529 (1966).

20-169. Young, R. A., and G. Black, J. Chem. Phys. 42, 3740 (1965).

20-170. Wallace, L., and D. M. Hunten, J. Geophys. Res. 73, 4813 (1968).

20-171. Filseth, S. V., A. Zia, and K. H. Welge, J. Chem. Phys. 52, 5502 (1970).

20-172. Watanabe, K., Adv. Geophys. 5, 153 (1958).

20-173. Zipf, E. C., Jr., Bull. Am. Phys. Soc. 12, 225 (1967).

20-174. Zipf, E. C., Jr., Bull. Am. Phys. Soc. 15, 418 (1970).

20-175. Chapman, S., Proc. Roy. Soc. A132, 353 (1931).

20-176. Young, R. A., and G. Black, J. Chem. Phys. 44, 3741 (1966).

20-177. Seaton, M. J., p. 289 of Reference 20-48.

20-178. Ingraham, J. C., and S. C. Brown, Phys. Rev. 138, A1015 (1965).

20-179. Henry, R., P. Burke, and A. L. Sinfailam, Phys. Rev. 178, 218 (1969).

20-180. Evans, W. F. J., and A. Vallance Jones, Can. J. Phys. 43, 697 (1965).

20-181. Hampson, R. F., Jr. and H. Okabe, J. Chem. Phys. 52, 1930 (1970).

20-182. Clark, I. D., and R. P. Wayne, Proc. Roy. Soc. A316, 539 (1970).

20-183. Filseth, S. V., F. Stuhl, and K. H. Welge, J. Chem. Phys. 52, 239 (1970).

20-184. Stuhl, F., and K. H. Welge, Can. J. Chem. 47, 1879 (1969).

20-185. Young, R. A., G. Black, and T. G. Slanger, J. Chem. Phys. 50, 309 (1969).

20-186. Carleton, N. P., F. J. LeBlanc, and O. Oldenberg, Bull. Am. Phys. Soc. 11, 503 (1966).

20-187. McGrath, W. D., and J. J. McGarvey, Planet. Space Sci. 15, 427 (1967).

20-188. Preston, K. F., and R. J. Cvetanovich, J. Chem. Phys. 45, 2888 (1966).

20-189. Yamazaki, H., and R. J. Cvetanovich, J. Chem. Phys. 40, 582 (1964).

20-190. Yamazaki, H., and R. J. Cvetanovich, J. Chem. Phys. 41, 3703 (1964).

20-191. Sullivan, J. O., and P. Warneck, J. Chem. Phys. 46, 953 (1967).

20-192. DeMore, W. B., and O. F. Raper, Astrophys. J. 139, 1381 (1964).

20-193. DeMore, W. B., and O. F. Raper, J. Chem. Phys. 44, 1780 (1964).

20-194. Izod, T., and R. P. Wayne, Chem. Phys. Letts. 4. 208 (1969).

20-195. DeMore, W. B., J. Chem. Phys. 52, 4309 (1970).

20-196. Clark, I. D., Chem. Phys. Letts. 5, 317 (1970).

20-197. Hunt, B. G., J. Geophys. Res. 71, 1385 (1966).

20-198. Hampson, J., Canadian Armaments Research and Development Establishment, Rept. TN 1627/64 (1964).

20-199. Hesstvedt, E., Geofys. Norveg. 27, 1 (1967).

20-200. Anderson, J., Ph. D. Dissertation, University of Colorado (1970).

20-201. Ohmholt, A., J. Atm. Terrestr. Phys. 10, 320 (1957).

20-202. Hunten, D. M., Ann. Geophys. 14, 167 (1958).

20-203. Narcisi, R. S., and A. D. Bailey, J. Geophys. Res. 7, 3687 (1965).

20-204. Fogel, M. Ya., Sov. Phys. - Usp. 3, 390 (1960).

20-205. Layton, J. K., J. Chem. Phys. 47, 1869 (1967).

20-206. Ferguson, E. E., F. C. Fehsenfeld, and J. Whitehead, J. Geophys. Res. S. P. 75, 4366 (1970).

20-207. Dalgarno, A., Can. J. Chem. 47, 1723 (1969).

20-208. Moiseiwitsch, B., and S. Smith, Revs. Mod. Phys. 40, 238 (1968).

20-209. Fite, W. L., R. F. Stebbings, and R. T. Brackmann, Phys. Rev. 116, 356 (1959).

20-210. Hils, D., H. Kleinpoppen, and H. Koschmieder, Proc. Phys. Soc. 89, 35 (1966).

20-211. Zapesochnyi, I. P., and L. L. Shimon, Optics Spectry. 19, 268 (1965).

20-212. Holt, H. K., and R. Krotkov, Phys. Rev. 144, 82 (1966).

20-213. Phelps, A. V., Phys. Rev. 99, 1307 (1955).

20-214. Stewart, D. T., and E. Gabathuler, Proc. Phys. Soc. A72, 287 (1958).

20-215. Stewart, D. T., Proc. Phys. Soc. A69, 437 (1956).

20-216. Chaney, E. L., and L. G. Christophorou, J. Chem. Phys. 51, 883 (1969).

20-217 Basco, N., and R. A. W. Norrish, Disc. Faraday Soc. 33, 99 (1962).

20-218. March, R., S. Furnival, and H. I. Schiff, Photochem. Photobiol. 4, 971 (1965).

20-219. Slanger, T. G., B. Wood, and G. Black, to be published (1971).

20-220. Anlauf, K., D. Maylotte, J. Polanyi, and R. Berstein, J. Chem. Phys. 51, 5716 (1969).

20-221. Polanyi, J., and D. Tardy, J. Chem. Phys. 51, 5717 (1969).

20-222. Bauer, E., and F. W. Cummings, J. Chem. Phys. 36, 618 (1962).

20-223. King, A. B., and C. Gatz, J. Chem. Phys. 37, 1566 (1962).

20-224. Kenty, C., J. Chem. Phys. 37, 1567 (1962).

20-225. Broida, H. P., J. Chem. Phys. 36, 444 (1962).

20-226. Sheridan, W. F., O. Oldenberg, and N. P. Carleton, in Atomic Collision Processes, M. R. C. McDowell, Ed., North-Holland Publishing Company, Amsterdam (1964); p. 440.

20-227. Hirsch, M. N., P. N. Eisner, and J. A. Selvin, C. C. Dewey Corp., Rept. R-173-4 (AD 607071) (1964).

20-228. Cher, M., and C. Hollingsworth, Can. J. Chem. 47, 1937 (1969).

20-229. Stebbings, R. F., J. Rutherford, and B. R. Turner, Planet. Space Sci. 13, 1125 (1965).

20-230. Donnally, B. L. et al, Phys. Rev. Letts. 12, 502 (1964).

20-231. Campbell, I. M., and B. A. Thrush, Chem. Communs. 12, 250 (1965).

20-232. Bauer, E., and M. Salkoff, J. Chem. Phys. 33, 1202 (1960).

20-233. Setser, D. W., and B. A. Thrush, Proc. Roy. Soc. A288, 275 (1965).

20-234. Kaskan, W. E., and R. A. Carabetta, General Electric Company, Final Report, Contract No. DA-31-124-ARO-D-214 (1965).

20-235. Bates, D. R., Earth is a Planet, University of Chicago Press, Chicago (1960); p. 576.

20-236. Belles, F. E., and M. R. Lauver, J. Chem. Phys. 40, 415 (1964).

20-237. Omidvar, K., Phys. Rev. 140, A26 (1965).

20-238. Seaton, M. J., Mon. Not. Roy. Astron. Soc. 127, 177 (1964).

20-239. Nicolaides, C., O. Sinanoglu, and P. Westhaus, Phys. Rev. A4, 1400 (1971).

# 21. ELECTRON COLLISION FREQUENCIES AND RADIO-FREQUENCY ABSORPTION*

A.V. Phelps, Joint Institute for Laboratory Astrophysics

(Latest Revision 26 May 1971)

## 21.1 INTRODUCTION

The purpose of this chapter is to present the data and formulas required for the calculation of the transmission of radio-frequency energy through weakly or strongly disturbed air of known composition. The data include plots and tabulations of the energy-dependent electron collision frequencies for the molecular and atomic components found in air at various temperatures. These data are discussed in Section 21.2. The formulas used for calculating the radio-frequency properties of electrons in gases are discussed in Section 21.3. Finally, approximations valid for weakly ionized dry air are discussed in Section 21.4. Electron-energy relaxation data are summarized in Section 21.5 and their use for the estimation of the collision frequency for non-thermal electrons is discussed in Section 21.6. Ion mobility data and their use in calculations of rf absorption and phase shift are discussed in Section 21.7.

## 21.2 ELECTRON COLLISION FREQUENCIES

Our present best estimates of the frequencies of momentum transfer collisions per molecule, $\nu_m(\epsilon)/N$, for electrons in various atmospheric gases are plotted as a function of electron energy $\epsilon$ in Figure 21-1 and are tabulated in Table 21-1. An attempt is made to indicate our degree of confidence in the results by showing the most reliable data (±20 percent or better) as solid curves, the data of intermediate reliability (factor of 2 or better) as long and short lines, and the least reliable (order of magnitude) as short dashes. The individual curves are discussed briefly below.

---

*Based in part on work done at the Westinghouse Research Laboratories and supported in part by the U.S. Army Research Office—Durham.

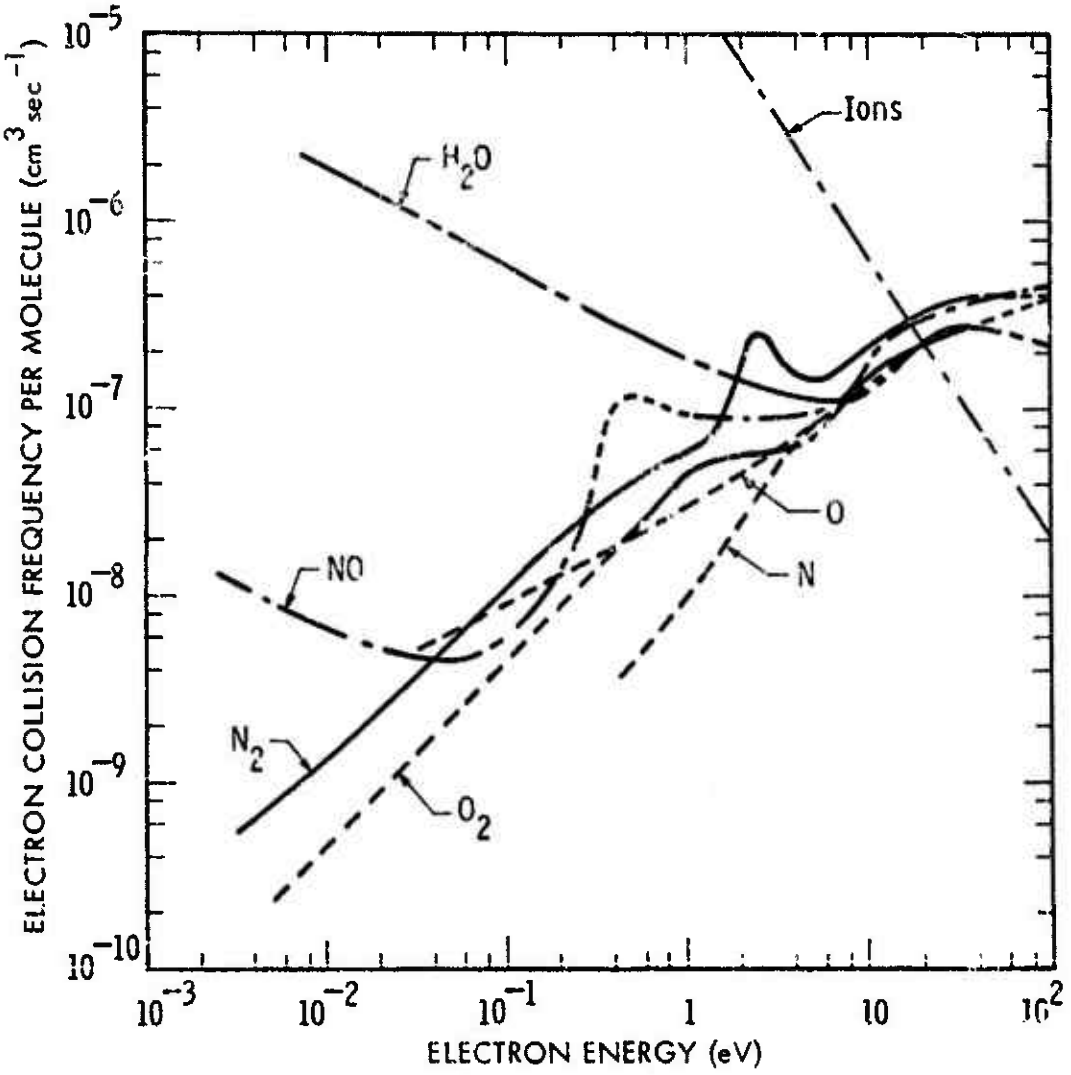


Figure 21-1. Electron collision frequencies in various atmospheric gases.

Table 21-1. Electron collision frequencies per molecule*

| $\epsilon$ (eV) | $N_2$ | $O_2$ | NO | O | N | $H_2O$ |
|---|---|---|---|---|---|---|
| .005 | 7.5(-10) | | 9.7(-9) | | | 2.85(-6) |
| .007 | 9.7(-10) | | 8.0(-9) | | | 2.35(-6) |
| .01 | 1.3(-9) | | 6.7(-9) | | | 1.93(-6) |
| .015 | 1.87(-9) | | 5.7(-9) | | | 1.57(-6) |
| .02 | 2.43(-9) | 1.2(-9) | 5.25(-9) | | | 1.36(-6) |
| .03 | 3.53(-9) | 1.7(-9) | 4.7(-9) | 6.0(-9) | | 1.10(-6) |
| .05 | 5.65(-9) | 2.8(-9) | 4.6(-9) | 7.2(-9) | | 8.5(-7) |
| .07 | 7.7(-9) | 4.0(-9) | 4.9(-9) | 8.5(-9) | | 7.2(-7) |
| .1 | 1.10(-8) | 5.0(-9) | 5.9(-9) | 1.02(-8) | | 6.0(-7) |
| .15 | 1.60(-8) | 6.5(-9) | 9.0(-9) | 1.3(-8) | | 4.85(-7) |
| .2 | 2.08(-8) | 8.6(-9) | 1.4(-8) | 1.5(-8) | | 4.15(-7) |
| .3 | 2.90(-8) | 1.32(-8) | 4.0(-8) | 1.8(-8) | | 3.4(-7) |
| .5 | 4.15(-8) | 2.16(-8) | 1.2(-7) | 2.4(-8) | 4.3(-9) | 2.63(-7) |
| .7 | 5.1(-8) | 3.05(-8) | 1.06(-7) | 2.8(-8) | 9.2(-9) | 2.25(-7) |
| 1.0 | 6.0(-8) | 4.65(-8) | 9.5(-8) | 3.5(-8) | 9.5(-9) | 1.93(-7) |
| 1.5 | 8.7(-8) | 5.5(-8) | 9.3(-8) | 4.4(-8) | 1.68(-8) | 1.64(-7) |
| 2.0 | 1.9(-7) | 5.75(-8) | 9.2(-8) | 5.2(-8) | 2.55(-8) | 1.48(-7) |
| 3 | 2.2(-7) | 6.1(-8) | 9.2(-8) | 6.6(-8) | 4.1(-8) | 1.30(-7) |
| 5 | 1.46(-7) | 7.3(-8) | 9.6(-8) | 9.3(-8) | 8.0(-8) | 1.17(-7) |
| 7 | 1.64(-7) | 1.02(-7) | 1.1(-7) | 1.17(-7) | 1.03(-7) | 1.13(-7) |
| 10 | 2.08(-7) | 1.48(-7) | 1.77(-7) | 1.52(-7) | 1.3(-7) | 1.24(-7) |
| 15 | 2.75(-7) | 1.93(-7) | 2.6(-7) | 2.1(-7) | 1.55(-7) | 1.74(-7) |
| 20 | 3.15(-7) | 2.2(-7) | 1.95(-7) | | | 2.27(-7) |
| 30 | 3.6(-7) | 2.6(-7) | 3.4(-7) | | | 2.70(-7) |

*1(-7) means $1 \times 10^{-7}$ $cm^3/sec$. As indicated in the text ond in Figure 21-1 the number of significant figures given is nat o measure of the reliability of the data.

### 21.2.1 Nitrogen

The momentum-transfer collision frequency data (Reference 21-1) shown for $N_2$ are expected to be accurate to about ±10 percent for electron energies between 0.003 and about 10 eV. For electron energies corresponding to temperatures between 150 and 2000 K the momentum-transfer collision frequency is reasonably well represented by a linear dependence on electron energy (Reference 21-2). The effect of rotationally and vibrationally excited states of $N_2$ on the collision frequencies expected at elevated gas temperatures has not been evaluated, but should be small for electron energies below about 1 eV and temperatures below 10,000 K.

### 21.2.2 Oxygen

The determination of momentum-transfer collision frequencies for electrons in $O_2$ at low energies is difficult because of large electron attachment coefficients. The most self-consistent results obtained thus far are from microwave measurements (Reference 21-3) of the conductivity following a pulsed discharge or a period of irradiation by high-energy particles. Unfortunately, it has not been possible to reconcile these results with published dc electron mobility measurements (References 21-4, 21-5). It appears that the collision frequency curve shown in Figure 21-1 for electron energies between 0 and about 2 eV is an average over a series of narrow resonances (References 21-4, 21-6). Such an average is probably sufficiently accurate for our present purposes. The microwave results (Reference 21-3) are shown for $\epsilon < 0.1$ eV. The results of beam experiments (References 21-7, 21-8) and swarm experiments (Reference 21-4) were used at higher energies. The presence of low-energy resonances in $O_2$ could possibly lead to changes in $\nu_m(\epsilon)$ with changes in rotational and vibrational temperatures (References 21-4, 21-6).

We note that the electron collision frequency shown for $O_2$ at energies corresponding to temperatures between 200 and 5000 K is also a linear function of electron energy. This means that mixtures of $O_2$ and $N_2$, e.g., dry air, can be analyzed using the linear energy dependence approximation. Available microwave results suggest that $O_2$ makes a smaller contribution to the collision frequency than estimated previously (References 21-2, 21-9, 21-10), i.e., the $O_2$ collision frequencies per molecule are 30-40 percent of those for $N_2$ rather than the 60-70 percent used in earlier calculations.

### 21.2.3 Argon

The collision frequency data (Reference 21-11) for Ar (not plotted) show that the 0.9 percent argon in air of sea-level composition makes less than a 2 percent contribution to the total electron collision frequency for any electron energy of ionospheric interest.

### 21.2.4 Corbon Dioxide

On the basis of $\nu_m(\epsilon)/N$ data (Reference 21-4) (not shown), the contribution of $CO_2$ to the total collision frequency for electrons in dry air of sea-level composition (0.03 percent) is only about 1 percent for electron energies of ionospheric interest. Since this mixing ratio is not likely to be exceeded at any altitude the contribution of $CO_2$ to the final $\nu_m(\epsilon)$ is neglected.

### 21.2.5 Woter Vapor

The very large $\nu_m(\epsilon)/N$ values (References 21-12 through 21-15) for low-energy electrons in $H_2O$ shown in Figure 21-1 mean that very small concentrations of $H_2O$ in air can significantly increase the electron collision frequency. Thus, 1 part of $H_2O$ in 300 parts of air, e.g., approximately 10 percent relative humidity at 300 K, will approximately double the electron collision frequency for thermal electrons. At electron energies corresponding to temperatures below about 5000 K, $\nu_m(\epsilon)/N$ varies approximately as the reciprocal of the square root of the electron energy. Note that this variation is quite different from that found for $N_2$ and $O_2$. At electron energies above 0.5 eV we expect the contribution of the $H_2O$ in air to the total collision frequency to be small compared to the contributions of $O_2$ and $N_2$.

### 21.2.6 Nitric Oxide

The values of $\nu_m(\epsilon)/N$ shown in Figure 21-1 for NO are based on an analysis of dc mobility data (References 21-13, 21-16) and on the assumption that at low electron energies $\nu_m(\epsilon)/N$ for electrons in NO is given by theoretical expressions based on a permanent dipole model (Reference 21-15). The results of microwave measurements (Reference 21-17) at electron noise temperatures between 1200 and 12,000 K lead to values of $\nu_m(\epsilon)/N$ which are much lower than the values shown in Figure 21-1 at energies near 1 eV.

### 21.2.7 Atomic Oxygen

The $\nu_m(\epsilon)/N$ curve shown in Figure 21-1 for atomic oxygen is based primarily on the "total" cross-section measured by electron-beam techniques (References 21-7, 21-18). These values are about the mean of the two microwave measurements of the momentum-transfer cross-section at the lower electron energies (Reference 21-19). Recent theory gives slightly larger values (Reference 21-20). In principle, measurements of free-free absorption and emission coefficients can be used to obtain elastic scattering data (Reference 21-21).

### 21.2.8 Atomic Nitrogen

As in the case of atomic oxygen the curve of $\nu_m(\epsilon)/N$ for N in Figure 21-1 is based on measurements (Reference 21-22) of the total scattering cross-section using electron-beam techniques. Recent theory (Reference 21-20) predicts a large low-energy resonance in the total scattering cross-section. However, free-free absorption coefficient measurements (Reference 21-21) show relatively little difference between the cross-sections for N and for O .

### 21.2.9 Hydroxyl

Since there are no experimental values for $\nu_m(\epsilon)/N$ for OH , we must rely entirely on theory (Reference 21-15). It is suggested that one use the same energy dependence as found for $H_2O$ but that the magnitude of $\nu_m(\epsilon)/N$ for OH be lowered by the square of the ratio of the dipole moments, i.e., by $(1.65/1.8)^2 = 0.84$. Thus, when moist air is heated, the conversion of $H_2O$ to OH will still result in large electron-neutral collision frequencies.

### 21.2.10 Positive and Negative Ions

Figure 21-1 shows the higher-energy portion of an approximate expression for $\nu_m(\epsilon)/N$ for positive ions. Laboratory experiments (Reference 21-23) are consistent with the relation:

$$\nu_{ei}(\epsilon)/N_i = 3.6\, T_e^{-3/2} \ln\left(2.0 \times 10^4\, T_e^{3/2}/N_i^{1/2}\right), \qquad (21\text{-}1)$$

where $N_i$ is the positive ion density. Note that theory (Reference 21-20) predicts that the scattering cross-section for ions depends upon the identity of the ion as well as its charge at high energies.

These predictions have not been extrapolated to the thermal energies of interest here or tested experimentally although free-free absorption theory (Reference 21-21) suggests that departures from the pure Coulomb scattering are small. The collision frequency for electrons and negative ions is assumed to be the same as for positive ions, although this question does not appear to have been investigated.

## 21.3 RADIO-FREQUENCY TRANSMISSION COEFFICIENTS

In this section the electron collision frequencies discussed in Section 21.2 are used to calculate the change in the dielectric coefficient, $\Delta K$, caused by the free electrons in the atmosphere. This change in the dielectric coefficient can be used to calculate the propagation constants appropriate to a given geometry, etc. (References 21-2, 21-24 through 21-26). The purpose of this section is to show how the energy dependence of $\nu_m(\epsilon)$ is taken into account in such calculations. We are concerned with integrals of the form (References 21-2, 21-24 through 21-26):

$$\Delta K = \frac{2}{3}\frac{\omega_{pe}^2}{\omega}\int_0^\infty \frac{[\Omega + i\nu_m(\epsilon)]}{[\nu_m^2(\epsilon) + \Omega^2]}\,\epsilon^{3/2}\,\frac{\partial f(\epsilon)}{\partial \epsilon}\,d\epsilon\,, \qquad (21\text{-}2)$$

where $\omega_{pe} = (ne^2/m\epsilon_o)^{1/2}$ is the plasma resonance frequency for electrons of density $n$, mass $m$, and charge $e$, $\epsilon_o$ is the dielectric constant of free space, $\omega$ is the angular frequency of the applied electric field, $\Omega = \omega$ or $\omega \pm \omega_{be}$, $\omega_{be} = eB/m$ is the cyclotron frequency for electrons in a magnetic field $B$, and $f(\epsilon)$ is the electron energy distribution function. Here $\int_0^\infty \epsilon^{1/2} f(\epsilon)d\epsilon = 1$. It is customary to assume that $f(\epsilon)$ is Maxwellian at a temperature $T_e$, i.e.:

$$f(\epsilon) = \frac{2}{\pi^{1/2}(kT_e)^{3/2}}\exp\left(-\frac{\epsilon}{kT_e}\right). \qquad (21\text{-}3)$$

The electron collision frequency to be used in Equation (21-2) is the sum of the collision frequencies for the neutral components of the gas. In many cases, e.g., weakly ionized dry air, it is sufficiently accurate to fit the resultant $\nu_m(\epsilon)$ data with an expression of the form:

$$\nu_m(\epsilon) = \nu_j[\epsilon/kT]^{j/2}\,. \qquad (21\text{-}4)$$

In the case of air containing small amounts of moisture, one must use the sum of several terms of the type given in Equation (21-4) in order to account properly for the low and intermediate energy behavior of $\nu_m(\epsilon)$ for electrons in $N_2$ and $O_2$, and at least one term to represent the $\nu_m(\epsilon)$ data for $H_2O$. In such cases, analytic expressions for $\nu_m(\epsilon)$ are simple to use only for $\Omega/\nu_m(kT) \gg 1$ and most calculations of $\Delta K$ have been carried out numerically. However, analytic techniques have been developed (Reference 21-25) which make it possible to handle polynomial expressions for $\nu_m(\epsilon)$.

When the electron-ion collision frequency given by Equation (21-1) becomes comparable with the sum of the $\nu_m(\epsilon)$ values for the neutral components, then Equation (21-2) is accurate only in the limit of large $\Omega/[\nu_m(\epsilon) + \nu_{ei}(\epsilon)]$. For gas mixtures for which Equation (21-4) is applicable for the neutral components, there are tables and graphs (Reference 21-26) which allow the evaluation of $\Delta K$ over a wide range of values of j and of fractional ionization.

## 21.4 WEAKLY IONIZED, DRY AIR

The collision frequency for weakly ionized, dry air can be approximated with reasonable accuracy by Equation (21-4) using j = 2, i.e., $\nu_m(\epsilon) = \nu_2(\epsilon/kT)$. The data of Figure 21-1 show that $\nu_m(\epsilon)/N = 1.03 \times 10^{-7}\ \epsilon\ cm^3/sec$ where N is the density of air at sea-level composition (Reference 21-27) and $\epsilon$ is in electron volts. Since the pressure p is related to the density by $p = NkT$, $\nu_2 = \nu_m(kT) = 8.6 \times 10^7\ p\ sec^{-1}$ when p is in torr. When the approximation $\nu_m(\epsilon) = \nu_2(\epsilon/kT)$ is substituted into Equation (21-2) one finds that:

$$\Delta K = \frac{\omega_{pe}^2}{\omega\Omega}\left[-i\left(\frac{5}{2}\right)\left(\frac{\Omega}{\nu_2}\right)\mathfrak{C}_{5/2}(\Omega/\nu_2) - \left(\frac{\Omega}{\nu_2}\right)^2 \mathfrak{C}_{3/2}(\Omega/\nu_2)\right]$$

$$= \left(\omega_{pe}^2/\omega\Omega\right)\left[-iA_2 - B_2\right], \qquad (21\text{-}5)$$

where the $\mathfrak{C}_p(X)$ functions have been tabulated by Dingle, Arnt, and Roy (Reference 21-28). The $A_2$ and $B_2$ functions are plotted in Figure 21-2 as a function of $\nu_2/\Omega$. For comparison purposes we show the corresponding functions (Reference 21-2), $A_o$ and $B_o$, calculated using Equations (21-2) and (21-3) under the previously popular assumption that j = 0 and $\nu(\epsilon) = \nu_o$, i.e., the assumption that electron collision frequency is independent of energy. The curves

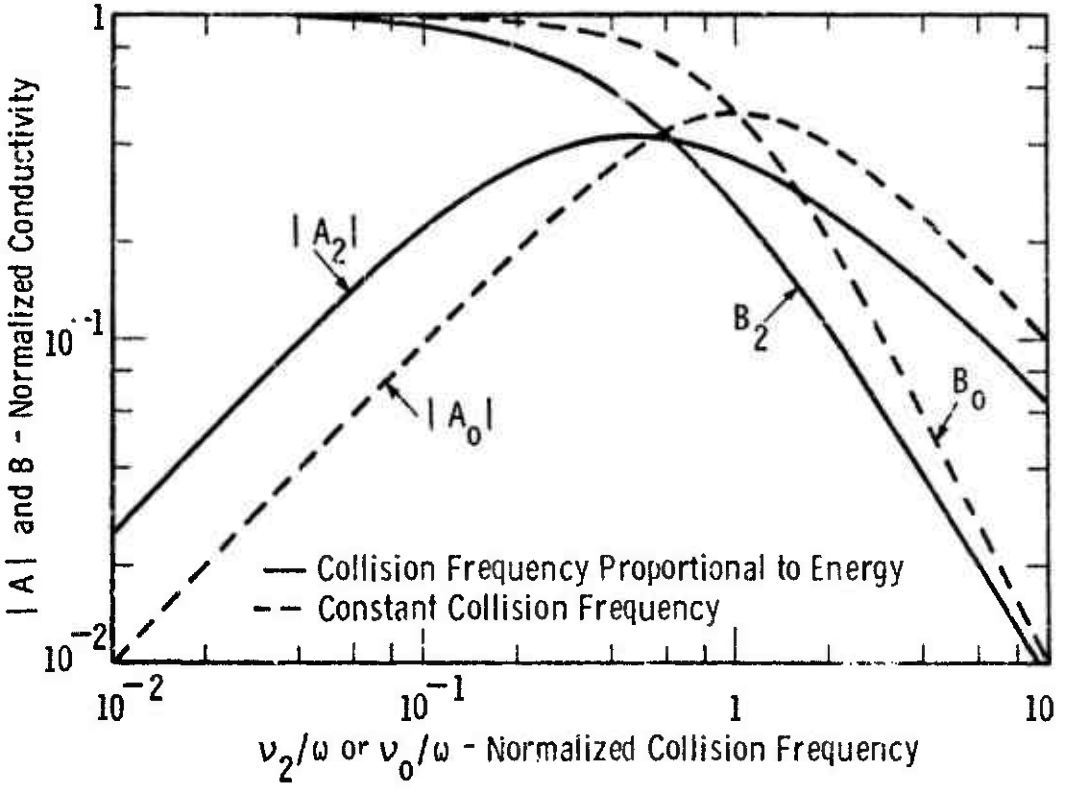


Figure 21-2. Real and imaginary parts of normalized conductivity showing effect of energy-dependent collision frequency.

of Figure 21-2 show that the use of the constant-collision-frequency assumption can lead to significant errors in the calculation of the change in the dielectric coefficient, $\Delta K$, and in the resultant propagation constants.

Ionospheric determinations (Reference 21-29) of electron collision frequencies are generally consistent with the collision frequencies given above. However, it seems unlikely that the gas pressures at the altitudes of significant ionospheric absorption are sufficiently well known to allow one to improve on the $\nu_m(\epsilon)/N$ values derived from the data of Figure 21-1. Some laboratory experiments (Reference 21-30) suggest values of $\nu_2$ for electrons in air which are 10-20 percent larger than those suggested here. This discrepancy needs to be investigated further.

## 21.5 ELECTRON ENERGY RELAXATION

Experimental studies of electron energy relaxation in gases of atmospheric interest include determinations of: a) the cross-sections for inelastic collisions using electron-beam (References 21-31, 21-32) and swarm (References 21-1, 21-4, 21-13) techniques; b) the efficiencies of production of radiation at moderately high gas densities (Reference 21-33); c) the relaxation of the electron noise temperature (Reference 21-34) at electron "temperatures" below about 1 eV; and d) the degree of ionospheric cross-modulation (References 21-29, 21-35). Theoretical studies include calculations (References 21-36, 21-37) of sets of inelastic cross-sections and "energy loss functions" and the application of these to the calculation of rates of excitation of visible and UV radiation resulting from high-energy electrons incident in air (References 21-32, 21-37, 21-38), of electron heating by electric fields (Reference 21-39), and of the excess of the electron temperature over the gas temperature under various ionospheric conditions (Reference 21-40).

There are various methods for expressing the results of the investigations of electron energy relaxation studies. The theoretical results for electron energies above roughly 1 eV are usually expressed in terms of the energy loss function $L(\epsilon)$, the cooling rate $d\epsilon/dt$, or the stopping power $d\epsilon/dx$ for monoenergetic electrons of energy $\epsilon$. These expressions for a gaseous species of density $N_i$ are related by:

$$\frac{1}{v}\frac{d\epsilon}{dt}\bigg|_i = \frac{d\epsilon}{dx}\bigg|_i = N_i L_i(\epsilon) = N_i \sum_j \epsilon_{ij}\sigma_{ij}(\epsilon) , \qquad (21\text{-}6)$$

where $\epsilon_{ij}$ and $\sigma_{ij}(\epsilon)$ are energy loss and excitation cross-sections for the $j^{th}$ state of species $i$. In the case of ionization, $\epsilon_{ij}$ is an average value dependent upon the secondary electron energy distribution. Measurements of these distributions for atmospheric gases have been reported only very recently (Reference 21-41).

At low electron energies the results of theoretical and experimental investigation are often expressed in terms of averages over the electron energy distribution. Thus, the rate of electron cooling is commonly written (References 21-1, 21-34, 21-35, 21-39, 21-42, 21-43) in forms equivalent to:

$$\frac{d\bar{\epsilon}}{dt} = -\nu_u(\epsilon_K)(\epsilon_K - kT_g) + Q , \qquad (21\text{-}7)$$

where $\bar{\epsilon}$ is the mean electron energy, $\epsilon_K$ is the characteristic energy of the electrons and for a Maxwellian energy distribution is equal to $kT_e$, $T_g$ is the gas temperature, and $\nu_u(\epsilon_K)$ is the rate coefficient for electron energy exchange with the gas. Q is the source term and may be due to secondary electrons or photoelectrons or to an electric field, which supplies energy to the electrons. At present, laboratory data for $\nu_u(\epsilon_K)$ are available only from measurements of the change in the electron energy caused by application of dc or radio-frequency electric fields (Reference 21-44). In the dc electric-field case, $\nu_u(\epsilon_K)$ has been called the electron energy exchange frequency and is defined (References 21-1, 21-43) as the ratio of the power input per electron $Q = ewE$ to the excess electron energy $(\epsilon_K - kT_g)$, where the electron drift velocity w and characteristic energy are the measured transport coefficients. In the radio-frequency case (Reference 21-34), the measurements are usually of the time constant for the relaxation of the electron noise "temperature" $T_n$. Conventionally, $\epsilon_K$ is replaced by $kT_n$ and $\nu_u$ by $\overline{G\nu}$, where G is the fractional energy loss per collision and $\nu$ is the electron collision frequency. When the electron collision frequency is small compared to the angular frequency and when the electron energy distribution is not Maxwellian, the ratio of $kT_n$ to $\epsilon_K$ may differ from unity by a significant (Reference 21-45), but generally unknown (Reference 21-46), factor.

The relationships among the functions $L(\epsilon)$, $\nu_u(\epsilon_K)$, and $\overline{G\nu}(T_n)$ are complicated by the fact that usually the electron energy distribution appropriate to a given value of $\nu_u$ or $\overline{G\nu}$ is not known. Sets of inelastic cross-sections or $L_{ij}(\epsilon)$ for low-energy electrons in a few gases have been obtained (References 21-1, 21-4, 21-13, 21-43) which are consistent with dc electron transport coefficients and which take into account the available theory and experimental data for monoenergetic electrons. Because of the large range of electron energies present in the transport coefficient or "swarm" experiments the curves of $\nu_u/N$ show considerably less structure than do the curves of $vL(\epsilon)$. Also, the value of $\epsilon_K$ at which the contribution of a given energy loss process to $\nu_u(\epsilon_K)$ is a maximum is usually lower than the energy at which $v\sigma_{ij}(\epsilon)$ reaches its maximum.

Recommended values of $\nu_u/N$ and of $vL_i(\epsilon)$ for various gases are shown in Figures 21-3 and 21-4 and are tabulated in Tables 21-2 and 21-3. Our degree of confidence in the values shown in the figures is indicated by solid curves (±20 percent or better), long and short dashes (factor of two), and short dashes (order of magnitude). Comments on the individual gases follow.

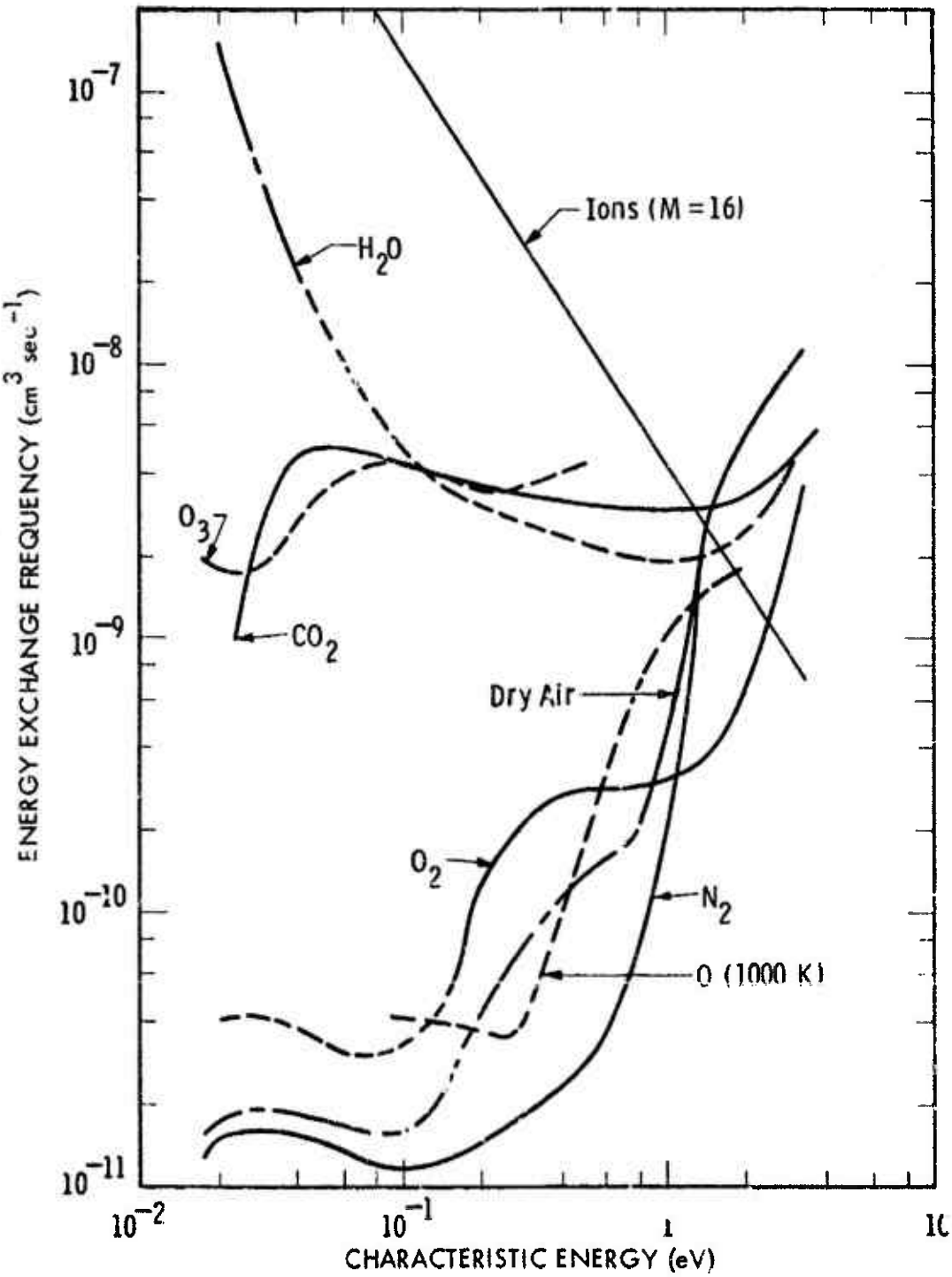


Figure 21-3. Electron energy exchange frequencies for various atmospheric gases.

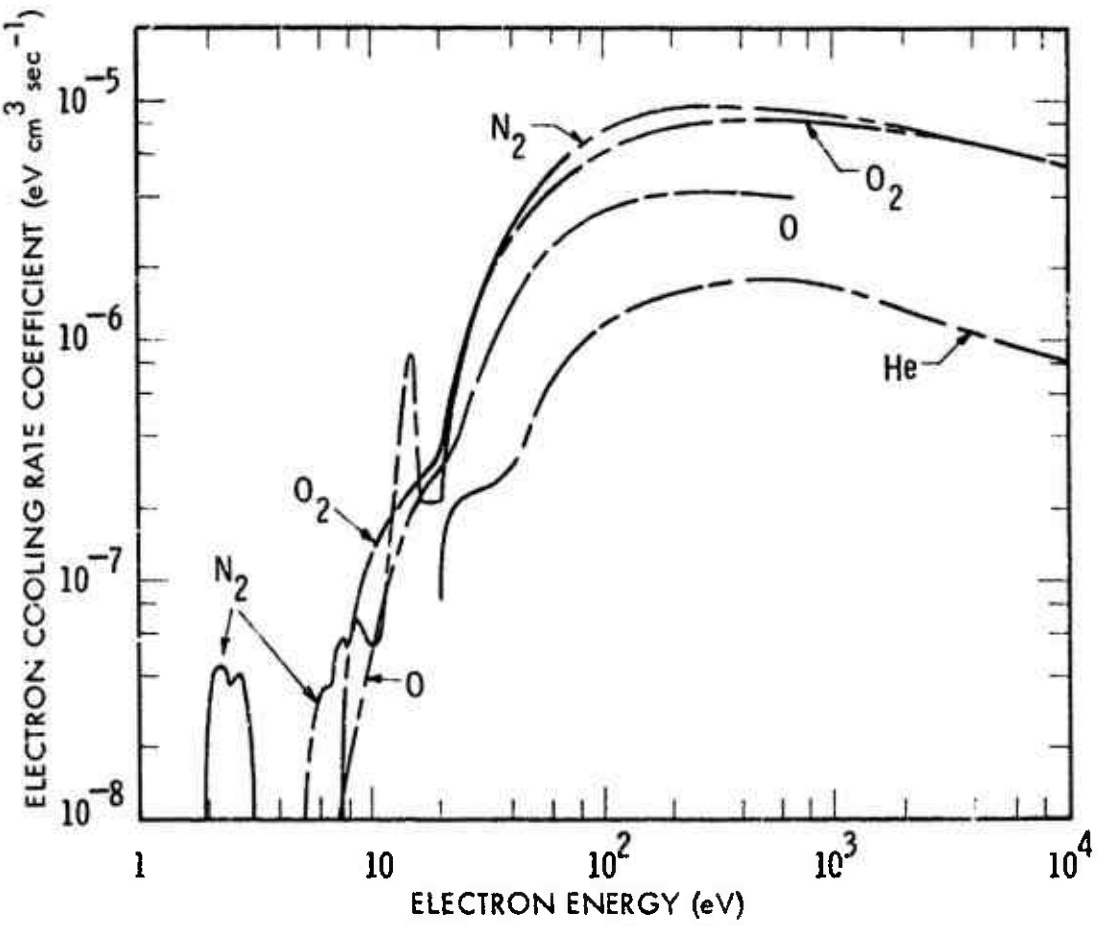


Figure 21-4. Electran cooling rates in atmaspheric gases.

Table 21-2. Electron energy exchange frequencies in atmospheric gases in $cm^3\ sec^{-1}$. Gas temperature is 200 K except for atomic oxygen which is at 1000 K.*

| $\epsilon_K$ | $N_2$ | $O_2$ | O | $H_2O$ | $CO_2$ | $O_3$ | Dry Air | NO |
|---|---|---|---|---|---|---|---|---|
| 1.72(-2) | 1.2(-11) | | | | 1.4(-10) | 2(-9) | 9.4(-12) | 1.6(-10) |
| 2(-2) | 1.5(-11) | | | 1.5(-7) | 5.1(-10) | 1.8(-9) | 1.2(-11) | 1.4(-10) |
| 3(-2) | 1.6(-11) | 8.0(-12) | | 4.4(-8) | 3.2(-9) | 1.9(-9) | 1.25(-11) | 1.03(-10) |
| 5(-2) | 1.4(-11) | 1.1(-11) | | 1.45(-8) | 4.9(-9) | 3.5(-9) | 1.1(-11) | 9.6(-11) |
| 7(-2) | 1.25(-11) | 1.7(-11) | | 8(-9) | 4.8(-9) | 4.2(-9) | 1.1(-11) | 7.9(-11) |
| 1(-1) | 1.17(-11) | 2.6(-11) | 4.1(-11) | 5(-9) | 4.4(-9) | 4.4(-9) | 1.25(-11) | 7.0(-11) |
| 1.5(-1) | 1.28(-11) | 5.3(-10) | 3.9(-11) | 3.6(-9) | 3.9(-9) | 3.9(-9) | 2.5(-11) | 1.4(-10) |
| 2(-1) | 1.47(-11) | 1.25(-10) | 3.6(-11) | 3.1(-9) | 3.7(-9) | 3.5(-9) | 4.5(-11) | 6(-10) |
| 3(-1) | 1.86(-11) | 2.15(-10) | 4.5(-11) | 2.7(-9) | 3.4(-9) | 3.9(-9) | 8(-11) | 2.6(-9) |
| 5(-1) | 4(-11) | 2.8(-10) | 2.0(-10) | 2.3(-9) | 3.1(-9) | 5.4(-9) | 1.4(-10) | 3.8(-9) |
| 7(-1) | 5.5(-11) | 2.9(-10) | 5.0(-10) | 2.0(-9) | 3.0(-9) | | 1.7(-10) | 3.4(-9) |
| 1 | 1.9(-10) | 3.1(-10) | 1.0(-9) | 1.9(-9) | 3.0(-9) | | 4.7(-10) | 3.0(-9) |
| 1.5 | 3(-9) | 4.1(-10) | 1.5(-9) | 2.1(-9) | 3.1(-9) | | 2.6(-9) | 7.5(-9) |
| 2 | 5.5(-9) | 7.2(-10) | 1.8(-9) | 2.5(-9) | 3.4(-9) | | 5.5(-9) | 1.3(-8) |
| 3 | 1.0(-8) | 2.6(-9) | | 4.3(-9) | 4.7(-9) | | 1.07(-8) | 1.8(-8) |

*1(-7) means $1 \times 10^{-7}\ cm^3/sec$.

Table 21-3. Electron cooling rate coefficient in eV $cm^3 sec^{-1}$.*

| $\epsilon$ (eV) | $N_2$ | $O_2$ | O | He |
|---|---|---|---|---|
| 1(4) | 5.3(-6) | 5.4(-6) | | 8.2(-7) |
| 5(3) | 6.4(-6) | 6.0(-6) | | 1.0(-6) |
| 2(3) | 8.0(-6) | 7.4(-6) | | 1.3(-6) |
| 1(3) | 8.8(-6) | 8.2(-6) | | 1.7(-6) |
| 5(2) | 9.3(-6) | 8.0(-6) | 4.0(-6) | 1.6(-6) |
| 2(2) | 9.4(-6) | 7.6(-6) | 4.0(-6) | 1.5(-6) |
| 1(2) | 7.6(-6) | 6.5(-6) | 3.6(-6) | 1.2(-6) |
| 5(1) | 4.3(-6) | 3.3(-6) | 2.1(-6) | 5.0(-7) |
| 3(1) | 1.6(-6) | 1.8(-6) | 8.1(-7) | 2.4(-7) |
| 2(1) | 2.1(-7) | 3.6(-6) | 3.1(-7) | |

*1(-7) means $1 \times 10^{-7} cm^3/sec$.

### 21.5.1 Nitrogen

Values of $\nu_u/N$ are available (Reference 21-1) for $N_2$ which are expected to be accurate to better than ± 10 percent for values of $\epsilon_K$ between 0.01 and 1 eV for a gas temperature of 77K and between 0.03 and 1 eV for 293K. The uncertainty is somewhat larger for $\epsilon_K$ values below 0.1 eV for intermediate temperatures, such as 200K, because of a lack of experimental data and the absence of numerical calculations (Reference 21-47). The accuracy of the $v\sum_j L_{ij}(\epsilon)$ values (Reference 21-37) for $N_2$ is unknown as the published experiments (References 21-31, 21-32) are incomplete. We have shown the values of $L(\epsilon)$ given by Dalgarno, McElroy, and Stewart (Reference 21-37) for energies below 500 eV, and those of Green and Peterson (Reference 21-37) for higher energies. Note that when calculations of $L_j(\epsilon)$ are made for $N_2$ (and other molecular gases) at elevated vibrational temperatures, it is important to allow for energy loss and gain in collisions with vibrationally excited states. At present our only source of such cross-sections is theory (Reference 21-48).

### 21.5.2 Molecular Oxygen

Values of $\nu_u/N$ for electrons in $O_2$ are available from dc swarm experiments (Reference 21-4) for $0.15 < \epsilon_K < 3$ eV with an estimated accuracy of better than ± 20 percent. At electron energies between 0.02 and 0.1 eV, measurements of $\overline{G\nu}$ in the afterglow of a microwave discharge (Reference 21-49) and theoretical calculations (Reference 21-50) of $\overline{G\nu}$ indicate a larger rate of electron energy loss for $O_2$ than for $N_2$. However, the theory (Reference 21-50) suggests a much more rapid variation in rotational excitation cross-section than do the microwave experiments (Reference 21-49). Figure 21-3 shows $\nu_u/N$ values which vary with $\epsilon_K$ as suggested by the microwave experiments (Reference 21-49) but which have been lowered somewhat in order to be consistent with the dc experiments (References 21-4, 21-5). The values of $vL_j(\epsilon)$ shown for $O_2$ were obtained as for $N_2$ except that it was necessary to apply a scale factor to the high-energy calculations in order to obtain agreement among the calculations at 500 eV. Recent investigations (Reference 21-51) have been concerned with the excitation of the vibrational and low-lying electronic states of $O_2$.

### 21.5.3 Atomic Oxygen

The only information available regarding the total rates of energy loss caused by atomic oxygen are the theoretical calculations (References 21-37, 21-52). Note that the values shown are for a gas temperature of 1000 K and were calculated using a Maxwellian electron energy distribution.

### 21.5.4 Water Vapor

Concentrations of water vapor such as those found in air near sea level have a large effect on the rates of energy relaxation for low-energy electrons. Values of $\nu_u/N$ shown in Figure 21-3 and Table 21-2 are calculated (Reference 21-13) from a set of momentum-transfer and inelastic cross-sections which, in turn, are chosen to be consistent with the theory (References 21-15, 21-43) for rotational excitation and with the very limited and badly scattered experimental data (References 21-12, 21-14).

### 21.5.5 Carbon Dioxide

Carbon dioxide is included in this compilation of data since the $\nu_u/N$ values (Reference 21-4) in $CO_2$ are large enough so that for

$0.03 < \epsilon_K < 0.1$ eV the 0.03 percent concentration of $CO_2$ in air increases the rate of electron energy loss by 10-15 percent. $CO_2$ is also of interest in connection with planetary atmospheres.

### 21.5.6 Helium

Energy loss functions for helium (Reference 21-37) can be calculated from available experimental data (References 21-31, 21-53).

### 21.5.7 Ozone

Because of its relatively large dipole moment and allowed infrared transition probabilities one expects relatively large values of $\nu_u/N$ for $O_3$ at low electron energies. The values cited in Figure 21-3 and Table 21-2 are estimated from theory (References 21-15, 21-43) and from a comparison of electron attachment coefficients in pure $O_3$ and in $O_3$-$CO_2$ mixtures (Reference 21-54).

### 21.5.8 Other Neutral Gases

Values of $\nu_u/N$ are available (References 21-4, 21-13, 21-34, 21-43) for CO and NO at energies below about 1 eV. A limited amount of data from which $\nu_u/N$ can be calculated is available for more complicated molecules (References 21-42, 21-43, 21-55).

### 21.5.9 Ions

Figure 21-3 shows a plot of an approximate expression for $\nu_u/N$ caused by the energy exchange between electrons and a typical positive ion, i.e., here $\nu_u/N \approx 2m\nu_{ei}/N$, and M is taken to be 16 amu. In addition, there may be a contribution resulting from the excitation of the rotational, vibrational, and electronic levels of the ions. Only a very limited amount of information (References 21-20, 21-53, 21-56) is available regarding these processes. Also, at electron and ion densities which may be considerably lower than those for which energy loss due to electron-ion scattering is important one must consider the sharing of electron energy among electrons (Reference 21-37). Thus, even though the energy loss rate caused by inelastic collisions may be large only for high electron energies, the effect of electron-electron interactions is to spread out, i.e., make more Maxwellian, the electron energy distribution and increase the effective rate at which electrons at all temperatures lose energy.

## 21.6 APPLICATION OF ELECTRON ENERGY LOSS DATA

The calculation of electron energy distribution functions and their use to predict radio-frequency absorption and rates of production of radiation is a rapidly developing field. However, the techniques are too complicated to be discussed in any detail here. Instead it will be shown how the direct experimental data of $\nu_u/N$ can be used to obtain an estimate of the electron energy distribution for low-energy electrons. First, we integrate Equation (21-7) to obtain the time required for electrons injected with energy $\epsilon_o$ to cool to $\epsilon_K$, i.e., for $Q = 0$:

$$t - t_o = \int_{\epsilon_K}^{\epsilon_o} \frac{d\bar{\epsilon}}{(\epsilon_K - kT)\,\nu_u(r_K)} \quad . \tag{21-8}$$

In order to evaluate Equation (21-8) we need to know the relationship between $\bar{\epsilon}$ and $\epsilon_K$. Since $\bar{\epsilon}/\epsilon_K$ is usually a slowly varying function of $\epsilon_K$, we will assume that the ratio is a constant which can be taken out of the integral (Reference 21-57). For a Maxwellian electron energy distribution $\bar{\epsilon}/\epsilon_K = 3/2$. Figure 21-5 shows the results of the calculation (Reference 21-58) of $\epsilon_K$ as a function of time for electrons in dry air. Thus, at an altitude of 70 km, where $N \approx 2 \times 10^{15}$ cm$^{-3}$, the time required for the $\epsilon_K$ values of electrons formed with energies above about 0.5 eV to reach a value 10 percent above thermal is about $2 \times 10^{-4}$ sec. This time is short compared to the lifetime against electron attachment of about 5 sec so that the electrons are expected to thermalize before they attach. At sea level ($N \approx 3.5 \times 10^{19}$ cm$^{-3}$), the time required for relaxation of $\epsilon_K$ to $1.1\ kT_g$ in dry air is about $2 \times 10^{-8}$ sec compared to a lifetime against attachment of about $1.6 \times 10^{-8}$ sec. However, the presence of only 1.5 percent $H_2O$ (roughly 50 percent relative humidity) reduces the time required for energy relaxation to within 10 percent of $kT_g$, to about $2.4 \times 10^{-9}$ sec. During the decay of $\epsilon_K$ to kT the electron transport coefficients, such as the radio-frequency attenuation, will be characteristic of the elevated value of $\epsilon_K$.

The transient solution following the injection of an impulse of energetic electrons calculated using Equation (21-8) can be used to calculate the steady-state average of measurable quantities such as the electron collision frequency which appears in the expressions for the rf attenuation. As an illustration, Figure 21-5 shows the values (Reference 21-59) of $\langle \nu_m \rangle / N$ calculated using the relation:

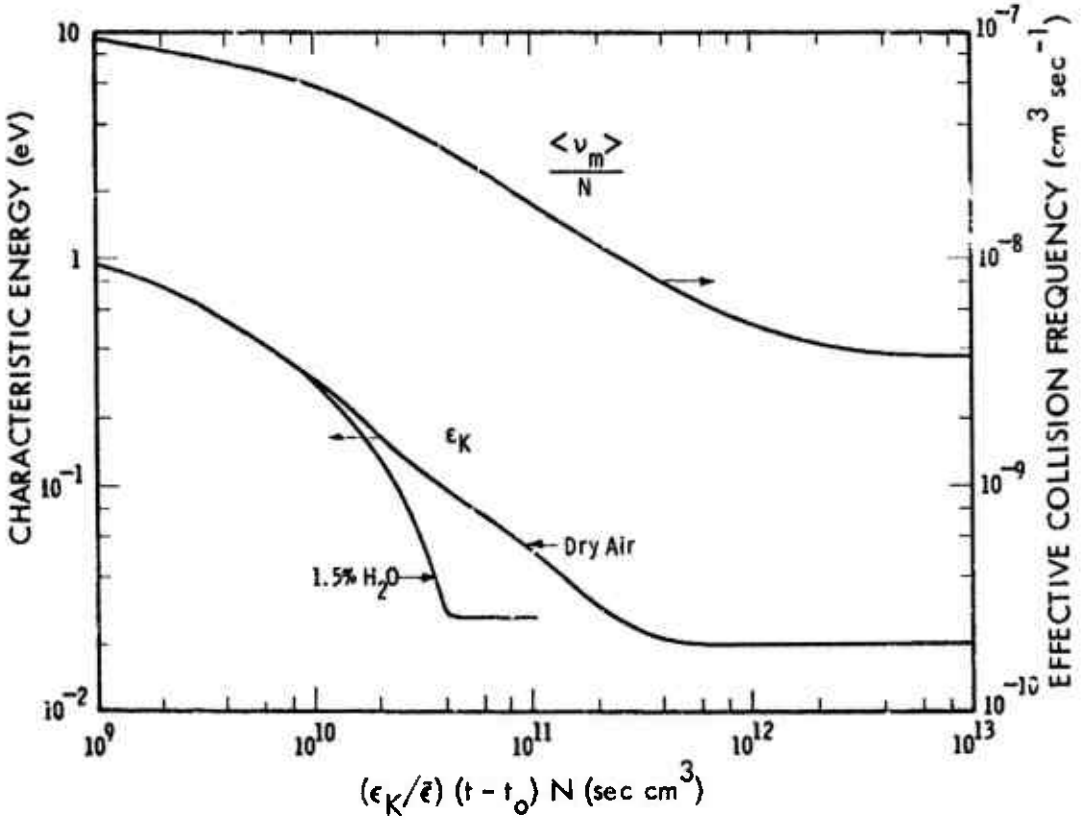


Figure 21-5. Relaxation of characteristic energy and momentum-transfer collision frequency for dry air at 230K and relaxation of characteristic energy in moist air (1.5 percent $H_2O$) at 300K.

$$\frac{\langle \nu_m \rangle}{N} = \frac{\nu_a}{\exp(-\nu_a t_o) - \exp(-\nu_a t)} \int_{t_o}^{t} \frac{\nu_m(\epsilon_K) \exp(-\nu_a t)\, dt}{N} . \quad (21\text{-}9)$$

Here $\nu_a$ is the frequency of electron attachment collisions. It is assumed to vary sufficiently slowly with $\epsilon_K$ so that the form of the electron energy distribution is not crucial. Here the rate of electron injection is assumed to be constant with time. In Figure 21-5 the attachment is assumed to be negligible over the time intervals of interest, i.e., $\nu_a t \ll 1$, so that Equation (21-9) becomes:

$$\frac{\langle \nu_m \rangle}{N} = \frac{1}{t-t_o} \int_{t_o}^{t} \frac{\nu_m(\epsilon_K) dt}{N} = \frac{1}{t-t_o} \int_{\epsilon_K}^{\epsilon_o} \frac{\nu_m(\epsilon_K) d\bar{\epsilon}}{N(\epsilon_K - kT)\nu_u(\epsilon_K)} . \quad (21\text{-}10)$$

This relation is analogous to the relations used previously (Reference 21-38) in calculating the rates of excitation in terms of the $L(\epsilon)$ functions. The errors introduced by the use of electron transport coefficients and energy distributions appropriate to the dc experiments rather than those for the actual decay period following electron injection are not known but are probably significantly less than a factor of two. It is suggested that the errors are of comparable uncertainty to those introduced by use of the "continuous approximation" of previous calculations. According to this approximation (References 21-37, 21-38) the electrons are assumed to lose their energy in small increments rather than in jumps equal to the excitation energies for the various inelastic processes. Obviously, further effort (Reference 21-60) is required in order to evaluate the accuracy of the available calculation techniques and to develop practical computational methods for more accurate calculations.

## 21.7 RADIO-FREQUENCY TRANSMISSION COEFFICIENTS FOR IONS

The prediction of change in dielectric constant and the radio-frequency transmission coefficients applicable in the presence of ions in atmospheric gases is made difficult because of: a) the lack of definitive information as to the identity of the ions; b) the difficulty of accurate ion-mobility measurements in the presence of fast ion-molecule reactions; and c) the apparent absence of a thorough investigation of the frequency dependence of the change in the dielectric constant caused by ions. Rocket-borne mass spectrometers (Reference 21-61) have shown that ions such as $H_3O^+$, $H_3O^+ \cdot (H_2O)_n$, $NO^+$, $O_2^+$, $N_2^+$, $NO_3^-$, and $NO_3^- \cdot (H_2O)_n$ are present in varying concentrations at altitudes above about 60 km. We therefore need to concern ourselves with the measured mobilities of these ions in gases of atmospheric interest. Since the momentum-transfer collision cross-sections for ions with various atmospheric molecules vary over a much smaller range than is the case for electrons, it is reasonable to consider scattering only by the major species, i.e., $N_2$, $O_2$, and O.

Suggested values for the mobilities of some of the positive and negative ions of interest are listed in Table 21-4. Most of the available laboratory data (References 21-62 through 21-68) are for a gas temperature of 300 K. Except for cases in which resonant charge transfer can occur, one expects that the thermal ion mobility $\mu_i$ will not deviate significantly from the relation (References 21-69, 21-70):

Table 21-4. Mobilities of ions in atmospheric gases.[a] Values shown are in units of $10^{19}$ $V^{-1}$ $cm^{-1}$ $sec^{-1}$.

| Ion | GAS | | | | | | | |
|---|---|---|---|---|---|---|---|---|
| | $N_2$ | Reference | $O_2$ | Reference | Air[b] | Reference | O | Reference |
| $N^+$ | (8.8)<br>8.0 | 21-63 | (9.4)[c] | | 8.2[c] | | (14.4) | |
| $N_2^+$ | 5.0 | 21-63 | (7.6)[c]<br>8.6[c] | 21-62 | 5.4[c] | | (12.5)[c] | |
| $N_3^+$ | (6.6)<br>6.1 | 21-63 | (6.9) | | 6.2 | | (11.5) | |
| $N_4^+$ | (6.2)<br>6.3 | 21-63 | (6.5) | | 6.3 | | (11.1) | |
| $O^+$ | (8.4)<br>8.6-10.0 | 21-62 | (9.0)<br>8.9 | 21-62 | (8.5)<br>9 | | 14.4 | 21-62 |
| $O_2^+$ | (7.0)<br>8.2 | 21-62 | 6.0 | 21-66 | 6.7 | 21-64 | 14-5 | 21-62 |
| $O_4^+$ | (6.1) | | (6.4) | | (6.1) | | (11.0) | |
| $NO^+$ | (7.1)<br>9.0 | 21-65 | (7.6) | | 9.4 | 21-64 | 14.8 | 21-62 |
| $H_3O^+$ | (8.0) | | (8.5) | | (8.1) | | (13.3) | |

Table 21-4. (Cont'd.)

| Ion | GAS | | | | | | | |
|---|---|---|---|---|---|---|---|---|
| | $N_2$ | Reference | $O_2$ | Reference | Air[b] | Reference | O | Reference |
| $H_3O^+ \cdot H_2O$ | (6.8) | | (7.1) | | (6.8) | | (11.8) | |
| $O_2^-$ | (7.0) | | 5.8 | 21-66 | 6.7 | | (12.0)[c] | |
| $O_3^-$ | (6.4) | | (6.7)<br>6.9 | 21-66 | (6.4) | | (11.5) | |
| $O_4^-$ | (6.1) | | (6.4)<br>5.8[d] | 21-66 | 6.0 | | (11.0)[c] | |
| $CO_3^-$ | (6.3) | | (6.4)<br>6.7 | 21-66 | (6.3) | | (11.0) | |
| $CO_4^-$ | (5.9) | | (6.2)<br>6.6 | 21-66 | (6.0) | | 10.8 | |
| $NO_2^-$ | (6.4) | | (6.7) | | (6.5) | | (11.4) | |
| $NO_3^-$ | (6.1) | | (6.4) | | (6.2) | | (11.0) | |
| $NO_3^- \cdot H_2O$ | (5.9) | | (6.1) | | (6.0) | | (10.8) | |

Notes:

[a] Values shown in parentheses are calculated using Equation (21-11) and polarizabilities at 11.9, 10.8 and 6.0 $a_o^3$ for $N_2$, $O_2$, and O, respectively. Most experimental values are for approximately 300 K.

Table 21-4. (Cont'd.)

Notes (Cont'd.):

[b] Dry air, sea-level compasition. Except where a reference is indicated these values were calculated using the value listed far $O_2$ und $N_2$ in Equation (21-12).

[c] Callision is accompanied by a fast two-body icn-malecule reaction.

[d] Here we have made use af the observation (References 21-66, 21-67) that the $O_2^-$ and $O_4^-$ mobilities are very nearly equal.

$$\mu_i N = \frac{9.66 \times 10^{+20}}{\sqrt{\alpha M_i}} \text{ cm}^{-1}\text{V}^{-1}\text{sec}^{-1} , \qquad (21\text{-}11)$$

where $\alpha$ is the atomic polarizability in units of $a_o^3$, $a_o$ is the Bohr radius, and $M_i$ is the reduced mass of the ion and neutral in units of the proton mass. In cases where experimental data are not available the ion mobilities are calculated using Equation (21-11) and are shown in parentheses in Table 21-4. The data of Table 21-4 show that values given by Equation (21-11) are low by a factor of $1.1 \pm 0.1$ for all except ions in their parent gas. Recently measured values (Reference 21-68) of the mobilities of hydrated positive and negative ions agree well with the predictions of Equation (21-11) for argon.

The mobility of an ion in a gas mixture can be calculated from the mobilities of that ion in the individual gases using the relation (Reference 21-71):

$$\mu N = \left[ \sum_j (\mu N)_j^{-1} \, (N_j/N) \right]^{-1} . \qquad (21\text{-}12)$$

This expression is used for the calculated values for air in Table 21-4.

The change in the dielectric constant caused by ions $\Delta K_i$ is customarily (References 21-72 through 21-75) written in a form equivalent to:

$$\Delta K_i = \frac{N_i e^2}{M_i \epsilon_0 \omega (\nu_i + j\Omega)} , \qquad (21\text{-}13)$$

where $N_i$, $M_i$, and $\nu_i$ are the density, mass, and collision frequency for a given ionic species. Here $\Omega = \omega$ or $\omega \pm \omega_{bi}$, where $\omega_{bi}$ is the ion cyclotron frequency. In the low-frequency limit:

$$\text{Im } \Delta K_i = N_i e^2 / M_i \epsilon_0 \nu_i \omega = N_i e \mu_i / \epsilon_0 \omega , \qquad (21\text{-}14)$$

where $\mu_i = e/M_i\nu_i$ is the ion mobility. In the case where the fre-

quency of momentum-transfer collisions is independent of the relative velocity, then $\nu_i$ is that frequency and $M_i$ is the reduced mass (References 21-75, 21-76). For ions in thermal equilibrium with the gas, calculations of ion mobility can be made using differential scattering cross-section data (Reference 21-75). However, there appears to have been no investigation of the consistency of rigorous theory with Equation (21-13) when used for the calculation of $\mathrm{Re}\,\Delta K_i$ or of the value of $\mathrm{Im}\,\Delta K_i$ when $(\mathrm{Re}\,\Delta K_i/\mathrm{Im}\,\Delta K_i)^2$ is other than a very small number. As a result one can only arbitrarily define the collision frequency (References 21-72 through 21-74) in terms of the dc mobility as $\nu_i = e/M_i\mu_i$. Here we use the reduced mass, although some authors use the ion mass (Reference 21-77).

The errors resulting from the use of Equation (21-13) for other than the low-frequency limit of $\mathrm{Im}\,\Delta K_i$ are unknown but are probably less than a factor of two. In many calculations of ionospheric absorption (Reference 21-72) the frequencies of interest are low enough and the gas densities are high enough so that it is unnecessary, and probably undesirable, to define an effective collision frequency for ions (Reference 21-73). It is of interest to note that in the low-frequency limit:

$$\mathrm{Re}\,\Delta K_i = N_i e^2/M_i\epsilon_0\nu_i^2 = N_i\mu_i^2 M_i/\epsilon_0 . \qquad (21\text{-}15)$$

Therefore, $\mathrm{Re}\,\Delta K_i$ is independent of the ion identity and mass in cases for which the mass dependence given by Equation (21-11) is valid, i.e., all ions except those moving in their parent gas.

Since the concentrations of ions and neutral species vary with altitude, it is not possible to assign a unique positive-ion mobility to the ionosphere. Based on the mobilities of Table 21-4, the apparent small systematic overestimates obtained using Equation (21-11), the measured ion compositions (Reference 21-61), and the neutral composition of the atmosphere (References 21-23, 21-78), one expects the average positive-ion mobility to decrease from about $7 \times 10^{19}$ $V^{-1}$ $cm^{-1}$ $sec^{-1}$ at 120 km ($NO^+$ in $N_2$, $O_2$, and O), to about $6.3 \times 10^{19}$ $V^{-1}$ $cm^{-1}$ $sec^{-1}$ at 70 km ($H_3O^+ \cdot H_2O$ in air). At about 30 km, measurements (Reference 21-79) give an average value of $(4.6 \pm 0.8) \times 10^{19}$ $V^{-1}$ $cm^{-1}$ $sec^{-1}$ while at sea level the measured values vary from 6.4 to $1.3 \times 10^{19}$ $V^{-1}$ $cm^{-1}$ $sec^{-1}$ or less, depending upon the "age" of the ion (References 21-80, 21-81). These mobilities can be used in Equation (21-14) so long as $\omega/N$ or $(\omega - \omega_{bi})/N$ is much less than

about $10^{-9}$ $cm^3 sec^{-1}$. At higher frequencies one can only estimate an effective collision frequency and use Equations (21-13) or (21-14) as discussed above.

## 21.8 SUMMARY

Although the data presented in Section 21.2 show that our knowledge of the electron collision frequency for some of the atoms and molecules expected in normal and disturbed air is poor, the collision frequencies for the more likely mixtures are probably known with much more accuracy than are the electron densities which are also used in the calculation of rf propagation coefficients. Further experimental studies of low-energy electron collisions in atomic and molecular oxygen would seem to be particularly worthwhile.

Electron energy relaxation data are still scarce and highly dependent on theory. Much experimental and theoretical work remains to be done to ensure that one has accurately included all of the important processes.

Experimental mobility data are available for some ions of interest, and theory can be used to estimate others, but better data are very desirable. The prediction of low-frequency rf attenuation caused by ions is much less dependent upon the mass of the ions than suggested by some investigators.

## REFERENCES

21-1. Engelhardt, A. G., A. V. Phelps, and C. G. Risk, Phys. Rev. 135, A1566 (1964). The rapid rise in the inelastic cross-section for $N_2$ between 21 and 25 eV which was postulated in this paper has not been detected by other experiments. Possible sources of error at the high E/N of significance here are the omission from the Boltzmann equation of terms corresponding to heating of the electrons produced by ionization and the departures from a nearly isotropic electron energy distribution.

21-2. Phelps, A. V., J. Appl. Phys. 31, 1723 (1960). See also Huxley, L. G. H., J. Atm. Terrestr. Phys. 16, 46 (1959).

21-3. Mentzoni, M.H., J. Res. Natl. Bur. Stds. 69D, 213 (1965); Veatch, G.E., J. T. Verdeyen, and J.H. Cahn, Bull. Am. Phys. Soc. 11, 496 (1966). Earlier results are those of van Lint, V.A.J., E.G. Wikner, and D.L. Trueblood, Bull. Am. Phys. Soc. 5, 122 (1960), and Fehsenfeld, F.C., J. Chem. Phys. 39, 1653 (1963).

21-4. Hake, R.D., Jr., and A.V. Phelps, Phys. Rev. 158, 70 (1967). Note that the momentum-transfer and inelastic cross-sections for $O_2$ given by A.V. Phelps in N.B.S. Tech. Note No. 211, Vol. 5 (1964) were the result of a very preliminary analysis and are no longer considered valid.

21-5. Nelson, D.R., and F.J. Davis, 23rd Gaseous Electronics Conference, Hartford, Connecticut (1970). Analysis of these low E/N drift velocity and longitudinal diffusion coefficient data should allow a better comparison of dc and microwave collision frequency and energy relaxation data.

21-6. Boness, M.J.W., and J.B. Hasted, Phys. Letts. 21, 526 (1966); Spence, D., and G.J. Schulz, Phys. Rev. A2, 1802 (1970).

21-7. Sunshine, G., B.B. Aubrey, and B. Bederson, Phys. Rev. 154, 1 (1967).

21-8. Salop, A., and N.N. Nakano, Phys. Rev. A2, 127 (1970).

21-9. Nicolet, M., Phys. Fluids 2, 95 (1959).

21-10. Shkarofsky, J.P., M.P. Bachynski, and T.W. Johnston, Planet.Space Sci. 6, 24 (1961).

21-11. Frost, L.S., and A.V. Phelps, Phys. Rev. 136, A1538 (1966).

21-12. Pack, J.L., R.E. Voshall, and A.V. Phelps, Phys. Rev. 127, 2084 (1962).

21-13. A consistent set of momentum-transfer and inelastic collision cross-sections have been obtained for $H_2O$ and NO by R.S. Cohen and A.V. Phelps (unpublished).

21-14. Takeda, S., and A. A. Dougal, J. Appl. Phys. 31, 412 (1960); Lowke, J. J., and J. A. Rees, Austral. J. Phys. 16, 447 (1963); Crompton, R. W., J. A. Rees, and R. L. Jory, Ibid. 18, 541 (1965); Ryzko, H., Proc. Phys. Soc. 85, 1283 (1965).

21-15. Altshuler, S., Phys. Rev. 107, 114 (1957); Mittelman, M. H., and R. E. von Holt, Phys. Rev. 140, A726 (1965); Crawford, O. H., A. Dalgarno, and P. B. Hays, Mol. Phys. 13, 191 (1967); Takayanagi, K., and Y. Itikawa, J. Phys. Soc. Japan 24, 160 (1968); Burt, P. B., W. E. Getty, and H. W. Graben, Phys. Letts. 29A, 261 (1969); Crawford, O. H., Chem. Phys. Letts. 2, 461 (1968). Altshuler's theory has been found to work well for electrons in CO at low energies (Reference 21-4) but to be low by approximately a factor of two (Reference 21-12) for $H_2O$. Note that the 13 percent "correction" proposed by Crawford et al is not valid because these authors did not carry the Chapman-Cowling type of procedure to a sufficiently high order of approximation. See Chapman, S., and T. G. Cowling, The Mathematical Theory of Non-Uniform Gases, 3rd Ed., Cambridge University Press, London (1952); p. 192.

21-16. Parkes, D. A., Thesis, Cambridge University, England (1965) (unpublished); Bailey V. A., and J. M. Someville, Phil. Mag. 17, 1169 (1934).

21-17. Mentzoni, M. H., and J. Donohoe, Can. J. Phys. 44, 693 (1966).

21-18. Neynaber, R. H., L. L. Marino, E. W. Rothe, and S. M. Trujillo, Phys. Rev. 123, 148 (1961).

21-19. Lin, S. C., and B. Kivel, Phys. Rev. 114, 1026 (1959); Diaber, J. W., and H. F. Waldron, Ibid. 151, 51 (1966). Our own efforts to reanalyze the data of Lin and Kivel using the $O_2$ and $N_2$ collision frequencies of Figure 21-1 lead to negative values for $\nu_m(\epsilon)/N$ for electrons in atomic oxygen.

21-20. Henry, R. J. W., P. G. Burke, and A. L. Sinfailam, Phys. Rev. 178, 218 (1969). Some of the theoretical calculations of momentum-transfer cross-sections for O have been discussed by C. J. Cook and D. C. Lorents. See Whitten, R. C., and I. G. Poppoff, Physics of the Lower Ionosphere, Prentice-Hall, Inc., Englewood Cliffs, N. J. (1965); Chap. 7.

21-21. Taylor, R. L., and G. Caledonia, J. Quant. Spectry. Radiative Transfer 9, 681 (1969). Earlier work is reviewed by Johnston, R. R., Ibid. 7, 815 (1967).

21-22. Neynaber, R. H., L. L. Marino, E. W. Rothe, and S. M. Trujillo, Phys. Rev. 129, 2069 (1963).

21-23. Chen, C. L., Phys. Rev. 135, A627 (1964).

21-24. Sen, H. K., and A. A. Wyller, J. Geophys. Res. 65, 3931 (1960); Budden, K. G., Radio Sci. 69D, 191 (1965).

21-25. Molmud, P., Phys. Fluids 7, 150 (1964).

21-26. Shkarofsky, I. P., Can. J. Phys. 39, 1619 (1961). Some of the relations given in this article have been stated in a different, but equivalent, form and applied to specific cases by Whitmer, R. F., and G. F. Herrmann, Phys. Fluids 9, 768 (1966).

21-27. COSPAR International Reference Atmosphere 1965, North Holland Publishing Co., Amsterdam (1965). See also Chapter 2 of this Handbook.

21-28. Dingle, R. B., D. Arnt, and S. K. Roy, Appl. Sci. Res. 6B, 155 (1956).

21-29. Kane, J. A., NASA Tech. Note 503 (1960); J. Geophys. Res. 64, 133 (1959); Jesperson, M., et al, Planet. Space Sci. 12, 543 (1964); Thane, E. V., and W. R. Piggott, J. Atm. Terrestr. Phys. 28, 721 (1966); Belrose, J. S., Ibid. 32, 567 (1970).

21-30. Carruthers, J. A., Can. J. Phys. 40, 1528 (1962).

21-31. Recent work is summarized by: Lassettre, E. N., Can. J. Chem. 47, 1733 (1969); Trajmar, S., J. K. Rice, and A. Kupperman, in Advances in Chemical Physics, I. Prigogine and S. A. Rice, Eds., John Wiley and Sons, Inc., New York (1970); Vol. 18.

21-32. Brinkman, R. T., and S. Trajmar, Ann. Geophys. 26, 201 (1970).

21-33. Davidson, G., and R. O'Neil, J. Chem. Phys. 41, 3946 (1964); Brocklehurst, B., and F. A. Downing, Ibid. 46, 2976 (1967); Hartman, P. L., Planet. Space Sci. 16, 1315 (1968); Holland, R. F., Bull. Am. Phys. Soc. 13, 897 (1968); Phys. Rev. 51, 3940 (1969).

21-34. Mentzoni, M. V., and R. V. Row, Phys. Rev. 130, 2312 (1963); Narasinga Rao, K. V., and R. L. Taylor, Phys. Letts. 27A, 296 (1968).

21-35. Smith, R. A., J. A. Bourne, E. G. Loch, and T. N. R. Coyne, Conf. Ground-Based Radio Wave Propagation Studies Lower Ionosph., Ottawa, Canada (1966); paper 3. 2. 1.

21-36. Dalgarno, A., Can. J. Chem. 47, 1723 (1969); Peterson, L. R., S. S. Prasad, and A. E. S. Green, Ibid. 47, 1774 (1969); Takayanagi, K., Repts Ionosph. Space Res. 19, 1, 16 (1965); Takayanagi, K., and T. Takahashi, Ibid. 20, 357 (1966).

21-37. Green, A. E. S., and L. R. Peterson, J. Geophys. Res. 73, 233 (1968); Dalgarno, A., M. B. McElroy, and A. I. Stewart, J. Atm. Sci. 26, 753 (1969), Landshoff, R. K., Lockheed Missiles and Space Corp., Report LMSC 3-27-67-1 (Vol. 4), DASA 1917-4 (1967); Rees, M. H., A. I. Stewart, and J. C. G. Walker, Planet. Space Sci. 17, 1997 (1969).

21-38. Peterson, L. R., Phys. Rev. 187, 105 (1969).

21-39. Carleton, N. P., and L. R. Megill, Phys. Rev. 126, 2089 (1962); Altshuler, S., J. Geophys. Res. 68, 4707 (1963). The results presented in Reference 21-1 show that the analyses of these references need to be repeated using more recent cross-section data.

21-40. Dalgarno, A., M.B. McElroy, M.H. Rees, and J.C.G. Walker, Planet. Space Sci. 16, 1371 (1968); Lane, N.F., and A. Dalgarno, J. Geophys. Res. 74, 3011 (1969); Whitten, R.C., J. Atm. Terrestr. Phys. 32, 1143 (1970).

21-41. Opal, C.B., W.K. Peterson, and E.C. Beaty, J. Chem. Phys. 55, 4100 (1971); Tisone, G.C., Bull. Am. Phys. Soc. 16, 202 (1971); Peterson, W.K., C.B. Opal, and E.C. Beaty, Ibid.

21-42. Huxley, L.G.H., and R.W. Crompton, in Atomic and Molecular Processes, D.R. Bates, Ed., Academic Press, New York (1962); Chap. 10.

21-43. Phelps, A.V., Revs. Mod. Phys. 40, 399 (1968); Takayanagi, K., Prog. Theoret. Phys. 40, 216 (1967); Takayanagi, K., and Y. Itikawa, in Advances in Atomic and Molecular Physics., D.R. Bates, Ed., Academic Press, Inc., New York (1970); Vol. 6, p. 105.

21-44. For recent measurements of energy relaxation at near-thermal energies see Warman, J.M., and M.C. Sauer, Jr., J. Chem. Phys. 52, 6428 (1970). The rate of electron energy relaxation is inferred from the time dependence of electron loss by attachment to $CCl_4$.

21-45. Fields, H., G. Bekefi, and S.C. Brown, Phys. Rev. 129, 506 (1963); Heylen, A.E.D., Proc. Phys. Soc. 79, 284 (1962).

21-46. As yet there are no useful theoretical studies of the effects of discrete electron energy losses on transient electron energy distributions and transport coefficients.

21-47. The available calculations of $\nu_u$ or $\overline{G\nu}$ for near-thermal electrons at various gas temperatures are correct only for conditions in which the electron energy distribution remains Maxwellian when the electron energy is raised above that of the gas by the applied field, e.g., in the case of strong electron-electron interaction. Thus, the thermal $\nu_u/N$ values measured and calculated numerically for $N_2$ for dc electric fields are only about half those given by Dalgarno,

A., and R.J. Moffett, Planet. Space Sci. 9, 439 (1962), even though the same inelastic collision cross-sections were used.

21-48. Chen, J.C.Y., J. Chem. Phys. 40, 3507 (1964); Phys. Letts. 45, 2710 (1966).

21-49. Mentzoni, M.H., and K.V. Narasinga Rao, Phys. Rev. Letts. 14, 779 (1965).

21-50. Geltman, S., and K. Takayanagi, Phys. Rev. 143, 25 (1966); see also Reference 21-43.

21-51. Konishi, A., K. Wakiya, M. Yamamoto, and H. Suzuki, J. Phys. Soc. Japan 29, 526 (1970); Cartwright, D.C., W. Williams, and S. Trajmar, Bull. Am. Phys. Soc. 15, 1518 (1970); Spence, D., and G.J. Schulz, Phys. Rev. A2, 1802 (1970).

21-52. Dalgarno, A., and T.C. Degges, Planet. Space Sci. 16, 125 (1968).

21-53. Moiseiwitsch, B.L., and S.J. Smith, Revs. Mod. Phys. 40, 238 (1968).

21-54. Stelman, D.S., and A.V. Phelps, DASA Symposium on Physics and Chemistry of the Upper Atmosphere, Stanford Research Institute (1969); J. Chem. Phys. (submitted, 1971).

21-55. Cottrell, T.L., and I.C. Walker, Quart. Revs. 20, 153 (1966).

21-56. Stabler, R.C., Phys. Rev. 131, 679 (1963); Sampson, D.H., Phys. Rev. 137, A4 (1965).

21-57. For an extremely narrow electron energy distribution and a rapidly increasing $Q_m(\epsilon)$, $\bar{\epsilon}/\epsilon_k$ can be (Reference 21-46) as low as 0.3. For molecular gases calculations (References 21-1, 21-4) show $1.1 < \bar{\epsilon}/\epsilon_k < 1.5$ but for Xe, $\bar{\epsilon}/\epsilon_k$ is (Reference 21-11) as low as 0.47).

21-58. Similar calculations have been made independently by C.E. Baum (unpublished).

21-59. The actual values of $\nu_{n1}(\epsilon_k)$ used in obtaining the upper curve of Figure 21-5 are those calculated from the readily available dc mobility, and are not those which should be used in calculations of the high-frequency limit of Equation (21-2). Therefore the values shown are significant primarily because they show that large values of $(t-t_o)N$ are required in order for the collision frequency to reach its thermal value.

21-60. Stewart, A. I., J. Geophys. Res. 75, 6333 (1970).

21-61. Narcisi, R. S., and A. D. Bailey, J. Geophys. Res. 70, 3687 (1965); Ann. Geophys. 22, 224 (1966); Narcisi, R. S., C. R. Philbrick, A. D. Bailey, and I. Delia Lucca, Conf. Meteorolog. Chem. Factors D-Region Aeronomy, University of Illinois (1969); R. S. Narcisi, R. S. (private communication).

21-62. Mason, E. A., Planet. Space Sci. 18, 137 (1970). The values quoted in Table 21-4 are for 200 K.

21-63. Moseley, J. T., R. M. Snuggs, D. W. Martin, and E. W. McDaniel, Phys. Rev. 178, 240 (1969).

21-64. Sinnott, G., D. E. Golden, and R. N. Varney, Phys. Rev. 170, 272 (1968).

21-65. Young, R. A., C. A. Gatz, R. L. Sharpless, and C. M. Ablow, Phys. Rev. 138, A359 (1965).

21-66. Snuggs, R. M., D. J. Volz, J. H. Schummers, D. W. Martin, and E. W. McDaniel, Bull. Am. Phys. Soc. 15, 433 (1970); Snuggs, R. M., Ph. D. Thesis, Georgia Institute of Technology (1970).

21-67. McKnight, L. G., Phys. Rev. A2, 762 (1970).

21-68. Young, C. E., D. Edelson, and W. E. Falconer, J. Chem. Phys. 53, 4295 (1970).

21-69. McDaniel, E. W., Collision Phenomena in Ionized Gases, John Wiley and Sons, Inc., New York (1964); Chapter 9; Smirnov, B. M., Usp. Fiz. Nauk. 92, 75 (1967) [translation: Sov. Phys.-Usp. 10, 313 (1967)].

21-70. Banks, P., Planet. Space Sci. 14, 1085, 1105 (1966).

21-71. Sandler, S. I., and E. A. Mason, J. Chem. Phys. 48, 2873 (1968); Biondi, M. A., and L. M. Chanin, Phys. Rev. 122, 843 (1961).

21-72. Crain, C. M., and H. G. Booker, J. Geophys. Res. 69, 4713 (1964); Thomas, L., J. Atm. Terrestr. Phys. 31, 991 (1969); Crain, C. M., Ibid. 32, 551 (1970).

21-73. Hirsh, M. N., G. M. Halpern, and N. S. Wolf, Bull. Am. Phys. Soc. 13, 199 (1968); Hirsh, M. N., N. S. Wolf, and G. M. Halpern, DASA Symposium on Physics and Chemistry of the Upper Atmosphere, Pittsburgh (1967).

21-74. Beauchamp, J. L., J. Chem. Phys. 46, 1231 (1967).

21-75. Chapman, S., and T. G. Cowling, The Mathematical Theory of Non-Uniform Gases, 3rd Ed., Cambridge University Press, London (1952); Chap. 19.

21-76. Wannier, G. H., Phys. Rev. 83, 281 (1951); Ibid 87, 795 (1952); Bell System Tech. J. 32, 170 (1953).

21-77. As an example of the uncertainty as to the proper ion collision frequency (Reference 21-70) one notes that in Reference 21-72 the ion mass is used to calculate the frequency (as for electrons) whereas Reference 21-76 uses the reduced mass.

21-78. Rees, M. H., J. C. G. Walker, and A. Dalgarno, Planet. Space Sci. 15, 1097 (1967).

21-79. Paltridge, G. W., J. Geophys. Res. 70, 2751 (1965).

21-30. Loeb, L. B., in Advances in Geophysics, H. E. Landsberg, and J. Van Mieghan, Eds., Academic Press, Inc., New York (1969); p. 223; Knoll, M., J. Eichmeier, and R. W. Sehön, in Advances in Electronics and Electron Physics, L. Marton, Ed., Academic Press, Inc., New York (1964); Vol. 19, p. 177.

21-81. Keller, G. E., J. Geophys. Res., Space Phys. 73, 3483 (1968); Ferguson, E. E., Revs. Geophys. 5, 305 (1967).

## GROUP D

## CHAPTERS ON DATA APPLICATION


CHAPTER 22 Deionization Solutions

CHAPTER 23 Problem Areas in Atmospheric Deionization

CHAPTER 24 Summery of Suggested Rate Constants

# 22. DEIONIZATION SOLUTIONS*

Capt. S.D. Rockwood, Air Force Weapons Laboratory
W.S. Knapp, General Electric—TEMPO
F.E. Niles, Ballistic Research Laboratories
(Latest Revision 1 September 1971)

## 22.1 INTRODUCTION

This chapter will document the results of several detailed calculations of the chemistry associated with the perturbed D, E, and F regions.

Some of these calculations will be devoted to exhibiting the advantages and disadvantages of different numerical methods. Others will attempt to identify, where possible, critical reactions of the regions studied. It is intended that these examples can serve both as a standard of comparison and as a guide for developing simplified schemes for future application.

## 22.2 MULTI-SPECIES CODES

### 22.2.1 D Region

Examples will be given of the multispecies code approach for solving the deionization kinetics of the D-region. The successes and limitations of such an approach will be discussed.

### 22.2.2 E and F Regions

The important role of the metastable states, especially $O(^1D)$, $N(^2D)$, and vibrationally excited $N_2$, in the process of deionization will be demonstrated. Further discussions will be given of the role played by excited states in determining the ultraviolet and X-ray pressure efficiencies, and the resulting coupling of hydrodynamics and chemistry.

---

*Editor's Note: A full chapter under this title will be prepared and distributed to authorized recipients of the Handbook at an early date. We present here an outline of the projected chapter, as proposed by the authors.

## 22.3 CODES FOR SYSTEMS

A description of the D-region lumped-parameter model developed from nuclear test data will be presented. This section will also include a discussion of the range of validity of the recombination parameter, $\alpha$ ,,defined at equilibrium as $\alpha \equiv q/n_e^2$, where $q(cm^{-3}\ sec^{-1})$ is an electron source, and $n_e(cm^{-3})$ is the electron number density.

# 23. PROBLEM AREAS IN ATMOSPHERIC DEIONIZATION

C.A. Blank, Defense Nuclear Agency
M.H. Bortner, General Electric Company
T. Baurer, General Electric Company
(Latest Revision 23 February 1972)

N. B. : This chapter was not ready for publication in time to be distributed with the rest of the Handbook. Chapter 23 will be prepared and distributed to authorized recipients of the Handbook at an early date.

# 24. SUMMARY OF SUGGESTED RATE CONSTANTS

M.H. Bortner, General Electric Company
R.H. Kummler, Wayne State University
T. Baurer, General Electric Company
(Latest Revision 24 September 1971)

## 24.1 INTRODUCTION

This chapter presents in Table 24-1 a summary of reactions, with suggested rate coefficients, relevant to the problems of atmospheric chemical recovery following a perturbation. The present generation of computers permits the convenient handling of large numbers of reactions in relation to the solution of such problems. Thus, one may now include in detailed calculations of this type, hundreds of individual reactions, and follow the complete histories of large numbers of individual species as atmospheric constituents. Many computer codes exist, e.g., the Keneshea code (Reference 24-1), which have been designed for the study of atmospheric reactions, and are capable of carrying out the appropriate calculations. Such codes are in use at various institutes and laboratories throughout the country. In order to promote communications among these installations it is convenient to have one standard set of rate coefficients which are recognized universally as valid for all common purposes, e.g., the comparative solution of test problems, or the complementary solution of different aspects of one large problem.

## 24.2 PRESENTATION OF REACTIONS AND RATE DATA

The reactions are listed in Table 24-1 in the same order as the reaction types given in Chapter 6 (Table 6-1), but the type numbers used are not the same in the two tabulations. Furthermore, where the authors of the various Chapters of this Handbook have recommended specific values for the reaction rate constants or coefficients, those values are used in Table 24-1. On the other hand, where such data are either uncertain or not available for particular reactions which are considered sufficiently important to be included, values of the rate constants or coefficients have been estimated, in most in-



Preceding page blank

stances by a committee of knowledgeable workers. These cases carry the notation (in the "Sources" column of the table) "HCE", or "Handbook Committee Estimate". THUS, A LARGE NUMBER OF THE REACTIONS LISTED ARE STILL PRIMARILY GUESSES. ONE SHOULD BE EXTREMELY CAREFUL NOT TO CONSIDER THESE RATES AS FINAL. In several cases the degree of uncertainty is based on the unavailability of any experimental data for the reaction considered. Where this is true, a notation "NED" ("No Experimental Data") is included among the applicable notes. Perhaps the latter label should have been applied to many more reactions in Table 24-1 than it has been.

It may be argued by some Handbook users that many of the reactions listed are not important. This is perhaps true under certain sets of conditions, in which case the reactions may be totally ignored, or alternatively their rates may be set equal to zero for coding purposes. However, under other, equally important circumstances, these same reactions may either contribute directly to or act as precursors of other processes which are influential within the given context. On the other hand, although the numbers of reactions and species included in the table are large, there certainly are some important omissions as well, since it can be anticipated that particular reactions, not yet thought to be of any importance to the deionization problem, or perhaps not yet even conceived of, may be found in the future to play some weighty role in the overall atmospheric chemical scheme.

In Table 24-1, the rate coefficients are presented in cgs units, i.e., in $sec^{-1}$, $cm^3 sec^{-1}$, and $cm^6 sec^{-1}$ for one-, two-, and three-body processes, respectively. Species densities are in $cm^{-3}$ and temperature in K. The letter "M" is used to represent a collision partner; unless specifically noted otherwise, it represents any possible species present and acting as catalyst. The numerical notation [-x] signifies multiplication by $10^{-x}$. Most rate functions "k" are represented by sets of numbers "a", "b", and "c", which refer in turn to the formulation:

$$k = a(T/300)^b \exp(-c/T),$$

where 300 in the first parenthesized term is the usual reference temperature (in K), unless another $T_{ref}$ is designated in the table. A few rate functions follow a more complex variation with temperature than that given above, or are dependent on other parameters as well, e.g.,

local species densities. These complex functions are presented in brackets, transcending the usual format of the table. Elsewhere, only the coefficient "a" is itself density-dependent rather than constant. Here, too, brackets are used.

A high degree of uncertainty for some of the data was implied in preceding paragraphs of this discussion. This uncertainty is particularly appropriate to the values of the exponent "b" in the above mathematical expression. For example, little or no experimental knowledge of the temperature dependence (to which "b" relates directly) is available for many exothermic reactions, which have been observed primarily at laboratory temperatures. Moreover, most of the reactions included in Table 24-1 are indeed exothermic, despite two recent trends, viz.: (a) an increasing emphasis within the atmospheric effects community on the study of high-temperature (including endothermic) processes; and hence (b) the inclusion of more endothermic reactions in the present edition of the Handbook than in its predecessor.

Wherever, in Table 24-1, $c \neq 0$, it follows that the rate constant at 300 K is unequal to the listed value of the "a" parameter; in all such cases the rate constant at 300 K, $k_{300}$, has been calculated from the three parameters and is listed in the "Notes" column. Such values are not to be construed as implying actual measurement at 300 K, unless specifically so stated in the table.

Finally, it should be noted that for a few reactions, e.g., XIX. 3-6, an unreasonably high value of the "a" parameter is tabulated. These appear to fit the available data (Reference 24-2), but more work is obviously needed. In some cases the reaction products are uncertain, and the noncommittal notation, "Products", is provided in the reaction equation itself, as an alternative to any guess or "guesstimate" as to the true identities of specific products.

Table 24-1. Reactions and suggested rate constants.

$k = a(T/300)^b e^{-c/T}$

| No. | Reaction | a | b | c | Notes | Sources |
|---|---|---|---|---|---|---|
| I. Radiative Recombination: | | | | | | |
| 1. | $O^+ + e \rightarrow O + h\nu$ | (3.5±1)[-12] | (-0.7±0.1) | 0 | | Chp. 16 |
| 2. | $N^+ + e \rightarrow N + h\nu$ | (3.5±1)[-12] | (-0.7±0.1) | 0 | | Chp. 16 |
| 3. | $H^+ + e \rightarrow H + h\nu$ | (3.5±1)[-12] | (-0.7±0.1) | 0 | | Chp. 16 |
| 4. | $O_2^+ + e \rightarrow O_2 + h\nu$ | (4)[-12±1] | (-0.7±0.5) | 0 | | HCE[a] |
| 5. | $N_2^+ + e \rightarrow N_2 + h\nu$ | (4)[-12±1] | (-0.7±0.5) | 0 | | HCE |
| 6. | $NO^+ + e \rightarrow NO + h\nu$ | (4)[-12±1] | (-0.7±0.5) | 0 | | HCE |
| II. Photoionization: | | | | | | |
| 1.a. | $O + h\nu \rightarrow O^+ (^4S) + e$ | | | | Wavelength and Flux Dependent | Chps. 12, 13 |
| b. | $\rightarrow O^+ (^2D) + e$ | | | | Wavelength and Flux Dependent | Chps. 12, 13 |
| c. | $\rightarrow O^+ (^2P) + e$ | | | | Wavelength and Flux Dependent | Chps. 12, 13 |

[a] Handbook Committee estimate (see text).

Table 24-1. (Cont'd.)

| No. | Reaction | a | b | c | Notes | Sources |
|---|---|---|---|---|---|---|
| II. | Photoionization (Cont'd.) | | | | | |
| 2.a. | $N_2 + h\nu \rightarrow N_2^+ + e$ | | | | Wavelength and Flux Dependent | Chps. 12, 13 |
| b. | $\rightarrow N^+ + e + N$ | | | | Wavelength and Flux Dependent | Chps. 12, 13 |
| 3.a. | $O_2 + h\nu \rightarrow O_2^+ + e$ | | | | Wavelength and Flux Dependent | Chps. 12, 13 |
| b. | $\rightarrow O^+ + e + O$ | | | | Wavelength and Flux Dependent | Chps. 12, 13 |
| 4. | $NO + h\nu \rightarrow NO^+ + e$ | | | | Wavelength and Flux Dependent | Chps. 12, 13 |
| III. | Three-Body Recombination: | | | | | |
| 1. | $X^+ + e + M \rightarrow$ Products | (1)[-26±1] | (-2.5) | 0 | $X^+$ and M are either atomic or molecular | Chp. 16 |
| 2. | $X^+ + e + e \rightarrow$ Products | (1)[-19] | (-4.5) | 0 | | Chp. 16 |
| IV. | Dissociative Recombination: | | | | | |
| 1.a. | $O_2^+ + e \rightarrow O + O$ | (2.1±0.2)[-7] | (-0.7±0.3) | 0 | $T = T_i = T_e$ | Chp. 16 |

Table 24-1. (Cont'd.)

| No. | Reaction | a | b | c | Notes | Sources |
|---|---|---|---|---|---|---|
| IV. | Dissociative Recombination (Cont'd.): | | | | | |
| 1.b. | $O_2^+ + e \rightarrow O + O$ | (2.1±0.2)[-7] | (-0.6±0.1) | 0 | Te Variation; $T = T_i = 300\,K$ | Chp. 16 |
| c. | $\rightarrow 1.46\,O(^3P) + 0.18\,O(^1D) + 0.36\,O(^1S)$ | | | | Overall at $T = 300\,K$ | Chp. 16 |
| 2.a. | $N_2^+ + e \rightarrow N + N$ | (2.7±0.3)[-7] | (-0.2±0.2) | 0 | T Variation | Chp. 16 |
| b. | $\rightarrow N + N$ | $\left(1.8^{+0.4}_{-0.2}\right)$[-7] | (-0.39) | 0 | $T_e$ Variation | Chp. 16 |
| c. | $\rightarrow N(^2D) + N(^4S)$ | | | | Overall | HCE |
| 3.a. | $NO^+ + e \rightarrow N + O$ | (4.0±3)[-7] | (-1.±0.2) | 0 | T = 200-300 K | Chp. 16 |
| b. | $\rightarrow N + O$ | (4.0±3)[-7] | (-0.5±0.1) | 0 | T = 300-4000 K | Chp. 16 |
| c. | $\rightarrow 0.75\,N(^2D) + 0.25\,N(^4S) + O(^3P)$ | | | | Overall | HCE |
| 4. | $N_3^+ + e \rightarrow N + N_2$ | (7±4)[-7] | (-1) | 0 | | HCE |
| 5. | $N_4^+ + e \rightarrow N_2 + N_2$ | (2±1)[-6] | (-1) | 0 | | Chp. 16 |
| 6. | $NO_2^+ + e \rightarrow$ Products | (5±4)[-7] | (-1±1) | 0 | | HCE |
| 7. | $NO^+ \cdot NO + e \rightarrow NO + NO$ | (1.7±0.5)[-6] | (-1) | 0 | | Chp. 16 |

Table 24-1. (Cont'd.)

| No. | Reaction | a | b | c | Notes | Sources |
|---|---|---|---|---|---|---|
| IV. | Dissociative Recombination (Cont'd.) | | | | | |
| 8. | $NO^+ \cdot H_2O + e \rightarrow NO + H_2O$ | (1)[-6] | (-1) | 0 | | HCE |
| 9. | $NO^+ \cdot (H_2O)_2 + e \rightarrow NO + 2H_2O$ | (2)[-6] | (-1) | 0 | | HCE |
| 10. | $NO^+ \cdot (H_2O)_3 + e \rightarrow NO + 3H_2O$ | (3)[-6] | (-1) | 0 | | HCE |
| 11. | $O_2^+ \cdot O_2 + e \rightarrow O_2 + O_2$ | (2±0.5)[-6] | (-1) | 0 | | Chp. 16 |
| 12. | $O_2^+ \cdot H_2O + e \rightarrow O_2 + H_2O$ | (1.5)[-6] | (-1) | 0 | | HCE |
| 13. | $H_3O^+ + e \rightarrow H_2O + H$ | (1.3±0.3)[-6] | $\left(-0.2^{+0.1}_{-0.4}\right)$ | 0 | | Chp. 16 |
| 14. | $H_3O^+ \cdot H_2O + e \rightarrow H + 2H_2O$ | (2.8±0.4)[-6] | $\left(-0.2^{+0.1}_{-0.4}\right)$ | 0 | | Chp. 16 |
| 15. | $H_3O^+ \cdot (H_2O)_2 + e \rightarrow H + 3H_2O$ | (5.1±0.7)[-6] | $\left(-0.2^{+0.1}_{-0.4}\right)$ | 0 | | Chp. 16 |
| 16. | $H_3O^+ \cdot (H_2O)_3 + e \rightarrow H + 4H_2O$ | (6.1±1.2)[-6] | $\left(-0.2^{+0.1}_{-0.4}\right)$ | 0 | | Chp. 16 |
| 17. | $H_3O^+ \cdot (H_2O)_4 + e \rightarrow H + 5H_2O$ | (7.4±1.5)[-6] | $\left(-0.2^{+0.1}_{-0.4}\right)$ | 0 | | Chp. 16 |
| 18.[b] | $H_3O^+ \cdot (H_2O)_5 + e \rightarrow H + 6H_2O$ | (9.3±2)[-6] | $\left(-0.2^{+0.1}_{-0.4}\right)$ | 0 | | Chp. 16 |
| 19. | $H_3O^+ \cdot OH + e \rightarrow$ Products | (3)[-6] | (-1) | 0 | | HCE |

[b] The analogous reactions for higher hydrates, i.e., $H_3O^+ \cdot (H_2O)_n + e$ where $n \geq 6$, may be treated kinetically as if n=5, viz., by using the rate coefficients for reaction 18.

Table 24-1. (Cont'd.)

| No. | Reaction | a | b | c | Notes | Sources |
|---|---|---|---|---|---|---|
| V. | Mutual Neutralization: | | | | | |
| 1. | $O^+ + O^- \rightarrow O + O$ | (2.7±1.3)[-7] | (-.5) | 0 | | Chp. 16 |
| 2. | $O_2^+ + O^- \rightarrow$ Products | (9.6±3.0)[-8] | (-.5) | 0 | | Chp. 16 |
| 3. | $O_2^+ + O_2^- \rightarrow$ Products | (4.2±1.3)[-7] | (-.5) | 0 | | Chp. 16 |
| 4. | $O_2^+ + NO_2^- \rightarrow$ Products | (4.1±1.3)[-7] | (-.5) | 0 | | Chp. 16 |
| 5. | $O_2^+ + NO_3^- \rightarrow$ Products | (1.3±0.5)[-7] | (-.5) | 0 | | Chp. 16 |
| 6. | $N_2^+ + O_2^- \rightarrow$ Products | (1.6±0.5)[-7] | (-.5) | 0 | | Chp. 16 |
| 7. | $NO^+ + O^- \rightarrow$ Products | (4.9±1.5)[-7] | (-.5) | 0 | | Chp. 16 |
| 8. | $NO^+ + NO_2^- \rightarrow$ Products | (3.5±2)[-7] | (-.5) | 0 | | Chp. 16 |
| 9. | $NO^+ + NO_3^- \rightarrow$ Products | (8.0±3.0)[-7] | (-.5) | 0 | Neither value can be recommended aver the ather. | Chp. 16 |
| | | (3.4±1.2)[-8] | (-.5) | 0 | | |
| 10. | $N^+ + O^- \rightarrow N + O$ | (2.6±0.8)[-7] | (-.5) | 0 | | Chp. 16 |
| 11. | $X^+ + Y^- \rightarrow$ Products | $\left(1^{+4}_{-0.9}\right)$[-7] | (-.5) | 0 | $X^+$ and $Y^-$ ore either atomic ar molecular. | HCE |

Table 24-1. (Cont'd.)

| No. | Reaction | a | b | c | Notes | Sources |
|---|---|---|---|---|---|---|
| VI. | Three-Body Ion-Ion Recombination: | | | | | |
| 1. | $X^+ + Y^- + M \rightarrow$ Products | (3±1)[-25] | (-2.5) | 0 | $X^+$, $Y^-$, and M are either atomic or molecular "air" species. | Chp. 16 |
| VII. | Radiative Attachment: | | | | | |
| 1. | $O + e \rightarrow O^- + h\nu$ | (1.3±0.1)[-15] | 0 | 0 | | Chp. 17 |
| 2. | $O_2 + e \rightarrow O_2^- + h\nu$ | (2)[-19±1] | 0 | 0 | | Chp. 17 |
| 3. | $O_3 + e \rightarrow O_3^- + h\nu$ | (1)[-17±2] | 0 | 0 | Slow compared with Reactions XI.2(a,b). | HCE |
| 4. | $NO_2 + e \rightarrow NO_2^- + h\nu$ | (1)[-17±2] | 0 | 0 | See Reaction IX.8. | HCE |
| 5. | $OH + e \rightarrow OH^- + h\nu$ | (1)[-15±1] | 0 | 0 | | Chp. 17 |
| VIII. | Photodetachment: | | | | | |
| 1. | $O^- + h\nu \rightarrow O + e$ | (1.4±0.1)[0] | 0 | 0 | These values are for normal-incidence, unattenuated solar flux at top of earth's atmosphere. | Chp. 17 |
| 2. | $O_2^- + h\nu \rightarrow O_2 + e$ | (0.33±0.1)[0] | 0 | 0 | | Chp. 17 |

Table 24-1. (Cont'd.)

| No. | Reaction | a | b | c | Notes | Sources |
|---|---|---|---|---|---|---|
| VIII. | Photodetachment (Cont'd.): | | | | | |
| 3. | $O_3^- + h\nu \rightarrow O_3 + e$ | (2±1)[-1] | 0 | 0 | Vary with altitudes and solar zenith angles. | Ref. 24-3 |
| 4. | $NO_2^- + h\nu \rightarrow NO_2 + e$ | (1)[-2±.] | 0 | 0 | | Chp. 17 |
| 5. | $OH^- + h\nu \rightarrow OH + e$ | (1)[0±1] | 0 | 0 | | Chp. 17 |
| IX. | Three-Body Attachment: | | | | | |
| 1. | $O + e + M \rightarrow O^- + M$ | (6.5)[-29] | (-2±0.5) | 9000 | NED[c] $k_{300} = 6.5[-42]$ | Calculated by detailed balance from data of Chp. 17, and JANAF Tables. |
| 2. | $O_2 + e + O \rightarrow O_2^- + O$ | (1)[-31±2] | 0 | 0 | NED | HCE |
| 3. | $O_2 + e + O_2 \rightarrow O_2^- + O_2$ | (1.4±0.2)[-29] | (-1) | 600 | T = 195-600 K $k_{300} = 1.9[-30]$ | Chp. 17 |
| 4. | $O_2 + e + N_2 \rightarrow O_2^- + N_2$ | (1±0.5)[-31] | 0 | 0 | | Chp. 17 |

[c] No experimental data (see text).

Table 24-1. (Cont'd.)

| No. | Reaction | a | b | c | Notes | Sources |
|---|---|---|---|---|---|---|
| IX. | Three-Body Attachment (Cont'd.): | | | | | |
| 5. | $O_2 + e + H_2O \rightarrow O_2^- + H_2O$ | (1.4±0.2)[-29] | 0 | 0 | T = 300-400 K | Chp. 17 |
| 6. | $O_2 + e + CO_2 \rightarrow O_2^- + CO_2$ | (3.3±0.7)[-30] | 0 | 0 | T = 300-525 K | Chp. 17 |
| 7. | $NO + e + M \rightarrow$ Products | (8)[-31] | 0 | 0 | M = NO | Chp. 17 |
| 8. | $NO_2 + e\ (+M) \rightarrow NO_2^-\ (+M)$ | (4)[-11] | 0 | 0 | Observed to be saturated 3-body process. k is the effective 2-body value. See Reaction VII.4. | Chp. 17 |
| X. | Collisional Detachment: | | | | | |
| 1. | $O^- + O_2 \rightarrow O + e + O_2$ | (2.3±1)[-9] | 0 | 26000 ±3000 | $T_i$ < 20,000 K $k_{300}$ = 1.0[-46] | Chp. 17 |
| 2. | $O^- + N_2 \rightarrow O + e + N_2$ | (2.3)[-9±0.5] | 0 | 26000 ±3000 | $T_i$ < 20,000 K $k_{300}$ = 1.0[-46] | Chp. 17 |
| 3.a. | $O_2^- + M \rightarrow O_2 + e + M$ | (1.9±0.4)[-12] | (1.5) | 4990 | M = $N_2$; T = 375-600 K $k_{300}$ = 1.1[-19] | Chp. 17 |

Table 24-1. (Cont'd.)

| No. | Reaction | a | b | c | Notes | Sources |
|---|---|---|---|---|---|---|
| X. | Collisional Detachment (Cont'd.): | | | | | |
| 3.b. | $O_2^- + M \rightarrow O_2 + e + M$ | (2.7±0.3)[-10] | (0.5) | 5590 | M = $O_2$; T = 375-600 K $k_{300}$ = 2.2[-18] | Chp. 17 |
| 4. | $O_2^- + O_2(a\,^1\Delta_g) \rightarrow O_2 + e + O_2$ | (2)[-10] | 0 | 0 | | Chps. 17, 20 |
| XI. | Dissociative Attachment: | | | | | |
| 1. | $O_2 + e \rightarrow O^- + O$ | - | - | - | k<<(1)[-16] for T<2000 K Endothermic $c > 40 \times 10^3$. Strong $T_v$ dependence (see Chp. 20). | Chp. 17 |
| 2.a. | $O_3 + e \rightarrow O^- + O_2$ | (9)[-12] | (1.5) | 0 | T = 200-300 K See Reaction VII.3 | Chp. 17 |
| b. | $\rightarrow O_2^- + O$ | 2.5[-4] | (-2±0.5) | 7200 | $k_{300}$ = 1.0[-14] | Calculated by detailed balance from data of Chp. 17 and JANAF Tables. |

Table 24-1. (Cont'd.)

| No. | Reaction | a | b | c | Notes | Sources |
|---|---|---|---|---|---|---|
| XII. | Assaciative Detachment: | | | | | |
| 1. | $O^- + O \rightarrow O_2 + e$ | (2±0.1)[-10] | 0 | 0 | | Chp. 17 |
| 2. | $O^- + O_2 \rightarrow O_3 + e$ | - | - | - | k < (5)[-15] at T = 300 K and $T_i$ = 300-10000 K Endothermic c ~ 5000 | Chp. 17 |
| 3. | $O^- + O_2(a\ ^1\Delta_g) \rightarrow O_3 + e$ | (3±2)[-10] | 0 | 0 | Cf. Reaction XV.1. | Chps. 17, 20 |
| 4. | $O^- + N \rightarrow NO + e$ | (2.2±.5)[-10] | 0 | 0 | | Chp. 17 |
| 5. | $O^- + N_2 \rightarrow N_2O + e$ | - | - | - | k < (1)[-12] at $T_i$ = 300 K | Chp. 17 |
| 6. | $O^- + NO \rightarrow NO_2 + e$ | (2±0.8[-10] | 0 | 0 | k = (3)[-10] $(T_i/300)^{-1}$ at $T_i$ = 300-2000 K | Chp. 17 |
| 7. | $O^- + O_3 \rightarrow O_2 + O_2 + e$ | - | - | - | Rate is slow, compared with Reaction XV.2. | HCE |
| 8. | $O^- + H_2 \rightarrow H_2O + e$ | (7.5±3)[-10] | 0 | 0 | | Chp. 17 |

Table 24-1. (Cont'd.)

| No. | Reaction | a | b | c | Notes | Saurces |
|---|---|---|---|---|---|---|
| XII. | Associative Detachment (Cant'd.): | | | | | |
| 9. | $O^- + CO \rightarrow CO_2 + e$ | (4.4±2)[-10] | 0 | 0 | | Ref. 24-4 |
| 10. | $O_2^- + O \rightarrow O_3 + e$ | (3±1.5)[-10] | 0 | 0 | | Chp. 17 |
| 11. | $O_2^- + N \rightarrow NO_2 + e$ | (5±1.5)[-10] | 0 | 0 | | Chp. 17 |
| 12. | $O_3^- + O \rightarrow O_2 + O_2 + e$ | $(1)\left[-11^{+1}_{-2}\right]$ | 0 | 0 | NED | HCE |
| 13. | $OH^- + O \rightarrow HO_2 + e$ | (2±0.6)[-10] | 0 | 0 | | Ref. 24-4 |
| 14. | $CO_3^- + O \rightarrow CO_2 + O_2 + e$ | - | - | - | Rate is slow, compared with Reoction XVI.18. | Chp. 17 |
| XIII. | Positive-Ion Charge Transfer: | | | | | |
| 1. | $O^+ + H \rightarrow O + H^+$ | (6.8)[-10] | 0 | 0 | | Chp. 18A |
| 2. | $O^+ + O_2 \rightarrow O + O_2^+$ | (2)[-11] | (-.5) | 0 | | Chp. 18A |
| 3. | $O^+(^2D) + O_2 \rightarrow O + O_2^+(c,A)$ | $(3)\left[-10^{+0.5}_{-1.0}\right]$ | 0 | 0 | | Chp. 20 |
| 4. | $O^+ + NO \rightarrow O + NO^+$ | - | - | - | Chp. 18A gives $k < (1.3)[-12]$ | Chp. 18A |

Table 24-1. (Cont'd.)

| No. | Reaction | a | b | c | Notes | Sources |
|---|---|---|---|---|---|---|
| XIII. | Positive-Ion Charge Transfer (Cont'd.): | | | | | |
| 5. | $O^+ + NO_2 \rightarrow O + NO_2^+$ | (1.6)[-9] | 0 | 0 | Data at 393 K | Chp. 18A |
| 6. | $O^+ + N_2O \rightarrow O + N_2O^+$ | (6.3)[-10] | 0 | 0 | Data at 393 K | Chp. 18A |
| 7. | $O^+ + H_2O \rightarrow O + H_2O^+$ | (2.3)[-9] | 0 | 0 | | Chp. 18A |
| 8. | $O^+(^2D) + N_2 \rightarrow O + N_2^+$ | (3)[-10±1] | 0 | 0 | | Chp. 20 |
| 9. | $N^+ + O \rightarrow N + O^+$ | (1)[-12] | 0 | 0 | | HCE |
| 10. | $N^+ + O_2 \rightarrow N + O_2^+$ | (3±1.5)[-10] | 0 | 0 | See Reaction XIV.5. | Chp. 18A |
| 11. | $N^+ + NO \rightarrow N + NO^+$ | (8±2.4)[-10] | 0 | 0 | | Chp. 18A |
| 12. | $N^+ + H_2O \rightarrow N + H_2O^+$ | (2.6)[-9] | 0 | 0 | | Chp. 18A |
| 13. | $N^+ + CO \rightarrow N + CO^+$ | (9±3)[-10] | 0 | 0 | | Ref. 24-5 |
| 14. | $N^+ + CO_2 \rightarrow N + CO_2^+$ | (1.3±0.4)[-9] | 0 | 0 | | Ref. 24-5 |
| 15. | $O_2^+ + NO \rightarrow O_2 + NO^+$ | (6.3±2.4)[-10] | 0 | 0 | | Chp. 18A |
| 16. | $O_2^+ + Na \rightarrow O_2 + Na^+$ | (6.7)[-10±1] | 0 | 0 | | Chp. 18A |

Table 24-1. (Cont'd.)

| No. | Reaction | a | b | c | Notes | Sources |
|---|---|---|---|---|---|---|
| XIII. | Positive-Ion Charge Transfer (Cont'd.): | | | | | |
| 17. | $O_2^+(a\,^4\Pi_u) + N_2 \rightarrow O_2 + N_2^+$ | (5)[-10] | 0 | 0 | | Chp. 18A |
| 18. | $N_2^+ + O \rightarrow N_2 + O^+$ | (6)[-12] | - | 0 | NED Chp. 18A gives $k < (1)[-11]$ | Calculated from upper atmaspheric data. (Ref. 24-6) |
| 19. | $N_2^+ + N \rightarrow N_2 + N^+$ | - | - | - | $k < (1)[-11]$ | Chp. 18A |
| 20. | $N_2^+ + O_2 \rightarrow N_2 + O_2^+$ | (5±1)[-11] | (-.5) | 0 | | Chp. 18A |
| 21. | $N_2^+ + NO \rightarrow N_2 + NO^+$ | (3.3±1.5)[-10] | 0 | 0 | | Chp. 18A |
| 22. | $N_2^+ + H_2O \rightarrow N_2 + H_2O^+$ | - | - | - | This reaction combined with Reaction XIV.15 add to $k=(2.2)[-9]$ | Chp. 18A |
| 23. | $N_2^+ + CO_2 \rightarrow N_2 + CO_2^+$ | (9±3)[-10] | 0 | 0 | | Ref. 24-5 |

Table 24-1. (Cont'd.)

| No. | Reaction | a | b | c | Notes | Sources |
|---|---|---|---|---|---|---|
| XIII. | Positive-Ion Charge Transfer (Cont'd.): | | | | | |
| 24. | $N_2^+ + Na \rightarrow N_2 + Na^+$ | (5.8)[-10] | 0 | 0 | | Chp. 18A |
| 25. | $NO^+ + Na \rightarrow NO + Na^+$ | (7.0)[-11] | 0 | 0 | | Chp. 18A |
| 26. | $NO_2^+ + NO \rightarrow NO_2 + NO^+$ | (2.9)[-10] | 0 | 0 | | Chp. 18A |
| 27. | $H^+ + O \rightarrow H + O^+$ | (3.8)[-10] | 0 | 0 | | Chp. 18A |
| 28. | $H^+ + NO \rightarrow H + NO^+$ | (1.9)[-9] | 0 | 0 | | Chp. 18A |
| 29. | $OH^+ + O_2 \rightarrow OH + O_2^+$ | (2)[-10] | 0 | 0 | | Chp. 18A |
| 30. | $H_2O^+ + O_2 \rightarrow H_2O + O_2^+$ | (2)[-10] | 0 | 0 | | Chp. 18A |
| 31. | $CO^+ + O \rightarrow CO + O^+$ | (1.4)[-10] | 0 | 0 | | Chp. 18A |

Table 24-1. (Cont'd.)

| No. | Reaction | a | b | c | Notes | Sources |
|---|---|---|---|---|---|---|
| XIII. | Positive-Ion Charge Transfer (Cont'd.): | | | | | |
| 32. | $CO^+ + NO \rightarrow CO + NO^+$ | (3.3)[-10] | 0 | 0 | | Chp. 18A |
| 33. | $CO_2^+ + O \rightarrow CO_2 + O^+$ | (1)[-10] | 0 | 0 | | Chp. 18A |
| 34. | $CO_2^+ + O_2 \rightarrow CO_2 + O_2^+$ | (5)[-11] | 0 | 0 | | Chp. 18A |
| 35. | $CO_2^+ + NO \rightarrow CO_2 + NO^+$ | (1.2)[-10] | 0 | 0 | | Chp. 18A |
| XIV. | Positive Ion-Atom Interchange: | | | | | |
| 1. | $O^+ + N_2 \rightarrow NO^+ + N$ | (1.2)[-12] | 0.5 | 0 | For $T_v(N_2) >$ 1200 K, see Chp. 20. | Chp. 18A |
| 2. | $O^+ + NO \rightarrow O_2^+ + N$ | - | - | - | $k < (1)[-12]$ | HCE |
| 3. | $O^+ + H_2 \rightarrow OH^+ + H$ | (2)[-9] | 0 | 0 | | Chp. 18A |
| 4. | $O^+ + CO_2 \rightarrow O_2^+ + CO$ | (1.1±0.7)[-9] | 0 | 0 | | Chp. 18A |
| 5. | $N^+ + O_2 \rightarrow NO^+ + O$ | (3)[-10] | 0 | 0 | See Reaction XIII.10. | Chp. 18A |

Table 24-1. (Cont'd.)

| No. | Reaction | a | b | c | Notes | Sources |
|---|---|---|---|---|---|---|
| XIV. | Positive Ion-Atom Interchange:(Cont'd.): | | | | | |
| 6. | $N^+ + H_2 \rightarrow NH^+ + H$ | (5.6)[-10] | 0 | 0 | | Chp. 18A |
| 7.a. | $O_2^+ + N \rightarrow NO^+ + O$ | (1.8±0.6)[-10] | 0 | 0 | | Chp. 18A |
| b. | $\rightarrow O^+ + NO$ | - | - | - | Endathermic by 0.163 eV. | |
| 8. | $O_2^+ + N_2 \rightarrow NO^+ + NO$ | $(1)\left[-16^{+1}_{-3}\right]$ | 0 | 0 | Chp. 18A gives $k < (1)[-15]$. | HCE |
| 9. | $O_2^+ + NO_2 \rightarrow NO^+ + O_3$ | (1)[-11±2] | 0 | 0 | | HCE |
| 10. | $O_2^+ + H_2 \rightarrow$ Products | - | - | - | $k < (1)[-11]$ | Chp. 18A |
| 11. | $O_2^+ + Na \rightarrow NaO^+ + O$ | (7.7)[-11] | 0 | 0 | | Chp. 18A |
| 12.a. | $N_2^+ + O \rightarrow NO^+ + N$ | (1.4±0.2)[-10] | 0 | 0 | | Chp. 18A |
| b. | $\rightarrow NO^+ + 0.5\,N(^4S) + 0.5\,N(^2D)$ | | | | Overall Reaction. | HCE |
| 13. | $N_2^+ + O_2 \rightarrow NO^+ + NO$ | (1)[-17±2] | 0 | 0 | | HCE |
| 14. | $N_2^+ + H_2 \rightarrow N_2H^+ + H$ | (1.7)[-9] | 0 | 0 | | Chp. 18A |

Table 24-1. (Cont'd.)

| No. | Reaction | a | b | c | Notes | Sources |
|---|---|---|---|---|---|---|
| XIV | Positive Ion-Atom Interchange (Cont'd.): | | | | | |
| 15. | $N_2^+ + H_2O \rightarrow N_2H^+ + OH$ | - | - | - | See Reaction XIII.22. | Chp. 18A |
| 16. | $NO^+ + O_3 \rightarrow NO_2^+ + O_2$ | (1)[-13±2] | 0 | 0 | | HCE |
| 17. | $N_3^+ + O_2 \rightarrow$ Products | (1.0±0.3)[-10] | 0 | 0 | Data at 200 K. Possible products include: (a) $NO^+ + O + N_2$; (b) $O_2^+ + N + N_2$; and (c) $NO_2^+ + N_2$, in roughly comparable magnitudes. | Chp. 18A |
| 18. | $N_4^+ + O_2 \rightarrow N_2 + N_2 + O_2^+$ | (4±1)[-10] | 0 | 0 | Data at 200 K. | Chp. 18A |
| 19. | $O_2^+ \cdot N_2 + O_2 \rightarrow O_4^+ + N_2$ | (5)[-11] | 0 | 0 | Minimum value; data at 80 K. | Chp. 18A |
| 20. | $O_4^+ + H_2O \rightarrow O_2^+ \cdot H_2O + O_2$ | (2.2)[-9] | 0 | 0 | | Chp. 18A |
| 21.a. | $O_2^+ \cdot H_2O + H_2O \rightarrow H_3O^+ + OH + O_2$ | (3)[-10] | 0 | 3000 | $k_{300} = 1.5[-14]$ | Chp. 18A |
| | $\rightarrow H_3O^+ \cdot OH + O_2$ | (1.9)[-9] | 0 | 0 | | Chp. 18A |
| 22. | $H_3O^+ \cdot OH + H_2O \rightarrow H_3O^+ \cdot H_2O + OH$ | (3.2)[-9] | 0 | 0 | | Chp. 18A |

Table 24-1. (Cont'd.)

| No. | Reaction | a | b | c | Notes | Sources |
|---|---|---|---|---|---|---|
| XIV. | Positive Ion-Atom Interchange (Cont'd.): | | | | | |
| 23. | $H_2O^+ + H_2O \rightarrow H_3O^+ + OH$ | (1.8)[-9] | 0 | 0 | | Chp. 18A |
| 24. | $NO^+ \cdot NO + H_2O \rightarrow NO^+ \cdot H_2O + NO$ | (1.4±0.3)[-9] | 0 | 0 | | Chp. 18A |
| 25. | $NO^+(H_2O)_3 + H_2O \rightarrow H_3O^+(H_2O)_2 + HNO_2$ | (7±2)[-11] | 0 | 0 | | Chp. 18A |
| 26. | $NO^+ \cdot CO_2 + H_2O \rightarrow NO^+ \cdot H_2O + CO_2$ | (1)[-9] | 0 | 0 | | Chp. 18A |
| 27. | $O_2^+ \cdot H_2O + O_2 \rightarrow O_2^+ \cdot O_2 + H_2O$ | (2)[-10] | 0 | 2300 | $k_{300} = 9.4[-14]$ | HCE |
| 28. | $O_2^+ \cdot H_2O + NO \rightarrow NO^+ + O_2 + H_2O$ | (1)[-10] | 0 | 0 | | HCE |
| 29. | $O_2^+ \cdot O_2 + O \rightarrow O_2^+ + O_3$ | (3±2)[-10] | 0 | 0 | | Chp. 18A |
| 30. | $O_2^+ \cdot O_2 + NO \rightarrow NO^+ + O_2 + O_2$ | (5)[-10] | 0 | 0 | | HCE |
| 31. | $NO^+ \cdot H_2O + NO \rightarrow NO^+ \cdot NO + H_2O$ | (2)[-10] | 0 | 2300 | $k_{300} = 9.4[-14]$ | Ref. 24-7 |
| 32. | $C^+ + O_2 \rightarrow CO^+ + O$ | (1.1±0.3)[-9] | 0 | 0 | | Ref. 24-8 |
| 33. | $C^+ + CO_2 \rightarrow CO^+ + CO$ | (1.8±0.6)[-9] | 0 | 0 | | Ref. 24-8 |
| 34. | $CO_2^+ + O \rightarrow CO + O_2^+$ | (1.6)[-10] | 0 | 0 | | Chp. 18A |
| 35. | $Fe^+ + O_3 \rightarrow FeO^+ + O_2$ | (1.5)[-10] | 0 | 0 | | Chp. 18A |

Table 24-1. (Cont'd.)

| No. | Reaction | a | b | c | Notes | Sources |
|---|---|---|---|---|---|---|
| XV. | Negative-Ion Charge Transfer: | | | | | |
| 1. | $O^- + O_2(a\ ^1\Delta_g) \rightarrow O_2^- + O$ | - | - | - | $k_{300} < (1)[-10]$ Cf. Reaction XII.3. | HCE |
| 2. | $O^- + O_3 \rightarrow O + O_3^-$ | (5.3±2)[-10] | 0 | 0 | See Reaction XII.7. | Chp. 18A |
| 3. | $O^- + NO_2 \rightarrow O + NO_2^-$ | (1.2)[-9] | 0 | 0 | | Chp. 18A |
| 4. | $O_2^- + O \rightarrow O_2 + O^-$ | - | - | - | $k < (1)[-10]$ | HCE |
| 5. | $O_2^- + O_3 \rightarrow 2O_2 + O_3^-$ | (4.0±1.3)[-10] | 0 | 0 | | Chp. 18A |
| 6. | $O_2^- + NO_2 \rightarrow O_2 + NO_2^-$ | (8)[-10] | 0 | 0 | | Chp. 18A |
| 7. | $O_2^- + NO_3 \rightarrow O_2 + NO_3^-$ | (5)[-10] | 0 | 0 | | HCE |
| 8. | $O_3^- + NO_2 \rightarrow O_3 + NO_2^-$ | (1.9)[-11] | 0 | 0 | Products uncertain; cf. Reaction XVI.5. | Chp. 18A |
| 9. | $O_3^- + NO_3 \rightarrow O_3 + NO_3^-$ | (5)[-10] | 0 | 0 | | HCE |
| 10. | $NO^- + O_2 \rightarrow NO + O_2^-$ | (5)[-10] | 0 | 0 | | Chp. 18A |

Table 24-1. (Cont'd.)

| No. | Reaction | o | b | c | Notes | Sources |
|---|---|---|---|---|---|---|
| XV. | Negative-Ion Charge Transfer (Cont'd.): | | | | | |
| 11. | $NO_2^- + NO_3 \rightarrow NO_2 + NO_3^-$ | (5)[-10] | 0 | 0 | | HCE |
| 12. | $H^- + NO_2 \rightarrow H + NO_2^-$ | (2.9)[-9] | 0 | 0 | | Chp. 18A |
| 13. | $OH^- + NO_2 \rightarrow OH + NO_2^-$ | (?)[-9] | 0 | 0 | | Chp. 18A |
| XVI. | Negative Ion-Atom Interchange: | | | | | |
| 1. | $O^- + N_2O \rightarrow NO^- + NO$ | (2±0.6)[-11] | 0 | 0 | | Chp. 18A |
| 2. | $O_3^- + O \rightarrow O_2^- + O_2$ | $(1)\left[-11^{+1}_{-2}\right]$ | 0 | 0 | NED | HCE |
| 3. | $O_3^- + N_2 \rightarrow N_2O^- + O_2$ | - | - | - | k < (1)[-15] | Chp. 18A |
| 4. | $O_3^- + NO \rightarrow NO_2^- + O_2$ | (1.0±0.3)[-11] | 0 | 0 | Ref. 18A-27 identifies products as $NO_3^-$ + O. This is probably incorrect. | Chp. 18A |
| 5. | $O_3^- + NO_2 \rightarrow NO_3^- + O_2$ | (2)[-11] | 0 | 0 | Cf. Reaction XV.8. | HCE |
| 6. | $O_3^- + CO_2 \rightarrow CO_3^- + O_2$ | (4.0±1.2)[-10] | 0 | 0 | | Chp. 18A |

Table 24-1. (Cont'd.)

| No. | Reaction | a | b | c | Notes | Sources |
|---|---|---|---|---|---|---|
| XVI. | Negative Ion-Atom Interchange (Cont'd.): | | | | | |
| 7. | $NO_2^- + O \rightarrow$ Products | - | - | - | k <(1)[-11] | Chp. 18A |
| 8. | $NO_2^- + N \rightarrow$ Products | - | - | - | k <(1)[-11] | Chp. 18A |
| 9. | $NO_2^- + O_3 \rightarrow O_2 + NO_3^-$ | (1.8)[-11] | 0 | 0 | | Chp. 18A |
| 10. | $NO_2^- + NO_2 \rightarrow NO_3^- + NO$ | (4)[-12] | 0 | 0 | | Chp. 18A |
| 11. | $NO_3^- + O \rightarrow$ Products | - | - | - | k <(1)[-11] | Chp. 18A |
| 12. | $NO_3^- + N \rightarrow NO_2^- + NO$ | - | - | - | k <(1)[-11] | Chp. 18A |
| 13. | $NO_3^- + NO \rightarrow NO_2^- + NO_2$ | - | - | - | k <(1)[-12]; see Reaction XVI.25. | Chp. 18A |
| 14. | $O_4^- + O \rightarrow O_3^- + O_2$ | (4)[-10] | 0 | 0 | $2O_2 + O^-$ may be a minor product channel. | Chp. 18A |
| 15. | $O_4^- + NO \rightarrow OONO^- + O_2$ | (2.5)[-10] | 0 | 0 | | Chp. 18A |
| 16. | $O_4^- + H_2O \rightarrow O_2^- \cdot H_2O + O_2$ | (1.4)[-9] | 0 | 0 | | Chp. 18A |
| 17. | $O_4^- + CO_2 \rightarrow CO_4^- + O_2$ | (4.3)[-10] | 0 | 0 | | Chp. 18A |

Table 24-1. (Cont'd.)

| No. | Reaction | a | b | c | Notes | Sources |
|---|---|---|---|---|---|---|
| XVI. | Negative Ion-Atom Interchange (Cont'd.): | | | | | |
| 18. | $CC_3^- + O \rightarrow O_2^- + CO_2$ | (8.0±2.4[-11] | 0 | 0 | See Reaction XII.14. | Chp. 18A |
| 19. | $CO_3^- + NO \rightarrow NO_2^- + CO_2$ | (9.0±3)[-12] | 0 | 0 | | Chp. 18A |
| 20. | $CO_3^- + NO_2 \rightarrow NO_3^- + CO_2$ | (8.0)[-11] | 0 | 0 | | Chp. 18A |
| 21. | $CO_4^- + O \rightarrow CO_3^- + O_2$ | (1.5)[-10] | 0 | 0 | $CO_2 + O_3^-$ may be a minor product channel. | Chp. 18A |
| 22. | $CO_4^- + NO \rightarrow OONO^- + CO_2$ | (4.8)[-11] | 0 | 0 | | Chp. 18A |
| 23. | $O_2^- \cdot H_2O + NO \rightarrow OONO^- + H_2O$ | (3.1)[-10] | 0 | 0 | | Chp. 18A |
| 24. | $O_2^- \cdot H_2O + CO_2 \rightarrow CO_4^- + H_2O$ | (5.8)[-10] | 0 | 0 | | Chp. 18A |
| 25. | $OONO^- + NO \rightarrow NO_2^- + NO_2$ | (1.5)[-11] | 0 | 0 | See Reaction XVI.13. | Chp. 18A |
| 26. | $CO_4^- + O_2 \rightarrow O_4^- + CO_2$ | (4.3)[-10] | 0 | 3000 | $k_{300} = 2.0[-14]$ | HCE |

Table 24-1. (Cont'd.)

| No | Reaction | a | b | c | Notes | Sources |
|---|---|---|---|---|---|---|
| XVII. | Radiative Positive-Ion-Neutral Association: | | | | | |
| 1. | $X^+ + Y \rightarrow XY^+ + h\nu$ | (1)[-17±2] | 0 | 0 | $X^+$ and Y are either atomic or molecular. | HCE |
| XVIII. | Three-Body Positive-Ion-Neutral Association: | | | | | |
| 1. | $O^+ + O + M \rightarrow O_2^+ + M$ | - | - | - | k < (1)[-30] | HCE |
| 2. | $O^+ + N + M \rightarrow NO^+ + M$ | - | - | - | k < (1)[-30] | HCE |
| 3. | $O^+ + N_2 + M \rightarrow NO^+ + N + M$ | (2.0)[-28] | $\left(-1^{+1}_{-2}\right)^d$ | 0 | From data at T = 82 K; M = He. Apparently $N_2O^+$ predissociates. | Chp. 18A |
| 4. | $O^+ + NO + M \rightarrow NO^+ + O + M$ | (1)[-29±2] | $\left(-1^{+1}_{-2}\right)^d$ | 0 | | HCE |
| 5. | $O_2^+ + O + M \rightarrow O_3^+ + M$ | (1)[-29±2] | $\left(-1^{+1}_{-2}\right)^d$ | 0 | | HCE |
| 6. | $N^+ + O + M \rightarrow NO^+ + M$ | (1)[-29±2] | $\left(-1^{+1}_{-2}\right)^d$ | 0 | | HCE |
| 7. | $N^+ + N + M \rightarrow N_2^+ + M$ | (1)[-29±2] | $\left(-1^{+1}_{-2}\right)^d$ | 0 | | HCE |
| 8. | $N_2^+ + N + M \rightarrow N_3^+ + M$ | (1)[-29±2] | $\left(-1^{+1}_{-2}\right)^d$ | 0 | | HCE |

[d] Value of "b" assigned via HCE.

Table 24-1. (Cont'd.)

| No. | Reaction | a | b | c | Notes | Sources |
|---|---|---|---|---|---|---|
| XVIII. | Three-Body Positive-Ian-Neutrol Assaciotian (Cont'd.): | | | | | |
| 9. | $N_2^+ + N_2 + M \rightarrow N_4^+ + M$ | (5.0)[-29] | $\left(-1^{+1}_{-2}\right)^d$ | 0 | From data at T = 300 K; M = $N_2$ | Chp. 18A |
| 10. | $NO^+ + O + M \rightarrow NO_2^+ + M$ | (5)[-2°±2] | $\left(-1^{+1}_{-2}\right)^d$ | 0 | | HCE |
| 11. | $N^+ + N_2 + M \rightarrow N_3^+ + M$ | (2±1)[-29] | $\left(-1^{+1}_{-2}\right)^d$ | 0 | | HCE |
| 12. | $NO^+ + N + M \rightarrow N_2O^+ + M$ | (1)[-29±2] | $\left(-1^{+1}_{-2}\right)^d$ | 0 | | HCE |
| 13. | $O_2^+ + O_2 + M \rightarrow O_4^+ + M$ | (2.7)[-30] | $\left(-1^{+1}_{-2}\right)^d$ | 0 | Fram data at 307 K; M = $O_2$ | Chp. 18A |
| 14. | $O_2^+ + N_2 + M \rightarrow O_2^+ \cdot N_2 + M$ | (2.9)[-29] | $\left(-1^{+1}_{-2}\right)^d$ | 0 | Fram data at T = 200 K; M = He | Chp. 18A |
| 15. | $O_2^+ + H_2O + M \rightarrow O_2^+ \cdot H_2O + M$ | (1.9)[-28] | $\left(-1^{+1}_{-2}\right)^d$ | 0 | Fram data at 296 K; M = $O_2$ | Chp. 18A |
| 16. | $NO^+ + NO + M \rightarrow NO^+ \cdot NO + M$ | (5.0)[-30] | $\left(-1^{+1}_{-2}\right)^d$ | 0 | Fram dato at 300 K; M = NO | Chp. 18A |
| 17. | $NO^+ + H_2O + M \rightarrow NO^+ \cdot H_2O + M$ | (1.5)[-28] | $\left(-1^{+1}_{-2}\right)^d$ | 0 | Fram data at 300 K; M = $N_2$ | Chp. 18A |

[d] Valve af "b" assigned via HCE.

Table 24-1. (Cont'd.)

| No. | Reaction | a | b | c | Notes | Sources |
|---|---|---|---|---|---|---|
| XVIII. | Three-Body Positive-Ion-Neutral Association (Cont'd.): | | | | | |
| 18. | $NO^+ \cdot H_2O + H_2O + M \rightarrow NO^+(H_2O)_2 + M$ | (1.1)[-27] | $\left(-1^{+1}_{-2}\right)^d$ | 0 | From data at 300 K; M = $N_2$ | Chp. 18A |
| 19. | $NO^+(H_2O)_2 + H_2O + M \rightarrow NO^+(H_2O)_3 + M$ | (1.6)[-27] | $\left(-1^{+1}_{-2}\right)^d$ | 0 | From data at 300 K; M = $N_2$ | Chp. 18A |
| 20. | $NO^+ + CO_2 + M \rightarrow NO^+ \cdot CO_2 + M$ | (2)[-29] | $\left(-1^{+1}_{-2}\right)^d$ | 0 | From data at 300 K; M = $CO_2$ | Chp. 18A |
| 21. | $H_3O^+ + H_2O + M \rightarrow H_3O^+ \cdot H_2O + M$ | (3.4)[-27] | $\left(-1^{+1}_{-2}\right)^d$ | 0 | From data at 300 K; M = $N_2$ | Chp. 18A |
| 22. | $H_3O^+ \cdot H_2O + H_2O + M \rightarrow H_3O^+(H_2O)_2 + M$ | (2.3)[-27] | $\left(-1^{+1}_{-2}\right)^d$ | 0 | From data at 300 K; M = $N_2$ | Chp. 18A |
| 23. | $H_3O^+(H_2O)_2 + H_2O + M \rightarrow H_3O^+(H_2O)_3 + M$ | (2.4)[-27] | $\left(-1^{+1}_{-2}\right)^d$ | 0 | From data at 300 K; M = $N_2$ | Chp. 18A |
| 24. | $H_3O^+(H_2O)_3 + H_2O + M \rightarrow H_3O^+(H_2O)_4 + M$ | (8.8)[-28] | $\left(-1^{+1}_{-2}\right)^d$ | 0 | From data at 307 K; M = $O_2$ | Chp. 18A |
| XIX. | Positive-Ion Collisional Dissociation: | | | | | |
| 1. | $O_2^+ \cdot O_2 + M \rightarrow O_2^+ + O_2 + M$ | (5)[-7] | (-1) | 5000 | $k_{300}$ = 2.9[-14] | Ref. 24-2 |

[d] Value of "b" assigned via HCE.

Table 24-1. (Cont'd.)

| No. | Reaction | a | b | c | Notes | Sources |
|---|---|---|---|---|---|---|
| XIX. | Positive-Ion Collisional Dissociation (Cont'd.): | | | | | |
| 2. | $NO^+ \cdot NO + M \rightarrow NO^+ + NO + M$ | (1)[-5] | (-1) | 7000 | $k_{300} = 7[-16]$ | Ref. 24-2 |
| 3. | $H_3O^+ \cdot OH + M \rightarrow H_3O^+ + OH + M$ | (1)[-1] | (-1) | 11,800 | $k_{300} = 8[-19]$ | Ref. 24-2 |
| 4. | $H_3O^+ \cdot H_2O + M \rightarrow H_3O^+ + H_2O + M$ | (8)[0] | (-1) | 18,000 | $k_{300} = 7[-26]$ | Ref. 24-2 |
| 5. | $H_3O^+(H_2O)_2 + M \rightarrow H_3O^+ \cdot H_2O + H_2O + M$ | (1)[-1] | (-1) | 11,200 | $k_{300} = 6[-18]$ | Ref. 24-2 |
| 6. | $H_3O^+(H_2O)_3 + M \rightarrow H_3O^+(H_2O)_2 + H_2O + M$ | (1)[-1] | (-1) | 8600 | $k_{300} = 4[-14]$ | Ref. 24-2 |
| 7. | $H_3O^+(H_2O)_4 + M \rightarrow H_3O^+(H_2O)_3 + H_2O + M$ | (3)[-3] | (-1) | 6000 | $k_{300} = 6[-12]$ | Ref. 24-2 |
| XX. | Radiative Negative-Ion-Neutral Association: | | | | | |
| 1. | $O^- + O_2 \rightarrow O_3^- + h\nu$ | (1)[-17±2] | 0 | 0 | | HCE |
| XXI. | Three-Body Negative-Ion-Neutral Association: | | | | | |
| 1. | $O^- + O_2 + M \rightarrow O_3^- + M$ | (1.1±0.1)[-30] | $\left(-1^{+1}_{-2}\right)^d$ | 0 | From data at 300 K; M = $O_2$ | Chp. 18A |
| 2. | $O^- + NO + M \rightarrow NO_2^- + M$ | (1)[-29±2] | $\left(-1^{+1}_{-2}\right)^d$ | 0 | | HCE |

[d] Value of "b" assigned via HCE.

Table 24-1. (Cont'd.)

| No. | Reaction | a | b | c | Notes | Sources |
|---|---|---|---|---|---|---|
| XXI. | Three-Body Negative-Ion-Neutral Association (Cont'd.): | | | | | |
| 3. | $O^- + CO_2 + M \rightarrow CO_3^- + M$ | (8.0)[-29] | $\left(-1^{+1}_{-2}\right)^d$ | 0 | From data at 300 K; M = $CO_2$ | Chp. 18A |
| 4. | $O_2^- + O_2 + M \rightarrow O_4^- + M$ | (3.5±0.5)[-31] | $\left(-1^{+1}_{-2}\right)^d$ | 0 | From data at 300 K; M = $O_2$ | Chp. 18A |
| 5. | $O_2^- + N_2 + M \rightarrow O_2^- \cdot N_2 + M$ | (3)[-32] | $\left(-1^{+1}_{-2}\right)^d$ | 0 | From data at 200 K; M = He | Chp. 18A |
| 6. | $O_2^- + CO_2 + M \rightarrow CO_4^- + M$ | (2.0)[-29] | $\left(-1^{+1}_{-2}\right)^d$ | 0 | From data at 300 K; M = $O_2$ | Chp. 18A |
| 7. | $NO_2^- + H_2O + M \rightarrow NO_2^- \cdot H_2O + M$ | (1.3)[-28] | $\left(-1^{+1}_{-2}\right)^d$ | 0 | From data at 300 K; M = NO | Chp. 18A |
| 8. | $O^- + N_2 + M \rightarrow N_2O^- + M$ | (3)[-31] | $\left(-1^{+1}_{-2}\right)^d$ | 0 | From data at 200 K; M = He | Chp. 18A |
| 9. | $O^- + H_2O + M \rightarrow O^- \cdot H_2O + M$ | (1.0)[-28] | $\left(-1^{+1}_{-2}\right)^d$ | 0 | From data at 300 K; M = $O_2$ | Chp. 18A |
| 10. | $O_2^- + H_2O + M \rightarrow O_2^- \cdot H_2O + M$ | (3)[-28] | $\left(-1^{+1}_{-2}\right)^d$ | 0 | From data at 300 K; M = $O_2$ | Chp. 18A |

[d] Value of "b" assigned via HCE.

Table 24-1. (Cont'd.)

| No. | Reaction | a | b | c | Notes | Sources |
|---|---|---|---|---|---|---|
| XXI. | Three-Body Negative-Ion-Neutrol Assaciation (Cant'd.): | | | | | |
| 11. | $O_3^- + H_2O + M \rightarrow O_3^- \cdot H_2O + M$ | (2.1)[-28] | $\left(-1^{+1}_{-2}\right)^d$ | 0 | Fram data at 300 K; M = $O_2$ | Chp. 18A |
| 12. | $O_2^- \cdot H_2O + H_2O + M \rightarrow O_2^-(H_2O)_2 + M$ | (4)[-28] | $\left(-1^{+1}_{-2}\right)^d$ | 0 | From data at 300 K; M = $O_2$ | Chp. 18A |
| XXII. | Negotive-Ion Collisional Dissaciation: | | | | | |
| 1. | $O_4^- + M \rightarrow O_2^- + O_2 + M$ | (1)[-3] | (-1) | 7500 | $k_{300}$ = 1.4[-14], but Ref. 24-9 gives 2.7[-14]. | Ref. 24-2 |
| XXIII. | Radiotive Neutral Recombinotian: | | | | | |
| 1.a. | $O+O \rightarrow O_2(^3\Sigma_u^+) + h\nu$ (Herzberg) | (2.4)[-21] | 0 | 0 | | Refs. 24-10, 24-11 |
| b. | $\rightarrow O_2(^1\Sigma_g^+) + h\nu$ (Atmaspheric) | (1.7)[-37]$n_{N_2}$ | 0 | 0 | | Ref. 24-11 |
| c. | $\rightarrow O_2(^3\Sigma_u^-) + h\nu$ (Schumann-Runge) | (2)[-17] | 0 | 12,100 | | Ref. 24-12 |
| 2.a. | $O + N \rightarrow NO(A^2\Sigma) + h\nu\,(\nu)$ | $\left\{1.2\times10^{-17}\left(\frac{T}{300}\right)^{-.35} + 2.1\times10^{-34} n_{N_2}\left(\frac{T}{300}\right)^{-1.24}\right\}$ | | | | Ref. 24-13 |

[d] Value of "b" assigned via HCE.

Table 24-1. (Cont'd.)

| No. | Reaction | a | b | c | Notes | Sources |
|---|---|---|---|---|---|---|
| XXIII. | Radiative Neutral Recombination (Cont'd.): | | | | | |
| 2.b. | $O + N \rightarrow NO(B^2\Pi) + h\nu(\delta)$ | $(3.1)[-34]n_{N_2}$ | (-1.4) | 0 | | Ref.24-13 |
| c. | $\rightarrow NO(C^2\Pi) + h\nu(\delta)$ | (6.8±3)[-18] | (-0.35) | 0 | | Ref.24-13 |
| 3. | $O + NO \rightarrow NO_2 + h\nu$ | (1.2±1)[-17] | (-2.0±0.5) | 0 | | Chp. 19 |
| 4. | $N + N \rightarrow N_2 + h\nu$ | (5±0.5)[-17] | (-0.90±0.05) | 0 | | Ref.24-14 |
| XXIV. | Neutral Photodissociation: | | | | | |
| 1.a. | $O_2 + h\nu \rightarrow O + O$ | | | | Flux and wavelength dependent. See Chapter 12. | |
| | $\rightarrow O + O(^1D)$ | | | | Schumann-Runge. Flux and wavelength dependent. See Chapter 12. | |
| 2. | $NO + h\nu \rightarrow N + O$ | | | | | |
| 3.a. | $O_3 + h\nu \rightarrow O + O_2$ | | | | | |
| b. | $\rightarrow O + O_2(a\ ^1\Delta_g)$ | | | | Flux and wavelength dependent. See Chapter 12. | |
| c. | $\rightarrow O(^1D) + O_2(a\ ^1\Delta_g)$ | | | | | |

Table 24-1. (Cont'd.)

| No. | Reaction | a | b | c | Notes | Sources |
|---|---|---|---|---|---|---|
| XXIV. | Neutral Photodissociation (Cont'd.): | | | | | |
| 3.d. | $O_3 + h\nu \rightarrow O(^1D) + O_2(b\ ^1\Sigma_g^+$ | | | | Flux and wavelength dependent. See Chapter 12. | |
| 4. | $NO_2 + h\nu \rightarrow O + NO$ | | | | | |
| 5.a. | $N_2O + h\nu \rightarrow N_2 + O$ | | | | | |
| b. | $\rightarrow N + NO$ | | | | | |
| 6. | $OH + h\nu \rightarrow O + H$ | | | | | |
| 7. | $H_2O + h\nu \rightarrow H + OH$ | | | | | |
| 8. | $HO_2 + h\nu \rightarrow OH + O$ | | | | | |
| 9. | $H_2O_2 + h\nu \rightarrow OH + OH$ | | | | | |
| 10. | $CO_2 + h\nu \rightarrow CO + O$ | | | | | |
| XXV. | Three-Body Neutral Recombination: | | | | | |
| 1. | $O + O + O \rightarrow O_2 + O(^1S)$ | $(1.5)[-34\pm1]$ | 0 | 0 | | Chp. 20 |
| 2. | $O + O + O_2 \rightarrow O_2(A^3\Sigma_u^+) + O_2$ | $(3)[-33\pm.3]$ | 0 | 0 | $\bar{1}$ = 1000 K | Chp. 20 |

Table 24-1. (Cont'd.)

| No. | Reaction | a | b | c | Notes | Sources |
|---|---|---|---|---|---|---|
| XXV. | Three-Body Neutral Recombination (Cont'd.): | | | | | |
| 3.a. | $O + O + N_2 \rightarrow O_2 + N_2$ | (3.0)[-33] | (-2.9±0.4) | 0 | | Chp. 19 |
| | | (3.9)[-34] | (-2.5±0.5) | 0 | $T_{Ref}$ = 3000 K | Chp. 19 |
| b. | $\rightarrow O_2(A^3\Sigma_u^+) + N_2$ | (2.1)[-37±1] | 0 | 0 | | Chp. 20 |
| c. | $\rightarrow O_2(b^1\Sigma_g^+) + N_2$ | (1.7)[-37±1] | 0 | 0 | | Chp. 20 |
| 4.a. | $N + N + N_2 \rightarrow N_2 + N_2$ | (7.6±2)[-34] | 0 | 500 ±200 | $k_{300}$ = 1.4[-34] | Chp. 19 |
| | | (4.6)[-33] | (-1.7) | 0 | $T_{Ref}$ = 3000 K | Chp. 19 |
| b. | $\rightarrow N_2 + N_2(B^3\Pi)$ | (1.4)[-33±1] | 0 | 0 | | Chp. 20 |
| 5. | $N + O + N_2 \rightarrow NO + N_2$ | (1.1±0.3)[-32] | (-0.5±0.2) | 0 | | Chp. 19 |
| 6. | $N + O + O \rightarrow NO + O(^1S)$ | (3)[-33±1] | 0 | 0 | | Chp. 20 |
| 7. | $N + O + N_2 \rightarrow NO(B^2\Pi) + N_2$ | (1)[-34±1] | 0 | 0 | | Chp.20 |
| 8. | $O + O_2 + N_2 \rightarrow O_3 + N_2$ | (5.5±2)[-34] | (-2.6±0.4) | 0 | | Chp. 19 |
| 9. | $O + N_2 + M \rightarrow N_2O + M$ | (1)[-34±2] | 0 | 7500 | $k_{300}$ = 1.4[-45] | HCE |
| 10. | $O + NO + N_2 \rightarrow NO_2 + N_2$ | (1.0±0.1)[-31] | (-2.5±0.3) | 0 | | Chp. 19 |
| 11. | $H + H + M \rightarrow H_2 + M$ | (8.3)[-33±0.5] | (-0.6±0.2) | 0 | | Ref.24-15 |

Table 24-1. (Cont'd.)

| No. | Reaction | a | b | c | Notes | Sources |
|---|---|---|---|---|---|---|
| XXV. | Three-Body Neutral Recombination (Cont'd.): | | | | | |
| 12. | $H + O_2 + N_2 \rightarrow HO_2 + N_2$ | (9±2)[-33] | 0 | 500±300 | $k_{300}$ = 1.7[-33] | Chp. 19 |
| 13. | $H + OH + M \rightarrow H_2O + M$ | (7±4)[-32] | 0 | 0 | T = 2000 K | Ref.24-16 |
| 14. | $CO + O + N_2 \rightarrow CO_2 + N_2$ | (1.4±0.3)[-35] | 0 | 0 | | Ref.24-17 |
| XXVI. | Neutral Collisional Dissaciation: | | | | | |
| 1. | $O_2 + O_2 \rightarrow O + O + O_2$ | (2.1±1)[-7] | (-1.5± 0.5) | 59,000 | T = 3000-5000 K | Ref.24-12 |
| 2. | $N_2 + N_2 \rightarrow N + N + N_2$ | (6.7±1.7)[-7] | (-1.6± 0.5) | 113,000 | T = 8000-15,000 K | Ref.24-18 |
| 3. | $N_2 + Ar \rightarrow N + N + Ar$ | (2.5±0.3)[-7] | (-1.6± 0.5) | 113,000 | T = 8000-15,000 K | Ref.24-18 |
| 4. | $NO + M \rightarrow N + O + M$ | (1.3±0.6)[-7] | (-1.5± 0.5) | 75,000 | T = 3000-8000 K; M = Ar, $O_2$, $N_2$ | Ref.24-19 |
| 5. | $O_3 + N_2 \rightarrow O + O_2 + N_2$ | (6.4±1.6[-10] | 0 | 11,400 | T = 200-1000 K; $k_{300}$ = 2[-26] | Ref.24-20 |

Table 24-1 (Cont'd.)

| No. | Reaction | a | b | c | Notes | Sources |
|---|---|---|---|---|---|---|
| XXVI. | Neutral Collisional Dissociation (Cont'd.): | | | | | |
| 6. | $O_3 + O_2(a\ ^1\Delta_g) \rightarrow O + O_2 + O_2$ | (4.5)[-11] | 0 | 2800±200 | T = 283-321 K; $k_{300}$=4[-15] | Ref.24-21 |
| 7. | $O_3 + O_2(b\ ^1\Sigma_g^+) \rightarrow O + O_2 + O_2$ | (6)[-13±1] | 0 | 0 | | Chp. 20 |
| XXVII. | Neutral Reorrangement: | | | | | |
| 1. | $O + N_2 \rightarrow NO + N$ | (1.0±0.3[-10] | 0 | 37,900±300 | $k_{300}$ = 1.1[-65] | Chp. 19 |
| 2. | $O + NO \rightarrow O_2 + N$ | (5.3±1.1)[-12] | 0 | 20,200±200 | $k_{300}$ = 3.1[-41] | Chp. 19 |
| 3. | $O + NO_2 \rightarrow NO + O_2$ | (1.6±0.5)[-11] | 0 | 300±150 | $k_{300}$ = 5.9[-12] | Chp. 19 |
| 4. | $O + N_2O \rightarrow NO + NO$ | (1.5±0.5)[-10] | 0 | 14,000±2000 | $k_{300}$ = 7.8[-31] | Chp. 19 |
| 5. | $O + N_2O \rightarrow O_2 + N_2$ | (5±2)[-11] | 0 | 14,000±2000 | $k_{300}$ = 2.6[-31] | Chp. 19 |
| 6.a. | $O + O_3 \rightarrow O_2 + O_2$ | (1.4±0.3)[-11] | 0 | 2220±200 | $k_{300}$ = 8.4[-15] | Chp. 19 |
| b. | $\rightarrow O_2 + O_2(a\ ^1\Delta_g)$ | (4.5)[-15±2] | 0 | 0 | | Chp. 20 |
| 7. | $O(^1D) + O_3 \rightarrow O_2 + O_2$ | (2.5±1)[-10] | 0 | 0 | | Ref.24-22 |
| 8. | $O(^1D) + H_2 \rightarrow OH + H$ | (3.5)[-10±1] | 0 | 0 | | Ref.24-23 |

Table 24-1. (Cont'd.)

| No. | Reaction | a | b | c | Notes | Sources |
|---|---|---|---|---|---|---|
| XXVII. | Neutral Rearrangement (Cont'd.): | | | | | |
| 9. | $O + OH \rightarrow H + O_2$ | (5±2)[-11] | 0 | 0 | Possibly b = 0.5 | Chp. 19 |
| 10. | $O + HO_2 \rightarrow OH + O_2$ | (1)[-11] | 0 | 0 | | Chp. 19 |
| 11. | $O(^1D) + H_2O \rightarrow OH + OH$ | (2±1)[-10] | 0 | 0 | | Ref. 24-24 |
| 12. | $N + O_2 \rightarrow NO + O$ | (2.4±0.3)[-11] | 0 | 4000±200 | $k_{300}$ = 3.9[-17] | Chp. 19 |
| 13. | $N(^2D) + O_2 \rightarrow NO + O$ | (7[illegible]-12] | (0.5) | 0 | | Chp. 20 |
| 14. | $N + O_2(a\ ^1\Delta_g) \rightarrow NO + O$ | (2.0±0.8)[-14] | 0 | 600 | Products uncertain; $k_{300}$ = 2.7[-15] | Ref. 24-25 |
| 15. | $N + NO \rightarrow N_2^{\ddagger}\ (v = 3\text{-}6) + O$ | (2.2±0.6)[-11] | 0 | 0 | | Chps. 19, 20 |
| 16.a. | $N + NO_2 \rightarrow N_2O + O$ | (8±1)[-12] | 0 | 0 | Chp. 19 gives a = (1.8±0.2)[-11] for overall reaction: $N + NO_2 \rightarrow$ Products. | Ref. 24-26 gives branching ratio. |
| b. | $\rightarrow NO + NO$ | (6±1)[-12] | 0 | 0 | | |
| c. | $\rightarrow N_2 + O + O$ | (2±1)[-12] | 0 | 0 | | |
| d. | $\rightarrow N_2 + O_2$ | (2±1)[-12] | 0 | 0 | | |

Table 24-1. (Cont'd.)

| No. | Reaction | a | b | c | Notes | Sources |
|---|---|---|---|---|---|---|
| XXVII. | Neutral Rearrangement (Cont'd.): | | | | | |
| 17. | $N + O_3 \rightarrow NO + O_2$ | (3.4)[-11] | (0.5) | 1200 | $k_{300}$ = (6)[-13] | Ref.24-27 |
| 18. | $NO + O_3 \rightarrow NO_2 + O_2$ | (9.5±1)[-13] | 0 | 1300±100 | $k_{300}$ = (1.3)[-14] | Chp. 19 |
| 19. | $NO + O_2 + NO \rightarrow NO_2 + NO_2$ | (1.1)[-38] | 0 | 480 | $k_{300}$ =(2.2)[-39] | Ref.24-28 |
| 20.a. | $NO_2 + O_3 \rightarrow NO_3 + O_2$ | (9.8)[-12] | 0 | 3500±300 | Values given are for the overall reaction: $NO_2+O_3 \rightarrow$ Products; $k_{300}$ = (8.5)[-17] | Ref.24-29 |
| b. | $\rightarrow NO + O_2 + O_2$ | | | | | |
| 21.a. | $H + O_3 \rightarrow OH + O_2$ | (2.6)[-11] | 0 | 0 | | Ref.24-30 |
| b. | $\rightarrow HO_2 + O$ | | | | | |
| 22. | $H + OH \rightarrow H_2 + O$ | (1.2)[-11] | 0 | 3650 | $k_{300}$ = 6.3[-17] | Ref.24-16 |
| 23.a. | $H + HO_2 \rightarrow OH + OH$ | - | - | - | $k \geq (1)[-11]$ | Ref.24-31 |
| b. | $\rightarrow H_2 + O_2$ | - | - | - | $k \geq (3)[-12]$ | Ref.24-31 |
| 24. | $H + H_2O_2 \rightarrow H_2 + HO_2$ | (3.9)[-11] | 0 | 4600 | $k_{300}$ = 9.0[-18] | Ref.24-32 |

Table 24-1. (Cont'd.)

| No. | Reaction | a | b | c | Notes | Sources |
|---|---|---|---|---|---|---|
| XXVII. | Neutral Rearrangement (Cont'd.): | | | | | |
| 25. | $OH + O_3 \rightarrow HO_2 + O_2$ | - | - | - | $k \geq 5[-13]$ | Ref.24-31 |
| 26. | $OH + OH \rightarrow H_2O + O$ | 5[-11] | 0 | 400 | $k_{300} = 1.3[-11]$ | Ref.24-33 |
| 27. | $OH + H_2 \rightarrow H_2O + H$ | 3.6[-11] | 0 | 2580 | $k_{300} = 6.7[-15]$ | Ref.24-16 |
| 28. | $OH + HO_2 \rightarrow H_2O + O_2$ | - | - | - | $k \geq (1)[-11]$ | Ref.24-31 |
| 29. | $OH + H_2O_2 \rightarrow H_2O + HO_2$ | (2)[-11] | 0 | 900 | $k_{300} = 1[-12]$ | Ref.24-32 |
| 30. | $HO_2 + HO_2 \rightarrow H_2O_2 + O_2$ | (3)[-12] | 0 | 0 | | Ref.24-34 |
| 31. | $CO + OH \rightarrow CO_2 + H$ | (7)[-13] | 0 | 540 | $k_{300} = 1.2[-13]$ | Ref.24-35 |
| XXVIII. | Radiative Electronic-State Deexcitation: | | | | | |
| 1. | $O(^1D) \rightarrow O + h\nu$ | (6.8±2)[-3] | 0 | 0 | | Chp. 20 |
| 2. | $O(^1S) \rightarrow O + h\nu$ | (1.35±0.4)[0] | 0 | 0 | Pressure-dependent | Chp. 20 |
| 3.a. | $N(^2D)_{3/2} \rightarrow N + h\nu$ | (1.6)[-5±0.3] | 0 | 0 | | Chp. 20 |
| b. | $N(^2D)_{1/2} \rightarrow N + h\nu$ | (7.1)[-6±0.3] | 0 | 0 | | Chp. 20 |

Table 24-1. (Cont'd.)

| No. | Reaction | a | b | c | Notes | Sources |
|---|---|---|---|---|---|---|
| XXVIII. Radiative Electronic-State Deexcitation (Cont'd.): | | | | | | |
| 4. | $N(^2P) \rightarrow N + h\nu$ | $(7.7)[-2\pm0.3]$ | 0 | 0 | | Chp. 20 |
| 5. | $O_2(a\ ^1\Delta_g) \rightarrow O_2 + h\nu$ | $(2.6\pm1.0)[-4]$ | 0 | 0 | Pressure-dependent | Chp. 20 |
| 6. | $O_2(b\ ^1\Sigma_g^+) \rightarrow O_2 + h\nu$ | $(8.3)[-2\pm0.3]$ | 0 | 0 | | Chp. 20 |
| 7.a. | $N_2(A^3\Sigma_u^+)(F_2) \rightarrow N_2 + h\nu$ | $(1.7)[-1\pm0.3]$ | 0 | 0 | | Chp. 20 |
| b. | $N_2(A^3\Sigma_u^+)(F_1, F_3) \rightarrow N_2 + h\nu$ | $(3.7)[-1\pm0.3]$ | 0 | 0 | | Chp. 20 |
| 8. | $NO(a^4\Pi) \rightarrow NO + h\nu$ | $(6.3)[0\pm0.3]$ | 0 | 0 | | Chp. 20 |
| 9. | $NO_2(^2B_1) \rightarrow NO_2 + h\nu$ | $(1.4\pm0.2)[+4]$ | 0 | 0 | | Chp. 20 |
| 10.a. | $O^+(^2D)_{5/2} \rightarrow O^+ + h\nu$ | $(4.8)[-5\pm0.3]$ | 0 | 0 | | Chp. 20 |
| b. | $O^+(^2D)_{3/2} \rightarrow O^+ + h\nu$ | $(1.7)[-4\pm0.3]$ | 0 | 0 | | Chp. 20 |
| 11.a. | $O^+(^2P)_{3/2} \rightarrow O^+ + h\nu$ | $(2.4)[-1\pm0.3]$ | 0 | 0 | | Chp. 20 |
| b. | $O^+(^2P)_{1/2} \rightarrow O^+ + h\nu$ | $(1.9)[-1\pm0.3]$ | 0 | 0 | | Chp. 20 |
| 12. | $N^+(^1D) \rightarrow N^+ + h\nu$ | $(4.0)[-3\pm0.3]$ | 0 | 0 | | Chp. 20 |
| 13. | $N^+(^1S) \rightarrow N^+ + h\nu$ | $(1.1)[0\pm0.3]$ | 0 | 0 | | Chp. 20 |

Table 24-1. (Cont'd.)

| No. | Reaction | a | b | c | Notes | Sources |
|---|---|---|---|---|---|---|
| XXIX. | Electronic State Photoexcitation: | | | | | |
| 1. | $O_2 + h\nu \rightarrow O_2(a\ ^1\Delta_g)$ | | | | Flux and wavelength dependent | |
| 2. | $O_2 + h\nu \rightarrow O_2(b\ ^1\Sigma_g^+)$ | | | | | |
| XXX. | Collisional Electronic-State Quenching: | | | | | |
| 1. | $O(^1D) + e \rightarrow O(^3P) + e$ | (1.5)[-9±1] | 0 | 0 | | Chp. 20 |
| 2. | $O(^1D) + N_2 \rightarrow O + N_2$ | (8.0±4)[-11] | 0 | 0 | For additional quenchants of $O(^1D)$, see Table 20-8. | Chp. 20 |
| 3. | $O(^1D) + O_2 \rightarrow O + O_2(b\ ^1\Sigma_g^+)$ | (7±2)[-11] | 0 | 0 | | Refs. 24-36, 24-37 |
| 4. | $O(^1D) + CO_2 \rightarrow O + CO_2$ | (3±1)[-12] | 0 | 0 | | Ref. 24-36 |
| 5. | $O(^1S) + e \rightarrow O(^3P) + e$ | (1.8)[-9±1] | 0 | 0 | Cf. Figure 20-9. | Chp. 20 |
| 6. | $O(^1S) + e \rightarrow O(^1D) + e$ | (4)[-10±1] | 0 | 0 | | Ref. 24-38 |
| 7. | $O(^1S) + O \rightarrow O + O$ | (1.8)[-13] | 0 | 0 | | Chp. 20 |
| 8. | $O(^1S) + O_2 \rightarrow O + O_2$ | (3±1)[-13] | 0 | 0 | | Refs. 24-39, 24-40, 24-41 |
| 9. | $O(^1S) + N_2 \rightarrow O + N_2$ | (1)[-16] | 0 | 0 | | Ref. 24-42 |

Table 24-1. (Cont'd.)

| No. | Reaction | a | b | c | Notes | Sources |
|---|---|---|---|---|---|---|
| XXX | Collisianal Electranic-State Quenching (Cant'd.): | | | | | |
| 10. | $O(^1S) + CO_2 \rightarrow O + CO_2$ | (3)[-13] | 0 | 0 | | Refs.24-40,24-41 |
| 11. | $O(^1S) + H_2O \rightarrow O + H_2O$ | (3±2)[-10] | 0 | 0 | | Refs.24-43,24-44 |
| 12. | $O^+(^2D) + e \rightarrow O^+ + e$ | (1)[-7±2] | 0 | 0 | | Ref.24-45 |
| 13. | $N(^2D) + e \rightarrow N + e$ | (5)[-10±1] | 0 | 0 | | Chp. 20 |
| 14. | $N(^2D) + N_2 \rightarrow N + N_2$ | (3±3)[-15] | 0 | 0 | | Ref.24-40 |
| 15. | $O_2(a\ ^1\Delta_g) + e \rightarrow O_2 + e$ | (1)[-11±1] | 0 | 0 | Cf. Figure 20-8. | Estimated by detailed balance calculation, from Ref. 24-46 and Fig. 20-8. |
| 16. | $O_2(a\ ^1\Delta_g) + O \rightarrow O_2 + O$ | - | - | - | $k \leq (1)[-16]$ For additional quenchants of $O_2(a\ ^1\Delta_g)$, see Table 20-6. | Chp. 20 (Table 20-6) |
| 17. | $O_2(a\ ^1\Delta_g) + O_2 \rightarrow O_2 + O_2$ | (2.4±0.2)[-18] | 0 | 0 | | Chp. 20 (Table 20-6) |

Table 24-1. (Cont'd.)

| No. | Reaction | a | b | c | Notes | Sources |
|---|---|---|---|---|---|---|
| XXX. | Collisional Electronic-State Quenching (Cont'd.): | | | | | |
| 18. | $O_2(a\ ^1\Delta_g) + O_3 \rightarrow O_2 + O_3$ | (3±2)[-15] | 0 | 0 | For additional quenchants of $O_2(a\ ^1\Delta_g)$, see Table 20-6. | Chp. 20 (Table 20-6) |
| 19. | $O_2(a\ ^1\Delta_g) + N_2 \rightarrow O_2 + N_2$ | - | - | - | k <(1.1)[-19] | Chp. 20 (Table 20-6) |
| 20. | $O_2(a\ ^1\Delta_g) + O_2(a\ ^1\Delta_g) \rightarrow O_2 + O_2(b\ ^1\Sigma_g^+)$ | (2)[-18±1] | 0 | 0 | | Ref. 24-47 |
| 21. | $O_2(b\ ^1\Sigma_g^+) + O_2 \rightarrow O_2 + O_2$ | (4.5±4)[-16] | 0 | 0 | | Ref. 24-39 |
| 22. | $O_2(b\ ^1\Sigma_g^+) + N_2 \rightarrow O_2 + N_2$ | (2.0±1.0)[-15] | 0 | 0 | | Ref. 24-39 |
| 23. | $N_2(A^3\Sigma) + O \rightarrow N_2 + O$ | - | - | - | k ≤(3)[-11] | Chp. 20 (Table 20-4) |
| 24. | $N_2(A^3\Sigma) + N \rightarrow N_2 + N$ | $(5)\left[-11^{+0}_{-1}\right]$ | 0 | 0 | | Chp. 20 (Table 20-4) |
| 25. | $N_2(A^3\Sigma) + O_2 \rightarrow N_2 + O_2$ | (3.8±2)[-12] | 0 | 0 | | Chp. 20 (Table 20-4) |

Table 24-1. (Cont'd.)

| No. | Reaction | a | b | c | Notes | Sources |
|---|---|---|---|---|---|---|
| XXX. | Collisional Electronic-State Quenching (Cont'd.): | | | | | |
| 26. | $N_2(A^3\Sigma) + NO \rightarrow N_2 + NO$ | (7±4[-11] | 0 | 0 | | Chp. 20 (Table 20-4) |
| 27. | $N_2^+(A^2\Pi) + N_2 \rightarrow N_2^+ + N_2$ | (1)[-9±1] | 0 | 0 | | Chp. 20 |
| 28. | $N_2^+(B^2\Sigma) + O_2 \rightarrow N_2^+ + O_2$ | (2)[-9±1] | 0 | 0 | | Chp. 20 |
| 29. | $N_2^+(B^2\Sigma) + N_2 \rightarrow N_2^+ + N_2$ | (6)[-10±1] | 0 | 0 | | Chp. 20 |
| XXXI. | Radiative Vibrational-State Deexcitation: | | | | | |
| 1. | $CO(v=1) \rightarrow CO(v=0) + h\nu$ | (3.3±0.3)[+1] | 0 | 0 | | Chp. 11 |
| 2. | $CO_2(001) \rightarrow CO_2(000) + h\nu$ | (4.00±0.20)[+2] | 0 | 0 | | Chp. 11 |
| XXXII. | Collisional Vibrational-State Quenching: | | | | | |
| 1. | $O_2(v=1) + M \rightarrow O_2(v=0) + M$ | $\left\{ \frac{2.5 \times 10^{-12}\, T \exp\left[-(2.95 \times 10^{5}/T)\right]^{1/3}}{\left(1 - e^{-2270/T}\right)} \right\}$ | | | $M = N_2$ or $O_2$; $T = 800\text{-}3200\,K$ | Chp. 20 (Table 20-5) |

Table 24-1. (Cont'd.)

| No. | Reaction | a | b | c | Notes | Sources |
|---|---|---|---|---|---|---|
| XXXII. | Collisional Vibrational-State Quenching (Cont'd.): | | | | | |
| 2. | $O_2(v=1) + O \rightarrow O_2(v=0) + O$ | $(5.7)[-12]$ | (-0.5) | 483 | T = 300-1700 K; $k_{300} = (1.1)[-12]$ | Chp. 20 (Table 20-5) |
| | | $1.7[-9]$ | 0 | 400 | T = 2000-4000 K | |
| 3. | $N_2(v=1) + O \rightarrow N_2(v=0) + O$ | $\dfrac{6.21 \times 10^{-14}\, T \exp\left[-(1.37 \times 10^5/T)\right]^{1/3}}{\left(1 - e^{-3390/T}\right)}$ or $\dfrac{3.43 \times 10^{-12}\, T \exp\left[-(3.74 \times 10^6/T)\right]^{1/3}}{\left(1 - e^{-3390/T}\right)}$ | | | T = 3000-4500 K | Chp. 20 (Table 20-2) |
| 4. | $N_2(v=1) + N_2 \rightarrow N_2(v=0) + N_2$ | $1.3 \times 10^{-11}\, T \exp\left[-(1.06 \times 10^7/T)\right]^{1/3}$ | | | T = 300-5000 K | Chp. 20 (Table 20-2) |
| XXXIII. | Collisional Vibrational Energy Exchange: | | | | | |
| 1. | $O_2(v=1) + H_2O \rightarrow O_2(v=0) + H_2O(010)$ | $(1.7)[-11 \pm 1]$ | (-0.5) | 0 | Endothermic by 39 $cm^{-1}$ (~0.005 eV) | Chp. 20 (Table 20-5 |

Table 24-1. (Cont'd.)

| No. | Reaction | a | b | c | Notes | Sources |
|---|---|---|---|---|---|---|
| XXXIII. Callisional Vibratianal Energy Exchange (Cont'd.): | | | | | | |
| 2. | $N_2(v=1)+O_2(v=0)\rightarrow N_2(v=0)+O_2(v=1)$ | $\left\{\frac{2.5\times10^{-7}\exp[-(1.82\times10^{7}/T)]^{1/3}}{\left(1-e^{-3390/T}\right)}\right\}$ | | | T = 1000-10,000 K | Chp. 20 (Table 20-2) |
| 3. | $N_2(v=1)+N_2(v=0)\rightarrow N_2(v=0)+N_2(v=1)$ | (3)[-13] | 0 | 0 | Case af resonant VV at T = 300 K. | Chp. 20 (Table 20-2) |
| 4. | $N_2(v=1)+CO_2(000)\rightarrow N_2(v=0)+CO_2(001)$ | (6±2)[-13] | (-0.5) | 0 | T = 300-1200 K | Chp. 20 (Table 20-2) |

## REFERENCES


24-1. Keneshea, T. J., Air Force Cambridge Research Laboratories, Rept. AFCRL-63-711 (1963).

24-2. Niles, F. E., private communication (1971).

24-3. Byerly, R., Jr., and E. C. Beaty, J. Geophys. Res. 76, 4596 (1971).

24-4. Ferguson, E. E., Accts. Chem. Research 3, 402 (1970).

24-5. Fehsenfeld, F. C., A. L. Schmeltekopf, and E. E. Ferguson, J. Chem. Phys. 44, 4537 (1966).

24-6. Biondi, M. A., private communication (1971).

24-7. Puckett, L. J., and M. W. Teague, J. Chem. Phys. 54, 2564 (1971).

24-8. Fehsenfeld, F. C., A. L. Schmeltekopf, and E. E. Ferguson, J. Chem. Phys. 45, 23 (1966).

24-9. Pack, J. L., and A. V. Phelps, Bull. Am. Phys. Soc. 16, 214 (1971).

24-10. McNeal, R. J., and S. C. Durana, J. Chem. Phys. 51, 2955 (1969).

24-11. Young, R. A., and G. Black, J. Chem. Phys. 44, 3741 (1966).

24-12. Sharma, R. D., and K. L. Wray, J. Chem. Phys. 54, 4578 (1971).

24-13. Gross, R. W. F., and N. Cohen, J. Chem. Phys. 48, 2582 (1968).

24-14. Gross, R. W. F., J. Chem. Phys. 48, 1302 (1968).

24-15. Ham, D. O., D. W. Trainor, and F. Kaufman, J. Chem. Phys. 53, 4395 (1970).

24-16. Baulch, D. L., D. D. Drysdale, and A. C. Lloyd, Leeds University High Temperature Reaction Rate Data Series, No. 2 (1968).

24-17. Slanger, T. G., and G. Black, J. Chem. Phys. 53, 3722 (1970).

24-18. Appleton, J. P., M. Steinberg, and D. J. Liquornik, J. Chem. Phys. 48, 599 (1968).

24-19. Wray, K. L., and J. D. Teare, J. Chem. Phys. 36, 2582 (1962).

24-20. Johnston, H. S., National Bureau of Standards, Rept. NSRDS-NBS-20 (1968).

24-21. Findlay, F. D., and D. R. Snelling, J. Chem. Phys. 54, 2750 (1971).

24-22. Gilpin, R., H. I. Schiff, and K. H. Welge, J. Chem. Phys. 55, 1087 (1971).

24-23. Donovan, R. J., D. Husain, and L. J. Kirsch, Chem. Phys. Letts. 6, 488 (1970).

24-24. Scott, P. M., and R. J. Cvetanovic, J. Chem. Phys. 54, 1440 (1971).

24-25. Wayne, R. P., Annals N. Y. Acad. Sci. 171, 199 (1970).

24-26. Phillips, L. F., and H. I. Schiff, J. Chem. Phys. 42, 3171 (1965).

24-27. Phillips, L. F., and H. I. Schiff, J. Chem. Phys. 36, 1509 (1962).

24-28. Greig, J. D., and P. G. Hall, Trans. Far. Soc. 63, 655 (1967).

24-29. Johnston, H. S., and D. M. Yost, J. Chem. Phys. 17, 286 (1949).

24-30. Phillips, L. F., and H. I. Schiff, J. Chem. Phys. 37, 1233 (1962).

24-31. Kaufman, F., Ann. Geophys. 20, 77 (1964).

24-32. Baulch, D. L., D. D. Drysdale, and A. C. Lloyd, Leeds University High Temperature Reaction Rate Data Series, No. 3 (1969).

24-33. Kaufman, F., private communication, modification of Reference 24-16 (1971).

24-34. Foner, S. N., and R. L. Hudson, Adv. Chem. 36, 34 (1962).

24-35. Baulch, D. L., D. D. Drysdale, and A. C. Lloyd. Leeds University High Temperature Reaction Rate Data Series, No. 1 (1968).

24-36. Noxon, J., J. Chem. Phys. 52, 1852 (1970).

24-37. Clark, I. D., Chem. Phys. Letts. 5, 317 (1970).

24-38. Seaton, M. J., in The Airglow and the Aurora, E. Armstrong and A. Dalgarno, Eds., Pergamon Press, London (1956); p. 289.

24-39. Zipf, E.C., Jr., Can. J. Chem. 47, 1863 (1969).

24-40. Black, G., T. G. Slanger, G. St. John, and R. A. Young. J. Chem. Phys. 51, 116 (1969).

24-41. Filseth, S. V., F. Stuhl, and K. H. Welge, J. Chem. Phys. 52, 239 (1970).

24-42. Clark, I. D., and R. P. Wayne, Proc. Roy. Soc. A316, 539 (1970).

24-43. Stuhl, F., and K. H. Welge, Can. J. Chem. 47, 1879 (1969).

24-44. Young, R. A., G. Black, and T. G. Slanger, J. Chem. Phys. 50, 309 (1969).

24-45. Dalgarno, A., private communication (1966).

24-46. Kummler, R. H., and M. H. Bortner, General Electric Company, Rept. TIS R67SD20 (1967).

24-47. Arnold, S. J., and E. A. Ogryzlo, Can. J. Phys. 45, 2053 (1967).

## APPENDICES

APPENDIX A SYMBOLS

APPENDIX B CONSTANTS

APPENDIX C CONVERSION FACTORS

APPENDIX D GLOSSARY

APPENDIX E SUBJECT INDEX

APPENDIX F SPECIES INDEX

APPENDIX G AUTHOR INDEX

APPENDIX H GENERAL REFERENCES

# APPENDIX A
# SYMBOLS

N. B.: Whenever applicable, chapter numbers in which a symbol is used are indicated in parentheses. In addition, wherever a particular symbol is also used for indexing, i.e., as a subscript, superscript, or parenthetical appendage to any other symbol, that fact is also indicated, along with the applicable chapter number(s).

| | |
|---|---|
| A | Electron affinity. |
| | Undesignated function of the medium (3). |
| | Designation in Figure 3-5, for minimum diffusivity value (3). |
| | Designation for unspecified chemical species (6, 19, 20). |
| | Thermodynamic work function (10). |
| | Einstein coefficient (11). |
| | Designation in Table 15-2, for beam-in-static-gas technique (15). |
| | Least-squares fit constant (16). |
| | Rate constant at the reference temperature, a characteristic term of the rate-constant function (19). |
| AB | Indexing use only; designation for a molecule AB (4). |
| AC | Alternating current. |
| $A_{ij}$ | Einstein coefficient for the i→j transition (11). |
| $A_o$ | Comparison imaginary function plotted in Figure 21-2 from Reference 21-2, assuming $j = 0$ and $\nu(\epsilon) = \nu_o$ (21). |
| $A_p$ | Daily geomagnetic index (5). |

A(v) Einstein coefficient for the vibrational transition $v \rightarrow v-1$ (11).

AZA Designation for Auroral Zone Absorption (5).

$A_2$ Imaginary function plotted in Figure 21-2, from Equation 21-5 (21).

a Rate constant at the reference temperature, usually 300 K, a characteristic term of the rate-constant function (6, 16, 19, 24).

Parameter defined in Equation 15-9 (15).

Indexing uses: species (3).
atomic (9).
ambipolar (9, 16).
trajectory point (15).
antisymmetric (15).
colliding species in the Firsov model (15).
attachment (21).

ac Alternating current.

$a_i$ Interaction or capture radius (15).

$a_o$ Bonding radius of hydrogenic species (11).

Radius of first Bohr orbit (15, 21).

av Indexing use only; average value (3, 11).

B Undesignated function of the medium (3).

Designation in Figure 3-5, for maximum diffusivity value (3).

Rotational constant (4, 11).

Designation for unspecified chemical species (6, 19, 20).

Recombination term in continuity equation (9).

Surface brightness of a radiating volume (11).

Designation in Table 15-2, for crossed-beam technique (15).

Least-squares fit constant (16).

B (cont'd) Designation in Figure 16-2, for work of Bardsley, Reference 16-28 (16).

Power of the pre-exponential thermal dependence, a characteristic term of the rate-constant function (19).

Magnetic field strength (21).

Indexing use: target species (15).

BH Designation for Birge-Hopfield system (9).

$B_o$ Comparison real function plotted in Figure 21-2, from Reference 21-2, assuming $j = 0$ and $\nu(\epsilon) = \nu_o$ (21).

B&T Designation in Figure 20-6, for work of Bauer and Tsang, Reference 20-143 (20).

$B_2$ Real function plotted in Figure 21-2, from Equation 21-5 (21).

b Power of the pre-exponential thermal dependence, a characteristic term of the rate-constant function (6, 16, 19, 24).

Parameter defined in Equation 15-10 (15).

Impact parameter (15).

Indexing uses: bound state of species (8).
trajectory point (15).
impact parameter (15).
colliding species in the Firsov model (15).
magnetic field (21).

$b_j$ Interaction or capture radius (15).

$|b_j|^2$ Capture probability (15).

buoy Indexing use only; buoyancy subrange (3).

$b_1$ Cut-off radius (15).

C Designation for unspecified chemical species (6, 19, 20).

Linear slope in a Boltzmann system (6).

Designation in Table 9-5, for chemical association process (9).

C (cont'd) Designation in Table 15-2, for fast-particle detection (15).

Constant ≅ 3.49 in the Thomas theory (15).

Least-squares fit constant (16).

$\mathfrak{C}_p(X)$ Integral function of X used in Equation 21-5 and explained and tabulated in Reference 21-28 (21).

c Speed of sound (3).

Speed of light (4, 7, 11).

Activation temperature of chemical reaction, a characteristic term of the rate-constant function (6, 19, 24).

Indexing uses: chemical change (3).
chemical energy (3).
cyclotron (7).
cone (7).
collisional (20).

$\bar{c}$ Mean thermal speed (3).

$\bar{c}_j$ Mean thermal speed of species "j" (3).

$c_o$ Speed of sound in unperturbed medium (3).

col Indexing use only; column (11).

crit Indexing use only; critical value (3).

$c_v$ Specific heat at constant volume per unit mass (3).

$c(\rho)$ $= \left|b_j(+\infty)\right|^2$ (15).

D Effective diffusion coefficient (3).

Dissociation energy (4).

Distance from nuclear burst measured along surface of earth (5).

Designation for unspecified chemical species (6).

Designation in Table 15-2, for slow-particle detection (15).

Least-squares fit constant (16).

D (cont'd) Diffusion coefficient (20).

Indexing uses: dielectric recombination (9).
dielectric dissociative recombination (9).
dissociation (10).

$D_a$ Ambipolar diffusion coefficient (9, 16).

DC Direct current.

$D_{eddy}$ Eddy diffusivity (3).

$D_m^j$ Molecular diffusion coefficient for species "j" (3).

$D_{nn}^j$ Turbulent molecular eddy diffusivity for species "j" (3).

$D_{nT}^j$ Turbulent thermal eddy diffusivity for species "j" (3).

$\underset{\sim}{D}_{nu}^j$ Turbulent diffusivity vector, from Equation 3-68a (3).

$D_{th}^j$ Thermal diffusion coefficient for species "j" (3).

$D_{mol}$ Molecular diffusivity (3).

$D_o$ Dissociation energy (17).

$D^T$ Thermal diffusion term (3).

$$\left.\begin{aligned}(D/Dt) &\equiv (\partial/\partial t) + \underset{\sim}{u}\cdot\nabla \\ (D_a/Dt) &\equiv (\partial/\partial t) + \underset{\sim}{u}_a\cdot\nabla\end{aligned}\right\}$$ Functional relationships (3).

d Length scale of motion (3).

Production rate factor (9).

Indexing uses: dissociation (4, 16).
dielectronic recombination (5, 8).
excited dielectronic state overlapping a continuum (8).

dc Direct current.

| | |
|---|---|
| E | Designation for East (3). |
| | State energy (4, 10). |
| | Collision energy in a Boltzmann system (6). |
| | Activation energy of reaction (6, 19). |
| | Energy (10, 15, 19, 20). |
| | Beam energy, in the method of Fleischmann, Dehmel, and Lee (15). |
| | Electric field strength (21). |
| | Indexing use: energy (6). |
| $E_a$ | Internal energy per unit mass of species "a" (3). |
| | Energy of antisymmetric state (15). |
| EA | Electron affinity (17, 18A). |
| $E_e$ | Kinetic energy of bound electron (15). |
| $E_f$ | Final electron energy in Bremsstrahlung (11). |
| $E_i$ | Initial electron energy in Bremsstrahlung (11). |
| | Ionization energy of projectile, in the method of Fleishmann, Dehmel, and Lee (15). |
| | Energy associated with charge state "i" (15). |
| $E_j$ | Energy associated with charge state "j" (15). |
| $E_{n\ell}$ | Binding energy of level $n\ell$ (11). |
| $E_o$ | Impact energy, in the Firsov model (15). |
| $E_{Ryd}$ | Binding energy of Rydberg level of hydrogenic species (11). |
| $E_s$ | Energy of symmetric state (15). |
| $E_t$ | Energy threshold for reaction in a Boltzmann system (6). |
| EUV | Designation for Extreme Ultraviolet (5). |

$E_{XA}$ Activation energy for collisional excitation ($X \rightarrow A$) reaction (20).

$E_1$ $= MR^2 (E_i/13.6)^2$, in the method of Fleischmann, Dehmel, and Lee (15).

Kinetic energy of incident ion before collision (15).

$E_2$ Kinetic energy of incident ion after collision (15).

e Ionic or electronic charge (7, 11, 15, 21).

Designation in Table 9-5, for photoelectron process (9).

Indexing uses: energy equation (3).
electron (4, 5, 7, 8, 11, 16, 20, 21, 22, 24).
electronic transition (11).
bound electron (15).
electron acting as third body (16).

eddy Indexing use only; eddy (3).

eff Indexing use only; effective (9, 15).

ex Indexing use only; excitation (4, 11).

F Solar flux at 10.7-cm wavelength (5).

Designation in Table 9-5, for fluorescence process (9).

Free energy (10).

Fraction of optically active molecules under irradiation, which are radiatively excited per second (11).

Designation on Page 18A-8, of work of Ferguson, from Reference 18A-9 (18A).

Designation on Page 18A-9, of work of Fehsenfeld et al, from Reference 18A-40 (18A).

$\underset{\sim}{F}$ Total external force per unit mass (3).

$\underset{\sim}{F}'$ Miscellaneous external forces acting on atmosphere (3).

$\underset{\sim}{F}_a$ External force per unit mass on species "a" (3).

$F(k)$ Turbulent power spectrum, in wavenumber space (3).

$F(k)_{Kolm}$ F(k) in the inertial subrange, according to Kolmogoroff's Law (3).

$f$ Oscillator strength or "f-number" of transition (11).

Range of reciprocal electron densities over which a linear variation with time is obtained, to within one percent (16).

Indexing uses: fluorescence (11).
final (11).

$f_o$ Resonant frequency (7).

$f_v$ Fraction of collisions having relative velocities between v and v+dv (6).

$f(X)$ Fractional atmospheric concentration of species "X" (4).

$f(\epsilon)$ Electron energy distribution function (21).

$G$ Fractional energy loss per collision (21).

$G(\ell, t)$ Probability for separation distance "$\ell$" between two particles (3).

GS Designation in Figure 16-2, of work of Gunton and Shaw, from Reference 16-7 (16).

$g$ Gravitational acceleration (2, 4).

Production rate factor (9).

Statistical weight (11).

Indexing use: gas-kinetic (21).

$\underset{\sim}{g}$ Gravitational force per unit mass (3).

gas Indexing use only; gas-kinetic (16).

$g_{ion}$ Statistical weight of ionic ground state (11).

$g_{n\ell}$ Statistical weight of a recombining level "$n\ell$" (11).

$g_n(\nu)$ Statistical weight of a recombining level in a hydrogenic species (11).

g(X) Electronic statistical weight of species "X" (4).

g(y) Firsov model parameter $\equiv \left[y^{0.1} - 1\right]$ (15).

H Pressure scale height (2).

Atmospheric scale height (3).

Magnetic field (7).

Scale height of atomic oxygen (9).

Enthalpy (10, 17, 19).

Total Hamiltonian (15).

Designation in Figure 16-1, of work of Hagen, from Reference 16-22 (16).

Designation on Page 18A-9, of work of Howard et al, from Reference 18A-12 (18A).

Scale height (20).

Indexing use: hydrogen atom (15).

Ha Designation in Figure 16-1, of work of Hackam, from Reference 16-19 (16).

HCE Designation for Handbook Committee Estimate (24).

H(X) Scale height of species "X" (4).

h Planck constant (3, 4, 6, 7, 11, 17, 19, 20, 24).

Altitude (4, 5).

Indexing use: altitude (4).

$\hbar$ Modified Planck constant, $h/2\pi$ (11, 15).

$h_{ii} \equiv (\phi_i, V_b\phi_i)$

$h_{ij} \equiv (\phi_i, V_a\phi_j)$ (15).

$h_{ji} \equiv (\phi_j, V_b\phi_i)$
$h_{jj} \equiv (\phi_j, V_a\phi_j)$ (15).

$\bar{h}_j^{-1}$ A measure of chemical effect in turbulence, from Equation 3-67a (3).

$h_o$ Turbopause altitude (4).

Indexing use: turbopause altitude (4).

horiz Indexing use only; horizontal (3).

$h_q$ Quenching height (9).

I Ionization potential (4, 15).

Photon flux after transmission (7).

Intensity of indicated radiation (9).

Geomagnetic dip angle (9).

Designation in Table 9-5, of ionic reaction process (9).

$I_{col}$ Line-of-sight column emission rate = line integral of $I_{vol}$ (11).

ICR Designation for Ion Cyclotron Resonance (7).

IGY Designation for International Geophysical Year (9).

$I_H$ Ionization potential (13.6 eV) of ground-state hydrogen atom (15).

Im Designation for imaginary portion of function (21).

$\mathrm{Im}\Delta K_i$ Imaginary portion of $\Delta K_i$, in the low-frequency limit (21).

$I_o$ Photon flux before transmission (7).

$I_o(\lambda)$ Incident light intensity (12).

IP Ionization potential (18A).

IR Infrared.

$I_{vol}$ Volume emission rate (11).

$I(\lambda)$ Transmitted light intensity (12).

$I_1$ Total number of primary or projectile species passing through target per unit time (15).

i $\sqrt{-1}$ (3, 21).

Charge condition at a point in the trajectory (15).

Indexing uses: species (2, 9, 20, 21).
directional components x, y, and z (3).
ionization (4, 10, 12, 14, 15).
ion (5, 11, 21, 24).
photoionization (7).
molecular ion (9).
ion-ion recombination or neutralization (9, 16).
state (11).
initial condition (11).
charge state (14).
initial charge on primary or projectile species (15).
charge condition at a trajectory point (15).
chemical process (16).
positive-ion (16, 21).

if Indexing use only; intermediate frequency (20).

$i_g$ Ion current (7).

ij Indexing use only; the transition i→j (11).

ion Indexing uses only; ion (11).
ion-kinetic (17).

ir Infrared.

J Effective rate coefficient for solar photodissociation of $O_2$ (3).

Solar flux (3).

Rotational quantum number (14).

J' Rotational quantum number (14).

j Charge condition at a point in the trajectory (15).

Vibrational level (21).

Indexing uses: species (3, 9, 13).
directional components x, y, and z (3).
state (11).
final charge on primary or projectile species (15).
charge condition at a trajectory point (15).
chemical process (16).
vibrational level (21).

K Eddy viscosity (3).

Equilibrium constant (5).

Designation in Figure 16-1, of work of Kasner, from Reference 16-20 (16).

Designation on Page 18A-8, of work of Kebarle, from Reference 18A-20 (18A).

Dielectric constant (21).

Indexing use: characteristic (21).

KB Designation in Figures 16-1 and 16-3, of work of Kasner and Biondi, from References 16-2 and 16-29, respectively (16).

$K_D$ Equilibrium constant for dissociation of diatomic molecules (10).

$K_i$ Equilibrium constant for ionization or electron detachment (10).

Dielectric constant as affected by ions (21).

Kolm Indexing use only; Kolmogoroff's Law (3).

$K_Q(v)$ Quenching rate for level "v" at a given total density and composition of quenchant (11).

$K_R(v)$ Chemical destruction rate for level "v" (11).

$K'$ Collisional rate (11).

$K'_{01}$ Collisional excitation rate (11).

$K'_{10}$ Collisional deexcitation rate (11).

$K$ Thermal conductivity coefficient (3).

$K_i$ Degree of ionization of plasma (3).

$k$ Wavenumber (3).

Boltzmann constant (4, 11, 20, 21).

Rate constant or rate-constant function, of chemical reaction, in the forward direction as written (6, 11, 18A, 19, 20, 24).

Total absorption coefficient (7).

Rate coefficient of ion-molecule reaction (8).

Total three-body recombination rate coefficient (16).

Indexing use: kinetic (4).

$\underset{\sim}{k}$ Wavenumber vector (3).

$k_g$ Upper limit of wavenumber for buoyancy subrange (3).

$k_i$ Photoionization coefficient (7).

Rate constant for inelastic scattering from species "i" (20).

$k^i_{3n}$ Rate coefficient for Thomson recombination, three-body neutral-molecule-stabilized, positive-ion-negative-ion recombination (16).

kin Indexing use only; kinetic (11).

$k_j(z)$ First-order rate constant for photoionization of species "j", at altitude "z" (13).

$k_M$ Rate constant for quenching reaction where "M" is the quenchant (20).

kn Reactive collision frequency (20).

$k(NO^+)$ Rate coefficient for $NO^+$ production (13).

$k_o$ $= 2\pi/L_o$ (3).

$k_r$ Rate constant for reverse reaction (18A).

$k_T$ Rate constant for a system having Maxwellian distribution (6, 14).

Absorption coefficient (12).

$k(v)$ Rate constant for formation of vibrationally excited species in level "v" (11).

$k_x$, $k_y$, $k_z$ Wavenumber directional components (3).

$k_\nu$ $= 2\pi/L_\nu = (\epsilon_\nu/\nu^3)^{1/4}$ (3).

$k_{10}$ Rate constant for deactivation of first vibrational level (20).

$k_{3e}$ Three-body recombination rate coefficient with electron as third body (16).

$k_{3n}$ Three-body recombination rate coefficient with neutral species as third body (16).

$k_{3r}$ Three-body recombination rate coefficient (16).

$k_{300}$ Rate constant at 300 K (24).

$k'$ Rate constant or rate-constant function of chemical reaction, in the reverse direction as written (6).

$k$ Boltzmann constant (3, 6).

L Designation for Lyman radiation (5).

Optical pathlength (13).

LBH Designation for Lyman-Birge-Hopfield system (9).

$L_{ij}(\epsilon)$ Inelastic cross-section for low-energy electron in gas (21).

$L_j$ Rate of process "j" leading to electron loss (16).

$L_j^{-1}$ A measure of the effect of wind shear in turbulence, in Equation 3-67b (3).

$L_j(\epsilon)$ Energy loss function for the jth vibrational level (21).

$L_o$ Length scale of large (turbulent) disturbances (3).

LT Designation in Figure 16-2, of work of Lin and Teare, from Reference 16-27 (16).

LTE Designation for Local Thermodynamic Equilibrium (4, 11).

Ly Designation for Lyman radiation (12).

$L(\epsilon)$ Energy loss function (21).

$L_\nu$ Length scale of the smallest of eddies (3).

$L_{2r}$ Rate of electron loss via two-body electron-ion recombination (16).

$L_{3r}$ Rate of electron loss via three-body electron-ion recombination (16).

$\ell$ Distance (3).

Charged rearrangement rate constant for negative ions (9)

Light path (12).

$\ell_m$ Gas-kinetic mean free path (3).

M Mean molecular weight (2).

Gram molecular weight (3).

Reduced molecular weight (6).

Designation for third body or collisional partner (6, 16, 17, 18A, 19, 20, 24).

Reduced mass of ion-molecule reaction pair (8).

M (cont'd) Projectile mass, in the method of Fleischmann, Dehmel, and Lee (15).

Designation for unspecified chemical species (17, 18A, 20).

Number density of collision partner (20).

Mass number (21).

MB Designation in Figures 16-1 and 16-3, of work of Mehr and Biondi, from Reference 16-21 (16).

Me Designation for unspecified metallic species (11).

$M_i$ Molecular weight of species "i" (2).

Mass number for an ionic species (21).

Reduced mass of ion + neutral pair (21).

$M_o$ Sea-level mean atmospheric molecular weight = 28.96 (2).

M(X) Mass of species "X" (4).

m Mean mass of an "air molecule" (3).

Unspecified function of altitude, time of day, and sunspot cycle (5).

Ionic mass (7, 15).

Concentration of attaching neutral species (9).

Mass of electron (21).

Indexing uses: equation of motion (3).
combining proportions (6).
molecular (9).
momentum-transfer (11, 21).
number of electrons stripped (15).

$m_a$ Molecular mass of species "a" (3).

$m_{av}$ Mass of average "air molecule" (3).

max Indexing use only; maximum (11).

| | |
|---|---|
| $m_e$ | Mass of electron (4, 11). |
| | Mass of bound electron on target atom (15). |
| $m_j$ | Molecular mass of species "j" (3). |
| mn | Indexing use only; mutual neutralization (16). |
| mol | Indexing use only; molecular (3). |
| $m_1$ | Mass of incident ion (15). |
| N | Number of observations (3). |
| | Brunt-Väisälä frequency (3). |
| | Electron concentration (9). |
| | Number of collisions per second per molecule at altitude (11). |
| | Total number of optically active molecules under irradiation (11). |
| | Designation for unspecified chemical species (16). |
| | Molecular density (21). |
| | Indexing use: neutral product (12). |
| $N_{col}$ | Column density of molecules under radiative excitation (11). |
| NED | Designation for No Experimental Data (24). |
| $N_{ex}$ | Total number of optically active molecules under irradiation which become excited (11). |
| $N_i$ | Positive-ion density (21). |
| $[N_j]$ | Concentration of species "j" (13). |
| $N^+$ | Positive-ion concentration (9). |
| $N_a^+$ | Density of atomic ions (9). |
| $N_{mi}^+$ | Density of molecular ions (9). |

$N^-$ Negative-ion concentration (9).

$n$ Species concentration (3).

Gas density (7).

Concentration of detaching neutral species (9).

Level of hydrogenic species into which recombination is taking place (11).

Density of absorbing gas (12).

≡ -b for certain recombination reactions (19).

Electron density (21).

Indexing uses: combining proportions (5, 6, 16, 17, 21, 24).
level of hydrogenic species (11).
final charge on initially neutral target species (13).
neutral species acting as third body (16).
electron noise (21).

$n_B$ Number density of target species (15).

$n_e$ Electron density (4, 5, 7, 8, 11, 15, 22).

$\langle n_e(t) \rangle$ Space-averaged electron density at time "t" (16).

$\langle n_e(0) \rangle$ Space-averaged electron density at zero time (16).

$n_e(\infty)$ Stationary electron density long after ionizing source is turned on (16).

$n_{eff}$ Number of electrons effectively available for ionization in the outer shell of projectile species, in the method of Fleischmann, Dehmel, and Lee (15).

$n_i$ Number density of species "i" (2, 20).

Ion density (11).

$n_j$ Number density of species "j" (3).

$n_j'$ Fluctuation of $n_j$ (3).

$\bar{n}_j$ Mean value of $n_j$ (3).

$n\ell$ A particular level into which radiative recombination is taking place (11).

Indexing use: level into which radiative recombination is taking place (11).

$n_{N_2}$ $N_2$ species density (24).

$n_o$ Loschmidt number (7, 12).

$n_s$ Density of stabilizing agent (16).

$n_{tot}$ Total species density (4).

n(X) Species density of "X" (4).

$n_1$ Vertical distribution of atomic-oxygen concentration (3).

$n_2$ Vertical distribution of molecular-oxygen concentration (3).

$n_+$ Positive-ion density (16).

$n_-$ Negative-ion density (16).

o Indexing uses: sea-level (2).
unperturbed-medium (3).
reference (3).
turbopause (4).
pre-magnetic storm (5).
pre-transmission (7).
resonant (7).
Loschmidt (7, 12).
standard-state (10).
band-origin (11).
atomic species (11).
incidence (12).
impact, in the Firsov model (15).
Bohr (15, 21).
collision-free (20).
free-space (21).
energy-independent (21).
pre-integration (21).

P — Designation on Page 18A-9, of work of Puckett and Teague, from Reference 18A-41 (18A).

P(b, u) — Probability for charge transfer on collision at impact parameter "b" and relative velocity "u" (15).

PCA — Designation for Polar Cap Absorption (5, 9).

$P_i$ — Rate of process "i" leading to electron production (16).

p — Pressure at altitude (2).

Pressure or partial pressure (3, 8, 10, 20, 21).

Indexing uses: combining proportions (6).
projectile species (15).
plasma (21).
half-integer spacing (21).

p' — Pressure for small perturbation or fluctuation (3).

$\bar{p}$ — Mean pressure (3).

$p_a$ — Partial pressure for species "a" (3).

$p_{N_2}$ — Pressure of $N_2$ (20).

$p_o$ — Pressure for unperturbed background (3).

pop — Indexing use only; population (4).

$p_1$ — Pressure at reference altitude (2).

Q — Diffusional rate (3).

Characteristic Q-number of a resonant cavity (7).

Partition function (11).

Cross-section (15).

Capture cross-section (15).

Source term (21).

Indexing use: quenching (11).

$Q_a$ Net rate of radiative heat absorption by species "a" (3).

$Q_c$ Net rate of chemical energy evolution per unit mass (3).

$Q_m(\epsilon)$ Source term for electron momentum-transfer collisions (21).

$Q_n$ Specific slow-ion production cross-section (15).

$Q_R$ Net rate of radiant energy absorption per unit mass (3).

$Q_{rot}(X)$ Rotational partition function for a rigid rotator (4).

$Q_v$ Vibrational partition function (11).

$Q_{vib}(X)$ Vibrational partition function for a harmonic oscillator (4).

$Q(X)$ Partition function of (molecular)species "X" (4).

$Q_{ii}^{0n}$ Ionization cross-section (ambiguous term) where i = j (15).

$Q_{ij}^{0n}$ Cross-section for collisional charge exchange in heavy-particle collisions, where i = n+j (15).

$Q_{10}^{01}$ Cross-section for collisional charge exchange where i = 1 (15).

$Q_+$ Total slow positive-charge production cross-section (15).

$Q_-$ Electron production cross-section (15).

$q$ Ion-pair production rate due to beta-particle ionization of air (5).

Electron production rate (9).

Bremsstrahlung radiation (11).

Electron source function (22).

Indexing use: quenching (9).

$\underset{\sim}{q}$ Total heat flux vector (3).

$\underset{\sim}{q}_a$ Heat flux carried by species "a" (3).

$q_o$ $= \sum_j \sigma_{0j} \approx \sigma_{01}$ at low energies (15).

$q_{v'v''}$ Franck-Condon factor for electronic transition involving $v = v'$ in excited state and $v = v''$ in ground state (11).

R Gas constant (2, 3, 19).

Designation in Table 9-5, for resonance scattering process (9).

Interaction distance, in the method of Fleischmann, Dehmel, and Lee (15).

Internuclear separation (15).

Indexing uses: radiant energy (3).
chemical destruction (11).

Re Reynolds number (3).

Designation for real portion of function (21).

$Re\Delta K_i$ Real portion of $\Delta K_i$, in the low-frequency limit (21).

Ri Richardson number (3).

$P_o$ Impact parameter, in the Firsov model (15).

Ryd Indexing use only; Rydberg (11).

$R_{\lambda\mu}$ Irradiance incident on volume element (11).

$R_{\lambda\mu e}$ Solar irradiance upon the atmosphere at center wavelength $\lambda_e$ of electronic transition (11).

r Radius of interaction (15).

Indexing uses: radiative recombination (8, 9).
recombination (16).
reference (16, 19).
reverse (18A).

$\underset{\sim}{r}$ Position vector measured from earth center (3).

Electron position vector, with respect to trajectory midpoint (15).

Indexing use: trajectory midpoint electron position vector (15).

$\vec{r}$ Space vector (16).

$\underset{\sim}{r}_a$ Electron position vector, with respect to trajectory point (15).

Indexing use: trajectory point electron position vector (15).

$\underset{\sim}{r}_b$ Electron position vector, with respect to trajectory point (15).

Indexing use: trajectory point electron position vector (15).

ref Indexing use only; reference (24).

rot Indexing use only; rotational (4, 11).

S Integrated band strength of transition (11).

Electron density shape factor (16).

Designation in Figure 16-2, of work of Stein et al, from Reference 16-26 (16).

Designation in Figure 16-3, of work of Sayers, from Reference 16-33 (16).

$S_{c;a}$ Rate of chemical production or loss of species "a" (3).

$\bar{S}_{c;j}$ Mean rate of chemical production or loss of species "j" (3).

$S_e$ Integrated band strength of electronic transition at its center wavelength $\lambda_e$ (11).

$S_{e;a}$ Effect of collisions and reactions on energy equation (3).

SID Designation for Sudden Ionospheric Disturbance (3).

SIGMAI Designation for total ionization cross-section (13).

SIGMAT Designation for total absorption cross-section (13).

$S_{ij} \equiv (\phi_i, \phi_j)$
$S_{ji} \equiv (\phi_j, \phi_i)$ (15).

$\underset{\sim}{S}_{m;a}$ Effect of collisions, including chemical effects, on equation of motion (3).

STAT Designation for statistical model (15).

s Indexing uses: shear (3).
solar continuum (11).
symmetric (15).
stabilizing agent (16).

solar Indexing use only; solar continuum (11).

T Temperature or kinetic temperature or translational temperature (2, 3, 4, 6, 8, 11, 14, 16, 17, 18A, 19, 20, 24).

Exospheric temperature (5).

Designation in Table 9-5, of excitation transfer process (9).

Kinetic energy operator (15).

Indexing uses: thermal (3).
total (12).

{T} Designation for simultaneous variation of $T_{gas}$, $T_i$, and $T_e$ (16).

$T_{av}$ Average kinetic temperature (11).

$T_d$ Dissociation temperature (4).

$T_e$ Electron temperature (5, 8, 16, 20, 21, 24).

$\{T_e\}$ Designation for variation of $T_e$ alone (16).

$T_{ex}$ Excitation temperature (4).

$T_g$ Gas-kinetic temperature (21).

$T_{gas}$ Gas-kinetic temperature (16).

$T_i$ Ionization temperature (4).

Ion-kinetic temperature (5, 24).

Positive-ion temperature (16).

| | |
|---|---|
| TID | Designation for Traveling Ionospheric Disturbance (3). |
| $T_{ion}$ | Ion-kinetic temperature (17). |
| $T_j$ | Effective temperature of species "j" (3). |
| $T_j'$ | Fluctuation of $T_j$ (3). |
| $\bar{T}_j$ | Mean value of $T_j$ (3). |
| $T_k$ | Kinetic temperature (4). |
| $T_{kin}$ | Kinetic temperature (11). |
| $T_M$ | Molecular-scale temperature (2). |
| TM | Indexing use only; normalization, in the method of Fleischmann, Dehmel, and Lee (15). |
| $T_n$ | Electron noise "temperature" (21). |
| TOF | Designation for Time-of-Flight (7). |
| $T_{pop}$ | Population temperature (4). |
| $T_r$ | Reference temperature (16, 19). |
| $T_{ref}$ | Reference temperature (24). |
| $T_{rot}$ | Rotational temperature (11). |
| $T_{tr}$ | Translational temperature (20). |
| $T_v$ | Vibrational temperature (4, 20, 24). |
| $T_{vib}$ | Vibrational temperature (11, 18A). |
| T-V | Designation for translational-vibrational energy transfer (11). |
| $T_+$ | Positive-ion temperature (16). |

$t$ Time (3, 5, 11, 15, 16, 19, 20, 21).

Indexing uses: threshold (6)
target species (15).

th Indexing use only; thermal (3).

$t_o$ Initial time of integration (21).

tot Indexing use only; total (4).

tr Indexing use only; translational (20).

$U_e$ Potential energy of bound electron (15).

UHF Designation for Ultra High Frequency (7).

UV Designation for Ultraviolet.

$u$ Speed (3).

$\equiv 2.855\ \theta/\lambda$ (11).

Relative velocity (15).

Radial component of relative velocity on collision, in the Firsov model (15).

Indexing uses: relative velocity (15).
energy exchange (21).

$\underset{\sim}{u}$ Velocity vector (3).

$\underset{\sim}{u}'$ Velocity vector for small perturbation or fluctuation (3).

$\underset{\sim}{\bar{u}}$ Mean velocity vector (3).

$\underset{\sim}{u}_a$ Velocity vector for species "a" (3).

$u_c$ Arbitrary reference velocity (3).

$u_i$ Directional components of velocity (3).

$\bar{u}_i$ Mean directional components of velocity (3).

$u_o$ Ionizational impact velocity, in the Firsov model (15).

uv Designation for ultraviolet.

$u_1$ Vertical component of diffusion velocity of atomic oxygen (3).

$u_2$ Vertical component of diffusion velocity of molecular oxygen (3).

V Volume (10).

$V_a(r_a)$ Potential centered on trajectory point (15).

$V_b(r_b)$ Potential centered on trajectory point (15).

VT Designation for vibrational-translational energy transfer (20).

V-T Designation for vibrational-translational energy transfer (11).

VV Designation for vibrational-vibrational energy transfer (20, 24).

V-V Designation for vibrational-vibrational energy transfer (11).

v Initial velocity (3).

Relative collisional velocity (6).

Vibrational level or quantum number (9, 11, 16, 20, 24).

Velocity (15, 21).

Indexing uses: constant volume (3).

vibrational (4, 11, 20, 24).

$\underset{\sim}{v}$ Velocity vector (15).

$\vec{v}$ Velocity vector (15).

v' Vibrational level in excited electronic state (11).

Vibrational level in unspecified electronic state (20).

| | |
|---|---|
| $v'v''$ | Indexing use only; electronic transition involving two states for which $v = v'$ and $v = v''$, respectively (11). |
| $v''$ | Vibrational level in ground electronic state (11). |
| | Vibrational level in unspecified electronic state (20). |
| $\bar{v}''$ | Mean number of vibrational quanta excited in ground electronic state through fluorescence (11). |
| $v_e$ | Velocity of bound electron on target atom (15). |
| $v'_e$ | Parameter defined in Equation 15-11 (15). |
| vib | Indexing use only; vibrational (4, 11, 18A). |
| $v_{max}$ | Maximum vibrational level (11). |
| vol | Indexing use only; volume (11). |
| $v_1$ | Velocity of incident ion (15). |
| $v'_1$ | Parameter defined in Equation 15-11 (15). |
| W | Designation for west (3). |
| | Designation for unspecified chemical species (6, 10). |
| WB | Designation in Figure 16-2, for work of Weller and Biondi, from Reference 16-24 (16). |
| W-K | Designation for Watson-Koontz system (9). |
| w | Electron drift velocity (21). |
| X | Designation for unspecified chemical species (6, 9, 10, 11, 14, 16, 17, 24). |
| | Indexing uses: chemical species (4, 8, 14).<br>functional (21). |
| [X] | Concentration of species "x" (11). |
| X' | Indexing use only; chemical species for product atom which may be in a bound excited state (8). |

XA — Indexing use only; electronic excitation (X → A) (20).

$[X(i)]$ — Number density of species "X" in the ith vibrational level (11).

$[X]_{col}$ — Column density of species "X" (11).

x — Wind direction (3).

Absorption pathlength (7).

Distance of primary or projectile species beam through target (15).

Distance (21).

Indexing uses: wind direction (3).
combining proportions (11).
ground-state (12).

$\bar{x}_j$ — Mean chemical reaction rate term, in Equation 3-68b (3).

$\underset{\sim}{\bar{x}}_j$ — Mean chemical reaction rate vector, in Equation 3-68c (3).

$x_o$ — $\equiv (b_1/a_o)(I/I_H)^{1/2} = \gamma b_1/a_o$ (15).

Y — Designation for unspecified chemical species (6, 9, 10, 11, 16, 17, 24).

y — Directional coordinate (3).

Normalized energy, in the Firsov model (15).

Indexing use: directional (3).

Z — Designation for unspecified chemical species (6, 10).

Altitude (9).

Number of collisions (11).

$Z_a$ — Nuclear charge on species "a", in the Firsov model (15).

$Z_b$ — Nuclear charge on species "b", in the Firsov model (15).

$Z_{ij}$ — Number of collisions per i → j transition (11).

$Z_p$ Number of charges on projectile species, in the method of Fleischmann, Dehmel, and Lee (15).

$Z_t$ Number of charges on target species, in the method of Fleischmann, Dehmel, and Lee (15).

$Z_1$ Number of charges on incident ion (15).

$Z_{10}$ Number of collisions required for translational-vibrational energy transfer (11).

$Z_{01}^{10}$ Number of collisions required for vibrational-vibrational energy transfer (11).

$z$ Altitude (2, 3, 13).

Indexing use: altitude (3, 13).

$z_o$ Reference altitude (3).

$z_1$ Reference altitude (2).

$\alpha$ Effective rate coefficient for three-body oxygen-atom recombination (3).

Molecular polarizability (8).

Total recombination rate coefficient (16).

Atomic polarizability (21)

Recombination parameter (21).

$\alpha_D$ Ion-electron recombination coefficient (9).

$\alpha_i^D$ Ion-electron dissociative recombination coefficient of molecular ion "i" (9).

$\alpha_d$ A numerical constant $\approx 1$ (3).

Ion-electron or dielectronic recombination coefficient (5, 8).

$\alpha_{eff}$ Effective recombination coefficient (9).

$\alpha_i$ Thermal diffusion coefficient of species "i" (2).

Ion-ion neutralization coefficient (9).

$\alpha^j$ Ion-ion recombination coefficient (9).

$\alpha(M^+)$ Recombination rate coefficient for $M^+$ (16).

$\alpha_{mn}$ Two-body mutual neutralization rate coefficient (16).

$\alpha_r$ Radiative recombination coefficient (8).

Radiative atomic-ion recombination coefficient (9).

$\alpha_v$ A numerical coefficient $\approx 1$ (3).

$\alpha_{2r}$ Two-body recombination coefficient (16).

$\alpha_{3e}$ Equivalent two-body rate coefficient for three-body electron-stabilized recombination (16).

$\beta$ Altitude-variant coefficient (5).

Electron attachment coefficient (9).

$\beta_1^j$ Non-isomeric molecular diffusivity term, in Equation 3-67c (3).

$\beta_2^j$ Non-isomeric turbulent diffusivity term, in Equation 3-67d (3).

$\vec{\Gamma}_e$ Electron vectorial current density (16).

$\gamma$ Ratio of specific heats (3).

Negative-ion chemical and collisional detachment coefficient (9).

$\equiv (I/I_H)^{1/2}$ (15).

$\Delta A$ Reaction work function (10).

$\Delta A_0^o$ Standard-state reaction work function at 0 K (10).

$\Delta a$, $\Delta b$, $\Delta c$ — Uncertainties in rate-constant function parameters a, b, and c, respectively (19).

$\Delta E$ — Excitation energy (4).

Reaction energy (10, 19).

Energy transferred on collision (15).

Indexing use: collisional-transfer energy (15).

$\Delta E_{if}$ — Radiant energy at intermediate frequency in the transitional energy range (20).

$\Delta E_0^\circ$ — Standard-state reaction energy at 0 K (10).

$\Delta F$ — Reaction free energy (10).

$\Delta F_0^\circ$ — Standard-state reaction free energy at 0 K (10).

$\Delta f_o$ — Resonant frequency shift (7).

$\Delta H$ — Reaction enthalpy (10, 17, 19).

$\Delta H_0^\circ$ — Standard-state reaction enthalpy at 0 K (10).

$\Delta K$ — Change in dielectric constant (21).

$\Delta K_i$ — Change in dielectric constant caused by ions (21).

$\Delta(pV)_0^\circ$ — Standard-state reaction work at 0 K (10).

$\Delta T$ — Temperature change in exosphere during magnetic storms (5).

$\Delta\lambda$ — Wavelength range (13).

Indexing use: wavelength range (13).

$\epsilon$ — Emission rate (11).

General normalized energy parameter, in the method of Fleischmann, Dehmel, and Lee (15).

$\epsilon$ (cont'd) Electron excitation energy, in the Firsov model (15).

Vibrational energy (20).

Electron energy (21).

Indexing use: electron energy (21).

$\bar{\epsilon}$ Mean electron energy (21).

$\epsilon_{ij}$ Energy loss cross-section for the jth state of species "i" (21).

$\epsilon_K$ Characteristic energy of electrons (21).

$\epsilon_o$ Ionization energy, in the Firsov model (15).

Dielectric constant of free space (21).

$\epsilon_\lambda$ Emission rate per unit wavelength range (11).

$\epsilon_\nu$ Molecular viscosity (3).

Emission rate per unit frequency range (11).

$\eta$ Fluorescence efficiency for electrons producing indicated radiation (9).

$\theta$ Angle between wind direction and north, or the axis of rotation of $\underset{\sim}{\Omega}$ (3).

Characteristic temperature (11).

Scattering angle (14).

$\theta_c$ Cone half-angle (7).

$\theta_v$ Characteristic vibrational temperature (20).

$\lambda$ Mixing length (3).

Wavelength (7, 11, 12, 13, 20).

$\equiv N^-/N$ (9).

Indexing uses: wavelength (11, 13).
light (12).

$\lambda_e$ Center wavelength of electronic transition (11).

$\lambda_o$ Wavelength at band origin (11).

$\lambda_\mu$ Wavelength of exciting irradiation (11).

$\mu$ Viscosity coefficient (3).

Reduced mass of collision (6).

Thermal mobility (21).

Indexing use: radiant medium (11).

$\mu_a$ Viscous coefficient of species "a" (3).

$\mu_{AB}$ Reduced mass of molecule AB (4).

$\mu_i$ Thermal mobility of ionic species (21).

$\nu$ Kinematic viscosity (3).

Frequency of light (6, 7, 17, 19, 20, 24).

Frequency of exciting irradiation (11).

Electron collision frequency (21).

Indexing uses: viscosity (3).
frequency (11).

$\nu'$ Vibrational quantum number for upper electronic state involved in transition (14).

$\nu''$ Vibrational quantum number for lower electronic state involved in transition (14).

$\nu_a$ Frequency of electron attachment collisions (21).

$\nu_{ei}(\epsilon)$ Frequency of electron-ion momentum-transfer collisions (21).

$\nu_f$ Frequency of fluorescing radiative output (11).

$\nu_i$ Collision frequency for ionic species (21).

$\nu_j$ Collision frequency for molecule in the jth vibrational level (21).

$\nu_m(\epsilon)$ Frequency of electron momentum-transfer collisions (21).

$\nu_o$ Wavenumber at band origin (11).

Energy-independent electron collision frequency (21).

$\nu_s$ Frequency of irradiating light in the solar continuum (11).

$\nu_{solar}$ Frequency of irradiating light in the solar continuum (11).

$\nu_u(\epsilon_K)$ Rate coefficient for electron energy exchange with gas, equal to electron energy exchange frequency in the dc electric-field case (21).

$\underset{\approx}{\pi}$ Total viscous stress tensor (3).

$\underset{\approx}{\pi}_a$ Viscous stress tensor of species "a" (3).

$\rho$ Density or total density (2, 5).

Mass density (3).

Negative-ion photodetachment rate (9).

Impact parameter (15).

$\rho'$ Mass density for small perturbation or fluctuation (3).

$\rho_a$ Mass density for species "a" (3).

$\rho_o$ Mass density for unperturbed background (3).

Density prior to magnetic storm (5).

$\sigma$ Reaction cross-section (6).

Absorption cross-section (7, 12).

Cross-section (14, 15, 18A).

$\sigma_E$ Monoenergetic cross-section (6).

$\sigma(E)_{i, i+1}$ Generalized cross-section for single electron loss, in the method of Fleischmann, Dehmel, and Lee (15).

$\sigma(E/E_1)_{TM}$ Normalized cross-section for single electron loss, in the method of Fleischmann, Dehmel, and Lee, and which equals $\sigma/\sigma_o$ of the Firsov model (15).

$\sigma^{eff}_{\Delta E}$ Effective cross-section for the transfer of energy $\Delta E$ (15).

$\sigma_i$ Photoionization cross-section (7).

Ionization cross-section (12).

Ionization cross-section for ions of positive charge state "i" (14).

$\sigma_{ij}$ Electron capture-and-loss cross-section (15).

$\sigma_{ij}(\epsilon)$ Excitation cross-section for the jth state of species "i" (21).

$\sigma(I, u)$ Cross-section for charge transfer at ionization potential "I" and relative velocity "u" (15).

$\sigma_{ix}$ Ion-product cross-section to the "X" state of the ion produced (12).

$\sigma_j(\Delta\lambda)$ Absorption cross-section of species "j" at wavelength range "$\Delta\lambda$" (13).

$\sigma'_j(\lambda)$ Ionization cross-section of species "j" at wavelength "$\lambda$" (13).

$\sigma_m$ Momentum-transfer cross-section (11).

$\sigma_N$ Neutral product cross-section (12).

$\sigma_{n\ell}(v)$ Cross-section for photoabsorption of initial state "$n\ell$" (11).

$\sigma_o$ A constant for atomic species (11).

Ionization cross-section on impact, in the Firsov model (15).

$\sigma_T(X)$ Total ionization cross-section for species "X" (14).

$\sigma_T(\lambda)$ Total absorption cross-section (12).

$\sigma_0$ Absorption cross-section for $O_2$ at zero atmosphere pressure, by extrapolation (Herzberg continuum) (12).

$\sigma_{01}$ $\approx \sum_j \sigma_{0j}$ at low energies (15).

$\sigma_{0j}$ Electron stripping cross-section from neutrals (15).

$\sigma_1$ Absorption cross-section for $O_2$ at one atmosphere pressure (Herzberg continuum) (12).

$\sigma_{1m}$ Cross-section for stripping "m" electrons in $N^+$ upon $N_2$ impact (15).

$\sigma_{10}$ $Q_{10}^{01}$ in the low-energy limit (15).

$\tau$ Time for onset of turbulent dispersion (3).

Recovery time (9).

Relaxation time, or the e-folding time of $\epsilon$ (20).

$\tau_c$ Effective lifetime for collisional deexcitation (20).

$\tau_j(\Delta\lambda)$ Optical depth in wavelength range "$\Delta\lambda$" for species "j" (13).

$\tau_o$ Collision-free radiative lifetime of excited species (20).

$\tau(\Delta\lambda)$ Optical depth in wavelength range "$\Delta\lambda$" (13).

$\Phi$ Rayleigh dissipation function (3).

$\Phi_z(\Delta\lambda)$ Local photon flux in the wavelength range "$\Delta\lambda$" at altitude "z" (13).

$\Phi_\infty(\Delta\lambda)$ Photon flux in the wavelength range "$\Delta\lambda$" at the top of the atmosphere (13).

$\phi$ Latitude (2, 3).

$\phi_i(\underset{\sim}{r}_a)$ Bound-state wavefunction for the charge state "i" at a trajectory point (15).

$\phi_i(\underset{\sim}{r}_a, \underset{\sim}{r})$ Wavefunction defined in Equation 15-18 (15).

$\phi_j(\underset{\sim}{r}_b)$ Bound-state wavefunction for the charge state "j" at a trajectory point (15).

$\phi_j(\underset{\sim}{r}_b, \underset{\sim}{r})$ Wavefunction defined in Equation 15-19 (15).

$\psi$ Total wavefunction (15).

$\Omega$ $\equiv \omega$ or $\omega \pm \omega_{be}$ or $\omega \pm \omega_{bi}$ (21).

$\underset{\sim}{\Omega}$ Angular velocity of earth's rotation (3).

$\omega$ Frequency (3).

Frequency of alternating electric field (7).

Angular frequency of applied electric field (21).

$\omega_a$ $\equiv c_o/2H$ (3).

$\omega_{be}$ Cyclotron frequency for electrons in a magnetic field (21).

$\omega_{bi}$ Cyclotron frequency for ions in a magnetic field (21).

$\omega_c$ Angular or cyclotron frequency of orbital motion (7).

$\omega_e$ Vibrational constant (4, 11).

$\omega_e x_e$ First anharmonic correction term (11).

$\omega_{pe}$ Plasma resonance frequency for electrons (21).

$\omega_s$ Wind shear (3).

Numbers used os indices:

0 Reference condition (3).

Temperature of 0 K (10, 19).

Zero atmosphere pressure (12).

Initial charge on neutral target species (15).

Zero time (16).

Functional (21).

| | |
|---|---|
| 01 | Excitation (11). |
| 1 | Reference condition (2). |
| | Atomic oxygen (3). |
| | Molecular (3). |
| | Vibrational level (10). |
| | One atmosphere pressure (12). |
| | Incident particles before collision (15). |
| | Cut-off (15). |
| | Stripping, in collision of $N^+$ on $N_2$ (15). |
| 10 | Deexcitation (11). |
| | Deactivation of first vibrational level (20). |
| 2 | Molecular oxygen (3). |
| | Turbulent (3). |
| | Vibrational level (10). |
| | Incident particles after collision (15). |
| | Number of electrons stripped, in collision of $N^+$ on $N_2$ (15). |
| | Two-body process (16). |
| | Functional (21). |
| 3 | Vibrational level (10). |
| | Number of electrons stripped, in collision of $N^+$ on $N_2$ (15). |
| | Three-body process (16). |
| 4 | Number of electrons stripped, in collision of $N^+$ on $N_2$ (15). |
| 300 | Temperature of 300 K (24). |

$\infty$ Top of atmosphere (13).

End of trajectory (15).

Designation of long time after ionizing source is turned on (16).

Miscellaneous symbols used as indices (where "X" is taken as an ananymous symbol modified by each index):

$X'$ Fluctuation or perturbation (3).

Miscellaneous (3).

Reverse (6).

Bound excited state (8).

Collisional (11).

Excited electronic state (11).

Ionization (13).

Secondary of a type (14).

Upper electronic state (14).

For special parameter (15).

Unspecified electronic state (20).

$X''$ Ground electronic state (11).

Lower electronic state (14).

Unspecified electronic state (20).

$\underset{\sim}{X}$ Vector (3, 15).

$\underset{\approx}{X}$ Tensor (3).

$\vec{X}$ Vector (15, 16).

$\overline{X}$ Mean (3, 11, 21).

$\langle X \rangle$ Space-averaged (16, 21).

$\{X\}$ Variation (3, 16).

| | |
|---|---|
| $[X]$ | Number density or concentration (3, 9, 10, 11). |
| $\|X\|$ | Absolute value (3, 15, 21). |
| $X^+$ | Positive-ion (9). |
| $X_+$ | Positive-charge (15).<br>Positive-ion (16). |
| $X^-$ | Negative-ion (9). |
| $X_-$ | Electron (15).<br>Negative-ion (16). |

# APPENDIX B
# CONSTANTS

| | |
|---|---|
| Atomic mass unit | $1.660 \times 10^{-24}$ g |
| Avogadro number | $6.0225 \times 10^{23}$ molecules $mole^{-1}$ |
| Base of natural logarithms | 2.7183 (Ln X = 2.3026 Log X) |
| Boltzmann constant | $1.3805 \times 10^{-16}$ erg $K^{-1}$ |
| Density of air at sea level | $1.293 \times 10^{-3}$ g $cm^{-3}$ |
| Electronic charge | $1.6021 \times 10^{-19}$ coul |
| | $4.803 \times 10^{-10}$ esu |
| Electronic mass | $9.109 \times 10^{-28}$ g |
| Fine structure constant | $7.30 \times 10^{-3}$ |
| Gas constant | 1.987 cal $mole^{-1}$ $K^{-1}$ |
| | $6.95 \times 10^{-1}$ $cm^{-1}$ $molecule^{-1}$ $K^{-1}$ |
| | 82.05 $cm^3$ atm $mole^{-1}$ $K^{-1}$ |
| | $8.61 \times 10^{-5}$ eV $molecule^{-1}$ $K^{-1}$ |
| | $8.3144 \times 10^{7}$ erg $mole^{-1}$ $K^{-1}$ |
| | $1.38 \times 10^{-16}$ erg $molecule^{-1}$ $K^{-1}$ |



Preceding page blank

| | |
|---|---|
| Gas constant (cont'd) | $1\ K^{-1}$ |
| | $1.987 \times 10^{-3}$ kcal mole$^{-1}$ K$^{-1}$ |
| | $8.205 \times 10^{-2}$ liter atm mole$^{-1}$ K$^{-1}$ |
| Gravitational acceleration | 980.665 cm sec$^{-2}$ |
| Loschmidt number | $2.69 \times 10^{19}$ molecules cm$^{-3}$ |
| Planck constant | $6.6256 \times 10^{-27}$ erg sec |
| Rydberg constant | $1.097 \times 10^{5}$ cm$^{-1}$ |
| Velocity of light in vacuum | $2.99793 \times 10^{10}$ cm sec$^{-1}$ |
| Velocity of sound in air at STP | 331.7 m sec$^{-1}$ |

# APPENDIX C
# CONVERSION FACTORS

## ALTITUDE

| | km | kft | statute miles | nautical miles |
|---|---|---|---|---|
| 1 kilometer | 1 | 3.281 | 0.6214 | 0.5396 |
| 1 kilofaot | 0.3048 | 1 | 0.1894 | 0.1645 |
| 1 statute mile | 1.609 | 5.280 | 1 | 0.8690 |
| 1 nautical mile | 1.853 | 6.080 | 1.1516 | 1 |

## ANGLE

| | minutes | degrees | radians | revalutians |
|---|---|---|---|---|
| 1 secand | $1.667 \times 10^{-2}$ | $2.778 \times 10^{-4}$ | $4.848 \times 10^{-6}$ | $7.72 \times 10^{-8}$ |
| 1 minute | 1 | $1.667 \times 10^{-2}$ | $2.909 \times 10^{-4}$ | $4.63 \times 10^{-6}$ |
| 1 degree | 60 | 1 | $1.745 \times 10^{-2}$ | $2.7 \times 10^{-3}$ |
| 1 radian | $3.44 \times 10^{3}$ | 57.30 | 1 | 0.1592 |
| 1 revalutian | $2.16 \times 10^{5}$ | 360 | 6.283 | 1 |

## CONCENTRATION

| | atm | moles liter$^{-1}$ | molecules cm$^{-3}$ | ppm | torr |
|---|---|---|---|---|---|
| 1 atmasphere | 1 | $0.122\ T^{-1}$ | $7.34 \times 10^{21}\ T^{-1}$ | $1 \times 10^{6}$ | 760 |
| 1 mole liter$^{-1}$ | $8.21\ T$ | 1 | $6.02 \times 10^{20}$ | $8.21 \times 10^{6}\ T$ | $6.24 \times 10^{3}\ T$ |
| 1 molecule cm$^{-3}$ | $1.36 \times 10^{-22}\ T$ | $1.66 \times 10^{-21}$ | 1 | $1.36 \times 10^{-16}\ T$ | $1.04 \times 10^{-19}\ T$ |
| 1 ppm | $1 \times 10^{-6}$ | $1.22 \times 10^{-7}\ T^{-1}$ | $7.33 \times 10^{15}\ T^{-1}$ | 1 | $7.6 \times 10^{-4}$ |
| 1 torr | $1.32 \times 10^{-3}$ | $1.61 \times 10^{-4}\ T^{-1}$ | $9.64 \times 10^{18}\ T^{-1}$ | $1.32 \times 10^{3}$ | 1 |

1 otmosphere (0 C) = $2.69 \times 10^{19}$ molecules cm$^{-3}$
(25 C) = $2.45 \times 10^{19}$ molecules cm$^{-3}$

1 torr (0 C) = $3.53 \times 10^{16}$ molecules cm$^{-3}$
(25 C) = $3.24 \times 10^{16}$ molecules cm$^{-3}$

1 ppm (0 C) = $2.69 \times 10^{13}$ molecules cm$^{-3}$
(25 C) = $2.45 \times 10^{13}$ molecules cm$^{-3}$

## CROSS-SECTION

$1\ cm^2 = 10^{24}$ barns $= 10^{18}$ megobarns

$1\ cm^2 = 3.54 \times 10^{16}\ cm^{-1}$ (at 1 torr, 0 C)

$o_o^2 = 2.80 \times 10^{-17}\ cm^2$

$\pi o_o^2 = 8.80 \times 10^{-17}\ cm^2$

ENERGY

| | eV [a] | ergs [a] | $cm^{-1}$ [a] | kcal $mole^{-1}$ [a] | Corresponding [b] Temperature (K) |
|---|---|---|---|---|---|
| 1 eV | 1 | $1.602 \times 10^{-12}$ | 8067.5 | 23.069 | 11,605. |
| 1 erg | $6.24 \times 10^{11}$ | 1 | $5.03 \times 10^{15}$ | $1.44 \times 10^{13}$ | $7.24 \times 10^{15}$ |
| 1 joule | $6.24 \times 10^{18}$ | $1 \times 10^{7}$ | $5.03 \times 10^{22}$ | $1.44 \times 10^{20}$ | |
| 1 jerk | $6.24 \times 10^{27}$ | $1 \times 10^{16}$ | $5.03 \times 10^{31}$ | $1.44 \times 10^{29}$ | |
| 1 $cm^{-1}$ (= 1 kayser) | $1.24 \times 10^{-4}$ | $1.99 \times 10^{-16}$ | 1 | $2.86 \times 10^{-3}$ | 1.44 |
| 1 kcal $mole^{-1}$ | $4.335 \times 10^{-2}$ | $6.95 \times 10^{-14}$ | 350. | 1 | 503. |
| 1 Rydberg | 13.605 | $2.18 \times 10^{-11}$ | $1.098 \times 10^{5}$ | 314. | $1.58 \times 10^{5}$ |
| 1 ton TNT | $2.6 \times 10^{28}$ | $4.2 \times 10^{16}$ | $2.1 \times 10^{32}$ | $6.0 \times 10^{29}$ | |
| 1 liter atm (0 C) | | $1.01 \times 10^{9}$ | | | |
| 1 watt sec | | $1 \times 10^{7}$ | | | |
| 1 Hartree | 27.210 | | | | |

Notes:

[a] In comparing eV, ergs, etc., with kcal $mole^{-1}$, the energy units must be regarded as being per molecule, i.e., as eV per molecule, erg per molecule, etc.

[b] This is the temperature which a gas would have if its molecules had an average translational energy per molecule of one unit, e.g., one eV, one erg, etc.

LENGTH (see also Altitude, Wavelength)

| | cm | meters | inches | feet |
|---|---|---|---|---|
| 1 A | $10^{-8}$ | $10^{-10}$ | $3.937 \times 10^{-9}$ | $3.281 \times 10^{-10}$ |
| 1 $\mu$m | $10^{-4}$ | $10^{-6}$ | $3.937 \times 10^{-5}$ | $3.281 \times 10^{-6}$ |
| 1 cm | 1 | $10^{-2}$ | 0.3937 | $3.281 \times 10^{-2}$ |
| 1 meter | 100 | 1 | 39.37 | 3.281 |
| 1 inch | 2.540 | $2.54 \times 10^{-2}$ | 1 | $8.33 \times 10^{-2}$ |
| 1 foot | 30.48 | 0.3048 | 12.0 | 1 |
| 1 astronomical unit = $1.495 \times 10^{11}$ miles | | | | |
| 1 Bohr unit = $5.2917 \times 10^{-1}$ A | | | | |

MASS

| | grams | ounces | pounds | tons |
|---|---|---|---|---|
| 1 gram | 1 | $3.53 \times 10^{-2}$ | $2.205 \times 10^{-3}$ | $1.10 \times 10^{-6}$ |
| 1 ounce | 28.35 | 1 | $6.25 \times 10^{-2}$ | $3.12 \times 10^{-5}$ |
| 1 pound | 453.6 | 16.0 | 1 | $5.0 \times 10^{-4}$ |
| 1 ton | $9.07 \times 10^{5}$ | $3.2 \times 10^{4}$ | $2.0 \times 10^{3}$ | 1 |

## PRESSURE

| | otm | bar | psi | torr |
|---|---|---|---|---|
| 1 atmosphere | 1 | 1.0133 | 14.70 | 760 |
| 1 bor | 0.9869 | 1 | 14.51 | 750 |
| 1 dyne $cm^{-2}$ | $9.87 \times 10^{-7}$ | $1 \times 10^{-6}$ | $1.45 \times 10^{-5}$ | $7.50 \times 10^{-4}$ |
| 1 inch Hg | $3.34 \times 10^{-2}$ | $3.38 \times 10^{-2}$ | 0.491 | 25.4 |
| 1 psi | $6.804 \times 10^{-2}$ | $6.91 \times 10^{-2}$ | 1 | 51.72 |
| 1 torr = 1 mmHg | $1.316 \times 10^{-3}$ | $1.33 \times 10^{-3}$ | $1.93 \times 10^{-2}$ | 1 |

## RADIANT FLUX

1 Rayleigh = $10^6$ photons $cm^{-2}$ $sec^{-1}$

## REACTION-RATE CONSTANTS

Bimoleculor:

k ($cm^3$ $malecule^{-1}$ $sec^{-1}$) x $6.02 \times 10^{20}$ = k (liter $male^{-1}$ $sec^{-1}$)

k (liter $mole^{-1}$ $sec^{-1}$) x $1.66 \times 10^{-21}$ = k ($cm^3$ $molecule^{-1}$ $sec^{-1}$)

k ($ppm^{-1}$ $min^{-1}$) x $2.27 \times 10^{-18}$ T = k ($cm^3$ $molecule^{-1}$ $sec^{-1}$)

k ($ppm^{-1}$ $sec^{-1}$) x $1.36 \times 10^{-16}$ T = k ($cm^3$ $molecule^{-1}$ $sec^{-1}$)

k ($ppm^{-1}$ $sec^{-1}$) x $4.05 \times 10^{-14}$ = k ($cm^3$ $molecule^{-1}$ $sec^{-1}$) at 25 C

k ($torr^{-1}$ $sec^{-1}$) x $1.04 \times 10^{-19}$ T = k ($cm^3$ $molecule^{-1}$ $sec^{-1}$)

k ($torr^{-1}$ $sec^{-1}$) x $2.84 \times 10^{-17}$ = k ($cm^3$ $molecule^{-1}$ $sec^{-1}$) at 0 C

k ($tarr^{-1}$ $sec^{-1}$) x $3.10 \times 10^{-17}$ = k ($cm^3$ $molecule^{-1}$ $sec^{-1}$) at 25 C

REACTION-RATE CONSTANTS (Cont'd.)

Termolecular:

$$k\ (cm^6\ molecule^{-2}\ sec^{-1}) \times 3.62 \times 10^{41} = k\ (liter^2\ mole^{-2}\ sec^{-1})$$

$$k\ (liter^2\ mole^{-2}\ sec^{-1}) \times 2.76 \times 10^{-42} = k\ (cm^6\ molecule^{-2}\ sec^{-1})$$

$$k\ (ppm^{-2}\ min^{-1}) \times 5.15 \times 10^{-36} T^2 = k\ (cm^6\ molecule^{-2}\ sec^{-1})$$

$$k\ (ppm^{-2}\ sec^{-1}) \times 1.85 \times 10^{-32} T^2 = k\ (cm^6\ molecule^{-2}\ sec^{-1})$$

$$k\ (ppm^{-2}\ sec^{-1}) \times 1.64 \times 10^{-27} = k\ (cm^6\ molecule^{-2}\ sec^{-1})\ at\ 25\,C$$

$$k\ (torr^{-2}\ sec^{-1}) \times 1.08 \times 10^{-38} T^2 = k\ (cm^6\ molecule^{-2}\ sec^{-1})$$

$$k\ (torr^{-2}\ sec^{-1}) \times 8.05 \times 10^{-34} = k\ (cm^6\ molecule^{-2}\ sec^{-1})\ at\ 0\,C$$

$$k\ (torr^{-2}\ sec^{-1}) \times 9.59 \times 10^{-34} = k\ (cm^6\ molecule^{-2}\ sec^{-1})\ at\ 25\,C$$

TEMPERATURE

$$T\,(C) = T\,(K) - 273.16$$
$$T\,(C) = [T\,(F) - 32]/1.8$$
$$T\,(C) = [T\,(R) - 491.7]/1.8$$

$$T\,(F) = 1.8\ T\,(C) + 32$$
$$T\,(F) = 1.8\ T\,(K) - 459.7$$
$$T\,(F) = T\,(R) - 459.7$$

$$T\,(K) = T\,(C) + 273.16$$
$$T\,(K) = [T\,(F) - 32]/1.8 + 273.16$$
$$T\,(K) = [T\,(R) - 491.7]/1.8 + 273.16$$

$$T\,(R) = 1.8\ T\,(C) + 491.7$$
$$T\,(R) = T\,(F) + 459.7$$
$$T\,(R) = 1.8\ [T\,(K) - 273.16] + 491.7$$

$$1\ C = 1\ K = 1.8\ F = 1.8\ R$$

## TIME

| | secs | mins | hrs | days |
|---|---|---|---|---|
| 1 shake | $1 \times 10^{-8}$ | | | |
| 1 second | 1 | $1.667 \times 10^{-2}$ | $2.77 \times 10^{-4}$ | $1.16 \times 10^{-5}$ |
| 1 minute | 60 | 1 | $1.667 \times 10^{-2}$ | $6.94 \times 10^{-4}$ |
| 1 hour | 3600 | 60 | 1 | $4.167 \times 10^{-2}$ |
| 1 day | $8.64 \times 10^{4}$ | $1.44 \times 10^{3}$ | 24 | 1 |

## VELOCITY

1 cm $sec^{-1}$ = $2.237 \times 10^{-2}$ mi $hr^{-1}$

1 ft $sec^{-1}$ = 30.48 cm $sec^{-1}$

1 ft $sec^{-1}$ = 0.6818 mi $hr^{-1}$

1 knot = 1 nautical mi $hr^{-1}$

1 knot = 51.5 cm $sec^{-1}$

1 knot = 1.689 ft $sec^{-1}$

1 mi $hr^{-1}$ = 44.70 cm $sec^{-1}$

1 mi $hr^{-1}$ = 1.467 ft $sec^{-1}$

VOLUME

| | $cm^3$ | $ft^3$ | $in^3$ |
|---|---|---|---|
| 1 $cm^3$ | 1 | $3.531 \times 10^{-5}$ | $6.102 \times 10^{-2}$ |
| 1 $ft^3$ | $2.832 \times 10^{4}$ | 1 | $1.728 \times 10^{3}$ |
| 1 $in^3$ | 16.39 | $5.787 \times 10^{-4}$ | 1 |
| 1 gallon | $3.785 \times 10^{3}$ | 0.1337 | 231 |
| 1 liter | 1000 | $3.531 \times 10^{-2}$ | 61.02 |

WAVELENGTH

| | A | cm | μm | nm |
|---|---|---|---|---|
| 1 A | 1 | $10^{-8}$ | $10^{-4}$ | $10^{-1}$ |
| 1 cm | $10^{8}$ | 1 | $10^{4}$ | $10^{7}$ |
| 1 μm | $10^{4}$ | $10^{-4}$ | 1 | $10^{3}$ |
| 1 nm | $10^{1}$ | $10^{-7}$ | $10^{-3}$ | 1 |

WAVELENGTH - ENERGY

$\lambda(A) \times E\ (eV) = 12{,}400.$

$\lambda\ (A) \times E\ (erg\ photon^{-1}) = 2 \times 10^{-8}$

# APPENDIX D
# GLOSSARY

Absorption Coefficient - The absorption coefficient, $k_\nu$ of a gas is defined by:

$$I_\nu = I_{o\nu} e^{-k_\nu x}, \quad \text{of frequency } \nu$$

where $I_{o\nu}$ is the intensity of the parallel light of frequency $\nu$ incident on the absorbing layer, $x$ is the thickness of the layer, and $I_\nu$ is the intensity of the transmitted light; both $I_{o\nu}$ and $I_\nu$, are in general functions of $\nu$, the frequency. The usual units of $k_\nu$ are $cm^{-1}$, although the concentration, n, is frequently eliminated by reporting a cross section; $k_\nu = \sigma_\nu n$.

Accuracy - The accuracy of a measurement refers to the probable departure from an absolute standard for that measurement; it may differ from the precision because of systematic errors inherent in the method.

Activation Energy - When rate coefficients for chemical reactions are correlated as a function of temperature by the relation:

$$k(T) = AT^b e^{-E/RT}$$

E is the empirical term called the activation energy; its value may be close to the more fundamental threshold energy for elementary chemical reactions.

Aeronomy - The science of the upper region of the atmosphere.

Airglow - Luminosity of the upper regions of the atmosphere. This includes dayglow, twilightglow and nightglow.

Ambipolar Diffusion - The high diffusion coefficient of electrons tends to create a charge separation when electrons diffuse more rapidly than ions toward regions of lower concentration. Electric forces created by the deviation from local charge equality tend to restore the balance by retarding the electrons and accelerating the positive ions. Both species of charged particles therefore diffuse with the same velocity without regard to sign, and therefore such diffusion is called ambipolar.

Association - The general term used to describe processes in which groups of atoms or molecules, charged or neutral, react to form molecules which are aggregates of the colliding bodies. Such processes can be two body but are generally stabilized by a third body.

Attachment - The process by which an electron is captured by a neutral atom or molecule to form a stable negative ion.

Aurora (aurora polaris) - rapidly varying displays of luminosity at high altitudes in the polar regions.

Auroral Regions - Regions between geomagnetic latitudes of 60° and the poles.

Auroral Zone - Regions within the auroral regions where auroras occur most often.

AZA - Auroral Zone Absorption events are associated with aurora particles and geomagnetic disturbances. The AZA is caused by bombardment of the upper atmosphere by charged particles (mainly electrons) guided into auroral latitudes by the earth's magnetic field.

Band Radiation - When observing molecular gases in absorption or emission under low dispersion, the spectra consist of more or less broad wavelength regions called bands, which are associated with many rotational transitions within a fixed electronic and vibrational transition.

Beam - a stream of well collimated particles usually at energies well above thermal and usually with a narrow range of energy distribution.

Biomolecular - This term indicates that the elementary reaction referred to occurs as the result of a two body collision. (compare second order)

Black Body Radiation - Idealized radiation which may be approached by the radiation emitted or absorbed by a small hole in a cavity wall. The energy density of such radiation is given by the Planck Law:

$$E(\nu)\, d\nu = \frac{8\pi h\nu^3}{c^3} \qquad \frac{d\nu}{(e^{h\nu/kT} - 1)}$$

The radiation is continuum and its intensity and the wavelength of its peak are a function of temperature.

Boltzmann Distribution - The Maxwell Boltzmann distribution may take on many equivalent forms. Perhaps the most popular expression of this distribution is the following: The number of molecules which have velocities with magnitudes within dv of v is given by:

$$n(v)\, dv = 4\pi N \left(\frac{m}{2\pi kT}\right)^{3/2} e^{-mv^2/2kT} v^2 dv$$

Bond Strength (energy) - The energy ($\Delta H$) required to form or break a bond between two atoms in a molecule is called the bond energy. In most cases, it is possible to express the heat of formation of a molecule as an additive property of the bonds forming the molecule, although the bond energy for a given type of bond will depend upon its chemical environment in the molecule in general.

Center of Mass Coordinates - Collision calculations in kinetic theory may be performed with considerable conceptual and mathematical simplification in the center of mass coordinate system. If $\vec{v}_1$ and $\vec{v}_2$ are the absolute velocities of particles 1 and 2 the following transformation may be made from the laboratory coordinate system of $\vec{v}_1$ and $\vec{v}_2$ to the center of mass coordinate system G and g:

$$\vec{G} = \frac{m_1 \vec{v}_1}{m_1 + m_2} + \frac{m_2 \vec{v}_2}{m_1 + m_2}$$

$$\vec{g} = \vec{v}_1 - \vec{v}_2$$

Since the Jacobian of the transformation is unity,

$$d\vec{G}\, d\vec{g} = d\vec{v}_1\, d\vec{v}_2$$

The three dimensional problem describing a spherical symmetrical two body collision can thereby be reduced to the equivalent one dimensional problem of describing the motion of one body in an effective potential field.

Center of mass collision energy - For chemical kinetics calculations, the relevant energy of a collision is the relative kinetic energy, $1/2\ \mu g^2$, where $\mu$ is the reduced mass of the two body collision and g is the magnitude of the relative velocity defined above. For a gas whose molecules have a Boltzmann distribution of peculiar velocity defined above. For a gas whose molecules have a Boltzmann distribution of peculiar velocities, the center of mass collision energy is distributed as:

$$P(K)\, dK = Ke^{-K}\, dK$$

where P(K) is the probability that a collision will have an energy within d K of K, and K is $1/2\ \mu g^2/kT$.

Charge Exchange - Usually used to mean charge transfer; sometimes used to mean either charge transfer or charged rearrangement.

Charge Transfer - a resction between two particles (usually sn ion and a neutral) in which an electron is transferred.

Charged Resrrangement - In this process, both electrons and atoms or groups of atoms are transferred and new species thereby createsd. In chapter 13 the term ion-molecule reaction is used for this.

Chemical Kinstics - Tho study of the rates and mechanisms at which chemical systems react.

Chromosphere - The region above the visible part of the sun in which much cnsrgy is absorbed.

Collision - Two-body - An encounter hetwesn two molecules is at best ill defined hecausc long rsngs forces are alwsys extsnt, although small. For conceptual purposes, comparisons may be made to the hard sphere model of kinetic theory, in which the two body collision frequency may be calculated to be: $Z = \bar{v}\ \sigma$, whsre $\bar{v}$ is tho average velocity and $\sigma$ is the cross section ($\pi R^2$) of the hard sphere.

Collision - Three-body - An simultaneous encounter between thres molecules is less well defined than the two body collision. However, using the model of a third body colliding witb the collision complex of two body collisions, a rate for three body collisions may be determined. Such a model is extremely sensitive to the choice of cross section.

Collision Frequency - This quantity is only well defined in the hard sphere model of kinetic theory in which the collision frequency, Z, is given by $Z = \bar{v}\ \sigma$, where $\bar{v}$ is the averaga velocity and $\sigma$ is the cross section, $\pi R^2$.

Collision Partner - A particle which takes part in a collisional reaction, but does not change chemically, its role being only a source of or sink for energy.

Concentration - The amount of species i per unit volume is called the concentration; most commonly in gas phase kinetics concentrations are expressed in units of molecules per c.

Continuum Radiation - Radiation emitted from or to an unquantitized (continuum) state is not discrete and is therefore called continuum radiation.

Cross Section - An effective area of a particle in a collision. A cross section for a specific process has the affect of including the probability that this process will occur during the collision.

D-Layer - The location of a peak or ledge in the electron density profile at about 75-80 km in the D-region (50-90 km).

Debris - See weapon debris.

Debye Length The characteristic length from a charged test particle beyond which other charged particles have a negligible effect on the trajectory of the test particle is called the Debye Length,

$$h = \left( \frac{e_o k T}{N_o e^2} \right)^{1/2}$$

where $e_o$ is the permittivity of free space.

Deexcitation - A process by which an excited species loses its excitation energy, such as radiation, quenching, energy transfer or chemical reaction.

Deionization - This term is applied to all processes which tend to decrease the ion and electron concentrations.

Density - The mass per unit volume is the density, $\rho$, with $\rho(r, t) = \sum_i n_i m_i$ where $n_i$ and $m_i$ are the number density and mass respectively of species i.

Detachment - The process by which an electron is released from a stable negative ion is called detachment.

Diffusion - The transport of species A relative to species B (or a bulk gas mixture) occurs as a result of a concentration gradient and is called ordinary diffusion, which is well described by Fick's first and second laws. This must be distinguished from pressure diffusion, thermal diffusion, and forced diffusion which are usually second order effects.

Diffusion Velocity - The diffusion velocity of chemical species j is the rate of flow of molecules j with respect to the mass average velocity of the bulk gas;

$$\vec{v}_j (\vec{r}, t) - \vec{v}_j \quad \vec{v}_o$$

Dissociation - The cleavage of a bond or bonds of a molecular species to produce smaller molecules or atoms is called dissociation.

Dissociation Energy - The energy required to dissociate a molecule in the zeroth vibrational and rotational states of an electronic state to a continuum state with zero relative translational energy is the dissociation energy.

Disturbed atmosphere - The atmosphere after the occurrence of a nuclear burst.

E - Layer - The location of a peak or ledge in the electron density profile at about 110 - 115 km in the E - region (90 - 160 km).

Elastic Collision - In an elastic collision, translational energy and momentum are conserved, and only translational energy is transferred.

Electron Affinity - The electron affinity of a molecule is the difference in the energies of the neutral molecule and its molecular ion when both species are in their lowest vibrational, rotational, nuclear, and electronic states. The definition (and the measurement) for an atom is not complicated by the vibrational and rotational problem.

Electron Density - In atmospheric chemistry problems, this term refers to the number of electrons per cc.

Electron Temperature - Because the electron energy distribution is highly sensitive to applied fields, the translational temperature of the electron population, defined by:

$$3/2\, k T_e = 1/2\, m_e \overline{v_e^2}$$

may be greatly different than the kinetic temperature, and must therefore sometimes be defined separately.

Electronic State - The solution to the wave equation is the wave function, which may be factored to an excellent approximation into electronic, vibrational, rotational, etc. parts. The electronic portion describes the orbital motion of the electrons and the different solutions represent different electronic states.

Electronic Temperature - After a strong perturbation, electronically excited species, especially of metastables, are deactivated slowly; therefore, the population will be higher than at equilibrium. The temperature calculated from a Boltzman distribution,

$$N_2/N_1 = g_2/g_1\ e^{-(E_2 - E_1)/kT}$$

will therefore yield a higher temperature.

Endothermic A physicochemical change is classified as endothermic if it is accompanied by the absorption of heat.

Energy Distribution - The energy distribution of an ensemble is described by a distribution function which predicts the number of particles with energies $E \pm dE$ per unit volume.

Equilibrium Constant - The product of the equilibrium concentrations of the products of a reaction divided by the product of the equilibrium concentrations of the reactants. It can be shown that this is also the ratio of the forward to reverse reaction rate constants, provided the products and reactants are in the same specified quantum states in both directions.

Escape Velocity - The velocity which is required by a body to escape from the earth's gravitational field.

Excitation - The process by which a molecule or atom is elevated to a quantum state other than the ground state.

Excited State - The general term which refers to quantum states other than ground. At equilibrium, there is a distribution of such states; even in the normal atmosphere, however, nonequilibrium sources exist such that larger concentrations of excited states are possible.

Exothermic - A physicochemical change is classified as exothermic if it is accompanied by the evolution of heat.

Exosphere - The outer regions of the earth's atmosphere from which atoms, if properly directed from their last collision and having sufficient energy to overcome gravity, escape to the interplanetary region.

$F_1$ Layer - The location of a peak or ledge in the electron density profile at about 180 km in the $F_1$ region (140 - 200 km).

$F_2$ Layer - The location of a peak in the electron density profile at about 300 km in the $F_2$ region (200 km and above).

Fireball - The luminous region of hot gases produced by a nuclear explosion. The term fireball may also be used to refer to the material initially heated to incandescence that has subsequently cooled. After the initial deposition of X-ray energy the fireball grows by radiation transport (radiative fireball). Eventually (after a few milliseconds at sea level and a few seconds at D-region altitudes) hydrodynamics becomes the dominant mechanism causing fireball growth.

Fission Yield - The energy released by fission processes following a nuclear explosion. This, plus the energy released by fusion processes, constitutes the total energy released by the weapon.

Geometric Altitude - The usual measured altitude.

Geopotential Altitude - An altitude scale which allows for the variation of gravity with height defined by

$$H = 1/G \int_0^Z g \, d z$$

where g is the acceleration due to gravity and G is a constant numerically equal to g at sea level. H can be shown to be given numerically by $Z R/(R + Z)$ where R is the earth radius.

Ground State - The lowest stable quantum state possible for a given molecule or atom. This term is most widely applied to the electronic structure since many molecules may have substantial populations in nonzero vibrational and rotational levels at equilibrium.

Heterosphere - The region of the atmosphere, above about 90 km, in which the relative concentrations of the major species changes as does the mean molecular weight.

Homosphere - The region of the atmosphere, below about 90 km, in which the relative concentrations of the major species remains nearly constant as does the mean molecular weight.

Impact Parameter - In a molecular encounter, the impact parameter is the distance of closest approach in the absence of a potential.

Impurity - An undesirable contaminant. In considering the earth's atmosphere, the term is often applied to any species involving elements other than nitrogen and oxygen.

Inelastic Collision - A collision in which translational energy and momentum are not conserved, but may be converted to internal energy and motion of one or more of the collision partners

Infrared Radiation - That portion of the electromagnetic radiation spectrum extending from about 7000 A to 1 mm. That below 20 $\mu$ is referred to as the near infrared radiation region; that portion above 20 $\mu$ is the far infrared region.

Initial Relative Velocity - The initial relative velocity of an encounter of molecule i with molecule j is given by:

$$\vec{g}_{ij} = v_i - v_j$$

where $v_i$ and $v_j$ are the linear velocities at infinite separation.

Intensity - Radiant flux emitted by a source per unit of solid angle (units e.g. watts $cm^{-2}$).

Ion Atom Interchange - A reaction between an ion and a neutral particle in which there is a rearrangement involving the transfer of one or more atoms and a new ion is formed. In Chapter IX the term ion molecule reaction is used for this.

Ion-Electron Recombination - The chemical reaction between a positive ion and an electron, leading to only neutral particles.

Ion-Ion Recombination - The mutual neutralization of a positive ion by a negative ion is called ion-ion recombination.

Ion Molecule Reaction - The reaction between a charged particle and a neutral species to yield charged and neutral products is called an ion molecule reaction. Often applied to the type of reaction between an a neutral species in which there is a rearrangement involving the transfer of one or more atoms.

Ionization - The process by which an electron may be ejected into the continuum from a molecule or atom.

Ionization Potential - The energy required to eject an electron from the ground state molecule or atom to the continuum with zero kinetic energy is called the ionization potential.

Ionosphere - The region of the atmosphere above 60 km in which there are appreciable numbers of ions.

Ionospheric Storm - A complex change, usually a decrease in atmospheric electron density, due to particles from a solar flare, most noticeable in the F region and lasting for hours.

Irradiance - The radiant flux per unit area, or the amount of energy per second which will be received by a surface of unit area which intercepts the emitted energy (units e.g. watts $cm^{-2}$); this must be distinguished from radiant emittance which refers to the radiant energy emitted from a source.

Kinetic Temperature - The translational or kinetic theory temporature is defined in terms of the mean peculiar kinetic energy,

$$3/2\,kT = 1/n \sum_i n_i \,(1/2\, m_i \overrightarrow{V_i^2})$$

at equilibrium.

Laboratory Coordinates - The coordinate system moving with the laboratory is referred to as the laboratory coordinate system.

Laboratory Energy - The kinetic energy of a particle relative to a coordinate system moving with the laboratory is referred to as the laboratory energy, since such an energy may be directly measured with reference to the laboratory.

Lifetime - The lifetime of an unstable or metastable species is defined as the time required to reach 1/e of the initial concentration in the absence of sources. The lifetime must be defined with respect to the process or processes depleting the state; thus in general an unstable species has a radiative lifetime, a quenching lifetime, $\tau_Q$, and perhaps a chemical reaction lifetime, and the overall lifetime $\tau_i$, may therefore be pressure dependent.

$$1/\tau = 1/\tau_{RAD} + 1/\tau_Q + \sum_i 1/\tau_i$$

The radiative lifetime, $\tau_{RAD}$, is the reciprocal Einstein coefficient for spontaneous emission, and is frequently referred to as the lifetime.

Line Radiation - The photon emitted in a transition from one bound energy state to another, lower bound energy state has the energy $h\nu$, which represents the energy difference between the two states within the limits imposed by the uncertainty principle. The observation of such emission with a spectrograph results in a single sharp line (although many such transitions simultaneously occurring may obscure this). Such emission is called line radiation.

Linear Velocity - The linear or absolute velocity $v_j$, of the species j is the velocity with respect to a fixed coordinate system. Its magnitude is called the molecular speed.

Magnetic Storm - A magnetic storm is an interval of pronounced magnetic activity. Many magnetic storms, particularly the big storms, begin suddenly and almost simultaneously, to within a minute, all over the earth. The sudden commencement is ascribed to the impact of (ionized) solar gas on the outer part of the geomagnetic field, at a distance of several earth radii. The intensity of a storm is usually rated according to the maximum range of the variation of the field components during the storm. However, a rating according to the maximum stormtime depression of the horizontal component is often preferred.

Mass Averaged Velocity - The mass averaged velocity, $v_o$, is defined by

$$\vec{v}_o(\vec{r}, t) = 1/\rho \sum_i n_i m_i \vec{v}_i,$$

where $\rho$ is the overall density and particular point $(\vec{r})$ and $\vec{v}_i$, is the linear velocity.

Mean Free Path - The distance which a molecule (atom) travels between collisions is referred to as its free path. The average free path is called the mean free path. Both terms are of course, well defined only in the hard sphere model.

Mesopause - The top of the mesosphere. There the temperature is a minimum. The thermosphere begins above here and atomic oxygen becomes a major constituent.

Mesosphere - The region of the atmosphere between about 50 and 85 km. The temperature decreases as the altitude increases in this region.

Minor Constituent - A species whose concentration is small relative to the concentration of similar types of species, i.e. neutrals or ions, is referred to as a minor constituent.

Mixing - The processes by which concentration gradients are eliminated are called mixing processes; molecular diffusion and turbulent mixing are important atmospheric mixing processes.

Mobility - The mobility of an ion is defined as its velocity in an electric field of unit strength. The usual units are $cm^2\ sec^{-1}\ volt^{-1}$.

Mono-Energetic - This term refers to a collection of particles whose kinetic energy distribution is extremely narrow, and in the ideal case is a delta function about the nominal energy.

Mutual Neutralization - The two body process by which a positive and a negative ion collide and produce only an electron transfer(and undoubtedly energy transfer) to obtain two neutral species:

$$X^+ + Y^- \rightarrow X + Y$$

is called mutual neutralization.

Negative Ion - A metastable atom or molecule which exists with an excess of electrons over protons and therefore has a net negative charge is a negative ion.

Neutral Recombination - The process by which neutral atoms or aggregates of atoms collide to form larger, more stable, molecules is referred to as neutral recombination. For most atmospheric neutral recombination, emission of a photon (radiative recombination) or stabilization by a third body is required.

PCA - Polar cap absorption events are associated with charged particles (mainly protons) ejected during an intense solar flare. The influx of protons with energies between approximately 10 Mev and 100 Mev lasts for several days after the cessation of the flare.

Peculiar Velocity - The peculiar velocity of a molecule of species j is defined as the velocity of the molecule with respect to the mass average velocity, $\vec{v}_o$

$$\vec{V}_j\ (\vec{v}_i, \vec{r}, t) = \vec{v}_j - \vec{v}_o$$

where $\vec{v}_j$ is the linear velocity.

Perturbed Atmosphere - The atmosphere as affected by a perturbing influence, especially as affected by a nuclear burst.

Photoabsorption - The absorption of electromagnetic radiation.

Photochemical - This term refers to the chemical effects of light, including the infrared and ultraviolet as well as the visible spectrum. Photochemistry is that branch of radiation chemistry dealing with lower energy radiation.

Photodissociation - The transition from a bound molecular state to a continuum associated with the fragments by absorption of a photon of light is termed photodissociation.

Photoexcitation - The transition from the ground state to a bound excited state (usually electronically excited) by the absorption of a photon is called photoexcitation.

Photoionization - The ejection of an electron from the bound state of an atom or molecule into the continuum by the absorption of a photon is photoionization.

Photosphere - The outer visible region of the sun.

Positive Ion - A stable atom or molecule which has lost an electron or electrons and therefore has a net positive charge is called a positive ion.

Precision - The precision of an experimental measurement performed a number of times refers to the reproducibility of the result as expressed by the standard deviation; the accuracy may be entirely different if systematic errors are presented.

Probability of a Collision - The average number of times a given particle will collide with other particles in a second.

Radiance - Radiant flux emitted by a source per unit of solid angle per unit area of projected surface (units e.g. watts $cm^{-2}$ $ster^{-1}$).

Radiation - The emission of electromagnetic energy.

Radiative Recombination - The association of two particles to form a single stable particle by a bimolecular reaction in which excess energy is disposed of by radiating.

Rate Constant - Empirically, the time derivative of a concentration, called a rate of reaction, is found to be proportional to the product of concentrations when the process is isothermal and the gases dilute. Thus,

$$R_i = \frac{dc_{ij}}{dt} = k_i \prod_{j=1}^{n} C_j$$

where n is the order of the ith reaction, $R_i$, the rate, and $C_j$, the concentration. The constant of proportionality, k, is called the rate constant, or the rate coefficient

Reaction Rate - In chemical kinetics, the time derivative of the concentration of a given species is called the rate of reaction of that species; it is also called the velocity or speed of the reaction.

Reaction Rate Constant - Rate Constant.

Recombination - A process by which unstable or metastable particles collide and form larger aggregates of stable atoms or molecules.

Recombination Coefficient - The rate constant of a recombination reaction.

Reentry - The entrance of a body of any size back into the atmosphere from which it previously exited. The body may only be returning to lower altitudes.

Relaxation - The approach toward equilibrium conditions.

Relaxation Time - When a system is slightly perturbed from an equilibrium state, the time required to return to 1/e of the initial perturbation is called the relaxation time.

Rotational Excitation - When a molecule contains more energy in rotational modes than would by predicted from the equipartition theory, then the molecule is said to be rotationally excited.

Rotational Temperature - Since the number density of molecules in the J level, N(J), is given by:

$$N(J) = N/Q_r \ (2J + 1) \ e^{-BJ(J+1)\,hc/kT}$$

and to a first approximation (for accuracy greater refinements are necessary), I(J), the intensity emitted (or absorbed) is proportional to N(J),a rotational temperature may be obtained from a plot of ln (I(J)/2J + 1) vs J(J + 1). Although rotational relaxation is rapid, chemiexcitation may cause a departure from the kinetic temperature, or make the term "temperature" meaningless.

Scale Height - Height differential over which density, or other extensive property, changes by a factor of e.

Scattering - Deflection by elastic collision.

Second Order Reaction - A reaction whose rate has an empirical dependence on the product of two concentrations and does not neceasarily imply a bimolecular reaction.

Solar Flare - A solar flare is a burst of "light" occuring in the chromosphere of the sun near a sunspot. Flares are divided into classes of importance (e.g. 1 -, 1, 1 +, . . . ) according to area and brightness. The average duration of a flare increases with importance (e.g., class 1 flares last about 20 minutes while class 3 flares last about 60 minutes). During some flares there is a marked increase in the flux of solar radiation in the far ultraviolet and soft x-ray regions of the spectrum.

Sporadic E-Layer - A peak in the electron density profile at about 100 km which is sometimes present.

Stratopause - The top of the stratosphere. Here there is a temperature maximum. The mesophere begins here.

Stratosphere - The region of the atmosphere between the tropopause (around 15 km) and the strstopause (about 50 km). The temperature increases with altitude throughout this region.

Stream - A rapid flow of particles, most of which are going in about the same direction. The conditions are such that the particles suffer collisions within the stream (as opposed to beam).

Swarm - A packet of charged particles moving under the influence of electric potential. The particles have a distribution of velocities and undergo many collisions.

S. I. D. - (Sudden Ionospheric Disturbance) - A sudden increase in the electron density, due to radiation from a solar flux, most noticeable in the D region, lasting for 20 to 90 minutes.

Temperature - The temperature of a system may be defined in several ways; at equilibrium all are equivalent. The establishment of equilibrium, however, isdifficult, and the possibility of nonequilibrium in reaction systems is high. It is therefore improper to define a temperature without an appropriate qualification. When one defines a elementary chemical reaction by specifying the complete quantum state of both reactants and products, then the important temperature is the kinetic or translational temperature.

Termolecular - This term indicates that the elementary reaction referred to occurs as the result of a three body collision; (compare third order).

Thermionic Emission - Emission of particles from a solid surface due to heating of the surface.

Thermopause - The upper limit of the thermosphere and lower limit of the mesosphere (about 400 km). Hence the temperature reaches a maximum.

Thermosphere - The region of the atmosphere between the mesopause (about 85 km) and thermopause (about 400 km). The temperature increases throughout this region.

Third Body - This term refers to the stabilizing particle in a three body collision which permits the conservation of translational momentum and energy in recombination reactions.

Third - Order Reaction - A reaction whose rate is empirically dependent on the product of three concentrations.

Three Body Recombination - A reaction between two particles to yield an aggregate (or complex) comprising both particles which is stablized by the collision with a third body. This is distinguished from a recombination which is stabilized by the emission of a photon of light.

Torr - The Torricelli, sbbrev. as Torr, is the unit of pressure equal to the weight of 1 mm. Hg.

Transition Probability - With the introuuction of an electromagnetic field interaction into the Schrodinger equation for s particle, a nonzero probability arises that a system originally in state $E_m$ will be found in state $E_n$ with an accompsnying absorption or emission of a photon of the electromagnetic radiation, $h\nu$, equal to $|E_n - E_m|/bc$.

Transmission - Energy or particles incident upon a system can be transmitted, refracted, scattered or absorbed. The fraction which passes through the system unaltered and undelayed is the transmission.

Tropopause - The upper limit of the troposphere. This varies with latitude being of the order of 15 km.

Troposphere - The region of the atmosphere from the surface to the tropopause the temperature decreases with increasing altitudes.

Ultraviolet Radiation - That portion of the electromagnetic spectrum with wavelengths of 4000 - 1700 Å , with the range from 1700 - 100 Å being termed the vacuum ultraviolet.

Uncertainty (in a rate constant) - The error in a rate constant is expressed herein as the uncertainty in the preexponential or constant factor, the uncertainty in the temperature dependence of the preexponential factor, and an uncertainty in the activation energy. Although in principle these uncertainties should be expressed in terms of the standard deviations, in practice, the errors are not independent and the quoted uncertainties represent the educated guess of the experimentalist or data analyst.

Vacuum Ultraviolet - That portion of the electromagnetic spectrum with wavelengths from about 1300Å to 100 Å, in which transitions between electronic levels of molecules and atoms sometimes occur is called the vacuum ultraviolet region because spectrographs must be evacuated to prevent absorption of the incident radiation.

Vibrational Excitation - If the population of a vibrational level or levels of a given species exceeds that which may be calculated from a Boltzmann distribution with the equilibrium temperature, then that species is said to be vibrationally excited.

Vibrational Temperature - Since vibrational relaxation is a much slower process than rotational and translational relaxation, a system which has been exposed to a disturbance may be expected to be vibrationally excited. When such a disturbance is created thermally, it frequently occurs that the I R. intensities (a measure of the vibrational level population) are distributed in accordance with the Boltzman distribution. In such cases, a "vibrational temperature" may be defined by the relation

$$N(v) = N/Q_v \; e^{-G_o(v)/kT}$$

so that a plot of $\ln I(v)$ vs. $G_o(v)$ should have a slope of $1/kT$, where $I(v)$ is the intensity of emission from the vibrational level v, and where the vibrational spacing is given by $G_o(v)$.

Visible Radiation - That portion of the electromagnetic spectrum with wavelengths from about 4000 - 7000 Å, to which the human eye is sensitive, is called the visible region.

Wave Functions - In quantum mechanics, the state of a system is described by the wave function, $\psi$, which depends on the particle coordinates and time, this function has the significance that $|\psi|^2 \, dV$ is the probability that at time, t, the system is located within $dV$ of V in the coordinate space.

Weapon Debris - The residue of a nuclear weapon after it has exploded. It consists of the materials used for the casing and other components of the weapon, the weapon carrier and associated structure, unexpended fissionable materials (isotopes of uranium and plutonium) and fission products. The term debris is also often used to refer only to the radioactive fission products.

Weapon Yield - The total effective energy released in a nuclear explosion. Usually expressed as a comparison to the energy released by the explosion of TNT (a 1 MT weapon release the same energy as an explosion of approximately one million tons of TNT). A 1 MT weapon releases $10^{15}$ calories or $4.2 \times 10^{22}$ ergs.

X - Ray Radiation or X-Radiation - That portion of the electromagnetic spectrum which extends from about 100 Å to $10^{-1}$ Å.

$\beta$ - Ray - High energy electrons emitted from decaying nuclear particles.

$\gamma$ - Ray Radiation - That portion of the electromagnetic spectrum which extends from about 1 A to $10^{-3}$ A.

# APPENDIX E
# SUBJECT INDEX


Absorption processes
  cross-sections for . . . . . 12-8, 12-11, 12-14
  photon . . . . . 12-3
  radio-frequency . . . . . 21-1
  types of . . . . . 12-2
Aeronomy, related to the natural atmosphere . . . . . 3-1
Afterglow studies . . . . . 7-1
Airglow
  known emissions for . . . . . 9-22
  spectrum of . . . . . 11-2
Associative detachment, data for 17-5
Atmosphere
  daytime
    fractional concentrations of the ionic species in . . . 4-4
  disturbed
    chemical kinetics of . . . . . 6-1
    chemical releases in . . . . . 5-19
    data gathering for . . . . . 6-16
    excited species in . . . . . 5-18
    ion-recombination processes in . . . . . 6-7
    metastable states in . . . . . 6-12
    natural causes . . . . . 5-1
    nuclear causes . . . . . 5-8
    reaction mechanisms in . . . . . 6-1
    temperature dependence in . . . . . 6-3
  natural
    concentrations in . . . . . 4-1
    dominant fluid motions in . . . . . 3-7
    energy balance in . . . . . 4-1, 4-10
    energy partition in . . . . . 4-8
    energy transfer in . . . . . 4-10
    fluid mechanics of . . . . . 3-1
    general . . . . . 2-1, 3-1
    population temperatures of . . . . . 4-1

Atmosphere (continued)
natural (continued)
turbulence in . . . . . 3-21, 3-31
vibrational population in . . . . . 4-10
wave motions in. . . . . 3-12
Atmospheric
diffusion coefficients . . . . . 3-30
emission, spectrum of . . . . . 11-3
measurements
data from . . . . . 9-1
results for various measurement parameters . . . . 9-15
types of . . . . . 9-2, 3
species, population temperatures of . . . . . 4-7
structure . . . . . 2-1
turbulence. . . . . 3-21
Attachment processes
dissociative . . . . . 17-5
radiative . . . . . 17-3
rate coefficients for . . . . . 9-19
three-body . . . . . 17-7
Band shapes . . . . . 11-35
Band widths . . . . . 11-35
Beam techniques . . . . . 7-11
Charge transfer processes . . . . . 8-7
ion-atom . . . . . 15-8
negative-ion . . . . . 18A-15
neutral metals . . . . . 18A-27
positive-ion . . . . . 18A-11
recombination . . . . . 16-1
Chemical
kinetics of the disturbed atmosphere . . . . . 6-1
releases in disturbed atmosphere . . . . . 5-19
Codes
multi-species . . . . . 22-1
systems . . . . . 22-2
ultraviolet deposition . . . . . 12-29
Coefficients
attachment . . . . . 9-19
calculated reaction. . . . . 20-31
diffusion . . . . . 3-30, 3-32
effective recombination rate . . . . . 9-14
effective two-body recombination . . . . . 16-9
electron cooling rate . . . . . 21-15

Coefficients (continued)
excitation-deexcitation . . . . . 20-32
ion-ion . . . . . 9-19
ion-neutral reaction rate . . . . . 9-17
neutral-neutral . . . . . 9-19
quenching . . . . . 9-29
radiative recombination . . . . . 8-2
recombination (in F-region) . . . . . 9-8
Collision
frequencies
in atmospheric gases . . . . . 21-2
electron . . . . . 21-1, 2, 3
measurements . . . . . 9-20
processes
data for . . . . . 17-8
definitions of . . . . . 15-2
experimental data for . . . . . 15-25
experimental methods for . . . . . 15-4
in the infrared . . . . . 11-10
kinetics of . . . . . 14-1, 15-1
parameters of . . . . . 11-12
theoretical methods for . . . . . 15-5
Conductivity, normalized . . . . . 21-9
Constituents, schematic heat budget
between 80 and 150 km . . . . . 4-11
Cross-sections
absorption . . . . . 12-11, 12-14
effective dissociation . . . . . 14-28
effective line excitation . . . . . 14-23
electron capture and loss . . . . . 15-16, 17
electron-impact excitation . . . . . 20-49
ionization . . . . . 12-11
mean zonal winds . . . . . 3-10
photochemical processes . . . . . 12-1
photoionization . . . . . 12-23, 12-25
photon . . . . . 12-6
stripping . . . . . 15-21, 22, 15-24
symbols for . . . . . 15-28
Data gathering from
afterglow studies . . . . . 7-2
atmospheric measurements . . . . . 9-1
beam techniques . . . . . 7-11
charge transfer . . . . . 8-7
disturbed atmosphere . . . . . 6-16

Data gathering from (continued)
drift-tube measurements . . . . . 7-9
electron impact . . . . . 8-10
electron-ion recombination . . . . . 8-1
ion cyclotron resonance . . . . . 7-8
ion-molecule reactions . . . . . 8-9
laboratory experimentation . . . . . 7-1
mass-spectrometer ion-source measurements . . . . 7-7
negative-ion removal . . . . . 8-6
photoionization . . . . . 8-11
photon measurements . . . . . 7-19
quenching collisions . . . . . 8-9
studies of irradiated air . . . . . 7-27
theoretical methods . . . . . 8-1
vibrational deactivation . . . . . 8-10
vibrational excitation . . . . . 8-11
Deexcitation processes . . . . . 20-1
energy stored in . . . . . 20-2
excited states of . . . . . 20-2
general considerations for . . . . . 20-1
lifetimes of . . . . . 20-2
rate coefficients for . . . . . 20-32
reaction rates for . . . . . 20-18
specific states of . . . . . 20-2
Deionization
problem areas . . . . . 23-1
solutions . . . . . 22-1
Detachment processes
associative . . . . . 17-5
collisional . . . . . 17-8
photo . . . . . 17-3
Diatomic molecules
lower electronic levels of . . . . . 10-40
vibrational energy levels of . . . . . 10-40
Diffusion coefficients
as a function of altitude . . . . . 3-30
as a function of time . . . . . 3-32
Dissociation . . . . . 10-4
Dissociative attachment, data for . . . . . 17-5
D-region
daytime ionization rate in . . . . . 5-6
effective recombination coefficients in . . . . . 9-8
electron density profiles of . . . . . 5-7

Drift-tube measurements . . . . . 7-9
Earthshine . . . . . 11-21
Electron
attachment processes
ionospheric significance of . . . . . 17-21
types of . . . . . 17-1
capture and loss, cross-sections for . . . . . 15-16, 17
collision frequencies . . . . . 21-1, 2, 3
cooling rate coefficients . . . . . 21-13, 21-15
energy
exchange frequencies . . . . . 21-12, 21-14
loss data . . . . . 21-18
relaxation . . . . . 21-10
density profiles . . . . . 5-17
D-region . . . . . 5-7
fireball . . . . . 5-12, 5-14
detachment processes
ionospheric significance of . . . . . 17-12
types of . . . . . 17-1
impact . . . . . 8-10, 20-46
ion recombination processes . . . . . 8-1
Electronic populations . . . . . 10-18 — 10-39
Emission spectra (atmospheric) . . . . . 11-3
Emissivities, calculated . . . . . 11-29, 30
Energies of formation . . . . . 10-11
Energy
absorption, altitude dependence of . . . . . 4-12
balance, in the upper atmosphere . . . . . 4-1
emission, altitude dependence of . . . . . 4-12
levels . . . . . 10-3
of atoms . . . . . 20-42
basic data . . . . . 10-1
of ions . . . . . 20-43
lower electronic . . . . . 10-40
of metallic ions . . . . . 20-42
of molecules . . . . . 20-42
vibrational . . . . . 10-40
Equilibrium constants . . . . . 10-1, 10-5
for dissociation . . . . . 10-49
for ionization of atoms . . . . . 10-50
for ionization of diatomic molecules . . . . . 10-50
for ionization (detachment) of negative ions . . . . . 10-49
E-region, effective recombination coefficients in . . . . . 9-8

Exchange frequencies . . . . . 21-12
Excitation processes . . . . . 20-1
collisional parameters . . . . . 11-12
effective line cross-sections of . . . . . 14-26
electron impact . . . . . 20-46
energy stored in . . . . . 20-2
excited states of . . . . . 20-2
general considerations for . . . . . 20-1
lifetimes of . . . . . 20-2
rate coefficients for . . . . . 20-32
reaction rates for . . . . . 20-18
specific states . . . . . 20-2
Excited
species, in disturbed atmosphere . . . . . 5-18
states
energy stored in . . . . . 20-2
lifetimes of . . . . . 20-2
reaction rates for . . . . . 20-18
Experimentation
afterglow studies . . . . . 7-2
beam techniques . . . . . 7-11
data gathering from . . . . . 7-1
drift-tube measurements . . . . . 7-9
ion cyclotron resonance . . . . . 7-8
mass-spectrometer ion-source measurements . . . . 7-7
for neutral reactions . . . . . 19-2
photon measurements . . . . . 7-19
summary of . . . . . 15-27
Fireball
electron densities for . . . . . 5-12, 5-14
temperatures for . . . . . 5-10
Flowing-afterglow apparatus . . . . . 7-6
Fluid
mechanics, of natural atmosphere . . . . . 3-1
motions
dominant in the natural atmosphere . . . . . 3-7
equations of . . . . . 3-2
Fluorescence efficiencies, as measured in auroras . . . . 9-24
F-region, effective recombination coefficients in . . . . 9-8
Gases (irradiated), apparatus used to study . . . . . 7-28
Gravity waves
evidence of . . . . . 3-17
generation and dissipation of . . . . . 3-19

Grotrian diagram (partial) . . . . . 10-42 — 10-45
Ion
atom charge transfer . . . . . 15-8
cyclotron resonance . . . . . 7-8
ion reactions, rate coefficients for . . . . . 9-19
mobilities . . . . . 21-21
molecule reactions . . . . . 8-9
neutral reactions . . . . . 18A-1
examples of . . . . . 18A-4
reaction rate coefficients for . . . . . 9-17
summary of reaction rate constants for . . . . . 18A-10
pair
density, due to prompt radiation . . . . . 5-15
production rates, from beta and gamma radiation . . 5-16
recombination processes, in disturbed atmosphere . . . 6-7
Ionic species, fractional concentrations in the
daytime atmosphere . . . . . 4-4
Ionization
daytime D-region rates . . . . . 5-6
due to medium-yield weapon . . . . . 5-14
first thresholds . . . . . 12-4
Ions (negative), stability of . . . . . 17-9
Infrared
collisional excitation processes in . . . . . 11-10
data . . . . . 11-6
radiative
excitation in . . . . . 11-20
processes in . . . . . 11-1
spectrum of high-altitude nuclear burst . . . . . 11-4, 5
Interchange processes
ion-atom
negative . . . . . 18A-19
positive . . . . . 18A-16
Irradiance . . . . . 11-22
Irradiated gases, studies of . . . . . 7-27
Kinetics of
atmospheric radiative processes in the infrared . . . . 11-1
high-energy heavy-particle collision processes . . . . 15-1
low-energy electron collision processes . . . . . 14-1
Loss frequencies . . . . . 20-45
Mass spectrometer
diagrams of . . . . . 7-3, 7-14
ion-source measurements . . . . . 7-7
microwave afterglow apparatus . . . . . 7-3

Metals (neutral), charge transfer to . . . . . 18A-27
Metastable states, in disturbed atmosphere . . . . . 6-12
Microwave afterglow mass-spectrometer apparatus . . . 7-3
Negative ions
  processes for
    atom-interchange . . . . . 18A-19
    charge transfer . . . . . 18A-15
    three-body . . . . . 18A-25
  removal of . . . . . 8-4
  stability of . . . . . 17-9, 10
$N_e$-h profiles. . . . . 5-9
Neutral
  metals, charge transfer to . . . . . 18A-27
  reactions
    discussions of . . . . . 19-4, 19-10
    experimental methods of . . . . . 19-2
    rate coefficients for . . . . . 9-19
  species, fractional concentrations in the atmosphere
    major . . . . . 4-2
    minor . . . . . 4-2
Nuclear
  atmosphere
    disturbed, environmental definitions of . . . . . 1-3
    perturbed . . . . . 5-8
  detonation (high-altitude), infrared spectrum of . . . 11-4, 5
Photochemical processes . . . . . 12-1, 13-1
  cross-section data for . . . . . 12-1
Photodetachment processes
  apparatus for study of. . . . . 7-26
  data for . . . . . 17-3
Photoionization . . . . . 8-11
  cross-sections . . . . . 12-23, 12-25
  solar . . . . . 13-1
Photon
  absorption processes . . . . . 12-3
  cross-section data . . . . . 12-6
  measurements . . . . . 7-19
Plasmas
  calculated emissivities of . . . . . 11-29, 30
  radiative processes in . . . . . 11-25
Population temperatures, of atmospheric species . . . . 4-7

Positive ions
processes for
atom-interchange . . . . . 18A-16
charge transfer . . . . . 18A-11
three-body . . . . . 18A-22
Potential energy curves . . . . . 10-46, 47. 48
Production rates (ion-pair), from beta and gamma radiation . . . . . 5-16
Quenching
collisions . . . . . 8-9
data . . . . . 20-28, 20-30
rate coefficients . . . . . 9-29
Radiative
lifetimes . . . . . 20-20
processes
attachment data for . . . . . 17-3
collisional . . . . . 8-4
in the infrared
excitation . . . . . 11-20
kinetics of . . . . . 11-1
in low-density plasmas . . . . . 11-25
recombination coefficients . . . . . 8-2
Radio-frequency absorption . . . . . 21-1
transmission coefficients . . . . . 21-7
for ions . . . . . 21-20
Rate coefficients
attachment . . . . . 9-19
deexcitation . . . . . 20-32
effective recombination . . . . . 9-14
electron cooling . . . . . 21-15
excitation . . . . . 20-32
ion-ion . . . . . 9-19
ion-neutral . . . . . 9-17
neutral-neutral . . . . . 9-19
quenching . . . . . 9-29
vibrational excitation . . . . . 20-48
Reaction
energies . . . . . 10-1
mechanisms, in disturbed atmosphere . . . . . 6-1
rate constants
excited species . . . . . 20-16
first order . . . . . 13-1
ion-neutral reactions . . . . . 18A-10

Reaction (continued)
rate constants (continued)
neutral reactions . . . . . 19-16
solar photoionization . . . . . 13-1
summary of . . . . . 24-4
vibrational excitation processes . . . . . 20-44
Recombination
coefficients
D-region . . . . . 9-8
E-region . . . . . 9-8
effective two-body . . . . . 16-19
F-region . . . . . 9-8
two-body electron-ion . . . . . 16-9
processes
charged particle . . . . . 16-1, 2, 16-6
collisional radiative . . . . . 16-19
effective two-body . . . . . 16-19
ctron-ion . . . . . 8-1
rate coefficients for . . . . . 9-14
Resonance fluorescence excitation . . . . . 11-40
Russek-Firsov models, comparison of . . . . . 15-26
Schumann-Runge bands, cross-section data in . . . . 12-9, 10
Solar
flux, incident on upper atmosphere . . . . . 13-5
photoionization rate constants . . . . . 13-1
ultraviolet intensities . . . . . 13-4
Spectral band shapes . . . . . 11-36 – 11-39
Spectrums
airglow . . . . . 11-2
atmospheric emission . . . . . 11-3
infrared of high-altitude nuclear burst . . . . . 11-4, 5
turbulent power . . . . . 3-24
Stripping cross-sections . . . . . 11-21, 22, 11-24
Temperature dependence, in disturbed atmosphere . . . . 6-3
Theoretical analysis
charge transfer . . . . . 8-7
data gathering from . . . . . 8-1
electron
impact . . . . . 8-10
ion recombination processes . . . . . 8-1
ion-molecule reactions . . . . . 8-9
negative-ion removal . . . . . 8-6

Theoretical analysis (continued)
photoionization . . . . . 8-11
quenching collisions . . . . . 8-9
vibrational
deactivation . . . . . 8-10
excitation . . . . . 8-11
Three-body attachment, data for . . . . . 17-7
Transmission coefficients
radio-frequency . . . . . 21-7
for ions . . . . . 21-20
Turbulence
effects on upper atmosphere chemistry . . . . . 3-31
in natural atmosphere . . . . . 3-21
Ultraviolet
deposition codes, photon cross-sections for . . . . . 12-29
solar intensities in . . . . . 13-1
Vibrational
deactivation . . . . . 8-10
excitation . . . . . 8-11
rate constants for . . . . . 20-44, 20-48
spacing, of triatomic molecules . . . . . 10-41
Water vapor, cross-sections of . . . . . 12-29
Wave motions, in the natural atmosphere . . . . . 3-12
Winds
cross-sections of . . . . . 3-10
horizontal components of . . . . . 3-11
speed spectra of . . . . . 3-19
vertical shears for . . . . . 3-11

# APPENDIX F
# SPECIES INDEX

N. B. : The entries are listed by chapter and page. For instance, the designation 5-7, 8 indicates the presence of information on pages 7 and 8 of Chapter 5, and 5-(6-9) designates information on pages 6 through 9 of Chapter 5. In a few cases, a species is treated continuously throughout an entire chapter; when this occurs, the chapter number is given. Where information is contained in a figure or table, the figure number or table number is given separately from the chapter and page numbers, which are used only for textual reference. Certain tables are subdivided, e.g., 16-1 into 16-1.1, 16-1.2, etc., and 24-1 into Roman Numeral categories. These subdivisions are included in the designations, where applicable, for greater clarity. Entries are listed alphabetically by standard chemical symbol, with the added features that the invented symbol "Me" is used to indicate metallic species generally, and that "air", "air ions", "electron", and "teflon" are entered as words, in their proper alphabetical order. Electronically excited states are listed either as specific state designations (in alphabetical and numerical order) where these are known, or by the use of the asterisk (*) to indicate electronic excitation generally. Vibrationally excited states are designated by the double-dagger (‡). Unless otherwise noted, all species listed are gas-phase species. A few solids and liquids are included, and are appropriately designated as such, viz., by the respective standard indicators (s) and (ℓ).

Ag Figure 15-2.

$Ag^+$ Page 15-36.



Preceding page blank

| | |
|---|---|
| Air | Pages 3-5, 33; 5-18; 7-27, 29; 17-7; 21-4, 5, (7-9), (16-18), 25.<br>Tables 11-2; 16-1.2; 21-2, 4; 24-1 (VI).<br>Figures 7-8; 9-2, 3; 21-3, 5. |
| Air Ions | Pages 16-21, 23.<br>Tables 16-1.1; 24-1 (VI). |
| Al | Pages 5-13; 7-20; 15-1, 21, 29.<br>Figures 5-10; 15-1, 5. |
| $Al^+$ | Pages 15-6, 15, 31, 35, 39, 44, 45, 47; 16-18; 20-18.<br>Table 16-1.1.<br>Figure 15-4. |
| $Al(CH_3)_3$ | Page 5-19. |
| AlO | Pages 11-23, 25.<br>Table 11-1. |
| $AlO^*$ | Page 11-25. |
| Ar | Pages 2-9, 10; 4-1; 10-2; 11-27; 15-21, 25, 34, 36, 37, 43; 16-14, 16, 17, 24; 17-3; 18A-9; 19-8, 9, 12; 21-5, 24.<br>Tables 10-1, 10; 15-1; 18A-5; 20-2, 6, 8; 24-1 (XXVI).<br>Figures 2-7; 4-1; 10-10; 14-10; 15-1, 2, 5. |
| $Ar^*$ | Table 10-10. |
| $Ar^+$ | Pages 15-31, 43; 16-18.<br>Tables 10-1, 11; 16-1.1. |
| $Ar^{+*}$ | Table 10-11. |
| $Ar^{++}$ | Page 15-43.<br>Table 10-1. |
| $Ar^{3+}$ | Page 15-43. |
| $Ar^{4+}$ | Page 15-43. |
| $Ar^{5+}$ | Page 15-43. |

| | |
|---|---|
| $Ar^{6+}$ | Page 15-43. |
| B | Figure 15-1. |
| $B^{+}$ | Page 16-18.<br>Table 16-1.1. |
| $B_2^{+}(B^2\Sigma)$ | Page 6-15. |
| Ba | Pages 5-19; 15-30; 20-7.<br>Table 20-10. |
| $Ba^{+}$ | Pages 15-33, 38, 42, 44, 46, 47.<br>Table 20-10. |
| $Ba^{+*}$ | Table 20-10. |
| $Ba^{++}$ | Pages 15-33, 42. |
| $Be^{+}$ | Pages 15-34; 16-18.<br>Tables 15-1; 16-1.1. |
| Br | Table 18A-2. |
| $Br^{-}$ | Page 16-21.<br>Tables 16-1.2; 18A-2. |
| $Br_2$ | Page 16-21. |
| $Br_2^{+}$ | Page 16-21.<br>Table 16-1.2. |
| C | Tables 8-2; 10-1, 3; 20-1.<br>Figures 7-7; 10-10; 15-1, 2; 20-1. |
| $C^{*}$ | Tables 10-3; 20-1.<br>Figure 20-1. |
| $C(^1D)$ | Table 20-1.<br>Figure 20-1. |
| $C(^1S)$ | Table 20-1. |

| | |
|---|---|
| $C(^5S)$ | Table 20-1. |
| C(s) | Page 10-2. |
| $C^+$ | Page 16-18.<br>Tables 10-1, 4; 16-1.1; 20-1; 24-1 (XIV).<br>Figures 14-24, 75, (77-79); 20-2. |
| $C^{+*}$ | Tables 10-4; 20-1.<br>Figures 14-24, 75, (77-79); 20-2. |
| $C^{++}$ | Table 20-1. |
| $C^-$ | Page 10-3.<br>Table 10-1.<br>Figure 10-9. |
| $CCl_4$ | Page 21-31. |
| $CHO^+$ | Tables 18A-1, 3. |
| $CH_4$ | Page 11-13.<br>Table 11-1.<br>Figure 11-1. |
| $CKO_2^+$ | See $K^+(CO_2)$. |
| CN | Table 20-10. |
| $CN^*$ | Table 20-10. |
| CN(A) | Table 20-10. |
| $CNO_3^+$ | See $NO^+(CO_2)$. |
| $CNaO_2^+$ | See $Na^+(CO_2)$. |
| CO | Pages 6-15; 11-35; 17-4; 21-17, 28.<br>Tables 10-1, 12; 11-1, 2; 17-2, 7; 18A-1, 3; 20-10; 24-1 (XII, XIII, XIV, XXIV, XXV, XXVII, XXXI).<br>Figures 10-8, 11; 11-3, 4, (11-14); 14-(21-28). |

| | |
|---|---|
| $CO^{\ddagger}$ | Tables 20-10; 24-1 (XXXI). |
| $CO^{*}$ | Table 10-12. |
| $CO(a\ ^{3}\Pi)$ | Table 10-12. |
| $CO(a'\ ^{3}\Sigma^{+})$ | Table 10-12. |
| $CO(A\ ^{1}\Pi)$ | Table 10-12. |
| $CO(d\ ^{3}\Delta)$ | Table 10-12. |
| $CO(e\ ^{3}\Sigma^{-})$ | Table 10-12. |
| $CO(I\ ^{1}\Sigma^{-})$ | Table 10-12. |
| $CO^{+}$ | Tables 10-1, 19; 18A-1; 20-10; 24-1 (XIII, XIV). |
| $CO^{+*}$ | Tables 10-19; 20-10. |
| $CO^{+}(A\ ^{2}\Pi)$ | Tables 10-19; 20-10. |
| $CO^{+}(B\ ^{2}\Sigma^{+})$ | Table 10-19. |
| $CO^{++}$ | Table 10-1.<br>Figure 14-22. |
| $CO_2$ | Pages 4-10, 13; 11-1, 11, 14, 34; 12-6, 16, 28; 13-2; 17-3, 4, 9, 12, 14; 18A-9, 10; 20-4, 15; 21-5, 16, 17.<br>Tables 10-1, 20; 11-1, 2; 12-2; 17-4, 5, 7; 18A-1, (3-6); 20-2, 6, 8, 10; 21-2; 24-1 (IX, XII, XIII, XIV, XVI, XVIII, XXI, XXIV, XXV, XXVII, XXX, XXXI, XXXIII). |
| $CO_2^{\ddagger}$ | Pages 4-13; 11-14.<br>Tables 10-20; 20-2; 24-1 (XXXI, XXXIII). |
| $CO_2^{+}$ | Page 9-11.<br>Tables 10-1, 20; 18A-1, 3; 24-1 (XIII, XIV).<br>Figures 14-(67-69). |
| $CO_2^{+\ddagger}$ | Table 10-20. |

| | |
|---|---|
| $CO_2^{+*}$ | Figures 14-(67-71). |
| $CO_2^{++}$ | Table 10-1. |
| $CO_2^-$ | Page 17-9. |
| $CO_3^-$ | Pages 17-2, 9, 12.<br>Tables 17-2, 4, 7; 18A-4, 6; 21-4; 24-1 (XII, XVI, XXI). |
| $CO_4^+$ | See $O_2^+(CO_2)$. |
| $CO_4^-$ | Pages 17-2, 9, 17.<br>Tables 17-7; 18A-4, 6; 21-4; 24-1 (XVI, XXI). |
| CSO | See OCS. |
| $C_2H_2$ | Page 16-17. |
| $C_2NaO_4^+$ | See $Na^+(CO_2)_2$. |
| $C_6H_6^+$ | Page 16-24. |
| Ca | Table 18A-7. |
| $Ca^+$ | Tables 18A-3, 5, 7.<br>Figure 20-1. |
| $Ca^{+*}$ | Tables 9-5; 20-10.<br>Figure 20-1. |
| $CaO^+$ | Table 18A-3. |
| $CaO_2^+$ | Table 18A-5. |
| Cl | Table 18A-2. |
| $Cl^+$ | Page 16-18.<br>Table 16-1.1. |
| $Cl^-$ | Table 18A-2. |
| Cs | Table 20-10. |

| | |
|---|---|
| $Cs^+$ | Pages 15-37, 41.<br>Table 20-10. |
| $D^-$ | Pages 16-22, 23.<br>Table 16-1.2. |
| $D_2$ | Page 16-24. |
| Electron | Chapters 17; 21.<br>Pages 4-6, 13; 5-(5-8), 19; 6-2, 3, (7-12), 14; 7-2, 4, 8, 11, 20, 23, 25, 27, 29; 8-(1-7), 10, 11; 9-1, 4, 6, (8-16), 30; 11-(25-33); 12-1, 5; 13-1; 15-1, (5-7), 20, 25, (29-47); 16-(1-21); 20-3, 5, 7, 8, 10, 11, (13-17); 22-2.<br>Tables 6-1; 8-(1-3); 9-1, 4; 12-1; 16-1.1; 18A-4; 20-7, 9, 10; 24-1 (I, II, III, IV, VII, VIII, IX, X, XI, XII, XXX).<br>Figures 4-3; 5-9; 7-6, 7; 9-1; 14-17; 16-(1-4); 20-(3-5), (7-9). |
| F | Page 17-18.<br>Table 17-7.<br>Figures 15-1, 2. |
| $F^+$ | Page 16-18.<br>Table 16-1.1. |
| Fe | Pages 11-20; 15-1, 21, 30; 20-7.<br>Table 18A-7.<br>Figures 15-1, 5. |
| $Fe^+$ | Pages 15-6, 15, 32, 35, 40, 44, 46, 47; 20-18.<br>Tables 18A-3, 5, 7; 24-1 (XIV).<br>Figures 15-3; 20-1. |
| FeO | Page 11-20.<br>Table 11-1. |
| $FeC^+$ | Tables 18A-3; 24-1 (XIV). |
| $FeO_2^+$ | Table 18A-5. |

| | |
|---|---|
| H | Pages 2-10; 6-8; 7-7; 8-(6-8); 10-4; 11-15, 17; 15-1, 18, 19; 19-3, 12; 20-16.<br>Tables 6-1; 8-2; 9-1, 5, 6; 10-1, 2; 12-2; 18A-(1-4), 7; 19-1; 20-10; 24-1 (I, IV, XIII, XIV, XV, XXIV, XXV, XXVII).<br>Figures 2-7; 10-1, 10; 14-1, 3, 4, 17; 15-1, 2. |
| $H^*$ | Tables 10-2; 20-10.<br>Figure 10-I. |
| $H(3\ ^2P)$ | Tables 9-5; 20-10. |
| $H(^2S)$ | Table 20-10. |
| $H^+$ | Pages 6-8; 7-17; 8-1, 8; 9-6, 8; 10-3; 16-18, 20, 22, 23.<br>Tables 8-1; 9-1; 10-1; 16-1.1, 1.2; 18A-1, 3, 7; 20-10; 24-1 (I, XIII).<br>Figures 14-3, 4, 64, 89; 16-4. |
| $H^-$ | Pages 7-17; 8-6, 7; 10-3; 16-22, 23; 17-2, 8.<br>Tables 10-1; 16-1.2; 17-3; 18A-2; 24-1 (XV).<br>Figures 10-9; 14-1, 16. |
| $HCO^+$ | See $CHO^+$. |
| $HNO_2$ | Page 18A-9.<br>Tables 18A-3, 4; 24-1 (XIV). |
| $HNO_3$ | Page 11-13.<br>Table 11-1. |
| $HO_2$ | Pages 11-16; 19-12; 20-16.<br>Tables 11-1; 19-1; 24-1 (XII, XXIV, XXV, XXVII). |
| $HO_2^-$ | Page 17-2. |
| HS | Table 18A-2. |
| $HS^-$ | Table 18A-2. |

$H_2$ — Pages 10-2; 11-31, 33; 16-17, 18, 24; 17-4; 19-4, 12; 20-16.
Tables 9-5; 10-1, 19; 17-4; 18A-3; 20-10; 24-1 (XII, XIV, XXV, XXVII).
Figures 10-8; 14-(12-20); 15-1, 2.

$H_2^{\ddagger}$ — Table 20-10.

$H_2^+$ — Page 16-18.
Tables 10-1, 19; 16-1.2.
Figures 14-13, 64, 89.

$H_2^{+\ddagger}$ — Page 16-18.

$H_2^-$ — Page 17-9.

$H_2NO_2^+$ — See $NO^+(H_2O)$.

$H_2NO_3^-$ — See $NO_2^-(H_2O)$.

$H_2NO_4^-$ — See $NO_3^-(H_2O)$.

$H_2O$ — Pages 4-15; 6-8; 9-11; 11-1, 11; 12-6, 29; 17-3, 4, 8, 12; 18A-2, 3, (8-10); 19-12; 20-15, 16; 21-5, 6, 8, 16, 18, 27, 28.
Tables 6-1; 10-1, 20; 11-1, 2; 12-2; 17-(3-5), 7; 18A-1, (3-7); 20-5, 6, 8, 10; 21-1, 2; 24-1 (IV, IX, XII, XIII, XIV, XVI, XVIII, XIX, XXI, XXIV, XXV, XXVII, XXX, XXXIII).
Figures 4-2, 8; 11-1; 12-17; 14-(62-65); 20-6; 21-1, 3, 5.

$H_2O^{\ddagger}$ — Page 4-15.
Tables 10-20; 20-5; 24-1 (XXXIII).

$H_2O^+$ — Tables 10-1, 20; 18A-1, 3, 7; 24-1 (XIII, XIV).
Figure 14-63.

$H_2O^{+\ddagger}$ — Table 10-20.

$H_2O^-$ — Page 17-9.

$H_2O_2$ — Table 24-1 (XXIV, XXVII).

$H_2O_2^-$ See $O^-(H_2O)$.

$H_2O_3^+$ See $O_2^+(H_2O)$.

$H_2O_3^-$ See $O_2^-(H_2O)$.

$H_2O_4^-$ See $O_3^-(H_2O)$.

$H_2SO_4(\ell)$ Page 19-4.

$H_3O$ Table 18A-7.

$H_3O^+$ Pages 9-11; 16-17; 18A-8; 21-20.
Tables 16-1.1; 18A-3, 5, 7; 21-4; 24-1 (IV, XIV, XVIII, XIX).

$H_3O^+(H_2O)$ Pages 18A-8; 21-25.
Tables 16-1.1; 18A-3, 5; 21-4; 24-1 (IV, XIV, XVIII, XIX).

$H_3O^+(H_2O)_2$ Pages 16-17; 18A-9.
Tables 16-1.1; 18A-3, 5; 24-1 (IV, XIV, XVIII, XIX).

$H_3O^+(H_2O)_3$ Tables 16-1.1; 18A-5; 24-1 (IV, XVIII, XIX).

$H_3O^+(H_2O)_4$ Tables 16-1.1; 18A-5; 24-1 (IV, XVIII, XIX).

$H_3O^+(H_2O)_5$ Page 16-17.
Tables 16-1.1; 24-1 (IV).

$H_3O^+(H_2O)_n$ Pages 9-11; 16-17; 18A-8; 21-20.
Tables 16-1.1; 24-1 (IV, XVIII, XIX).

$H_3O^+(OH)$ Page 18A-8.
Tables 18A-3; 24-1 (IV, XIV, XIX).

$H_3O_2^-$ See $OH^-(H_2O)$.

$H_3PO_4(\ell)$ Page 19-4.

$H_4NO_3^+$ See $NO^+(H_2O)_2$.

$H_4O_2^+$ See $H_3O^+(OH)$.

| | |
|---|---|
| $H_4O_4^-$ | See $O_2^-(H_2O)_2$. |
| $H_5O_2^+$ | See $H_3O^+(H_2O)$. |
| $H_6NO_4^+$ | See $NO^+(H_2O)_3$. |
| $H_6O_5^-$ | See $O_2^-(H_2O)_3$. |
| $H_7O_3^+$ | See $H_3O^+(H_2O)_2$. |
| $H_8O_6^-$ | See $O_2^-(H_2O)_4$. |
| $H_9O_4^+$ | See $H_3O^+(H_2O)_3$. |
| $H_{10}O_7^-$ | See $O_2^-(H_2O)_5$. |
| $H_{11}O_5^+$ | See $H_3O^+(H_2O)_4$. |
| $H_{13}O_6^+$ | See $H_3O^+(H_2O)_5$. |
| $H_{2n}NO_{n+3}^-$ | See $NO_3^-(H_2O)_n$. |
| $H_{2n}O_{n+2}^-$ | See $O_2^-(H_2O)_n$. |
| $H_{n+3}O_{n+1}^+$ | See $H_3O^+(H_2O)_n$. |
| He | Pages 2-9, 10; 4-1; 7-4, 10, 23; 8-4; 11-33; 15-1; 16-12, 14, 15, 17, 20, 21, 24; 18A-4, 7, 9; 19-12; 20-15; 21-17.<br>Tables 8-2; 9-1, 3, 5; 12-2; 16-1.1, 1.2; 18A-1, 5, 6; 20-8, 10; 21-3; 24-1 (XVIII, XXI).<br>Figures 2-7; 4-1; 7-3, 6; 15-1, 2; 21-4. |
| $He^*$ | Table 20-10. |
| $He(^3P)$ | Table 9-5. |
| $He(2\ ^1S)$ | Table 20-10 |
| $He(^3S)$ | Tables 9-5; 20-10. |
| $He^+$ | Pages 8-3; 15-45, 46; 16-18, 20, 22, 23; 18A-3, 4.<br>Tables 9-1, 3, 5; 16-1.1; 18A-1; 20-10. |

$He_2^+$ Page 16-20.
Tables 16-1.1; 18A-1.

Hg Page 20-7.

I Pages 15-21; 19-3.
Table 18A-2.
Figures 15-5, 7.

$I^+$ Pages 15-37, 41.
Table 15-1.

$I^-$ Page 16-21.
Tables 16-1.2; 18A-2.

$I_2$ Page 16-21.

$I_2^+$ Page 16-21.
Table 16-1.2.

K Pages 15-21, 29.
Table 8-2.
Figures 15-2, 5, 8.

$K^*$ Table 9-5.

$K^+$ Pages 15-32, 35, 40; 16-18.
Tables 15-1; 16-1.1; 18A-3, 5.

$K^+(CO_2)$ Table 18A-5.

$KO^+$ Table 18A-3.

Kr Pages 15-30; 16-24.
Table 20-8.
Figures 15-1, 2.

$Kr^+$ Pages 15-32, 36, 40.

Li Page 15-1.
Table 8-2.
Figures 15-1, 2.

$Li^*$ Table 9-5.

| | |
|---|---|
| $Li^+$ | Page 16-18.<br>Table 16-1.1. |
| Me | Pages 11-20; 20-7. |
| $Me^+$ | Pages 20-7, 18. |
| MeO | Pages 11-20, (23-25). |
| $MeO^‡$ | Pages 11-23, 24. |
| $MeO^*$ | Page 11-24. |
| $MeO^{*‡}$ | Page 11-24. |
| $MeO_2$ | Page 11-20. |
| $MeO_x$ | Page 11-19. |
| $MeO_x^‡$ | Page 11-19. |
| Mg | Table 18A-7. |
| $Mg^+$ | Pages 16-18; 18A-6.<br>Tables 16-1.1; 18A-3, 5, 7.<br>Figure 20-1. |
| $MgO^+$ | Page 18A-6.<br>Table 18A-3. |
| $MgO_2^-$ | Table 18A-5. |
| N | Pages 4-13; 5-18; 6-7, 8, 14, 15; 7-7; 8-8, 10, 12; 2; 10-4; 11-18, 31, 32; 12-6, 24, 30; 15-1, 5, 21, 25, 29; 16-10, 11, 24, 25; 17-6; 18A-4, 5; 19-2, 3, 6, 7, 10, 13, 14; 20-(3-5), 7, 9, 10, 14, 15, 17; 21-6.<br>Tables 6-1; 8-2; 9-(2-6); 10-1, 5; 12-2, 6a, 6b, 8a, 8b; 17-4, 7; 18A-1, (3-5), 7; 19-1, 20-1, 3. 4, 6, 9, 10; 21-1; 24-1 (I, II, IV, V. XII, XIV, XVI, XVIII, XXIII, XXIV, XXV, XXVI, XXVII, XXVIII, XXX).<br>Figures 4-1; 10-2, 5, 6, 10; 12-12; 14-5, 6; 15-1, 2; 20-1, 5; 21-1. |

| | |
|---|---|
| $N^*$ | Pages 20-10, 15.<br>Tables 10-5; 20-1, 10.<br>Figures 10-2; 20-1, 5. |
| $N(^2D)$ | Pages 5-8, 17, 18; 6-15; 11-18; 20-10; 22-1.<br>Tables 9-(4-6); 12-6a, 6b; 20-1, 10; 24-1 (IV, XIV, XXVII, XXVIII, XXX).<br>Figures 10-5, 6; 12-12; 20-1, 5. |
| $N(^2P)$ | Page 20-10.<br>Tables 9-5, 6; 12-6a, 6b; 20-1, 10; 24-1 (XXVIII).<br>Figures 10-5, 6; 12-12; 20-1, 5. |
| $N(^4P)$ | Tables 9-5, 6; 20-1. |
| $N^+$ | Pages 8-2, 8; 15-22, 25, 31, 34, 39, 43, 45, 46; 16-18, 22; 18A-4; 20-15.<br>Tables 9-2, 3; 10-1, 6; 12-8a, 8b; 14-3; 15-1; 16-1.1, 1.2; 18A-1, 3, 7; 20-1; 21-4; 24-1 (I, II, V, XIII, XIV, XVIII, XXVIII).<br>Figures 10-5, 6; 12-12; 14-11, 39, 90; 15-9; 20-2. |
| $N^{+*}$ | Page 20-15.<br>Tables 10-6; 14-[illegible] 20-1.<br>Figures 14-39; 20-2. |
| $N^+(^1D)$ | Tables 20-1; 24-1 (XXVIII).<br>Figures 12-12; 20-2. |
| $N^+(^1S)$ | Tables 20-1; 24-1 (XXVIII).<br>Figure 12-12. |
| $N^{++}$ | Pages 15-22, 43.<br>Table 10-1.<br>Figure 14-11 |
| $N^{3+}$ | Page 15-43. |
| $N^-$ | Figure 10-5. |
| $NH^+$ | Tables 18A-3; 24-1 (XIV). |
| $NH_2^-$ | Page 7-9. |

| | |
|---|---|
| $NH_3$ | Table 11-1. |
| NO | Pages 4-13, 15; 5-18; 6-8, 15; 8-5; 10-4; 11-1, 14, 19, 25; 12-6, 24, 30; 13-1, 2; 16-(10-12), 14, 22; 17-2, 4, 6, 7, 9, 12; 18A-2, 7, 9; 19-6, 7, 10, 11, 13, 14; 20-3, 7, 8, 10, 14; 21-5, 17, 27.<br>Tables 6-1; 9-2, 4, 31; 10-1, 15; 11-1, 2; 12-2, 9a, 9b; 17-4, 5, 7; 18A-(1-7); 19-1; 20-1, 2, 4, 10; 21-1, 2; 24-1 (I, II, IV, IX, XII, XIII, XIV, XV, XVI, XVIII, XIX, XXI, XXIII, XXIV, XXV, XXVI, XXVII, XXVIII, XXX).<br>Figures 4-2, 8; 5-4; 10-6, 8, 11; 11-3, 4; 12-13; 14-(42-44); 20-1; 21-1. |
| $NO^{\ddagger}$ | Page 11-18.<br>Table 20-2.<br>Figure 10-6. |
| $NO^{*}$ | Tables 10-15; 20-1, 10.<br>Figures 10-6; 20-1. |
| $NO(a\ ^4\Pi)$ | Tables 10-15; 20-1; 24-1 (XXVIII).<br>Figures 10-6; 20-1. |
| $NO(a\ ^4\Pi)^{\ddagger}$ | Figure 20-1. |
| $NO(A\ ^2\Sigma^+)$ | Page 6-15.<br>Tables 9-5; 10-15; 11-2; 20-1, 10; 24-1 (XXIII).<br>Figures 10-6; 20-1. |
| $NO(A\ ^2\Sigma^+)^{\ddagger}$ | Table 20-10.<br>Figure 20-1. |
| $NO(b\ ^4\Sigma^-)$ | Table 10-15.<br>Figure 10-6. |
| $NO(B\ ^2\Pi)$ | Pages 6-15; 8-5.<br>Tables 10-15; 20-1, 10; 24-1 (XXIII, XXV).<br>Figure 10-6. |
| $NO(B'\ ^2\Delta)$ | Page 8-5.<br>Figure 10-6. |

| | |
|---|---|
| $NO(C\ ^2\Pi)$ | Tables 10-15; 24-1 (XXIII).<br>Figure 10-6. |
| $NO(D\ ^2\Sigma^+)$ | Table 10-15.<br>Figure 10-6. |
| $NO(E\ ^2\Sigma^+)$ | Figure 10-6. |
| $NO(F\ ^2\Delta)$ | Figure 10-6. |
| $NO(G\ ^2\Sigma^-)$ | Figure 10-6. |
| $NO(H\ ^2\Sigma^+)$ | Figure 10-6. |
| $NO(H'\ ^2\Pi)$ | Figure 10-6. |
| $NO(K\ ^2\Pi)$ | Figure 10-6. |
| $NO(M\ ^2\Sigma^+)$ | Figure 10-6. |
| $NO(S\ ^2\Sigma^+)$ | Figure 10-6. |
| $NO(^2\Phi_i)$ | Figure 10-6. |
| $NO^+$ | Pages 4-6; 5-7; 6-7, 8, 14, 15; 8-5; 9-11, 12, 31; 13-3, 4; 16-5, 7, (10-12), 14, 17, 22, 24; 18A-5, 6, 9, 10; 20-5, 7, 10, 17; 21-20, 25.<br>Tables 9-(2-4); 10-1, 16; 11-1; 12-9a, 9b; 13-3, 5, 7; 16-1.1, 1.2; 18A-1, 3, 5, 7; 20-1, 3, 9, 10; 21-4; 24-1 (I, II, IV, V, XIII, XIV, XVIII, XIX).<br>Figures 4-3, 4; 10-6; 11-3, 4; 16-2; 20-1, 2. |
| $NO^{+\ddagger}$ | Page 11-18.<br>Figures 10-6; 20-1. |
| $NO^{+*}$ | Tables 10-16; 20-1.<br>Figures 10-6; 20-2. |
| $NO^+(a\ ^3\Sigma^+)$ | Tables 10-16; 12-9a, 9b; 20-1.<br>Figures 10-6; 20-2. |
| $NO^+(a\ ^3\Sigma^+)^\ddagger$ | Figure 20-2. |

| | |
|---|---|
| $NO^+(A\ ^1\Pi)$ | Tables 10-16; 12-9a, 9b.<br>Figure 10-6. |
| $NO^+(A'\ ^1\Sigma^-)$ | Tables 10-16; 12-9a, 9b.<br>Figures 10-6; 20-2. |
| $NO^+(b\ ^3\Pi)$ | Tables 10-16; 12-9a, 9b; 20-1.<br>Figures 10-6; 20-2. |
| $NO^+(b'\ ^3\Sigma^-)$ | Tables 10-16; 12-9a, 9b.<br>Figures 10-6; 20-2. |
| $NO^+(w\ ^3\Delta)$ | Tables 10-16; 12-9a, 9b; 20-1.<br>Figures 10-6; 20-2. |
| $NO^+(W\ ^1\Delta)$ | Tables 10-16; 12-9a, 9b.<br>Figure 10-6. |
| $NO^+(CO_2)$ | Pages 18A-9, 10.<br>Tables 18A-3, 5; 24-1 (XIV, XVIII). |
| $NO^+(H_2O)$ | Pages 18A-9, 10.<br>Tables 18A-3, 5; 24-1 (IV, XIV, XVIII). |
| $NO^+(H_2O)_2$ | Page 18A-9.<br>Tables 18A-5; 24-1 (IV, XVIII). |
| $NO^+(H_2O)_3$ | Page 18A-9.<br>Tables 18A-3, 5; 24-1 (IV, XIV, XVIII). |
| $NO^+(NO)$ | Pages 16-10, 11, 14, 16.<br>Tables 16-1.1; 18A-3, 5; 24-1 (IV, XIV, XVIII, XIX). |
| $NO^+(N_2)$ | Page 20-8.<br>Table 18A-5. |
| $NO^+(O_2)$ | Table 18A-5. |
| $NO^{++}$ | Table 10-1. |
| $NO^-$ | Page 17-2.<br>Tables 10-1, 19; 17-5, 7; 18A-2, 4; 24-1 (XV, XVI).<br>Figure 10-6. |

$NON_2^+$ See $NO^+(N_2)$.

$NO_2$ Pages 5-18; 6-2; 16-16, 22; 17-6, 9; 18A-7, 9; 19-10, 11, 14.
Tables 9-5; 10-1, 20; 11-1; 12-2; 17-2, 4, 5, 7; 18A-1, 2, 4; 19-1; 20-1, 8; 24-1 (VII, VIII, IX, XII, XIII, XIV, XV, XVI, XXIII, XXIV, XXV, XXVII, XXVIII).

$NO_2^{\ddagger}$ Table 10-20.

$NO_2^*$ Page 19-11.
Tables 20-1; 24-1 (XXVIII).

$NO_2^+$ Page 18A-9.
Tables 10-1, 20; 18A-1; 24-1 (IV, XIII, XIV, XVIII).

$NO_2^{+\ddagger}$ Table 10-20.

$NO_2^-$ Pages 16-22, 24; 17-2, 9, 12; 18A-7.
Tables 10-1, 20; 16-1.2; 17-2, 5, 7; 18A-2, 4, 6; 21-4; 24-1 (V, VII, VIII, IX, XV, XVI, XXI).

$NO_2^{-\ddagger}$ Table 10-20.

$NO_2^-(H_2O)$ Tables 18A-6; 24-1 (XXI).

$NO_3$ Pages 18A-7; 19-14.
Tables 6-1; 19-1; 24-1 (XV, XXVII).

$NO_3^+$ See $NO^+(O_2)$.

$NO_3^-$ (Cf. $OONO^-$) Pages 5-5; 16-22; 17-2, 9, 12, 13; 18A-7; 21-20.
Tables 16-1.2; 17-2, 7; 18A-2, 4; 21-4; 24-1 (V, XV, XVI).

$NO_3^-(H_2O)$ Table 21-4.

$NO_3^-(H_2O)_n$ Pages 5-5; 17-2, 13; 21-20.

$N_2$ Pages 2-9, 10; 4-1, 8, 13; 6-8, 14, 15; 8-11, 12; 9-4, 12, 13, 31; 10-2, 4, 11-13, 14, 18, 27, 32; 12-6, 16, 17, 30; 13-(1-4); 14-1; 15-1, 21, 22, 25, (34-38); 16-8, 10, 22, 24; 17-3, 5, 8; 18A-(3-5), 7, 9; 19-4, (7-10), (12-14); 20-(3-10), 13, (15-17); 21-4, 5, 8, 15, 20, 25, 26, 28, 31; 22-1.
Tables 9-2, 3, 6, 7; 10-1, 13; 11-2; 12-(2-4), 6a, 6b; 13-1, 2, 4, 6; 14-(1-3), 15-1; 16-1.2; 17-(4-6); 18A-1, (3-7); 19-1; 20-1, 2, (4-6), (8-10); 21-(1-4); 24-1 (I, II, IV, IX, X, XII, XIII, XIV, XVI, XVIII, XXI, XXIII, XXIV, XXV, XXVI, XXVII, XXVIII, XXX, XXXII, XXXIII).
Figures 2-7; 4-1, 4, 8; 10-5, 8, 11; 12-7; 14-(29-41); 15-1, 2, (6-9); 20-1, 3, 4, 6; 21-1, 3, 4.

$N_2^{\ddagger}$ Pages 4-13; 5-17; 6-7; 11-14, 34; 19-7, 14; 20-(3-6); 21-4; 22-1.
Tables 9-6; 20-2, 3, 10; 24-1 (XXVII, XXXII, XXXIII).
Figures 10-5; 20-1, 3, 4.

$N_2^{*}$ Pages 20-3, (6-8).
Tables 10-13; 20-1, 10.
Figures 10-5; 20-1.

$N_2(a\ ^1\Pi_g)$ Tables 9-5, 6; 10-13; 20-1, 10.
Figure 10-5.

$N_2(a\ ^1\Pi_g)^{\ddagger}$ Table 20-10.

$N_2(a'\ ^1\Sigma_u^-)$ Tables 10-13; 20-1.
Figure 10-5.

$N_2(A\ ^3\Sigma_u^+)$ Pages 6-15; 20-3, (6-8).
Tables 9-6, 7; 10-13; 20-1, 4, 10; 24-1 (XXVIII, XXX).
Figures 10-5; 20-1.

$N_2(A\ ^3\Sigma_u^+)^{\ddagger}$ Pages 20-3, 7.
Figure 20-1.

$N_2(b'\ ^1\Sigma_u^+)$ Figure 10-5.

$N_2(B\ ^3\Pi_g)$ Pages 6-15; 20-6, 7.
Tables 9-5, 6; 10-13; 20-1, 10; 24-1 (XXV).
Figures 10-5; 20-1.

$N_2(B\ ^3\Pi_g)^{\ddagger}$ Figure 20-1.

$N_2(B'\ ^3\Sigma_u^-)$ Page 20-7.
Tables 9-5; 10-13; 20-1.
Figure 10-5.

$N_2(C\ ^3\Pi_u)$ Pages 20-6, 7.
Tables 9-5, 6; 20-10.
Figure 10-5.

$N_2(C\ ^3\Pi_u)^{\ddagger}$ Table 20-10.

$N_2(C'\ ^3\Pi_u)$ Figure 10-5.

$N_2(D\ ^3\Sigma_u^+)$ Page 20-7.

$N_2(E\ ^3\Sigma_g^+)$ Page 20-7.
Figure 10-5.

$N_2(h\ ^1\Sigma_u^+)$ Tables 9-6; 12-6a.

$N_2(w\ ^1\Delta_u)$ Tables 10-13; 20-1.
Figure 10-5.

$N_2(W\ ^3\Delta_u)$ Page 20-7.
Tables 10-13; 20-1.

$N_2(^1\Pi_u)$ Tables 12-6a, 6b.

$N_2(^5\Pi_u)$ Figure 10-5.

$N_2^+$ Pages 6-15; 8-12; 9-4, 11, 21, 31; 13-1, 3, 4; 14-1; 15-5, 43; 16-7, 8, 10, 18, 22; 18A-(4-7); 20-(6-10), 15, 17; 21-20.
Tables 9-2, 3, 6; 10-1, 14; 13-3, 5, 7; 14-1, 2; 16-1.1, 1.2; 18A-1, 3, 5, 7; 20-1, 9, 10; 21-4; 24-1 (I, II, IV, V, XIII, XIV, XVIII, XXX).
Figures 10-5; 12-7; 14-(30-37), 90; 16-1; 20-2.

$N_2^{+\ddagger}$ Pages 16-8; 20-10.
Figures 10-5; 20-2.

$N_2^{+*}$ Pages 20-8, 9.
Tables 10-14; 20-1, 10.
Figures 10-5; 20-2.

$N_2^+(A\ ^2\Pi_u)$ Pages 6-15; 20-6, 8, 9, 17.
Tables 9-5, 6; 10-14; 12-6a, 6b; 14-1; 20-1, 10; 24-1 (XXX).
Figures 10-5; 12-7; 14-(30-33); 20-2.

$N_2^+(A\ ^2\Pi_u)^\ddagger$ Page 20-17.
Figure 20-1.

$N_2^+(B\ ^2\Sigma_u^+)$ Pages 20-6, (8-10), 17.
Tables 9-5, 6; 10-14; 12-6a, 6b; 14-2; 20-1, 9, 10; 24-1 (XXX).
Figures 10-5; 12-7; 14-(34-37).

$N_2^+(C\ ^2\Sigma_u^+)$ Page 18A-4.
Table 10-14.
Figure 10-5.

$N_2^+(D\ ^2\Pi_g)$ Table 10-14.
Figure 10-5.

$N_2^+(^2\Delta_u)$ Figure 10-5.

$N_2^+(^4\Delta_u)$ Pages 20-8, 9.
Table 10-14.
Figure 10-5.

$N_2^+(^2\Pi_u)$ Figure 10-5.

$N_2^+(^4\Pi_g)$ Figure 10-5.

$N_2^+(^4\Pi_u)$ Figure 10-5.

$N_2^+(^2\Sigma_u^-)$ Figure 10-5.

$N_2^+(^4\Sigma_g^+)$ Figure 10-5.

$N_2^+(^4\Sigma_u^+)$ Pages 20-8, 9.
Tables 10-14; 20-1.
Figure 10-5.

$N_2^+(^4\Sigma_u^-)$ Table 10-14.
Figure 10-5.

$N_2^{++}$ Table 10-1.

$N_2^-$ Pages 4-13; 17-9; 20-3.
Figure 10-5.

$N_2^{-\ddagger}$ Figure 10-5.

$N_2H^+$ Tables 18A-1, 3; 24-1 (XIV).

$N_2O$ Pages 17-4, 6; 19-13, 14.
Tables 10-1, 20; 11-1; 12-2; 17-4; 18A-1, 4, 5, 7; 19-1; 20-2, 10; 24-1(XII, XIII, XVI, XXIV, XXV, XXVII).
Figures 11-1; 14-(82-88).

$N_2O^\ddagger$ Tables 10-20; 20-2, 10.

$N_2O^*$ Page 4-13.

$N_2O^+$ Tables 10-1, 20; 18A-1, 5, 7; 24-1 (XIII, XVIII).
Figures 14-(83-85).

$N_2O^{+\ddagger}$ Table 10-20.

$N_2O^{+*}$ Figures 14-(83-85).

$N_2O^-$ Page 17-9.
Tables 18A-4, 6; 24-1 (XVI, XXI).

$N_2O_2^+$ See $NO^+(NO)$ and $O_2^+(N_2)$.

$N_2O_2^-$ See $O_2^-(N_2)$.

$N_2O_3^+$ See $O_2^+(N_2O)$.

| | |
|---|---|
| $N_3^+$ | Pages 16-7, 8, 10; 20-9.<br>Tables 18A-3; 21-4; 24-1 (IV, XIV, XVIII). |
| $N_4^+$ | Pages 16-7, 10, 16; 18A-7.<br>Tables 16-1.1; 18A-1, 3, 5; 21-4; 24-1 (IV, XIV, XVIII).<br>Figure 16-1. |
| Na | Pages 5-19; 18A-3, 6; 20-7.<br>Tables 8-2; 9-6; 18A-1, 3, 7; 20-10; 24-1 (XIII, XIV).<br>Figures 15-2; 20-1. |
| $Na^*$ | Tables 9-5; 20-1, 10. |
| $Na^+$ | Pages 16-18, 23; 18A-6; 20-18.<br>Tables 16-1.1; 18A-1, 3, 5, 7; 24-1 (XIII).<br>Figure 20-1. |
| $Na^+(CO_2)$ | Table 18A-5. |
| $Na^+(CO_2)_2$ | Table 18A-5. |
| $NaO^+$ | Tables 18A-3; 24-1 (XIV). |
| Ne | Pages 15-25, 43, 44; 16-8, 10, 11, 14, 16, 24.<br>Tables 8-2; 15-1.<br>Figures 15-1, 2. |
| $Ne^*$ | Page 16-8. |
| $Ne^+$ | Pages 15-34, 39, 43; 16-18.<br>Table 16-1.1. |
| $Ne^{++}$ | Page 15-43. |
| $Ne^{3+}$ | Page 15-43. |
| $Ne^{4+}$ | Page 15-43. |
| $Ne^{5+}$ | Page 15-43. |
| $Ne_2^+$ | Page 16-16. |

| | |
|---|---|
| O | Pages 2-9, 10; 3-33, 34; 4-13, 15; 5-18; 6-2, 8, 12, 14, 15; 7-7; 8-7, 8, 10, 11; 9-12, 13, 15, 30, 31; 10-4; 11-13, (16-20), 31, 32; 12-6, (8-23), 30; 13-1, 3, 4; 15-1, 6, 15, 25, (29-33); 16-10, 11, 16; 17-2, 6, 9, 12, 14; 18A-5, 6, 8; 19-(2-14); 20-3, 6, 7, (10-12), (14-18); 21-6, 16, 20, 25, 29.<br>Tables 6-1; 8-2; 9-(2-6); 10-1, 8; 12-(1-5), 7a, 7b, 8a, 8b; 13-1, 2, 4, 6; 15-2; 17-(1-4), 6, 7; 18A-(1-4), 6, 7; 19-1; 20-1, 2, (4-7), 9, 10; 21-(1-4); 24-1 (I, II, IV, V, VII, VIII, IX, X, XI, XII, XIII, XIV, XV, XVI, XVIII, XXIII, XXIV, XXV, XXVI, XXVII, XXVIII, XXX, XXXII).<br>Figures 2-7; 4-1, 7; 10-3, 6, 7, 10; 12-(8-10); 14-2, (7-9); 15-(1-4); 20-1, 4, 6, 9; 21-1, 4. |
| $O^*$ | Pages 12-(17-23).<br>Tables 10-8; 12-5; 20-1, 7, 10.<br>Figures 10-3; 12-8, 9; 20-1, 9. |
| $O(^1D)$ | Pages 4-13; 5-17, 18; 6-15; 8-10; 12-9, 21, 27, 28; 16-16; 19-14; 20-3, 4, 12, (14-16); 22-1.<br>Tables 9-(5-7); 12-3, 5, 7a, 7b; 20-1, 7, 8, 10; 24-1 (IV, XXIV, XXVII, XXVIII, XXX).<br>Figures 4-2, 4, 5; 10-6, 7, 10; 20-1, 9. |
| $O(4\ ^3P)$ | Table 9-5. |
| $O(^5P)$ | Table 9-6. |
| $O(^1S)$ | Pages 5-18; 8-10; 9-31; 12-21; 16-16; 19-14; 20-4, 14, 15.<br>Tables 9-(5-7); 12-7a, 7b; 20-1, 7, 10; 24-1 (IV, XXV, XXVIII, XXX).<br>Figures 10-6, 7; 12-10; 20-1, 9. |
| $O(^3S)$ | Tables 9-5, 6; 20-1. |
| $O(^5S)$ | Tables 9-5, 6; 20-1.<br>Figure 20-1. |
| $O^+$ | Pages 4-6; 6-7, 14, 15; 8-2, 8; 9-(11-13), 15; 10-4; 12-14, 21; 13-3, 4; 15-31, 34, 39, (43-45), 47; 16-18, 22, 23; 18A-5; 20-5, 11, (15-17). |

| | |
|---|---|
| $O^+$ (Cont'd.) | Tables 9-2, 3, 5, 6; 10-1, 9; 12-1, 7b, 8a, 8b; 13-3, 5, 7; 16-1.1, 1.2; 18A-1, 3, 5, 7; 20-1, 3; 21-4; 24-1 (I, II, V, XIII, XIV, XVIII, XXVIII, XXX). |
| | Figures 4-3, 4; 10-4, 6, 7; 12-8, 10, 11; 14-8, 64, 73, 74; 20-2, 4. |
| $O^{+*}$ | Pages 12-20, 21; 20-(15-17).<br>Tables 10-9; 20-1.<br>Figures 10-4; 12-(8-11); 20-2. |
| $O^+(^2D)$ | Pages 6-15; 12-20; 20-8, (16-18).<br>Tables 9-3, 6; 12-8a, 8b; 20-1, 9, 10; 24-1 (II, XIII, XXVIII, XXX).<br>Figures 10-7; 12-8, 9, 11; 14-73; 20-2. |
| $O^+(^2P)$ | Pages 12-21; 20-16, 17.<br>Tables 9-6; 12-8a, 8b; 20-1; 24-1 (II, XXVIII).<br>Figures 12-(9-11). |
| $O^+(^4P)$ | Figure 14-74. |
| $O^{++}$ | Page 15-43.<br>Tables 10-1; 12-1. |
| $O^{3+}$ | Page 15-43. |
| $O^-$ | Pages 5-7; 6-12, 14; 8-7; 9-15, 30; 10-3; 11-25; 16-22, 23; 17-2, 4, 5, 8, 9, 12, 13; 18A-3; 20-11, 13.<br>Tables 10-1, 7; 16-1.2; 17-(1-4), 6, 7; 18A-2, 4, 6; 20-10; 24-1 (V, VII, VIII, IX, X, XI, XII, XV, XVI, XX, XXI).<br>Figures 10-6, 7, 9; 14-2. |
| $O^{-*}$ | Table 10-7. |
| $O^-(CO_2)$ | See $CO_3^-$. |
| $O^-(H_2O)$ | Tables 18A-6; 24-1 (XXI). |
| OCS | Page 19-6. |

| | |
|---|---|
| OH | Pages 7-7; 11-1, 16, 17; 17-2, 18A-8; 19-3, 12; 20-16; 21-6.<br>Tables 6-1; 10-1, 19; 11-1; 17-(1-3); 18A-(1-3); 19-1; 20-10; 24-1(VII, VIII, XIII, XIV, XV, XIX, XXIV, XXV, XXVII).<br>Figure 4-6. |
| $OH^{\ddagger}$ | Pages 11-(15-17).<br>Tables 9-5; 20-10. |
| $OH^{*}$ | Page 12-29.<br>Tables 10-19; 20-10. |
| $OH^{+}$ | Tables 10-1, 19; 18A-1, 3; 24-1 (XIII, XIV).<br>Figure 14-64. |
| $OH^{+*}$ | Table 10-19. |
| $OH^{-}$ | Page 17-2.<br>Tables 10-1, 19; 17-1, 2, 7; 18A-2, 4; 24-1 (VII, VIII, XII, XV). |
| $OH^{-}(H_2O)$ | Table 17-7. |
| $OONO^{-}$<br>(Cf. $NO_3^{-}$) | Page 18A-7.<br>Tables 18A-4; 24-1 (XVI). |
| $O_2$ | Pages 2-9, 10; 3-33, 38; 4-1, 6, 8, 10, 15; 5-19; 6-2, 8, 12, 14, 15; 8-11; 9-12, 15, 30; 10-2, 4; 11-(13-20), 27, 32, 33; 12-(6-16), 20, 27 28, 30; 13-1, 3, 4; 15-1, 21, 34, 36, (39-43), 46, 47; 16-14, 15, 17, 22, 23; 17-2, 4, (6-8), 12, 14, 17; 18A-(5-9); 19-(4-6), (8-14); 20-6, (9-18); 21-4, 5, 8, 16, 20, 25, 27, 28.<br>Tables 9-2, 4, 6, 7; 10-1, 17; 11-2; 12-(1-4), 7a, 7b; 13-1, 2, 4, 6; 15-1; 16-1.2; 17-(1-7); 18A-(1-7); 19-1; 20-1, 2, (4-6), (8-10); 21-(1-4); 24-1 (I, II, IV, VII, VIII, IX, X, XI, XII, XIII, XIV, XV, XVI, XVIII, XIX, XX, XXI, XXII, XXIII, XXIV, XXV, XXVI, XXVII, XXVIII, XXIX, XXX, XXXII, XXXIII).<br>Figures 2-7; 3-7; 4-1, 4, (6-8); 10-7, 8, 11; 11-(8-10); 12-(1-6); 14-(45-61); 15-1, 2, (6-8); 20-1, 4 (6-8); 21-1, 3, 4. |

| | |
|---|---|
| $O_2^{\ddagger}$ | Pages 4-15; 8-11; 11-19; 19-7, 14; 20-11, 18; 21-4, 16.<br>Tables 9-3; 20-2, 5, 10; 24-1 (XXXII, XXXIII).<br>Figures 10-7; 20-1, 6, 7. |
| $O_2^{*}$ | Pages 20-12, 18; 21-16.<br>Tables 10-17; 12-1; 20-1, 10.<br>Figures 10-7; 20-1, 8. |
| $O_2(a\ ^1\Delta_g)$ | Pages 5-8, 18; 6-15; 11-19; 12-6, 7, 14, 16, 27, 28; 13-2; 17-8; 18A-3; 19-5, 14; 20-12, 13.<br>Tables 9-(5-7); 10-17; 12-2; 17-4, 6; 20-1, 6, 10; 24-1 (X, XII, XV, XXIV, XXVI, XXVII, XXVIII, XXIX, XXX).<br>Figures 4-2, 4, 5; 5-4; 10-7; 20-1, 8. |
| $O_2(a\ ^1\Delta_g)^{\ddagger}$ | Figure 20-1. |
| $O_2(A\ ^3\Sigma_u^+)$ | Page 20-12.<br>Tables 9-5; 10-17; 20-1, 10; 24-1 (XXIII, XXV).<br>Figure 10-7. |
| $O_2(A\ ^3\Sigma_u^+)^{\ddagger}$ | Table 20-10. |
| $O_2(b\ ^1\Sigma_g^+)$ | Pages 6-15; 11-19; 12-16; 19-5, 14; 20-12, 13.<br>Tables 9-(5-7); 10-17; 20-1, 10; 24-1 (XXIII, XXIV, XXV, XXVI, XXVIII, XXIX, XXX).<br>Figures 10-7; 20-1, 8. |
| $O_2(b\ ^1\Sigma_g^+)^{\ddagger}$ | Page 20-12.<br>Figure 20-1. |
| $O_2(B\ ^3\Sigma_u^-)$ | Page 20-12.<br>Tables 10-17; 20-1; 24-1 (XXIII).<br>Figures 10-7; 20-1. |
| $O_2(B\ ^3\Sigma_u^-)^{\ddagger}$ | Figure 20-1. |
| $O_2(c\ ^1\Sigma_u^-)$ | Page 20-12.<br>Tables 10-17; 20-1.<br>Figure 10-7. |
| $O_2(C\ ^3\Delta_u)$ | Tables 10-7; 20-1.<br>Figure 10-7. |

$O_2^+$ Pages 4-6; 5-7; 6-15; 8-12; 9-11, 12, 31; 13-3, 4; 15-43; 16-7, (14-16), 18, 22; 18A-(5-8); 20-9, 10, 14, 17; 21-20.
Tables 9-2; 10-1, 18; 12-1, 7a, 7b; 13-3, 5, 7; 16-1.1, 1.2; 18A-1, 3, 5, 7; 20-1, 7, 9, 10; 21-4; 24-1 (I, II, IV, V, XIII, XIV, XVIII, XIX).
Figures 4-3, 4; 10-7; 12-5; 14-(46-58), 64; 16-3; 20-2.

$O_2^{+\ddagger}$ Page 16-14.
Figures 10-7; 20-2.

$O_2^{+*}$ Page 20-9.
Tables 10-18; 20-1, 10.
Figures 10-7; 20-2.

$O_2^+(a\ ^4\Pi_u)$ Pages 6-15; 16-14, 16; 20-9, 17.
Tables 9-6; 10-18; 12-7a, 7b; 18A-1; 20-1; 24-1 (XIII).
Figures 10-7; 12-6; 14-(54-58); 20-2.

$O_2^+(a\ ^4\Pi_u)^\ddagger$ Page 20-17.
Figure 20-2.

$O_2^+(A\ ^2\Pi_u)$ Pages 6-15; 20-17.
Tables 10-18; 12-7a, 7b; 20-1; 24-1 (XIII).
Figures 10-7; 12-6; 14-(47-53); 20-2.

$O_2^+(A\ ^2\Pi_u)^\ddagger$ Figure 20-2.

$O_2^+(b\ ^4\Sigma_g^-)$ Pages 6-15; 20-9.
Tables 9-6; 10-18; 12-7a, 7b; 20-1.
Figures 10-7; 12-5; 14-(54-58).

$O_2^+(c\ ^4\Sigma_u^-)$ Figure 10-7.

$O_2^+(^2\Delta_g)$ Figure 10-7.

$O_2^+(^2\Sigma_g^-)$ Figures 10-7; 12-5.

$O_2^+(^2\Phi_u)$ Figure 10-7.

$O_2^+(CO_2)$ Table 18A-5.

| | |
|---|---|
| $O_2^+(H_2O)$ | Page 18A-8.<br>Tables 18A-3, 5; 24-1 (IV, XIV, XVIII). |
| $O_2^+(N_2)$ | Tables 18A-3, 5; 24-1 (XIV, XVIII). |
| $O_2^+(N_2O)$ | Table 18A-5. |
| $O_2^+(O_2)$ | See $O_4^+$. |
| $O_2^{++}$ | Table 10-1. |
| $O_2^-$ | Pages 5-7; 6-12; 9-30; 16-22; 17-2, 4, (7-9), (12-14); 18A-3, 7; 20-13.<br>Tables 9-4; 10-1, 19; 12-1; 16-1.2; 17-1, 2, (4-7); 18A-2, 4, 6; 20-10; 21-4; 24-1 (V, VII, VIII, IX, X, XI, XII, XV, XVI, XXI, XXII).<br>Figures 10-7, 9. |
| $O_2^-(CO_2)$ | See $CO_4^-$. |
| $O_2^-(H_2O)$ | Pages 17-2, 9, 17.<br>Tables 17-7; 18A-4, 6; 24-1 (XVI, XXI). |
| $O_2^-(H_2O)_2$ | Tables 17-7; 18A-6; 24-1 (XXI). |
| $O_2^-(H_2O)_3$ | Table 17-7. |
| $O_2^-(H_2O)_4$ | Table 17-7. |
| $O_2^-(H_2O)_5$ | Table 17-7. |
| $O_2^-(H_2O)_n$ | Page 17-16. |
| $O_2^-(N_2)$ | Tables 18A-6; 24-1 (XXI). |
| $O_2^-(O_2)$ | See $O_4^-$. |
| $O_3$ | Pages 4-15; 5-18; 6-2, 12; 9-30; 11-1, 11, 15, 17, 19; 12-6, 24, 27; 17-2, 4, 9, 12; 18A-6, 8; 19-2, (4-8), 14; 20-12, 13; 21-17.<br>Tables 10-1, 20; 11-1; 12-2; 17-(1-4), 7; 18A-(2-4); 19-1; 20-6, 10; 21-2; 24-1 (VII, VIII, XI, XII, XIV, XV, XVI, XXIV, XXV, XXVI, XXVII, XXX).<br>Figures 4-2, 7, 8; 11-1, 2; 12-14, 15; 21-3. |

| | |
|---|---|
| $O_3^{\ddagger}$ | Page 11-19.<br>Table 10-20. |
| $O_3^{+}$ | Page 16-14.<br>Tables 10-1, 20; 24-1 (XVIII). |
| $O_3^{+\ddagger}$ | Table 10-20. |
| $O_3^{-}$ | Pages 17-2, 9, 12.<br>Tables 10-1, 20; 17-1, 2, 4, 7; 18A-2, 4, 6; 21-4; 24-1 (VII, VIII, XII, XV, XVI, XX, XXI). |
| $O_3^{-\ddagger}$ | Table 10-20. |
| $O_3^{-}(H_2O)$ | Tables 18A-6; 24-1 (XXI). |
| $O_4^{*}$ | Page 20-13. |
| $O_4^{+}$ | Pages 16-14, 16; 18A-(6-8).<br>Tables 16-1.1; 18A-3, 5; 21-4; 24-1 (IV, XIV, X III, XIX). |
| $O_4^{-}$ | Pages 17-9, 14, 17; 18A-7.<br>Tables 17-7; 18A-4, 6; 21-4; 24-1 (XVI, XXI, XXII). |
| $P^{+}$ | Page 16-18.<br>Table 16-1.1. |
| $PH_2^{-}$ | Page 7-9. |
| Pt | Page 7-22. |
| $Rb^{+}$ | Page 15-36. |
| $S^{+}$ | Page 16-18.<br>Table 16-1.1. |
| $SF_5^{-}$ | Page 17-18.<br>Table 17-7. |
| $SF_6$ | Pages 17-17, 18.<br>Table 17-7. |

| | |
|---|---|
| $SF_6^-$ | Pages 16-24; 17-18.<br>Table 17-7. |
| SH | See HS |
| $SH^-$ | See $HS^-$. |
| $Sb^+$ | Pages 15-37, 41. |
| $Si^+$ | Pages 4-15; 16-18; 18A-5; 20-18.<br>Tables 9-3; 18A-3.<br>Figure 20-1. |
| $SiO^+$ | Pages 18A-5; 20-18.<br>Tables 9-3; 16-1.1; 18A-3. |
| Sr | Page 15-21.<br>Figures 15-1, 2, 5, 7. |
| $Sr^+$ | Pages 15-36, 40.<br>Table 15-1. |
| Teflon(s) | Page 19-4. |
| Te | Figure 15-1. |
| U | Pages 15-1, 21, 25.<br>Figures 15-2, 6. |
| $U^+$ | Pages 15-25, 38, 42.<br>Table 15-1. |
| UO | Table 11-1. |
| W | Page 7-22. |
| Xe | Pages 7-22; 15-30; 16-24.<br>Tables 16-1.2; 20-8.<br>Figures 15-1, 2. |
| $Xe^+$ | Pages 15-32, 37, 41. |

# APPENDIX G
# AUTHOR INDEX*

Aarsnes, K.: 9-104

Aarts, J. F. M.: 14-(3687), (4220)

Aberth, W. H.: 7-48, 63; 16-53, 54, 55, 56, 59, 60, 61

Ablow, C. M.: 21-65

Abraham, G.: 20-62

Abramowitz, S.: 11-14

Accardo, C. A.: 9-51

Ackerman, M.: 7-35; 12-13; 13-13, 15

Ackerman, R. A.: 20-158

Acquista, N.: 11-13

Adams, K. B.: 10-46

Adams, N. G.: 17-43; 18-38, 45

Aikin, A. C.: 9-55, 98

Aitken, K. L.: 7-56; 16-63

Akasofu, S. I.: 9-14

---

* Included in Chapters 3 and 14 are supplementary bibliographies. Those works listed in Chapter 3 are listed in alphabetical order by senior author. Those listed in Chapter 14 are listed in parentheses by a JILA (Joint Institute for Laboratory Astrophysics) Information Center number which should be used in any correspondence with JILA or the authors of Chapter 14.

Papers and books of general interest in the field of coverage of Chapter 3, i.e., aside from the specific reference to material quoted in the text, are designated by an asterisk, *.

Alberti, F.: 12-38

Albritton, D. L.: 7-25; 10-55; 17-36; 18-13, 14; 20-163

Ali, A. W.: 12-55; 15 (Author); 20-64

Al-Joboury, M. I.: 7-79, 80

Allen, E. F.: 5-31

Allison, A. C.: 8-35, 41

Allison, S. K.: 15-1, 2

Altshuler, S.: 21-15

Amdur, I.: 7-34

Amme, R. C.: 20-130

Anderson, A. D.: 11-49

Anderson, H. C.: 3 (Supp.)*

Anderson, J. B.: 6-19; 20-200

Ankudinov, V. A.: 15-52

Anlauf, K.: 11-27; 20-220

Appleton, E. V.: 9-1

Appleton, J. A.: 12-41

Appleton, J. P.: 24-18

Archer, D.: 5 (Author)

Armstrong, E. B.: 20-48; 24-38

Arnold, J.: 6-16

Arnold, S. J.: 20-168; 24-47

Arnt, D.: 21-28

Arshadi, M.: 17-42

Arthurs, A. M.: 8-34

Ashby, R. A.: 12-38

Ashmore, P. G.: 19-33

Asundi, R. K.: 10-30; 14-(743), (938), (2763)

Attwood, D.: 19-37

Aubrey, B. B.: 21-7

Awajobi, O. A.: 9-34

Axworthy, A. E., Jr.: 19-4

Bachynski, M. P.: 21-10

Badger, R. M.: 20-32

Bahr, J. L.: 12-88

Baiamonte, V.: 6-17

Bailey, A. D.: 9-19, 27; 17-10; 20-203; 21-61

Bailey, D. K.: 9-22

Bailey, T. L.: 17-25

Bailey, V. A.: 21-16

Bair, E.: 6-17

Baisley, V. C.: 12-72

Baker, A. D.: 7-78

Baker, C.: 7-78

Baker, D. M.: 3-33; 20-166

Baker, K.: 20-166

Baldeschwieler, J. D.: 7-22

Baldwin, R. R.: 19-33

Bamford, C. H.: 11-18 (Ed.)

Banks, P.: 21-70

Bardsley, J. N.: 8-15, 21, 61, 64; 11-66; 16-28; 17-39, 60

Barrow, R. F.: 10-32

Barth, C. A.: 9-74, 92; 19-35; 20-69

Bascc, N.: 20-217

Bates, D. R.: 4-4 (Ed.); 7-9 (Ed.), 57 (Ed.), 89 (Ed.); 8-1, 4, 6, 7, 8, 9, 10, 12, 14, 16, 17, 25, 26, 30; 9-25; 11-68, 69; 15-2 (Ed.), 4, 19, 20 (Ed.), 32; 16-42 (Ed.), 43; 17-21; 20-4, 43, 76, 235

Baulch, D. L.: 15-54; 24-15, 35, 32

Baum, C. E.: 21-58

Baurer, E.: 3 (Author)-2, 44; 4 (Author)-14, 15; 20-6, 7, 55, 56, 80, 143, 222, 232

Baurer, T.: 1 (Author); 6 (Author); 19-37; 23 (Author); 24 (Author)

Bayes, K.: 20-135

Beaty, E. C.. 10-36; 17-5, 44, 45; 21-41; 24-3

Beauchamp, J. L.: 7-20, 21; 21-74

Becker, R. A.: 7-70; 12-42

Bederson, B.: 7-2 (Ed.), 58 (Ed.); 21-7

Bekefi, G.: 21-45

Bell, G.: 15-13

Belles, F. E.: 20-236

Belon, A. E.: 9-11

Belrose, J. S.: 5-14; 9-95; 21-29

Belyaev, V. A.: 7-61

Benesch, W.: 10-52; 20-19

Bennett, R. A.: 17-40, 62

Bennett, W. R.: 20-46 (Ed.)

Benson, S. W.: 19-4

Berkowitz, J.: 7-85; 17-58

Berlande, J.: 16-47

Berning, W. W.: 9-53

Bernstein, R.: 20-220

Berry, R. E.: 16-40

Berry, R. S.: 7-64; 8-75; 10-14, 43; 16-62

Bethe, H. A.: 11-44

Bethke, G. W.: 12-15

Beyer, R. A.: 18-65, 66

Beynon, W. J. G.: 9-58 (Ed.), 62 (Ed.)

Biaume, F.: 12-13

Biberman, L. M.: 11-50

Biondi, M. A.: 7-1, 2, 3, 26, 27, 28; 8-15; 9-26, 28, 32; 16 (Author)-1, 2, 4, 8, 10, 12, 14, 15, 16, 21, 24, 29, 30, 37; 17-28, 31; 18-23, 24; 21-71; 24-6

Bird, R. B.: 3-4*; 4-18; 20-96; 11-22

Birely, J. H.: 7-38; 9-5

Birkinshaw, K.: 7-15

Bitterman, S.: 11-20; 20-82

Bjelland, B.: 9-99

Black, G.: 6-18; 9-122, 126, 130; 12-22; 20-121, 136, 150, 169, 176, 185, 219; 24-11, 17, 40, 44

Blake, A. J.: 12-9, 33, 88

Blake, H. A.: 9-18, 64

Blank, C. A.: 1 (Author); 23 (Author)

Blickensderfer, R. P.: 17-64

Blumen, W.: 3-38

Boerboom, A. J. H.: 14-(1782)

Boese, R. W.: 20-33

Bohme, D. K.: 8-39; 17-43; 18-5, 7, 8, 26, 36, 38, 45

Bohr, N.: 15-11, 12

Boksenberg, A.: 14-(1106)

Bolden, R. C.: 7-11

Bomke, H. A.: 9-18, 64

Boness, M. J. W.: 10-59; 21-6

Bonnet, R. M.: 13-12

Bonomo, F. S.: 11-8

Booker, H. G.: 21-72

Born, G. H.: 16-45

Borst, W. L.: 11-4; 14-(4080), (4125)

Bortner, M. H.: 1 (Author); 3 (Supp.)*; 4 (Author)-1, 2, 12, 14; 6 (Author)-1, 2, 20, 21; 11-43; 16-65; 20-56, 95, 162, 164; 23 (Author); 24 (Author)-46

Bourdeau, R. E.: 9-55

Bourene, M.: 19-50

Bourne, J. A.: 21-35

Bowen, I. S.: 10-44; 12-86

Bowers, M. T.: 7-21

Bowhill, S. A.: 9-60

Boyle, J. W.: 11-36

Brackman, R. T.: 8-66; 15-8, 9, 10, 43, 44, 46; 14-(320), (323); 17-16; 20-133, 138, 209

Bradbury, J. N.: 9-66

Bragin, Yu. A.: 9-90

Branscomb, L. M.: 5-29; 7-88, 89, 90; 10-12, 31; 14-(2904); 17-1, 2, 3, 4, 5, 8, 37

Bransden, B. H.: 8-33

Brauman, J. I.: 7-23

Breig, E. L.: 11-30

Breshears, D.: 4-18; 11-22; 20-96

Brewer, L.: 10-18

Brezhnev, B. G.: 7-61

Briglia, D. D.: 14-(1410), (1451), (1460)

Brinton, H. C.: 9-29, 83

Brix, P.: 10-28

Broadfoot, A. L.: 20-104

Brocklehurst, B.: 21-33

Broida, H. P.: 7-93; 20-225

Brooks, C. T.: 19-33

Brooks, J. N.: 11-21

Brouillard, F.: 7-62

Brown, G. M.: 9-58 (Ed.), 62 (Ed.)

Brown, H. L.: 7-27, 28; 18-24

Brown, R. L.: 8-74

Brown, S. C.: 16-16; 20-178; 21-45

Browne, J. C.: 8-23

Browne, J. D.: 8-41

Brueckner, K. A.: 17-13

Brundle, C. R.: 7-78

Bryant, D. A.: 9-104

Bubert, H.: 20-27

Bucel'nikova, N. S.: 14-(766); 17-15

Budzinski, E. E.: 9-69

Bunn, F. E.: 11-1

Burch, D. S.: 19-36

Burgers, J. M.: 3-5

Burgess, A.: 8-3; 11-54; 15-20

Burhop, E. H. S.: 16-48

Burke, P. G.: 8-45, 47; 20-179; 21-20

Burns, D. J.: 14-(1214), (3246)

Burns, K.: 10-46

Burrow, P. D.: 20-71

Burt, J. A.: 17-36; 18-13; 20-163

Burt, P. B.: 21-15

Buttrill, S. E.: 7-20

Byerly, R., Jr.: 10-36; 17-44; 24-3

Bykhouoskii, V. K.: 8-40

Cadle, R. D.: 6-11; 20-51

Cahill, R. W.: 11-37

Cahn, J.H.: 21-3
Cairns, R.B.: 7-76; 12-26, 27, 48, 75, 80, 89; 13-16
Caledonia, G.: 11-67; 21-21
Calfee, R.F.: 11-5
Callear, A.B.: 11-18; 20-73
Camac, M.: 11-10
Campbell, E.S.: 19-6
Campbell, I.M.: 19-21, 57; 20-231
Caplinger, E.: 14-(1268)
Carabetta, R.A.: 11-43; 20-234
Carleton, N.P.: 14-(992); 20-16, 127, 186, 226; 21-39
Carlston, C.E.: 15-46
Carrier, G.: 10-9
Carrington, T.: 20-65
Carroll, P.K.: 12-14, 59
Carruthers, J.A.: 21-30
Carter, V.L.: 12-11, 24, 43
Cartwright, D.C.: 8-48; 20-112, 113, 114, 115
Carver, J.H.: 12-9, 33, 88
Castellano, E.: 19-8
Celotta, R.J. et al: 10-27; 17-40, 62
Cermak, V.: 7-51; 8-36; 20-120, 126
Cetiner, E.: 5-14
Chamberlain, G.E.: 14 (Author)
Chamberlain, J.W.: 9-108; 11-26; 20-47, 152
Champion, K.S.W.: 2 (Author); 16-17
Chaney, E.L.: 20-216
Chanin, L.M.: 17-28; 21-71
Chantry, P.J.: 17-17, 50, 61

Chapman, S.: 3-19*, 58, 59; 9-14; 20-175; 21-15, 75

Charters, P. E.: 11-28

Chasseriaux, J. M.: 3 (Supp.)

Chen, C. L.: 17-61; 21-23

Chen, J. C. Y.: 8-20, 22, 54, 59; 17-24; 20-60, 140; 21-48

Cher, M.: 20-228

Cheret, M.: 16-46, 47

Chibisov, M. I.: 11-64; 17-38

Childs, W.: 20-34

Chilton, C. J.: 9-54

Chimonas, G.: 3-39

Ching, B. K.: 7-70; 12-42

Christophorou, L. G.: 17-48; 20-216

Chubb, T. A.: 9-73

Chupka, W. A.: 7-17; 17-58

Churchill, D. R.: 11-62

Ciolkowski, S.: 19-37

Clark, I. D.: 9-120; 12-39; 20-154, 156, 159, 181, 196; 24-37, 42

Clark, M. A.: 9-107

Clark, T. C.: 20-78

Clarke, E. M.: 14-(2784), (2954)

Clayton, C. R.: 17-60

Clough, S. A.: 11-11

Clow, R. P.: 7-24

Clyne, M. A. A.: 19-10, 18, 26, 32, 40, 56

Cohen, N.: 24-13

Cohen, R. S.: 21-13

Cohen, V. W.: 7-58 (Ed.)

Colegrove, D. G.: 3-60, 61

Colgate, S. O.: 7-34
Collins, C. B.: 11-72
Comeaux, A. R.: 7-84; 15-46
Comes, F. J.: 12-49, 57
Compton, D. M. J.: 18-22
Compton, R. N.: 17-48
Conneely, M. J.: 8-47
Conner, J. P.: 9-54
Connor, T. R.: 16-14
Conrath, B. J.: 11-41
Conway, D. C.: 17-45
Cook, C. J.: 7-63; 16-53; 20-20
Cook, G. R.: 7-70; 10-29; 12-17, 29, 31, 42; 20-160
Cooper, J.: 17-11
Copeland, G. E.: 20-40
Copsey, M. J.: 7-5
Corrigan, S. J. B.: 14-(1566), (1771)
Cosby, P.: 20-141
Cottrell, T. L.: 21-55
Courtier, G. M.: 9-104
Cowling, T. G.: 21-15, 75
Coyne, T. N. R.: 21-35
Craggs, J. D.: 14-(357), (938)
Craig, R. A.: 3 (Supp.)
Crain, C. M.: 21-72
Crawford, O. H.: 21-15
Crompton, R. W.: 21-42
Cummings, F. W.: 20-80, 222
Curran, R. K.: 17-20

Curtiss, C. F.: 3-4*

Cvetanovich, R. J.: 20-188, 189, 190; 24-24

Dale, F.: 7-47; 18-17, 55

Dalgarno, A.: 6-3, 4, 10; 7-51; 8 (Author)-6, 19, 23, 32, 35, 36, 41, 50, 51, 69; 9-24, 37, 40, 85, 102, 105, 138, 139; 12-47; 15-16, 18, 31, 33; 16-42; 17-21; 20-48, 77, 92, 111, 207; 21-15, 36, 37; 21-40, 47, 52, 78; 24-38, 45

Dance, D. F.: 7-54; 14-(2788), (2790); 17-37

Danilov, A. D.: 3-66*

Davies, K.: 3-33

Davidovitz, P.: 20-71

Davidson, G. T.: 9-4; 21-33

Davidson, N.: 19-5

Davis, F. J.: 21-5

Decker, L. J.: 19-11

Degen, V.: 10-54; 20-35

Degges, T. C.: 11-35; 15-16; 21-52

de Heer, F. J.: 7-92; 14-(1281), (1782), (3687), (4220)

Dehmel, R. C.: 15-29, 30

de Jager, C.: 5-2 (Ed.)

Delcroix, J. L.: 3-1*

Delgreco, F. P.: 11 (Author)

Della Lucca, L.: 9-19; 17-10; 21-61

Deloche, R.: 16-45, 47

DeMore, W. B.: 12-70; 20-192, 193, 195

Denkov, Yu. N.: 8-65

Despain, A.: 20-166

Detwiler, C. R.: 13-11

Diaber, J. W.: 21-19

Dibeler, V. H.: 10-33, 35

Dick, K. A.: 9-110

Dickinson, P. H. G.: 9-31

Dickinson, R. E.: 3-25*, 26*

Dingle, R. B.: 21-28

Ditchburn, R. W.: 8-67; 12-8

Dmitriev, I. S.: 15-50, 51, 56

Doering, J. P.: 16-5

Doherty, R. H.: 9-135

Dolder, K. T.: 7-52, 53; 14-(261), (4344)

Donahue, T. M.: 9-56, 137, 140; 11-4

Donley, J. L.: 9-55

Donnally, B. L.: 20-230

Donohoe, J.: 21-17

Donovan, R. J.: 20-45; 24-23

Doolittle, P. H.: 12-32

D'Orazio, L. A.: 17-41

Dorfman, L. M.: 19-19

Dorman, F. H.: 10-20, 23

Dougal, A. A.: 21-14

Doughty, N. A.: 11-56

Douglas, A. E.: 10-17

Dowell, J. T.: 20-144

Downing, F. A.: 21-33

Drayson, S. R.: 4-7

Dressler, K.: 10-26

Drysdale, D. D.: 19-54; 24-16, 32, 35

Dunkin, D. B.: 9-78, 84, 88; 17-43, 51; 18-4, 5, 7, 8; 4-5, 38, 43, 48, 50, 56

Dunn, G. H.: 7-55, 58; 14-(2171), (2772)

Durana, S. C.: 24-10

Durden, D.A.: 18-19, 20

Dutsch, H.U.: 12-65

Dyce, R.B.: 5-20

Eather, R.H.: 9-10, 111, 112, 115

Eckart, C.* 3-18*

Edelson, D.: 21-68

Edmonds, R.S.: 9-53

Edquist, O., et al: 10-53; 20-28

Ehrhardt, H.: 7-85; 14-(3252); 15-59

Eichmeier, J.: 21-80

Eisner, P.N.: 7-94, 95, 96; 16-51; 20-227

Ekin, J.W., Jr.: 17-23

Elder, F.A.: 17-50

Eliassen, A.: 3 (Supp.)*

Elleman, D.D.: 7-21

Ellison, M.A.: 5-13

Elzer, A.: 12-49, 57

Endow, N.: 19-25

Engelhardt, A.G.: 20-61; 21-1

Englander-Golden, P.: 14-(1105), (1410), (1459)

Entemann, E.A.: 7-60; 18-57

Epstein, E.S.: 4-7

Erastov, E.M.: 7-61

Eriksson, K.B.S.: 10-40, 42, 45; 12-83

Estermann, I.: 7-9(Ed.), 57 (Ed.); 15-20 (Ed.)

Evans, E.W.: 16-36

Evans, J.E.: 9 (Author)-8, 15, 16, 21

Evans, J.S.: 12-23

Evans, J. V.: 4-3; 5-7, 8; 6-5

Evans, W. F. J.: 9-119; 12-34; 20-148, 180

Evanson, K. M.: 19-36

Everhart, E.: 15-53

Ewing, G. E.: 17-64

Eyring, H.: 16-71

Fabian, W.: 12-12

Faire, A. C.: 16-17

Falconer, W. E.: 21-68

Fano, W.: 20-5

Farmer, A. J. D.: 12-12

Farragher, A. L.: 7-10; 18-10

Fastie, W. G.: 9-103

Fateeva, L. N.: 15-50, 51, 56

Fedele, D.: 3-7*

Fedorenko, N. V.: 15-5, 6

Fehsenfeld, F. C.: 4-21; 6-6; 7-9; 9-30, 78, 81, 82, 84, 88, 133; 17-7, 22, 27, 36, 43, 49, 51; 18-4, 5, 6, 7, 8, 9, 13, 32, 34, 35, 36, 38, 39, 40, 42, 43, 47, 48, 49, 50, 52, 53, 54, 56, 58, 59, 62; 20-89, 163, 206; 21-3; 24-5, 8

Feinberg, R. M.: 11-10

Feldman, E.: 4-17

Fenimore, C. P.: 19-38

Ferguson, E. E.: 4-21; 6-6; 7-9, 51; 8-36; 9-30, 78, 81, 84, 88; 17-7, 22, 27, 43, 51, 54, 67; 18 (Author)-4, 5, 6, 7, 8, 9, 14, 31, 32, 35, 36, 38, 40, 42, 43, 44, 45, 47, 48, 49, 50, 52, 53, 54, 56, 58, 59, 62; 20-89, 206; 21-81; 24-4, 5, 8

Fessenden, R. W.: 17-32

Field, F. H.: 7-12

Fields, H.: 21-45

Filseth, S. V.: 20-171, 183; 24-41

Findlay, F.: 20-157; 24-21

Findlay, J. A.: 9-83

Fineman, M. A.: 14-(2784), (2954); 20-134

Fink, E. H.: 20-39

Finkelnberg, W.: 11-48

Finlayson, N.: 6-16; 20-168

Firsov, O. B.: 15-36, 37, 38

Fisher, E. R.: 4-15; 20-7, 55, 62, 63, 87, 94

Fite, W. L.: 7-2 (Ed.), 8, 10; 8-66; 14-(320), (323); 15 (Author)-8, 9, 10, 28, 44, 45, 46, 47, 49; 17-16; 18-10, 30; 20-86, 133, 138, 209

Flannery, M. R.: 8-26

Fleischmann, H. H.: 15-29, 30

Florance, E. J.: 15-31

Florance, E. T.: 15-16, 17, 18

Flugge, R.: 20-149

Flugge, S.: 3 (Supp.)(Ed.)*; 7-74 (Ed.); 11-48 (Ed.); 12-1 (Ed.)

Fogel, Ya. M.: 14-(4083); 15-52; 20-204

Folkestad, K.: 9-72

Foner, S. N.: 20-103; 24-34

Fontijn, A.: 11-40; 19-29

Ford, H. W.: 19-25

Fortin, C.: 20-157

Fouracre, R. A.: 18-3

Fowler, R. G.: 14-(2923); 20-23

Francis, W. E.: 8-29; 15-35

Frankevich, E. L.: 7-13

Franklin, J. L.: 7-12

Frazier, P. A.: 11-56
Freedman, E.: 19-28
Friedman, L.: 7-51; 8-36
Frihagen, J.: 5-7 (Ed.); 9-132 (Ed.)
Frimout, D.: 13-13
Frisov, O. B.: 11-64
Froben, F. W.: 20-27
Frommhold, L.: 16-4, 15; 17-25
Frosch, R.: 20-24
Frost, D. C.: 7-81
Frost, L. S.: 21-11
Fueno, T.: 16-71
Furnival, S.: 20-218
Futrell, J. H.: 7-24, 14, 15

Gabathuler, E.: 20-214
Gadsden, M.: 9-125
Gaily, T. D.: 16-64
Galomb, D.: 5-31
Garcia, J. D.: 15-21, 26, 27, 28
Garcia-Munoz, M.: 15-2
Gardner, J. L.: 12-88
Gardner, M. E.: 16-66
Garnett, S. H.: 20-78, 79
Garrett, D. L.: 13-10
Garriott, O. K.: 3-12*; 5-21; 9-36
Garstang, R. H.: 20-13
Gattinger, R. L.: 6-9; 20-147
Gatz, C.: 20-223; 21-65

Gauvin, H. P.: 11-3

Geballe, R.: 17-26

Geltman, S.: 8-56; 11-55, 56; 17-12; 21-50

Gentry, W. R.: 7-50

George, J. D.: 13 (Author)

Georges, T. M.: 3-27 (Ed.)*, 32*

Gerjuoy, E.: 8-49; 15-26, 27, 28

Getty, W. E.: 21-15

Ghormley, J. A.: 11-36

Giese, C. F.: 7-42, 44, 45

Giesecke, A. A.: 9-64

Giguere, P. A.: 10-63

Gilbody, H. B.: 15-58, 61

Gille, J. C.: 3-23*, 24, 46

Gilmore, F. R.: 1 (Author); 10 (Author)-51; 17-52; 20 (Author)-6, 7, 9

Gilpin, R.: 24-22

Gioumousis, G.: 8-37; 11-62

Gislason, E. A.: 7-50

Giver, L. P.: 20-33

Glad, S.: 10-39

Glasstone, S.: 5-23

Glennon, B. M.: 20-8

Gluckstern, R.: 15-14

Glupe, G.: 14-(589)

Godske, C. L.: 3-56*

Goldan, P. D.: 9-30; 18-45, 52; 20-109

Goldberg, L.: 13-8

Golden, D. E.: 18-25; 20-68; 21-64

Goldman, A.: 11-8

Goldstein, R.: 12-19

Golub, S.: 17-6

Gonfalone, A.: 16-46, 47

Good, A.: 18-19, 20

Good, R. E.: 11-32

Goodall, C. V.: 16-32

Goody, R. M.: 3 (Supp.)*

Gottlieb, B.: 4-9

Gould, R.: 8-3

Graben, H. W.: 21-15

Gray, E. P.: 16-3

Greaves, C.: 16-9

Green, A. E. S.: 20-69, 70; 21-36, 37

Green, J. A.: 16-35

Greene, E. F.: 7-35

Greene, J. S., Jr.: 15 (Author)-7

Greig, J. D.: 24-28

Griem, H. R.: 11-46, 49

Grigorev, A. N.: 15-39

Grones, G. V.: 5-1

Gross, R. W. F.: 24-13, 14

Grotrian, W.: 10-4

Grünberg, R.: 17-34

Gryzinski, M.: 15-22, 23, 24, 25

Guerin, F.: 20-25

Gunton, R. C.: 9 (Author)-33, 89; 16-7, 26; 17-31

Gush, H. P.: 11-1

Gustafasson, G.: 9-52

Gutman, D.: 17-58

Guttman, A.: 11-7

Haas, R.: 14-(684)

Hackman, R.: 16-19

Haddad, G.: 12-9, 12

Haerendel, G.: 5-32, 34

Hagen, G.: 7-65, 66; 16-22

Hake, R. D.: 21-4

Hall, J. L.: 7-87; 17-11, 40, 62

Hall, L. A.: 13-1, 7

Hall, P. G.: 24-28

Halpern, G. M.: 16-50; 21-73

Ham, D. O.: 24-15

Hamlin, D. A.: 11-34

Hampson, J.: 20-198

Hampson, R. F.: 20-181

Hanel, R. A.: 11-41

Hansen, W. B.: 3-60, 61; 9-75, 77

Hanson, H. P.: 14-(2784), (2954)

Harang, O.: 5-30

Hargreaves, J. K.: 9-48

Harris, A. K.: 9-18, 64

Harris, K. K.: 3-30

Harrison, H. J.: 7-86; 14-(974)

Harrison, M. F. A.: 7-52, 53, 54, 56; 14-(261), (2788), (2790); 16-63, 64; 17-37

Harteck, P.: 12-10

Hartman, P. L.: 21-33

Hartunian, R. A.: 19-30

Haslett, J.: 20-167

Hasted, J.B.: 7-29, 30; 8-39; 15-3, 42; 17-25; 18-26, 27; 20-161; 21-6

Hays, P.B.: 21-15

Head, C.E.: 20-21

Headrick, D.: 20-149

Heffter, J.L.: 3-57

Heicklen, J.: 6-14, 15

Heimerl, J.: 7-26; 18-23, 63, 64

Helbing, R.K.B.: 7-41

Hemsworth, R.S.: 7-11

Henderson, W.R.: 8-66; 17-16; 20-86, 138

Hendl, R.G.: 3-38

Henry, R.J.W.: 8-45, 51, 69, 70, 71, 73; 12-46, 47, 51, 52, 56, 58; 20-179; 21-20

Herm, R.R.: 7-38

Herman, K.: 10-63

Herman, Z.: 7-49

Herrmann, G.F.: 21-26

Herron, J.T.: 10-37; 12-84; 19-23

Herschbach, D.R.: 7-38, 39; 20-67

Herzberg, G.: 10-2, 6, 15, 28, 34, 50; 12-79; 17-53

Herzenberg, A.: 8-20, 21, 58, 61, 63; 17-24, 35

Herzfeld, K.F.: 20-74; 11-17

Hessenaur, H.: 17-34

Hesser, J.E.: 20-22

Hesstvedt, E.: 3 (Supp.); 20-199

Hewitt, E.W.: 19-30

Hewitt, L.W.: 9-95

Heylen, A. E. D.: 21-45

Hibbert, A.: 8-47

Hicks, G. T.: 9-73

Hidalgo, M. B.: 8-72

Hils, D.: 20-210

Hines, C. O.: 3-22 (Ed.)*, 29, 39; 20-52

Hinnov, E.: 11-70; 16-44

Hinteregger, H. E.: 13-1, 7

Hirschfelder, J. O.: 3-4*

Hirschberg, J. G.: 16-44

Hirsh, M. N.: 7-94, 95, 96; 16-50, 51; 20-227; 21-73

Hochanadel, C. J.: 11-36

Hochstim, A. R.: 3 (Supp.) (Ed.)*

Hodges, R. R.: 3-42, 51; 9-94

Holland, D. H.: 11-62

Holland, R. F.: 14-(2785); 20-29; 21-33

Hollingsworth, C.: 20-228

Hollstein, M.: 20-18

Holt, H. K.: 20-212

Holt, O.: 9-99

Holzer, W., et al: 10-61

Houston, R. E.: 9-70

Howard, C. J.: 18-11, 12

Huber, K. P.: 10-25

Hudson, R. D.: 7-73; 12-7, 11, 24, 43

Hudson, R. L.: 24-34

Huffman, R. E.: 5-10; 7-69, 72; 12 (Author)-5, 18, 26, 28, 36, 37 44, 53, 59, 72, 78; 13 (Author)-6

Hughes, B. M.: 17-65

Huise, W. H.: 9-64

Humphrey, C. H.: 11-62

Humphreys, C. J.: 10-47

Hunt, B. G.: 6-8; 9-136; 20-197

Hunten, D. M.: 9-12, 91, 101, 119, 121, 123; 12-40; 20-42, 84, 104, 148, 170, 202

Hunter, D. M.: 12-34, 67

Huppi, E. R.: 11-2

Hurst, G. S.: 17-48

Hushfar, F.: 11-33

Husian, D.: 20-45; 24-23

Huxley, L. G. H.: 21-2, 42

Hyatt, D.: 7-16

Hyslop, J.: 8-34

Inghram, M. G.: 17-50

Ingraham, J. C.: 20-178

Inn, E. C. Y.: 12-63

Intezarova, E. I.: 19-42

Isaacson, L.: 20-107

Isberg, H. B. S.: 12-83

Isler, R. C.: 9-103

Itikawa, Y.: 8-55; 21-15, 43

Iwata, M.: 10-19

Izod, T. P. J.: 12-71; 20-194

Jacchia, L. G.: 5-2, 4, 5

Jacox, M.: 11-6

Jaffe, S. B.: 6-19

Jamshidi, E.: 4-19

Janev, R. K.: 8-24

Jarmain, W. R.: 20-36

Jenkins, F. A.: 12-82

Jespersen, M.: 5-16; 9-99, 100; 21-29

Jesperson, N.: 9-67

Jeunehomme, M.: 20-17, 26, 38, 41

John, T. L.: 11-57

Johnsen, R.: 7-26, 27, 28; 16-37; 18-23, 24

Johnson, A. W.: 20-23

Johnson, F. S.: 3-60, 61; 4-9

Johnson, L. C.: 11-70

Johnson, R. G.: 9-8, 66

Johnston, H. S.: 19-46, 58; 20-30; 24-20, 29

Johnston, T. W.: 21-10

Joki, E. G.: 9 (Author)

Jones, A. Vallance: 9-119; 12-34; 20-147, 148, 180

Jones, G. W.: 19-38

Jones, I. T. N.: 20-146

Jones, P. R.: 15-53

Jones, W. M.: 19-5

Jordon, J. E.: 7-34

Jory, R. L.: 21-14

Jundi, Z.: 8-26

Jursa, A. S.: 12-77

Justus, C. G.: 3-10

Kane, J. A.: 9-72, 96, 98, 99; 21-29

Kaneko, Y.: 7-29, 31; 18-29

Kanomata, I.: 7-31; 18-29

Kappe, V. T.: 14-(4083)

Karzas, W. J.: 11-47

Kaskan, W. E.: 20-234

Kasner, W. H.: 16-2, 13, 20, 29, 30

Katayama, D. J.: 12-78

Kaufman, F.: 6-13; 7-6; 18-11, 12; 19 (Author)-2, 11, 13, 15, 17 24, 27, 31, 34, 45, 53, 55; 20-31, 135; 24-15, 31, 33

Kay, J.: 17-47

Kebarle, P.: 17-42, 66; 18-19, 20

Keck, J. C.: 8-26; 10-9

Keller, G. E.: 18-65, 66; 21-81

Kellogg, W. W.: 3-55

Kelso, J. R.: 6-13; 19-13, 15, 17, 24, 28

Kenahan, J. A.: 10-13

Keneshea, T. J.: 3-64, 3 (Supp.); 4-8; 13 (Author)-4; 24-1

Kennealy, J. P.: 11 (Author)-16

Kenty, C.: 20-119, 224

Kerr, D. E.: 16-3

Kerstetter, J. D.: 7-49

Kerwin, L.: 20-131

Ketcheson, R. D.: 19-43

Keyser, L.: 19-53; 20-31

Khare, S. P.: 8-12; 9-138

Khazan, S. M.: 15-39

Kiefer, J. H.: 11-23; 19-9; 20-142

Kiefer, L. J.: 12-6; 14 (Author)

King, A. B.: 20-223

Kingston, A. E.: 8-7, 8, 9, 10; 15-4; 16-43

Kingston, E.: 11-68, 69

Kirsch, L. J.: 24-23

Kishko, S. M.: 14-(3387)

Kistemaker, J.: 14-(1281), (1782)

Kistiakowsky, G. B.: 19-12; 20-78, 79

Kivel, B.: 11-60, 63; 21-19

Klein, F. S.: 19-23

Klein, M. M.: 8-13; 17-13

Kleinpoppen, H.: 20-210

Kleinschmidt, E.: 3 (Supp.)*

Klodowski, H. F.: 10-62

Klots, C. E.: 17-57

Knapp, W. S.: 5 (Author)-26; 22 (Author)

Knopf, H.: 8-31

Knudsen, W. C.: 3-30; 9-76

Kobayashi, N.: 7-31; 18-29

Kochanski, A.: 3-14

Kockarts, G.: 4-10; 12-13

Kondratiev, V. N.: 19-42

Konishi, A.: 21-51

Korol, V. I.: 14-(3387)

Koschmieder, H.: 20-210

Koval, A. G.: 14-(4083)

Kozlov, S. I.: 9-46

Kramers, H. A.: 11-45

Krause, H. F.: 20-86

Krauss, M.: 8-62

Kregel, M. O.: 17-31

Kreuger, A. J.: 11-38

Krezenski, D. C.: 19-44

Krotkov, R.: 20-212

Kruger, C.H.: 20-97

Krupenie, P.H.: 10-49

Kuckes, A.F.: 16-44

Kuethe, A.M.: 3-6

Kuhn, W.R.: 3 (Supp.); 11-19

Kumar, V.: 12-88

Kummler, R.H.: 3 (Supp.)*; 4 (Author)-1, 2, 13, 14; 6-2; 11-43; 20 (Author)-56, 63, 94, 95, 162, 164; 24 (Author)-46

Kunde, V.G.: 11-41

Kupperman, A.: 21-31

Kurepa, M.V.: 14-(743), (938)

Kurzius, S.: 11-40

Kurzweg, L.: 15-9

Kyle, T.G.: 11-8

Lagangren, C.R.: 10-11

Laider, K.J.: 20-3

Lambert, J.D.: 4-4; 11-18

Lampe, F.W.: 7-12

Landmark, B.: 5-12 (Ed.); 9-62, 67, 72, 99

Landon, S.A.: 8-26

Landshoff, R.K.: 15-40; 21-37

Lane, N.F.: 21-40

Larrabee, J.C.: 12-18, 26, 28, 36, 37, 44, 50, 53, 59, 72; 13-6

Larrabee, J.S.: 5-10

Larson, L.E.: 9-70

Lassettre, E.N.: 21-31

Latter, R.: 5-25; 11-47

Latimer, I.D.: 9-105; 14-(1564), (1771)

Lauver, M. R. : 20-236

Lawrence, G. M. : 14-(4326); 20-11, 14

Layton, J. K. : 7 (Author); 15-45, 46, 47, 54; 20-205

Le Blanc, F. J. : 20-186

Le Breton, P. R. : 7-39

Le Calve, J. : 19-50

Lee, A. R. : 20-127

Lee, S. K. : 15-30

Lee, Y. T. : 7-39, 50

Lefebvre-Brion, H. : 20-25

Leighton, F. : 19-7

Leighton, P. A. : 12-62

Le Levier, R. E. : 5-25, 29; 9-45; 17-8

Leovy, C. : 3-36, 47; 4-5, 6

Lerfald, G. M. : 9-48

Leu, M. T. : 16-37

Levchenko, Yu. Z. : 15-39

Levine, J. : 17-40, 62

Levine, S. : 20-31

Lewis, B. R. : 12-12

Lewis, J. T. : 8-16

Lewis, P. : 4-17

Lichten, W. : 20-5, 99

Liemohn, H. G. : 3 (Supp.)

Lifshitz, C. : 17-65

Light, J. C. : 20-65

Liller, W. : 3-13

Lin, C. C. : 14-(2923)

Lin, S. C. : 16-27; 21-19

Lindalen, H. R.: 9-104
Linder, F.: 14-(3252)
Lindhard, R. S.: 15-12
Lindzen, R. S.: 3-19*, 50
Lineberger, W. C.: 7-91; 18-1
Lineberger, W. E.: 7-4
Linnett, J. W.: 19-33
Linson, L. M.: 5-33
Liquornik, D. J.: 24-18
Liston, S. K.: 10-35
Litovitz, T. A.: 20-74
Liu, C. H.: 3-45; 7-93
Llewellyn, E. J.: 9-119; 12-34; 20-148
Lloyd, A. C.: 19-54; 24-16, 32
Lo, H. H.: 15-9, 10, 44, 48, 49
Loch, R. G.: 21-35
Lockey, C. W. A.: 3 (Supp.)
Loeb, L. B.: 21-80
Lokan, K. H.: 12-12
Lomax, J. B.: 5-28
London, J.: 3 (Supp.); 11-19
Lorents, D. C.: 7-48, 63; 16-53; 20-18, 110; 21-20
Lowke, J. J.: 21-14
Lundell, O. R.: 19-43
Lust, R.: 5-32
Lutz, R. W.: 11-23; 19-9; 20-142
Lynch, R.: 10-4, 43

MacDonald, R. G.: 11-27, 28
Mackie, J. C.: 10-14, 43
Magee, J. K.: 15-40
Magee, J. L.: 21-37
Magnuso, G. D.: 15-46
Mahadevan, P.: 15-46
Mahan, B. H.: 7-50; 16-5, 52, 56
Mairer, W. B.: 7-42, 43; 20-29
Malaviya, V.: 8-14
Mandl, F.: 8-21, 58, 61, 64; 11-66; 17-39
Mapleton, R. A.: 8-30; 15-19
March, R.: 20-218
Marino, L. L.: 7-36; 14-(978); 21-18, 22
Marmo, F. F.: 12-60
Marovich, E.: 9-125
Marr, G. V.: 7-71, 75; 12-2
Marriott, R.: 8-43
Martin, D. W.: 7-25; 18-28; 21-63, 66
Marton, L. L.: 15-3 (Ed.)
Maseide, K.: 9-67, 104
Mason, E. A.: 8-31; 21-62, 71
Massey, H. S. W.: 8-2, 25; 9-25; 16-48; 17-21
Masson, A. J.: 7-16
Mastrup, F. N.: 12-19
Mathias, A.: 6-12
Matsunaga, F. M.: 12-30, 61, 73; 13-5
Matuura, N.: 9-80
Mayr, H. G.: 9-83
Mayer, J. E.: 10-7

Mayer, M. G.: 10-7

Maylotte, D.: 20-220

McCarroll, R.: 15-32

McComber, H. K.: 15-18, 31

McConkey, J. W.: 9-105; 10-13; 14-(1214), (1504), (3246), (3981)

McCormac, B. M.: 5-30 (Ed.), 34 (Ed.); 9 (Ed.)-3, 5, 8, 21, 86, 101, 114; 11-3 (Ed.)

McCrumb, J. L.: 19-45

McDaniel, E. W.: 7-25, 51; 8-36; 17-22; 18-28; 21-63, 66, 69

McDermott, D. P.: 5-1

McDiarmid, I. B.: 9-69

McDonald, J. D.: 7-39

McDowell, C. A.: 7-81

McDowell, M. R. C.: 15-59 (Ed.); 20-130

McEachron, R. P.: 11-56

McElhinney, M. W.: 9-59

McElroy, A. D.: 10-62

McElroy, M. B.: 3-69; 9-85, 91, 102, 123; 12-40, 67; 20-42, 111, 128; 21-37, 40

McFarland, M.: 18-48, 56

McGarvey, J. J.: 12-54; 20-187

McGee, J.: 6-14

McGowan, J. W.: 7-84; 14-(2784), (2954); 20 (Author)-1, 6, 131, 132

McGowan, S.: 16-69

McGrath, W. D.: 12-54; 20-187

McIlwain, C. E.: 9-113

McIver, R. T.: 7-23

McKenny, D. J.: 19-18

McNeal, R. J.: 9-5; 10-29; 20-160; 24-10

McNesby, F. R.: 12-68

McKinnon, P. J.: 9-51

McKnight, L. G.: 18-37; 21-67

McWhirter, R. W. P.: 8-9; 11-68; 16-43

Meaburn, G. M.: 19-50

Mechtley, E. A.: 9-20

Mecke, R.: 20-34

Megill, L. R.: 5-15; 7-29; 18-26; 20-161, 166, 167; 21-39

Mehlhorn, W.: 14-(589)

Mehr, F. J.: 7-3; 16-21

Meinel, A. B.: 9-14

Meira, L. G., Jr.: 9-93

Mende, S. B.: 9-10, 115

Mentall, J. E.: 20-86

Mentzoni, M. H.: 16-18, 31; 21-3, 17, 34, 49

Merrill, P. W.: 10-5

Metzger, P. H.: 7-70; 9-107; 12-17, 29

Meyer, C. B.: 19-29

Meyerott, R. E.: 9-8, 15, 21

Michels, H. H.: 11-42

Midgley, J. E.: 3 (Supp.)

Mies, F. H.: 8-62

Miescher, E.: 10-26

Miller, J. H.: 20-33

Miller, R. E.: 9-103

Miller, T. M.: 7-25; 18-28

Milligan, D. E.: 11-6

Millikan, R.: 20-83

Minnhagen, L.: 10-38, 48

Minnis, C. M.: 9-58

Mirza, I. M.: 14-(3524), (3769)

Mitra, A. P.: 9-42, 61

Mitra, S. K.: 5-11; 9-23

Mittelman, M. H.: 21-15

Mjolsness, R. C.: 8-53, 57; 11-59

Moe, O. K.: 3-3; 4-11

Moffett, R. J.: 8-26, 50; 21-47

Moiseiwitsch, B.: 20-208; 21-53

Moller, C. K.: 10-17

Molmud, P.: 21-25

Monin, A. S.: 3 (Supp.)

Moore, A. F.: 5-2 (Ed.)

Moore, C. E.: 10-3, 5

Moran, T.: 20-141

Morgan, J. E.: 4-16; 19-16, 20; 20-54

Morgan, L. A.: 8-47

Morrison, J. D.: 10-20, 23

Moruzzi, J. L.: 17-23; 18-68

Moseley, J.: 8-18; 16-55, 56, 57, 58, 59, 60, 61; 21-63

Mosely, J. T.: 18-28

Moseman, M.: 18-9, 40, 42, 45

Moses, H. A.: 15-53

Mosher, R. L.: 18-17

Motley, R. W.: 16-44

Mott, N. F.: 8-2

Mottl, J.: 12-81

Moursund, A. L.: 7-35

Moustafa, H. R.: 14-(1782)

Mulcahy, M. F. R.: 19-48

Murcray, D. G.: 11-21

Murgatroyd, R. J.: 3-9, 3 (Supp.)-4 listings

Murphy, E. A.: 3-40

Murphy, R. E.: 11-12

Muschlitz, E. E.: 17-25; 20-44

Myers, B. F.: 11-34

Myers, G. H.: 19-27

Nagy, A. F.: 11-24; 20-58

Nagy, R.: 4-13

Nakano, N. N.: 21-8

Nakata, R. S.: 12-73

Nakayama, T.: 12-81

Narasingarao, K. V.: 21-34, 48

Narayanamurti, V.: 10-60

Narcisi, R. S.: 5-17, 18, 19; 9-19, 27; 17-10; 20-203; 21-61

Natason, G. L.: 16-70

Nelson, D. R.: 21-5

Nesbit, L. E.: 17-45

Nestorov, G.: 9-41, 50, 57

Neynaber, R. H.: 7 (Author)-37, 57, 59; 14-(978), (1268); 21-18, 22

Nicholls, R.: 20-12, 36, 37

Nicolaides, C.: 20-239

Nielson, D. L.: 5-28

Nielson, S. E.: 16-40

Nikitin, E. E.: 8-40

Nikolaev, L. N.: 15-50, 51, 56

Niles, F. E.: 3 (Supp.); 17-9; 22 (Author); 24-2

Nisbet, J. S.: 9-38

Nishimura, H.: 14-(1700), (1838), (3024)

Nobgen, J.W.: 10-62

Norman, G.E.: 11-50

Norrish, R.A.W.: 20-217

Norton, A.S.: 20-100

Norton, R.B.: 9-39, 92; 20-90

Noxon, J.F: 9-129; 11-39; 12-20; 20-116, 151, 165; 24-36

Nudelman, C.: 19-6

Nussbaum, G.H.: 15-57

Obayashi, T.: 5-22; 9-63

O'Brien, B.J.: 9-111

O'Bryan, C.L.: 12-78

Obukhoff, A.M.: 3 (Supp.)

Ogawa, M.: 7-70; 10-22; 12-25, 31

O'Grady, B.V.: 20-79

Ogryzlo, E.O.: 6-16; 20-168; 24-47

Ohmholt, A.: 20-201

Okabe, H.: 12-68; 20-181

Oldenberg, O.: 14-(992); 20-186, 226

Olmsted, J.: 20-100

Olson, R.E.: 8-18; 16-57, 58

O'Malley, T.F.: 6-7; 8-15, 65; 17-12, 18; 18-33; 20-91, 139

Omholt, A.: 5-30 (Ed.), 34 (Ed.); 9-2 (Ed.), 65, 68, 117

Omidvar, K.: 20-237

O'Neill, R.: 4-20; 21-33; 11-25

Ong, P.P.: 7-30; 8-39; 18-26, 27

Oort, A.H.: 3-48

Opal, C.B.: 21-41

Opik, U.: 8-67

Oskam, H.: 16-11

Otto, W.R.: 15-46

Oya, H.: 9-63

Pack, J.L.: 7-32; 17-14, 45; 18-61; 21-12; 24-9

Page, F.M.: 17-47

Paltridge, G.W.: 21-79

Pantoja, A.: 9-64

Parez, J.: 7-97

Parkes, D.A.: 17-30; 18-67; 19-31; 21-16

Parkinson, T.M.: 9-128, 140

Parkinson, W.H.: 13-11

Parthasarathy, R.: 9-71

Pastiels, R.: 13-13

Paul, E., Jr.: 10-47

Paulsen, D.E.: 5-10; 12-26; 13-6

Paulson, J.F.: 7 (Author)-47; 17-59; 18-17, 18, 55, 60

Payzant, J.D.: 17-66

Peacher, J.L.: 8-22; 20-140

Peart, B.: 14-(4344)

Peatman, W.B.: 7-64; 16-62

Peden, J.A.: 7-10, 15-28; 18-10

Pederson, B.M.: 9-100

Peek, M.: 9-106; 11-71

Peetermans, W.: 4-10

Pekeris, C.L.: 10-10

Penner, S.S.: 11-13

Percival, I.C.: 15-20

Perner, D.: 19-50

Person, J.C.: 16-52

Peters, T.: 11-48

Petersen, O.: 9-99

Peterson, J.R.: 7-63; 8-18; 16-53, 54, 55, 56, 57, 58, 59, 60, 61; 20-110

Peterson, L.R.: 21-36, 37, 38

Peterson, R.: 20-18

Peterson, W.K.: 21-41

Petrie, W.: 20-106

Pharo, M.W., III: 9-83

Phelps, A.V.: 7-32; 17 (Author)-14, 19, 23, 28, 29, 32, 45; 18-61, 68; 20-61, 213; 21 (Author)-1, 2, 4, 11, 12, 13, 43, 54; 24-9

Philbrick, C.R.: 9-19; 21-61

Phillips, L.F.: 4-16; 19-14, 16, 39; 20-53, 54; 24-26, 27, 30

Pichanick, F.M.T.: 7-58 (Ed.)

Piddington, J.H.: 9-2

Pierce, E.T.: 5-24

Piggott, W.R.: 21-29

Pikus, I.M.: 15 (Author)

Pilipenko, D.V.: 15-52

Pitteway, M.L.V.: 3-41

Pitts, J.N.: 20-158

Pivovar, L.I.: 15-39

Podney, W.N.: 3-44

Pohl, R.D.: 10-69

Polanyi, J.C.: 11-27, 28; 20-56, 220, 221

Poppoff, I.G.: 9 (Author)-43, 44, 53, 131; 21-20

Porter, G.: 7-12 (Ed.); 19-2 (Ed.)

Poss, E.: 7-96

Prabhakara, C.: 11-41

Prasad, S.S.: 21-36

Preston, K. F.: 20-188

Price, W. C.: 7-82

Priester, W.: 5-1, 3, 4 (Ed.)

Prigogine, I.: 21-31 (Ed.)

Proshchak, L. I.: 14-(4083)

Puckett, L. J.: 7-4; 17-31; 18-1, 41, 64; 24-7

Purcell, J. D.: 13-10, 14

Quinn, T. P.: 9-38

Quiroz, R. S.: 3 (Supp.)(Ed.)

Rai, D. B.: 9-71

Raizer, Yu. P.: 9-46; 11-61

Raper, O.: 12-70; 20-192, 193

Rapp, D.: 8-29; 14-(1105), (1410), (1451), (1459), (1460); 15-35; 20-72

Ratcliffe, J. A.: 20-49

Rawer, K.: 3-8 (Ed.)*

Reasoner, D. L.: 9-111

Ree, T.: 16-71

Rees, J. A.: 21-14

Rees, M. H.: 9-11, 139; 21-37, 40, 78

Reeves, E. M.: 13-11

Reeves, R. R.: 12-10

Reid, G. C.: 9-132, 134

Reid, R. H. G.: 4-22; 5-12, 13

Reinhardt, P. W.: 17-48

Reinhardt, W. P.: 8-47

Rice, J. K.: 21-31

Rice, S. A.: 21-31 (Ed.)

Richter, J.: 11-51

Riley, J. F.: 11-37

Rishbeth, H.: 3-12; 9-17, 36

Risk, C. G.: 20-61; 21-1

Robb, W. D.: 8-47

Roberts, J. R.: 11-58

Robinson, G.: 20-24

Rockwood, S. D.: 22 (Author)

Rogers, J. W.: 11-33

Rogers, W. A.: 16-30

Rol, F. K.: 7-60; 18-57

Romick, G. J.: 9-11, 116

Rony, P. R.: 19-3

Rose, P. H.: 15-57

Rose, T. L.: 7-49

Rosen, N.: 15-34

Rosenberg, N. W.: 3-10, 11, 3 (Supp.); 5-31

Rosenstock, H. M.: 10-33

Rosner, D. E.: 19-1

Ross, J.: 7-33 (Ed.), 35; 20-44 (Ed.)

Rothe, E. W.: 7-36, 41, 59; 14-(978), (1268); 21-18, 22

Row, R. V.: 21-34

Roy, S. K.: 21-28

Rundle, H. N.: 9-86

Rundle, H. W.: 18-11, 12

Rundel, R. D.: 7-56; 14-(2788), (2790); 16-63; 17-37

Ruppel, H. M.: 11-59

Russek, A.: 15-41

Russell, M. E.: 7-17

Rutherford, J. A.: 7-8, 46; 18-21, 22, 46, 69; 20-108, 129, 229

Ryan, K.R.: 7-14, 15; 18-48

Rybner, J.: 9-99

Ryding, G.: 15-57

Ryzko, H.: 21-14

St. John, G.: 16-6; 20-122, 125, 136; 24-40

St. John, R.M.: 14-(2923), (3710)

Sakai, H.: 13-5

Salkoff, M.: 20-232

Salop, A.: 21-8

Salpeter, E.E.: 11-44

Sampson, D.H.: 8-53, 57; 21-56

Samson, J.A.R.: 7-67, 76; 12-27, 31, 48, 75, 80, 89, 90

Sandler, S.I.: 21-71

Sandlin, G.D.: 13-14

Sanford, B.P.: 9-114

Sappenfield, D.: 11-53, 71

Sauer, M.C., Jr.: 19-19, 49; 21-44

Saum, K.A.: 10-52

Savage, B.D.: 20-11

Sawina, J.M.: 18-37

Saxman, A.C.: 15-57

Sayers, J.J.: 7-5; 8-28; 9-31; 16-33, 49, 67; 18-2

Scarborough, J.: 17-42

Schaffner, S.: 9-74

Scheibe, M.: 11-62; 16-26

Schexnayder, C.J.: 12-23

Schiff, H.I.: 4-16; 6-12; 7-7; 9-30, 84; 10-37; 12-84; 17-7, 36; 18-13; 19-14, 16, 20, 29, 39, 41, 43; 20-53, 54, 167, 218; 24-22, 26, 27, 30

Schlapp, D. M.: 9-97

Schmeltekopf, A. L.: 6-6; 7-9; 9-30, 78, 84, 88; 10-55; 17-7, 22, 27; 18-4, 14, 32, 43, 49, 52, 53, 56; 20-88, 89; 24-5, 8

Schmidtke, G.: 13-7

Schneider, B.: 8-75

Schoen, R. I.: 7-77, 83; 12-3, 32

Schofield, K.: 19-59

Schram, B. L.: 14-(1281), (1863)

Schubert, K. E.: 12-32

Schuler, D. Z.: 11-52

Schulz, G. J.: 8-60; 10-58, 59; 14-(324), (984), (1289), (2763); 17-50; 20-59, 102, 144, 145; 21-6, 51

Schumacher, H. J.: 19-8

Schummers, J. H.: 21-66

Schurin, B.: 11-11

Schutten, J.: 14-(1782)

Schwartz, S.: 20-30

Schweinfurth, R. A.: 2 (Author)

Scott, P. M.: 24-24

Searcy, A. W.: 10-18

Sears, R. D.: 5-27; 20-93

Seaton, M. J.: 8-44, 46; 11-54; 16-41; 20-177, 238; 24-38

Segal, G. A.: 17-60

Sehön, R. W.: 21-80

Seino, K.: 9-20

Selley, N. J.: 19-33

Selvin, J. A.: 20-227

Selwyn, P. A.: 3 (Author)

Ser, C. L.: 21-24

Setser, D. W.: 20-233

Seward, D.: 10-60

Shafer, C.: 17-45

Sharma, R. D.: 24-12

Sharp, G. W.: 3-30

Sharp, R. D.: 9-116

Sharp, T. E.: 14-(1451); 20-72

Sharp, W. E.: 9-109

Sharpless, R. L.: 21-65

Shaw, J. J.: 7-11

Shaw, T. M.: 9-33; 16-7, 26; 17-31

Shefov, N. N.: 11-29

Shemansky, D.: 20-15, 16, 20

Sheppard, D. J.: 9-18, 64

Shere, K. D.: 3-37

Sheridan, J. R.: 16-56; 20-18

Sheridan, W. F.: 14-(992); 20-226

Shimazaki, T.: 3-62, 63

Shimon, L. L.: 20-211

Shkarofsky, J. P.: 21-10, 26

Shore, B. W.: 8-5

Shuler, K. E.: 20-46 (Ed.), 65

Siebert, M.: 3-20*

Siegal, M. W.: 7-87; 10-24; 17-11, 40, 62

Silk, J.: 8-74

Silver, D. M.: 19-27

Simpson, F. R.: 14-(3981)

Sinanoglu, O.: 20-239

Sinfailan, A. L.: 8-45; 20-179; 21-20

Sinnott, G.: 18-25; 21-64

Skouli, G.: 9-104

Skuhenich, V. V.: 14-(3387)

Slanger, T. G.: 9-130; 12-74; 20-121, 136, 150, 185, 219; 24-17, 40, 44

Slevin, J. A.: 7-94, 95

Slovli, G.: 9-72

Smirnov, B. M.: 17-38; 21-69

Smith, A. C. H.: 7-54; 14-(1268), (2790); 15-58, 59, 60

Smith, D.: 7-5; 16-32; 18-2, 3

Smith, F. L.: 9-87

Smith, I. W. M.: 19-51

Smith, K.: 8-47

Smith, L. G.: 3-67; 9-51

Smith, M.: 20-8

Smith, P. T.: 14-(18), (225)

Smith, R. A.: 17-25; 21-35

Smith, S. J.: 7-90; 17-2, 3, 20-208; 21-53

Smyth, K. C.: 7-23

Snelling, D.: 6-17; 20-157; 24-21

Snow, W. R.: 7-8

Snuggs, R. M.: 21-63, 66

Sokai, H.: 12-61

Someville, J. M.: 21-16

Speier, F.: 12-49

Spence, D.: 10-58; 20-145; 21-6, 51

Spizzichino, A.: 3-34

Srivastava, B. N.: 14-(3524), (3769), (3943)

Sroka, W.: 14-(3833), (4336)

Stabler, R. C.: 21-56

Stair, A. T., Jr.: 11-2, 3, 31, 33

Stanton, P. N.: 14-(3710)

Starr, V. P.: 3-52*

Starr, W. L.: 20-85

Stebbings, R. F.: 7-46; 15-45, 46, 58, 59, 60; 20-108, 129, 137, 209, 229

Stedman, D. H.: 19-56

Steele, F. K.: 9-54

Steer, R. P.: 20-158

Stein, J. A.: 12-24

Stein, R. P.: 16-26

Stein, S.: 8-49

Steinberg, M.: 24-18

Steiner, B.: 17-6

Stelman, D.: 17-19; 21-54

Stevenson, D. R.: 8-37

Stewart, A. I.: 9-102; 21-37, 60

Stewart, A. L.: 8-68, 69; 12-47

Stewart, D. T.: 14-(333); 20-214, 215

Stoicheff, B. P.: 10-56

Stolarski, R. S.: 4-13; 11-24; 20-58

Stormer, C.: 9-13

Street, K.: 20-100

Strobel, D. F.: 3-69; 9-91

Studniarz, S. A.: 7-47

Stuhl, F.: 9-127; 20-183, 184; 24-41, 43

Sugden, T. M.: 16-35; 17-30

Sullivan, J. O.: 12-21; 20-191

Summers, H. P.: 8-11

Sunshine, G.: 21-7

Suzuki, H.: 21-51

Swider, W., Jr.: 13-3

Swift, D. W.: 9-49

Syverson, M. W.: 16-26

Takahashi, T.: 21-36

Takamine, T.: 10-19

Takayanagi, K.: 8-42, 52, 55, 56; 20-75; 21-15, 36, 43, 50

Takeda, S.: 21-14

Tal'roze, V. L.,: 7-13

Tanaka, Y.: 10-19, 22; 12-18, 28, 36, 37, 44, 50, 59, 63

Tančić, A. R.: 8-24

Tannenwald, L. M.: 11-62

Tardy, D.: 20-221

Tate, J. T.: 14-(18)

Taubenheim, J.: 9-50, 57

Taylor, A.: 3-41, 48

Taylor, H. A.: 9-29

Taylor, H. S.: 8-65; 17-60

Taylor, R. L.: 10-14, 43; 11-20, 67; 20-82; 21-21, 34

Tchen, C. M.: 3 (Author)-43, 53, 68

Teague, M. W.: 17-31; 18-41; 24-7

Teare, J. D.: 16-27; 24-19

Teplova, Ya. A.: 15-50, 51, 56

Thane, E. V.: 21-29

Theard, L. P.: 16-23

Theobald, K.: 9-106

Theon, J. C.: 3-28

Thomas H.: 15-15

Thomas, L.: 5-9; 9-39; 20-90; 21-72

Thompson, B. A.: 12-10

Thompson, K. R.: 11-14

Thompson, W. P.: 19-30

Thomson, J. J.: 8-27; 16-68

Thonemann, P. C.: 7-52, 53; 14-(2o1)

Thrane, E.: 5-16 (Ed.)

Thrush, B. A.: 19-10, 18, 21, 26, 32, 40, 57; 20-123, 231, 233

Tiernan, T. O.: 17-65

Tilford, S. G.: 10-21

Tinsley, B. A.: 9-79

Tipper, C. F. H.: 11-18 (Ed.)

Tisone, G.: 14-(2904); 17-3, 37; 21-41

Toistoy, P. N.: 3 (Supp.)*

Tousey, R.: 13-9, 10

Tozer, B. A.: 14-(357)

Trainor, D. W.: 24-15

Trajmar, S.: 20-112, 113; 21-31, 32, 51

Treanor, C. E.: 20-81

Trefftz, E.: 8-5

Troim, J.: 9-98

Trozzolo, A. M.: 20 (Ed.)-153

Trueblood, D. L.: 7-97; 17-33; 21-3

Trujillo, S. M.: 7-37, 59; 14-(978), (1268); 21-18, 22

Tsang, S. C.: 20-143

Tsao, C. W.: 7-50

Tucker, W.: 8-3

Tuckwell, H. C.: 8-76

Turner, B. R.: 7-46; 8-38; 15-55, 60; 18-21, 22, 69, 70; 20-108, 129, 229

Turner, D. W.: 7-78, 79, 80, 82

Tverskoi, P. N.: 3 (Supp.)*

Twiddy, N. D.: 7-11

Tyler, B. J.: 19-33

Ulwick, J. C.: 9-9

Ung, A. Y. M.: 12-74

Urbach, H. B.: 19-7

Utterback, N. G.: 7-40; 20-130

Vallance-Jones, A.: 6-9

Valley, S. L.: 3-15 (Ed.)*; 5-3 (Ed.); 7-69 (Ed.)

van den Hulst, H. C.: 5-2 (Ed.)

Vanderhoff, J. A.: 18-63

Van der Hoven, J.: 3-49

Vanderslice, J. T.: 8-31

van der Wiel, M. J.: 14-(1281)

van Lint, V. A. J.: 7-8, 97; 16-25; 17-33; 21-3

Van Zyl, B.: 7-55; 14-(2171), (2772)

Varney, R. N.: 18-25; 21-64

Vasseur, G.: 3-31

Vaughan, A. L.: 14-(17)

Veatch, G. E.: 21-3

Vedeneyev, V. I. et al: 17-68

Verdeyen, J. T.: 21-3

Victor, G. A.: 8-13; 15-16, 33

Vigroux, E.: 12-64, 66

Villarjo, D.: 17-50

Vincenti, W. G.: 20-97

Voigt, P. A.: 11-58

Volland, H.: 9-47

Volpi, G. G.: 19-12

Volz, D. J.: 21-66

Von Holt, R. E.: 21-15

Von Rosenberg, C. W., Jr.: 11-15

Von Zahn, U.: 3-65

Vorburger, T. V.: 17-44

Voshall, R. E.: 17-32, 45; 21-12

Vroom, D. A.: 7 (Author)-81, 84, 92; 14-(3687)

Wakiya, K.: 21-51

Waldron, H. F.: 21-19

Waldteufel, P.: 3-31

Walker, I. C.: 17-56; 21-55

Walker, J.: 4-13

Walker, J. A.: 10-33, 35

Walker, J. C. G.: 9-139; 11-24 20-57, 58; 21-37, 40, 78

Walker, R. E.: 17-63

Wallace, L.: 9-121; 10-57; 20-105, 128, 152, 170

Wallace, R. W.: 7-23

Walt, M.: 9-3, 16 (Ed.)

Walton, D. S.: 14-(4344)

Wand, R. H.: 3-35

Wannier, G. H.: 21-76

Warke, C. S.: 16-39

Warman, J. M.: 17-32; 21-44

Warneck, P.: 7-18, 19; 12-21; 17-55; 18-15, 16; 20-191

Watanabe, K.: 12-4, 16, 30, 60, 61, 73, 76, 77, 81, 85; 13-5; 20-172

Watts, J. M.: 9-48

Wayne, R. P.: 9-120; 12-35, 39, 69, 71; 19-40; 20-146, 154, 156, 159, 181, 194; 24-25, 42

Webb, T. G.: 15-16, 18, 31, 33

Webb, W. L.: 3 (Supp.) (Ed.)*

Wecker, M. S.: 19-37

Weeks, L. H.: 3-67; 9-51

Weiner, J.: 7-64; 16-62

Weissler, G. L.: 7-74; 12-1, 31

Welge, K. H.: 9-127; 20-39, 171, 183, 184; 24-22, 41, 43

Welker, J.: 15-26, 27

Weller, C. S.: 9-32; 16-8, 24; 17-31

Welsh, J.: 18-55

Wentink, T.: 20-107

Westenberg, A. A.: 17-63; 19-38

Westhaus, P.: 20-239

Whipple, F. J.: 3-13

Whitaker, W. A.: 15-7

White, D.: 20-83

Whitehead, J. D.: 4-21; 9-81; 20-206

Whitlock, R. F.: 20-32

Whitmer, R. F.: 21-26

Whitten, R. C.: 9 (Author)-24, 40, 43, 44, 53, 131; 20-92, 21-20, 40

Widing, K. G.: 13-14

Widom, B.: 10-8

Wiese, W. L.: 20-8

Wikner, E. G.: 17-33; 21-3

Wilkes, M. V.: 3-21*

Wilkins, R. L.: 16-38

Wilkinson, P. G.: 10-21

Williams, D. J.: 19-48
Williams, R. L.: 8-73
Williams, W.: 20-112, 113; 21-51
Williams, W. J.: 11-21
Wilson, K. R.: 7-38
Wilson, L. N.: 16-36
Wilson, W. E.: 19-47
Windelmann, R. W.: 5-20
Winer, A.: 20-155
Winkler, C.: 20-2
Winters, H. F.: 20-101
Withbrae, G. L.: 4-22
Wittkower, G. H.: 15-57, 61
Wojtowicz, J. A.: 19-7
Wolf, F. A.: 8-38; 18-70
Wolf, N. S.: 16-50; 21-73
Wolfgang, R.: 7-49
Woo, S. B.: 17-5, 44
Wood, B.: 20-219
Wood, R. H.: 17-41
Woodgate, S. S.: 7-22
Woodward, B. W.: 7-91
Woolsey, J. M.: 14-(1214), (3246)
Workman, J. B.: 5-33
Worley, R. E.: 12-82
Wray, K. L.: 4-17; 11-15; 19-9, 22; 20-124; 24-12, 19
Wright, A.: 20-2, 32
Wu, H. L.: 20-19
Wyatt, M. E.: 7-97; 16-25

Yamamoto, M.: 21-51

Yamazaki, H.: 20-189, 190

Yamdagni, R.: 17-66

Yeh, K. C.: 3-45

Yonezawa, T.: 9-35

Yoshino, K.: 12-87

Yost, D. M.: 19-58; 24-29

Young, C. E.: 21-68

Young, L. A.: 11-9

Young, N.: 8-14

Young, P. A.: 12-8

Young, R. A.: 6-18; 9-122, 124, 126, 130; 12-22, 74; 16-6; 20-118, 121, 122, 125, 136, 150, 169, 176, 185; 21-65; 24-11, 40, 44

Zapesochnyi, I. P.: 20-211

Zare, R. N.: 7-55; 10-55; 17-11

Zaslowsky, J. A.: 19-7

Zel'dovich, Y. B.: 11-61

Zelikoff, M.: 12-76; 20-50

Zener, C.: 15-34

Zia, A.: 20-171

Ziemba, F. P.: 15-53

Zimmerman, S. P.: 3-11, 54, 64

Zipf, E. C.: 9-118, 128, 140; 11-4; 14-(4080), (4125); 16-34; 19-53; 20-10, 117, 173, 174; 24-39

# APPENDIX H
# GENERAL REFERENCES

Advances in Chemical Physics series, John Wiley, New York.

Albritton, D. L., A. L. Schmeltekopf, and R. N. Zare, Diatomic Franck-Condon Factors, Harper and Row, New York (1972).

Annual Reviews of Physical Chemistry series.

Armstrong, E. B., and A. Dalgarno, Eds., The Airglow and Aurorae, Pergamon Press, London (1956).

Ausloos, P. J., Ed., Ion-Molecule Reactions in the Gas Phase, Advances in Chemistry Series No. 58, American Chemical Society, Washington (1966).

Bahn, G. S., Reaction Rate Compilation for the H-O-N System, Gordon and Breach, New York (1968).

Bamford, C. H., and C. F. H. Tipper, Eds., Comprehensive Chemical Kinetics III, Elsevier, New York (1969).

Bates, D. R., Earth is a Planet, University of Chicago Press, Chicago (1950).

Bates, D. R. et al, Eds., Advances in Atomic and Molecular Physics series, Academic Press, New York (1965 et seq.).

Bates, D. R., Ed., Atomic and Molecular Processes, Academic Press, New York (1962).

Baulch, D. L., D. D. Drysdale, and A. C. Lloyd, High Temperature Reaction Rate Data series, Leeds University, Leeds (1968 et seq.).

Bederson, B., and W. L. Fite, Eds., Methods of Experimental Physics, Academic Press, New York (1968).

Bederson, B., V. W. Cohen, and F. M. T. Pichanick, Eds., Atomic Physics, Plenum Press, New York (1969).

Bethe, H. A., and E. E. Salpeter, Quantum Mechanics of One and Two Electron Systems, Academic Press, New York (1957).

Beynon, W. J. G., and G. M. Brown, Eds., Solar Eclipses and the Ionosphere, Pergamon Press, New York (1956).

Burgers, J. M., Flow Equations for Composite Gases, Academic Press, New York (1969).

Cadle, R. D., Ed., Chemical Reactions in the Lower and Upper Atmosphere, Interscience, New York (1961).

Chamberlain, J. W., Physics of the Aurora and Airglow, Academic Press, New York (1961).

Chapman, S., and T. G. Cowling, The Mathematical Theory of Non-Uniform Gases, 3rd Ed., Cambridge University Press, London (1952).

COSPAR International Reference Atmosphere, North-Holland, Amsterdam (1965).

Cottrell, T. L., The Strengths of Chemical Bonds, Butterworths, London (1954).

Craig, R. A., The Upper Atmosphere: Meteorology and Physics, Academic Press, New York (1965).

Danilov, A. D., Chemistry of the Ionosphere, Plenum Press, New York (1970).

Defense Atomic Support Agency, Ionospheric Measurement Instrumentation: A Survey, DASIAC SR 32; DASA 1583 (1965).

Delcroix, J. L., Plasma Physics, John Wiley, New York (1965).

Dushman, S., Scientific Foundations of Vacuum Technique, John Wiley, New York (1949).

Eckart, C., Hydrodynamics of Oceans and Atmospheres, Pergamon Press, New York (1960).

Flügge, S., Ed., Handbuch der Physik, Springer-Verlag, Berlin.

Franklin, J. L., Ed., Ion-Molecule Reactions, Plenum Press, New York (1972).

Frihagen, J., Ed., Electron Density Profiles in Ionosphere and Exosphere, North-Holland, Amsterdam (1966).

Gaydon, A. G., Dissociation Energies and Spectra of Diatomic Molecules, Chapman & Hall, London (1953).

Glasstone, S., Ed., The Effects of Nuclear Weapons, U. S. Government Printing Office, Washington (1962).

Goody, R. M., Atmospheric Radiation. I. Theoretical Basis, Oxford University Press, London (1964).

Green, A. E. S., Ed., The Middle Ultraviolet, John Wiley, New York (1966).

Griem, H. R., Plasma Spectroscopy, McGraw-Hill, New York (1964).

Grotrian, W., Graphische Darstellung der Spektren von Atomen und Ionen mit Ein, Zwei, und Drei Valenzelektronen, Springer-Verlag, Berlin (1928).

Hasted, J. B., Physics of Atomic Collision, Butterworths, Washington (1964).

Herzberg, G., Atomic Spectra and Atomic Structure, Dover Publications, New York (1944).

Herzberg, G., Spectra of Diatomic Molecules, 2nd Ed., Van Nostrand, New York (1950).

Herzberg, G., Electronic Spectra of Polyatomic Molecules, Van Nostrand, Princeton, New Jersey (1966).

Herzfeld, K. F., and T. A. Litovitz, Absorption and Dispersion of Ultrasonic Waves, Academic Press, New York (1959).

Hines, C. O. et al, Eds., Physics of the Earth's Upper Atmosphere, Prentice-Hall, Englewood Cliffs, New Jersey (1965).

Hirschfelder, J. O., C. F. Curtiss, and R. B. Bird, Molecular Theory of Gases and Liquids, John Wiley, New York (1954).

Hochstim, A. R., Ed., Bihliography of Chemical Kinetics and Collision Processes, Plenum Press, New York (1969).

Hochstim, A. R., Ed., Kinetic Processes in Gases and Plasmas, Academic Press, New York (1969).

International Symposia on Combustion, The Combustion Institute, Pittsburgh.

Ivanov-Kholodnyi, G. S., and G. M. Nikol'skii, The Sun and the Ionosphere, translated from the Russian, U. S. Department of Commerce National Technical Information Service, NASA TT F-654; TT 70-50184, Springfield, Virginia (1972).

Joint Army-Navy-Air Force Thermochemical Panel, JANAF Thermochemical Tables, Dow Chemical, Midland, Michigan (1960 et seq.).

Katz, J. J., and E. Rabinowitch, The Chemistry of Uranium, National Nuclear Energy Series, Division VIII—Volume 5, Dover, New York (1951).

Laidler, K. J., Chemical Kinetics of the Excited States, Oxford University Press, London (1955).

Landmark, B., Ed., Advances in Upper Atmosphere Research, Pergamon Press and the MacMillan Co., New York and London (1963).

Landsberg, H. E., and J. Van Mieghan, Eds., Advances in Geophysics, Academic Press, New York (1969).

Leighton, P. A., Photochemistry of Air Pollution, Academic Press, New York (1961).

Lochte-Holtgreven, W., Ed., Plasma Diagnostics, North-Holland, Amsterdam (1968).

Loeb, L. B., Fundamental Processes of Electrical Discharge in Gases, John Wiley, New York (1939).

Margenau, H., and G. M. Murphy, The Mathematics of Physics and Chemistry, Van Nostrand, New York (1943).

Marr, G. V., Photoionization Processes in Gases, Academic Press, New York (1967).

Marton, L. L., Ed., Advances in Electronics and Electron Physics series, Academic Press, New York.

Massey, H. S. W., Negative Ions, Cambridge University Press, Cambridge (1950).

Massey, H. S. W., and E. H. S. Burhop, Electronic and Ionic Impact Phenomena, Oxford University Press, London (1952).

Mayer, J. E., and M. G. Mayer, Statistical Mechanics, John Wiley, New York (1940).

McCormac, B. M., Ed., Aurora and Airglow, Reinhold, New York (1967).

McCormac, B. M., Ed., The Radiating Atmosphere, Reidel, Dordrecht, Holland (1971).

McCormac, B. M., and A. Omholt, Eds., Atmospheric Emissions, Reinhold, New York (1969).

McDaniel, E. W., Collision Phenomena in Ionized Gases, John Wiley, New York (1964).

McDaniel, E. W. et al, Ion-Molecule Reactions, John Wiley, New York (1970).

McDowell, M. R. C., Ed., Atomic Collision Processes, North-Holland, Amsterdam (1964).

Menzel, D. H., Ed., Selected Papers on the Transfer of Radiation, Dover, New York (1966).

Mitra, S. K., The Upper Atmosphere, The Asiatic Society, Calcutta (1952).

Moore, C. E., Atomic Energy Levels, Circular 467, Vols. I, II, III, National Bureau of Standards, Washington (1949 et seq.).

Mott, N. F., and H. S. W. Massey, The Theory of Atomic Collisions, 3rd Ed., Oxford University Press, London (1965).

National Standard Reference Data System publications, National Bureau of Standards (NSRDS-NBS), Washington.

Noyes, W. A., Jr., and P. A. Leighton, The Photochemistry of Gases, Dover, New York (1966).

Oak Ridge National Laboratory, Atomic and Molecular Processes Information Center, Bibliography of Atomic and Molecular Processes.

Penner, S. S., Quantitative Molecular Spectroscopy and Gas Emissivities, Addison-Wesley, Reading, Massachusetts (1959).

Progress in Reaction Kinetics series, Pergamon Press, New York.

Radiation Chemistry Data Center, Biweekly Lists of References in Radiation Chemistry, University of Notre Dame, Notre Dame, Indiana (1968 et seq.).

Ratajczak, E., and A. F. Trotman-Dickenson, Supplementary Tables of Bimolecular Gas Reactions, University of Wales Institute of Science and Technology, Department of Education and Science, London (1970).

Ratcliffe, J. A., Ed., Physics of the Upper Atmosphere, Academic Press, New York (1960).

Rawer, K., Ed., Winds and Turbulence in Stratosphere, Mesosphere, and Ionosphere, North-Holland, Amsterdam (1968).

Rishbeth, H., and O. K. Garriott, Introduction to Ionospheric Physics, Academic Press, New York (1969).

Ross, J., Ed., Molecular Beams, Interscience, New York (1966).

Samson, J. A. R., Techniques of Vacuum Ultraviolet Spectroscopy, John Wiley, New York (1967).

Sawyer, R. A., Experimental Spectroscopy, Dover, New York (1963).

Seaton, M. J., Atomic and Molecular Processes, Academic Press, New York (1962).

Shuler, K. E., and W. R. Bennett, Eds., Chemical Lasers, Applied Optics, Supplement 2, Volume 4 (1965).

Sinnott, G. A., Bibliography of Ion-Molecule Reaction Rate Data, JILA Information Center Report No. 9, University of Colorado, Boulder (1969).

Sobolev, V. V., A Treatise on Radiative Transfer, Van Nostrand, Princeton, New Jersey (1963).

Starr, V. P., Physics of Negative Viscosity Phenomena, McGraw-Hill, New York (1968).

Steacie, E. W. R., Atomic and Free Radical Reactions, 2nd Ed., Reinhold, New York (1954).

Stormer, C., The Polar Aurora, Oxford University Press, London (1955).

Thrane, E., Ed., Electron Density Distribution in the Ionosphere and Exosphere, North-Holland, Amsterdam (1964).

Trozzolo, A. M., Ed., Singlet Molecular Oxygen and Its Role in Environmental Sciences, Annals of the New York Academy of Sciences, Volume 171, Article 1 (1970).

Turner, D. W. et al, Molecular Photoelectron Spectroscopy, Interscience, London (1970).

Tverskoi, P. N., Physics of the Atmosphere: A Course in Meteorology, translated from the Russian, U. S. Department of Commerce Clearing House, N66-23462, Government Printing Office, Washington (1965).

United States Standard Atmosphere Supplement 1966, Government Printing Office, Washington (1966).

Valley, S. L., Ed., Handbook of Geophysics and Space Environments, McGraw-Hill, New York (1965).

Vedeneyev, V. I. et al, Bond Energies, Ionization Potentials, and Electron Affinities, St. Martin's Press, New York (1966).

Vincenti, W. G., and C. H. Kruger, Physical Gas Dynamics, John Wiley, New York (1965).

Walt, M., Ed., Auroral Phenomena—Experiments and Theory, Stanford University Press, Stanford, California (1965).

Webb, W. L., Ed., Stratospheric Circulation, Academic Press, New York (1969).

Whitten, R. C., and I. G. Poppoff, Physics of the Lower Ionosphere, Prentice-Hall, Englewood Cliffs, New Jersey (1965).

Wilkes, M. V., Oscillations of the Earth's Atmosphere, Cambridge University Press, Cambridge (1949).

Wright, A., and C. Winkler, Active Nitrogen, Academic Press, New York (1968).

Zel'dovich, Y. B., and Yu. P. Raizer, Physics of Shock Waves and High Temperature Hydrodynamic Phenomena, Academic Press, New York (1966).

Zelikoff, M., Ed., The Threshold of Space, Pergamon Press, New York (1957).